Applied Ecology and Environmental Research

International Scientific Journal

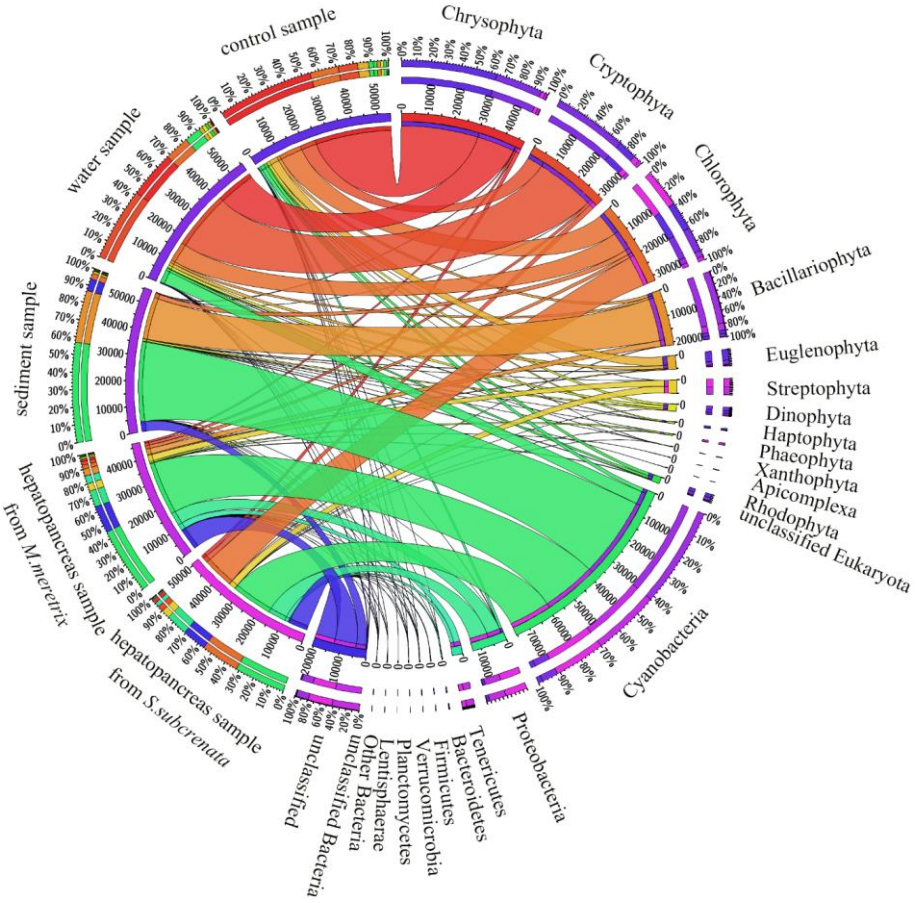

VOLUME 19 * NUMBER 6 * 2021

Published: November 30, 2021
http://www.aloki.hu
ISSN 1589 1623 / ISSN 1785 0037
DOI: http://dx.doi.org/10.15666/aeer

CHEMICAL CHARACTERIZATION OF COMMON MILKWEED (*ASCLEPIAS SYRIACA* L.) ROOT EXTRACTS AND THEIR INFLUENCE ON MAIZE (*Zea mays* L.), SOYBEAN (*Glycine max* (L.) Merr.) AND SUNFLOWER (*Helianthus annuus* L.) SEED GERMINATION AND SEEDLING GROWTH

POPOV, M.[1] – PRVULOVIĆ, D.[2] – ŠUĆUR, J.[2] – VIDOVIĆ, S.[3] – SAMARDŽIĆ, N.[1] – STOJANOVIĆ, T.[1] – KONSTANTINOVIĆ, B.[1*]

[1]*Department of Plant and Environmental Protection, Faculty of Agriculture, University of Novi Sad, Trg Dositeja Obradovića 8, 21102 Novi Sad, Republic of Serbia (phone: +381-21-485-3500)*

[2]*Department of Field and Vegetable Crops, Faculty of Agriculture, University of Novi Sad, Trg Dositeja Obradovića 8, 21102 Novi Sad, Republic of Serbia (phone: +381-21-485-3500)*

[3]*Department of Biotechnology and Pharmaceutical Engineering, Faculty of Technology, University of Novi Sad, Bulevar Cara Lazara 1, 21102 Novi Sad, Republic of Serbia (phone: +381-21-485-3619)*

[*]*Corresponding author*
e-mail: bojan.konstantinovic@polj.edu.rs; phone: +381-21-485-3315

(Received 8th Apr 2021; accepted 19th Jul 2021)

Abstract. The *Asclepias syriaca* L. is an invasive weed species which continuously occurs in numerous populations in the ruderal and agricultural land in Serbia. The aim of the study was to examine the antioxidant capacity of the *A. syriaca* water and methanol extracts and investigate the effects of the selected extracts towards the seed germination, growth, seedlings development and oxidative stress parameters of maize (*Zea mays* L.), soybean (*Glycine max* (L.) Merr.) and sunflower (*Helianthus annuus* L.). The water extract exhibited the higher total tannin content and superoxide free radical scavenging activity, while the methanol extract had a higher antioxidant capacity (measured by FRAP, DPPH and ABTS assays). The total tannin content ranged from 0.252 (methanol extract) to 0.805 (water extract) mg GAE/g. The water extract showed a significant germination inhibition in the tested plants, while no inhibition was noted in the case of the methanol extract compared with the control. However, both of the tested extracts types significantly reduced shoot and root length in case of all the tested plants.
Keywords: *Asclepias syriaca, allelopathy, growth inhibition, antioxidant capacity*

Introduction

The common milkweed (*Asclepias syriaca* L.) occured as an invasive weed in Central and Eastern Europe (Mojzes and Kalapos, 2015) and spread through the extensive areas where it formed new ecosystems (Kelemen et al., 2016). Except being common in abandoned arable land and deforested clearings (Szilassi et al., 2019), as well as on the sand grassland (Bakacsy, 2019), this weed species favours fields and plantations of the agricultural crops (Bakacsy and Bagi, 2020). Many scientific papers confirm the problem of the common milkweed presence in agricultural crops, as well as the cause of the yield reduction of the crops such as: great millet, maize, alfalfa, wheat, sorghum and soybean (Cramer and Burnside, 1982; Bhowmik, 1994; Hartzler and Buhler, 2000). In the past decades in Serbia a continuous presence of the weed species *A. syriaca* has been

http://www.aloki.hu ● ISSN 1589 1623 (Print) ● ISSN 1785 0037 (Online)
DOI: http://dx.doi.org/10.15666/aeer/1906_42194230

established in the neglected orchards and vineyards, along the roads and railway lines, as well as on the dams and other ruderal habitats where it most frequently forms uniform associations, or it occurs with other weed species and *A. syriaca* being the most predominant. From there it spreads to the arable land where it forms "oases", especially in maize, sunflower, soybean, rapeseed, orchards and vineyards (Dolmagić, 2010).

The allelopathic effect of *A. syriaca* was determined by Le Tourneau et al. (1956) who reported that the water extract of the aerial plant parts at the concentration of 2 g dry weight per 100 mL of water inhibits the seed germination, as well as the length of coleoptile and hypocotyl of the Mida wheat. Rasmussen (1975) subsequently found that the water extracts obtained from *A. syriaca* leaf inhibited the seedling growth of the cultivated sorghum (*Sorghum bicolor* L.). More recently, Narwal et al. (2000) established that the water extract from the fresh root inhibits the germination of *Amaranthus retroflexus* L., *Chenopodium album* L. and *Lepidium sativum* L. Similarly, Beres and Kazinczi (2000) found that *A. syriaca* water extract reduces the maize germination by 34%, as well as hinders the germination of sunflower and soybean seeds. The same extract was found to induce fresh weight production increase in wheat. According to Szilágyi et al. (2018), the water extract of the *A. syriaca* stem in the concentration of 8 g/100 mL inhibited the garden cress (*Lepidium sativum* L.) seed germination, which was also noted in case of the 4 and 8 g/100 mL concentrations of the leaf water extract.

The common milkweed is a perennial plant with rhizomatic root, which is effective in the vegetative propagation of the plant (Bagi, 2008). Considering its powerful root, large leaf area, effective seed dispersion and clonal spread, drought tolerance (Szitár et al., 2018), as well as the allelopathic properties, this weed can be competitive in case of the other less aggressive plant species (Borders and Lee-Mäder, 2014).

The analyses of the *A. syriaca* chemical composition indicate that the whole plant is the source of polyphenols, oils and hydrocarbon polymers. In 48 *A. syriaca* populations studied by Campbell (1983) the presence of polyphenol + oil was noted in 4.7−14.4% of the dry weight samples, while 0.2−1.2% contained hydrocarbon polymers. In addition, the presence of phenolic acids (*p*-hydroxybenzoic, *p*-coumaric, protocatechuic and caffeic acid) in *A. syriaca* leaves and flowers was determined by the TLC and HPLC methods. The mentioned author also found that the flowers contain gallic acid, while *α*-resorcylic, vanilla and chlorogenic acid were obtained from the leaves. Sikorska et al. (2000) subsequently established that the conjugated forms of phenolic acids predominate in the *A. syriaca* plant.

All the aerial plant parts, as well as the root, contain cardenolide glycosides identified as syriobioside, syrioside, syriogenin, xysmalogenin, desglucouzarin, uzarigenin and uzarin, as well as proteins, fitosterols and vitamin C. The resins, waxes, rubber, oil, enzymes, terpens and hydrocarbons are considered to be the main components of the *A. syriaca* latex (Sikorska et al., 2000). The cardenolides, the bitter-tasting steroids, exhibit toxic effects in animals that consume the plant because they interrupt the Na-K flux in animal cells (Malcolm, 1991).

Given the increasing prevalence of *A. syriaca* in agroecosystems the aim of this paper was to establish whether the water and methanolic extract of *A. syriaca* root has a negative effect towards the seed germination, the growth and the seedlings development of the most important field crops (maize, sunflower and soybean), and whether the extracts cause oxidative stress for the studied plants.

http://www.aloki.hu ● ISSN 1589 1623 (Print) ● ISSN 1785 0037 (Online)
DOI: http://dx.doi.org/10.15666/aeer/1906_42194230

Materials and Methods

Sampling and extracts preparation

The study was conducted in 2019 by using the root samples of the *A. syriaca* collected in May of the same year from the banks of the Danube (45°15'39" N; 19°52'00" E) and dried at 40°C for 5 days in the dryer, after which they were ground into powder and stored at 2°C until the analysis. The bioassay experiment was carried out two months later, in July, by dispersing the 40 g of the dry root mass in 1 L of the distilled water for 24 hours in a shaker (GFL, Schuttelapparate Shakers, Germany, Model 3015) in the dark. The resulting water extract at the concentration level of 0.04 g/mL, which was marked as WAT, was filtered according to the method described by Chon et al. (2003) and used for making further diluents in order to get 4 final tested concentrations: 0.04, 0.03, 0.02 and 0.01 g/mL.

The methanolic solution was prepared by dispersing 40 g of the dry root mass in 1 L of 95% methanol at 24°C for 24 hours in a shaker (GFL, Schuttelapparate Shakers, Germany, Model 3015) in the dark, followed by filtering using the same procedure as for the WAT. After that the methanol was evaporated to the absolutely dry matter which had been diluted in 1 L of the distilled water and marked as 0.04 g/mL MET. From this dilution, three other diluents were made in order to get 4 final tested concentrations: 0.04, 0.03, 0.02 and 0.01 g/mL.

The WAT and the MET extracts were used for further bioassays under the assumption that the WAT extracts absorb more bioactive compounds than the MET extracts, which presumably could be the cause of the greater inhibition of the seed germination and shoot and root length of the tested plants by the WAT extracts.

For the laboratory examination of the allelopathic effect of *A. syriaca* root extracts the soybean (sort Balkan), sunflower (P-251) and maize (hybrid NS 5053) seeds were used. Each extract was diluted with distilled water to obtain the 0.01, 0.02, 0.03 and 0.04 g/mL concentrations. For each of the four tested concentrations, as well as for the controls, four replicates were done by placing 25 maize, soybean and sunflower seeds separately in the Petri dishes (Ø 12 mm) on a filter paper soaked with 8 mL of the particular extract concentration, i.e. distilled water in case of controls. The whole experiment was carried out twice. Prior to commencing the experiment, all seeds were sterilized via the Voll et al. (2005) method. The seeds were allowed to germinate in a temperature-controlled chamber at 24°C during a 12-hour light period, after which the temperature was reduced to 20°C for a 12-hour dark period, while maintaining the average air humidity at 65%. The allelopathic activity of the *A. syriaca* root on the maize, soybean and sunflower crops was determined by measuring the seedling shoot and root length (Marinov-Serafimova et al., 2007), as well as by recording the number of the germinated seeds, 7 days after the start of the experiment. After that the plants were collected for the oxidative stress analysis. The germination percentage was calculated using the following formula (*Eq.1*):

$$GP(\%) = \frac{GS \times 100}{TSS} \qquad \text{(Eq.1)}$$

In *Equation 1*, *GP* is the germination percentage, *GS* represents the number of the germinated seeds, while the *TSS* stands for the total seeds sown.

http://www.aloki.hu ● ISSN 1589 1623 (Print) ● ISSN 1785 0037 (Online)
DOI: http://dx.doi.org/10.15666/aeer/1906_42194230

Chemical analysis of the Asclepias syriaca root extract

One gram of the dry plant material was extracted overnight with 50 mL of 70% methanol. The water extracts were prepared with boiling distilled water. The extracts were centrifuged, filtered and kept in the refrigerator until the analysis.

The contents of the total phenolic (TP) compounds and total tannins (TT) in extracts were determined using a Folin-Ciocalteu colorimetric method (Nagavani and Raghava Rao, 2010). The amount of TP and TT was calculated as a gallic acid equivalent (GAE) from the calibration curve of the gallic acid standard solutions. The obtained results were expressed in milligrams of the gallic acid equivalents per 1 g of the dry plant weight (mg GAE/g).

The ferric-reducing antioxidant power (FRAP) assay was carried out according to the procedure reported by Valentão et al. (2002). The ABTS (2,20-Azino-bis (3-Ethylbenzothiazoline-6-Sulfonic Acid)) assay was based on a method described by Miller et al. (1993). The scavenging of the free radicals was evaluated in a DPPH (2,2-diphenyl-1-picrylhydrazyl) acetone solution (Lai and Lim, 2011). The degree of the solution discoloration indicates the scavenging efficiency of the added substance. The total antioxidant activity (TAA) of plant extracts was performed by phosphomolybdenum method as reported by Kalaskar and Surana (2014). The standard curves for FRAP, ABTS, DPPH and TAA assays were plotted using the trolox solution. The standard curve was constructed using the different concentrations of the acetone solution of the trolox and the results were expressed as mg trolox equivalents per gram of dry plant material (mg TE/g). The superoxide free radical (O_2^-) scavenging activity was carried out by the NBT (nitroblue tetrazolium) test (Kalaskar and Surana, 2014). The results were expressed as the percentage (%) of the inhibition of O_2^- production during 15 minutes.

The obtained data are reported as the average values for at least three independent replications for all of the performed assays.

Biochemical analysis of the tested plants

For the determination of the biochemical parameters 2 g of the fresh plant material (soybean, sunflower and maize) treated with 0.02 and 0.04 g/mL of the WAT, as well as for the control, were homogenized in 10 mL of the phosphate buffer (0.1 M, pH 7.0). After the centrifugation, the supernatants (soybean, sunflower and maize extracts) were used for the biochemical analyses. The biochemical analyses were carried out spectrophotometrically using an UV/VIS spectrophotometer (Thermo Scientific Evolution 220 (USA)).

The superoxide dismutase (SOD) (EC 1.15.1.1) activity was assayed according to the method of Mandal et al. (2008) which was slightly modified by measuring its ability to inhibit the photochemical reduction of the nitro blue tetrazolium (NBT) chloride. One unit of the SOD activity was defined as the amount of enzymes required to inhibit reduction of the NBT by 50%. The activity of the enzyme was expressed in U/g of fresh weight (FW). The amount of removed superoxide anion radicals was determined by the method of Misra and Fridovich (1972). The total amount of removed superoxide anion radicals was given in nmol O_2 per g of fresh weight (nmol O_2/g FW). The malondialdehyde (MDA) content, an end product of the lipid peroxidation process, was measured at 532 nm using the thiobarbituric acid (TBA) test (Mandal et al., 2008). The total amount of the TBA-reactive substances was given in nmol of MDA equivalents per g of fresh weight (nmol MDA/g FW).

http://www.aloki.hu ● ISSN 1589 1623 (Print) ● ISSN 1785 0037 (Online)
DOI: http://dx.doi.org/10.15666/aeer/1906_42194230

Statistical analysis

For biochemical analysis of the tested plants all measurements were performed in triplicates. The values of the biochemical parameters were expressed as the average value ± standard error and tested by ANOVA followed by the comparison of the average values by Duncan's multiple range test ($p<0.05$). The data were analyzed using TIBC STATISTICA version 13.5.0.17. The same statistical analysis was used in order to determine the statistical significance of the maize, sunflower and soybean shoot and root length inhibition as the dependent variables and the water and methanol *A. syriaca* root extract concentrations as the independent variable, as well as for the seed germination of the tested plants as the dependent variable.

Results and Discussion

Chemical analysis of the Asclepias syriaca root extracts

The content of the total phenolics, tannins and antioxidant capacity of the water and methanol extracts of the *A. syriaca* roots are shown in *Table 1* where the average values and standard deviation are shown. Regarding the extraction solvent significant differences were found in the content of most measured chemical parameters in the extracts of the *A. syriaca* roots ($p<0.05$). No significant differences were observed in TP content and TAA of water and methanol extracts. It is observed that water extracts possess a significantly higher ($p<0.05$) TT content and a higher superoxide free radical (O_2^-) scavenging activity measured by NBT assay (51.92%) compared with the extraction with 70% methanol (12.39%). The TT contents in the examined extracts ranged from 0.252 (methanol extract) to 0.805 (water extract) mg GAE/g. The methanol extract of the *A. syriaca* roots possess a higher antioxidant capacity in comparison with the water extract measured by FRAP, DPPH and ABTS assays.

Table 1. *The content of the phenolic compounds and the antioxidant capacity of the water and methanol extracts of the A. syriaca roots presented as the average value ± standard deviation*

	Total phenolics (mgGAE/g)	**Total tannins (mgGAE/g)**	**FRAP (mgTE/g)**	**DPPH (mgTE/g)**	**ABTS (mgTE/g)**	**TAA (mgTE/g)**	**NBT assay (%)**
Water extract	2.104 ± 0.057[a]	0.805 ± 0.073[a]	2.441 ± 0.058[a]	1.000 ± 0.322[a]	2.469 ± 0.162[a]	105.184 ± 14.202[a]	79.41 ± 1.52[a]
Methanol extract	2.046 ± 0.080[a]	0.252 ± 0.085[b]	3.085 ± 0.071[b]	1.557 ± 0.050[b]	3.069 ± 0.145[b]	94.535 ± 3.581[a]	51.92 ± 1.44[b]

The values followed by the same letter are at the same level of the statistical significance for $p<0.05$

Effect of Asclepias syriaca root extracts on the bioassay test species

The applied *A. syriaca* WAT concentrations exhibited a significant germination inhibition in maize, soybean and sunflower seeds in comparison with the control group. The higher WAT concentrations have induced the notable decrease in the percentage of the germinated sunflower and maize seeds. The similar results were obtained by Nádasy et al. (2018) who noticed that 7.5% water extract of the *A. syriaca* root reduced the maize germination by 20%.

http://www.aloki.hu ● ISSN 1589 1623 (Print) ● ISSN 1785 0037 (Online)
DOI: http://dx.doi.org/10.15666/aeer/1906_42194230

Nevertheless, the MET extracts have shown no inhibition regarding the seed germination of any of the tested plants (*Fig. 1*).

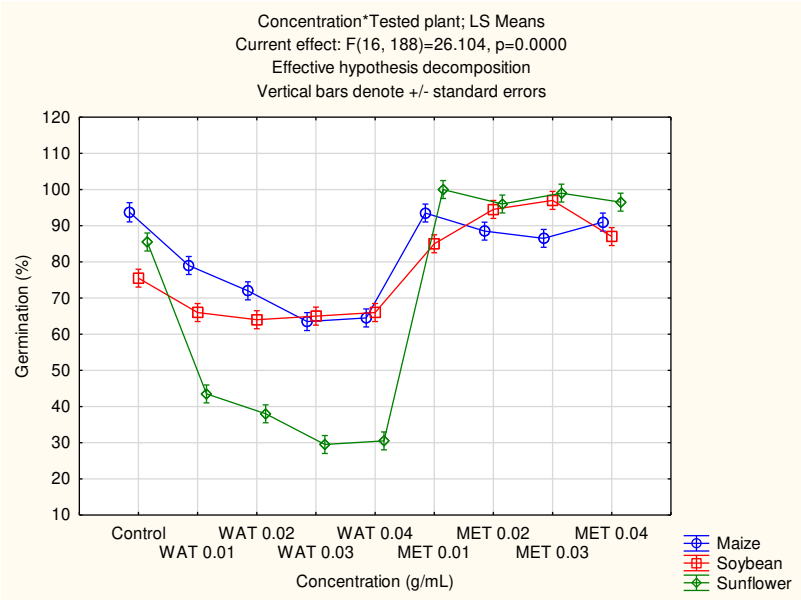

Figure 1. *The effect of the Asclepias syriaca root extracts on the maize, soybean and sunflower seeds germination (%)*

The effects of the different WAT and MET concentrations showed the high statistical differences regarding the maize shoot (p_{sl}=0.0000 for p<0.01) and root length (p_{rl}=0.0000 for p<0.01). Duncan's post hoc test confirmed the tested statistically significant differences and emphasized the similar shoot and root inhibition induced by 0.02, 0.03 and 0.04 g/mL of the MET (*Fig. 2*).

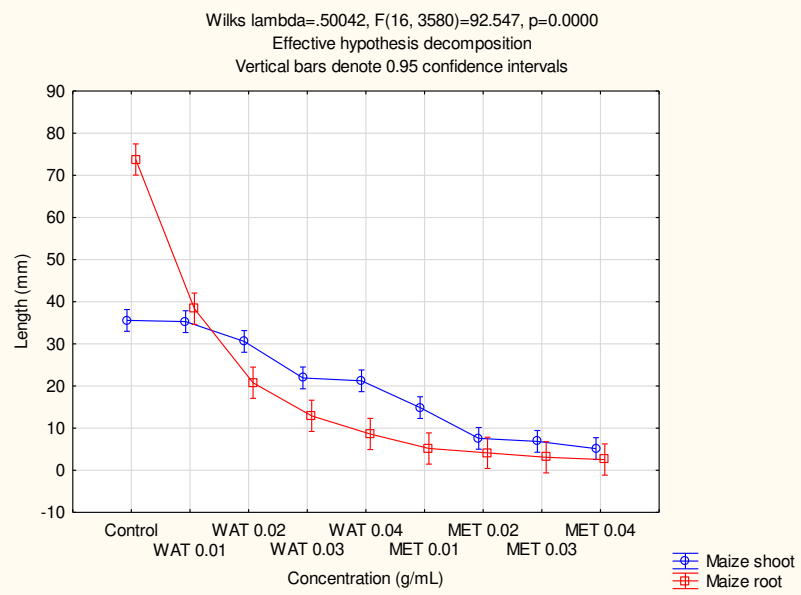

Figure 2. *The effect of the water and methanol A. syriaca root extracts on the shoot and root length of the maize*

http://www.aloki.hu ● ISSN 1589 1623 (Print) ● ISSN 1785 0037 (Online)
DOI: http://dx.doi.org/10.15666/aeer/1906_42194230

In case of the soybean, the effects of the different WAT and MET concentrations were similar as in the previous case, where high statistical differences were determined for both the shoot (p_{sl}=0.0000 for p<0.01) and root length (p_{rl}=0.0000 for p<0.01). According to the Duncan's post hoc test high statistically significant differences in shoot and root inhibition were observed for 0.04 g/mL of the MET, followed by 0.02, 0.03 and 0.04 g/mL of the WAT concentrations (*Fig. 3*).

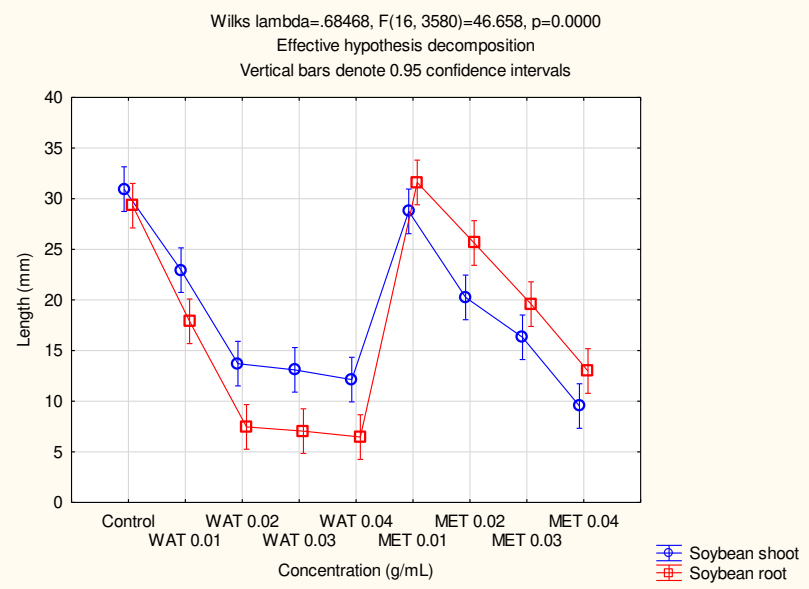

Figure 3. *The effect of water and methanol A. syriaca root extracts on shoot and root length of soybean*

Comparing the effects of the different WAT and MET concentrations, high statistical differences were observed considering the sunflower shoot (p_{sl}=0.0000 for p<0.01) and root length (p_{rl}=0.0000 for p<0.01). Duncan's post hoc test confirmed the tested statistical significances and highlighted the similar shoot and root inhibition induced by the 0.03 and 0.04 g/mL of the WAT and 0.02, 0.03 and 0.04 g/mL of the MET (*Fig. 4*).

Biochemical analysis of the tested plants

The significant decrease in the activity of the SOD was detected in sunflower seedlings after the treatment with 0.02 g/mL of the WAT. On the other hand, in the soybean seedlings the higher concentration of the WAT (0.04 g/mL) significantly increased the activity of the SOD. In the maize seedlings there was no significant difference in the activity of the SOD in the treated seedlings compared with the seedlings from the control group.

The total amount of the removed superoxide anion radicals was significantly higher in all treated seedlings after the treatment with the higher concentration (0.04 g/mL) of the WAT.

The accumulation of malondialdehyde (MDA) was notably higher in maize and soybean seedlings after the treatment with the higher concentration of the WAT (0.04 g/mL). In the maize seedling the amount of MDA was 301 nmol MDA/g FW, while the amount of MDA in the soybean seedling was 284 nmol MDA/g FW. The

http://www.aloki.hu ● ISSN 1589 1623 (Print) ● ISSN 1785 0037 (Online)
DOI: http://dx.doi.org/10.15666/aeer/1906_42194230

accumulation of the MDA indicates that 0.04 g/mL of the WAT expresses the negative effect against the maize and soybean seedlings inducing oxidative stress accompanied by the induction of the lipid peroxidation process. In the sunflower seedlings there was no significant increase in the lipid peroxidation intensity. The obtained results are shown in *Table 2*.

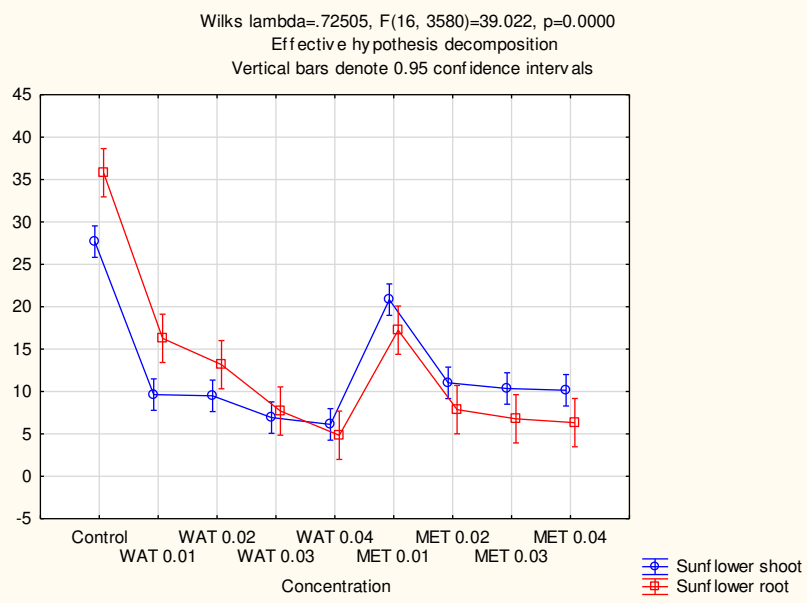

Figure 4. *The effect of the A. syriaca water and methanol root extracts concentrations on the sunflower shoot and root length*

Table 2. *The effect of the two tested concentrations of the Asclepias syriaca water extracts and the control on the activity of the antioxidant enzymes, as well as on the MDA content in the seedlings of the maize, soybean and sunflower presented as the average value ± standard deviation*

Tested plant	Variable	LP nmol MDA/g FW	SOD U/g FW	nmol O_2/g FW
maize	control	44.273±0.685^{a}	44.745±0.579^{a}	5.835±0.568^{a}
	0.02 g/mL	43.151±3.952^{a}	47.339±0.556^{a}	75.970±3.905^{b}
	0.04 g/mL	301.613±4.927^{e}	46.249±1.220^{a}	80.392±0.810^{b}
soybean	control	57.511±4.312^{b}	1.993±0.065^{e}	101.954±11.459^{b}
	0.02 g/mL	66.335±1.425^{c}	2.858±0.260^{e}	129.852±82.732^{b}
	0.04 g/mL	284.412±7.513^{d}	22.899±14.134^{b}	241.929±4.500^{c}
sunflower	control	42.179±4.094^{a}	21.507±0.919^{b}	88.575±6.710^{b}
	0.02 g/mL	40.758±0.648^{a}	12.333±3.444^{c}	102.849±3.683^{b}
	0.04 g/mL	40.011±0.565^{a}	22.335±5.096^{b}	226.798±19.858^{c}

The values followed by the same letter are at the same level of the statistical significance for $p<0.05$

The chemical composition analysis of the *A. syriaca* extract revealed the presence of the phenolic compounds. The total phenolic and tannin content was higher in the *A. syriaca* root WAT extract compared with MET extract. The negative effect of the WAT on the lipid peroxidation process in maize and soybean seedlings was probably

http://www.aloki.hu ● ISSN 1589 1623 (Print) ● ISSN 1785 0037 (Online)
DOI: http://dx.doi.org/10.15666/aeer/1906_42194230

caused by the phenolics and other toxic plant secondary metabolites presented in *A. syriaca* root.

The results of the other authors indicate that the yield losses could be due to phytotoxins produced by *A. syriaca*. Rasmussen (1975) reported that the water extracts from the fresh *A. syriaca* leaves inhibited the growth of the grain sorghum seedlings. Cramer and Burnside (1982) found that water extracts of *A. syriaca* shoot and root significantly reduced the germination percentage, hypocotyl length and the radicle length of sorghum. Even though, as allelochemicals, phenols occupy a significant place in the scientific literature (Einhellig, 2004), some characteristics of this group of compounds do not correspond with the allelochemical concept. For example, cinnamic acid is universally present in all higher plants, while benzoic acids are found in all examined *Magnoliophyta* (Dalton, 1999). Moreover, they are an integral part of the soil to which they are delivered via root secretions, as well as through microbiological activities involved in the degradation of plant residues, which are considered to perform a major impact on the free phenols level in the soil (Blum, 2004). Although the allelopathic effect of the phenols has been extensively studied (Inderjit, 1996), in most cases these compounds are present as a mixture. Similarly, it is likely that more than one compound induces the allelopathy reaction (Einhellig, 2004). Different compounds have varying toxicity, similar modes of action, or affect cellular functions in several different ways, due to which they do not exhibit a typical herbicidal effect. Their individual concentrations in the soil are usually lower than in laboratory conditions and are insufficient for significant allelopathic activity. It is assumed that the intensity of the phenolic compounds allelopathic activity in the natural conditions depends solely on their combination and on the ratio of their quantities, although the possible synergism among the compounds has not yet been proven.

The extensive body of literature on the organic acids possible mechanisms of action, especially phenolic acids, exists (Rice, 1984; Einhellig, 2002; Prasad and Devi, 2002). The available evidence indicates that the root cell membrane is the primary site of action, similar to contact herbicides. This root cell membrane disorder leads to the impairment of its normal functioning and thus results in the interruption of the nutrient and water absorption or energy accumulation (Einhellig, 1995; Blum et al., 1999; Einhellig, 2002; Prasad and Devi, 2002). Hence, there is no universal plant response to the inhibitory concentration of these allelochemicals in relation to, for example, natural stresses. The phenolic acids act as the systemic herbicides since they are absorbed through the roots and gradually translocated throughout the entire plant (Glass and Böhm, 1971; Harper and Balke, 1981; Lehman and Blum, 1999).

Conclusion

The applied *A. syriaca* water extract concentrations exhibited a significant germination inhibition in maize, soybean and sunflower seeds, while the MET extracts did not inhibit seed germination of any of the three tested plants. Also, all the concentrations of the studied water extract caused the inhibition to the epicotyl and hypocotyl increase of the three tested plants seedlings, with the exception of the lowest concentration of the WAT extract (0.01) which had no significant influence on the shoot length. The MET extract in all of the tested concentrations inhibited the shoot and root length of the tested plants, with the exception of the lowest concentration of the MET extract (0.01) which had no significant influence on the shoot length of soybean.

http://www.aloki.hu ● ISSN 1589 1623 (Print) ● ISSN 1785 0037 (Online)
DOI: http://dx.doi.org/10.15666/aeer/1906_42194230

The activity of the SOD was significantly decreased in sunflower seedlings treated with 0.02 g/mL of the *A. syriaca* water extract, while it was notably increased in the soybean seedlings treated with 0.04 g/mL of the same extract. In case of the maize seedlings a significant difference in the activity of the SOD compared with the control group was not observed.

The total amount of removed superoxide anion radicals was significantly higher in all of the treated seedlings after the treatment with the higher concentration (0.04 g/mL) of the *A. syriaca* water extract.

The MDA accumulation was notably higher in maize (301 nmol MDA/g FW) and soybean seedlings (284 nmol MDA/g FW) treated with 0.04 g/mL of the *A. syriaca* water extract, which implicates that the mentioned water extract concentration induced oxidative stress, both with the induction of the lipid peroxidation process in maize and soybean seedlings. In the sunflower seedlings there was no significant increase in the lipid peroxidation intensity.

As it was mentioned before, in the natural conditions, the presence of the *A. syriaca* significantly reduces the crop yield. This adverse effect can be attributed to the competitive relationship between weeds and crops. Still, the levels of the secondary metabolites from the *A. syriaca* root should be subjected to a detailed evaluation, as well as its allelopathic effect in case of other crops.

Considering numerous consequences of the continuous pesticide use the modern agriculture has a task to maintain the quality and the quantity of the crop production while minimizing pesticide application and soil erosion. The concept of allelopathy applied in the modern agricultural production could be of great importance in achieving that important task. Since allelochemicals affect the growth and the yield of the cultivated crops, as well as the present weed populations, the further research considering allelopathy could contribute to finding the alternative ways for the weed management. The possible way of using allelopathy in agriculture implies the production of natural fertilizers with herbicidal activity based on allelochemicals.

REFERENCES

[1] Bagi, I. (2008): Common milkweed (*Asclepias syriaca* L.). – In: Botta-Dukát, Z., Balogh, L. (eds.) The Most Important Invasive Plants in Hungary. Hungarian Academy of Sciences, Institute of Ecology and Botany, Vácrátót, Hungary.

[2] Bakacsy, L. (2019): Invasion impact is conditioned by initial vegetation states. – Community Ecology 20: 11-19.

[3] Bakacsy, L., Bagi, I. (2020): Survival and regeneration ability of clonal common milkweed (*Asclepias syriaca* L.) after a single herbicide treatment in natural open sand grasslands. – Scientific Reports 10: 14222.

[4] Beres, I., Kazinczi, G. (2000): Allelopathic effects of shoot extracts and residues of weeds on field crops. – Allelopathy Journal 7(1): 93-98.

[5] Bhowmik, P. C. (1994): Biology and control of common milkweed (*Asclepias syriaca*). – In: Duke, S. A. (ed.) Reviews of Weed Science. Weed Science Society of America, Champaign, Illinois.

[6] Blum, U. (2004): Fate of Phenolic allelochemicals in soils – the role of soil and rhizosphere microorganisms. – In: Macias, F. A., Galindo, J. C. G., Molinillo, J. M. G., Cutler, H. G. (eds.) Allelopathy. Chemistry and Mode of Action of Allelochemicals. CRC Press, Boca Raton.

http://www.aloki.hu ● ISSN 1589 1623 (Print) ● ISSN 1785 0037 (Online)
DOI: http://dx.doi.org/10.15666/aeer/1906_42194230

[7] Blum, U., Shafer, S. R., Lehman, M. (1999): Evidence for inhibitory allelopathic interactions involving phenolic acids in field soils: Concepts vs. an experimental model. – Critical Reviews in Plant Sciences 18(5): 673-693.
[8] Borders, B., Lee-Mäder, E. (2014): Milkweeds: A Conservation Practitioner's Guide. – In: Conner, M., Morris, S. (eds.) Plant Ecology, Seed Production Methods, and Habitat Restoration Opportunities. The Xerces Society for invertebrate conservation, Broadway, Portland.
[9] Campbell, T. A. (1983): Chemical and agronomic evaluation of common milkweed, *Asclepias syriaca*. – Economic botany 37(2): 174-180.
[10] Chon, S. U., Kim, Y. M., Lee, J. C. (2003): Herbicidal potential and quantification of causative allelochemicals from several Compositae weeds. – Weed research 43(6): 444-450.
[11] Cramer, G. L., Burnside, O. C. (1982): Distribution and interference of common milkweed (*Asclepias syriaca*) in Nebraska. – Weed Science 30(4): 385-388.
[12] Dalton, B. R. (1999): The occurrence and behavior of plant phenolic acids in soil environments and their potential involvement in allelochemical interference interactions: Methodological limitations in establishing conclusive proof for allelopathy. – In: Inderjit, K. M., Dakshimi, M., Foy, L. C. (eds.) Principle and Practices in Plant Ecology Allelochemical Interactions. CRC Press LLC, Boca Raton.
[13] Dolmagić, A. (2010): Preliminarna ispitivanja o mogućnosti suzbijanja ciganskog perja (*Asclepias syriaca* L.) - u usevu soje. – Biljni lekar 38(1): 42-49.
[14] Einhellig, F. A. (1995): Allelopathy - Current Status and Future Goals. – In: Inderjit, K. M., Dakshini, M., Einhellig, F. A. (eds.) Allelopathy: Organisms, Processes and Applications. ACS Symposium Series, American Chemical Society, Washington DC.
[15] Einhellig, F. A. (2002): The physiology of allelochemical action: clues and views. – In: Reigosa, M. J., Pedrol, N. (eds.) Allelopathy: From Molecules to Ecosystems. Science Publishers, Inc., Enfield.
[16] Einhellig, F. A. (2004): Mode of allelochemical action of phenolic compounds. – In: Macias, F. A., Galindo, J. C. G., Molinillo, J. M. G., Cutler, H. G. (eds.) Allelopathy. Chemistry and Mode of Action of Allelochemicals. CRC Press, Boca Raton.
[17] Glass, A. D. M., Böhm, B. A. (1971): The uptake of simple phenols by barley roots. – Planta 100(2): 93-105.
[18] Harper, J. R., Balke, N. E. (1981): Characterization of the inhibition of K^+ absorption in oat roots by salicylic acid. – Plant Physiology 68(6): 1349-1553.
[19] Hartzler, R. G., Buhler, D. D. (2000): Occurrence of common milkweed (*Asclepias syriaca*) in cropland and adjacent areas. – Crop Protection 19(5): 363-366.
[20] Inderjit, K. (1996): Plant phenolics in allelopathy. – The Botanical Review 62(2): 186-202.
[21] Kalaskar, M. G., Surana, S. J. (2014): Free radical scavenging, immunomodulatory activity and chemical composition of *Luffa acutangula* var. *Amara* (Cucurbitaceae) pericarp. – Journal of the Chilean Chemical Society 59(1): 2299-2302.
[22] Kelemen, A., Valkó, O., Kröel-Dulay, G., Deák, B., Török, P., Tóth, K., Miglécz, T., Tóthmérész, B. (2016): The invasion of common milkweed (*Asclepias syriaca*) in sandy old-fields - is it a threat to the native flora? – Applied Vegetation Science 19: 218-224.
[23] Lai, H. Y., Lim, Y. Y. (2011): Evaluation of antioxidant activities of the methanolic extracts of selected ferns in Malaysia. – International Journal of Environmental Science and Development 2(6): 442-447.
[24] Le Tourneau, D., Fails, G. D., Heggeness, H. G. (1956): The effect of water extracts of plant tissue on germination of seeds and growth of seedlings. – Weeds 4(4): 363-368.
[25] Lehman, M. E., Blum, U. (1999): Evaluation of ferulic acid uptake as a measurement of allelochemical dose: effective concentrations. – Journal of Chemical Ecology 25(11): 2585-2600.
[26] Malcolm, S. B. (1991): Cardenolide-mediated interactions between plants and herbivores. – In: Rosenthal, G. A., Berenbaum, M. R. (eds.) Herbivores: Their Interactions with Secondary Metabolites. Academic Press, San Diego, CA, USA.

http://www.aloki.hu ● ISSN 1589 1623 (Print) ● ISSN 1785 0037 (Online)
DOI: http://dx.doi.org/10.15666/aeer/1906_42194230

[27] Mandal, S., Mitra, A., Mallick, N. (2008): Biochemical characterization of oxidative burst during interaction between *Solanum lycopersicum* and *Fusarium oxysporum* f. *sp. lycopersici*. – Physiological and Molecular Plant Pathology 72(1): 56-61.
[28] Marinov-Serafimova, P., Dimitrova, T. S., Golubinova, I., Ilieva, A. (2007): Study of suitability of some solutions in allelopathic researches. – Herbologia 8(1): 1-10.
[29] Miller, N. J., Rice-Evans, C., Davies, M. J., Gopinathan, V., Milner, A. (1993): A novel method for measuring antioxidant capacity and its application to monitoring and antioxidant status in premature neonates. – Clinical Science 84: 407-412.
[30] Misra, H. P., Fridovich, I. (1972): The Role of Superoxide Anion in the Autoxidation of Epinephrine and a Simple Assay for Superoxide Dismutase. – Journal of Biological Chemistry 247: 3170-3175.
[31] Mojzes, A., Kalapos, T. (2015): Plant-Derived Smoke Enhances Germination of the Invasive Common Milkweed (*Asclepias syriaca* L.). – Polish Journal of Ecology 63(2): 280-285.
[32] Nádasy, E., Pásztor, G., Béres, I., Szilágyi, G. (2018): Allelopathic effects of *Abutilon theophrasti, Asclepias syriaca* and *Panicum ruderale* on maize. – Tagungsband 28. Deutsche Arbeitsbesprechung über Fragen der Unkrautbiologie und -bekämpfung, 27.02.-01.03.2018, Braunschweig, Deutschland, pp. 453-457.
[33] Nagavani, V., Raghava Rao, T. (2010): Evaluation of antioxidant potential and identification of polyphenols by RP-HPLC in *Michelia champaca* flowers. – Advances in Biological Research 4(3): 159-168.
[34] Narwal, S. S., Hoagland, R. E., Dilday, R. H., Reigosa, M. J. (2000): Allelopathy in Ecological Agriculture and Forestry. – Proceedings of the III International Congress on Allelopathy in Ecological Agriculture and Forestry, 18-21 August, Dharwad, India, pp. 1-9.
[35] Prasad, M. N. V., Devi, S. R. (2002): Physiological basis for allelochemical actions of ferulic acid. – In: Reigosa, M. J., Pedrol, N. (eds.) Allelopathy: From Molecules to Ecosystems. Science Publishers, Inc., Enfield.
[36] Rasmussen, J. A. (1975): Non-competitive effects of common milkweed, *Asclepias syriaca* L., on germination and growth of grain sorghum. – The American Midland Naturalist Journal 94(2): 478-483.
[37] Rice, E. L. (1984): Allelopathy. – Academic Press, Orlando.
[38] Sikorska, M., Matławska, I., Głowniak, K., Zgórka, G. (2000): Qualitative and quantitative analysis of phenolic acid in *Asclepias syriaca* L. – Acta Poloniae Pharmaceutica 57(1): 69-72.
[39] Szilágyi, A., Radócz, L., Tóth, T. (2018): Allelopathic effect of invasive plants (*Eriochloa villosa*, *Asclepias syriaca*, *Fallopia x bohemica*, *Solidago gigantea*) on seed germination. – Acta Agraria Debreceniensis (74): 179-182.
[40] Szilassi, P., Szatmári, G., Pásztor, L., Árvai, M., Szatmári, J., Szitár, K., Papp, L. (2019): Understanding the Environmental Background of an Invasive Plant Species (*Asclepias syriaca*) for the Future: An Application of LUCAS Field Photographs and Machine Learning Algorithm Methods. – Plants 8(12): 593.
[41] Szitár, K., Kröel-Dulay, G., Török, K. (2018): Invasive *Asclepias syriaca* can have facilitative effects on native grass establishment in a water-stressed ecosystem. – Applied Vegetation Science 21: 607-614.
[42] Valentão, P., Fernandes, E., Carvalho, F., Andrade, P. B., Seabra, R. M., Bastos. M. L. (2002): Antioxidative properties of cardoon (*Cynara cardunculus* L.) infusion against superoxide radical, hydroxyl radical, and hypochlorus acid. – Journal of Agricultural and Food Chemistry 50(17): 4989-4993.
[43] Voll, E., Voll, C. E., Filho, R. V. (2005): Allelopathic effects of aconitic acid on wild poinsettia (*Euphorbia heterophylla*) and morningglory (*Ipomoea grandifolia*). – Journal of Environmental Science and Health Part B 40(1): 69-75.

http://www.aloki.hu ● ISSN 1589 1623 (Print) ● ISSN 1785 0037 (Online)
DOI: http://dx.doi.org/10.15666/aeer/1906_42194230

FOXTAIL MILLET (*SETARIA ITALICA* (L.) P. BEAUVOIS) QUALITY RESPONSE TO FERTILIZER LEVELS, HERBICIDE, AND SELENIUM

YANG, Y. J.[1] – GUO, M. J[1] – PANG, Y. F.[1] – SHAO, Q. L.[1] – WU, Y. Z.[1] – ZHAO, H. M.[1] – JI, A. Q.[1] – MA, J. H.[1] – SONG, X. E.[2] – SUN, C. Q.[3] – YANG, X. F.[1] – FENG, Z. W.[4*]

[1]*College of Biological Sciences and Technology, Jinzhong University, Jinzhong 030600, China (phone: +86-351-398-5785)*

[2]*Key Laboratory of Crop Chemical Regulation and Chemical Weed Control, Agronomy College, Shanxi Agricultural University, Taigu 030801, China (phone: +86-354-628-9272)*

[3]*Institute of Crop Sciences, Shanxi Academy of Agricultural Sciences, Taiyuan 030031, China (phone: +86-351-712-3700)*

[4]*Technology Department, Shanxi Academy of Agricultural Sciences, Taiyuan 030031, China (phone: +86-351-707-3254)*

**Corresponding author*
e-mail: yyj1210@sina.com

(Received 19th Apr 2021; accepted 30th Aug 2021)

Abstract. Foxtail millet (*Setaria italica* (L.) P. Beauvois) is a high-nutrition food source. It is commonly consumed in Africa, Asia, Central America, and South America. The key to popularize high-quality foxtail millet in accordance with local conditions is quantifying the impacts of cultivation conditions on its quality. Here, we determined the effects of different fertilizer levels nitrogen (N), tetraphosphorus decaoxide (P_2O_5), and potassium oxide (K_2O), tribenuron-methyl (TBM) herbicide, and *selenium* (Se) on the quality of foxtail millet Jingu 54 using a quadratic general rotation combination design. The first principal component, which could explain 57.41% of the total variance of grain quality, was chosen as the comprehensive quality of Jingu 54 via principal component analysis. The effects of fertilizer levels and Se on comprehensive quality of Jingu 54 were significant ($P < 0.05$), except for TBM. The effects of N × K_2O, N ×TBM, and K_2O × TBM interactions reached significance for the comprehensive quality of Jingu 54 ($P < 0.05$). The grain quality of Jingu 54 was predict by regression equation ($P = 0.0048$, $R^2 = 0.8451$). Recommended cultivation conditions are 108.31 kg ha^{-1}, 94.80 kg ha^{-1}, 105.03 kg ha^{-1}, 88.08 g ha^{-1}, and 18.48 g ai ha^{-1} for N, P_2O_5, K_2O, Se, and TBM, respectively. The maximum predicted comprehensive quality of Jingu 54 was 56.85. This study lays a theoretical foundation for achieving high quality Jingu 54 in the field.

Keywords: *Jingu 54, comprehensive quality, principal component analysis, response surface methodology, tribenuron-methyl herbicide*

Introduction

Foxtail millet (*Setaria italica* (L.) P. Beauvois) is known as the first of five cereals grain has high nutritional value (Sachdev et al., 2021). It is second only to wheat and maize in dry farming of north China and characterized by small genome, short growth cycle and tolerance to drought stress (Jones and Liu, 2009; Yang et al., 2012; Veeranagamallaiah et al., 2008). Some studies have investigated the effects of cultivation conditions on crop quality in wheat (Zörb et al., 2018; Xia et al., 2019), maize (Chilimba, et al., 2012; Guo et al., 2020), and rice (Chen and Chen, 2019; Huang,

http://www.aloki.hu ● ISSN 1589 1623 (Print) ● ISSN 1785 0037 (Online)
DOI: http://dx.doi.org/10.15666/aeer/1906_42314249

2020), but few have examined the cultivation conditions on quality of foxtail millet. Moreover, existing studies have focused on the relationship between individual quality indicators of foxtail millet and individual cultivation conditions by using statistical methods such as simple correlation analysis, which lacks comprehensiveness and is insufficient at explaining the complex interaction between different factors (Powers et al., 2020).

Principal component analysis (PCA) is a widely used statistical method for reducing variable dimensionality. Actually, as a multivariate correlation method, PCA disintegrates a few of inter-correlated variables into smaller sets of clusters which are composed of variables with lower or no degree of correlation (Anju and Banerjee, 2012). Similarly, as a statistical modeling and analysis technique, response surface methodology (RSM) is very popular in optimizing multiple variables (Mao et al., 2018; Montgomery, 2008). Hence, RSM has widespread application prospects in processing biotechnology, such as protein extraction, biofuel production, fermentation, and enzyme immobilization (Feng and Zhang, 2020; Abdel-Fattah et al., 2002; Liu et al., 2003; Adinarayana and Ellaiah, 2002). Moreover, RSM had been used on seedlings, and canola (*Brassica napus* L.) (Dong et al., 2011; Koocheki et al., 2014) culture, Chinese white poplar (Populus tomentosa Carr.). However, its application in optimization of foxtail millet cultivation conditions is barely explored.

Improper fertilization levels and fertilization methods will reduce the efficiency of fertilizers and also increase environmental pollution, thus hampering the quality of foxtail millet. The effects of nitrogen (N), phosphorus (P), potassium (K), and their interaction on the quality of millet have rarely been reported. In addition, exogenous selenium (Se) can increase the content of lutein in tomato (Pezzarossa et al., 2013). It was reported that foliar application Se increased the concentration of iron and zinc in colored-grain wheat (Xia et al., 2019). Whether Se addition also benefits the quality of foxtail millet and affects yellow pigment content in foxtail millet grains is unknown. Finally, while the effect of herbicides on yield components has been reported (Guo et al., 2019; Suganthi et al., 2013; Robinson et al., 2013), its impact on the quality of foxtail millet is not well-understood.

The foxtail millet variety used in this study is Jingu 54, which was breeded from Jingu 21 (a dominant foxtail millet in China) and Jingu 20 (high yielding and drought tolerance). Jingu 54 show a specific characteristic in high yielding, quality and Se enrichment. However, the sown area of Jingu 54 in Shanxi province is about 0.5 million acres. The object of this study was to (1) obtain a comprehensive quality measurement of foxtail millet Jingu 54 by PCA, and (2) assess the effects of fertilizer levels, tribenuron-methyl (TBM) herbicide, and Se on quality of foxtail millet. We carried out field experiments based on 5-factor-5-level quadratic general rotary combination design. Based on the experimental results, the optimal cultivation conditions were determined, thus providing a guidance for future quality improvement of foxtail millet.

Materials and methods

Experimental site and materials

Field experiments were carried out in the Agricultural Experimental Station of Shanxi Agricultural University in Taigu County, Jinzhong City, Shanxi, China. An average annual rainfall of 462.9 mm and 9.9 °C of the annual average temperature are

http://www.aloki.hu ● ISSN 1589 1623 (Print) ● ISSN 1785 0037 (Online)
DOI: http://dx.doi.org/10.15666/aeer/1906_42314249

owned by the study site which has a temperate continental climate. The meteorological data of the experimental locations throughout the growth season of foxtail millet (May-September) in 2019 are shown in *Table 1*.

Table 1. *Meteorological data of the experimental sites during growing season of foxtail millet (May-September) in 2019*

Month	Precipitation (mm)	Temperature (℃)		≥ 20 ℃ accumulated temperature (℃)	Sunshine hours (h)
		Min	Max		
5	30.1	2.6	35.1	329.1	277.0
6	41.6	12.7	35.2	708.0	224.2
7	63.8	12.1	37.0	768.8	229.9
8	42.2	10.5	33.8	706.8	214.0
9	73.9	7.4	34.2	218.4	217.0

The test variety was the foxtail millet Jingu 54. Strawberries were cultivated for rotation with foxtail millet Jingu 54 in the experimental site. Soil texture was red sandy loam and with a medium organic matter content (17.9 g kg^{-1}). Soil texture was characteristic of red sandy loam and a medium organic matter content (17.9 g kg^{-1}). Soil pH was 8.2. Soil involves original soil-available K_2O (93 mg kg^{-1}), N (76 mg kg^{-1}), and P_2O_5 (29 mg kg^{-1}) (Soil Survey Staff, 2014).

Experimental design

Quadratic general rotation combination design with a 5-factor-5-level was implemented to optimize fertilizer levels (N, P_2O_5, and K_2O), herbicide, and Se. The five independent factors (x_1 to x_5) were studied at five different levels (coded: −2, −1, 0, + 1, and + 2, respectively) (*Table 2*), at the central point with six repetitions and two replications at the axial and factorial points, respectively (*Table 3*). The recommended applicable dose of the herbicide was form 13.5 g ha^{-1} to 22.5 g ha^{-1}. A total of 32 treatment combinationswith three replications were run in a completely randomized block design and protection rows were set around the experimental site. Each plot was 3 m × 6 m in size. The plant density and the apllied row distance were 330,000 plants per hectare and 23 cm, respectively. The best combination in 2019 was chosen for the verification test in 2020, planting on May 18, with a plot size of 6 m ×6 m = 36 m^2 and 6 plots.

Table 2. *Levels and codes of five experimental factors*

Code	N (kg ha^{-1})	P_2O_5 (kg ha^{-1})	K_2O (kg ha^{-1})	Se (g ha^{-1})	Tribenuron-methyl (g ai ha^{-1})
–2	0	0	0	0	0
–1	69	36	37.5	60	20
0	138	72	75	120	40
1	207	108	112.5	180	60
2	276	144	150	240	80
Δj	69	36	37.5	60	20

http://www.aloki.hu ● ISSN 1589 1623 (Print) ● ISSN 1785 0037 (Online)
DOI: http://dx.doi.org/10.15666/aeer/1906_42314249

Table 3. *Program and experimental results of quadratic general rotation design for quality traits comprehensive quality of foxtail millet*

No	x_1	x_2	x_3	x_4	x_5	Protein (%)	Fat (%)	Yellow pigment (mg kg^{-1})	Folic acid (ug g^{-1})	Se (ug kg^{-1})	Alkali	Gel	Amylose	PC1
1	1	1	1	1	1	9.9	5.28	11.48	1.76	48.59	2.6	95.43	16.46	50.72
2	1	1	1	-1	-1	10.96	5.6	12.25	1.79	48.59	3.31	99.7	17.76	54.15
3	1	1	-1	1	-1	10.47	4.5	10	1.86	49.15	2.98	85	14	43.88
4	1	1	-1	-1	1	10.15	5.28	11.56	1.83	50.07	2.76	95.43	16.6	50.58
5	1	-1	1	1	-1	9.95	4.96	11.13	1.89	49.15	2.64	91.15	15.88	48.07
6	1	-1	1	-1	1	10.55	5.49	12.2	1.85	48.04	3.04	98.16	17.67	53.29
7	1	-1	-1	1	1	9	4.99	11.01	1.87	50.26	2	91.5	15.69	47.51
8	1	-1	-1	-1	-1	10.72	4.83	10.6	1.8	48.96	3.15	89.44	14.99	46.93
9	-1	1	1	1	-1	9.05	5.45	12.22	1.83	46	2.04	97.65	17.7	52.95
10	-1	1	1	-1	1	9.41	5.28	11.39	1.72	48.78	2.27	95.43	16.32	50.40
11	-1	1	-1	1	1	9.63	5.23	11.67	1.83	46.93	2.42	94.74	16.79	50.87
12	-1	1	-1	-1	-1	10.66	5.46	11.89	1.77	48.22	3.11	97.82	17.15	52.76
13	-1	-1	1	1	1	9.44	4.68	10.31	1.84	49.52	2.29	87.39	14.52	44.97
14	-1	-1	1	-1	-1	9.08	5.5	12.02	1.75	46.93	2.05	98.33	17.37	52.86
15	-1	-1	-1	1	-1	9.52	5.15	11.46	1.86	49.15	2.35	93.72	16.43	49.57
16	-1	-1	-1	-1	1	10.01	5.21	11.44	1.76	46.56	2.67	94.4	16.4	50.65
17	-2	0	0	0	0	9.63	5.41	12.07	1.81	46	2.42	97.14	17.45	52.73
18	2	0	0	0	0	10.5	4.91	10.83	1.87	51	3	90.47	15.38	47.18
19	0	-2	0	0	0	9.6	5.32	11.91	1.78	48.78	2.4	95.94	17.18	51.33
20	0	2	0	0	0	10.8	5.59	11.99	1.7	48.41	3.2	99.53	17.31	53.74
21	0	0	-2	0	0	11.15	5.19	11.29	1.82	49.33	3.44	94.23	16.15	50.20
22	0	0	2	0	0	9.11	5.47	12.14	1.84	47.11	2.07	97.99	17.56	52.79
23	0	0	0	-2	0	10.01	5.4	12.27	1.9	47.11	2.67	96.97	17.78	52.78
24	0	0	0	2	0	10.39	5.05	11.52	1.89	49.89	2.93	92.35	16.54	49.14
25	0	0	0	0	-2	10.09	5.65	12.37	1.84	46	2.73	100.38	17.95	54.86
26	0	0	0	0	2	9.68	5.17	11.38	1.83	49.33	2.45	93.89	16.29	49.59
27	0	0	0	0	0	11.62	5.65	12.4	1.8	48.22	3.75	100.38	18.01	54.99
28	0	0	0	0	0	11.81	5.62	12.6	1.83	49.52	3.87	99.87	18.34	54.77
29	0	0	0	0	0	10.61	5.74	12.59	1.81	48.78	3.07	101.58	18.31	55.30
30	0	0	0	0	0	11.37	5.72	12.73	1.86	48.78	3.58	101.24	18.56	55.59
31	0	0	0	0	0	12	5.49	12.25	1.81	48.59	4	98.16	17.76	53.78
32	0	0	0	0	0	11.18	6	13	1.79	47.48	3.45	105	19	57.99

x_1 – N, x_2 – P_2O_5, x_3 – K_2O, x_4 –Se, x_5 –tribenuron-methyl, PC1-the first principal component

Uniform seeds were sown on May 6, 2019 using a 2BX-3 small seeder (College of Engineering, Shanxi Agricultural University). Seedlings with at least three fully expanded leaves were thinned in accordance with plant spacing. One half of N was applied as a basal fertilizer, and the other half as a top-dressing at the jointing-booting stage. K_2O and P_2O_5 were sereved as supplement natural fertilizers. Fertilizers included urea (N 46%), triple superphosphate (P_2O_5 42%), and sulfate of potash (K_2O 50%). Different dosages of TBM herbicide (10%) and water as control were applied on foxtail millet Jingu 54 seedlings at five-leaf stage. Different dosages of selenite selenium (Na_2SeO_3) were sprayed on the leaf surface during the filling stage. Plots were irrigated and prepared by rotary tillage before sowing. Weed control was undertaken by inter-tillage twice during the experimental period.

The response surface design, which (1) significantly reduces the number of experiments (n = 32) without loss of information when compared to the 5-factor-5-level

http://www.aloki.hu ● ISSN 1589 1623 (Print) ● ISSN 1785 0037 (Online)
DOI: http://dx.doi.org/10.15666/aeer/1906_42314249

full factorial design ($n = 5^5$); (2) simultaneously analyzes the effects of linear, quadratic, and interaction terms of target factors; and (3) obtains a prediction model with a curved surface, is the main advantage of the current study. Although the orthogonal design may decrease the number of trials as well, it only examines the isolated experimental sites one at a time. In contrast, the response surface design enables for ongoing analysis of the experimental levels throughout the optimization process. The latter approach may produce equal variances at experimental sites with equal distance to the center point, overcoming the limitation of orthogonal design methods and improving optimization accuracy. Using a response surface design, optimal conditions for comprehensive quality of foxtail millet can be found. The research took into account all interactions between fertilizer levels, Se, and herbicide, yielding more accurate findings than prior studies that just looked at single-factor impacts (Yang et al., 2018).

Measurement

The gel consistency was determined using a method described by Tran et al. (2011) with slight modifications. Finely grounded foxtail millet grain (100 mg) in duplicate were putted into 13 mm × 100 mm tubes which were respectively filled with 200 μL ethyl alcohol (95%), 0.025% thymol blue, 2.5 mL 0.15 N KOH. The tubes were mixed using a Vortex Genie mixer and then placed in a vigorously boiling water bath for 8 min, held at room temperature for 5 min, and cooled in an ice water bath for 20 min. After this, tubes were laid horizontally on a light box on top of graphing paper. Measure the distance that the gel migrated in the tube after 1 h.

The amylose content in foxtail millet starches was determined according to the procedure of the American Association of Cereal Chemists (2000).

The alkali digestion value was measured from twenty intact and fully mature foxtail millet grains of uniform size that were placed in a Petri dish. 10 mL 1.7% potassium hydroxide (KOH) solution was added to each Petri dish until the grains were completely submerged. The grains remained dispersed to facilitate decomposition and covered with a lid. The samples were placed in a 30 °C thermostat incubator (BIC-300, Shanghai Boxun Industry & Commerce Co., Ltd. Medical Equipment Factory) for 6 h and the decomposition of each grain was then observed. The degree of decomposition was recorded according to *Table 4*. The alkali digestion value was calculated as follows: $A = \sum (G \times N)/7$, where A is alkali digestion value, G is grade of each grain, and N is number of grains at the same degree.

Table 4. *Standard for alkali digestion value of foxtail millet grain samples*

Standard	Degree of decomposition	Definition
1	Grain unchanged	White core in grain
2	Grain expanded	White core in grain, with powdery ring
3	Grain expanded, with incomplete or narrow ring	White core in grain, with flocculent or nebulous ring
4	Grain enlarged, with complete and wide ring	Cotton white core in grain, with nebulous ring
5	Grain cracked, with complete and wide ring	Cotton white core in grain, with clear ring
6	Grain partially dispersed and dissolved, blended with ring	Cloud white core in grain, with no ring
7	Grain completely dispersed	Both core and ring disappeared in grain

The crude protein and fat content of grain samples were determined by the methods described in Association of Official Analytical Chemists (AOAC, 2000). Percentage

http://www.aloki.hu ● ISSN 1589 1623 (Print) ● ISSN 1785 0037 (Online)
DOI: http://dx.doi.org/10.15666/aeer/1906_42314249

crude protein (CP%) was determined by the Kjeldahl method and calculated based on the percentage N (N%) obtained: CP% = N% × 6.25. Fat content (%) was detected by the Soxhlet extraction technique.

Total 500 mg finely grounded foxtail millet grain (was acid-digested with 5 mL 70% superior-grade pure nitric acid and 2 mL 30% hydrogen peroxide to measure Se. With ultrapure water (18.2 MΩ cm^{-1}) the digested samples were diluted to 25 mL. We analyzed the concentration of Se in the digestion solution by atomic fluorescence spectrometry (AFS-933, Beijing Jitian Instrument Co., Ltd.).

Folic acid was determined in exactly 2.5 g foxtail millet grain. Sample was weighed into 25 mL 0.1 mol L^{-1} *potassium dihydrogen phosphate* (KH_2PO_4) and incubated in a 50 °C thermostat water bath for 8 h. The sample was then centrifuged in a high-speed refrigerated centrifuge (Neofuge 15R, Shanghai Lishen Scientific Equipment Co., Ltd.) at 5000 rpm for 10 min. The supernatant was collected, followed by addition of 0.5 g aniline-treated activated C. The mixture was thoroughly vortexed and then heated to boiling in a water bath (DK-S26, Shanghai Jinghong Experimental Equipment Co., Ltd.) for 10 min. The sample was filtered and the supernatant was discarded. The residue was washed five times with 7 mL 3% ammonia: 70% ethanol. The eluate was evaporated and concentrated to 5 mL, followed by addition of 1 mL 2% glacial acetic acid. Thereafter, 0.04% potassium permanganate ($KMnO_4$) was added dropwise until the color of the solution no longer changed. Furthermore, 3% hydrogen peroxide (H_2O_2) was added until the color of $KMnO_4$ faded. The solution was diluted to a volume of 10 mL. The fluorescence intensity was measured using a fluorescence spectrophotometer (BioSpectrometer fluorescence, Germany Eppendorf) at Ex = 370 nm and Em = 443 nm (Shao et al., 2014).

The content of grain yellow pigment was determined using the method described by Ning et al. (2016). The absorbance was measured at 450 nm using a spectrophotometer (UV-2400, Shanghai Sunny Hengping Scientific Instrument Co., Ltd.).

Statistical analysis

All treatments were performed at triplicate and results presented as mean values. We collected the crops (2 m × 2 m) in the middle of each plot for lab analysis to minimize the marginal impact. Using SAS 9.4 software (SAS Institute Inc., Cary, NC, USA), all data analysis were processed. Comprehensive quality of foxtail millet was obtained by principal component analysis (PCA). Quadratic regression model was used for optimizing the cultivation conditions of foxtail millet for fertilizer levels, herbicide and Se. Effects of factorial interactions on grain quality were based on contour plots with Graphpad prism 8.0.

Results

PCA of quality indicators of foxtail millet

To analyze the relationship between the cultivation conditions and grain quality of foxtail millet, PCA was used. Only two eigenvalues were > 1 and explained 82.34% of the total variance in grain quality (*Table 5*). As a result, the first two eigenvalues were picked out for further analysis; other small but non-zero eigenvalues were discarded to set up some potential contributing source factors. From the rotated component matrix (*Table 6*), it was noticeable that all quality parameters were clearly illustrated by the

http://www.aloki.hu ● ISSN 1589 1623 (Print) ● ISSN 1785 0037 (Online)
DOI: http://dx.doi.org/10.15666/aeer/1906_42314249

first two principal components. The first principal component (PC1) explained 57.41% of the variance including protein, fat, folic acid, gel consistency, amylase, alkali digestion value, yellow pigment, and Se. Obviously, the second principal component (PC2), accounting for 24.92% of the variance, had high loadings for protein, Se, and alkali digestion value. Consequently, PC1 was chosen to represent the comprehensive quality of foxtail millet.

Table 5. *Eigenvalues, contribution, and cumulative contribution of the correlation matrix of indicators for comprehensive quality of foxtail millet*

Principal component	Eigenvalue	Contribution proportion (%)	Cumulative (%)
F1	4.5926	57.4080	57.4080
F2	1.9943	24.9285	82.3365
F3	0.9334	11.6670	94.0035
F4	0.4571	5.7140	99.7175
F5	0.0225	0.2818	99.9993
F6	0.0000	0.0004	99.9997
F7	0.0000	0.0002	99.9999
F8	0.0000	0.0001	100.0000

Table 6. *Eigenvectors of selected principal components for comprehensive quality of foxtail millet*

Quality indexes	Eigenvector	
	F1	F2
protein	0.2246	0.6032
fat	0.4583	-0.0798
Yellow pigment	0.4522	-0.0800
Folic acid	-0.1509	0.1444
Se	-0.2182	0.4753
Alkali digestion value	0.2243	0.6033
Gel consistency	0.4582	-0.0803
Amylose	0.4522	-0.0790

Effects of fertilizer levels, Se and hericide on grain comprehensive quality of foxtail millet

Except for TBM, the effects of fertilizer levels and Se on comprehensive quality of foxtail millet were significant ($P < 0.05$). The effect on comprehensive quality was the most significant for Se ($P = 0.0014$), followed by N ($P = 0.0135$), K_2O ($P = 0.0180$), and P_2O_5 ($P = 0.0341$) (*Table 7*). In the design range, the effects of the five factors on comprehensive quality showed a parabolic trend, yet with various patterns (*Fig. 1*). With increasing K_2O, comprehensive quality first increased rapidly; when K_2O exceeded 0.5, the quality showed a slow decline. With increasing P_2O_5 and N, comprehensive quality climbed slightly and then gradually decreased. With increasing Se and TBM, comprehensive quality increased slightly and then plummeted.

http://www.aloki.hu ● ISSN 1589 1623 (Print) ● ISSN 1785 0037 (Online)
DOI: http://dx.doi.org/10.15666/aeer/1906_42314249

Table 7. *Test of significance for the coefficients of regression equation for comprehensive quality of foxtail millet*

Term	Sum of square	DF	Mean square	Partial correlation	F-value	P-value
x_1	18.3750	1	18.3750	-0.6631	8.6328	0.0135*
x_2	12.4416	1	12.4416	0.5891	5.8452	0.0341*
x_3	16.4011	1	16.4011	0.6418	7.7054	0.0180*
x_4	38.4054	1	38.4054	-0.7882	18.0434	0.0014**
x_5	6.7416	1	6.7416	-0.4728	3.1673	0.1027
$x_1 \times x_1$	60.8736	1	60.8736	-0.8498	28.5992	0.0002**
$x_2 \times x_2$	18.5659	1	18.5659	-0.6650	8.7225	0.0131*
$x_3 \times x_3$	32.6839	1	32.6839	-0.7633	15.3553	0.0024**
$x_4 \times x_4$	41.4913	1	41.4913	-0.7995	19.4932	0.0010**
$x_5 \times x_5$	22.3593	1	22.3593	-0.6989	10.5047	0.0079**
$x_1 \times x_2$	1.8225	1	1.8225	-0.2687	0.8562	0.3746
$x_1 \times x_3$	25.0000	1	25.0000	0.7186	11.7453	0.0057**
$x_1 \times x_4$	2.6082	1	2.6082	-0.3166	1.2254	0.2919
$x_1 \times x_5$	25.8064	1	25.8064	0.7241	12.1242	0.0051**
$x_2 \times x_3$	1.9600	1	1.9600	0.2779	0.9208	0.3579
$x_2 \times x_4$	1.0712	1	1.0712	0.2092	0.5033	0.4928
$x_2 \times x_5$	0.0016	1	0.0016	-0.0083	0.0008	0.9786
$x_3 \times x_4$	1.5006	1	1.5006	-0.2454	0.7050	0.4190
$x_3 \times x_5$	14.2884	1	14.2884	-0.6156	6.7129	0.0251*
$x_4 \times x_5$	0.1190	1	0.1190	0.0711	0.0599	0.8174

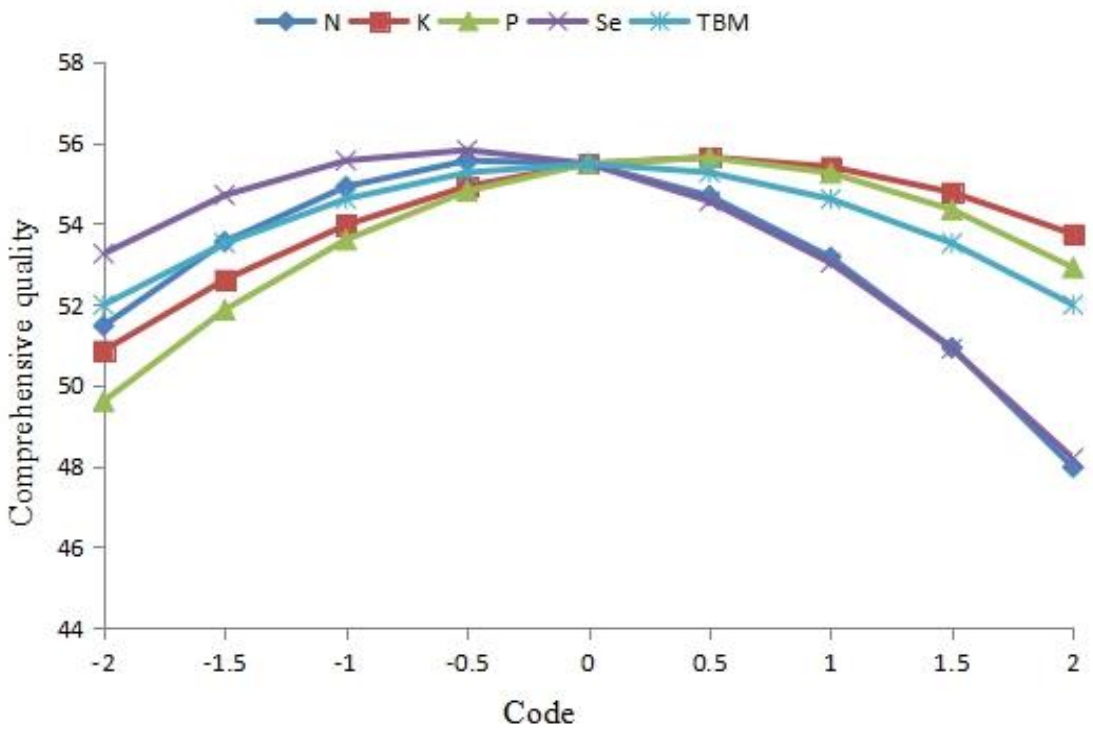

Figure 1. *Effects of single factors on comprehensive quality of Jingu 54*

http://www.aloki.hu ● ISSN 1589 1623 (Print) ● ISSN 1785 0037 (Online)
DOI: http://dx.doi.org/10.15666/aeer/1906_42314249

The effects of N × K_2O, N ×TBM, K_2O ×TBM interactions reached statistical significance for comprehensive quality of foxtail millet (*Table 7*). The contour plots (*Fig. 2*) were mapped to show the interactive effects of N × K_2O, N ×TBM, K_2O ×TBM.

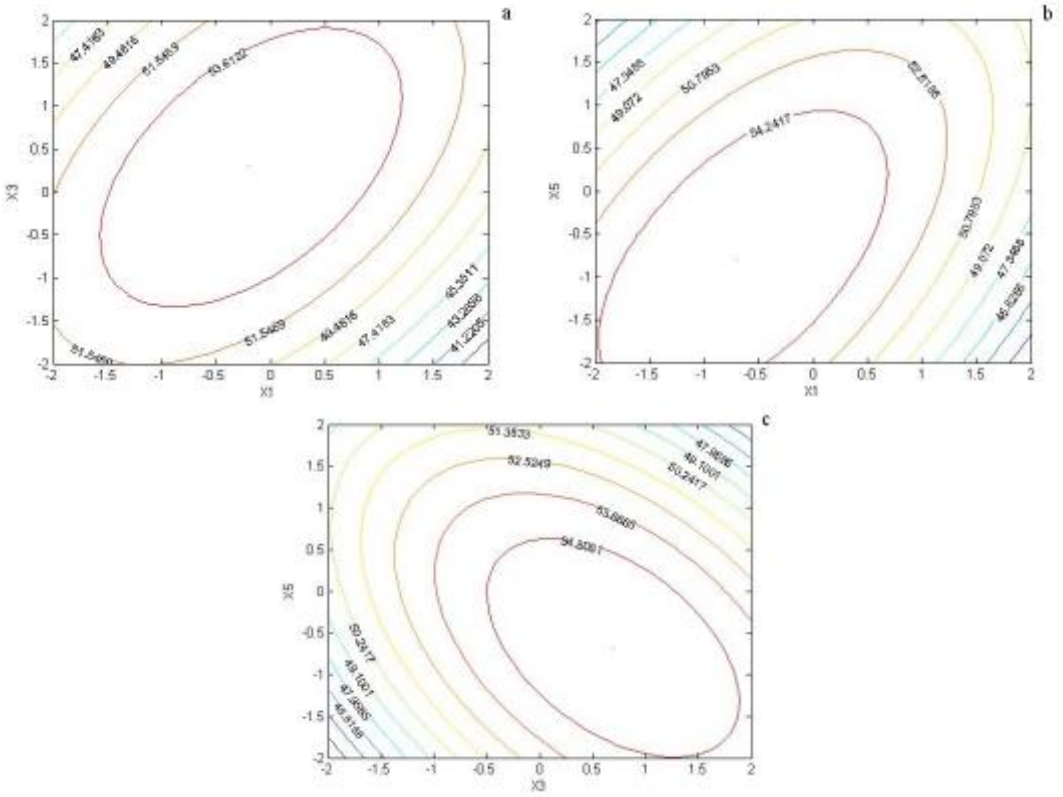

Figure 2. *Significant effects of factor interactions on comprehensive quality of Jingu 54. a: N × K_2O; b: N ×TBM; c: K_2O × TBM*

When P_2O_5, TBM and Se were fixed at the zero level, the comprehensive quality of foxtail millet decreased and then increased with the increase of N and K_2O (*Fig. 2a*). The effect of N was greater at higher K_2O levels than at lower K_2O levels. At lower N levels, enriching K_2O caused little change in the comprehensive quality; at higher N levels, comprehensive quality first increased rapidly and then decreased slowly with the increase of K_2O.

When P_2O_5, K_2O, and Se were fixed at the zero level, increasing N caused a dramatic comprehensive quality increase at high TBM levels, but not at low TBM levels. With continued increase in N application, there was a downward trend in comprehensive quality (*Fig. 2b*). When TBM levels was increased at lower N levels, the comprehensive quality first increased slowly and then decreased rapidly. An opposite trend was observed in the comprehensive quality with increasing TBM levels at higher N levels.

When N, P_2O_5, and Se were fixed at the zero level, comprehensive quality began to increase quickly and then dropped as TBM levels were increased at an appropriate (or lower) level of K_2O. When TBM levels were reduced at higher K_2O levels, comprehensive quality was rapidly increased after a slow reduced (*Fig. 2c*).

http://www.aloki.hu ● ISSN 1589 1623 (Print) ● ISSN 1785 0037 (Online)
DOI: http://dx.doi.org/10.15666/aeer/1906_42314249

Response of comprehensive quality of foxtail millet to fertilizer, herbicide and Se

To obtain a practicable and effective model, the actual responses should be suitable for existing linear, two factor interactions, cubic, or quadratic model. The quadratic model was selected and validated in the analysis of variance. The results included Fisher variation ratio (*F* value), probability value (*P* value), lack of fit, and adjusted *R*-squared (R_{Adj}^2). The second-order polynomial equation for grain quality follows:

$$y = 55.48 - 0.88x_1 + 0.72x_2 + 0.83x_3 - 1.27x_4 - 0.53x_5 - 1.44x_1^2 - 0.80x_2^2 - 1.06x_3^2 - 1.19x_4^2 - 0.87x_5^2 - 0.34x_1x_2 + 1.25x_1x_3 - 0.40x_1x_4 + 1.27x_1x_5 + 0.35x_2x_3 + 0.26x_2x_4 - 0.01x_2x_5 - 0.31x_3x_4 - 0.95x_3x_5 + 0.09x_4x_5 \quad \text{(Eq.1)}$$

where *y* is the predicted response of grain quality and x_1, x_2, x_3, x_4, and x_5 are coded values of N level, P_2O_5 level, K_2O level, Se level, and TBM level, respectively.

The statistical significance of *Equation 1* was evaluated by an *F*-test. The F-test of the response surface variances showed that the equation (R^2_{adj} was 0.8451) was statistically valid ($P < 0.05$), and lack of fit item test was not significant ($P > 0.05$). The optimal values of the selected factors in their respective coded values were: $x_1 = -0.4303$, $x_2 = 0.6334$, $x_3 = 0.8007$, $x_4 = -0.5320$, and $x_5 = -1.0761$. Accordingly, the actual N level, P_2O_5 level, K_2O level, Se level, and TBM level were 108.31 kg ha^{-1}, 94.80 kg ha^{-1}, 105.03 kg ha^{-1}, 88.08 g ha^{-1}, and 18.48 g ai ha^{-1}, respectively. The maximum predicted comprehensive quality of foxtail millet was 56.85. Multivariate quadratic regression indicated that the relationship between the five factors and comprehensive quality of Jingu 54 was significant, which can be used for forecast of production.

Verification of Jingu 54 cultivation conditions

The theoretically optimum combination was not included in the 32 experimental treatment combinations developed in 2019. Six plots with an area of 6 m × 6 m were chosen in May 2020 to further validate the optimum conditions of 108.31 kg ha^{-1}, 94.80 kg ha^{-1}, 105.03 kg ha^{-}1, 88.08 g ha^{-1}, and 18.48 g ha^{-1} for N, P_2O_5, K_2O, selenium, and tribenuron-methyl, respectively. The comprehensive quality of Jingu 54 was 57.46, and the error with the projected value was 1.07 percent, which was extremely near to the model value, confirming the model's practicability.

Discussion

Cultivation conditions have a significant impact on the grain quality of foxtail millet. Existing research on the connection between cultivation circumstances and foxtail millet quality has often relied on simple correlation analysis, which cannot show the intricate interaction of internal regulation (Powers et al., 2020). Multiple statistical analyses were used in this study to gradually show that fertilizer levels, herbicide, and Se influence the grain quality of foxtail millet.

Both the quality indicators of foxtail millet and the growing circumstances were multidimensional factors in the research. As a result, determining optimum cultivation conditions influencing grain quality of foxtail millet proved challenging. PCA was initially utilized in the research to get the main component reflecting the comprehensive quality of foxtail millet. Furthermore, the most important cultivation factors influencing foxtail millet quality were identified, and an optimum connection model was developed

http://www.aloki.hu ● ISSN 1589 1623 (Print) ● ISSN 1785 0037 (Online)
DOI: http://dx.doi.org/10.15666/aeer/1906_42314249

using regression analysis. The optimum growing conditions were established, and the impacts of one-factor and two-factor interaction on comprehensive quality of foxtail millet were investigated. The above-mentioned progressive system analysis is also a quantitative comparison study of the development trend in a dynamic process. This technique overcomes the drawbacks of utilizing single indicators and methodologies, having limited and dispersed cultivation circumstances, and a lack of thorough research and assessment of the crop-cultivation connection. As a result, the results reached here are more trustworthy and may better represent the real circumstances, which meet the requirements of this research. Furthermore, the findings provide a logical decision-making foundation for future research and analysis of foxtail millet.

Foxtail millet grain quality is a multifaceted characteristic that includes nutritional quality, as well as cooking and eating quality (Suman et al., 2015). Based on the PCA findings, we chose PC1 to represent the comprehensive quality of foxtail millet since it contributed 57.41 percent of the total variance. This component comprised nutritional quality (protein, fat, yellow pigment, folic acid, and Se) as well as cooking and eating quality (gel consistency, amylase, alkali digestion value), and therefore accurately reflected the foxtail millet quality.

Reasonable fertilization settings may enhance crop quality while reducing nutrient loss and avoiding possible environmental issues (Wang et al., 2011). Our findings revealed that single factors N, P, and K had a substantial impact on the comprehensive quality of Jingu 54, and that the quality rose initially and then declined as fertilization increased (Li, 2008). This may be because enhanced soil fertility raised the pace of grain filling, delayed the appearance of the filling phase, extended the filling time, and accelerated the accumulation of nitrogen, phosphorus, and assimilates in grains, all of which are beneficial to grain quality formation (Li, 2008). Nitrogen and potassium may boost photosynthetic capacity, enhance pigments that absorb light energy, improve carbohydrate synthesis and transformation, and boost grain nutritional quality. However, overuse of a particular nitrogen fertilizer resulted in a decrease in quality (Wang et al., 2011). Tang et al. (2019) obtained similar results while researching the potential function of nitrogen fertilizer in rice quality regulation. Guo et al. (2020) demonstrated that judicious nitrogen fertilizer application may enhance the concentration of certain nutritional components in maize kernel and improve its quality. Zòrb et al. (2018) demonstrated that nitrogen fertilizer aided protein accumulation in wheat. Chen and Chen (2019) discovered that phosphate fertilizer may enhance the amount of starch, crude protein, and amino acids in rice, as well as boost phosphorus absorption in rice and straw. Results indicated that the impact of N, P, and K on foxtail millet quality was at the following sequence N > P > K, which was inconsistent with previous finding on beta-carotene and lutein of foxtail millet (Dong et al., 2018). The explanation for the discrepancy may be because the research was more thorough in its assessment of the plant's overall quality, including lutein.

Appropriate nitrogen, phosphorus, and potassium ratios may significantly enhance crop growth and development, accelerate the accumulation and transit of photosynthetic products after anthesis, and improve grain nutritional quality (Wang et al., 2010). According to the findings, the combination between N and K had a substantial impact on the quality of Jingu 54. When the potassium level is low, an excessively high nitrogen level will result in a decrease in quality, while when the potassium level is high, the higher the nitrogen level is within a specific range, the better the quality. The findings indicated that crop quality could not be improved in the presence of low

http://www.aloki.hu ● ISSN 1589 1623 (Print) ● ISSN 1785 0037 (Online)
DOI: http://dx.doi.org/10.15666/aeer/1906_42314249

nitrogen, but that quality deteriorated significantly as potassium treatment increased, suggesting that excessive potassium application should be avoided in the presence of low nitrogen. Because N and K complement each other in the process of plant metabolism, maintaining the proper N/K ratio is essential to guarantee excellent quality (Wang et al., 2011). But the effects of the interaction of phosphorus, nitrogen, and potassium did not reach statistical significance for comprehensive quality of Jingu 54. There are many studies on the use of N, P, and K fertilizers in combination, although most of them focus on the impact of fertilization on crop yield or fertilizer efficiency. According to Wang et al. (2010) the interaction of N and P had a substantial impact on rice production, while the interaction of N and K was not significant. Wang et al. (2011) demonstrated that when the K level was low, a high N level resulted in a lower yield, while a higher N level in a specific range resulted in a greater yield, which was comparable to the findings of our research. However, research on the effect of N, P, and K interactions on crop quality is limited, making it difficult to determine a reasonable fertilization ratio for crop quality. This research provides a certain reference for the investigation of the effects of combined application of nitrogen, phosphorus, and potassium on crop quality.

This study revealed a significant role of Se in the comprehensive quality of Jingu 54. In consistent with our finding, previous studies have shown that exogenous Se can increase the content of lutein in tomato (Pezzarossa et al., 2013). Similarly, Se (at 0-810 kg ha^{-1}) increased the content of lutein in carrots by 94.2% (Biacs et al., 1995). However, other trials have shown that exogenous Se has no effect on the content of lutein in cabbage (Lefsrud et al., 2006) or tomato (Pezzarossa et al., 2014). The reason for the inconsistency of these results may be due to the concentrations of exogenous Se and/or the characteristics of the target crop. So far, there are few reports on the effect of Se on foxtail millet, especially regarding to their yellow pigment content. Previous investigation on corn shows that Se application on leaf surface does not influence mineral content in corn kernels (Wang et al., 2013). Studies on various crops such as corn (Chilimba et al., 2012), wheat (Broadley et al., 2010), and rice (Boldrinet et al., 2013) showed that the Se content in the grain has a linear relationship to the concentration of exogenous Se. This research also found that when selenium content rose, the quality of Jingu 54 improved at first, then declined. To avoid the negative health consequences of deficiency or excessive selenium intake appropriate dose should be chosen when applying selenium fertilizer to crops, so that selenium may completely exercise its biological activities of anti-oxidation and immune promotion (Boldrinet et al., 2013). The combination of selenium with nitrogen, phosphorus, potassium, and herbicide did not achieve a significant level of influence on the comprehensive quality. But most of them adopted orthogonal design without analyzing the interaction between factors (Long et al., 2019).

Weed competition has become an important limiting factor for crop growth and development, with chemical herbicides controlling weeds in the field while also reducing crop yields and quality (Iqbal et al., 2019; Javaid and Tanveer, 2013). Because yield and quality are two determinants of millet value (Chauhan and Openga, 2012), it is critical to investigate the effects of herbicides. The findings indicated that the quality of Jingu 54 rose initially and subsequently deteriorated as TBM herbicide concentration increased. Malalgoda et al. (2020) discovered that incorrect administration of fensulfuron-methyl may have a serious impact on agricultural seed protein content. The impact of herbicide stress on agricultural seed mineral content was suggested by Gugala

http://www.aloki.hu ● ISSN 1589 1623 (Print) ● ISSN 1785 0037 (Online)
DOI: http://dx.doi.org/10.15666/aeer/1906_42314249

et al. (2010, 2012) and Ning et al. (2015). The interaction between TBM and N (and K) had a substantial effect on the comprehensive quality of Jingu 54 in this research. The quality of Jingu 54 improved quickly initially and then declined slowly as TBM concentration increased at high nitrogen levels, indicating that nitrogen may mitigate pesticide damage at specific concentrations. When TBM was raised to a specific level at high potassium levels, the quality of Jingu 54 dropped quickly, which may be attributable to the suppression of potassium on TBM degradation (Huang, 2020). The effect of herbicides on crop quality can only be fully appreciated via a comprehensive investigation of soil and crop nutritional status, which necessitates further research.

Conclusion

It is the first time to report the effects of different fertilizer levels (N, P_2O_5, and K_2O), TBM herbicide, and Se on comprehensive quality of foxtail millet Jingu 54. The optimal application of N, P, K, Se and herbicides could reduce waste, reduce pollution, and protect the ecological environment without affecting the quality of foxtail millet. Additionally, foxtail millet grain was reported to be enriched with Se through exogenous Se under the foliar application of Se. Our study established a multivariate quadratic regression model of comprehensive quality, which showed statistical significance and thus could be used for production prediction. Based on the regression model, optimal cultivation conditions were obtained for Jingu 54 under the following experimental conditions: N level, P_2O_5 level, K_2O level, Se level, and TBM level as 108.31 kg ha^{-1}, 94.80 kg ha^{-1}, 105.03 kg ha^{-1}, 88.08 g ha^{-1}, and 18.48 g ai ha^{-1}, respectively. The maximum predicted comprehensive quality of foxtail millet was 56.85. Our study provides a valuable practice for the optimized cultivation management and targeted planting of high-quality foxtail millet. Because of the impact of soil environment and fertilization, the development of grain quality is a complicated process that has to be researched more thoroughly.

Acknowledgments. The study was supported by the Key Research and Development General Project in Shanxi Province, China (201703D221009-1), the Key Research and Development General Project in Shanxi Province, China (201903D221075), the Key Research and Development General Project in Shanxi Province, China (201903D221030), the Shanxi Science and Technology Development Project of Universities (2019L0884) , maker team of Jinzhong University (jzxycktd2019027) and Innovation team of Jinzhong University (jzxyjscxtd202108) .

REFERENCES

[1] Abdel-Fattah, Y. R., Abdel-Fattah, W. R., Zamilpa, R., Pierce, J. R. (2002): Numerical modelling of ferrous-ion oxidation rate in *Acidithiobacillus ferroxidans* ATCC 23270: optimization of culture conditions through statistically designed experiments. – Acta Microbiologica Polonica 51: 225-235.

[2] Adinarayana, K., Ellaiah, P. (2002): Response surface optimization of the critical medium components for the production of alkaline protease by a newly isolated. – Journal of Pharmaceutical Sciences 5: 272-278.

[3] American Association of Cereal Chemists (2000): AACC International Approved Methods. 9th Ed. – American Association of Cereal Chemists (AACC) International, St. Paul, Minnesota.

http://www.aloki.hu ● ISSN 1589 1623 (Print) ● ISSN 1785 0037 (Online)
DOI: http://dx.doi.org/10.15666/aeer/1906_42314249

[4] Anju, M., Banerjee, D. K. (2012): Multivariate statistical analysis of heavy metals in soils of a Pb-Zn mining area, India. – Environmental Monitoring and Assessment 184: 4191-4206.
[5] AOAC (2000): Official Methods of Analysis. 17th Ed. – Association of Official Analytical Chemists (AOAC), Gaithersburg, Maryland.
[6] Biacs, P. A., Daood, H. G., Kadar, I. (1995): Effect of Mo, Se, Zn, and Cr treatments on the yield, element concentration, and carotenoid content of carrot. – Journal of Agricultural and Food Chemistry 43: 589-591.
[7] Boldrin, P. F., Faquin, V., Ramos, S. J., Boldrin, K. V. F., Avila, F. W., Guilherme, L. R. G. (2013): Soil and foliar application of Se in rice biofortification. – Journal of Food Composition and Analysis 31: 238-244.
[8] Broadley, M. R., Alcock, J., Alford, J. (2010): Se biofortification of high-yielding winter wheat by liquid or granular Se fertilisation. – Plant and Soil 332: 5-18.
[9] Chauhan, B. S., Opeňa, J. L. (2012): Effect of tillage systems and herbicides on weed emergence, weed growth, and grain yield in dry-seeded rice systems. – Field Crops Research 137: 56-69.
[10] Chen, S. P., Chen, J. D. (2019): Effects of different phosphorus application rates on yield, quality and phosphate fertilizer utilization efficiency of rice submission date. – Anhui Agricultural Sciences Bulletin 25(13): 57-58, 109 (in Chinese).
[11] Chilimba, A. D. C., Young, S. D., Black, C. R. (2012): Agronomic biofortification of maize with Se (Se) in Malawi. – Field Crops Research 125: 118-128.
[12] Dong, W., Qin, J., Li, J. Y., Zhao, Y., Nie, L. S. (2011): Interactions between soil water content and fertilizer on growth characteristics and biomass yield of Chinese white poplar (Populus Tomentosa Carr.) seedlings. – Soil Science and Plant Nutrition 57(2): 303-312.
[13] Dong, Q. N., Liu, Y. F., Cheng, L. P., Guo, E., Shan, Y. G., Zhang, M. P. (2018): Effect of different fertilization conditions on the content of β-carotene and latein in foxtail millet. – Journal of Nuclear Agricultural Science. 32(5): 1003-1008 (in Chinese).
[14] Feng, Y. N., Zhang, X. F. (2020): Polysaccharide extracted from Huperzia serrata using response surface methodology and its biological activity. – International Journal of Biological Macromolecules 157: 267-275.
[15] Gugala, M., Zarzecka, K. (2010): The effect of weed control methods on magnesium and calcium content in edible pea seeds (Pisum sativum L.). – Journal of Elementology 15: 269-280.
[16] Gugala, M., Zarzecka, K., Mystkowska, I. (2012): Potato tuber content of magnesium and calcium depending on weed control methods. – Journal of Elementology 17: 247-254.
[17] Guo, M. J., Song, X. E., Shen, J., Wang, J. M., Zhao, X. T., Liu, S. G., Dong, S. Q., Yuan, X. Y., Wen, Y. Y., Guo, P. Y., Shi, X. X., Shi, Y. F. (2019): Precision orientation herbicide spraying against weeds in plastic-mulched fields of spring hybrid millet. – Emirates Journal of Food and Agriculture 31(11): 837-846.
[18] Guo, S., Chen, Y. H., Chen, X. C., Chen, Y. L., Tang, Y., Yang, L., Wang, L., Qin, Y. S., Li, M. S., Chen, F. J., Lui, G. h., Gu, R. L., Yuan, L. X. (2020): Grain mineral accumulation changes in Chinese maize cultivars released in different decades and the responses to nitrogen fertilizer. – Front Plant Science 10: 1662.
[19] Huang, X. H. (2020): Exploring the Agronomic Effect of Nitrogen and Phosphorus Fertilizers and Herbicides Quinclorac in the Double-Season Rice Region of Jiangxi Province. – Zhejiang University, Hangzhou (in Chinese).
[20] Iqbal, M. F., Shad, G. M., Feng, Y. L., Liu, M. C., Wag, S., Lu, X. R., Iqbal, Z., Tarig. M. (2019): Efficacy of postemergence herbicides for controlling curled Dock (RUMEX CRISPUS L.) in wheat crops. – Applied Ecology and Environmental Research 17(6): 12753-12766.
[21] Javaid, M. M., and Tanveer, A. (2013): Optimization of application efficacy for post herbicides with adjuvants on three-cornered jack (Emex australis Steinheil) in wheat. – Weed Technology 27: 437-444.

http://www.aloki.hu ● ISSN 1589 1623 (Print) ● ISSN 1785 0037 (Online)
DOI: http://dx.doi.org/10.15666/aeer/1906_42314249

[22] Jones, M. K., Liu, X. (2009): Origins of agriculture in East Asia. – Science 324: 730-731.
[23] Koocheki, A., Mahallati, M. N., Moradi, R., Mansoori, H. (2014): Optimizing water, N and crop density in canola cultivation using response surface methodology and central composite design. – Soil Science and Plant Nutrition 60(2): 286-298.
[24] Lefsrud, M. G., Kopsell, D. A., Kopsell, D. E. (2006): Kale carotenoids are unaffected by, whereas biomass production, elemental concentrations, and Se accumulation respond to, changes in Se fertility. – Journal of Agricultural and Food Chemistry 54: 1764-1771.
[25] Li, J. Q. (2008): Study on the influencing mechanisms of nitrogen and phosphorus nutrients on maize yield and quality in rainfed lands of the loess plateau. – Plant Nutrition and Fertilizer Science 14(6): 1042-1047 (in Chinese).
[26] Liu, C., Liu, Y., Liao, W., Wen, Z., Chen, S. (2003): Application of statistically-based experimental designs for the optimization of nisin production from whey. – Biotechnology Letters 25: 877-882.
[27] Long, S. F., Wang, M., Wu, D. M., Liu, B., Huang, F. X., Xing, D. Y., Zhu, J. Q. (2019): Effect of combined application of selenium nitrogen phosphorus and potassium fertilizers on yield, appearance quality and selenium uptake of Paddy rice. – Journal of Yangtze University (Natural Science Edition) 16(1): 66-71, 124 (in Chinese).
[28] Malalgoda, M., Ohm, J. B., Howatt, K. A., Green, A., Simsek, S. (2020): Effects of pre-harvest glyphosate use on protein composition and shikimic acid accumulation in spring wheat. – Food Chemistry 332: 127422.
[29] Mao, K. J., Huang, P., Zhang, L., Yu, H. S., Zhou, X. Z., Ye, X. Y. (2018): Optimisation of extraction conditions for total saponins from Cynanchum wallichii using response surface methodology and its anti-tumour effects. – Natural Product Research 32(18): 2233-2237.
[30] Montgomery, D. C. (2008): Design and Analysis of Experiments. 7th Ed. – John Wiley & Sons, New York.
[31] Ning, N., Yuan, X. Y., dong, S. Q., Wen, Y. Y., Guo, Z. P., Guo, M. J., Guo, P. Y. (2015): Grain yield and quality of foxtail millet (*Setaria italica* L.) in response to tribenuron-methyl. – Plos One 10(11): e0142557.
[32] Ning, N., Yuan, X. Y., Dong, S. Q., Wen, Y. Y., Gao, Z. P., Guo, M. J. (2016): Increasing Se and yellow pigment concentrations in foxtail millet (*Setaria italica* L.) grain with foliar application of Selenite. – Biological Trace Element Research 170: 245-252.
[33] Pezzarossa, B., Rosellinia, I., Malorgio, F. (2013): Effect of Se enrichment of tomato plants on ripe fruit metabolism and composition. – Acta Horticultural 1012: 247-251.
[34] Pezzarossa, B., Rosellinia, I., Borghesib, E. (2014): Effects of Se-enrichment on yield, fruit composition and ripening of tomato (*Solarium lycopersicum*) plants grown in hydroponics. – Scientia Horticulturae 165: 106-110.
[35] Powers, D. N., Trunfio, N., Velugula-Yellela, S. R., Angart, P., Faustino, A., Agarabi, C. (2020): Multivariate data analysis of growth medium trends affecting antibody glycosylation. – Biotechnology Progress 36(1): e2903.
[36] Robinson, A. P., Simpson, D. M., Johnson, W. G. (2013): Response of glyphosate-tolerant soybean yield components to dicamba exposure. – Weed Science 61: 526-536.
[37] Sachdev, N., Goomer, S., Singh, L. R. (2021): Foxtail millet: a potential crop to meet future demand scenario for alternative sustainable protein. – Journal of the Science of Food and Agriculture 101(3): 831-842.
[38] Shao, L. H., Wang, L., Bai, W. W., Liu, Y. J. (2014): Evaluation and analysis of folic acid content in millet from different ecological regions in Shanxi province. – Journal of Integrative Agriculture 47: 1265-1272.
[39] Soil Survey Staff (2014): Keys to Soil Taxonomy. 12th Ed. – USDA-NRCS, Washington, DC.

http://www.aloki.hu ● ISSN 1589 1623 (Print) ● ISSN 1785 0037 (Online)
DOI: http://dx.doi.org/10.15666/aeer/1906_42314249

[40] Suganthi, M., Muthukrishnan, P., Chinnusamy, C. (2013): Influence of early post emergence sulfonylurea herbicides on growth, yield parameters, yield and weed control efficiency in sugarcane. – Agronomy Journal 12: 59-63.
[41] Suman, V., Sarita, S., Neha, T. (2015): Comparative study on nutritional and sensory quality of barnyard and foxtail millet food products with traditional rice products. – Food Science and Technology Research 52: 5147-5155.
[42] Tang, S., Zhang, H. X., Liu, W. Z., Dou, Z., Zhou, Q. Y., Chen, W. Z., Wang. S. H., Ding, Y. F. (2019): Nitrogen fertilizer at heading stage effectively compensates for the deterioration of rice quality by effecting the search-related properties under elevated temperatures. – Food Chemistry 277: 455-462.
[43] Tran, N. A., Daygon, V. D., Resurreccion, A. P., Cuevas, R. P., Corpuz, H. M., Fitzgerald, M. A. (2011): A single nucleotide polymorphism in the Waxy gene explains a significant component of gel consistency. – Theoretical and Applied Genetics 123: 519-525.
[44] Veeranagamallaiah, G., Jyothsnakumari, G., Thippeswamy, M., Chandra Obul Reddy, P., Surabhi, G. K., Sriranganayakulu, G. (2008): Proteomic analysis of salt stress responses in foxtail millet (Setaria italica L. cv. Prasad) seedlings. – Plant Science 175: 631-641.
[45] Wang, C. A., Zhang, W. X., Zhao, L., Zhao, X. Z., Hou, W. P., Gao, L. W., Wang, B. L. (2010): Effect of amount of nitrogen, phosphorus and potassium fertilizer application on yield and quality of rice. – Journal of Jilin Agricultural Sciences 35(1): 28-33 (in Chinese).
[46] Wang, W. N., Lu, J. W., He, Y. Q., Li, X. H., Li, H. (2011): Effect of N, P, K fertilizer application on grain yield quality nutrient uptake and utilization of rice. – Chinese Journal of Rice Science 25(6): 645-653 (in Chinese).
[47] Wang, J. W., Wang, Z. H., Mao, H. (2013): Increasing Se concentration in maize grain with soil or foliar-applied selenite on the Loess Plateau in China. – Field Crops Research 150: 83-90.
[48] Xia, Q., Yang, Z. P., Xue, N. W., Dai, X. J., Zhang, X., Gao, Z. Q. (2019): Effect of foliar application of selenium on nutrient concentration and yield of colored-grain wheat in China. – Applied Ecology and Environmental Research 17(2): 2187-2202.
[49] Yang, X. Y., Wan, Z. W., Perry, L., Lu, H. Y., Wang, Q., Zhao, C. H. (2012): Early millet use in northern China. – Proceedings of the National Academy of Sciences America 109: 3726-3730.
[50] Yang, Y. J., Zhang, J. H., Chen, L. J., Ji, A. Q., Zhao, H. M., Guo, P. Y. (2018): Effects of fertilizer levels and plant density on chlorophyll content, chlorophyll fluorescence and grain yield of *Setaria italica*. – International Journal of Agriculture Biology 20: 737-744.
[51] Zörb, C., Ludewig, U., Hawkesford, M. J. (2018): Perspective on wheat yield and quality with reduced nitrogen supply. – Trends Plant Science 23(11): 1029-1037.

http://www.aloki.hu ● ISSN 1589 1623 (Print) ● ISSN 1785 0037 (Online)
DOI: http://dx.doi.org/10.15666/aeer/1906_42314249

APPENDIX

Figure A1. *A diagram of the used experimental design (a quadratic general rotation combination design with a 5-factor-5-level was used, with 32 treatments and three replications). 96 units were run in a fully randomized block design, with protection rows placed around the experimental location)*

3 m × 6 m			Protection row			
Protection row	5 ($A_4B_2C_4D_4E_2$)	Aisle	30 ($A_3B_3C_3D_3E_3$)	Aisle	14 ($A_2B_2C_4D_2E_2$)	Protection row
	7 ($A_4B_2C_2D_4E_4$)		28 ($A_3B_3C_3D_3E_3$)		17 ($A_1B_3C_3D_3E_3$)	
	32 ($A_3B_3C_3D_3E_3$)		24 ($A_3B_3C_3D_5E_3$)		12 ($A_2B_4C_2D_2E_2$)	
	25 ($A_3B_3C_3D_3E_1$)		13 ($A_2B_2C_4D_4E_4$)		26 ($A_3B_3C_3D_3E_5$)	
	10 ($A_2B_4C_4D_2E_4$)		1 ($A_4B_4C_4D_4E_4$)		22 ($A_3B_3C_5D_3E_3$)	
	21 ($A_3B_3C_1D_3E_3$)		31 ($A_3B_3C_3D_3E_3$)		9 ($A_2B_4C_4D_4E_2$)	
	16 ($A_2B_2C_2D_2E_4$)		7 ($A_4B_2C_2D_4E_4$)		18 ($A_5B_3C_3D_3E_3$)	
	8 ($A_4B_2C_2D_2E_2$)		2 ($A_4B_4C_4D_2E_2$)		29 ($A_3B_3C_3D_3E_3$)	
	12 ($A_2B_4C_2D_2E_2$)		27 ($A_3B_3C_3D_3E_3$)		17 ($A_1B_3C_3D_3E_3$)	
	9 ($A_2B_4C_4D_4E_2$)		23 ($A_3B_3C_3D_1E_3$)		2 ($A_4B_4C_4D_2E_2$)	
	1 ($A_4B_4C_4D_4E_4$)		5 ($A_4B_2C_4D_4E_2$)		27 ($A_3B_3C_3D_3E_3$)	
	4 ($A_4B_4C_2D_2E_4$)		15 ($A_2B_2C_2D_4E_2$)		6 ($A_4B_2C_4D_2E_4$)	
	26 ($A_3B_3C_3D_3E_5$)		11 ($A_2B_4C_2D_4E_4$)		30 ($A_3B_3C_3D_3E_3$)	
	18 ($A_5B_3C_3D_3E_3$)		8 ($A_4B_2C_2D_2E_2$)		19 ($A_3B_1C_3D_3E_3$)	
	25 ($A_3B_3C_3D_3E_1$)		16 ($A_2B_2C_2D_2E_4$)		32 ($A_3B_3C_3D_3E_3$)	
	13 ($A_2B_2C_2D_4E_2$)		4 ($A_4B_4C_2D_2E_4$)		15 ($A_2B_2C_2D_4E_2$)	
	3 ($A_4B_4C_2D_4E_2$)		6 ($A_4B_2C_4D_2E_4$)		24 ($A_3B_3C_3D_5E_3$)	
	28 ($A_3B_3C_3D_3E_3$)		19 ($A_3B_1C_3D_3E_3$)		1 ($A_4B_4C_4D_4E_4$)	
	22 ($A_3B_3C_5D_3E_3$)		14 ($A_2B_2C_4D_2E_2$)		32 ($A_3B_3C_3D_3E_3$)	
	30 ($A_3B_3C_3D_3E_3$)		9 ($A_2B_4C_4D_4E_2$)		16 ($A_2B_2C_2D_2E_4$)	
	21 ($A_3B_3C_1D_3E_3$)		25 ($A_3B_3C_3D_3E_1$)		11 ($A_2B_4C_2D_4E_4$)	
	3 ($A_4B_4C_2D_4E_2$)		11 ($A_2B_4C_2D_4E_4$)		7 ($A_4B_2C_2D_4E_4$)	
	27 ($A_3B_3C_3D_3E_3$)		2 ($A_4B_4C_4D_2E_2$)		20 ($A_3B_5C_3D_3E_3$)	
	20 ($A_3B_5C_3D_3E_3$)		28 ($A_3B_3C_3D_3E_3$)		29 ($A_3B_3C_3D_3E_3$)	
	6 ($A_4B_2C_4D_2E_4$)		26 ($A_3B_3C_3D_3E_5$)		8 ($A_4B_2C_2D_2E_2$)	
	23 ($A_3B_3C_3D_1E_3$)		5 ($A_4B_2C_4D_4E_2$)		31 ($A_3B_3C_3D_3E_3$)	
	17 ($A_1B_3C_3D_3E_3$)		22 ($A_3B_3C_5D_3E_3$)		3 ($A_4B_4C_2D_4E_2$)	
	31 ($A_3B_3C_3D_3E_3$)		15 ($A_2B_2C_2D_4E_2$)		21 ($A_3B_3C_1D_3E_3$)	
	4 ($A_4B_4C_2D_2E_4$)		24 ($A_3B_3C_3D_5E_3$)		14 ($A_2B_2C_4D_2E_2$)	
	20 ($A_3B_5C_3D_3E_3$)		10 ($A_2B_4C_4D_2E_4$)		19 ($A_3B_1C_3D_3E_3$)	
	18 ($A_5B_3C_3D_3E_3$)		12 ($A_2B_4C_2D_2E_2$)		23 ($A_3B_3C_3D_1E_3$)	
	13 ($A_2B_2C_4D_4E_4$)		29 ($A_3B_3C_3D_3E_3$)		10 ($A_2B_4C_4D_2E_4$)	
Protection row						

The numbers in the table are treatment codes, which are the same as the treatment codes in *Table 2* of the main text. A_1, A_2, A_3, A_4, and A_5 correspond to nitrogen fertilizer levels of 0, 69, 138, 207, and 276 kg ha^{-1} correspondingly; B_1, B_2, B_3, B_4, and B_5 equate to 0, 36, 72, 108, and 144kg ha^{-1} of phosphate fertilizer, respectively; C_1, C_2, C_3, C_4, and C_5 equate to 0, 37.5, 75, 112.5, and 150kg ha^{-1} of potash fertilizer, respectively; D_1, D_2, D_3, D_4, and D_5 equate to 0, 60, 120, 180, and 240kg ha–1 of selenium fertilizer, respectively ; E_1, E_2, E_3, E_4, and E_5 correspond to 0, 20, 40, 60, and 80g ai ha^{-1} of the various herbicide levels

http://www.aloki.hu ● ISSN 1589 1623 (Print) ● ISSN 1785 0037 (Online)
DOI: http://dx.doi.org/10.15666/aeer/1906_42314249

Figure A2. *The photos of the experimental culture or equipment*

APPLIED ECOLOGY AND ENVIRONMENTAL RESEARCH 19(6):4231-4249.
http://www.aloki.hu ● ISSN 1589 1623 (Print) ● ISSN 1785 0037 (Online)
DOI: http://dx.doi.org/10.15666/aeer/1906_42314249

http://www.aloki.hu ● ISSN 1589 1623 (Print) ● ISSN 1785 0037 (Online)
DOI: http://dx.doi.org/10.15666/aeer/1906_42314249

EFFECT OF DROUGHT ON MORPHOLOGICAL AND PHYSIOLOGICAL DEVELOPMENT OF BREAD WHEAT (*Triticum aestivum* L.) GENOTYPES AT PRE AND POST HEADING PERIOD

ALBAYRAK, O.[1*] – BAYHAN, M.[2] – OZKAN, R.[2] – AKINCI, C.[3] – YILDIRIM, M.[3]

[1-3]*Dicle University, Faculty of Agriculture, Department of Field Crops, Diyarbakir, Turkey*

[2]*100/2000 CoHE PhD Scholarship Program Student, Dicle University, Faculty of Agriculture, Department of Field Crops, Diyarbakir, Turkey*

[*]*Corresponding author*
e-mail: ondera@dicle.edu.tr; phone: +90-412-241-1000; fax: +90-412-241-1048

(Received 9th May 2021; accepted 3rd Sep 2021)

Abstract. The goal of the study was to determine the effect of drought on the bread wheat genotypes at pre-and post-heading stage. This research was conducted for two years in 2017-2018 and 2018-2019 wheat growing season at Dicle University Faculty of Agriculture Research and Application Field in Diyarbakir, Turkey. Two check varieties (Empire and Pehlivan) and 8 CIMMYT bread wheat lines were used as materials in the study. Significant differences in all features such as heading stage, chlorophyll content (SPAD), normalized difference vegatation index (NDVI), leaf area index (LAI), plant height, grain weight and grain yield between the genotypes were identified. Based on the results of the correlation analysis performed over the two-year average data; grain yield was found to be correlated with an increase of all the characteristics studied during the pre-heading period when drought stress were encountered. In terms of grain yield, late varieties are resistant to stress that occurs prior to heading, while early varieties have become advantageous after heading. According to the results of the study, ideal genotypes with high yield and stability are expected to have moderate heading stage in environments where precipitation fluctuates from year to year due to climate change.
Keywords: *bread wheat, drought, stress, heading, yield*

Introduction

Drought, one of the environmental stress factors, is the most important factor limiting crop production in rain-based agricultural areas in most of the world. Appropriate criteria should be developed for genotype evaluation to better understand how and in what way drought affects wheat yield in different development stages. Through this way, progress can be made towards the development of higher competitive genotypes, which will better respond to the dominant form of drought in area with certain ecological conditions (Ayranci, 2012). Drought tolerance in cool season cereals is rightly related to plants' ability to root deeply. The response of each genotype to drought varies depending on the stage of development. Drought in the early stages of development, decreases plant height, leaf area and number of fertile tiller; drought between stem elongation and spike formation, decreases number of fertile flowers in the spikelet, fertile spikelet in the spike and fertile spike; drought in the heading stage, decreases the number of grain in the spike; drought after flowering causes weight loss in the grain, while drought during the grain filling period leads to loss of grain in the tips and bottoms of the spike by increasing intra-spike competition in terms of sharing the insufficient assimilates (Kutlu and Kinaci, 2010).

The effects of both heat and drought stress are expected to increase in dry-farming regions such as Central America, North Africa , Central Asia, Western Asia and Western

http://www.aloki.hu ● ISSN 1589 1623 (Print) ● ISSN 1785 0037 (Online)
DOI: http://dx.doi.org/10.15666/aeer/1906_42514263

Australia in the near future (IPCC, 2012). In Mediterranean climate regions, wheat is mostly grown in arid and semi-arid areas without irrigation, and plants are exposed to drougt and high temperatures during grain growth, resulting in major yield reductions. While the world population density rises day by day and the arable land declines, crop losses due to high temperatures have become increasingly critical in meeting the growing demand for food. The most important issue in plant breeding studies for drought tolerance is identifying the morphological and physiological response mechanisms used by plants to withstand water deficiency and drought. Developing the reactions of plants to stress caused by high temperatures and water deficiency, as aimed in this research, can be the basis for drought tolerance studies and can be used as a selection criterion for the selection of resistant plants. Today, there is a need to develop new wheat varieties that show high performance under drought and high heat stress. This need can only be met by focusing on crop and plant physiology features through interdisciplinary cooperation (Yildirim et al., 2009a).

In a study by Qaseem et al. (2019) was aimed to quantify effects of drought, heat and combined heat and drought during reproductive stage on wheat yield. Grain yield was reduced by 56.47%, 53.05% and 44.66% under combined heat and drought, heat and drought treatment, respectively.

Drought stress is a major abiotic stress factor, constraining wheat production and quality worldwide. Additionally, grain yield under stress and non-stress environments were highly correlated with the mean productivity, the geometric mean productivity, stress tolerance index, yield index, harmonic mean, drought resistance index and modified stress tolerance index (Ali and El-Sadek, 2016).

In this research, the effects of physiological and morphological properties on grain yield in bread wheat were investigated under conditions of drought that occurred before and after heading stage.

Materials and methods

This research was conducted for two years in 2017-2018 and 2018-2019 wheat growing season at Dicle University Faculty of Agriculture Research and Application Field in Diyarbakir (37° 53' North and 40° 16' East), Turkey. Two check varieties (Empire and Pehlivan) and 8 CIMMYT bread wheat lines were used as materials in the study.

The results of some physical and chemical analysis of the soil of the experiment area are given in *Table 1*. The clay content of the soils is high and heavy. In addition, there are no significant problems with pH, salinity and groundwater. The soil of the trial area is low in organic matter, alkaline (pH 7.9) and clayey.

Some climate data are given in *Table 2* for the two years (2017-2018, 2018-2019) that the study was conducted in. The first year of this study, while in the pre-heading period (December-April), plants received 268.40 mm of precipitation, in the same period the precipitation amounted to 604.80 mm in the second year. Since the average precipitation amount at the pre-heading stage was 429.50 mm over long term, the first year was exceptionally dry and the second year was exceptionally rainy. The precipitation was 172.20 mm during the 1st year of the study in the post-heading period (May-June), with the precipitation 46.80 mm in the 2nd year of the study. Since the total long-term average precipitation amount is 52.20 mm in this period, the area where the study is conducted is subject to terminal drought stress.

http://www.aloki.hu ● ISSN 1589 1623 (Print) ● ISSN 1785 0037 (Online)
DOI: http://dx.doi.org/10.15666/aeer/1906_42514263

Table 1. *Soil analysis results of the experiment area*

Physical and Chemical Properties		Depth of soil		
		0-30 cm	30-60 cm	60-90 cm
pH		7.7	7.9	7.8
P_2O_5 (%)		0.42	--	--
Organic matter (%)		1.67	1.67	--
Lime (%)		7.8	7.8	8.7
EC (dS/m)		0.48	0.37	0.42
Soil structure	Sand (%)	10	12	12
	Silt (%)	24	22	21
	Clay (%)	66	66	67
	Class Structure	C	C	C
Field Capacity (g/10 g)		35.5	35.2	36.4
Fading point (g/100 g)		25.5	25.3	27
Volume weight (g/cm3)		1.19	1.25	1.27
İnf. Speed (mm/h)		8		

Table 2. *The average monthly rainfall (mm) and temperature (^0C)*

STAGE	Months	Average Temperature (°C)			Precipitation (mm)		
		2017-2018	2018-2019	Long years	2017-2018	2018-2019	Long years
PRE HEADING	October	17.00	18.90	17.30	1.00	35.00	32.20
	November	10.10	10.20	9.50	21.20	59.00	54.20
	December	5.80	6.30	3.90	12.80	78.00	71.40
	January	5.20	3.80	1.70	86.60	67.60	70.30
	February	7.60	5.40	3.60	86.40	77.40	68.00
	March	12.30	8.20	8.40	11.60	135.20	65.10
	April	15.90	11.80	13.80	48.80	152.60	68.30
	Average	9.48	7.62	6.82	44.57	94.97	66.22
	Total	73.90	64.60	58.20	268.40	604.80	429.50
POST HEADING	May	19.40	20.10	19.20	157.80	45.80	44.10
	June	26.50	28.30	26.20	14.40	1.00	8.10
	Average	22.95	24.20	22.70	86.10	23.40	26.10
	Total	45.90	48.40	45.40	172.20	46.80	52.20

Although the pre-heading period was much hotter in the first year than the seasonal averages, the grain filling period was in seasonal norms. In the second year, except for the booting period, the pre-heading period was marginally above the seasonal average, while it was seen as stressful after the spike emergence (*Table 2*). The analysis of climate data shows that two different environments are formed. In this scenario, pre-heading period, the first year was assessed as extremely drought and heat stressful and high rainy and suitable climate post-heading period. In the second year, on the contrary of the first year, it was accepted as the environment with high rainfall and partially heat stressed for pre-heading, and moderate hot stress environment post-heading stage. Water content in the soil is high in the second year, based on the 239 mm of precipitation received before planting in the first year.

The experiment was established in both years with 4 replication according to the randomized completed block design. The parcel area was set to be 6 m^2 (0.2 m x 5 m x 6 rows) (*Figure 1*). Sowing was carried out in the first year on 15 December and the second year on 5 February, with a trial sowing machine, 500 seeds density per square meter. As a sowing fertilizer of 6 kg da^{-1} nitrogen (N) and 6 kg da^{-1} phosphorus (P_2O_5) was applied,

http://www.aloki.hu ● ISSN 1589 1623 (Print) ● ISSN 1785 0037 (Online)
DOI: http://dx.doi.org/10.15666/aeer/1906_42514263

while 6 kg da^{-1} nitrogen (N) at stem eleongation. In the study, for weed control (narrow and broad-leaved) were applied fenoxaprop-p-ethyl and Tribenuron-Methyl active substances herbicides. Harvesting was done in both years on July 17 by harvesting a 5 m^2 area with the plot combine harvester. The heading stage in the characteristics examined was calculated as the number of days between the planting date and the period during which the spike appeared at 1/2 in half of the plants in the plot. Plant height was determined by measuring the distance between the soil surface and the top spikelet tip in 10 plants in the plot by meter. The grain yield was calculated by weighing the seeds harvested with the parcel combine harvester and later counting one thousand grain (g) in the grain counting machine. The normalized difference vegatation index (NDVI) has been calculated using Trimple Green Seeker (Trimble Navigation Limited, Sunnyvale, CA, USA), ranging between 0.00-0.99. The SPAD value (chlorophyll content) of the physiological properties examined in the study was measured with the SPAD-502 chlorophyll meter (Minolta Camera Co., Japan) device, and the leaf area index (LAI) was measured with the LAI-2000 (LI-COR, Lincoln, NE) device. SPAD, LAI and NDVI measurements were performed during the heading period, in sunny weather and between 11:00 and 14:00h, when there was no wind.

Figure 1. *Images of the research field*

Using JUMP Pro 13 statistical package software the data of the analyzed features were subjected to variance analysis and and the differences between the averages were revealed by LSD testing.

Results and discussion

Heading stage (day)

There were important variations between the bread wheat genotypes for the heading stage obtained by evaluating the amount of time spent from the emergence to the heading. The heading stage varied between 130.0-133.3 days in the first year and 96.3-105.3 days

http://www.aloki.hu ● ISSN 1589 1623 (Print) ● ISSN 1785 0037 (Online)
DOI: http://dx.doi.org/10.15666/aeer/1906_42514263

in the second year (*Table 3*). It was observed that DZ20-9 line with 130.0 days in first year and DZ20-3 line with 96.25 days in second year were the earliest genotype. The Pehlivan variety and DZ20-6 line were the most late genotypes in the first and second years, respectively. According to the average results of both years, the heading stage varied between 113.4-119.1 days and the DZ20-3 line was determined to be the earliest genotype. The fact that genotypes have different values for their heading stage in two years may be attributable to the emergence delay due to the first year's severe drought and genotypes having different biological characteristics. The fact that the earliness feature extends the grain filling time allows for greater assimilation accumulation in the grain and supports yield increase. According to the two-year average results; while the yield of the late varieties was low, it was determined that the medium-early varieties had high yields (*Table 3*). Yildirim et al. (2005) also notes that there is an increase in grain yield of early varieties. Blum (2010) shows that the earliness feature (early flowering) is the mechanism of drought escape, especially in the late developmental periods, however, late flowering implies higher yield potential, and early genotypes may experience decreased yields in environments where the drought arrival period is unpredictable, and therefore earlyness reported that it can be used to optimize phenology in more predictable environments. Yavas (2010) stated that wheat genotypes were started earlier heading in drought stress than stress-free conditions.

SPAD value (chlorophyll content)

SPAD measurements have demonstrated a strong association with chlorophyll derived from plants. There was no difference between bread wheat genotypes in both years in terms of chlorophyll content and SPAD values ranged between 44.63-51.08 in the first year and 41.93-46.75 in the second (*Table 3*). The fact that the genotype x year interaction is insignificant and that the genotypes with high chlorophyll content give similar results in both years reveal that this parameter is mostly under genotypic control and that the SPAD meter device can be used safely in selection by breeders. It is reported that by using the SPAD meter as a selection criterion in breeding programs, a genetic improvement in yield can be achieved (Yildirim et al., 2009b).

Yildirim et al. (2013) reported that the SPAD meter can be used in the selection of plants with high yield potential in both normal and heat stress conditions according to the measurements made during the milk grain growth stage in the bread wheat F_2 segregation progenies. In the study of Yildirim et al. (2009b) on the use possibilities of chlorophyll content and canopy temperature in durum wheat breeding, they stated that there is a broad variation between genotypes and the chlorophyll content of each genotype may vary depending on the time of plant development. They determined that a genotype with low chlorophyll content among the different hybrid genotypes could increase the chlorophyll content in later ages of the plant. They reported that this could alter the ranking between genotypes by growing periods, and therefore it would be beneficial to perform selection in more than one period, rather than in a single measurement period. The SPAD value was found to be correlated with leaf chlorophyll and nitrogen, and critical values for maximum shoot growth were 53 when low water was given, and 44 for excess water values (Barraclough and Kyte, 2001).

http://www.aloki.hu ● ISSN 1589 1623 (Print) ● ISSN 1785 0037 (Online)
DOI: http://dx.doi.org/10.15666/aeer/1906_42514263

Table 3. *Mean values for heading stage, SPAD, NDVI and LAI value of bread wheat genotypes*

Genotypes	Heading stage(day)			SPAD value			NDVI value			LAI value		
	2017-2018	2018-2019	Mean of years	2017-2018	2018-2019	Mean of years	2017-2018	2018-2019	Mean of years	2017-2018	2018-2019	Mean of years
DZ20-3	130.50 bc	96.25 d	113.42 e	47.28	44.37	45.82	0.32	0.56 cd	0.44 de	0.88	1.23 ab	1.05
DZ20-4	130.25 bc	97.50 cd	113.88 de	46.4	44.38	45.39	0.31	0.56 cd	0.44 e	0.63	1.05 b	0.84
DZ20-5	130.75 bc[1]	102.00 ab	116.38 bc	50.78	46.37	48.57	0.33	0.57 cd	0.45 c-e	0.78	1.13 b	0.95
DZ20-6	133.00 a	105.25 a	119.13 a	46.9	44.78	45.84	0.39	0.64 ab	0.51 ab	1.13	1.08 b	1.10
DZ20-7	133.00 a	99.75 bc	116.33 bc	48.43	41.93	45.18	0.34	0.55 cd	0.44 c-e	0.95	1.13 b	1.04
DZ20-8	131.00 bc	104.25 a	117.63 ab	48.17	42.55	45.36	0.37	0.59 b-d	0.48 bc	0.83	1.08 b	0.95
DZ20-9	130.00 c	97.75 cd	113.88 de	44.63	46.73	45.68	0.36	0.59 bc	0.48 b-d	0.87	1.08 b	0.97
DZ20-10	131.00 bc	100.00 bc	115.50 cd	46.43	43.53	44.98	0.35	0.54 d	0.44 c-e	1.03	0.73 c	0.88
Empire	131.75 ab	99.50 b-d	115.63 cd	48.95	46.75	47.85	0.36	0.57 cd	0.46 c-e	0.80	1.15 b	0.98
Pehlivan	133.25 a	105.00 a	119.13 a	51.08	43.73	47.4	0.39	0.66 a	0.52 a	0.95	1.50 a	1.23
Mean	131.45 A	100.72 B	116.087	47.9	44.51	46.21	0.35 B	0.58 A	46.63	0.88	1.11	0.10
LSD	1.74	3.32	1.82	-	-	-	-	0.047	0.04	-	0.30	-
P	**	**	**	-	-	-	-	**	**	-	**	-
CV(%)	0.91	2.21	1.56	7.11	7.36	6.99	12.57	5.17	8.15	27.52	22.52	22

LSD, least significant difference; [1]: Means with the same letter are not significantly different; CV, coefficient of variation; P, Significance levels:*, $P<0.05$; **, $P<0.01$

http://www.aloki.hu ● ISSN 1589 1623 (Print) ● ISSN 1785 0037 (Online)
DOI: http://dx.doi.org/10.15666/aeer/1906_42514263

NDVI value

Spectral reflectance indices are valuable instruments for assessing the process of photosynthesis. NDVI is one of the commonly used canopy indices as an indicator of the surface green area which the plant covers and is directly related to the yield of grain (Kizilgeci et al., 2018). The NDVI has been associated with a variety of factors, including crop nutrient shortage, grain production, and long-term water stress. However, rather than representing the influence of a single component, NDVI must be seen as a composite measure of plant development that incorporates several plant growth variables (Verhults and Govaerst, 2010). The difference in NDVI value between genotypes was negligible in the first year, while significant was in the second year (*Table 3*). During the first year the NDVI value ranged from 0.31-0.39 and in the second year from 0.54-0.66. Pehlivan and DZ20-6 genotypes had the highest value in both years in terms of NDVI ranking. The lowest-value genotype were DZ20-10 at second year.

Looking at the two-year average values, NDVI ranged between 0.44 and 0.52 and genotypes with the highest value were similar in both years. The low NDVI values of the first year compared to the second year can be explained by the drought stress experienced in the first year of the study. The drought experienced in this period resulted in poor plant growth, decreased number of leaves, and shortened plant height. As a result, the vegetation density in the plot remained weak and the NDVI measurements were adversely affected by this situation. In this regard, NDVI measurements may not be effective in disclosing the difference between genotypes in drought environments before heading stage. Masuda et al. (2002) stated that the production of chlorophyll varied depending on the growth conditions of the plant, and that the amount of chlorophyll decreased under adverse conditions. It has been reported that there is a significant relationship between NDVI and biomass in wheat under full irrigation, supporting irrigation and rainfed conditions, particularly in the early periods between tillering and the start of the stem elengation period, and this relationship has disappeared in later periods and also an important relationship between the yield and NDVI values in rainfall and support irrigation has been reported (Savasli et al., 2012). Crusiol et al. (2017) stated that several factors such as the stage of measurement, the type of sensor and the environment affect the NDVI value.

LAI (leaf area index) value

In wheat, the leaf area index (LAI) gradually increases and quickly after emergence, reaching its peak value 2-3 weeks before flowering and gradually decreases as a result of leaf loss caused by maturity (Koc and Barutcular, 2000). In the first year of the study, analysis of variance of leaf area index of genotypes was found to be statistically insignificant, whereas in the second year of the study, it was statistically significant. Leaf area index values ranged between 0.63-1.13 in the first year and 0.73-1.50 in the second year. The highest leaf area index value was obtained in the from variety Pehlivan with 1.50. Drought experienced in the early stages of development in the first year of the study, resulting in a decrease in plant height, leaf area and fertile tiller.

While the LAI value varies depending on the plant's genotype and period of development (Kizilgeci et al., 2017), it is more important to determine the appropriate values for each genotype rather than the low or high LAI value, and it is recommended that varieties with a high HFA value be selected when more biomass is intended (Yildirim et al., 2018). The leaf area of the plants is significant in arid and semi-arid areas where

http://www.aloki.hu ● ISSN 1589 1623 (Print) ● ISSN 1785 0037 (Online)
DOI: http://dx.doi.org/10.15666/aeer/1906_42514263

water is inadequate in terms of resistance to drought. Varieties which do not have large leaf areas are preferred especially in arid areas (Okursoy, 2005).

Plant height (cm)

Average values of bread wheat genotypes for plant height are given in Table 4. In both years of the study, the difference between genotypes was found to be statistically significant. Plant height of genotypes varied between 37.6 and 44.2 cm in the first year and between 80.4 and 97.4 cm in the second year. In the study, the highest plant height values were obtained from DZ20-6 and DZ20-9 lines in the first year and from Empire variety with 97.4 cm in the second year. Whereas in the first year the average plant height of the genotypes was 40.2 cm, in the second year it was 87.8 cm and a double value was observed compared with the first year. The differences in plant height between the two years may be attributed to the drought stress of the plants due to inadequate rainfall prior to heading in the 2017-2018 season of the experiment, and precipitation in the second year prior to heading was twice as high as in the previous year. It has been stated that water stress during the tillering period causes a decrease in plant height (Baloch et al., 2007). Plant height decreases due to low rainfall and high average temperature (Mut et al., 2006). Different studies showed that bread wheat's plant height decreased under the drought stress seen in different growth stages, and this decrease showed variability depending on the drought period and severity (Shamsi et al., 2010). Akinci (2003) stated that the plant height ranged between 51.6 and 113.7 cm in its study of 26 varieties of bread wheat.

Grain weight (g)

Thousand grain weight is a trait that is influenced by multiple genes, and varies depending on the genotype and environment (Dogan and Kendal, 2012). Thousand grain weights of the genotypes ranged from 27.22 to 35.67 g in the first year and from 26.57 to 34.0 g in the second year, and the variance between the varieties in both years was statistically important. Looking at *Table 4*, it is shown that the maximum grain weight value in the first year was obtained from the DZ20-6 line at 35.67 g, and the lowest grain weight value was obtained from the DZ20-8 genotype at 27.22 g. *Table 4* reveals that the highest thousand grain weight value was obtained from a DZ20-6 line of 35.67 g in the first year and the lowest thousand grain weight from the DZ20-8 genotype with 27.22 g. DZ20-4 was the highest thousand grain with a weight of 34.0 g in the second year, while DZ20-8 gave a weight of 26.57 g for the lowest grain weight. On average, grain weight were between 26.89 g and 31.78 g based on the two-year findings of the study. Although it was very dry and hot before heading period in the first year, after spike emergence high rainfall caused thousands of grain weights to grow. It has been recorded in studies of varieties and lines of bread wheat that thousands of grain weights ranged from 29.9-49.7 g (Sahin et al., 2005).

Grain yield (kg ha^{-1})

In both years, variations between different wheat genotypes were found to be statistically significant at a level of 1% (*Table 4*). The highest grain yield was obtained from DZ20-6 line with 14.78 kg ha^{-1} in the first year of the study, while the lowest grain yield was obtained from the genotypes DZ20-3 (8.05 kg ha^{-1}) and DZ20-4 (8.690 kg ha^{-1}). The highest yield was obtained in the second year from DZ20-9 line at 30,09 kg ha^{-1},

http://www.aloki.hu ● ISSN 1589 1623 (Print) ● ISSN 1785 0037 (Online)
DOI: http://dx.doi.org/10.15666/aeer/1906_42514263

while the lowest yield was obtained from DZ20-6 genotype at 20.12 kg ha^{-1}. Two-year average grain yield data varied between 15.98-20.97 kg ha^{-1} and DZ20-7 and DZ20-9 genotypes yielded the highest grain yield. In a study conducted under similar conditions, the grain yield of bread wheat varieties varied between 29.96 kg ha^{-1} and 73.29 kg ha^{-1} (Yildirim et al., 2005). In the first growing season, the low total precipitation before heading caused drought stress and a very low yield of grain. In the second year of the study, flowering and grain filling period was negatively affected due to insufficient rainfall after the heading. The drought experienced in this period reduced the yield potential by causing both shortening of the grain filling period and the sterility of the upper spikelets. In the second year, despite the dry period after spiking, the higher grain yield in the first year may have been caused by the remobilization of the reserves accumulated in the stems and leaves before spiking. Early drought in wheat, it was recorded, has less impact than the drought in late development period and reduces the number of tillering, drought before heading stage reduces the number of fertile spikes, the number of spike grains and grain yield and the lowest yield is attributed to drought during grain filling (Abayomi and Wright, 1999).

Table 4. *Mean values for plant height, grain weight and grain yield*

Genotypes	Plant height (cm)			Grain weight (g)			Grain yield (t ha^{-1})		
	2017-2018	2018-2019	Mean of years	2017-2018	2018-2019	Mean of years	2017-2018	2018-2019	Mean of years
DZ20-3	37.6 e	91.87 ab	64.73 b-d	29.61 ef	32.30 ab	30.95 a	8.05 e	23.91 b	15.98 e
DZ20-4	38.95 de	81.20 e	60.08 e	29.17 ef	34.00 a	31.58 a	8.69 e	28.11 a	18.40 b-d
DZ20-5	40.87 b[1]	84.55 e	62.71 c-e	28.57 fg	26.61 c	27.59 b	13.59 b	24.17 b	18.88 bc
DZ20-6	44.2 a	80.45 e	62.33 d-e	35.67 a	26.98 c	31.32 a	14.79 a	20.12 c	17.45 c-e
DZ20-7	41.2 b	91.07 bc	66.13 ab	30.26 d-f	32.67 ab	31.46 a	11.59 c	30.35 a	20.97 a
DZ20-8	37.8 de	84.70 de	61.25 e	27.22 g	26.57 c	26.89 b	11.54 c	21.44 bc	16.49 e
DZ20-9	42.8 a	90.60 b-d	66.70 ab	31.81 cd	32.02 ab	31.91 a	11.48 c	30.09 a	20.79 a
DZ20-10	40.65 bc	90.85 bc	65.75 a-c	30.81 c-e	30.46 b	30.64 a	10.27 d	28.70 a	19.49 ab
Empire	39.23 cd	97.40 a	68.31 a	32.32 bc	31.23 ab	31.78 a	11.78 c	28.58 a	20.18 ab
Pehlivan	38.7 de	85.33 c-e	62.02 de	33.88 b	27.17 c	30.53 a	11.01 c-d	22.31 bc	16.66 de
Mean	40.20 B	87.80 A	64.00	30.93	30	30.47	11.28 B	25.78 A	18.53
LSD	1.58	6.03	3.03	1.72	2.74	1.61	1.07	3.53	1.80
P	**	**	**	**	**	**	**	**	**
CV(%)	2.71	5.06	4.74	3.84	6.53	5.28	6.53	9.44	9.7

LSD, least significant difference; [1]: Means with the same letter are not significantly different; CV, coefficient of variation; P, Significance levels:*, $P<0.05$; **, $P<0.01$

The DZ20-6 line, which yielded the highest yield in the dry first year, increased by 36.06 percent in the second year and was more stable but yielded lower than other genotypes, according to *Figure 2* showing the yield order of genotypes by rainfall amount. DZ20-7 lines, which yielded 11.59 kg ha^{-1} in the first year, increased by 161.94% in the second year and yielded 30.35 kg ha^{-1}. This shows that this genotype has a general resistance to drought before and after heading. Among the genotypes, the DZ20-4 genotype with an increase of 223% was the most positive response to the total amount of precipitation before heading. Jana et al. (1990) reported that frequency of wheat population with early heading, early maturity and long grain filling period are considered as indicators of increase tolerance to drought. This strategy may be valid if stress is

http://www.aloki.hu ● ISSN 1589 1623 (Print) ● ISSN 1785 0037 (Online)
DOI: http://dx.doi.org/10.15666/aeer/1906_42514263

experienced throughout entire development period or before reproductive period. In this way, late-heading genotypes get the maximum yield during the first dry year because they continue to be stay-green throughout the growing stages and are better able to take advantage of late rains.

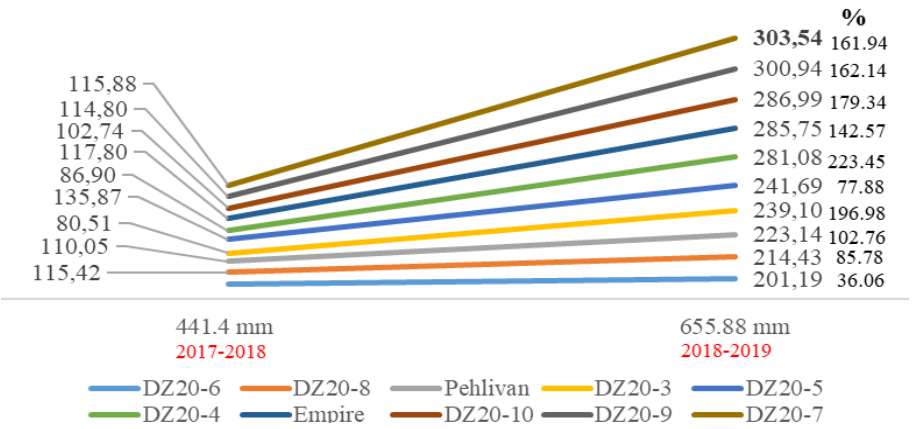

Figure 2. *Two-season rainfall and seasonal yield changes*

Correlation analysis among investigated parameters

The increase in all properties had a positive effect on the grain yield in the first year when drought and heat stress occurred in the pre-heading period, and a positive and significant relationship was found between grain yield and SPAD, plant height and thousand grain weight characteristics, in the second year (*Table 5*). Late genotypes provided a yield advantage in the first year due to the drought during the pre-heading period, whereas early genotypes were found to be advantageous in the second year due to drought after heading. Karaman et al. (2014) examined the relationship between physiological parameters and grain yield in some bread wheat varieties and found a strong association between grain yield and NDVI measurement. Yildirim et al. (2018) reported that grain yield was associated with NDVI and LAI among the physiological characteristics examined in bread wheat, but there was no significant relationship between grain yield and SPAD. Sakin et al. (2015) reported that there is a positive and significant relationship between grain yield and plant height in bread wheat, and the grain yield of tall varieties is high.

Table 5. *The correlations between parameters*

Parameters	**LAI Value**		**Plant height (cm)**		**NDVI Value**		**Heading stage (day)**		**SPAD Value**		**Grain weight (g)**	
	Year-I	Year II	Year-I	Year II	Year-I	Year II	Year-I	Year II	Year-I	Year II	Year-I	Year II
Plant height (cm)	0.71**	0.17										
NDVI Value	0.81**	0.60**	0.76**	-0.02								
Heading stage(day)	0.69**	0.22	0.53**	-0.24	0.66**	0.49**						
SPAD Value	0.49**	0.14	0.52**	0.19	0.63**	0.09	0.59**	0.21				
Grain weight (g)	0.59**	-0.07	0.54**	0.39*	0.58**	-0.33*	0.64**	-0.65**	0.28	0.16		
Grain yield (kg ha^{-1})	0.66**	0.03	0.75**	0.51**	0.76**	-0.2	0.61**	-0.09	0.53**	0.52**	0.52**	0.59**

http://www.aloki.hu ● ISSN 1589 1623 (Print) ● ISSN 1785 0037 (Online)
DOI: http://dx.doi.org/10.15666/aeer/1906_42514263

Conclusion

Wheat yield varies depending on the annual precipitation as well as the distribution of precipitation. During the years of the research, the difference in the amount of precipitation in the wheat growing season before and after the heading offered an opportunity to test the genotype responses to different conditions.

When comparing late genotypes to early genotypes, it has been shown that the late genotypes are more productive in the dry season when there is precipitation during the grain filling phase.

To achieve stability and high yield potential in environments where seasonal precipitation fluctuates as a result of climate change, it would be beneficial to make the variety recommendation with mid-early varieties that produce the highest yield in both seasons rather than early and late genotypes.

Based on the findings, it will be possible to recommend to farmers mid-early genotypes DZ20-7 and Empire, which have demonstrated general stability and good production, as well as to assess them as parent in breeding studies.

Testing multiple genotypes in different locations will allow researchers to give a more accurate genotype recommendation to growers.

REFERENCES

[1] Abayomi, Y. A., Wright, D. (1999): Osmotic potential and temperature effects on germination of spring wheat (*Triticum aestivum* L.) genotypes. – Tropical Agriculture (Trinidad) 76(2): 120-125.

[2] Akinci, C. (2003): Comparison of some varieties and lines of bread and durum wheat. – 5th Field Crops Congress of Turkey, 13- October 17, 2003, Field Crops Breeding, pp. 426-430.

[3] Ali, M. B., El-Sadek, A. N. (2016): Evaluation of drought tolerance indices for wheat (*Triticum aestivum* L.) under irrigated and rainfed conditions. – Communications in Biometry and Crop Science 11: 77-89.

[4] Ayranci, R. (2012): Determination of yield, physiological, morphologıcal and quality parameters in bread wheat genotypes to be used in different drought types. – The Graduate School of Natural and Applied Science of Selcuk University, the Degree of Doctor of Philosophy in Department of Field Crops, Konya.

[5] Baloch, M. J., Veesar, N. F. (2007): Identification of plant traits for characterization of early maturing upland cotton varieties. – Pakistan Journal of Scientific and Industrial Research (Pak. J. Sci. & Ind. Res.) 50: 128-132.

[6] Barraclough, P. B., Kyte, J. (2001): Effect of water stress on chlorophyll meter readings in winter wheat. – In: Horst, W. J. et al. (eds.) Plant Nutrition. Developments in Plant and Soil Sciences 92: 722-723. Springer, Dordrecht. https://doi.org/10.1007/0-306-47624-X_350.

[7] Blum, A. (2010): Plant breeding for water-limited environments. – Springer, London, 210p.

[8] Crusiol, L. G. T., de Fátima Corréa Carvalho, J., Sibaldelli, R. N. R. (2017): NDVI variation according to the time of measurement, sampling size, positioning of sensor and water regime in different soybean cultivars. – Precision Agric 18: 470-490. https://doi.org/10.1007/s11119-016-9465-6.

[9] Dogan, Y., Kendal, E. (2012): Determination of grain yield and some quality traits of some bread wheat (*Triticum aestivum* L.) genotypes in Diyarbakir ecological conditions. – YYU J Agr Sci 23(3): 199-208.

[10] IPCC. (2012): Managing the risks of extreme events and disasters to advance climate change adaptation. – In: Field, C. B. et al. (eds.) A special report of working groups I and II of the intergovernmental panel on climate change. Cambridge University Press, Cambridge, UK, and New York, NY, USA, 582p.

http://www.aloki.hu ● ISSN 1589 1623 (Print) ● ISSN 1785 0037 (Online)
DOI: http://dx.doi.org/10.15666/aeer/1906_42514263

[11] Jana, S., Srivastava, J. R., Damania, A. B., Clarce, J. M., Yang, R. C., Pecetti, L. (1990): Phenotypicdiversity and associations of some drought-related characters in durum wheat in the Mediterranean region. – In: Srivastava, J. P., Damania, A. B. (eds.) Wheat Genetic Resources: Meeting Diverse Needs. John Wiley and Sons, England, pp. 27-44. https://doi.org/10.2135/cropsci1991.0011183X003100060018x.

[12] Karaman, M., Akinci, C., Yildirim, M. (2014): Investigation of the relationship between grain yield with physiological parameters in some bread wheat varieties. – Trakya University Journal of Natural Sciences 15(1): 41-46.

[13] Kizilgeci, F., Akinci, C., Albayrak, O., Yildirim, M. (2017): Relationships of grain yield and some quality parameters with physiological parameters in some triticale advanced lines. – Igdır Univ. J. Inst. Sci. & Tech. 7(1): 337-345. DOI: https://doi.org/10.21597/jist.2017127446.

[14] Kizilgeci, F., Yildirim, M., Akinci, C., Albayrak, O., Sessiz, U., Tazebay, N. (2018): Evaluation of relationships between yield and yield components with physiological parameters in barley (*Hordeum vulgare* L.) genotypes. – DUFED 7(2): 61-66.

[15] Koc, M., Barutcular, C. (2000): Relationship between leaf area index at anthesis and yield in wheat under Cukurova conditions. – Turkish Journal of Agriculture and Forestry 24(5): 585-594. https://dergipark.org.tr/tr/pub/tbtkagriculture/issue/11655/138764.

[16] Kutlu, I., Kinaci, G. (2010): Evaluation of drought resistance indicates for yield and its components in three triticale cultivars. – Journal of Tekirdag Agricultural Faculty 7(2): 95-103.

[17] Masuda, T., Polle, J. E. W., Melis, A. (2002): Biosynthesis and distribution of chlorophyll among the photosystems during recovery of the green alga Dunaliella salina from irradiance stress. – Plant Physiol. 128: 603-614.

[18] Mut, Z., Albayrak, S., Tongel, O. (2006): Determination of grain yield and some traits of triticale (*Xtriticosecal*e *Wittmack*) lines. – Ankara University Faculty Of Agriculture, Agricultural Sciences Journal 12(1): 56-64.

[19] Okursoy, H. (2005): Determination of the economic irrigation level in Trakya conditions. – Trakya University Institute of Science, Master's Thesis, 80p., Tekirdag.

[20] Qaseem, M. F., Qureshi, R., Shaheen, H. (2019): Effects of Pre-Anthesis Drought, Heat and Their Combination on the Growth, Yield and Physiology of diverse Wheat (*Triticum aestivum* L.) Genotypes Varying in Sensitivity to Heat and drought stress. – Sci Rep 9: 6955. https://doi.org/10.1038/s41598-019-43477-z.

[21] Sahin, M., Aydogan, S., Akcacik, A. G., Taner, S. (2005): The evaluation on alveograf analysis of some bread wheat genotypes improved for the Central Anatolia. – Tagem journals 2: 1-9.

[22] Sakin, M. A., Naneli, İ., Goy, A. G., Ozdemir, K. (2015): Determination of yield and yield components of some bread wheat (*Triticum aestivum* L.) varieties at Tokat-Zile conditions. – Journal of Agricultural Faculty of Gaziosmanpasa University 32(3): 119-132. doi:10.13002/jafag927.

[23] Savasli, E., Cekic, C., Onder, O., Dayioglu, R., Kalayci, H. M. (2012): Evaluation of some bread wheat cultivars and advanced breeding lines for yield, biomass and vegetation index. – TABAD 5(2): 33-37. DOI: 10.13140/RG.2.1.4568.5522.

[24] Shamsi, K., Petrosyan, M., Noor-Mohammadi, G. (2010): The role of water deficit stress and water use efficiency on bread wheat cultivars. – J. Appl. Biosci. 35: 2325-2331.

[25] Verhulst, N., Govaerts, B. (2010): The normalized difference vegetation index (NDVI) GreenSeeker handheld sensor: Toward the integrated evaluation of crop management. Part A: Concepts and case studies. – Mexico, D.F.; CIMMYT.

[26] Yavas, I. (2010): The determination of drought resistance characters in Aegean Region's wheat cultivars. – Ph.D. Thesis, Department of Field Crops, 103p. Aydın.

[27] Yildirim, A., Sakin, M. A., Gokmen, S. (2005): Evaluation of some common bread wheat cultivars advanced and breeding lines for yield and yield components. – Gaziosmanpasa University Journal of the Faculty of Agriculture 22(1): 63-72.

http://www.aloki.hu ● ISSN 1589 1623 (Print) ● ISSN 1785 0037 (Online)
DOI: http://dx.doi.org/10.15666/aeer/1906_42514263

[28] Yildirim, M., Bahar, B., Yucel, C., Genc, I. (2009a): Plant temperature variations in Cimmyt wheat yield experiment sets. – Turkey VIII. Field Crops Congress, 19-22 October 2009, Hatay, pp. 427-432.
[29] Yildirim, M., Akinci, C., Barutcular, C. (2009b): Applicability of canopy temperature depression and chlorophyl content in durum wheat breeding. – Anadolu J. Agric. Sci. 24: 158-166.
[30] Yildirim, M., Koc, M., Akinci, C., Barutcular, C. (2013): Variations in morphological and physiological traits of bread wheat diallel crosses under timely and late sowing conditions. – Field Crops Research 140: 9-17. https://doi.org/10.1016/j.fcr.2012.10.001.
[31] Yildirim, M., Kizilgeci, F., Akinci, C., Albayrak, O. (2018): Correlation analysis of LAI, SPAD, NDVI, CT with grain yield and quality traits of some bread wheat genotypes at heading stages. – Anatolia International Multidisciplinary Studies Congress, 22-29 December 2018, Diyarbakır, pp. 853-857.

http://www.aloki.hu ● ISSN 1589 1623 (Print) ● ISSN 1785 0037 (Online)
DOI: http://dx.doi.org/10.15666/aeer/1906_42514263

EFFECT OF DIFFERENT PLANT DENSITIES ON GROWTH PARAMETERS AND DRY MATTER ACCUMULATION IN COTTON (*Gossypium hirsutum* L.)

BEYYAVAS, V. – HALILOGLU, H.*

Department of Field Crops, Faculty of Agriculture, Harran University, Osmanbey Campus, Sanliurfa 63050, Turkey

**Corresponding author*
e-mail: haliloglu@harran.edu.tr; phone: +90-530-205-0794

(Received 10th May 2021; accepted 30th Aug 2021)

Abstract. This study was carried out to determine the effects of various plant densities on growth parameters and dry matter accumulation in cotton (*Gossypium hirsutum* L.). Field experiments was conducted on the experimental site of Field Crops Department in Faculty of Agriculture, University of Harran. The Stoneville-453 cotton variety was used as plant material. Experimental layout was randomized blocks with 3 replications in the two years of experiment. Plant densities (PD) were 70 × 5 cm (PD1, 28 plants per m^2), 70 × 20 cm (PD2, 7 plants per m^2) and 35 × 5 cm (PD3, 57 plants per m^2). Plant height (cm), number of nodes (pieces), height to nod ratio (HNR, piece), stem diameter (cm), stem dry matter accumulation (g), leaf dry matter accumulation (g), flower dry matter accumulation (g), total dry matter accumulation (g), number of leaves (pieces), leaf area index (LAI) at 60th, 75th, 90th, 105th and 120th days from sowing and yields during harvest period were determined. The plant height, number of nodes, stem diameter, flower, leaf, stem and total dry matter accumulation weights were higher in the PD2 treatment, while LAI and yields were higher in PD3 treatment.
Keywords: *biomass, leaf area index, management factors, row spacing, high yield formation*

Introduction and literature review

Genetic potential of a variety, environmental conditions and cultural processes in crop production are the major factors affecting crop yield. Plant density in cotton cultivation is one of the most important variables affecting yield per unit area and increasing profitability. Proper plant density and fertilizer management are the most important factors to obtain high cotton yield (Bednarz et al., 2006; Tariq et al., 2018). Previous studies revealed that extreme high or low plant density causes a significant decrease in cotton yield. The cotton is extremely responsive to management factors, therefore, optimum density of cotton plants may vary depending on location, environment, cultivar and preferences of growers (Silvertooth et al., 1999; Dong et al., 2006a, b). However, the final lint yield of cotton was reported as stable across a wide range of plant population densities (Bednarz et al., 2000; Siebert et al., 2006).

Some studies reported that fiber yield increases with higher plant density per unit area (Mao et al., 2015) and plant density has a positive effect on yield increase (Zhi et al., 2016), while some studies indicated that plant density has no impact on cotton yield (Ren et al., 2013). Optimum plant density is a key determinant of high yield formation in cotton. The growth and development of plants can provide a beneficial micro-environment (canopy temperature, relative humidity and light transmittance) for high yield (Yang et al., 2014).

Kerby et al. (1990) reported that the dry matter content during the first squaring, first flowering, peak blooming and boll opening periods was higher under

http://www.aloki.hu ● ISSN 1589 1623 (Print) ● ISSN 1785 0037 (Online)
DOI: http://dx.doi.org/10.15666/aeer/1906_42654280

increased plant densities. In addition, leaf area index, dry matter accumulation and the number of bolls per unit area increased with decreasing row spacing (Samani et al., 1999).

The density of cotton population significantly affects layout of canopy, interception of light and eventually development of bolls. In addition, plant height, photosynthetic efficiency of leaves, plant architecture and boll sizes are also affected by number of plants per unit area (Hussain et al., 2000; Siebert et al., 2006). Lint yield and leaf area index increase with the increase in plant density, however, leaf area of single leaves is reduced (Gwathmey and Clement, 2010).

Distribution of assimilates between vegetative and reproductive organs has a significant impact on cotton yield (Reta-Sánchez and Fowler, 2002; Jones et al., 1996; Kerby et al., 1993). Studies indicating the importance of biomass accumulation and its distribution among reproductive organs for cotton yield (Saleem et al., 2010; Bange and Milroy, 2004; Wells and Meredith, 1984) were mostly carried out under extensive agricultural practices and using non-transgenic cotton varieties.

Production of high amount of biomass is needed for cotton yield and ratio of biomass among reproductive organs affects the cotton yield (Bange and Milroy, 2004). The cotton plants accumulate high vegetative biomass. The accumulation of biomass increases in early growth stages with the availability of more light to lower parts (Khan et al., 2020), while it decreases in the last growth stages due to shedding of fruits and leaves (Zhi et al., 2016; Khan et al., 2017).

Leaf area or leaf area index is considered an important indicator of growth, which is defined as the net increase in dry matter content for unit leaf area at unit time. The plant leaf area depends on the number of leaves on a plant, the average single leaf area, and the photosynthetic functional length of the leaves. The effects of these three features on the leaf area may vary depend on genetic structure of the variety and environmental conditions (Reddy and Reddy, 1992). The increase in leaf area index of cotton plants is slow in the first periods of the growing period, while increases rapidly later and can reach the highest level at the growing period of about 100 days (Wullschleger and Oosterhuis, 1992). The LAI which generally varies between 3.7 and 5.2, gradually decreases in later periods due to the leaf losses caused by the increase in the generative development of plants and leaf aging (Reta-Sánchez and Fowler, 2002).

Even though this study was conducted in 2006 and 2007 years, plant densities related to inter-row and intra-row spacings differ from region to region and machine or manual harvesting types in cotton cultivation areas. For this reason, this study still maintains its importance.

This study was carried out to determine the effects of different plant densities on the growth parameters of cotton and the changes in dry matter accumulation until harvest.

Materials and methods

Stoneville-453 cotton variety (*Gossypium hirsutum* L.) was used as plant material in the study. The Stoneville-453 cotton variety was breed by the Stoneville Seed Company and registered in 1988 (Calhoun et al., 1997). The variety, certified to be used in the Sanliurfa region in 1995, is preferred by farmers, especially due to medium early and high gin efficiency (42%) (Harem, 2010).

http://www.aloki.hu ● ISSN 1589 1623 (Print) ● ISSN 1785 0037 (Online)
DOI: http://dx.doi.org/10.15666/aeer/1906_42654280

Experimental site

Field experiments were conducted in Eyyubiye Campus of Harran University, and the experimental site is located in Harran Plain, Sanliurfa (37°08' North and 38°46' east, ASL 465 m) close to Syrian border in Turkey (*Fig. 1*).

Average temperature values during cotton growth period (April-November) in 2006 was between 11.4 and 33.4 °C and it was between 12.6 and 34.0 °C in 2007. Total precipitation in 2006 (April-November) varied from 0 to 81.1 mm, while it varied from 0 to 49.2 mm in 2007 (*Table 1*).

Table 1. *Some important meteorological data of the experimental field (Anonymous, 2007b)*

Months	Years	Av. max temp. (°C)	Av. min temp. (°C)	Av. temp. (°C)	Av. relative humidity (°C)	Av. total precip. (mm)
April	First year	23.2	12.3	17.8	62.9	81.1
	Second year	18.8	8.8	13.1	66.5	49.2
	Long term averages	22.0	10.0	15.9	56.0	49.2
May	First year	30.4	16.9	23.8	45.9	17.4
	Second year	31.1	19.5	25.4	54.0	8.8
	Long term averages	28.6	15.0	22.0	45.0	26.0
June	First year	38.0	22.8	30.8	40.8	0.3
	Second year	37.2	23.0	30.4	36.9	0.8
	Long term averages	34.4	20.2	27.9	32.4	3.0
July	First year	38.5	24.9	32.2	45.5	0.3
	Second year	40.8	27.0	34.0	31.3	8.0
	Long term averages	38.6	26.8	33.1	29.7	0.6
August	First year	40.4	26.0	33.4	44.6	-
	Second year	39.3	25.4	32.2	41.9	3.2
	Long term averages	38.1	23.6	31.2	32.3	0.9
September	First year	32.3	22.4	27.2	42.3	-
	Second year	36.0	22.0	28.4	36.4	-
	Long term averages	33.8	19.8	26.7	35.1	1.1
October	First year	25.9	12.8	20.6	61.5	42.5
	Second year	28.4	16.5	21.6	47.7	25.9
	Long term averages	26.9	14.2	20.1	44.8	23.8
November	First year	16.3	7.7	11.4	57.5	26.2
	Second year	18.3	8.6	12.6	58.2	15.4
	Long term averages	18.6	8.3	12.8	59.0	45.7

The soil of experimental field is alluvial, deep, and high in lime and potassium, while, poor in phosphorus content. Soil samples were taken from a depth of 0-20 cm in 2006 and 2007 before planting.

The clay content of the soil samples were 56.50 and 59.04%, pH value was 7.76 and 7.66, organic matter content was 1.59 and 1.45%, and lime content was 25.4 and 23.7%, respectively (*Table 2*).

http://www.aloki.hu ● ISSN 1589 1623 (Print) ● ISSN 1785 0037 (Online)
DOI: http://dx.doi.org/10.15666/aeer/1906_42654280

Figure 1. *The map of the experimental field*

Table 2. *Some physical and chemical soil properties of the experimental field (Anonymous, 2007a)*

Soil properties	First year	Second year
Clay (%)	56.50	59.04
Silt-loam (%)	22.70	22.72
Sand (%)	20.80	18.24
pH	7.76	7.66
Lime ($CaCO_3$) (%)	25.40	23.70
Total salt (%)	0.052	0.068
Organic matter (%)	1.59	1.45

Experimental design

Cotton seeds were planted on May 15 in 2006 and 2007. The experiment was conducted as a completely randomized block design with three replications. Each plot consisted of 4 rows with 10 m length. The plots were fertilized to provide 160 kg N ha^{-1} and 80 kg P ha^{-1} phosphorus. Half of nitrogen and all of phosphorus were applied using 20.20.0 compound fertilizer during planting and the other half of nitrogen was applied using ammonium nitrate (33% N) fertilizer at the beginning of flowering.

Traditionally, 70 × 20 cm of planting density is applied in the region where the experiments were carried out. In this study, different planting densities applied so as to determine interactions of the yield and some growth parameters with plant densities.

Following the sufficient emergence, the number of plants were decreased to arrange plant density to 70 × 5 cm (PD1, 28 plants m^{-2}), 70 × 20 cm (PD2, 7 plants m^{-2}) and 35 × 5 cm (PD3, 57 plants m^{-2}) (*Fig. 2*). Total of 900 mm irrigation water was applied in 2006 and 2007 with 9 furrow irrigations. All necessary agricultural practices during growing periods were carried out conventionally. Aphids (*Aphiss gossypii*), leafhopper (*Empoasca spp*), silverleaf whitefly (*Bemisia tabaci Genn*.) and cotton bollworm (*Heliothis armigera* Hübn.) were observed in 2006 and 2007; therefore, pesticides were applied considering the economic damage thresholds. Against aphids (*Aphiss gossypii*) insecticide (40% Dimethoate active substance) with dose of 1000 cc ha^{-1}, against

http://www.aloki.hu ● ISSN 1589 1623 (Print) ● ISSN 1785 0037 (Online)
DOI: http://dx.doi.org/10.15666/aeer/1906_42654280

leafhopper (*Empoasca ssp*) and whitefly (*Bemisia tabaci* Genn) 200 g ha^{-1} of Acetamiprid and 600 cc ha^{-1} of Esfenvalerate, and against greenworm (*Heliothus armigera* Hübn.) 200 g ha^{-1} of Acetamiprid and 2000 cc ha^{-1} of Cloropyrifos were mixed and applied.

Figure 2. *An image from the experiment field*

Cotton plant growth parameters

The plant height, stem diameter, leaf number, number of nodes, height to node ratio (HNR) and leaf area index (LAI) of randomly selected 10 plants from each plot were determined at 60 (T1), 75 (T2), 90 (T3), 105 (T4) and 120 (T5) days after planting (DAP) according to Montgomery (1997).

Biomass accumulation and partitioning

These plants were then separated into three parts as reproductive structures (flowers), leaves and stems, and dried separately. Total dry matter weights were calculated by summing the dry matter weights of plant parts. Samples were oven dried at 70 ℃ for 72 h until attaining a constant weight (Wells and Meredith, 1986; Kandil et al., 2004).

Daily dry matter production was calculated using the following equation explained by Board (2000):

$$BBO = W2 - W1 / T1 - T2$$

W1: Dry weight of plants at T1 (g $plant^{-1}$), W2: Dry weight of plants at T2 (g $plant^{-1}$), T1: The time when the dry matter weight determined during the first growing period (day), T2: The time when the dry matter weight determined during the second growing period (day).

Leaf area index (LAI)

Leaf area index was calculated using the following equation explained by Board (2000):

Leaf area index (LAI) = total leaf area of plant (cm^2) / total area covered by a plant (cm^2)

http://www.aloki.hu ● ISSN 1589 1623 (Print) ● ISSN 1785 0037 (Online)
DOI: http://dx.doi.org/10.15666/aeer/1906_42654280

Seed cotton yield

The yields for experimental plots were determined by harvesting two rows in the middle after removing 1 m on each side to remove edge effect. Seed cotton yield per hectare was calculated using the mean yield value obtained for plots.

Data analysis

The field experiment was conducted in randomized block design, however, the data obtained for plant growth parameters except the seed cotton yield were analyzed in the statistical program of MINITAB 18.1 according to the split plots in the randomized blocks. The averages were grouped using the Tukey-HSD test.

Results and discussion

Variance analysis indicated a significant difference between years; therefore, the data of each year were presented separately.

Plant height (cm)

The highest plant height in 2006 (78.71 cm) was obtained in the PD2 plant density treatment, while the highest plant height in 2007 was recorded in PD1 and PD3 plant densities (65.97 cm and 65.30 cm). In the first year of the field experiment, the plant height decreased in parallel with the increase in plant density per m^{-2} (*Table 3*). The results recorded in the first year are in accordance with findings of Khan et al. (2020), Clawson et al. (2006) and Gwathmey and Clement (2010) who reported a decrease in plant height with the increase in plant density. In contrast to the plant heights in the first year, plant height increased with the increase in plant density in the second year. Similar to the results of second year, Kaggwa-Asiimwe et al. (2013) and Beyyavas et al. (2018) also indicated an increase in plant height with the increase in plant density. The differences in relationship between plant height and plant density may be attributed to the differences in climate and environmental conditions of the experimental sites.

The highest plant height in 2006 during plant growth period examined was reached at T5 (97.14 cm) and in 2007 at T4 and T5 times (78.42 cm and 79.65 cm). The cotton plant has an indeterminate growth habit (Tariq et al., 2018), therefore, the plant height regularly increases with the progress in time.

Number of nodes (pcs plant^{-1})

The highest number of nodes in 2006 and 2007 was obtained in PD2 plant density (17.34 and 14.90 pcs plant^{-1}). Our findings are consistent with the findings of Clawson et al. (2006) and Gwathmey and Clement (2010) who reported that wide row distance in cotton cultivation increased the number of nodes per plant.

The highest number of nodes per plant in both years (18.81 and 17.83 pcs plant^{-1}) was recorded in at T5 time (*Table 3*). Since cotton has an indeterminate growth pattern, the number of nodes is increasing proportionally with increase in plant height.

The number of nodes vary according to genetics of the plant, fertilization, irrigation and cultural practices. In particular, excessive nitrogen fertilization and irrigation applications may cause an increase in plant height and, as a result, an increase in the number of nodes.

http://www.aloki.hu ● ISSN 1589 1623 (Print) ● ISSN 1785 0037 (Online)
DOI: http://dx.doi.org/10.15666/aeer/1906_42654280

Table 3. *The effect of different plant densities and growth times in cotton on plant height (cm), number of nodes (pcs plant^{-1}), height to node ratio (HNR) and stem diameter (cm)*

Treatments		Plant height (cm)		Number of nodes (pcs plant^{-1})		Height to node ratio (HNR)		Stem diameter (cm)	
		2006	**2007**	**2006**	**2007**	**2006**	**2007**	**2006**	**2007**
Plant density	PD1	75.22 ^{b*}	65.97 ^{a*}	15.64 ^{b*}	14.14 ^{b*}	4.72 ^{a*}	4.63 ^{a*}	0.81 ^{b*}	0.71 ^{b*}
	PD2	78.71 ^{a}	63.07 ^{b}	17.34 ^{a}	14.90 ^{a}	4.47 ^{b}	4.20 ^{b}	1.11 ^{a}	1.43 ^{a}
	PD3	74.58 ^{b}	65.30 ^{a}	15.23 ^{b}	13.91 ^{b}	4.77 ^{a}	4.60 ^{a}	0.76 ^{b}	0.71 ^{b}
Times	T1	40.00 ^{e}	36.05 ^{d}	11.21 ^{d}	9.30 ^{d}	3.60 ^{c}	3.92 ^{c}	0.65 ^{d}	0.47 ^{c}
	T2	66.62 ^{d}	54.53 ^{c}	15.07 ^{c}	14.22 ^{c}	4.42 ^{b}	3.84 ^{c}	0.75 ^{cd}	0.67 ^{b}
	T3	84.95 ^{c}	75.24 ^{b}	17.41 ^{b}	14.56 ^{c}	4.89 ^{a}	5.17 ^{a}	0.76 ^{c}	0.86 ^{a}
	T4	92.13 ^{b}	78.42 ^{a}	17.84 ^{b}	15.69 ^{b}	5.19 ^{a}	4.99 ^{a}	1.04 ^{b}	0.87 ^{a}
	T5	97.14 ^{a}	79.65 ^{a}	18.81 ^{a}	17.83 ^{a}	5.16 ^{a}	4.46 ^{b}	1.27 ^{a}	1.91 ^{a}
	F values								
PD		12.83**	7.42**	55.13**	13.53**	5.39*	17.06**	76.60**	44.54**
T		844.49**	699.31**	245.33**	295.74**	53.04**	63.61**	90.05**	116.54**
PD × T		12.55**	19.83**	5.03*	13.00**	3.59**	1.12^{ns}	0.85^{ns}	6.82**

*Means that do not share a letter are significantly different. *p ≤ 0.05, **p ≤ 0.01, ns: non-significant
PD1: 70 × 5 cm, PD2: 70 × 20 cm, PD3: 35 × 5 cm

Height to node ratio (HNR)

The highest HNR in both years of the experiment was obtained in PD1 (4.72 and 4.63 pcs plant^{-1}) and PD3 (4.77 and 4.60 pcs plant^{-1}) treatments. The increase in plant density caused an increase in plant height a consequently to the HNR (*Table 3*).

The HNR in both years increased proportionally to the increase in the number of days. The HNR in 2006 was ranked from low to high as T1 (3.60 cm) < T2 (4.42 cm) < T3 (4.89 cm) < T5 (5.16 cm) < T4 (5.19 cm), and in 2007 T2 (3.22 cm) < T1 (3.92 cm) < T5 (4.46 cm) < T4 (4.99 cm) < T3 (5.17 cm). The HNR peaked in T3 and T4 times, which are the flowering peak and boll development periods, and slightly decreased after the cut-out period. The HNR in this study are coincide with the findings of Birgul (2008) and Celik et al. (2009) who reported that the HNR was 2.6 at the squaring stage, 3.4 at the beginning of flowering, 4.6 at the flowering peak, 5.1 in the cut-out period, 5.04 in the boll opening period and 4.84 in the harvest period. The results can be associated with the consumption of nutrients in the development of more bolls with the formation of flowers and bolls in the generative period after certain vegetative development period. Therefore, plants continue generative development rather than vegetative growth (Kerby et al., 1993).

Stem diameter (cm)

The stem diameter of the plants in the PD2 (1.11 and 1.43 cm) treatment was higher in both years of the experiment compared to the other two plant densities. The result can be explained by the fact that plant in wide row plantings benefit from the competitive environment better and the plant uptake and use more nutrients. In both years of the experiment, the stem diameter increased proportionally with the increase in the number of days. The stem diameter of cotton plants by the time was T1 < T2 < T3 < T4 < T5,

http://www.aloki.hu ● ISSN 1589 1623 (Print) ● ISSN 1785 0037 (Online)
DOI: http://dx.doi.org/10.15666/aeer/1906_42654280

respectively (*Table 3*). Zhang et al. (2016) reported that stem diameter increased as plant density decreased.

Flower dry matter weight (g plant^{-1})

The highest flower dry matter accumulation in both years of the experiment was obtained in PD2 (49.36 and 44.48 g) treatment. The decrease in the number of plants per m^{-2} in wide row plantings improved the utilization of competitive environment and nutrients in plant development. Our results are in agreement with those reported by Khan et al. (2020), who stated that flower dry matter accumulation decreases with the increase in plant density. Similarly, Yang et al. (2014) indicated that accumulation of flower biomass decreased in high and low plant densities.

The flower dry matter accumulation increased proportionally with increase in the number of days (*Table 4*). The results are similar to the findings of Dai et al. (2015), who reported that dry matter accumulations gradually increased with plant growth. The highest flower dry matter accumulation in 2006 was obtained at T5 time (82.01 g), while T3 (45.22 g), T4 (41.98 g) and T5 (50.86 g) times were in the same group in 2007. This result reveals that plants produce flower dry matter in proportionally with the progress in generative period. The flower dry matter weight in total dry matter weight in 2006 was ranked as PD1 (46%) > PD3 (44%) > PD2 (37%) and in 2007, PD2 (58%) > PD1 (55%) > PD3 (39%) (*Table 2*). In terms of time, the flower dry matter weight in total dry matter weight in 2006 was ranked as T1(%6) < T2 (%16) < T3 (%40) < T5 (%46) < T4 (%47); in 2007, T1 (%4) < T2 (%13) < T5 (%62) < T4 (%54) < T3 (%69). The flowers and boll dry matter accumulation in total dry matter at T3 time (90th day), which coincides with the flowering peak and boll development period, was higher in 2007 compared to the other times examined.

Table 4. *The effect of different plant densities and growth times in cotton on flower dry matter weight (g plant^{-1}), leaf dry matter weight (g plant^{-1}), stem dry matter weight (g plant^{-1}) and total dry matter weight (g plant^{-1})*

Treatments		Flower dry matter weight (g plant^{-1})		Leaf dry matter weight (g plant^{-1})		Stem dry matter weight (g plant^{-1})		Total dry matter weight (g plant^{-1})	
		2006	**2007**	**2006**	**2007**	**2006**	**2007**	**2006**	**2007**
Plant density	PD1	33.40 ^{b*}	29.91 ^{b*}	17.98 ^{b*}	13.93 ^{a*}	21.31 ^{b*}	10.93 ^{b*}	72.69 ^{b*}	54.77 ^{b*}
	PD2	49.36 ^{a}	44.48 ^{a}	46.05 ^{a}	16.01 ^{a}	37.11 ^{a}	15.85 ^{a}	132.52 ^{a}	76.34 ^{a}
	PD3	33.80 ^{b}	10.85 ^{c}	21.85 ^{b}	8.73 ^{b}	21.75 ^{b}	7.98 ^{b}	77.40 ^{b}	27.56 ^{c}
Times	T1	0.85 ^{c}	0.49 ^{b}	7.88 ^{c}	8.32 ^{c}	5.01 ^{c}	3.23 ^{b}	13.74 ^{c}	12.04 ^{b}
	T2	6.44 ^{c}	3.52 ^{b}	18.21 ^{c}	12.22 ^{bc}	15.58 ^{bc}	11.47 ^{a}	40.23 ^{c}	27.21 ^{b}
	T3	41.79 ^{b}	45.22 ^{a}	38.52 ^{ab}	8.56 ^{c}	25.12 ^{b}	11.51 ^{a}	105.43 ^{b}	65.29 ^{a}
	T4	63.17 ^{ab}	41.98 ^{a}	31.94 ^{b}	19.20 ^{a}	38.00 ^{a}	16.07 ^{a}	133.11 ^{b}	77.25 ^{a}
	T5	82.01 ^{a}	50.86 ^{a}	46.59 ^{a}	16.13 ^{ab}	49.93 ^{a}	15.66 ^{a}	178.53 ^{a}	82.65 ^{a}
	F values								
PD		4.84*	17.29**	40.41**	24.29**	16.48**	15.93**	2.46**	12.84**
T		43.48**	21.60**	25.42**	23.44**	38.56**	16.12**	15.15**	26.72**
PD × T		1.06^{ns}	4.06**	4.18**	5.19**	2.12^{ns}	1.21^{ns}	0.72*	4.35**

*Means that do not share a letter are significantly different. *p ≤ 0.05, **p ≤ 0.01, ns: non-significant
PD1: 70 × 5 cm, PD2: 70 × 20 cm, PD3: 35 × 5 cm

http://www.aloki.hu ● ISSN 1589 1623 (Print) ● ISSN 1785 0037 (Online)
DOI: http://dx.doi.org/10.15666/aeer/1906_42654280

Leaf dry matter weight (g plant^{-1})

Leaf dry matter accumulation in the PD2 (46.05 and 16.01 g) was higher than the other two densities in both years of the experiment. The results indicated that plants benefited better from the competitive environment with the decrease in the number of plants per m^2 in wide row plantings and plants utilized the nutrients more efficiently in development. In contrast to our findings, Khan et al. (2020) reported that higher number of plants per unit area in dense planting caused higher vegetative growth and increase in total and vegetative biomass. Leaf dry matter accumulation increased proportionally with the increase in the number of days (*Table 4*). The highest dry matter accumulation in 2006 was obtained at T5 time (46.59 g) and in 2007 at time T4 (19.20 g). The results revealed that physiological recession period started at T4 time in 2006 due to climate and environmental conditions and it was between T3 and T5 times in 2007. The ratio of leaf dry matter weight in total dry matter weight in 2006 was ranked as PD2 (35%) > PD3 (28%) > PD1 (25%); in 2007, as PD2 (39%) > PD1 (25%) > PD3 (21%) (*Table 2*). In terms of the times, the ratio of leaf dry matter weight in total dry matter weight in 2006 was ranked as T1 (57%) > T2 (45%) > T5 (26%) > T4 (24%) > T3 (8%), and in 2007, T1 (69%) > T2 (45%) > T4 (25%) > T5 (20%) > T3 (13%).

Stem dry matter weight (g plant^{-1})

Stem dry matter accumulation in both years of the trial with PD2 treatment (37.11 and 15.85 g) was higher compared to the other two plant density treatments. The results revealed that decreasing the number of plants per m^2 in wide row plantings improved the use of the competitive environment, and plants utilized nutrients better in development. The results were contradicting to the findings of Khan et al. (2020) who indicated that the total and vegetative biomass increased with the increase in the number of plants per unit area due to high vegetative growth. The stem dry matter accumulation increased proportionally with the increase in the number of days (*Table 4*). The highest stem dry matter accumulation in 2006 was recorded at T4 (38.00 g) and T5 (49.93 g), and in 2007, it was obtained at T2, T3, T4 and T5. The stem diameters at T2, T3, T4 and T5 were statistically similar and included in the same group. However, the results revealed that plants entered to the physiological recession period between T4 and T5 due to the climate and environmental conditions. In terms of planting density, the ratio of stem dry matter weight in total dry matter weight in 2006 was ranked as PD1 (29%) > PD2 (28%) > PD3 (28%); in 2007, it was ranked as PD3 (29%) > PD2 (21%) > PD1 (20%) (*Table 2*). In terms of the times examined, the ratio of stem dry matter weight in total dry matter weight in 2006 was ranked as T2 (39%) > T1 (36%) > T4 (29%) > T5 (28%) > T3 (24%); in 2007, it was ranked as T2 (42%) > T1 (27%) > T4 (21%) > T5 (19%) > T3 (18%).

Total dry matter weight (g plant^{-1})

The PD2 treatment provided higher total dry matter weight (132.52 and 76.34 g) in both years of the experiment compared to the other two plant densities (*Fig. 3*). The low plant density increased the use of light, nutrients and water, and consequently the plant growth. In addition, higher number of bolls, flowers, leaves and fruiting branches were formed per plant in low density planting. Therefore, total dry matter accumulation per plant was also increased in low plant density. Similarly, Kerby et al. (1990) reported higher dry matter accumulation under lower number of plant per unit area. In contrast to

http://www.aloki.hu ● ISSN 1589 1623 (Print) ● ISSN 1785 0037 (Online)
DOI: http://dx.doi.org/10.15666/aeer/1906_42654280

our findings, Ali et al. (2009) indicated that dry matter accumulation increased proportionally with the increase in planting density. Rahman et al. (2013) reported that the dry matter ratio per unit area in a plant density of 30 cm was 323.32 g m^{-2} which decreased to 257.18 g m^{-2} at a plant density of 50 cm in soybean. The results attributed to the dry matter production and accumulation in the side branches by encouraging the formation of side branches in low plant densities. The increase in the number of side branches causes increase dry matter content in low plant population compared to the normal plant population and also causes more nodes and fruit formation (Carpenter and Board, 1997). High plant density increases plant total biomass, while the individual biomass of a cotton plant decreases (Khan et al., 2019). The results for vegetative and reproductive dry mass obtained in our study are contradicting to the findings of Afzal et al. (2018) who stated that total dry matter production in low density was 19.32% lower than high density plantings.

The results showed that total dry matter accumulation increased with the increase in the number of days (*Table 4*). The dry matter accumulation of the plant in 2006 and 2007 increased proportionally from the vegetative period to the end of the generative period (T1 < T2 < T3 < T4 < T5) (*Fig. 4*).

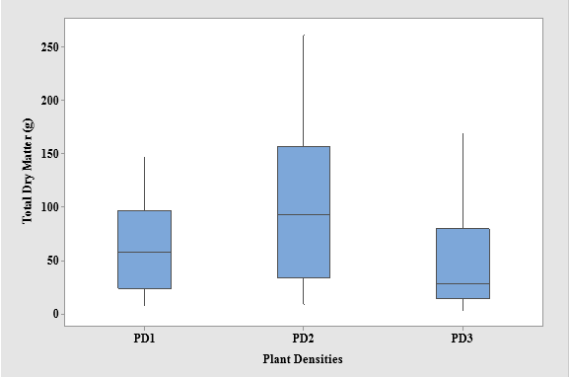

Figure 3. *Total dry matter weight at different plant densities*

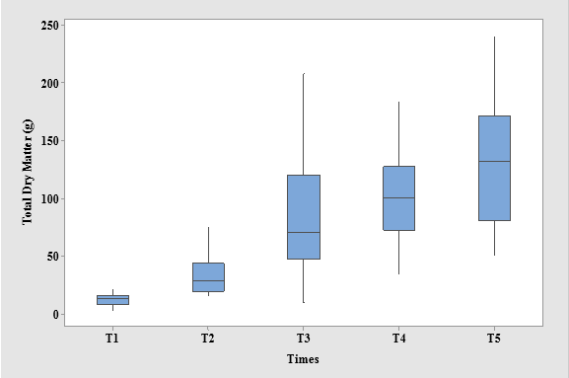

Figure 4. *Total dry matter weight at different plant growth times*

Daily dry matter production in 2006 between T1-T2 period was 1.77 g $plant^{-1}$, between T2-T3 period 4.35 g $plant^{-1}$, between T3-T4 period 1.85 g $plant^{-1}$ and between T4-T5 period 3.03 g $plant^{-1}$. The daily dry matter production in 2007 between T1-T2

http://www.aloki.hu ● ISSN 1589 1623 (Print) ● ISSN 1785 0037 (Online)
DOI: http://dx.doi.org/10.15666/aeer/1906_42654280

periods was 1.01 g plant^{-1}, between T2-T3 period 2.54 g plant^{-1}, between T3-T4 0.80 g plant^{-1}, and between T4-T5 0.36 g plant^{-1}. The daily dry matter production in both years of the trial reached the highest level between T1 and T2. This can be explained by the highest growth and development of cotton plants, as well as the highest flowering and fruiting development.

Leaf area index (LAI)

The PD3 (57 plants m^{-2}) in both years of the trial produced higher leaf area index (11.55 and 12.66) than other plant density treatments (*Fig. 5*). Leaf area index ranged from 1.48 to 12.66.

It can be observed that the leaf area index values increased proportionally from the vegetative period to the end of the generative period (T1 < T2 < T3 < T4 < T5) in both years of the experiment (*Fig. 6*). Gwathmey and Clement (2010) and Yao et al. (2017) stated that leaf area index increase with the increase in plant density; however, an individual leaf area may be reduced in high plant density.

The LAI in both years increased proportionally with the increase in the number of days (*Table 5*). The results reported in previous studies are consistent with our findings. For example; Zhang et al. (1962) reported that LAI value reached 6.12 in 400000 plants ha^{-1} plant density, while LAI was 3.82 in 200000 plant ha^{-1} plant density.

Rahman and Hossain (2011) stated that the leaf area index value increased with the increase of plant density. In their research while leaf area index was observed 2.45 per 20 plants m^{-2}, 3.69 per 60 plants m^{-2}. Samani et al. (1999) reported that the leaf area index and dry matter accumulation unit area increased with the decrease of row spacing. Zhang et al. (2016) and Wang et al. (2016) reported that a relatively higher leaf area index (LAI) occurs at higher plant densities.

Table 5. *The effect of different plant densities and growth times on the leaf area index (LAI), number of leaves (pcs plant^{-1}) and seed cotton yield (kg ha^{-1})*

Treatments		**Leaf area index (LAI)**		**Number of leaves (pcs plant^{-1})**		**Seed cotton yield (kg ha^{-1})**	
		2006	**2007**	**2006**	**2007**	**2006**	**2007**
Plant density	PD1	4.49 ^{b*}	4.48 ^{b*}	31.73 ^{b*}	32.40 ^{b*}	477.31 ^{c}	6010.33 ^{b*}
	PD2	2.02 ^{c}	1.48 ^{c}	43.10 ^{a}	43.50 ^{a}	522.62 ^{b}	5294.67 ^{c}
	PD3	11.55 ^{a}	12.66 ^{a}	28.43 ^{b}	28.31 ^{b}	575.90 ^{a}	7096.00 ^{a}
Times	T1	2.64 ^{d}	2.23 ^{c}	20.50 ^{c}	21.72 ^{c}		
	T2	5.84 ^{c}	6.29 ^{b}	33.56 ^{b}	33.44 ^{b}		
	T3	6.82 ^{b}	6.48 ^{b}	30.61 ^{b}	33.66 ^{b}		
	T4	6.94 ^{b}	7.66 ^{ab}	52.39 ^{a}	55.50 ^{a}		
	T5	7.88 ^{a}	8.38 ^{a}	35.00 ^{b}	37.51 ^{b}		
				F values			
PD		953.41**	460.57**	20.33**	20.23**	268.65**	958.88**
T		96.12**	47.01**	27.51**	25.98**		
PD × T		25.97**	15.95**	2.95*	2.68*		

*Means that do not share a letter are significantly different. *p ≤ 0.05, **p ≤ 0.01
PD1: 70 × 5 cm, PD2: 70 × 20 cm, PD3: 35 × 5 cm

http://www.aloki.hu ● ISSN 1589 1623 (Print) ● ISSN 1785 0037 (Online)
DOI: http://dx.doi.org/10.15666/aeer/1906_42654280

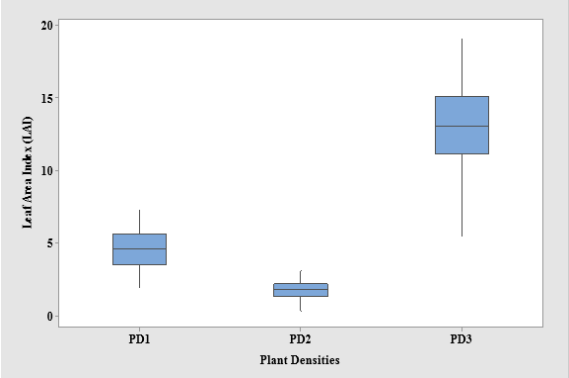

Figure 5. *Leaf area index at different plant densities*

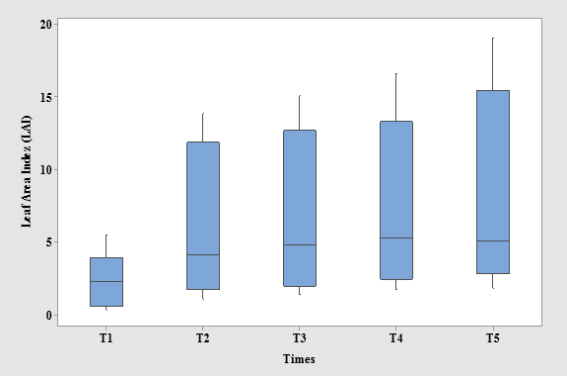

Figure 6. *Leaf area index at different growth times*

Number of leaves (pcs plant^{-1})

The number of leaves (43.10 and 43.50 pcs plant^{-1}) in PD2 treatment was higher in both years compared to the other two plant densities (*Table 5*). Similarly, Khan et al. (2020) stated that the number of leaves per plant is affected by the plant density and the number of leaves decreases with increasing density. In addition, the decrease in the number of plants per m^2 in wide row plantings improved the utilization of competitive environment, nutrients were used better in plant development, and thus more leaves were formed. The number of leaves in 2006 from low to high was ranked as T1 (20.50) < T3 (30.61) < T2 (33.56) < T5 (35.00) < T4 (52.39). In 2007, the number of leaves was ranked as T1 (21.72) < T2 (33.44) < T3 (33.86) < T5 (37.51) < T4 (55.50). The highest number of leaves in both years of the experiment was obtained at T4 (105th day). Although the number of leaves per plant generally increased from T1 to T4 period, decreased at T5 period. This situation can be explained by the slowing of vegetative development due to physiological maturation and senescence of the plant.

Seed cotton yield (kg ha^{-1})

In both years of the experiment, the yield increased with the increase in the number of plants per m^2 (*Table 5*). The yield in PD3, narrow planting, was higher in both years (5759 and 7096 kg ha^{-1}) compared to the yield recorded in other plant density treatments (*Figs. 7-8*).

http://www.aloki.hu ● ISSN 1589 1623 (Print) ● ISSN 1785 0037 (Online)
DOI: http://dx.doi.org/10.15666/aeer/1906_42654280

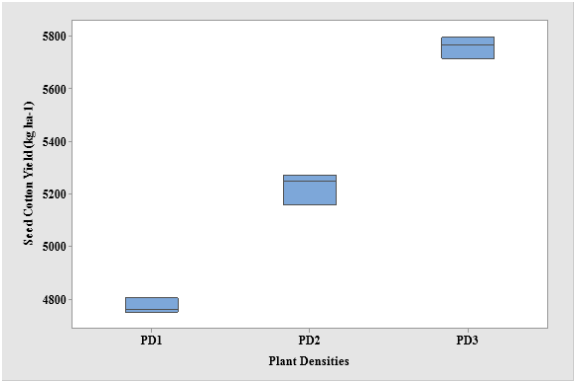

Figure 7. *Seed cotton yield at different plant densities (kg ha^{-1}) (first year)*

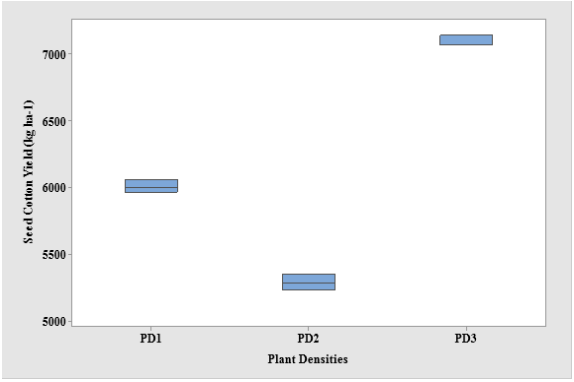

Figure 8. *Seed cotton yield at different plant densities (kg ha^{-1}) (second year)*

The yield per plant was decreased or the total dry matter accumulation per plant was lower in dense plantings, however, the increase in the number of plants per unit area caused an increase in total yield. The increase in the number of plants in a unit area up to a certain number decreased the yield per plant, however total yield increased.

Zhang et al. (2016) reported that the seed cotton yield (5908, 6158 and 6074 kg ha^{-1}) increased with the increase of plant density (12, 18 and 24 plant m^{-2}), which is consistent with our results.

Conclusions

The results indicated that the growth parameters examined were affected by the plant density treatments tested in the experiment. The PD2 treatment (7 plants per m^{-2}) caused higher plant height, number of nodes, stem diameter, flower, leaf, stem and total dry matter weights, while PD3 treatment (57 plants per m^{-2}) yielded higher LAI and yield compared to the other plant density treatments. The decrease in the number of plants per m^{-2} in wide row plantings improved the benefit from the competitive environment and increased the use of light, water and nutrients in plant development. However, the increase in the number of plants per unit area had a positive effect on yield. Excessive plant density can cause plants to receive less light, increase in disease and pest populations, and difficulties in planting and especially harvesting.

http://www.aloki.hu ● ISSN 1589 1623 (Print) ● ISSN 1785 0037 (Online)
DOI: http://dx.doi.org/10.15666/aeer/1906_42654280

Plant density varies from each region to region due to factors such as genetic structure, climate and soil conditions, fertilization, irrigation, cultural practices and harvesting method. Therefore, the most suitable plant density in the regions where cotton is grown should be determined according to the results of the researches

REFERENCES

[1] Afzal, M. N., Tariq, M., Ahmad, M., Mubeen, K., Khan, M. A., Afzal, M. U., Ahmad, S. (2018): Dry matter, lint mass and fiber properties of cotton in response to nitrogen application and planting densities. – Pakistan Journal of Agricultural Research 32(2): 229-240.

[2] Ali, H., Afzal, M. N., Muhammad, D. (2009): Effect of sowing dates and plant spacing on growth and dry matter partitioning in cotton (*Gossypium hirsutum* L.). – Pakistan Journal Botany 41(5): 2145-2155.

[3] Anonymous (2007a). GAP Agricultural Research Institute. – Sanliurfa, Turkey.

[4] Anonymous (2007b). Meteorological Data Obtained from Sanliurfa Meteorological Station. – Sanliurfa, Turkey.

[5] Bange, M. P., Milroy, S. P. (2004): Growth and dry matter partitioning of diverse cotton genotypes. – Field Crops 87: 73-87.

[6] Bednarz, C. W., Bridges, D. C., Brown, S. M. (2000): Analysis of cotton yield stability across population densities. – Agronomy Journal 92: 128-135.

[7] Bednarz, C. W., Nichols, R. L., Brown, S. M. (2006): Plant density modifications of cotton within-boll yield components. – Crop Science 46: 2076-2080.

[8] Beyyavas, V., Yilmaz, A., Haliloglu, H. (2018): The effect of different plant densities and mepiquat chloride application on cotton (*Gossypium hirsutum* L.) yield and yield components in normal sowing time. – Journal of Agricultural Faculty of Mustafa Kemal University 23(2): 262-273.

[9] Birgul, I. H. (2008): Determination of fiber characteristics for different harvesting dates and plant growth parameters in some cotton (*Gossypium hirsutum* L.) varieties. – Harran University Graduate School of Natural and Applied Sciences Department of Field Crops. MSc. Thesis. Sanliurfa, Turkey.

[10] Board, J. E. (2000): Light interception efficiency and light quality effect yield compensation of soybean at low plant populations. – Crop Science 40: 1285-1294.

[11] Calhoun, D. S., Bowman, D. T., May, O. L. (1997): Pedigrees of Upland and Pima Cotton Cultivars Released between 1970 and 1995. – Division of Agriculture, Forestry and Veterinary, Medicine Communications, Mississippi State University. U.S.A.

[12] Carpenter, A. C., Board, J. E. (1997): Growth dynamic factors controlling soybean stability across plant populations. – Crop Science 37(5): 1520-1526.

[13] Celik, I., Onal, I., Cetinkaya, M. (2009): Evaluation of plant growth characteristics of cotton cultivar Çukurova-1518 by plant monitoring techniques in Antalya conditions. – Derim 26(2): 42-56.

[14] Clawson, E. L., Cothren, J. T., Blouin, D. C. (2006): Nitrogen fertilization and yield of cotton in ultra-narrow and conventional row spacings. – Agronomy Journal 98: 72-79.

[15] Dai, j., Li, W., Tang, W., Zhang, D., Li, Z., Lu, H., Eneji, A. E., Dong, H. (2015): Manipulation of dry matter accumulation and partitioning with plant density in relation to yield stability of cotton under intensive management. – Field Crops Research 180: 207-215.

[16] Dong, H. Z., Li, W. J., Tang, W., Li, Z. H., Zhang, D. M. (2006a): Crop/Stress physiology effects of genotypes and plant density on yield, yield components and photosynthesis in BT transgenic cotton. – J. Agron. Crop Sci. 139: 132-139.

http://www.aloki.hu ● ISSN 1589 1623 (Print) ● ISSN 1785 0037 (Online)
DOI: http://dx.doi.org/10.15666/aeer/1906_42654280

[17] Dong, H., Li, W., Tang, W., Li, Z., Zhang, D., Niu, Y. (2006b): Yield, quality and leaf senescence of cotton grown at varying planting dates and plant densities in the Yellow River Valley of China. – Field Crops Research 98: 106-115.
[18] Gwathmey, C. O., Clement, J. D. (2010): Alteration of cotton source–sink relations with plant population density and mepiquat chloride. – Field Crops Research 116: 101-107.
[19] Harem, E. (2010): Cotton Varieties Registered in Turkey. – GAP Agricultural Research Institute. Publication No: 165. Sanliurfa, Turkey.
[20] Hussain, S., Farid, Z. S., Anwar, M., Gill, M. I., Baugh, M. D. (2000): Effect of plant density and nitrogen on the yield of seed cotton variety CIM-443. – Sarhad J. Agri. 16: 143-147.
[21] Jones, M. A., Wells, R., Guthrie, D. S. (1996): Cotton response to seasonal pattern of flower removal: II. Growth and dry matter allocation. – Agronomy Journal 36: 639-645.
[22] Kaggwa-Asiimwe, R., Andrade-Sanchez, P., Wang, G. (2013): Plant architecture influences growth and yield response of upland cotton to population density. – Field Crops Research 145: 52-59.
[23] Kandil, A. A., Badawi, M. A., El-Moursy, S. A., Abdou, U. M. A. (2004): Effect of planting dates, nitrogen levels, and bio-fertilization treatment on 1: Growth attributes of suger beet (*Beta vulgaris* L.). – Scietif. J. King. Faisal Uni. 5(2): 227-237.
[24] Kerby, T. A., Cassman, K. G., Keeley, M. (1990): Genotypes and plant densities for narrow-row cotton systems. II. Leaf area and dry-matter partitioning. – Crop Science 30: 649-653.
[25] Kerby, T. A., Keeley, M., Watson, M. (1993): Variation in Fiber Development as Affect by Source to Sink Relationships. – In: Herber, D. J., Richter, D. A. (eds.) Cotton Physiology Conference. Pron. Beltwide Cotton Conf., New Orleans, LA. 10-14 Jan, 1993. Natl. Cotton Counc., Memphis, TN, pp. 1248-1251.
[26] Khan, A., Wang, L., Ali, S., Tung, S. A., Hafeez, A., Yang, G. (2017): Optimal planting density and sowing date can improve cotton yield by maintaining reproductive organ biomass and enhancing potassium uptake. – Field Crops Research 214: 164-174.
[27] Khan, A., Kong, X., Najeeb, U., Zheng, J., Kean, D., Tan, Y., Akhtar, K., Munsif, F., Zhou, R. (2019): Planting density induced changes in cotton biomass yield, fiber quality, and phosphorus distribution under beta growth model. – Agronomy-Basel 9(9): 1-18.
[28] Khan, N., Han, Y., Xing, F., Feng, L., Wang, Z., Wang, G., Yang, B., Fan, Z., Lei, Y., Xiong, S., Li, X., Li, Y. (2020): Plant density influences reproductive growth, lint yield and boll spatial distribution of cotton. – Agronomy-Basel 10(14): 1-17.
[29] Mao, L., Zhang, L., Evers, J. B., Werf, W., Liu, S., Zhang, S., Wang, B., Li, Z. (2015): Yield components and quality of intercropped cotton in response to mepiquat chloride and plant density. – Field Crops Research 179: 63-71.
[30] Montgomery, D. C. (1997): Design and Analysis of Experiments. 4th Ed. – Wiley, New York.
[31] Rahman, M., Hossain, M. (2011): Plant density effects on growth, yield and yield components of two soybean varieties under equidistant planting arrangement. – Asian Journal of Plant Sciences 10(5): 278-286.
[32] Rahman, M. M., Rahman, M. M., Hossain, M. M. (2013): Effect of Row Spacing and Cultivator on The Growth and Seed Yield of Soybean (*Glycine max* [L.] Merill) in Kharif-II Season. – The Agriculturists 11(1): 33-38.
[33] Reddy, K. R., Reddy, V. R. (1992): Temperature Effects on early season cotton growth and development. – Agronomy Journal 84(2): 229-237.
[34] Ren, X., Zhang, L., Du, M., Evers, J. B., Werf, W., Tian, X., Li, Z. (2013): Managing mepiquat chloride and plant density for optimal yield and quality of cotton. – Field Crops Research 149: 1-10.
[35] Reta-Sánchez, D. G., Flowler., J. L. (2002): Canopy light environment and yield of narrow-row cottons as affected by canopy architecture. – Agronomy Journal 94: 1317-1323.

http://www.aloki.hu ● ISSN 1589 1623 (Print) ● ISSN 1785 0037 (Online)
DOI: http://dx.doi.org/10.15666/aeer/1906_42654280

[36] Saleem, M. F., Bilal, M. F., Awais, M., Shahid, M. Q., Anjum, S. A. (2010): Effect of nitrogen on seed cotton yield and fiber qualities of cotton (*Gossypium hirsutum* L.) cultivars. – J. Anim. Plant Sci. 20(1): 23-27.
[37] Samani, M. R. K., Khajehpour, M. R., Ghavaland, A. (1999): Effects of row spacing and plant density on growth and dry matter accumulation in cotton in Isfahan. – Iranian Journal of Agr. Sci. 29(4): 667-679.
[38] Siebert, J. D., Stewart, A. M., Leonard, B. R. (2006): Comparative growth and yield of cotton planted at various densities and configurations. – Agronomy Journal 98: 562-568.
[39] Silvertooth, J. C., Edmisten, K. L., McCarty, W. H. (1999): Production Practices. – In: Smith, C. W. (ed.) Cotton: Origin, History, Technology, and Production. John Wiley and Sons, Inc. New York, pp. 463-465.
[40] Tariq, M., Afzal, M. N., Muhammad, D., Ahmad, S., Shahzad, A. N., Kiran, A., Wakeel, A. (2018): Relationship of tissue potassium content with yield and fiber quality components of Bt cotton as influenced by potassium application methods. – Field Crops Research 229: 37-43.
[41] Wang, Q., Han, S., Zhang, L., Zhang, D., Werf, W. V. D., Evers, J. B., Sun, H., Su, Z., Zhang, S. (2016): Density responses and spatial distribution of cotton yield and yield components in jujube (*Zizyphus jujube*)/cotton (*Gossypium hirsutum*) agroforestry. – Europ. J. Agronomy 79: 58-65.
[42] Wells, R., Meredith, W. R. Jr. (1984): Comparative growth of obsolete and modern cotton cultivars: II. Reproductive dry matter partitioning. – Crop Science 24: 863-868.
[43] Wells, R., Meredith, W. R. (1986): Normal vs. okra leaf yield interactions in cotton. – Crop Science 26: 223-232.
[44] Wullschleger, S. D., Oosterhuis, D. M. (1992): Canopy leaf area development and age-class dynamic in cotton. – Crop Science 3(2): 451-456.
[45] Yang, G. Z., Luo, X. J., Nie, Y. C., Zhang, X. L. (2014): Effects of plant density on yield and canopy micro environment in hybrid cotton. – Journal of Integrative Agriculture 13: 2154-2163.
[46] Yao, H., Zhang, Y., Yi, X., Zuo, W., Lei, Z., Sui, L., Zhang, W. (2017): Characters in light-response curves of canopy photosynthetic use efficiency of light and N in responses to plant density in field-grown cotton. – Field Crops Research 203: 192-200.
[47] Zhang, R. Z., Tian, L., Zheng, J. L. (1962): LAI and high-yield properties on soybean. – J. Northeast Agric. Coll. 3: 1-7.
[48] Zhang, D., Luo, Z., Liu, S., Li, W., Tang, W., Dong, H. (2016): Effects of deficit irrigation and plant density on the growth, yield and fiber quality of irrigated cotton. – Field Crops Research 197: 1-9.
[49] Zhi, X. Y., Han, Y. C., Li, Y. B., Wang, G. P., Du, W. L., Li, X. X., Mao, S. C., Lu, F. (2016): Effects of plant density on cotton yield components and quality. – J. Integr. Agric. 15: 1469-1479.

http://www.aloki.hu ● ISSN 1589 1623 (Print) ● ISSN 1785 0037 (Online)
DOI: http://dx.doi.org/10.15666/aeer/1906_42654280

PROSPECTS FOR DIATOMS IDENTIFICATION USING METAGENOMICS: A REVIEW

ALINDONOSI, A. R.[1*] – BAESHEN, M. N.[1] – ELSHARAWY, N. T.[1,2]

[1]*Department of Biology, College of Science, University of Jeddah, Jeddah 21598, Saudi Arabia*

[2]*Departement of Food Hygiene, Faculty of Veterinary Medicine, New Valley University, Egypt*

[*]*Corresponding author*
e-mail: aalindonosi.stu@uj.edu.sa

(Received 26th May 2021; accepted 3rd Sep 2021)

Abstract. The marine environment is the largest ecosystem, richest in biodiversity and biological activity. Diatoms are almost omnipresent and common in the plankton and benthos in both freshwater and marine environments. They have a major influence on their environment whereas representing a significant part in primary production and carbon fixation in marine ecosystems. Microscopic examination and cell culture technique have been applied to detect, isolate and study the diatom species. On the other hand, molecular methods have contributed to overcome the drawbacks of the classical methods and also to accomplish the research objectives more efficiently. Metagenomics is an advanced molecular method utilizing direct collected microbial samples and has been used in various fields of microbial studies. It provides obvious details on the taxonomy, biodiversity, ecology and further information around the potential functions. Consequently, it can explore the biochemical components that have significant importance in various biotechnology, ecology, biomedicine and industry applications. This review focused on the effectiveness of the metagenomics method for exploring microbial communities and recruiting this to discover the diatom community.
Keywords: *microbial communities, genomic, sea water, molecular technique, gene markers*

Introduction

Diatoms are silicified, ubiquitous and highly abundant microalgae that are rich in minerals, metabolites and various biochemical compounds. These compounds have significant roles in various fields such as industry, pharmaceutics, biotechnology, and biodegradation (Vanelslander et al., 2009). Some species are used in the biomonitoring of ecological assessment as a response to the environmental fluctuations and changes in water habitats (Poikane et al., 2016). Diatoms have been described and characterized traditionally based on morphological characteristics (Falasco et al., 2009), by microscopic examination which does not require cultivation in a laboratory. Furthermore, valuable biochemical components of diatoms have been detected through growing, isolating and studying characteristics of the species after being cultivated under laboratory conditions (Araújo and Garcia, 2005). Despite the long history of the study of diatom diversity and the numerous researches about its importance, knowledge on the diversity of diatoms and their potential applications still limited. Consequently, the ecological conditions and various interactions related to them continue to be misleading.

In the 1980s, molecular techniques were applied to diatom studies for the first time (Medlin et al., 1988). Molecular phylogenetic researches have been widely performed to overcome morphological limitations to identify and classify diatoms (Evans et al., 2007; Jahn et al., 2007; Mann et al., 2010; Moniz and Kaczmarska, 2010). Powered by advances in the technology of next-generation sequencing, metagenomics has the possibility to explore the taxonomic and functional diversity of the microbes sampled from a certain

http://www.aloki.hu ● ISSN 1589 1623 (Print) ● ISSN1785 0037 (Online)
DOI: http://dx.doi.org/10.15666/aeer/1906_42814298

natural environment. Moreover, metagenomic analysis aims to determine the genome sequences of uncultivable and rare microbes, for describing microbial ecosystems and for discovering the novel genes and gene products (Wrighton et al., 2012; Yatsunenko et al., 2012; Albertsen et al., 2013).

This review shows the traditional methods used in diatom community studies and obstacles that hindered the advancement of diatoms' researches and applications. In addition, it illustrates the metagenomic approach as an alternative method to diatoms discovery and discusses the potential capabilities and applications.

General information of diatoms

Diatoms (Bacillariophyta) represent one of the most common and high diversity group of microalgae and have an important role in the food web and ecosystems (Mann, 1999). They are photosynthetic, microscopic, unicellular and eukaryotic microalgae (McLaughlin, 2012). There are more than 200,000 species of diatoms reported worldwide (Mann and Droop, 1996), but only about 12.000 species have been defined (Guiry, 2012).

Diatoms are almost omnipresent, they exist wherever water is present, in water bodies and terrestrial ecosystems as well as in aerosols (Jahn et al., 2007). They occur in terrestrial environments such as mosses, wet rocks and soils (Falasco et al., 2014; Tofilovska et al., 2014). Most of diatoms are common in the plankton and benthos in all aquatic habitats including freshwater and marine (Smol and Stoermer, 2010), except the warmest and most hypersaline environments (Round et al., 1990). Benthic diatoms are found in large quantities on the surface of intertidal sediments that are covered with water at high tide and exposed to the atmosphere within low tide status (Admiraal, 1984; Round et al., 1990; Haubois et al., 2005). Their dominant and diversity in the tidal flats contribute to the maintenance of the functional ecosystems such as primary production, algal biomass, nutrient cycling and sediment stabilization (Admiraal, 1984; Sullivan and Moncreiff, 1988; Underwood and Kromkamp, 1999).

The wide distribution of diatoms makes them fitting tools for a variety of applications both, as living and fossils organisms (Atazadeh and Sharifi, 2010). Marine diatoms contribute to around 40% of the total primary production in marine ecosystems and 20% of global carbon fixation. They feed the food chains of aquacultures with sufficient levels of amino acids and vitamins (Brown, 1991). Moreover, diatoms contain a high abundance of diverse biochemical compounds that make them important sources for applications in various fields (Caldwell, 2009; Falkowski et al., 1998). Some strains have been selected as the best candidates for biofuel production (D'Ippolito et al., 2015). Biochemical compounds are also used in other applications such as in therapeutic (e.g. anticancer and anti-tuberculosis) (Lauritano et al., 2018; Hussein and Abdullah, 2020), for foods, food supplements and nutrition industries (Chauton et al., 2015). In addition, they can be applied for biomineralization, biomaterials synthesis, degradation of wastes, and nanotechnology (Dolatabadi and de la Guardia, 2011; Jamali et al., 2012). Besides, diatoms play role in forensic science as one of independent techniques used to diagnose a cause of death by drowning (Levkov et al., 2017). Some species, especially benthic diatoms, are highly sensitive to changes in the condition of the environment. Therefore, they are used as bio-indicators for the ecological assessment of water habitats around the globe (Stevenson and Smol, 2015; Poikane et al., 2016).

http://www.aloki.hu ● ISSN 1589 1623 (Print) ● ISSN1785 0037 (Online)
DOI: http://dx.doi.org/10.15666/aeer/1906_42814298

Traditional methods applied for studying diatoms

Many of the studies depended on the traditional methods to determine taxonomic information, cellular composition and the functional roles of diatoms. Despite the long history of the study of diatom diversity and the numerous studies about its importance, the information on the diversity of benthic diatoms still limited.

Microscopy examination

Morphological taxonomic identification is the traditional methodology for determining the diatoms used to date. This method is performed by microscopic inspection of the outline and details of the silicified frustule or valve (Shape, Raphe, Puncta and Cingula), and the examination slid is prepared according to the condition of the study sample (McLaughlin, 2012). The morphological method is distinguished by its ability to examine the sample directly without the need for culture, and to identify a large majority of the taxa and lower taxonomic levels, until genus and species, shown in (*Fig. 1A*) (Falasco et al., 2009; Rivera et al., 2018).

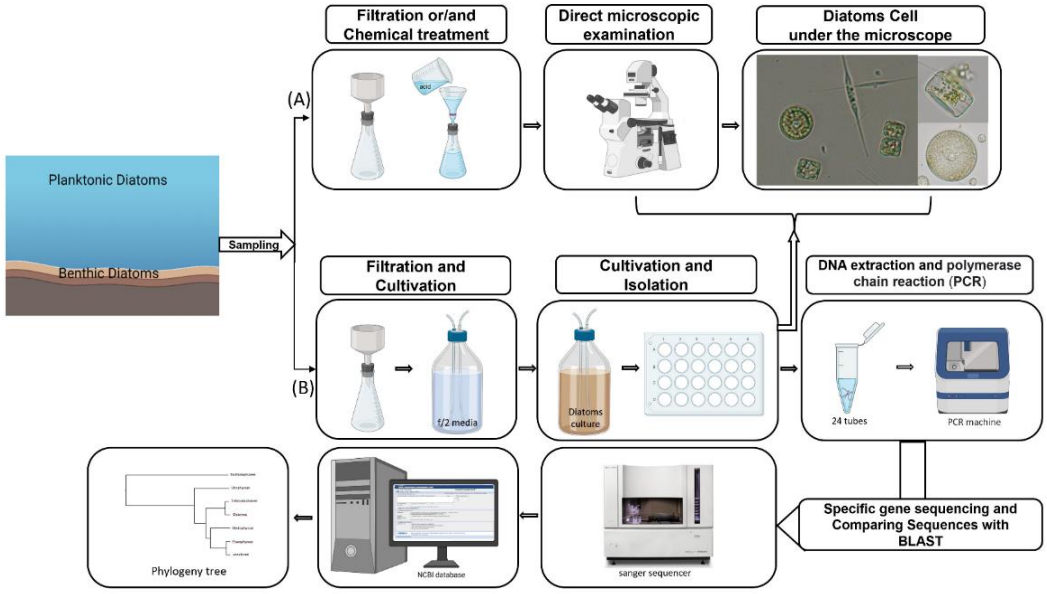

Figure 1. *Illustration of the steps of the traditional method for studying diatom species; (A) Microscopic examination, (B) Cultivation and Sanger sequencing*

However, the morphological method is an impediment for continuous studies for several reasons: 1) depends on the simple forms and small size of benthic diatoms. Also, challenges arise when differentiating between morphologically near species, 2) it needs an extensive experience, 3) requires a great deal of time and effort (Sullivan and Currin, 2002; Brotas and Plante-Cuny, 2003; Underwood and Barnett, 2006; Kahlert et al., 2012). In addition, before applying morphological analysis, some samples need to be treated with acidic treatment, because these samples contain a lot of sediment particles and organic material. As a result, this processing removes all organic material and makes it impossible to know whether the frustules of diatoms are dead or alive (Baldi et al., 2011).

http://www.aloki.hu ● ISSN 1589 1623 (Print) ● ISSN1785 0037 (Online)
DOI: http://dx.doi.org/10.15666/aeer/1906_42814298

Cell culture technique

Diatom cells can be used for numerous applications of biotechnology such as using silicon originated from frustules in aquaculture, using of intracellular and extracellular metabolites extracted from the cells in cosmetic, industrial and pharmaceutical applications (Lebeau and Robert, 2002). Given the importance of diatoms, species cultivation is the reliable method for growing, isolating and studying the characteristics of the species and its valuable components. This method is based on preparing an artificial environment in the laboratory, with suitable ingredients for culturing diatoms (*Fig. 1B*). In addition, the procedure for the culture involves other aspects such as maintenance of the culture in the laboratory scale, as well as control the quantity and quality of products throughout careful control of environmental factors and conditions, such as temperature, aeration, availability of nutrient, pH and light intensity, and their constant supply to the aqua farmers in different phases of growth (Lebeau and Robert, 2003; Perumal et al., 2015). Cell culture technique may be able to grow individual species that have not been well defined, to isolate those important for biotechnology or to increase cells number for species to be studied (Nanjappa et al., 2013).

Although culturing diatoms has many advantages, there are many drawbacks that make it a tedious and costly process, such as 1) imbalance of any component of the media leads to the limitation of diatom growth, 2) it requires certain light intensity and photoperiod, 3) it causes overproduction of the beneficial products with a decrease in biomass production as a consequence of metabolic stress conditions, 4) some species may not grow in the presence of others or they may appear transparent (Sullivan and Currin, 2002; Lebeau and Robert, 2003; Kahlert et al., 2012; D'Ippolito et al., 2015). In addition, microalgae are generally challenging in axenic culture without any contamination (Ashokkumar et al., 2015).

Microscopy examination and cell culture technique are the conventional approaches that have been used extensively in the taxonomy and biotechnology. Nevertheless, there were many studies needed more examinations, such as chemical, physical and biochemical tests and statistical analysis, to complete the results of the study. Despite that, these methods are still used up to date.

Molecular approaches

To identify and characterize the taxonomy of cultured and uncultured diatoms, there is a need for molecular methods that are more effective, more accurate, rapid and highly specific for the detection of diatom species, as an alternative method to microscopic examination (Siaut et al., 2007; Nguyen et al., 2011). Such morphologically similar species are not necessarily similar in their genetic content, therefore these methods provide precise identification at the species level. Accordingly, protein expression is different within species. Sanger sequencing is one of these approaches based on PCR sequencing of a specific gene, where it can accurately read an average length of 800 base pairs. These methods rely on the extraction, storage, amplification and sequencing of DNA from environmental samples (*Fig. 1B*) (Lear et al., 2018). Therefore, using the Sanger sequencing method is suitable for individual gene sequencing from a pure culture containing a single strain. In addition, this method can be run for 96 individual specimens at one time (Kim et al., 2014). Sanger sequencing has been used to study the diversity of microalgal communities but in low-diversity environments (Aliaga Goltsman et al., 2009; Bates et al., 2012; Park et al., 2015). Although this technique is in use, yet it does not fit

http://www.aloki.hu ● ISSN 1589 1623 (Print) ● ISSN1785 0037 (Online)
DOI: http://dx.doi.org/10.15666/aeer/1906_42814298

large-scale experiments and the complex microbial communities study. As such, sequencing technologies were developed to coincide with the modern studies that have focused on microbiota and microbiome (Turnbaugh et al., 2007; Thursby and Juge, 2017; Song et al., 2018). Furthermore, metagenomics is a powerful molecular approach used for the comprehensive analysis of microbial community which replaces a series of traditional studies.

Metagenomics

Metagenomic analysis is an advanced molecular method that offers comprehensive portraits of microbial communities isolated directly from their environment (Dutilh, 2014; Kumar Awasthi et al., 2020). It provides more significant data and a deep insight into the taxonomic composition and diversity, functional genes, novel genes exploration, the structure and organization of genomes, metabolic products and biocatalysts, which were difficult to find through classical laboratory methods as the conditions were optimized for those finding which missed a lot of important aspects to human needs and knowledge (Tringe et al., 2005; Felczykowska et al., 2015; Roumpeka et al., 2017). Metagenomics is primarily a microbial community science, with a primary emphasis on describing and predicting the interactions between different populations of microbes and the interaction between species or among species (Marx, 2013).

Nevertheless, metagenomics is a culture-independent analysis of the genomic content of entire microbiome into their structure and function in a given environment (Handelsman et al., 1998). It depends on two procedures which are next-generation sequencing (NGS) and bioinformatics (*Fig. 2*). NGS provides millions to billions of nucleotide short reads in massively parallel analysis and high-throughput with low cost (Metzker, 2010; Mardis, 2011). These sequencing outputs are digital and hence enable direct quantitative comparisons through bioinformatics tools (Kulski, 2015; Jünemann et al., 2017). Therefore, this combination produces huge data obtained from environmental DNA and processes it to provide an obvious perception of their biosynthesis.

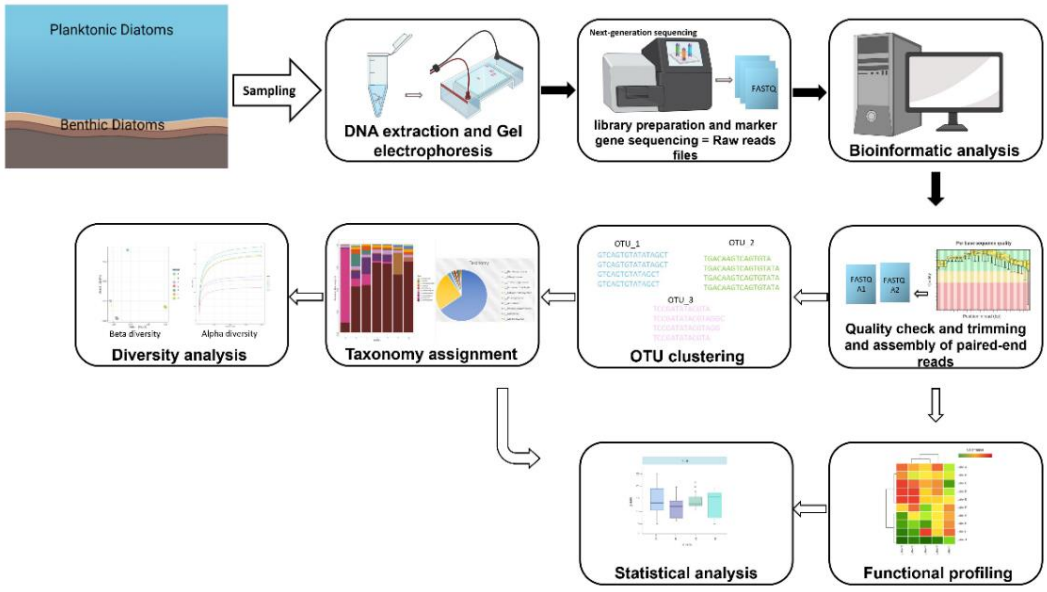

Figure 2. *Schematic illustrates the amplicon metagenomics workflow for studying diatom community*

http://www.aloki.hu ● ISSN 1589 1623 (Print) ● ISSN1785 0037 (Online)
DOI: http://dx.doi.org/10.15666/aeer/1906_42814298

Marine microbial metagenomics

Communities of microorganisms- archaea, bacteria, viruses, phages, fungi, microalgae and other eukaryotic microorganisms- are an integral part of, and play important roles in, various ecosystems. The marine environment is the largest ecosystem, richest with biodiversity and biological activity (Zhao, 2011; Felczykowska et al., 2012). The microbial community was estimated in the oceans which host about 3.6 $x10^{29}$ microbial cells. While soil represents the most diverse environment contained 2.6 x 10^{29} cells of the bacterial community (Torsvik and Øvreås, 2002; Sogin et al., 2006). As for the human level, the intestine is the most densely part of the microbial community in the human body, where bacterial counts reaching $10^{12\text{-}14}$ cells (Prescot et al., 1999; Tremaroli and Bäckhed, 2012; De Mandal et al., 2014). Although of the numerous studies on microbes and their ecological importance, the marine microbial community is still not completely exploited yet. The main reason for not characterizing these microbes is the difficulties in detecting under microscopy and in reproducing or culturing microbes by classical techniques under laboratory conditions (Epstein, 2013).

Nowadays, metagenomics can be considered an advance technology to investigate genetic information of marine microbiome (Barone et al., 2014). The taxonomy of metagenomics aims to detect the exact species of microbes and to classify the data of various microbial groups through the analysis of specific genes that reside in a given environment (Kumar Awasthi et al., 2020). Metagenomics can recognize the microbial genes that carry out specific functions and can detect the ecological factors that shape the microbial diversity of community structures (Delmont et al., 2011). Moreover, it contributes to found microbial fingerprints of diverse environments (Behzad et al., 2016). Using metagenomics term was began when Handelsman and colleagues extracted the collection of microbial DNA from soil samples (Handelsman et al., 1998). For 20 years, metagenomics has been used to explore microbial communities in soil, marine water, activated sludge, animal waste and, human and animal guts (Poroyko et al., 2010; Beale et al., 2018; Cabral et al., 2018; Cai et al., 2018; Lekunberri et al., 2018; Yang et al., 2018). For example, Hess et al. (2011) applied high-throughput sequencing to analyze the samples from the rumen of fistulated cows samples in an extended metagenomic study. They discovered more than 2.5 million novel genes and the nearly entire genomes of 15 microorganisms that had never cultured in the laboratory. They also recorded exceeding 27,000 putative carbohydrate-active enzymes with cellulolytic function (Hess et al., 2011). Besides, metagenomic studies provide significant visualization into previously unidentified terrestrial and marine microorganisms (Daniel, 2005; Simon and Daniel, 2011).

High-throughput sequencing

Metagenomics depend on NGS which works on the principle of high-throughput sequencing (HTS) that was successfully implemented in the microbial community environment, where it becomes essential in studies on genomics, epigenomics and transcriptomics (Sogin et al., 2006). There are two major methods based on high-throughput sequencing for studying the microbiome: whole-genome-shotgun (WGS) and marker-gene (amplicon) metagenomics. WGS is sequencing complete genomes of all microorganisms in a certain environment at a single time. In contrast, the sequencing-based on marker gene targets a specific region of gene for microbial community existent in an ecological sample (*Fig. 2*) (Pérez- et al., 2020). Both approaches are suitable option

http://www.aloki.hu ● ISSN 1589 1623 (Print) ● ISSN1785 0037 (Online)
DOI: http://dx.doi.org/10.15666/aeer/1906_42814298

applicable in different conditions according to the target study. Nevertheless, marker gene analysis is useful for long- term projects or studies due to the fact that it consumes mostly short time, because of their low cost, and the simplicity and easiness of analyzing results for large numbers of samples, compared to WGS (Knight et al., 2018).

Generally, high- throughput sequencing involves PCR amplification of a marker gene using primers designed according to the marker. All genetic markers are conserved genes including one or more hypervariable regions, which can be used to discriminate different or closely related lineages. The ideal marker (1) composed of a short sequence which amplified and sequenced easily during one read following a standardised laboratory technique, (2) the global primers is flanked by the conserved region, and (3) it has the ability which resolving the different organism's species (Stoeckle, 2003; Hebert et al., 2003; Moritz and Cicero, 2004). Various gene regions have been used as markers for different microorganisms. The mitochondrial cytochrome oxidase I gene (cox1 or COI) has been used for the analysis of eukaryotes communities (Seifert et al., 2007; Stern et al., 2010). The widest marker that contributes to studying microbial diversity and community structures is nuclear-encoded small subunit ribosomal RNA genes (SSU-rRNA). This marker includes the 16S rRNA gene (16S rDNA) and the 18S rRNA gene (18S rDNA) that has been used extensively to examine prokaryotic and eukaryotic diversity, respectively (Janda and Abbott, 2007; Zhan et al., 2013; Hugerth et al., 2014; Saghaï et al., 2015; Groendahl et al., 2017; Yergeau et al., 2017; Winand et al., 2019). Furthermore, another nuclear marker is the internal transcribed spacer region (ITS), which is a common one in the fungal community study (Tedersoo et al., 2010; Schoch et al., 2012; Kemler et al., 2013; Nilsson et al., 2013), and already been used as a marker in some protists (Stern et al., 2010; Molins et al., 2018). To study photosynthetic microorganisms, microalgae, the chloroplast gene encoding, ribulose-1,5-bisphosphate carboxylase large-subunit (rbcL) is utilized as a molecular marker (Patel et al., 2018; Pujari et al., 2019).

Marker genes of diatoms

For diatom communities, the 18S rRNA gene, COI, ITS and rbcL already have shown potential for use as marker (Moniz and Kaczmarska, 2009). Nevertheless, two markers of them are more useful to analysis diatom communities, 18S rRNA gene and rbcL gene, because they are less heterogeneous between individuals when distinguishing between species (Mann et al., 2010; Zimmermann et al., 2011). The highly conserved region, 18S rRNA gene, uses for deep phylogenetic analyses and biodiversity screening. It contains nine highly variable regions; V1 to V9, but V4 and V9 regions are the best candidates (Stoeck et al., 2010; Pawlowski et al., 2012; Zimmermann et al., 2015). Both of them are the most variable regions of the 18S rRNA gene, however, the V4 region is strongly approximated to the variability of the entire 18S gene (Dunthorn et al., 2012). The V4 represents the largest and most complex of the highly variable regions within the 18S locus, while its length ranges 390–410 bp long fragment of the 1800 bp long 18S rRNA gene (Nelles et al., 1984; Nickrent and Sargent, 1991). The efficiency of using the V4 region in environmental studies is due to its ease of amplification with the universal primers and its ability identification to the species level. The 18S rRNA gene is distinguished by its high representation in databases and more extensive compared with other genetic markers (Zimmermann et al., 2011).

On the other side, rbcL marker also demonstrated the ability to distinguish among diatom taxa and study of the phylogenetic (Trobajo et al., 2010; MacGillivary and

http://www.aloki.hu ● ISSN 1589 1623 (Print) ● ISSN1785 0037 (Online)
DOI: http://dx.doi.org/10.15666/aeer/1906_42814298

Kaczmarska, 2011; Rimet et al., 2018; An et al., 2018). Use the rbcL gene as a genetic marker is recommend due to its ease of amplification and alignment, and low susceptibility to contamination by heterotrophic pollutants (Evans et al., 2007; MacGillivary and Kaczmarska, 2011). Furthermore, it affords better resolution recognition of diatom species than 18S rRNA, in addition to it lacks long branch artefacts among its phylogeny and not influenced by sequencing errors (Beszteri et al., 2001; Lenaïg Kermarrec et al., 2013; An et al., 2017). Despite of it is appropriate as a marker for the study of taxonomy and phylogenetic analyses of benthic diatoms, it is more conserved than the 18S rRNA gene and failed to cluster the entire diatoms assemblage (Guo et al., 2015; An et al., 2017).

Metagenomics- next-generation sequencing applied in diatoms study

Next-generation sequencing (NGS) is the most effective technique to analyze diatom community structures and functions, where render it possible in a short time, less effort and minimal cost (Visco et al., 2015). It enables the rapid and accurate classification of benthic diatom and contributes extremely to study the biodiversity. It can also reveal hidden and small cells that cannot appear under the microscope (Zhan et al., 2013). NGS includes various platformers and three of them were commoly applied in diatom studies, Roche 454 System, Ion torrent and Illumina sequencer.

The 454 pyrosequencing was applied to study microbial communities in various environments for different purposes (Tedersoo et al., 2010; Cheval et al., 2011; Mayo et al., 2014; Groendahl et al., 2017). It was a convenient tool for the taxonomic characterization of diatom communities and within the context of biomonitoring (Zimmermann et al., 2011; Kermarrec et al., 2013; Lenaïg Kermarrec et al., 2014; Nanjappa et al., 2014; Piredda et al., 2018). Ion Torrent Personal Genome Machine (PGM) has been used for structure and function analyses of fungal, bacterial and archaeal communities (Whiteley et al., 2012; Kemler et al., 2013; Groendahl et al., 2017). Most diatoms studies that applied HTS by Ion Torrent machine, targeted rbcL gene, compared the ability of the molecular approach to assess the composition of diatom community, quality indices (the Specific Pollution sensitivity Index (SPI)) score and ecological status, to the ones generated by the morphology-based method (Rivera et al., 2017; Rivera et al., 2018; Bailet et al., 2019). The third platform which used for studying diatom was Illumina platform, it which has been used combined with the rbcL in most studies to explore the structure and diversity of diatom community with estimating the environmental condition and the effect of spatial and temporal changes on diversity and distribution of communities (Rimet et al., 2019; Tapolczai et al., 2019). Recently, most studies are targeted to describe benthic diatoms communities by using Illumina sequencer with rbcL or 18S rRNA gene (An et al., 2018, 2020; Mora et al., 2019; Bailet et al., 2020; Huang et al., 2020; Stoof-Leichsenring et al., 2020).

Metagenomics applications

Identification of microbial communities is followed by detecting their functional genes and metabolic activities, therefore, leading to employment of microbes to useful various applications. Metagenomics is an effective tool to achieve that and reveal the secrets of countless microbial communities. The metagenomic approach has the potential to improve knowledge in various fields, such as biomedicine, Agriculture, pharmaceutical, industrial and ecological applications (*Fig. 3*).

http://www.aloki.hu ● ISSN 1589 1623 (Print) ● ISSN1785 0037 (Online)
DOI: http://dx.doi.org/10.15666/aeer/1906_42814298

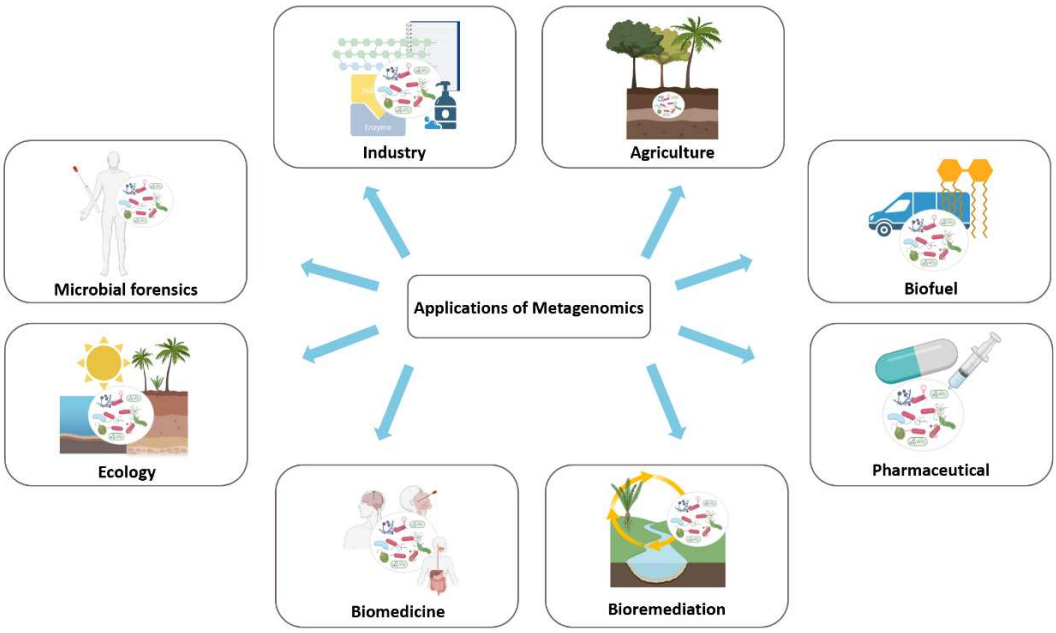

Figure 3. *The various fields of metagenomic applications*

In biomedical sciences, metagenomics has been used to develop strategies of novel diagnostic and treatment after describing the human microbiome role in healthy and patient individuals and also in populations. Zhao et al. (2021) presented a description of the relationship between the gut microbiome of patients with lung cancer and the clinical outcomes of chemotherapy based on the metagenomic analysis. Although most of the natural and bioactive compounds of marine microbes remain unknown to date, metagenomics was able to identify microbial communities, that have diverse biosynthetic capacities, and then the uncovering some distinct biocatalysts that were used in biotechnological applications (Turnbaugh and Gordon, 2008; Jeon et al., 2009; Coughlan et al., 2015). It was also utilized for explorating enzymes from nature to be taken advantage of in industrial applications, such as cellulase, lipase and protease (Lopez-Lopez et al., 2014; Schröder et al., 2014; Pessoa et al., 2017). Furthermore, metagenomics has been used in marine biomonitoring field through study the microbial community during an intense dinoflagellate bloom (Nowinski et al., 2019). Using the metagenomic method in agriculture applications helped in monitoring the ecological status and the early detection of problems affecting the microbial population in agricultural environments (Goss-Souza et al., 2019). In addition to these applications, there is a wide spectrum of research areas that have utilized metagenomics.

Accordingly, it is expected that diatom applications based on metagenomics will discover completely unknown components, functions and characteristics for various diatom species, as well as detailed information on previously studied functions with other methods.

Conclusion

Marine ecosystems tend to be rich in bioactive compounds produced by various marine microorganisms. Diatoms are one of the most common and more active microorganisms

http://www.aloki.hu ● ISSN 1589 1623 (Print) ● ISSN1785 0037 (Online)
DOI: http://dx.doi.org/10.15666/aeer/1906_42814298

found in the seawater. They have, however, received insufficient attention due to used classical methods limitations. The advancement of molecular methods and their effectiveness for detecting microbial communities contributed to improve the output of microbial studies. Since the majority of marine microbes are not cultivable, the metagenomic method holds great promise for discovering their communities and novel applicable compounds of significant biological activities. It is expected that metagenomics will be used increasingly in the future to detect previously unknown diatom communities and to broaden the scope of diatom applications. Nevertheless, even with substantial advances in the development of molecular tools used for the assessments and monitoring of microbial diversity, the morphological approach remains critical in the eco-genomic era in species identification and detection. Finally, further research in metagenomics field is expected to provide new fascinating discoveries and exciting findings.

Acknowledgements. This work was financed by the corresponding author only and was not carried out within any framework of the project. The authors declared that the present study was performed in absence of any conflict of interest. This summary statement will be ultimately published as the article is accepted.

REFERENCES

[1] Admiraal, W. (1984): The ecology of estuarine sediment-inhabiting diatoms. – Progress in Phycological Research 3: 269-322.

[2] Albertsen, M., Hugenholtz, P., Skarshewski, A., Nielsen, K. I., Tyson, G. W., Nielsen, P. H. (2013): Genome sequences of rare, uncultured bacteria obtained by differential coverage binning of multiple metagenomes. – Nature Biotechnology 31: 533-538.

[3] Aliaga Goltsman, D. S., Denef, V. J., Singer, S. W., VerBerkmoes, N. C., Lefsrud, M., Mueller, R. S., Dick, G. J., Sun, C. I., Wheeler, K. E., Zemla, A., Baker, B. J., Hauser, L., Land, M., Shah, M. B., Thelen, M. P., Hettich, R. I., Banfield, J. F. (2009): Community genomic and proteomic analyses of chemoautotrophic iron-oxidizing "Leptospirillum rubarum" (Group II) and "Leptospirillum ferrodiazotrophum" (Group III) bacteria in acid mine drainage biofilms. – Applied and Environmental Microbiology 75(13): 4599-4615.

[4] An, S. M., Choi, D. H., Lee, J. H., Lee, H., Noh, J. H. (2017): Identification of benthic diatoms isolated from the eastern tidal flats of the Yellow Sea: Comparison between morphological and molecular approaches. – PLoS ONE 12(6): e0179422.

[5] An, S. M., Choi, D. H., Lee, H., Lee, J. H., Noh, J. H. (2018): Next-generation sequencing reveals the diversity of benthic diatoms in tidal flats. – Algae 33(2): 167-180.

[6] An, S. M., Choi, D. H., Noh, J. H. (2020): High-throughput sequencing analysis reveals dynamic seasonal succession of diatom assemblages in a temperate tidal flat. – Estuarine, Coastal and Shelf Science 237: 106686.

[7] Araújo, S. D. C., Garcia, V. M. T. (2005): Growth and biochemical composition of the diatom Chaetoceros cf. wighamii brightwell under different temperature, salinity and carbon dioxide levels. I. Protein, carbohydrates and lipids. – Aquaculture 246: 405-412.

[8] Ashokkumar, S., Manimaran, K., Kim, K. (2015): Cultivation and Identification of Microalgae (Diatom). – In: Kim, S. K., Chojnacka, K. (eds.) Marine Algae Extracts: Processes, Products, and Applications. John Wiley & Sons 2: 59-78.

[9] Atazadeh, I., Sharifi, M. (2010): Algae as bioindicators. – Lambert Academic Publishing House.

[10] Bailet, B., Bouchez, A., Franc, A., Frigerio, J-M., Keck, F., Karjalainen, S-M., Rimet, F., Schneider, S., Kahlert, M. (2019): Molecular versus morphological data for benthic

http://www.aloki.hu ● ISSN 1589 1623 (Print) ● ISSN1785 0037 (Online)
DOI: http://dx.doi.org/10.15666/aeer/1906_42814298

diatoms biomonitoring in Northern Europe freshwater and consequences for ecological status. – Metabarcoding and Metagenomics 3: 21-35.

[11] Bailet, B., Apothéloz-Perret-Gentil, L., Baričević, A., Chonova, T., Franc, A., Frigerio, J-M., Kelly, M., Mora, D., Pfannkuchen, M., Proft, S., Ramon, M., Vasselon, V., Zimmermann, J., Kahlert, M. (2020): Diatom DNA metabarcoding for ecological assessment: Comparison among bioinformatics pipelines used in six European countries reveals the need for standardization. – Science of the Total Environment 745: 140948.

[12] Baldi, F., Facca, C., Marchetto, D., Nguyen, T. N. M., Spurio, R. (2011): Diatom quantification and their distribution with salinity brines in coastal sediments of Terra Nova Bay (Antarctica). – Marine Environmental Research 71: 304-311.

[13] Barone, R., De Santi, C., Esposito, F. P., Tedesco, P., Galati, F., Visone, M., Di Scala, A., De Pascale, D. (2014): Marine metagenomics, a valuable tool for enzymes and bioactive compounds discovery. – Frontiers in Marine Science 1: 38.

[14] Bates, S. T., Berg-Lyons, D., Lauber, C. L., Walters, W. A., Knight, R., Fierer, N. (2012): A preliminary survey of lichen associated eukaryotes using pyrosequencing. – Lichenologist 44: 137-146.

[15] Beale, D. J., Crosswell, J., Karpe, A. V., Metcalfe, S. S., Morrison, P. D., Staley, C., Ahmed, W., Sadowsky, M. J., Palombo, E. A., Steven, A. D. L. (2018): Seasonal metabolic analysis of marine sediments collected from Moreton Bay in South East Queensland, Australia, using a multi-omics-based approach. – Science of the Total Environment 631-632: 1328-1341.

[16] Behzad, H., Ibarra, M. A., Mineta, K., Gojobori, T. (2016): Metagenomic studies of the Red Sea. – Gene 576: 717-723.

[17] Beszteri, B., Ács, É., Makk, J., Kovács, G., Márialigeti, K., Kiss, K. T. (2001): Phylogeny of six naviculoid diatoms based on 18S rDNA sequences. – International Journal of Systematic and Evolutionary Microbiology 51(4): 1581-1586.

[18] Brotas, V., Plante-Cuny, M. R. (2003): The use of HPLC pigment analysis to study microphytobenthos communities. – Acta Oecologica 24: S109-S115.

[19] Brown, M. R. (1991): The amino-acid and sugar composition of 16 species of microalgae used in mariculture. – Journal of Experimental Marine Biology and Ecology 145: 79-99.

[20] Cabral, L., Pereira de Sousa, S. T., Lacerda Junior, G. V., Hawley, E., Andreote, F. D., Hess, M., de Oliveira, V. M. (2018): Microbial functional responses to long-term anthropogenic impact in mangrove soils. – Ecotoxicology and Environmental Safety 160: 231-239.

[21] Cai, L., Chen, T.-B., Zheng, S.-W., Liu, H.-T., Zheng, G.-D. (2018): Decomposition of lignocellulose and readily degradable carbohydrates during sewage sludge biodrying, insights of the potential role of microorganisms from a metagenomic analysis. – Chemosphere 201: 127-136.

[22] Caldwell, G. (2009): The Influence of Bioactive Oxylipins from Marine Diatoms on Invertebrate Reproduction and Development. – Marine Drugs 7: 367-400.

[23] Chauton, M. S., Reitan, K. I., Norsker, N. H., Tveteras, R., Kleivdal, H. T. (2015): A techno-economic analysis of industrial production of marine microalgae as a source of EPA and DHA-rich raw material for aquafeed: Research challenges and possibilities. – Aquaculture 436: 95-103.

[24] Cheval, J., Sauvage, V., Frangeul, L., Dacheux, L., Guigon, G., Dumey, N., Pariente, K., Rousseaux, C., Dorange, F., Berthet, N., Brisse, S., Moszer, I., Bourhy, H., Manuguerra, C. J., Lecuit, M., Burguiere, A., Caro, V., Eloit, M. (2011): Evaluation of high-throughput sequencing for identifying known and unknown viruses in biological samples. – Journal of Clinical Microbiology 49: 3268-3275.

[25] Coughlan, L. M., Cotter, P. D., Hill, C., Alvarez-Ordóñez, A. (2015): Biotechnological applications of functional metagenomics in the food and pharmaceutical industries. – Frontiers in Microbiology 6: 672.

http://www.aloki.hu ● ISSN 1589 1623 (Print) ● ISSN1785 0037 (Online)
DOI: http://dx.doi.org/10.15666/aeer/1906_42814298

[26] D'Ippolito, G., Sardo, A., Paris, D., Vella, F. M., Adelfi, M. G., Botte, P., Gallo, C., Fontana, A. (2015): Potential of lipid metabolism in marine diatoms for biofuel production. – Biotechnology for Biofuels 8: 28.
[27] Daniel, R. (2005): The metagenomics of soil. – Nature Reviews Microbiology 3: 470-478.
[28] De Mandal, S., Sanga, Z., Nachimuthu, S. K. (2014): Metagenomic analysis of bacterial community composition among the cave sediments of Indo-Burman biodiversity hotspot region. – PeerJ PrePrints 2: 631.
[29] Delmont, T. O., Robe, P., Cecillon, S., Clark, I. M., Constancias, F., Simonet, P., Hirsch, P. R., Vogel, T. M. (2011): Accessing the soil metagenome for studies of microbial diversity. – Applied and Environmental Microbiology 77(4): 1315-1324.
[30] Dolatabadi, J. E. N., de la Guardia, M. (2011): Applications of diatoms and silica nanotechnology in biosensing, drug and gene delivery, and formation of complex metal nanostructures. – TrAC Trends in Analytical Chemistry 30: 1538-1548.
[31] Dunthorn, M., Klier, J., Bunge, J., Stoeck, T. (2012): Comparing the hyper-variable V4 and V9 regions of the small subunit rDNA for assessment of ciliate environmental diversity. – Journal of Eukaryotic Microbiology 59: 185-187.
[32] Dutilh, B. E. (2014): Metagenomic ventures into outer sequence space. – Bacteriophage 4: e979664.
[33] Epstein, S. S. (2013): The phenomenon of microbial uncultivability. – Current Opinion in Microbiology 16: 636-642.
[34] Evans, K. M., Wortley, A. H., Mann, D. G. (2007): An assessment of potential diatom "barcode" genes (cox1, rbcL, 18S and ITS rDNA) and their effectiveness in determining relationships in Sellaphora (Bacillariophyta). – Protist 158: 349-364.
[35] Falasco, E., Blanco, S., Bona, F., Gom, J., Hlúbiková, D., Novais, M. H., Hoffmann, L., Ector, L. (2009): Taxonomy, morphology and distribution of the Sellaphora stroemii complex (Bacillariophyceae). – Fottea 9: 243-256.
[36] Falasco, E., Ector, L., Isaia, M., Wetzel, C. E., Hoffmann, L., Bona, F. (2014): Diatom flora in subterranean ecosystems: A review. – International Journal of Speleology 43: 231-251.
[37] Falkowski, P. G., Barber, R. T., Smetacek, V. (1998): Biogeochemical controls and feedbacks on ocean primary production. – Science 281: 200-206.
[38] Felczykowska, A., Bloch, S. K., Nejman-Faleńczyk, B., Barańska, S. (2012): Metagenomic approach in the investigation of new bioactive compounds in the marine environment. – Acta Biochimica Polonica 59: 501-505.
[39] Felczykowska, A., Krajewska, A., Zielińska, S., Łos, J. M. (2015): Sampling, metadata and DNA extraction - Important steps in metagenomic studies. – Acta Biochimica Polonica 62: 151-160.
[40] Goss-Souza, D., Mendes, L. W., Borges, C. D., Rodrigues, J. L. M., Tsai, S. M. (2019): Amazon forest-to-agriculture conversion alters rhizosphere microbiome composition while functions are kept. – FEMS Microbiology Ecology 95(3): fiz009.
[41] Groendahl, S., Kahlert, M., Fink, P. (2017): The best of both worlds: A combined approach for analyzing microalgal diversity via metabarcoding and morphology-based methods. – PLoS ONE 12: 1-15.
[42] Guiry, M. D. (2012): How many species of algae are there? – Journal of Phycology 48: 1057-1063.
[43] Guo, L., Sui, Z., Zhang, S., Ren, Y., Liu, Y. (2015): Comparison of potential diatom 'barcode' genes (The 18S rRNA gene and ITS, COI, rbcL) and their effectiveness in discriminating and determining species taxonomy in the Bacillariophyta. – International Journal of Systematic and Evolutionary Microbiology 65: 1369-1380.
[44] Handelsman, J., Rondon, M. R., Brady, S. F., Clardy, J., Goodman, R. M. (1998): Molecular biological access to the chemistry of unknown soil microbes: A new frontier for natural products. – Chemistry and Biology 5: R245-R249.

http://www.aloki.hu ● ISSN 1589 1623 (Print) ● ISSN1785 0037 (Online)
DOI: http://dx.doi.org/10.15666/aeer/1906_42814298

[45] Haubois, A. G., Sylvestre, F., Guarini, J. M., Richard, P., Blanchard, G. F. (2005): Spatio-temporal structure of the epipelic diatom assemblage from an intertidal mudflat in Marennes-Oléron Bay, France. – Estuarine, Coastal and Shelf Science 64: 385-394.
[46] Hebert, P. D. N., Ratnasingham, S., DeWaard, J. R. (2003): Barcoding animal life: Cytochrome c oxidase subunit 1 divergences among closely related species. – Proceedings of the Royal Society, Series B: Biological Sciences 270: S96-S99.
[47] Hess, M., Sczyrba, A., Egan, R., Kim, T.-W. (2011): Metagenomic discovery of biomass-degrading genes and genomes from cow rumen. – Science 463: 463-467.
[48] Huang, S., Herzschuh, U., Pestryakova, L. A., Zimmermann, H. H., Davydova, P., Biskaborn, B. K., Shevtsova, I., Stoof-Leichsenring, K. R. (2020): Genetic and morphologic determination of diatom community composition in surface sediments from glacial and thermokarst lakes in the Siberian Arctic. – Journal of Paleolimnology 64: 225-242.
[49] Hugerth, L. W., Muller, E. E. L., Hu, Y. O. O., Lebrun, L. A. M., Roume, H., Lundin, D., Wilmes, P., Andersson, A. F. (2014): Systematic design of 18S rRNA gene primers for determining eukaryotic diversity in microbial consortia. – PLoS ONE 9: e95567.
[50] Hussein, H. A., Abdullah, M. A. (2020): Anticancer Compounds Derived from Marine Diatoms. – Marine Drugs 18: 356.
[51] Jahn, R., Zetzsche, H., Reinhardt, R., Gemeinholzer, B. (2007): Diatoms and DNA barcoding: A pilot study on an environmental sample. – In: Kusber, W., Jahn, R. (ed.) Proceedings of the 1st Central European Diatom Meeting, Botanic Garden and Botanical Museum Berlin-Dahlem, pp. 63-68.
[52] Jamali, A. A., Akbari, F., Ghorakhlu, M. M., de la Guardia, M., Khosroushahi, A. Y. (2012): Applications of diatoms as potential microalgae in nanobiotechnology. – BioImpacts 2: 83-89.
[53] Janda, J. M., Abbott, S. L. (2007): 16S rRNA gene sequencing for bacterial identification in the diagnostic laboratory: Pluses, perils, and pitfalls. – Journal of Clinical Microbiology 45: 2761-2764.
[54] Jeon, J. H., Kim, J. T., Kim, Y. J., Kim, H.-K., Lee, H. S., Kang, S. G., Kim, S.-J., Lee, J.-H. (2009): Cloning and characterization of a new cold-active lipase from a deep-sea sediment metagenome. – Applied Microbiology and Biotechnology 81: 865-874.
[55] Jünemann, S., Kleinbölting, N., Jaenicke, S., Henke, C., Hassa, J., Nelkner, J., Stolze, Y., Albaum, S. P., Schlüter, A., Goesmann, A., Sczyrba, A., Stoye, J. (2017): Bioinformatics for NGS-based metagenomics and the application to biogas research. – Journal of Biotechnology 261: 10-23.
[56] Kahlert, M., Kelly, M., Albert, R.-L., Almeida, S., Besta, T., Blanco, S., Coste, M., Denys, L., Ector, L., Fránková, M., Hlubikova, D., Ivanov, P., Kennedy, B., Marvan, P., Mertens, A., Miettinen, J., Picinska-Faltynowicz, J., Tison-Rosebery, J., Tomés, E., Vilbaste, S., Vogel, A. (2012): Identification versus counting protocols as sources of uncertainty in diatom-based ecological status assessments. – Hydrobiologia 695: 109-124.
[57] Kemler, M., Garnas, J., Wingfield, M. J., Gryzenhout, M., Pillay, K.-A., Slippers, B. (2013): Ion Torrent PGM as tool for fungal community analysis: A case study of endophytes in eucalyptus grandis reveals high taxonomic diversity. – PLoS ONE 8(12): e81718.
[58] Kermarrec, L., Franc, A., Rimet, F., Chaumeil, P., Humbert, J. F., Bouchez, A. (2013): Next-generation sequencing to inventory taxonomic diversity in eukaryotic communities: A test for freshwater diatoms. – Molecular Ecology Resources 13(4): 607-619.
[59] Kermarrec, L., Bouchez, A., Rimet, F., Humbert, J. F. (2013): First Evidence of the Existence of Semi-Cryptic Species and of a Phylogeographic Structure in the Gomphonema parvulum (Kützing) Kützing Complex (Bacillariophyta). – Protist 164: 686-705.
[60] Kermarrec, L., Franc, A., Rimet, F., Chaumeil, P., Frigerio, J.-M., Humbert, J.-F., Bouchez, A. (2014): A next-generation sequencing approach to river biomonitoring using benthic diatoms. – Freshwater Science 33(1): 349-363.

http://www.aloki.hu ● ISSN 1589 1623 (Print) ● ISSN1785 0037 (Online)
DOI: http://dx.doi.org/10.15666/aeer/1906_42814298

[61] Kim, K. M., Park, J. H., Bhattacharya, D., Yoon, H. S. (2014): Applications of next-generation sequencing to unravelling the evolutionary history of algae. – International Journal of Systematic and Evolutionary Microbiology 64: 333-345.
[62] Knight, R., Vrbanac, A., Taylor, B. C. (2018): Best practices for analysing microbiomes. – Nature Reviews Microbiology 16: 410-422.
[63] Kulski, J. K. (2015): Next-Generation Sequencing - An Overview of the History, Tools, and "Omic " Applications. – In: Kulski, J. K. (ed.) Next generation sequencing-advances, applications and challenges. Croatia: InTech, pp. 3-60.
[64] Kumar Awasthi, M., Ravindran, B., Sarsaiya, S., Chen, H., Wainaina, S., Singh, E., Liu, T., Kumar, S., Pandey, A., Singh, L., Zhang, Z. (2020): Metagenomics for taxonomy profiling: tools and approaches. – Bioengineered 11: 356-374.
[65] Lauritano, C., Martín, J., de la Cruz, M., Reyes, F., Romano, G., Ianora, A. (2018): First identification of marine diatoms with anti-tuberculosis activity. – Scientific Reports 8: 2284.
[66] Lear, G., Dickie, I., Banks, J. (2018): Methods for the extraction, storage, amplification and sequencing of DNA from environmental samples. – New Zealand Journal of Ecology 42: 10-50A.
[67] Lebeau, T., Robert, J. M. (2002): Diatom cultivation and biotechnologically relevant products. Part II: Current and putative products. – Applied Microbiology and Biotechnology 60: 624-632.
[68] Lebeau, T., Robert, J. M. (2003): Diatom cultivation and biotechnologically relevant products. Part I: Cultivation at various scales. – Applied Microbiology and Biotechnology 60: 612-623).
[69] Lekunberri, I., Balcázar, J. L., Borrego, C. M. (2018): Metagenomic exploration reveals a marked change in the river resistome and mobilome after treated wastewater discharges. – Environmental Pollution 234: 538-542.
[70] Levkov, Z., Williams, D. M., Nikolovska, D., Tofilovska, S., Cakar, Z. (2017): The use of diatoms in forensic science: advantages and limitations of the diatom test in cases of drowning. – In: Williams, M., Hill, T., Boomer, I. et al. (eds.) The Archaeological and Forensic Applications of Microfossils: A Deeper Understanding of Human History. The Micropalaeontological Society, Special Publications. Geological Society of London, pp. 261-277.
[71] Lopez-Lopez, O., Cerdan, M., Siso, M. (2014): New Extremophilic Lipases and Esterases from Metagenomics. – Current Protein & Peptide Science 15: 445-455.
[72] MacGillivary, M. L., Kaczmarska, I. (2011): Survey of the Efficacy of a Short Fragment of the rbcL Gene as a Supplemental DNA Barcode for Diatoms. – Journal of Eukaryotic Microbiology 58: 529-536.
[73] Mann, D. G., Droop, S. J. M. (1996): Biodiversity, biogeography and conservation of diatoms. – Biogeography of Freshwater Algae, pp. 19-32.
[74] Mann, D. G. (1999): The species concept in diatoms. – Phycologia 38: 437-495.
[75] Mann, D. G., Sato, S., Trobajo, R., Vanormelingen, P. (2010): DNA barcoding for species identification and discovery in diatoms. – Cryptogamie Algologie 31(4): 557-577.
[76] Mardis, E. R. (2011): A decade's perspective on DNA sequencing technology. – Nature 470: 198-203.
[77] Marx, C. J. (2013): Can You Sequence Ecology? Metagenomics of Adaptive Diversification. – PLOS Biology 11: e1001487.
[78] Mayo, B., Rachid, C., Alegria, A., Leite, A. M. O., Peixoto, R. S., Delgado, S. (2014): Impact of Next Generation Sequencing Techniques in Food Microbiology. – Current Genomics 15(4): 293-309.
[79] McLaughlin, R. B. (2012): An introduction to the Microscopical Study of Diatoms. – Edited by John Gustav Delly and Steve Gill 445.
[80] Medlin, L., Elwood, H. J., Stickel, S., Sogin, M. L. (1988): The characterization of enzymatically amplified eukaryotic 16S-like rRNA-coding regions. – Gene 71: 491-499.

http://www.aloki.hu ● ISSN 1589 1623 (Print) ● ISSN1785 0037 (Online)
DOI: http://dx.doi.org/10.15666/aeer/1906_42814298

[81] Metzker, M. L. (2010): Sequencing technologies - the next generation. – Nature Reviews Genetics 11: 31-46.
[82] Molins, A., Moya, P., García-Breijo, F. J., Reig-Arminana, J., Barreno, E. (2018): A multi-tool approach to assess microalgal diversity in lichens: Isolation, Sanger sequencing, HTS and ultrastructural correlations. – Lichenologist 50: 123-138.
[83] Moniz, M. B. J., Kaczmarska, I. (2009): Barcoding diatoms: Is there a good marker? – Molecular Ecology Resources 9: 65-74.
[84] Moniz, M. B. J., Kaczmarska, I. (2010): Barcoding of Diatoms: Nuclear Encoded ITS Revisited. – Protist 161: 7-34.
[85] Mora, D., Abarca, N., Proft, S., Grau, J. H., Enke, N., Carmona, J., Skibbe, O., Jahn, R., Zimmermann, J. (2019): Morphology and metabarcoding: A test with stream diatoms from Mexico highlights the complementarity of identification methods. – Freshwater Science 38: 448-464.
[86] Moritz, C., Cicero, C. (2004): DNA Barcoding: Promise and Pitfalls. – PLoS Biology 2: e354.
[87] Nanjappa, D., Kooistra, W. H. C. F., Zingone, A. (2013): A reappraisal of the genus Leptocylindrus (Bacillariophyta), with the addition of three species and the erection of Tenuicylindrus gen. nov. – Journal of Phycology 49: 917-936.
[88] Nanjappa, D., Audic, S., Romac, S., Kooistra, W. H. C. F., Zingone, A. (2014): Assessment of species diversity and distribution of an ancient diatom lineage using a DNA metabarcoding approach. – PLoS ONE 9: e103810.
[89] Nelles, L., Fang, B. L., Volckaert, G., Vandenberghe, A., De Wachter, R. (1984): Nucleotide sequence of a crustacean 18S ribosomal RNA gene and secondary structure of eukaryotic small subunit ribosoraal RNAs. – Nucleic Acids Research 12: 8749-8768.
[90] Nguyen, T. N. M., Berzano, M., Gualerzi, C. O., Spurio, R. (2011): Development of molecular tools for the detection of freshwater diatoms. – Journal of Microbiological Methods 84: 33-40.
[91] Nickrent, D. L., Sargent, M. L. (1991): An overview of the secondary structure of the V4 region of eukaryotic small-subunit ribosomal RNA. – Nucleic Acids Research 19: 227-235.
[92] Nilsson, R. H., Tedersoo, L., Abarenkov, K. (2013): Fungal community analysis by high-throughput sequencing of amplified markers - a user' s guide. – New Phytologist 199: 288-299.
[93] Nowinski, B., Smith, C. B., Thomas, C. M., Moran, M. A. (2019): Microbial metagenomes and metatranscriptomes during a coastal phytoplankton bloom. – Scientific Data 6: 1-7.
[94] Pachiappan, P., Prasath, B. B., Perumal, S. (2015): Isolation and Culture of Microalgae Perumal. – Advances in Marine and Brackishwater Aquaculture, pp. 166-181.
[95] Park, C. H., Kim, K. M., Elvebakk, A., Kim, O. S., Jeong, G., Hong, S. G. (2015): Algal and fungal diversity in Antarctic lichens. – The Journal of Eukaryotic Microbiology 62(2): 196-205.
[96] Patel, A., Chaudhary, S., Syed, B. A., Gami, B., Patel, P., Patel, B. (2018): Rbcl Marker Based Approach for Molecular Identification of Arthrospira and Dunaliella Isolates from Non-Axenic Cultures. – Journal of Genetics and Genetic Engineering 2: 24-34.
[97] Pawlowski, J., Audic, S., Adl, S., Bass, D., Belbahri, L., Berney, C., et al. (2012): CBOL Protist Working Group: Barcoding Eukaryotic Richness beyond the Animal, Plant, and Fungal Kingdoms. – PLoS Biology 10: e1001419.
[98] Pérez, A. E., Gomez, L., Buchrieser, C. (2020): Metagenomic approaches in microbial ecology: an update on genome and marker gene sequencing analyses. – Microbial Genomics 6(8): mgen000409.
[99] Pessoa, T. B. A., Rezende, R. P., Marques, E. d et al. (2017): Metagenomic alkaline protease from mangrove sediment. – Journal of Basic Microbiology 57: 962-973.
[100] Piredda, R., Claverie, J. M., Decelle, J., et al. (2018): Diatom diversity through HTS-metabarcoding in coastal European seas. – Scientific Reports 8: 1-12.

http://www.aloki.hu ● ISSN 1589 1623 (Print) ● ISSN1785 0037 (Online)
DOI: http://dx.doi.org/10.15666/aeer/1906_42814298

[101] Poikane, S., Kelly, M., Cantonati, M. (2016): Benthic algal assessment of ecological status in European lakes and rivers: Challenges and opportunities. – Science of the Total Environment 568: 603-613.
[102] Poroyko, V., White, J. R., Wang, M., et al. (2010): Gut microbial gene expression in mother-fed and formula-fed piglets. – PLoS ONE 5.
[103] Prescot, L. M., Harley, J. P., Klein, D. A. (1999): Microbiology 4th Edition. – WCB. McGraw Hill New York, London.
[104] Pujari, L., Wu, C., Kan, J., et al. (2019): Diversity and spatial distribution of chromophytic phytoplankton in the bay of bengal revealed by RuBisCO Genes (rbcL). – Frontiers in Microbiology 10: 1501.
[105] Rimet, F., Abarca, N., Bouchez, A., et al. (2018): The potential of High-Throughput Sequencing (HTS) of natural samples as a source of primary taxonomic information for reference libraries of diatom barcodes. – Fottea 18: 37-54.
[106] Rimet, F., Gusev, E., Kahlert, M., et al. (2019): Diat.barcode, an open-access curated barcode library for diatoms. – Scientific Reports 9: 15116.
[107] Rivera, S. F., Vasselon, V., Jacquet, S., et al. (2017): Metabarcoding of lake benthic diatoms: from structure assemblages to ecological assessment. – Hydrobiologia 807: 37-50.
[108] Rivera, S. F., Vasselon, V., Ballorain, K., et al. (2018): DNA metabarcoding and microscopic analyses of sea turtles biofilms: Complementary to understand turtle behavior. – PLoS ONE 13: 1-20.
[109] Roumpeka, D. D., Wallace, R. J., Escalettes, F., et al. (2017): A review of bioinformatics tools for bio-prospecting from metagenomic sequence data. – Frontiers in Genetics 8: 23.
[110] Round, F. E., Crawford, R. M., Mann, D. G. (1990): Diatoms: biology and morphology of the genera. – Cambridge University Press, Cambridge, UK.
[111] Saghaï, A., Zivanovic, Y., Zeyen, N., et al. (2015): Metagenome-based diversity analyses suggest a significant contribution of non-cyanobacterial lineages to carbonate precipitation in modern microbialites. – Frontiers in Microbiology 6: 797.
[112] Schoch, C. L., Seifert, K. A., Huhndorf, S., et al. (2012): Nuclear ribosomal internal transcribed spacer (ITS) region as a universal DNA barcode marker for Fungi. – Proceedings of the National Academy of Sciences of the United States of America 109: 6241-6246.
[113] Schröder, C., Elleuche, S., Blank, S., Antranikian, G. (2014): Characterization of a heat-active archaeal β-glucosidase from a hydrothermal spring metagenome. – Enzyme and Microbial Technology 57: 48-5.
[114] Seifert, K. A., Samson, R. A., DeWaard, J. R., et al. (2007): Prospects for fungus identification using CO1 DNA barcodes, with Penicillium as a test case. – Proceedings of the National Academy of Sciences of the United States of America 104: 3901-3906.
[115] Siaut, M., Heijde, M., Mangogna, M., et al. (2007): Molecular toolbox for studying diatom biology in Phaeodactylum tricornutum. – Gene 406: 23-35.
[116] Simon, C., Daniel, R. (2011): Metagenomic analyses: Past and future trends. – Applied and Environmental Microbiology 77: 1153-1161.
[117] Smol, J. P., Stoermer, E. F. (2010): The diatoms: applications for the environmental and earth sciences. – Cambridge University Press, Cambridge, UK.
[118] Sogin, M. L., Morrison, H. G., Huber, J. A., et al. (2006): Microbial diversity in the deep sea and the underexplored "rare biosphere". – Proceedings of the National Academy of Sciences of the United States of America 103: 12115-12120.
[119] Song, E. J., Lee, E. S., Nam, Y. D. (2018): Progress of analytical tools and techniques for human gut microbiome research. – Journal of Microbiology 56: 693-705.
[120] Stern, R. F., Horak, A., Andrew, R. L., et al. (2010): Environmental barcoding reveals massive dinoflagellate diversity in marine environments. – PLoS ONE 5.
[121] Stevenson, R. J., Smol, J. P. (2015): Use of Algae in Ecological Assessments. – Freshwater Algae of North America: Ecology and Classification, pp. 921-962.

http://www.aloki.hu ● ISSN 1589 1623 (Print) ● ISSN1785 0037 (Online)
DOI: http://dx.doi.org/10.15666/aeer/1906_42814298

[122] Stoeck, T., Bass, D., Nebel, M., et al. (2010): Multiple marker parallel tag environmental DNA sequencing reveals a highly complex eukaryotic community in marine anoxic water. – Molecular Ecology 19: 21-31.
[123] Stoeckle, M. (2003): Taxonomy, DNA, and the bar code of life. – BioScience 53: 796-797.
[124] Stoof-Leichsenring, K. R., Dulias, K., Biskaborn, B. K., et al. (2020): Lake-depth related pattern of genetic and morphological diatom diversity in boreal Lake Bolshoe Toko, Eastern Siberia. – PLOS ONE 15: 0230284.
[125] Sullivan, M. J., Moncreiff, C. A. (1988): Primary Production of Edaphic Algal Communities in a Mississippi Salt Marsh 1. – Journal of Phycology 24: 49-58.
[126] Sullivan, M. J., Currin, C. A. (2002): Community structure and functional dynamics of benthic microalgae in salt marshes. – Concepts and controversies in tidal marsh ecology, pp. 81-106.
[127] Tapolczai, K., Keck, F., Bouchez, A., Rimet, F., Kahlert, M., Vasselon, V. (2019): Diatom DNA Metabarcoding for Biomonitoring: Strategies to Avoid Major Taxonomical and Bioinformatical Biases Limiting Molecular Indices Capacities. – Frontiers in Ecology and Evolution 7: 409.
[128] Tedersoo, L., Nilsson, R. H., Abarenkov, K., Jairus, T., Sadam, A., Saar, I., Bahram, M., Bechem, E., Chuyong, G., Köljalg, U. (2010): 454 Pyrosequencing and Sanger sequencing of tropical mycorrhizal fungi provide similar results but reveal substantial methodological biases. – New Phytologist 188(1): 291-301.
[129] Thursby, E., Juge, N. (2017): Introduction to the human gut microbiota. – Biochemical Journal 474: 1823-1836.
[130] Tofilovska, S., Wetzel, C. E., Ector, L., Levkov, Z. (2014): Observation on *Achnanthes* Bory *sensu stricto* (Bacillariophyceae) from subaerial habitats in Macedonia and comparison with the type material of *A. coarctata* (B rébisson ex W. S mith) G runow, *A. coarctata var. sinaensis*. – Fottea 14: 15-42.
[131] Torsvik, V., Øvreås, L. (2002): Microbial diversity and function in soil: From genes to ecosystems. – Current Opinion in Microbiology 5: 240-245.
[132] Tremaroli, V., Bäckhed, F. (2012): Functional interactions between the gut microbiota and host metabolism. – Nature 489: 242-249.
[133] Tringe, S. G., Von Mering, C., Kobayashi, A., Salamov, A. A., Chen, K., Chang, H. W., Podar, M., Short, J. M., Mathur, E. J., Detter, J. C., Bork, P., Hugenholtz, P., Rubin, E. M. (2005): Comparative metagenomics of microbial communities. – Science 308: 554-557.
[134] Trobajo, R., Mann, D. G., Clavero, E., Evans, K. M., Vanormelingen, P., McGregor, R. (2010): The use of partial cox1, rbcL and LSU rDNA sequences for phylogenetics and species identification within the nitzschia palea species complex (bacillariophyceae). – European Journal of Phycology 45: 413-425.
[135] Turnbaugh, P. J., Ley, R. E., Hamady, M., Fraser-Liggett, C. M., Knight, R., Gordon, J. I. (2007): The Human Microbiome Project. – Nature 449: 804-810.
[136] Turnbaugh, P. J., Gordon, J. I. (2008): An Invitation to the marriage of metagenomics and metabolomics. – Cell 134: 708-713.
[137] Underwood, G., Kromkamp, J. (1999): Primary Production by Phytoplankton and Microphytobenthos in Estuaries. – In: Nedwell, D. B., Raffaelli, D. G. (eds.) Advances in EcologicalResearch. Elsevier: Academic Press, London, pp. 93-153.
[138] Underwood, G. J. C., Barnett, M. (2006): What determines species composition in microphytobenthic biofilms. – In: Kromkamp, J. (ed.) Functioning of Microphytobenthos in Estuaries. The Netherlands: Royal Netherlands Academy of Arts and Sciences, pp. 121-138.
[139] Vanelslander, B., De Wever, A., Van Oostende, N., Kaewnuratchadasorn, P., Vanormelingen, P., Hendrickx, F., Sabbe, K., Vyverman, W. (2009): Complementarity effects drive positive diversity effects on biomass production in experimental benthic diatom biofilms. – Journal of Ecology 97: 1075-1082.

http://www.aloki.hu ● ISSN 1589 1623 (Print) ● ISSN1785 0037 (Online)
DOI: http://dx.doi.org/10.15666/aeer/1906_42814298

[140] Visco, J. A., Apothéloz-Perret-Gentil, L., Cordonier, A., Esling, P., Pillet, L., Pawlowski, J. (2015): Environmental monitoring: inferring the diatom index from next-generation sequencing data. – Environmental science & technology 49(13): 7597-7605.
[141] Whiteley, A. S., Jenkins, S., Waite, I., Kresoje, N., Payne, H., Mullan, B., Allcock, R., O'Donnell, A. (2012): Microbial 16S rRNA Ion Tag and community metagenome sequencing using the Ion Torrent (PGM) Platform. – Journal of Microbiological Methods 91: 80-88.
[142] Winand, R., Bogaerts, B., Hoffman, S., Lefevre, L., Delvove, M., Van Braekel, J., Fu, Q., Roosens, N. H. C., De Keersmaecker, S. C. J., Vanneste, K. (2019): Targeting the 16S rRNA Gene for Bacterial Identification in Complex Mixed Samples: Comparative Evaluation of Second (Illumina) and Third (Oxford Nanopore Technologies) Generation Sequencing Technologies. – International Journal of Molecular Sciences 21(1): 298.
[143] Wrighton, K. C., Thomas, B. C., Sharon, I., Miller, C. S., Castelle, C. J., VerBerkmoes, N. C., Wilkins, M. J., Hettich, R. L., Lipton, M. S., Williams, K. H., Long, P. E., Banfield, J. F. (2012): Fermentation, hydrogen, and sulfur metabolism in multiple uncultivated bacterial phyla. – Science 337(6102): 1661-1665.
[144] Yang, Y., Wu, H., Dong, S., Jin, W., Han, K., Ren, Y., Zeng, M. (2018): Glycation of fish protein impacts its fermentation metabolites and gut microbiota during in vitro human colonic fermentation. – Food Research International 113: 189-196.
[145] Yatsunenko, T., Rey, F. E., Manary, M. J. (2012): Human gut microbiome viewed across age and geography. – Nature 486: 222-227.
[146] Yergeau, E., Michel, C., Tremblay, J., Niemi, A., King, T. L., Wyglinski, J., Lee, K., Greer, C. W. (2017): Metagenomic survey of the taxonomic and functional microbial communities of seawater and sea ice from the Canadian Arctic. – Scientific Reports 7: 42242.
[147] Zhan, A., Hulák, M., Sylvester, F., Huang, X., Adebayo, A., Abbott, C. L., Adamowicz, S. J., Heath, D. D., Cristescu, M. E., Macisaac, H. J. (2013): High sensitivity of 454 pyrosequencing for detection of rare species in aquatic communities. – Methods in Ecology and Evolution 4: 558-565.
[148] Zhao, X.-Q. (2011): Genome-Based Studies of Marine Microorganisms to Maximize the Diversity of Natural Products Discovery for Medical Treatments. – Evidence-Based Complementary and Alternative Medicine 2011: 11.
[149] Zhao, Z., Fei, K., Bai, H., Wang, Z., Duan, J., Wang, J. (2021): Metagenome association study of the gut microbiome revealed biomarkers linked to chemotherapy outcomes in locally advanced and advanced lung cancer. – Thoracic Cancer 12(1): 66-78.
[150] Zimmermann, J., Jahn, R., Gemeinholzer, B. (2011): Barcoding diatoms: Evaluation of the V4 subregion on the 18S rRNA gene, including new primers and protocols. – Organisms Diversity and Evolution 11: 173-192.
[151] Zimmermann, J., Glöckner, G., Jahn, R., Enke, N., Gemeinholzer, B. (2015): Metabarcoding vs. morphological identification to assess diatom diversity in environmental studies. – Molecular Ecology Resources 15(3): 526-542.

http://www.aloki.hu ● ISSN 1589 1623 (Print) ● ISSN1785 0037 (Online)
DOI: http://dx.doi.org/10.15666/aeer/1906_42814298

TWO SAINFOIN (*ONOBRYCHIS VICIIFOLIA* SCOP.) CULTIVARS DIFFER IN THEIR RESPONSES TO NEUTRAL AND SALINE-ALKALI STRESS DURING SEED GERMINATION AND EARLY SEEDLING GROWTH

LI, S. J.[1] – ZHU, Y. H.[1] – WHITE, J. F.[2] – WEI, M.[1] – WU, G. Q.[1*]

[1]*School of Life Science and Engineering, Lanzhou University of Technology, Lanzhou 730050, China*
(phone: +86-931-297-6650; fax: +86-931-297-3367)

[2]*Department of Plant Biology, Rutgers University, New Brunswick, NJ 08901, USA*

**Corresponding author*
e-mail: gqwu@lut.edu.cn; phone: +86-931-297-6060

(Received 27th Jun 2021; accepted 20th Sep 2021)

Abstract. Salinity is one of the major environmental factors limiting plant growth and development. Two cultivars (the native "Gansu," GS; and the imported "Italian," IT) of sainfoin (*Onobrychis viciifolia* Scop.) were exposed to two neutral salts (NaCl and Na_2SO_4) and two alkaline salts (Na_2CO_3 and $NaHCO_3$) at concentrations ranging from 0-300 mM. After seven days seed germination rates and radicle and hypocotyl lengths were compared. Exposure only to 50 mM neutral salts did not affect significantly relative germination rates compared to control (0 mM). In contrast, higher concentrations of neutral salts and alkaline salts significantly inhibited germination rates and reduced radicle and hypocotyl lengths. Although the two cultivars were visually similar in appearance and had similar patterns in response to saline and alkaline stresses, GS had relatively higher threshold germination concentration compared to IT, and the radicles and hypocotyls of seedlings grown under NaCl and Na_2SO_4 were longer than for IT, indicating that GS is more salt-tolerant. Under neutral salt stress, the recovery germination percentage increased with higher salt concentration. However, under alkaline salt stress, the recovery germination percentage sharply decreased with increasing salt concentration. These results suggest that the damage caused by alkaline salts is more severe than those caused by neutral salts. The present study provides novel insights into the responses of seed germination to different types of salinity in an important forage species.
Keywords: *forage, germination rate, hypocotyl, radical, physiological response*

Introduction

Abiotic stress seriously affects plant growth and development, resulting in crop failure and reducing average crop yields worldwide (Muscolo et al., 2014; Khalil et al., 2016; Partheeban et al., 2017; Niu et al., 2018). Salinity is one of the most important abiotic factors and impacts almost every aspect of plant biochemistry and physiology, from seed germination and seedling growth to the final production and yield from mature crops (Lu et al., 2010; Gebremedhn and Berhanu, 2013; Radic et al., 2019). Exposure of seeds to saline conditions may compromise subsequent seedling establishment (Albuquerque and Carvalho, 2003; Ahmadvand et al., 2012). Indeed, salinization has already affected over 800 million hectares of land, approximately 6% of the total land area worldwide (Munns and Tester, 2008; Wu et al., 2015a).

Assessing salt tolerance of seed germination is extremely important because successful establishment depends entirely on seed germination, and seeds with more

http://www.aloki.hu ● ISSN 1589 1623 (Print) ● ISSN 1785 0037 (Online)
DOI: http://dx.doi.org/10.15666/aeer/1906_42994311

rapid germination under saline conditions are expected to establish faster and accumulate more biomass (Gorai and Neffati, 2007; Petrovic et al., 2016). One of the most common experiments to study seed germination sensitivity to salinity involves the application of NaCl, Na_2SO_4, Na_2CO_3, and $NaHCO_3$ to seed and seedling media (Zahra et al., 2011; Idris and Ali, 2015; Hu et al., 2018; Li and Zhao, 2018).

Sainfoin (*Onobrychis viciifolia* Scop.) is one of the most bloat-safe forage legume crops with high tannin levels, and it is renowned for its medicinal value to grazing animals (Mohajer et al., 2014). Recently, various studies have characterized the environmental preferences, agronomy, plant-microbial interactions, and crop protection of sainfoin (Okcu and Topaloglu, 2019). Sainfoin is an important forage species in agriculture preferred by farmers over other forage legumes. It is widely distributed throughout the arid and semi-arid areas of northern China, Europe, and Russia (Baldinger et al., 2014; Wu et al., 2017; Cirujeda et al., 2019). Since meat products have become more popular as people's living standards have improved, increasing forage crops will be crucial in increasing livestock production. However, in some areas, development of forage crops is negatively affected by abiotic stress. As a result, forage plants may become the focus of breeding programs, particularly for developing salt-tolerant varieties. For sainfoin cultivation, the most important problem is poor germination (Okcu and Topaloglu, 2019), which always results in undesirable establishment and, occasionally, in crop failure (Abbasdokht et al., 2014; Radic et al., 2019). Our previous studies showd that low salt (5-50 mM NaCl) did not affect plant growth of sainfoin, whereas high salt (100 and 200 mM) significantly limited its growth (Wu et al., 2017). Recently, it was reported that the damages caused by alkaline (Na_2CO_3) stress on the growth of sainfoin plants were more serious than those caused by saline-alkaline (NaCl: Na_2CO_3) stress (Wu et al., 2021). However, the studies on effects of neutral and alkaline salts on seed germination and early seedling growth of sainfoin have been rarely performed.

The objective of this work was to investigate and compare the effects of two common salt stress factors, neutral salinity (NaCl and Na_2SO_4) and alkaline salinity (Na_2CO_3 and $NaHCO_3$), on seed germination and seedling growth of two sainfoin cultivars. The results of the present study would not only provide novel insights into the responses of seed germination to different types of salinity in forage species, but also provide a practical basis for improvement and utilization of saline soil.

Materials and methods

Plant materials

This study was carried out in the Lab of Plant Physiology and Ecology at Lanzhou University of Technology, Lanzhou, Gansu Province, China, from March through December, 2019. The seeds of sainfoin (*O. viciifolia* Scop.) cultivars "Gansu" (GS, native breed) and "Italian" (IT, imported breed) were purchased from Lanzhou Nongfeng Seed and Seedling Technology Co., Ltd. and Gansu Mammoth Agriculture Co., Ltd., respectively. The seeds of these two cultivars are very similar and cannot be distinguished based on appearance. The masses of 1000 seeds of GS and IT were 23.03 and 21.07 g, respectively. Prior to the experiment, excessively large or small seeds were discarded, and seeds of uniform size were collected for the germination experiments. Seeds were kept in a cold chamber at 4 °C until the start of the experiments.

http://www.aloki.hu ● ISSN 1589 1623 (Print) ● ISSN 1785 0037 (Online)
DOI: http://dx.doi.org/10.15666/aeer/1906_42994311

Germination test

A total of four salinity types (NaCl, Na_2SO_4, Na_2CO_3, and $NaHCO_3$) were applied. Seeds of GS and IT were exposed to two neutral salinities (NaCl and Na_2SO_4) and two alkaline salinities (Na_2CO_3 and $NaHCO_3$) at 0, 50, 100, 200, 250, and 300 mM during a seven-day period and their germination assessed.

Seeds were first surface sterilized in a 3% sodium hypochlorite solution for 8 min, then rinsed with the sterile distilled water five times, soaked in the distilled water for 12 h, and briefly dried on filter paper. Fifty seeds were randomly placed on 9-cm diameter Petri dishes with three layers of filter paper wetted with 12 mL of the treatment solutions. The filter paper and solutions were changed each day. Petri dishes were randomly placed in the dark in a precision incubator that maintained the temperature at 18 °C. Three independent replicates were conducted for each treatment.

After 7 d of salt exposure, ungerminated seeds were transferred to Petri dishes with only distilled water and incubated at 18 °C for an additional 6 d.

Data collection

Seeds were considered to have germinated when their radicle length was at least 1 mm. The number of seeds germinated on each Petri dish was recorded daily during the seven-day salinity exposure. The hypocotyl and radicle lengths were measured using a ruler on the seventh day. The germination rate (GR) was calculated according to Hu et al. (2018) as

$$GR(\%) = \frac{a}{b} \times 100 \quad \text{(Eq.1)}$$

where a is the number of germinated seeds and b is the number of total seeds per treatment. The recovery germination percentage (RGP) was calculated as

$$RGP(\%) = \frac{c}{d} \times 100 \quad \text{(Eq.2)}$$

where c is the number of newly germinated seeds in recovery test, and d is the number of seeds transferred to the distilled water treatment (Zhang et al., 2014).

Statistical analysis

Data analysis was performed using SPSS 22.0 (Chicago, USA). Two-way and three-way ANOVAs using salinity type, salinity concentration, and cultivar, as the factors were performed to analyze the differences among the four salinity types, the seven salinity concentrations, the two cultivars, and their interactions. Duncan's Multiple Range tests were used to determine significant differences between means at the $P < 0.05$ level.

Results

Effects of neutral and alkaline salts on seed germination rate

We compared the effects of different concentrations of neutral salinities (NaCl and Na_2SO_4) and alkaline salinities ($NaHCO_3$ and Na_2CO_3) on the time courses of seed germination (*Figs. 1* and *2*).

http://www.aloki.hu ● ISSN 1589 1623 (Print) ● ISSN 1785 0037 (Online)
DOI: http://dx.doi.org/10.15666/aeer/1906_42994311

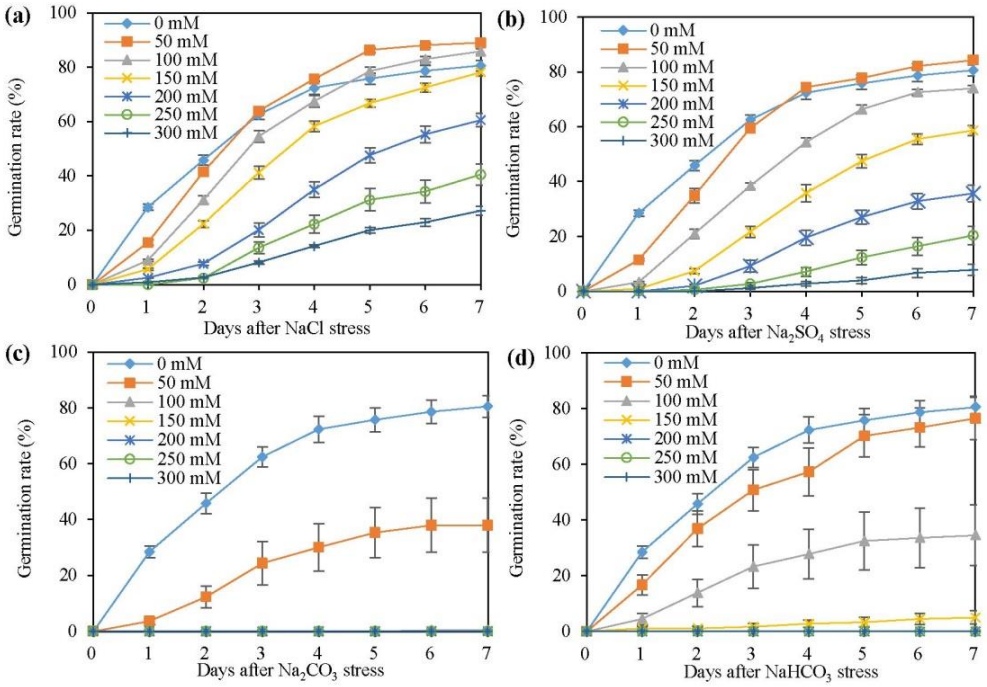

Figure 1. *Time course of seed germination of the sainfoin cultivar "Gansu" (GS) subjected to NaCl (a), Na_2SO_4 (b), Na_2CO_3 (c), and $NaHCO_3$ (d) in various concentrations (0, 50, 100, 150, 200, 250, and 300 mM) during a seven-day period. Fifty seeds were pooled in each replicate (n = 3). Values are mean ± standard error (SE), and error bars represent SE*

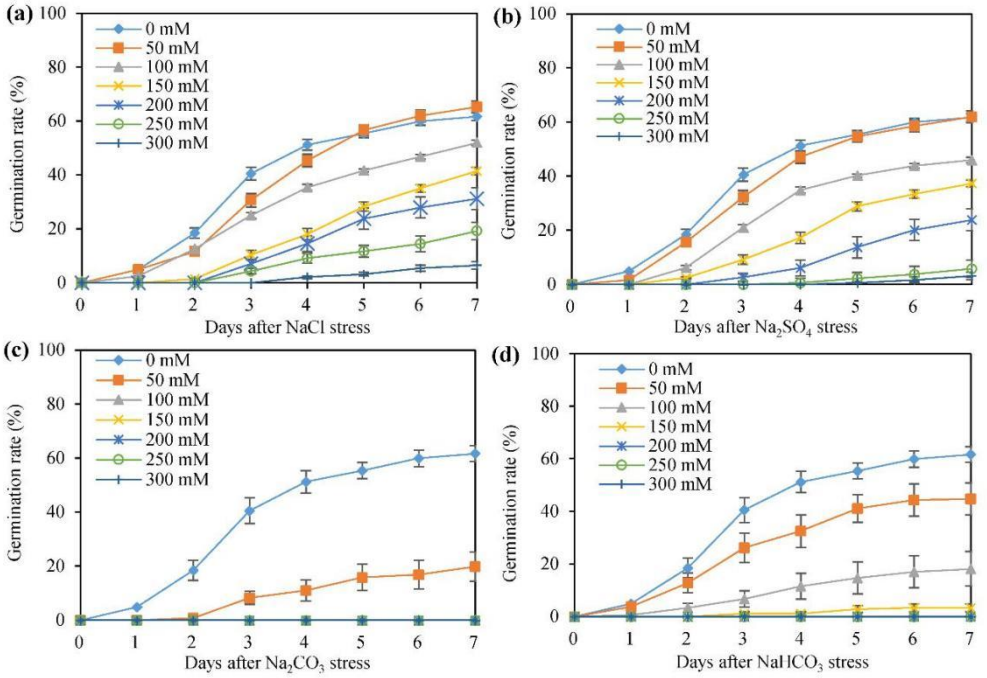

Figure 2. *Time course of seed germination of the sainfoin cultivar "Italian" (IT) subjected to NaCl (a), Na_2SO_4 (b), Na_2CO_3 (c), and $NaHCO_3$ (d) in various concentrations (0, 50, 100, 150, 200, 250, and 300 mM) during a seven-day period. Fifty seeds were pooled in each replicate (n = 3). Values are mean ± standard error (SE), and error bars represent SE*

http://www.aloki.hu ● ISSN 1589 1623 (Print) ● ISSN 1785 0037 (Online)
DOI: http://dx.doi.org/10.15666/aeer/1906_42994311

GS had a higher rate of seed germination than IT under both normal (no added salts) and saline treatments. At the end of the experiment on the seventh day, the highest germination rate under NaCl exposure for both cultivars occurred with the 50 mM NaCl treatment, followed by 100 mM in GS and 0 mM in IT. Germination rates were significantly reduced by higher salt concentrations in both GS (200, 250, and 300 mM) and IT (100, 150, 200, 250, and 300 mM) compared to control (0 mM) (*Figs. 1a* and *2a*). Under Na_2SO_4 treatments, the concentration of 50 mM did not affect germination rate in either GS or IT, while higher concentrations (100–300 mM) significantly decreased germination rate in both cultivars compared to the control (0 mM) (*Figs. 1b* and *2b*). Under 50 mM Na_2CO_3 treatment, GS began to germinate on the first day, while IT did not begin to germinate until the third day. By the seventh day, the 50 mM concentration of Na_2CO_3 significantly reduced gemination rates of GS and IT by 52.9% and 67.9%, respectively, compared to the 0 mM control concentration, whereas high concentrations (100-300 mM) completely inhibited germination in both cultivars (*Figs. 1c* and *2c*). Under $NaHCO_3$ treatment, germination rates were reduced significantly both in GS and IT by 50 mM concentration over a seven-day period compared to the 0 mM control. Exposure to 100 mM $NaHCO_3$ observably decreased germination rates in GS and IT to levels significantly lower than at a concentration of 50 mM. Both cultivars maintained lower germination rates when exposed to 150 mM $NaHCO_3$, and germination was almost completely inhibited under high concentrations (200, 250, and 300 mM) of $NaHCO_3$ throughout the seven days of treatment (*Figs. 1d* and *2d*).

The effects of salt exposure on relative gemination rate in the two cultivars were further analyzed. Under neutral salts (NaCl and Na_2SO_4), the relative germination rates both in GS and IT remained unchanged at 50 mM, but relative germination rate decreased significantly with increasing salt concentration from 100 to 300 mM (*Fig. 3a, b*).

Interestingly, the relative germination rate of GS was higher than IT under both NaCl and Na_2SO_4 treatments. Furthermore, Na_2SO_4 had a stronger inhibitory effect on seed gemination than NaCl, especially at high concentrations. Under alkaline salts (Na_2CO_3 and $NaHCO_3$), the increasing of salt concentration reduced significantly the relative germination rates, reaching zero at 100 mM Na_2CO_3 and 200 mM $NaHCO_3$ (*Fig. 3c, d*), indicating that Na_2CO_3 more strongly inhibited seed germination than $NaHCO_3$. The relative germination rate of GS was significantly higher than that of IT when exposed to 50 and 100 mM $NaHCO_3$ (*Fig. 3d*). Moreover, the results of the two-way ANOVA showed that the effects of salinity type, salinity concentration, and their interaction on germination rates were significant in GS. However, in IT, both salt type and salt concentration had significant effects on germination of IT, but the interaction between salt type and salt concentration was not significant (*Table 1*).

Table 1. *Two-way ANOVA of effects of salinity type and salinity concentration on germination rate and lengths of the hypocotyl and radicle in two sainfoin cultivars, "Gansu" (GS) and "Italian" (IT), exposed to salinity stress*

Variable and source of variation	GS			IT		
	Germination rate	Hypocotyl length	Radicle length	Germination rate	Hypocotyl length	Radicle length
Salinity type (df = 3)	24.685**	14.698**	27.350**	7.886**	29.865**	1.036
Salinity concentration (df = 6)	62.195**	54.182**	123.842**	62.236**	63.289**	23.219**
Salinity type × concentration (df = 18)	3.130**	6.363**	3.310**	1.536	4.466**	1.345

*$P < 0.05$; **$P < 0.01$

http://www.aloki.hu ● ISSN 1589 1623 (Print) ● ISSN 1785 0037 (Online)
DOI: http://dx.doi.org/10.15666/aeer/1906_42994311

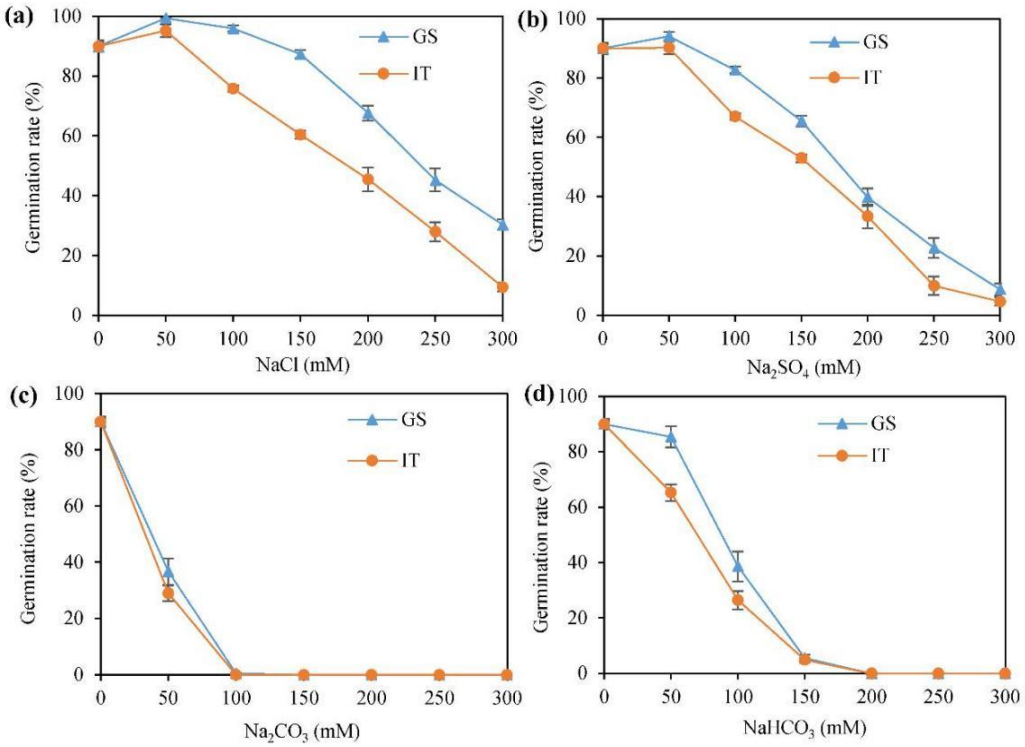

Figure 3. *Germination rates of seeds in two sainfoin cultivars "Gansu" (GS) and "Italian" (IT) after subjected with NaCl (a), Na_2SO_4 (b), Na_2CO_3 (c), and $NaHCO_3$ (d) of various concentrations (0, 50, 100, 150, 200, 250, and 300 mM) for 7 d. Fifty seeds were pooled in each repeat (n = 3). Values are mean ± standard error (SE) and error bars represent SE*

Effect of neutral and alkaline salts on growth of hypocotyl and radicle in two sainfoin cultivars during seed germination

To explore effects of different kinds of salts on seedling growth after seed germination, the lengths of hypocotyl and radicle were measured at the end of the 7-day salt exposure. As shown in *Table 2*, under neutral salts, all concentrations (50-300 mM) significantly reduced the lengths of hypocotyl and radicle in both GS and IT compared to the control (0 mM).

At the same salt concentration, the reduction of hypocotyl and radicle lengths by NaCl was less than by Na_2SO_4 in both cultivars. For example, at 300 mM NaCl and Na_2SO_4, hypocotyl length in GS was reduced by 89.9% and 94.9%, respectively, compared to control (0 mM). Under Na_2CO_3 stress, the minimum concentration needed to completely inhibit growth of both the hypocotyl and the radicle was 150 mM in GS, but only 100 mM in IT. However, under $NaHCO_3$ stress, the minimum concentration to completely inhibit growth was 200 mM in both cultivars (*Table 2*). The results of a two-way ANOVA showed that the effects of salt type, salt concentration, and the salt type × concentration interaction were significant for both hypocotyl length and radicle length in GS, but only for hypocotyl length in IT. Salinity type and salinity concentration had significant effects on radicle length in IT, but their interactive effect was not significant (*Table 1*). Further analysis showed that the hypocotyl and radicle growth under salinity stress varied among cultivars, salinity types, and salinity concentrations (*Table 3*).

http://www.aloki.hu ● ISSN 1589 1623 (Print) ● ISSN 1785 0037 (Online)
DOI: http://dx.doi.org/10.15666/aeer/1906_42994311

Table 2. *Effects of NaCl, Na_2SO_4, Na_2CO_3, and $NaHCO_3$ of various concentrations (0, 50, 100, 150, 250, and 300 mM) on growth of hypocotyl and radicle after seed germination in two sainfoin cultivars, "Gansu" (GS) and "Italian" (IT)*

Stress		GS		IT	
Salinity type	**Concentration (mM)**	**Hypocotyl length (mm)**	**Radicle length (mm)**	**Hypocotyl length (mm)**	**Radicle length (mm)**
NaCl	0	26.33 ± 6.46^{a}	82.56 ± 10.67^{a}	24.00 ± 5.61^{a}	74.78 ± 15.72^{a}
	50	14.22 ± 7.64^{b}	57.78 ± 12.57^{b}	14.78 ± 3.59^{b}	59.00 ± 8.27^{b}
	100	5.00 ± 1.93^{c}	49.56 ± 6.24^{c}	7.33 ± 3.87^{c}	41.67 ± 8.07^{c}
	150	5.00 ± 3.16^{c}	41.00 ± 7.22^{d}	7.33 ± 4.24^{c}	37.22 ± 8.75^{c}
	200	3.33 ± 0.50^{c}	25.67 ± 3.70^{e}	3.78 ± 1.39^{cd}	19.44 ± 6.38^{d}
	250	3.33 ± 0.86^{c}	10.33 ± 5.07^{f}	3.11 ± 0.92^{d}	11.44 ± 6.12^{de}
	300	2.67 ± 1.00^{c}	6.11 ± 2.36^{f}	1.22 ± 0.44^{d}	1.78 ± 0.83^{e}
Na_2SO_4	0	26.33 ± 6.46^{a}	82.56 ± 10.67^{a}	20.67 ± 2.87^{a}	72.00 ± 12.41^{a}
	50	12.22 ± 2.22^{b}	45.78 ± 10.45^{b}	8.00 ± 4.47^{b}	47.17 ± 7.80^{b}
	100	7.11 ± 3.01^{c}	39.89 ± 7.18^{b}	4.00 ± 1.41^{c}	35.17 ± 7.78^{b}
	150	3.44 ± 0.88^{d}	26.11 ± 3.75^{c}	2.83 ± 0.75^{c}	25.5 ± 7.71^{bc}
	200	3.11 ± 1.26^{d}	14.44 ± 7.41^{d}	2.83 ± 0.75^{c}	15.5 ± 1.97^{cd}
	250	2.11 ± 0.60^{d}	9.56 ± 3.84^{de}	2.75 ± 1.25^{c}	5.75 ± 1.89^{de}
	300	1.33 ± 0.50^{d}	4.00 ± 1.22^{e}	1.00 ± 0.00^{c}	2.00 ± 1.15^{e}
Na_2CO_3	0	24.00 ± 1.87^{a}	74.89 ± 5.22^{a}	24.00 ± 1.87^{a}	74.89 ± 7.29^{a}
	50	10.88 ± 2.31^{b}	11.00 ± 1.82^{b}	10.44 ± 0.95^{b}	10.22 ± 3.59^{b}
	100	1.00 ± 0.00^{c}	1.33 ± 0.33^{c}	-	-
	150	-	-	-	-
$NaHCO_3$	0	24.00 ± 1.87^{a}	74.89 ± 5.22^{a}	24.00 ± 1.87^{a}	74.89 ± 7.29^{a}
	50	18.75 ± 1.50^{ab}	18.13 ± 2.02^{b}	13.67 ± 1.84^{b}	11.67 ± 2.72^{b}
	100	15.71 ± 1.14^{bc}	5.71 ± 0.80^{c}	17.00 ± 1.22^{b}	4.33 ± 1.08^{b}
	150	10.00 ± 1.22^{c}	4.50 ± 0.95^{c}	4.40 ± 0.92^{c}	6.00 ± 1.54^{b}
	200	-	-	-	-

Columns with different lowercase letters indicate significant differences at $P < 0.05$ (Duncan's test)

Table 3. *A three-way ANOVA analysis of effects of salinity types, concentrations and cultivars on germination rates of seeds, and lengths of hypocotyls and radicles in sainfoin exposed to salinity stresses*

	Fv	**Fs**	**Fc**	**Fv × s**	**Fv × c**	**Fs × c**	**Fv × s × c**
df	1	3	6	3	6	18	18
Germination rate	318.878**	56.006**	198.717**	6.746**	2.123*	6.956**	1.791*
Radicle length	0.221	33.282**	111.598**	7.848**	2.125*	8.340**	2.187*
Hypocotyl length	0.355	8.523**	76.845**	2.326	2.002	1.984*	1.410

Fv, comparison of two sainfoin cultivars; Fs, comparison of two types of salinity; Fc, comparison of four concentrations of salinity; Fs × c, comparison of two kinds of salinity and four concentrations of salinity; Fv × c, comparisons of two cultivars and four concentrations of salinity; Fs × v × c, comparisons of two cultivars, two kinds of salinity, and four concentrations of salinity
$^{*}P < 0.05$; $^{**}P < 0.01$

Seed germination recovery in two sainfoin cultivars after different types of salts stresses

To evaluate how harmful different types of salts and different salt concentrations were on seeds, the seeds ungerminated after seven days of salt treatment were transferred to distilled water, and germination recovery was tested. As shown in

http://www.aloki.hu ● ISSN 1589 1623 (Print) ● ISSN 1785 0037 (Online)
DOI: http://dx.doi.org/10.15666/aeer/1906_42994311

Figure 4, after Na_2SO_4 exposure, germination recovery increased with increasing salt concentration from 50 to 300 mM in both cultivars, and the among of increase was significantly less in IT than in GS.

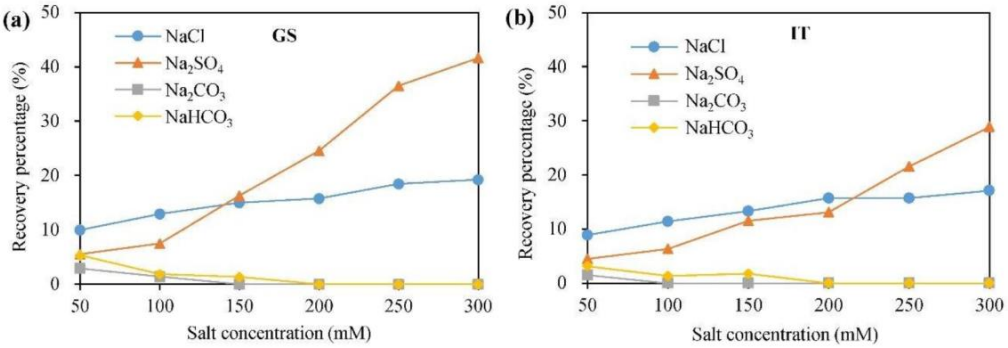

Figure 4. *Recovery germination of seeds in two sainfoin cultivars "Gansu" (GS) (a) and "Italian" (IT) (b) subjected with NaCl, Na_2SO_4, Na_2CO_3, and $NaHCO_3$ of various concentrations (50, 100, 150, 200, 250, and 300 mM) for 7 d*

After NaCl stress, the recovery germination percentage (RGP) maintained the stable levels with increasing salt concentration in both GS and IT. Compared to the two neutral salts, after exposure to two alkaline salts, RGP significantly declined with increasing salt concentration. Although germination recovery also occurred in alkaline salt treatments, RGP was very low, and the maximum RGP was only 5%. The RGP reached zero when the concentration of Na_2CO_3 was 100 and 150 mM in IT and GS, respectively. However, recovery germination did not occur in either GS or IT when concentrations of $NaHCO_3$ exceeded 200 mM (*Fig. 4a, b*). These results suggest that alkaline salinities are more harmful to seeds of both sainfoin cultivars than neutral salinities.

Threshold and critical salt concentrations for the germination of seeds and growth of hypocotyl and radicle in two sainfoin cultivars under different types of salts stresses

As shown in *Table 4*, both threshold and critical salinity concentrations for seed germination were relatively higher under neutral salts than under alkaline salts for both cultivars. Under neutral salts, GS exhibited higher threshold concentrations of 200 mM NaCl and 150 mM Na_2SO_4 and higher critical concentrations of 250 mM NaCl and 200 mM Na_2SO_4, whereas IT showed relatively lower threshold and critical concentrations. Under alkaline salts, GS displayed the same threshold and critical concentrations as IT in both Na_2CO_3 and $NaHCO_3$ conditions (*Table 4*).

Discussion

The different effects of neutral and alkaline salinities on seed germination and recovery of two sainfoin cultivars

Both neutral and alkaline salts inhibited seed germination, with germination significantly reduced with increasing salt concentrations (*Figs. 1* and *2*). For example, the germination rate of GS under 50 mM of neutral salts was as high as the control

http://www.aloki.hu ● ISSN 1589 1623 (Print) ● ISSN 1785 0037 (Online)
DOI: http://dx.doi.org/10.15666/aeer/1906_42994311

(0 mM) (>80%) (*Fig. 1a, b*), and the length of the radicle and hypocotyl exceeded 12 and 45 mm, respectively (*Table 2*). However, few seeds germinated (<30%) at a concentration of 300 mM (*Fig. 1a, b*), and the lengths of the hypocotyl and radical at this high salt concentration were reduced by more than 90% (*Table 2*). In alkaline salinities, hypocotyl and radicle length were reduced to zero (*Table 2*). Similar results were also found in *Haloxylon ammodendron* (Huang et al., 2003), in which the germination rate gradually declined with increasing salinity concentrations.

Table 4. *The threshold and critical salt concentration for the seed germination, and the hypocotyl and radicle growth in two sainfoin cultivars "Gansu" (GS) and "Italian" (IT) exposed to different salts stresses*

Cultivars	Salinity	Threshold salinity concentration (mM)			Critical salinity concertation (mM)		
		Germination	Hypocotyl	Radicle	Germination	Hypocotyl	Radicle
GS	NaCl	200	50	50	250	100	150
	Na_2SO_4	150	50	50	200	50	100
	Na_2CO_3	50	50*	50*	50	50	50
	$NaHCO_3$	100	100	50*	100	100	50
IT	NaCl	150	50	50	250	100	150
	Na_2SO_4	100	50	100	200	50	100
	Na_2CO_3	50	50	50*	50	50	50*
	$NaHCO_3$	100	50	50*	100	150	50

Threshold salinity concentration is defined as the highest level of salinity resulting in non-significant decrease, and the critical salinity concertation is defined as the level of salinity resulting in a 50% decrease of seed germination or lengths of hypocotyls and radicles. "*" represents significant decrease compared to the control from 50 mM salinity concentration

It is well-known that neutral salts and alkaline salts impose distinct types of stresses (Shi and Sheng, 2005). Plants exposed to alkaline conditions experienced not only ionic stress but also high pH stress, which aggravates the effects of ionic toxicity and osmotic stress on seeds and damages the seed embryo (Yang et al., 2009). In the present study, the differences between neutral and alkaline salinities were further investigated. It is clear that alkaline salinity was more harmful than neural salinity to sainfoin seed germination and seedling growth (*Table 2*). Both GS and IT cultivars had higher germination under neutral salinities (NaCl and Na_2SO_4) than under alkaline salinities ($NaHCO_3$ and Na_2CO_3). Under Na_2CO_3, seeds germinated only at a concentration of 50 mM. Similarly, under $NaHCO_3$ stress, germination did not occur at concentrations exceeding 150 mM. However, at even 300 mM concentrations of NaCl and Na_2SO_4 seeds still germinated (*Figs. 1* and *2*). Additionally, sainfoin exhibited a relatively higher threshold concentration of neutral salts than alkaline salts during germination. The threshold concentrations of NaCl and Na_2SO_4 for GS germination were 200 and 150 mM, while the corresponding thresholds of alkaline salts (Na_2CO_3 and $NaHCO_3$) were 50 and 100 mM, respectively. However, for germination of the IT cultivar, the critical concentrations of NaCl and Na_2SO_4 were 250 and 200 mM, while the corresponding critical concentrations of alkaline salts (Na_2CO_3 and $NaHCO_3$) were 50 and 100 mM, respectively (*Table 4*). These results suggest that damage caused by alkaline salts is more serious than those caused by neutral salts. In previous studies, it was observed that the damage due to alkaline salts are often more complex, and the

http://www.aloki.hu ● ISSN 1589 1623 (Print) ● ISSN 1785 0037 (Online)
DOI: http://dx.doi.org/10.15666/aeer/1906_42994311

process and degree of damage, as well as the breakdown of ecological performance, are more severe than those due to neutral salts (Yang et al., 2009).

In the neutral salt treatments, the recovery germination percentage increased with increasing salt concentration (*Fig. 4*). For instance, the recovery percentages in GS increased from 5% to 40% under Na_2SO_4, with the maximum recovery germination percentage occurring after exposure to 300 mM, indicating that neutral salts only temporarily inhibited seed germination in sainfoin. However, under alkaline salt stress, the recovery germination percentage sharply decreased with increasing salt concentrations. In addition, both cultivars exhibited lower recovery germination percentage in alkaline conditions compared to neutral salinity conditions (*Fig. 4*). These results implied that alkaline salinity not only temporarily inhibited seed germination but also led to prolonged toxicity.

The different tolerance to salt stresses in two sainfoin cultivars

Both neutral and alkaline salinity stresses led to reduced germination rate with increasing salt concentration. The reduction in germination was proportional to the concentration of Na^+, with more Na^+ leading to lower rates of germination (Hu et al., 2018). Under neutral salt conditions, the germination curve of 250 mM in NaCl almost coincided with that of Na_2SO_4 at 200 mM in both GS and IT. Similarly, under alkaline conditions, the germination curve of 50 mM in Na_2CO_3 was almost the same as that of $NaHCO_3$ at 100 mM (*Figs. 1a, b* and *2a, b*). These results demonstrated that Na^+ might be toxic to seed germination. Na^+ has been reported to have a physiological role in seedlings of sugar beet (Wu et al., 2015b), and high absorption of Na^+ inhibited and decreased germination rate (Carpýcý et al., 2009). Toxicity of Na^+ may therefore be the main cause of reduced germination with increasing salinity concentration.

Salt tolerance has been shown to differ during seed germination and vary among different plant varieties (Hu et al., 2018). Although GS and IT exhibited a very similar appearance and displayed the same patterns of response to saline and alkaline stresses, there were nonetheless obvious differences in salt tolerance between the two cultivars. GS was more tolerant to neutral salt stress during germination, as the germination rate showed a relatively higher threshold concentration compared to IT (*Table 4*). Additionally, the radicles and hypocotyls of seedlings grown under NaCl and Na_2SO_4 were also longer in GS than in IT. These results confirmed that GS was more tolerant to NaCl and Na_2SO_4. However, both GS and IT experienced sharp reductions in germination at higher concentrations of alkaline salts (*Fig. 3*), which was exemplified by the lower critical concentration at 50 mM Na_2CO_3 and at 100 mM $NaHCO_3$ (*Table 4*). These results implied that sainfoin is extremely sensitive to alkaline conditions.

It is well documented that the role of the seed coat is to protect the embryo from harmful environmental conditions (Wierzbicka and Obidzińska, 1998; Yang et al., 2012). The effect of abiotic stress on seed germination of different crop cultivars depends upon different seed structures (Wierzbicka and Obidzińska, 1998; Ashraf and Foolad, 2005). In general, a solid seed coat can protect the seed embryo from salt toxicity, particularly because of its wide variability in structure compared to other tissues or organs (Wierzbicka and Obidzińska, 1998). The seed coat, therefore, is the major barrier to salinity stress, and it prevents embryo toxicity prior to seed coat degradation by the germinating embryonic roots (Hu et al., 2018). As the two sainfoin cultivars have similar structures of seeds, the reason for the stronger salinity tolerance

http://www.aloki.hu ● ISSN 1589 1623 (Print) ● ISSN 1785 0037 (Online)
DOI: http://dx.doi.org/10.15666/aeer/1906_42994311

of GS compared to that of IT may be attributed to its higher quality seeds (i.e. the heavier mass of 100 seeds), which can hold more dry matter and more energy in the seed embryo.

Conclusions

Different types of salts inhibited seed germination and growth of hypocotyls and radicles, with increasing inhibition with increasing salt concentrations. Salts affected sainfoin germination and early growth in the following order: Na_2CO_3 > $NaHCO_3$ > Na_2SO_4 > NaCl. Neutral salinity only temporarily inhibited germination, whereas alkaline salinity temporarily inhibited germination during exposure but also proved toxic to sainfoin seeds even after removal of the salts. Thus, the effects of neutral salinity and alkaline salinity were different, and damage due to alkaline salinity was more severe than that of neutral salinity. GS seeds germinated and grew more rapidly compared to IT seeds under saline-alkaline stress, suggesting that GS is more salt-tolerant. However, the molecular mechanisms underling the response of sainfoin to saline-alkaline stress need to be addressed in the future research.

Acknowledgements. This research was funded by the National Natural Science Foundation of China, grant number 31860404; Science and Technology Department of Gansu Province, grant number 21YF5FA082; Lanzhou Science and Technology Bureau, grant number 2017-4-94. We would like to thank all the people involved in this project and the reviewers who provided constructive comments. We would also like to thank Dr. Adam Roddy at Yale University for his assistance with English language and grammatical editing.

REFERENCES

[1] Abbasdokht, H.; Gholami, A.; Asghari, H. (2014): Halopriming and hydropriming treatments to overcome salt and drought stress at germination stage of corn (*Zea mays* L.). – Desert 19: 27-34.

[2] Ahmadvand, G.; Soleimani, F.; Saadatian, B.; Pouya, M. (2012): Effects of seed priming on germination and emergence traits of two soybean cultivars under salinity stress. – International Journal of Applied and Basic Sciences 3: 234-241.

[3] Albuquerque, F. E.; Carvalho, N. M. (2003): Effect of the type of environmental stress on the emergence of sunflower (*Helianthus annus* L.), soybean (*Glycine max* (L.) Merril) and maize (*Zea mays* L.) seeds with different levels of vigor. – Seed Science & Technology 31: 465-479.

[4] Ashraf, M.; Foolad, M. R. (2005): Pre-sowing seed treatment - A shotgun approach to improve germination, plant growth, and crop yield under saline and non-saline conditions. – Advances in Agronomy 88: 223-271.

[5] Baldinger, L.; Hagmüller, W.; Minihuber, U.; Matzner, M.; Zollitsch, W. (2014): Sainfoin seeds in organic diets for weaned piglets-utilizing the protein-rich grains of a long-known forage legume. – Renewable Agriculture and Food Systems 31: 12-21.

[6] Carpýcý, E. B.; Celýk, N.; Bayram, G. (2009): Effects of salt stress on germination of some maize (*Zea mays* L.) cultivars. – African Journal of Biotechnology 8: 4918-4922.

[7] Cirujeda, A.; Marí, A. I.; Murillo, S.; Aibar, J.; Pardo, G.; Solé-Senan, X. O. (2019): May the inclusion of a legume crop change weed composition in cereal fields? Example of sainfoin in Aragon (Spain). – Agronomy 9: 134.

http://www.aloki.hu ● ISSN 1589 1623 (Print) ● ISSN 1785 0037 (Online)
DOI: http://dx.doi.org/10.15666/aeer/1906_42994311

[8] Gebremedhn, Y.; Berhanu, A. (2013): The role of seed priming in improving seed germination and seedling growth of maize (*Zea mays* L.) under salt stress at laboratory conditions. – African Journal of Biotechnology 12: 6484-6490.
[9] Gorai, M.; Neffati, M. (2007): Germination responses of Reaumuria vermiculata to salinity and temperature. – Annals of Applied Biology 151: 53-59.
[10] Hu, H.; Liu, H.; Liu, F. (2018): Seed germination of hemp (*Cannabis sativa* L.) cultivars responds differently to the stress of salt type and concentration. – Industrial Crops and Products 123: 254-261.
[11] Huang, Z.; Zhang, X.; Zheng, G.; Gutterman, Y. (2003): Influence of light, temperature, salinity and storage on seed germination of *Haloxylon ammodendron*. – Journal of Arid Environments 55: 453-464.
[12] Idris, Y. A.; Ali, S. A. M. (2015): Response of maize (*Zea mays* L.) to sodium chloride stress at early growth stages. – International Journal of Agronomy and Agricultural Research 6: 68-74.
[13] Khalil, C.; Houssein, B. E.; Hassan, B.; Fouad, M. (2016): Comparative salt tolerance study of some acacia species at seed germination stage. – Asian Journal of Plant Sciences 15: 66-74.
[14] Li, X.; Zhao, W. Z. (2018): Effects of salt-alkaline mixed stresses on seed germination and seeding growth of *Bassia dasyphylla* in desert region. – Journal of Desert Research 38: 300-306.
[15] Lu, S. W.; Li, T. L.; Jiang, J. (2010): Effects of tomato fruit under Na^+-salt and Cl^--salt stresses on sucrose metabolism. – African Journal of Agricultural Research 5: 2227-2231.
[16] Mohajer, S.; Taha, R. M.; Lay, M. M.; Esmaeili, A. K.; Khalili, M. (2014): Stimulatory effects of gamma irradiation on phytochemical properties, mitotic behaviour, and nutritional composition of sainfoin (*Onobrychis viciifolia* Scop.). – The Scientific World Journal 2014: 1-9.
[17] Munns, R.; Tester, M. (2008): Mechanisms of salinity tolerance. – Annual Review of Plant Biology 59: 651-81.
[18] Muscolo, A.; Sidari, M.; Anastasi, U.; Santonoceto, U.; Maggio, A. (2014): Effect of PEG-induced drought stress on seed germination of four lentil genotypes. – Journal of Plant Interactions 9(1): 354-363.
[19] Niu, Y.; Yang, X. Y.; Dai, C. F.; Wang, B. W.; Ren, G. L.; Wu, J. L.; Wang, F. B.; Chen, X. H. (2018): Related indices selection of soybean salt tolerance at germination and seedling stages. – Soybean Science 37: 216-223.
[20] Okcu, M.; Topaloglu, F. N. (2019): Effect of different gibberellic acid doses treatment on seed germination of wild sainfoin (*Onobrychis vichfolia*). – Fresenius Environmental Bulletin 28: 1062-1068.
[21] Partheeban, C.; Chandrasekhar, C. N.; Jeyakumar, P.; Ravikesavan, R.; Gnanam, R. (2017): Effect of PEG induced drought stress on seed germination and seedling characters of maize (*Zea mays* L.) genotypes. – International Journal of Current Microbiology and Applied Sciences 6: 1095-1104.
[22] Petrovic, G.; Jovicic, D.; Nikolic, Z.; Tamindzic, G.; Ignjatov, M.; Milosevic, D.; Milosevic, B. (2016): Comparative study of drought and salt stress effects on germination and seedling growth of pea. – Genetika 48: 373-381.
[23] Radic, V.; Balalic, I.; Jacimovic, G.; Nastasic, A.; Savic, J.; Marjanovic-Jeromela, A. (2019): Impact of drought and salt stress on seed germination and seedling growth of maize hybrids. – Genetika 51: 743-756.
[24] Shi, D.; Sheng, Y. (2005): Effect of various salt-alkaline mixed stress conditions on sunflower seedlings and analysis of their stress factors. – Environmental and Experimental Botany 54: 8-21.
[25] Wierzbicka, M.; Obidzińska, J. (1998): The effect of lead on seed imbibition and germination in different plant species. – Plant Science 137: 155-171.

http://www.aloki.hu ● ISSN 1589 1623 (Print) ● ISSN 1785 0037 (Online)
DOI: http://dx.doi.org/10.15666/aeer/1906_42994311

[26] Wu, G. Q.; Shui, Q. Z.; Wang, C. M.; Zhang, J. L.; Yuan, H. J.; Li, S. J.; Liu, Z. J. (2015a): Characteristics of Na^+ uptake in sugar beet (*Beta vulgaris* L.) seedlings under mild salt conditions. – Acta Physiologiae Plantarum 37: 1-13.
[27] Wu, H.; Shabala, L.; Liu, X.; Azzarello, E.; Zhou, M.; Pandolfi, C.; Pandolfi, C.; Chen, Z.; Bose, J.; Mancuso, S.; Shabala, S. (2015b): Linking salinity stress tolerance with tissue-specific Na^+ sequestration in wheat roots. – Frontiers in Plant Science 6: 71.
[28] Wu, G. Q.; Jia, Z.; Liu, H. L.; Wang, C. M.; Li, S. J. (2017): Effect of salt stress on growth, ion accumulation, and distribution in sainfoins (*Onobrychis viciaefolia*) seedlings. – Pratacultural Science 34: 1661-1668.
[29] Wu, G. Q.; Li, H., Zhu, Y. H., Li, S. J. (2021): Comparative physiological response of sainfoin (*Onobrychis viciaefolia*) seedlings to alkaline and saline-alkaline stress. – Journal of Animal and Plant Sciences. 31(4): 1028-1035.
[30] Yang, C. W.; Zhang, M. L.; Liu, J.; Shi, D. C.; Wang, D. L. (2009): Effects of buffer capacity on growth, photosynthesis, and solute accumulation of a glycophyte (wheat) and a halophyte (*Chloris virgata*). – Photosynthetica 47: 55-60.
[31] Yang, X.; Baskin, J. M.; Baskin, C. C.; Huang, Z. (2012): More than just a coating: ecological importance, taxonomic occurrence and phylogenetic relationships of seed coat mucilage. – Perspectives in Plant Ecology Evolution & Systematics 14: 434-442.
[32] Zahra, K.; Ifar, M.; Motamedi, M. (2011): Effects of NaCl salinity on maize (*Zea mays* L.) at germination and early seedling stage. – African Journal of Biotechnology 11: 298-304.
[33] Zhang, H.; Zhang, G.; Lu, X.; Zhou, D.; Han, X. (2014): Salt tolerance during seed germination and early seedling stages of 12 halophytes. – Plant and Soil 388: 229-241.

http://www.aloki.hu ● ISSN 1589 1623 (Print) ● ISSN 1785 0037 (Online)
DOI: http://dx.doi.org/10.15666/aeer/1906_42994311

THE IMPACT OF THE ECOHYDROLOGIC CONDITIONS OF THREE GORGES RESERVOIR ON THE SPAWNING ACTIVITY OF FOUR MAJOR CHINESE CARPS IN THE MIDDLE OF YANGTZE RIVER, CHINA

GUO, W. X.* – JIN, Y. G. – ZHAO, R. C. – WANG, H. X.

[1]*North China University of Water Resources and Electric Power, Zhengzhou 450045, China*

[2]*Key Laboratory of Water Resources Conservation and Intensive Utilization in Yellow River Basin of Henan Province, Zhengzhou 450045, China*

**Corresponding author*
e-mail: whxzju@163.com; phone: +86-135-9257-3656

(Received 2nd Jun 2020; accepted 29th Jul 2021)

Abstract. Black carp (*Mylopharyngodon piceus*), grass carp (*Ctenopharyngodon idella*), silver carp (*Hypophthalmichthys molitrix*) and bighead carp (*Aristichthys nobilis*) are the four major Chinese carps and are migratory fishes living in rivers and lakes in the Yangtze River of China. The flow regime alternation of rivers has an impact on the spawning and reproduction conditions of four major Chinese carps in the lower reaches of the Three Gorges Reservoir. To investigate the changes in hydrological conditions and spawning and reproduction performances of four major Chinese carps during their spawning period before and after impoundment of Three Gorges Reservoir, a quantitative analysis of the relevance between such hydrological parameters as flow, water level, sediment concentration and water temperature of Yichang Station and larva runoff of the four species during their spawning period was carried out. As suggested by the results, when four major Chinese carps are spawning, the proper hydrological parameters would be 11,000-15,000 m^3/s for flow, 43.0-46.0 m for water level, 0.01-0.21 kg/m^3 for sediment concentration and 4-8 d for water rise, and 22-24℃ for water temperature. Among those values, water rise and sediment concentration appear to be in significant positive correlation with the larvae abundance of four major Chinese carps, and thus remain critical factors. After the impoundment of Three Gorges Reservoir, the declining trend in flow, water level and water temperature during the spawning period of four major Chinese carps is not significant when compared with that in sediment concentration (by over 98%). The spawning and reproduction time of four species also gets retarded due to the late-coming proper water temperature, so does the spawning scale. The proportions of four carps also change a lot, with *silver* carp ascending to be at the highest ratio among them. This study can provide a reference for the protection of important fishes in the lower reaches of Three Gorges Reservoir.

Keywords: *Three Gorges Reservoir, Yichang Station, eco-hydrological conditions, four major Chinese carps, spawning ground*

Introduction

In past decades, hydraulic engineering, a much-disputed human activity, is gaining more and more attention (Ban et al., 2014). On one hand, it does bring economic benefits such as flood control, irrigation, power generation, shipping, industry and urban domestic water to human beings (Poff et al., 1997; Jiang et al., 2014); on the other, it also changes

http://www.aloki.hu ● ISSN 1589 1623 (Print) ● ISSN1785 0037 (Online)
DOI: http://dx.doi.org/10.15666/aeer/1906_43134330

the natural hydrological conditions of rivers and overturns their original continuity, producing some negative effect on the species composition and adaptability of biocoenosis within the reaches in question (Cai et al., 2018; Grill et al., 2019). As the hydraulic engineering development gets enhanced, the original hydrological conditions of rivers will definitely suffer a more severe impact, and the balance of riverine ecosystem will be thus destroyed (Xue et al., 2017). As a result, to study the impact of hydraulic engineering development on hydrological conditions and ecology of rivers turns out to be a hot spot in the current riverine eco-hydrology research field (Li et al., 2011; Wang et al., 2018).

Three Gorges Reservoir is situated at the middle reaches of Yangtze River. Within its downstream segment from Yichang to Chenglingji, there is a spawning site for the important commercial fishes, namely "four major Chinese carps" which accounts for 42.7% of total spawning capacity along the River. This is one of the most important natural reproduction zones for Chinese carps in Yangtze River (Guo et al., 2011; Li et al., 2013). The impoundment at Three Gorges Reservoir has produced a significant effect on the spawning and reproduction of four major Chinese carps, which is analyzed by some scholars. Li et al. (2012) deduced the principal hydrological parameters affecting spawning activity of fishes by figuring out the flow demand of four major Chinese carps in Yangtze River by using the variational method. By defining a series of water temperature parameters, Cai et al. (2017) analyzed the change in reproduction time of four major Chinese fishes and water temperature parameters before and after the impoundment of Three Gorges Reservoir and suggested that low temperature of discharging water may be held responsible for the delay of reproduction time. Peng et al. (2012) revealed the possible adverse effect of dissolved gas supersaturation resulting from post-impoundment flood discharge at Three Gorges Reservoir on the spawns and larval fishes of four major Chinese carps. Apart from those, there are also some other related studies (Zhao et al., 2012; Yang et al., 2017).

Fish conservation has been the focus of discussion on many environmental issues. The construction of reservoir dam has changed the natural rhythm of surface runoff, resulting in significant changes in the physical environment, chemical environment, biome structure and function of river ecosystem (Chen et al., 2017; Herath et al., 2020). According to statistics, 85 of the 113 major rivers in Canada, the United States, Europe and the former Soviet Union were affected by major construction, resulting in changes in downstream hydrological processes, fragmentation or disappearance of aquatic habitats, and declining fish diversity and resource levels (Li et al., 2018). Over the past hundred years, dam construction has led to the threat or extinction of nearly 1,800 species of identifiable freshwater fish worldwide (Agostinho et al., 2008; Dai et al., 2017). At present, the impact of hydropower development on fish has become the focus of attention of all sectors of society, and the protection of fish habitat has become an important part of the ecological protection system of hydropower engineering construction (Feng et al., 2013; Zhang et al., 2017, 2018).

http://www.aloki.hu ● ISSN 1589 1623 (Print) ● ISSN1785 0037 (Online)
DOI: http://dx.doi.org/10.15666/aeer/1906_43134330

Since a majority of previous studies concentrate on single hydrological parameter, whereas spawning and reproduction behaviors of four major Chinese carps are under the influence of multiple factors. In this study, the hydrological parameters and the larvae runoff monitoring data downstream Three Gorges Reservoir were investigated to evaluate the impact of the eco-hydrologic conditions of Three Gorges Reservoir on the spawning activity of four major Chinese carps. Our objectives were (1) to determine the correlation between the hydrological conditions and the spawning activity of four major Chinese carps; (2) to analyze the variation of hydrological conditions during spawning period of four major Chinese carps before and after impoundment at Three Gorges Reservoir; (3) to assess the impacts of Three Gorges Reservoir on the spawning and reproduction activities of four major Chinese carps. The study can provide a theoretical basis for rvierine ecosystem protection of the Yangtze River.

Study area and methods

Sampling location and time

The present study selected the spawning site of four major Chinese carps in lower reaches of Three Gorges Reservoir as the research area. Ever since the founding of the People's Republic of China, three influential investigations concerning the reproductive habits, spawns, larval fish development, spawning site distribution, and spawning scale of four major Chinese carps have been conducted during 1958-1966, 1981-1986 and 1997-2010, respectively. During those investigations, a great number of monitoring data were generated. In accordance with a survey by Institute of Hydrobiology, there were altogether 30 spawning sites for four major Chinese carps in Tianjia Township from Chongqing to Hubei before Gezhou Dam Hydro-Junction was built, among which 11 were located in the segment from Yichang to Chenglingji with 42.7% of total spawning quantity along the river. Those spawning sites are the habitats of spawning and reproduction for four major Chinese carps with critical ecological functions and constitute important eco-functional regions in the biological resources of Yangtze River. After Gezhou Dam was completed, the major spawning sites above the dam include Xinshi Township, Pingshan, Anbian, Chongqing, Changshou, Wuling, Gaojia Township, Zhongxian County, Wushan, Badong and Liantuo, while those below the dam are Yichang-Zhicheng Cross-section, Jingshan-Jianli Cross-section, Chenglingji-E'Cheng-Wuxue Cross-section, Jiujiang-Hukou-Pengze Cross-section. From Yichang to Chenglingji along Yangtze River, there are 10 spawning sites for four major Chinese carps, among which 9 are located at Jianli and the cross-sections above it. The relative positions of spawning sites are demonstrated in *Fig. 1*.

http://www.aloki.hu ● ISSN 1589 1623 (Print) ● ISSN1785 0037 (Online)
DOI: http://dx.doi.org/10.15666/aeer/1906_43134330

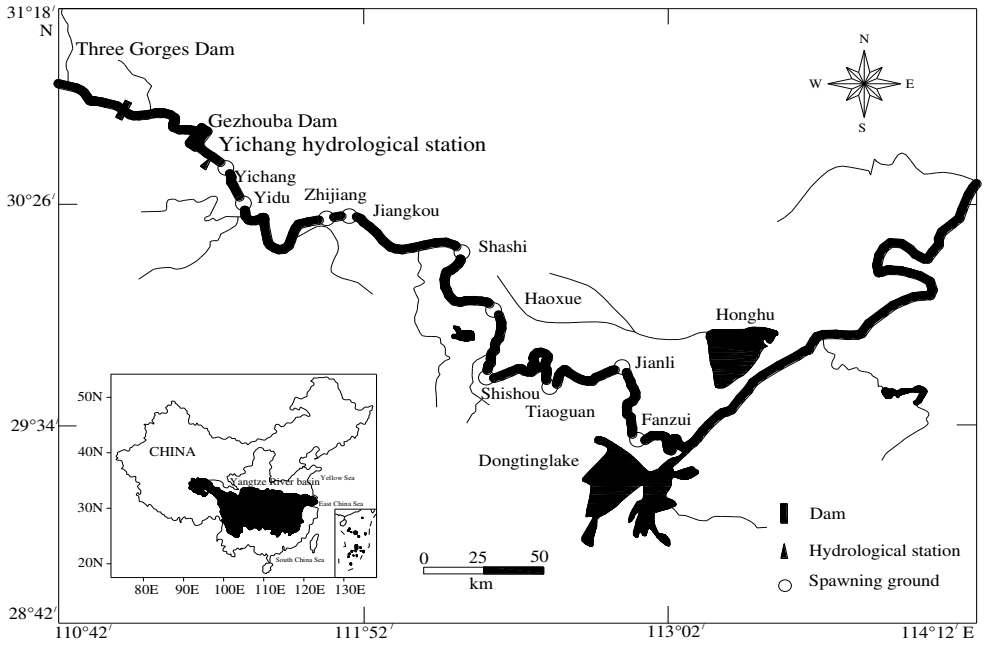

Figure 1. *Distribution of spawning sites of four major Chinese carps in middle reaches of Yangtze River*

In the Yangtze River, silver carp usually reproduce in late April to early July, and middle May to middle June is the best time for breeding (Yi et al., 1988). The breeding activity of bighead carp is usually from May to July, slightly later than that of silver carp. The reproductive period of grass carp is usually earlier than that of black carp. Generally spawning begins in late April or early May and ends in late June or early July. The spawning period of black carp is from May to July, a little later than that of grass carp and silver carp. Spawning requirements of four major Chinese carps are specific and rigorous: they typically spawn in large and turbid rivers; the lowest water temperature for spawning is 18°C, with a peak occurring at 21–24°C; an increase in the river flow is the key triggering factor to spawning. Eggs and larvae need to drift in the freeflowing river reaches for at least 100 km until they grow large enough to migrate into the nursery habitats of connecting lakes, such as Dongting Lake and Poyang Lake (Zhang et al., 2000; Chen et al., 2009).

The spawning grounds of four major Chinese carps are generally located in the area of curved river, wide and narrow river surface and complicated riverbed topography, or there are sandbars and reefs in the middle of the river, or sandy beaches and rocky beaches along the river. In these regions, the flow direction and velocity are various, and the flow pattern is extremely turbulent. Special environmental conditions form complex and diverse flow characteristics, which provide the environmental factors needed for the fish to spawn. *Figure 2* are the photos of the typical spawning grounds.

http://www.aloki.hu ● ISSN 1589 1623 (Print) ● ISSN1785 0037 (Online)
DOI: http://dx.doi.org/10.15666/aeer/1906_43134330

Figure 2. *The photos of typical spawning grounds*

Data and statistical analysis

Survey and monitoring of carps' larvae

Every year from 1997 to 2005, sampling was conducted daily between May 1 and June 30. Samples were collected twice daily, once between 9:00 and 11:00, and once between 15:00 and 17:00. The gears used for capture of larvae were a ring net and a trap net. A ring net was used to gather larvae and eggs from different water depths. The ring net consisted of a round mouth formed by a steel loop (diameter=50 cm; area=0.1963 m^2), a conical net and a collection bucket. The netting was made of fine silk with the grid size of 0.5 mm. A steel frame supported the whole body. A flow meter was fixed in the mouth of the net. A large weight was attached to the bottom of the frame to assist sinking the net into the flowing water. Trap nets were used to collect eggs and larvae from near water surface in littoral areas.

The underlying data for this study are measured hydrological data and seedling monitoring data for the spawning period of fish in protected areas for 2009-2016, and the sources and related processing of the data are as follows: Since 2009, the Yangtze River Fisheries Research Institute of the Chinese Academy of Aquatic Sciences has carried out routine monitoring of fish resources in protected areas, including the monitoring points of the early fish resources in the upper reaches of the Yangtze River in the Jiangjin district of several river sections (E106°15°, N29°18'), fish eggs are collected from May 1 to July 10, each day from 09:00-11:00 a.m. and 15:00-17:00 p.m.

http://www.aloki.hu ● ISSN 1589 1623 (Print) ● ISSN1785 0037 (Online)
DOI: http://dx.doi.org/10.15666/aeer/1906_43134330

Data processing and evaluation

The field data should record the parameters of water depth, current velocity and sediment of each fish sample. Fish samples were clearly classified by species and age, and their length and weight were recorded. At the same time, other habitat parameters such as type of deep pool, cover or shelter were recorded. *Figure 3* is the distribution of the current velocity in the spawning ground of a certain fish in a river. Unless the observed data is very large, the frequency distribution curve will not be very smooth, so the data can be grouped by a certain width of interval to increase the smoothness of the curve. The formula of interval width is shown in (1). The fitness curve can be obtained from the midpoint of each interval of a simple continuous frequency histogram. Smooth the curve further if necessary (*Figure 3*). The data can also be standardized by dividing by the maximum of the curve to get a fitness of 0 ~ 1. *Table 1* shows the results of an analysis of a field observation.

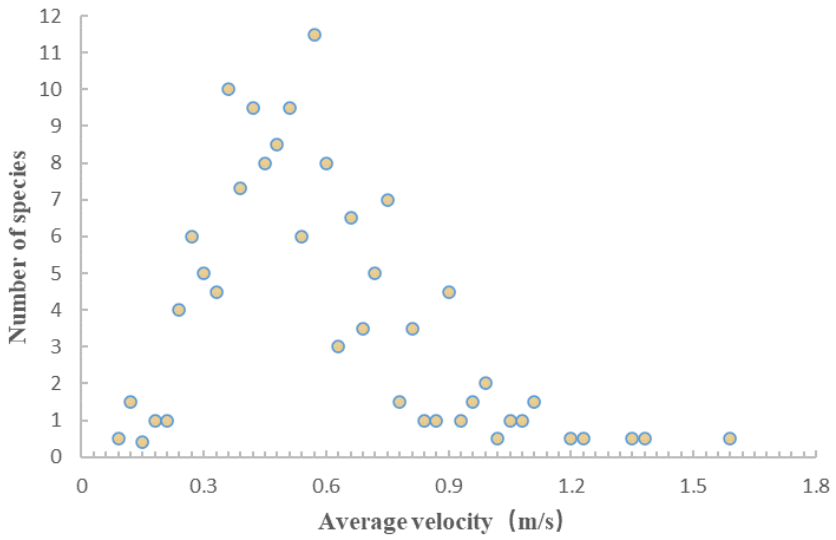

Figure 3. *Velocity distribution in fish spawning ground*

Table 1. *Field observation data and preference function of fish depth preference*

Depth /cm	Area /m^2	Number	N/N_{max}	A/A_{max}	N_{norm}/A_{norm}	Preference	Smoothing Preference
0~10	100	0	0	1.00	0	0	0
10~20	70	19	0.51	0.70	0.73	0.37	0.50
20~30	50	37	1.00	0.50	2.00	1.00	1.00
30~40	45	31	0.84	0.45	1.86	0.93	1.00
40~50	60	25	0.68	0.60	1.13	0.56	0.60
50~60	40	13	0.35	0.40	0.88	0.44	0.45
60~70	30	5	0.14	0.30	0.45	0.23	0.30
70~80	25	3	0.08	0.25	0.32	0.15	0.15
80~90	20	3	0.08	0.20	0.41	0.20	0.15
90~100	10	0	0	0.10	0	0	0

http://www.aloki.hu ● ISSN 1589 1623 (Print) ● ISSN1785 0037 (Online)
DOI: http://dx.doi.org/10.15666/aeer/1906_43134330

The formula for interval width is

$$I=\frac{R}{I+3.908\lg N} \quad \text{(Eq.1)}$$

Formula: I for the best spacing size, R for the observed value range, n for the observed number of species.

The frequency data for habitat use need only be plotted at simple locations based on measured data, while the habitat preference function must include the availability of different habitat quality, as shown in *Table 1*. The number of individuals divided by the proportion of the total habitat area (or volume) in some ranges can yield very different fitness curves. If the proportion of a category is too small, the ratio may be too large, so species abundance and area need to be standardized first.

In this study, the hydrological data about Yichang Station in lower reaches of Yangtze River were placed under an analysis. This hydrological station is of the control station of Three Gorges Reservoir, which can well reflect the change characters of the flow at the four major Chinese carps' spawning sites in the lower reaches of Yangtze River. Besides, the data about water level, flow rate, water temperature and sediment concentration at Yichang Station (during 1956-2016) have a long history and are thus highly representative. The four major Chinese carps in the downstream Jianli cross-section of Three Gorges Reservoir were selected here as the research objects. This cross-section is situated at about 210 km downstream from Yichang, and the spawning site extended by 25 km. The hydrological data about Yichang Station were collected from Hydrological Yearbook of Yangtze River, while the larvae runoff monitoring data from Yangtze River Three Gorges Ecological and Environmental Monitoring Bulletin (during 1997-2016).

Results

Analysis of correlation between the spawning and reproduction of four major Chinese carps and the hydrological conditions

From 1997 to 2016, altogether 26 batches of four major Chinese carps were monitored as spawning in corresponding sites of Jianli, and the water level, flow rate, sediment concentration and water temperature data of that day were either measured or collected on site for an analysis of the average, minimum, maximum values as well as the suitable range of flow rate during the spawning period of four major Chinese carps (*Table 2*).

To conduct statistics of suitable range of flow rate during spawning period of four major Chinese carps, the spawning frequency of those fishes in the major flow rate characteristics were recorded to obtain the frequency curves of all the hydrological characteristic indicators as shown in *Fig. 4*.

As revealed by an analysis of four major Chinese carps' spawning and reproduction conditions, the spawning activity of them is almost all done during flooding season.

http://www.aloki.hu ● ISSN 1589 1623 (Print) ● ISSN1785 0037 (Online)
DOI: http://dx.doi.org/10.15666/aeer/1906_43134330

Flooding is a process containing changes in a string of hydrological elements, including elevated water level and flow, accelerated flow rate, reduced transparency, and disorderly flow state, during which flow rate is accelerated so that four major Chinese carps are stimulated to become mature and parent fishes begin spawning and discharging seminal fluid. As the water levels lowers and flow rate decelerates, most of the reproductive activities come to a stop.

Table 2. *Principal hydrological characteristics of spawning cross-sections for four major Chinese carps*

Eigenvalues	Flow (m^3/s)	Water level (m)	Sediment concentration (kg/m^3)	Water temperature (℃)	Rise rate of flow ($m^3/s \cdot d$)	Rise rate of water-level (m/d)	Flooding period (d)
Means	17529	45.17	0.378	23.4	1615	0.54	7
Minimum	7958	41.4	0.003	20.9	120	0.06	2
Maximum	34700	49.88	1.41	25.8	5675	1.60	15
Standard deviation	5695	1.9	0.44	1.3	1523	0.39	3
Suitable range	11000-15000	43-46	0.01-0.21	22-24	100-1000	0.3-0.55	4-8

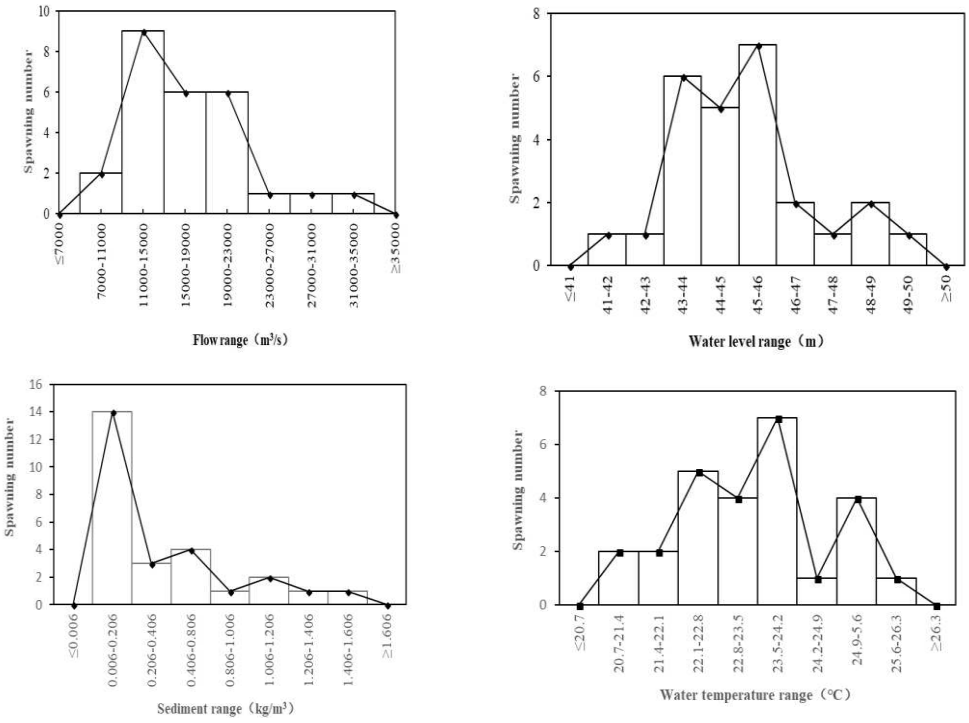

Figure 4. *Frequency curves of the hydrological indicators*

http://www.aloki.hu ● ISSN 1589 1623 (Print) ● ISSN1785 0037 (Online)
DOI: http://dx.doi.org/10.15666/aeer/1906_43134330

To quantify the relation between spawning quantity of four major Chinese carps and hydrologically influential factors, we fitted the larvae runoff and hydrological factors during spawning period. The fitting relationship between larvae runoff and flooding period can be expressed as $y = 1.1842x - 0.4614$ with a coefficient of association of 0.58 and is significant positive (*Fig. 5*), and that between larvae runoff and sediment concentration expressed as $y = 7.4458 + 1.8296$ with a coefficient of association of 0.58 and is significant positive (*Fig. 6*). The correlations between larvae runoff and other hydrological indicators are less significant. It can be thus inferred that flooding period and sediment concentration are two important factors affecting the spawning quantity of four major Chinese carps.

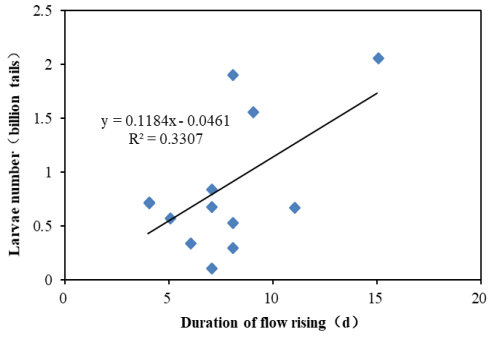

Figure 5. *The correlation curve of Duration of flow rising vs. larvae number*

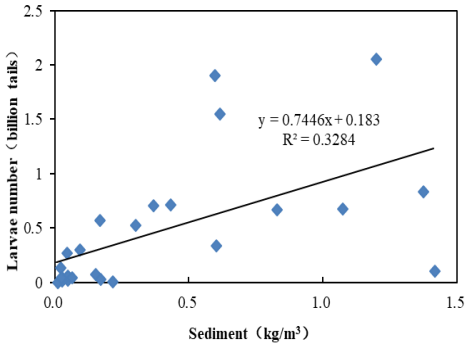

Figure 6. *The correlation curve of sediment vs. larvae number*

Change in hydrological conditions during spawning season of four major Chinese carps before and after impoundment at Three Gorges Reservoir

This study highlights the change in the flow rate, water level, water temperature and sediment concentration of Yichang Station during the prosperous spawning months, May and June, of four major Chinese carps before and after the impoundment by Three Gorges Reservoir. To check the significance of change trend in all the hydrological factors during spawning season of four major Chinese carps, Mann-Kendall trend test was performed and the results are provided in *Table 3*. According to the results of test, there is no significant change in the flow rate during the spawning season of four major Chinese carps, but water level, water temperature and sediment concentration change considerably. Water level and water temperature in May passed 95% confidence test at a significant declining trend and while water level in June and sediment concentration in May and June passed 99% confidence test with a significant declining trend. It can be thus seen that during the spawning season of four major Chinese carps, such hydrological factors as

http://www.aloki.hu ● ISSN 1589 1623 (Print) ● ISSN1785 0037 (Online)
DOI: http://dx.doi.org/10.15666/aeer/1906_43134330

water level, water temperature and sediment concentration undergo a significant change which can be attributed to the impoundment at Three Gorges Reservoir.

Table 3. *Analytic table of hydrological indicators' trend at Yichang Station during spawning season of four major Chinese carps*

Hydrological indicators	Month	Z_c	Rulebook	Trend
Flow	May	0.34	$\|Z_c\| < 1.96$	Increase
	June	-0.29	$\|Z_c\| < 1.96$	Decrease
Water level	May	-2.40	$1.96 < \|Z_c\| < 2.58$	Decrease*
	June	-3.90	$\|Z_c\| > 2.58$	Decrease**
Water temperature	May	-2.19	$1.96 < \|Z_c\| < 2.58$	Decrease*
	June	-1.78	$\|Z_c\| < 1.96$	Decrease
Sediment concentration	May	-7.95	$\|Z_c\| > 2.58$	Decrease**
	June	-5.69	$\|Z_c\| > 2.58$	Decrease**

* Significant trend at 0.05 confidence level; ** Significant trend at 0.01 confidence level

To analyze the hydrological impact of impoundment at Three Gorges Reservoir on spawning season of four major Chinese carps in 2003, we summarized and analyzed the change in all the hydrological elements before and after the impoundment at Three Gorges Reservoir (*Table 4*). It can be inferred from *Table 3* that after impoundment at Three Gorges Reservoir, all the hydrological factors displayed a declination in varying degrees. The average flow rate in June of several years dropped by 960 m^3/s (5.32%) when compared with that before dam construction; average water level in May and June of several years declined by 8.24% and 3.15%, respectively; the declination in sediment concentration was most striking by being 98.11% (0.52 kg/m^3) and 97.94% (0.95 kg/m^3) in May and June, respectively. Therefore, water level doesn't affect much the spawning and reproduction of four major Chinese carps. The declination in flow rate in May does inhibit the river flow during the spawning season of those fishes, but water temperature drop directly postpones their spawning time so that they have greatly reduced time for spawning. The dramatic decrease in sediment concentration may change the riverbed configuration in spawning sites of those carps, affecting their habitat conditions and thus their spawning and reproduction in a negative way.

Change in spawning and reproduction of four major Chinese carps before and after impoundment at Three Gorges Reservoir

Analysis of four major Chinese carps' spawning time before and after impoundment at Three Gorges Reservoir

On the basis of spawning monitoring data about four major Chinese carps in past years, the spawning activity of those fishes begins as early on April 28 and late on May 10 and

http://www.aloki.hu ● ISSN 1589 1623 (Print) ● ISSN1785 0037 (Online)
DOI: http://dx.doi.org/10.15666/aeer/1906_43134330

ends as early on June 15 and late on July 5. The spawning and reproduction of four major Chinese carps was found to be closely related to water temperature which mainly ranges between 14℃ and 30℃ from late April to late July at Yichang Hydrological Station. In natural conditions, four major Chinese carps begin spawning at 18℃ and remain most actively reproductive at 20-24℃, but end the activity when the temperature is below 18℃. *Fig. 7* illustrates the change in lowest water temperature at Yichang Station during the spawning and reproduction period of four major Chinese.

Table 4. *Hydrological condition of spawning grounds of four major Chinese carps at the Yichang station in May and June*

Month		Flow (m^3/s)	Water level (m)	Water temperature (℃)	Sediment concentration (kg/m^3)
May	Per-impact	11560	41.22	21.24	0.53
	Post-impact	12315	40.98	19.49	0.01
	Change	755	-0.24	-1.75	-0.52
	Change degree	6.53%	-0.59%	-8.24%	-98.11%
June	Per-impact	18060	43.62	23.47	0.97
	Post-impact	17100	42.66	22.73	0.02
	Change	-960	-0.96	-0.74	-0.95
	Change degree	-5.32%	-2.20%	-3.15%	-97.94%

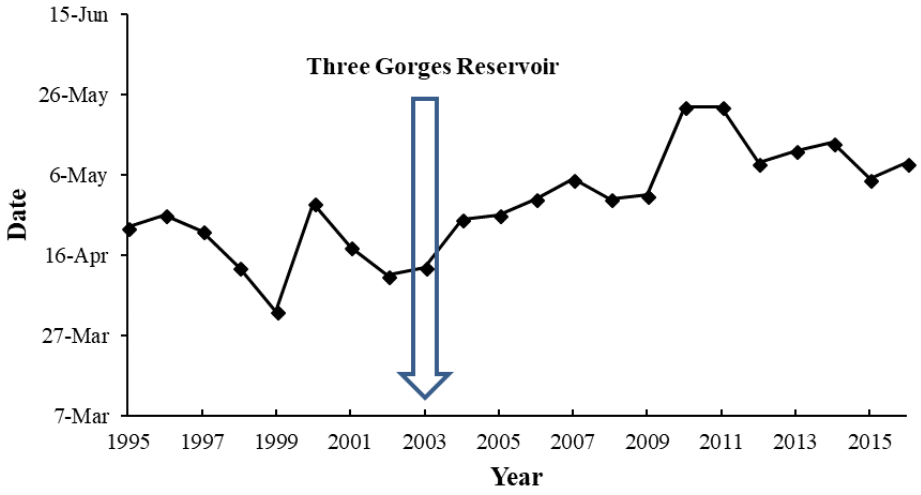

Figure 7. *Change in date of the lowest water temperature during spawning and reproduction season of four major Chinese carps over the years*

By checking the change in date on which daily average water temperature is stabilized at 18℃ during spawning and reproduction period of four major Chinese carps before and

http://www.aloki.hu ● ISSN 1589 1623 (Print) ● ISSN1785 0037 (Online)
DOI: http://dx.doi.org/10.15666/aeer/1906_43134330

after impoundment at Three Gorges Reservoir, we can find that during this period, little change occurs in term of effect of impoundment by the dame on the water temperature. After Three Gorges Reservoir begins impoundment, the water temperature at Yichang Station in April and May is lower than that in natural state before the impoundment by 2℃. During 2004-2008, when four major Chinese carps begin spawning and reproduction, the date on which daily average temperature of Yichang Station gets stabilized at 18℃ are April 25, 26, 30, May 5 and April 30, respectively, later than that before impoundment by 10 days or so. During 2009-2013, the dates are May 10, 23, 23, 9 and 12, respectively, later than that after the impoundment by 10 days. Therefore, the impoundment at Three Gorges Reservoir does cause a postponement in the spawning and reproductive activities of four major Chinese carps, and the average postponement is about 20 days. It produces certain effect on their spawning activity which is postponed from the late April before impoundment to middle and late May and even early June after that.

Analysis of spawning scale of four major Chinese carps before and after the impoundment at Three Gorges Reservoir

In accordance with 1997 Yangtze River Three Gorges Project Ecological and Environmental Monitoring Bulletin from Chongqing to Tianjia Township, among which 11 are located from Chongqing to Yichang and 11 in the 400 km Yichang-Chenglingji Cross-section downstream of the dam reservoir area, and 8 in Chenglingji-Wuxue Cross-section. Before the impoundment at Three Gorges Reservoir, the larval fishes on Jianli cross-section mainly come from the spawning sites of four major Chinese carps above Gezhou Dam and reached a peak in term of spawning quantity in 1986 with larvae runoff being 7.2 billion. The larvae runoff monitoring results about four major Chinese carps on Jianli cross-section before and after the impoundment by Three Gorges Reservoir are derived from Yangtze River Three Gorges Project Ecological and Environmental Monitoring Gazette over the years (1997-2016) and provided in *Fig. 8*.

http://www.aloki.hu ● ISSN 1589 1623 (Print) ● ISSN1785 0037 (Online)
DOI: http://dx.doi.org/10.15666/aeer/1906_43134330

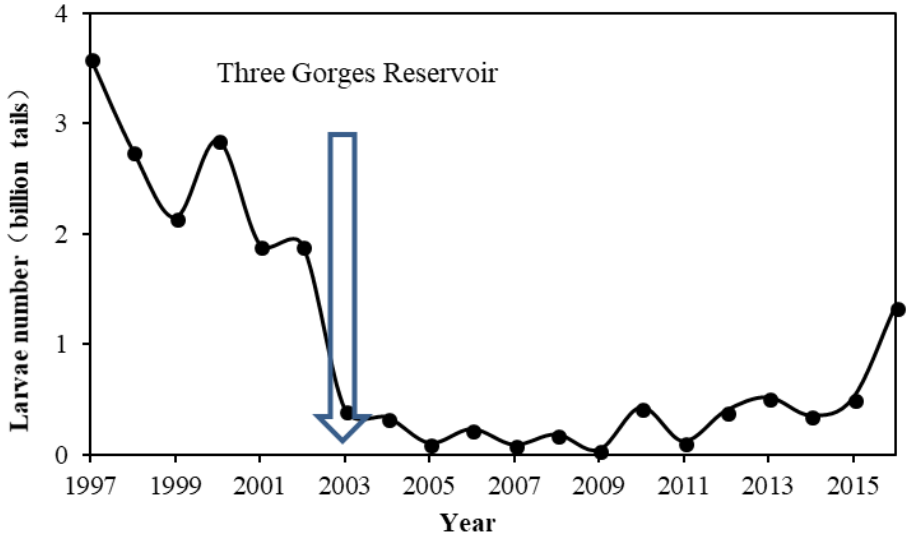

Figure 8. *The monitoring results of four major Chinese carps' larvae runoff at the Jianli cross-section*

As revealed in *Fig. 8*, after impoundment is initiated at Three Gorges Reservoir, significant adverse effect has been produced on the spawning and reproduction of four major Chinese carps. The larvae runoff during 2003-2016 displays a notable drop from 2.52 billion before impoundment to 0.29 billion after that. Since the larval fishes on Jianli cross-section are from the spawning sites in Yichang, Yidu, Jiangkou, Shishou and Diaoguan, the larvae runoff on this cross-section is found to be in dramatic declination with the lowest value (0.042 billion only) showing in 2009, and no larval flood was detected for the first time in 2005. In 2010, 0.43 billion larval fishes were detected, which are significantly higher than that in 2009. The major overlying reason is that a lot of original parent fishes were released in Shishou and Jianli cross-sections in this year and great flood peaks appeared in late June and early July. In order to promote spawning and reproduction among four major Chinese carps, ecological scheduling experiments have been launched at Three Gorges Reservoir since 2011. According to the experiments, when four major Chinese carps begin spawning and reproduction, the discharged flow of dam is underregulated. As suggested by the monitoring results, the effect of ecological scheduling is obvious and the spawning scale of those four major Chinese carps gets improved. The larvae runoff during 2012-2016 was 0.397 billion, 0.52 billion, 0.355 billion, 0.51 billion and 1.34 billion, respectively.

Analysis of spawning fish composition among four major Chinese carps before and after impoundment at Three Gorges Reservoir

On the basis of data from several monitoring activities targeting four major Chinese carps in the history as well as those in recent four years, the composition of larval fishes of four major Chinese carps on Jianli-Sanzhou cross-section is demonstrated in *Fig. 9*.

http://www.aloki.hu ● ISSN 1589 1623 (Print) ● ISSN1785 0037 (Online)
DOI: http://dx.doi.org/10.15666/aeer/1906_43134330

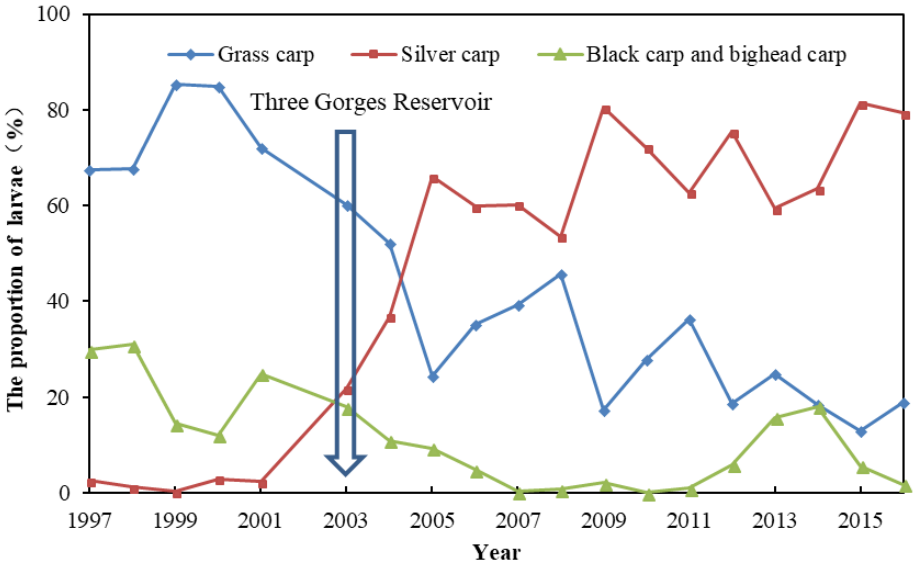

Figure 9. *The fry type of four major Chinese carps at the Jianli cross-section*

As shown in *Fig. 9*, before impoundment at Three Gorges Reservoir, the fishes on Jianli cross-section are mainly composed of grass carp and black carp, in which the former was overwhelming. The proportions of silver carp, black carp and bighead carp kept declining. By comparison, after the impoundment was started at Three Gorges Reservoir, great change occurred to the compositions of fishes in this cross-section, for the proportion of silver carp among larval fishes kept rising and reached 80.5% and 79.3%, respectively, in 2009 and 2016; the proportion of grass carp declined from 60.2% in 2003 to 18.9% in 2016; and the proportions of black carp and bighead carp were reduced to the lowest value (<2%).

Discussion

The correlation between the spawning and reproduction of four major Chinese carps and the hydrological conditions

Hydrological factors affecting the reproduction of four major Chinese carps

Studies have shown that the key hydrological indicators affecting the reproduction of domestic fish are flow rate growth and flood duration (Feng et al., 2013; Xie et al., 2015). In this study, the response relationship between the early resources of the four major Chinese carps to the hydrological process was analyzed, and it was also concluded that there was a significant positive correlation between the number of domestic fish eggs and the flow growth rate during the flood process. When the duration of rising water was 3 d, the number of eggs and seedlings of domestic fish was low, and when the duration of rising water was 4 d or above, the number of eggs and seedlings of domestic fish was relatively high. Therefore, within a certain range of flow growth rate, the larger flow growth rate is beneficial to the reproduction of the four major Chinese carps. When the

http://www.aloki.hu ● ISSN 1589 1623 (Print) ● ISSN1785 0037 (Online)
DOI: http://dx.doi.org/10.15666/aeer/1906_43134330

flood duration is too low, it cannot achieve the purpose of stimulating domestic fish to lay eggs.

The role of ecological dispatch in the breeding of domestic fish in the Jianli section

Four major Chinese carps in the spring water temperature rose to more than 18 degrees C to start spawning, 15 to 20 degrees C process for four major Chinese carps glands from stage 3 to stage 4 has an important impact, after more than 20 degrees C, or even higher water temperature of 21 degrees C, the sexual gland development of domestic fish will be quickly completed, sexual maturity of the four major Chinese carps pro-fish began to concentrate on breeding. During the ecological dispatch period from 2013 to 2017, the water temperature in the section of the River reached 18 degrees C, and heated up one by one, and then reached more than 20 degrees C, and the water temperature during the ecological dispatch period reached the basic requirements of the spawning water temperature of domestic fish.

According to the analysis of this study, when the ecological scheduling time of the Three Gorges Reservoir was in late June, the ecological scheduling promoted the formation of an effective water-inflation process in the Jianli River. The duration of water-inflation reached 4 d and above, and the flow growth rate reached 1600-2833 $m^3/(s \cdot d)$, which would stimulate the concentrated reproduction of domestic fish. The scholar has comprehensively analyzed the eco-environmental flow demand of domestic fish in the middle reaches of the Yangtze River before and after the operation of the Three Gorges (Li et al., 2015). It was considered that the normal reproduction of domestic fish was from June 15 to July 20 every year, and the flood rate was 900-3100 $m^3/(s \cdot d)$. The conclusion of this study is within this range, and on this basis, the duration and growth rate of water inflation are further quantified. The results of this study can be used as an ecological regulation scheme for the breeding activities of the four major Chinese carps in the Jianli section of the Three Gorges Reservoir.

Conclusions

According to an analysis of frequency curves of major hydrological factors during spawning and reproduction period of four major Chinese carps, the proper flow rate for spawning and reproduction activities of those carps is 11,000-15,000 m^3/s, the proper flow rate rising amplitude is 5,000-13,000 m^3/s, proper daily flow rate rising speed is 100-1,000 m^3/s d, and the proper flooding period is 4-8 d. Among those hydrological factors, flooding period is in significant positive correlation with the spawning and reproductive quantity of four major Chinese carps with a correlation coefficient of 0.58. The proper water level is 43.0-46.0 m, proper rising range for water level is 2.0-4.0 m and proper daily rising range is 0.3-0.55 m/d. The proper sediment concentration is 0.01-0.21 kg/m^3. The spawning quantity of those fishes and sediment concentration are in significant positive relation with correlation efficient being 0.57. The proper water

http://www.aloki.hu ● ISSN 1589 1623 (Print) ● ISSN1785 0037 (Online)
DOI: http://dx.doi.org/10.15666/aeer/1906_43134330

temperature range for spawning and reproduction of four major Chinese carps is 22-24℃. This last factor is not a critical one affecting the spawning and reproduction quantity of those carps, but it does influence the initial spawning and reproduction time of them.

In May and June, the monthly average flow rate, water level, water temperature and sediment concentration in Yichang section display a declining trend, among which the first three don't drop dramatically while the last one falls significantly at a confidence level over 95%. The sediment concentration declines by 0.52 kg/m^3 and 0.95 kg/m^3 in May and June after the impoundment, and the declination is over 98% of the pre-impoundment values. The great reduction in sediment concentration may change the riverbed structure of spawning sites for four major Chinese carps and produce a negative effect on the habitat conditions of them and further affect their spawning and reproduction activities.

An analysis of the spawning and reproduction conditions of four major Chinese carps in the middle reaches of Yangtze River reveals the number of spawning sites falls from 28 in the 1970s to present 8. The spawning scale also displays a dramatic declination, for as suggested by the cross-section monitoring results in Jianli, the spawning scale goes from 7.2 billion in 1986 to 0.52 billion now and even reaches 0.042 billion in 2009. In the larvae composition among four major Chinese carps, silver carp enjoys an absolute advantage, while the number of grass carp declines and that of dark carp and bighead carp drops sharply. The spawning and reproduction are also postponed with initial date postponed from the middle April in the past to the present middle May and spawning peak from the past middle May to the present late June.

In the future, we should combine engineering, non-engineering and management measures to comprehensively propose fish restoration and protection measures.

Acknowledgments. This work was supported by the National Nature Science Foundation of China (No. 51679090, 51609085, 51779094); the National Natural Science Foundation of Henan, China (No. 162102110015, 152300410113); Guizhou Water Resources Technology Project（KT202008).

Conflicts of Interests. The authors declare no conflicts of interests.

REFERENCES

[1] Agostinho, A. A., Pelicice, F. M., Gomes, L. C. (2008): Dams and The Fish Fauna of the Neotropical Region: Impacts and Management Related to Diversity and Fisheries. – Brazilian Journal of Biology 68(4): 1119-1132.

[2] Ban, X., Jiang, L. Z., Zeng, X. H., Du, Y., Xiao, F., Ling, F. (2014): Quantifying The Spatio-Temporal Variation of Flow and Sediment in The Middle Yangtze River After the Impoundment of the Three Gorges. – Advances in Water Science 25(2): 650-657. (In Chinese).

http://www.aloki.hu ● ISSN 1589 1623 (Print) ● ISSN1785 0037 (Online)
DOI: http://dx.doi.org/10.15666/aeer/1906_43134330

[3] Cai, Y. P., Yang, Z., Xu, W. (2017): Effect of Water Temperature Variation After Impoundment of the Three Gorges Reservoir on The Four Major Chinese Carps. – Advanced Engineering Sciences 49(1): 70-77. (In Chinese).
[4] Cai, H. Y., Piccolroaz, S., Huang, J. Z., Liu, Z. Y., Liu, F., Toffolon, M. (2018): Quantifying The Impact of the Three Gorges Dam on The Thermal Dynamics of the Yangtze River. – Environ. Res. Lett. 13(5): 054016.
[5] Chen, W., Olden, J. D. (2017): Designing Flows to Resolve Human and Environmental Water Needs in a Dam-Regulated River. – Nature Communications 8(1): 2158.
[6] Dai, M., Wang, J., Zhang, M., Chen, X. (2017): Impact of The Three Gorges Project Operation on The Water Exchange Between Dongting Lake and The Yangtze River. – International Journal of Sediment Research 32(4): 506-514.
[7] Feng, L., Hu, C. M., Chen, X. L., Zhao, X. (2013): Dramatic Inundation Changes of China's Two Largest Freshwater Lakes Linked to The Three Gorges Dam. – Environmental Science & Technology 47(17): 9628-9634.
[8] Grill, G., Lehner, B., Thieme, M., Geenen, B., Tickner, D., Antonelli, F., Maced, H. E. (2019): Mapping The World's Free-Flowing rivers. – Nature 569: 215-221.
[9] Guo, W. X., Wang, H. X., Xu, J. X., Xu, J. X. (2011): Effects of Three Gorges Reservoir on The Downstream Eco-Hydrological Regimes During the Spawning of Important Fishes. – Journal of Hydroelectric Engineering 30(03): 22-26. (In Chinese).
[10] Herath, I. K., Wu, S., Ma, M., Huang, P. (2020): Reservoir CO_2 Evasion Flux and Controlling Factors of Carbon Species Traced by Δ13cdic at Different Regulating Phases of a Hydro-Power Dam. – Science of the Total Environment 698: 134184.
[11] Jiang, L. Z., Ban, X., Wang, X., Cai, X. (2014): Assessment of Hydrologic Alterations Caused by the Three Gorges Dam in the Middle and Lower Reaches of Yangtze River, China. – Water 6: 1419-1434.
[12] Li, Q., Yu, M., Lu, G., Cai, T., Xia, Z., Ren, L. (2011): Impacts of the Gezhouba and the Three Gorges Reservoirs on the Sediment Regime of the Yangtze River. – Hydrol. 403: 224-233.
[13] Li, Q. Q., Qin, H., Chen, G. C., Wang, B. (2012): Analysis on Hydrologic Alternation of Middle Yangtze River and its Impact on Fish. – Yangtze River 43(11): 87-89. (In Chinese).
[14] Li, J., Xia, Z. Q., Dai, H. C., Yi, W. (2013): Effect of the Three Gorges Reservoir Initial Filling on Downstream Habitat Suitability of the Typical Fishes. – Journal of Hydraulic Engineering 44(8): 892-900. (In Chinese).
[15] Li, C., Zhou, J., Ouyang, S., Wang, C., Liu, Y. (2015): Water Resources Optimal Allocation Based on Large-Scale Reservoirs in the Upper Reaches of Yangtze River. – Water Resour Manage. 29(7): 2171-2187.
[16] Li, Z., Ma, J., Guo, J., Paerl, H. W., Brookes, J. D., Xiao, Y., Fang, F., Ouyang, W., Lu, L. (2018): Water Quality Trends in the Three Gorges Reservoir Region Before and After Impoundment (1992-2016). – Ecohydrology & Hydrobiology 203: 1-11.
[17] Peng, Q. D., Liao, W. G., Li, C., Yu, X. Z. (2012): Impacts of Four Major Chinese Carps' Natural Reproduction in the Middle Reaches of Yangtze River by Three Gorges Project Since the Impoundment. – Advanced Engineering Sciences 44(S2): 228-232. (In Chinese).
[18] Poff, N. L., Allan, J. D., Bain, M. B., Karr, J. R., Prestegaard, K. L., Richter, B. D., Sparks, R. E., Stromberg, J. C. (1997): The Natural Flow Regime. – Bioscience 47: 769-784.
[19] Wang, Y., Zhang, N., Wang, D., Wu, J., Zhang, X. (2018): Investigating the Impacts of Cascade Hydropower Development on The Natural Flow Regime in The Yangtze River, China. – Total Environ 624: 1187-1194.
[20] Xie, Y. H., Yue, T., Chen, X. S., Feng, L., Deng, Z. M. (2015): The Impact of Three Gorges Dam on the Downstream Eco-Hydrological Environment and Vegetation Distribution of East Dongting Lake. – Ecohydrology 8(4): 738-746.

http://www.aloki.hu ● ISSN 1589 1623 (Print) ● ISSN1785 0037 (Online)
DOI: http://dx.doi.org/10.15666/aeer/1906_43134330

[21] Xue, L. Q., Zhang, H., Zhang, L. C., Chi, Y. X., Sun, C. (2017): Impact of Water Conservancy Projects on Eco-Hydrological Regime of Tarim River Based on Improved RVA Method. – Journal of Hehai Unviersity (Natural Sciences) 45(3): 189-196. (In Chinese).

[22] Yang, Z., Gong, Y., Dong, C., Qiao, H., Chen, X. J., Tang, H. Y. (2017): Temporal and Spatial Distribution of the Four Major Chinese Carp Species in Three Gorges Reservoir During the Normal Operating Period. – Journal of Hydroecology 38(5): 72-79. (In Chinese).

[23] Zhang, J., Sun, M., Deng, Z., Lu, J., Wang, D., Chen, L., Liu, X. (2017): Runoff and Sediment Response to Cascade Hydropower Exploitation in the Middle and Lower Han River, China. – Mathematical Problems in Engineering, ID: 8785236.

[24] Zhang, J., Feng, L., Chen, L., Wang, D., Dai, M., Xu, W., Yan, T. (2018): Water Compensation and its Implication of the Three Gorges Reservoir for The River-Lake System in The Middle Yangtze River, China. – Water 10(8): 10081011.

[25] Zhao, Y., Zhou, J. Z., Xu, K., Zhao, N. (2012): Ecological Operation of Three Gorges Reservoir for Protection of Four Major Chinese Carps Spawning. – Advanced Engineering Sciences 44(4): 45-50. (In Chinese).

http://www.aloki.hu ● ISSN 1589 1623 (Print) ● ISSN1785 0037 (Online)
DOI: http://dx.doi.org/10.15666/aeer/1906_43134330

ASSESSMENT OF THE IMPACT OF LAND USE CHANGES ON NET PRIMARY PRODUCTIVITY USING HUMAN APPROPRIATION OF NET PRIMARY PRODUCTIVITY IN ANJI, CHINA

HUANG, Y.[1] – CHEN, S. L.[2*] – JIANG, H.[3] – CHEN, W. J.[4] – MO, X. H.[5]

[1]*School of Cyber Security, Jinling Institute of Technology, No. 99 Hongjin Road, Nanjing 211169, Jiangsu, China*

[2]*College of Economics and Management, Nanjing Forestry University, No. 159 Longpan Road, Nanjing 210037, Jiangsu, China*

[3]*International Institute for Earth System Science, Nanjing University, No. 163 Xianlin Road, Nanjing 210023, Jiangsu, China*

[4]*School of Software Engineering, Jinling Institute of Technology, No. 99 Hongjin Road, Nanjing 211169, Jiangsu, China*

[5]*School of Computer Engineering, Jinling Institute of Technology, No. 99 Hongjin Road, Nanjing, 211169, Jiangsu China*

**Corresponding author*
e-mail: slchen@njfu.edu.cn

(Received 6th Jun 2021; accepted 3rd Sep 2021)

Abstract. The land use changes (LUC) have altered the vegetation net primary productivity (NPP). Human appropriation of net primary productivity resulting from LUC ($HANPP_{luc}$) can be used to quantify the consequence of LUC on vegetation NPP. $HANPP_{luc}$ is defined as the difference between the potential and actual NPP availability in ecosystems. Based on the Thornthwaite Memorial model, CASA model, and multiple linear regression, this paper estimated the potential and actual NPP, explored the temporal and spatial changes of $HANPP_{luc}$, and analyzed the impact of LUC on vegetation NPP in Anji, China. There was a significant increasing trend in annual $HANPP_{luc}$ from 1984 to 2014. The total mean value of $HANPP_{luc}$ was 155 Gg C $year^{-1}$, while $HANPP_{luc}$ per unit was 82 ± 54 g C m^{-2} $year^{-1}$. The growth of Moso bamboo (*Phyllostachys pubescens*) forests area caused an increase of 33.5 Gg C $year^{-1}$ in NPP. However, the urbanization was the main reason for the decrease of NPP, which resulted in a decrease of 97.9 Gg C $year^{-1}$ in NPP. This study quantified the impact of LUC on vegetation NPP, and provided key data for urban landscape planning, Moso bamboo management, and regional ecological carbon cycle models.
Keywords: *potential NPP, CASA model, Thornthwaite Memorial model, Moso bamboo forests, urbanization*

Introduction

The Northern Hemisphere atmospheric CO_2 concentration has been successively rising at an increasing rate, mainly due to the continued burning of fossil fuels and land use changes (LUC) (IPCC, 2013). By fixing atmospheric CO_2, the forest ecosystems and cropland ecosystems mitigate the rise in CO_2, and play important roles in the global carbon cycle. The economy in the subtropical region of China has developed rapidly since 1978, and the economic achievement of China is mainly belonged to the subtropical region (Shi et al., 2020). The rapid economic development had accelerated the process of urbanization, and the area of urban land had increased significantly, which led to the

http://www.aloki.hu ● ISSN 1589 1623 (Print) ● ISSN 1785 0037 (Online)
DOI: http://dx.doi.org/10.15666/aeer/1906_43314348

decrease in the area of forests and croplands. This is verified by the data on the subtropical region of China, where the area of urban land had increased by 4.9% of the total area, while the area of forests and croplands had decreased about 15.1% of the total area during the period 1980-2018. The urbanization has decreased the carbon sequestration ability of the forests and croplands (Chen et al., 2020; Mahbub et al., 2019). Thus, some obvious questions arise: how to monitor and evaluate the carbon fixation ability of the ecosystems, and how to quantify the impact of urbanization on carbon sequestration.

Moso bamboo (*Phyllostachys pubescens*) forests are common in the subtropical region of China, covering approximately 3.9 million ha of area, and account for 74% of the Chinese bamboo forests area and 80% of the world's bamboo forests area (Song et al., 2016). Over the last 30 years, the area of Moso bamboo forests had increased significantly, and the rate of increase was approximately 3% (Chen et al., 2018; Song et al., 2013). The Moso bamboo growing pattern is greatly different from other forest types and accumulate large amounts of carbon (Cao et al., 2019). How to evaluate the carbon sequestration ability of the Moso bamboo forests, and analyze the impact of the growth of bamboo forests area on carbon sequestration are problems faced by ecologists.

Net primary productivity (NPP), which is equal to the difference between the amount of carbon absorbed by plant photosynthesis and the carbon released by plant respiration, can reflect the carbon fixation ability of plants (Garbulsky and Paruelo, 2004). Therefore, quantifying the consequence of LUC on vegetation NPP will guide urbanization, control the decrease of ecosystem NPP, and mitigate the climate warming trends (Foley et al., 2005). Human appropriation of net primary productivity resulting from LUC ($HANPP_{luc}$) can be used to quantify the consequence of LUC on vegetation NPP, and has been widely used worldwide (Haberl et al., 2014; Huang et al., 2020; Weinzettel et al., 2019). $HANPP_{luc}$ is the loss of potential NPP due to LUC, and is defined as the difference between potential and actual NPP availability in ecosystems. Potential NPP (NPP_{pot}) is the NPP of native ecosystems that would most likely exist in the absence of human activities, while actual NPP (NPP_{act}) is the NPP of current ecosystems. As a percentage of NPP_{pot}, the global $HANPP_{luc}$ varied between 4% and 56% during the period 1990-2015 (Haberl et al., 2014, 2007; Plutzar et al., 2016; Pritchard et al., 2018; Saikku et al., 2015). In China, $HANPP_{luc}$ varied between 6% and 26% of NPP_{pot} during the period 2000-2015 (Chen et al., 2015; Huang et al., 2020; Lin et al., 2016). How to simulate NPP_{act} and NPP_{pot} are key problems for $HANPP_{luc}$ estimation.

The Carnegie-Ames-Stanford approach (CASA) model is a widely used method for NPP_{act} estimation in China, and the simulated NPP_{act} was consistent with the observed NPP (Chen et al., 2017; Xu and Wang, 2016; Zhang et al., 2016). At present, empirical models that use correlations between climate data and measured NPP at individual sites have been widely used for NPP_{pot} estimation (Lin et al., 2016). Based on Liebig's Law of Minimum, the Miami model uses temperature and precipitation to estimate NPP_{pot} (Gang et al., 2014; Zhang et al., 2015). NPP_{pot} is not only related to temperature and precipitation, but also to other environmental factors. Actual evapotranspiration is used by the Thornthwaite Memorial model to estimate NPP_{pot} (Liu et al., 2019; Yin et al., 2020). The Chikugo model is the function of precipitation and net surface radiation (Chen et al., 2015).

The accuracy of measured NPP_{pot} directly affected the accuracy of empirical models. The core zone in a nature reserve is designed to strictly protect ecosystems, and minimize disturbance by human activities (Geneletti and Duren, 2008). The ecosystem

http://www.aloki.hu ● ISSN 1589 1623 (Print) ● ISSN 1785 0037 (Online)
DOI: http://dx.doi.org/10.15666/aeer/1906_43314348

in the core zone is considered to be a natural ecosystem that is undisturbed by humans (Zhang et al., 2017b). Therefore, the NPP_{act} in the core zone would be considered to be the NPP_{pot}. However, the NPP_{pot} estimation models based on the correlations between NPP_{pot} in the core zone and climate data has not been reported.

Given the above scientific challenges, this study used the CASA model to simulate the NPP_{act}. Based on the core zone in the nature reserve, the NPP_{pot} estimation models for the different forest types were established using multiple linear regression. Anji and TianMu Mountain Nature Reserve, located in eastern subtropical China (see *Fig. 1a*), were selected as test region. The forest types in Anji and the core zone in TianMu Mountain Nature Reserve are similar, and these are Moso bamboo forests (MBF), subtropical broadleaf forests (SBF), and subtropical needle leaf forests (SNLF). Based on the core zone in TianMu Mountain Nature Reserve, the NPP_{pot} estimation models for the three forest types were established using the correlations between the measured NPP_{pot} and temperature, precipitation, and solar radiation. The NPP_{pot} in the croplands was estimated by the Thornthwaite Memorial model. The objectives of this study were to (1) estimate the NPP_{act} and NPP_{pot} in Anji, (2) explore the temporal and spatial changes of $HANPP_{luc}$ in Anji, and (3) analyze the impact of LUC on vegetation NPP.

Materials and methods

Study area

Anji and the core zone in TianMu Mountain Nature Reserve are located in northwestern Zhejiang Province, China (see *Fig. 1b*). The area of the core zone in TianMu Mountain Nature Reserve and Anji are about 598 and 188601 ha. The forest types in Anji and the core zone in TianMu Mountain Nature Reserve are the MBF, SBF, and SNLF (see *Fig. 1c* and *d*). The SBF consists of the following six different tree species: *Cyclobalanopsis glauca*, *Castanopsis sclerophylla*, *Castanopsis sclerophylla*, *Castanopsis eyrei*, *Schima superba*, and *Quercus fabri*. The five different tree species in the SNLF are *Pinus massoniana*, *Cryptomeria fortune*, *Pseudolarix amabilis*, *Pinus taiwanensis* and *Cunninghamia lanceolata*.

The Moso bamboo growing pattern is greatly different from other forest types. It can reach maximum height (10-20 m) in 2-4 months, and accumulate large amounts of carbon (Cao et al., 2019). The Moso bamboo is widely distributed in Anji, and the area of it increased significantly during the period 1984-2014. The croplands also exists in Anji, however, the area of the croplands, SBF, and SNLF has been decreased at a rapid rate due to the urbanization and increase of MBF.

Design of $HANPP_{luc}$ estimation procedure

$HANPP_{luc}$ is defined as the difference between NPP_{pot} and NPP_{act}. The CASA model was used to calculate NPP_{act} in Anji and the core zone in TianMu Mountain Nature Reserve from 1984 to 2014. In order to estimate NPP_{pot}, we assumed that: (1) Because no human activity is permitted in the core zone in a nature reserve (Hull et al., 2011), for the MBF, SBF and SNLF, the NPP_{act} in the core zone in TianMu Mountain Nature Reserve would be considered to be NPP_{pot}; (2) According to Tobler's first law (TFL) of geography (Waters, 2017), the NPP_{pot} in degraded regions should be equal to that in non-degraded regions when the degraded and non-degraded regions have similar natural conditions (Lin et al., 2016). The forest types in Anji and the core zone in TianMu

http://www.aloki.hu ● ISSN 1589 1623 (Print) ● ISSN 1785 0037 (Online)
DOI: http://dx.doi.org/10.15666/aeer/1906_43314348

Mountain Nature Reserve are similar. Therefore, the NPP_{pot} in the MBF, SBF and SNLF in Anji would be considered to be equal to that in the core zone in TianMu Mountain Nature Reserve.

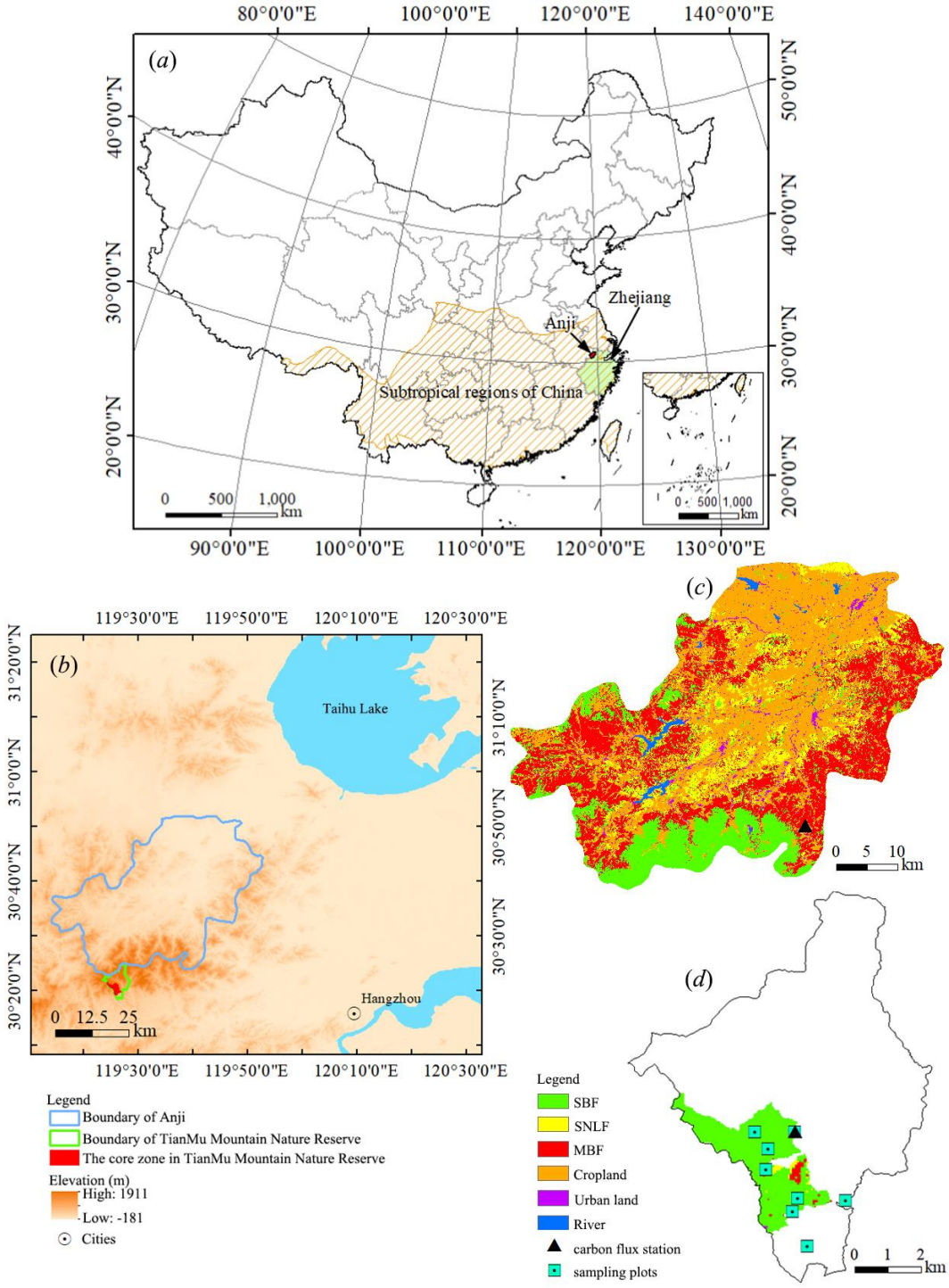

Figure 1. *Location of (a) subtropical region of China and (b) Anji and the core zone in TianMu Mountain Nature Reserve, and the land cover maps in (c) Anji and (d) the core zone in TianMu Mountain Nature Reserve. The cyan square points are the plots of in-situ NPP observation, and the black triangle points are the carbon flux stations using the eddy covariance observation systems to measure NPP*

http://www.aloki.hu ● ISSN 1589 1623 (Print) ● ISSN 1785 0037 (Online)
DOI: http://dx.doi.org/10.15666/aeer/1906_43314348

Figure 2 shows the process of the $HANPP_{luc}$ estimation. Firstly, based on the meteorological data, NDVI, and land cover maps, the CASA model was used to estimate the NPP_{act} in Anji and the core zone in TianMu Mountain Nature Reserve from 1984 to 2014. Secondly, based on the CASA-simulated NPP_{act}, meteorological data, and land cover maps in the core zone in TianMu Mountain Nature Reserve, the NPP_{pot} estimation models for the SBF, SNLF, and MBF were established using multiple linear regression. Thirdly, according to assumption 2, based on the meteorological data and land cover map in 1984, the NPP_{pot} in the SBF, SNLF, and MBF in Anji was simulated using the NPP_{pot} estimation models for the three forest types. Fourthly, based on the meteorological data and land cover map in 1984, the Thornthwaite Memorial model was used to estimate the NPP_{pot} in the croplands in Anji. Finally, the $HANPP_{luc}$ in Anji was calculated as the difference between NPP_{pot} and NPP_{act}.

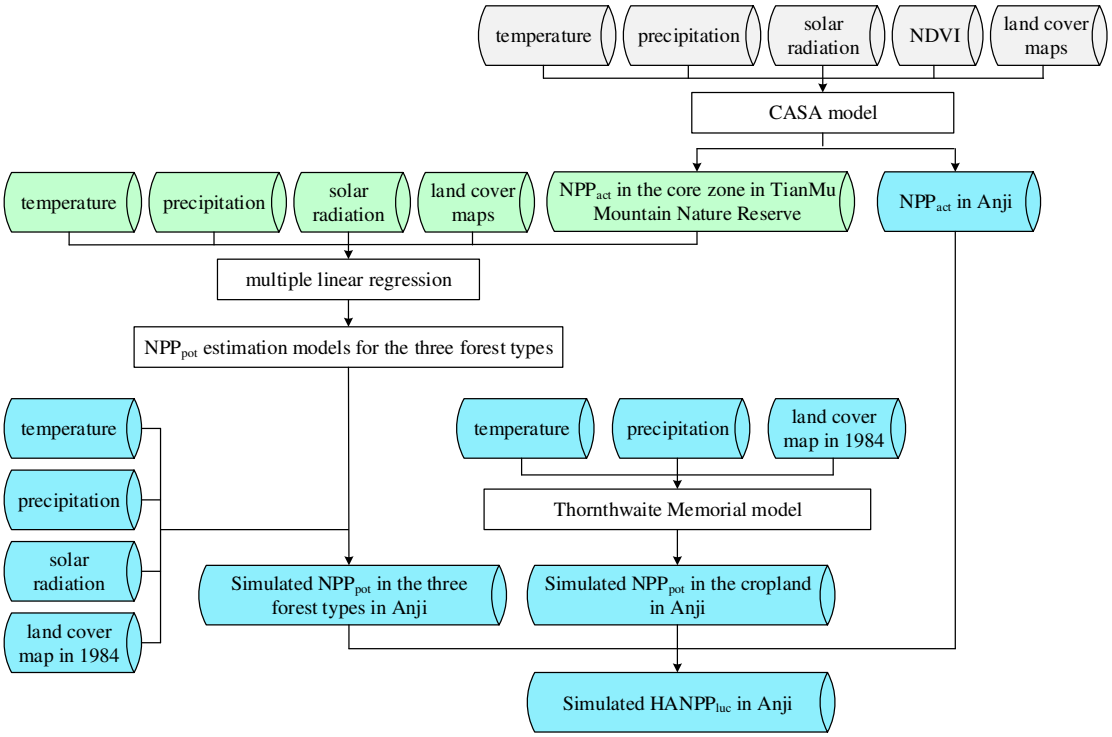

Figure 2. *Flowchart of $HANPP_{luc}$ estimation. The gray cylinders are the datasets in Anji and the core zone in TianMu Mountain Nature Reserve, the green cylinders are the datasets in the core zone in TianMu Mountain Nature Reserve, and the blue cylinders are the datasets in Anji*

Input data

The datasets we used for $HANPP_{luc}$ estimation are the meteorological datasets, NDVI, and land cover maps. The meteorological datasets, including monthly temperature, monthly precipitation, and monthly solar radiation, were provided by China Meteorological Administration (http://data.cma.cn/). The meteorological datasets are quality controlled, and the percentage of correct data is approaching to 100%. The meteorological datasets were also resampled to match the spatial resolution of $HANPP_{luc}$ using ordinary kriging method. The NDVI provided by AVHRR Global Inventory Modeling and Mapping Studies (GIMMS) group was used for NPP_{pot} estimation. The NDVI3g dataset was downloaded from NASA Ames Ecological

http://www.aloki.hu ● ISSN 1589 1623 (Print) ● ISSN 1785 0037 (Online)
DOI: http://dx.doi.org/10.15666/aeer/1906_43314348

Forecasting Lab (https://ecocast.arc.nasa.gov/data/pub/gimms/3g.v1/), and then was resampled to match the spatial resolution of $HANPP_{luc}$ using ordinary kriging method. The land cover maps in Anji were derived from Landsat MSS and OLI scenes using the supervised Maximum-Likelihood classification (Chen et al., 2020).

Field work

In Tianmu Mountain Nature Reserve, eight sampling plots were selected to validate the NPP of the actual vegetation (see the cyan square points in *Fig. 1d*), and the size of each plot is 20 m×20 m. There were four sampling plots in the SBF, three sampling plots in the SNLF, and one sampling plot in the MBF. At each sampling plots, the mean heights, breast diameters and crown diameters of stand-grown trees were derived from the field investigations which carried out during the period 2005-2010.

In the SBF in Tianmu Mountain Nature Reserve, there was one carbon flux observation station which using the eddy covariance observation systems to measure NPP (Chen et al., 2017). The carbon flux observation station was established in 2012, and the measured NPP has been obtained since 2013. In Anji, there was also one carbon flux observation station in the MBF (see *Fig. 1c*). The carbon flux observation station was established in 2010, and the measured NPP has been obtained since 2011. Details can be found in Chen et al. (2020).

$HANPP_{luc}$ estimation

$HANPP_{luc}$ is the loss of the potential NPP due to LUC (g C m^{-2} $year^{-1}$), and can be calculated as:

$$HANPP_{luc} = NPP_{pot} - NPP_{act} \quad \text{(Eq.1)}$$

where NPP_{pot} is the NPP of the potential natural vegetation that would most likely exist in the absence of human-led land use (g C m^{-2} $year^{-1}$), and NPP_{act} is the NPP of the actual vegetation (g C m^{-2} $year^{-1}$).

NPP_{act} estimation

The CASA model was used to estimate the NPP_{act}. The monthly value of NPP_{act} can be calculated as (Field et al., 1995; Potter et al., 1993):

$$NPP_{act} = 0.5 \times S \times FPAR \times T_{\varepsilon} \times W_{\varepsilon} \times LUE_{max} \quad \text{(Eq.2)}$$

where S is the total solar radiation reaching the earth's surface (MJ $month^{-1}$). FPAR is the fraction of photosynthetically active radiation and was calculated following the procedure of Zhu et al. (2006). T_{ε} is the temperature stress indicator, W_{ε} is the water stress indicator. The equations of T_{ε} and W_{ε} can be found in Potter et al. (1993). LUE_{max} is the maximum light-use efficiency of the vegetation (g C MJ^{-1}), and the values of LUE_{max} for the MBF, SBF, SNLF, and croplands can be found in Chen et al. (2020).

NPP_{pot} estimation

The Thornthwaite Memorial model was used for the NPP_{pot} estimation in the croplands. The Thornthwaite Memorial model uses the relationship between actual

http://www.aloki.hu ● ISSN 1589 1623 (Print) ● ISSN 1785 0037 (Online)
DOI: http://dx.doi.org/10.15666/aeer/1906_43314348

evapotranspiration and carbon fixation to estimate NPP_{pot} (Lieth, 1975; Liu et al., 2019). The yearly value of NPP_{pot} can be calculated as:

$$NPP_{pot} = 3000[1 - e^{-0.0009695(V-20)}] \quad \text{(Eq.3)}$$

$$V = \frac{1.05Prec}{\sqrt{1+(1.05Prec/L)^2}} \quad \text{(Eq.4)}$$

$$L=300+25Temp+0.05Temp^3 \quad \text{(Eq.5)}$$

where V is the mean annual actual evapotranspiration (mm), $Prec$ is the mean annual precipitation (mm), L is annual maximum evapotranspiration (mm), and $Temp$ is mean annual temperature (℃).

The NPP_{pot} was affected by the temperature, precipitation, and solar radiation in Anji and the core zone in TianMu Mountain Nature Reserve (see *Table 1*). Therefore, the NPP_{pot} estimation models for the SBF, SNLF, and MBF were established using multiple linear regression. The multilinear regression equation is

$$NPP_{pot} = a \times T_a + b \times P + c \times S + d \quad \text{(Eq.6)}$$

where T_a is the mean monthly temperature (°C), P is the monthly precipitation (mm), S is the monthly solar radiation (MJ month^{-1}), a, b, c, and d are the regression coefficients.

Table 1. *Pearson correlation coefficient (R) between NPP_{pot} and temperature (T_a), precipitation (P), and solar radiation (S) for each forest type*

Forest type	T_a	P	S
SBF	0.81*	0.28*	0.82*
SNLF	0.79*	0.27*	0.80*
MBF	0.82*	0.29*	0.83*

*At 5% signification level

Land use transition matrix

The land use transition matrix was used to detect the transition of different land cover type during the period 1984-2014 (Lü et al., 2020). The area of one land cover type in the year 1984 can be calculated as:

$$A_{i+}=\sum_{j=1}^{n} A_{ij} \quad \text{(Eq.7)}$$

where A_{ij} $(i \neq j)$ is the area of the land cover type that was converted from type i to type j between 1984 and 2014, n is the number of land cover type, A_{ii} is the area of the land cover type that showed the persistence of type i between 1984 and 2014.

The area of the land cover type that was occupied by type j in the year 2014 is

$$A_{+j}=\sum_{j=1}^{n} A_{ij} \quad \text{(Eq.8)}$$

http://www.aloki.hu ● ISSN 1589 1623 (Print) ● ISSN 1785 0037 (Online)
DOI: http://dx.doi.org/10.15666/aeer/1906_43314348

Changing trend

The slope of linear regression equation was used to calculate the $HANPP_{luc}$ changing trend during the period 1984-2014, and can be calculated as:

$$slope = \frac{n \times \sum_{i=1}^{n} (i \times HANPP_{luc_i}) - \sum_{i=1}^{n} i \times \sum_{i=1}^{n} HANPP_{luc_i}}{n \times \sum_{i=1}^{n} i^2 - (\sum_{i=1}^{n} i)^2} \quad \text{(Eq.9)}$$

where n is the number of years ($n = 31$), $HANPP_{luc_i}$ is the $HANPP_{luc}$ in the year i. A positive slope value indicates that the $HANPP_{luc}$ is in an upward trend, and a negative slope value means that the $HANPP_{luc}$ is in a decreasing trend.

Results

Spatial pattern of LUC

Figure 3 shows the LUC in Anji during the period 1984-2014. The land use transition matrix was obtained using *Equations 7–8* (*Table 2*). Over the last 31 years, there was about 57.8% of the total area of Anji where the land cover type were not changed. The area of MBF increased from 30.4% of the total area of Anji in 1984 to 43.7% in 2014, while the area of SBF and SNLF decreased about 7317 and 5666 ha. The area of croplands also decreased about 25324 ha due to the urban expansion, and the area of urban land increased from 2.0% of the total area of Anji in 1984 to 8.5% in 2014. The area of river increased about 809 ha during the period 1984-2014.

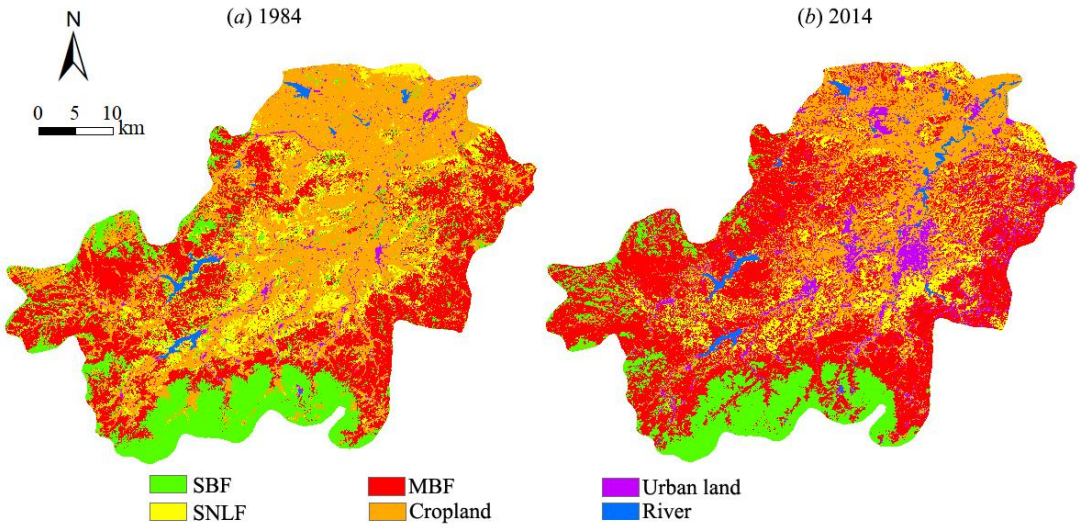

Figure 3. *The land cover maps in the year (a) 1984 and (b) 2014*

NPP_{act} estimation and validation

The NPP_{act} in Anji and TianMu Mountain Nature Reserve were simulated by the CASA model (see *Eq. 2*). The observed NPP_{act} at the eight sampling plots in Tianmu Mountain Nature Reserve were used to validate the simulated NPP_{act} (see *Fig. 4a*). The results show that the simulated annual NPP_{act} was largely consistent with the observed NPP_{act} ($R^2 = 0.91$, $p < 0.01$), and the value of RMSE was 73 g C m^{-2} $year^{-1}$.

http://www.aloki.hu ● ISSN 1589 1623 (Print) ● ISSN 1785 0037 (Online)
DOI: http://dx.doi.org/10.15666/aeer/1906_43314348

Table 2. *Land use transition matrix (unit: ha) of Anji during the period 1984-2014*

	SBF	SNLF	MBF	Croplands	Urban	River
SBF	18,215	667	10,335	1,330	523	118
SNLF	656	8,763	9,528	3,484	918	23
MBF	2,472	4,592	43,211	3,949	3,192	33
Croplands	2,513	3,638	19,359	35,551	9,365	838
Urban	14	45	214	1,505	1,852	155
River	2	0	9	121	226	1,621

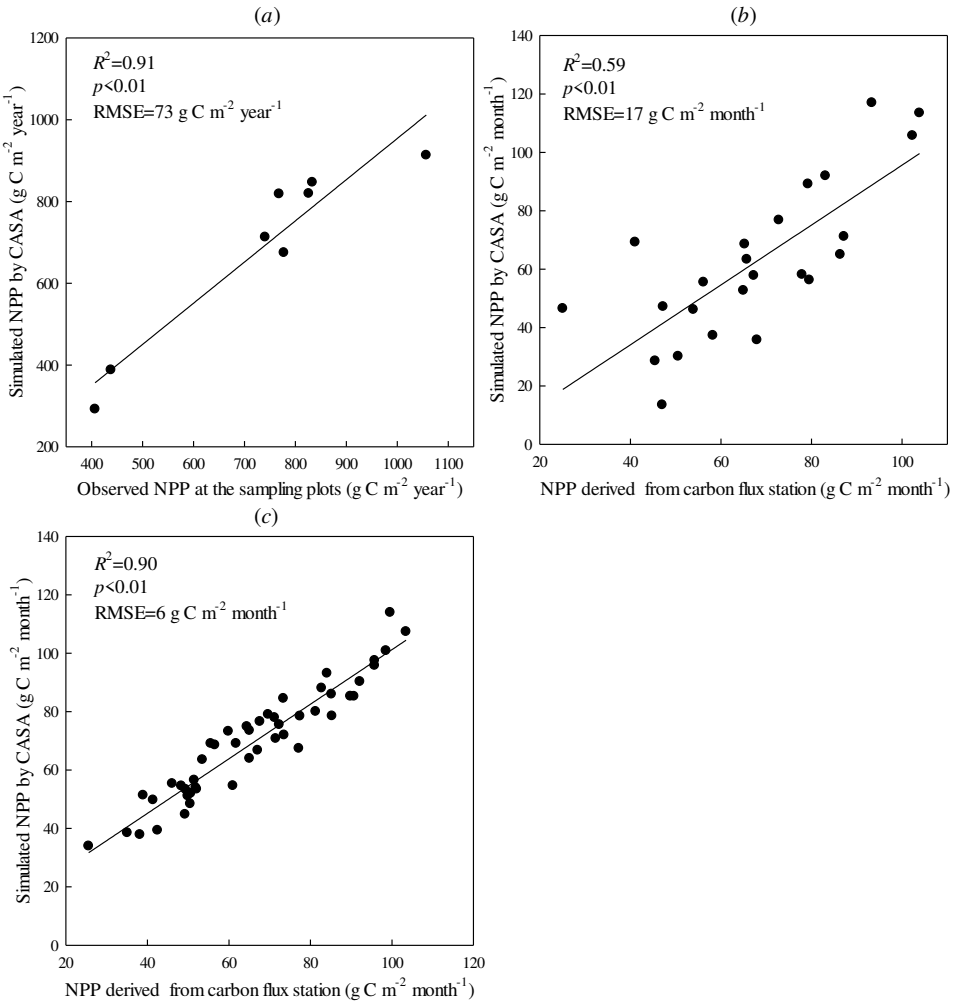

Figure 4. *Comparison of (a) the simulated annual NPP with the observed NPP at the eight sampling plots in Tianmu Mountain Nature Reserve, and comparison of the simulated monthly NPP with the NPP derived from the carbon flux stations (b) from 2013 to 2014 in TianMu Mountain Nature Reserve and (c) from 2011 to 2014 in Anji*

The NPP_{act} derived from the eddy covariance observation systems in TianMu Mountain Nature Reserve (see *Fig. 4b*) and Anji (see *Fig. 4c*) were also used to validate the simulated NPP_{act}. The results show that the monthly NPP_{act} simulated by CASA model was largely consistent with the NPP_{act} derived from the eddy covariance

http://www.aloki.hu ● ISSN 1589 1623 (Print) ● ISSN 1785 0037 (Online)
DOI: http://dx.doi.org/10.15666/aeer/1906_43314348

observation systems ($R^2 \geq 0.59$, $p < 0.01$). Therefore, the NPP_{act} simulated by CASA model can be used for $HANPP_{luc}$ estimation.

NPP_{pot} estimation and validation

The NPP_{pot} in the croplands in Anji from 1984 to 2014 was simulated by the Thornthwaite Memorial model (see *Eqs. 3–5*). According to Tobler's first law (TFL) of geography, the NPP_{pot} in the SBF, SNLF, and MBF in Anji would be considered to be equal to that in the core zone in TianMu Mountain Nature Reserve. Based on the monthly CASA-simulated NPP_{act}, temperature (T_a), precipitation (P), and solar radiation (S) for eight months (January, February, April, May, July, August, October, and November) from 1984 to 2014 in the core zone in TianMu Mountain Nature Reserve, the NPP_{pot} estimation models for the SBF, SNLF, and MBF were established using multiple linear regression (see *Table 3*).

Table 3. *The NPP_{pot} estimation models for each forest type*

Forest type	NPP_{pot} estimation models	R^2	*p*
SBF	$NPP_{pot}=2.26\times T_a-0.02\times P+0.29\times S-69.90$	0.74	< 0.01
SNLF	$NPP_{pot}=1.96\times T_a-0.02\times P+0.27\times S-62.38$	0.71	< 0.01
MBF	$NPP_{pot}=2.54\times T_a-0.01\times P+0.28\times S-70.60$	0.76	< 0.01

T_a: temperature, P: precipitation, S: solar radiation

The monthly mean CASA-simulated NPP_{act} for four months (March, June, September and December) from 1984 to 2014 in the core zone in TianMu Mountain Nature Reserve was used to validate the simulated monthly mean NPP_{pot} of the three forest types (see *Fig. 5*). The results show that the simulated NPP_{pot} was consistent with the CASA-simulated NPP_{act} ($R^2 \geq 0.68$, $p < 0.01$).

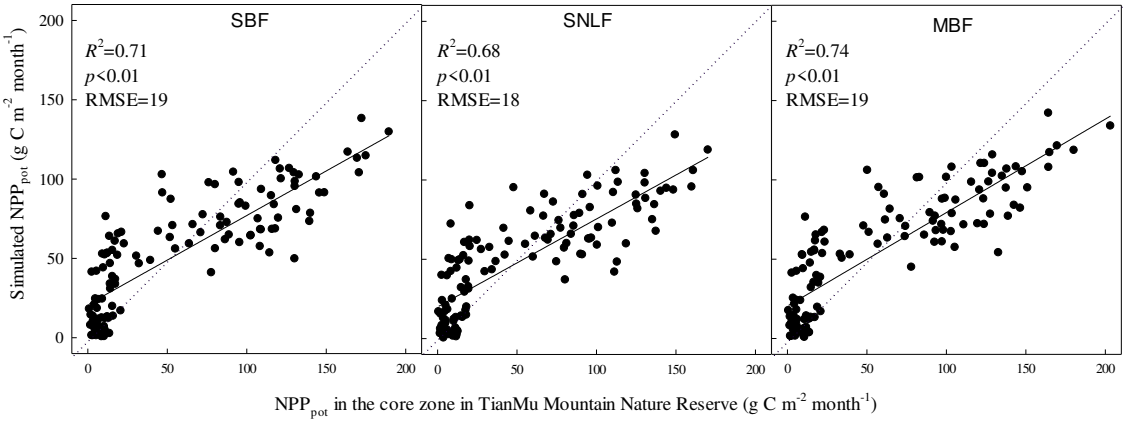

Figure 5. *Comparison of the simulated NPP_{pot} with the NPP_{pot} in the core zone in TianMu Mountain Nature Reserve*

$HANPP_{luc}$ interannual variability

The $HANPP_{luc}$ in Anji from 1984 to 2014 were calculated using *Equation 1*. Using *Equation 9,* we can find that there was a significant increasing trend with the rate of

http://www.aloki.hu ● ISSN 1589 1623 (Print) ● ISSN 1785 0037 (Online)
DOI: http://dx.doi.org/10.15666/aeer/1906_43314348

2 g C m^{-2} $year^{-1}$ in annual $HANPP_{luc}$, increasing from 1 g C m^{-2} $year^{-1}$ in 1984 to 48 g C m^{-2} $year^{-1}$ in 2014 (see *Fig. 6*). The highest annual $HANPP_{luc}$ appeared in 2007, with the value of 248 g C m^{-2} $year^{-1}$, while the lowest annual $HANPP_{luc}$ appeared in 1984, with the value of 1 g C m^{-2} $year^{-1}$. The annual averaged $HANPP_{luc}$ was 82 g C m^{-2} $year^{-1}$, and it means that the NPP_{act} decreased about 82 g C m^{-2} $year^{-1}$ due to the LUC.

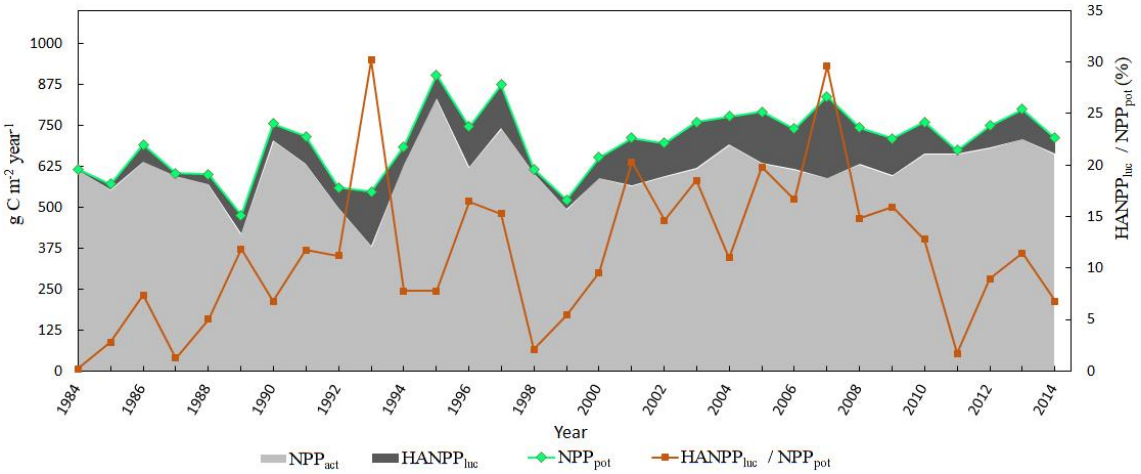

Figure 6. *Interannual changes in the annual NPP_{act}, $HANPP_{luc}$, NPP_{pot}, and $HANPP_{luc}/NPP_{pot}$ in Anji during the period 1984-2014*

The increase of $HANPP_{luc}$ is also visible in the increase of $HANPP_{luc}$ as a percentage of NPP_{pot} (i.e. $HANPP_{luc}/NPP_{pot}$), which increased from 0.2% in 1984 to 6.7% in 2014. The highest annual $HANPP_{luc}/NPP_{pot}$ also appeared in 2007, with the value of 29.6%, while the lowest annual $HANPP_{luc}/NPP_{pot}$ appeared in 1984, with the value of 0.2%. The annual averaged $HANPP_{luc}/NPP_{pot}$ was 11%, which means that the NPP_{act} decreased about 11% of the NPP_{pot} due to the LUC during the period 1984-2014.

Figure 6 also shows that there was a significant upward trends in the annual NPP_{act} in Anji, and the rate of increase was 3.0 g C m^{-2} $year^{-1}$. The annual NPP_{act} varied between 382 and 833 g C m^{-2} $year^{-1}$, and annual averaged NPP_{act} was 614 g C m^{-2} $year^{-1}$. There was also a significant upward trends in the annual NPP_{pot} in Anji, and the rate of increase was 5.4 g C m^{-2} $year^{-1}$. The annual NPP_{pot} varied between 474 and 903 g C m^{-2} $year^{-1}$, and annual averaged NPP_{pot} was 697 g C m^{-2} $year^{-1}$.

Spatial pattern of $HANPP_{luc}$

In Anji, the total mean value of $HANPP_{luc}$ was 155 Gg C $year^{-1}$, while $HANPP_{luc}$ per unit was 82 ± 54 g C m^{-2} $year^{-1}$ from 1984 to 2014. The $HANPP_{luc}$ in central Anji were higher than those in other regions (see *Fig. 7a*). In general, the positive $HANPP_{luc}$, i.e. NPP_{pot} was higher than NPP_{act}, appeared in northern, southern and central Anji, while the negative $HANPP_{luc}$ appeared in eastern and western Anji. The area of the negative $HANPP_{luc}$ regions was 73723 ha, accounting for 39% of Anji area. The MBF is widely distributed in those regions, NPP_{act} was higher than NPP_{pot} because of MBF management like the On and Off-year management and fertilization (Chen et al., 2018; Zhang et al., 2017a).

Although there was an increasing trend in the annual $HANPP_{luc}$, the changing trends showed a large spatial heterogeneity (see *Fig. 7b*). The $HANPP_{luc}$ increased in northern

http://www.aloki.hu ● ISSN 1589 1623 (Print) ● ISSN 1785 0037 (Online)
DOI: http://dx.doi.org/10.15666/aeer/1906_43314348

and central Anji because of the urbanization and decrease of croplands. The area where the $HANPP_{luc}$ increased significantly was 11342 ha, accounting for 6% of Anji area (see *Fig. 7c*). *Figure 7b* also illustrates that the $HANPP_{luc}$ decreased in the northern, southern and central Anji due to land cover changes to highly productive land type (MBF). The area where the $HANPP_{luc}$ decreased significantly was 13232 ha, accounting for 7% of Anji area (see *Fig. 7c*).

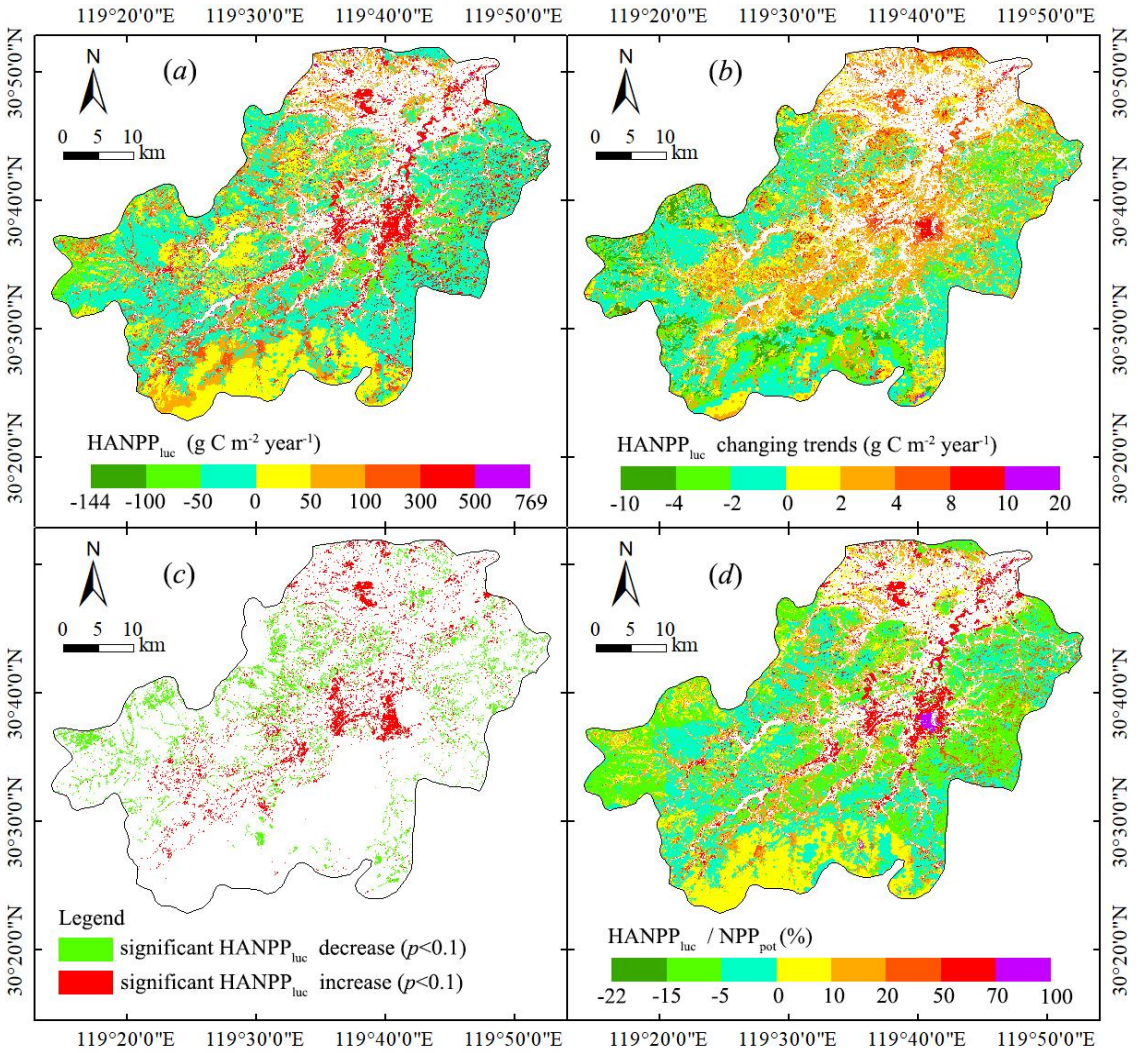

Figure 7. *Spatial distributions of (a) annual $HANPP_{luc}$, (b) changing trends in $HANPP_{luc}$, (c) significant $HANPP_{luc}$ change ($p < 0.1$), and (d) annual averaged $HANPP_{luc}/NPP_{pot}$ from 1984 to 2014 in Anji*

Over the 31 years, the mean value of the ratio between $HANPP_{luc}$ and NPP_{pot} (i.e. $HANPP_{luc}/NPP_{pot}$) was 11 ± 7%. The positive $HANPP_{luc}/NPP_{pot}$ values were distributed in the northern, southern and central Anji (see *Fig. 7d*), and the highest value of $HANPP_{luc}/NPP_{pot}$ appeared in central Anji due to land cover changes to urban land. The negative $HANPP_{luc}/NPP_{pot}$ values appeared in eastern and western Anji, and the lowest value of $HANPP_{luc}/NPP_{pot}$ was in eastern Anji because of land cover changes to highly productive land type (MBF).

http://www.aloki.hu ● ISSN 1589 1623 (Print) ● ISSN 1785 0037 (Online)
DOI: http://dx.doi.org/10.15666/aeer/1906_43314348

Discussion

Comparison with previous work

Compared with previous work (see *Table 4*), the simulated NPP_{pot} in Anji was similar to the result in the core zone in Tianmu Mountain Nature Reserve (Chen et al., 2017), karst areas of south China (Lin et al., 2016), and coastal areas of Jiangsu (Zhang et al., 2015). However, the simulated NPP_{pot} was lower than the result in Zhejiang reported by Pan (2020), and was higher than the result in Yangtze River Delta reported by Huang (2020).

For SBF, the simulated NPP_{pot} in Anji was similar to the result in the core zone in Tianmu Mountain Nature Reserve (Chen et al., 2017), Zhejiang (Sun, 2009), Gannan (Zou et al., 2011), and China (Lin et al., 2012). For SNLF, the simulated NPP_{pot} in Anji was similar to the result in the core zone in Tianmu Mountain Nature Reserve (Chen et al., 2017), Zhejiang (Sun, 2009), and global tropical and subtropical needle leaf forests (Medková et al., 2017). Our result was higher than the result in cold temperate needle leaf forests in China reported by Ren (2017). For MBF, the simulated NPP_{pot} in Anji was similar to the result in the core zone in Tianmu Mountain Nature Reserve (Chen et al., 2017). However, it was lower than the result in Wuyishan Biosphere Reserve (Li et al., 2006). For croplands, the simulated NPP_{pot} in Anji was higher than the result in global croplands (Haberl et al., 2007).

Table 4. *Overview of previous work on NPP_{pot} at different scale*

Work	Study scale	Time period	NPP_{pot} (g C m^{-2} $year^{-1}$)
This study	Anji, China	1984-2014	697 ± 100
Chen et al., 2017	The core zone in Tianmu Mountain Nature Reserve	1984-2014	720 ± 114
Lin et al., 2016	Karst areas of south China	2000-2013	400-850
Zhang et al., 2015	Coastal areas of Jiangsu, China	2000-2010	603-832
Pan and Xu, 2020	Zhejiang, China	1981-2015	896
Huang et al., 2020	Yangtze River Delta, China	2005-2015	424-631
This study	SBF in Anji	1984-2014	775 ± 106
Chen et al., 2017	SBF in the core zone in Tianmu Mountain Nature Reserve	1984-2014	717 ± 120
Sun, 2009	SBF in Zhejiang	1981-1998	500-800
Zou et al., 2011	SBF in Gannan	1950-2000	733
Lin et al., 2012	SBF in China	1961-2006	534-847
This study	SNLF in Anji	1984-2014	720 ± 97
Chen et al., 2017	SNLF in the core zone in Tianmu Mountain Nature Reserve	1984-2014	665 ± 94
Medková et al., 2017	Global tropical and subtropical NLF	2000	735
Sun, 2009	SNLF in Zhejiang	1981-1998	500-800
Ren et al., 2017	Cold temperate NLF in China	1982-2012	430
This study	MBF in Anji, China	1984-2014	805 ± 108
Chen et al., 2017	MBF in the core zone in Tianmu Mountain Nature Reserve	1984-2014	731-784
Li et al., 2006	MBF in Wuyishan Biosphere Reserve	1993	826
This study	Croplands in Anji, China	1984-2014	670 ± 63
Haberl et al., 2007	Global croplands	2000	611

NLF: needle leaf forests

http://www.aloki.hu ● ISSN 1589 1623 (Print) ● ISSN 1785 0037 (Online)
DOI: http://dx.doi.org/10.15666/aeer/1906_43314348

During the period 1984-2014, the annual $HANPP_{luc}$ varied between 1 and 248 g C m^{-2} $year^{-1}$, with the mean value of 82 ± 54 g C m^{-2} $year^{-1}$ (see *Table 5*). Our results were similar to the results in the regions where the geographic and climatic conditions are similar to Anji (Huang et al., 2020; Zhang et al., 2015). The national $HANPP_{luc}$ values from previous studies were also compared with the annual $HANPP_{luc}$ in Anji, and the results show that our results were similar to the results in China (Chen et al., 2015) and New Zealand (Fetzel et al., 2014). However, the result was higher than the global result reported by Haberl (2007).

In Anji, the ratio between $HANPP_{luc}$ and NPP_{pot} (i.e. $HANPP_{luc}/NPP_{pot}$) varied between 0.2% and 29.6%, with the mean value of 11 ± 7%. Our results were similar to the results in the regions where the geographic and climatic conditions are similar to Anji (Huang et al., 2020; Zhang et al., 2015). The result was also similar to the result in Karst areas of south China (Lin et al., 2016). As shown in *Table 5*, distinct differences in $HANPP_{luc}/NPP_{pot}$ are found in different countries and regions. The $HANPP_{luc}/NPP_{pot}$ in China was higher than that in East Asia or Europe (Chen et al., 2015; Haberl et al., 2007; Plutzar et al., 2016), and was similar to the result in Central Asia (Huang et al., 2018). The variation of the $HANPP_{luc}/NPP_{pot}$ in New Zealand or global terrestrial ecosystems was larger than that in China (Fetzel et al., 2014; Haberl et al., 2014). The $HANPP_{luc}/NPP_{pot}$ in Anji was lower than that in China, this is mainly caused by the increase of the area of forest types, increasing from 59% in 1984 to 66% in 2014 (see *Table 2*).

Table 5. *Overview of previous work on $HANPP_{luc}$ at different scale*

Quantity	Study scale	Time period	Results	References
$HANPP_{luc}$ (g C m^{-2} $year^{-1}$)	Anji, China	1984-2014	82 ± 54	This study
	Zhejiang, China	2005-2015	71	Huang et al., 2020
	Coastal areas of Jiangsu, China	2000-2010	-23-100	Zhang et al., 2015
	Yangtze River Delta, China	2005-2015	26-102	Huang et al., 2020
	China	2001-2010	45-121	Chen et al., 2015
	New Zealand	1860-2005	11-96	Fetzel et al., 2014
	Global	2000	4	Haberl et al., 2007
$HANPP_{luc}/NPP_{pot}$	Anji, China	1984-2014	11 ± 7%	This study
	Coastal areas of Jiangsu, China	2000-2010	-11%-32%	Zhang et al., 2015
	Yangtze River Delta, China	2005-2015	6%-19%	Huang et al., 2020
	Karst areas of south China	2000-2013	13%-22%	Lin et al., 2016
	China	2001-2010	11%-26%	Chen et al., 2015
	East Asia	2000	5%	Haberl et al., 2007
	Central Asia	1979-2012	0.3%-22%	Huang et al., 2018
	Europe	1990-2006	11%	Plutzar et al., 2016
	New Zealand	1860-2005	4%-37%	Fetzel et al., 2014
	Global	2000	4%-55%	Haberl et al., 2014

Impact of land use changes on NPP

Based on the $HANPP_{luc}$ and transition of different land cover types during the period 1984-2014 (see *Table 2*), the $HANPP_{luc}$ changes resulting from LUC were calculated

http://www.aloki.hu ● ISSN 1589 1623 (Print) ● ISSN 1785 0037 (Online)
DOI: http://dx.doi.org/10.15666/aeer/1906_43314348

(see *Table 6*). MBF has a strong capacity for carbon sequestration (Cao et al., 2019; Chen et al., 2020). Therefore, because of the increase of the MBF, which increased about 25207 ha during the period 1984-2014, the $HANPP_{luc}$ in the MBF decreased from 49.0 Gg C $year^{-1}$ in 1984 to 15.5 Gg C $year^{-1}$ in 2014. It means that the NPP increased about 33.5 Gg C $year^{-1}$ due to the increase of MBF.

Table 6. *The $HANPP_{luc}$ (Unit: Mg C $year^{-1}$) resulting from LUC during the period 1984-2014 in Anji*

Type	SBF	SNLF	MBF	Croplands	Urban	River	Total
SBF	19,192	138	1,481	-390	3,612	637	24,670
SNLF	503	-2,523	-4,211	-2,782	5,757	111	-3,145
MBF	3,449	1,770	15,600	701	27,369	129	49,018
Croplands	3,484	1,059	4,358	2,953	49,732	4,267	65,853
Urban	-91	-215	-1,631	-9,480	0	0	-11,417
River	-45	0	-93	45	0	0	-93
Total	26,493	228	15,504	-8,952	86,469	5,144	

The area of the SBF decreased about 7316 ha during the period 1984-2014, while the $HANPP_{luc}$ in the SBF increased from 24.7 Gg C $year^{-1}$ in 1984 to 26.5 Gg C $year^{-1}$ in 2014. It means that the NPP decreased about 1.8 Gg C $year^{-1}$. The area of the SNLF decreased about 5666 ha, which caused the NPP decrease of 3.4 Gg C $year^{-1}$. The area of the urban land increased about 12291 ha, which caused the NPP decrease of 97.9 Gg C $year^{-1}$. The area of the river increased about 809 ha, and it led to a decrease of 5.2 Gg C $year^{-1}$ in the NPP.

The area of the croplands decreased about 25323 ha during the period 1984-2014, and the area of the croplands occupied by MBF, SBF, or SNLF was about 16739 ha. In the vast majority of the global terrestrial ecosystems, converting croplands to forests increases NPP (Krausmann et al., 2013). As a consequence, the NPP increased 7.5 Gg C $year^{-1}$.

Conclusion

Based on the CASA model and the Thornthwaite Memorial model, this paper calculated the NPP_{act} and NPP_{pot} in Anji during the period 1984-2014, explored the temporal and spatial changes of $HANPP_{luc}$ in Anji, and analyzed the impact of LUC on vegetation NPP. The main findings are as follows:

(1) Over the 31 years, there was an increasing trend in the annual $HANPP_{luc}$, but the changing trends showed a large spatial heterogeneity. The $HANPP_{luc}$ increased in northern and central Anji because of the urbanization and decrease of the croplands. While the $HANPP_{luc}$ decreased in northern, southern and central Anji due to land cover changes to highly productive land type (MBF).

(2) In general, the $HANPP_{luc}$ in central Anji were higher than those in other regions. The positive $HANPP_{luc}$, i.e. NPP_{pot} was higher than NPP_{act}, appeared in northern, southern and central Anji, while the negative $HANPP_{luc}$ appeared in eastern and western Anji.

(3) The increase of the MBF led to an increase in NPP, while converting croplands to forests also increased NPP. However, the increase of the urban land and river caused the

http://www.aloki.hu ● ISSN 1589 1623 (Print) ● ISSN 1785 0037 (Online)
DOI: http://dx.doi.org/10.15666/aeer/1906_43314348

NPP decreasing significantly. Our results indicate that MBF is a good substitute for wood due to its strong capacity for carbon sequestration, and we also should control of the expansion of urban land.

The long-term forecasting and evaluation of the temporal and spatial changes of $HANPP_{luc}$ has more important significance for land use management, and it is our future studies.

Acknowledgements. This work was supported by the Jiangsu Provincial Department of Education Foundation of China [Grant number 2020SJA0541]; the Major Project of the Philosophy and Social Science Foundation of the Jiangsu Higher Education Institutions of China [Grant number 2021SJZDA130]; and the Ministry of Education Foundation of China [Grant number 19JZD023]; and Scientific Research Foundation for Talented Scholars of Jinling Institute of Technology (under grant JIT-B-202031).

REFERENCES

[1] Cao, L., Coops, N. C., Sun, Y., Ruan, H., Wang, G., Dai, J., She, G. (2019): Estimating canopy structure and biomass in bamboo forests using airborne LiDAR data. – ISPRS Journal of Photogrammetry and Remote Sensing 148: 114-129.

[2] Chen, A., Li, R., Wang, H., He, B. (2015): Quantitative assessment of human appropriation of aboveground net primary production in China. – Ecological Modelling 312: 54-60.

[3] Chen, S., Jiang, H., Jin, J., Wang, Y. (2017): Changes in net primary production in the Tianmu Mountain Nature Reserve, China, from 1984 to 2014. – International Journal of Remote Sensing 38: 211-234.

[4] Chen, S., Jiang, H., Cai, Z., Zhou, X., Peng, C. (2018): The response of the net primary production of Moso bamboo forest to the On and Off-year management: a case study in Anji County, Zhejiang, China. – Forest Ecology and Management 409: 1-7.

[5] Chen, S., Jiang, H., Chen, Y., Cai, Z. (2020): Spatial-temporal patterns of net primary production in Anji (China) between 1984 and 2014. – Ecological Indicators 110.

[6] Fetzel, T., Gradwohl, M., Erb, K.-H. (2014): Conversion, intensification, and abandonment: a human appropriation of net primary production approach to analyze historic land-use dynamics in New Zealand 1860–2005. – Ecological Economics 97: 201-208.

[7] Field, C. B., Randerson, J. T., Malmström, C. M. (1995): Global net primary production: combining ecology and remote sensing. – Remote Sensing of Environment 51: 74-88.

[8] Foley, J. A., Defries, R., Asner, G. P., Barford, C., Bonan, G., Carpenter, S. R., Chapin, F. S., Coe, M. T., Daily, G. C., Gibbs, H. K., Helkowski, J. H., Holloway, T., Howard, E. A., Kucharik, C. J., Monfreda, C., Patz, J. A., Prentice, I. C., Ramankutty, N., Snyder, P. K. (2005): Global consequences of land use. – Science 309: 570-574.

[9] Gang, C., Zhou, W., Chen, Y., Wang, Z., Sun, Z., Li, J., Qi, J., Odeh, I. (2014): Quantitative assessment of the contributions of climate change and human activities on global grassland degradation. – Environmental Earth Sciences 72: 4273-4282.

[10] Garbulsky, M. F., Paruelo, J. M. (2004): Remote sensing of protected areas to derive baseline vegetation functioning characteristics. – Journal of Vegetation Science 15: 711-720.

[11] Geneletti, D., Duren, I. V. (2008): Protected area zoning for conservation and use: a combination of spatial multicriteria and multiobjective evaluation. – Landscape and Urban Planning 85: 97-110.

[12] Haberl, H., Erb, K. H., Krausmann, F., Gaube, V., Bondeau, A., Plutzar, C., Gingrich, S., Lucht, W., Fischer-Kowalski, M. (2007): Quantifying and mapping the human

http://www.aloki.hu ● ISSN 1589 1623 (Print) ● ISSN 1785 0037 (Online)
DOI: http://dx.doi.org/10.15666/aeer/1906_43314348

appropriation of net primary production in earth's terrestrial ecosystems. – Proc Natl Acad Sci USA 104: 12942-12947.

[13] Haberl, H., Erb, K.-H., Krausmann, F. (2014): Human appropriation of net primary production: patterns, trends, and planetary boundaries. – Annual Review of Environment and Resources 39: 363-391.

[14] Huang, X., Luo, G., Han, Q. (2018): Temporospatial patterns of human appropriation of net primary production in Central Asia grasslands. – Ecological Indicators 91: 555-561.

[15] Huang, Q., Zhang, F., Zhang, Q., Ou, H., Jin, Y. (2020): Quantitative assessment of the impact of human activities on terrestrial net primary productivity in the Yangtze River delta. – Sustainability 12.

[16] Hull, V., Xu, W., Liu, W., Zhou, S., Viña, A., Zhang, J., Tuanmu, M.-N., Huang, J., Linderman, M., Chen, X., Huang, Y., Ouyang, Z., Zhang, H., Liu, J. (2011): Evaluating the efficacy of zoning designations for protected area management. – Biological Conservation 144: 3028-3037.

[17] IPCC (2013): Climate Change 2013: The Physical Science Basis. Contribution of Working Group I to the Fifth Assessment Report of the Intergovernmental Panel on Climate Change. – Cambridge University Press, Cambridge UK, New York.

[18] Krausmann, F., Erb, K.-H., Gingrich, S., Haberl, H., Bondeau, A., Gaube, V., Lauk, C., Plutzar, C., Searchinger, T. D. (2013): Global human appropriation of net primary production doubled in the 20th century. – Proc Natl Acad Sci USA 110: 10324-10329.

[19] Li, Z. J., Lin, P., He, J. Y., Yang, Z. W., Lin, Y. M. (2006): Silicon's organic pool and biological cycle in moso bamboo community of Wuyishan Biosphere Reserve. – J Zhejiang Univ Sci B 7: 849-857.

[20] Lieth, H. (1975): Modeling the Primary Productivity of the World. – In: Lieth, H., Whittaker, R. H. (eds.) Primary Productivity of the Biosphere. Springer, New York, pp. 237-264.

[21] Lin, D., Yu, H., Lian, F., Wang, J.-a., Zhu, A. X., Yue, Y. (2016): Quantifying the hazardous impacts of human-induced land degradation on terrestrial ecosystems: a case study of karst areas of south China. – Environmental Earth Sciences 75.

[22] Lin, H., Zhao, J. U. N., Liang, T., Bogaert, J. A. N., Li, Z. (2012): A classification indices-based model for net primary productivity (Npp) and potential productivity of vegetation in China. – International Journal of Biomathematics 05: 1-23.

[23] Liu, Y., Zhang, Z., Tong, L., Khalifa, M., Wang, Q., Gang, C., Wang, Z., Li, J., Sun, Z. (2019): Assessing the effects of climate variation and human activities on grassland degradation and restoration across the globe. – Ecological Indicators 106.

[24] Lü, D., Gao, G., Lü, Y., Xiao, F., Fu, B. (2020): Detailed land use transition quantification matters for smart land management in drylands: an in-depth analysis in Northwest China. – Land Use Policy 90.

[25] Mahbub, R. B., Ahmed, N., Rahman, S., Hossain, M. M., Sujauddin, M. (2019): Human appropriation of net primary production in Bangladesh, 1700–2100. – Land Use Policy 87.

[26] Medková, H., Vačkář, D., Weinzettel, J. (2017): Appropriation of potential net primary production by cropland in terrestrial ecoregions. – Journal of Cleaner Production 150: 294-300.

[27] Pan, J., Xu, B. (2020): Modeling spatial distribution of potential vegetation NPP in China. – Chinese Journal of Ecology 39: 1001-1012.

[28] Plutzar, C., Kroisleitner, C., Haberl, H., Fetzel, T., Bulgheroni, C., Beringer, T., Hostert, P., Kastner, T., Kuemmerle, T., Lauk, C., Levers, C., Lindner, M., Moser, D., Müller, D., Niedertscheider, M., Paracchini, M. L., Schaphoff, S., Verburg, P. H., Verkerk, P. J., Erb, K.-H. (2016): Changes in the spatial patterns of human appropriation of net primary production (HANPP) in Europe 1990–2006. – Regional Environmental Change 16: 1225-1238.

http://www.aloki.hu ● ISSN 1589 1623 (Print) ● ISSN 1785 0037 (Online)
DOI: http://dx.doi.org/10.15666/aeer/1906_43314348

[29] Potter, C. S., Randerson, J. T., Field, C. B., Matson, P. A., Vitousek, P. M., Mooney, H. A., Klooster, S. A. (1993): Terrestrial ecosystem production: a process model based on global satellite and surface data. – Global Biogeochemical Cycles 7: 811-841.
[30] Pritchard, R., Ryan, C. M., Grundy, I., van der Horst, D. (2018): Human appropriation of net primary productivity and rural livelihoods: findings from six villages in Zimbabwe. – Ecological Economics 146: 115-124.
[31] Ren, z., Zhu, H., Shi, H., Liu, X. (2017): Spatiotemporal-distribution pattern variation of net primary productivity in potential natural vegetation and its response to climate and topography in China. – Acta Agrestia Sinica 25: 474-485.
[32] Saikku, L., Mattila, T., Akujärvi, A., Liski, J. (2015): Human appropriation of net primary production in Finland during 1990–2010. – Biomass and Bioenergy 83: 559-567.
[33] Shi, T., Yang, S., Zhang, W., Zhou, Q. (2020): Coupling coordination degree measurement and spatiotemporal heterogeneity between economic development and ecological environment—empirical evidence from tropical and subtropical regions of China. – Journal of Cleaner Production 244.
[34] Song, X., Peng, C., Zhou, G., Jiang, H., Wang, W., Xiang, W. (2013): Climate warming-induced upward shift of Moso bamboo population on Tianmu Mountain, China. – Journal of Mountain Science 10: 363-369.
[35] Song, X., Peng, C., Zhou, G., Gu, H., Li, Q., Zhang, C. (2016): Dynamic allocation and transfer of non-structural carbohydrates, a possible mechanism for the explosive growth of Moso bamboo (Phyllostachys heterocycla). – Scientific Reports 6.
[36] Sun, G. (2009): Simulation of potential vegetation distribution and estimation of carbon flux in China from 1981 to 1998 with LPJ dynamic global vegetation model. – Climatic and Environmental Research 14: 341-351.
[37] Waters, N. (2017): Tobler's First Law of Geography. – In: International Encyclopedia of Geography: People, the Earth, Environment and Technology. Wiley-Interscience, New York.
[38] Weinzettel, J., Vačkářů, D., Medková, H. (2019): Potential net primary production footprint of agriculture: a global trade analysis. – Journal of Industrial Ecology 23: 1133-1142.
[39] Xu, H.-j., Wang, X.-p. (2016): Effects of altered precipitation regimes on plant productivity in the arid region of northern China. – Ecological Informatics 31: 137-146.
[40] Yin, L., Dai, E., Zheng, D., Wang, Y., Ma, L., Tong, M. (2020): What drives the vegetation dynamics in the Hengduan Mountain region, southwest China: climate change or human activity? – Ecological Indicators 112.
[41] Zhang, F., Pu, L., Huang, Q. (2015): Quantitative assessment of the human appropriation of net primary production (HANPP) in the coastal areas of Jiangsu, China. – Sustainability 7: 15857-15870.
[42] Zhang, T., Peng, J., Liang, W., Yang, Y., Liu, Y. (2016): Spatial-temporal patterns of water use efficiency and climate controls in China's Loess Plateau during 2000-2010. – The Science of the Total Environment 565: 105-122.
[43] Zhang, J., Lv, J., Li, Q., Ying, Y., Peng, C., Song, X. (2017a): Effects of nitrogen deposition and management practices on leaf litterfall and N and P return in a Moso bamboo forest. – Biogeochemistry 134: 115-124.
[44] Zhang, L., Luo, Z., Mallon, D., Li, C., Jiang, Z. (2017b): Biodiversity conservation status in China's growing protected areas. – Biological Conservation 210: 89-100.
[45] Zhu, W., Pan, Y., He, H., Yu, D., Hu, H. (2006): Simulation of maximum light use efficiency for some typical vegetation types in China. – Chinese Science Bulletin 51: 457-463.
[46] Zou, D., Feng, Q., Liang, T. (2011): Research on Grassland Classification and NPP in Gannan Region. – Remote Sensing Technology and Application 26: 577-583.

http://www.aloki.hu ● ISSN 1589 1623 (Print) ● ISSN 1785 0037 (Online)
DOI: http://dx.doi.org/10.15666/aeer/1906_43314348

IMIDACLOPRID TOXICITY: EFFECTS ON THE CLASTOGENIC RESPONSE OF CARP (*CYPRINUS CARPIO*) FRY

ISPIR, U.[1] – OZCAN, M.[2*]

[1]*Turgut Ozal University, Doğanşehir Vahap Küçük Vocational School, Department of Aquaculture, Malatya 44210, Turkey*

[2]*Kahramanmaras Sütçü Imam University, Agriculture Faculty, Department of Fisheries, Kahramanmaras 46040, Turkey*

[*]*Corresponding author*
e-mail: mikailozcan@ksu.edu.tr; phone: +90-344-300-2097; fax: +90-344-300-2002

(Received 31st Mar 2020; accepted 20th Sep 2021)

Abstract. The article aimed to determine the effects of different doses of Imidacloprid on carp (*Cyprinus carpio*) fries, in order to determine whether their response could be used for the bioindication of the substance in aquatic environments in Turkey. The fish (weight 0.34±0.03 g, total length 2.97±0.21 cm) were subjected to 2.8 and 5.6 mg/l of Imidacloprid concentration for 96 and 168 h. A drop of blood from the caudal vein of carp was obtained and smeared on clean dry slide. Micronucleus (MN) and nuclear abnormality (NAs) analysis were carried out on erythrocytes. The frequency of micronucleus and nuclear abnormality observed varied significantly among the treated individuals ($p<0.05$). Imidacloprid led to negative alterations in the MN and NAs.
Keywords: *carp, Cyprinus carpio, Imidacloprid, micronucleus, nuclear abnormality*

Introduction

The environmental mutagens have been classified into three groups, such as, living, physical and chemical mutagens (Manna, 1982, 1983). The consequences of these pollutions on fish and shellfish have been studied by toxicologists. The exploratory, research in this field has identified it as an important environmental problem, all over the world. The effectiveness of these chemicals on the hereditary components of living organisms were categorised in genetic toxicology (Bickham et al., 2000; Iturburu et al., 2017). Brusick (1980) reported that even if many toxic substances damage the genetic material in nonspecific manner, the effect of these agents are highly specific on nucleic' acid. Hence these are capable of producing harmful effect at sublethal level.

The Imidacloprid can persist in soil, with 7-353 days for thiamethoxam and a half-life (28 - 1250 days) of neonicotinoids highly variable which varies greatly among soil type and other factors, (Goulson, 2013; Ansoar-Rodríguez et al., 2015). Also, depending on soil and rainfall conditions, 2.4% to nearly 80% of the mass of neonicotinoids (including Imidacloprid) could make their way into water bodies (Kurwadkar et al., 2013; Ansoar-Rodríguez et al., 2015; Bonmatin et al., 2015). Due to its presence in various environments, inhabited by large numbers of organisms, toxicological studies are extremely important. Thus, the use of living organisms (bioindicator), capable of somehow indicating the presence of stresses generated by environmental pollutants (Carneiro and Takayanagui, 2009; Abdel-Mohsien and Mahmoud, 2015), is one way to monitor the negative effects in the environment. Due to the presence of significant levels that have been detected in water, it is very

http://www.aloki.hu ● ISSN 1589 1623 (Print) ● ISSN 1785 0037 (Online)
DOI: http://dx.doi.org/10.15666/aeer/1906_43494355

important to conduct studies on the effects of Imidacloprid on aquatic organisms as bioindicators. Fish are widely to this end because their capacity to accumulate contaminants and show physiological, biochemical, histological or differentiated cell response (Fontanetti et al., 2012). These organisms may indicate variations in tolerance to environmental conditions created by the use of pesticides, including genetic change, which makes them excellent indicators with a high application for monitoring environmental genotoxicity (Yohannes et al., 2014).

The micronucleus (MN) assay has been used as a measure of genotoxicity in fish under laboratory and field conditions. The formation of nuclear abnormalities (NAs) such as lobed, blebbed, and notched nuclei described by several authors have been reported in fish erythrocytes as a consequence of exposure to environmental and chemical contaminants with cytotoxic, genotoxic, mutagenic or carcinogenic activity. The micronucleus test in fish has the potential to detect clastogenic and aneugenic effects of environmental agents in aqueous media. Because teleost erythrocytes are nucleated, MN have been scored in fish erythrocytes as a measure of clastogenic activity (Heddle et al., 1983; Al-Sabti and Metcalfe, 1995; Fenech et al., 2003; Machado Da Rocha et al., 2009).

Paralichthys olivaceus, in vitro cytotoxicity median inhibitory concentrations of 38.5 mg/L to 41.9 mg/L of technical imidacloprid were reported, whereas other species like *Oncorhynchus mykiss* and *Cyprinus carpio* presented 96-h LC50 values of 211 mg/L and 280 mg/L, respectively. Other negative effects, like the alteration of the neurobehavioral function in early-life and adult zebrafish (Crosby et al., 2015) or the stress syndrome in juvenile *Oryzias latipes* (Sanchez Bayo and Goka, 2005), have been described. Other vertebrates also suffer imidacloprid effects. For example, increased DNA damage in human peripheral blood lymphocytes exposed in vitro to 20 mM imidacloprid (5 mg/L) have been reported (Costa et al., 2009).

There was no published report on clastogenic effect of Imidacloprid on carp fry. Based on the observations from literature survey, it was investigated to study the toxic effect of Imidacloprid on erythrocytes of carp, *C. carpio*.

Materials and Methods

Fish and chemical supply

Fish samples, weighing 0.34±0.03 g, were obtained from the Keban Fish Breeding Unit of IX. Region Directorate, the State Hydraulic Works in Turkey. They were brought to the laboratory and acclimated to laboratory conditions for 14 days. Water temperature in the tank was maintained at 24.0 ± 1.0 °C using a heater. Fishes were fed with pellet feeds during acclimating. Fish were fed *ad libitum* with a commercial feed throughout the experiments. Fish were stocked in 3 groups (25 fish/per group) in the tanks supplied.

The first group was maintained in tap water as a control group. The fish in group 2 and 3 were exposed to 2.8 and 5.6 mg/l of Imidacloprid (N-{1-[(6-chloro-3-pyridyl) methyl]-4,5-dihydroimidazol-2-yl} nitramide) concentration for 96 and 168 h (7 days). The entire experiment was repeated two independent times; each replicate for each group contained twenty-five fish, for a total of 150 fish. At the 96 h and 168 h of the test, the fish were anaesthetized in an anaesthetic matter (50 ppm, benzocaine) and a drop blood was taken from the caudal vein. Water quality parameters were monitored daily for each tank.

http://www.aloki.hu ● ISSN 1589 1623 (Print) ● ISSN 1785 0037 (Online)
DOI: http://dx.doi.org/10.15666/aeer/1906_43494355

Micronucleus assay

The slides were prepared by smearing one drop of blood on clean microscopic slides, fixed in methanol for 10 min and left to air-dry at room temperature and finally stained with 5% Giemsa in Sorenson buffer (pH 6.9) for 20 min. A total of 1000 erythrocytes were examined for each specimen under the light microscope. For the scoring of micronuclei, the following criteria were adopted from Fenech et al. (2003). The diameter of the MN should be less than one-third of the main nucleus. MN should be separated from or marginally overlap with main nucleus as long as there is clear identification of the nuclear boundary. MN should have similar staining as the main nucleus.

Statistical analysis

The one-way analysis of variance (ANOVA), Duncan's Multiple Range Test was employed to compare the mean differences in MN frequency between control and different exposure periods and, in between successive exposure periods.

Results

Imidacloprid exposure elicited hyperactivity characterized by opercula movement, erratic swimming, loss of equilibrium, hanging in the water vertically and gasping for air. However, no fish died after the 168 h period of exposure to different Imidacloprid doses.

Results of micronucleus assays with carp are shown in *Tables 1, 2* and *Figures 1, 2*. In the 2.8 mg/L Imidacloprid group, the micronuclei cell number were not significantly different ($p>0.05$). As shown in the figure, Imidacloprid treatment significantly increased the micronucleus frequency in blood ($P<0.05$) in 5.6 mg/L treatment group. For the concentration of 5.6 mg/L Imidacloprid, the number of micronuclei cell was significantly higher than control after exposure of 168h, whereas the micronuclei abnormalities did not show any increase in relation to the control group up to 96 hours (*Fig. 3*). The number of nuclear abnormality (NA) moderate increased both 96h and 168 h in 5.8 mg/L Imidacloprid group.

Table 1. *Mean values of micronuclei frequencies in blood of fishes treaed with Imidacloprid*

	96h	**168h**
Control	1.72±0.12	1.74±0.11
2.8 mg/L	1.69±0.09	1.73±0.13
5.6 mg/L	$1.93±0.19^{a,b}$	$2.28±0.20^{a,b}$

Table 2. *Mean values of binuclei frequencies in blood of fishes treaed with Imidacloprid*

	96h	**168h**
Control	0.11±0.01	0.14±0.02
2.8 mg/L	0.09±0.01	0.13±0.03
5.6 mg/L	0.12±0.02	0.14±0.02

http://www.aloki.hu ● ISSN 1589 1623 (Print) ● ISSN 1785 0037 (Online)
DOI: http://dx.doi.org/10.15666/aeer/1906_43494355

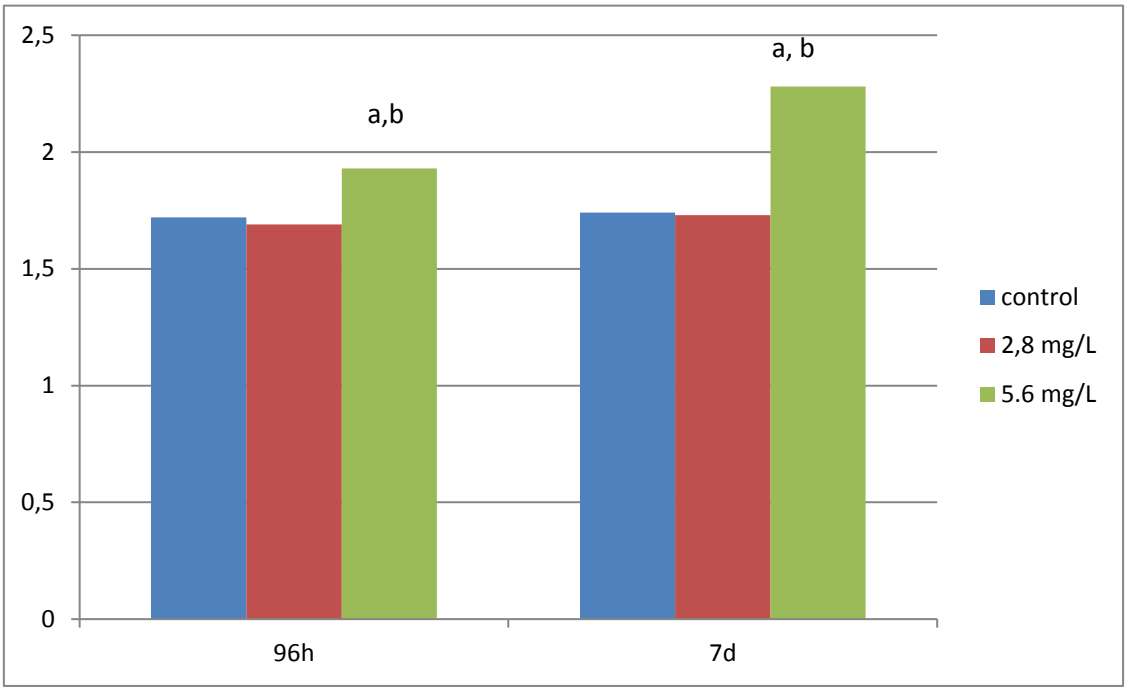

Figure 1. *The erythrocytes from carp exposed to imidacloprid. (A) normal erythrocytes (B) micronucleus*

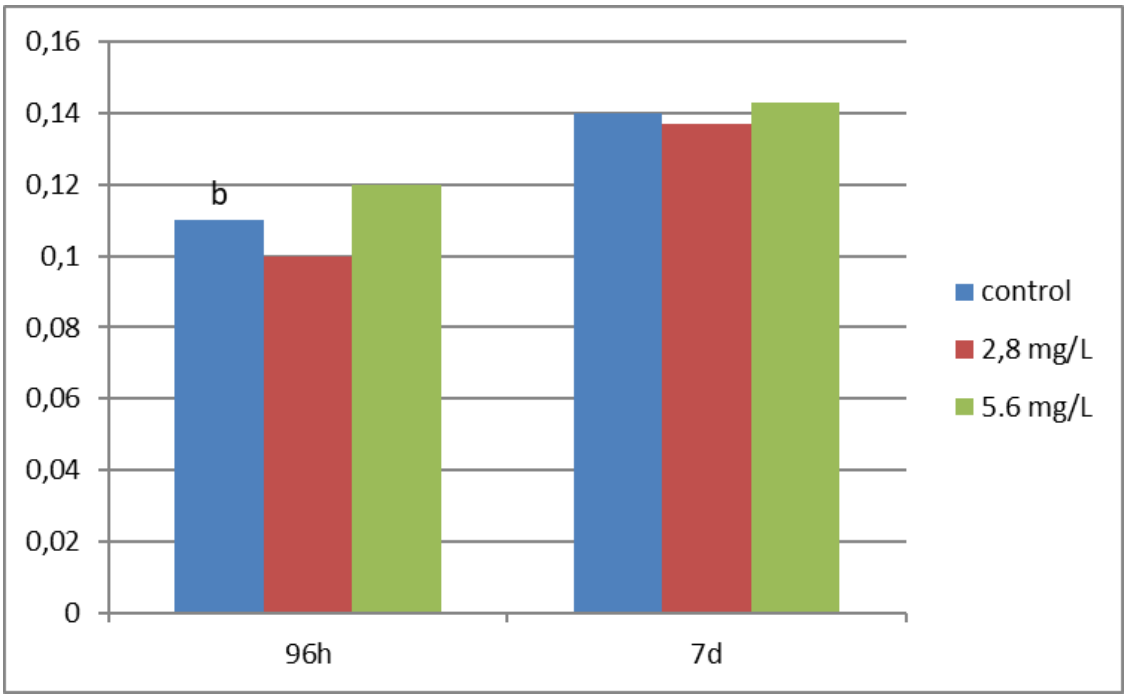

Figure 2. *Mean values of binuclei frequencies in blood of fishes treaed with Imidacloprid*

http://www.aloki.hu ● ISSN 1589 1623 (Print) ● ISSN 1785 0037 (Online)
DOI: http://dx.doi.org/10.15666/aeer/1906_43494355

(A)

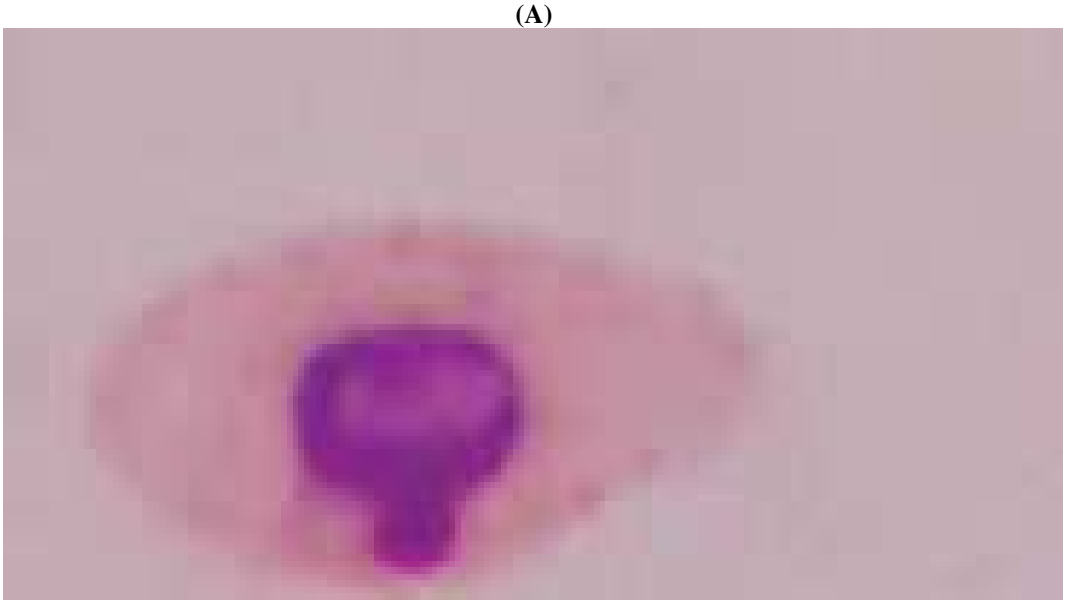

(B)

Figure 3. *The erythrocytes from carp exposed to imidacloprid. (A) normal erythrocytes (B) micronucleus*

Discussion

In the commercial formulation bioassay all fish exposed to 10 000mg/L İmidacloprid died after 3 h (Iturburu et al., 2017). In this study, Imidacloprid exposure elicited hyperactivity characterized by opercula movement, erratic swimming, loss of equilibrium, hanging in the water vertically and gasping for air. However, no fish died after the 168 h period of exposure to different Imidacloprid doses.

This study, Imidacloprid caused a dose-dependent increase in the frequency of MN and other NAs, which was statistically significant ($p < 0.05$) in the highest concentration evaluated (5.6 mg/L) compared to the control (*Tables 1, 2* and *Figs. 1, 2*). The results obtained in this study corroborate other pesticide studies using different species of fish, such as the evaluation of Imidacloprid (1-[(6-chloro-3-pyridinylmethyl]-N-nitro-2-

http://www.aloki.hu ● ISSN 1589 1623 (Print) ● ISSN 1785 0037 (Online)
DOI: http://dx.doi.org/10.15666/aeer/1906_43494355

imidazolidinimine; CASN˚138261-41-3; molecular formula C9H10ClN5O2), Aficida® and Endosulfan insecticides in fish erythrocytes from *Oreochromis niloticus* (Perciformes, Cichlidae), *Cnesterodon decemmaculatus* (Poeciliidae) and *Carassius carassius* (Cyprinidae) by the MN test (Candioti et al., 2010; Dar et al., 2015; Ansoar-Rodríguez et al., 2015). These studies demonstrate the effectiveness of fish and the MN test as a model for the biomonitoring of aquatic ecosystems that may be affected by pesticides.

At 100 mg/L and 1000 mg/L the imidacloprid micronucleus frequency was significantly higher than its negative control. Conversely, in the active ingredient bioassay the micronucleus frequency was significantly higher at 1000 mg/L imidacloprid in relation to its negative control (Iturburu et al., 2017). This study, for the concentration of 5.6 mg/L Imidacloprid, the number of micronuclei cell was significantly higher than control after exposure of 168 h, whereas the micronuclei abnormalities did not show any increase in relation to the control group up to 96 hours (*Fig. 3*). The number of nuclear abnormality (NA) moderate increased both 96 h and 168 h in 5.8 mg/L Imidacloprid group.

Conclusion

Considering the genotoxic effects of Imidacloprid on *C. carpio* as obtained in this study by MN, there is serious apprehension about the potential danger of this drug to aquatic organisms. However, detailed studies using other assays having different end points may be needed to confirm the mutagenic and genotoxic status of the Imidacloprid and further explore the mechanism and interactions with the DNA metabolism in different aquatic organisms, especially fish.

Acknowledgment. This work was presented as an oral presentation at the 2nd International Conference on Civil and Environmental Engineering (Cappadocia-2017), May 8 – 10, 2017, Nevşehir, Turkey.

Ethical Approval. All animal studies were approved by the Animal Ethics Committee of Kahramanmaraş Sütçü Imam University, Faculty of Agriculture (KSÜZİRHADYEK) and Research Institute (Protocol number: 2016/5-1).

REFERENCES

[1] Abdel-Mohsien, H. S., Mahmoud, M. A. M. (2015): Accumulation of Some Heavy Metals in Oreochromis niloticus from the Nile in Egypt: Potential Hazards to Fish and Consumers. – Journal of Environmental Protection 6: 1003-1013.

[2] Al-Sabti, K. C. D. (1995): Metcalfe. Fish micronuclei for assessing genotoxicity in water. – Mutat. Res. 343: 121-135.

[3] Ansoar-Rodríguez, Y., Christofoletti, C. A., Marcato, A. C., Correia, J. E., Bueno, O. C., Malaspina, O., Fontanetti, C. S. (2015): Genotoxic Potential of the Insecticide Imidacloprid in a Non-Target Organism (*Oreochromis niloticus*-Pisces). – Journal of Environmental Protection 6: 1360-1367.

[4] Bickham, J. W., Sandhu, S., Hebert, P. D. N., Chikhi, L., Athwal, R. (2000): Effects of chemical contaminants on genetic diversity in natural populations: Implications for biomonitoring and ecotoxicology. – Mutat Res 463: 33-51.

[5] Bonmatin, J. M., Giorio, C., Girolami, V., Goulson, D., Kreutzweiser, D. P., Krupke, C., Liess, M., Long, E., Marzaro, M., Mitchell, E. A. D., Noome, D. A., Simon-Delso, N.,

http://www.aloki.hu ● ISSN 1589 1623 (Print) ● ISSN 1785 0037 (Online)
DOI: http://dx.doi.org/10.15666/aeer/1906_43494355

Tapparo, A. (2015): Environmental fate and exposure; neonicotinoids and fipronil. – Environ Sci Pollut Res 22: 35-67.

[6] Brusick, D. J. (1980): Principles of genetic toxicology (First edition). – Plenum Press, New York, 279p.

[7] Candioti, J. V., Soloneski, S., Larramendy, M. L. (2010): Genotoxic and Cytotoxic Effects of the Formulated Insecticide Aficida® on *Cnesterodon decemmaculatus* (Jenyns, 1842) (Pisces: Poeciliidae). – Mutation Research 703: 180-186.

[8] Carneiro, R. M. A., Takayanagui, A. M. M. (2009): Estudos sobre bioindicadores vegetais e poluição atmosférica por meio de revisão sistemática da literatura. – Revista Brasileira de Ciências Ambientais 13: 26-44.

[9] Costa, C., Silvari, V., Melchinib, A., Catania, S., Heffronc, J. J., Trovato, A., De Pasquale, R. (2009): Genotoxicity of imidacloprid in relation to metabolic activation and composition of the commercial product. – Mutat Res 672(1): 40-44.

[10] Crosby, E. B., Bailey, J. M., Oliveri, A. N., Levin, E. D. (2015): Neurobehavioral impairments caused by developmental imidacloprid exposure in zebrafish. – Neurotoxicol Teratol 49: 81-90.

[11] Dar, S. A., Yousuf, A. R., Balkhi, M. H., Ganai, F. A., Bhat, F. A. (2015): Assessment of Endosulfan Induced Genotoxicity and Mutagenicity Manifested by Oxidative Stress Pathways in Freshwater Cyprinid Fish Crucian Carp (*Carassius carassius* L.). – Chemosphere 120: 273-283.

[12] Fenech, M., Chang, W. P., Kirsch-Volders, M., Holland, N., Bonassi, S., Zeiger, E. (2003): HUMN project: Detailed description of the scoring criteria for the cytokinesis-block micronucleus assay using isolated human lymphocyte cultures. – Mutat. Res. 534: 65-75.

[13] Fontanetti, C. S., Souza, T. S., Christofoletti, C. A. (2012): Sustainable Water Management in the Tropics and Subtropics-and Case Studies in Brazil. – The Role of Biomonitoring in the Quality Assessment of Water Resources 3: 975-1005.

[14] Goulson, D. (2013): Review: An Overview of the Environmental Risks Posed by Neonicotinoid Insecticides. – Journal of Applied Ecology 50: 977-987.

[15] Heddle, J. A., Hite, M., Jrkhart, B., Macgregor, J., Salamone, M. (1983): The induction of micronuclei as a measure of genotoxicity. – Mutat. Res. 123: 61-118.

[16] Iturburu, F. G., Zömısch, M., Panzerı, A. M., Crupkın, A. C., Contardo-Jara, V., Pflugmacher, S., Menone, M. L. (2017): Uptake, distribution in different tissues, and genotoxicity of imidacloprid in the freshwater fish *Australoheros facetus*. – Environmental Toxicology and Chemistry 36(3): 699-708.

[17] Kurwadkar, S. T., Dewinne, D., Wheat, R., McGaha, D. G., Mitchell, F. L. (2013): Time Dependent Sorption Behavior of Dinotefuran, Imidacloprid and Thiamethoxam. – Journal of Environmental Science and Health (Part B) 48: 237-242.

[18] Machado Da Rocha, C. A., Dos Santos, R. A., De Oliveira Bahia, M., Da Cunha, L. A., Ribeiro, H. F., Burbano, R. M. R. (2009): The Micronucleus Assay in Fish Species as an Important Tool for Xenobiotic Exposure Risk Assessment - A Brief Review and an Example Using Neotropical Fish Exposed to Methylmercury. – Reviews in Fisheries Science 17(4): 478-484.

[19] Manna, G. K. (1982): The new horizon of mutagenesis. – Curr. Sci. 51: 1087-1093.

[20] Manna, G. K. (1983): Cytogenetics studies on fishes and amphibia. – In: Genetical Research in India, XV Intern. Congr. Genet. New Delhi, India, 12-21. ICAR, pp. 244-273.

[21] Sanchez Bayo, F., Goka, K. (2005): Unexpected effects of zinc pyrithione and imidacloprid on Japanese medaka fish (*Oryzias latipes*). – Aquat Toxicol 74: 285-293.

[22] Yohannes, Y. B., Ikenaka, Y., Saengtienchai, A., Watanabe, K. P., Nakayama, M. M., Ishizuka, M. (2014): Concentrations and Human Health Risk Assessment of Organochlorine Pesticides in Edible Fish Species from a Rift Valley Lake-Lake Ziway, Ethiopia. – Ecotoxicology and Environmental Safe 106: 95-101.

http://www.aloki.hu ● ISSN 1589 1623 (Print) ● ISSN 1785 0037 (Online)
DOI: http://dx.doi.org/10.15666/aeer/1906_43494355

ENHANCING SUSTAINABILITY AND FODDER PRODUCTION OF LOWLAND PASTURES THROUGH FENCING AND CONSERVATION AGRICULTURE IN ARID AGRO-PASTORAL ECOSYSTEMS

TLILI, A.[1] – FETOUI, M.[2] – BEN SALEM, F.[1] – LOUHAICHI, M.[3] – NEFFATI, M.[1] – TARHOUNI, M.[1*]

[1]*Institut des Régions Arides. Laboratoire des Ecosystèmes Pastoraux et Valorisation des Plantes Spontanées et des Microorganismes Associés, University of Gabes, 4100 Médenine, Tunisia*

[2]*Institut des Régions Arides, Laboratoire d'économie et Sociétés Rurales, University of Gabes, 4100 Médenine, Tunisia*

[3]*International Center for Agricultural Research in the Dry Areas (ICARDA), Tunis, Tunisia*

[*]*Corresponding author*
e-mail: medhtarhouni@yahoo.fr

(Received 15th Mar 2021; accepted 30th Aug 2021)

Abstract. The short-term fencing effects on vegetation in dryland landscape depressions are analyzed and the economic performance of grazing-only and integrated grazing with cropping in regard to land capital are compared. The goal is to suggest efficient strategic choices and more profitable land allocation of lowlands in dry areas. To analyze the vegetation, 12 cages each 2 m² were installed at three sides of a depression (4 east, 4 middle and 4 west side). Natural vegetation was recorded in the inside and outside cages during the spring of 2015, 2016 and 2018. Pastoral productivity was also calculated. To study the economic performance of cropping systems, local owner-farmers representing three cropped areas (1, 3 and 9 ha) were interviewed using socioeconomic surveys. The main results showed that short-term fencing increased diversity (24% to 61% in the middle cages). This improvement is due to annuals and the recruitment of palatable perennials. Economic evaluation showed that grazing is more profitable than integrated management, except for diversified and large cropped areas. The strategic recommendations for efficient, profitable and sustainable lowland allocation are short-term fencing with grazing-only in small depressions, and diversified crops mixed with grazing in larger depressions.
Keywords: *rangeland management, economic performance, drylands, landscape depressions, Marab*

Introduction

During the last few decades, climate change and overexploitation have destroyed natural resources and dramatically changed many ecosystem services (Vijaya Venkataraman et al., 2012; Hoffmann et al., 2014). Impacts on ecosystems can be environmental, economic and social, particularly in the most vulnerable semi-arid and arid areas (Schilling et al., 2012; Grimm et al., 2013). In these areas, ecological balance has been destabilized by human pressure and changes in land use and abiotic stresses, consequently affecting biodiversity and resilience capacity (Aïdoud et al., 2006; Eskandari et al., 2016; Zhang et al., 2016). Despite their fragility, these large areas are occupied by almost 38% of the world's human population. They contribute to carbon sequestration, combat desertification, and maintain livestock farming (Lal, 2002; Reynolds et al., 2007). Apart from its position in the food chain as the primary producer, spontaneous vegetation plays an important role in the prevention of soil degradation and erosion, maintenance of soil structure and fertility, and regulation of water flows and

http://www.aloki.hu ● ISSN 1589 1623 (Print) ● ISSN 1785 0037 (Online)
DOI: http://dx.doi.org/10.15666/aeer/1906_43574371

climate (Alcamo, 2003; Hoffmann et al., 2014). Many natural ecosystems are disturbed following their conversion to farmland and selective exploitation. Grazing, animal breeding and seasonal cropping are the main agricultural activities affecting dryland ecosystems. These land uses have changed during recent decades due to intensification and increases in productivity, following changes in human population density and progress in cultivation techniques, mechanization and agrichemicals. Overgrazing occurs in some localities when the stocking rate is exceeded, and rangeland availability is reduced by plowing or water deficits (Ouled-Belgacem et al., 2013). Hence, human activities and poor land management, particularly overgrazing, exacerbated by climate change constitute the main causes of ecosystem degradation (FAO, 2006; Tietjen and Jeltsch, 2007; Carmona et al., 2013; Hoffmann et al., 2014).

To avoid this decline, strategic management, conservation techniques and sustainable use should be pursued. Various solutions have been developed to preserve pastoral areas in Southern Tunisia, with a focus on rehabilitation and pastoral enhancement techniques and interventions. Fencing is one of the most well-known and traditionally widely practiced techniques for rangeland management in Tunisia and elsewhere around the world (Nefzaoui and Mourid, 2008; Squires et al., 2009; Gamoun et al., 2018; Ouled-Belgacem, 2018).

This technique, locally known as *gdel*, consists of leaving part of a rangeland to rest (without grazing) for a period of two to four years depending on the ecosystem capacity to recover and rainfall conditions, to reconstitute plant cover, reduce soil erosion and increase fodder production, soil organic matter ,and biodiversity (Ouled-Belgacem, 2012). Landscape depressions, known as *marab* in Arabic, constitute one of the better-integrated agro-pastoral systems with good edaphic and hydrologic properties. These agro-pastoral systems bring together the agricultural activities of grazing and cropping.

However, instabilities shaped by these activities can lead to disturbed vegetation structure, principally revealed by a decline in perennial plants (Hubbell et al., 1999; Slimani and Aïdoud, 2004). Several approaches to local management have been applied to reduce degradation by enhancing some marginalized resources (e.g., revegetation using pastoral halophytes and alternative feeds in scarce seasons) and re-adjusting the ecological balance (Temel et al., 2015; Ayeb et al., 2016; Tlili et al., 2018).

To mitigate ecosystem degradation and reduce forage deficiency requires improving our knowledge of the specificities of agro-pastoral systems. Furthermore, the grazing and cropping combination must be analyzed to show the environmental impacts and economic efficiency. In this context, the present work aims to assess free grazing and fencing impacts on natural vegetation and to compare the economic performance of grazing-only and integrated grazing with cropping to suggest optimal choices and more profitable and sustainable land allocation for arid lowland depressions.

Materials and Methods

Study site

The study was in the Samaliete region, southern Tunisia (33°18′08.26″N, 10°55′30.11″E; *Figure 1*). It is characterized by an arid Mediterranean climate with high temperature variability and precipitation patterns. The mean annual precipitation is about 165 mm with an average annual temperature of 21.4° C (according to climate data for the period 1991–2016; https://climateknowledgeportal.worldbank.org). The rainiest months are December and January and the driest are June and July. Soils in this region are

http://www.aloki.hu ● ISSN 1589 1623 (Print) ● ISSN 1785 0037 (Online)
DOI: http://dx.doi.org/10.15666/aeer/1906_43574371

calcareous with gypsic materials in the surface. Skeletal-gypsic soils are found in the surrounding areas, but the middle of depressions are characterized by deep, sandy soil. Some dwarf shrubs (e.g. *Gymnocarpos decander* Forssk. and *Anthyllis henoniana* Coss. Ex Batt.), forbs and grasses dominate the natural vegetation cover of the region.

Historically, the region has been devoted to grazing sheep and goats with some cultivated field crops during rainy years (cereals and legumes).

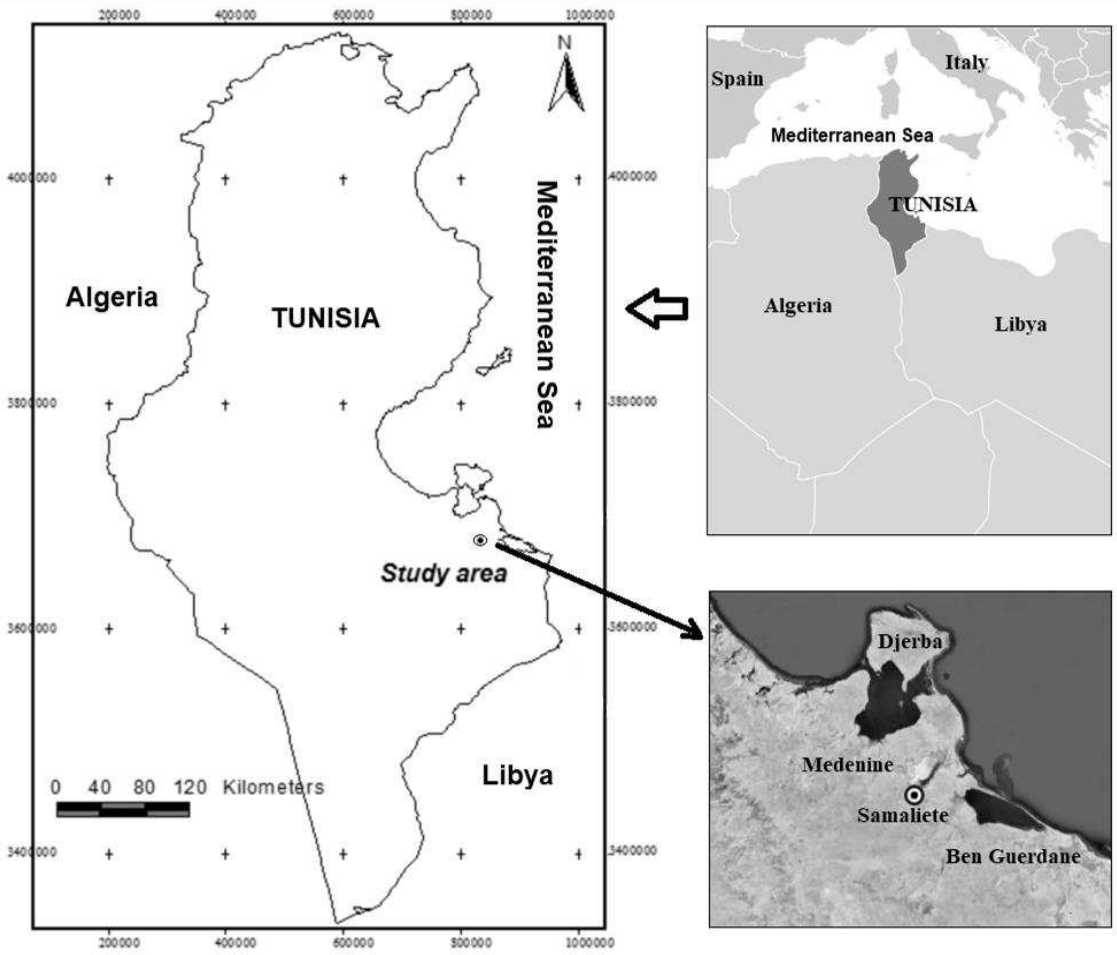

Figure 1. *Geographical location of the study site*

Experimental design

The experimental protocol was established on three sides of one lowland depression (east, middle and west side) in March 2015 (spring). The east and west sides of the depression were sloping (10%) but the middle was flat (about 50 m width, cropped area). On each side, four replicate-rectangular cages (each 50 cm high, 2 m^2 area and 15 m apart) were installed to protect vegetation from grazing animals, including small rodents (*Figure 2*, *Figure 3*). Four other rectangular quadrats (2 m^2 each, control) were installed and kept open to free grazing. Some ecological indicators such as flora richness and density were monitored during the springs of 2015, 2016 and 2018 inside and outside the cages.

http://www.aloki.hu ● ISSN 1589 1623 (Print) ● ISSN 1785 0037 (Online)
DOI: http://dx.doi.org/10.15666/aeer/1906_43574371

Figure 2. *Cage design and the overall view of the experimental depression*

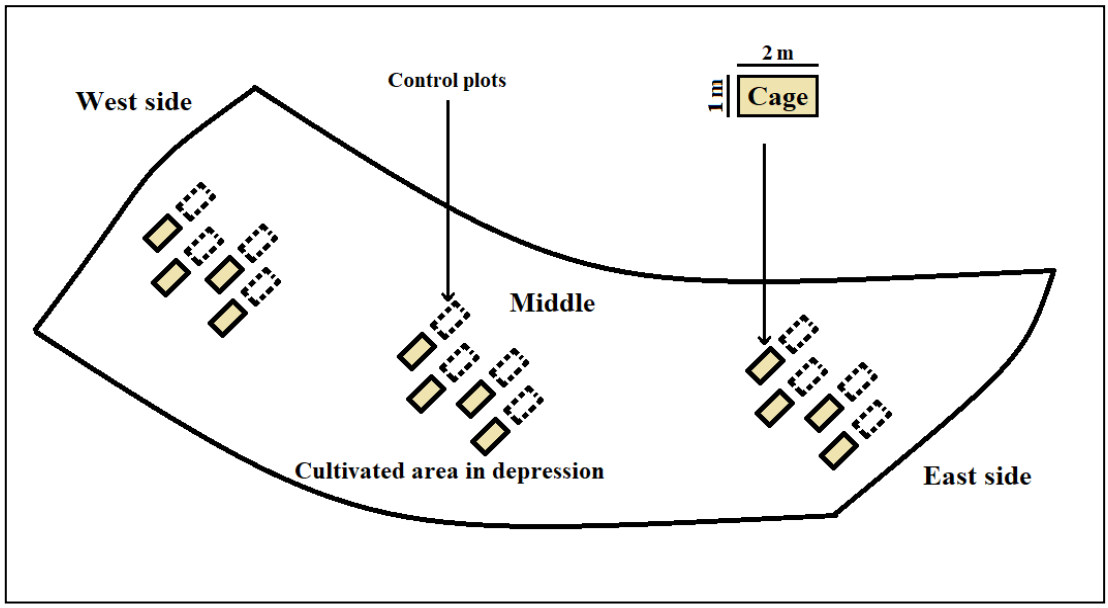

Figure 3. *Cage locations and experimental design for the vegetation measurement in the west, middle and east sides of the studied depression*

Vegetation monitoring

The grazing value (i.e. pastoral production) measurements were taken during the spring of 2015, 2016 and 2018, using the quadrat point method as described by Daget and Poissonnet (1971) and Floret (1988). Four lines (20 m length each) were monitored on each side of the depression. Every 20 cm along the tape, a fine pin was inserted in the ground and all vegetation and ground contacts were noted. In parallel, inside and outside cages, flora richness and density of perennial and annual species were evaluated, on each aspect/side during the study periods (*Table 1*).

The majority of plant species were identified in the field, and samples of unidentified species were collected and identified in the laboratory using reference books and taxonomic databases. Plant diversity between the monitored plots (*Table 1*) was determined using Jaccard's similarity index (S_J) as described by Roux and Roux (1967) (*Eq. 1*).

http://www.aloki.hu ● ISSN 1589 1623 (Print) ● ISSN 1785 0037 (Online)
DOI: http://dx.doi.org/10.15666/aeer/1906_43574371

Table 1. *Respective codes of the monitored plots within the depression over seasons*

Codes	Aspects/Sides	Grazing treatments	Spring of
EO1	East	Outside	2015
EO2	East	Outside	2016
EO3	East	Outside	2018
MO1	Middle	Outside	2015
MO2	Middle	Outside	2016
MO3	Middle	Outside	2018
WO1	West	Outside	2015
WO2	West	Outside	2016
WO3	West	Outside	2018
EI1	East	Inside	2015
EI2	East	Inside	2016
EI3	East	Inside	2018
MI1	Middle	Inside	2015
MI2	Middle	Inside	2016
MI3	Middle	Inside	2018
WI1	West	Inside	2015
WI2	West	Inside	2016
WI3	West	Inside	2018

$$S_J\,(x, y) = \frac{c}{(a + b - c)} \qquad \text{(Eq. 1)}$$

where a is the number of species in cage x, b is the number of species in cage y and c is the number of common species between x and y. The vegetation cover (VC) was:

$$VC = \frac{n}{N} \times 100 \qquad \text{(Eq. 2)}$$

With n the number of hits of all plant species and N the total number of hits. Thereafter, specific frequency of presence (SFP) was calculated as:

$$SPF_i = \frac{n_i}{N} \times 100 \qquad \text{(Eq. 3)}$$

With n_i the number of hits of the i^{th} species. The specific contribution of presence (SCP) of i^{th} species was:

$$SCP_i = \frac{SFP_i}{\sum_{i=1}^{n} SFP} \times 100 \qquad \text{(Eq. 4)}$$

The grazing value (GV) was then calculated:

$$GV = 0.2 \times \sum_{i=1}^{n} (SCP_i \times Is_i) \times VC \qquad \text{(Eq. 5)}$$

http://www.aloki.hu ● ISSN 1589 1623 (Print) ● ISSN 1785 0037 (Online)
DOI: http://dx.doi.org/10.15666/aeer/1906_43574371

where Is_i is the acceptability index of i^{th} species (Le Houérou and Ionesco, 1973). Finally, pastoral productivity (*P*) was obtained according to Aïdoud et al. (1983):

$$\boldsymbol{P}\ (\text{FU ha}^{-1}\ \text{year}^{-1}) = \quad \mathbf{7.52 \times} \boldsymbol{GV} \qquad \text{(Eq. 6)}$$

where FU is the forage unit, (one FU is the equivalent of 1 kg of barley).

Socioeconomic surveys

The field investigations were coupled with socioeconomic surveys with four owners of neighboring cropped depressions. Only these four owners are still in the region due to rural exodus. The objective of the surveys was to evaluate owner incomes (cropped systems) in comparison with owners only grazing. The four evaluated crops were barley (1 ha), barley and lentil (both in 1 ha), barley and lentil (both in 3 ha) and barley, wheat and lentil (all in 9 ha).

Interviews were conducted by the research team during the spring of 2015 (rainy year, 167.8 mm) and 2016 (dry year, 61.9 mm). The questionnaire had four sections: (i) household demographic information, (ii) agricultural systems, (iii) farm economic analysis and, (iv) community-identified problems assessment. Each interview lasted on average 1 hour. The data was coded and cleaned using Excel and data analysis was carried out using SPSS software.

Economic evaluation

Annual grazing incomes of 1 ha depressions (*GI*) in rainy and dry years (respectively 2015 and 2016) were calculated as:

$$\boldsymbol{GI} = \quad \boldsymbol{P} \times \mathbf{0.14} \qquad \text{(Eq. 7)}$$

where 0.14 is the local price of 1 kg of barley (in Euro).

After crop harvesting during the rainy year (2015), the economic benefits from small (1 ha), medium (3 ha) and large (9 ha) plowed depressions were calculated. The economic efficiency and profitability of land allocation in four different lowland systems were then evaluated, taking into account the land capital (i.e. small, medium and large plowed areas), the crop diversification and the land allocation (i.e. grazed and cropped lands).

To investigate the economic performance and efficiency of each surveyed lowland farm, a set of economic indicators were calculated. These indicators were (i) total rainfed crop gross product, total cost (i.e. input and labor costs) and overall gross margin (crop income), (ii) efficiency of the production process (EPP) (gross product-inputs/gross product), to assess the overall economic efficiency of each farm, and (iii) the total income for the integrated crop and grazing systems for a period of four years. Note that in southern Tunisia the long-term frequency of rain is about 1 rainy/3 dry years per four-year period (Ouessar et al., 2006). The total incomes for the grazing-only systems for four years were calculated to assess the profitability of the different farming systems and to identify more profitable land allocation.

http://www.aloki.hu ● ISSN 1589 1623 (Print) ● ISSN 1785 0037 (Online)
DOI: http://dx.doi.org/10.15666/aeer/1906_43574371

Statistical analysis

After testing normality (Shapiro–Wilk test) to verify homogeneity of variance, means were log-transformed. One-way ANOVAs were performed to separately compare density, richness and productivity under grazing, aspects and years effect. Two-way and three-way ANOVAs were used to test the interactions of these factors. Diversity analysis was carried out using the Jaccard similarity index between cages. All statistical analyses were performed using SPSS 20.0 software.

Results

Flora richness

The number of annual and perennial species in the inside and outside cages are presented in *Table 2*. The highest number of annuals was found in the middle of the depression (16.3 ± 3.4 species) and on the eastern side for perennials (9.8 ± 2.1 species). The lowest number of annuals occurred in spring 2016 inside cages on the east side of the depression, with 6.5 ± 2.5 species. During this same season, 4 ± 1.2 perennial species were found in the outside cages on the western side. In general, annuals were dominant in the inside and outside cages compared to perennials. Only annual forbs on the eastern side of the depression showed a significant difference ($F = 6.41$; $p < 0.05$) between outside (10 ± 3.6) and inside cages (5.3 ± 2.1), in spring 2016. The highest number of shrubs was on the east side of the depression and the lowest in the middle. This was due to plowing effects.

Table 2. *Flora richness of inside and outside cages in the Samaliete depression during the spring of 2015, 2016 and 2018*

	Spring	Inside			Outside		
		East	Middle	West	East	Middle	West
Annual forbs	2015	10.3 ± 6.3	13.5 ± 2.7A	10.5 ± 3.1	9.8 ± 2.2A	13.3 ± 2.6	11.0 ± 3.6A
	2016	5.3 ± 2.1*	7.0 ± 1.4B	7.8 ± 2.9	10.0 ± 3.6A*	7.3 ± 3.2	7.5 ± 2.6AB
	2018	4.5 ± 1.3	6.8 ± 2.1B	7.3 ± 1.7	5.0 ± 1.4bB	9.0 ± 3.2a	5.8 ± 0.5abB
Annual grasses	2015	2.0 ± 1.6A	2.8 ± 0.9A	2.0 ± 0.8	1.8 ± 0.5	2.8 ± 0.5A	2.8 ± 0.9
	2016	1.3 ± 0.9AB	0.8 ± 0.5B	1.3 ± 0.1	0.8 ± 0.5	1.3 ± 0.5B	1.3 ± 0.5
	2018	0.8 ± 0.5B	1.5 ± 0.6B	0.8 ± 0.9	1.0 ± 1.2	1.8 ± 1.3AB	2.0 ± 1.4
Total annuals	2015	12.3 ± 7.5	16.3 ± 3.4A	12.5 ± 3.7	11.5 ± 2.1A	16.0 ± 2.2A	13.8 ± 4.3A
	2016	6.5 ± 2.5	7.8 ± 1.3B	9.0 ± 3.6	10.8 ± 3.9A	8.8 ± 3.3B	8.8 ± 3.0AB
	2018	5.3 ± 1.5b	8.3 ± 2.1aB	8.0 ± 1.4a	5.5 ± 1.7B	10.0 ± 3.4AB	7.0 ± 0.8B
Perennial forbs	2015	3.0 ± 1.12B	4.3 ± 2.2	3.5 ± 1.3	5.5 ± 3.1	5.0 ± 1.8	3.0 ± 1.4AB
	2016	5.5 ± 1.9A	4.0 ± 0.8	3.6 ± 1.7	6.0 ± 2.2a	3.5 ± 2.1b	2.3 ± 0.9bB
	2018	5.5 ± 1.7A	4.0 ± 1.4	6.3 ± 1.7	7.0 ± 1.2	5.3 ± 3.6	5.3 ± 1.7A
Perennial grasses	2015	0.5 ± 0.5	1.0 ± 1.1	1.0 ± 1.2	0.3 ± 0.5	0.8 ± 0.5	0.0
	2016	0.0	0.3 ± 0.5	0.5 ± 0.5	0.3 ± 0.5	0.8 ± 0.5	0.3 ± 0.5
	2018	0.3 ± 0.5	0.5 ± 0.5	0.5 ± 0.6	0.25 ± 0.50	0.5 ± 0.6	0.3 ± 0.5
Shrubs	2015	2.5 ± 1.3	0.8 ± 0.9	1.0 ± 1.1	2.0 ± 0.8a	0.0 b	1.0 ± 0.8ab
	2016	2.3 ± 0.6a	0.3 ± 0.5b	1.5 ± 0.6a	2.5 ± 1.0a	0.0 b	1.5 ± 0.6ab
	2018	2.5 ± 1.3	1.0 ± 0.8	1.0 ± 0.8	2.5 ± 1.3a	0.3 ± 0.5b	1.3 ± 0.5ab
Total perennials	2015	5.8 ± 1.9B	5.5 ± 2.9	5.0 ± 1.8	7.8 ± 4.0	5.8 ± 2.2	4.0 ± 1.4
	2016	7.8 ± 2.6A	4.5 ± 0.6	5.3 ± 2.2	8.8 ± 3.0a	4.3 ± 2.2b	4.0 ± 1.2b
	2018	8.3 ± 2.9A	5.5 ± 2.4	7.8 ± 2.8	9.8 ± 2.1	6.0 ± 3.9	6.8 ± 1.9

a/b indicate significant differences between the depression sides during the same year; A/B indicate significant differences between years for the same side, according to Student–Newman–Keuls test. (*) indicates a significant difference between inside and outside cages for the same side and year. Values are means ± SD (n = 4)

http://www.aloki.hu ● ISSN 1589 1623 (Print) ● ISSN 1785 0037 (Online)
DOI: http://dx.doi.org/10.15666/aeer/1906_43574371

Plant density

Annual and perennial plant densities of inside and outside cages on the east, middle and west sides of the depression during the three years (2015, 2016 and 2018) are shown in *Figure 4*. The highest annual density was in the outside cages in the middle of the depression during spring 2015 (131.88 plants.m^{-2}), and the lowest in the inside cages on the east side during spring 2018 (7.5 plants.m^{-2}). For perennial density, the ANOVA showed a significant difference between years (outside cages on the east side: $p < 0.05$; between sides, outside cages in 2016: $p < 0.05$). The interaction of factors was not significant. However, there were significant differences for annual density between inside and outside cages only in the middle of the depression in spring 2016 ($p < 0.05$). Also, inter-annual significant differences were noted in the middle of the depression in both inside and outside cages on the one hand, and outside cages on the western side on the other hand. The main difference between aspects was found in the outside cages during the three years. No interaction between factors was noted.

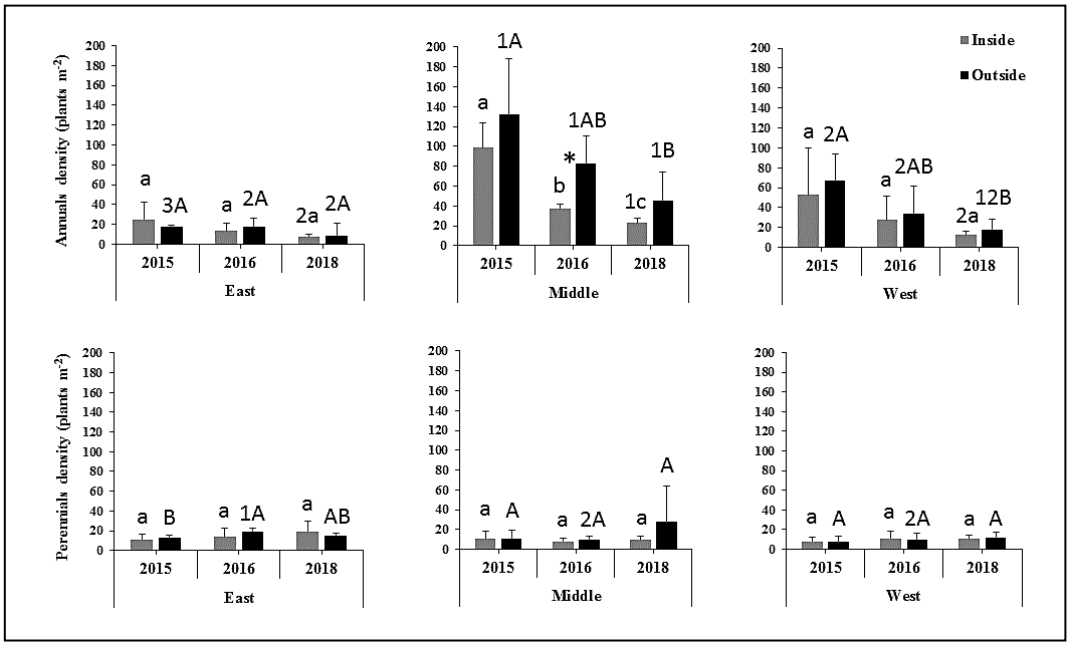

Figure 4. *Annual and perennial densities (plant.m^{-2}) inside and outside cages in the east, the middle and the west side of the Samaliete depression during the spring 2015, 2016 and 2018. a/b/c and A/B indicate significant differences between years inside and outside cages, respectively, in the same aspect; 1/2/3 indicate significant differences between sides in the same year, according to the Duncan test. (*) indicates significant difference between inside and outside cages for the same side and year; values are means ± SD (n = 4)*

Diversity

Jaccard's similarity index between the inside and outside cages is shown in *Table 3*. The highest index (0.76) was noted between the middle inside (MI1) and outside cages (MO1) in spring 2015, indicating that 76% of plant species were common to MI1 and MO1. The lowest index (0.17) was between the middle inside cages in spring 2016 (MI2) and eastern outside cages in spring 2018 (EO3). This indicates that the biggest difference in the floristic composition was between MI2 and EO3 (i.e. MI2–EO3). The main results

http://www.aloki.hu ● ISSN 1589 1623 (Print) ● ISSN 1785 0037 (Online)
DOI: http://dx.doi.org/10.15666/aeer/1906_43574371

of this index indicate floristic homogeneity in the middle of the depression. Some indices exceeded 0.5, indicating that more than 50% of plant species were common between the cages. Within the same site, similarity indexes were higher in spring 2015 with 0.63, 0.76 and 0.58 for EI1–EO1, MI1–MO1 and WI1–WO1, respectively. The similarity indices decreased in spring 2016 to 0.48 for EI2–EO2 and MI2–MO2. In spring 2018, similarities were lower with 0.41, 0.39 and 0.52 for EI3–EO3, MI3–MO3 and WI3–WO3, respectively. These results suggest that after three years of fencing, flora diversity had increased in all sites of the depression.

Table 3. *Jaccard's similarity index inside and outside cages in the Samaliete depression. The index between inside and outside cages in the same location and year are indicated with bolded numbers*

	EO1	**EO2**	**EO3**	**MO1**	**MO2**	**MO3**	**WO1**	**WO2**	**WO3**	**EI1**	**EI2**	**EI3**	**MI1**	**MI2**	**MI3**	**WI1**	**WI2**	**WI3**
EO1	1.00																	
EO2	0.58	1.00																
EO3	0.48	0.49	1.00															
MO1	0.44	0.45	0.28	1.00														
MO2	0.34	0.41	0.28	0.51	1.00													
MO3	0.36	0.31	0.36	0.48	0.41	1.00												
WO1	0.52	0.40	0.27	0.59	0.46	0.44	1.00											
WO2	0.37	0.48	0.31	0.50	0.67	0.37	0.56	1.00										
WO3	0.45	0.36	0.43	0.42	0.37	0.58	0.51	0.44	1.00									
EI1	**0.63**	0.44	0.32	0.52	0.36	0.40	0.62	0.42	0.48	1.00								
EI2	0.50	**0.48**	0.34	0.40	0.43	0.28	0.42	0.46	0.37	0.49	1.00							
EI3	0.36	0.39	**0.41**	0.32	0.25	0.46	0.31	0.28	0.36	0.31	0.28	1.00						
MI1	0.48	0.43	0.32	**0.76**	0.49	0.43	0.60	0.51	0.40	0.60	0.48	0.35	1.00					
MI2	0.28	0.34	0.17	0.48	**0.48**	0.28	0.36	0.52	0.30	0.33	0.52	0.25	0.49	1.00				
MI3	0.31	0.31	0.39	0.31	0.25	**0.39**	0.25	0.28	0.36	0.29	0.28	0.46	0.35	0.28	1.00			
WI1	0.67	0.50	0.40	0.59	0.46	0.47	**0.58**	0.53	0.51	0.62	0.53	0.35	0.60	0.39	0.35	1.00		
WI2	0.50	0.55	0.35	0.50	0.51	0.35	0.46	**0.58**	0.41	0.49	0.68	0.33	0.51	0.61	0.29	0.64	1.00	
WI3	0.47	0.45	0.51	0.44	0.35	0.54	0.40	0.35	**0.52**	0.40	0.35	0.54	0.45	0.29	0.45	0.49	0.41	1.00

EO, east outside; MO, middle outside; WO, west outside; EI, east inside; MI, middle inside; and WI, west inside. 1, 2 and 3 correspond to years 2015, 2016 and 2018, respectively

Productivity and economic evaluation

Rangeland production of the grazed area in the Samaliete depression significantly differed ($p < 0.05$) between the rainy (2015) and dry (2016) years, with 172.42 ± 79.99 and 91.34 ± 41.67 FU ha^{-1} year^{-1}, respectively. The lowland systems showed differences among the four farms in terms of economic performance and EPP, but also in terms of farming system (grazing-only and integrated grazing and cropping; *Table 4*). Farm 4 showed the largest rainfed crop income per hectare (141 EUR/ha), followed by farm 2 (10 EUR/ha). The other two small and medium farms (1 and 3) had negative values of −213 and −6 EUR/ha. However, farm 1 followed farm 4 in terms of EPP.

The diversification of crops (barley, wheat and lentil) had a positive impact on the income of farms 4 and 2. This observation did not apply to farm 3, possibly due to the high cost of paid labor on this farm, used especially for harvesting. The land capital also played an important economic role wherein farm 4 (9 ha) had the largest crop income

http://www.aloki.hu ● ISSN 1589 1623 (Print) ● ISSN 1785 0037 (Online)
DOI: http://dx.doi.org/10.15666/aeer/1906_43574371

(565 EUR, 141 EUR/ha). However, farm 3 had a much lower income (3 ha and −6 EUR/ha) than farm 2 (1 ha and 10 EUR/ha).

Table 4. *Characterization and differences in term of economic performance and efficiency of the production process between the four landscape depression farm) in the Samaliete region*

	Farm 1	**Farm 2**	**Farm 3**	**Farm 4**
Total area (ha)	1	1	3	9
Farming system (rainy year)	**Wheat**	**Wheat + lentil**	**Wheat + barley + lentil**	**Wheat + barley + lentil**
Cropped area (wheat and barley) (ha)	0.35	0.35	1	3
Cropped area (lentil) (ha)	0.1	0.1	0.35	1
Grazing area (ha)	0.55	0.55	1.65	5
Inputs (EUR)	17	34	92	207
Labor costs (EUR)	82	88	252	405
Total costs (EUR)	99	122	344	614
Total costs (EUR /ha)	220	271	255	154
Total crop gross product (EUR)	70	126	336	1179
Total crop gross product (EUR /ha)	155	281	248	295
Crop income (EUR) (rainy year)	-29	5	-8	565
Crop income (EUR /ha) (rainy year)	-65	10	-6	141
Grazing income (if with crops) (rainy year) (EUR)	13	13	39	118
Grazing income (if grazing only) (rainy year) (EUR)	24	24	71	213
Grazing income (EUR) (dry year)	12	12	37	112
Total income (crop and grazing) (1 rainy year) (EUR)	-16	18	31	683
Total income (crop and grazing) (4 years) (EUR)	21	55	143	1018
Total income (grazing only) (4 years) (EUR)	61	61	183	548
Profit of grazing only (4 years) (EUR)	40	6	40	-470
Efficiency of the production process (%) (gross product-inputs/gross product)	75	73	72	82

Discussion

Overall, human population increase has generated unsustainable land use practices by destroying the natural balance and transforming pastures to crop–livestock systems (Tomlinson et al., 2002; Sanderson et al., 2013). These transformations vary according to social, climatic, edaphic and ecologic aspects. Lowland depressions in arid and semi-arid areas are natural spaces that have undergone remarkable management changes. These landscape depressions constitute valuable areas for agriculture due to their hydrologic characteristics and soil fertility (Louhaichi et al., 2012; Hassan et al., 2017).

Our results showed that flora richness increased following fencing, with a dominance of annuals. Perennials had lower numbers in the middle of the depression, attesting to the negative effect of plowing. In the outside cages, the most common annual species in all depression sides during the three years were *Anacyclus cyrtolepidiodes* Pomel., *Asphodelus tenuifolius* Cav., *Echium humile* Desf., *Fagonia glutinosa* Del., *Filago germanica* L., *Plantago ovata* Forssk. and *Schismus barbatus* (L.) Thell. The common perennial plants were *Argyrolobium uniflorum* (Decne.) Jaub. & Spach, *Deverra tortuosa* (Desf.) DC., *Erodium glaucophyllum* (L.) L'Hér., *Helianthemum sessiliflorum* (Desf.) Pers, *Herniaria fontanesii* J. Gay and *Linaria aegyptiaca* (L.) Dum. Cours. Inside cages,

http://www.aloki.hu ● ISSN 1589 1623 (Print) ● ISSN 1785 0037 (Online)
DOI: http://dx.doi.org/10.15666/aeer/1906_43574371

the most found species (more than 75%) were *Anthyllis henoniana* Coss. Ex Batt., *Cynodon dactylon* (L.) Pers., *Gymnocarpos decander* Forssk., *Helianthemum kahiricum* (Delile), *Hippocrepis bicontorta* Loisel and *Reaumuria vermiculata* (L.).

The majority of perennial species in the outside cages were unpalatable or of low palatability and only occasionally palatable. The dominant species in the inside cages were palatable and very palatable perennial plants. After short-term fencing (3 years), unpalatable perennials were frequent in the outside cages, but in the inside cages there were increases in palatable and very palatable perennial species.

Comparable studies stated that overgrazing can influence vegetation structure, reducing perennial species richness, especially by losing the most palatable ones, usually replaced by unpalatable and annual species (Noy-Meir, 1995; Peer et al., 2001; Louhaichi et al., 2009, 2012; Tarhouni et al., 2010). Decreasing richness reduces the regeneration ability of rangelands and their resilience capacity by reducing seed production (Louhaichi et al., 2012). Bochet (2015) suggested that, in arid and semi-arid patchy ecosystems, plant seeds can be transported by surface runoff and reach more favorable sites for installation. Lowland depressions can be a suitable refuge area for seed germination and plant growth. However, this opportunity can be lost if depression areas are overgrazed and continuously plowed during rainy years.

Fencing had no effect on perennial plant density, but annual density increased in the middle. This can likely be explained by the abundance of unpalatable perennials in the outside cages, with the regeneration of palatable species in the protected cages or by the plowing effects favoring annual plants. These results corroborate the findings of Louhaichi et al. (2012) concerning the increase of plant density with fencing followed by an increase in annual forbs and grasses with a lower degree of perennial shrubs and semi-shrubs. Hassan et al. (2017) also reported that plant density increased in protected areas in arid lowland pastures with a dominance of annuals from three main botanical families: Poaceae, Asteraceae and Brassicaceae. Generally, ecosystem regeneration takes time depending on rainfall, seed bank, seed sources, competition between species, severity of disturbance and grazing regime (Pakeman and Small, 2005).

Similarly, species diversity increased greatly following short-term fencing in the middle and on the eastern side of the depression, with less increase evident on the western side. The diversity restitution in the middle is explained by the favorable conditions with good water status without grazing. Low diversity in the east and west sides can be explained by factors such as runoff (decreasing the soil moisture) and sun radiation (Louhaichi et al., 2012; Hassan et al., 2017). Plant diversity is considered the best indicator of health and resilience capacity of ecosystems. Without grazing, plant community recovery depends on precipitation, soil fertility and vegetation composition and physiognomy of woody or herbaceous species (Zhang, 1998). At low soil fertility, high annual species diversity was observed in protected Mongolian grasslands (Gough and Marrs, 1990).

This study shows that short-term fencing with at least one rainy year on arid landscape depressions can improve rangeland productivity by avoiding the negative impact of overgrazing. Nevertheless, grazing intensity is not the only factor determining the profitability of these agro-pastoral systems, and farm size and crop type are also influential. Farm size and stocking rate are among the main factors affecting the adoption of environmental policies and crop-livestock management (Shideed et al., 2007). Consequently, effects of size and crop type on farm economic performance were studied, and an economic evaluation was applied.

http://www.aloki.hu ● ISSN 1589 1623 (Print) ● ISSN 1785 0037 (Online)
DOI: http://dx.doi.org/10.15666/aeer/1906_43574371

The comparison of economic efficiency of land allocation between the studies depression suggests that g-razing only (non-fenced and non-cropped rangelands) in a 4-year period (3 years dry and 1 rainy year) is more profitable than integrating grazing with crops (non-fenced and cropped rangelands) on small and medium farms. In the case of large plowed areas, integrating grazing and crops is more economically efficient, especially with crop diversification. In addition to these economic impacts, the association between livestock husbandry and crop production could be considered as a form of response to climatic and socio-environmental risks and uncertainties in southern Mediterranean arid regions (Sraïri et al., 2017). In this case, we have to take into account the possible negative impact of plowing on sustainability of rangelands.

Special attention should be given to the most profitable farms to increase their economic performance and promote their sustainability. Attention should also be given to promoting and consolidating the productive choices that demonstrate their effectiveness, especially in small and medium lowlands, to produce diversified crops with high added value. The aim is to increase and secure farm income by developing diversified crops with high added value (e.g. vegetables and arboriculture) while modifying the rotation and adoption of new crops and reducing others that are less profitable or extending the cultivated area. The extension of cultivated areas can be done by improving water access through investing in the introduction of drip irrigation (occasionally subsidized by the state). These findings are consistent with previous research showing that crop diversification improves the performance of farming systems, enhances resilience and offers food security to households (Darnhofer et al., 2010; Souissi et al., 2018). The effectiveness of this strategy depends on the availability of farm assets, particularly wells, tractors, finance and family labor.

Conclusion

This study was carried out to investigate the vegetation composition and structure after fencing and to compare the incomes of management types (grazing-only and cropping with continuous grazing) in arid lowland depressions. The overall goal is the promotion of better pastoral, livestock and cropping management to meet population needs while protecting critical ecosystems. Results suggest that short-term fencing improved vegetation structure and pastoral productivity. Using landscape depressions as non-fenced rangelands (grazing-only) is more profitable than integrating grazing with cropping in small and medium areas, while integrated management (grazing with large-area cropping), especially with crop diversification, appeared to be more profitable than grazing-only. In summary, the better use of landscape lowlands in arid areas, having a high productivity compared to highlands, requires consideration of grazing intensity, minimum profitable plowing area and crop diversification. Fencing on sloping sides of depressions increased their fodder production. Protection of some lowland areas could enhance biodiversity. These recommendations are meant to inform decision making in rangeland management projects in arid lands around the world. In future works, the evaluation of carbon sequestration in lowlands could help inform climate change mitigation and adaptation measures.

Acknowledgements. This work was supported by the Arid Regions Institute of Médenine (IRA, Tunisia) budget, the International Center for Agricultural Research in the Dry Areas (ICARDA, Tunis), the OPEC fund for international development (OFID) and the CGIAR Research Program on Livestock (CRP Livestock). Authors acknowledge Scriptoria for English editing and anonymous reviewers for their valuable suggestions.

http://www.aloki.hu ● ISSN 1589 1623 (Print) ● ISSN 1785 0037 (Online)
DOI: http://dx.doi.org/10.15666/aeer/1906_43574371

REFERENCES

[1] Aïdoud, A., Le Floc'h, E., Le Houérou, H. N. (2006): Les steppes arides du nord de l'Afrique. – Sécheresse 17(1): 19-30.
[2] Aïdoud, A., Nedjraoui, D., Djebaili, S., Poissonet, J. (1983): Evaluation des ressources pastorales dans les hautes plaines steppiques du Sud Oranais: Productivité et valeur pastorale des parcours. – Bulletin de la Société d'histoire naturelle de l'Afrique du nord 13: 33-46.
[3] Alcamo, J. (2003): Ecosystems and Human Well-Being: A Framework for Assessment. A Report of the Conceptual Framework Working Group of the Millennium Ecosystem Assessment. – Island Press, Washington, DC.
[4] Ayeb, N., Seddik, M., Atti, N., Atigui, M., Fguiri, I., Barmat, A., Arroum, S., Addis, M., Hammadi, M., Khorchani, T. (2016): Growth, feed intake and carcass characteristics of indigenous goats fed local resources in Tunisian arid land. – Animal Production Science 56(11): 1842-1848.
[5] Bochet, E. (2015): The fate of seeds in the soil: a review of the influence of overland flow on seed removal and its consequences for the vegetation of arid and semiarid patchy ecosystems. – Soil 1(1): 131-146.
[6] Carmona, C. P., Röder, A., Azcárate, F. M., Peco, B. (2013): Grazing management or physiography? Factors controlling vegetation recovery in Mediterranean grasslands. – Ecological Modelling 251: 73-84.
[7] Daget, P., Poissonet, J. (1971): Une méthode d'analyse phytologique des prairies. Critères d'application. – Annales Agronomiques 22(1): 5-41.
[8] Darnhofer, I., Bellon, S., Dedieu, B., Milestad, R. (2010): Adaptiveness to enhance the sustainability of farming systems. A review. – Agronomy for Sustainable Development 30(3): 545-555.
[9] Eskandari, H., Borji, M., Khosravi, H., Mesbahzadeh, T. (2016): Desertification of forest, range and desert in Tehran province, affected by climate change. – Solid Earth 7(3): 905-915.
[10] FAO. (2006): Livestock's Long Shadow. Environmental Issues and Options. – In: Steinfeld, H., Gerber, P., Wassenaar, T., Castel, V., Rosales, M., de Haan, C. (eds.) FAO, LEAD initiative. FAO: Rome, Italy.
[11] Floret, Ch. (1988): Méthodes de Mesure de la Végétation Pastorale. Pastoralisme et Développement. – CIHEAM: Montpellier Cedex.
[12] Gamoun, M., Werner, J., Louhaichi, M. (2018): Traditional grazing-management practice makes an impact in southern Tunisia. – Retrieved from: http://www.icarda.org/dryWire/traditional-grazing-management-practice-makes-impact-southern-tunisia. (Accessed, 27 October 2020).
[13] Gough, M. W., Marrs, R. H. (1990): A comparison of soil fertility between semi-natural and agricultural plant communities: Implications for the creations of species-rich grassland on abandoned agricultural land. – Biological Conservation 51(2): 83-96.
[14] Grimm, N. B., Chapin III, F. S., Bierwagen, B., Gonzalez, P., Groffman, P. M., Luo, Y., Melton, F., Nadelhoffer, K., Pairis, A., Raymond, P. A., Schimel, J., Williamson, C. E. (2013): The impacts of climate change on ecosystem structure and function. – Frontiers in Ecology and Environment 11(9): 474-482.
[15] Hassan, S., Ates, S., Kaabneh, A., Louhaichi, M. (2017): The effect of grazing exclusion on vegetation characteristics and plant community structure in arid lowland pastures. – Retrieved from: http://om.ciheam.org/om/pdf/a114/00007551.pdf. (Accessed, 27 october 2020).
[16] Hoffmann, I., From, T., Boerma, D. (2014): Ecosystem services provided by livestock species and breeds, with special consideration to the contributions of small-scale livestock keepers and pastoralists. – Rome: FAO. Retrieved from: http://www.fao.org/3/a-at598e.pdf. (Accessed, 27 october 2020).

http://www.aloki.hu ● ISSN 1589 1623 (Print) ● ISSN 1785 0037 (Online)
DOI: http://dx.doi.org/10.15666/aeer/1906_43574371

[17] Hubbell, S. P., Foster, R. B., O'Brien, S. T., Harms, K. E., Condit, R., Wechsler, B., Wright, S. J., De Lao, S. L. (1999): Light-cap disturbances, recruitment limitation, and tree diversity in a neotropical forest. – Science 283(5401): 554-557.
[18] Lal, R. (2002): Carbon sequestration in dryland ecosystems of west Asia and North Africa. – Land Degradation & Development 13(1): 45-59.
[19] Le Houérou, H. N., Ionesco, T. (1973): Palatabilité des espèces végétales de la Tunisie steppique (indices spécifiques). – Project FAO/TUN - 71/525. Rome: FAO, Division Production et Protection des Plantes.
[20] Louhaichi, M., Salkini, A. K., Petersen, S. L. (2009): Effect of small ruminant grazing on the plant community characteristics of semi-arid Mediterranean ecosystems. – International Journal of Agriculture and Biology 11(6): 681-689.
[21] Louhaichi, M., Ghassali, F., Salkini, A. K., Petersen, S. L. (2012): Effect of sheep grazing on rangeland plant communities: case study of landscape depressions within Syrian arid steppes. – Journal of Arid Environments 79: 101-106.
[22] Nefzaoui, A., El Mourid, M. (2008): Rangeland Improvement and Management in Arid and Semi-Arid Environments of West Asia and North Africa. – Cairo: ICARDA. http://hdl.handle.net/10625/44380.
[23] Noy-Meir, I. (1995): Interactive effects of fire and grazing on structure and diversity of Mediterranean grasslands. – Journal of Vegetation Science 6(5): 701-710.
[24] Ouessar, M., Tâamallah, H., Ouled Begacem, A. (2006): Un environnement soumis à des fortes contraintes climatiques. – In: Genin, D., Guillaume, H., Ouessar, M., Ouled-Belgacem, A., Romagny, B., Sghaier, M., Taamallah, H. (eds.) Entre désertification et développement: La Jeffara tunisienne. Cérès éditions, Tunis (Tunisie), pp.23-32.
[25] Ouled-Belgacem, A. (2012): Rangeland resting. – In: Schwilch, G., Hessel, R., Verzandvoort, S. (eds.) Desire for Greener Land. Options for sustainable land management in drylands. Bern, Switzerland, and Wageningen, The Netherlands: University of Bern - CDE, Alterra - Wageningen UR, ISRIC - World Soil Information and CTA - Technical Centre for Agricultural and Rural Cooperation, pp.169-172.
[26] Ouled-Belgacem, A. (2018): Rangeland restoration and management in relation to land tenure and vegetation type: the revival of the resting "*gdel*" technique in southern Tunisia. – ICARDA Technical Report. https://hdl.handle.net/20.500.11766/8276. (Accessed, 27 october 2020).
[27] Ouled-Belgacem, A., Tarhouni, M., Louhaichi, M. (2013): Effect of protection on plant community dynamics in the Mediterranean arid zone of southern Tunisia: a case study from Bou Hedma National Park. – Land Degradation & Development 24(1): 57-62.
[28] Pakeman, R. J., Small, J. L. (2005): The role of the seed bank, seed rain and the timing of disturbance in gap regeneration. – Journal of Vegetation Science 16(1): 121-130.
[29] Peer, T., Millinger, A., Gruber, J. P., Hussain, F. (2001): Vegetation and altitudinal zonation in relation to the impact of grazing in the steppe lands of the Hindu Kush Range (N-Pakistan). – Phytocoenologia 31(4): 477-498.
[30] Reynolds, J. F., Smith, D. M., Lambin, E. F., Turner, B. L., Mortimore, M., Batterbury, S. P., Downing, T. E., Dowlatabadi, H., Fernandez, R. J., Herrick, J. E., Sannwald, E. H., Jiang, H., Leemans, R., Lynam, T., Maestre, F. T., Ayarza, M., Walker, B. (2007): Global desertification: building a science for dryland development. – Science 316(5826): 847-851.
[31] Roux, G., Roux, M. (1967): À propos de quelques méthodes de classification en phytosociologie. – Revue de Statistique Appliquée 15(2): 59-72.
[32] Sanderson, M. A., Archer, D., Hendrickson, J., Kronberg, S., Liebig, M., Nichols, K., Schmer, M., Tanaka, D., Aguilar, J. (2013): Diversification and ecosystem services for conservation agriculture: Outcomes from pastures and integrated crop–livestock systems. – Renewable Agriculture and Food Systems 28(2): 129-144.
[33] Schilling, J., Freier, K. P., Hertig, E., Scheffran, J. (2012): Climate change, vulnerability and adaptation in North Africa with focus on Morocco. – Agriculture Ecosystems & Environment 156: 12-26.

http://www.aloki.hu ● ISSN 1589 1623 (Print) ● ISSN 1785 0037 (Online)
DOI: http://dx.doi.org/10.15666/aeer/1906_43574371

[34] Shideed, K., El Mourid, M., Alary, V., Laamari, A., Nefzaoui, A. (2007): Enabling policy environment to enhance uptake of natural resources management technologies in marginal drylands: empirical evidence from Morocco and Tunisia. – In: King, C., Bigas, H., Zafar, A. (eds.) Proceedings of the Joint International Conference "Desertification and the International Policy Imperative". Algiers (Algeria) 17–19 December 2006, pp.201-212.
[35] Slimani, H., Aïdoud, A. (2004): Desertification in the Maghreb: a case study of an Algerian high-plain steppe. – In: Marquina, A. (ed.) Environmental Challenges in the Mediterranean 2000–2050. NATO Science Series 37: 93-108.
[36] Souissi, I., Boisson, J. M., Mekki, I., Therond, O., Flichman, G., Wery, J., Belhouchette, H. (2018): Impact assessment of climate change on farming systems in the South Mediterranean area: A Tunisian case study. – Regional Environmental Change 18(3): 637-650.
[37] Squires, V. R., Lu, X., Lu, Q., Wang, T., Yang, Y. (2009): Degradation and Recovery in China's Pastoral Lands. – CABI, Wallingford, UK.
[38] Sraïri, M. T., M'ghar, F. A., Benidir, M., Bengoumi, M. (2017): Analyse typologique de la diversité et des performances de l'élevage oasien. – Cahiers Agricultures 26(1): 15005.
[39] Tarhouni, M., Ben Salem, F., Belgacem, A. O., Neffati, M. (2010): Acceptability of plant species along grazing gradients around watering points in Tunisian arid zone. – Flora 205(7): 454-461.
[40] Temel, S., Surmen, M., Tan, M. (2015): Effects of growth stages on the nutritive value of specific halophyte species in saline grasslands. – Journal of Animal and Plant Sciences 25(5): 1419-1428.
[41] Tietjen, B., Jeltsch, F. (2007): Semi-arid grazing systems and climate change: a survey of present modelling potential and future needs. – Journal of Applied Ecology 44(2): 425-434.
[42] Tlili, A., Tarhouni, M., Cerdà, A., Louhaichi, M., Neffati, M. (2018): Comparing yield and growth characteristics of four pastoral plant species under two salinity soil levels. – Land Degradation & Development 29(9): 3104-3111.
[43] Tomlinson, K. W., Hearne, J. W., Alexander, R. R. (2002): An approach to evaluate the effect of property size on land-use options in semi-arid rangelands. – Ecological Modelling 149(1-2): 85-95.
[44] VijayaVenkataRaman, S., Iniyan, S., Goic, R. (2012): A review of climate change, mitigation and adaptation. – Renewable & Sustainable Energy Reviews 16(1): 878-897.
[45] Zhang, M., Wu, J., Tang, Y. (2016): The effects of grazing on the spatial pattern of elm (*Ulmus pumila* L.) in the sparse woodland steppe of Horqin Sandy Land in northeastern China. – Solid Earth 7(2): 631-637.
[46] Zhang, W. (1998): Changes in species diversity and canopy cover in steppe vegetation in Inner Mongolia under protection from grazing. – Biodiversity and Conservation 7(10): 1365-1381.

http://www.aloki.hu ● ISSN 1589 1623 (Print) ● ISSN 1785 0037 (Online)
DOI: http://dx.doi.org/10.15666/aeer/1906_43574371

INVENTORY OF SOME INTRODUCED AND INVASIVE PLANT SPECIES IN SOME GOVERNORATES OF THE KINGDOM OF SAUDI ARABIA

ALJEDDANI, G. S.[1] – AL-HARBI, N. A.[2] – AL-QAHTANI, S. M.[2] – EL-ABSY, K. M.[2,3*] – ABDULLATIF, B. M.[4] – DAHAN, T. E.[5]

[1]*Department of Biology, College of Science, University of Jeddah, Jeddah, Saudi Arabia*

[2]*University College of Tayma, Tabuk University, Tayma, Saudi Arabia*

[3]*Eco-physiology Unit, Plant Ecology and Ranges Department, Desert Research Center, Cairo, Egypt*

[4]*Omdurman Islamic University, Khartoum, Sudan*

[5]*University of Bisha, Bisha, Saudi Arabia*

**Corresponding author*
e-mail:k.alabssi@ut.edu.sa

(Received 27th Apr 2021; accepted 4th Sep 2021)

Abstract. This investigation revealed that there are 42 species belonging to fifteen families in eleven governorates of KSA. The highest number (seven) and percentage (20.60%) of introduced species were recorded in Dammam and Riyadh, while, the lowest values were recorded in the regions of Al-Baha, Al-Ghat and Jizan (one and 2.94%). As for Al-Baha a large number of introduced species (nineteen, 46.34%) were recorded, nearly half of the number of species examined, while no invasive species were recorded in Bisha, Dammam, and Tabuk. The life growth of the introduced species ranges from trees to young weeds. Phanerophytes (45%) had the highest proportion of life expectancy for the introduced plants, followed by Therophyte (40%) and Chamaephytes (15%), while the highest percentage (63%) among life ratios of the introduced and invasive plants was recorded for Therophyte, and the percentage of life growth of introduced plants indicates the dominance of herbs among other life forms. Regarding the total growth of life, the highest recorded percentage was in herbs (50%), followed by shrubs (19.05%), trees (16.67%), bush (9.52%) and grass (4.76%). The biological growth of weeds was dominant for the invasive plant species, followed by trees in the introduced species, and shrubs and trees in the introduced and invasive species. These indicate that the annual species and invasive weeds are better adapted to the environmental conditions in the studied areas in KSA.
Keywords: *inventory, plants, biodiversity, introduced, invasive, regions, KSA*

Introduction

Invasive alien species (IAS) are a leading threat causing the mass extinction of native species around the world. In response to this issue, the international community in October 2010 at Nagoya, Japan established several objectives concerning the Convention of Biological Diversity (CBD), with the 9th target focusing on establishing measures to prevent the introduction and incorporation of IAS by 2020 for all signatories (CBD, 2010, 2001). Invasive species are primarily spread by human activities, often unintentionally. Over the past few centuries, the range of plant species colonizing areas outside their native habitats has risen dramatically. (Seebens et al., 2017). Current findings documented in a study by the world bank imply that changing climate leads to the dissemination and thus further intensifies the influence of such

http://www.aloki.hu ● ISSN 1589 1623 (Print) ● ISSN 1785 0037 (Online)
DOI: http://dx.doi.org/10.15666/aeer/1906_43734388

species. Due to invasive species, more than $1 billion dollars was lost yearly in the US and $1.5 trillion dollars globally (Globalization101, 2020).

In the different ecosystems across KSA only, it has been estimated that the number of alien and naturalized species was 2284 (Thomas, 2011). KSA flora comprises of 48 foreign species, of which 9 species have been identified for the first time by KSA, as well as human intrusion in ecological systems, such as the eviction of naturally grown plants from intensely vegetated areas for road establishment (Kingston and Waldren, 2003). Invasive plants are progressively broadening their existence in various ecosystems, such as roadsides, desolated areas, barren lands, agricultural areas, landfill sites, forest lands, etc., because of the lack of sustainable threats and intensified responsiveness. Competition between invasive and endemic species intensifies for water, sunlight, space and nutrients, and natural ecosystems can be disrupted by dispersing of invasive species. (USDA, 2020). An invader plant is a native or foreign species that have a disruptive impact on the growth and production of commercial plant species, triggering specific management issues, or grows where it is not desired (Le Roux, 1981). Invasive plants are often naturalized species that develop fertile offspring at significant distances from the parent plants, usually in very significant numbers (for clades propagating by seeds and other reproductive structures, the estimated scales are more than a hundred meters in less than 5 decades.; more than 2 m per year for clades distributing by roots, stolons, rhizomes or subterranean stems) accordingly they have the opportunity to disseminate across vast regions (Richardson et al., 2000). These species, independently and sometimes at unprecedented rates, are able to flourish, reproduce and disperse across the landscape (van Wilgen et al., 2001). Invasive species can be found in natural or semi-natural ecosystems and endanger indigenous biodiversity (IUCN, 1999). Invasive species have now become a worldwide challenge to the ecosystem, culture and the economy, endangering biodiversity, altering the balance of ecosystems and growing environmental devastation. (Levine et al., 2003). After ecosystem defragmentation, this is the second-largest factor for loss of biodiversity. (Gaertner et al., 2009). Invasive plants are significant threats to the stability of the ecosystem and biodiversity, where 80% of endangered species extinctions are due to invasions of non-native species worldwide. (Pimentel et al., 2005). Invasive plants could indeed dramatically change biodiversity by replacing the range of native vegetation, insects, and microbial communities with invasive plants, thus obstructing ecosystem infrastructure. By altering the nutrient cycle and soil pH, invasive species alter the ecology of a given ecosystem (Drenovsky et al., 2007), where lowered pH might indeed decrease the availability of nutrients leading to reduced growth of native plants, especially in habitats with poor nutrient availability.

Ecosystem services are the benefits that human derives from ecosystems, like food, fiber and water provision, nutrient cycling, water and air purification (carbon sequestration), as well as erosion prevention, pests, distribution regimes, recreation and tourism (Diaz et al., 2007; Naidoo and Ricketts, 2008). Invasive species frequently have harmful environmental effects on the habitats they enter (Pejchar and Mooney, 2009). Invasive plants severely decrease the crop yields (Pimentel et al., 2000) and values of agricultural lands, causing loss of forages, decreased rangeland productivity and fodder value due to invasion of pastures, in certain circumstances, soil carbon reserves have diminished (Eviner et al., 2010), leading to increased fire incidence, range, and vehemence (Mack et al., 2000), loss of aesthetic elegance in gardens and landscapes as well as the imposition of substantial expenses on the world economy (Vila et al., 2011).

http://www.aloki.hu ● ISSN 1589 1623 (Print) ● ISSN 1785 0037 (Online)
DOI: http://dx.doi.org/10.15666/aeer/1906_43734388

Invasive plant species have an impact on the diversity of native species, impacting the abundance of water by reducing the flow of water in a system already heavily constrained by water (Mark and Dickinson, 2008), impairing the availability of soil nutrients and increasing the occurrence of many other groups of pests (Mack et al., 2000) as well as disordered morphology of riparian areas of the water bodies, contributing to changes in flood frequency and intensity (Zavaleta, 2000) and increased soil erosion. Comparatively, after a foreign plant has occupied an ecosystem, by altering the light, solar radiation and temperature levels in the infiltrated places, it affects the characteristics of that area. For a variety of animals, the nature and affordability of food, shelter, nesting places sunning sites and rests have changed. Plant invasions have meaningfully undermined innate diversity by plummeting the abundance (by 43.5%), diversity (by 50.7%), and vitality (by 41.7%) of denizen plant species and the appropriateness (by 16.5%) and multiplicity (by 17.5%) of animal species (Vila et al., 2010). Invasive plant species control is a global request to help the offset of damaging consequences and empower the restoration of natural biodiversity (Hulme, 2006) through their exclusion from invaded habitats (Blanchard and Holmes, 2008). Given different biological properties, the issue of alien species control can be identified as the question of how to allocate vital resources among different management efforts (protection, monitoring, and regulation) over space and time, the management target of minimizing the financial and ecological harm incurred by invasive species and the management costs (Büyüktahtakın and Haight, 2018). This present investigation was conducted to discover, identify, and to make an inventory of the introduced and invasive plants in some governorates of the Kingdom of Saudi Arabia (KSA), in addition, warning about them as a threat to the local plant species diversity and flora of KSA.

Materials and methods

Some of the introduced plant species and invasive introduced plant species were restricted during the year 2020 in eleven governorates of the Kingdom, every governorate was given a code from 1-11, respectively (1-Al-Baha, 2- Al Ghat, 3- Bisha, 4- Buraidah, 5- Dammam, 6- Fayfa 7- Jizan, 8- Jeddah, 9- Tabuk, 10- Taif, 11 Riyadh). As shown in *Figure 1,* and the plant species and families to which they belong were defined using the following references (Chaudhary, 1999, 2000, 2001) and the website GBIF (*Table 1*).

Table 1. *The GPS coordinates of eleven governorates in the KSA*

No.	Regions	Latitude	Longitude
1	Al-Baha	20° 16’ 20.1864’’ N	41° 26’ 28.5036’’ E
2	Al Ghat	26° 01’ 21.60” N	44° 57’ 23.39” E
3	Bisha	19° 58’ 34.8672’’ N	42° 35’ 24.6012’’ E
4	Buraidah	26° 21’ 33.2316’’ N	43° 58’ 54.5232’’ E
5	Dammam	26° 23’ 57.3000’’ N	49° 59’ 3.6960’’ E
6	Fayfa	17 16’ 00’’ N	43 06’ 00’’ E
7	Jizan	16° 54’ 34.8588’’ N	42° 34’ 4.4472’’ E
8	Jeddah	21° 32’ 35.9988’’ N	39° 10’ 22.0044’’ E
9	Tabuk	28° 23’ 0.6288’’ N	36° 33’ 58.2876’’ E
10	Taif	21° 16’ 13.01” N	40° 24’ 56.99” E
11	Riyadh	24° 42’ 48.7872’’ N	46° 40’ 31.0656’’ E

http://www.aloki.hu ● ISSN 1589 1623 (Print) ● ISSN 1785 0037 (Online)
DOI: http://dx.doi.org/10.15666/aeer/1906_43734388

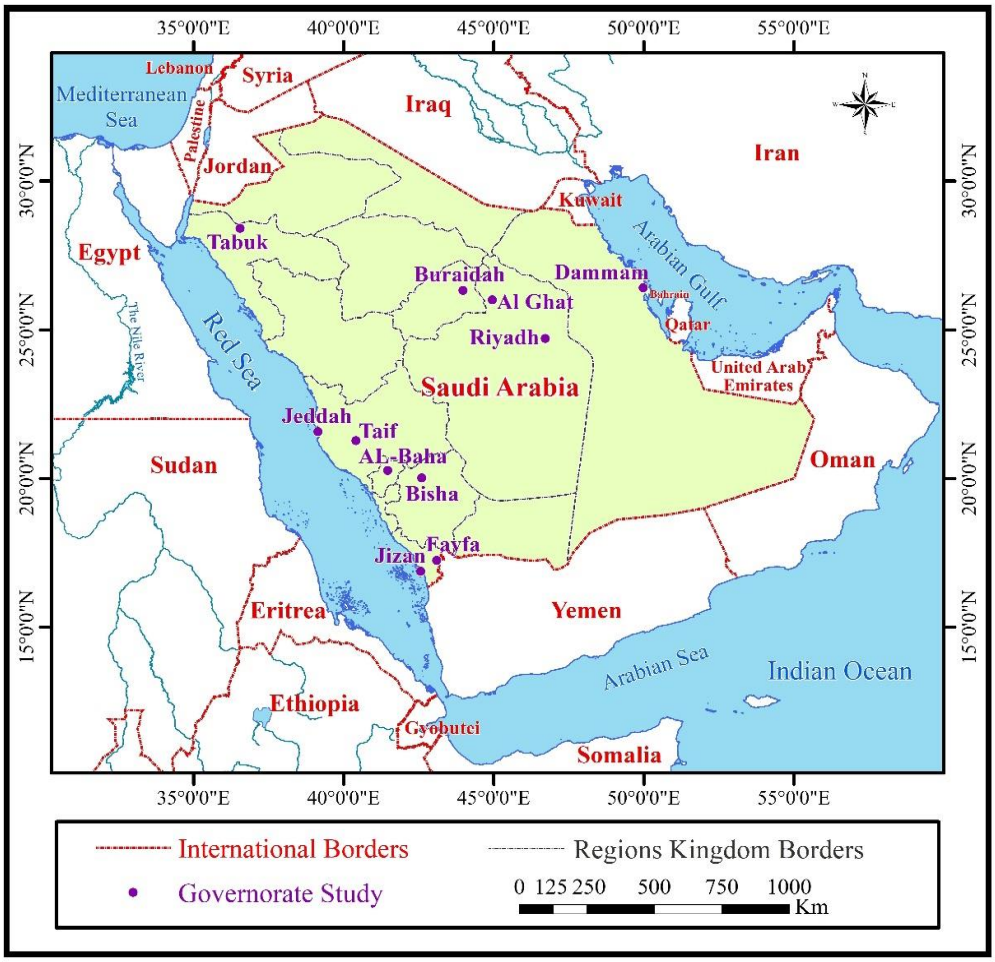

Figure 1. *Saudi Arabia map displaying the locations of the plant species being studied*

Statistical analysis

Cluster analysis for introduced and invasive plant species based on Euclidean distances was performed by Ward's method. The Principal Component Analysis (PCA) method explained by Harman (1976) was followed in the extraction of the components for eleven regions based on the presence and absence of introduced and invasive plant species. The percentage variability explained by each component was determined (Harman, 1976; Sharma, 1996). The data were subjected to descriptive statistics and PCA as well as biplot graphical display. Multivariate statistical techniques were executed using a computer software program PAST version 4.03 (Hammer et al., 2020).

Results

Investigation of many governorates in Saudi Arabia (Al-Baha, Al Ghat, Bisha, Buraidah, Dammam, Fayfa, Jizan, Jeddah, Tabuk, Taif, Riyadh,), revealed the presence of forty-two species in the eleven governorates as shown in *Table 2*. These species belong to fifteen families. Amaranthaceae and Asteraceae are the most common families among the investigated families (7 species, each); followed by Fabaceae with 6 species, Aizoaceae with 4 species, and Cactaceae, Solanaceae, and Euphorbiaceae with

http://www.aloki.hu ● ISSN 1589 1623 (Print) ● ISSN 1785 0037 (Online)
DOI: http://dx.doi.org/10.15666/aeer/1906_43734388

3 species each, followed by Poaceae with 2 species. While Annonaceae, Papaveraceae, Heliotropiaceae, Cucurbitaceae and Verbenaceae, Primulaceae and Potamogetonaceae are represented by 1 species. *Prosopis juliflora* (Sw.) was the most common species, it was recorded in 6 governorates (Al-Baha, Al Ghat, Buraidah, Jizan, Jeddah, Riyadh) of variable ecological conditions (*Table 2*).

Table 2. *List of presence (+) and absence (-) and the number int. and int. & inv. plant species and their families in the studied governorates*

Plant species	Families	Governorates										
		1	2	3	4	5	6	7	8	9	10	11
Acacia ampliceps Maslin	Fabaceae	-	-	-	+	-	-	-	-	-	-	-
Acacia salicina Lindl.	Fabaceae	-	-	-	+	-	-	-	-	-	-	-
Alternanthera pungens Kunth	Amaranthaceae	+	-	-	-	-	-	-	-	-	-	-
Amaranthus albus L.	Amaranthaceae	-	-	-	-	-	-	+		+	+	-
Amaranthus hybridus L.	Amaranthaceae	+	-	-	-	-	-	-	-	+	-	-
Amaranthus spinosus L.	Amaranthaceae	-	-	-	-	-	-	+	-	-	-	-
Annona squamosa L.	Annonaceae	-	-	-	-	-	-	-	-	-	-	+
Argemone ochroleuca Sweet	Papaveraceae	+	-	+	-	-	+	-	-	+	-	+
Atriplex suberecta I. Verd.	Amaranthaceae	-	-	-	-	+	-	-	-	-	-	-
Conyza bonariensis (L.) Cronq.	Asteraceae	-	-	-	-	-	-	-	-	-	-	+
Cylindropuntia rosea (DC.) Backeb.	Cactaceae	+	-	-	-	-	-	-	-	-	-	-
Datura innoxia Mill.	Solanaceae	+	+	-	+	-	-	-	-	+	-	+
Datura stramonium L.	Solanaceae	+	-	-	-	-	-	-	-	-	-	+
Eclipta prostrata L.	Asteraceae	+	-	-	-	-	-	-	-	-	-	-
Euphorbia heterophylla L.	Euphorbiaceae	-	-	-	-	+	-	-	-	-	-	-
Euphorbia maculata L.	Euphorbiaceae	-	-	-	-	-	-	-	-	-	-	-
Euphorbia prostrata Aiton	Euphorbiaceae	-	-	-	-	-	-	-	-	-	+	-
Heliotropium curassavicum L.	Heliotropiaceae	+	-	-	-	+	-	-	-	-	+	+
Imperata cylindrica (L.) P. Beauv.	Poaceae	-	-	-	-	-	-	-	+	-	-	-
Kali turgida (Dumort.) Gutermann	Amaranthaceae	+	-	-	-	-	-	-	-	-	-	-
Lantana camara L.	Verbenaceae	+	-	-	-	-	-	-	-	-	-	+
Leucaena leucocephala (Lam.) de Wit	Fabaceae	-	-	-	-	-	-	-	-	-	+	+
Lysimachia arvensis subsp. Arvensis	Primulaceae	-	+	-	-	-	-	-	-	-	-	-
Momordica balsamina L.	Cucurbitaceae	-	-	-	-	+	-	-	-	-	-	-
Nicotiana glauca Graham	Solanaceae	+	-	+	-	-	+	-	-	-	-	-
Opuntia ficus-indica (L.) Mill.	Cactaceae	+	-	-	-	-	-	-	-	+	-	-
Opuntia stricta (Haw.) Haw.	Cactaceae	+	-	-	-	-	+	-	-	+	-	-
Parkinsonia aculeata L.	Fabaceae	-	-	-	-	-	-	-	-	+	-	-
Phragmites australis (Cav.) Steud.	Poaceae	-	-	-	-	-	-	+	+	-	-	-
Potamogeton perfoliatus L.	Potamogetonaceae	-	-	-	-	-	-	-	-	-	+	-
Prosopis juliflora (Sw.) DC.	Fabaceae	+	+	-	+	-	+	+	-	-	+	-
Prosopis koelziana Burkart	Fabaceae	-	-	-	-	-	-	-	-	-	+	-
Salicornia europaea L.	Amaranthaceae	-	-	-	-	+	-	-	-	-	-	-
Sesuvium portulacastrum L.	Aizoaceae	-	-	-	-	+	-	-	-	-	+	-
Sesuvium sesuvioides (Fenzl) Verdc.	Aizoaceae	-	-	-	-	-	+	-	-	-	-	-
Sesuvium verrucosum Raf.	Aizoaceae	-	-	-	-	+	-	+	-	-	-	-
Tagetes minuta L.	Asteraceae	+	-	-	-	-	-	-	-	-	-	-
Tridax procumbens L.	Asteraceae	+	-	-	-	-	-	-	-	-	-	+
Verbesina encelioides (Cav.) A. Gray	Asteraceae	+	-	-	-	-	-	-	-	+	-	-
Xanthium spinosum L.	Asteraceae	+	-	-	-	-	-	-	-	-	-	-
Xanthium strumarium L.	Asteraceae	+	+	-	-	-	-	-	-	-	-	-
Zaleya pentandra (L.) C. Jeffrey	Aizoaceae	+	-	-	-	-	-	-	-	-	-	-

http://www.aloki.hu ● ISSN 1589 1623 (Print) ● ISSN 1785 0037 (Online)
DOI: http://dx.doi.org/10.15666/aeer/1906_43734388

On the other hand, *Table 3* clarified the numbers and percentage of introduced and introduced and invasive plants growing in different governorates. The highest number and percentage of introduced species were recorded in Dammam and Riyadh (7 species with 20.60% each). On the other hand, the lowest number and percentage of introduced plants were recorded in Al-Baha, Al- Ghat, and Jizan, 1 species with 2.94% each. Nonetheless, Jeddah, Buraidah, Tabuk, Taif, and Viva recorded 4, 3, and 2 species with 11.76%, 8.82, and 5.88% respectively.

Table 3. *Number and percentage of the presence of introduced and invasive plant species in some studied governorates*

Plant Species / Governorates	Introduced		Introduced & invasive	
	Number	Percentage %	Number	Percentage %
Al-Baha	1	2. 94	19	46.34
Al Ghat	1	2.94	3	7.31
Bisha	2	5.88	0	0
Buraidah	3	8.82	1	2.44
Dammam	7	20.60	0	0
Fayfa	2	5.88	7	17.07
Jizan	1	2.94	4	9.76
Jeddah	4	11.76	1	2.44
Tabuk	3	8.82	0	0
Taif	3	8.82	5	12.20
Riyadh	7	20.60	1	2.44
Total	34	100	41	100

Concerning, introduced and invasive plants (*Table 3*), in Al-Baha a high number of species and hence percentage (19, 46.34%) was recorded, almost half the number of investigated species. While no invasive species was reported in Bisha, Dammam, and Tabuk. Moreover, it was clarified that the life growth of introduced species ranges from trees to small grass. These include 4-Trees (*A. ampliceps* Maslin, *A. salicina* Lindl., *A. squamosa* L. and *P. aculeata* L. twelve herbs, two bushes, one shrub and two grasses (*P. australis* and *I. cylindrica*) on the other hand, among introduced and invasive plants 3 Trees (*L. leucocephala* (Lam.) de Wit, *O. ficus-indica* (L.) Mill and *O. stricta* (Haw.) Haw, ten herbs, two bushes seven shrubs and no grasses were recorded (*Table 4*). At the level of life form, nine Phanerophytes, eight Therophyte and three Chamaephytes were recorded in introduced plants. While four Phanerophytes, fourteen Therophytes and four Chamaephytes registed in introduced and invasive plants. Moreover, the percentage of life form of introduced plants (*Table 5*) showed that Phanerophytes and Therophyte had the highest percentage (45% and 40%) respectively while Chamaephytes were represented by 15%. Concerning the percentage life form of introduced and invasive plants, it indicated that the highest percentage was recorded in Therophyte among other life forms (63%), while Phanerophytes and Chemophytes shared the same percentage (18%). Percentage of life growth of introduced plants as is represented in *Table 6*, indicated the domination of herbs among other life growth, following the trend: herbs (57.14%) > trees (19.05%) > bush = grass (9.52%, each) and shrub (4.76%). The percentage of life growth of introduced and invasive plants (*Table 7*) followed a

http://www.aloki.hu ● ISSN 1589 1623 (Print) ● ISSN 1785 0037 (Online)
DOI: http://dx.doi.org/10.15666/aeer/1906_43734388

different trend but also with the domination of herbs. Herbs were recorded in the highest number and no grass was reported. (Herbs (45%) > shrub (32%) > tree (14%) > bush (9%) > grass (0%).) In general, as is represented in *Table 6,* a total of forty-two species were found in the study area as introduced and invasive plants. In form of life form, Therophytes were recorded as the dominant life form, with a percent of more than half the investigated species (52.38%), followed by Phanerophytes (30.95%) and then Chamaephytes (16.67%), (*Table 8*), In terms of a total of life growth, on the other hand, it was showed that the highest number recorded was in herbs 21 species, with a percent of half the number of all studied plants (50%), t followed by shrubs (8, 19.05%), trees (7, 16.67%), bush (4, 9.52%) and grass (2, 4.76) (*Table 8*).

Table 4. *List of introduced and invasive plant species and their families (type, life form and life growth) in some governorates study*

Plant species	Type	Life form	Life growth
Acacia ampliceps Maslin	Introduced	Phanerophyes	Tree
Acacia salicina Lindl.	Introduced	Phanerophyes	Tree
Alternanthera pungens Kunth	Introduced & Invasive	Therophytes	Herb
Amaranthus albus L.	Introduced & Invasive	Therophytes	Bush
Amaranthus hybridus L.	Introduced & Invasive	Therophytes	Bush
Amaranthus spinosus L.	Introduced	Therophytes	Big weed
Annona squamosa L.	Introduced	Phanerophyes	Tree
Argemone ochroleuca Sweet	Introduced	Therophytes	Herb
Atriplex suberecta I. Verd.	Introduced & Invasive	Therophytes	Shrub
Conyza bonariensis (L.) Cronq.	Introduced	Therophytes	Herb
Cylindropuntia rosea (DC.) Backeb.	Introduced & Invasive	Therophytes	Shrub
Datura innoxia Mill.	Introduced & Invasive	Therophytes	Shrub
Datura stramonium L.	Introduced & Invasive	Therophytes	Shrub
Eclipta prostrata L.	Introduced & Invasive	Chamaephytes	Herb
Euphorbia heterophylla L.	Introduced	Chamaephytes	Herb
Euphorbia maculata L.	Introduced	Chamaephytes	Herb
Euphorbia prostrata Aiton	Introduced	Chamaephytes	Herb
Heliotropium curassavicum L.	Introduced & Invasive	Chamaephytes	Herb
Imperata cylindrica (L.) P. Beauv.	Introduced	Phanerophyes	Grass
Kali turgida (Dumort.) Gutermann	Introduced & Invasive	Therophytes	Herb
Lantana camara L.	Introduced &Invasive	Therophytes	Shrub
Leucaena leucocephala (Lam.) de Wit	Introduced &Invasive	Phanerophyes	Tree
Lysimachia arvensis subsp. Arvensis	Introduced	Therophytes	Bush
Momordica balsamina L.	Introduced	Phanerophyes)	Herb
Nicotiana glauca Graham	Introduced& Invasive	Phanerophyes)	Shrub or small tree
Opuntia ficus-indica (L.) Mill.	Introduced &Invasive	Chamaephytes	Tree
Opuntia stricta (Haw.) Haw.	Introduced &Invasive	Chamaephytes	Tree
Parkinsonia aculeata L.	Introduced	Phanerophyes	Tree
Phragmites australis (Cav.) Steud.	Introduced	Phanerophyes	Grass
Potamogeton perfoliatus L.	Introduced	Phanerophyes	Herb
Prosopis juliflora (Sw.) DC.	Introduced & Invasive	Phanerophytes	Shrub to small tree
Prosopis koelziana Burkart	Introduced	Phanerophytes	Shrub to small tree

http://www.aloki.hu ● ISSN 1589 1623 (Print) ● ISSN 1785 0037 (Online)
DOI: http://dx.doi.org/10.15666/aeer/1906_43734388

Salicornia europaea L.	Introduced	Therophytes	Herb
Sesuvium portulacastrum L.	Introduced	Therophytes	Herb
Sesuvium sesuvioides (Fenzl) Verdc.	Introduced	Therophytes	Herb
Sesuvium verrucosum Raf.	Introduced	Therophytes	Herb to shrub
Tagetes minuta L.	Introduced & Invasive	Therophytes	Herb
Tridax procumbens L.	Introduced & Invasive	Therophytes	Herb
Verbesina encelioides (Cav.) A. Gray	Introduced &Invasive	Therophytes	Herb
Xanthium spinosum L.	Introduced &Invasive	Therophytes	Herb
Xanthium strumarium L.	Introduced & Invasive	Therophytes	Herb
Zaleya pentandra (L.) C. Jeffrey	Introduced & Invasive	Therophytes	Herb

Table 5. *Each percentage of the presence of introduced and invasive plant species, life form in some governorates of the Kingdom of Saudi Arabia*

Life form / Type	Phanerophytes		Therophyte		Chamaephytes		Total No.	Total P.%
	No.	P.%	No.	P. %	No.	P. %		
Introduced	9	45	8	40	3	15	20	100
Introduced & Invasive	4	18.18	14	63.64	4	18.18	22	100

Table 6. *Each percentage of the presence of introduced and invasive plant species, Life growth in some governorates of the Kingdom of Saudi Arabia*

Life / Growth type	Tree		Herb		Bush		Shrub		Grass		Total No.	Total P.%
	No.	P.%	No.	P.%	No.	P. %	No.	P.%	No.	P.%		
Introduced	4	20	11	55	2	10	1	5	2	10	20	100
Introduced & Invasive	3	13.63	10	45.45	2	9.10	7	31.82	0	0	22	100

Table 7. *Total percentage of the presence of introduced and invasive plant species Life growth in some governorates of the Kingdom of Saudi Arabia*

Life growth	Tree	Herb	Bush	Shrub	Grass	Total
Number	7	21	4	8	2	42
Percentage %	16.67	50	9.52	19.05	4.76	100%

Table 8. *Total percentage of the presence of introduced and invasive plant species life form in some governorates of the Kingdom of Saudi Arabia*

Life form	Phanerophytes	Therophytes	Chamaephytes	Total
Number	13	22	7	42
percentage	30.95%	52.38%	16.67%	100%

Multivariate statistical technique

For the determination of the similarities and differences among introduced and invasive plant species based on the presence and absence of them in some governorates

http://www.aloki.hu ● ISSN 1589 1623 (Print) ● ISSN 1785 0037 (Online)
DOI: http://dx.doi.org/10.15666/aeer/1906_43734388

of the KSA, cluster analysis with the Ward method was used. According to the cluster analysis, the introduced and invasive plant species were divided into eight clusters (*Fig. 2*). The tree diagram had exhibited the least distances or dissimilarity between the introduced and invasive plant species inside each cluster. While the high distances of these species are found among the eight clusters. Both the first and the seventh clusters consisted of two species. While each of the second, third, and sixth clusters comprised of five types. Each of the fourth and eighth clusters consisted of seven types and the fifth cluster of nine types. *Figure 2* indicates that there are identical or similar species in their presence and absence in the study regions within all eight clusters except for the seventh cluster, for example, the two species *Amaranthus hybridus* and *Opuntia ficus-indica* in the eighth cluster as well as the species *Zaleya pentandra*, *Alternanthera pungens*, *Cylindropuntia rosea*, *Eclipta prostrata*, *Kali turgida*, *Tagetes minuta* and *Xanthium spinosum* in the fifth cluster. On the other hand, the species *Euphorbia maculata* was not observed in any of the studied regions.

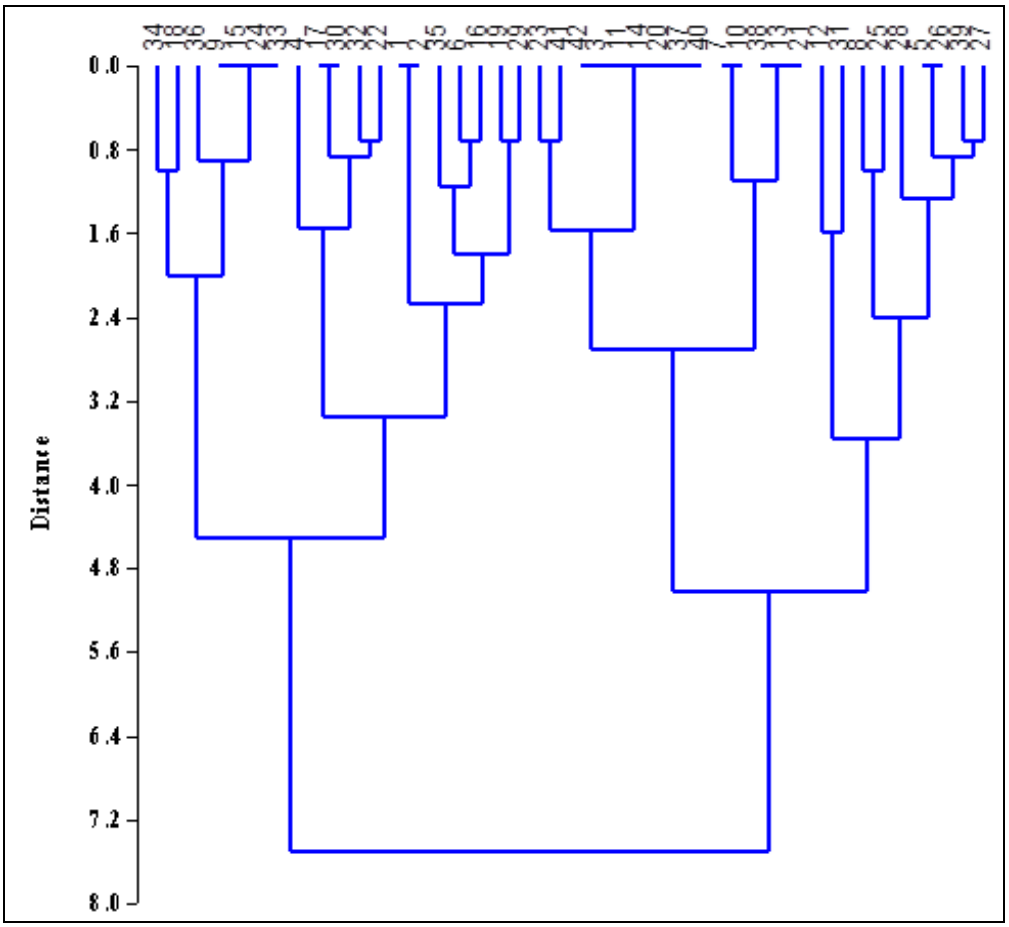

Figure 2. *Tree diagram for introduced and invasive plants species using ward's method. 1: A. ampliceps; 2: A. salicina; 3: A. pungens; 4: A. albus; 5: A. hybridus; 6: A. spinosus; 7: A. squamosa; 8: A. ochroleuca; 9: A. suberecta; 10: C. bonariensis; 11: C. rosea; 12: D. innoxia; 13: D. stramonium; 14: E. prostrata; 15: E. heterophylla; 16: E. maculata; 17: E. prostrata; 18: H. curassavicum; 19: Icylindrica; 20: K. turgida; 21: L. camara; 22: L. leucocephala; 23: L. arvensis; 24: M. balsamina; 25: N. glauca; 26: O. ficus-indica; 27: O. stricta; 28: P. aculeata; 29: P. australis; 30: P. perfoliatus; 31: P. juliflora; 32: P. koelziana; 33: S. europaea; 34: S. portulacastrum; 35: S. sesuvioides; 36: S. verrucosum; 37: T. minuta; 38: T. procumbens; 39: V. encelioides; 40: X. spinosum; 41: X. strumarium; 42: Z. pentandra*

http://www.aloki.hu ● ISSN 1589 1623 (Print) ● ISSN 1785 0037 (Online)
DOI: http://dx.doi.org/10.15666/aeer/1906_43734388

Principal component analysis (PCA)

PCA is a multivariate statistical approach that reduces the complex data by turning the number of interrelated variables into a smaller number of variables called principal components. Hence, it has been used to understand the relationship among the eleven studied regions based on the presence and absence of introduced and invasive plant species in these regions. The first five main PCAs extracted had larger eigenvalues than one (Eigenvalue > 1) which contributed to 69.36% of the accumulative variation of the original variables (*Table 9*). While the other PCAs extracted had eigenvalues less than one (Eigenvalue < 1). The results demonstrated that the PCA1 and PCA contributed to 35.95% of the total variability with Al-Baha, Bisha, Jizan, and Taif regions in the PCA1 and with AlGhat, Buraidah, and Jeddah regions in the PCA2. The first two PCAs had principally featured the eleven regions in various groups; consequently, PCA1 and PCA2 were harnessed to construct a biplot (*Fig. 3*).

Table 9. *PCA results for eleven regions based on presence and absence of introduced and invasive plant species*

Regions	PCA1	PCA2	PCA3	PCA4	PCA5
Al-Baha	0.47	-0.11	-0.20	-0.17	-0.06
Al Ghat	0.19	0.54	-0.28	-0.03	-0.05
Bisha	0.42	-0.18	0.42	0.27	0.11
Buraidah	0.15	0.56	-0.24	0.01	-0.02
Dammam	-0.33	-0.14	0.00	0.45	-0.29
Fayfa	0.20	-0.16	-0.33	0.17	0.75
Jizan	0.44	0.12	0.42	0.30	-0.07
Jeddah	-0.14	0.47	0.41	0.03	0.07
Tabuk	-0.19	0.11	0.44	-0.47	0.43
Taif	0.34	0.02	0.06	-0.12	-0.26
Riyadh	-0.16	0.25	-0.03	0.58	0.26
Eigen value	2.24	1.72	1.47	1.19	1.02
Explained variance	20.33	15.62	13.32	10.85	9.24
Cumulative variance	20.33	35.95	49.27	60.12	69.36

The relationships among different eleven regions based on the presence and absence of introduced and invasive plant species are graphically displayed in a biplot of PCA1 and PCA2 (*Fig. 3*). A highly positive correlation was found between L3 and L6, L7 and L8, L2 and L4 as well as L1 and L3. The positive and low association between all possible pairs of the regions 1;2;3;4;6;9 were observed. Also, the low positive correlations were recorded for the L7 region with 2, 4, and 10 as well as for the L11 region with 1 and 3. On the other hand, the other relationships were either very low or negative between the regions under study. This could be due to the existence of a relationship between these invasive species and the environmental conditions of these areas, especially the local species.

Discussion

Out of 13000 vascular plant species, 4% of plants are outside their original range in the world (Van Kleunen et al., 2015). The two American continents are considered to be

http://www.aloki.hu ● ISSN 1589 1623 (Print) ● ISSN 1785 0037 (Online)
DOI: http://dx.doi.org/10.15666/aeer/1906_43734388

the main habitat for all the basic invasive species found in the Kingdom of Saudi Arabia. During the past decade, the urbanization in KSA has led to the introduction of many invasive, exotic, and harmful plant species (Al-Harthi et al., 2019).

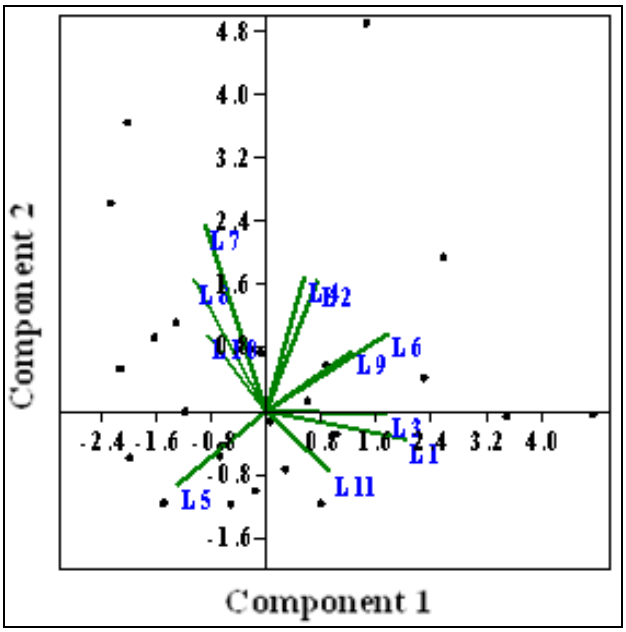

Figure 3. *Biplot graph on the basis of the first two principal component axes of eleven regions according to the presence and absence of introduced and invasive plants species. L1: Al-Baha; L2: Al Ghat; L3: Bisha; L4: Buraidah; L5: Dammam; L6: Fayfa; L7: Jizan; L8: Jeddah; L9: Tabuk; L10: Taif; L11: Riyadh*

The governorates under study differed in the number and percentage of invasive plants, due to the difference in climate and soil, in addition to the fact that these plants found an appropriate habitat for growth in these areas. Plant growth changes with altering resource availability, the effect of plants on soil properties and soil feedbacks (Wang et al., 2020). Perhaps the success of these invasive plants in these areas is due to the assumption unavailability of the natural enemy (Keane and Crawley, 2002), contains new weapons (Callaway and Aschehoug, 2000), the evolution of increased competitiveness (Blossey and Notzold, 1995), plant-soil feedback (Klironomos, 2002) and resource availability (Wang et al., 2020), or the presence of some different mechanisms enhancing the invasion of alien plants (Qin et al., 2013). The environment and diversity variables showed a difference among habitats in the Kingdom of Saudi Arabia and environmental changes, as drought, heat, and an increase in CO_2 and nitrogen can lead to a change in soil and plant growth (Pugnaire et al., 2019), which leads to the spread of invasive plants in these areas. The results showed that the highest percentage of invasive plants was found in Al-Baha region, which confirms the high invasion of these plants in this region. Invasive plant species menace local biodiversity, but whether alien species can competitively replace local species is still in dispute (Catford, 2018). Huang et al. (2016) reported that invasive species may not outperform native plants under resource limitation. There are several methods of controlling invasive species that have been adopted in countries with experience in this field, such as mechanical control, prescribed burning and chemical control (Berhanu and Tesfaye,

http://www.aloki.hu ● ISSN 1589 1623 (Print) ● ISSN 1785 0037 (Online)
DOI: http://dx.doi.org/10.15666/aeer/1906_43734388

2006). Chemical control is not recommended to preserve the environment from pollution despite its proven effectiveness and success.

The invasive species *P. juliflora* is generally found in the northwest, north, eastern and central regions of KSA, especially disturbed sites, or amongst secondary plants predominated by some other shrubs. (Thomas et al., 2010). The invasive species *P. juliflora* is spreading rapidly and compete with natural vegetation in the KSA due to rapid growth, resistance to drought, and ability to reproduce and spread successfully under drought conditions, in addition to the loss of the ecosystem to its natural immunity to resistance against such invasive species (Rogers, 2000; Berhanu and Tesfaye, 2006). Consequently, this species is considered very dangerous and has a negative impact on the biological diversity of the Kingdom of Saudi Arabia (Shiferaw et al., 2004). As explained by Thomas et al. (2010), that the invasive species *P. juliflora* has invaded most of the localities in inland sites in the Saudi Jazan region, which will have harmful effects on the local plants in this region. Harding and Bate (1991) reported that Invasive *Prosopis* species are spreading rapidly in arid regions as well as in areas of high rainfall and groundwater in South Africa. Invasive *P. juliflora* trees form dense thickets that are difficult to penetrate and not use the land for various agricultural practices (Harding and Bate, 1991), as well as interfere with mustering and injure livestock in Saudi Arabia (Thomas et al., 2016) and Africa (Berhanu and Tesfaye, 2006). Invasive plant species have been reported to have faster growth rates than native plant species (Ramula et al., 2008). Some plant species are rare in their native regions, but highly invasive in other regions, such as *Acacia baileyana*, *Eucalyptus globulus*, *Impatiens parviflora* and *Centaurea solstitialis* (Catford, 2018). As a result of the multiple introductions of invasive plant species, genetically more diverse invasive species can arise and become more widespread (Oduor et al., 2015). Thus, the environmental adjustment of the introduced plant species can be indorsed by different introductions (Oduor et al., 2016). The different methods of reproduction play an important role in preserving certain genetic groups and thus the continuation of the natural hybridization process (Rebman and Pinkava, 2001), among these methods are sexual (self-fertility) and vegetative reproduction as well as the adventive embryo that led to the spread of invasive species in the kingdom, especially *Opuntia ficus-indica* and *Opuntia stricta* species. From these data, three types of life forms (Therophyte, Chamaephytes, and Phanerophytes) were identified for the invasive plant species in the KSA. The Phanerophytes life form recorded the highest percentage of the introduced types, followed by Therophyte and Chamaephytes. While, Therophyte life form was registered with the highest percentage of the introduced and invasive plants, followed by Phanerophytes and Chamaephytes equally. The results also showed that the life growth of herbs life was dominant for the invasive plant species, followed by trees in the introduced types, and shrubs and trees in the introduced and invasive types. These results indicate that the annual (Therophyte) and herb invasive species adapt better to the environmental conditions in the studied regions of the KSA. Perhaps the reason for the spread of invasive annual species is due to the method of propagation by seed or vegetative growth. The life form of wild species was adequately adapted from annual species through the study system by Nelis (2012). Under abiotic stress conditions, both grass and perennial invasive species adapt and have higher growth and spread rates (Nelis, 2012), and in regions with poor soils, thin grasses are more common and widespread than other plant species (Grime, 2001). Invasive plant species are frequently characterized by evolving adaptations in their exotic areas, and this adaptation appears

http://www.aloki.hu ● ISSN 1589 1623 (Print) ● ISSN 1785 0037 (Online)
DOI: http://dx.doi.org/10.15666/aeer/1906_43734388

after 20 years (Oduor et al., 2016). Nelis (2012) explained that the botanical characteristics of the life form may explain the differences in the processes underlying the dynamics of the plant populations, and the rate of growth and immigration of plant populations can be predicted by the life form. Thomas et al. (2016) reported that except for the species dominance which negatively correlated, invasive and alien species positively correlated with altitude and most of the indices of diversity in regions. A correlation was found between invasive species and several local species in the KSA, but these correlations are not fixed in all cases.

Conclusion

It was many ways in which these plants were introduced to the KSA, such as the seasons of Hajj, or for food, or medicinal purposes, decorations, etc., as well as the increase in international trade and travel, through occasional means, or human disturbances in natural habitats such as removal of native plants from heavily cultivated areas for road constructions, which is an agent change and a threat to local biodiversity, the environment, society, the economy, and the ecosystem. Therefore, in the future, laws must be established to limit the introduction and use of these plants and be under the supervision of the Ministry of Agriculture, and the community should be encouraged to use local plants. In addition to working on early detection and monitoring of new and emerging invasive plant species they can also be resisted by mechanical, biological, or chemical methods, especially before flowering and fruiting stages.

Acknowledgments. The authors thank to all those who contributed and supported this research through personal contact and provided us with the data: Abrahim Al-Dakhil from Buraydah, Ali Al-Zahrani from Al-Baha, Luluah. Almasoudi from Taif, Mshary Alowid from Dammam, Yahya Masrahi from Jazan, Sultan Alodhidan from Al-Ghat, Eisa AlFaify from Fayfa and Najat Bukhari from Riyadh, in addition to the researchers participating in this research from Tabuk, Bisha and Jeddah.

REFERENCES

[1] Al-Harthi, S. T. S., Al-Qahtani, A. M., Al-Munqedhi, B. M. (2019): Alien plants in Western region, Saudi Arabia. – Journal of Agricultural, Environmental and Veterinary Sciences 3(3): 82-90. https://doi.org/10.26389/AJSRP.S140419.

[2] Berhanu, A., Tesfaye, G. (2006): The Prosopis dilemma, impacts on dryland biodiversity and some controlling methods. – Journal of the Drylands 1(2): 158-164.

[3] Blanchard, R., Holmes, P. M. (2008): Riparian vegetation recovery after invasive alien tree clearance in the Fynbos Biome. – South African Journal of Botany 74: 421-431. https://doi.org/10.1016/j.sajb.2008.01.178.

[4] Blossey, B., Notzold, R. (1995): Evolution of increased competitive ability in invasive nonindigenous plants: a hypothesis. – Journal of Ecology 83: 887-889. https://doi.org/10.2307/22614 25.

[5] Büyüktahtakın, E., Haight, R. G. (2018): A review of operations research models in invasive species management: state of the art, challenges, and future directions. – Annals of Operations Research, Springer 271: 357-403. DOI: 10.1007/s10479-017-2670-5.

[6] Callaway, R. M., Aschehoug, E. T. (2000): Invasive plants versus their new and old neighbors: a mechanism for exotic invasion. – Science 290: 521-523. https://doi.org/10.1126/scien ce.290.5491.521.

http://www.aloki.hu ● ISSN 1589 1623 (Print) ● ISSN 1785 0037 (Online)
DOI: http://dx.doi.org/10.15666/aeer/1906_43734388

[7] Catford, J. A., Bode, M., Tilman, D. (2018): Introduced species that overcome life history tradeoffs can cause native extinctions. – Nat Commun 9: 2131. https://doi.org/10.1038/s41467-018-04491-3.
[8] CBD (Convention on Biological Diversity) (2010): Strategic plan for biodiversity 2011–2020. – https://www.cbd.int (accessed 21 Oct. 2020).
[9] CBD News (2001): Convention on Biological Diversity. – http://www.biodiv.org/programmes/cross-cutting/alien/default.asp.
[10] Chaudhary, S. A. (1999): Flora of the Kingdom of the Saudi Arabia, Vol. I. – Ministry of Agriculture and Water, Riyadh.
[11] Chaudhary, S. A. (2000): Flora of the Kingdom of the Saudi Arabia (Part 3), Vol. II. – Ministry of Agriculture and Water, Riyadh.
[12] Chaudhary, S. A. (2001): Flora of the Kingdom of the Saudi Arabia (Part 2), Vol. II. – Ministry of Agriculture and Water, Riyadh.
[13] Diaz, S., Lavorel, S., Chapin, F. S., Tecco, P. A., Gurvich, D. E., Grigulis, K. (2007): Functional Diversity - at the Crossroads between Ecosystem Functioning and Environmental Filters. – In: Canadell, J. G., Pataki, D., Pitelka, L. (eds.) Terrestrial Ecosystems in a Changing World. IGBP series. Springer-Verlag, Berlin, pp. 81-92.
[14] Drenovsky, R. E., Batten, K. M. (2007): Invasion by *Aegilops triuncialis* (Barb Goatgrass) slows carbon and nutrient cycling in a serpentine grassland. – Biological Invasions 9: 107-116. DOI: 10.1007/s10530-006-0007-4.
[15] Eviner, V. T., Hoskinson, S. A., Hawkes, C. V. (2010): Ecosystem impacts of exotic plants can feed back to increase invasion in western U.S. rangelands. – Rangelands 31: 21-31. DOI: 10.2111/RANGELANDS-D-09-00005.1.
[16] Gaertner, M., Breeyen, A. D., Hui, C., Richardson, D. M. (2009): Impacts of alien plant invasions on species richness in Mediterranean-type ecosystems: a meta-analysis. – Progress in Physical Geography 33: 319-338.
[17] Globalization101 (2020): The Global Spread of Invasive Species. – https://www.globalization101.org/the-global-spread-of-invasive-species/ (accessed 21 Oct. 2020).
[18] Grime, J. P. (2001): Plant Strategies, Vegetation Processes, and Ecosystem Properties. – John Wiley and Sons, New York.
[19] Hammer, Ø., Harper, D. S. T., Ryan, P. D. (2020): Paleontological statistics software package for education and data analysis. – Palaeontologia Electronica 4(1): 9 pp.
[20] Harding, G. B., Bate, G. C. (1991): The occurrence of invasive Prosopis species in the north-western Cape, South Africa. – South African Journal of Science 87: 188-192.
[21] Harman, H. H. (1976): Modern Factor Analysis. 3rd Ed. – University of Chicago Press, Chicago.
[22] Huang, Q. Q., Shen, Y. D., Li, X. X., Li, S. L., Fan, Z. W. (2016): Invasive Eupatorium catarium and Ageratum conyzoides benefit more than does a common native plant from nutrient addition in both competitive and non-competitive environments. – Ecological Research 31: 145-152. https://doi.org/10.1007/s1128 4-015-1323-x.
[23] Hulme, P. E. (2006): Beyond control: wider implications for the management of biological invasions. – Journal of Applied Ecology 43: 835-847.
[24] IUCN (International Union for the Conservation of Nature) (1999): IUCN guidelines for the prevention of biodiversity loss due to biological invasion. – Species 31/32: 28-42.
[25] Keane, R. M., Crawley, M. J. (2002): Exotic plant invasions and the enemy release hypothesis. – TRENDS in Ecology & Evolution 17: 164-170. https://doi.org/10.1016/s0169-5347(02)02499-0.
[26] Kingston, N., Waldren, S. (2003): The plant communities and environmental gradients of Pitcairn Island: the significance of invasive species and the need for conservation management. – Annals of Botany 92: 31-40. DOI: 10.1093/aob/mcg106.
[27] Klironomos, J. N. (2002): Feedback with soil biota contributes to plant rarity and invasiveness in communities. – Nature 417: 67-70. https://doi.org/10.1038/41706 7a.

http://www.aloki.hu ● ISSN 1589 1623 (Print) ● ISSN 1785 0037 (Online)
DOI: http://dx.doi.org/10.15666/aeer/1906_43734388

[28] Le Roux, P. J. (1981): Plant Invader Species in Pine Plantations in South Africa. – In: Van de Venter, H. A., Mason, M. (eds.) Proc. of the 4th National WEEDS Conference of South Africa. Pretoria, South Africa, 27-29 January 1981. A. A. Balkema, Cape Town, pp. 155-168.

[29] Levine, J. M., Vila, M., Antonio, C. M., Dukes, J. S., Grigulis, K., Lavorel, S. (2003): Mechanisms underlying the impacts of exotic plant invasions. – Proceedings of the Royal Society of London. Series B: Biolog. Sci. 270(1517): 775-781. https://doi.org/10.1098/rspb.2003.2327.

[30] Mack, R. N., Simberloff, D., Lonsdale, W. M., Evans, H., Clout, M., Bazzaz, F. A. (2000): Biotic invasions: causes, epidemiology, global consequences, and control. – Ecological Applications 3(1): 689-710. https://doi.org/10.1890/1051-0761(2000)010[0689:BICEGC]2.0.CO;2.

[31] Mark, A. F., Dickinson, K. J. M. (2008): Maximizing water yields with indigenous non-forest vegetation: a New Zealand perspective. – Ecology and the Environment 6(1): 25-34. DOI: 10.1890/060130.

[32] Naidoo, R., Balmford, A., Costanza, R., Fisher, B., Green, R. E., Lehner, B., Malcolm, T. R., Ricketts, T. H. (2008): Global mapping of ecosystem services and conservation priorities. – Proceedings of the National Academy of Sciences 105(28): 9495-500. DOI: 10.1073/pnas.0707823105.

[33] Nelis, L. C. (2012): Life form and life history explain variation in population processes in a grassland community invaded by exotic plants and mammals. – PLoS ONE 7(8): e42906. https://doi.org/10.1371/journal.pone.0042906.

[34] Oduor, A. M. O., Gomez, J. M., Herrador, M. B. and Perfectti, F. (2015): Invasion of Brassica nigra in North America: distributions and origins of chloroplast DNA haplotypes suggest multiple introductions. – Biological Invasions 17: 2447-2459. https://doi.org/10.1007/s10530-015-0888-1.

[35] Oduor, A. M. O., Leimu, R., van Kleunen, M. (2016): Invasive plant species are locally adapted just as frequently and at least as strongly as native plant species. – Journal of Ecology 104: 957-968. https://doi.org/10.1111/1365-2745.12578.

[36] Pejchar, L., Mooney, H. A. (2009): Invasive species, ecosystem services and human wellbeing. – Trends in Ecology & Evolution 24: 497-504. https://doi.org/10.1016/j.tree.2009.03.016.

[37] Pimentel, D., Lach, L., Zuniga, R., Morrison, D. (2000): Environmental and economic costs of nonindigenous species in the United States. – Bioscience 50(1): 53-65. DOI: 10.1641/0006-3568(2000)050[0053:EAECON]2.3.CO;2.

[38] Pimentel, D., Zuniga, R., Morrison, D. (2005): Update on the environmental and economic costs associated with alien invasive species in the United States. – Ecological Economics 52:(3) 273-288. https://doi.org/10.1016/j.ecolecon.2004.10.002.

[39] Pugnaire, F. I., Morillo, J. A., Penuelas, J., Reich, P. B., Bardgett, R. D., Gaxiola, A., Wardle, D. A., van der Putten, W. H. (2019): Climate change effects on plant-soil feedbacks and consequences for biodiversity and functioning of terrestrial ecosystems. – Science advances 5(11), [aaz1834]. https://doi.org/10.1126/sciadv.aaz1834.

[40] Qin, R., Zheng, Y., Valiente-Banuet, A., Callaway, R. M., Barclay, G. F., Pereyra, C. S., Feng, Y. (2013): The evolution of increased competitive ability, innate competitive advantages, and novel biochemical weapons act in concert for a tropical invader. – New Phytologist 197: 979-988. https ://doi.org/10.1111/nph.12071.

[41] Ramula, S., Knight, T. M., Burns, J. H., Buckley, Y. M. (2008): General guidelines for invasive plant management based on comparative demography of invasive and native plant populations. – Journal of Applied Ecology 45: 1124-1133. https://doi.org/10.1111/j.1365-2664.2008.01502.x.

[42] Rebman, J. P., Pinkava, D. J. (2001): Opuntia cacti of North America: An Overview. – The Florida Entomologist 84(4): 474-483. https://doi.org/10.2307/3496374.

http://www.aloki.hu ● ISSN 1589 1623 (Print) ● ISSN 1785 0037 (Online)
DOI: http://dx.doi.org/10.15666/aeer/1906_43734388

[43] Richardson, D. M. (1988): Forestry trees as invasive aliens. – Conservation Biology 12(1): 18-26. DOI: 10.1111/j.1523-1739.1998.96392.x.
[44] Richardson, D. M., Pysek, P., Rejmánek, M., Barbour, M. G., Panetta, F. D., West, C. J. (2000): Naturalization and invasion of alien plants: concepts and definitions. – Diversiety and Distributions 6: 93-107. https://doi.org/10.1046/j.1472-4642.2000.00083.x.
[45] Rogers, K. E. (2000): The Magnificent Mesquite. – Univ. of Texas Press, Austin.
[46] Seebens, H., Blackburn TM., Dyer, E. E., Genovesi, P., Hulme, P. E., et al. (2017): No saturation in the accumulation of alien species worldwide. – Nature Communications 8: 1-9. doi: 10.1038/ncomms14435.
[47] Sharma, S. (1996): Applied Multivariate Techniques. 2nd Ed. – John Wiley and Sons, New York.
[48] Shiferaw, H., Teketay, D., Nemomissa, S., Assefa, F. (2004): Some biological characteristics that foster the invasion of Prosopis juliflora (Sw.) DC. at Middle Awash Rift Valley Area, north-eastern Ethiopia. – Journal of Arid Environments 58(2): 135-154. https://doi.org/10.1016/j.jaridenv.2003.08.011.
[49] Thomas, J. (2011): Onward (continuously updated). Plant diversity of Saudi Arabia, King Saud University. – http://plantdiversityofsaudiarabia.info/Biodiversity-Saudi-Arabia/Flora/Checklist/Cheklist.htm (accessed 21 Oct. 2020).
[50] Thomas, J., Alfarhan, A. H., Samraoui, B., Sivadasan, M., Bukhari, N., Al-Atar, A. A. (2010): Floristic composition of the Farasan Archipelago in SE Red Sea and its affinities to phytogeographical regions. – Arab Gulf Journal of Scientific Research 28(2): 79-90.
[51] Thomas, J., El-Sheikh, M. A., Alfarhan, A. H., Alatar, A. A., Sivadasan, M., Basahi, M., Al-Obaid, S., Rajakrishnan, R. (2016): Impact of alien invasive species on habitats and species richness in Saudi Arabia. – Journal of Arid Environments 127: 53-65. http://dx.doi.org/10.1016/j.jaridenv.2015.10.009.
[52] USDA (2020): Invasive plants. – https://www.fs.fed.us/wildflowers/invasives/#:~:text=What is an Invasive Plant,or harm to human health (accessed 21 Oct. 2020).
[53] Van Kleunen, M., Dawson, W., Essl, F. et al. (2015): Global exchange and accumulation of non-native plants. – Nature 525: 100-103. https://doi.org/10.1038/nature14910.
[54] Van Wilgen, B. W., Richardson, D. M., Le Maitre, D. C., Marais, C., Magadlela, D. (2001): The economic consequences of alien plant invasions: examples of impacts and approaches to sustainable management in South Africa. – Environment Development and Sustainability 3(2): 145-168. DOI: 10.1023/A: 1011668417953.
[55] Vila, M., Basnou, C., Pyšek, P., Josefsson, M., Genovesi, P., Gollasch, S., Nentwig, W., Olenin, S., Roques, A., Roy, D., Hulme, P., Partners, D. (2010): How well do we understand the impacts of alien species on ecosystem services? A pan-European cross-taxa assessment. – Frontiers in Ecology and the Environment 8: 135-144. DOI: 10.1890/080083.
[56] Wang, Y., Ni, G., Hou, Y., Wang, Q., Huang, Q. (2020): Plant–soil feedbacks under resource limitation may not contribute to the invasion by annual Asteraceae plants. – Oecologia 194: 165-176. https://doi.org/10.1007/s00442-020-04756-z.
[57] Zavaleta, E. (2000): The economic value of controlling an invasive shrub. – AMBIO 29(8): 462-467. DOI: 10.1579/0044-7447-29.8.462.

http://www.aloki.hu ● ISSN 1589 1623 (Print) ● ISSN 1785 0037 (Online)
DOI: http://dx.doi.org/10.15666/aeer/1906_43734388

PHYTOPLANKTON COMMUNITY STRUCTURE AND ITS RELATIONSHIP WITH ENVIRONMENTAL FACTORS IN TAIHU NATIONAL WETLAND PARK IN NORTHEAST CHINA

CHAI, Y. H.[1#] – YU, T. Y.[2#] – SUN, X.[3] – WEI, H.[4*] – YU, H. X.[2*]

[1]*Aulin College, Northeast Forestry University, Harbin 150040, China*

[2]*College of Wildlife and Protected Area, Northeast Forestry University, Harbin 150040, China*

[3]*College of Fisheries and Life Science, Dalian Ocean University, Dalian 116023, China*

[4]*School of Business, Beijing Union University, Beijing 100101, China*

[#] *Co-first authors*
These authors contributed to the work equally.

[*]*Corresponding authors*
e-mail: heng.wei@buu.edu.cn (Wei, H.); china.yhx@163.com (Yu, H. X.)

(Received 28th Apr 2021; accepted 29th Jul 2021)

Abstract. In order to understand the community structure of phytoplankton and its relationship with environmental factors in Taihu National Wetland Park in northeast China, a study was conducted in Taihu in September 2020. The results showed that there were 39 species of phytoplankton belonging to 27 genera and 6 phyla, among which Chlorophyta was the most abundant (20 species). The abundance and biomass of 5# and 6# sampling sites were significantly higher than other sampling sites, which may be caused by eutrophication. In Taihu National Wetland Park, the dominant species were *Merismopedia minima*, *Aphanizomenon flosaquae*, *Synedra acus*, *Synura*.sp and *Scenedesmus quadricauda*. Phytoplankton community structure in autumn in Taihu National Wetland Park were mainly influenced by pH, NO_3^--N, and water temperature. This research can provide a scientific basis for biodiversity protection and pollution control in Taihu National Wetland Park.
Keywords: *phytoplankton, biodiversity, richness, correlation, spatiality*

Introduction

According to Chalar (2009), the Earth's ecosystem is experiencing an unprecedented rate of biodiversity loss as a result of global climate change, eutrophication, and overexploitation of natural resources. Aquatic ecosystems especially lakes are vulnerable and the loss of biodiversity may have catastrophic consequences, such as algal blooms (Cardinale et al., 2012; Weyhenmeyer et al., 2013). Phytoplankton, which forms the base of food web in lakes, is particularly sensitive to variations in environmental factors (Mulvenna et al., 2012; Weyhenmeyer et al., 2013). Their community structure-like composition, abundance and biomass are affected by biotic factors, as well as abiotic factors like temperature, salinity, pH, nutrients and electrical conductivity (Oduor and Schagerl, 2007; Schagerl and Oduor, 2008; Oren, 2011). Investigations of phytoplankton communities in different ecosystem types have been carried out by different researchers in China (Ma and Yu, 2013; Sun et al., 2019; Ma et al., 2021).

Taihu National Wetland Park is located in the east of Tailai County. The wetland park receives water from direct precipitation. It also receives inflow from domestic sewage and industrial wastewater from Tailai County (Lin, 2002). Before 1990's, the wetland

http://www.aloki.hu ● ISSN 1589 1623 (Print) ● ISSN1785 0037 (Online)
DOI: http://dx.doi.org/10.15666/aeer/1906_43894402

park was seriously polluted because of the inflow of wastewater from Tailai paper mill. However, after the paper mill was banned from discharging its wastewater into the wetland, the water quality of Taihu National Wetland Park improved to a certain extent. In the recent years, the development of tourism and the influence of nearby residents' activities as a result of increase in human population have led to deterioration of the water quality in the wetland. As it currently stands, the water quality of the lake is in deplorable state. Although studies on planktons have been conducted in most of the aquatic systems in China (Sun et al., 2010; Yang et al., 2011; Shi et al., 2015), work of community structure of phytoplankton and their relationship to environmental variable of Taihu National Wetland Park is, however, lacking. So, this study will help fill the lacunae in scientific understanding of the community structure of this unique ecosystem. Moreover, this study will provide some reference for ecological restoration and management of the Wetland Park.

Materials and methods

Study area and sampling sites

The study was conducted in Taihu National Wetland Park which lies on E123˚25'14.17"~E123˚29'00.97", N46˚24'12.10"~N46˚21'15.10" in northeast China (Chen et al., 2018). Taihu National Wetland Park covers an area of approximately 1365 hm^2 and it lies in an area which is under the influence of temperate continental monsoon climate zone. This study area receives an annual average precipitation of 360 mm with an annual mean temperature of about 4.2 ℃. The wetland is important for water supply, flood control, tourism and recreation, and aquaculture.

All samples were collected 3 times from 8 sampling sites of Taihu National Wetland Park in September (autumn) in 2020. The site included 1# located in the ditch close to Taihu, sites 2# and 3# were located in the sewage treatment plant, site 4# was located in the "reclaimed water" inlet of the sewage treatment plant, and sites 5-8# were located in the middle of the Taihu National Wetland Park (*Table 1, Figure 1*).

Table 1. *Location of sampling sites in Taihu National Wetland Park*

Sampling sites	Coordinate	Sampling sites	Coordinate
1#	46°21′56″N123°26′32″E	5#	46°23′03″N123°26′14″E
2#	46°22′18″N123°26′42″E	6#	46°23′04″N123°26′20″E
3#	46°22′25″N123°26′15″E	7#	46°23′02″N123°27′13″E
4#	46°22′20″N123°26′50″E	8#	46°23′30″N123°26′51″E

Sample collection and analysis

At each sampling site water temperature (WT), pH, ammonia nitrogen (NH_4^+-N) and nitrate nitrogen (NO_3^--N) were measured using a Multi parameter water quality analyzer (YSI 6600, YSI Inc., USA) while water transparency (SD) was determined using a 20 cm Secchi disk. Whole water samples from the same site were collected and transported to the laboratory for analysis of total nitrogen (TN), total phosphorus (TP) and chemical oxygen demand (COD_{Cr}). Total nitrogen (TN), TP and COD_{Cr} were analyzed according to the standard methods for China (MEP (Ministry of Environmental Protection, 2002).

http://www.aloki.hu ● ISSN 1589 1623 (Print) ● ISSN1785 0037 (Online)
DOI: http://dx.doi.org/10.15666/aeer/1906_43894402

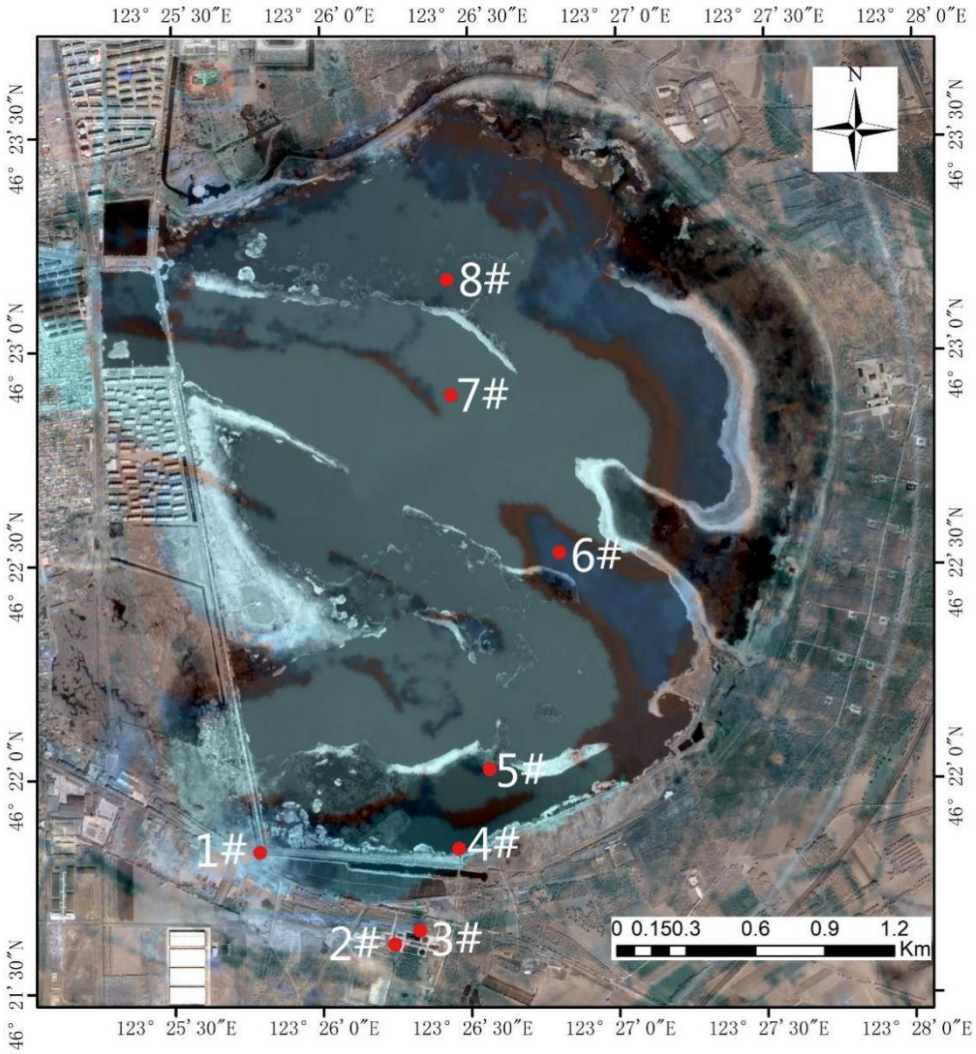

Figure 1. *Map of Taihu National Wetland Park Showing the distribution of sampling sites*

Replicates of phytoplankton samples (1 L at each site) were collected, put in a labeled bottle and immediately fixed with Lugol's solution. The phytoplankton samples were allowed to sediment for 48 h and then concentrated to 30 mL. Phytoplankton were identified by referring to the identification key of Hu (2006) and counted using an inverted microscope (Leica Microsystems, German) at 400× magnification. Phytoplankton diversity, richness and dominance were determined for each sampling sites using number of taxa, total number of individuals per taxa and relative abundance of each taxon over the sampling period respectively. Biomass of the phytoplankton was computed by dividing wet weight (mg) obtained from length–weight relation of the species to the volume of water (L) filtered (Sun et al., 2010). Shannon-Weaver diversity index (Shannon and Weiner 1948) was used to calculate diversity as follows:

$$H = -\sum[(\frac{n}{N}) * (\ln \frac{n}{N})] \quad \text{(Eq.1)}$$

where n = number of individuals of a taxon; N = total number of individual in a site. This index takes into account both the numbers of taxa and their relative abundance.

http://www.aloki.hu ● ISSN 1589 1623 (Print) ● ISSN1785 0037 (Online)
DOI: http://dx.doi.org/10.15666/aeer/1906_43894402

Taxon richness was calculated using Margalefs Index (D) (Clarke and Warwick, 1994):

$$D = (S - 1) / \ln N \quad \text{(Eq.2)}$$

where S is the total number of species, N is the total number of individuals of all species, and P_i is the proportion of the number of individuals of the i-th species in the total number of individuals.

Species dominance was computed according to the formula proposed by as follows:

$$y = f_i \times P_i \quad \text{(Eq.3)}$$

where, y is the dominance, P_i is the proportion of the i-th species in the total number of individuals, f_i is the frequency of the species at each sampling time. When $y > 0.02$, it is defined as the dominant species. *Table 2* below shows the water quality evaluating criteria based on the diversity indices.

Table 2. *Diversity Index Water Quality Evaluation Standard*

Index	Pollution index		
Shannon-Weaver Diversity index(H')	0-1 Heavy	1-3 Medium	＞3 Light
Margalef Richness index(D)	0-1 Heavy	1-3 Medium	＞3 Light

Data analyses

The data was analyzed using SPSS 17.0 (SPSS, 2008) and Microsoft Excel window 2007. Before analysis, the Kolmogorov-Smirnov method was used to test whether data were normally distributed, and the Bartlett test was performed to assess the homogeneity of variance. The data that did not meet the normality test was log transformed. One-way ANOVA was used to test the difference of the measures variable (environmental variables, phytoplankton diversity, richness and dominance) among sites. Relationships between phytoplankton species and environment variables were analyzed using the detrended correspondence analysis and redundancy analysis (RDA) using CANOCO 4.5 software (Microcomputer Power, New York, USA). Monte Carlo simulations with 499 permutations were used to test the significance of the physical–chemical variables in explaining the biomass of phytoplankton functional groups data in the RDA. Figures were drawn using Microsoft excel.

Results

Physical–chemical variables

The mean spatial values of physical–chemical factors recorded among the sampling sites within the study period are presented in *Table 3*. The average WT was 18.62 ºC with the relative highest value of 20 ºC being recorded in site 1#. The values of pH measured in this wetland park were in the side of alkalinity (basic). TN, TP, NH_4^+-N, NO_3^--N and CODcr differed significantly among the sites. TN, TP, NH_4^+-N and NO_3^--N were significantly higher in site 2# with a mean value of 6.62, 0.67, 11.26 and 1.23 mg/L, respectively. Similarly, CODcr was significantly higher in site 2# (*Table 2*).

http://www.aloki.hu ● ISSN 1589 1623 (Print) ● ISSN1785 0037 (Online)
DOI: http://dx.doi.org/10.15666/aeer/1906_43894402

Classification which was done according to the *Environmental Quality Standard for Surface Water* (GB3838-2002), showed that with exception of NO_3^-N which belongs to Class IV water quality, all the remaining measured variables belong to Class V water quality.

Table 3. *Water quality measurement results of Taihu National Wetland Park (unit: except water temperature and pH, the rest are all mg/L)*

Sampling site	WT(°C)	pH	NH_4^+-N	NO_3^--N	TN	TP	COD_{Cr}
1#	20	8.74	1.26	0.62	1.67	0.26	22.8
2#	18	8.25	11.26	1.23	6.62	0.67	29.6
3#	18	8.93	3.26	0.53	4.88	0.34	22.3
4#	19	9.17	2.21	0.59	4.82	0.27	20.2
5#	19	9.03	1.22	0.52	4.92	0.25	19.3
6#	19	9.32	0.96	0.39	3.46	0.18	2.6
7#	18	9.28	1.09	0.42	3.13	0.21	2.2
8#	18	9.11	1.06	0.46	2.95	0.18	2.3
Average value	18.62	8.98	2.79	0.59	4.06	0.30	15.2
GB3838-2002			V	IV	V	V	V

Phytoplankton species composition and their spatial distribution

In the current study, a total of 39 species of phytoplankton belonging to 27 genera and in 6 classes were identified. Chlorophyta was the most with 20 species, accounting for 51.28%; bacillariophyta was the second with 11 species accounting for 28.21%; Cyanophyta has 4 species, accounting for 10.26%; Euglenophyta has 2, accounting for 5.13%; Chrysophyta and cryptophyta had 1 each which accounted for 5.13% altogether.

Spatially, sampling site 5# had the highest number of species (31 species), followed by 6# (24 species) and the site with the least species number was 1# (*Figure 2*). The abundance and biomass of phytoplankton measured in the Taihu National Wetland Park was significantly different among sampling sites (*Figure 3*). There was spatial significant difference in abundance and biomass distribution among sampling sites (*Figure 3*). The abundance of the phytoplankton ranged between 141.6×10^4ind./L ~ 4311.6×10^4ind./L, with the highest value of 4311.6×10^4ind./L recorded in site 5# while the least (141.6×10^4ind./L) was measured at site 1#. The phytoplankton biomass measured ranged between 0.39 mg / L and 21.24 mg / L,with the highest value of 21.24 mg / L measured at site 6# and the lowest of 0.39 mg / L at site 1#.

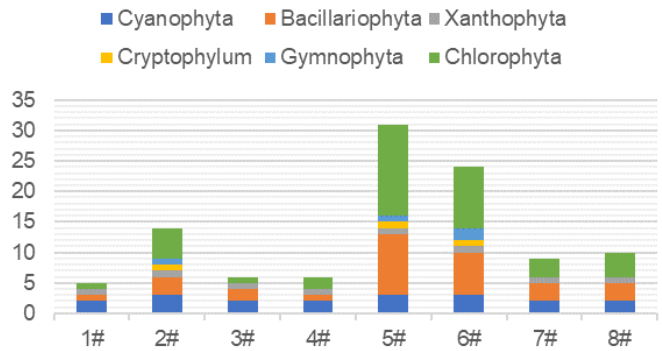

Figure 2. *Number of phytoplankton species at sampling sites in Taihu National Wetland Park in autumn*

http://www.aloki.hu ● ISSN 1589 1623 (Print) ● ISSN1785 0037 (Online)
DOI: http://dx.doi.org/10.15666/aeer/1906_43894402

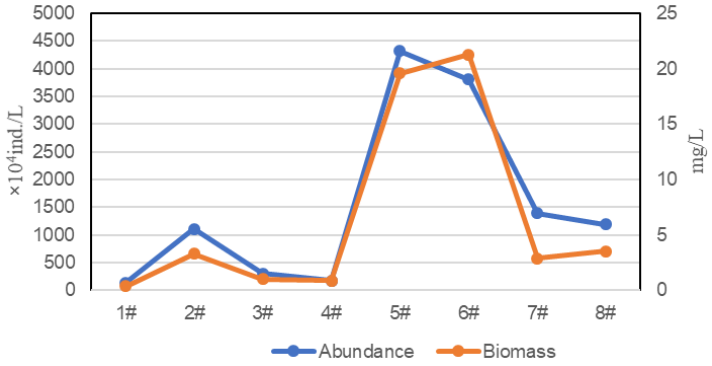

Figure 3. *Phytoplankton abundance and biomass in Taihu National Wetland Park*

Phytoplankton species diversity, richness and dominance

Phytoplankton community attributes such as diversity, richness and dominance often give important clues of the functional status or health of aquatic system. From the results, Shannon Weaver index ranged from 1.041 to 2.371 in the study area while; Margalef richness index ranged from 0.838 to 3.665 (*Table 4 and Figure 4*). Spatially, site 5# had the highest value of phytoplankton diversity of (2.371) while site 1# with a value of 1.041 was the least. Similarly, the taxon richness was significant higher in site 5# with a value of 3.665 and the least was observed in site 1# with a value of 0.838. Moreover, it is apparent that, Taihu National Wetland Park belongs to medium-heavy pollution type (*Table 4*).

Table 4. *The diversity index and pollution evaluation of phytoplankton sampling points in Taihu National Wetland Park in autumn*

Sampling site	*H'*	Assessment	*D*	Assessment
1#	1.041	Medium pollution	0.838	Heavy pollution
2#	1.248	Medium pollution	1.903	Medium pollution
3#	1.492	Medium pollution	0.901	Heavy pollution
4#	1.171	Medium pollution	1.001	Medium pollution
5#	2.371	Medium pollution	3.665	Light pollution
6#	2.229	Medium pollution	2.853	Medium pollution
7#	1.045	Medium pollution	1.134	Medium pollution
8#	1.287	Medium pollution	1.305	Medium pollution
Average value	1.486	Medium pollution	1.7	Medium pollution

Dominant species are defined by the dominance y > 0.02. The dominant species and their dominance of phytoplankton in Taihu National Wetland Park are shown in *Table 5*. In this study, the dominant species were *Schizosaccharum tenuiflorum*, filamentous alga bloom and *Scenedesmus giraldii,* belong to the indicator algae of eutrophic water body, and their dominance degrees are 0.675, 0.041 and 0.058, respectively.

When the occurrence of a species is greater than 65, then the species is regarded as a common species (Occurrence frequency>65%). *Table 6* shows the common species recorded during the study period in Taihu National Wetland Park. Seven common species belonging into 4 classes were observed in the wetland. These species are *Merismopedia minima*, *Aphanizomenon flosaquae*, *Cyclotella meneghiniana* and *Scenedesmus quadricauda*. These species are all indicator of eutrophic water body.

http://www.aloki.hu ● ISSN 1589 1623 (Print) ● ISSN1785 0037 (Online)
DOI: http://dx.doi.org/10.15666/aeer/1906_43894402

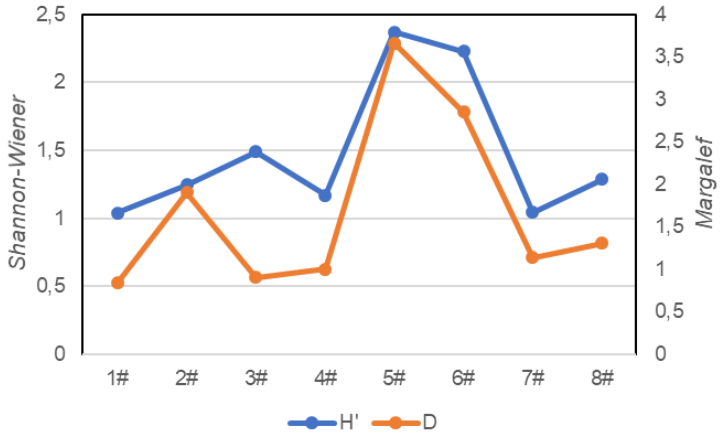

Figure 4. *Phytoplankton taxon characteristics determined at the sites in the Taihu National Wetland Park*

Table 5. *The dominant species of phytoplankton in Taihu National Wetland Park in autumn*

Dominant species	Occurrence frequency	Dominance
Merismopedia minima	1	0.675
Aphanizomenon flosaquae	1	0.041
Synedra acus	1	0.023
Synura.sp.	1	0.062
Scenedesmus quadricauda	1	0.058

Table 6. *Common species of phytoplankton in autumn in Taihu National Wetland Park*

Phylum	Species
Cyanophyta	*Merismopedia minima* *Aphanizomenon flosaquae*
Bacillariophyta	*Synedra acus* *Cyclotella meneghiniana*
Chrysophyta	*Synura.sp.*
Chlorophyta	*Ankistrodesmus angustus* *Scenedesmus quadricauda*

Relationship between environmental variables and some major phytoplankton species

RDA was carried out to determine the relationship between the abundance of the main functional species (*Table 7*) and environmental factors. The Monte Carlo test was significant for the first axis and all canonical axes ($p < 0.001$), suggesting that these environmental variables are important factors in explaining the group compositions. From *Figure 5*, NO_3^--N(0.8692) was the main positive correlation factor, TP (0.7523) was the second main positive correlation factor, and NH_4^+-N(0.6867) and COD_{Cr}(0.5641) also had significant positive correlation, while pH (-0.7595) in negative correlation factors had significant correlation. Water temperature (WT) was weakly but positive related to most of the phytoplankton species. From *Figure 6*, temperature and pH did not differ

http://www.aloki.hu ● ISSN 1589 1623 (Print) ● ISSN1785 0037 (Online)
DOI: http://dx.doi.org/10.15666/aeer/1906_43894402

significantly between the sites, therefore, these parameters could not influence the community structure.

Table 7. *Species and numbers of phytoplankton in the RDA ordination chart*

No.	Latin name	No	Latin name
L1	*Merismopedia minima*	Y1	*Cryptomonas ovate*
L2	*Merismopedia marssonii*	LU1	*Euglena oxyuris*
L3	*Phormidium allorgei*	LV1	*Chlamydomonas globosa*
L4	*Aphanizomenon flosaquae*	LV2	*Ankistrodesmus angustus*
G1	*Melosira granulata*	LV3	*Scenedesmus quadricauda*
G2	*Synedra acus*	LV4	*Selenastrum minutum* (Nag). Coll
G3	*Synedra amphicephala*	LV5	*Kirchneriella lunaris*
G4	*Synedra ulna*	LV6	*Dictyosphaerium pulchellum*
G5	*Cyclotella meneghiniana*	LV7	*Crucigenia tetrapedia*
G6	*Navicula exigua*	LV8	*Cosmarium obtusatum*
H1	*Synura.sp.*		

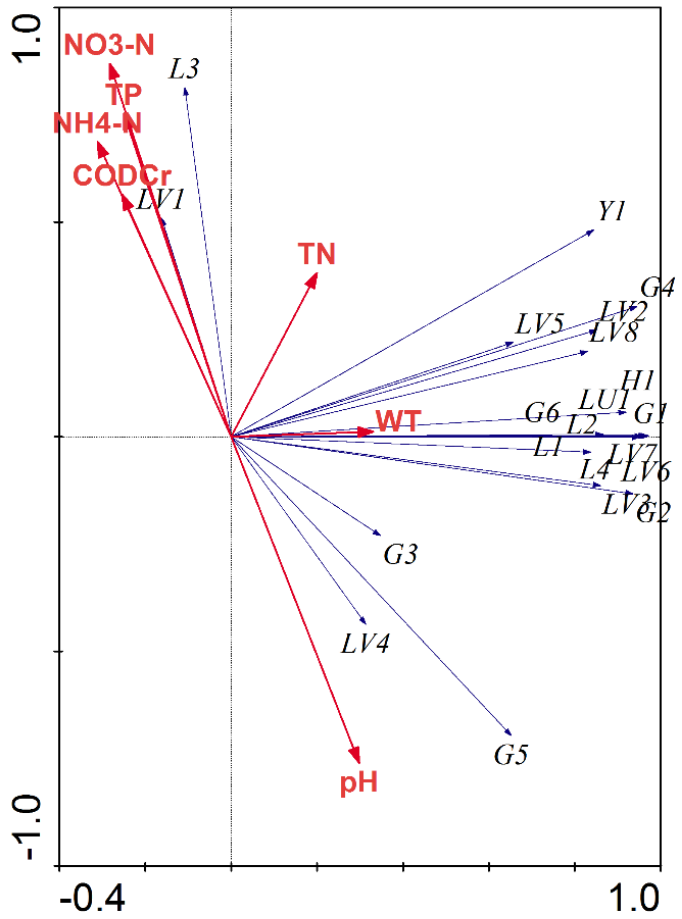

Figure 5. *RDA analysis chart of phytoplankton species and environmental factors. Water temperature (WT), pH,total nitrogen (TN), total phosphorus (TP), ammonia nitrogen (NH_4^+-N) and nitrate nitrogen (NO_3^--N) and Chemical Oxygen Demand (CODcr)*

http://www.aloki.hu ● ISSN 1589 1623 (Print) ● ISSN1785 0037 (Online)
DOI: http://dx.doi.org/10.15666/aeer/1906_43894402

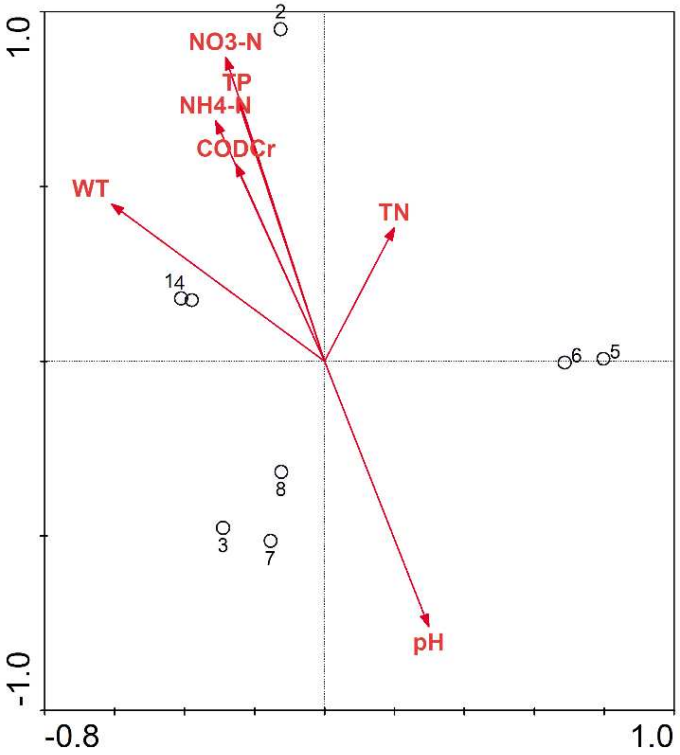

Figure 6. *RDA analysis chart of sampling sites and environmental factors. Water temperature (WT), pH,total nitrogen (TN), total phosphorus (TP), ammonia nitrogen (NH_4^+-N) and nitrate nitrogen (NO_3^--N) and Chemical Oxygen Demand (CODcr).*

Discussion

Variables such as dissolved gases, water temperature, pH, phosphates, nitrates, conductivity among many others including various physical properties (gases and solids solubility) are very important for growth and dispersal of phytoplankton (Mahar et al., 2000; Toma, 2011; Ma et al., 2019). Water temperature which is one of the important variables that influence growth of phytoplankton communities in aquatic system did not differ significantly. Water temperature not only influences the growth and distribution of phytoplankton in aquatic ecosystems, but also influences solubility of gases, water stratification, conductivity and pH (Sharm and Michael, 1987). The measured pH of lake varied between 8.25 to 9.32 during the study period. The values showed that the water of Taihu National Wetland Park was alkaline in nature.

Nutrients, especially phosphorus and nitrogen, are important for healthy growth of phytoplankton in aquatic systems. Plant can absorb nitrogen both as nitrate and ammonia. The concentrations of ammonia nitrogen, total nitrogen and total phosphorus went beyond class IV requirements of Environmental Quality Standards for Surface Water (National standards of the People's Republic of China) (GB3838-2002). The concentration data of total nitrogen and total phosphorus exceeded the limit values of eutrophication indicators proposed by OECD. Spatially, sites 2# and 3# had significant higher values of the nutrients concentration. This could be attributed by the fact that the site was located on a sewage treatment plant. Sites 5# to 8# recorded the lowest concentration values of nutrients probable because they were located within the wetland where the wetland plants and soil acted as filters of the nutrients.

http://www.aloki.hu ● ISSN 1589 1623 (Print) ● ISSN1785 0037 (Online)
DOI: http://dx.doi.org/10.15666/aeer/1906_43894402

In aquatic ecosystem, phytoplankton community structure often changes with the change of environment factors (Ouyangxb and Han, 2007; Li et al., 2014). Diversity indices has often been used to evaluate water pollution and phytoplankton community status. In this study, Shannon Weaver diversity index (*H'*) was used to assess the diversity of phytoplankton spatial and also see whether environmental factors had an impact on the community structure. The study showed that the diversity index ranges from 1.041 to 2.371, with an average of 1.486. Species richness measured in this study ranged from 0.838 to 3.665, with an average of 1.7. Sites 5# and 6# which were light and medium polluted respectively had high diversity and richness values. According to the Intermediate Disturbance Hypothesis (IDH) theory, high diversity occurs at sites experiencing moderate levels of disturbance due to competition hierarchy of species. At low levels of disturbance or pollution, more competitive organisms will push subordinate species to extinction and dominate the ecosystem hence low diversity (Dial and Roughgarden, 1998). Those sites which were located far away from where the sewage treatment plant was had low phytoplankton diversity and richness. This implies that the distribution of phytoplankton species in Taihu National Wetland Park is uneven and the stability of community structure is unstable. Moreover, the fact that *Schizosaccharum tenuiflorum*, filamentous alga bloom and *Scenedesmus giraldii* were dominant implies that this wetland park could be facing serious pollution and also the concentration of organic matter is high (Liang et al., 2019).

The relationships between environmental variables and phytoplankton species were determined in this study. Water temperature (WT) was positively related to the abundance and biomass of the most phytoplankton species. According to Srifa (2010), water temperature is a factor that can positively or negatively affect the growth of some plankton species. Moreover, the rate of photosynthesis of phytoplankton is promoted by the rising water temperature, which accelerates the accumulation of biomass (Gong et al., 2020). The growth rate of phytoplankton is generally low in acidic water and higher in weak alkaline water (You et al., 2007). In this study, the pH value fluctuated from 8.25 to 9.32, which was beyond the pH value range of weak alkaline water, which might likely limit the growth and development of phytoplankton. Moreover, the results of RDA analysis showed that there was a significant negative correlation between pH and *Synedra amphicephala*, *Cyclotella meneghiniana* and *Selenastrum minutum* (Nag). Coll, which was consistent with the above phenomenon.

Nutrient enrichment will stimulate the growth of phytoplankton in relation to its abundance and biomass in various aquatic systems. Phytoplankton in different plant classes have different requirement for nutrition of phosphorus and nitrogen. Nitrogen species such as nitrate, nitrite and ammonia nitrogen, which are equilibrated with each other, can also affect phytoplankton community structure. The results of RDA analysis showed that there was a significant positive correlation between sampling site 2# and NO_3^--N (*Fig. 6*), and the dominant species in this sampling site, *Phormidium allorgei* and *Chlamydomonas globosa*, also showed a significant positive correlation with NO_3^--N and TP. This may be due to the fact that sampling site 2# is located in a sewage treatment plant with serious nitrogen and phosphorus pollution, and its ecological environment is conducive for the growth and development of *Phormidium allorgei* and *Chlamydomonas globosa*, which can be used as indicator species for mesotrophic-eutrophic water. Nutrients such as N and P are important for the growth of phytoplankton, and at particular concentrations can influence the growth of phytoplankton (Elmgren and Larsson, 2001). Sun et al. (2008) note that increase concentrations of N and P at a given range can promote

http://www.aloki.hu ● ISSN 1589 1623 (Print) ● ISSN1785 0037 (Online)
DOI: http://dx.doi.org/10.15666/aeer/1906_43894402

the growth of phytoplankton. This, therefore implies that nutrients factors in the wetland can effectively control the abundance and biomass of phytoplankton species through bottom-up effects.

Conclusion

In this study, a total of 39 species of phytoplankton were detected in Taihu National Wetland Park and Cyanophyta was dominant in some areas. The dominant species of phytoplankton in this survey are *Merismopedia minima* and *Aphanizomenon flosaquae* of Cyanophyta, *Synedra acus* of Bacillariophyta, *Synura.sp.* of Chrysophyta and *Scenedesmus quadricauda* of Chlorophyta. According to the evaluation of water quality based on physical and chemical indexes and phytoplankton diversity indexes, Taihu National Wetland Park is generally moderately to severely polluted, especially near the outlet of sewage treatment plant. Water temperature, nitrogen and phosphorus nutrients, and pH value are the key factors affecting phytoplankton community structure. Therefore, the above-mentioned environmental factors should be considered in the future treatment of water pollution in Taihu National Wetland Park.

Acknowledgements. The authors are grateful to the people that helped with all aspects of the fieldwork. This study was supported by the central government supports the reform and development fund projects of local colleges and universities "Research on integrated technology innovation of sustainable utilization of cold water fish resources industrialization" (2020GSP14), and Key research topics of economic and social development in Heilongjiang Province (20309).

REFERENCES

[1] Cardinale, B. J., Duffy, J. E., Gonzalez, A., Hooper, D. U., Perrings, C., Venail, P., Narwani, A., Mace, G. M., Tilman, D., Wardle, D. A. (2012): Biodiversity loss and its impact on humanity. – Nature 486: 59-67.

[2] Chalar, G. (2009): The use of phytoplankton patterns of diversity for algal bloom management. – Limnologica 39: 200-208.

[3] Chen, N., Wang, Y., Yang, T., Yu, H., Ma, C. (2018): Characteristics of functional group and evaluation of water quality of summer phytoplankton in the Tai Lake. – Journal of Northeast Forestry University 46: 69-73. (in Chinese with English abstract).

[4] Clarke, K. R., Warwick, R. M. (1994): Change in marine communities: an approach to statistical analysis and interpretation. – United Kingdom: Plymouth marine laboratory, Natural environment research council.

[5] Dial, R., Roughgarden, J. (1998): Theory of marine communities: the intermediate disturbance hypothesis. – Ecology 79: 1412-1424.

[6] Elmgren, R., Larsson, U. (2001): Nitrogen and the Baltic Sea: managing nitrogen in relation to phosphorus. – The Scientific World Journal 1: 371-377.

[7] Gong, F., Li, G., Wang, Y., Liu, Q., Huang, F., Yin, K., Gong, J. (2020): Spatial shifts in size structure, phylogenetic diversity, community composition and abundance of small eukaryotic plankton in a coastal upwelling area of the northern South China Sea. – Journal of Plankton Research 42: 650-667.

[8] Hu, H. (2006): The freshwater algae of China: systematics, taxonomy and ecology. – Science Press.

[9] Li, H., Liu, Y., Fan, Y., Guo, C. (2014): Community structure characteristics of phytoplankton in Tongjiang of the Sanjiang Plain Wetland. – Chinese Bulletin of Botany 49: 440. (in Chinese with English abstract).

http://www.aloki.hu ● ISSN 1589 1623 (Print) ● ISSN1785 0037 (Online)
DOI: http://dx.doi.org/10.15666/aeer/1906_43894402

[10] Liang, Y., Zhang, G., Wan, A., Zhao, Z., Wang, S., Liu, Q. (2019): Nutrient-limitation induced diatom-dinoflagellate shift of spring phytoplankton community in an offshore shellfish farming area. – Marine pollution bulletin 141: 1-8.
[11] Lin, Z. (2002): Analysis of Water Environmental Change in Taihu Watershed. – Journal of Lake Science 14: 111-116. (in Chinese with English abstract).
[12] Ma, C., Yu, H. (2013): Phytoplankton community structure in reservoirs of different trophic status, Northeast China. – Chinese journal of oceanology and limnology 31: 471-481.
[13] Ma, C., Chula, M. P., Yu, H., Sun, X., Liang, L., Al-Ghanim, K., Mahboob, S. (2019): Spatial and temporal variation of phytoplankton functional groups in extremely alkaline Dali Nur Lake, North China. – Journal of Freshwater Ecology 34: 91-105.
[14] Ma, C., Zhao, C., Mwagona, P. C., Li, Z., Liu, Z., Dou, H., Zhou, X., Bhadha, J. H. (2021): Bottom-up and top-down effects on phytoplankton functional groups in Hulun Lake, China. – In: Annales de Limnologie-International Journal of Limnology, EDP Sciences, p. 3.
[15] Mahar, M., Baloch, W., Jafri, S. (2000): Diversity and seasonal occurrence of planktonic rotifers in Manchar Lake, Sindh, Pakistan. – Pakistan Journal of Fisheries 1: 25-32.
[16] MEP. (2002): China's national standard: GB3838-2002: Environmental quality standards for surface water. – Ministry of Environmental Protection C.
[17] Mulvenna, V., Dale, K., Priestly, B., Mueller, U., Humpage, A., Shaw, G., Allinson, G., Falconer, I. (2012): Health risk assessment for cyanobacterial toxins in seafood. – International journal of environmental research and public health 9: 807-820.
[18] Oduor, S., Schagerl, M. (2007): Phytoplankton photosynthetic characteristics in three Kenyan Rift Valley saline-alkaline lakes. – Journal of Plankton Research 29: 1041-1050.
[19] Oren, A. (2011): Thermodynamic limits to microbial life at high salt concentrations. – Environmental microbiology 13: 1908-1923.
[20] Ouyangxb, H., Han, B. (2007): Water quality and phytoplankton community in the Qiyeshi Reservoir after water diversion from Dongjiang River. – Journal of Lake Sciences 19: 204-211.
[21] Schagerl, M., Oduor, S. (2008): Phytoplankton community relationship to environmental variables in three Kenyan Rift Valley saline-alkaline lakes. – Marine and Freshwater Research 59: 125-136.
[22] Shannon, C. E., Weiner, W. (1948): A mathematical theory of communication. – Publ. University of Illinois Press, Urbana.
[23] Sharm, B., Michael, R. G. (1987): Review of taxonomic studies on freshwater Cladocera from India with remarks on biogeography. – Hydrobiologia 145: 29-33.
[24] Shi, Y. Q., Sun, S., Zhang, G. T., Wang, S. W., Li, C. L. (2015): Distribution pattern of zooplankton functional groups in the Yellow Sea in June: a possible cause for geographical separation of giant jellyfish species. – Hydrobiologia 754: 43-58.
[25] Srifa, A. (2010): Factors controlling zooplankton dynamics in a subtropical lake during cyanobacterial bloom events. – University of Florida.
[26] Sun, X., Dong, S., Tang, Z. (2008): Influences of nutrients and illuminace on phytoplankton community structure. – South China Fish Sci. 4: 5-13. (in Chinese with English abstract).
[27] Sun, S., Huo, Y., Yang, B. (2010): Zooplankton functional groups on the continental shelf of the yellow sea. – Deep Sea Research Part II: Topical Studies in Oceanography 57: 1006-1016.
[28] Sun, X., Mwagona, P. C., Shabani, I. E., Hou, W., Li, X., Zhao, F., Chen, Q., Zhao, Y., Liu, D., Li, X. (2019): Phytoplankton functional groups response to environmental parameters in Muling River basin of northeast China. – In: Annales de Limnologie-International Journal of Limnology. EDP Sciences, p. 17.
[29] Toma, J. J. (2011): Physical and chemical properties and algal composition of Derbendikhan lake, Sulaimania, Iraq. – Current World Environment 6: 17-27.

http://www.aloki.hu ● ISSN 1589 1623 (Print) ● ISSN1785 0037 (Online)
DOI: http://dx.doi.org/10.15666/aeer/1906_43894402

[30] Weyhenmeyer, G. A., Peter, H., Willén, E. (2013): Shifts in phytoplankton species richness and biomass along a latitudinal gradient–consequences for relationships between biodiversity and ecosystem functioning. – Freshwater Biology 58: 612-623.
[31] Yang, M., Bi, Y., Hu, J., Zhu, K., Zhou, G., Hu, Z. (2011): Seasonal variation in functional phytoplankton groups in Xiangxi Bay, Three Gorges Reservoir Chinese. – Journal of Oceanology and Limnology 29: 1057-1064.
[32] You, L., Cui, L., Liu, Z., Yang, B., Huang, Z. (2007): Correlation analysis of parameters in algal growth. – Environmental Science & Technology 30: 42-44.

http://www.aloki.hu ● ISSN 1589 1623 (Print) ● ISSN1785 0037 (Online)
DOI: http://dx.doi.org/10.15666/aeer/1906_43894402

APPENDIX

Appendix 1. *List of phytoplankton in Taihu National Wetland Park*

Phylum	**Family**	**Genus**	**Species**
Cyanophyta	Merismopediaceae	*Merismopedia*	*Merismopedia minima*
			Merismopedia marssonii
	Phormidioideae	*Phormidium*	*Phormidium allorgei*
	Nostocaceae	*Aphanizomenon*	*Aphanizomenon flosaquae*
Bacillariophyta	Fragilariaceae	*Fragilaria*	*Fragilaria brevistriata*
		Synedra	*Synedra acus*
			Synedra amphicephala
			Synedra ulna
	Coscinodiscaceae	*Diatoma*	*Diatoma vulgare*
		Melosira	*Melosira granulata*
		Cyclotella	*Cyclotella meneghiniana*
	Naviculaceae	*Navicula*	*Navicula exigua*
			Navicula dicephala
	Gomphonemaceae	*Gomphonema*	*Gomphonema constrictum*
	Cymbellaceae	*Cymbella*	*Cymbella ventricosa*
Euglenophyta	Euglenaceae	*Euglena*	*Euglena oxyuris*
		Strombomonas	*Strombomonas schauinslandii*
Cyanophyta	Chlamydomonadaceae	*Chlamydomonas*	*Chlamydomonas globosa*
	Chlorellaceae	*Ankistrodesmus*	*Ankistrodesmus angustus*
			Ankistrodesmus acicularis
			Ankistrodesmus falcatus
		Chodatella	*Chodatella quadriseta*
		Selenastrum	*Selenastrum gracile*
			Selenastrum minutum (Nag). coll
		Kirchneriella	*Kirchneriella lunaris*
	Scenedesmaceae	*Scenedesmus*	*Scenedesmus bijuga*
			Scenedesmus dimorphus
			Scenedesmus quadricauda
			Scenedesmus platydiscus
		Coelastrum	*Coelastrum microporum*
		Crucigenia	*Crucigenia quadrata*
			Crucigenia tetrapedia
	Volvocaceae	*Pandorina*	*Pandorina morum*
	Pediastraceae	*Pediastrum*	*Pediastrum birtadiatum*
			Pediastrum tetras
	Dictyosphaeraceae	*Dictyosphaerium*	*Dictyosphaerium pulchellum*
	Desmidiaceae	*Cosmarium*	*Cosmarium obtusatum*
Chrysophyta	Synuraceae	*Synura*	*Synura.sp*
Cryptophyta	Cryptomonadaceae	*Cryptomonas*	*Cryptomonas ovata*

http://www.aloki.hu ● ISSN 1589 1623 (Print) ● ISSN1785 0037 (Online)
DOI: http://dx.doi.org/10.15666/aeer/1906_43894402

SIGNIFICANCE OF INTRA ANNUAL FLUCTUATIONS IN SOME SELECTED CONIFERS FROM A DRY TEMPERATE AREA (KALAM FOREST DIVISION), KHYBER PAKHTUNKHWA, PAKISTAN: A DENDROCHRONOLOGICAL ASSESSMENT

MUHAMMAD, S.* – TAYYAB, M. – AKRAM, N. – MALIK, S. M. – AWAN, U. F. – KHAN, Z. – HASNAIN, M. – ZAHID, M. – RASOOL, K. – KHAIRDIN, A.

Dendrochronology Lab., Department of Botany, Government College University, Lahore 54000, Pakistan

**Corresponding author*
e-mail: dr.sohaibmuhammad@gcu.edu.pk

(Received 28th Apr 2021; accepted 20th Aug 2021)

Abstract. Dendrochronological potential of some gymnosperms was determined by dividing a study site into 9 stands. 76 samples of *Abies pindrow* with maximum age of 698 years having 149.3 cm diameter, 23 samples of *Taxus baccata* with maximum age of 479 years having 137.2 cm diameter, 4 samples of *Pinus roxburghii* with maximum age of 218 years having 19.2 inches diameter and 2 samples of *Cedrus deodara* were obtained. All species were crossdated successfully by Skeleton Plot Model. Among them, mean growth of *A. pindrow* was 0.05-0.27 cm per year while for *T. baccata* it was 0.15-0.24 cm per year. Moreover, regression analysis between age and dbh was ($y = 0.0847x + 4.0756$), ($R^2 = 0.921$) in 3rd stand and ($y = 11.108x-41.174$), ($R^2 = 0.8424$) in 2nd stand of *A. pindrow* and *T. baccata* respectively. The maximum value observed was in the 3rd stand of *T. baccata* species which showed better correlation as compared to the rest of the stands. Strong correlation was also observed between TRW and difference of earlywood and latewood cell mass in all species. *A. pindrow* showed maximum value as ($y = 1.1397x + 0.1873$), ($R^2 = 0.9972$).
Keywords: *skeleton plot, Abies pindrow, Cedrus deodara, Pinus roxburghii, Taxus baccata*

Introduction

Dendrochronology, "the study of tree time," is a multidisciplinary science that dates annual tree rings to their exact year formation to investigate prehistorical, historical and modern events (Palmer et al., 2011; Cook and Kairiukstis, 2010). It is applied in various subfields like climatology, ecology, forestry, fire history, geology, hydrology, volcanology and many other disciplines (Nash, 2002). Trees are intimately bound to environment as they record natural (temperature and precipitation) or unnatural (human induced) events or processes which can be seen in varying patterns of tree ring widths (Ali et al., 2021). Year to year climate variation induces variability in volume of wood that the tree produces in most geographic regions. When environmental conditions become favorable, trees respond by creating large volume of wood and produce less volume of wood in other years when conditions are unfavorable for growth (Sun et al., 2016; Panyushkina, 2011). Coniferous forests are important natural resources to sustain life in tropical, subtropical and temperate regions throughout the globe as they have economic and ecological importance. Among them, Kalam Forest Division (dry temperate area) is also geographically vulnerable to climate change due to environmental and some anthropogenic activities. The study was conducted in Kalam Forest division with objective to determine dendrochronological potential (age and

http://www.aloki.hu ● ISSN 1589 1623 (Print) ● ISSN 1785 0037 (Online)
DOI: http://dx.doi.org/10.15666/aeer/1906_44034419

growth rate studies) and to develop tree ring chronologies of conifers by SPM (Skeleton Plot Model) Method (Speer, 2010) (*Fig. 1*).

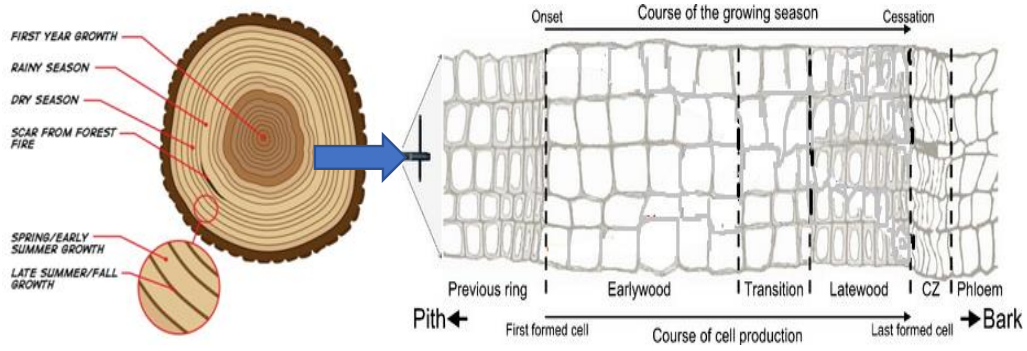

Figure 1. *Annual ring fluctuations (earlywood and latewood) and anthropogenic behavior*

Chronology development by skeleton plot model

Skeleton Plot Model is one of most appropriate and extensively used method by dendrochronologists to crossdate the tree samples which is the "procedure of matching ring width variations." Skeleton Plot, "Plot of vertical bars in which bar length is inversely related to tree ring width, is used to identify the double or false rings which occurs if seasonal growth is interrupted by severe climatic conditions, diseases or other agents and is later resumed a second growth layer, visible and added in during one growth season (Copenheaver et al., 2006). Such additional layer is false ring, which is simply a band of latewood cells between latewood part of previous ring and early wood part of next ring (Nash, 2002). As temperate trees (conifers) develop rings yearly so, patterns of tree ring widths are matched and compared in similar and dissimilar geologic regions (Vasconcellos et al., 2019; Speer, 2010).

Pakistan is more vulnerable to climate change due to environmental factors changing forest types (Bajwa et al., 2015) inducing health problems (Gosling et al., 2009), as well as reducing the oxygen levels in the sea (Shaffer et al., 2009). These changes are not uniform throughout globe and vary with change in regional temperature and precipitation so, dendrochronology helps to examine the past climate as well as to predict future climate by annual rings of trees (Shah et al., 2019). Many researchers have been engaged and are working in above mentioned areas. Muhammad et al. (2021) determined age and growth rate of pines. Ahmed and Naqvi (2005), Khan et al. (2008), Ahmed et al. (2009) determined dendrochronological potential of some gymnosperms from Swat, Dir, Chitral, Mansehra and Azad Kashmir, Pakistan. Khan (2011) determined dendrochronological potential of *C. deodara* and *Pinus gerardiana*. Wahab (2011) also estimated age and growth rates of conifers from Dir, Pakistan. Khan et al. (2013) developed tree ring chronologies and used in forest management, past climate investigation, wildfire and other hydrological aspects. The objectives of study were: (1) to estimate age and growth rate of selected conifers (*A. pindrow*, *T. baccata*, *P. roxburghii* and *C. deodara*); (2) to determine relationships, if any, between diameter/age, diameter/growth rate and between seasonal parts of annual rings of trees; (3) to determine correlation between different parameters to model meaningful relationships in form of regression analysis; (4) to develop Skeleton Plot Model of all

http://www.aloki.hu ● ISSN 1589 1623 (Print) ● ISSN 1785 0037 (Online)
DOI: http://dx.doi.org/10.15666/aeer/1906_44034419

samples, composite skeleton plot of climatically sensitive trees and their matching with master skeleton plots and raising their master chronologies.

Study site

Kalam Forest Division is geographically known as Swat Kohistan (*Fig. 2*), an independent Forest Division from last 5 decades as it was a part of Swat Forest Division in previous times. It consists of two tehsils known as Kalam and Behrain and covers an area about 3182.9272 km^2. The site is climatically very sensitive as it lies in dry temperate zone, too much cold at high elevations causes migration of people to bottom of valley to fulfil their needs and survival. Here temperature and precipitation varies with altitude and appears in form of rain and snow. Rain falls from December to May as its average record is 492 mm and annual record is 423.56 cm (Iqbal, 2014).

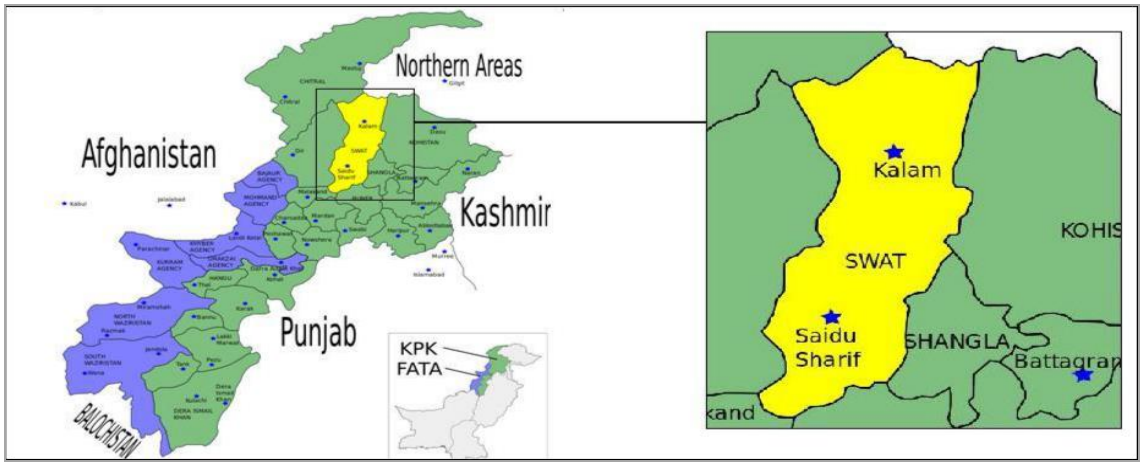

Figure 2. *Divisional boundaries of Kalam Forest Division*

Materials and methods

Sample collection, processing and measurement

Four conifer species were targeted for sample collection namely *A. pindrow, T. baccata*, *P. roxburghii* and *C. deodara* (*Fig. 3*). Subjective sampling was performed in the field and those individual trees were selected that were present on high and low elevation sites, steep slopes and well drained soils because they could possess the tree rings significantly sensitive to regional climate and cross dating could be performed successfully (Ahmed, 2014). Cores were obtained from healthy, rigid and unbranched trees by Swedish increment borers at height as 1.3 m or 4.3 ft. A total of 105 cores were obtained from 51 different trees in 2019. The cores were preserved in plastic straws to maintain alignment of cores. The ends of straws were covered with paper tape and holes created in trees were refilled by wax to protect them from any fungal or pathogen disease (Wahab et al., 2008). The diameter at breast height (dbh) of each tree was measured by dbh measuring tape (Hart and Grissino-Mayer, 2008). Later on, cores were mounted on wooden frames with glue and were allowed to dry. Sander machine fitted with different grades of sand papers (80, 100, 120, 150, 180, 320 and 400 grit, depending upon particular species) was used to make smooth and fine surface of cores. It was proceeded until suitable polished surface was achieved after varnish coat (Phipps,

http://www.aloki.hu ● ISSN 1589 1623 (Print) ● ISSN 1785 0037 (Online)
DOI: http://dx.doi.org/10.15666/aeer/1906_44034419

1985). Velmex measuring system (TA4021H1) having connection with computer installed with J2X software was used. All samples were measured one by one with respect to earlywood, latewood and total ring width (Volney and Mallet, 1992; Yamaguchi, 1991). All samples were crossdated successfully by skeleton plot method and further statistical analysis was performed.

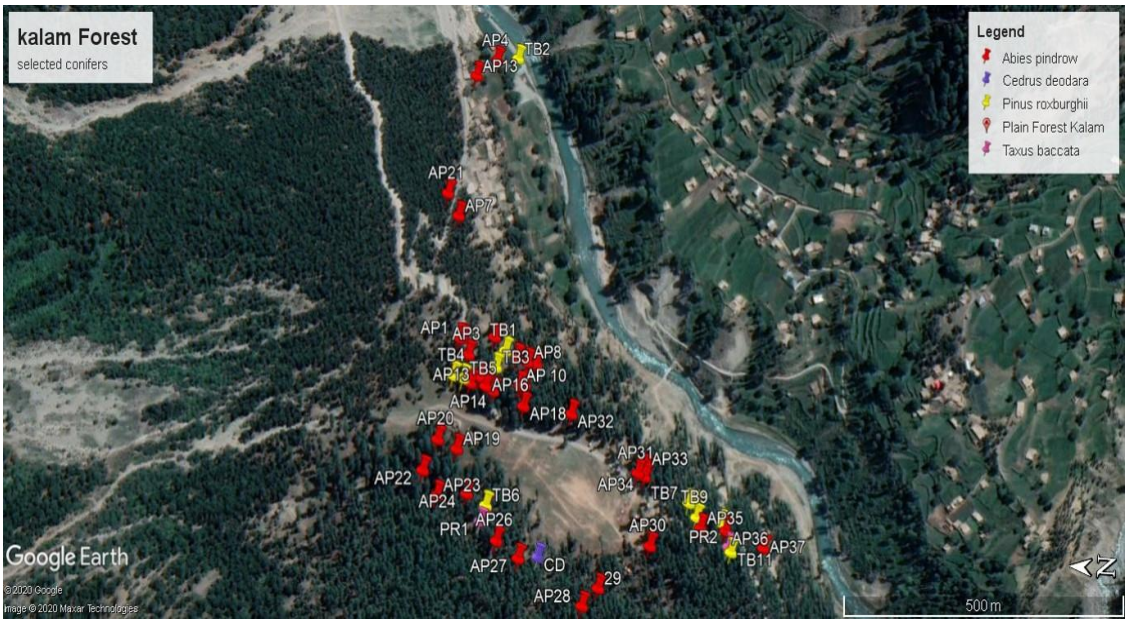

Figure 3. *GPS points of selected conifers location in Kalam Forest Division KP, Pakistan*

Results

Dendrochronological potential of above-mentioned species was determined by dividing study site into different stands and their relationships were determined by different parameters.

Age and growth rate determination

Age of all trees was estimated from nine stands of study site as shown in *Table 1*. The oldest tree was *A. pindrow* with 698 years age and 149.3 cm diameter. The youngest tree was 63 years of age with 73.15 cm diameter. An age of 479 years with 137.2 cm diameter was recorded in *T. baccata* as maximum age in this particular species while youngest was 113 years old having 45.72 cm diameter. In case of *P. roxburghii*, the maximum and minimum age was estimated as 218 years and 68 years with 48.76 cm, 67.05 cm diameter respectively. *C. deodara* was found to be minimal as regional climate and other topographic features of site were found to be unfavorable for this particular species.

Growth rate of all trees was also determined from this dry temperate area as shown in respective table. The maximum and minimum growth rate of *A. pindrow* was 0.48 cm/year and 0.05 cm/year. It was maximum as 0.06 cm/year in case of *T. baccata* while minimum was 0.12 cm/year. *P. roxburghii* also showed maximum and minimum growth rate as 0.15 cm/year and 0.10 cm/year respectively. Overall, *T. baccata* was found to be denser in study site and its growth rate was also recorded as maximum as 0.66 cm/year.

http://www.aloki.hu ● ISSN 1589 1623 (Print) ● ISSN 1785 0037 (Online)
DOI: http://dx.doi.org/10.15666/aeer/1906_44034419

Table 1. *Age and growth rate studies of conifers*

Species	Earlywood (mm)		Latewood (mm)		Age (years)		Mean growth (mm)		Growth rate (cm/year)	
	Max.	Min.	Max.	Min.	Max.	Min.	Max.	Min.	Max.	Min.
A. pindrow	4.7	0.55	0.53	0.13	698	63	0.16	0.02	0.48	0.05
T. baccata	6.5	1.22	0.71	0.14	479	113	0.24	0.06	0.66	0.12
P. roxburghii	1.45	1	0.24	0.14	218	68	0.05	0.04	0.15	0.10

Seasonal dynamics

Tree ring width (TRW) and its parts (earlywood and latewood) were also measured (*Fig. 1*). The maximum TRW measurement was 4.86 mm and 0.69 mm as minimum in case of *A. pindrow*. The early and latewood part was 4.70 mm, 0.53 mm and 0.53 mm, 0.13 mm respectively. In case of *T. baccata,* TRW was 6.64 mm and 1.37 mm as maximum and minimum. The early and latewood part was 6.5 mm, 1.2 mm and 0.71 mm, 0.41 mm respectively *P. roxburghii* showed TRW value as 1.66 mm and 1.11 mm and early latewood parts were 1.45 mm, 1.00 mm and 0.24 mm, 0.14 mm wide respectively.

Correlations between dbh/age, dbh/growth rate, TRW and difference of earlywood, latewood cell mass

Correlations of all species were determined (*Table 2*). Diameter at breast height (dbh) of *A. pindrow* showed positive significant correlation with age (*Fig. 4a*) while it was positive/negative correlated with growth rate (*Fig. 4b*). *T. baccata* showed positive correlation between dbh and age (*Fig. 5a*) and negative between dbh and growth rate (*Fig. 5b*) and it was found to be highly negative in *P. roxburghii* trees (*Fig. 6a, b*). Moreover, the correlation was also observed between tree ring width and difference of early, latewood cell mass. It was observed highly positive in all selected species gymnosperms (*Figs. 4c, 5c, 6c*). The maximum value was observed in 5th stand of *A. pindrow* (*Fig. 4c*).

Table 2. *Correlation and regression analysis between dbh/age, dbh/growth rate and TRW/early & latewood cell mass*

Species	Parameter	Correlation (R^2)	Regression
A. pindrow	Dbh/age	0.921	y = 0.0847x + 4.0756
	Dbh/growth rate	0.4126	y = -339.62x + 84.091
	TRW/Difference of earlywood and latewood cell mass	0.9972	y = 1.1397x + 0.1873
T. baccata	Dbh/age	0.8424	y = 11.108x-41.174
	Dbh/growth rate	0.4055	y = -134.69x + 55.873
	TRW/Difference of earlywood and latewood cell mass	0.9646	y = 0.9417x + 0.8654
P. roxburghii	Dbh/age	0.6296	y = -11.806x + 414.67
	Dbh/growth rate	0.0909	y = -130.91x + 29.018
	TRW/Difference of earlywood and latewood cell mass	0.8943	y = 1.1081x + 0.285

http://www.aloki.hu ● ISSN 1589 1623 (Print) ● ISSN 1785 0037 (Online)
DOI: http://dx.doi.org/10.15666/aeer/1906_44034419

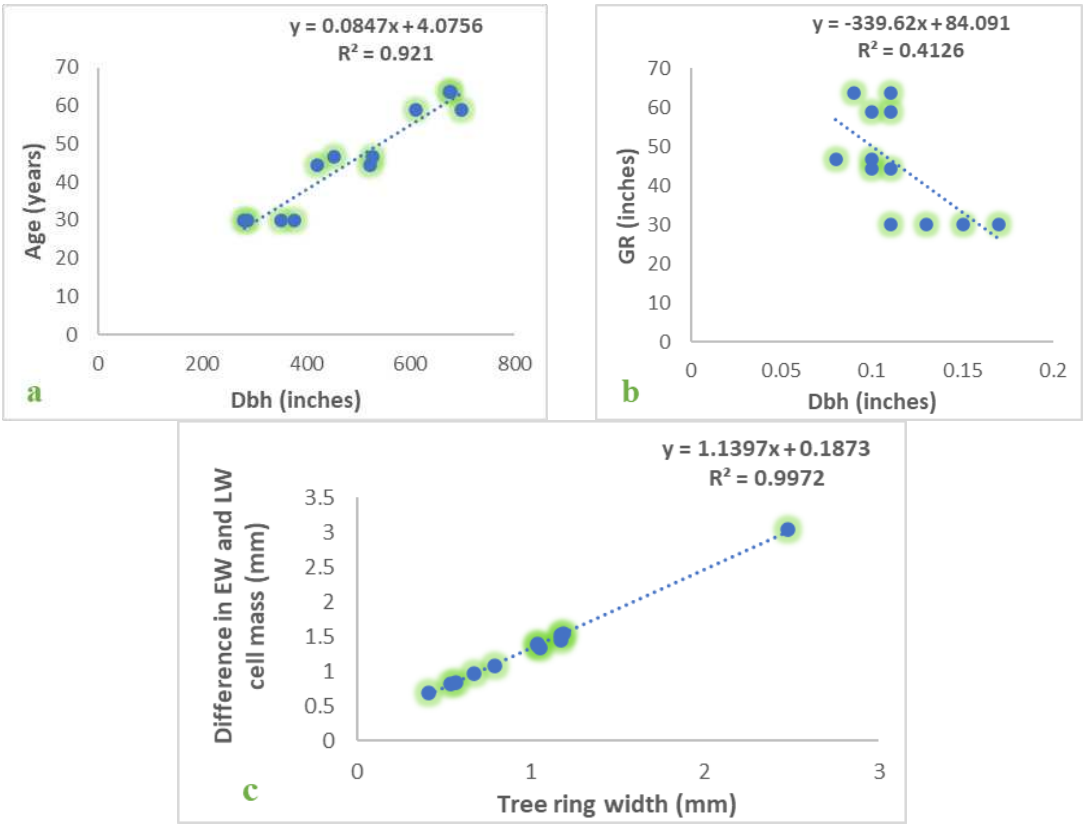

Figure 4. *Correlation studies of A. pindrow*

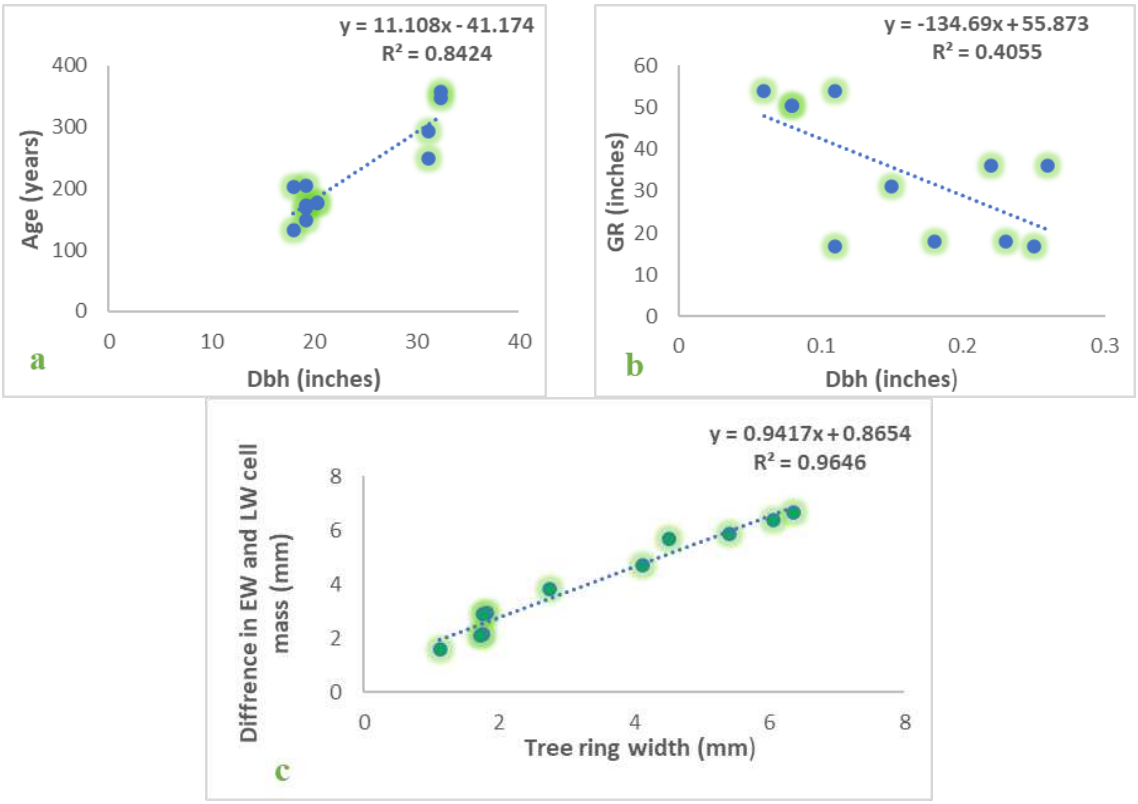

Figure 5. *Correlation studies of T. baccata*

http://www.aloki.hu ● ISSN 1589 1623 (Print) ● ISSN 1785 0037 (Online)
DOI: http://dx.doi.org/10.15666/aeer/1906_44034419

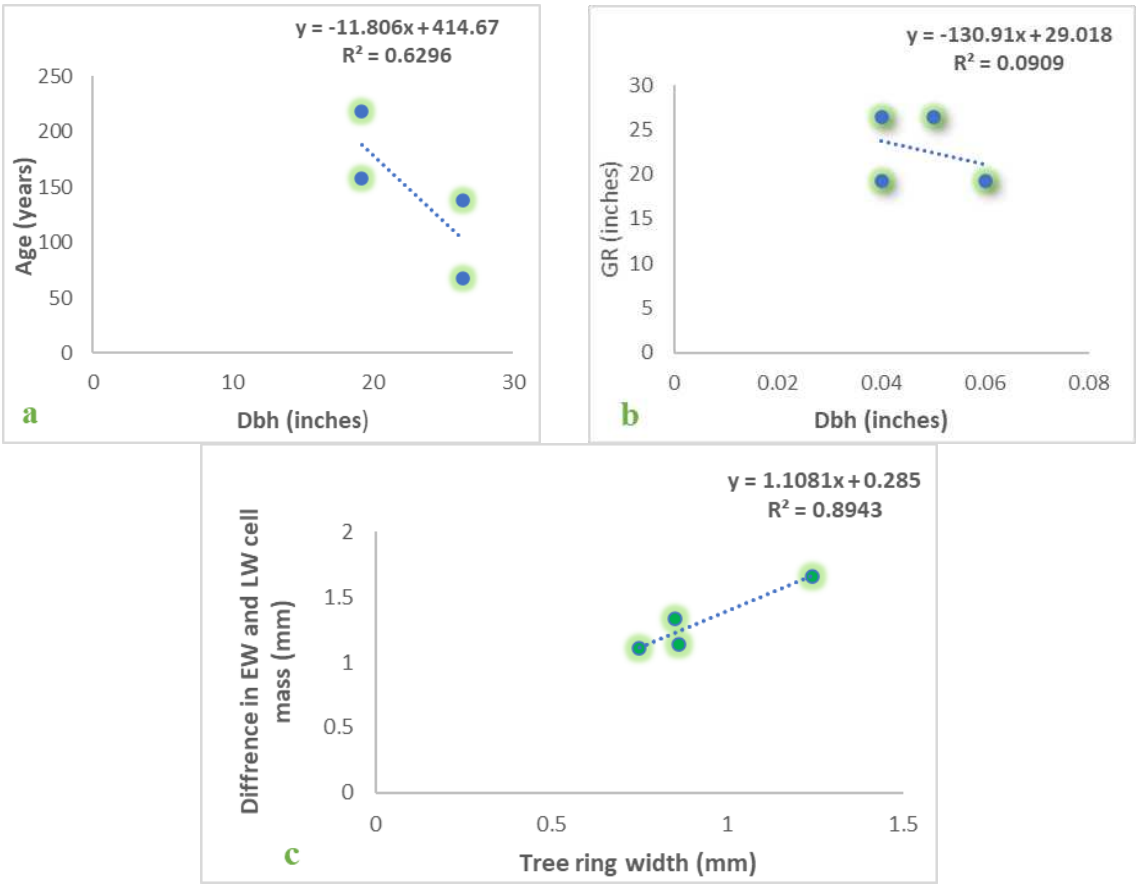

Figure 6. *Correlation studies of P. roxburghii*

Skeleton plot model

The fundamental principle of dendrochronology is crossdating which is simply crossmatching of tree ring width patterns among the species of similar and dissimilar geologic regions. It was applied to all trees either they showed complacent or sensitive growth patterns (*Table 3*). It was best represented by sensitive trees (*Fig. 7*) as they produced rings yearly or seasonally and responded well to climate fluctuations by creating larger and smaller rings while complacent trees produced rings of similar widths, as their growth was not affected by seasonal climate fluctuations. The samples showed sensitivity as they obtained from high and low elevation sites, steep slopes and well drained soils while others showed complacent nature as they were obtained from poor drained soils and near bank of river (Swat River, Pakistan).

Table 3. *Tree ring matching patterns (chronology development) between samples of same trees through ***SPM method*

Sample codes	Tree life span	Matching pattern		No. of matched years	GPS coordinates
		Narrow ring years	Wide ring years		
A. pindrow					
AP1 and AP1'	1929-2019AD	1998, 1999	----	2	N:35.51123 E:72.60368
AP2 and AP2'	1888-2019AD	1905-1927, 1933-1945, 1947-1974, 1995-1998, 2010-2019	----	78	N:35.51118 E:72.60368

http://www.aloki.hu ● ISSN 1589 1623 (Print) ● ISSN 1785 0037 (Online)
DOI: http://dx.doi.org/10.15666/aeer/1906_44034419

AP3 and AP3'	1926-2019AD	1967, 1978, 1984, 1985, 1991-1993, 2000, 2010, 2011	----	10	N:35.51107 E:72.60342
AP4 and AP4'	1926-2019AD	1967, 1968, 1982, 1983, 1992, 2001-2003, 2013, 2018, 2019	----	11	N:35.51095 E:72.60850
AP7 and AP7'	1933-2019AD	1946, 1964, 1996, 1997, 2009, 2010	1977-1986	16	N:35.51068 E:72.60374
AP11 and AP11'	1817-2019AD	1931-1934, 1985-1989, 1994, 2018, 2019	----	12	N:35.51031 E:72.60343
AP12 and AP12'	1897-2019AD	1936-1938, 1981-1983, 1989, 2001-2003, 2005-2008, 2010-2019	----	24	N:35.51080 E:72.60860
AP13 and AP13'	1819-2019AD	1944, 1953-1961, 2015, 2018, 2019	----	13	N:35.51014 E:72.60337
AP14 and AP14'	1846-2019AD	1903, 1904, 1937, 1938, 1943-1946, 1951-1974, 2007-2014, 2019	1900, 1901, 1983-1993, 1998-2003	59	N:35.51000 E:72.60334
AP15 and AP15'	1830-2019AD	1915-1924, 1936-1945, 1968-1973, 1995-1997	1948, 2005-2007	33	N:35.51024 E:72.60297
AP16 and AP16'	1857-2019AD	1879-1882, 1889, 1900, 1907-1912, 1958-1965, 1973-1987, 1990-1993	1946, 1947, 2005-2009	46	N:35.51020 E:72.60298
AP17 and AP17'	1879-2019AD	1926-1945, 1973-1977, 1979-1985, 1999, 2000, 2011-2019	----	43	N:35.51016 E:72.60300
AP18 and AP18'	1930-2019AD	1983, 1984, 1986, 1989-1991, 2001-2005, 2018, 2019	1982, 1995-1999	19	N:35.51127 E:72.60818
AP21 and AP21'	1922-2019AD	1959-1963, 1975-1977, 1982, 1983, 1998-2001, 2010-2012, 2016-2019	----	21	N:35.51101 E:72.60296
AP22 and AP22'	1942-2019AD	1983, 1998-2000, 2016-2019	----	8	N:35.51086 E:72.60307
AP23 and AP23'	1897-2019AD	1940-1947, 1952-1954, 1982, 1983, 1987-1989, 2001-2019	----	35	N:35.51077 E:72.60293
AP24 and AP24'	1910-2019AD	1948, 1949, 1975, 1980, 1998, 2018, 2019	----	7	N:35.51065 E:72.60280
AP25 and AP25'	1900-2019AD	1940, 1947, 1984, 1967-1973, 1999, 2011, 2018, 2019	----	14	N:35.51016 E:72.60265
AP26 and AP26'	1859-2019AD	1926-1931, 1933, 1938-1942, 1944-1947, 1949, 2001, 2009-2015, 2018, 2019	1911-1924	41	N:35.51115 E:72.60189
AP27 and AP27'	1929-2019AD	2001	----	1	N:35.51145 E:72.80202
AP28 and AP28'	1859-2019AD	1904, 1970, 1975, 1981-1986, 1996, 2002-2007, 2010-2019	1936, 1937, 1998-2001	32	N:35.51158 E:72.80608
AP29 and AP29'	1879-2019AD	1975, 1976, 2012-2019	----	10	N:35.51164 E:72.60152
AP30 and AP30'	1801-2019AD	1820-1828, 1857-1865, 1872-1876, 1929-1931, 1945-1951, 1960, 1961, 1964-1966, 1996-1999, 2002-2005, 2009-2019	1897-1903, 1936, 1910-1914	70	N:35.51140 E:72.60114
AP31 and AP31'	1872-2019AD	1911, 1915, 1916, 1943-1953, 1959-1999	2005-2014	65	N:35.51095 E:72.60119
AP32 and AP32'	1679-2019AD	1729-1755	1760-1767, 1783-1835, 1837-2019	271	N:35.51064 E:72.60100
AP35 and AP35'	1775-2019AD	1838-1840, 1844-1852, 1856-1870, 1881-1900, 1906-1910, 1913-1956, 1958, 1961, 1962, 1965, 1973, 1974, 1976-1978, 1981-1992, 1996-2004, 2018, 2019		128	N:35.51045 E:72.60047
AP36 and AP36'	1806-2019AD	1977-2004, 2007, 1881-1890, 1898-1951, 1969-1974, 2018, 2019	1953-1967	115	N:35.51010 E:72.60021
AP38 and AP38'	1834-2019AD	1907-1913, 1915, 1927-1930, 1932-1945, 1948-1953, 1964, 1965, 1974-1977, 2002-2019	----	56	N:35.50907 E:72.59952
AP39 and AP39'	1802-2019AD	1930-1950, 1983-2019, 1964-1973	1908-1918	89	N:35.50883 E:72.59981

http://www.aloki.hu ● ISSN 1589 1623 (Print) ● ISSN 1785 0037 (Online)
DOI: http://dx.doi.org/10.15666/aeer/1906_44034419

AP40 and AP40'	1815-2019AD	1977, 1980-1982, 2012, 2013	1977	7	N:35.50805 E:72.80054
AP41 and AP41'	1833-2019AD	1946-1950, 1960, 1975, 1976, 1984-1989, 1987, 1993-2000, 2012-2014	----	26	N:35.50829 E:72.60169
AP42 and AP42'	1898-2019AD	1934-1939	----	6	N:35.50940 E:72.60258
AP43 and AP43'	1944-2019AD	1992-1999	----	8	N:35.50817 E:72.60177
AP44 and AP44'	1903-2019AD	1925-1949, 1956-1962, 1977-2005	1976	62	N:35.50818 E:72.60164
AP48 and AP48'	1891-2019AD	1988-1994, 2008-2019	----	19	N:35.50685 E:72.60086
AP50 and AP50'	1876-2019AD	2019-1990, 1933, 1932	----	32	N:35.50980 E:72.60096
T. baccata					
TB5	1953-2019AD	----	----	---	N:35.51085 E:72.60382
TB6 and TB6'	1918-2019AD	1978, 1979	----	2	N:35.51063 E:72.60875
TB8 and TB8'	1985-2019 AD	----	2016-2013, 2009, 2001, 2000, 1999, 1998	9	N:35.51050 E:72.60353
TB9 and TB9'	1950-2019AD	2018, 2019	----	2	N:35.51061 E:72.60857
TB10 and TB10'	1932-2019AD	1960, 1961, 1963, 1964, 2018, 2019	1954, 1992, 1993	9	N:35.51063 E:72.60325
TB19 and TB19'	1966-2019AD	1998-2000, 2018, 2019	1993	6	N:35.51128 E:72.60306
TB20 and TB20'	1953-2019AD	1997, 2018, 2019	----	3	N:35.51113 E:72.60306
TB33 and TB33'	1903-2019AD	2019-1996, 1998, 1987	----	24	N:35.51113 E:72.60303
TB45 and TB45'	1894-2019AD	1951, 1971-1982, 1989-1995, 2008-2011, 2016-2019	----	28	N:35.51065 E:72.60102
TB46 and TB46'	1899-2019AD	1972, 1973, 1979, 1980, 1996-2000	2006-2008	12	N:35.51065 E:72.60102
TB47 and TB47'	1859-2019AD	1904-1909, 1932-1934, 1960-1966	1998-2019	38	N:35.50746 E:72.60127
TB49 and TB49'	1874-2019AD	1938-1940, 1956, 1992, 1993, 1997, 1998, 2004-2008, 2010-2019	1970	24	N:35.50734 E:72.60123
P. roxburghii					
PR34 and PR34'	1814-2019AD	1827, 1828, 1918-1923, 1929, 1932-1939, 1940, 1942, 1943, 1992, 1993, 1998-2000, 2007, 2008, 2018, 2019	1887-1906	49	N:35.51072 E:72.60047
PR51 and PR51'	1877-2019AD	1985-1988, 2004-2019	1995-1998	24	N:35.50680 E:72.60061
C. deodara					
CD37and CD37'	1783-2019AD	1860-1864, 1905, 1932-1936, 1945-1947, 1949, 1951-1954, 1959-1960, 1970-1988, 1998-2010, 2013-2019	----	60	N:35.50980 E:72.60024

After crossdating all the core samples, composite skeleton plots of the most sensitive trees were made between two cores of each individual tree which highlighted the most sensitive years of growth. These plots were matched with the master skeleton plot and master chronology was developed as shown in *Figure 7a-h*.

Composite skeleton plots, master skeleton plots and master chronologies of sensitive trees were presented in *Figure 7*.

http://www.aloki.hu ● ISSN 1589 1623 (Print) ● ISSN 1785 0037 (Online)
DOI: http://dx.doi.org/10.15666/aeer/1906_44034419

AP1 & AP3 (1931-2019 AD)

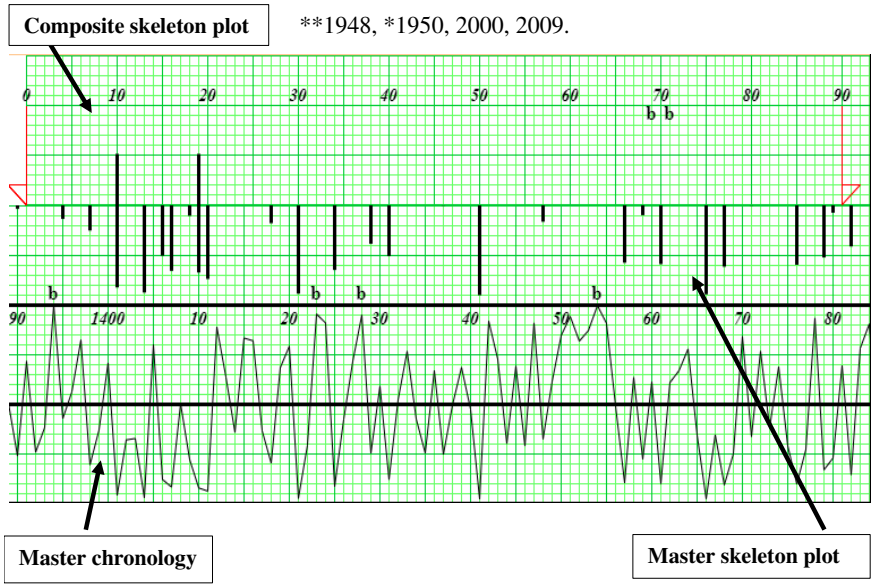

a

AP4 & AP7 (1928-2019 AD)

*1934-1937, *1940, 1948, 2010, 2009

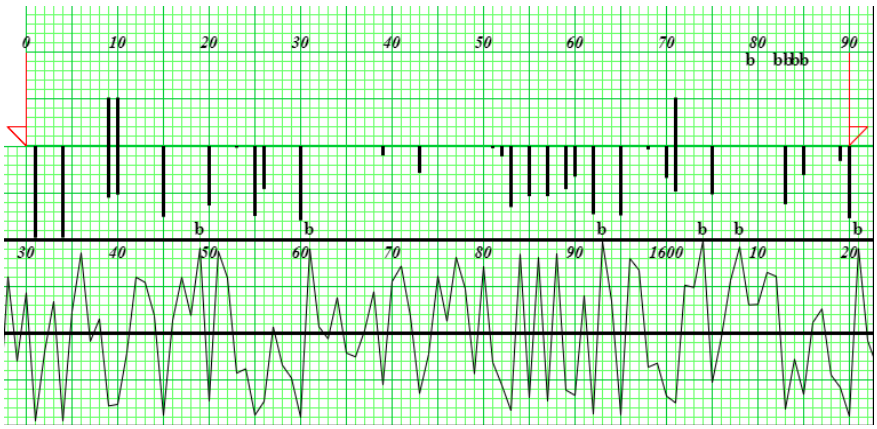

b

AP12 & AP13' (1897-2019 AD)

1957-1961, 1976, 1978, 1983, 1987, 1988, 2015, 2018.

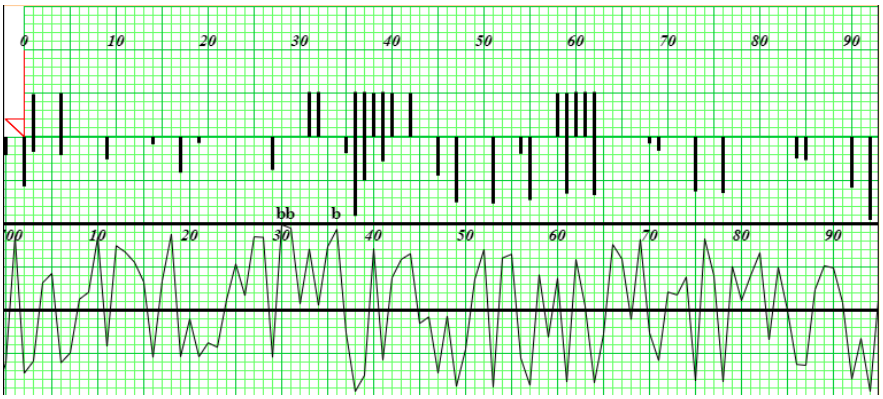

c

http://www.aloki.hu ● ISSN 1589 1623 (Print) ● ISSN 1785 0037 (Online)
DOI: http://dx.doi.org/10.15666/aeer/1906_44034419

AP15 &AP18' (1887-2019 AD)

*1956, 1979-1981, 2000-2003.

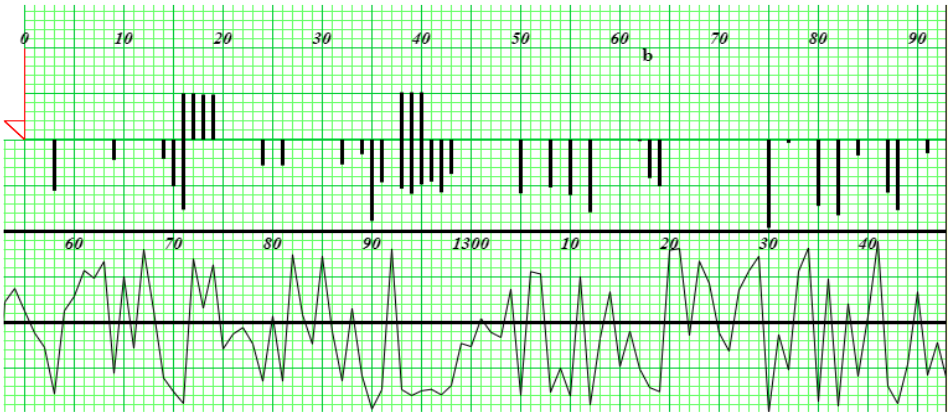

d

AP22 & AP24 (1911-2019 AD)

*(1958, 1959, 1961), 1975, 1983, 1998, 2017, 2018.

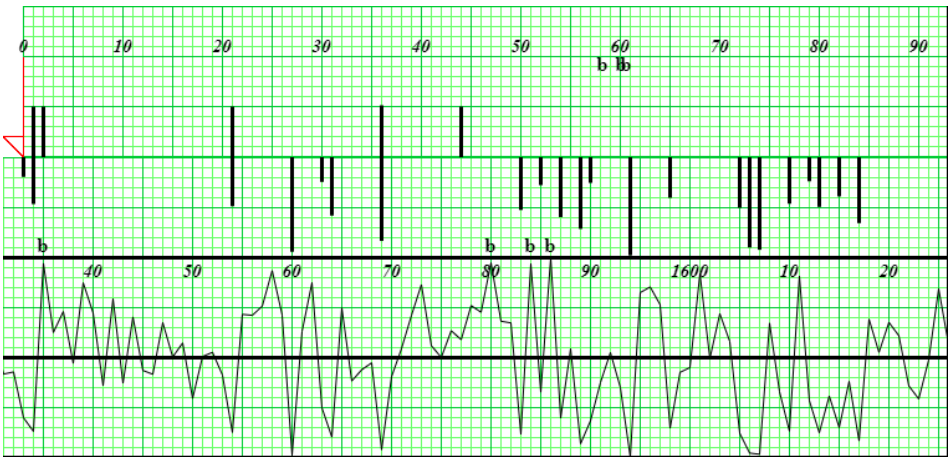

e

AP27 & AP42' (1898-2019 AD)

*1967, 2001.

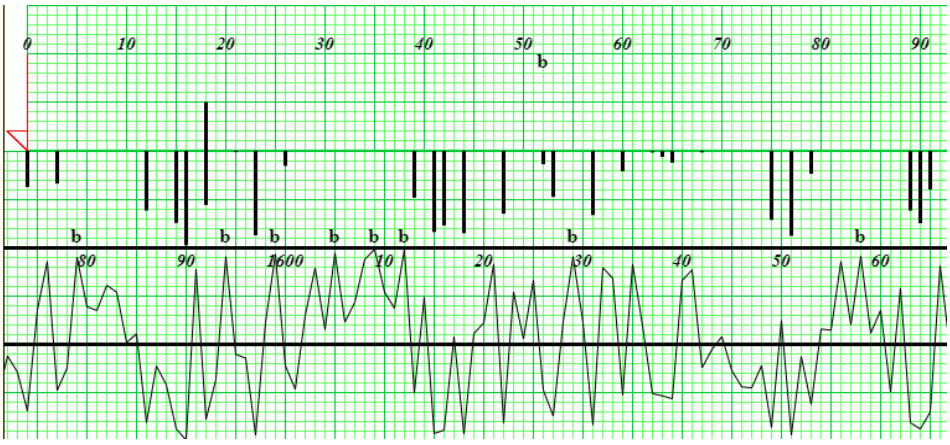

f

http://www.aloki.hu ● ISSN 1589 1623 (Print) ● ISSN 1785 0037 (Online)
DOI: http://dx.doi.org/10.15666/aeer/1906_44034419

TB5 & TB9 (1963-2019 AD)

** (1977, 1978, 1980, 1992, 1994, 1997, 2004, 2005, 2010), 2018.

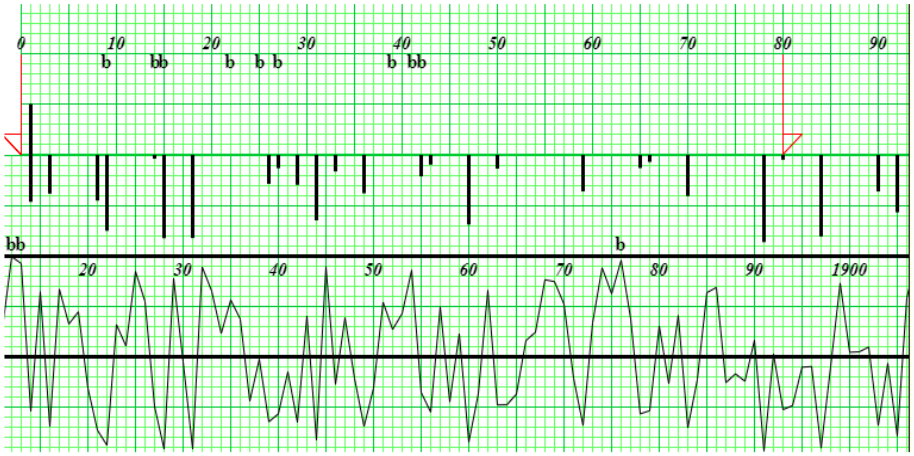

g

TB19' & TB20 (1953-2019 AD)

1997, 1998, 2000, 2018.

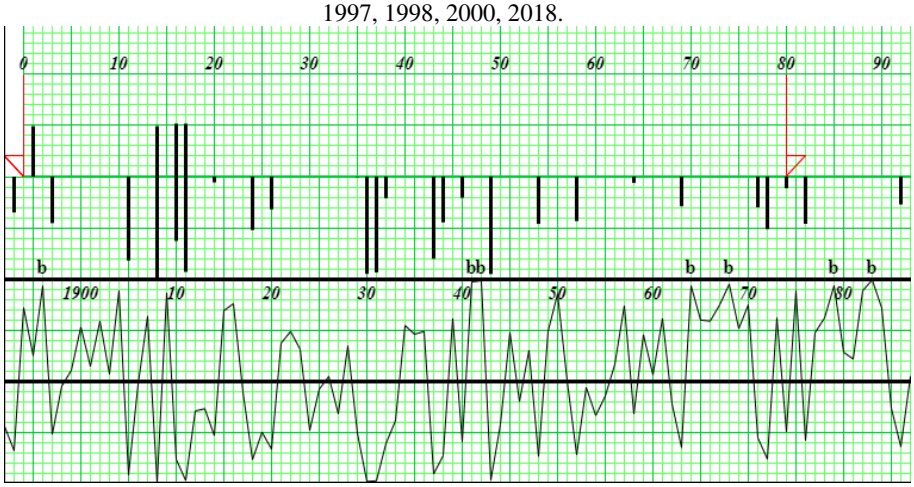

h

Figure 7. *(a-h) Most sensitive growth years of trees, representation through composite skeleton plot and their matching with master skeleton plot and master chronology*

Discussion

Conifers population increases with increase in forest resources and particular species have wide range of distribution. The nature of any forest is determined by interaction of many physical and biological factors resulted in species distribution in particular geographical region depending upon resource requirements in tolerant sites where it makes necessity for survival (Glatzel, 2009; Shaheen et al., 2015). Thus, present study focuses on age and growth rate determination and intra annual fluctuations between different species by graphical representation. In this way, chronology was prepared by Skeleton Plot Model after identification of climate sensitive years in selected species (Sheppard, 2002).

Environmental factors are very important in determining species dominancy at site such as sufficient light, nutrition, moisture and other edapho climate features. So, *A. pindrow* was found to be in large number as edapho climate features favored its growth

http://www.aloki.hu ● ISSN 1589 1623 (Print) ● ISSN 1785 0037 (Online)
DOI: http://dx.doi.org/10.15666/aeer/1906_44034419

while *T. baccata*, *P. roxburghii, C. deodara* was found to be minimal which may due to some anthropogenic activities like cutting, logging, fire and overgrazing.

Age and growth rate studies

Maximum and minimum age and growth rate of all selected conifers is presented in *Table 1*. Age and growth rate varies with elevation variation, from species to species and even among the similar species of similar sites. Many researchers have been engaged and are investigating dendrochronological potential from Pakistan and around the globe. Ahmed et al. (1990) reported age of *P. wallichiana*, 112 years with 20.5 cm dbh from dry temperate area of Takhtesuleman and moist temperate area like Khanaspur, Ayubia and Murree with different diameters, 58 cm, 65 cm, 58 cm dbh. *A. pindrow* showed an age of 103 years and 105 years with 71.2 and 92 cm dbh respectively from Murree site. An oldest *A. pindrow* was recorded with age of 277 years and 89 cm diameter from Ayubia. *C. deodara* was found to be oldest with age of 533 years and 180 cm dbh from Chitral site. The present study revealed the dominancy of *A. pindrow* with maximum age of 698 years and 149.3 cm diameter from Kalam Forest Division. Some other researchers from other countries determined dendrochronological potential of trees. Mccarthy and Weetman (2006) determined age of *Abies balsames* with 264 years black and white spruce with 264 and 247 years respectively from Canada. Muhammad et al. (2019) determined age of *C. deodara* from Kashmir Point Murree, Pakistan. Moreover, age of *Pondesera* was also determined, 618, 613 and 330 years from different sites of California by Youngblood et al. (2004). In the present study, we determined age of *A. pindrow*, *T. baccata* and *P. roxburghii,* 698 years with 149.3 cm dbh, 479 years with 137.16 cm and 218 years with 48.76 cm dbh respectively. *C. deodara* was found in minimum quantity due to reduced competition among trees and illegal cutting and burning of trees. So, significant positive correlation was observed in age and dbh among different species. Age may increase or decrease with increase of diameter as species lie in different geographical positions. Moreover, it was not observed an effective parameter for age variation as regional climate also favors the growth of conifers after Scipioni et al. (2021) and Ahmed et al. (2011).

Maximum and minimum growth rate of all species is presented in *Table 1*. Growth rate of conifers is also affected by availability of forest resources such as moisture content, favorable temperature and precipitation, adequate nutrients and prevention from natural or unnatural disasters after Ahmed et al. (2012). Among selected species *T. baccata* was found to be with maximum growth rate as environmental factors favored its growth and development. However, growth rate of rest species was also observed reasonable but not responded like *T. baccata.* Siddiqui et al. (2013) observed slow growth rate of *A. pindrow* from moist temperate area. Ahmed and Sarangzai (1992) determined growth rate of *P. wallichiana,* 2.5 cm/years from Murree. Ahmed et al. (2009) also determined as 1.7 cm/years in *P. wallichiana* from Dir. *A. pindrow* and *C. deodara* was observed with faster growth rate from Dir and Naran areas. In present study, *T. baccata* was observed with maximum growth rate, 0.66 cm/year while it was 0.05 and 0.10 cm/year as maximum in *A. pindrow* and *P. roxburghii* respectively.

Correlations study

Many researchers observed significant positive correlation between age and diameter from different sites of world. Ahmed and Sarangzai (1991) obtained such positive correlation in all selected species. However, Ahmed et al. (1990) did not find significant

http://www.aloki.hu ● ISSN 1589 1623 (Print) ● ISSN 1785 0037 (Online)
DOI: http://dx.doi.org/10.15666/aeer/1906_44034419

relationship between these parameters in *Juniperus excela* from Baluchistan, Pakisan. Moreover, Wahab et al. (2008) did not observe such positive relationship in *Picea smithiana*. Ahmed et al. (2009) did not find such correlation four species i.e., *A. pindrow, P. wallichiana, C. deodara* and *Picea smithiana* but they observed positive relation in *P. roxburghii*. In the present study, *A. pindrow*, *T. baccata* and *C. deodara* showed positive correlation while *P. roxburghii* showed highly negative correlation between age and diameter.

Growth rate was also observed non-significant by various researches. Muhammad et al. (2021) did not observe significant correlation between dbh and growth rate in *C. deodara* from Murree, Pakistan. Wahab et al. (2008) also observed negative relationship between dbh and growth rate in *P. smithiana* from conifers of Afghanistan Forest. *A. pindrow, P. wallichiana* and *C. deodara* also showed highly significant negative correlation between dbh and growth rate by Siddiqui et al., 2013. Ahmed et al. (2012) observed strongest response by rainfall. All selected species showed highly negative correlation between dbh and growth rate in present findings as shown in *Figures 4b, 5b, 6b.*

Conclusion

Kalam Valley, located at the junction of three mountains (Hindukush, Himalaya, and Karakoram), has a special topography, according to the researchers. The alpine peaks in the area vary in elevation from 1900 to 4600 m. Conifers grow taller as a result of edaphoclimate factors such as harsh winters, acidic soil, altitude variation, salts, sand, silt, and organic matter. Briefly to conclude, the study site was densely covered with *A. pindrow* as huge number of this species was observed while *C. deodara* was observed as minimal due to some anthropogenic disturbances. Significant positive correlation was observed between age and diameter in all species except *P. roxburghii* after Ahmed and Sarangzai (1991) while no such significant relationship was observed between diameter and growth rate after Wahab et al. (2008). Moreover, environmental factors mainly temperature, precipitation and rainfall also favored age and growth rate of these conifers and *T. baccata* responded well to these climatic variations as maximum growth rate was recorded in this species after Ahmed et al. (2012). A lot of reasons (deforestation, burning of wood as to fulfil needs of coal, overgrazing, town planning, and frequent forest fires) have placed the study site under biological stress due to *C. deodara* was observed a few in number. The chronology presented in results clearly depicted highly sensitive tree rings which were distinct indications of growth rate variations during development of trees. The developed chronologies signify the sensitivity of conifers of dry temperate study region towards diverse climatic factors and could be analyzed to predict future seasonal climate variations. Some highly recommended steps can be followed to conserve species habitat (natural biodiversity) through traditional practices such as:

- Need of awareness and management of forests to regain their valuable potential regarding to scientific research projects.
- Implementation of Forest rules to avoid from illegal cutting, burning and chopping by providing alternative fuel resources.
- Old age trees of study site such as *A. pindrow, T. baccata,* particularly *C. deodara* (national tree of Pakistan) etc. must be declared as cultural heritage of country.
- Ecotourism must be developed to promote cultural and economic significance by working with international counterparts, to acquire global exposure.

http://www.aloki.hu ● ISSN 1589 1623 (Print) ● ISSN 1785 0037 (Online)
DOI: http://dx.doi.org/10.15666/aeer/1906_44034419

Acknowledgements. Authors are very grateful to Mr. Naveed Shehzad, Hassan Nawaz and Amir Ali for help in Field work and all anonymous referees for their valuable comments and suggestions that have significantly increased the quality of manuscript.

REFERENCES

[1] Ahmed, M. (2014): The Science of Tree Rings: Dendrochronology. – Qureshi Art Press, Nazimabad, Karachi, pp. 95-108.
[2] Ahmed, M., Sarangzai, A. M. (1991): Dendrochronological approach to estimate age and growth rate of various species from Himalayan region of Pakistan. – Pakistan Journal of Botany 23(1): 78-89.
[3] Ahmed, M., Sarangzai, A. M. (1992): Dendrochronological potential of a few tree species from Himalayan region of Pakistan, a preliminary investigation. – Pakistan Journal of Pure and Applied Sciences 11(2): 65-72.
[4] Ahmed, M., Naqvi, S. H. (2005): Tree ring chronologies of *Picea smithiana* (Wall) Boiss, and its quantitative vegetation description from Himalayan region of Pakistan. – Pakistan Journal Botany 37(3): 697-707.
[5] Ahmed, M., Nagi, E. E., Wang, E. L. M. (1990): Present state of Juniper in Rodhmallazi forest of Baluchistan. Pakistan. – Pakistan Journal of Forestry 227-236.
[6] Ahmed, M., Wahab, M., Khan, N., Siddiqui, M. F., Khan, M. U., Hussain, S. T. (2009): Age and growth rates of some gymnosperms in Pakistan. A dendrochronological approach. – Pakistan Journal of Botany 41(2): 849-860.
[7] Ahmed, M., Palmer, J., Khan, N., Wahab, M., Fenrick, P., Esper, J., Cook, E. (2011): The dendroclimatic potential of conifers from Northern Pakistan. – Dendrochronologia 29(2): 77-88.
[8] Ahmed, M., Khan, N., Wahab, M., Zafar, M. U., Palmer, J. (2012): Climate/growth correlations of tree species in the Indus Basin of the Karakoram range, north Pakistan. – International Association of Wood Anatomists 33(1) 51-56.
[9] Ali, M., Asad, F., Zhu, H., Ahmed, M., Sigdel, S. R., Huang, R., Sharma, S., Liang, E., Hussain, I., Yaseen, T. (2021): Dendrochronological investigation of selected conifers from Karakoram-Himalaya, Northern Pakistan. – Pakistan Journal of Botany 53(3) 1091-1099.
[10] Bajwa, G. A., Shahzad, M. K., Satti, H. K. (2015): Climate change and its impacts on growth of blue pine (*Pinus wallichiana*) in Murree forest division, Pakistan. – Science Technology and Development 34(1): 27-34.
[11] Cook, E. R., Kairiukstis, L. A. (2010): Methods of Dendrochronology: Applications in the Environmental Sciences. – Kluwer Academic Publishers, Dordrecht.
[12] Copenheaver, C. A., Pokorski, E. A., Currie, J. E., Abrams, M. D. (2006): Causation of false ring formation in *Pinus banksiana*: a comparison of age, canopy class, climate and growth rate. – Forest Ecology and Management 236: 348-355.
[13] Glatzel, G. (2009): Mountain forests in a changing World, an Epilogue. – Mountain Research and Development 29: 188-190.
[14] Gosling, S. N., Lowe, J. A., McGregor, G. R., Pelling, M., Lalamud, B. D. (2009): Association between elevated atmospheric temperature and human mortality: a critical review of the literature. – Climate Change 92: 299-341.
[15] Hart, J. L., Grissino-Mayer, H. D. (2008): Vegetation patterns and dendroecology of a mixed hard wood forest on the Cumberland Plateau: implications for stand development. – Forest Ecology and Management 225: 1960-1975.
[16] Iqbal, H. (2014): Divisional Profile of Kalam Forest Division. – Kalam Forest Division, Madyan Swat.
[17] Khan, N. (2011): Vegetation ecology and dendrochronology of Chitral. – Ph.D Thesis, Department of Botany, Federal Urdu University, Gulshan-e-Iqbal, Karachi.

http://www.aloki.hu ● ISSN 1589 1623 (Print) ● ISSN 1785 0037 (Online)
DOI: http://dx.doi.org/10.15666/aeer/1906_44034419

[18] Khan, N., Ahmed, M., Wahab, M. (2008): Dendrochronological potential of *Picea smithiana* (Wall) Boiss. from Afghanistan. – Pakistan Journal of Botany 40(3): 1063-1070.
[19] Khan, N., Ahmed, M., Shahid, S. S. (2013): Climatic signal in Tree ring chronologies of *Cedrus deodara* from Chitral Hindukush range of Pakistan. – Geochronometria 40(3): 195-207.
[20] McCarthy, J. W., Weetman, G. (2006): Age and size structure of gap-dynamics, old-growth boreal stands in Newfoundland. – Silva Fennica 40: 209-230.
[21] Muhammad, S., Tayyab, M., Khan, Z., Malik, S. M., Akram, N. (2019): Age and growth rate studies of *Cedrus deodara* (Roxb. ex D. Don) around Kashmir point Reserve Forest of Tehsil Murree. – International Journal of Biosciences 15(3): 458-465.
[22] Muhammad, S., Hasnain, M., Tayyab, M., Khan, Z., Rasool, K. (2021): Dendrochronological potential of blue pine (*Pinus wallichiana* A.B. Jacks.) of Kuldana Reserve Forest of Tehsil Murree, Pakistan. – Pakistan Journal of Science 73(1): 130-137.
[23] Nash, S. E. (2002): Archeological tree ring dating at the millennium. – Journal of Archeological Research 10(3): 243-266.
[24] Palmer, J., Ahmed, M., Khan, Z. (2011): Application of tree-ring research in Pakistan. – Federal Urdu University of Arts, Science and Technology Journal of Biology 1(1): 19-25.
[25] Panyushkina, I. P. (2011): Dendrochronology. McGraw Hill Encyclopedia of Science & Technology, 11th Ed. – McGraw Hill, New York, pp. 1-11.
[26] Phipps, R. L. (1985): Collecting, Preparing, Crossdating and Measuring Tree Increment Cores. – U.S. Geological Survey, Washington, DC, pp. 35-40.
[27] Scipioni, M. C., Fontana, C., Oliveira, J. M., Junior, L. S., Roig, F. A., Tomazello-Filho, M. (2021): Effects of cold conditions on the growth rates of a subtropical conifer. – Dendrochronologia 68: 125858.
[28] Shaffer, G., Olsen, S. M., Pederson, G. O. P. (2009): Long term ocean oxygen depletion in response to carbon dioxide emissions from fossil fuels. – Nature Geoscience 2: 105-109.
[29] Shah, H., Jehan, N., Rehman, S. S., Bukhari, S. S. B. (2019): Comparative study of climate change and its impact on ring-widths of spruce (*Picea smithiana)* at Kalam and Kaghan Forest Divisions, Khyber Pakhtunkhwa, Pakistan. – Sarhad Journal of Agriculture 35(3): 788-797.
[30] Shaheen, H., Sarwar, R., Firdous, S. S., Dar, M. E., Ullah, Z., Khan, S. M. (2015): Distribution and structure of conifers with special emphasis on *Taxus baccata* in moist temperate Forests of Kashmir Himalayas. – Pakistan Journal of Botany 47(SI): 71-76.
[31] Sheppard, P. R. (2002): Web-based tools for teaching dendrochronology. – Journal of Natural Resources and Life Sciences Education 31: 123-129.
[32] Siddiqui, M. F., Shaukat, S. S., Ahmed, M., Khan, N., Khan, I. A. (2013): Vegetation environment relationship of conifer dominating forests of moist temperate belt of Himalayan and Hindukush regions of Pakistan. – Pakistan Journal of Botany 45: 577592.
[33] Speer, J. H. (2010): Fundamentals of Tree Ring Research. – University of Arizona Press, Tucson.
[34] Sun, Y., Wang, L., Yin, H. (2016): Influence of climatic factors on tree-ring maximum latewood density of *Picea schrenkiana* in Xinjiang, China. – Frontiers in Earth Science 10(1): 126-134.
[35] Vasconcellos, T. J. M., Filho, T., Callado, C. H. (2019): Dendrochronology and Dendroclimatology of Ceiba apeciosa (A. St. Hil) Ravenna (Malvaceaea) exposed to urban pollution in Rio de Jeneiro city, Brazil. – Dendrochronologia 53: 104-113.
[36] Volney, W. J. A., Mallet, K. I. (1992): Light rings and the age of jack pine trees. – Canadian Journal of Forest Research 22: 2011-2013.
[37] Wahab, M. (2011): Population dynamics and dendrochronological potential of pine tree species from District Dir. – Ph.D. thesis. Department of Botany, Federal Urdu University, Gulshan-e-Iqbal, Karachi.

http://www.aloki.hu ● ISSN 1589 1623 (Print) ● ISSN 1785 0037 (Online)
DOI: http://dx.doi.org/10.15666/aeer/1906_44034419

[38] Wahab, M., Ahmed, M., Khan, N. (2008): Phytosociology and dynamics of some pine forests of Afghanistan. – Pakistan Journal of Botany 40: 1071-1079.
[39] Yamaguchi, D. K. (1991): A simple method for cross-dating increment cores from living trees. – Canadian Journal of Forest Research 21: 414-416.
[40] Youngblood, A., Max, T., Coe. K. (2004): Stand structure in east side old-growth forests of Oregon and northern California. – Forest Ecology and Management 199: 191-217.

http://www.aloki.hu ● ISSN 1589 1623 (Print) ● ISSN 1785 0037 (Online)
DOI: http://dx.doi.org/10.15666/aeer/1906_44034419

EFFECTS OF DIET COMPOSITION ON CONSUMPTION, LIVE BODY WEIGHT AND LIFE SPAN OF WORKER HONEY BEES (*Apis mellifera* L.)

OSKAY, D.

Tekirdağ Namık Kemal University, Agriculture Faculty, Department of Agricultural Biotechnology, 59030 Tekirdağ, Turkey
(e-mail: doskay@nku.edu.tr; phone: +90-282-250-2292; fax: +90-282-250-9929)

(Received 22nd Apr 2021; accepted 20th Sep 2021)

Abstract. Due to current threats such as climate change, emerging diseases, and agricultural chemical use, honey bees are struggling to obtain adequate uncontaminated nectar and pollen for survival. Under these conditions, beekeepers feed their colonies with pollen and honey substitutes. In this study, several experimental diets were examined and compared with pollen and honey substitutes used by the beekeepers. The effects of the diets on consumption, live body weight and lifespan of groups of adult worker honey bees were investigated under laboratory conditions. "Natural-like" diet was used as control. Solid food with different amounts of protein and enzymatically prepared liquid food, enzymatically prepared liquid food with added caffeine, colored non-enzymatically prepared liquid food were tested. Pollen substitute protein levels were 0.4 to 10%. Solid food with low protein diet was consumed less, and resulted in low live body weight and low survival in comparison to control and higher protein amounts. Bees fed with enzymatically prepared liquid food with added caffeine group showed more activity but did not attain significantly higher survival ratio than bees fed only enzymatically prepared liquid food. This study discusses role of protein content and food preparation in the management of honey bee colonies.
Keywords: *nutrition, substitutes, protein, sugar, beekeeping*

Introduction

Nutrition has a significant impact on animal health, disease resistance, and ability to survive. Honey bee nutrition is a popular issue in beekeeping on a global scale (Pudasaini et al., 2020). Honey provides energy for honey bees (*Apis mellifera* L.), while pollen provides protein and is required for larval and adult stage growth.

Climate change, diseases, agricultural chemicals and habitation loss affect honey bees negatively (Brown et al., 2016). Currently, honey bees have difficulty to finding enough uncontaminated nectar and pollen (Hladun et al., 2012, 2015; Silici et al., 2016). This is essential for their survival. Even when pollen is available, not all pollen provides an adequate quantity of nutrition for colony development (Pernal and Currie, 2000). Furthermore, honey bee foraging opportunities are limited throughout the year due to environmental factors such as temperature, humidity, light intensity, solar irradiation values, wind, rain, and flower patches (Farrar, 1934; Burrill and Dietz, 1981; Winston, 1987). Under these conditions, beekeepers feed their colonies with pollen and honey substitutes. In order to grow honey bee colony population, rearing brood, queens, drones, successful overwintering, and increase honey production, supplementary diets are needed (Herbert, 1992; Goodwin et al., 1994; Koç and Karacaoğlu, 2004). Several studies have been conducted in order to develop an ideal supplemental protein diet for honey bees that is healthy, extremely wealthy in required nutrients, and easily accepted. Previous studies have examined the effects of protein- and carbohydrate-rich supplement foods on colony development, lifespan, brood, honey, production performance, wax construction and honey bee biology (Herbert et al., 1977, 1992; Doull, 1980; Winston et al., 1983;

http://www.aloki.hu ● ISSN 1589 1623 (Print) ● ISSN1785 0037 (Online)
DOI: http://dx.doi.org/10.15666/aeer/1906_44214430

Cremonez et al., 1998; Mattila and Otis, 2006; Dastouri and Maheri-Sis, 2007; Cappelari et al., 2009; Basualdo et al., 2013, 2014; Kumar and Agrawal, 2014; Gemeda, 2014; Pande et al., 2015; Frias et al., 2016; Paiva et al., 2016; Almaida-Dias et al., 2018; Mohammad et al., 2020; Adgaba et al., 2020; Mahbob et al., 2021). Manning et al. (2007) demonstrated that soy protein shortens the life span of honey bees, implying that soy proteins are less appealing to honey them. Therefore, soy protein has not used in this study.

Danihlik et al. (2018) examined changes in immune system characteristics in bees given various pollen diets. Their results on the significance of protein content in the bee diet have practical consequences for rethinking the value of protein supplementation in the sugar-based diet given to bee colonies, as well as its effect on bee and colony health and successful wintering capability. Scientific study is ongoing to find out the impact of compounds that provide critical nutrition to honey bees. Vrabie et al. (2019) supplemented honey bee colonies with whey protein and observed an increase in brood development of 13.1-14.5 percent and acacia honey yield of 24.7-44.8 percent.

Scientists all around the globe have developed several substitute meal recipes for bees based on the nutritional content of honey and pollen, acceptability, digestibility, and affordability of materials. This may assist to keep all colony characteristics stable enough to take full benefit of the next nectar flow season. However, a globally recognized standard balanced diet for commercial beekeeping is still needed (Paray et al., 2021).

Three honey and three pollen substitutes were used under laboratory conditions to better understand the effects of different kinds of honey and pollen substitutes on bees, as well to determine their impact on adult bee live body weight, feed consumption and life span. The live body weight difference across age groups with different honey, pollen substitutions, and effect of phagostimulants such as caffeine are examined in this study for the first time.

Material and Method

Rearing conditions and modalities of treatment

Capped brood combs with emerging bees were collected in May 2016 from 20 honey bee colonies led by sister queens at Tekirdag Namik Kemal University apiaries (Tekirdag, Turkey). These brood combs were incubated overnight at hive temperatures and humidity (35°C, 75% humidity, and no light) to simulate the hive environment for providing 1 day old bees. Bees that had just emerged were carefully brushed into a wide plastic basin and mixed.

The size of the cages was 14 cm x 13 cm x 8.3 cm and the volume was 1.5 L. A wide section of the cages was glued to the floor, and 4 ventilation holes were opened, up to a diameter of 2 cm. and a height of 4 cm. above the floor. The top of the cage also had an opening of 4 cm diameter. Side ventilation holes of the cage were covered with wiremesh (fly screen) and silicone. 100 individual bees were placed inside the transparent plastic cages (14 x 13 x 8.3 cm) and returned to the incubator (75% humidity and 35°C temperature); as in Evans et al. (2009).

Each cage represented one of 6 treatment groups. 100 one-day old worker bees placed in each group cage. All food was provided to bees in a free-choice feeding system in Eppendorf culture vials (15 mL) with small holes that allow bees to enter in tubes. The feed vials were replaced every three days.

http://www.aloki.hu ● ISSN 1589 1623 (Print) ● ISSN1785 0037 (Online)
DOI: http://dx.doi.org/10.15666/aeer/1906_44214430

A “natural–like” diet was utilized in the experiment. Honey and fresh pollen were gathered from University apiaries honey bee colonies. Honey and fresh pollen were stored in a glass jar. Honey was maintained at ambient temperature throughout the experiment, whereas pollen was stored at -18 °C.

Two different pollen substitute diets were experienced: two containing higher levels of crude protein and another one with a lower protein content. 10% protein pollen substitute was a mixture of inactive bread yeast extract powder, powdered beet sugar, inverted sugar syrup (70% sugar, 30% water), sunflower honey and sunflower seed oil. 0.4% pollen substitute was a commercial food containing soybean flour.

Three different honey substitute diets were tested for the experiment. Inverted sugar syrup (enzymatically prepared liquid food) was produced by dissolving beet sugar in water and by addition of invertase enzyme. The inverted sugar syrup was mixed and stored at 40°C temperature for 36 hours. It was fed to caged bees within one week of production. Caffeine powder was supplied from Sigma-Aldrich Co. LLC. 1 mM caffeine concentration was used for enzymatically prepared liquid food for the added caffeine group (Wright et al., 2013). Colored non-enzymatically prepared liquid food was acquired commercially.

A: "natural-like" diet used as control (honey and pollen).

B: solid food with 0.4% protein (pollen substitute).

C: solid food with 10% protein (pollen substitute).

D: Enzymatically prepared liquid food (sugar syrup).

E. Enzymatically prepared liquid food with some caffeine (sugar syrup).

F: Colored non-Enzymatically prepared liquid food (sugar syrup).

The quantity of consumed food was measured every 3 days, before each fill up, by weighing the solid and liquid foods remaining in the feeder vials, and as compared to the weight of the full feeder at the start. The alteration in milligrams was transformed to microliters (1 μL = 1.22 mg of sugar syrup) and divided by the number of surviving bees (Renzi et al., 2016). The total amount of solid and liquid food consumed was calculated after 24 days.

Because the live body weight parametry had not previously been studied in honey bee worker bee feeding research, the solid food with 10% protein feed group (C) was chosen to represent the protein feed group for comparison with the control group when designing the experimental groups, while enzymatically prepared liquid food (D) and colored non-enzymatically prepared liquid food (F) were chosen to represent the protein feed group for comparison with the control group. One, twelve, twenty-four days old live bees collected from cages were placed in different size of tubes, weighed with a precision scale and placed back in their cages alive. Ten live worker bees from each group were chosen at random for live body weight measurements. Every day, dead bees were gathered and counted from the cages.

Data analyses

The impact of nutritional treatments on solids, liquids, food consumption, and body weight was evaluated using two-way ANOVA. For the six diet applications, the Kaplan-Meier survival test was used for the life span of honey bees (Kleinbaum and Mitchel, 1996; Wang et al., 2014). Graphpad Prism 6.0 software (GraphPad software, San Diego, USA) was used to conduct statistical analysis.

http://www.aloki.hu ● ISSN 1589 1623 (Print) ● ISSN1785 0037 (Online)
DOI: http://dx.doi.org/10.15666/aeer/1906_44214430

Results

Live body weight

The effects of the dietary treatments on live body weight performance are shown in *Figure 1*. When the experiment started the mean live body weights in treatment groups "natural-like" diet used as control (A), solid food with 10% protein (C), enzymatically prepared liquid food (D), colored non-enzymatically prepared liquid food (F) at one day of age was, 89.77±1.71 mg, 90.66±1.58 mg, 90.22±1.39 mg, and 89.77±1.39 mg, respectively. There were no significant differences among groups ($F_{1.24}$=2.16, P >0.05). The mean live body weights in treatment groups A, C, D and F at 12 days of age were, 136.40±14.75 mg, 128.60±16.29 mg, 106.60±16.06 mg, and 99.80±15.80 mg. There was a significant difference among groups (P<0.05). There was not a statistical difference between "natural -like" diet used as control (A) and solid food with 10% protein (C) (P>0.05). There was not a statistical difference between enzymatically prepared liquid food (D), colored non-enzymatically prepared liquid food (F) (P>0.05). There was a significant difference between protein (A and C) and carbohydrate diet groups (D and F) (P<0.05).

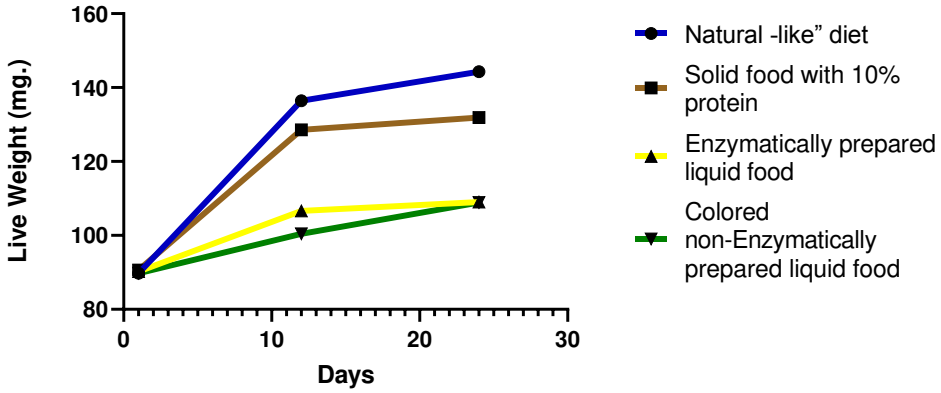

Figure 1. *Live body weight (mg) of caged worker bees fed with different diets*

The mean live body weights in treatment groups A, C, D, F at 24 days of age were, 144.33±9.34 mg, 131.90±23.64 mg, 109±4.82 mg, and 108.88±18.78 mg. There was not a statistical difference between "natural -like" diet used as control (A) and solid food with 10% protein (C) (P>0.05). In addition, there wasn't a statistical difference between enzymatically prepared liquid food (D), colored non-enzymatically prepared liquid food (F) (P>0.05). A significant difference was found between protein (A and C) and carbohydrate diet groups (D and F) diet groups (P<0.05). Highest live body weight was the control group. An inverted syrup without enzyme group was lowest live weight.

Solid food consumption quantity

The effects of the dietary treatments on solid food consumption by bees in groups "natural-like" diet (A), solid food with 0.4% protein (B), and solid food with 10% protein (C) are shown in *Figure 2*. Solid food consumption was measured every 3 days through 21 days. Mean of daily solid food consumption in treatment groups A, C and B during the three weeks of the experiment were, 20.61±10.33 µg, 14.42±11.45 µg, and 0±0, respectively.

http://www.aloki.hu ● ISSN 1589 1623 (Print) ● ISSN1785 0037 (Online)
DOI: http://dx.doi.org/10.15666/aeer/1906_44214430

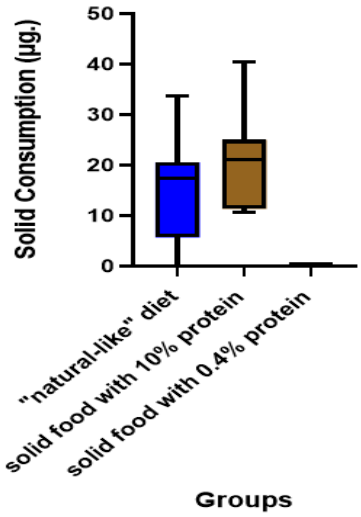

Figure 2. *Daily solid food consumption (µg) per bee at the 21 days of caged worker bees fed with different diets*

Highest consumption was for "natural-like" diet among the solids but there is no significant difference between "natural-like" diet (A) and solid food with 10% protein groups (C) ($F_{1.21}$= 9.85, P>0.05). There was no solid feed consumption at solid food with 0.4% protein group (B). Bees consumed only enzymatically prepared liquid food.

Liquid food consumption quantities

The effects of the dietary treatments on liquid consumption food groups, "natural-like" diet used as control (A), enzymatically prepared liquid food (D), enzymatically prepared liquid food with some caffeine (E), colored non-Enzymatically prepared liquid food (F) (A, D, E and F) performance is shown in *Figure 3*. Liquid food consumption was measured every 3 days during the 21 days. Mean of daily liquid food consumption in treatment groups A, D, F and E through the three weeks of the experiment were, 26.47±14.99 µL, 37.50±15.86 µL, 29.87±18.41 µL and 41.96± 15.34 µL respectively. Diet quality had no effect on daily liquid food consumption from the 1st to the 21st day of treatment ($F_{1.21}$= 1.32, P>0.05). There was also no significant relation among food consumption amounts. Highest consumption was enzymatically prepared liquid food with some caffeine (E) among the liquid foods. Lowest consumption was honey among the liquid foods.

The life span of honey bee

The mean of life span days in treatment groups "natural-like" diet used as control (A), solid food with 0.4% protein (B), solid food with 10% protein (C), enzymatically prepared liquid food (D), enzymatically prepared liquid food with some caffeine (E), colored non-enzymatically prepared liquid food (F) was 24.6±1.38, 23.25±2.60, 29.01±1.86, 22.56±1.98, 23.28±3.14 and 19.92±3.07, respectively. There were significant differences among groups (P<0.001). Bees fed with solid food with 10% protein (C) showed the best survival. There was no significant difference between bees fed "natural-like" diet (A) and bees fed with solid food with 10% protein (C) (P>0.05). There was no significant difference among enzymatically prepared liquid food (D), solid food with 0.4% protein

http://www.aloki.hu ● ISSN 1589 1623 (Print) ● ISSN1785 0037 (Online)
DOI: http://dx.doi.org/10.15666/aeer/1906_44214430

(B) and enzymatically prepared liquid food with some caffeine (E) ($P>0.05$). Colored non-enzymatically prepared liquid food (F) showed the lowest survival that was significantly different than other groups ($P<0.001$). Bees fed with higher protein ratio groups showed significantly different survival results than bees fed with only syrups in terms of average lifespan ($X^2=44.59$, $P<0.001$) (*Figure 4*).

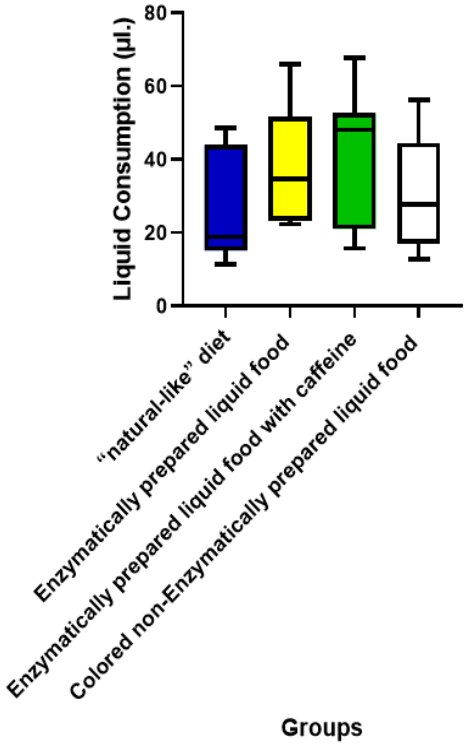

Figure 3. *Daily Liquid food consumption (µL) of caged worker bees fed with different liquid diets*

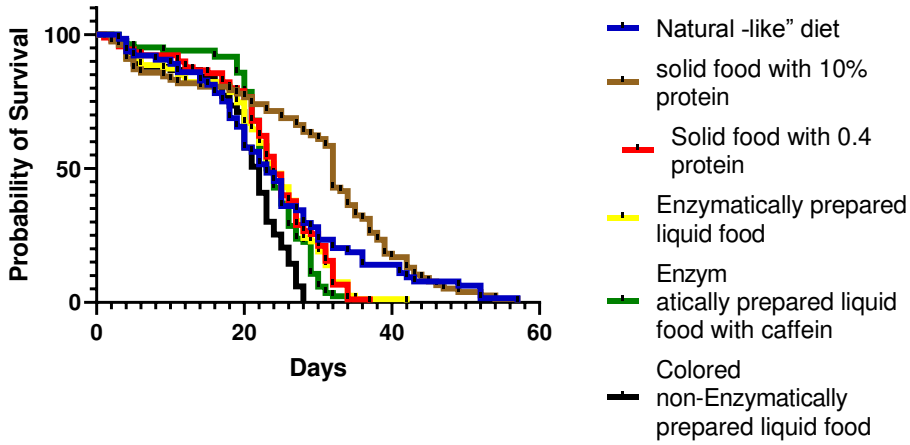

Figure 4. *Survival of newly emerged bees caged and fed a variety of diets under incubator settings. Foods were controlled, "natural-like" diet used as control (A), solid food with 0.4% protein (B), solid food with 10% protein (C), enzymatically prepared liquid food (D), enzymatically prepared liquid food with some caffeine (E), colored non-enzymatically prepared liquid food (F)*

http://www.aloki.hu ● ISSN 1589 1623 (Print) ● ISSN1785 0037 (Online)
DOI: http://dx.doi.org/10.15666/aeer/1906_44214430

Discussion

The results obtained in this study, with respect to live body weight, food consumption, and life span, are in agreement with the pollen and honey substitute effects reported by Dastouri and Maheri-Sis (2007) and Basualdo et al. (2013, 2014). Kumar et al. (2014) remarked that bee body weight is not efficient method of calculating the protein rank of bees provided with high level–protein-content pollen (HLCP) and low level–protein-content pollen (LLCP). Content of HLCP and LLCP protein ratio were 29% and 10%. In this study, content of high level protein diets were %10, "natural -like" diet. When it was compared live body weight with liquid food without protein and solid food with 10% protein groups it was a significant difference between groups. It means that live body weight parameter would use depend of protein ratio level of diet.

The study's key result is that bees fed pollen and a 10% pollen substitute had the highest survival rate, whereas bees fed only inverted sugar syrup had the shortest lifespan.

The current study's findings contradict those of Pirk et al. (2010), who demonstrated that bees fed carbohydrate survived better than bees fed pollen substituted with sugar. In their study, they have used casein as a protein source. Additionally, Altaye et al. (2010) demonstrated that while casein diets increased survival and Feed-Bee® diets decreased it, royal jelly diets increased ovarian activation and casein diets decreased it.

The findings confirm that a high-protein diet has a positive effect on live body weight in bees sampled on the 12^{th} and 24^{th} days, which correlates to the age of maximum body growth in worker bees.

Gregorc et al. (2019) conducted a 9-day surviver test on bees fed in cages with various pollen substitute ratios. According to the research, there were extremely fast bee mortality in the groups given 50% and 40% pollen substitute feed. As a result, they suggested that high protein diets should be avoided in adult bees.

Bees foraging at a feeder containing 1 M sucrose with caffeine made more visits than bees foraging at a feeder containing an equivalent molarity sucrose without caffeine, according to Couvillon et al. (2015). Also, caffeine increases the tendency and rate of recurrence of individual bee waggle dancing. In this experiment, enzymatically prepared liquid food with some caffeine (E) bees didn't any significant differences than other liquid groups about live body weight, consumption and surviving. While changing their food in the cages, the bees in the enzymatically prepared liquid food with some caffeine group move and run more than the bees in the other groups. These motions, however, have not been quantified.

Conclusion

Present results demonstrate that %10 protein ratio can be used in feed patties for feeding colonies in spring and autumn season for colony nutrition management.

Supplemental feeding is generally used by beekeepers to sustain colony maintenance strategy to promote up their honey bee colonies when nectar and pollen sources are scarce in nature or in agriculturally plants cultivated, but the dietary basis of protein and carbohydrate supplement issue has not been studied sufficiently. In this research, prepared pollen (Group C) and honey (Group D and E) substitutes gave rational results based on honey bee ecology and physiology. Given that climate change, urbanization, agricultural chemicals, diseases, and pests will all have a detrimental impact on honey bees in the future, greater emphasis should be given to nutritional research. There is a need for substitute food studies that incorporate vitamins, minerals, lipids, prebiotics, and

http://www.aloki.hu ● ISSN 1589 1623 (Print) ● ISSN1785 0037 (Online)
DOI: http://dx.doi.org/10.15666/aeer/1906_44214430

probiotics in addition to the carbohydrate and protein sources utilized in bee substitute diets.

The impact of naturally occurring secondary metabolites, such as caffeine, on honey bee behavior and metabolism should be investigated.

Acknowledgements. The author would like to thank Yılmaz Berk Koru, Gizem Sönmez Oskay, and Mustafa Degermenci for their assistance in gathering the data.

REFERENCES

[1] Adgaba, N., Al-Ghamdi, A., Tadesse, Y., Mohammed, S. E. A., Al-Attal, Y. (2020): Brood-Rearing Enhancing Potential of Manually Packed Pollen Feeding in Comparison with Pollen and Pollen Supplements in Patty Forms. – Journal of Apicultural Science 64(2): 189-198.

[2] Almaida-Dias, J. M., Morais, M. M., Francoy, T. M., Pereira, R. A., Turcatto, A. P., De Jong, D. (2018): Fermentation of a pollen substitute diet with bee bread microorganisms increases diet consumption and hemolymph protein levels of honey bees (*Hymenoptera: Apidae*). – Sociobiology 65(4): 760-765. doi: 10.13102/ sociobiology.v65i4.3293.

[3] Altaye, S. Z., Pirk, C. W., Crewe, R. M., Nicolson, S. W. (2010): Convergence of carbohydrate-biased intake targets in caged worker honeybees fed different protein sources. – Journal of Experimental Biology 213(19): 3311-3318.

[4] Basualdo, M., Barragan, S., Vanagas, L., Garcia, C., Solana, H., Rodriguez, E., Bedascarrasbure, E. (2013): Conversion of high and low pollen protein diets into protein in worker honey bees (*Hymenoptera: Apidae*). – Journal of Economic Entomology 106: 1553-1558. doi: 10.1603/EC12466.

[5] Basualdo, M., Barragan, S., Antunez, K. (2014): Bee bread increases honeybee haemolymph protein and promote better survival despite causing higher Nosema ceranae abundance in honeybees. – Environmental Microbiology Reports 6: 396-400. doi: 10.1111/1758-2229.12169.

[6] Brown, M. J., Dicks, L. V., Paxton, R. J., Baldock, K. C., Barron, A. B., Chauzat, M. P., Li, J. (2016): A horizon scan of future threats and opportunities for pollinators and pollination. – Peer J 4: e2249.

[7] Burrill, R. M., Dietz, A. (1981): The response of honey bees to variations in solar radiation and temperature. – Apidologie 12: 319-328.

[8] Cappelari, F. A., Turcatto, A. P., Morais, M. M., De Jong, D. (2009): Africanized honey bees more efficiently convert protein diets into hemolymph protein than do Carniolan bees (*Apis mellifera carnica*). – Genetics and Molecular Research 8: 1245-1249. doi: 10.4238/vol8-4gmr628.

[9] Couvillon, M. J., Al Toufailia, H., Butterfield, T. M., Schrell, F., Ratnieks, F. L., Schürch, R. (2015): Caffeinated forage tricks honeybees into increasing foraging and recruitment behaviors. – Current Biology 25(21): 2815-2818.

[10] Cremonez, T. M., De Jong, D., Bitondi, M. M. G. (1998): Quantification of hemolymph proteins as a fast method for testing protein diets for honey bees (Hymenoptera: Apidae). – J. Econ. Entomol. 91: 1284-1289.

[11] Danihlík, J., Škrabišová, M., Lenobel, R., Šebela, M., Omar, E., Petřivalský, M., Brodschneider, R. (2018): Does the pollen diet influence the production and expression of antimicrobial peptides in individual honey bees? – Insects 9(3): 79.

[12] Dastouri, M. R., Maheri-Sis, N. (2007): The effect of replacement feeding of some protein sources with pollen on honey bee population and colony performance. – J. Anim. Vet. Adv. 6: 1258-1261.

http://www.aloki.hu ● ISSN 1589 1623 (Print) ● ISSN1785 0037 (Online)
DOI: http://dx.doi.org/10.15666/aeer/1906_44214430

[13] Doull, K. M. (1980): Relationships between consumption of a pollen supplement, honey production and brood rearing in colonies of honeybees *Apis mellifera* L. II. – Apidologie 11: 367-374.
[14] Evans, D. J., Chen, P. Y., Prisco, G., Pettis, J., Williams, V. (2009): Bee cups: single-use cages for honey bee experiments. – Journal of Apicultural Research and Bee World 48(4): 300-302.
[15] Farrar, C. L. (1934): Bees must have pollen. – Glean. Bee Cult. 62: 276-278.
[16] Frias, B. E. D., Barbosa, C. D., Lourenço, A. P. (2016): Pollen nutrition in honey bees (*Apis mellifera*): impact on adult health. – Apidologie 47(1): 15-25.
[17] Gemeda, T. K. (2014): Testing of effect of dearth period supplementary feeding of honeybee (*Apis mellifera*) on brood development and honey production. – International Journal of Advance Research 2(11): 319-324.
[18] Goodwin, R. M., Ten Houten, A., Perry, J. H. (1994): Effect of feeding pollen substitutes to honey bee colonies used for kiwifruit pollination and honey production. – New Zealand J. Crop. Hort. 22: 459-462.
[19] Gregorc, A., Sampson, B., Knight, P. R., Adamczyk, J. (2019): Diet quality affects honey bee (Hymenoptera: Apidae) mortality under laboratory conditions. – Journal of Apicultural Research 58(4): 492-493.
[20] Herbert, E. W., Shimanuki, H., Caron, D. (1977): Optimum protein levels required by honey bees (Hymenoptera: Apidae) to initiate and maintain brood rearing. – Apidologie 8: 141-146. doi: 10.1051/apido:19770204.
[21] Herbert, E. W. (1992): Honey bee nutrition. – In: Graham, J. M. (ed.) The hive and the honey bee. – Dadant and Sons, Hamilton, IL. pp. 197-233.
[22] Hladun, K. R., Smith, B. H., Mustard, J. A., Morton, R. R., Trumble, J. T. (2012): Selenium toxicity to honey bee (*Apis mellifera* L.*)* pollinators: effects on behaviors and survival. – PloS one 7(4): e34137.
[23] Hladun, K. R., Parker, D. R., Trumble, J. T. (2015): Cadmium, copper, and lead accumulation and bioconcentration in the vegetative and reproductive organs of *Raphanus sativus*: implications for plant performance and pollination. – Journal of Chemical Ecology 41(4): 386-395.
[24] Kleinbaum, D. G., Mitchel, K. (1996): Statistics for Biology and Health (survival analysis, second edition). – Springer science + Business Media, Inc.
[25] Koç, A. U., Karacaoglu, M. (2004): Effects of rearing season on the quality of queen honeybees (*Apis mellifera* L.) raised under the conditions of Aegean Region. – Mellifera 4(7): 34-37.
[26] Kumar, R., Agrawal, O. P. (2014): Comparative performance of honeybee colonies fed with artificial diets in Gwalior and Panchkula region. – Journal of Entomology and Zoology Studies 2(4): 104-107.
[27] Mahbob, M., Adahm, M., Mohamed, A. R., Rania-Qurash, S. (2021): A fermented Pollen Substitute Diet Affects Wax Construction by Honey Bee Workers (*Apies mellifera* L.). – Egyptian Academic Journal of Biological Sciences A, Entomology 14(2): 1-11.
[28] Manning, R., Rutkay, A., Eaton, L., Dell, B. (2007): Lipid-enhanced pollen and lipid-reduced flour diets and their effect on the longevity of honey bees (*Apis mellifera* L.). – Australian Journal of Entomology 46(3): 251-257.
[29] Mattila, H. R., Otis, G. W. (2006): The effects of pollen availability during larval development on the behavior and physiology of spring-reared honey bee workers. – Apidologie 37: 533-546.
[30] Mohammad, R. H. S., Sari, M., Tahmasbi, G., Chaji, M. (2020): The effects of different levels of protein and silymarin on the population growth and Hypopharyngeal gland surface of honey bee workers (*Apis mellifera meda*). – Biotechnology in Animal Husbandry 36(3): 341-358.

http://www.aloki.hu ● ISSN 1589 1623 (Print) ● ISSN1785 0037 (Online)
DOI: http://dx.doi.org/10.15666/aeer/1906_44214430

[31] Paiva, J. P. L. M., Paiva, H. M., Esposito, E., Morais, M. M. (2016): On the effects of artificial feeding on bee colony dynamics: a mathematical model. – Plos One 11: e0167054. doi: 10.1371/ journal.pone.0167054.
[32] Pande, R., Karnatak, A. K., Pande, N. (2015): Development of nectar supplements for death period management of honeybees (*Apis mellifera* L.) colonies in foothills of Shivalik range of Himalayan. – The Bioscan 10(4): 1599-1603.
[33] Paray, B. A., Kumari, I., Hajam, Y. A., Sharma, B., Kumar, R., Albeshr, M. F., Khan, J. M. (2021): Honeybee nutrition and pollen substitutes: A review. – Saudi Journal of Biological Sciences 28(1): 1167.
[34] Pernal, S. F., Currie, R. W. (2000): Pollen quality of fresh and 1-year-old single pollen diets for worker honey bees (*Apis mellifera* L.). – Apidologie 31: 387-409.
[35] Pirk, C. W., Boodhoo, C., Human, H., Nicolson, S. W. (2010): The importance of protein type and protein to carbohydrate ratio for survival and ovarian activation of caged honeybees (*Apis mellifera* scutellata). – Apidologie 41(1): 62-72.
[36] Pudasaini, R., Dhital, B., Chaudhary, S. (2020): Nutritional requirement and its role on honeybee: a review. – Journal of Agriculture and Natural Resources 3(2): 321-334.
[37] Renzi, M. T., Rodríguez-Gasol, N., Medrzycki, P., Porrini, C., Martini, A., Burgio, G., Maini, S., Sgolastra, F. (2016): Combined effect of pollen quality and thiamethoxam on hypopharyngeal gland development and protein content in *Apis mellifera*. – Apidologie 47: 779.
[38] Silici, S., Uluozlu, O. D., Tuzen, M., Soylak, M. (2016): Honeybees and honey as monitors for heavy metal contamination near thermal power plants in Mugla, Turkey. – Toxicology and Industrial Health 32(3): 507-516.
[39] Vrabie, V., Derjanschi, V., Ciochină, V., Vrabie, E. (2019): The use of whey for honey bee feeding and obtaining of proteincarbohydrate bee feed. – In: Scientific Papers Series D, Animal Science 62: 105-110.
[40] Wang, H., Zhang, S. W., Zeng, Z. J., Yan, W. Y. (2014): Nutrition affects longevity and gene expression in honey bee (*Apis mellifera* L.) workers. – Apidologie 45(5): 618-625.
[41] Winston, M. L. (1987): The Biology of the Honey Bees. – Harvard University Press, London, UK.
[42] Winston, M. L., Chalmers, W. T., Lee, P. C. (1983): Effects of two pollen substitutes on brood mortality and length of adult life in the honey bee. – Journal of Apicultural Research 22: 49-52.
[43] Wright, G. A., Baker, D. D., Palmer, M. J., Stabler, D., Mustard, J. A., Power, E. F., Stevenson, P. C. (2013): Caffeine in floral nectar enhances a pollinator's memory of reward. – Science 339(6124): 1202-1204.

http://www.aloki.hu ● ISSN 1589 1623 (Print) ● ISSN1785 0037 (Online)
DOI: http://dx.doi.org/10.15666/aeer/1906_44214430

THE EFFECT OF GROWING MEDIA AND HUMIC ACID TREATMENTS ON SOME PLANT PROPERTIES OF PURSLANE (*Portulaca oleracea* L.)

UGUR, A.[1*] – KOCAMANOGLU, C.[2]

[1]*Agricultural Faculty, Department of Horticulture, Ordu University, 52200 Ordu, Turkey*

[2]*Ordu Eskipazar Agricultural Credit Cooperative, 52100 Ordu, Turkey*

[*]*Corresponding author*
e-mail: atnanugur@gmail.com; phone: +90-452-226-5200 - 6237; fax: 90-452-234-6632

(Received 4th May 2021; accepted 3rd Sep 2021)

Abstract. Growing medium in soilless culture is important due to its effects on plant nutrition. In this study, the effects of growing environment and humic acid on yield and quality in purslane cultivation were investigated. The study was carried out in laboratories of Ordu University, Department of Horticulture and under greenhouses conditions (Merzifon provinces). Peat, perlite medium, 2:1 peat/perlite, 1:1 peat/perlite and 1:2 peat/perlite mixtures were used as growing medium in plastic sowing pot. Seeds were sown on the 6th of April. Throughout the study, all cultural processes were carried out to ensure that the crops reached marketable harvest size and plants were harvested on 24 May. The yield, shoot height, shoot diameter, oxalic acid and nitrate contents were determined for the harvested plants. Plant yields varied between 1957-3113 g per square meters depending on the growing medium. Parallel to the humic acid application dose, plant yield increased by 6.21-12.08%. Similarly, the shoot height, shoot diameter and leaf oxalic acid contents increased with humic acid applications. Leaf nitrate contents were determined with 1512 mg/100 g in the lowest 1:1 peat/perlite medium. The highest nitrate value was determined as 2343 mg/100 g nitrate content in 100% perlite medium.
Keywords: *leaf, nitrate, oxalic acid, Portulaca oleracea L., quality*

Introduction

Purslane (*Portulaca oleracea* L.) is an annual herbaceous plant of Portulacaceae family. Purslane is a common weed and grows abundantly in vegetable gardens as it gets hotter via generating various tiny, black poppy-like seeds. The plant has found a large growing area in tropical and subtropical regions throughout the world as it grows fast, is self-compatible and generates various seeds that do not fade away for a long time. Called purslane in USA, the plant is also known as portulak, porcellana, glistrida, antrakla, adrahni, rigla, verdolaga, pigweed, beldroega, little hogweed, red root, tuchenitsa, pursle and semizotu in different parts of the world. There are records and documents indicating that the plant has been used in the Arabian Peninsula and Mediterranean basin since the Middle Age. The plant was called as "mad vegetable" in the Middle Age as it shoots and grew fast. Purslane has stood out in the recent years due to its content of phytochemicals, vitamins and minerals (Simopoulos et al., 1992; Palaniswamy et al., 2000; Petropoulos et al., 2016; Alu'datt et al., 2019). It's preventing oxidation and thus antioxidant capacity enhancing properties have been determined in the oil industry (Mousavi et al., 2015). It is used in public health due to its antitumor, hypoglycemic, antiscorbutic, antiseptic, antispasmodic, diuretic, antioxidant, antidiabetic, antibacterial, antitussive, anti-inflammatory and wound healing properties (Dkhil et al., 2011). On the other hand, experimental studies were carried out on its medical effects. As it contains alpha linolenic acid, which is omega-3 oil acid found in fish and certain algae, its consumption has risen

http://www.aloki.hu ● ISSN 1589 1623 (Print) ● ISSN1785 0037 (Online)
DOI: http://dx.doi.org/10.15666/aeer/1906_44314441

(Simopoulos et al., 1992; Palaniswamy et al., 2002). Its consumption is more preferred compared to fish as it has a more reasonable odor, is affordable and grown in plenitude in any ecological environment. It is generally consumed like spinach in Turkish cuisine; used in patties with different types of cheese and in salads and garnitures and as an appetizer with garlic and yoghurt. However, purslane contains a significant amount of oxalic acid (Palaniswamy et al., 2004). Normally all plants contain oxalic acid but certain types especially greens have a higher oxalic acid content. Oxalic acid generates insoluble salts by combining with acid iron and calcium and prevents their usefulness. Especially people with kidney diseases should be careful while consuming the vegetables containing oxalic acid (Simopoulos et al., 1992; Palaniswamy et al., 2004).

Ecological factors, fertilizing, growing conditions and genetic factors affect plant development and their chemical content (Palaniswamy et al., 2000). Purslane is grown in gardens in March-September when insolation is frequent albeit varying by ecologies and can be grown in greenhouses when soil and field conditions are not appropriate. In addition, greenhouse cultivation is carried out for healthier and homogeneous plant growth against the possible negative effects of diseases and pests, rain and wind (Pandey and Pandey, 2015). It is not very competitive against other plants. Plant development gets weaker in shady medium and scraggily developing plants are not durable against diseases and pests. When external conditions do not allow plant development, growing the plant in greenhouses provides advantages for both competition against other species and plant development. In soilless systems, the growing medium affects the plant length, dry and wet weights as well as crude fiber, protein, lipid and ash contents (Alu'datt et al., 2019). In soilless growing, certain organic and inorganic based media are used. Humic acid has effects such as inducing useful microorganisms in addition to the features of chelation, buffering, cation exchange capacity and nutrient ingestion in the growing medium (Abdel-Razzak and El-Sharkawy, 2013). Use of humic acid is preferred in soil and soilless plant growing due to its direct and indirect effects in plant development. In this study, effect of humic acid applications in peat and perlite mixtures of different ratios on plant development and certain chemical contents of purslane.

Material and Methods

Plant material and equipment

In the study, standard seeds of Salonica purslane species (Istanbul Seed) were used. The plants were grown under maximum/minimum temperatures of 26/15°C in greenhouse conditions. Plants were grown in plastic pots 50x20x17 cm in size and 11 liters in volume.

Growing medium

Different mixture ratios of perlite (Akper Mining Co., Çankiri/Turkey) and peat (Basissubsrat 2, Stender Group, Germany) medium was used in the study. These media are given below (*Table 1*).

Seeds were homogenously sown on the media filled to sowing pots with a calculation of 0.6 g per square meters on April 6. Following the sowing, seeds were coated with a covering material (peat) of 1 cm height. Plant development in pots was left to its natural course, and no number of plants was equalized.

http://www.aloki.hu ● ISSN 1589 1623 (Print) ● ISSN1785 0037 (Online)
DOI: http://dx.doi.org/10.15666/aeer/1906_44314441

Table 1. *Growing media and its contents*

Media	Contents
Medium 1	Peat (100%)
Medium 2	2:1 Peat:Perlite
Medium 3	1:1 Peat:Perlite
Medium 4	1:2 Peat:Perlite
Medium 5	Perlite (100%)

Humic acid applications and fertilizing

HumElit 18 (Kutahya Chemical, Turkey) humic acid of leonardite origin was used in the study. Humic acid was applied by providing irrigation water following the seed sowing. 0.1%, 0.2%, 0.3% and control solutions (water) of humic acid were used as testing factor and the prepared solutions were applied with a calculation of 2.500 cc per m^2. As chemical fertilizer, 10-8-10 kg of N-P-K (Nitrogen, Phosphorus and Potassium) was fertilized per decare. Nitrogenous (CAN- calcium ammonium nitrate) and potassic (potassium sulfate) fertilizers were used evenly in two times on the day of seed sowing and 15^{th} day respectively and phosphorus (TSP-triple superphosphate) fertilizer was applied once on the day of sow seeding. All cultural procedures such as weed removal and irrigation (twice a week) were duly performed till harvesting.

Harvesting of the plants

On 48^{th} day following the seed sowing (beginning of blooming), the plants were harvested from 1-2 cm above the root collar by means of a sharp knife. The following quality analyses were carried out on the harvested plants.

Plant yield: The harvested plants were weighed on scales of 0.01 precision and the yield was determined.

Shoot length: The distance between the butt and the growing end of 5 shoots randomly selected from each application was measured by ruler and the shoot length (cm) was determined accordingly.

Shoot diameter: The shoots were measured from 1 cm above their butt by means of digital caliper and the shoot diameter (mm) was determined by averaging these values.

Determining nitrate content: 5 grams of plant sample were crashed in a porcelain garlic press with distilled water. Inside of the garlic press was washed by using 100 ml purified water and drained into the volumetric flask with white band filter paper and thus the samples were diluted 10 times. 0.5 ml sample was taken into tubes from filtered agent and 1 ml 5% salicylic acid was added and the mixture was mixed in the vortex and then cooled. After adding 10 ml NaOH solution on it, the new mixture was also mixed in the vortex and then cooled. Then, the samples were read at a wavelength of 410 nm via the spectrophotometer and nitrate nitrogen of the plant was determined (Cataldo et al., 1975).

Determining oxalic acid values: The oxalic acid content was discovered via the spectrophotometer by Victoria Blue B indicator. 4 ml of paint solution, Victoria Blue B (1×10^{-4} mol/L) solution, potassium dichromate solution (0.030 mol/L) and sulfuric acid solution were taken and a mixture of 100 ml was obtained and this mixture was awaited under a water bath of 600 °C for 9 minutes after mixing it thoroughly and then cooled under tap water for 2 minutes. 20 hours before the reading, 0.05 grams of dry and ground purslane was put in plastic test tubes of 50 ml and 50 ml distilled water was added onto it. Half an hour before the reading, it was awaited in water bath (60 °C) for 10 minutes

http://www.aloki.hu ● ISSN 1589 1623 (Print) ● ISSN1785 0037 (Online)
DOI: http://dx.doi.org/10.15666/aeer/1906_44314441

and left for cooling. The filtrate was filtered with filter paper and then 3950 µl paint solution was added onto 50 µl sample taken from this filtrate. Then, the samples were awaited under a water bath of 60 °C for 9 minutes and oxalic acid was ensured to react with Victoria Blue B. Absorbance values of the samples cooled under running tap water were measured at a wavelength of 610 nm via the spectrophotometer without delay. Oxalic acid content was measured in $mg.g^{-1}$ dry weight through the regression equation obtained by standard oxalic acid solutions with the known concentrations prepared in the same manner (Yan et al., 2004).

Statistical analysis

The study was based on three repetitions according to the random plots trial design. The data were statistically analysed through JUMP packaged software. Each pot was considered to be an application repetition. The meaningful differences between applications and interaction values were determined to have a $p<0.05$ level of significance in LSD multiple comparison test. Since all interaction effects were found to be insignificant, application effects were discussed separately.

Results and Discussion

Plant yield

Effect of growing media and humic acid doses on plant yield of purslane given *Figure 1*.

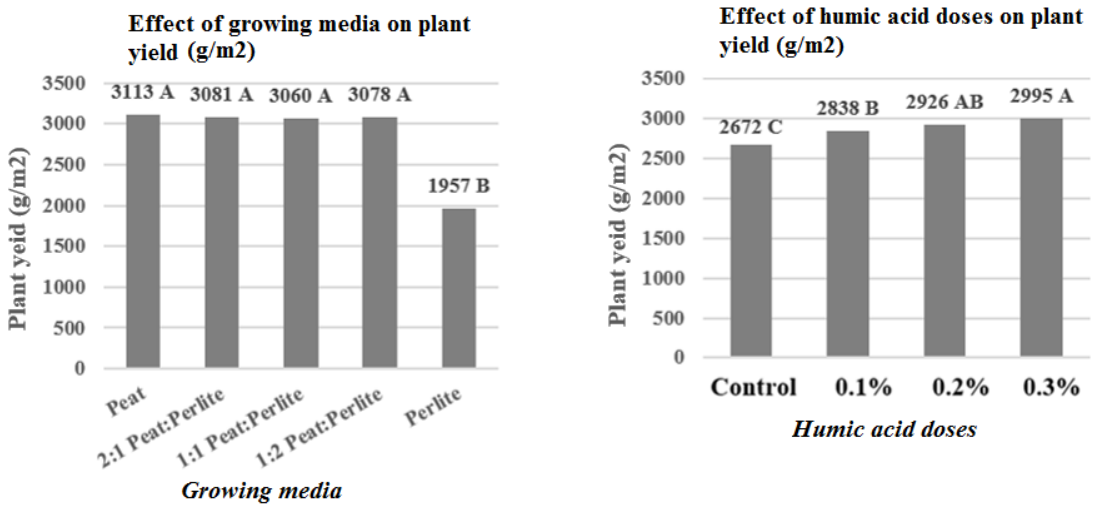

Figure 1. *Effect of growing media and humic acid doses on plant yield of purslane. Different letters on the column indicate significant differences at P< 0.05 according to LSD test*

In the study, growing media and humic acid doses led to changes in plant yields of the purslane plants. Scrutinizing the plant yields by growing media, all peat-containing mixtures were included in the same statistical group and had higher plant yields compared to the perlite medium. Plant yields of the plants growing in the perlite yield decreased by up to 36% compared to those grown in other growing medium. It was determined by Cros et al. (2007) in their studies testing the effects of different growing medium for purslane that plant yield decreased by 53% in the perlite medium compared to the peat medium.

http://www.aloki.hu ● ISSN 1589 1623 (Print) ● ISSN1785 0037 (Online)
DOI: http://dx.doi.org/10.15666/aeer/1906_44314441

Sezer and Ugur (2016) reported that the highest and lowest plant yields were obtained in peat medium and perlite medium respectively for the red sorrel plants grown in different growing media. Kaymak (2013) found out that plant yield of different nitrogen sources for the purslane varied between 1295 g and 1524 g per square meter. Similarly, Fontana et al. (2006) established that rational change and quantity of different nitrogen sources changed plant yield of purslane by 714-1807 g per square meter. Karkanis and Petropoulos (2017) reported that plant yield of purslane genotypes per square meter varied 1523 to 2800 g. In the previous studies, lower plant yields were found out for the perlite medium compared to organic growing medium in terms of growing of different vegetable species. It is considered that perlite is less effective for plant development compared to media of organic origin as it is an inert (chemically inactive agent) medium. Due to this reason, plant yield was identified to be lower in the perlite medium compared to peat and peat-mixture media. On the other hand, harvesting time is another factor affecting the plant yield of green vegetables. In our study, the plant was harvested on the 48th day following the seed sowing. Hence the purslane plants were harvested on the 20th day following the seed sowing in the study conducted by Fontana et al. (2006) which gave lower plant yield values. In the meantime, it is also possible for the ecology to affect the plant yield. Indeed, Oztekin et al. (2020) stated in their study that fertilization and temperature are effective in plant yield and earliness in purslane. The fact that the plant yield was determined to be 1295-1524 g per square meters in the study conducted by Kaymak (2013) in Erzurum province that has a harsher climate compared to Merzifon (Amasya) where we grew purslane indicates that the ecology directly affects plant development. Application doses of humic acid also affected the plant yields. As the application doses increased, so did the plant yields. A humic acid dose of 0.3% gave us the highest plant yield. As humic acid increases water and nutrient ingestion from the soil, positively affects the useful organisms on the soil, induces enzyme activities and growing hormones due to its general characteristics higher plant yield values were obtained by application of it (Ekinci et al., 2015).

Shoot length

Effect of growing media and humic acid doses on shoot length of purslane given *Figure 2*.

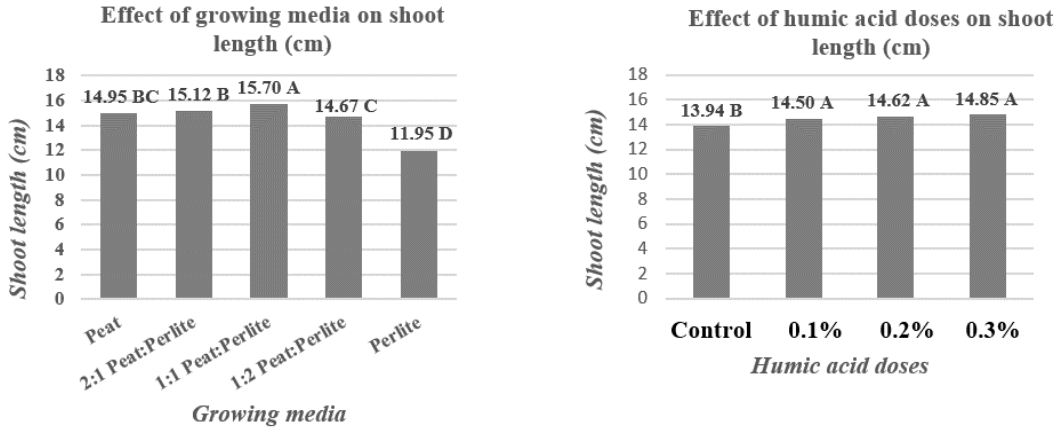

Figure 2. *Effect of growing media and humic acid doses on shoot length of purslane. Different letters on the column indicate significant differences at P< 0.05 according to LSD test*

http://www.aloki.hu ● ISSN 1589 1623 (Print) ● ISSN1785 0037 (Online)
DOI: http://dx.doi.org/10.15666/aeer/1906_44314441

It was observed that there were statistical differences in the shoot length of the purslane plants by the growing media and humic acid applications ($p<0.05$). Humic acid applications were included in the same group statistically and increased the shoot length compared to the control. The best results in terms of shoot length of the growing media were obtained from 1:1 peat/perlite mixture and it was identified that it yielded a shoot length approximately 31% higher than the perlite medium. Considering the shoot lengths in terms of growing medium, it was observed that the perlite medium and 1:1 peat/perlite medium yielded the worst and best results respectively. The peat medium and peat-containing media yielded higher shoot lengths compared to the perlite medium. This is not only related to peat but also caused by its ventilation and water retention properties compared to the perlite medium. Sezer and Ugur (2016) reported that the peat medium yielded increases up to 142-151% for the leaf stalk length of red sorrel compared to the perlite medium. This, as stated before, is related to the fact that peat is a medium of organic origin and allows using nutrients more.

Effects of the humic acid doses on the shoot length of the purslane plants were similar to those on plant yields. The lowest shoot length was determined in the control application and humic acid applications had an increasing effect on the shoot lengths. The shoot length tended to increase depending on the increase in humic acid doses but effects of the application doses were determined to be similar. However, humic acid applications were found out to be non-effective on the plant development. In such studies, causes such as the application method, inappropriate application doses and contents of commercial preparations might prevent observation of the anticipated effect. It is clear that humic acid has positive influence on the metabolism in terms of its general effects albeit varying by plant species. Scrutinizing the studies on the shoot lengths of the purslane, Egea-Gilabert et al. (2014) reported that the plant length varied 9.3 to 15.4 cm in commercial and local purslane genotypes. Palaniswamy et al. (2004) stated that the shoot length of the purslane was 27.4-30.7 cm and 41.3-44.3 cm in 8-leaf and 16-leaf phases respectively. Santos et al. (2016) found out that the plant length of purslane varied 10.2 to 20.4 cm by nitrogenous fertilizing. In our study, the shoot lengths were 11.35 to 15.81 cm. It was observed that our shoot lengths were lower compared to similar studies. Higher plant or shoot length values measured in other studies were caused by the fact that the plants bloomed and reached to full development phase in terms of plant lengths in such studies. As the shoots were harvested prior to blooming of the plants in our study, the plant shoots did not reach to their final forms.

Shoot diameter

Effect of growing media and humic acid doses on shoot diameter of purslane given *Figure 3*.

It was found out that the growing media and humic acid applications led to statistically meaningful changes in the shoot diameters of the purslane ($p<0.05$). 2:1 peat/perlite medium yielded the highest shoot diameter of 3.88 mm and the lowest shoot diameter of 2.98 mm was measured in the perlite medium. In our study, the shoot diameters of the purslane varied 2.87 to 4.17 mm. Petropoulos et al. (2015) stated in their researches on different purslane genotypes that the shoot diameter varied 6.21 to 10.65 mm. It is clear that these findings are much higher than the results of our study. This margin is caused by the fact that Petropoulos et al. (2015) measured the plants in the further growing phases of the plants. Scrutinizing the shoot diameter values by growing medium, the perlite medium yielded the lowest values as was the case in the shoot length. The peat/perlite

http://www.aloki.hu ● ISSN 1589 1623 (Print) ● ISSN1785 0037 (Online)
DOI: http://dx.doi.org/10.15666/aeer/1906_44314441

(2:1) mixture yielded the highest shoot diameter and it was followed by the peat and peat/perlite (1:1) mixture. As indicated by Cros et al. (2007), purslane's yielding the best and worst plant development results in the peat and perlite media respectively is consistent with our findings. The peat/perlite (2:1) mixture's yielding the highest shoot diameter might be caused by plants' growing a tad slower in the peat medium thanks to ventilation provided by perlite. Shoot diameter of the purslane was directly affected by the humic acid application. Humic acid applications ensured increases up to 10% in the shoot diameter values compared to the control. A humic acid dose of 0.3% yielded the highest shoot diameter value of 3.74 mm. Existence of more dominant/binding testing factors depending on the application purpose may prevent observing possible effects of humic acid. Hence, it was difficult to determine the effects of humic acid applications on germination due to higher germination results observed in the germination study conducted by the researches with a seed of stronger vigor.

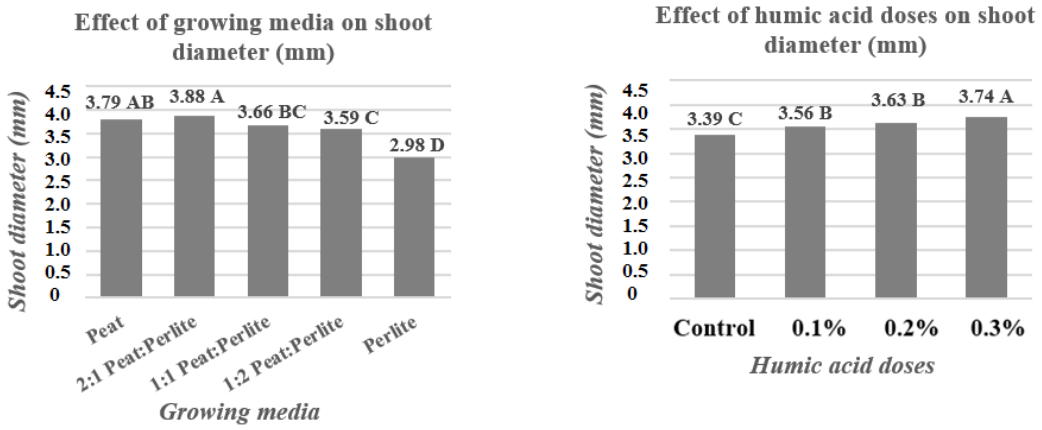

Figure 3. *Effect of growing media and humic acid doses on shoot diameter of purslane. Different letters on the column indicate significant differences at P< 0.05 according to LSD test*

Leaf oxalic acid values

Effect of growing media and humic acid doses on leaf oxalic acid values of purslane given *Figure 4*.

Humic acid application doses and growing media were determined to effect change of oxalic acid contents of the purslane plants ($p<0.05$). The lowest oxalic acid content was measured in control plants and the plants on which humic acid doses of 0.2% and 0.3% were applied yielded the highest oxalic acid content. These results are backed by the findings of Palaniswamy et al. (2004) indicating that oxalic acid content of purslane was higher by use of nitrate fertilizers and in early development phase of the plant. On the other hand, the researches stated that oxalic acid content of 622.5 mg/100 g in the leaves of plantlets was reduced down to 148.8 mg/100 g in case of late harvesting. Egea-Gilabert et al. (2014) found out that oxalic acid content of the purslane genotypes was 155-274 mg/100 g. It was established in the study conducted by Petropoulos et al. (2015) in Greece with 6 purslane genotypes that oxalic acid content was 371-753 mg/100 g. It was discovered in the study carried out by Kaskar et al. (2008) that the purslane genotypes of Turkish and Spanish origin had oxalic acid contents of 450.28-615.40 mg/100 g. Making a more general assessment, Moreau and Savage (2009) stated that oxalic acid content of vegetables, hard-shells, fruits and wild plants varied in a large range.

http://www.aloki.hu ● ISSN 1589 1623 (Print) ● ISSN1785 0037 (Online)
DOI: http://dx.doi.org/10.15666/aeer/1906_44314441

According to the statements of the researches, plants had oxalic acid contents varying by 225 to 1294 mg/100 g. The findings of our study seem to be consistent with Petropoulos et al. (2015). Similarly, the value of 622.5 mg/100g determined for early plant development by Palaniswamy et al. (2004) resembles to the findings of our study to a great extent. It is believed that the plants of Egea-Gilabert et al. (2014) yielded lower oxalic acid contents as they had higher biomasses at the harvesting time and their shoots had harder tissues. This belief is supported by the conclusion of "decreasing oxalic acid content in purslane in late harvests" (Palaniswamy et al., 2004). At the same time, the suggestion of Moreau and Savage (2009) regarding possible effects of growing conditions on oxalic acid content of purslane may help us explaining the effects of the growing medium. Although higher oxalic acid contents were measured for the plants grown in the peat medium providing faster plant development, lower oxalic acid content of the plants grown in 2:1 peat/perlite medium compared to those grown in 1:2 peat/perlite medium makes it more difficult to reach to a definite conclusion. We believe that increase in oxalic acid content of purslane depending on humic acid application doses is related to plant development rate. High doses of humic acid may cause a decrease in oxalic acid content, as the plants are in more active growth due to the increase in mineral and water uptake to the plant. The oxalic acid content determined by Moreau and Savage (2009) in plants growing under sunny (10.72 mg/g) and shady (12.34 mg/g) conditions partially supports our suggestion.

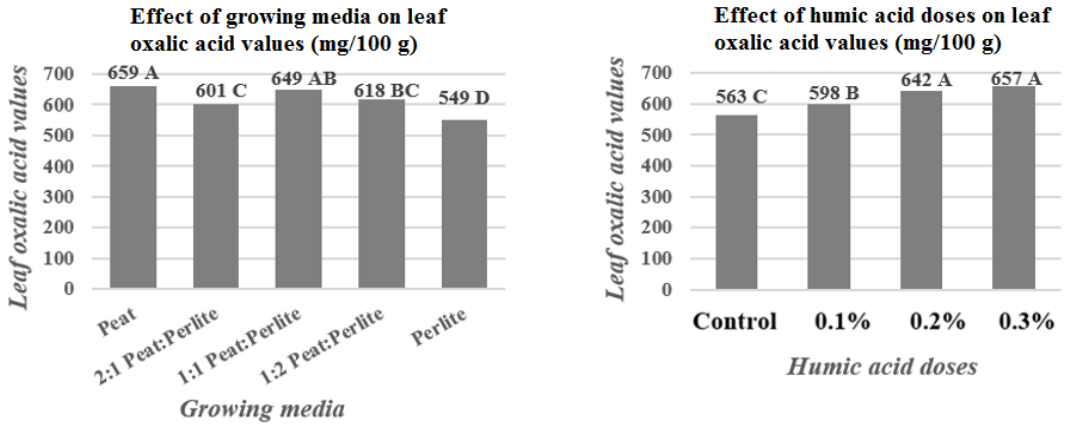

Figure 4. *Effect of growing media and humic acid doses on leaf oxalic acid values of purslane. Different letters on the column indicate significant differences at P< 0.05 according to LSD test*

Leaf nitrate values

Effect of growing media and humic acid doses on leaf nitrate values of purslane given *Figure 5*.

Although nitrate accumulation of purslane increased in direct proportion to the humic acid application dose, this increase was determined to be statistically insignificant. Considering the nitrate accumulation by growing medium, nitrate accumulation was measured to be lower in the peat-containing media. In our study, the plants grown in 1:1 peat/perlite medium yielded the lowest nitrate accumulation in terms of media. Corre and Breimer (1979) stated that purslane should be classified as a highly nitrogenous vegetable with its nitrate content higher than 2500 mg/kg in terms of wet weight. Kaskar et al. (2008) reported that the nitrate content varied 1285 to 2552.84 ppm

http://www.aloki.hu ● ISSN 1589 1623 (Print) ● ISSN1785 0037 (Online)
DOI: http://dx.doi.org/10.15666/aeer/1906_44314441

(128.5-255.28 mg/100 g) in the purslane genotypes of Turkish and Spanish origins. Egea-Gilabert et al. (2014) established a nitrate accumulation of 1.13-3.95 g/kg in the purslane. Franco et al. (2011) stated that the nitrate content of purslane under salty condition was 101.7-188.6 mg/100 g and nitrate content increased depending on the decrease in light exposure. On the other hand, Kaymak (2013) reported that nitrate content of purslane varied by nitrogenous fertilizer form and such fertilizers led to more nitrate accumulation in the plants compared to urea and ammonium fertilizers. In this study, nitrate content of the purslane was measured to be 123.2-143.5 mg/100 g. Our results seem to be a tad higher than the previous findings. We believe that nitrate accumulation was a bit higher in our study as it was carried out in April-May that had less light exposure compared to the summer months. The nitrate accumulation determined to be 144.3-243.3 mg/100 g according to the results of our study resembles to the results of the previous studies to a great extent.

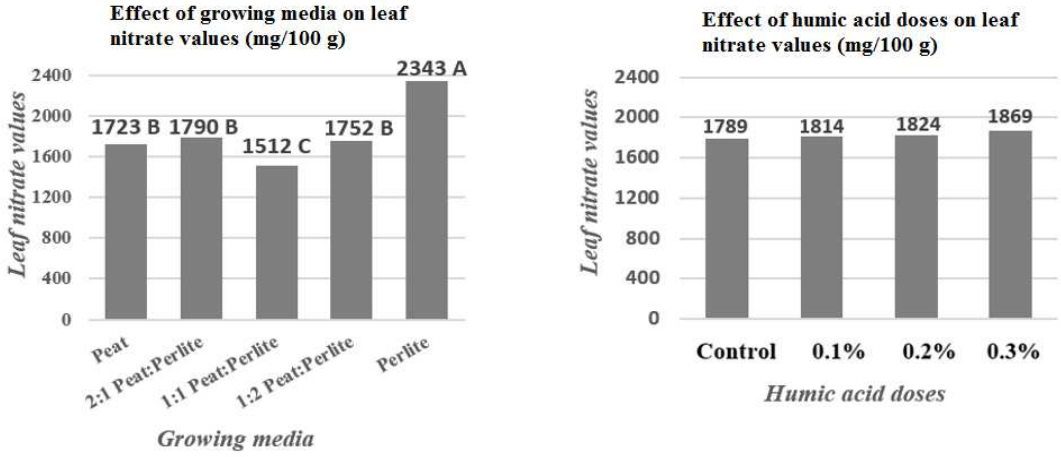

Figure 5. *Effect of growing media and humic acid doses on leaf nitrate values of purslane. Different letters on the column indicate significant differences at P< 0.05 according to LSD test*

Conclusions

In the study, no significant problem was observed for purslane growing under the greenhouse conditions of our region in terms of diseases and pests. As we grew these plants in a mid-season, plant development was affected and it was observed that the plants tended to bloom to create seeds as the temperature increased. Yield and leaf quality of the plants vary by the growing medium. The growing media other than 100% perlite produced similar yield values. 1:1 peat/perlite mixture stood out by its yield values, low nitrate and oxalic acid contents and certain quality parameters such as generating long and fresh shoots (lower shoot diameter). When the perlite medium, known for its chemical inertness, was used alone, worse yielding and quality results were obtained but it might be useful to use it as a growing medium for the soilless culture as it has positive effects in terms of low concentration, physical flexibility, low heat transmission and especially water retention and medium ventilation when used with peat. As a result of this study, use of 1:1 peat/perlite mixture as the growing medium and a humic acid dose of 0.3% for growing are recommended for agricultural sustainability, productivity and a healthy growing process. However, testing genotypes at higher humic acid doses according to different growing periods and harvest times may allow for a better understanding of the subject.

http://www.aloki.hu ● ISSN 1589 1623 (Print) ● ISSN1785 0037 (Online)
DOI: http://dx.doi.org/10.15666/aeer/1906_44314441

Acknowledgements. The authors thank the Ordu University Scientific Research Projects Coordination Unit for their support within the scope of the project numbered TF-1233.

REFERENCES

[1] Abdel-Razzak, H. S., El-Sharkawy, G. A. (2013): Effect of biofertilizer and humic acid applications on growth, yield, quality and storability of two garlic (*Allium sativum* L.) cultivars. – Asian Journal of Crop Science 5: 48-64.

[2] Alu'datt, M. H., Rababah, T., Alhamad, M. N., Al-Tawaha, A., Al-Tawaha, A. R., Gammoh, S., Ereifej, K. I., Al-Karaki, G., Hamasha, H. R., Tranchant, C. C., Kubow, S. (2019): Herbal yield, nutritive composition, phenolic contents and antioxidant activity of purslane (*Portulaca oleracea* L.) grown in different soilless media in a closed system. – Industrial Crops and Products 141: 111746.

[3] Cataldo, D. A., Haroon, L. E., Schrader, L. E., Youngs, V. L. (1975): Rapid colorimetric determination of nitrate in plant tissue by nitration of salicylic acid. – Communications in Soil Science and Plant Analysis 6: 71-80.

[4] Corre, W. J., Breimer, T. (1979): Nitrate and nitrites in vegetables. – Pudoc, Wageningen, Netherlands, p. 75.

[5] Cros, V., Sánchez, J. J. M., Franco, J. A. (2007): Good yields of common purslane with a high fatty acid content can be obtained in a peat-based floating system. – HortTechnology 17: 14-20.

[6] Dkhil, M. A., Abdel Moniem, A. E., Al-Quraishy, S., Saleh, R. A. (2011): Antioxidant effect of purslane (*Portulaca oleracea*) and its mechanism of action. – Journal of Medicinal Plant Research 5(9): 1589-1563.

[7] Egea-Gilabert, C., Ruiz-Hernández, M. V., Parra, M. A., Fernández, J. A. (2014): Characterization of purslane (*Portulaca oleracea* L.) accessions: suitability as ready-to-eat product. – Scientia Horticulturae 172: 73-81.

[8] Ekinci, M., Esringu, A., Dursun, A., Yildirim, E., Turan, M., Karaman, M. R., Arjumend, T. (2015): Growth, yield, and calcium and boron uptake of tomato (*Lycopersicon esculentum* L.) and cucumber (*Cucumis sativus* L.) asaffected by calcium and boron humate application in greenhouse conditions. – Turkish Journal of Agriculture and Forestry 39(5): 613-632.

[9] Fontana, E., Hoeberechts, J., Nicola, S., Cros, V., Palmegiano, G. B., Peiretti, P. G. (2006): Nitrogen concentration and nitrate/ammonium ratio affect yield and change the oxalic acid concentration and fatty acid profile of purslane (*Portulaca oleracea* L.) grown in a soilless culture system. – Journal of the Science of Food and Agriculture 86: 2417-2424.

[10] Franco, J. A., Cros, V., Vicente, M. J., Martínez-Sánchez, J. J. (2011): Effects of salinity on the germination, growth, and nitrate contents of purslane (*Portulaca oleracea* L.) cultivated under different climatic conditions. – The Journal of Horticultural Science and Biotechnology 86(1): 1-6.

[11] Karkanis, A. C., Petropoulos, S. A. (2017): Physiological and growth responses of several genotypes of common Purslane (*Portulaca oleracea* L.) under Mediterranean semi-arid conditions. – Notulae Botanicae Horti Agrobotanici Cluj-Napoca 45(2): 569-575.

[12] Kaskar, C., Fernández, J. A., Ochoa, J., Niñirola, D., Conesa, E., Tuzel, Y. (2008): Agronomic behaviour and oxalate and nitrate content of different purslane cultivars (*Portulaca oleracea*) grown in a hydroponic floating system. – Acta Horticulture 807: 521-526.

[13] Kaymak, H. C. (2013): Effect of nitrogen forms on growth, yield and nitrate accumulation of cultivated purslane (*Portulaca oleracea* L.). – Bulgarian Journal of Agricultural Science 19: 444-449.

http://www.aloki.hu ● ISSN 1589 1623 (Print) ● ISSN1785 0037 (Online)
DOI: http://dx.doi.org/10.15666/aeer/1906_44314441

[14] Moreau, A. G., Savage, G. (2009): Oxalate content of purslane leaves and the effect of combining them with yoghurt or coconut products. – Journal of Food Composition and Analysis 22: 303-306.
[15] Mousavi, S. R. J., Niazmand, R., Shahidi Noghabi, M. (2015): Antioxidant activity of purslane (*Portulaca oleracea* L.) seedhydro-alcoholic extract on the stability of soybean oil. – Journal of Agricultural Science and Technology 17: 1473-1480.
[16] Oztekin, G. B., Uludag, T., Tuzel, Y. (2020): Impact of nutrient solution concentration on baby leaf purslane production in floating system. – Acta Horticulture 1273: 65-74.
[17] Palaniswamy, U. R., McAvoy, R. J., Bible, B. B. (2000): Omega-3-fatty acid concentration in *Portulaca oleracea* is altered by nitrogen source in hydroponic solution. – Journal of the American Society for Horticultural Science 125(2): 190-194.
[18] Palaniswamy, U. R., Bible, B. B., McAvoy, R. J. (2002): Effect of nitrate: ammonium nitrogen ratio on oxalate levels of purslane. – Trends in New Crops and New Uses 11(5): 453-455.
[19] Palaniswamy, U. R., Bible, B. B., McAvoy, R. J. (2004): Oxalic acid concentrations in Purslane (*Portulaca oleraceae* L.) is altered by the stage of harvest and the nitrate to ammonium ratios in hydroponics. – Scientia Horticulturae 102(2): 267-275.
[20] Pandey, S., Pandey, A. (2015): Greenhouse technology. – International Journal of Research-Granthaalayah 3(9): 1-3.
[21] Petropoulos, S. A., Karkanis, A., Fernandes, A., Barros, L., Ferreira, I. C., Ntatsi, G., Petrotos, K., Lykas, C., Khah, E. (2015): Chemical composition and yield of six genotypes of common purslane (*Portulaca oleracea* L.): an alternative source of Omega-3 fatty acids. – Plant Foods for Human Nutrition 70(4): 420-426.
[22] Petropoulos, S. A., Karkanis, A., Martins, N., Ferreira, I. C. F. R. (2016): Phytochemical composition and bioactive compounds of common purslane (*Portulaca oleracea* L.) as affected by crop management practices. – Trends in Food Science & Technology 55: 1-10.
[23] Santos, R. V., Machado, R. M. A., Alves-Pereira, I., Ferreira, R. M. A. (2016): The influence of nitrogen fertilization on growth, yield, nitrate and oxalic acid concentration in purslane (*Portulaca oleracea*). – Acta Horticulture 1142: 299-304.
[24] Sezer, M., Ugur, A. (2016): The effect of growing medium and organic fertilizing on some yield properties of the sorrel (*Rumex acetosella* L.). – 6th International Conference of Ecosystems, June 2-6, Tirana, Albania.
[25] Simopoulos, A. P., Norman, H. A., Gillapsy, J. E., Duke, J. A. (1992): Common purslane: A source of omega-3 fatty acids and antioxidants. – Journal of the American College of Nutrition 11: 374-382.
[26] Yan, Z. Y., Xing, G. M., Li, Z. X. (2004): Quantitative determination of oxalic acid using victoria blue B based on a catalytic kinetic spectrophotometric method. – Microchimica Acta 144(1-3): 199-205.

http://www.aloki.hu ● ISSN 1589 1623 (Print) ● ISSN1785 0037 (Online)
DOI: http://dx.doi.org/10.15666/aeer/1906_44314441

MAPPING AND MONITORING OF URBAN SPRAWL TO PROMOTE SUSTAINABLE URBANIZATION USING GEOSPATIAL TECHNIQUES

KHAN, M. R.[1] – AMIN, M.[2*] – AHMAD, Z.[2] – SAGIN, J.[3]

[1]*School of Environmental Science, Charles Sturt University, Albury, Australia*

[2]*Institute of Geo-Information & Earth Observation, PMAS Arid Agriculture University, Rawalpindi, Pakistan*

[3]*The Environment & Resource Efficiency Cluster (EREC), Nazarbayev University, Nur-Sultan, Kazakhstan*

[*]*Corresponding author*
e-mail: m.amin@uaar.edu.pk

(Received 6th May 2021; accepted 29th Jul 2021)

Abstract. Urbanization is a global phenomenon, but in undeveloped countries like Pakistan, urban sprawl ratio has proliferated. Non-systematic development, increased migration, and sharp population growth have been predominant factors. These variables boosted the population and resulted in quickly built-up areas in the Peshawar district. The present research was to investigate spatial and temporal change in the urban sprawl from 2000 to 2018. Remotely sensed data and Maximum Likelihood Classification were used to investigate the urban sprawl. Remotely sensed data is fundamentally appropriate for providing information and characteristics for urban land cover on spatial and temporal scales. The results show that the total urban built-up areas were 54.39 km^2, 54.62 km^2, 64.64 km^2, 69.65 km^2 and 77.39 km^2 with annual growth rates of 0.084%, 3.06%, 1.43% and 3.3%, respectively, in 2000, 2005, 2010, 2015 and 2018. The overall accuracy of the classified imagery was 80 %. Our finding of analysis shows that major changes were detected in the built-up area of Peshawar during this 18-year time period. According to the Peshawar Development Authority report, in 2017 the total urban built-up area was 84km^2 while our analysis shows that the total built area was 77 km^2. The primary driving force for the development was education, health, and microeconomic centers, and the population shift to the Peshawar district from neighboring tribal regions because of military operations. It has been recommended that hyper spectral imagery would be useful for monitoring the urban expansion of larger cities.
Keywords: *predominant factors, spatial and temporal, remote sensing, Maximum Likelihood Classification, hyper spectral imagery*

Introduction

The term urban in Pakistan can be used when the population living in an area of any region is more than 5,000 persons, and they are subject to specific parameters including municipal services, socio-economic basis and access to basic facilities (Mehmood et al., 2016). The total urban population divided by the total population of the area is the formula to measure the urbanization of that region (Wen and Ren, 2017). Urban expansion is when the population expands outward from both the city and its suburb to peripheral areas to minimum-density as well as sometimes auto-dependent rural land growth (Gillham, 2002). In other words, urban expansion is the outer dispersion of urban areas to suburbs – meaning from a high bulk area to a low-density area. This urban sprawl happens due to the spread of the built-up areas onto the rural land (Foody, 2002; Jat et al., 2008).

Half of the world's population is living in metropolitan areas and cities. This ratio was about 33% in 1960 and is predicted to reach up to 70% by 2050 (Mehmood et al.,

http://www.aloki.hu ● ISSN 1589 1623 (Print) ● ISSN1785 0037 (Online)
DOI: http://dx.doi.org/10.15666/aeer/1906_44434457

2016). Globally, big cities in all developed and developing countries, have lost their green areas or forest lands due to the very rapid conversion of agricultural land into the built-up areas (Dadras et al., 2015).

The main factors which cause urban expansion are a high standard of living, living and property expenditures, a developed transportation system, and basic health facilities such as hospitals etc. (Solé-Ollé et al., 2008). In developing countries, the rapid and uncontrolled population growth causes serious complications, such as a shortage of a nutritious food supply, unplanned settlements, ecological issues, and smog, all of which destroy of natural structure the area (Sudhira et al., 2004).

Approximately one-third of Pakistan's population lives in big cities. Pakistan's urbanization rate has grown from 4.9 to 6.5% per year in the last 40 years. Between 1951 and 1991, the overall population grew by 236 percent, while the urban population rose by 49.5 percent. Urbanization has resulted in two mega-cities Karachi (estimated to be 8-10 million), Lahore (approximately 5 million) and six cities with residents of one million (Qadeer, 1996).

Unplanned urbanization is also causing a huge problem in Peshawar. Due to the migration of Afghan refugees and IDP's from tribal areas, rapid urbanization took place in Peshawar district and urban areas grew and extended rapidly (Raziq et al., 2016). Urban settlements have expanded, and new urban areas have emerged in newly urbanized areas including Regi Model Town, Hayatabad Township, and a number of local projects. The transformation of this agricultural land into the built-up area damaged the agricultural industry and caused food scarcity at the local level (Rahim et al., 2015a). The Peshawar Development Authority might need to create a better development management system as well as a plan with only a sustainable development goal.

The urban area of Peshawar district is growing very quickly in terms of both population as well as spatial development. Because of this rapid spread, a large number of difficulties have emerged. In this circumstance, this study will concentrate on the rapid growth and unplanned development and illegal encroachment. Because of the growth and expansion in the city area, the peripheral zone, and green belt or farming land has very rapidly converted into a built-up area. The rapid sprawl of urban areas has led to a swift rise in land and property values. The main objectives of this research were to study the spatial and temporal trend of urban sprawl of Peshawar and to find out the causes of urban sprawl and the role of RS and GIS for future planning.

Role of GIS and RS for sustainable urbanization

The application of RS and GIS offers an effective scientific method to detect trends in land-use and determine their effects on the environment, which cannot be supported by fieldwork, and monitoring approaches by the authorities. Instead of wasting money on traditional methods, national and city, governments should incorporate RS and GIS technology to evaluate the extent, growth rate, and direction of land-use shifts. The emergence of satellite imagery has introduced valuable information sources for all those interested in urban planning. Sustainable land development projects must be built to determine the future direction and the trends of urban development in order to reduce the amount of farmland losses through urban planning. Governments can then implement policies and ideas to tackle the uncontrolled growth of city extension. RS and GIS applications are strong tools to support the decision-making process for controlling urban development.

http://www.aloki.hu ● ISSN 1589 1623 (Print) ● ISSN1785 0037 (Online)
DOI: http://dx.doi.org/10.15666/aeer/1906_44434457

As a consequence, growing research attention has focused on mapping and measuring urban development using remote sensing (RS) and other approaches (Goetz, 2013). RS and GIS knowledge can be used proficiently in the investigation and cataloging of urban expansion and land use land cover changes as well as monitoring the growth of any city area (Shirazi and Kazmi, 2014). To monitor urban sprawl and to determine sustainable urbanization, precise and accurate data or information about urban sprawl patterns is needed (He et al., 2010). Remote sensing plays a vital role and technically efficient and widely used in the study of urban expansion. Over the last few years, remote sensing technologies have emerged, especially because of their low cost, broad spatial swath width, temporal resolution and powerful data acquisition capability. Thus, urban researchers and urban planners have been urged to use remote sensing data to track Spatio-temporal Land Use Land Cover (LULC) variation and city area growth (Seilheimer et al., 2007). For example, the application of Geo-informatics and remote sensing in studies of urban expansion in China have provided more effective and better results when gathering urban land use information (Zeng et al., 2008).

Materials and methods

Study area

Peshawar is one of the oldest and largest capital cities of Khyber Pakhtunkhwa. The Peshawar district is situated in the wide-ranging valley of Peshawar close to the eastern end of the historic Khyber Pass. *Figure 1* represents the location map of the study area, Peshawar lies, 33° 41′ to 34° 12′ North latitude, and from 71° 27′ to 71° 47′ East longitude. The Peshawar district occupies a total land area of about 1,255 km^2. Winter season usually occurs from the middle of November until mid-March. Summer runs from May until September. The local economy is supplemented by agricultural processing, manufacturing and industry. It is the regional epicenter for commercial and educational organizations and other utilities of the province. In the 1961 census report, 29% of the total urban population lived in Peshawar district. According to the 1998 census report, 33% of the population was found in urban areas of Peshawar as compared to the total population (PCO, 1998). After 1978, the relocation of Afghan migrants triggered the urban growth rate in the Peshawar city and in the 1998 census, the population reached 2.01 million without Afghan refugees (Turton and Marsden, 2002). Another factor seems to be that the sex ratio is 106.5 while the annual growth rate was 4% between 1998-2017. As well, a number of dynamic business activities play a vital role in the expansion of the city (PCO, 2017).

Data collection and processing

Data collection was obtained from both primary and secondary sources. Remotely sensed multispectral satellite imagery of the 30 ×30 m spatial resolution Landsat series was downloaded from the United States Geological Survey (USGS; http:/landsat.usgs.gov) for the corresponding path (151/) row (36 and 37) for the Peshawar district. The images were downloaded for the year 2000, 2005, 2010,2015 and 2018. The secondary data included detailed population information of the Peshawar district from 1998 and 2017 census reports. The methodological flow chart of the study is shown in *Figure 2*.

http://www.aloki.hu ● ISSN 1589 1623 (Print) ● ISSN1785 0037 (Online)
DOI: http://dx.doi.org/10.15666/aeer/1906_44434457

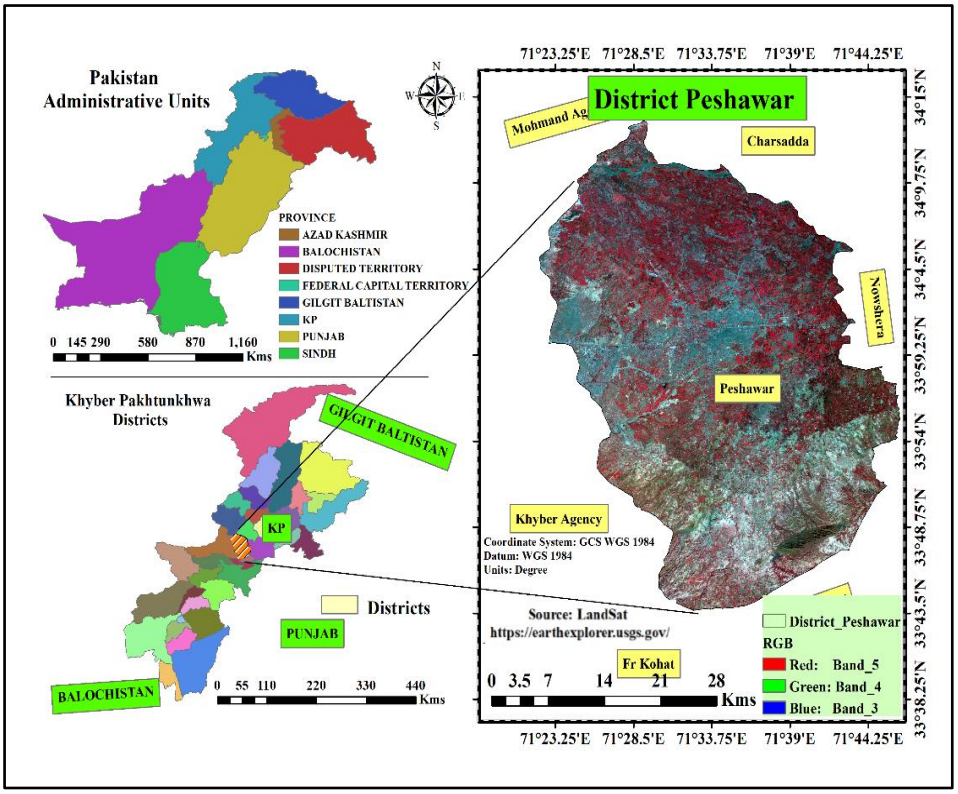

Figure 1. *Locational Map of Peshawar District*

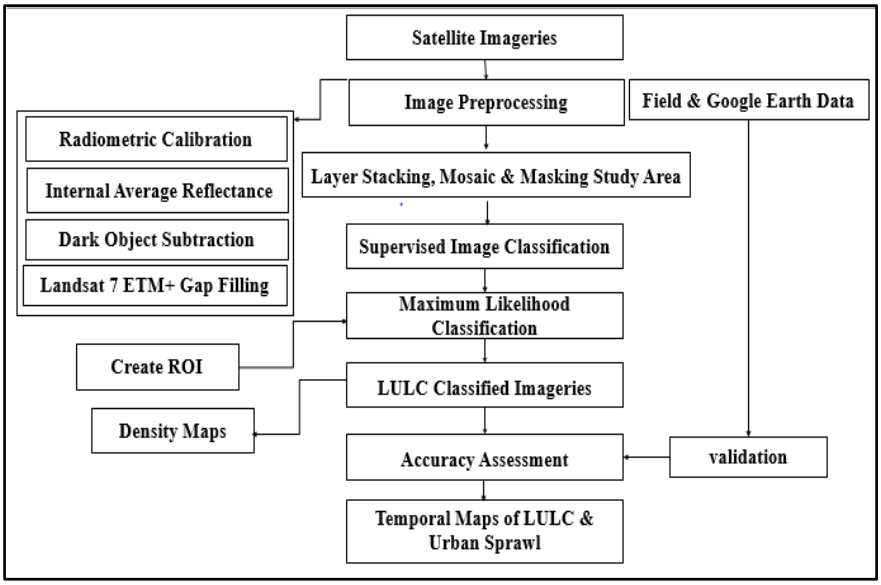

Figure 2. *Flow Chart of Methodology*

First of all, the atmospheric correction was implemented by using radiometric correction, gap filling, IAR reflectance, and DOS technique to bring entire images to common reference spectral characteristics by using ENVI classic 5.3 software (ENVI Version, 2009). Then, GIS was used to evaluate patterns and trends of land use in order

http://www.aloki.hu ● ISSN 1589 1623 (Print) ● ISSN1785 0037 (Online)
DOI: http://dx.doi.org/10.15666/aeer/1906_44434457

to understand variations in urban development. The study area was masked from images with help from the territorial boundary of the Peshawar District. Satellite images have been analyzed in depth to evaluate possible land use classes. Five distinguishable land use classes were recognized and named: urban/built-up, vegetation, barren land, water bodies and areas under shadow regime (*Table 1*). Supervised classification using the MLC algorithm was performed for the categorization of multiple images (Ahmad and Quegan, 2012). The inherent problem in MLC techniques such as mixing between barren and built-up was addressed by the texture difference between the buildup class and the barren land class. Built-up area has rough texture while barren land has a smooth texture. Also, some random polygon samples of built area were taken on google earth to correlate with classified imageries of Landsat, which was classified through MLC. To improve the classification accuracy, a knowledge-based expert method was used for post-classification improvement of primary classified images (Foody, 2002; Zeng et al., 2008). The accuracy assessment of classified images was completed using field data. For the year 2018, 100 points were collected during the study area survey. More than 75 points for each year were randomly created on classified images of different years and validated with Google Earth for the years 2000, 2005, 2010 and 2015 complete detail are in *Table 2*. Finally, an error matrix was created. Maximum likelihood classification was applied to extract classified images and to map urban extensions over a period of 18 years.

Table 1. *Different Land Use Land Cover description*

Class Name	Description
Urban/built-up	built-up, commercial and service area, manufacturing, transportation etc.
Agriculture farms	Cropland, agricultural farms, greenhouses other trees, etc.
Bare land	Bare and exposed areas and soil
Water bodies	Rivers, canals and water ponds
shadow regime	areas under terrain shadow and low elevation as compared to surrounding area

Results and discussion

Results obtained from image analysis in *Figure 3* show the amount of change over the 18-year period, where a significant portion of the agricultural and barren land was converted into the built-up area.

Built-up area

To estimate the probable land use classes, satellite images were thoroughly examined (Fonji and Taff, 2014; Mahboob and Iqbal, 2015), by using Arc Map software, we were able to estimate LULC temporal change for various years. This included approximately 195.71 km^2 in 2000, 281 km^2 in 2005, 251 km^2 in 2010 and then an increase to 483 km^2 in 2015 while in 2018 it covered 511 km^2 of the Peshawar District (see *Figure 3* below). *Figure 4* represents the Land use /Land cover classes of Peshawar district. Urban sprawl occurred in all directions from the main city, but most growth was directed south and west at the ring road and Chamkani Peshawar. Most growth was in town 3 and town 4. The built-up area increased along the main road network of Peshawar city. This increase was due to either people affected by the flood in 2010 or the approximately 2.5 million Afghani Refugees who migrated to Pakistan during the Soviet Union attack on Afghanistan from 1979 to 1989 (Turton and Marsden, 2002). From 2009 to 2012, there

http://www.aloki.hu ● ISSN 1589 1623 (Print) ● ISSN1785 0037 (Online)
DOI: http://dx.doi.org/10.15666/aeer/1906_44434457

were around 3 million IDPs (Internally Displaced Persons) in Khyber Pakhtunkhwa (KP) mainly coming from the districts of Federally Administered Tribal Areas (FATA). In addition, one million people were relocated inside because of the flooding and about 5 million from Military operations against militants or Taliban in FATA. The number of IDP registered in KP was more than 3 million from 2009 to 2010 and it further increased from three lakhs up to seven lakhs in KP at the end of 2012. Nearly 43% of the registered IDPs lived in Peshawar (Roehrs, 2015). As indicated by the trend recorded in the 2017 census during the last period of 20 years, the rate of urban growth has accelerated in recent years. A socio-economic factor is one of the main causes of urban sprawl in Peshawar. Peshawar is Khyber Pakhtunkhwa's largest city, a major commercial and economic hub, and an integral role of the province's economy. Historically, Peshawar served as a gateway to Central Asia for traders and visitors (PCO, 2017).

Table 2. *Overall percentage accuracy of the image classification of Peshawar derived from Landsat*

Landsat ETM+ 2000 (classification accuracy: 86.67%)					
	Built-Up	Vegetation	Barren land	Water Bodies	Shadow Regime
Built-Up	12	00	03	00	00
Vegetation	00	21	04	00	00
Barren land	01	01	27	01	00
Water Bodies	00	00	00	03	00
Shadow Regime	00	00	00	00	02
Landsat TM+ 2005 (classification accuracy: 81.33%)					
	Built-Up	Vegetation	Barren land	Water Bodies	Shadow Regime
Built-Up	14	01	03	00	00
Vegetation	01	20	02	00	01
	01	03	25	00	01
Water Bodies	00	00	01	02	00
Shadow Regime	00	00	00	00	00
Landsat TM+ 2010 (classification accuracy: 82.66%)					
	Built-Up	Vegetation	Barren land	Water Bodies	Shadow Regime
Built-Up	22	00	03	00	00
Vegetation	02	16	02	00	00
Barren land	01	02	17	00	01
Water Bodies	00	01	00	05	01
Shadow Regime	00	00	00	00	02
Landsat OLI+ 2015 (classification accuracy: 80%)					
	Built-Up	Vegetation	Barren land	Water Bodies	Shadow Regime
Built-Up	25	02	03	00	00
Vegetation	02	05	02	00	00
Barren land	02	01	29	00	01
Water Bodies	00	01	00	01	00
Shadow Regime	00	00	00	00	01
Landsat OLI+ 2015 (classification accuracy: 90%)					
	Built-Up	Vegetation	Barren land	Water Bodies	Shadow Regime
Built-Up	28	00	02	00	00
Vegetation	03	37	02	00	00
Barren land	00	03	20	00	00
Water Bodies	00	00	00	04	00
Shadow Regime	00	00	00	00	01

http://www.aloki.hu ● ISSN 1589 1623 (Print) ● ISSN1785 0037 (Online)
DOI: http://dx.doi.org/10.15666/aeer/1906_44434457

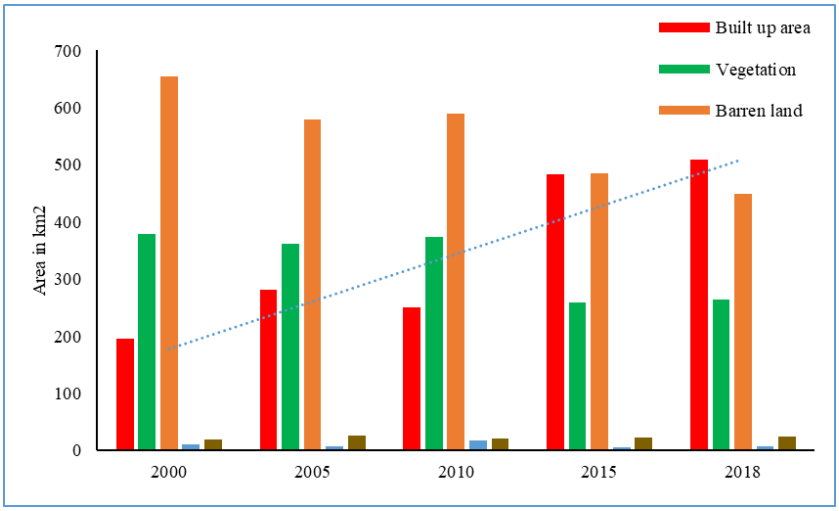

Figure 3. *LULC Change in District Peshawar 2000-2018*

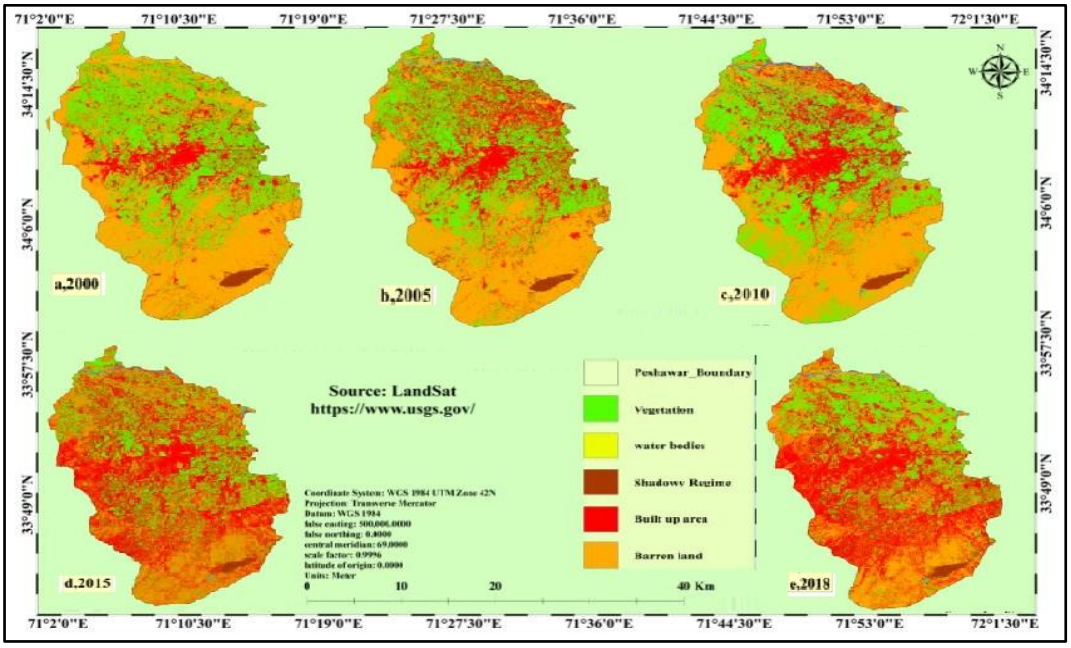

Figure 4. *LULC Classification of Peshawar District (a) 2000, (b) 2005, (c) 2010, (d) 2015, (e) 2018*

Agricultural farms

The study showed a huge decrease in the available agricultural land within the Peshawar district. The area of farmland was 379 km^2 in 2008, 361 km^2 in 2005, 373 km^2 in 2010 and it further decreased down to 259 km^2 in 2015, while a minor increase of 04 km^2 occurred in 2018. Ghaffar stated that the frequency of land loss due to urban development has been rising at an alarming rate, so it needs to be managed and monitored (Ahmed Khan Jatoo et al., 2016).

http://www.aloki.hu ● ISSN 1589 1623 (Print) ● ISSN1785 0037 (Online)
DOI: http://dx.doi.org/10.15666/aeer/1906_44434457

Barren land

The results of this study show that the barren area declined from 655 km^2, 578 km^2, 590 km^2, 485.47 km^2 as well as 448.59 km^2, respectively in 2000, 2005, 2010, 2015 and 2018. One significant decline in this class was 115 km^2 while in total, barren land was reduced by 207 km^2 in the 18-year period from 2000 to 2018.

Most of the land use for urban development was empty space in the town and leftover land between adjacent buildings. Eventually, the forested areas have also been transformed into the built-up zone (Ahmad and Goparaju, 2016).

It is clearly observed that in Peshawar, a decline in agricultural and barren land is due to the development of buildings, roads, houses and new residential communities in these areas.

Water bodies and shadow regime

Figure 3 also indicates that the total land area occupied by water class has a mixed value from 2000 to 2018, but there was a 07 km^2 increase in 2010 due to massive flood occurrences in Peshawar. However, after the flood, a rapid decline occurred. Similarly, the shadow regime area of approximately 24 km^2 covered the southern part of the Peshawar district.

Figure 3 shows the results for LULC in Peshawar district from 2000 to 2018. Results show that the built-up area extends from 195.71 km^2 to 281 km^2 between 2000 and 2005, while a 30 km^2 decrease occurred in 2010 due to the devastating floods of 2010. The built-up area increased by almost 232 km^2 in the five years from 2010 to 2015. A considerable decrease occurred during 2000 – 2018 in vegetation and barren land by 115 km^2 and 207 km^2, respectively. While water bodies covered 0.15 km^2 and the area under shadow cover was zero km^2 in 2000. In 2005, the built-up area covered 54.62 km^2, which increased by 10 km^2 in 2010. The built-up area further increased to 69.65 km^2 in 2015. The built-up area rapidly increased in the next three years to 77.39 km^2 (2015 to 2018).

The transformation of agricultural land into urban use may create a number of issues including political, cultural, environmental as well as social insecurity (Peerzado et al., 2018).

The built-up area has rapidly increased due to the growth of the indigenous population and the migration of people from rural areas to urban centers as shown in *Figure 4*. The trend line shows increase in built up area of Peshawar city which is the strong evidence of urban expansion in Peshawar city. This migration of Afghan refugees and people from the tribal regions due to the Taliban insurgency played a vital role in Peshawar city expansion and urban sprawl. In 2009 to 2012, there were around 3m IDPs in KP, mainly from other areas of KP Province and some districts of FATA (Roehrs, 2015). An additional 19m people have been moved inside by the flooding and earthquakes as about 5m by the armed fight against militants or Taliban in FATA and some districts of KP. The number of IDP register in Khyber Pakhtunkhwa over 3m from 2009 to 2010, currently, the number of registered IDP's was 774,594 in KP at the end of 2012. Nearly 43% of registered IDPs lived in Peshawar (Roehrs, 2015).

Each of the Classified Map was matched with positional or field data to evaluate the accurateness of the classified image that is done with the supervised classification algorithm. The reference data were used for data organized by collecting through a random sample method with the help of field information and Google earth application

http://www.aloki.hu ● ISSN 1589 1623 (Print) ● ISSN1785 0037 (Online)
DOI: http://dx.doi.org/10.15666/aeer/1906_44434457

to detect the particular location of the point and compare the classified accuracy with historical imageries of google Earth of Peshawar district. While for year of 2018, detail filed survey was conduct. *Table 2* represents the overall accuracy of district Peshawar imagery Classification of the 2018 year was 90%. User accuracy for built-up area class, vegetation, bare land, and water class as well as the Shadow regime were 93.33%, 88.10%, 86.96%, and 100%, respectively. While Producer Accuracy for the above same classes were 90%, 92%, 83%, 100% and 100% for the 2018 year of District Peshawar.

For the maximum likelihood classification for Peshawar district, in *Figure 5* shows the urban areas in 2000, 2005, 2010, 2015 and 2018. In 2000, the total area covered by Peshawar city was 93 km^2. In which, 54 km^2, 12 km^2, and 26 km^2 was covered by urban/built-up, Vegetation, and barren land, respectively. Linear line represents the built-up growth trend from the year of 2000 to 2018 respectively.

Figure 5. *Temporal Change in land use and land cover in Peshawar city*

As Raziq et al. (2016) stated, significant changes were noted in the region under development areas were grew steadily by 26.59 percent, but there was a significant decline in agricultural and barren land between 1999 and 2016.

In 1998, population census data was available, showing a 3.29 percent annual growth rate. For 2000, 2005, 2010, and 2015, the population was estimated using the annual growth rate and census data from 1998. Then, using 2017 census data and a 3.99 percent annual growth rate, estimate the population for 2018. A hypothetical linear trend between the five interval census years is represented by the diagonal line which shows increases in population in the Peshawar city (DCR, 2017) (*Figure 6*).

The overall patterns and variations of land-use change in Fez have been analyzed by categorizing the area of land that has been changed from forest and agricultural land to land used for residential areas (El Garouani et al., 2017). *Figure 7* shows that most of the urban growth in the Peshawar district was unplanned. About 70% of the cultivated land area and 50% of barren land were lost in the 18-year time period (2000-18). This loss was due to rapid and unplanned urban growth in Peshawar. Therefore, supposing the decline of farming land continued at the same rate, the remaining 4% of Peshawar urban cultivated land would probably reach zero in the next few years. *Figure 7* demonstrates the loss of different land use land cover types in the 18 years from 2000 to 2018 because of urban sprawl. This will possibly destroy and reduce the limited farming lands, water assets, and biodiversity in the study area. The total planned area of district Peshawar is

http://www.aloki.hu ● ISSN 1589 1623 (Print) ● ISSN1785 0037 (Online)
DOI: http://dx.doi.org/10.15666/aeer/1906_44434457

30.99 km^2 which includes, Hayatabad Sector, Peshawar Cantonment, and the University of Peshawar having an area of 13.35 km^2, 3.64 km^2, and 4.00 km^2, respectively.

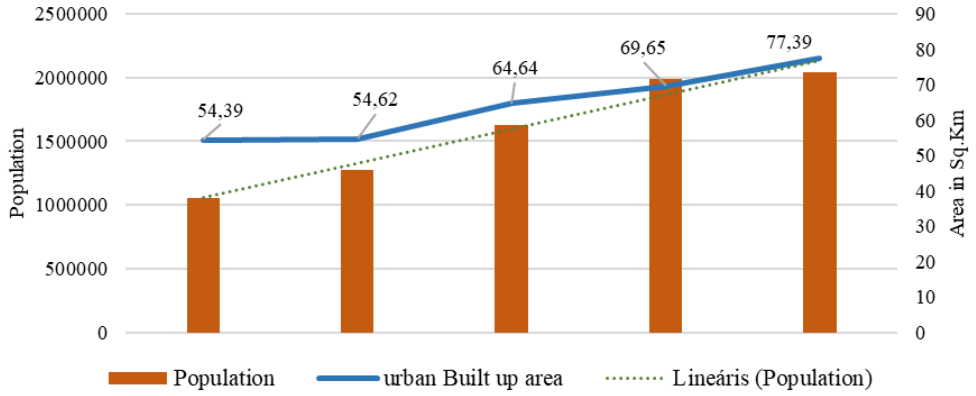

Figure 6. *Temporal Change in land use and land cover in Peshawar city*

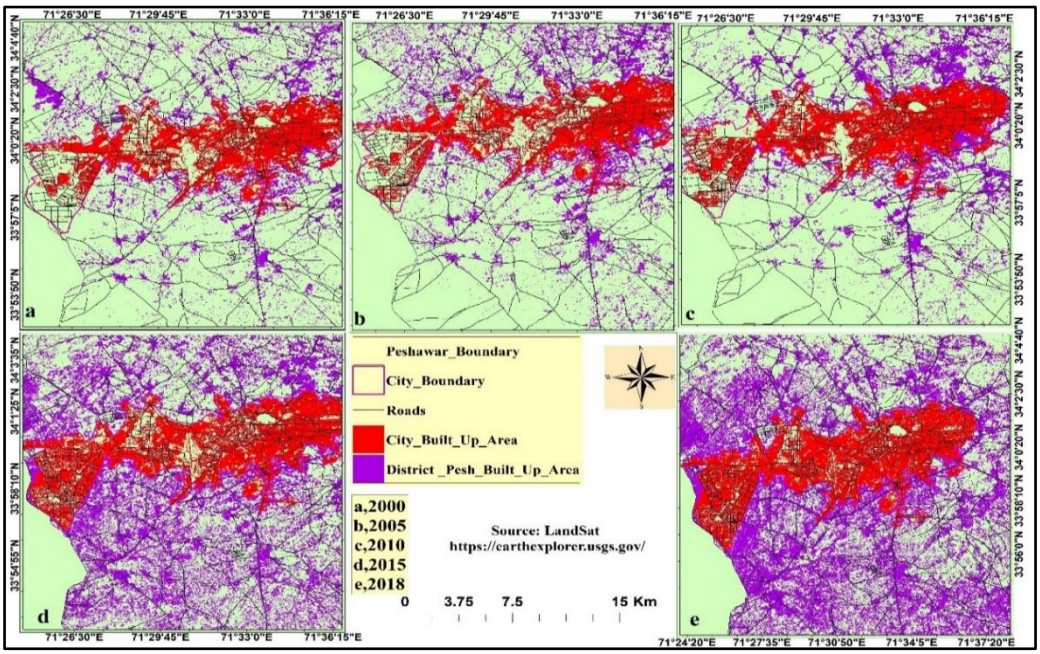

Figure 7. *Built-up area expansion in the last 18 years in different direction in the Peshawar city*

The statistic results from the calculation of temporal change in land use land cover shows that the built-up area has been growing at an annual growth rate of 0.084%, 3.06%, 1.43% and 3.33% during the periods of 2000–2005, 2005–2010, 2010-2015 and 2015-2018, respectively in the Peshawar city with interval of five years but from 2015 to 2018 for three years (*Table 3*). *Table 4* shows the detail change matrix i.e. the nature of change from one class to another class during 2000-2018.

For urban expansion in the city of Peshawar KP using multi-temporal Landsat data, classification findings indicate that over the last two periods, major increases occurred in the built-up area while there was a rapid decline in agricultural and barren land (Raziq et al., 2016).

http://www.aloki.hu ● ISSN 1589 1623 (Print) ● ISSN1785 0037 (Online)
DOI: http://dx.doi.org/10.15666/aeer/1906_44434457

Table 3. *Inter-censual growth rate of urban area of Peshawar*

S.No	Years	Change (Km^2)	Change % age	Time Span	Growth Rate
1	2000-2005	0.23	0.42	5 year	0.084
2	2005-2010	10.02	15.34	5 year	3.06
3	2010-2015	5.01	7.19	5 year	1.43
4	2015-2018	7.79	10	3 year	3.33

Table 4. *Change matrix from one class to another class during 2000-2018*

LULC Classes	2000		2005		2010		2015		2018	
	UL	C or DL	UL	C or DL	UL	C or DL	UL	C or DL	UL	C or DL
Built up	54.39	195.71	54.62	281	64.64	251.01	69.65	483.87	77.39	509.66
Vegetation	379.18	12.02	361	14.63	373.03	5.59	247.3	6.73	243.85	3.87
Barren Land	651.06	26.49	578.28	23.75	590.01	23.11	485.47	16.71	448.59	12.11
water Bodies	10.8	0.15	8	0	17.12	0.11	5.35	0	6.46	0
Shadow Regime	17.71	0.07	25.87	0.01	21.3	0	23.25	0	39.23	0

LULC: Land Use & Land Cover, UL: At Urban Level, C or DL: At City or District Level

Built-up area densities of Peshawar city

Map density values are calculated by dividing the number of built-in pixels to the actual number of pixels in the kernel. It converts the land cover class to a density category when applied to a classified satellite image (see *Figure 8*). Based on the density scale, it can be additionally classified into low (<20), low medium (21-40), medium (41-60), medium high (61-80) and high-density (>81) % built up area (*Fig. 8*). On this basis, the relative percentage of each class was calculated. The calculation of the built-up density resulted in the distribution of high, medium-high, medium and low-medium and low-density groups in Peshawar city. The high density of built-up areas may denote the compact and more clustered form of the built-up pattern, followed by the medium high class, whereas medium density would refer to the comparatively less dense built-up areas. Low medium class and low density of broadly and sparsely spaced built-up zones also exist. In *Figure 8*, the red and blue colors represent a high and medium high-density category, which expanded rapidly from 2000 to 2018, especially in the south-west direction. This was likely due to the development of road and transportation networks and the small industrial area in the city.

Major causing factors of urban sprawl in Peshawar

In comparison to demographic figures of the district, the 1998 census report total population was 2,019,000 while in the 2017 census total population of Peshawar was 4,269,079 (DCR, 1998, 2017). Urban development also refers to many relevant factors such as construction, transportation, sanitation system, deforestation, water supply as well as industrial processes. Such factors are directly or indirectly related to the urban extension, there are 2018 public and private schools, 616 public and private universities respectively. There 18 major public as well as a private hospital and 52 dispensaries (Saleem Adnan, 2017).

http://www.aloki.hu ● ISSN 1589 1623 (Print) ● ISSN1785 0037 (Online)
DOI: http://dx.doi.org/10.15666/aeer/1906_44434457

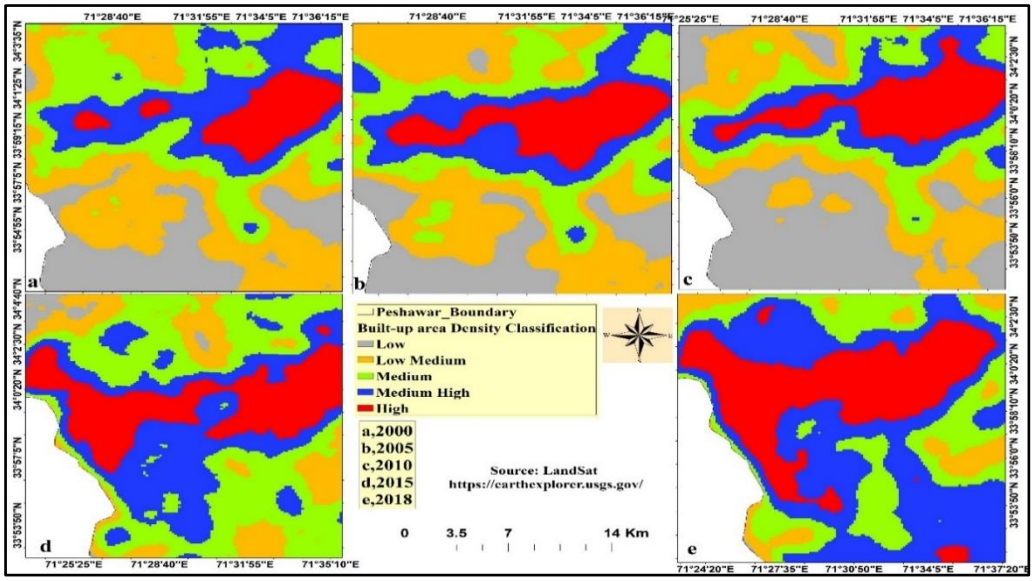

Figure 8. *Classification of built-up area densities of Peshawar city*

Three million afghan refuge migrated to Peshawar in 1979 due to country war and terror situations (Turton, 2000), where 31,284 registered families were still living in Peshawar. From 2009 to 2012, approximately 3 million IDPs migrated from different areas of the KPK Province to Peshawar and some districts of FATA. An additional 19 million people have been moved inside by the flooding and earthquakes. About 5 million were migrated due to armed fight against militants or Taliban in FATA and some districts of KPK (Roehrs, 2015).

Conclusions

Various local administrations, particularly those at the urban level, do not have a team of professionals that can observe land expansion that is quickly taking place all over Peshawar city. By using the combination of RS data and GIS techniques to analyze the nature, growth rate and location of land-use variations, local governments can recognize cities and towns that are overtaking a lot of valuable agricultural and cultivated land. They can then formulate strategies and guidelines to deal with such uncontrolled development. The integration of RS and GIS is a powerful tool and decision-support system for urban development. Remote sensing and GIS provide an effective and systematic way to monitor land-use variations and estimate their influences on the environment, which cannot be provided by fieldwork and government reporting methods. It has been found that the increase in built-up area over several 5-year intervals was 0.42%, 15.34%, 7.19% and 10% from 2000 to 2005, 2005 to 2010, 2010-2015 and 2015 to 2018, respectively. Urban sprawl is mainly seen in the western and southern parts of Peshawar city along the roadside. The westward increase was mainly due to Afghan refugees, IDP's from tribal territories and hazardous floods in the northern part of Peshawar. The study found that many buildings and built-up sites were developed on valuable good quality cultivated and barren land. As food supply is a chief factor of sustainable expansion, it is essential to ensure that unwarranted urban growth can be prevented as much as possible on valuable agricultural land. The results acquired from this Landsat imagery show that the land cover

http://www.aloki.hu ● ISSN 1589 1623 (Print) ● ISSN1785 0037 (Online)
DOI: http://dx.doi.org/10.15666/aeer/1906_44434457

type arrangement of an urban area and highly urbanized areas can be effectively identified using a carefully built methodology for image analysis. This technique should be applied at a global scale, given its dependence on moderate spatial resolution image data and the combination of standard image processing procedures. Changes in the composition can also be identified over time as a basis for analyzing the complexity of urban development, but the precision of this analyzes depends heavily on the quality of the original images of the forms of land cover. Furthermore, other causal factors, such as socio-economic conditions, government funding for public projects, the extent of industrialization, barriers and distances from major locations, can also be considered in future research for urban sprawl modeling. To mitigate the amount of agricultural loss from urbanization, a sustainable land development strategy that guides the future direction and trend of urban growth needs to be implemented.

The study's results have conceptual and methodological significance; future research will focus on the entire city of Peshawar, as well as the environmental and socio-ecological aspects of urban sprawl. This future research study will help in urban planning and the development of a sustainable metropolis in Khyber Pakhtunkhwa, Pakistan. This will help to establish a sustainable strategy to protect useful agricultural land from urbanization and to organize the time and geographical coordinates of urban development.

REFERENCES

[1] Ahmad, A., Quegan, S. (2012): Analysis of Maximum Likelihood Classification Technique on Landsat 5 TM Satellite Data of Tropical Land Covers. – 2012 IEEE Conference, pp. 280-285.

[2] Ahmad, F., Goparaju, L. (2016): Analysis of Urban Sprawl Dynamics Using Geospatial Technology in Ranchi City, Jharkhand, India. – Journal of Environmental Geography 9(1-2): 7-13. https://doi.org/10.1515/jengeo-2016-0002.

[3] Ahmed Khan Jatoo, W., Chen, J. F., Saengkrod, W., Mastoi, A. G. (2016): Urbanization in Pakistan: Challenges and Way Forward (Options) For Sustainable Urban Development. – Proceedings of the 4th International Conference on Energy, Environment and Sustainable Development (EESD 2016). http://eesd.muet.edu.pk/sites/default/files/imagecache/EESD_2016_paper_243.pdf.

[4] Dadras, M., Shafri, H. Z. M., Ahmad, N. (2015): Spatio-temporal analysis of urban growth from remote sensing data in Bandar Abbas city, Iran. – The Egyptian Journal of Remote Sensing and Space Sciences 18(1): 35-52. https://doi.org/10.1016/j.ejrs.2015.03.005.

[5] El Garouani, A., Mulla, D. J., El Garouani, S., Knight, J. (2017): Analysis of urban growth and sprawl from remote sensing data: Case of Fez, Morocco. – International Journal of Sustainable Built Environment 6(1): 160-169. https://doi.org/10.1016/j.ijsbe.2017.02.003.

[6] ENVI (2009): ENVI User's Guide. – Pennsylvania State University.

[7] Fonji, S. F., Taff, G. N. (2014): Using satellite data to monitor land-use land-cover change in North-eastern Latvia. – SpringerPlus 3(1): 1-15. https://doi.org/10.1186/2193-1801-3-61.

[8] Foody, G. M. (2002): Status of land cover classification accuracy assessment. – Remote Sensing of Environment 80(1): 185-201.

[9] Gillham, O. (2002): The limitless city: a primer on the urban sprawl debate. – Island Press.

[10] Goetz, A. (2013): Suburban sprawl or urban centres: Tensions and contradictions of smart growth approaches in Denver, Colorado. – Urban Studies 50(11): 2178-2195.

http://www.aloki.hu ● ISSN 1589 1623 (Print) ● ISSN1785 0037 (Online)
DOI: http://dx.doi.org/10.15666/aeer/1906_44434457

[11] He, C., Shi, P., Xie, D., Zhao, Y. (2010): Improving the normalized difference built- up index to map urban built-up areas using a semiautomatic segmentation approach. – Remote Sensing Letters 1(4). https://doi.org/10.1080/01431161.2010.481681
[12] Jat, M. K., Garg, P. K., Khare, D. (2008): Monitoring and modelling of urban sprawl using remote sensing and GIS techniques. – International Journal of Applied Earth Observation and Geoinformation 10(1): 26-43. https://doi.org/10.1016/j.jag.2007.04.002.
[13] Majd, M. S., Mans, L. (2012): Maximum Likelihood Classification of Single High-resolution Polarimetric SAR Images in Urban Areas. – https://doi.org/10.1127/1432-8364/20.
[14] Mehmood, R., Mehmood, S. A., Butt, M. A., Younas, I., Adrees, M. (2016): Spatiotemporal Analysis of Urban Sprawl and Its Contributions to Climate and Environment of Peshawar Using Remote Sensing and GIS Techniques. – Journal of Geographic Information System 08(02): 137-148. https://doi.org/10.4236/jgis.2016.82013.
[15] PCO. (1998): 6th Population and Housing census survey. – District Census Report of Peshawar: Pakistan Census Organization.
[16] PCO. (2017): 7th Population and Housing census survey. – District Census Report of Peshawar: Pakistan Census Organization.
[17] Peerzado, M. B., Magsi, H., Sheikh, M. J. (2018): Land use conflicts and urban sprawl: Conversion of agriculture lands into urbanization in Hyderabad, Pakistan. – Journal of the Saudi Society of Agricultural Sciences. https://doi.org/10.1016/j.jssas.2018.02.002.
[18] Qadeer, M. A. (1996): An assessment of Pakistan's urban policies, 1947-1997. – Pakistan Development Review 35(4 PART 2): 443-465. https://doi.org/10.30541/v35i4iipp.443-465.
[19] Rahim, A., Khan, K., Jamal, R., Tariq, N., Akif, A. (2015): The Spatial and Temporal Variation in the Ground Water Potential Due to Urbanization in the Peshawar Regime of Pakistan. – Science International 27(3): 2225-2233.
[20] Raziq, A., Xu, A., Li, Y. (2016): Monitoring of Land Use/Land Cover Changes and Urban Sprawl in Peshawar City in Khyber Pakhtunkhwa: An Application of Geo- Information Techniques Using of Multi-Temporal Satellite Data. – Journal of Remote Sensing & GIS 5: 4. https://doi.org/10.4172/2469-4134.1000174.
[21] Roehrs, A. C. (2015): The Refugee Dilemma: Afghans in Pakistan between expulsion and failing aid schemes. – Afghanistan Analysts Network, September 2018, 1-11.
[22] Salem Adnan, Q. F. (2017): Urban Policy and Planning Unit - Provincial Land Use Plan (PLUP). – Planning and Development Department Government of Khyber Pakhtunkhwa Final Land Use Plan of District Peshawar (Issue 306). https://urbanpolicyunit.gkp.pk/provincial-land-use-plan-phase-2/.
[23] Seilheimer, T. S., Wei, A., Chow-Fraser, P., Eyles, N. (2007): Impact of urbanization on the water quality, fish habitat, and fish community of a Lake Ontario marsh, Frenchman's Bay. – Urban Ecosystems 10(3): 299-319.
[24] Shirazi, S., Kazmi, S. (2014): Analysis of Population Growth and Urban Development in Lahore-Pakistan using Geospatial Techniques: Suggesting some future Options. – South Asian Studies 29: 269-280. http://pu.edu.pk/images/journal/csas/PDF/20 Safdar Shirazi_29_1.pdf.
[25] Solé-Ollé, A., Hortas-Rico, M. (2008): Does Urban Sprawl Increase the Costs of Providing Localpublic Services? Evidence from Spanish Municipalities. – Documents De Treball De L'Ieb 6: 1-33.
[26] Sudhira, H. S., Ramachandra, T. V., Jagadish, K. S. (2004): Urban sprawl: Metrics, dynamics and modelling using GIS. – International Journal of Applied Earth Observation and Geoinformation 5(1): 29-39. https://doi.org/10.1016/j.jag.2003.08.002.
[27] Turton, D., Marsden, P. (2002): Taking Refugees for a Ride? The politics of refugee return to Afghanistan. – The Afghanistan Research and Evaluation Unit (AREU).

http://www.aloki.hu ● ISSN 1589 1623 (Print) ● ISSN1785 0037 (Online)
DOI: http://dx.doi.org/10.15666/aeer/1906_44434457

[28] Wen, F., Ren, L. (2017): The measurement of urbanization level based on entity space: A case study of JingJinJi region, China. – MATEC Web of Conferences, 100. https://doi.org/10.1051/matecconf/201710005046.
[29] Zeng, F., Cui, K., Xie, Z., Wu, L., Liu, M., Sun, G., Lin, Y., Luo, D., Zeng, Z. (2008): Phthalate esters (PAEs): Emerging organic contaminants in agricultural soils in peri-urban areas around Guangzhou, China. – Environmental Pollution 156(2): 425-434. https://doi.org/10.1016/j.envpol.2008.01.045.

http://www.aloki.hu ● ISSN 1589 1623 (Print) ● ISSN1785 0037 (Online)
DOI: http://dx.doi.org/10.15666/aeer/1906_44434457

PHENOTYPIC TRAITS OF *BROMUS INERMIS* LEYSS AND ENVIRONMENTAL FACTORS ON THE NORTH SLOPE OF THE TIANSHAN MOUNTAINS

GONG, K. – JIN, G. L.* – WANG, Y. X. – LI, C. J. – YUE, Y. H. – HAN, W. Q. – LIU, W. H. – WU, X. E.

College of Grassland and Environmental Sciences, Xinjiang Agricultural University/Key Laboratory of Grassland Resources and Ecology of Xinjiang, Urumqi 830052, China (e-mail: 1538095879@qq.com – K. Gong; phone: +86-185-9907-7363)

**Corresponding author*
e-mail: jguili@126.com; phone: +86-189-0991-0602

(Received 11th May 2021; accepted 4th Sep 2021)

Abstract. The adaptability of plants to heterogeneous environments demonstrates their phenotypic plasticity, and their responses to the environment are reflected mainly in their phenotypic traits and biomass allocation strategies. We selected 5 regions from west to east on the north slope of the Tianshan Mountains in Xinjiang to collect *Bromus inermis,* and the results showed that there were significant differences in phenotypic traits and biomass allocation patterns from west to east, indicating that this species has a strong ability to adapt to heterogeneous environments. The plant height, leaf characteristics and reproductive characteristics of *B. inermis* in the central study area were superior to of plants in other areas. The vegetative organs of *B. inermis* had greater variability and more biomass than the other organs, while the aboveground organ biomass showed a close relationship with the aboveground biomass allocation; the stem biomass distribution was the most representative of this relationship. We concluded that, in heterogeneous environments, *B. inermis* adjusts its phenotypic traits and biomass allocation mostly in response to differences in climate. In the study area, *B. inermis* adapted to guarantee its asexual growth and reduced its investment in sexual reproduction, which is in line with the reproductive mode of this rhizomatous plant.
Keywords: *heterogeneous environments, biomass allocation, ecological adaptability*

Introduction

Many plants grow in different heterogeneous environments within the geographical range to which they are adapted, and their organs undergo different degrees of variation in response to different environmental factors in their habitat in order to maintain plant growth and reproduction. In recent years, a new research perspective based on phenotypic traits has been used to focus on the influence of the relationship between different organs and habitats on growth and reproduction (Peltonen-Sainio et al., 2011; Sadras and Slafer, 2012; Slafer et al., 2014). Scholars have found that the leaves of plants at lower elevations are larger and that the morphological variation of flowers at higher elevations is more obvious (Olowa et al., 2018). The different forms of plant fruits and seeds correspond to the level of stress experienced by the maternal plant during its growth and development. Under severe water stress and the loss of its deciduous leaves, the production of no dehiscent fruit in Cruciferae plants will increase. Plants with strong phenotypic plasticity can live in a variety of habitats, which provides them with more opportunities to reproduce in complex environments and avoid various types of risk (Lu et al., 2012).

During the process of plant growth, the availability of resource inputs is reflected in the response and adaptability of plant development and reproduction in relation to the environment. When plant growth is affected by a lack of soil resources such as water or

http://www.aloki.hu ● ISSN 1589 1623 (Print) ● ISSN 1785 0037 (Online)
DOI: http://dx.doi.org/10.15666/aeer/1906_44594475

nutrients, the plant will allocate more biomass to the roots (Xu et al., 2012). Conversely, if the plant is constrained by light resources, the plant will allocate more biomass to the leaves to ensure consistent light intake by the plant (Luo et al., 2012). These changes represent the response of plants to stressful environments, and differences in location and elevation can also lead to different biomass allocation patterns within the same plant species. One elevation-related change that has been commonly found in previous studies is that with increasing elevation, alpine plants allocate more biomass to their belowground parts, leading to a significant decline in stem biomass (Olowa et al., 2018). This response indicates that as the elevation increases, the amount of energy the environment provides for plant growth decreases, as does the amount of energy the plants themselves need. Therefore, to ensure their survival, plants must allocate more resources to their reproductive organs, complete their life cycle and thereby increase the reproductive rate of the population (Yang et al., 2020).

Plants respond to different environments by changing their phenotypes or adjusting their biomass allocation patterns, which indicates that the organ area and volume of plants are two factors determining plant access to resources (Bradshaw, 1965; Pang and Lercher, 2015). Scholars have often used comparative morphology and biological mathematics to analyse and evaluate the phenotypic traits of plants, distinguish the morphological differences between different germplasms, classify their status and groupings, and finally select qualified breeding materials to provide high-quality materials for cultivation (Duruflé et al., 2019).

Environmental factors are often considered important statistical parameters in explaining the influence of heterogeneity on phenotypic variations among different environments (Zheng et al., 2019). However, we found that environmental impacts can be observed as the differences in plant traits between geographic populations. The influence of genetic variation is typically more concentrated in the interior of a population than at the edge of the population range. Character variation also occurs within and between geographic populations in total variation models, leading to gradual changes in plant growth (Morgenstern, 2011; McKown et al., 2014).

Xinjiang is located in Central Asia and the Central Asian desert transition or intersection area. Natural *Bromus inermis* is distributed across a broad longitudinal and latitudinal range in a mountainous region, and there are notable topographic and atmospheric differences in the environment within this range. Therefore, the phenotypic traits and biomass allocation strategies of *B. inermis* have evolved to adapt to these environments under the influence of many factors. The characteristic ecological adaptability of this group has resulted in the development of a rich germplasm resource gene pool. *B. inermis* has the same adaptive characteristics as *Leymus chinensis*, *Dactylis glomerata* and other plants of similar research value (Li et al., 2015; Zhang et al., 2015; Wang et al., 2011); in addition, other relevant studies on herbage have been published in recent years (Zhao et al., 2016; Ott et al., 2017; Yuan et al., 2019).

B. inermis is a perennial rhizomatous grass that is traditionally used for grazing or fodder. Wild *B. inermis* is distributed in the temperate regions of Asia, Europe and North America and is widely distributed in many regions of China. Natural *B. inermis* in Xinjiang is distributed mainly within a range that is 1500 ~ 2400 m north of the Tianshan Mountains, 92.986° ~ 80.766° east longitude, 43.074° ~ 48.701° north latitude, and mostly in meadow grassland. Previous studies have shown that *B. inermis* exhibits high growth adaptability after invading other grasslands and could perform a series of life activities, such as settlement and expansion, by changing its phenotypic

http://www.aloki.hu ● ISSN 1589 1623 (Print) ● ISSN 1785 0037 (Online)
DOI: http://dx.doi.org/10.15666/aeer/1906_44594475

traits and biomass allocation strategies (Salesman and Thomsen, 2011; Stotz et al., 2016; Ott et al., 2017); it can also occupy an important ecological niche in mixed plantings (Ulrich and Perkins, 2014; Biligetu and Coulman, 2011). After artificial stress, it can actively adjust its own structure to avoid growth retardation by responding rapidly to various influencing factors (Woodis and Jackson, 2010; Lermi et al., 2018; Majidi et al., 2017). In conclusion, *B. inermis* shows strong adaptability in both natural and human conditions, which has enabled the population to expand and reproduce by changing its phenotype. However, the physiological traits of *B. inermis* have not yet been examined in detail. In this study, the following questions were addressed: (1) Are there differences in phenotypic characteristics among different natural populations of *B. inermis*? (2) What are the effects of climatic factors and soil factors on *B. inermis*?

Material and methods

Study sites

B. inermis is widely distributed in Jilin, Liaoning, Inner Mongolia, Hebei, Shanxi, Shandong, Jiangsu, Shaanxi, Gansu, Qinghai, Xinjiang, Xizang, Yunnan, Sichuan, Guizhou and other provinces (regions) in China. It mainly grows in meadow steppe, alpine meadow and mountain meadow environments. It is the dominant species in mountain meadow ecosystems at 1 000 ~ 3 500 m. It has become an important cultivated forage in arid and cold regions of China.

The study was performed on the north slope of the Tianshan Mountains (80.910-93.755° E, 43.109-43.836° N), where there is a typical distribution of *B. inermis*. The north slope of the Tianshan Mountains, including the western, central and eastern sections of the Tianshan Mountain foothills, is located in the north of the Tarim Basin, where the terrain is high in the south and low in the north. The distinct topography influences the local climatic conditions mainly by causing differences in temperature and rainfall, which have an impact on the growth and reproduction of plant populations. Therefore, it is appropriate to study the adaptive growth of plants in different regions of the Tianshan Mountains.

From west to the east along the mountain, we selected 5 grasslands in which *B. inermis* was the dominant species or a subdominant species. The selected grasslands were located in Zhaosu County, Hutubi County, Urumqi County, Qitai County and Balikun County. All the selected grasslands are protected by fences and are not disturbed by livestock feeding (*Figs. 1* and *2*).

Experimental design

In the 5 selected regions, we need to accurately determine the distribution range of *B. inermis*. According to the actual distribution, three sample plots were evenly arranged along the elevation range of the distribution area, and each sample plot was 10 × 10 m. Geographic information on each sample plot was recorded, including longitude, latitude and elevation. Complete single plants (including roots) representing the average level of the plot were randomly extracted from the plot, and 30 plants were extracted from each plot, yielding a total of 90 samples of *B. inermis* from the 3 plots at different elevations.

Because the elevation fluctuates greatly in the Tianshan Mountains, the elevation of each region is not the same, and the differences are large. We uniformly refer to the sites in each region as the low-elevation, medium-elevation and high-elevation sites to

http://www.aloki.hu ● ISSN 1589 1623 (Print) ● ISSN 1785 0037 (Online)
DOI: http://dx.doi.org/10.15666/aeer/1906_44594475

describe the specific distribution location of *B. inermis* in each area, rather than the actual elevation range. Therefore, the high-elevation site in one region may be lower than the low-elevation site in another region, but this is does not influence our comparison. We only pay attention to the relationship between different elevation positions in a single region.

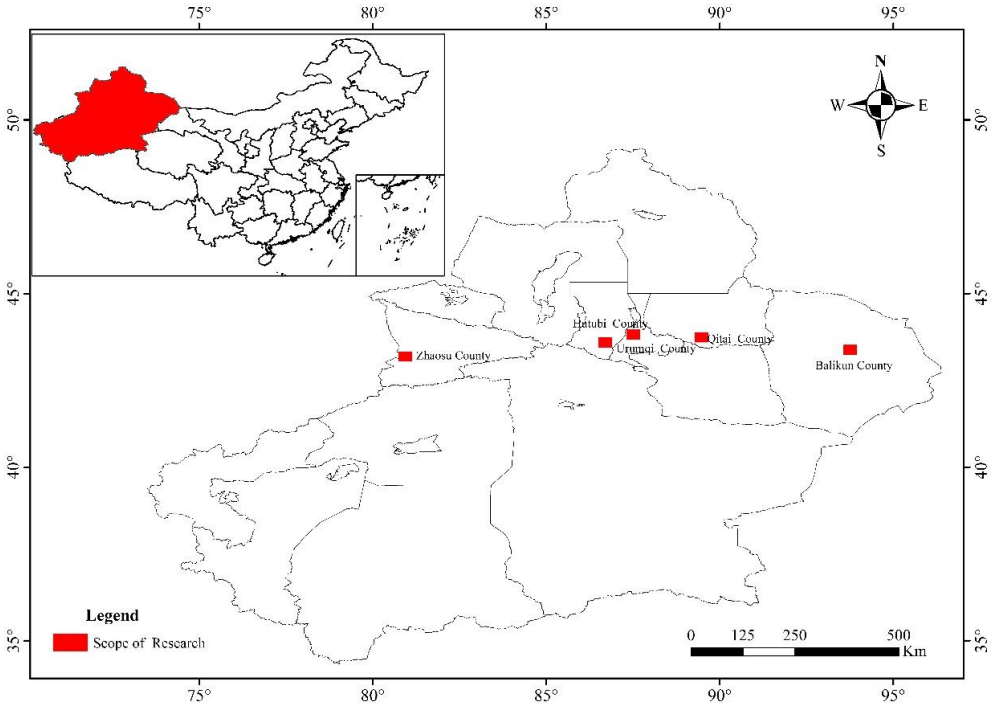

Figure 1. *Map of the study sites*

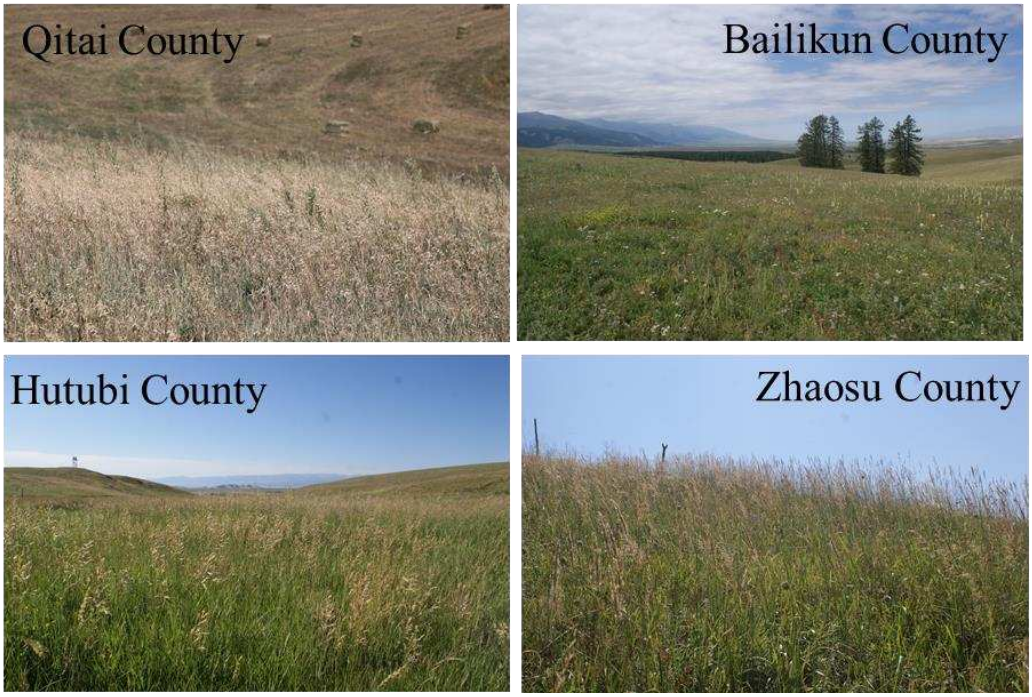

Figure 2. *Research area status*

http://www.aloki.hu ● ISSN 1589 1623 (Print) ● ISSN 1785 0037 (Online)
DOI: http://dx.doi.org/10.15666/aeer/1906_44594475

Climatic and edaphic data

The meteorological data of the five selected regions, including annual mean temperature and annual precipitation, were calculated using the interpolation method based on 30 years of data (1989-2019) provided by the meteorological stations of The National Meteorological Data Center of China. It is important to note that we have calculated the averages of the meteorological data for each region's meteorological data. Therefore, we use meteorological data for each region rather than for each elevation. The changes in elevation are not associated with dramatic differences in geographical location, and the climatic factors change little; thus, we do not use these data (*Table 1*).

Table 1. *Geographic information and meteorological information for the sampling area*

Origin	Elevation (m)		Longitude	Latitude	Annual average temperature (°)	Average annual precipitation (mm)
Zhaosu County	Low	1790	E 80.910°	N 43.109°	5.9	559.6
	Medium	1980	E 80.914°	N 43.111°		
	High	2100	E 80.922°	N 43.170°		
Hutubi County	Low	1574	E 87.329°	N 43.836°	7.3	193.8
	Medium	1598	E 87.035°	N 43.514°		
	High	1616	E 87.330°	N 43.836°		
Urumqi County	Low	1630	E 87.029°	N 43.516°	1.3	257.0
	Medium	1670	E 87.040°	N 43.502°		
	High	1960	E 87.042°	N 43.483°		
Qitai County	Low	1574	E 89.329°	N 43.836°	7.8	185.0
	Medium	1810	E 89.600°	N 43.617°		
	High	1853	E 89.587°	N 43.625°		
Bailikun County	Low	2107	E 93.751°	N 43.329°	2.4	230.8
	Medium	2206	E 93.754°	N 43.328°		
	High	2298	E 93.755°	N 43.327°		

Three soil samples from the 0-5 cm, 5-10 cm and 10-15 cm layers were taken in each sample plot. The samples were first combined, and then the soil samples were prepared by quartering. Each quartered sample was air-dried and then sieved through a 1 mm sieve to remove chunks of rock and plant roots. The soil pH was measured by using a potentiometer. The organic matter content (soil organic carbon) was measured by the potassium dichromate heating method. The total nitrogen was measured by the Kjeldahl procedure. The total phosphorus was measured by the Mo-Sb colorimetric method (*Table 2*).

Table 2. *Soil physical and chemical characteristics in the sampling area*

Origin	PH	N (g/kg)	P (g/kg)	K (g/kg)
Zhaosu County	7.01 ± 0.18	4.98 ± 0.45	0.03 ± 0.003	11.82 ± 2.46
Hutubi County	7.64 ± 0.16	4.97 ± 0.52	0.03 ± 0.003	9.90 ± 0.27
Urumqi County	7.39 ± 0.05	2.59 ± 1.23	0.03 ± 0.003	8.54 ± 0.01
Qitai County	6.90 ± 0.47	5.67 ± 0.91	0.04 ± 0.003	10.67 ± 0.27
Bailikun County	7.61 ± 0.16	4.92 ± 1.48	0.04 ± 0.006	10.09 ± 0.01

http://www.aloki.hu ● ISSN 1589 1623 (Print) ● ISSN 1785 0037 (Online)
DOI: http://dx.doi.org/10.15666/aeer/1906_44594475

Phenotypic index determination

We selected 12 phenotypic indicators to measure in *B. inermis*, including the reproductive branch height, vegetative branch height, stem diameter, spike length, root length, leaf length, leaf width, inflorescence length, and inflorescence width. The leaf index and inflorescence index were measured 3 times. We also counted the tiller number in each plot and recorded the thousand-grain weight for the sampled plants.

Biomass determination

The *B. inermis* plants that had been measured were carefully cut into stems, leaves, spikes and roots. Each part of the plant was weighed separately, and the undried weight of each component was recorded.

The root mass ratio (RMR, root weight/total plant weight), leaf mass ratio (LMR, leaf weight/total plant weight), spike mass ratio (SMR, spike weight/total plant weight), belowground storage organ biomass ratio (belowground storage organ weight/total plant weight), and aboveground biomass ratio (shoot weight/total plant weight) were calculated. The nutrient acquisition organ biomass ratio (root weight, stem weight and leaf weight/total plant weight) and the reproductive component organ biomass ratio (spike weight/total plant weight) were also calculated.

Data analysis

The F test was used to preliminarily verify the assumption of homogeneity. Then, ANOVA was used to analyse the differences between the phenotypic morphological indexes and component biomass indexes in the different regions. Multiple comparison analyses were performed on the trait differences in *B. inermis* among the 3 elevations and 5 regions, and the variation coefficients of each index in the 5 regions were calculated. The differences in biomass allocation to plant components (belowground and aboveground biomass, vegetative biomass and reproductive biomass) among regions were analysed. Principal component analysis (PCA) was used to evaluate the main trait factors that influenced the traits of *B. inermis*, and the relevance of variables was determined according to the direction, orientation and magnitude of their vectors. The response of the biomass of the abovementioned components to the biomass allocation was analysed by linear regression.

Results

The influence of region and elevation on trait indexes

The altitudinal gradient and the different regions had different effects on the phenotypic growth of *B. inermis* (*Table 3*). Elevation significantly influenced the main stem diameter but had no effect on the other indexes. However, the phenotypes still varied among elevation levels. Six indexes gradually increased with elevation, such as the leaf length, inflorescence width, thousand-grain weight, leaf mass ratio, supporting organ biomass ratio and spike mass ratio, with an increase range of 5.57%-19.75% and an average growth rate of 10.26%. However, the vegetative branch height, reproductive branch height and ear length reached their maximum at the medium elevation, with an average increase of 9.53% over the lowest values. The remaining 3 indexes, tiller number, stem diameter and leaf width, reached their maximum values at

http://www.aloki.hu ● ISSN 1589 1623 (Print) ● ISSN 1785 0037 (Online)
DOI: http://dx.doi.org/10.15666/aeer/1906_44594475

low elevations, with an average growth rate of 18.72%. Additionally, the effects of region and elevation on tiller number and stem diameter were not significant. In summary, the growth rate of *B. inermis* at low elevations is faster than that at high elevations, while the biomass accumulation of *B. inermis* at high elevations is greater than that at low elevations.

Table 3. *Mean values (±SE) and significance levels from the two-way ANOVA of trait indexes*

Variable	Elevation			ANOVA		
	Low	Medium	High	Region (R)	Elevation (E)	R×E
Tiller number	2.83 ± 2.75	1.79 ± 1.67	2.35 ± 2.28	ns	ns	ns
Reproductive branch height	88.02 ± 22.33	91.54 ± 18.76	83.13 ± 28.85	*	ns	*
Vegetative branch height	25.97 ± 13.95	28.90 ± 14.63	28.45 ± 20.12	**	ns	ns
Leaf length	1.97 ± 0.60	1.82 ± 0.45	1.83 ± 0.53	*	*	ns
Leaf width	10.95 ± 4.01	12.41 ± 5.45	12.50 ± 5.04	**	ns	ns
Spike length	4.54 ± 1.76	4.23 ± 1.718	3.81 ± 1.04	**	ns	ns
Root length	12.27 ± 6.85	11.16 ± 5.38	11.62 ± 4.75	ns	ns	ns
Inflorescence length	12.91 ± 4.42	13.83 ± 3.67	13.27 ± 5.97	***	ns	*
Inflorescence width	20.14 ± 4.72	19.66 ± 4.19	18.61 ± 5.02	ns	ns	ns
Stem diameter	2.06 ± 0.81	2.17 ± 0.71	2.17 ± 0.77	ns	ns	ns
Thousand-grain weight	2.42 ± 0.44	2.56 ± 0.44	2.59 ± 0.29	***	ns	**
SBR	36.23 ± 14.43	38.00 ± 16.83	39.61 ± 17.83	ns	ns	ns
LMR	38.20 ± 15.30	37.46 ± 16.36	35.30 ± 15.95	ns	ns	ns
RMR	16.83 ± 11.72	14.15 ± 10.70	16.94 ± 11.93	*	ns	ns
SMR	8.07 ± 6.74	7.72 ± 7.17	8.15 ± 8.17	*	ns	ns

*Significant correlation at the < 0.05 level. **Significant correlation at the < 0.01 level

In contrast, the various regions had a more significant influence on phenotype and biomass than the different elevations and had a significant influence on all indicators except tiller number, root length, spikelet traits, and stem and root biomass. However, these indicators were not significantly influenced by the interactive effect of region and elevation, indicating that these indicators may be more influenced by genetic variation than by environmental factors. Among the trait indexes, spike length and thousand-grain weight were the most significantly influenced by region ($P < 0.01$). As shown in *Table 4,* the spike length and thousand-grain weight in Urumqi County were significantly higher than those in the other regions and were higher than the minimum values by 96.27% and 37.88%, respectively. They first increased and then decreased from west to east along the north slope of the Tianshan Mountains, and the height index, leaf index and grain quality also showed the same pattern. However, the stem diameter and root length in Hutubi County were significantly higher than those in other regions, with an average increase of 45.75% above the minimum value. The results indicated that there were more significant differences in *B. inermis* between regions than between elevations, suggesting the main influences on *B. inermis* phenotype and biomass are regional. At the same time, it can be seen that the *B. inermis* plants in the central part of the north slope of the Tianshan Mountains are tall, with a high leaf area, few leaves, and large panicle grains; therefore, these plants have more potential for genetic development than those from other areas.

http://www.aloki.hu ● ISSN 1589 1623 (Print) ● ISSN 1785 0037 (Online)
DOI: http://dx.doi.org/10.15666/aeer/1906_44594475

Table 4. *Mean values (±SE) of indicators among different regions*

Variable	Region				
	Zhaosu County	**Hutubi County**	**Urumqi County**	**Qitai County**	**Balikun County**
Reproductive branch height	78.92 ± 17.93b	106.89 ± 16.30c	107.34 ± 25.93c	69.93 ± 10.81a	76.09 ± 15.59ab
Vegetative branch height	28.44 ± 14.06b	40.83 ± 10.72c	44.36 ± 19.68c	16.59 ± 7.14a	19.19 ± 6.75a
Stem diameter	1.51 ± 0.29a	2.27 ± 0.48c	2.19 ± 0.65b	1.67 ± 0.31a	1.90 ± 0.46b
Leaf length	7.64 ± 1.88a	15.42 ± 3.36c	16.19 ± 3.95c	8.87 ± 2.19a	11.81 ± 5.30b
Leaf width	2.75 ± 0.62a	3.92 ± 0.85b	5.96 ± 1.94d	3.75 ± 0.80b	4.56 ± 1.05c
Root length	9.72 ± 5.86a	13.73 ± 5.08c	12.07 ± 4.91bc	11.27 ± 6.36ab	11.73 ± 5.64abc
Spike length	8.82 ± 3.03a	16.60 ± 3.32d	17.31 ± 5.05d	10.75 ± 2.74b	13.35 ± 2.90c
Thousand-grain weight	2.38 ± 0.23a	2.51 ± 0.31a	3.03 ± 0.32b	2.49 ± 0.40a	2.20 ± 0.12a
LMR	14.31 ± 10.44a	14.44 ± 14.61a	13.68 ± 11.27a	15.35 ± 9.74a	21.95 ± 9.01b
SMR	5.89 ± 4.89a	3.64 ± 3.85a	10.67 ± 6.04b	10.43 ± 7.87b	9.03 ± 9.84b

Different lowercase letters above the columns indicate significant differences at $P < 0.05$

Variation in phenotypic indicators and biomass allocation within the 5 regions

Comparing traits within each region along the north slope of the Tianshan Mountains revealed that each index varied greatly (*Table 5*) but that the variation within each region did not exhibit regularity. Overall, the phenotypic traits of *B. inermis* on the north slope of the Tianshan Mountains were different, but the degree of variation was small. The variation in biomass allocation was very small within all regions and overall. Moreover, when there were differences among regions, the differences were not in the main indexes of concern. The variation range of the 11 trait indexes among all regions ranged from 0.126 to 0.700. Among them, the degree of variation in the tiller number, root length and vegetative branch height (vegetative organ traits) was high, at 0.541, 0.485 and 0.397, respectively; the degree of variation in the panicle length and spikelet width (reproductive organs) was also high, at 0.261 and 0.274, respectively.

Table 5. *The coefficient of variation for each index in the 5 regions and the total coefficient of variation for each index*

Variable	Region					Total coefficient of variation
	Zhaosu County	**Hutubi county**	**Urumqi County**	**Qitai County**	**Balikun County**	
Tiller number	0.462	0.539	0.355	0.700	0.647	0.541
Reproductive branch height	0.227	0.152	0.242	0.155	0.205	0.196
Vegetative branch height	0.494	0.263	0.444	0.43	0.352	0.397
Leaf length	0.191	0.210	0.297	0.186	0.244	0.226
Leaf width	0.247	0.218	0.244	0.247	0.449	0.281
Spike length	0.225	0.216	0.325	0.213	0.230	0.242
Root length	0.603	0.370	0.407	0.564	0.481	0.485
Inflorescence length	0.343	0.200	0.292	0.255	0.218	0.261
Inflorescence width	0.227	0.177	0.334	0.174	0.175	0.217
Stem diameter	0.296	0.356	0.332	0.126	0.261	0.274
Thousand-grain weight	0.097	0.123	0.107	0.163	0.056	0.109
SBR	0.047	0.037	0.041	0.039	0.045	0.021
LMR	0.049	0.043	0.054	0.038	0.036	0.020
RMR	0.077	0.110	0.087	0.067	0.043	0.034
SMR	0.088	0.115	0.060	0.080	0.115	0.044

http://www.aloki.hu ● ISSN 1589 1623 (Print) ● ISSN 1785 0037 (Online)
DOI: http://dx.doi.org/10.15666/aeer/1906_44594475

Effect of region on the biomass of each plant component

The biomass distribution ratios for the reproductive biomass and nutrient acquisition biomass of *B. inermis* were determined for the different regions (*Fig. 3a*). The biomass allocation to nutrient acquisition organs in all 5 regions was greater than 80%, and there were significant differences among regions ($P < 0.05$). *B. inermis* in Urumqi County, Qitai County and Balikun County allocated significantly more biomass to reproductive components than that in Zhaosu County and Hutubi County. In summary, in the five *B. inermis* regions, more biomass was allocated the stem, leaf and root to ensure adequate nutrient storage and growth in *B. inermis*.

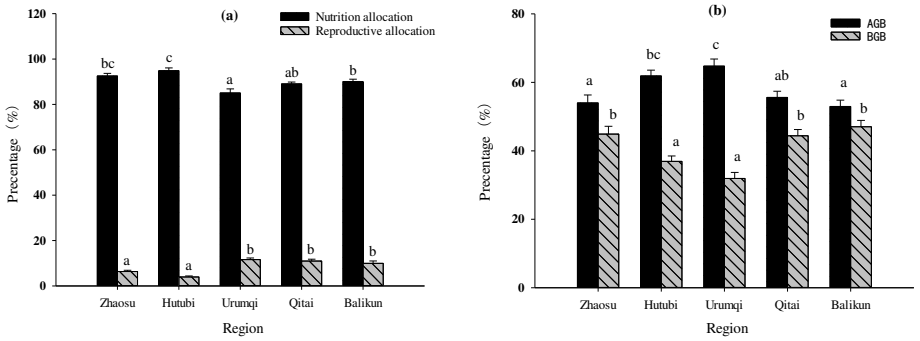

Figure 3. *(a) Reproductive and nutrient-acquiring biomass and (b) aboveground biomass and belowground biomass in the five regions. Different lowercase letters above the columns indicate significant differences at $P < 0.05$*

The aboveground and belowground biomass of *B. inermis* in different regions (*Fig. 3b*) exhibited different patterns. Aboveground biomass was significantly higher than belowground biomass ($P < 0.05$), and the highest proportion of aboveground biomass was observed in Urumqi County (64.75%). The highest proportion of belowground biomass was in Balikun County, at 47.04% of the total biomass. The belowground biomass values in Urumqi County and Hutubi County were significantly lower those that in other regions ($P < 0.05$). Thus, along the north slope of the Tianshan Mountains from west to east, the aboveground biomass distribution of *B. inermis* first increased and then decreased, while the belowground biomass showed the opposite trend. The results showed that the habitat in the central part of the study region was more favourable to the growth of the aboveground parts of *B. inermis*; as a result, the yield of the forage parts of *B. inermis* was increased. In the western and eastern parts of the study area, the belowground biomass was higher than in the central part to ensure adequate water and nutrients for *B. inermis*.

The response of each indicator to environmental factors

Climate factors had more influence on the *B. inermis* phenotype and biomass than soil factors (*Table 6*). In terms of topographic factors, elevation had an extremely significant correlation with each index except root length and spike mass ratio. The results of the differential analysis showed that the leaf width, root length and spikelet length reached maximum values at the lowest elevation, and the correlation analysis was consistent with these results. There was no correlation between the thousand-grain

http://www.aloki.hu ● ISSN 1589 1623 (Print) ● ISSN 1785 0037 (Online)
DOI: http://dx.doi.org/10.15666/aeer/1906_44594475

weight, root mass ratio and geographical location, while the correlations between vegetative branch height, leaf mass ratio, spike mass ratio and geographical location were weak; the correlations of the other indexes were generally highly significant. Most of the indicators for *B. inermis* reached maximum values in the central part of the study area, and the indicators did not show a trend of gradually increasing or decreasing with increasing latitude from west to the east on the north slope of the Tianshan Mountains.

Similarly, in the correlation analysis, most indicators were correlated with the latitude, but the correlation coefficients of these relationships were small. The average annual temperature was not correlated with root length or spike length, and the average annual precipitation was not correlated with leaf length or spike width; these climate factors were correlated with the other indexes for *B. inermis*. The average annual temperature and average annual precipitation had little influence on the reproductive components and storage components of *B. inermis* and were more strongly correlated with plant size and biomass traits. The vegetative branch height decreased with increasing N and K in the soil. Similarly, an increase in N also decreased the thousand-grain weight, while an increase in K decreased the stem mass ratio and increased the leaf mass ratio. The correlations between reproductive branch height and leaf width, spike length, stem diameter and thousand-grain weight were highly significant.

Table 6. *Correlations between phenotypic traits of Bromus inermis and geographical factors*

Trait	Climatic factor					Edaphic factor		
	Elevation	Longitude	Latitude	AMT	AMP	N	K	PH
Tiller number	0.197**	0.114*	-0.145**	0.165**	-0.181**	0.036	0.208	0.075
Reproductive branch height	-0.330**	-0.130**	0.171**	-0.515**	0.417**	-0.054	-0.216	0.070
Vegetative branch height	-0.280**	-0.301**	0.042	-0.589**	0.509**	-0.286*	-0.486**	0.221
Leaf length	-0.236**	0.181**	0.278**	-0.143**	0.052	0.142	0.051	0.200
Leaf width	-0.221**	0.181**	0.282**	-0.291**	0.0148**	-0.120	-0.056	0.316*
Spike length	-0.176**	0.313**	0.181**	-0.065	-0.080	-0.186	0.110	0.483**
Root length	-0.109*	0.095*	0.167**	-0.027	-0.005	-0.032	0.031	-0.220
Inflorescence length	-0.225**	0.222**	0.326**	-0.244**	0.103*	0.077	0.032	0.225
Inflorescence width	0.212**	0.218**	-0.121*	0.269**	-0.290**	-0.144	0.041	0.221
Stem diameter	0.406**	0.504**	-0.160**	0.318**	-0.439**	0.068	0.181	0.303*
Thousand-grain weight	-0.433**	-0.186	0.127	-0.430**	0.372*	-0.407**	-0.282	0.415**
SBR	-0.256**	-0.243**	0.105*	-0.371**	0.362**	-0.208	-0.358**	0.142
LMR	0.194**	0.204**	-0.061	0.198**	-0.222**	0.143	0.287**	-0.129
RMR	0.127**	0.059	-0.071	0.225**	-0.180**	0.162	0.179	-0.233
SMR	0.101*	0.165**	0.043	0.169**	-0.188**	-0.105	-0.003	0.276

The correlation between aboveground biomass and aboveground components

The yield of *B. inermis*, as a good forage, is provided by the aboveground portion of the plant, which we measure as the aboveground biomass. Biomass is the content of the overall expression. To explore the relationship between the total biomass and the biomass of aboveground components is of great significance in exploring the influence of the environment on the growth of components and how it is reflected in the yield. Aboveground biomass showed a significant positive correlation with stem biomass, leaf biomass and spike biomass, and their responses to aboveground biomass showed a linear pattern (*Fig. 4*). With the increase in aboveground biomass, the biomass allocated to the

http://www.aloki.hu ● ISSN 1589 1623 (Print) ● ISSN 1785 0037 (Online)
DOI: http://dx.doi.org/10.15666/aeer/1906_44594475

aboveground components increased; the increase in stem biomass was the most obvious, followed by the increases in leaf and spike biomass. The results showed that when the aboveground biomass of *B. inermis* increased, the stem obtained more resources to promote plant growth; however, the spike began to need the majority growth resources during the middle of the growth period, so the biomass allocated to the stem decreased.

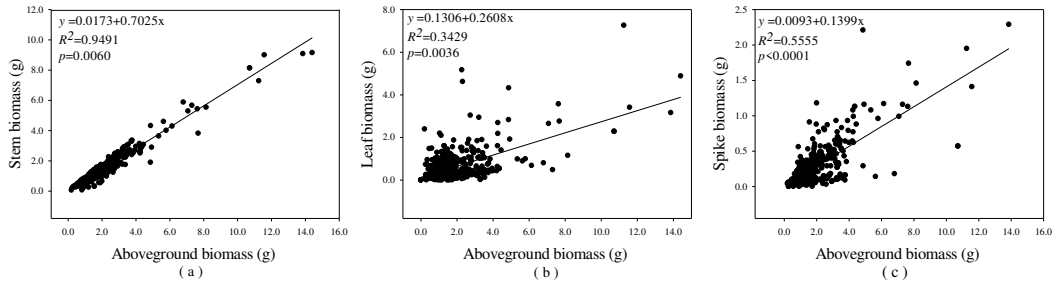

Figure 4. *Relationship between aboveground biomass and stem biomass (a), leaf biomass (b), and spike biomass (c)*

Discussion

Adaptability of phenotypic traits to the environment

The long-term interaction between plants and the environment is reflected in the external form of plants as they minimize the negative impacts of adverse environments (Meng et al., 2007). We observed varying degrees of difference in individual phenotypic plasticity in *B. inermis* within the same mountain range and in different environments. Therefore, plants should be considered in the context of various factors when discussing their ability to respond to heterogeneous environments by, for example, changing their phenotypic characteristics and component biomass allocation. However, first, we need to understand the similarities and differences in plant phenotypic characteristics and biomass allocation. Geographical location controls the combination of and differences in environmental factors, and the responses of plants along geographical gradients represent a model for a "natural experiment" (Stotz et al., 2017). We adopted an in situ sampling method, which is one of the most convenient ways to study the phenotypic variation of plants in their natural state. It can help us to effectively understand the environmental factors that affect the variation in natural populations and to explore the ecological effects of these factors more effectively (Bobowicz and kowa, 1986).

Vegetation is densely distributed on the north slope of the Tianshan Mountains, but there are substantial climate differences and an uneven distribution of species across the mountain range from east to west. Therefore, studying the ecological adaptability of the same plant in different locations is the foundation for further exploring the potential of the plant. In this study, the differences in the phenotypic characteristics and biomass allocation of natural *B. inermis* were mainly regional, while the different elevations had little effect on these factors.

Our results showed that the degree of variation in the 11 phenotypic traits of natural *B. inermis* varied widely. This result is not surprising, as *B. inermis* is a cross-pollinated forage plant that exhibits variations in its offspring (Copete et al., 2018). Among them, the degrees of variation in nutrient acquisition traits (tiller number and root length) and

http://www.aloki.hu ● ISSN 1589 1623 (Print) ● ISSN 1785 0037 (Online)
DOI: http://dx.doi.org/10.15666/aeer/1906_44594475

growth traits (vegetative branch height and reproductive branch height) were relatively large. In other studies, we found that plant height was a strong indicator of the ability of a plant to adapt to climate change. During drought periods, upward stem growth is affected, which hinders an increase in plant height. Differences in water availability among different environments are an important factor leading to differences in plant height (Wang et al., 2010). We also found that tiller number, root length, spikelet traits, and stem and root biomass distribution did not change significantly among different environments, indicating that these traits were more stable. The degree of variation reflects the potential for variation in these traits in plants. Traits with a greater degree of variation are more suitable for research and are preferred as research materials, while more stable traits can provide materials for breeding. The principal component values of the traits indicated that the source of plant differences was the region, which is consistent with the ANOVA results described above. In the study of phenotypic traits, we found that the growth characteristics of reproductive branches, such as height, are the main factors affecting the differences in *B. inermis*; this finding is in line with trends in the genetic diversity of agronomic traits among gramineous grasses (Hao et al., 2011). In general, the phenotypic traits of *B. inermis* in the central section of the north slope of the Tianshan Mountains were superior to those of *B. inermis* in the eastern and western sections, indicating that these phenotypic traits exhibited certain regional adaptations.

Plants often need to change their phenotypic traits to respond and adapt to the heterogeneity of the environment during their long-term growth process. The correlation between environmental factors and plant traits indicates the response of the plant traits to the environment. The results of this study showed that most of the trait indicators were significantly correlated with geographical factors; most of these correlations were very significant correlations, though only a few indicators were correlated with soil factors. The relationship between traits and geographical factors is a focus of ecological research, and differences in temperature, rainfall and light factors lead to heterogeneity in the environmental conditions for plant growth. Testing plant performance under different environmental conditions can differentiate the optimal environment for plants from a suboptimal environment and determine the combination of traits that ensures the competitiveness of plants in both environments as well as the conditions at which the resource utilization rate of plants is highest. These methods can also be used to obtain plants suitable for increasing the range of a species, and this information is very useful for studying plant breeding for further range expansion.

Biomass allocation adaptation capacity

Biomass is an important indicator of the interaction between plants and the environment, and it is also the embodiment of plants' adaptability to the environment as well as their growth and development patterns. In addition, the biomass of individuals and components also reflects the capacity of an ecosystem to obtain energy (Michel et al., 2015). Vegetation responds to the availability of various resources through a variety of complex regulation systems, thus effectively improving the utilization efficiency of the entire ecosystem for limited resources (Stotz et al., 2017). To effectively adapt to the heterogeneity of the environment, the distribution of the total plant biomass to each component is not fixed. Rather, biomass allocation must be based on the influence of light, temperature, water, nutrients and other abiotic factors in the region, as well as on other plants in the community. Therefore, biomass allocation can be used as an indicator of the plant response to the environment, as it reflects whether the habitat is conducive

http://www.aloki.hu ● ISSN 1589 1623 (Print) ● ISSN 1785 0037 (Online)
DOI: http://dx.doi.org/10.15666/aeer/1906_44594475

to plant growth. Previous studies have obtained results regarding the biomass allocation of gramineous plant components under heterogeneous environments that are mostly similar to the results of this study (Zhao et al., 2018). The biomass input to stems and roots was greater than that to other components in different environments in this study, but some studies have shown that other plants allocate more biomass to their leaves than to their roots (Yang et al., 2009).

Nongrazed pastures were selected for this study, and the growth of plants was affected mainly by the natural environment. The results of the correlation analysis in this study show that the correlations of the environmental factors elevation, annual average temperature and annual average precipitation with the biomass distribution were stronger than others. Changes in elevation can cause differences in temperature and rainfall, so in the final analysis, the biomass allocation was affected mainly by these two factors. Tyree's study found that under insufficient water conditions, plants increased their biomass allocation to the stem mainly to reduce cavitation in the xylem (Hong et al., 2017) and stored more water to alleviate the water penetration that might occur in the stem. In this experiment, the stem biomass allocation ratio varied greatly among the different environments, which indicated that the water conditions were not consistent; the differences in the root biomass allocation ratio among different regions also corroborated this finding.

The results for the aboveground biomass and aboveground component biomass in this study confirmed that the biomass allocation to the stem was more closely related to the total aboveground biomass than the biomass allocation to other plant components. In a number of simulated-rainfall experiments, it was found that a reduction in rainfall was beneficial to the growth of belowground plant parts because the reduction in water stimulated the uptake of water by roots, thus increasing the biomass of roots and the absorption of nutrients such as nitrogen and phosphorus (Liu et al., 2018). Decreases in rainfall have no significant effect on overall plant biomass because while plants will increase their root biomass under low-water conditions, they will also reduce their leaf biomass to avoid excessive water loss from evapotranspiration. In this study, the leaf biomass remained relatively stable across the 5 regions, which represents a resource allocation strategy for plants in unique environments (Huxman et al., 2004).

Previous studies have found that an increase in temperature is conducive to the accumulation of plant biomass and that plants are more inclined to allocate biomass to their aboveground parts, especially the stems, under warmer conditions (Wal and Stien, 2016). The aboveground biomass is not only related to the CO_2 fixation ability of a plant but is also closely related to the total biomass of the plant; the accumulation of belowground biomass is conducive to the absorption of water and nutrients. In a study of the effects of temperature on plants, it was found that a high belowground biomass/aboveground biomass ratio was an adaptive strategy for cold environments (Ma et al., 2010) because low temperature inhibited the root turnover rate, resulting in an increase in belowground biomass (Yang et al., 2009). In this study, the aboveground biomass of *B. inermis* in Hutubi County and Urumqi County was larger than that in other counties, and the total biomass was also higher than that in the other areas. This was due to the abundant rainfall and light in these two counties; determining whether the *B. inermis* (smooth brome) growing in these areas has special growth characteristics and whether it can become a source of high-quality breeding varieties will require further research (Chen and Zhang, 2012). The distribution of aboveground biomass and belowground biomass in *B. inermis* in the other three regions was relatively balanced,

http://www.aloki.hu ● ISSN 1589 1623 (Print) ● ISSN 1785 0037 (Online)
DOI: http://dx.doi.org/10.15666/aeer/1906_44594475

which ensured a supply of sufficient nutrients and water to meet the demands of reproductive growth (Mateus H et al., 2015).

Plants, by adjusting the allocation of their biomass, balance their investment in each organ across different environments. The aboveground and belowground biomass and the balance of nutrient acquisition and reproductive biomass show the distribution of different resource acquisition strategies of plants of the same species. In this study, we found that plants respond to the environment more through the plasticity of their phenotypic traits than by adjusting their biomass allocation.

Conclusion

According to our field investigation experiments, significant phenotypic characteristic variation was observed between different regions, and little variation was observed within regions. Habitat heterogeneity also affected the geographic variation of the phenotypic traits of *B. inermis*. Some traits were strongly affected by environmental effects, among which the vegetative branch height, leaf width, panicle characteristics and stem diameter are suitable for studies that need to be sensitive to environmental effects. More resources were invested in vegetative organs than in nutrient acquisition organs, which indicated that plants were more inclined to regenerate and expand their population through asexual reproduction. The aboveground organs were closely related to the aboveground biomass allocation, which was more conducive to plants adapting to an environment with frequent temperature and water changes by coordinating their various organs.

This study provides basic information regarding the phenotypic diversity of *B. inermis* and its potential breeding sources. *B. inermis* in the central part of the north slope of the Tianshan Mountains showed obvious advantages. It is the most promising germplasm resource identified in this study due to its high plant height, wide leaves and high material yield. *B. inermis* has the ability to adapt to different environments, which suggests that it has the ability to withstand local and global climate changes. Further field experiments will help to reveal the phenotypic adaptability of *B. inermis* in different environments and will provide a reference for future work on phenotypic gene mapping and gene screening.

Acknowledgements. The authors would like to acknowledge the contributions and support of College of Grassland and Environmental Sciences, Xinjiang Agricultural University, Key Laboratory of Grassland Resources and Ecology of Xinjiang.

Author contributions. Jin, G. L. conceived the ideas; Gong, K. conducted the experiments and prepared samples. L.W.H. and G.K. collected the data; L.W.H. and G.K. analysed the data; G.K. wrote the manuscript. All authors contributed critically to the drafts.

Funding information. This research was funded by the Grassology Peak Discipline Foundation of the Xinjiang Uygur Autonomous Region, China (CXGFXK-2019-03), China Forage and Grass Research System (CARS34).

Conflict of interests. The authors declare that they have no conflict of interests.

REFERENCES

[1] Biligetu, B., Coulman, B. (2011): Leaf area expansion and net photosynthetic rate of three bromegrass (Bromus) species. – Photosynthetica 49(3): 478-480.

http://www.aloki.hu ● ISSN 1589 1623 (Print) ● ISSN 1785 0037 (Online)
DOI: http://dx.doi.org/10.15666/aeer/1906_44594475

[2] Bobowicz, M. A., Krzakowa, M. (1986): Anatomical differences between Pinus mugs Truro populations from the Tarts Mts. expressed in needle traits and in needle and cone traits together. – Acta Societatis Botanicorum Poloniae 55(2): 275.
[3] Bradshaw, A. D. (1965): Evolutionary significance of phenotypic plasticity in plants. – Advances in Genetics 13(1): 115-155.
[4] Chen, J. H., Zhang, Y. M. (2012): Strategies for biomass allocation of two desert plant species under water stress. – Arid Zone Research 29(03): 432-439.
[5] Copete, A., Moreno, R., Cabrera, A. (2018): Characterization of a world collection of Agropyron cristatum accessions. – Genet Resour Crop Evol. 65: 1455-1469.
[6] Duruflé, H., Ranocha P., Mbadinga, D. M, et al. (2019): Phenotypic trait variation as a response to altitude-related constraints in Arabidopsis populations. – Frontiers in Plant Science 10.
[7] Hao, F., Xu, Z., Li, P., et al. (2011): Genetic diversity of Bromus inermis on agronomic traits. – Pratacultural Science 28(05): 769-776.
[8] Hong, J. J., Liu, S., Glover, P., et al. (2017): Mathematical and experimental investigation of water migration in plant xylem. – J Bionic Eng 14(4): 622-630.
[9] Huxman, T. E., Smith, M. D., Fay, P. A., et al. (2004): Convergence across biomes to a common rain-use efficiency. – Nature 429: 651-654.
[10] Lermi, A. G., Erdogdu, Altinok, S. (2018): The effects of chemical and organic fertilizer applications on forage yield and quality of smooth brome (Bromus inermis L.) under irrigated and non-irrigated conditions. – Applied Ecology and Environmental Research 16(5): 6087-6094.
[11] Li, X., Liu, Z., Wang, Z., et al. (2015): Pathways of Leymus chinensis individual aboveground biomass decline in natural semiarid grassland induced by overgrazing: a study at the plant functional trait scale. – Plos One 10(5): 192-205.
[12] Liu, H., Mi, Z., Lin, L., et al. (2018): Shifting plant species composition in response to climate change stabilizes grassland primary production. – Proceedings of the National Academy of Sciences of the United States of America 115(16), 4051-4056.
[13] Lu, J. J., Tan, D. Y., Baskin, J. M., et al. (2012): Phenotypic plasticity and bet-hedging in a heterocarpic winter annual/spring ephemeral cold desert species of Brassicaceae. – Oikos 121, 357-366.
[14] Luo, Y. J., Wang, X. K., Zhang, X. Q., et al. (2012): Root: shoot ratios across China's forests: forest type and climatic effects. – Forest Ecology and Management 269: 19-25.
[15] Ma, W. L., Shi, P. L., Li, W. H., et al. (2010): Changes in individual plant traits and biomass allocation in alpine meadow with elevation variation on the Qinghai-Tibetan Plateau. – Science in China Series C: Life Sciences 53(9): 1142-1151.
[16] Majidi, M. M., Bahrami, S., Abtahi, M., et al. (2017): Genetic analysis of seed-related traits in smooth bromegrass (Bromus inermis) under well-watered and water-stressed conditions. – Grass and Forage Science 72(1).
[17] Mateus, H. V., Agustin, Z., Ariadne, F. L., et al. (2015): Semi-determinate growth habit adjusts the vegetative-to-reproductive balance and increases productivity and water-use efficiency in tomato (Solanum lycopersicum). – Journal of Plant Physiology, 177: 11-19.
[18] McKown, A. D., Guy, R. D., Klapste, J. (2014): Geographical and environmental gradients shape phenotypic trait variation and genetic structure in Populus trichocarpa. – New Phytol 201(4): 1263-1276.
[19] Meng, T. T., Ni, J., Wang, G. H. (2007): Plant functional traits, environments and ecosystem functioning. – Journal of Plant Ecology 31: 150-165.
[20] Michel, Loïc, N., et al. (2015): Selective top-down control of epiphytic biomass by amphipods from Posidonia oceanica meadows: implications for ecosystem functioning. – Belgian Journal of Zoology 145(2): 83-93
[21] Morgenstern, M. (2011): Geographic Variation in Forest Trees: Genetic Basis and Application of Knowledge in Silviculture. – University of British Columbia Press, Vancouver, pp. 3-18.

http://www.aloki.hu ● ISSN 1589 1623 (Print) ● ISSN 1785 0037 (Online)
DOI: http://dx.doi.org/10.15666/aeer/1906_44594475

[22] Olowa, L. F., Lalisan, J. A., Ma, R. (2018): Leaves of Tectaria dissecta ((G. Forst.) Lellinger) collected from three elevations in Tinago Falls, Iligan City exhibit morphological variation using fractal analysis. – Electronic J Biol 13: 4.
[23] Ott, J. P., Butler, J. L., Rong, Y. (2017): Greater bud outgrowth of Bromus inermis than Pascopyrum smithii under multiple environmental conditions. – Journal of Plant Ecology 10(3): 518-527.
[24] Pang, T. Y., Lercher, M. (2015): Evolution of complex phenotypes through successions of adaptive steps. Quantitative Biology. – arXiv: Populations and Evolution Corpus ID: 1744841
[25] Peltonen-Sainio, P., Jauhiainen, L., Hakala, K. (2011): Crop responses to temperature and precipitation according to long-term multi-location trials at high-latitude conditions. – Journal of Agricultural Science 149(1): 49-62.
[26] Sadras, V. O., Slafer, G. A. (2012): Environmental modulation of yield components in cereals: heritabilities reveal a hierarchy of phenotypic plasticities. – Field Crops Research 127: 215-224.
[27] Salesman, J. B., Thomsen, M. (2011): Smooth brome (Bromus inermis) in tallgrass prairies: a review of control methods and future research directions. – Ecological Restoration 29(4): 374-381.
[28] Slafer, G. A., Savin, Sadras, V. O. (2014): Coarse and fine regulation of wheat yield components in response to genotype and environment. – Field Crops Research 9(3): 158-169.
[29] Stotz, G. C., Gianoli, E., Patchell, M. J., et al. (2017): Differential responses of native and exotic plant species to an invasive grass are driven by variation in biotic and abiotic factors. – Journal of Vegetation Science 28(2): 325-336.
[30] Ulrich, E., Perkins, L. (2014): Bromus inermis and Elymus canadensis but not Poa pratensis demonstrate strong competitive effects and all benefit from priority. – Plant Ecology 215(11): 1269-1275.
[31] Wal, R., Stien, A. (2016): High-arctic plants like it hot: a long-term investigation of between-year variability in plant biomass. – Ecology 95(12).
[32] Wang, Y. H., Yu, F. H., Dong, M., et al. (2010): Growth and biomass allocation of Lolium perenne seedlings in response to mechanical stimulation and water availability. – Annales Botanici Fennici 47(5): 367-372.
[33] Wang, R. Z., Huang, W. W., Chen, L., et al. (2011): Anatomical and physiological plasticity in Leymus chinensis (Poaceae) along large-scale longitudinal gradient in Northeast China. – PLoS ONE 6(11): 374-381.
[34] Woodis, J. E., Jackson, R. D. (2010): The effects of clipping height and frequency on net primary production of Andropogon gerardii (C4 grass) and Bromus inermis (C3 grass) in greenhouse experiments. – Grass and Forage Science 63. https://doi.org/10.1111/j.1365-2494.2008.00653.x.
[35] Xu, X., Niu, S. L., Sherry, R. A., et al. (2012): Interannual variability in responses of belowground net primary productivity (NPP) and NPP partitioning to long-term warming and clipping in a tallgrass prairie. – Global Change Biology 18: 1648-1656.
[36] Yang, Y. H., Fang, J. Y., Ji, C. J., et al. (2009): Above- and belowground biomass allocation in Tibetan grasslands. – Journal of Vegetation 1: 177-184.
[37] Yang, X. P., Li, P., Dong, C. F., et al. (2020): Studies on the dynamics of above-ground biomass and nutritive values of annual ryegrass and common oat. – Acta Agrestia Sinica 28(01): 149-158.
[38] Yuan, J., Wang, P., Yang, Y. (2019): Effects of simulated herbivory on the vegetative reproduction and compensatory growth of Hordeum brevisubulatum at different ontogenic stages. – International Journal of Environmental Research and Public Health 16(9): 1663-1671.

http://www.aloki.hu ● ISSN 1589 1623 (Print) ● ISSN 1785 0037 (Online)
DOI: http://dx.doi.org/10.15666/aeer/1906_44594475

[39] Zhang, J., Li, X., Zhuang, L., et al. (2015): Growth forms of Leymus chinesis (Poaceae) at the different developmental stages of the natural population. – Plant Species Biology 29(3): 263-271.
[40] Zhao, N. X., Zhang, L. H., Zhao, T. T., et al. (2016): Trait differentiation among Stipa krylovii populations in the Inner Mongolia Steppe region. – Flora 223: 90-98.
[41] Zhao, P. P., Li, G. Q., Shao, W. S., et al. (2018): Influence of herbivore exclusion on the soil seed bank and the aboveground vegetation characteristics of Agropyron mongolicun dominant desert steppe grassland. – Acta Prataculturae Sinica 27(1): 42-52.
[42] Zheng, S., Zhu, H., Wang, X. R., et al. (2019): Environment-dependent phenotypic variation of Osmanthus fragrans. – Journal of Nanjing Forestry University (Natural Sciences Edition).

http://www.aloki.hu ● ISSN 1589 1623 (Print) ● ISSN 1785 0037 (Online)
DOI: http://dx.doi.org/10.15666/aeer/1906_44594475

SELECTIVE FEEDING OF TWO BIVALVE SPECIES ON THE PHYTOPLANKTON COMMUNITY IN AN AQUACULTURE POND REVEALED BY HIGH-THROUGHPUT SEQUENCING

QIAO, L.[1] – REN, C.[2] – SUN, X.[1] – SONG, K.[1] – LI, T.[1*] – MU, X.[3]

[1]*Key Laboratory of Sustainable Utilization of Technology Research for Fishery Resource of Zhejiang Province, Zhejiang Marine Fisheries Research Institute, Zhoushan 316012, China*

[2]*Marine Science and Technology College, Zhejiang Ocean University, Zhoushan, Zhejiang 316000, China*

[3]*Fishery Resource and Environment Research Center, Chinese Academy of Fishery Sciences, Beijing 100141, China*

**Corresponding author*
e-mail: litiejun1982@126.com; phone: +86-580-2299-886

(Received 26th May 2021; accepted 3rd Sep 2021)

Abstract. Filtering bivalves consume microalgae throughout their life cycles, and for several decades, the selective feeding of bivalves on phytoplankton has been an active area of research in the fields of bivalve physiology and ecology. However, owing to the limitations of detection methods, there is comparatively little data available regarding the in situ food composition of suspension-feeding bivalves. In this study, conducted in December 2020, we used high-throughput sequencing of the 23S rRNA gene to characterize the phytoplankton community within the gut contents of the bivalves *Meretrix meretrix* and *Scapharca subcrenata* reared in the same aquaculture ponds. Phytoplankton from six phyla were identified in hepatopancreas samples obtained from *M. meretrix*, among which, Cyanophyta was found to be the predominant group, followed by Bacillariophyta. Seven phyla of phytoplankton were detected in the hepatopancreas samples obtained from *S. subcrenata*, among which, Cyanophyta and Chlorophyta were dominant. Ivlev's electivity index was used to evaluate the feeding selectivity of the bivalves. The results indicated that *M. meretrix* showed a preferential selection for Cyanophyta and Bacillariophyta, whereas *S. subcrenata* preferentially selected Xanthophyta, Cyanophyta, and Chlorophyta. At the genus level, *M. meretrix* showed a preference for 12 genera, including *Phormidium*, *Pleurocapsa*, *Skeletonema*, *Synechococcus*, and *Planktothricoides*, whereas *S. subcrenata* showed a preferential selection for 16 genera, including *Tetraselmis*, *Pleurocapsa*, and *Planktothricoides*.
Keywords: *mariculture, Meretrix meretrix, Scapharca subcrenata, 23S rRNA gene, feeding selectivity*

Introduction

Bivalves are the predominant mariculture species in China (Mao et al., 2019), with bivalve production in 2019 amounting to approximately 14.39 million tons, which accounted for more than 69% of China's total mariculture production (CFSY, 2020). Bivalves not only affect phytoplankton community structure but also enhance sediment nutrient cycling via benthic–pelagic coupling (Newell, 2004; Smyth et al., 2013; Murphy et al., 2016), and accordingly play key functional roles in aquatic ecosystems. Bivalves can exert "top-down" grazer control on phytoplankton and filter other organic matter, thereby increasing the amount of light reaching the sediment surface, which in turn has the effect of reducing the dominance of phytoplankton production and extending the depth to which ecologically important benthic plants such as benthic microalgae can grow (Newell and Ott, 1999; Newell, 2004). Conversely, bivalves can also exert "bottom-up" nutrient control on phytoplankton production. The nitrogen and

http://www.aloki.hu ● ISSN 1589 1623 (Print) ● ISSN 1785 0037 (Online)
DOI: http://dx.doi.org/10.15666/aeer/1906_44774491

phosphorus excreted by bivalves and regenerated from their biodeposits are recycled back into the water column, thereby supporting further phytoplankton production (Newell, 2004). Given their ecological and economic importance, suspension-feeding bivalves have been extensively studied.

Meretrix meretrix and *Scapharca subcrenata* are important commercial bivalve species consumed in China (CFSY, 2020), for which live microalgae are a fundamental food source. In this regard, previous studies have revealed that bivalves are characterized by feeding selectivity (Ward and Shumway, 2004; Rosa et al., 2018). Certain bivalves have been found to distinguish their food from various types of particles, preferentially ingesting particles of a suitable size and nutrient content, while rejecting low-quality or unwanted material, thus optimizing energy intake (Ward and Shumway, 2004). Elucidating the food preferences of suspension-feeding bivalves is essential for enhancing existing models of bivalve growth and, consequently, to gain a better understanding of the dynamics of the ecosystems they dominate (Pales Espinosa et al., 2016). Accordingly, the mechanisms used by suspension-feeding bivalves to capture and ingest high-quality food from a mixture of particles of various sizes and physicochemical properties have for several decades been a major area of biological oceanographic research (Ward and Shumway, 2004; Rosa et al., 2018).

Several methodological approaches, including microscopic examination, pigment-based method, isotope labeling method, real-time fluorescent quantitative PCR (qPCR), have been adopted for assessing the selective feeding of bivalves (Ward and Shumway, 2004; Rosa et al., 2018). In addition to being highly laborious and time-consuming, direct microscopy rarely enables accurate identification of similar taxa and small cells (Manoylov, 2014). In particular, food contents are often partially digested and morphologically altered, which accordingly hinders the acquisition of relevant information in the case of gut analyses (Sautour et al., 2000). Furthermore, pigment-based methods are notably sensitive to pigment breakdown, and chlorophyll pigments tend to be broadly class-specific rather than specific to particular species (Irigoien et al., 2004). In addition, pigment-based methods do not yield data for heterotrophic prey (Nejstgaard et al., 2008). Although the aforementioned two methods can be used in in situ studies, investigations of the selective feeding of bivalves have been hampered by the inaccurate and laborious identification and counting of microalgal species. Although isotopic labeling has been used to provide information on the feeding preferences of bivalves (Brillant and MacDonald, 2002; Fukumori et al., 2008), this technique is both a time-consuming and expensive approach to distinguishing microalgal species. Moreover, the use of stable isotope tracers does not precisely reflect the in situ food composition of predators in the natural environment (Schmidt et al., 2003). qPCR has the notable advantages of strong specificity, high sensitivity, good repeatability, and accuracy, and has been successfully applied to assess the selective feeding of bivalve larvae based on species-specific primers targeting microalgal 18S rDNA sequences (Liao et al., 2017). This technique is mainly used for qualitative and quantitative detection of known bait microalgae, which although suitable for ingestion experiments in the laboratory, cannot be effectively applied in characterizing the diets of bivalves in the natural environment. Consequently, the prevailing lack of information regarding in situ diets can largely be attributed to methodological deficiencies that have hindered our understanding of the selective feeding of bivalves. Nevertheless, in recent years, the rapid development of modern molecular biological techniques has offered new approaches for examining the in situ food composition of organisms (Jedlicka et al.,

http://www.aloki.hu ● ISSN 1589 1623 (Print) ● ISSN 1785 0037 (Online)
DOI: http://dx.doi.org/10.15666/aeer/1906_44774491

2017; Su et al., 2018). High-throughput sequencing is now more rapid, has higher throughput, is less costly, and has obvious advantages over the traditional methods of studying in situ bivalve diets.

In this study, we performed high-throughput sequencing of the 23S rRNA gene to investigate the composition of phytoplankton in the hepatopancreases of *M. meretrix* and *S. subcrenata* reared in aquaculture ponds, along with samples of pond water and sediments. The objectives of this study were to analyze the composition of phytoplankton within the gut contents of *M. meretrix* and *S. subcrenata*, and thereby characterize the feeding selectivity of these two bivalve species on phytoplankton in the natural environment.

Materials and methods

Ethical statement

All experiments conducted in this study were carried out in accordance with the Care and Use of Laboratory Animals guidelines formulated by the Ministry of Science and Technology of China. The protocol used in this study was approved by the Institutional Animal Care and Use Committee of Zhejiang Marine Fisheries Research Institute.

Sample collection

To examine the composition of phytoplankton potentially available as sources of food for the two bivalve species *M. meretrix* and *S. subcrenata*, we collected ambient four water samples and two sediment samples from two ponds at the Daishan Dongsha Aquafarm located in Zhoushan City, Zhejiang Province (30°18′50″N; 122°8′32″E), in December 2020. Control samples were collected from an area of the ponds devoid of bivalves. Biological samples of *M. meretrix* and *S. subcrenata* were collected simultaneously and stored at −4 °C for a short period of time prior to dissection.

Sample preparation

Samples of pond water (1 L) were filtered through 0.22 μm Millipore membranes, and membranes containing the filtered plankton were flash frozen and stored at −80 °C until used for DNA analysis. Sediment samples were sub-packaged into microtubes and stored at −80 °C until used for DNA analysis. To reduce diet profile differences among the bivalve individuals, the hepatopancreases of 10 individuals were pooled as a single composite sample for each pond, homogenized with a pestle in 5 mL microtubes, and stored at -80 °C until used for DNA analysis.

High-throughput sequencing of phytoplankton and bioinformatic analysis

Total genomic DNA was extracted from all samples using a FastDNA spin kit for soil (MP Biomedicals, OH, USA), following the manufacturer's instructions. The quality of the DNA was verified by gel electrophoresis on 0.5% agarose gels, and DNA concentrations were determined using a NanoDrop spectrophotometer (NanoDrop Technologies, Wilmington, DE, USA). The primers p23SrV_f1 (5′-GGA CAG AAA GAC CCT ATG AA-3′) and p23SrV_r1 (5′-TCA GCC TGT TAT CCC TAG AG-3′) were used to amplify the 23S rDNA gene (Sherwood and Presting, 2007). Purified PCR

http://www.aloki.hu ● ISSN 1589 1623 (Print) ● ISSN 1785 0037 (Online)
DOI: http://dx.doi.org/10.15666/aeer/1906_44774491

products were sequenced at Majorbio Bio-Pharm Technology Co. Ltd. (Shanghai, China) using the MiSeq platform (Illumina, San Diego, USA).

The 23S rDNA sequences were processed using the QIIME (version 1.91) software package. The original sequence data were sorted into valid reads after demultiplexing and quality filtering, and the high-quality sequences thus obtained were clustered into operational taxonomic units (OTUs) with an identity threshold of 97%, using UPARSE (version 7.1 http://drive5.com/uparse/) with a novel "greedy" algorithm that performs simultaneous de novo-based chimera filtering and OTU clustering. The taxonomy of a representative sequence of each OTU was assigned using the Basic Local Alignment Search Tool (BLAST) in the NCBI database (http://www.ncbi.nlm.nih.gov). Following the exclusion of bacteria (all non-cyanobacteria) and unclassified sequences, phytoplankton sequences were selected for analysis of community composition based on taxonomic information.

The sequencing data used in this study have been archived in the Sequence Read Archive (SRA) of the NCBI database under accession number SRP307598.

Feeding selectivity analysis

The selectivity of bivalves with respect to feeding on phytoplankton was evaluated using Ivlev's electivity index (E) (Ivlev, 1961), calculated using the following formula:

$$E = (r_i - p_i)/(r_i + p_i) \quad \text{(Eq.1)}$$

In *Equation 1*, r_i is the relative abundance of phytoplankton in the hepatopancreas sample from bivalves, and p_i is the relative abundance of similar items in pond water. The calculated values of E range from -1.0 to + 1.0, with $-1.0 \leq E \leq -0.3$ indicating the avoidance or inaccessibility of a prey item, $-0.3 < E < 0.3$ indicating random selection from the environment, and $0.3 \leq E \leq 1.0$ indicating active selection (Strauss, 1979; Puig et al., 2001).

Results

High-throughput sequencing data

A total of 290,347 raw reads with an average read length of 368 nucleotides were obtained based on the high-throughput Illumina sequencing of all samples. After quality and chimera assessments and the removal of low-quality reads, a total of 263,314 clean reads and 334 OTUs were obtained (*Table 1*). Taxa were assigned to the representative sequences of each OTU using the NCBI database. On the basis of the taxonomic information thus obtained, the sequences were annotated to 20 different phyla (*Fig. 1*). In the control sample, Chrysophyta sequences accounted for the highest proportion of the total sequences (54.86%), followed by Chlorophyta (16.33%) and Cryptophyta (11.15%). In water samples, Cryptophyta showed the highest relative abundance (41.49%), followed by Chrysophyta (26.69%) and Chlorophyta (14.06%), whereas dominant phyla in the sediment samples were Cyanobacteria (56.88%) and Bacillariophyta (30.08%). In the hepatopancreas samples obtained from *M. meretrix*, Cyanobacteria (45.36%), and Proteobacteria (11.28%) were found to be dominant, whereas in samples obtained from *S. subcrenata*, Cyanobacteria (31.88%), Chlorophyta (23.89%), and Proteobacteria (13.67%) were predominant (*Fig. 1*). Following the

http://www.aloki.hu ● ISSN 1589 1623 (Print) ● ISSN 1785 0037 (Online)
DOI: http://dx.doi.org/10.15666/aeer/1906_44774491

exclusion of bacteria (all non-cyanobacteria), zooplankton, macroalgae, and unclassified sequences, the remaining 216,910 sequences were assigned to the phytoplankton taxa (*Table 1*). The number of phytoplankton sequences was randomly rarefied to the number of sequences present in the sample with the lowest amount, which was used in further analyses of community composition and diversity.

Table 1. *The numbers of sequences in quality control analysis*

Samples	Raw reads	Clean reads	Total OTUs	Phytoplankton reads
Control sample	62,630	54,962	152	52,716
Water sample	62,914	55,651	175	54,314
Sediment sample	64,269	55,506	219	51,362
Hepatopancreas sample from *Meretrix meretrix*	47,655	46,595	78	26,854
Hepatopancreas sample from *Scapharca subcrenata*	52,879	50,602	87	31,665
Sum	290,347	263,314	334	216,910

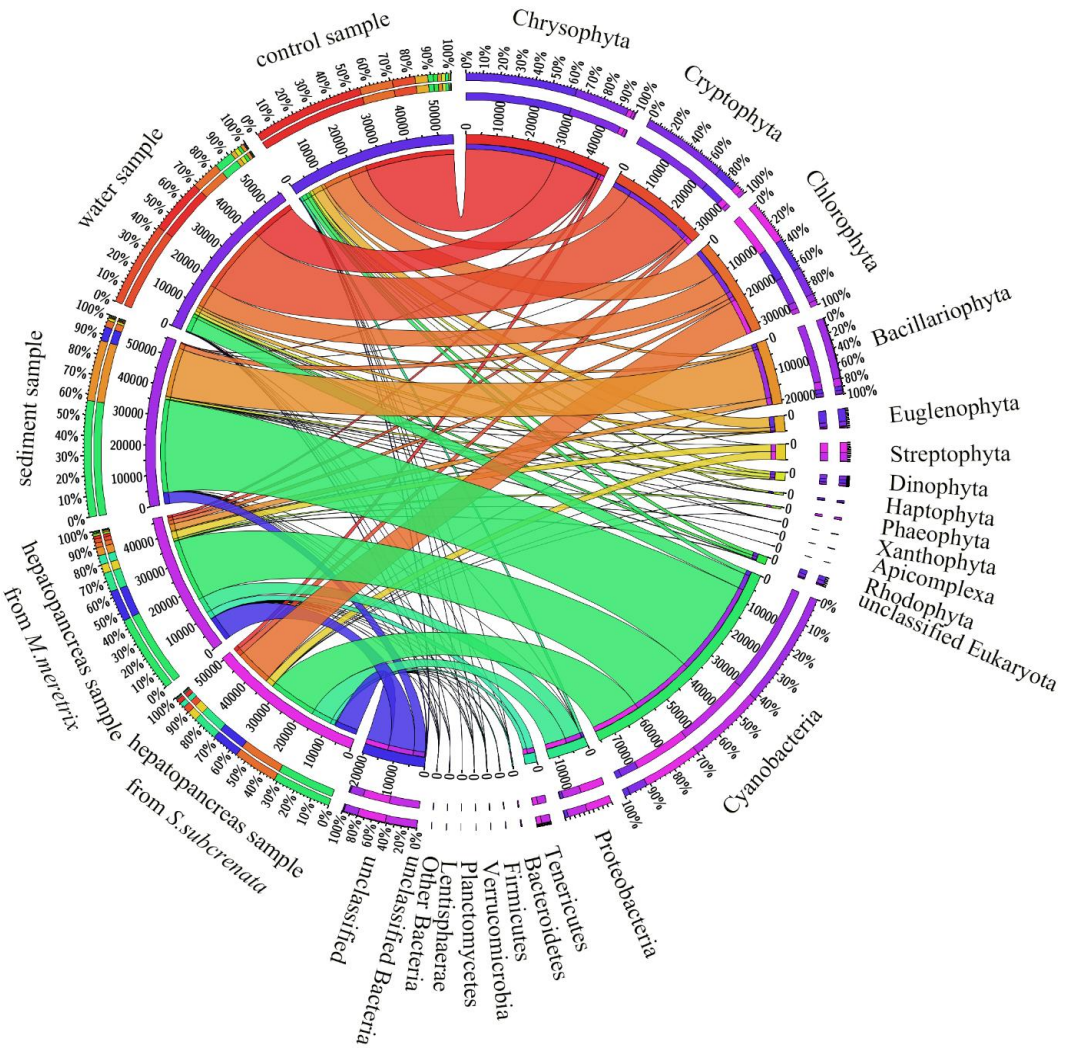

Figure 1. *Circular representation of sequences assigned to 20 phyla and unclassified groups of phytoplankton*

http://www.aloki.hu ● ISSN 1589 1623 (Print) ● ISSN 1785 0037 (Online)
DOI: http://dx.doi.org/10.15666/aeer/1906_44774491

Phytoplankton community composition

At the phylum level, we identified a total of nine phyla based on high-throughput sequencing, namely, Cyanophyta, Chrysophyta, Chlorophyta, Cryptophyta, Bacillariophyta, Euglenophyta, Dinophyta, Haptophyta, and Xanthophyta (*Fig. 2a*). In the control sample, Chrysophyta was found to be the predominant group, accounting for 57.48% of the total phytoplankton community, followed by Chlorophyta (16.96%) and Cryptophyta (11.53%). In the water samples, Cryptophyta showed the highest relative abundance (46.00%), followed by Chrysophyta (25.39%) and Chlorophyta (14.21%), and in the sediment samples, Cyanophyta and Bacillariophyta comprised the largest proportions of phytoplankton, with relative abundances of 62.26% and 31.65%, respectively. No representatives of Xanthophyta were detected in sediment samples. In the hepatopancreas samples obtained from *M. meretrix*, only six phyla were identified, with Cyanophyta being the predominant group (76.36%), followed by Bacillariophyta (8.71%). No representatives of the phyla Dinophyta, Haptophyta, and Xanthophyta were detected in these samples. Seven phyla (excluding Euglenophyta and Haptophyta) were detected in the hepatopancreas samples of *S. subcrenata*, with Cyanophyta (60.22%) and Chlorophyta (32.08%) being characterized as the most prominent groups.

At the genus level, we identified 57 genera based on high-throughput sequencing. In the control sample, *Pseudopedinella* was found to be the predominant group, accounting for 57.34% of the total phytoplankton, followed by *Ostreococcus* (13.37%). In the water samples, *Teleaulax* and *Pseudopedinella* represented the largest proportions of phytoplankton, with relative abundances of 43.48% and 25.28%, respectively, whereas large proportions of *Synechococcus* (55.52%) and *Skeletonema* (18.89%) were present in the sediment samples. In the hepatopancreas samples obtained from *M. meretrix*, *Synechococcus* (40.53%) and *Phormidium* (16.47%) were the predominant genera, whereas large proportions of *Planktothricoides*, *Tetraselmis*, *Pleurocapsa*, and *Synechococcus* were detected in the hepatopancreas samples obtained from *S. subcrenata*, with relative abundances of 25.46%, 24.75%, 20.95%, and 10.27%, respectively (*Fig. 2b*).

Feeding selectivity of bivalves

The feeding selectivity of bivalves on phytoplankton was evaluated based on Ivlev's electivity index (*Fig. 3*). At the phylum level, the index values indicated that *M. meretrix* showed preferential selection for Cyanophyta (0.80) and Bacillariophyta (0.68), whereas it tends to avoid Dinophyta (-1.00), Haptophyta (-1.00), Xanthophyta (-1.00), Cryptophyta (-0.81), Chrysophyta (-0.77), and Chlorophyta (-0.44), and appears to consume Euglenophyta according to availability. Comparatively, *S. subcrenata* was found to preferentially select Xanthophyta (0.82), Cyanophyta (0.75), and Chlorophyta (0.39), but appeared to avoid Euglenophyta (-1.00), Haptophyta (-1.00), Dinophyta (-0.92), Cryptophyta (-0.84), Chrysophyta (-0.79), and Bacillariophyta (-0.70). At the genus level, *M. meretrix* showed a preference for 12 genera and a neutral response to 28 genera (*Table 2*), whereas *S. subcrenata* showed a preferential selection for 16 genera but a neutral response to 27 genera (*Table 2*). Among the dominant genera in the samples (*Fig. 2b*), *M. meretrix* appears to actively select *Phormidium* (1.00), *Pleurocapsa* (0.98), *Skeletonema* (0.89), *Synechococcus* (0.68), *Planktothricoides* (0.48), and avoids *Pseudopedinella* (-1.00), *Tetraselmis* (-1.00), *Ostreococcus* (-1.00), *and Teleaulax* (-0.89). *S. subcrenata* actively selects *Tetraselmis* (1.00), *Pleurocapsa*

http://www.aloki.hu ● ISSN 1589 1623 (Print) ● ISSN 1785 0037 (Online)
DOI: http://dx.doi.org/10.15666/aeer/1906_44774491

(0.99), *Planktothricoides* (0.99), and avoids *Pseudopedinella* (-1.00), *Ostreococcus* (-1.00), *Teleaulax* (-0.88), *and Skeletonema* (-0.37), whereas *Synechococcus* is selected according to availability.

Table 2. *Selectivity of Meretrix meretrix and Scapharca subcrenata for phytoplankton at the genus level. Symbols "+", "-" and "/" indicates active selection, avoidance and random selection, respectively*

Genus	*M. meretrix*	*S. subcrenata*
Synechococcus	+	/
Pseudopedinella	-	-
Teleaulax	-	-
Pleurocapsa	+	+
Skeletonema	+	-
Planktothricoides	+	+
Tetraselmis	-	+
Ostreococcus	-	-
Phormidium	+	/
Eutreptiella	/	-
Cyanobium	+	+
Picochlorum	+	+
Haslea	-	-
Gloeotilopsis	+	+
Microchloropsis	+	+
Micromonas	-	-
Halamphora	-	-
Nostoc	+	-
Kryptoperidinium	-	-
Proteomonas	/	/
Chrysochromulina	-	-
Actinocyclus	-	-
Synechocystis	+	+
Lyngbya	-	+
Microcoleus	+	/
Pyramimonas	-	-
Oscillatoria	/	+
Anabaena	/	+
Jaaginema	-	+
Nitzschia	-	-
Cyanobacterium	/	+
Pseudoscourfieldia	-	/
Bathycoccus	-	-
Vaucheria	/	+
Chondrocystis	/	+
Lusitaniella	/	+
Thermosynechococcus	-	-
Trichodesmium	-	-
Nephroselmis	-	-
Heterosigma	-	-
Marsupiomonas	-	-
Picocystis	-	-
Euglena	-	-
Tisochrysis	-	-
Mychonastes	-	-
Spirulina	-	-
Resultomonas	-	-
Dangeardinia	-	-

http://www.aloki.hu ● ISSN 1589 1623 (Print) ● ISSN 1785 0037 (Online)
DOI: http://dx.doi.org/10.15666/aeer/1906_44774491

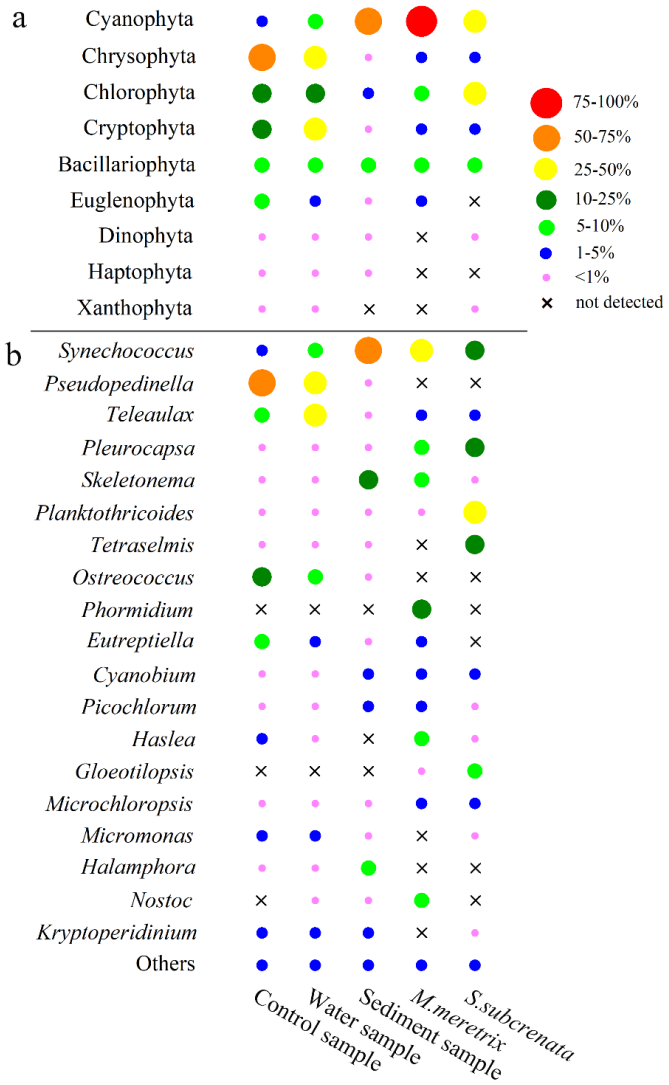

Figure 2. *Relative abundance of taxa in the phytoplankton community at the phylum (a) and genus (b) levels identified using high-throughput sequencing. The size of the circles shows proportions of sequences from each sample*

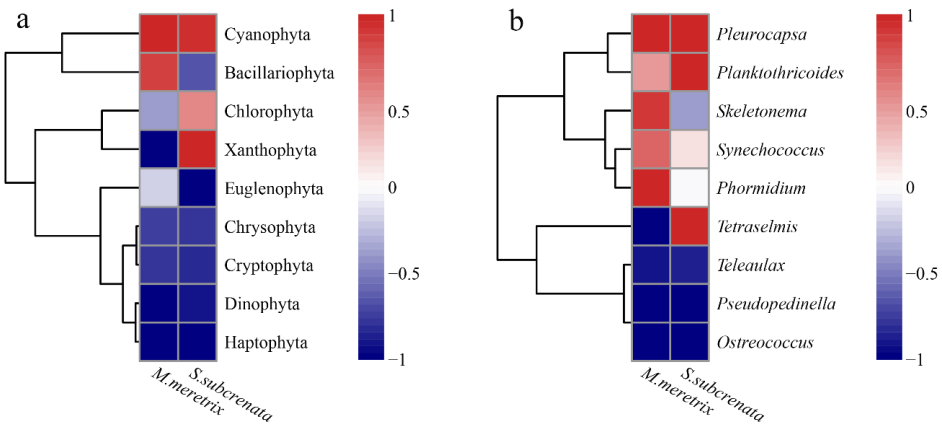

Figure 3. *Heatmaps showing bivalve feeding selectivity on phytoplankton at the phylum (a) and genus (b) levels*

APPLIED ECOLOGY AND ENVIRONMENTAL RESEARCH 19(6):4477-4491.
http://www.aloki.hu ● ISSN 1589 1623 (Print) ● ISSN 1785 0037 (Online)
DOI: http://dx.doi.org/10.15666/aeer/1906_44774491

Discussion

During the course of their lifetime, bivalves feed exclusively on Phytoplankton, the availability of which is a key factor in determining growth and development, and is also an important factor affecting the sustainable development of aquaculture. The accuracy and precision of the methods used to analyze diets make an important contribution to theoretical studies of feeding, which is also vital to the application of research results in the practice of ecological aquaculture. In recent years, there have been notable advances with respect to the methodology used for dietary analyses (Leray et al., 2013; Leal et al., 2016; Hirai et al., 2017), with high-throughput sequencing being increasingly more widely used by researchers, given its high efficiency. A number of marker genes (including 16S rRNA, 18S rDNA, and ITS) have been employed to characterize the feeding habits and intestinal microbial communities of aquatic animals (Borsodi et al., 2017; Su et al., 2018; Yeh et al., 2020). The universal plastid amplicon (UPA), a fragment of the plastid 23S rRNA gene, can be used not only to eliminate the interference of bivalve host genes but also to identify both eukaryotic algae and cyanobacteria, which are widely used to study phytoplankton community structure and diversity (Sherwood and Presting, 2007; Li et al., 2016; Qiao et al., 2019). In the present study, we used sequences of the 23S rDNA gene as a marker, analyzed based Illumina sequencing, to assess the feeding preference of *M. meretrix* and *S. subcrenata* on phytoplankton in the same aquacultural ponds, knowledge of which is essential for gaining an understanding of aquatic food webs and facilitating the ecosystem-based management of aquaculture.

In this study, we identified six phytoplankton phyla in hepatopancreas samples obtained from *M. meretrix* (*Fig. 2a*), among which, Cyanophyta was found to be the predominant group, followed by Bacillariophyta. Comparatively, seven phyla were detected in the hepatopancreas of *S. subcrenata*, with Cyanophyta and Chlorophyta featuring predominantly (*Fig. 2a*). In this regard, previous studies of the gut contents of more than 200 bivalve species (Hunt, 1925; Nelson, 1927, 1947; Hillman, 1965) have indicated that diatoms constitute the primary food source of bivalves (Rosa et al., 2018). We speculate that the disparity between these findings and those of the present study could be attributable to differences in the detection methods used. A majority of the previous studies have tended to use traditional microscopic techniques, amongst which light microscopy has notable limitations with respect to the identification and classification of phytoplankton with small cell sizes, particularly pico-sized and some small nano-sized phytoplankton (Manoylov, 2014; Qiao et al., 2019). In the present study, we identified the two algal genera *Synechococcus* and *Phormidium* as being dominant in the hepatopancreas samples obtained from *M. meretrix*, the diameters of which have previously been determined as ranging from 0.6 to 2.1 μm (Herdman et al., 2001) and 0.7 to 6.3 μm (Marquardt and Palinska, 2007), respectively. In the hepatopancreas samples from *S. subcrenata*, we detected large proportions of the genera *Planktothricoides*, *Tetraselmis*, *Pleurocapsa*, and *Synechococcus*. Previous studies on the ultrastructure of *Planktothricoides*, *Tetraselmis*, and *Pleurocapsa* have shown that these three algal genera have respective length and width dimensions of 1.86 to 5.96 μm and 2.83 to 13.70 μm; 6 to 16 μm and 4 to 10.5 μm; and 1.5 μm and 0.2 μm (Wujek, 1979; Hori et al., 1986; Tawong, 2017). Given these size ranges, these algae could easily evade detection by light microscopy. In recent years, an increasing number of studies have examined the contributions of picoplankton and other small particles (<4 μm) to bivalve growth (LeBlanc et al., 2012; Strøhmeier et al., 2012; Sonier et al., 2016). These picoplankton are operationally defined as particles ranging in size from

http://www.aloki.hu ● ISSN 1589 1623 (Print) ● ISSN 1785 0037 (Online)
DOI: http://dx.doi.org/10.15666/aeer/1906_44774491

0.2 to 2 μm, among which are included cyanobacteria and small eukaryotes that can numerically dominate the seston (Rosa et al., 2018). Consequently, it is quite conceivable that the contribution of pico-sized and small nano-sized phytoplankton to bivalve energetics is notably higher than previously reported.

Different bivalves have been found to have differing feeding preferences (Rosa et al., 2018). For example, Shumway et al. (1985) have applied flow cytometric techniques (FCM) to study particle capture in *Ostrea edulis* and demonstrated that this species preferentially captures the dinoflagellate *Prorocentrum minimum* over a similarly sized diatom (*Phaeodactylum tricornutum*) and cryptophyte (*Chroomonas salina*). In juvenile scallops of three species (*Placopecten magellanicus*, *Patinopecten yessoensis*, and *Argopecten irradians*) simultaneously fed a total of six algal clones, clearance rates were monitored using FCM, the results of which indicated that in scallops fed natural assemblages of particles, clearance rates varied between species, with *Placopecten* generally having higher uptake rates for all three size classes of particles (3–5 μm, 5–8 μm, > 8 μm) followed by *Argopecten* and *Patinopecten*. For the 8-μm size class of particles, *Argopecten* was found to have the highest clearance rate (Shumway et al., 1997). In laboratory feeding experiments conducted by Tang et al. (2006), of the authors provided *M. meretrix* with five different species of marine microalgae (*Isochrysis galbana*, *Dunaliella* sp., *Phaeodactylum tricornutum*, *Platymonas subcordiformis*, and *Pavlova viridis*), both singly and in various mixtures, and accordingly found that the larvae of this bivalve were characterized by selective feeding behavior, with a preference for *I. galbana*. In the present study, we found that *M. meretrix* showed a clear preference for Cyanophyta (*Phormidium*, *Pleurocapsa*, *Synechococcus*) and Bacillariophyta (*Skeletonema*), whereas *S. subcrenata* preferentially selected Xanthophyta (*Vaucheria*), Cyanophyta (*Pleurocapsa* and *Planktothricoides*), and Chlorophyta (*Tetraselmis*) (*Fig. 3; Table 2*).

The selective feeding of bivalves on phytoplankton is potentially associated with multiple factors, including cell size and shape and the quality, quantity, and availability of food (Tang et al., 2006; Chen et al., 2015; Rosa et al., 2013, 2015, 2018). Feeding selectivity based on particle size has been found to differ among bivalve species, and is probably dependent on bivalve ctenidial architecture and laterofrontal cilia/cirri microstructure (Rosa et al., 2018). In this regard, mussels have a filibranchiate homorhabdic ctenidium with large compound laterofrontal cirri that are highly efficient with respect to capturing particles ranging in size from 4 μm to 10 μm (Riisgård, 1988; Rosa et al., 2015, 2018). Compared with mussels, oysters have a pseudolamellibranchiate heterorhabdic ctenidium with well-developed laterofrontal cirri (Owen and McCrae, 1976; Ribelin and Collier, 1977), which generally have a higher capture efficiency for particles that are larger in size by more than 3 μm (Rosa et al., 2018). Moreover, scallops have a filibranchiate heterorhabdic ctenidium with a single row of laterofrontal cilia (Owen and McCrae, 1976; Beninger, 1991) and have been reported to have low capture efficiency for 2–7 μm particles (Møhlenberg and Riisgård, 1978; Riisgård, 1988).

In addition to cell size, the feeding behavior of some bivalves might also be associated with a requirement for certain essential nutrients (Caers et al., 1999; Tang et al., 2006; Chen et al., 2015). For example, studies have shown that higher eicosapentaenoic acid and arachidonic acid levels in the diet appear to have a positive effect on the total hemocyte count, granulocyte percentage, phagocytic rate, oxidative activity, and immunity of bivalves (Delaporte et al., 2003, 2006). Microalgae commonly used as aquaculture feeds include *Phormidium*, *Skeletonema*, *Thalassiosira*,

http://www.aloki.hu ● ISSN 1589 1623 (Print) ● ISSN 1785 0037 (Online)
DOI: http://dx.doi.org/10.15666/aeer/1906_44774491

Tertraselmis, *Pavlova*, *Isochrysis*, and *Nannochloropsis*, which are noted for their high nutritional value, particularly their high contents of polyunsaturated fatty acids (Muller-Feuga et al., 2003; Thajuddin and Subramanian, 2005). In addition, phytoplankton motility may influence the feeding preferences of bivalves. In the present study, we observed that both *M. meretrix* and *S. subcrenata* appeared to avoid consuming *Pseudopedinella* and *Teleaulax* (*Fig. 3*; *Table 2*), even though these two genera were predominant groups in the assessed water samples (*Fig. 2b*). The phytoplankton in these two genera are characterized by flagella, which play an important motility-related role by pulling cells in a forward direction (Heimann et al., 1989; Laza-Martínez et al., 2012; Gerea et al., 2016). This motility presumably enables the cells to evade capture by bivalves, and conceivably accounts for their higher relative abundance in water samples.

It should be noted that the findings of the present study are based on only a single sampling survey conducted on water samples and organisms collected from aquaculture ponds, and consequently, we have not been able to assess differences in the feeding selectivity of bivalves during different periods of aquaculture. Accordingly, it is necessary to carry out continuous monitoring surveys to examine differences in the feeding selectivity of different bivalve species during the different stages of culture. Nevertheless, the findings of this study do provide a useful foundation for future studies on the feeding selectivity of bivalves in natural environments using high-throughput sequencing technology.

Conclusions

In this study, we performed high-throughput sequencing to characterize the phytoplankton compositions of water and sediments and gut contents of the bivalves *M. meretrix* and *S. subcrenata* in samples collected from aquaculture ponds. In the water samples, we found Cryptophyta to have the highest relative abundance, followed by Chrysophyta and Chlorophyta, whereas in sediment samples, Cyanophyta and Bacillariophyta comprised a large proportion of the phytoplankton population. Phytoplankton within six phyla were identified in hepatopancreas samples obtained from *M. meretrix*, among which, Cyanophyta was found to be the predominant group, followed by Bacillariophyta. Similarly, we detected seven phyla of phytoplankton in hepatopancreas samples obtained from *S. subcrenata*, among which, Cyanophyta and Chlorophyta predominated. Using Ivlev's electivity index to evaluate the feeding selectivity of the two bivalve species, we established that *M. meretrix* preferentially selects phytoplankton within the phyla Cyanophyta and Bacillariophyta, whereas *S. subcrenata* was characterized by a preference for Xanthophyta, Cyanophyta, and Chlorophyta. At the genus level, *M. meretrix* showed a preference for 12 genera, including *Phormidium*, *Pleurocapsa*, *Skeletonema*, *Synechococcus*, and *Planktothricoides*, whereas *S. subcrenata* preferentially selects 16 genera, among which were *Tetraselmis*, *Pleurocapsa*, and *Planktothricoides*. In the future study, it is necessary to carry out continuous monitoring surveys to examine differences in the feeding selectivity of different bivalve species during the different stages of culture.

Acknowledgements. This study was supported by the Science and Technology Planning Project of Zhejiang Marine Fisheries Research Institute (HYS-ZY-202101), the Start-up Foundation for Doctors of Zhejiang Ocean University (11034150220004), and the Natural Science Foundation of Zhejiang Province (LQ20D030002).

http://www.aloki.hu ● ISSN 1589 1623 (Print) ● ISSN 1785 0037 (Online)
DOI: http://dx.doi.org/10.15666/aeer/1906_44774491

REFERENCES

[1] Beninger, P. G. (1991): Structures and Mechanisms of Feeding in Scallops: Paradigms and Paradoxes. – In: Shumway, S. E. (ed.) An International Compendium of Scallop Biology and Culture. Baton Rouge, LA, pp. 331-340.
[2] Borsodi, A. K., Szabó, A., Krett, G., Felfldi, T., Boros, G. (2017): Gut content microbiota of introduced bigheaded carps (*Hypophthalmichthys* spp.) inhabiting the largest shallow lake in Central Europe. – Microbiological Research 195: 40-50.
[3] Brillant, M., MacDonald, B. A. (2002): Postingestive selection in the sea scallop (*Placopecten magellanicus*) on the basis of chemical properties of particles. – Marine Biology 141(3): 457-465.
[4] Caers, M., Coutteau, P., Sorgeloos, P. (1999): Dietary impact of algal and artificial diets, fed at different feeding rations, on the growth and fatty acid composition of *Tapes philippinarum* (L.) spat. – Aquaculture 170(3): 307-322.
[5] CFSY (2020): China Fishery Statistical Yearbook. – China Agriculture Publishing House, Beijing.
[6] Chen, S. M., Tseng, K. Y., Huang, C. H. (2015): Fatty acid composition, sarcoplasmic reticular lipid oxidation, and immunity of hard clam (*Meretrix lusoria*) fed different dietary microalgae. – Fish and Shellfish Immunology 45(1): 141-145.
[7] Delaporte, M., Soudant, P., Moal, J., Lambert, C., Samain, J. F. (2003): Effect of a mono-specific algal diet on immune functions in two bivalve species - *Crassostrea gigas* and *Ruditapes philippinarum*. – Journal of Experimental Biology 206(Pt 17): 3053-3064.
[8] Delaporte, M., Soudant, P., Moal, J., Giudicelli, E., Lambert, C., Séguineau, C., Samain, J. (2006): Impact of 20:4n-6 supplementation on the fatty acid composition and hemocyte parameters of the pacific oyster *Crassostrea gigas*. – Lipids 41: 567-576.
[9] Fukumori, K., Oi, M., Doi, H., Okuda, N., Yamaguchi, H., Kuwae, M., Miyasaka, H., Yoshino, K., Koizumi, Y., Omori, K., Takeoka, H. (2008): Food sources of the pearl oyster in coastal ecosystems of Japan: evidence from diet and stable isotope analysis. – Estuarine Coastal and Shelf Science 76(3): 704-709.
[10] Gerea, M., Saad, J. F., Izaguirre, I., Queimalinos, C., Unrein, F. (2016): Presence, abundance and bacterivory of the mixotrophic algae *Pseudopedinella* (Dictyochophyceae) in freshwater environments. – Aquatic Microbial Ecology 76(3): 219-232.
[11] Heimann, K., Benting, J., Timmermann, S., Melkonian, M. (1989): The flagellar developmental cycle in algae: two types of flagellar development in uniflagellate algae. – Protoplasma 153(1-2): 14-23.
[12] Herdman, H., Castenholz, R. W., Waterbury, J. B., Rippka, R. (2001): Form-Genus XIII. Synechococcus. – In: Boone, D. R., Castenholz, R. W. (eds.), Bergey's Manual of Systematic Bacteriology. Springer-Verlag, New York, pp. 508-512.
[13] Hillman, R. E. (1965): The American oyster, Crassostrea virginica gmelin. – Chesapeake Science 6: 199.
[14] Hirai, J., Hidaka, K., Nagai, S., Ichikawa, T. (2017): Molecular-based diet analysis of the early post-larvae of Japanese sardine *Sardinops melanostictus* and Pacific round herring *Etrumeus teres*. – Marine Ecology Progress 564(564): 99-113.
[15] Hori, T., Norris, R. E., Chihara, M. (1986): Studies on the ultrastructure and taxonomy of the *Genustetraselmis* (Prasinophyceae). – The Botanical Magazine, Tokyo 99(1): 123-135.
[16] Hunt, O. D. (1925): The food of the bottom fauna of the Plymouth fishing grounds. – Journal of the Marine Biological Association of the United Kingdom 13: 560-599.
[17] Irigoien, X., Meyer, B., Harris, R., Harbour, D. (2004): Using HPLC pigment analysis to investigate phytoplankton taxonomy: the importance of knowing your species. – Helgoland Marine Research 58(2): 77-82.

http://www.aloki.hu ● ISSN 1589 1623 (Print) ● ISSN 1785 0037 (Online)
DOI: http://dx.doi.org/10.15666/aeer/1906_44774491

[18] Ivlev, V. S. (1961): Experimental Ecology of the Feeding of Fish. – Yale University Press New Haven, CT.
[19] Jedlicka, J., Vo, A., Almeida, R. (2017): Molecular scatology and high-throughput sequencing reveal predominately herbivorous insects in the diets of adult and nestling Western Bluebirds (*Sialia mexicana*) in California vineyards. – The Auk 134(1): 116-127.
[20] Laza-Martínez, A., Arluzea, J., Miguel, I., Orive, E. (2012): Morphological and molecular characterization of *Teleaulax gracilis* sp. nov. and *T. minuta* sp. nov. (Cryptophyceae). – Phycologia 36(1): 37-52.
[21] Leal, M. C., Ferrier-Pagès, C. (2016): Molecular trophic markers in marine food webs and their potential use for coral ecology. – Marine Genomics 29: 1-7.
[22] Leblanc, A., Arnold, A. A., Genard, B., Nadalini, J. B., Heine, M., Marcotte, I., Tremblay, R., Sleno, L. (2012): Determination of isotopic labeling of proteins by precursor ion scanning liquid chromatography/tandem mass spectrometry of derivatized amino acids applied to nuclear magnetic resonance studies. – Rapid Communications in Mass Spectrometry 26(10): 1165-1174.
[23] Leray, M., Yang, J. Y., Meyer, C. P., Mills, S. C. (2013): A new versatile primer set targeting a short fragment of the mitochondrial COI region for metabarcoding metazoan diversity: application for characterizing coral reef fish gut contents. – Frontiers in Zoology 10(1): 1-14.
[24] Li, G., Dong, H., Hou, W., Wang, S., Jiang, H., Yang, J., Wu, G. (2016): Temporal Succession of Ancient Phytoplankton Community in Qinghai Lake and Implication for Paleo-environmental Change. – Scientific Reports 6: 19769.
[25] Liao, K., Chen, W., Zhang, R., Zhou, H., Yan, X. (2017): qPCR analysis of bivalve larvae feeding preferences when grazing on mixed microalgal diets. – Plos One 12(6): e0180730.
[26] Manoylov, K. M. (2014): Taxonomic identification of algae (morphological and molecular): species concepts, methodologies, and their implications for ecological bioassessment. – Journal of Phycology 50(3): 409-424.
[27] Mao, Y., Lin, F., Fang, J., Fang, J., Li, J., Du, M. (2019): Bivalve Production in China. – In: Smaal, A., Ferreira, J., Grant, J., Petersen, J., Strand, Ø. (eds.) Goods and Services of Marine Bivalves. Springer, Cham.
[28] Marquardt, J., Palinska, K. A. (2007): Genotypic and phenotypic diversity of cyanobacteria assigned to the genus *Phormidium* (Oscillatoriales) from different habitats and geographical sites. – Archives of Microbiology 187(5): 397-413.
[29] Møhlenberg, F., Riisgård, H. U. (1978): Efficiency of particle retention in 13 species of suspension feeding bivalves. – Ophelia 17: 239-246.
[30] Muller-Feuga, A., Moal, J., Kaas, R. (2003): The Microalgae of Aquaculture. – In: Stottrup, J. G., McEvoy, L. A. (eds.) Live Feeds in Marine Aquaculture. Blackwell Science, Oxford, pp. 206-252.
[31] Murphy, A. E., Anderson, I. C., Smyth, A. R., Song, B., Luckenbach, M. W. (2016): Microbial nitrogen processing in hard clam (*Mercenaria mercenaria*) aquaculture sediments: the relative importance of denitrification and dissimilatory nitrate reduction to ammonium (DNRA). – Limnology and Oceanography 61(5): 1589-1604.
[32] Nejstgaard, J. C., Frischer, M. E., Simonelli, P., Troedsson, C., Brakel, M., Adiyaman, F., Sazhin, A. F., Artigas, L. F. (2008): Quantitative PCR to estimate copepod feeding. – Marine Biology 153(4): 565-577.
[33] Nelson, T. C. (1927): The mechanism of feeding in the oyster. – Proceedings of the Society for Experimental Biology and Medicine 21: 166-168.
[34] Nelson, T. C. (1947): Some contributions from the land in determining conditions of life in the sea. – Ecological Monographs 17: 337-346.

http://www.aloki.hu ● ISSN 1589 1623 (Print) ● ISSN 1785 0037 (Online)
DOI: http://dx.doi.org/10.15666/aeer/1906_44774491

[35] Newell, R. I. (2004): Ecosystem influences of natural and cultivated populations of suspension-feeding bivalve molluscs: a review. – Journal of Shellfish Research 23(1): 51-62.
[36] Newell, R. I. E., Ott, J. A. (1999): Macrobenthic Communities and Eutrophication. – In: Malone, T. C., Smadlaka, N. A., Malej, A., Harding, L. W. Jr. (eds.) Ecosystems at the Land–Sea Margin: Drainage Basin to Coastal Sea. Coastal and Estuarine Comparisons series. American Geophysical Union, Washington, DC.
[37] Owen, G., Mccrae, J. M. (1976): Further studies on the latero-frontal tracts of bivalves. – Proceedings of the Royal Society of London 194(1117): 527-544.
[38] Pales Espinosa, E., Cerrato, R. M., Wikfors, G. H., Allam, B. (2016): Modeling food choice in the two suspension-feeding bivalves, *Crassostrea virginica* and *Mytilus edulis*. – Marine Biology 163(2): 1-13.
[39] Puig, S., Videla, F., Cona, M. I., Monge, A. S. (2001): Use of food availability by guanacos (*Lama guanicoe*) and livestock in Northern Patagonia (Mendoza, Argentina). – Journal of Arid Environments 47: 291-308.
[40] Qiao, L., Chang, Z., Li, J., Chen, Z., Yang, L., Luo, Q. (2019): Phytoplankton community structure and diversity in the indoor industrial aquaculture system for *Litopenaeus vannamei* revealed by high-throughput sequencing and morphological identification. – Aquaculture Research 50: 2563-2576.
[41] Ribelin, B. W., Collier, A. (1977): Studies on the gill ciliation of the American oyster *Crassostrea virginica* (gmelin). – Journal of Morphology 151(3): 439-449.
[42] Riisgård, H. U. (1988): Efficiency of particle retention and filtration rate in 6 species of northeast American bivalves. – Marine Ecology Progress Series 45(3): 217-223.
[43] Rosa, M., Ward, J. E., Shumway, S. E., Wikfors, G. H., Pales-Espinosa, E., Allam, B. (2013): Effects of particle surface properties on feeding selectivity in the eastern oyster *Crassostrea virginica* and the blue mussel *Mytilus edulis*. – Journal of Experimental Marine Biology & Ecology 446: 320-327.
[44] Rosa, M., Ward, J. E., Ouvrard, M., Holohan, B. A., Espinosa, E. P., Shumway, S. E., Allam, B. (2015): Examining the physiological plasticity of particle capture by the blue mussel, *Mytilus edulis* (L.): confounding factors and potential artifacts with studies utilizing natural seston. – Journal of Experimental Marine Biology and Ecology 473: 207-217.
[45] Rosa, M., Ward, J. E., Shumway, S. E. (2018): Selective capture and ingestion of particles by suspension-feeding bivalve molluscs: a review. – Journal of Shellfish Research 37(4): 727-746.
[46] Sautour, B., Artigas, L. F., Delmas, D., Herbland, A., Laborde, P. (2000): Grazing impact of micro- and mesozooplankton during a spring situation in coastal waters off the Gironde estuary. – Journal of Plankton Research 22(3): 531-552.
[47] Schmidt, K., Atkinson, A., Stübing, D., Mcclelland, J. W., Montoya, J. P., Voss, M. (2003): Trophic relationships among Southern Ocean copepods and krill: some uses and limitations of a stable isotope approach. – Limnology and Oceanography 48(1): 277-289.
[48] Sherwood, A. R., Presting, G. G. (2007): Universal primers amplify a 23S rDNA plastid marker in eukaryotic algae and cyanobacteria. – Journal of Phycology 43(3): 605-608.
[49] Shumway, S. E., Cucci, T. L., Newell, R. C., Selvin, R., Guillard, R. R. L., Yentsch, C. M. (1985): Flow cytometry: a new method for characterization of differential ingestion, digestion and egestion by suspension feeders. – Marine Ecology Progress Series 24: 201-204.
[50] Shumway, S. E., Cucci, T. L., Lesser, M. P., Bourne, N., Bunting, B. (1997): Particle clearance and selection in three species of juvenile scallops. – Aquaculture International 5(1): 89-99.
[51] Smyth, A. R., Geraldi, N. R., Piehler, M. F. (2013): Oyster-mediated benthic-pelagic coupling modifies nitrogen pools and processes. – Marine Ecology Progress Series 493: 23-30.

http://www.aloki.hu ● ISSN 1589 1623 (Print) ● ISSN 1785 0037 (Online)
DOI: http://dx.doi.org/10.15666/aeer/1906_44774491

[52] Sonier, R., Filgueira, R., Guyondet, T., Olivier, F., Meziane, T., Starr, M., LeBlanc, A. R., Comeau, L. A. (2016): Picoplankton contribution to *Mytilus edulis* growth in an intense culture environment. – Marine Biology 163: 73-85.
[53] Strauss, R. E. (1979): Reliability Estimates for Ivlev's Electivity Index, the Forage Ratio, and a Proposed Linear Index of Food Selection. – Transactions of the American Fisheries Society 108(4): 344-352.
[54] Strøhmeier, T., Strand, Ø., Alunno-Bruscia, M., Duinker, A., Cranford, P. J. (2012): Variability in particle retention efficiency by the mussel *Mytilus edulis*. – Journal of Experimental Marine Biology and Ecology 412: 96-102.
[55] Su, M., Liu, H., Liang, X., Gui, L., Zhang, J. (2018): Dietary analysis of marine fish species: enhancing the detection of prey-specific DNA sequences via high-throughput sequencing using blocking primers. – Estuaries and Coasts 41(2): 1-12.
[56] Tang, B., Liu, B., Wang, G., Tao, Z., Xiang, J. (2006): Effects of various algal diets and starvation on larval growth and survival of *Meretrix meretrix*. – Aquaculture 254(1-4): 526-533.
[57] Tawong, W. (2017): Diversity of the potential 2-methylisoborneol-producing genotypes in Thai strains of *Planktothricoides* (cyanobacteria). – Brazilian Archives of Biology and Technology 60: e17160567.
[58] Thajuddin, N., Subramanian, G. (2005): Cyanobacterial biodiversity and potential applications in biotechnology. – Current Science 89(1): 47-57.
[59] Ward, J. E., Shumway, S. E. (2004): Separating the grain from the chaff: particle selection in 720 suspension- and deposit-feeding bivalves. – Journal of Experimental Marine Biology and Ecology 300: 83-130.
[60] Wujek, D. E. (1979): Intracellular bacteria in the blue-green alga *Pleurocapsa minor*. – Transactions of the American Microscopical Society 98(1): 143-145.
[61] Yeh, H. D., Questel, J. M., Maas, K. R., Bucklin, A. (2020): Metabarcoding analysis of regional variation in gut contents of the copepod *Calanus finmarchicus* in the North Atlantic Ocean. – Deep Sea Research Part II Topical Studies in Oceanography 180: 104738.

http://www.aloki.hu ● ISSN 1589 1623 (Print) ● ISSN 1785 0037 (Online)
DOI: http://dx.doi.org/10.15666/aeer/1906_44774491

COMPARISON OF PLANT FUNCTIONAL TRAITS BETWEEN WILD AND REINTRODUCED *SINOJACKIA HUANGMEIENSIS*, A RARE AND ENDANGERED PLANT

REN, Z. K.[1] – WANG, S. T.[2] – YANG, T.[2] – JIANG, M. X.[2*] – DU, K. B.[1*]

[1]*College of Horticulture and Forestry Sciences, Huazhong Agricultural University, Wuhan 430070, Hubei, China*

[2]*Key Laboratory of Aquatic Botany and Watershed Ecology, Wuhan Botanical Garden, Chinese Academy of Sciences, Wuhan 430074, China*

[*]*Corresponding authors*
e-mail: mxjiang@wbgcas.cn; kebingdu@mail.hzau.edu.cn

(Received 29th May 2021; accepted 4th Sep 2021)

Abstract. *Sinojackia huangmeiensis* is a rare and endangered plant in China. To help protect *S. huangmeiensis*, we have implemented its reintroduction via augmentation and translocation. Here, we compared the morphological, anatomical, and ecophysiological traits of leaves of wild and reintroduced (augmented and translocated) plants. Leaf thickness, leaf area, and dry matter content of the trunk leaves were highest for augmented plants, intermediate for wild plants, and lowest for translocated plants. Specific leaf area of the trunk leaves was largest for translocated plants, intermediate for wild plants, and smallest for augmented plants. The ratio of palisade tissue to spongy tissue in trunk leaves was lower in both augmented plants and translocated plants than in wild plants. The maximum photosynthetic rate of augmented and translocated plants was similar and higher than that of wild plants. Water-use efficiency was highest for wild plants and lowest for augmented plants. We found that *S. huangmeiensis* was a mesophyte. It could tolerate a wide range of light conditions and had strong ecophysiological adaptability. Our findings suggest that *S. huangmeiensis*, and perhaps other endangered plants that have narrow distributions and that produce sprouts, can be transplanted with trunk and sprouts together in order to increase their survival.
Keywords: *ecophysiological traits, mesophyte, morphological and anatomical traits, sprout, augmentation, translocation*

Introduction

With population growth and urbanization, human activities directly and indirectly have led to a heightened risk of extinction for about 20% of plants in the world (Sharrock and Wyse Jackson, 2017). In China, about 12% of the 35000 species of higher plants (bryophytes, ferns and seed plants) are under threat (Qin and Zhao, 2017). Because these threatened plants are important parts of ecosystems, they require conservation.

There are three approaches to plant conservation: in situ conservation, ex situ conservation, and reintroduction. Reintroduction is the deliberate establishment of individuals of a species in an area or habitat where it has become extirpated with the aim of establishing a viable, self-sustaining population. Plant reintroduction can involve the establishment of an extirpated species in a relatively intact habitat or it can be part of the restoration of a degraded habitat (Maunder, 1992). As a conservation measure, reintroduction is more effective than simple in situ conservation and single ex situ conservation, and can save and protect extremely small populations of wild plants (Yang et al., 2020). The three types of reintroduction include augmentation (adding

http://www.aloki.hu ● ISSN 1589 1623 (Print) ● ISSN 1785 0037 (Online)
DOI: http://dx.doi.org/10.15666/aeer/1906_44934504

more individuals to an existing population), restitution or reintroduction (reintroducing individuals to a population that has disappeared in an area), and translocation (Liu et al., 2015; Ren, 2020). While augmentation and reintroduction increase the abundance of the species in the native area, translocation can introduce the species to a new area. To date, more than 1000 plant reintroduction studies have been reported in the world. These studies have investigated physiological ecology, morphological anatomy, and functional traits (Catoni and Gratani, 2013); population dynamics, genetic diversity, and population persistence (Maschinski and Haskins, 2012; Taylor et al., 2017; Ren, 2020); and levels from the organ to the individual, population, metapopulation, and ecosystem (Seddon, 2010; Godefroid and Vanderborght, 2011). The main reproductive materials used in plant reintroductions are seeds, seedlings, grafted seedlings, cutting seedlings, tissue culture seedlings, and rarely, sprouting seedlings (Bond and Midgley, 2001; Ren, 2020).

Some woody plants can also regenerate naturally by producing seeds and by sprouting (Lu et al., 2020). Sprouting can increase the stability of plant populations under adversity (del Tredici, 2001; Lu et al., 2020). Researchers have speculated that the production of multiple sprouts by one root system increases a plant's ability to resist competition and herbivory early in the regeneration process (Pigott, 1989; Lu et al., 2020). The survival and growth of sprouts are affected by canopy tree species and microhabitat properties (Ahrens and Newton, 2008). For understory plants, basal sprouting is an important mechanism for promoting both survival under closed-canopy conditions and vegetative expansion when a canopy gap develops. At exposed sites or near the limits of a species range, the production of basal sprouts allows plants to spread into adjacent areas, thereby circumventing the difficult process of seedling establishment (Del Tredici, 2001).

Sinojackia huangmeiensis is a small deciduous tree or shrub in the family Styracaceae. It has a high ornamental value because of its flowers and fruit (*Fig. 1*). It is endemic to China and its wild individuals are currently distributed only in the secondary forest in the Longganhu National Wetland Nature Reserve, Huangmei County, Hubei Province (Wang et al., 2018). The distribution of *S. huangmeiensis* is narrow, with an area of only about 0.33 ha. Because of habitat destruction, logging, termite grazing, hard peel of fruits, and poor germination, only 501 individuals have been found in the field, and these face a high risk of extinction (Wei et al., 2018). *S. huangmeiensis* is a rare and endangered species and is listed as one of the 120 plant species with extremely small populations in China (Wang et al., 2018).

Figure 1. *The flowers and fruits of Sinojackia huangmeiensis*

http://www.aloki.hu ● ISSN 1589 1623 (Print) ● ISSN 1785 0037 (Online)
DOI: http://dx.doi.org/10.15666/aeer/1906_44934504

Previous studies have shown that the wild population of *S. huangmeiensis* can naturally recruit new individuals, but its age structure includes only a low proportion of young individuals, and every wild individual produces sprouts (Wang et al., 2018). The population has a clustered distribution (Luo et al., 2016), and its genetic diversity is low (Ruan et al., 2012; Zhao et al., 2016; Gao et al., 2018; Dong et al., 2020). In the same community, the leaf functional traits of *S. huangmeiensis* vary among different microhabitats (Wang et al., 2019). The seed setting rate and germination rate of *S. huangmeiensis* are very low (Zhang et al., 2008). However, it can be propagated via cuttings. The fruit size of the wild *S. huangmeiensis* plants is similar to that of ex situ conserved plants (Liu et al., 2018). To date, there have been no reintroduction studies of *S. huangmeiensis*, or studies that have compared the morphological, anatomical, and ecophysiological traits of wild plants and reintroduced plants (including sprouts). Investigation of these variables should help explain the success or failure of *S. huangmeiensis* reintroduction and the plant's potential adaptive mechanisms.

In this study of *S. huangmeiensis*, we compared the morphological, anatomical, and ecophysiological traits of wild plants, augmented plants, and translocated plants. We attempted to answer the following three questions: (1) Does *S. huangmeiensis* have a wide or narrow range of light intensity preference? (2) How do the morphological, anatomical, and ecophysiological traits of leaves differ between "trunk leaves" (those that extend from the trunk) and "sprout leaves" (those that extend from sprouts)? and (3) To what extent are reintroduced plants ecologically adaptable? The results should provide useful information for the protection and utilization of *S. huangmeiensis*.

Materials and methods

Study area

The study was concurrently conducted at three sites. The first site was the core area of the Longanhu National Nature Reserve, Huangmei County, Hubei Province, central China (29°59' N, 116°01' E, hereafter referred to as LGH or the wild population site). LGH is an original distribution area of *S. huangmeiensis*. It has a subtropical monsoon climate, with a mean annual temperature of 17.3℃ and a total annual rainfall of 1431 mm. The altitude is about 31 m. LGH has a red soil, and its climax plant community is subtropical evergreen broad-leaved forest (Liu et al., 2018). The second site was at the experimental area of the Longanhu National Nature Reserve (hereafter referred to as AUG or the augmentation site). Augmentation was conducted to increase the number of individuals near the wild population, and these individuals were derived from cuttings from different wild individuals so as to provide genetic diversity. The distance between the core area and experimental area was about 300 m. The third site was at the Wuhan Botanical Garden (30º32'N, 114º24'E, hereafter referred to as WBG or the translocation site), Wuhan City, Hubei Province, China. WBG is about 200 km from the original distribution area of *S. huangmeiensis*. It also has a subtropical monsoon climate, with a mean annual temperature of 17.1℃ and a total annual rainfall of 1308 mm. The altitude is about 80 m. WBG has a red soil (Liu et al., 2018). The climate at WBG is colder and dryer than that at LGH and AUG. We hoped to successfully translocate *S. huangmeiensis* to WBG in order to establish a new population and also to enable the assessment of climate effects on this species.

http://www.aloki.hu ● ISSN 1589 1623 (Print) ● ISSN 1785 0037 (Online)
DOI: http://dx.doi.org/10.15666/aeer/1906_44934504

Sample plant selection

In August 2020, three wild plants (including sprouts) were selected at the LGH site, and three augmented plants were selected at the AUG site; the latter augmented plants were 3 years old and were derived from cuttings. The augmented plants were also watered in the dry season and fertilized once each year. Three translocated plants (including sprouts) were selected at the WBG site; these translocated plants were 10 years old cuttings seedlings planted under the plantation canopy and that were growing naturally without a fence (*Fig. 2*).

Figure 2. *The habitat of wild, augmented, and translocated S. huangmeiensis plants at three sites (From left to right)*

The height, diameter at breast height, trunk diameter at the soil surface, and crown width of each of the nine *S. huangmeiensis* trees were measured in the field, and the numbers of sprouts were counted. The habitat characteristics of the sites and the plant traits are listed in *Table 1*.

Measurement of morphological and anatomical traits

In August 2020, we counted the sprouts and fruits for each of the three *S. huangmeiensis* trees at each site, and we used a Vernier caliper to measure the diameter of 10 fruits from each tree. A Vernier caliper was also used to measure the thickness of 10 leaves from each trunk and sprout of each tree at each site. We also collected 20 mature leaves from the trunk and one sprout of each *S. huangmeiensis* plant; these were transported in an ice chest to the laboratory where leaf area, leaf dry matter content, specific leaf area, and the thickness of palisade tissue and spongy tissue were measured; tissue thickness was measured by making freehand slices (Soudzilovskaiaa et al., 2013; Ren et al., 2019).

http://www.aloki.hu ● ISSN 1589 1623 (Print) ● ISSN 1785 0037 (Online)
DOI: http://dx.doi.org/10.15666/aeer/1906_44934504

Table 1. *The habitat and description of wild, augmented, and translocated S. huangmeiensis plants at three sites. Values are means + SD of three trees per site*

Variable	Site		
	LGH (wild plants)	AUG (augmented plants)	WBG (translocated plants)
Vegetation	Secondary forest	Field	Plantation
Dominant species	*Cinnamomum camphora* (L.) Presl, *Pinus elliottii*, *Magnolia zenii* Cheng	-	*Quercus acutissima*, *Ilex cornuta*, *Celtis sinensis*
Light transmittance (%)	9.2±2.9	100±0	8.2±1.6
Soil type	Red soil	Red soil	Red soil
Number of individuals measured	3	3	3
Age (years)	-	3	10
Diameter at breast height (cm)	5.6±1.3	2.9±0.4	5.8±1.5
Trunk diameter (cm)	7.1±2.3	4.6±0.6	7.1±2.0
Height (m)	3.2±0.7	2.2±0.3	2.6±0.6

Measurement of ecophysiological traits

The light saturation point (LSP), light compensation point (LCP), light-saturated net photosynthetic rate (Pmax), dark respiration rate (RD), and water-use efficiency (WUE) were measured on one mature leaf of the trunk and one mature leaf of a sprout of each of the three trees at the LGH, AGU, and WBG sites. A portable photosynthesis apparatus (Lci-T, Bioscientific Ltd., UK) was used to measure the light response curves of leaves on a sunny morning between 8:30 and 12:00 am in August 2020. The chamber temperature was set at 25°C and the reference CO_2 concentration was set at 400 μmol mol^{-1}, which were similar to the ambient environment. In order from strong to weak, the light intensity was manually set at 1600, 1400, 1200, 1000, 800, 600, 400, 200, 100, 50, 20, and 0 $\mu mol \cdot m^{-2} \cdot s^{-1}$ (Nijs et al., 1997; Dubois et al., 2007; Wang et al., 2016).

We harvested 10 more mature leaves from each of the three trees at each site to analyze leaf pigment contents. Leaf discs (0.6 cm in diameter) were immersed in 80% acetone and were kept in the dark at 4°C for 5 d. The light absorption of the extract was measured at 663, 645, and 440 nm with a UV-visible spectrophotometer (UV-3802, Unico, China), and the contents of chlorophyll a (Chl a), chlorophyll b (Chl b), and carotenoids (Car) were calculated. The ratio of chlorophyll a / b and the ratio of carotenoids to chlorophyll (Car / Chl) were also calculated (Wang et al., 2016).

Measurement of light transmittance under the forest canopy

The light transmittance under the forest canopy was also measured at each site. Because of the great heterogeneity of light under the forest canopy, the Digital Lux Meter (TES 1332a, Taiwan, China) was used to measure the light intensity outside the forest and at 9 points under the forest canopy. The light transmittance (%) was calculated from the light intensity under the forest canopy and the light intensity outside the forest (Ouyang et al., 2021).

http://www.aloki.hu ● ISSN 1589 1623 (Print) ● ISSN 1785 0037 (Online)
DOI: http://dx.doi.org/10.15666/aeer/1906_44934504

Statistical analysis

We used one-way analysis of variance (ANOVA) to test the differences in the leaf functional traits (i.e., morphological, anatomical, and ecophysiological traits) among the wild, augmented, and translocated *S. huangmeiensis* plants. We used a paired-sample t-test to compare traits between the leaves on the trunk vs. leaves on the sprout; this was done separately for the wild site and the reintroduction site. Statistical significance was set at $P<0.05$. Unless noted otherwise, means and standard deviations (SD) are presented. All analyses were conducted using the statistical program SPSS 25.0 (IBM Inc., Chicago, USA) and Excel 2003.

Results

Comparison of functional traits of trunk leaves at three sites

There were significant differences in morphological and anatomical traits among wild, augmented, and translocated plants (*Table 2*). The leaf thickness, area, and dry matter content of the trunk leaves were highest for augmented plants, intermediate for wild plants, and lowest for translocated plants. The specific leaf area of the trunk leaves was highest for translocated plants, intermediate for wild plants, and lowest for augmented plants. The ratio of palisade tissue to spongy tissue in trunk leaves was higher for wild plants than for augmented or translocated plants.

Table 2. *Morphological and anatomical properties of Sinojackia huangmeiensis at three sites*

Property	Site		
	LGH (wild plants)	AUG (augmented plants)	WBG (translocated plants)
Leaf thickness (mm)	0.156±0.015^{b}	0.200±0.015^{a}	0.128±0.008^{c}
Leaf area (cm^2)	24.80±2.60 ^{b}	28.12±1.89 ^{a}	15.96±0.61 ^{c}
Leaf dry matter content ($mg\ g^{-1}$)	321.02±47.58 ^{b}	388.86±11.19 ^{a}	260.34±13.54 ^{c}
Specific leaf area ($cm^2 \cdot g^{-1}$)	23.05±6.11 ^{b}	11.89±0.31 ^{c}	35.90±3.15 ^{a}
Thickness of palisade tissue (μm)	48.04±11.41 ^{b}	60.19±16.26 ^{a}	29.30±3.80 ^{c}
Thickness of spongy tissue (μm)	46.90±9.41 ^{b}	73.95±14.79 ^{a}	39.17±2.03 ^{c}
Palisade tissue/spongy tissue	1.02±0.78 ^{a}	0.81±0.53 ^{b}	0.75±0.13 ^{b}
Number of sprouts (individual)	21±6 ^{a}	0±0 $^{c\#}$	6±4 ^{b}
Number of fruits (individual)	79±19 ^{b}	145±28 ^{a}	37±2 ^{c}
Diameter of fruit (mm)	11.66±1.61 ^{b}	15.54±2.15 ^{a}	9.84±0.54 ^{c}

Note: In this table, traits for leaves are based on trunk leaves. Values are means ± SE, $n = 10$. # means "Sprouts were cut off". Within each row, different lowercase letters indicate significant differences between sites at $P<0.05$

http://www.aloki.hu ● ISSN 1589 1623 (Print) ● ISSN 1785 0037 (Online)
DOI: http://dx.doi.org/10.15666/aeer/1906_44934504

The number of sprouts was much higher for wild plants than for translocated or augmented plants. The number of fruits and the diameter of fruits of were largest for augmented plants, intermediate for wild plants, and smallest for translocated plants (*Table 2*).

Most of the ecophysiological traits of the trunk leaves significantly differed among wild, augmented, and translocated plants (*Table 3*). The Chl a / Chl b ratio of leaves at the three sites was > 3, and was highest for the augmented plants. The Car / Chl values of leaves at the three sites were generally similar. The light saturation point was highest for the augmented plants and was lowest for the wild plants. The light compensation point was lowest for translocated plants and highest for augmented plants. The maximum photosynthetic rate was similar for the augmented and translocated plants and was higher for the latter two kinds of plants than for the wild plants. The water-use efficiency was highest for the wild plants and lowest for the augmented plants.

Table 3. *Ecophysiological traits of Sinojackia huangmeiensis leaves*

Trait	Site		
	LGH (wild plants)	AUG (augmented plants)	WBG (translocated plants)
Chl *a* (mg g^{-1})	2.46±0.04^{b}	1.49±0.09^{c}	2.70±0.33^{a}
Chl *b* (mg g^{-1})	0.53±0.04^{b}	0.27±0.02^{c}	0.64±0.05^{a}
Chl a/Chl b	4.64±0.04^{b}	5.52±0.05^{a}	4.22±0.09^{c}
Car (mg g^{-1})	0.68±0.03^{a}	0.41±0.02^{b}	0.72±0.03^{a}
Car/Chl	0.23±0.01^{a}	0.23±0.01^{a}	0.22±0.01^{a}
LSP (μmol m^{-2} s^{-1})	511.80±54.60^{c}	2245.07±784.02^{a}	948.70±412.00^{b}
LCP (μmol m^{-2} s^{-1})	21.23±4.05^{b}	37.36±0.44^{a}	17.48±7.41^{c}
P_{max} (μmol m^{-2} s^{-1})	5.14±1.54^{b}	6.01±0.76^{a}	6.04±1.58^{a}
R_D (μmol m^{-2} s^{-1})	3.39±0.56^{c}	3.72±0.25^{b}	7.26±1.07^{a}
WUE (μmol $mmol^{-1}$)	138.87±19.81^{a}	79.81±0.88^{c}	105.31±21.26^{b}

Note: In this table, traits for leaves are based on trunk leaves. Chl *a* - chlorophyll *a*; Chl *b* - chlorophyll *b*; Chl - chlorophyll. Car – carotenoid. LSP – light saturation point; LCP – light compensation point; P_{max} – maximum photosynthetic rate; R_D – dark respiration rate; WUE – water-use efficiency. Values are means ± SE, $n = 3$. Within each row, different lowercase letters indicate significant differences between sites at $P<0.05$

Comparison of functional traits of trunk leaves vs. sprout leaves

For translocated plants, the leaf area, Car content, and Car/Chl were higher for trunk leaves than for sprout leaves ($P < 0.05$); none of the other traits differed between trunk leaves and sprout leaves of translocated plants (*Table 4*). For wild plants, none of the morphological or ecophysiological traits significantly differed for trunk leaves vs. sprout leaves ($P > 0.05$).

http://www.aloki.hu ● ISSN 1589 1623 (Print) ● ISSN 1785 0037 (Online)
DOI: http://dx.doi.org/10.15666/aeer/1906_44934504

Table 4. *Comparisons of morphological and ecophysiological traits of trunk leaves vs. sprout leaves of Sinojackia huangmeiensis at a site with wild plants and at a site with translocated plants*

Variable	LGH (wild plants)		WBG (translocated plants)	
	Trunk leaves	Sprout leaves	Trunk leaves	Sprout leaves
Blade thickness (mm)	0.16±0.01^{a}	0.10±0.01^{a}	0.13±0.01^{A}	0.11±0.01^{A}
Leaf area (cm^2)	24.80±2.60^{a}	22.99±3.63^{a}	15.96±0.61^{A}	8.86±1.19^{B}
Specific leaf area ($cm^2 \cdot g^{-1}$)	23.05±6.11^{a}	25.67±8.05^{a}	35.90±3.15^{A}	48.83±3.65^{A}
Leaf dry matter content ($mg\ g^{-1}$)	321.02±47.58^{a}	297.73±46.89^{a}	260.34±13.54^{A}	167.58±18.59^{A}
LSP ($\mu mol\ m^{-2}\ s^{-1}$)	511.80±54.60^{a}	514.79±43.69^{a}	948.70±412.00^{A}	743.47±225.81^{A}
LCP ($\mu mol\ m^{-2}\ s^{-1}$)	21.23±4.05^{a}	16.85±2.37^{a}	17.48±7.41^{A}	15.10±2.14^{A}
P_{max} ($\mu mol\ m^{-2}\ s^{-1}$)	5.14±1.54^{a}	4.38±1.09^{a}	6.04±1.58^{A}	3.12±1.84^{A}
R_D ($\mu mol\ m^{-2}\ s^{-1}$)	3.39±0.56^{a}	5.28±1.57^{a}	7.26±1.07^{A}	3.55±1.52^{A}
WUE ($\mu mol\ mmol^{-1}$)	138.87±19.81^{a}	93.26±9.56^{a}	105.31±21.26^{A}	69.20±20.98^{A}
Chl *a* (mg g–1)	2.46±0.04^{a}	2.32±0.48^{a}	2.70±0.33^{A}	1.40±0.11^{A}
Chl *b* ($mg\ g^{-1}$)	0.53±0.04^{a}	0.58±0.12^{a}	0.64±0.05^{A}	0.60±0.10^{A}
Car ($mg\ g^{-1}$)	0.68±0.03^{a}	0.60±0.12^{a}	0.72±0.03^{A}	0.18±0.00^{B}
Car/Chl	0.23±0.01^{a}	0.21±0.01^{a}	0.22±0.01^{A}	0.09±0.01^{B}

Note: Chl a - chlorophyll a; Chl b - chlorophyll b; Chl - chlorophyll. Car – carotenoid. LSP – light saturation point; LCP – light compensation point; Pmax – maximum photosynthetic rate; RD – dark respiration rate; WUE – water-use efficiency. Values are means ± SE, n = 3. For each trait within each site, different letters (lowercase for site LGH and uppercase for site WBG) indicate significant differences between trunk leaves vs. shoot leaves at P<0.05

Discussion

Sinojackia huangmeiensis tolerates a wide range of light intensities

There were significant differences in morphological, anatomical, and ecophysiological traits among the three sites. The values for most of these traits tended to be highest for the wild plants (at site LGH), intermediate for the translocated plants (at site WBG), and lowest for the augmented plants (at site AUG). The results showed that wild, augmented, and translocated *S. huangmeiensis* plants can grow in an environment with 10-100% light transmittance. This indicates that *S. huangmeiensis* can endure both shady and sunny conditions. In addition, the Chl a / Chl b values of the leaves at the three sites were greater than 3, and the light compensation points were low, indicating that *S. huangmeiensis* is a mesophyte. These results are consistent with a previous report that found that *S. huangmeiensis* is shade tolerant but can also grow under strong light (Liang et al., 2007). Based on our results, we suggest that young seedlings or cuttings be kept in a shaded environment; once they are mature, these plants can be transplanted into a full-light environment. Light intensity does not influence plant's survival and distribution but influence plant's growth performance.

http://www.aloki.hu ● ISSN 1589 1623 (Print) ● ISSN 1785 0037 (Online)
DOI: http://dx.doi.org/10.15666/aeer/1906_44934504

The distribution of Sinojackia huangmeiensis is narrow but its morphological, anatomical, and ecophysiological adaptability is substantial

Sinojackia huangmeiensis showed strong morphological, anatomical, ecophysiological adaptability based on plant functional traits of wild and reintroduced (augmented and translocated) plants. Leaf thickness, leaf area, and dry matter content of the trunk leaves were highest for augmented plants, intermediate for wild plants, and lowest for translocated plants. Specific leaf area of the trunk leaves was largest for translocated plants, intermediate for wild plants, and smallest for augmented plants. The ratio of palisade tissue to spongy tissue in trunk leaves was lower in both augmented plants and translocated plants than in wild plants. The number and the diameter of fruits were largest in augmented plants, intermediate in wild plants, and lowest in translocated plants. The maximum photosynthetic rate of augmented and translocated plants was similar and higher than that of wild plants. Light saturation and compensation points were highest for augmented plants; the light saturation point was lowest for wild plants; and the light compensation point was lowest for translocated plants. Water-use efficiency was highest for wild plants and lowest for augmented plants. For translocated plants, leaf area, Car content, and Car/Chl were significantly higher for trunk leaves than for sprout leaves.

At the time of this study, a total of 501 wild individuals of *S. huangmeiensis* were growing naturally and with protection at the LGH site in the Longanhu National Nature Reserve. In the experimental area of the nature reserve (the AUG site), the augmented seedlings were continuously pruned, irrigated during droughts, and occasionally fertilized. According to genetic diversity data (Zhao et al., 2016; Gao et al., 2018; Dong et al., 2020), we selected 3 individuals from different genetic diversity groups for cuttings, and planted these cuttings at the AUG site, so as to achieve ex situ conservation of the full genetic diversity of this species. The temperature and rainfall were lower at the translocation site (the WBG site) than at the LGH site, but light transmittance was similar. The translocated plants grew well at the WBG site, and produced flowers, fruits, and sprouts. This indicates that *S. huangmeiensis* can survive and achieve asexual and sexual reproduction in Wuhan. We also introduced 3-year-old cutting seedlings with sprouts of *S. huangmeiensis* to Yantai, Shandong Province (120°35’ E, 37°26’ N, total annual rainfall = 525 mm, annual average temperature = 13.4℃) and Guangzhou, Guangdong Province (112°57’ E, 23°35’ N, total rainfall = 1612 mm, annual average temperature = 20.8℃); the plants survived in both places, but did not blossom or bear fruit in the past 3 years (unpublished data). Our findings suggest that *S. huangmeiensis* has strong adaptability and may survive under future climate conditions. Two other rare and endangered plants in South China, Manglietia longipedunculata and Euryodendron excelsum, also have narrow distribution ranges and strong ecophysiological adaptability (Ren et al., 2016, 2019). It is only because of their narrow distribution and human interference that they are endangered. The endangered state of these species could be relieved by their artificial reintroduction and translocation.

For ex situ conservation and reintroduction, transplanting of the trunk and associated sprouts may improve the success rate

Sinojackia huangmeiensis can simultaneously propagate via by producing seeds and by sprouting. Through sprouting regeneration, *S. huangmeiensis* is conducive to resist

http://www.aloki.hu ● ISSN 1589 1623 (Print) ● ISSN 1785 0037 (Online)
DOI: http://dx.doi.org/10.15666/aeer/1906_44934504

interference and adverse environment, and through both seedling and sprouting regeneration, *S. huangmeiensis* expands the distribution area. Thus, the natural regeneration of the population can be carried out normally (Wang et al., 2018).

Sprouting can increase the persistence of reintroduced plants. Sprout growth and sprout longevity are usually greater under sunny than shady conditions (Lu et al., 2020). Sprout regeneration is common in forest ecosystems (del Tredici, 2001) and in the regeneration of some rare and endangered plant populations (Du et al., 2018). Tilia cordata populations in northern England, for example, can last for thousands of years through sprouting regeneration (Pigott, 1989). Du et al. (2018) reported that sprouting plays an important role in regeneration of the Magnolia sinostellata population in China. Most research on persistence of reintroduced plants has focused on the importance of safe sites, seed and seedling banks, dispersal, and germination (Lu et al., 2020). The role of sprouting of *S. huangmeiensis* as a form of persistence in conservation and management of plant species has mostly been neglected. Sprouts are resistant to disturbance and catastrophe, can tolerate long periods with little or no recruitment, and tend to preserve genetic diversity. According to an earlier study, populations of sprouting plants experiencing the loss of pollinators and dispersers can persist for long periods (Bond and Midgley, 2001).

Conclusion

Sinojackia huangmeiensis is rare and endangered because of human disturbance, its narrow distribution, low genetic diversity, limited dispersal by animals, and low germination rate. *S. huangmeiensis* has a wide range of light intensity preference. The maximum photosynthetic rate of reintroduced plants is higher than that of wild plants. Water-use efficiency of wild plants is higher than that of reintroduced plants. *S. huangmeiensis* can propagate via seeds and sprouts. Although the sprout leaves are less ecologically adaptable than trunk leaves, the ecological adaptability of the trunk and sprout leaves is complementary and thereby increases overall plant adaptability and persistence. As a plant that can grow under a wide range of light conditions and that produces both trunks and sprouts, *S. huangmeiensis* has a potentially wide distribution area and can adapt, at least to some degree, to global climate change. In the future, *S. huangmeiensis* can be effectively protected through in situ conservation, ex situ conservation, and reintroduction. For its ex situ conservation and reintroduction, translocating sprouts along with the trunk should increase survival rate and persistence. Conservation translocation can also be used to overcome the plant's dispersal limitations under climate change. The reintroduction of this species requires continuous monitoring.

Acknowledgements. We thank Deputy director Guoxun Chen and Mr Nan Wang for help in the field in the Longanhu National Nature Reserve. This work was supported by Huazhong Agricultural University (No.202110504038).

REFERENCES

[1] Ahrens, G. R., Newton, M. (2008): Root dynamics in sprouting tanoak forests of southwestern Oregon. – Canadian Journal of Forest Research 38: 1855-1866.

http://www.aloki.hu ● ISSN 1589 1623 (Print) ● ISSN 1785 0037 (Online)
DOI: http://dx.doi.org/10.15666/aeer/1906_44934504

[2] Bond, W. J., Midgley, J. J. (2001): Ecology of sprouting in woody plants: the persistence niche. – Trends in Ecology & Evolution 16: 45-51.
[3] Catoni, R., Gratani, L. (2013): Morphological and physiological adaptive traits of Mediterranean narrow endemic plants: The case of *Centaurea gymnocarpa* (Capraia Island, Italy). – Flora 208: 174-183.
[4] Del Tredici, P. (2001): Sprouting in temperate trees: A morphological and ecological review. – Botanical Review 67: 121-140.
[5] Dong, H. J., Wang, H. Y., Li, Y. L., Yu, J. J. (2020): The complete chloroplast genome sequence of *Sinojackia huangmeiensis* (Styracaceae). – Mitochondrial DNA Part B 5: 715-717.
[6] Du, Y. X., Wu, W. J., Ji, Z. L., Zhang, D. (2018): Analysis on morphological characters of sprouts of the endangered plant *Magnolia sinostellata*. – Ecological Science 37: 152-156.
[7] Dubois, J.-J. B., Fiscus, E. L., Booker, F. L., Flowers, M. D., Reid, C. D. (2007): Optimizing the statistical estimation of the parameters of the Farquhar–von Caemmerer-Berry model of photosynthesis. – New Phytologist 176: 402-414.
[8] Gao, L., Gao, P., Li, S. S. (2018): Germplasm genetic diversity of *Sinojackia huangmeiensis* populations based on ISSR markers. – Molecular Plant Breeding 16(18): 6017-6022.
[9] Godefroid, S., Vanderborght, T. (2011): Plant reintroductions: the need for a global database. – Biodiversity Conservation 20: 3683-3688.
[10] Liang, Y., Wang, M., Guo, J., Zhou, S. M., Wang, L. (2007): Morphologies and structures of seedlings and their phylogenies for three species in three genera of ranunculaceae. – Acta Botanic Boreali-Occid Sinica 27: 1357-1363.
[11] Liu, H., Ren, H., Liu, Q., Wen, X. Y., Maunder, M., Gao, J. Y. (2015): The conservation translocation of threatened plants as a conservation measure in China: A review. – Conservation. Biology 29: 1537-1551.
[12] Liu, M. T., Wei, X. Z., Jiang, M. X. (2018): Comparison of fruit traits between wild and ex situ populations of *Sinojackia huangmeiensis*. – Plant Science Journal 36: 354-361.
[13] Lu, D. L., Zhu, J. J., Wang, G. F. (2020): Resprouting of tree species: A research review. – Chinese Journal of Ecology 39: 4178-4184.
[14] Luo, M. C., Shi, Q. Z., Yang, J. J., Zhang, C. T. (2016): Study on natural population of *Sinojackia huangmeiensis* in Hubei Province. – Journal of Anhui Agricultural Sciences 44: 67-68.
[15] Maschinski, J., Haskins, K. E. (2012): Plant Reintroduction in a Changing Climate: Promises and Perils. – Island Press, Washington DC.
[16] Maunder, M. (1992): Plant reintroduction: an overview. – Biodiversity Conservation1 1: 51-61.
[17] Nijs, I., Ferris, R., Blum, H. (1997): Stomatal regulation in a changing climate: a field study using free air temperature increase (FATI) and free air CO2 enrichment (FACE). – Plant Cell Environ 20: 1041-1050.
[18] Ouyang, K. T., Ren, H., Xu, Z. H., Wang, F. G., Zhang, Q. M., Liu, S. Z., Guo, Q. F. (2021): Habitat characteristics and population structure of *Dipteris chinensis*, a relict plant in China. – Applied Ecology and Environmental Research 19(3): 1939-1951.
[19] Pigott, C. D. (1989): Factors controlling the distribution of *Tilia cordata* Mill at the northern limits of its geographical range. – New Phytologist 112: 1175-121.
[20] Qin, H., Zhao, N. L. (2017): Evaluating the threat status of higher plants in China. – Biodiversity Science 25: 689-695.
[21] Ren, H. (2020): Conservation and Reintroduction of Rare and Endangered Plants in China. – Springer, Singapore, 233p.
[22] Ren, H., Liu, H., Wang, J., Yuan, L. L., Cui, X. D., Zhang, Q. M., Fu, L., Chen, H. F., Zhong, W. C., Yang, K. M., Guo, Q. F. (2016): The use of grafted seedlings increases the

http://www.aloki.hu ● ISSN 1589 1623 (Print) ● ISSN 1785 0037 (Online)
DOI: http://dx.doi.org/10.15666/aeer/1906_44934504

success of conservation translocations of *Manglietia longipedunculata* (Magnoliaceae), a critically endangered tree. – Oryx 50: 437-445.

[23] Ren, H., Yi, H. L., Zhang, Q. M., Wang, J., Wen, X. Y., Guo, Q. F., Liu, H. (2019): Morphological, anatomical and physiological traits of *Euryodendron excelsum* as affected by conservation translocation (augmentation vs. conservation introduction) in South China. – Photosynthetica 57: 217-225.

[24] Ruan, Y. M., Zhang, J. J., Yao, X. H., Huang, H. W., Ge, J. W. (2012): Genetic diversity and fine-scale spatial genetic structure of different life history stages in a small, isolated population of *Sinojackia huangmeiensis* (Styracaceae). – Biodiversity Science 20: 460-469.

[25] Seddon, P. J. (2010): From reintroduction to assisted colonization: moving along the conservation translocation spectrum. – Restoration Ecology 18: 796-802.

[26] Sharrock, S., Wyse Jackson, P. (2017): Plant conservation and the sustainable development goals: a policy paper prepared for the global partnership for plant conservation. – Annual. Mossouri Botanical Garden 102: 290-302.

[27] Soudzilovskaiaa, N. A., Elum, T. G., Onipchenko, V. G., Shidakov, I., Salpagarova, F. S., Khubiev, A. B., Tekeev, D. K., Cornelissen, J. H. C. (2013): Functional traits predict relationship between plant abundance dynamic and long-term climate warming. – PNAS 110: 18180-18184.

[28] Taylor, G., Canessa, S., Clarke, R. H., Ingwersen, D., Ewen, D. J. G. (2017): Is reintroduction biology an effective applied science? – Trends in Ecology & Evolution 32: 873.

[29] Wang, Y., Shao, L., Wang, J., Ren, H., Liu, H., Zhang, Q. M., Guo, Q. F., Chen, X. W. (2016): Comparison of morphological and physiological characteristics in two phenotypes of a rare and endangered plant, *Begonia fimbristipula* Hance. – Photosynthetica 54: 381-389.

[30] Wang, S. T., Wu, H., Liu, M. T., Jiang, M. X. (2018): Community structure and dynamics of a remnant forest dominated by a plant species with extremely small population (*Sinojackia huangmeiensis*) in central China. – Biodiversity Science 26: 99-109.

[31] Wang, S. T., Xu, Y. Z., Yang, T., Jiang, M. X. (2019): Impacts of microhabitats on leaf functional traits of the wild population of *Sinojackia huangmeiensi*. – Biodiversity Science 28: 277-288.

[32] Wei, X. Z., Liu, M. T., Wang, S. T., Jiang, M. X. (2018): Seed morphological traits and seed element concentrations of an endangered tree species displayed contrasting responses to waterlogging induced by extreme precipitation. – Flora 246: 19-25.

[33] Yang, J., Cai, L., Liu, D. T., Chen, G., Sun, W. B. (2020): China's conservation program on plant species with extremely small populations (PSESP): progress and perspectives. – Biological Conservation 244: 108535.

[34] Zhao, J., Tong, Y. Q., Ge, T. M., Ge, J. W. (2016): Genetic diversity estimation and core collection construction of *Sinojackia huangmeiensis* based on novel microsatellite markers. – Biochemical Systematics and Ecology 64: 74-80.

[35] Zhang, J. J., Ye, Q. G., Yao, X. X., Zhang, S. J., Huang, H. W. (2008): Preliminary studies on the floral biology, breeding system and reproductive success of *Sinojackia huangmeiensi*, an endangered plant in a fragmented habitat in Hubei Province, China. – Chinese Journal of Plant Ecology 32: 743-750.

http://www.aloki.hu ● ISSN 1589 1623 (Print) ● ISSN 1785 0037 (Online)
DOI: http://dx.doi.org/10.15666/aeer/1906_44934504

THE EFFECT OF AMINO ACID L-ALPHA PROLINE AND NITROGEN BACTERIA *AZOTOBACTER VINELANDII* ON THE CONTENT OF MICROELEMENTS AGAINST THE BACKGROUND OF MINERAL NITROGEN FERTILIZATION

PŁAZA, A.* – RZĄŻEWSKA, E.

Siedlce University of Natural Sciences and Humanities, Faculty of Agrobioengineering and Animal Husbandry, Siedlce, Poland

**Corresponding author*
e-mail: anna.plaza@uph.edu.pl

(Received 31st May 2021; accepted 3rd Sep 2021)

Abstract. The aim of the research was to determine the effect of L-alpha prolina and *Azotoba vinelandii* against the background of mineral nitrogen fertilization on the content of microelements in spring wheat grain. Field research work was conducted on a family-owned farm located in Krzymosze. The following two factors were examined: I biological preparations: control where no biological preparations were applied, L-alpha prolina, *Azotoba vinelandii*, L-alpha prolina+*Azotobacter vinelandii*; II mineral nitrogen fertiliser regime: non-fertilised control, 60 kg N∘ha^{-1}, 90 kg N∘ha^{-1}, 120 kg N∘ha^{-1}. Spring wheat grain was sampled to determine microelements. The obtained results revealed that the application of biofertilizers increased iron and zinc contents but reduced manganese and copper concentrations in spring wheat grain. The highest content of iron and zinc, and the lowest concentration of manganese and copper were recorded in spring wheat grain after application of L-alpha prolina +*Azotoba vinelandii* biological preparations with a dose of mineral nitrogen fertilization of 90 kg N ha^{-1}.
Keywords: *nitrogen bacteria, mineral content, grain, fertilization, biostimulator*

Introduction

Due to the occurrence of years with a shortage of precipitation and high temperature in Poland, cereal crops do not yield consistently and bring lower yields than expected. Thus, climate warming poses threats to arable crops (Radkowski and Radkowska, 2013; Colla et al., 2014; Du Jardin, 2015). To combat this adverse climate change, biological methods must be used in developing a system of sustainable agriculture. One of the ways is the use of biostimulants, which have a positive effect on the growth and development of plants and have a protective function for cells, which makes plants resistant to rainfall deficiency during the growing season (Michalak and Chojnacka, 2013; Calvo et al., 2014; Du Jardin, 2015). A good biological substance may be the amino acid L-alpha proline, which is easily absorbed by plants. Proline is the most widely distributed metabolite that accumulates under stress conditions (Delauney and Verma, 1993) the significance of this accumulation in osmotic adjustment in plants is still debated and varies from species to species (Hoai et al., 2003). According to Qotob et al. (2019) data obtained could be concluded that the using of plant growth regulators as a proline reduced the consumption of mineral fertilizers. There are no studies determining the effect of this amino acid on the chemical composition of grain for consumption. Moreover, in sustainable agriculture it is recommended to limit the use of mineral nitrogen fertilization, in favor of biological nitrogen. The use of nitrogen bacteria is not only a source of nitrogen for plants, but also improves the chemical, biological and physical properties of the soil. This enables plants to take up other nutrients, including micronutrients, which are so important in the human

http://www.aloki.hu ● ISSN 1589 1623 (Print) ● ISSN1785 0037 (Online)
DOI: http://dx.doi.org/10.15666/aeer/1906_45054514

diet, especially when used together with biostimulants (Calvo et al., 2014; Muhammed et al., 2016). Bacteria stimulate the growth of the root system, which improves the plant's water and nutrient management. The climate changes that have been noticeable over the last few years, resulting in seasonal droughts, require the intensification of the search for new, but at the same time cheap and pro-environmental solutions, leading to an increase in the use of water by crops. A new solution is the use of bacterial preparations. These goals can be implemented within the framework of the European Green Deal, which assumes the protection of the soil environment by 2030, e.g. by limiting mineral nitrogen fertilization by 20%. Taking into account the advantages of using biological preparations in plant cultivation, research was undertaken to determine the effect of the amino acid L-alpha proline and nitrogen bacteria *Azotobacter vinelandii* on the background of mineral nitrogen fertilization on the content of microelements in the grain of spring wheat grown in changing weather conditions.

Materials and Methods

A field experiment was conducted in 2017-2019 on a family owned farm located in Krzymosze (52° 03' 27''N, 22° 33' 74''E) near Siedlce, Poland. The experimental soil was Stagnic Luvisol (soil classification according to WRB). Available macroelement contents were as follows: P 8.2 mg 100 g^{-1} soil, K 18.7 mg 100 g^{-1} soil and Mg 4.8 mg 100 g^{-1}soil. Microelement contents amounted to: Mn 131 mg⊙kg^{-1} soil, Cu 4.9 mg⊙kg^{-1} soil, Zn 5.5 mg⊙kg^{-1} soil and Fe 845 mg⊙kg^{-1} soil. The mineral nitrogen contents were $N\text{-}NH_4$ + 4.97 mgkg^{-1} of soil and $N\text{-}NO_3$ – 78.4 mg kg^{-1} of soil. Soil reaction was neutral and humus content was 1.88%. Chemical analyzes of the soil were performed at the Chemical and Agricultural Station in Warsaw. The experiment was set up with three replicates. The size of the plot for the collection was 16 m^2. Spring wheat was sown at a row spacing of 11 cm. The following two factors were examined: (I) biological preparations: control where no biological preparations were applied, L-alpha prolina 2 g⊙ha^{-1}, *Azotoba vinelandii* 1 l⊙ha^{-1}, L-alpha prolina 2 g⊙ha^{-1}+ 1 *Azotoba vinelandii*; (II) mineral nitrogen application regime: non-fertilised control, 60 kg N⊙ha^{-1} (preplant), 90 kg N⊙ha^{-1} (60 kg N⊙ha^{-1} preplant + 30 kg N⊙ha^{-1} at the stem elongation stage), 120 kg N⊙ha^{-1} (60 kg N⊙ha^{-1} preplant + 30 kg N⊙ha^{-1} at the stem elongation stage + 30 kg N⊙ha^{-1} – foliar application of 8% urea solution applied as the stage of initial ear formation). Spring wheat cv. Mandaryna was preceded by maize. After harvesting the forecrop, pre-winter plowing was performed, and spring crops were sown before wheat. Phosphorus and potassium fertiliser rates were chosen based on soil availability and amounted to 30.8 and 99.6 kg⊙ha^{-1} of P and K, respectively. Mineral nitrogen regime was as described for factor II above. Mineral nitrogen fertilization before sowing and in the shooting stage (BBCH 30) was applied in the form of 34% ammonium nitrate. On the other hand, foliar fertilization with 46% urea in the form of an 8% solution in the heading stage (BBCH 50). Spring wheat was sown in early April at the rate of 500 grains per 1 m^2. Biofertilizers were applied once at the stage of spring wheat tillering (BBCH 20). First biological preparation contains the *Azotobacter vinelandii* MVY-010 (1x10 CFU/l) a biological product intended for increasing nitrogen content in the soil. Contains non-symbiotic, free-living soil bacterium *Azotobacter vinelandii*, which effectively assimilates the atmospheric nitrogen and extracts bioactive substances that improve the development of plants, and polysaccharide alginates having influence on the formation of water-resistant units in the soil. Second biological preparation contains the L-α proline (purity, 5%) a

http://www.aloki.hu ● ISSN 1589 1623 (Print) ● ISSN1785 0037 (Online)
DOI: http://dx.doi.org/10.15666/aeer/1906_45054514

biostimulator increasing the natural resistance of plants to the stress. It contains L-α proline 5 (amino acid) easily assimilated by plants that has a multiple effect on the growth and development of plants and performs a protective function of cells as well as helps to adapt to adverse environmental conditions. L-α proline balances the metabolism processes of vital substances and compensates their shortage. Biological preparations should be dissolved in water and sprayed with 250 l ha^{-1} of water. The distributor of biological preparations in Poland is PHU Biotel Sp. zoo. Dzikowice 87, 67-300 Szprotawa. During the plantation, the herbicide Gold 450 SC at a dose of 1.25 l ha^{-1}, fungicide (the first treatment Bumper Super 490 EC at the dose of 1 l ha^{-1}; the second treatment Falcon 460 EC 0.6 l ha^{-1}) and the growth regulator Cerone were used. 480 SL 0.75 l ha^{-1}. Spring wheat was harvested in early August. During spring wheat harvest, grain was sampled to perform chemical analyses. From each plot after the grain was harvested, a representative sample with a volume of 250 g was taken. Determinations included selected macroelements (Fe, Zn, Cu and Mn) by means of Inductively Coupled Plasma Optical Emission Spectrometry (ICP-OES). Mn (FAAS), Cu (FAAS), Zn (FAAS) and Fe (FAAS). Then the plant material was taken up in acids in a microwave digestor Milesone Ethos Plus. The content of micronutrients was determined in the mineralisation by emission spectrometry with excitation in inductively coupled plasma and an optical detector (ICP OES), using an emission spectrometer Perkin Elmer Optima 8300. The assay was performed in triplicate. The results for each characteristic were subjected to analysis of variance (ANOVA). Comparison of means for significant sources of variation was achieved by means of Tukey's test at the significance level of $P \leq 0.05$. ANOVA with regression was calculated for mineral nitrogen application and content of micronutrients. Significance was tested using Fisher-Snedecor test at significance level at $P \leq 0.05$ and $P \leq 0.01$ (Hill and Lewicki, 2006). All the calculations were performed in STATISTICA®, version 12.0.

Results and Discussion

In *Table 1* described significance of the effects in ANOVA (2017-2019).

Table 1. *Significance of the effects in ANOVA , results from 2017-2019 years*

Source of variability	Trait -content of:			
	Iron	**Cooper**	**Manganese**	**Zinc**
Year	ns	ns	ns	**
Biological preparation	***	***	***	***
Nitrogen application	***	***	***	**
Year*Biological preparation	ns	ns	ns	ns
Year*Nitrogen application	ns	ns	ns	ns
Biological preparation*Nitrogen application	*	**	ns	ns
Year*Biological preparation*Nitrogen application	ns	ns	ns	ns
Variability coefficient V%	4.98	4.36	4.07	5.16

ns- non significant, * significant at p <0.05, significant at p<0.01, significant at p<0.001

http://www.aloki.hu ● ISSN 1589 1623 (Print) ● ISSN1785 0037 (Online)
DOI: http://dx.doi.org/10.15666/aeer/1906_45054514

Iron content in spring wheat grain was significantly affected by the experimental factors and their interaction (*Table 2*).

Table 2. *Iron content in spring wheat grain (means across 2017-2019), mg kg^{-1} DM*

Biological preparatons (A)	Mineral nitrogen fertiliser regime (B), kg N◎ha^{-1}				Means
	Control	60	90	120	
Control	34.23a*	37.48a	36.21a	35.44a	35.84D
L-alpha proline	41.12b	49.44a	54.17a	51.12a	48.96C
Azotoba vinelandii	55.25b	62.31a	68.53a	65.43a	62.88B
L-alpha proline + *Azotobacter vinelandii*	98.21c	109.17b	118.50a	112.17ab	109.5A
Means	57.21C	64.60B	69.35A	66.04AB	-

*Values in columns followed by the same small letter and values in rows followed by the same capital letter do not differ significantly at P<0.05

The regression line between fertilization of mineral nitrogen and iron content in grain spring wheat showed that increasing the dose of nitrogen to 90 kg ha^{-1} increased the iron content in spring wheat grain. The maximum iron content in spring wheat grain was obtained with the use of mineral nitrogen fertilization in the dose of 99.5 kg Nha^{-1} (*Figure 1*).

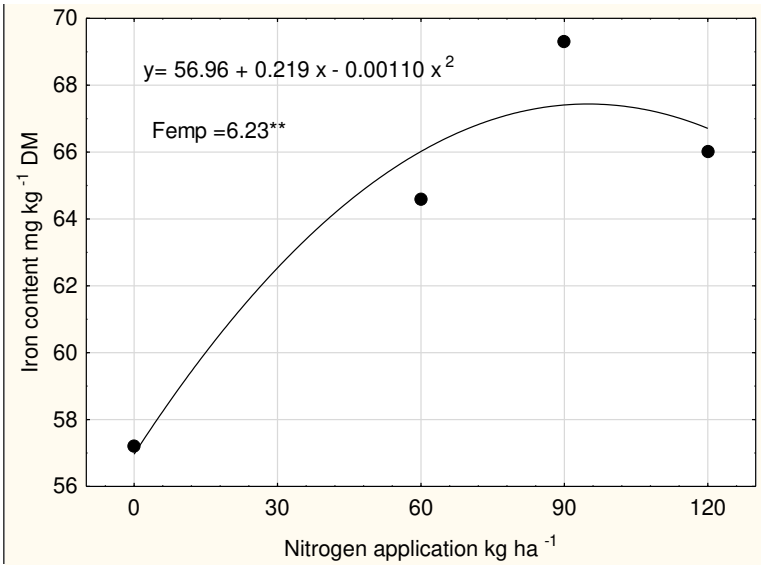

Figure 1. *Regression line between ferilization of mineral nitrogen (x) and iron content in grain (y), mean for 2017-2019 years*

Iron concentration was the lowest in control spring wheat grain produced with mineral nitrogen input and no biological product application. Also Johansson et al. (2001), Sułek and Cacak-Pietrzak (2008), Gondek and Gondek (2010) as well as Buczek et al. (2011) found the lowest iron content in cereal grain following an application of the highest mineral fertiliser rates. High mineral fertiliser rates, including nitrogen, pose a threat to the natural environment. This leads to pollution of groundwater with nitrates, and

http://www.aloki.hu ● ISSN 1589 1623 (Print) ● ISSN1785 0037 (Online)
DOI: http://dx.doi.org/10.15666/aeer/1906_45054514

contributes to poorer crop yield quality due to, among others, less iron which is a valuable microelement (Gondek and Gondek, 2010). In the present study, an application of biofertilizers, in particular *Azotoba vinelandii* and L-alpha proline + *Azotobacter vinelandii*, increased iron content in spring wheat grain. L-alpha proline and *Azotobacter vinelandii*are microbiological products containing, respectively, the nitrifying bacteria *Azotobacter vinelandii*, and the essential amino acid L-alpha proline. Mona et al. (2012) have demonstrated that the nitrifying bacteria *Azotobacter chroococum* and *Azospirillum* brastlensel contribute to an increase in the wheat grain content of Fe compared with control. A possible explanation is that microorganisms metabolise and then mineralize organic matter, which introduces into circulation the elements which are essential in plant nutrition, including iron which is a microelement so important for human health (Srinivas et al., 2002; Mahamed and Kaharia, 2012). In the experiment reported here, an application of L-alpha proline significantly reduced Fe content in spring wheat grain compared with the bacteria based product. It is due to the fact that bacteria-free L-alpha proline contains only an amino acid which contributes to a lower release of Fe from the soil environment. In the present work, nitrogen fertilisation at lower rates, that is 60 and 90 kg N⊙ha^{-1}, resulted in Fe increase in spring wheat grain compared with control. It was also confirmed that an application of the highest nitrogen rate contributed to a decline in the iron content in spring wheat grain, which was due to the fact that too high nitrogen rates cause soil environment degradation, and reduce microelement uptake by plants. In turn, low mineral nitrogen rates positively affect soil microorganisms which decompose organic matter and release minerals, including iron, for uptake by plants. In the present work, an interaction was confirmed indicating that the highest iron concentration was determined in the grain of spring wheat treated with accompanied by an L-alpha proline + *Azotobacter vinelandii* application of 90 kg N⊙ha^{-1}. It can be explained by the fact that an application of products containing the bacteria *Azotobacter vinelandii*, which reduce elemental nitrogen from the air, and the amino acid L-alpha proline, accompanied by nitrogen fertiliser at the rate of 90 kg ⊙ha^{-1} create favourable conditions for the growth and development of spring wheat, which results in iron accumulation in spring wheat grain. In contrast, an application of the highest nitrogen rate negatively affects the soil environment, similarly to lack of nitrogen fertilisation in the control unit, which resulted in the lowest iron concentration in spring wheat grain.

Statistical analysis demonstrated a significant influence of the experimental factors on manganese content in spring wheat grain (*Table 3*).

Table 3. *Manganese content in spring wheat grain (means across 2017-2019), mg kg^{-1} DM*

Biological preparations (A)	**Mineral nitrogen fertiliser regime (B), kg N⊙ha^{-1}**				**Means**
	Control	60	90	120	
Control	74.81c	76.23c	78.31c	84.81c	78.54A
L-alpha proline	70.12b	73.21b	74.39b	76.20b	73.48B
Azotoba vinelandii	68.85b	71.10b	73.14b	77.34b	72.61B
L-alpha proline + *Azotobacter vinelandii*	63.87a	65.14a	66.38a	69.15a	66.14C
Means	69.41C	71.42BC	73.06B	76.88A	-

*Values in columns followed by the same small letter and values in rows followed by the same capital letter do not differ significantly at P<0.05

http://www.aloki.hu ● ISSN 1589 1623 (Print) ● ISSN1785 0037 (Online)
DOI: http://dx.doi.org/10.15666/aeer/1906_45054514

The regression line between fertilization of mineral nitrogen and manganese content in grain spring wheat showed that increasing the dose of nitrogen from 60 to 120 kg ha^{-1} increased the manganese content in spring wheat grain (*Figure 2*).

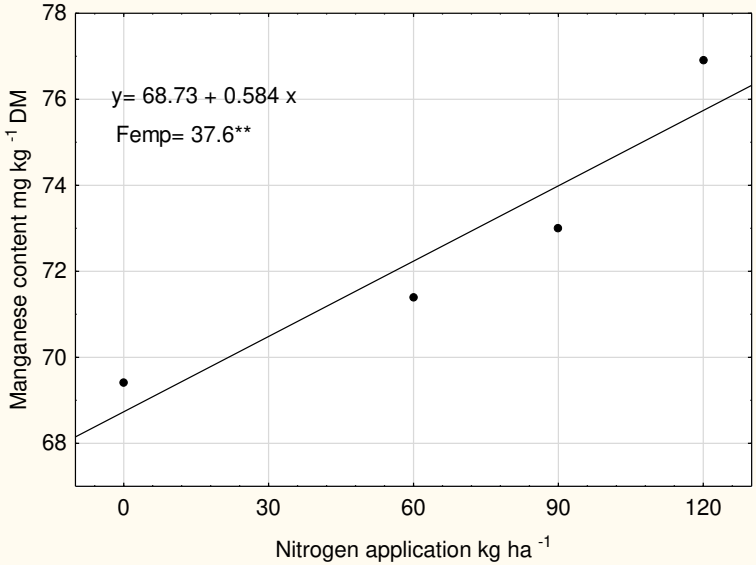

Figure 2. *Regression line between ferilization of mineral nitrogen (x) and manganese content in grain (y), mean for 2017-2019 years*

The highest concentration of this element was recorded in the grain of spring wheat grown in the control plot where no biofertilizers had been applied. Also research by Johansson et al. (2001), Wang and Malhi (2008) and Jarecki (2019) revealed the highest manganese content in the grain of cereals cultivated using mineral fertiliser input only. In the present study, an application of biofertilizers contributed to a significant decline in Mn concentration in spring wheat grain compared with control. The lowest manganese content was recorded in the grain of spring wheat treated with the two biofertilizers L-alpha proline + *Azotobacter vinelandii*. It agrees with findings reported by Mona et al. (2012) and Muhammad et al. (2016) who demonstrated that, following an application of nitrifying bacteria, there was observed a decline in the wheat grain content of Mn. It was due to the fact that bacteria have a positive effect on an accumulation of organic matter in which manganese is accumulated. In the experiment reported here, L-alpha proline or *Azotobacter vinelandii* applied separately increased Mn content in spring wheat grain but its concentration in grain was significantly lower compared with control wheat grain. Nitrogen fertiliser regime significantly affected manganese content in spring wheat grain. An application of increasing nitrogen rates was followed by an increase in the spring wheat grain content of manganese. The highest concentration of this microelement was recorded in the grain of spring wheat fertilised with 120 kg N◎ha^{-1}. Also Buczek et al. (2011) as well as Jarecki et al. (2019) demonstrated that mineral fertilisation contributed to an increase in the cereal grain content of Mn. A possible explanation is that an application of excessive mineral fertiliser rates leads to soil environment degradation due to reduction in humus which accumulates Mn.

Zn content in spring wheat grain was significantly affected by the experimental factors (*Table 4*).

http://www.aloki.hu ● ISSN 1589 1623 (Print) ● ISSN1785 0037 (Online)
DOI: http://dx.doi.org/10.15666/aeer/1906_45054514

The regression line between fertilization of mineral nitrogen and zinc content in grain spring wheat showed that increasing the dose of nitrogen to 60 kg ha^{-1} increased the zinc content in spring wheat grain. The maximum zinc content in spring wheat grain was obtained with the use of mineral nitrogen fertilization in the dose of 67.59 kg Nha^{-1} (*Figure 3*).

Table 4. *Zinc content in spring wheat grain (means across 2017-2019), mg kg^{-1} DM*

Biological preparations (A)	Mineral nitrogen fertiliser regime (B), kg N◎ha^{-1}				Means
	Control	60	90	120	
Control	17.94a	19.42a	18.56a	18.14a	18.52D
L-alpha proline	20.37b	23.74b	25.10b	22.75b	22.99C
Azotoba vinelandii	25.92c	27.12c	29.31c	26.40c	27.19B
L-alpha proline+*Azotobacter vinelandii*	28.41d	29.83d	31.47d	29.05d	29.69A
Means	23.16C	25.03AB	26.11A	24.09BC	-

*Values in columns followed by the same small letter and values in rows followed by the same capital letter do not differ significantly at P<0.05

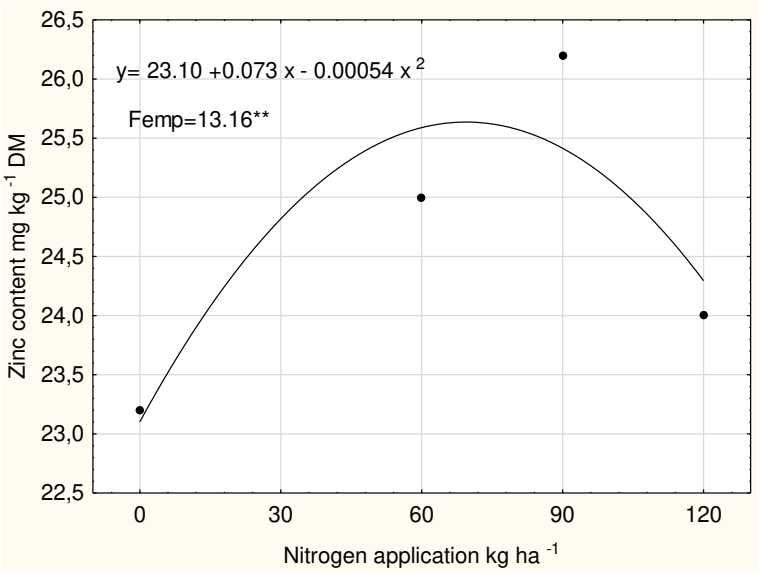

Figure 3. *Regression line between fertilization of mineral nitrogen (x) and zinc content in grain (y), mean for 2017-2019 years*

Zinc plays an important part in plant metabolism. Both the shortage and excess of this element leads to reduced plant growth and development (Srinivals et al., 2002; Sharma et al., 2004; Luo et al., 2013). In the present work, the lowest zinc content was recorded in control spring wheat grain produced without an application of biological products. By contrast, when applied, the products contributed to an increase in Zn content in spring wheat grain. The highest concentration of zinc was determined in the grain of spring wheat treated with L-alpha proline + *Azotobacter vinelandii*. It can be explained by the fact that nitrifying bacteria present in the *Azotoba vinelandii* positively influence the soil content of organic matter, which after mineralisation releases Zn as confirmed in the study

http://www.aloki.hu ● ISSN 1589 1623 (Print) ● ISSN1785 0037 (Online)
DOI: http://dx.doi.org/10.15666/aeer/1906_45054514

by Mona et al. (2012) whore corded similar relationships following an application of other strains of nitrifying bacteria. In the experiment reported here, nitrogen fertilisation up to the rate of 90 kg N◎ha^{-1} increased Zn concentration in spring wheat grain. However, the highest nitrogen rate was followed by a decline in zinc content in spring wheat grain, which agrees with find in s reported by Sułek and Cacak-Pietrzak (2008) as well as Barczak et al. (2018).

Statistical analysis demonstrated a significant impact of the experimental factors and their interaction on copper content in spring wheat grain (*Table 5*).

Table 5. *Copper content in spring wheat grain (means across 2017-2019), mg kg-1 DM*

Biological preparations (A)	**Mineral nitrogen fertiliser regime (B), kg N◎ha^{-1}**				**Means**
	Control	60	90	120	
Control	4.73c	5.12c	5.79b	6.31a	5.49A
L-alpha proline	4.32c	4.69bc	4.83ab	5.18a	4.76B
Azotoba vinelandii	4.11b	4.26ab	4.37ab	4.59a	4.33C
L-alpha proline+*Azotobacter vinelandii*	3.84a	4.07a	4.19a	4.31a	4.10C
Means	4.25D	4.54C	4.80B	5.10A	-

*Values in columns followed by the same small letter and values in rows followed by the same capital letter do not differ significantly at P<0.05

The regression line between fertilization of mineral nitrogen and cooper content in grain spring wheat showed that increasing the dose of nitrogen from 60 to 120 kg ha^{-1} increased the cooper content in spring wheat grain (*Figure 4*).

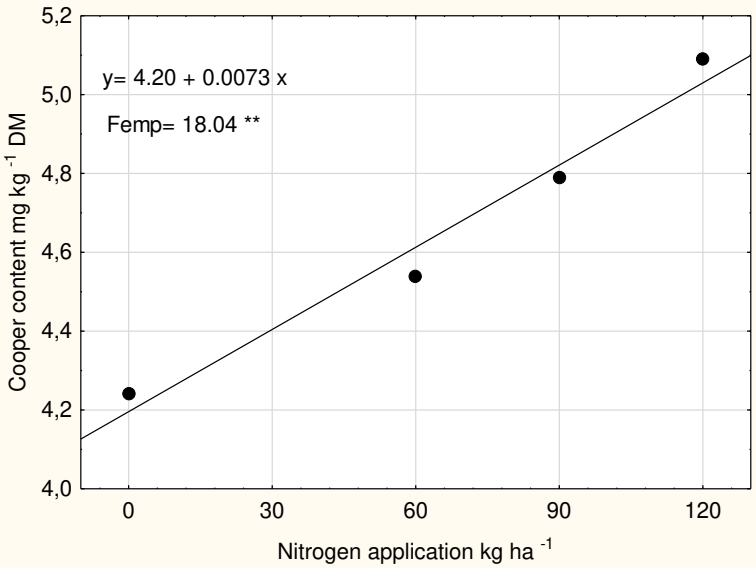

Figure 4. *Regression line between ferilization of mineral nitrogen (x) and cooper content in grain (y), mean for 2017-2019 years*

The highest copper content was determined in the grain of control spring wheat which had been treated with no biofertilizers. An application of the products, particularly

http://www.aloki.hu ● ISSN 1589 1623 (Print) ● ISSN1785 0037 (Online)
DOI: http://dx.doi.org/10.15666/aeer/1906_45054514

Azotoba vinelandii and L-alpha proline + *Azotobacter vinelandii*, contributed to adecline in copper concentration in spring wheat grain. Bacteria *Azotobacter vinelandii* which positively affect an accumulation of soil organic matter. The organic matter accumulates an excessive Cu amount, which provides protection against too much copper being take up by the plants, the notion confirmed in the study by Mona et al. (2012) and Chennappa et al. (2017) who applied other nitrifying bacteria strains.

In the present work, increasing nitrogen fertiliser rates contributed to an increase in the spring wheat grain content of Cu. Also research by Johansson et al. (2001), Buczek et al. (2011) and Jarecki et al. (2019) demonstrated that increasing nitrogen fertiliser rates produced an increase in copper content in cereal grain. However, the values were lower than WHO/FAO standards and thus posed no threat to human and animal health (2012). In the experiment reported here, an interaction was confirmed indicating the at the highest copper content was recorded in control spring wheat grain fertilised with 120 kg N◎ha^{-1}, it being the lowest following treatment with L-alpha proline + *Azotobacter vinelandii* without nitrogen fertiliser input.

Conclusions

1. The weather conditions significantly differentiated the content of micronutrients in the spring wheat grain. An application of biofertilizers increased iron and zinc contents, and reduced the concentration of manganese and copper in spring wheat grain.
2. Increasing nitrogen fertiliser rates, up to 90 kg N◎ha^{-1}, contributed to an increase in the spring wheat grain content of the examined microelements.
3. The highest content of iron and zinc, and the lowest concentration of manganese and copper were recorded in spring wheat grain after application of L-alpha proline + *Azotobacter vinelandii* biological preparations with a dose of mineral nitrogen fertilization of 90 kg N ha^{-1}.
4. In conditions of sustainable agriculture, it is recommended to cultivate spring wheat with the use of the amino acid L-alpha proline with the bacteria *Azotobacter vinelandii*, at the level of mineral nitrogen fertilization with 90 kg N ha^{-1}, for broad agricultural practice.
5. Research should continue on the use of other strains of nitrogen bacteria and growth promoters in the cultivation of spring wheat.

REFERENCES

[1] Barczak, B., Klikocka, H., Kozera, W., Knapowski, T. (2018): Assessment of the effect of sulphur fertilization on oat grain yield and micronutrient uptake. – J. Elem. 23(1): 45-56. https://doi.org/10.5601/jelem.2017.22.1.1318.

[2] Buczek, J., Bobrecka-Jamro, D., Jarecki, W. (2011): Yield and quality of grain of selected spring wheat cultivars depending on the dose and the time of nitrogen application. – Frag. Agron. 28(4): 7-15.

[3] Calvo, P., Nelson, L., Kloepper, J. W. (2014): Agricultural uses of plant biostimulants. – Plant Soil. 383: 3-41. https://doi.org/10.1007/s11104-014-2131-8.

[4] Chennappa, G., Naik, M. K., Amaresh, Y. S., Nagaraja, H., Sreenivasa, M. Y. (2017): Azotobacter: A Potential Biofertilizer and Bioinoculants for Sustainable Agriculture. – In: Panpatte, D., Jhala, Y., Vyas, R., Shelat, H. (eds.) Microorganisms for green revolution. Microorganism for Sustainability 6, Springer.

http://www.aloki.hu ● ISSN 1589 1623 (Print) ● ISSN1785 0037 (Online)
DOI: http://dx.doi.org/10.15666/aeer/1906_45054514

[5] Colla, G., Rouphael, Y., Canaguier, R., Svecova, E., Cardarelli, M. (2014): Biostimulant action of a plant-derived protein hydrolysate produced through enzymatic hydrolysis. – Front. Plant Sci. 5: 448. https://doi.org/10.3389/fpls.2014.0044.
[6] Delauney, A. J., Verma, D. P. S. (1993): Proline biosynthesis and osmoregulation in plants. – The Plant Journal 4: 215-223. https://doi.org/10.1046/j.1365-313X.1993.04020215.x.
[7] Du Jardin, P. (2015): Plant biostimulants: Definition, concept, main categories and regulation. – Sci. Hort. 196: 3-14. https://doi.org/10.1016/j.scienta.2015.09.021.
[8] Gondek, K., Gondek, A. (2010): The influence of mineral fertilization on the field and content of selected macro and microelements in spring wheat. – J. Res. Appl. Agric. Eng. 55(1): 30-36.
[9] Hill, T., Lewicki, P. (2006): Statistics: methods and applications. A comprehensive reference for science, industry and date mining. – StatSoft, ISBN 1-884233-59-7.
[10] Hoai, N. T. T., Shim, I. S., Kobayashi, K., Kenji, U. (2003): Accumulation of some nitrogen compounds in response to salt stress and their relationships with salt tolerance in rice (*Oryza sativa* L.) seedlings. – Plant Growth Regul. 41: 159-164.
[11] Jarecki, W., Buczek, J., Bobrecka-Jamro, D. (2019): Response of facultative cultivars of spring wheat to autumn sowing and foliar fertilization. – J. Elem. 24(2): 817-828. https://doi.org/10.5601/jelem.2018.23.4.1726.
[12] Johansson, E., Prieto-Linde, M. L., Jönsson, J. (2001): Effects of wheat cultivar and nitrogen application on storage protein compositioand bread-making quality. – Cereal Chem. 78(1): 19-25. https://doi.org/10.1094/CCHEM.2001.78.1.19.
[13] Luo, Y. W., Xie, W. H., Jin, X. X., Wang, Q., He, Y. J. (2013): Effects of germination on iron, zinc, calcium, manganese, and copper availability from cereals. – CyTa300 J. Food. 12(1): 22-26. https://doi.org/10.1080/19476337.2013.782071.
[14] Mahamed, H. H., Kaharia, M. (2012): Assessment of some heavy metals in vegetables, cereals and fruits in Saudi Arabian markets. – Egyp. J. Aqua. Res. 38: 31-37.
[15] Michalak, I., Chojnacka, K. (2013): Use of extract from Baltic seaweeds produced by chemical hydrolysis in plant cultivation. – Przem. Chem. 92: 1046-1049.
[16] Mona, E. E., Eman, R. H., Heba, S. S. (2012): Biofertilizers and/or some micronutrients role on wheat plants grown on newly reclaimed soil. – Afric. J. Ecol. 50: 464-475. https://doi.org/10.1111/j.1365-2028.2012.01342.x.
[17] Muhammad, I. R., Liyakat, H. M., Tanvir, S., Tatal, A., Iqbal, M. I., Mohammad, O. (2016): Bacteria and fungi can contribute to nutrients bioavailability and aggregate formation in degraded soils. – Microbiological Res. 183: 26-41. https://doi.org/10.1016/j.micres.2015.11.007.
[18] Qotob, M. A., Nasef, M. A., Elhakim, H. K. A., Shaker, O. G., Habashy, N. R., Abdelhamid, I. A. (2019): Integrated effect of plant growth regulators with boron sources on some biological parameters of sugar beet. – bioRxiv 839068; doi:https://doi.org/10.1101/839068.
[19] Radkowski, A., Radkowska, I. (2013): Effect of foliar application of growth biostimulant on quality and nutritive value of meadow sward. – Ecol. Chem. Eng. A. 20: 1205-1211. https://doi.org/10.2428/ecea.2013.20(10)110.
[20] Sharma, O. P., Bangar, S., Rajesh Jain, K. S., Sharma, P. K. (2004): Heavy metals accumulation in soil irrigated by municipal and industrial effluent. – J. Environ. Sci. Eng. 46(1): 65-73.
[21] Srinivas, N., Vinod Kumar, B., Suresh Kumar, K. (2002): Lead Pollution in Roadside Plant in Visakhapatnam. – J Envir. Stud. Pol. 5(1): 63-68.
[22] Sułek, A., Cacak-Pietrzak, G. (2008): Formation the quality characteristics of spring wheat varieties depending on nitrogen fertilization. – Frag. Agron. 25(1): 400-409.
[23] Szmigiel, A., Oleksy, A., Kołodziejczyk, M. (2014): Effect of nitro gen fertilization on quality and quantity in spring wheat. – EJPAU 17(2): 1.
[24] Wang, Z., Li, S., Malhi, S. (2008): Effects of fertilization and other agronomic measures on nutritional quality of crops. – J. Sci. Food Agric. 88: 7-23.

http://www.aloki.hu ● ISSN 1589 1623 (Print) ● ISSN1785 0037 (Online)
DOI: http://dx.doi.org/10.15666/aeer/1906_45054514

THE EFFECT OF DIFFERENT AFFORESTATION TREE SPECIES ON PLANT DIVERSITY AFTER 50 YEARS ON MOUNT TAI, CHINA

ZHOU, J.[1] – GAO, Y.[2,3*] – WANG, Y.[2] – ZHAO, Y. J.[4]

[1]*School of Life Sciences, Qufu Normal University, Jining 273 165, China*
(e-mail: jingzhou-2004@163.com)

[2]*Shandong Provincial Key Laboratory of Water and Soil Conservation and Environmental Protection, College of Resources and Environment, Linyi University, Linyi 276 005, China*
(e-mail: wangyunsd@163.com)

[3]*Linyi Scientific Exploration Laboratory, Linyi 276 037, China*

[4]*College of Agriculture and Forestry, Linyi University, Linyi 276005, China*
(e-mail: zhaoyanjie1882@126.com)

[*]*Corresponding author*
e-mail: gaoyuan1182@tom.com

(Received 4th Jun 2021; accepted 3rd Sep 2021)

Abstract. The degree of forest vegetation restoration and reconstruction and the impact of different afforestation tree species on plant diversity in Mount Tai, China were evaluated. We selected 6 kinds of 50-year-old plantations along Tianwai village, Hongmen, Tianzhu peak and Taohuayuan lines. The results show that: 1) *Robinia pseudoacacia* plantation has significantly lower tree layer richness, Shannon-Wiener diversity and Simpson diversity than other plantations; *Pinus tabulaeformis* and larch tree plantations have significantly lower shrub layer Shannon -Wiener and Simpson diversity than other plantations, *Pinus tabulaeformis* and *Pinus densiflora* have significantly lower Pielou evenness than the other four plantations; *Pinus tabulaeformis* plantation and *Platycladus orientalis* plantation have significantly lower herb layer richness than the other four plantations, while *Pinus tabulaeformis* plantation has significantly lower Shannon-Wiener diversity and Simpson diversity than the other five plantations. 2) Species richness, Shannon-Wiener diversity and Simpson diversity of tree and shrub layers are all presented from highest to lowest in the following order: Mount Meng > Mount Tai > Mount Yi, while Mount Tai plantation has the highest herb layer species richness, Shannon-Wiener diversity and Simpson diversity. These results provide basis for the regulation and prediction of regional forest vegetation restoration and reconstruction in the future.

Keywords: *vegetation restoration, plant diversity, shrub layer, 50-year-old plantations, Mount Tai, plantation, plant diversity, soil, 50-year Forest Establishment*

Introduction

Biodiversity provides the basis for maintaining the stability of ecosystem structure and function (Wang et al., 2016), which represents one core issue in plant ecology (Kazakou et al., 2008). Changes in species diversity in the process of vegetation restoration reflect the degree of vegetation restoration, which is also a result of the combined effects of ecological processes such as community environmental evolution, population intrusion and diffusion (Kapás et al., 2020), and competition. Excessive studies have confirmed that plantation forests can effectively prevent land degradation and promote vegetation restoration (Depauw et al., 2019), but different initial afforestation tree species will lead to significantly different plant community structures and species diversity of plantation

http://www.aloki.hu ● ISSN 1589 1623 (Print) ● ISSN1785 0037 (Online)
DOI: http://dx.doi.org/10.15666/aeer/1906_45154526

forests (Togonidze and Akhalkatsi, 2015). Studies have shown that the use of exotic species for afforestation will weaken the natural restoration of native plants and reduce plant diversity of the community (Xue et al., 2016). However, studies also found that use of exotic species for afforestation can contribute to biodiversity conservation and protect successional tree species in the later stage, which will eventually be restored to native zonal vegetation and exotic species will be withdrawn (Assandri et al., 2016). Plantation forests are superior to enclosed forests in terms of biodiversity conservation potential, and its species of harmful plants are also fewer compared to the latter (Huang et al., 2015). To maintain stability of plantation forest ecosystem and maximize its functions, species diversity research after vegetation restoration is particularly important. There is a need to evaluate the vegetation restoration and reconstruction processes and effects based on the principle of biodiversity (Lindenmayer et al., 2018). For plantation forest more than 50 years old, dynamics research on vegetation restoration and reconstruction is ever more urgent due to the scarcity of samples (Chi et al., 2004; Fan et al., 2008; Gao et al., 2011).

Due to its complex and diverse ecological environmental conditions, the mountainous region has become a germplasm bank for species survival, reproduction and preservation (Tian and Li, 2012). Mount Tai, standing on the North China Plain, is the highest mountain in Shandong. Rich in wild plant resources, it is the mountain with the most diverse vegetation, and the highest number of endemic plant species in Shandong Province (Su et al., 2018), which is a dual heritage of world culture and nature, World Geopark, National Key Cultural Relics Protection Unit, National Key Scenic Spot and National 5A Tourist Attraction. The research on Mount Tai vegetation began with the front forest vegetation investigation of Mount Tai by the East China Forestry Investigation Team in 1950, the Mount Tai Vegetation Investigation Team of Botanical Geography Training Class of East China Normal University in 1956, and the Geobotany Investigation Team of Shandong University in 1957 (Kyohou, 1958). After more than 60 years of inheritance, there have been studies on plant diversity in some forest types (Chen et al., 2019) and some forest farms (Kuswanda et al., 2019).

Based on previous studies, this paper intends to conduct a field investigation on 50-year restoration and reconstruction of six main afforestation tree species in Mount Tai, evaluate the status and extent of forest vegetation restoration and reconstruction, and examine the impact of different afforestation tree species on plant diversity, thus providing a basis for the regulation and prediction of regional forest vegetation restoration and reconstruction in the future.

Materials and methods

Overview of the sample plot

Mount Tai is located in the middle of Shandong, China, with geographic coordinates of 36°05'–36°15'N, 117°05'–117°24' E, covering an area of 426 km^2. The main peak, Yuhuangding, with an altitude of 1545 m, is the highest peak in Shandong. The mountain is mainly composed of complex rock-crystalline gneiss and metamorphic granite, with a small amount of limestone and sandy shale. The soil types are mainly brown soil, ordinary acid brown soil, mountain dark brown soil and mountain shrubby meadow soil, with ordinary acid brown soil as the most common type. The climate is warm-temperate continental monsoon climate with four distinct seasons and sufficient sunlight. The annual average temperature is about 5.3 ℃ at the mountain top and 12.8 ℃ at the mountain foot. The average annual rainfall is about 1 125 mm at the mountain top, and 600 mm at

http://www.aloki.hu ● ISSN 1589 1623 (Print) ● ISSN1785 0037 (Online)
DOI: http://dx.doi.org/10.15666/aeer/1906_45154526

the mountain foot. The forest coverage rate is about 81.5%, and the main vegetation is *Pinus tabuliformis* forest, *Platycladus orientalis* forest, *Pinus densiflora* forest, *Pinus thunbergii* forest, *Quercus acutissima* forest, *Robinia pseudoacacia* forest and *Quercus variabilis* forest (Fu et al., 2009; Ma et al., 2010; Zhang et al., 2011). The map of the location of the sampling site was shown in *Figure S1*. The phenological differences between the studied species were shown in *Table S1*. We measured soil nutrients and the data was shown in *Table 1*. And soil nutrient detection methods refer to Donald (2020).

Table 1. *Soil nutrients in sample plots*

	Organic matter g·kg^{-1}	**Total nitrogen g·kg^{-1}**	**Total phosphorus g·kg^{-1}**	**Total potassium g·kg^{-1}**	**Hydrolytic nitrogen mg·kg^{-1}**	**Available phosphorus mg·kg^{-1}**	**Available potassium mg·kg^{-1}**
PT forest	81.0±11.3	3.3±0.3	1.5±0.2	11.7±0.7	235.9±44.8	83.6±7.5	70.3±7.8
PO forest	19.7±6.1	1.1±0.3	0.5±0.1	8.9±0.8	87.0±27.0	39.2±16.8	59.8±9.7
RP forest	37.3±6.2	2.3±0.4	0.8±0.1	7.7±0.5	194.7±43.6	32.2±7.0	69.8±16.4
PD forest	44.3±6.4	2.3±0.2	1.3±0.1	12.2±0.9	176.2±35.7	60.8±10.8	79.4±8.0
LK forest	72.9±7.5	4.0±0.2	1.8±0.1	10.2±0.6	528.5±207.2	81.4±2.7	92.9±22.2
PA forest	35.7±2.9	2.1±0.2	0.9±0.2	3.8±0.5	190.9±24.0	27.8±5.6	69.0±10.7

PT forest = *Pinus tabulaeformis* forest, PO forest = *Platycladus orientalis* forest, RP forest = *Robinia pseudoacacia* forest, PD forest = *Pinus densiflora* forest, LK forest = *Larix kaempferi* forest PA forest = *Pinus armandii* Franch. forest

Field investigation

The field investigation covered Tianwai Village route, Hongmen route, Tianzhu Peak route and Taohuayuan route. 50-year-old middle-aged forest was selected as the sample plot, and typical sampling method was taken for the forest investigation (Fang et al., 2004; Yu et al., 2009). A total of 42 sample plots were set up in the field, with a dimension of 30 m × 20 m. The selected sample plots are neat and can represent basic characteristics of the community.

The community level is divided into tree layer, shrub layer and herb layer for hierarchical statistics. According to investigation specifications for plant species diversity in mountainous areas (Fang et al., 2004) and method specifications for the inventory of plant communities (Yu et al., 2009), statistical specifications of the plot stratification are decided as: tree layer, 30 m × 20 m; shrub layer, 15 m × 15 m, located at the center of the sample plot, 1; herb layer, 1 m × 1 m, located at the four corners of the sample plot, 4. In tree layer measurement, record species and numbers of all woody plants with (DBH) ≥ 5 cm and DBH of each wood; in shrub layer measurement, record species, numbers of all woody plants with DBH < 5 cm and DBH of each wood, including arbor seedlings, saplings and woody vines.

Data processing

Four general diversity indexes are selected for calculation and analysis of plant diversity (Fang et al., 2004; Yu et al., 2009): Richness Index (S, Equation 1), Shannon-Wiener Diversity Index (H, Equation 2), Simpson Diversity Index (P, Equation 3) and Pielou Evenness Index (E, Equation 4). The calculation formulas are:

http://www.aloki.hu ● ISSN 1589 1623 (Print) ● ISSN1785 0037 (Online)
DOI: http://dx.doi.org/10.15666/aeer/1906_45154526

$$S = \text{plant species in the sample plot} \quad \text{(Eq.1)}$$

$$H = -\sum_{i=1}^{S} P_i lnP_i \quad \text{(Eq.2)}$$

$$P = 1 - \sum_{i=1}^{S} P_i^2 \quad \text{(Eq.3)}$$

$$E = H / \ln S \quad \text{(Eq.4)}$$

where, P_i is the ratio of the importance value of the $_i$-th species to the total importance value of all species in the sample plot, importance value of shrub layer = (relative significance + relative density + relative frequency)/3, and importance value of herb layer = (relative height + relative density + relative frequency)/3.

Statistical analysis

The differences in plant diversity between forest types are analyzed by single factor method and T test. The inter-layer and intra-layer plant diversity correlation is interpreted by principal component analysis. Data analysis and chart production are completed using SPSS 17.0 and Excel 2003.

Results

Species diversity of six plantation forests in Mount Tai after 50 years of establishment

Species diversity of tree layer

Tree Species detected in the individual plots were shown in *Table S2*. Tree layer plant richness index, Shannon-Wiener diversity index, and Simpson diversity index present relatively consistent characteristics. That is, Robinia pseudoacacia plantation has significantly lower value than the other five plantation forests (P<0.05), while *Pinus tabulaeformis* plantation, *Platycladus orientalis* plantation, *Pinus densiflora* plantation, *Pinus armandi* plantation and larch tree plantation are not significantly different from each other (*Figure 1A1–Figure 1A3*). There is no significant difference in Pielou evenness index of the 6 plantations in Mount Tai (*Figure 1A4*).

Species diversity of shrub layer

Shrub layer plant richness index is not significantly different among the six plantations (*Figure 1B1*). *Pinus tabulaeformis* plantation and larch tree plantation have significantly lower Shannon-Wiener and Simpson diversity indexes than the other four species (P<0.05), *Platycladus orientalis* plantation, *Robinia pseudoacacia* plantation, *Pinus densiflora* plantation and *Pinus armandi* plantation are not significantly different from each other (*Figure 1B2-Figure 1B3*). *Pinus tabuliformis* plantation and *Pinus densiflora* plantation have significantly lower Pielou evenness index than the other four plantations (P<0.05). *Platycladus orientalis* plantation, *Robinia pseudoacacia* plantation, *Pinus armandi* plantation and larch tree plantation are not significantly different from each other (*Figure 1B4*).

http://www.aloki.hu ● ISSN 1589 1623 (Print) ● ISSN1785 0037 (Online)
DOI: http://dx.doi.org/10.15666/aeer/1906_45154526

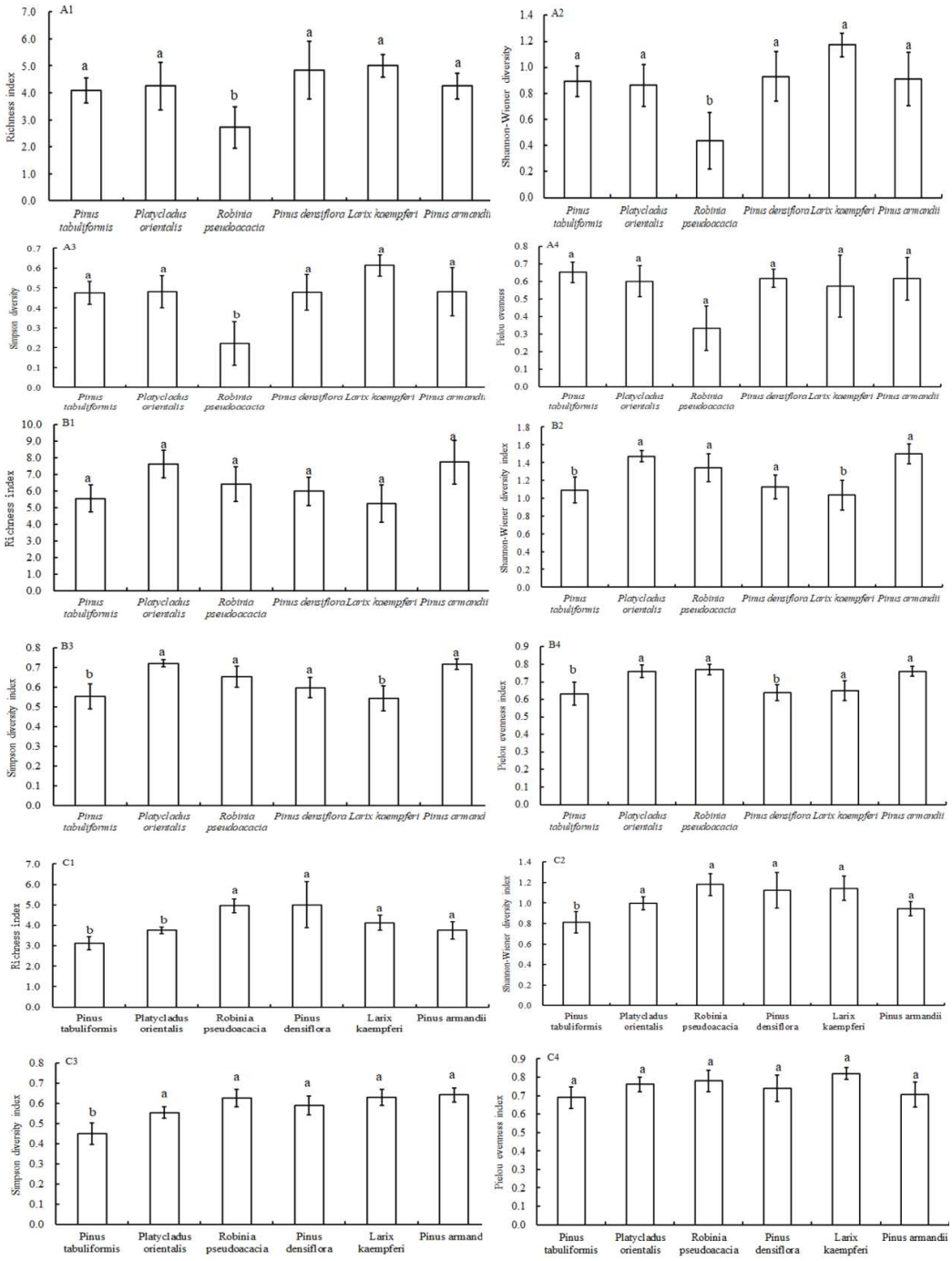

Figure 1. *The richness index, Shannon-Wiener diversity index, Simpson diversity index and Pielou evenness index of the tree layer (A1–A4), shrub layer (B1–B4) and herb layer (C1–C4) of the 6 main plantations in Mount Tai (Mean ± standard error) Different lowercase letters indicate significant differences among plantations (P<0.05)*

Species diversity of herb layer

In herb layer, *Pinus tabulaeformis* plantation and *Platycladus orientalis* plantation have significantly lower richness index than the other four plantations (P<0.05), while *Robinia pseudoacacia* plantation, *Pinus densiflora* plantation, *Pinus armandi* plantation

http://www.aloki.hu ● ISSN 1589 1623 (Print) ● ISSN1785 0037 (Online)
DOI: http://dx.doi.org/10.15666/aeer/1906_45154526

and larch tree plantation are not significantly different from each other (*Figure 1C1*). Pinus tabulaeformis plantation has significantly lower Shannon-Wiener and Simpson diversity indexes than the other five plantations (P<0.05), *Platycladus orientalis* plantation, *Robinia pseudoacacia* plantation, *Pinus densiflora* plantation, *Pinus armandi* plantation and larch tree plantation are not significantly different from each other (*Figure 1C2–Figure 1C3*). There is no significant difference in Pielou evenness index between the 6 plantations in Mount Tai (*Figure 1C4*).

Correlation analysis of tree, shrub and herb species diversity

The four inter-layer diversity indexes of tree layer, shrub layer and herb layer of Mount Tai plantations are all significantly positively correlated and inter-layer richness index, Shannon-Wiener diversity index and Simpson diversity index show significant positive correlation between shrub layer and herb layer (*Table 2*).

Table 2. *Correlation of species diversity of tree, shrub and herb in the Taishan plantation*

	T−S	T−H	T−P	T−E	S−S	S−H	S−P	S−E	H−S	H−H	H−P	H−E
T−S	1.00											
T−H	0.89**	1.00										
T−P	0.80**	0.98**	1.00									
T−E	0.53**	0.77**	0.83**	1.00								
S−S	0.15	0.14	0.12*	0.02	1.00							
S−H	0.08	0.08	0.06	-0.06	0.88**	1.00						
S−P	0.05	0.08	0.07	-0.02	0.74**	0.96**	1.00					
S−E	-0.00	0.05	0.05	-0.01	0.32*	0.68**	0.81**	1.00				
H−S	-0.16	-0.24	-0.30*	-0.23	0.32*	0.35**	0.31*	0.19	1.00			
H−H	0.01	-0.09	-0.18	-0.19	0.36**	0.38**	0.35**	0.19	0.86**	1.00		
H−P	0.01	-0.07	-0.16	-0.21	0.35**	0.36**	0.33*	0.19	0.69**	0.87**	1.00	
H−E	0.07	-0.02	-0.09	-0.14	0.23	0.22	0.22	0.07	0.38**	0.72**	0.71**	1.00

T-S, tree layer richness index; T-H, tree layer Shannon-Wiener diversity index; T-P, tree layer Simpson diversity index; T-E, tree layer Pielou evenness index; S-S, shrub Layer richness index; S-H, shrub layer Shannon-Wiener diversity index; S-P, shrub layer Simpson diversity index; S-E, shrub layer Pielou evenness index; H-S, herb layer richness index; H−H, Shannon-Wiener diversity index of herb layer; H−P, Simpson diversity index of herb layer; H−E, Pielou evenness index of herb layer, *, P<0.05; **, P<0.01

Differences in plant diversity between Mount Tai, Mount Meng and Mount Yi plantations

Species richness index

The species richness indexes of tree layer and shrub layer are both presented as that of Mount Meng plantation> Mount Tai plantation> Mount Yi plantation (p <0.05), while that of herb layer is presented as that of Mount Tai plantation> Mount Meng plantation> Mount Yi plantation (P<0.05) (*Figure 2A*).

http://www.aloki.hu ● ISSN 1589 1623 (Print) ● ISSN1785 0037 (Online)
DOI: http://dx.doi.org/10.15666/aeer/1906_45154526

Shannon-Wiener diversity index

Shannon-Wiener diversity index of tree layer and shrub layer is presented as that of Mount Meng plantation> Mount Tai plantation> Mount Yi plantation (P<0.05), while the herb layer is presented as that of Mount Tai plantation> Mount Yi plantation> Mount Meng plantation. Lin (P<0.05) (*Figure 2B*).

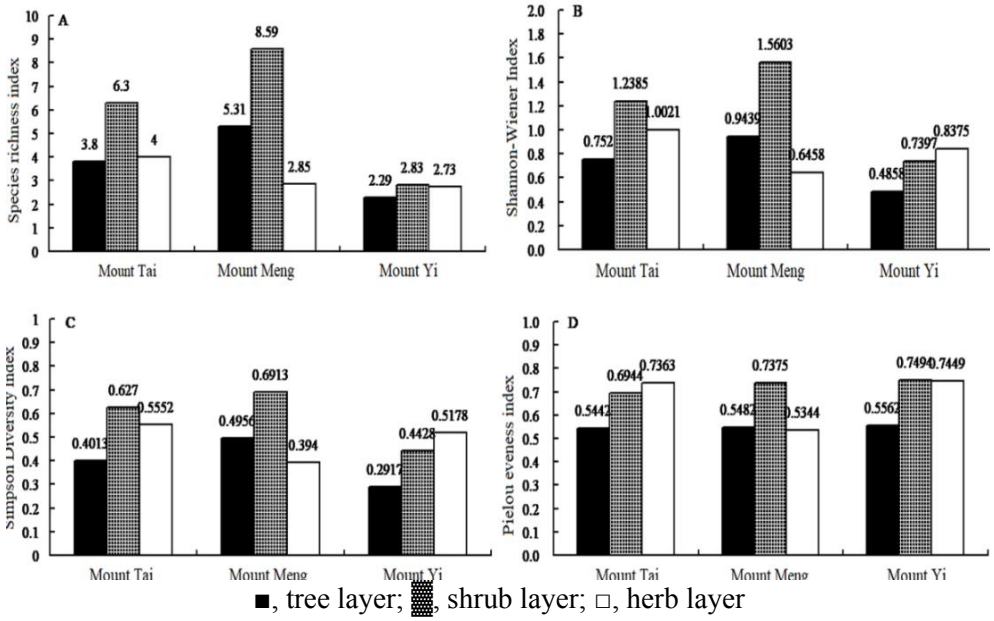

Figure 2. *The abundance index (A), Shannon-Wiener diversity index (B), Simpson diversity index (C), and Pielou evenness index (D) of the tree layer and shrub layer of Taishan, Mengshan and Yishan plantations and herb layer difference*

Simpson diversity index

Simpson diversity index of tree layer and shrub layer is presented as that of Mount Meng plantation> Mount Tai plantation> Mount Yi plantation, while the herb layer is presented as that of Mount Tai plantation> Mount Yi plantation> Mount Meng plantation (*Figure 2C*).

Pielou eveness index

Pielou evenness indexes of tree layer and shrub layer are both presented as that of Mount Yi plantation> Mount Meng plantation> Mount Tai plantation, while the herb layer is presented as that of Mount Yi plantation>T Mount Tai plantation> Mount Meng plantation (*Figure 2D*).

Discussion

Most of the existing vegetation in Mount Tai is plantation forest after the founding of the People's Republic of China, with a few natural forests and secondary forests. The six main plantations are subjected to dual influence of vegetation evolution history and interference from human activities. The vegetation types, plant communities and species diversity are mainly affected by artificial afforestation in the early stage and tourism

http://www.aloki.hu ● ISSN 1589 1623 (Print) ● ISSN1785 0037 (Online)
DOI: http://dx.doi.org/10.15666/aeer/1906_45154526

activities and natural succession in the later period. The six plantations in Mount Tai have been enclosed for 50 years. Under strict and effective local forestry management, soil and water conservation is fine, the forest coverage rate is significantly increased, plant species are significantly increased, so the forest vegetation is restored and rebuilt smoothly, but different plantations differ greatly.

Robinia pseudoacacia plantation in Mount Tai has significantly lower tree layer richness index, Shannon-Wiener diversity index and Simpson diversity index than the other five plantations. This may be due to the inhibition of *Robinia pseudoacacia* forest growth on the understory (Wu et al., 2017). Therefore, we should carry out thinning management for the existing stands with high canopy density in time to promote the growth of lower vegetation, reasonably allocate trees, shrubs and grasses, enrich the community hierarchy and improve the ecological function of *Robinia pseudoacacia* forest. *Pinus tabulaeformis* plantation and larch tree plantation have significantly lower shrub layer Shannon -Wiener diversity index and Simpson diversity index than the other four plantations, *Pinus tabulaeformis* plantation and *Pinus densiflora* have significantly lower Pielou evenness index than the other four plantations; *Pinus tabulaeformis* plantation and *Platycladus orientalis* plantation have significantly lower herb layer richness index than the other four plantations, while *Pinus tabulaeformis* plantation has significantly lower Shannon-Wiener diversity index and Simpson diversity than the other five plantations. On the whole, among the six main plantations in Mount Tai, *Robinia pseudoacacia* plantation has the lowest plant diversity in the tree layer, while *Pinus tabulaeformis* plantation has the lowest plant diversity in the shrub and herb layers. This result was inconsistent with our previous research in Mengshan mountain, which may be caused by the difference of afforestation time, geographical location, soil and climate between the two mountains (Gao et al., 2009).

The four inter-layer diversity indexes of tree layer, shrub layer and herb layer of Mount Tai plantations are all significantly positively correlated, while inter-layer richness index, Shannon-Wiener diversity index and Simpson diversity index show significant positive correlation between shrub layer and herb layer.

According to the investigation, the six main plantations in Mount Tai display sparseness within the trees and simplification of the community appearance, which may be due to the different growth habits and reproduction strategies of plants. For example, perennial forbs have strong tolerance and cushion against disturbances, while shrubs and semi-shrubs are sensitive to interference (Zheng et al., 2008; Gao, 2009). Species richness index, Shannon-Wiener diversity index and Simpson diversity index of tree layer and shrub layer are all presented as that of Mount Meng plantation> Mount Tai plantation> Mount Yi plantation, while Mount Tai plantation has the highest herb layer species richness index, Shannon-Wiener diversity index and Simpson diversity index, though it has the lowest tree layer and shrub layer Pielou evenness index. The understory shrub and herb layer vegetation generally features shade tolerance and fast growth rate, which can easily form a thick and dense evergreen understory shrub and herb layer in the forest ecosystem, thus limiting the natural regeneration of trees, and restricting forest regeneration to a certain extent (Kobayashi et al., 2010).

Conclusion

In the current study, the degree of forest vegetation restoration and reconstruction and the impact of different afforestation tree species on plant diversity in Mount Tai, China

http://www.aloki.hu ● ISSN 1589 1623 (Print) ● ISSN1785 0037 (Online)
DOI: http://dx.doi.org/10.15666/aeer/1906_45154526

were evaluated. Compared with previous studies, this paper further discusses the effect of different after station tree species on plant diversity after 50 years on Mount Tai, China. Plantation in Mount Tai obviously has the function of protecting and improving soil particle and pore structure. The preservation and improvement of soil structure and function has become an indispensable prerequisite for the success of artificial afforestation in Mount Tai. Further research should focus on the differences of microbial communities and functional microorganisms in rhizosphere and bulk soil of afforestation tree species.

Funding. Funded by the Fund of Shandong Provincial Key Laboratory of Water and Soil Conservation and Environmental Protection, Linyi University [NO. STKF201906], the National Natural Science Foundation of China for Young Scholars [NO. 41807053], and National Natural Science Foundation of China [NO. 32071630].

REFERENCES

[1] Assandri, G., Bogliani, G., Pedrini, P., Brambilla, M. (2016): Land-use and bird occurrence at the urban margin: implications for planning and conservation. – North-Western Journal of Zoology 13(1): e161601.
[2] Chen, L., Han, W., Liu, D., Liu, G. (2019): How forest gaps shaped plant diversity along an elevational gradient in wolong national nature reserve? – Journal of Geographical Sciences 29(7): 1081-1097.
[3] Depauw, L., Perring, M. P., Brunet, J., Maes, S. L., Verheyen, K. (2019): Interactive effects of past land use and recent forest management on the understorey community in temperate oak forests in South Sweden. – Journal of Vegetation Science 30(5): 917-928.
[4] Donald, C., Phillimon, N., Henry, M., Felix, C. (2020): Fire alters the availability of soil nutrients and accelerates growth of Eucalyptus grandis in Zambia. – Journal of Forestry Research 31: 1637-1645.
[5] Fan, B., Sang, W. G., Li, G. Q., Liu, R. G., Chen, L. Z., Wang, K. (2008): Long-term protection effects of national reserve to forest vegetation in 4 decades: biodiversity change analysis of major forest types in Changbai Mountain Nature Reserve, China. – Science in China 10: 948.
[6] Fang, J., Shen, Z., Tang, Z., Wang, Z. (2004): The Protocol for the Survey Plan for Plant Species Diversity of China's Mountains. – Biodiversity Science 12(1): 5-9.
[7] Gao, Y. (2009): Effect of tourism on species composition in Mount Meng, Shandong Province. – World Sci-Tech Research and Development 31(4): 708-710.
[8] Gao, Y., Chen, Y., Dong, H., Hao, J., Ci, H. (2011): Vegetation and species diversity change analysis in 50 years in Tashan Mountain, Shandong Province, China. – Acta Ecologica Sinica 31(20): 5984-5991.
[9] Huang, X. R., He, F., Pang, S. L., Hou, Y. R., Lu, G. D. (2015): Understory biodiversity of plantations on karst mountains in Guangxi and its relation to environmental factors. – Chinese Journal of Ecology 34(11): 3024-3033.
[10] Kapás, R., Plue, J., Kimberley, A., Cousins, S. (2020): Grazing livestock increases both vegetation and seed bank diversity in remnant and restored grasslands. – Journal of Vegetation Science 31(6): 1053-1065.
[11] Kazakou, E., Dimitrakopoulos, P. G., Baker, A., Reeves, R. D., Troumbis, A. Y. (2008): Hypotheses, mechanisms and trade-offs of tolerance and adaptation to serpentine soils: From species to ecosystem level. – Biological Reviews 83(4): 495-508.
[12] Kobayashi, T., Shimano, K., Muraoka, H. (2010): Effect of light availability on the carbon gain of beech (Fagus crenata) seedlings with reference to the density of dwarf bamboo

http://www.aloki.hu ● ISSN 1589 1623 (Print) ● ISSN1785 0037 (Online)
DOI: http://dx.doi.org/10.15666/aeer/1906_45154526

(Sasa kurilensis) in an understory of Japan Sea type beech forest. – Plant Species Biology 19(1): 33-46.
[13] Kyohou, G. Y. (1958): The vegetation of Chaoyang Dong, Taishan, and its vicinity. – Journal of Shandong University: natural science 8(1): 243-256.
[14] Lindenmayer, D., Blanchard, W., Crane, M., Michael, D., Sato, C. (2018): Biodiversity benefits of vegetation restoration are undermined by livestock grazing. – Restoration Ecology 26(06): 1157-1164.
[15] Su, Y., Li, J., Qiu, J., Jin, Z., Fang, X., Chao, Y., Wang, J., Zhou, H. (2018): Current situation investigation and analysis of medicinal plant resources in Mount Tai area. – Chinese Wild Plant Resources 37(5): 1006-9690.
[16] Tian, Z., Li, Z. (2012): The vertical distribution of vegetation patterns and its relationship with environment factors at the northern slope of Ili River Valley: a bimodal distribution pattern. – Acta Ecologica Sinica 32(4): 1151-1162.
[17] Togonidze, N., Akhalkatsi, M. (2015): Variability of plant species diversity during the natural restoration of the subalpine birch forest in the Central Great Caucasus. – Turkish Journal of Botany 39: 458-471.
[18] Wang, S., Loreau, M., Jordan, F. (2016): Biodiversity and ecosystem stability across scales in metacommunities. – Ecology Letters 19(5): 510-518.
[19] Wu, D., Jiao, W., Yu, W. (2017): Species composition and community characteristics of 15-year-old Robinia pseudoacacia forest and natural vegetation in Ansai, Shaanxi province. – Research of Soil and Water Conservation 24(4): 12-16.
[20] Xue, S., Zhu, F., Kong, X., Wu, C., Huang, L., Huang, N., Hartley, W. (2016): A review of the characterization and revegetation of bauxite residues (red mud). – Environmental Science & Pollution Research 23(2): 1120-1132.
[21] Yu, D., Jiang, Y., Wang, Z., Zheng, C., Zhu, J., Wang, X., Shen, H., Fang, J., Tang, Z., He, J. (2009): Methods and protocols for plant community inventory. – Biodiversity Science 17(6): 533-548.
[22] Zheng, W., Zhu, J., Pan, C. (2008): Effect of tourism disturbance intensity on plant species diversity of meadow community in Kanasi Nature Reserve. – Acta Agrestia Sinica 16(6): 624-629, 635.

APPENDIX

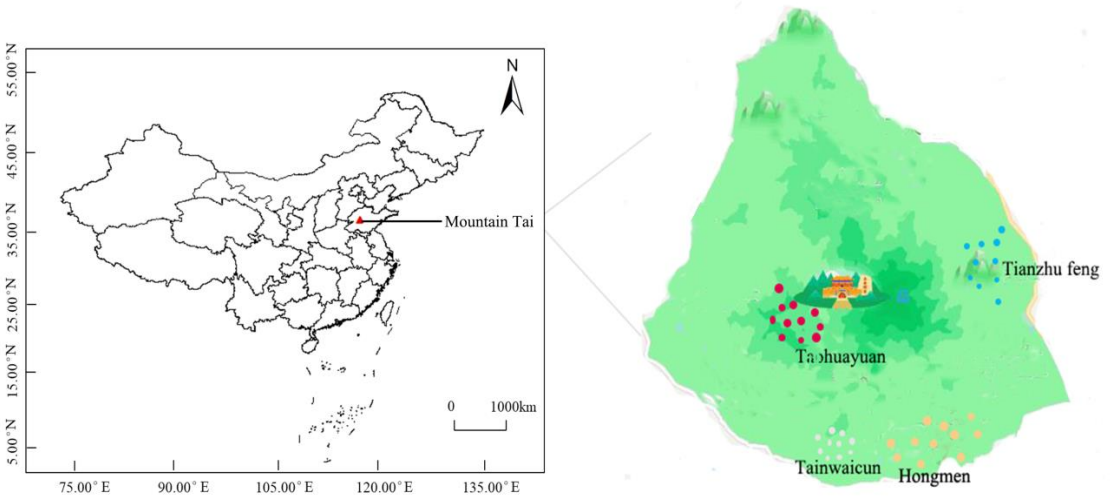

Figure S1. *The map of the location of the sampling sites*

http://www.aloki.hu ● ISSN 1589 1623 (Print) ● ISSN1785 0037 (Online)
DOI: http://dx.doi.org/10.15666/aeer/1906_45154526

Table S1. *Phenological differences between the studied species*

	Average DBH (cm)	Forest canopy density (%)	Tree density (/ha)
PT forest	20.43	76	567
PO forest	11.63	73	1000
RP forest	15.03	81	733
PD forest	16.97	75	800
LK forest	18.33	92	1033
PA forest	19.42	86	900

PT forest = *Pinus tabulaeformis* forest, PO forest = *Platycladus orientalis* forest, RP forest = *Robinia pseudoacacia* forest, PD forest = *Pinus densiflora* forest, LK forest = *Larix kaempferi* forest PA forest = *Pinus armandii* Franch. forest

Table S2. *Species detected in the individual plots*

PT forest	PO forest	RP forest	PD forest	LK forest	PA forest
Pinus bungeana Zucc. et Endi	*Platycladus orientalis (Linn.) Franco*	*Pinus densiflora Sieb. et Zucc.*	*Platycladus orientalis (Linn.) Franco*	*Pinus densiflora Sieb. et Zucc.*	*Grewia biloba G. Don var.parviflora (Bunge)H.-M*
Platycladus orientalis (Linn.) Franco	*Pinus densiflora Sieb. et Zucc.*	*Ailanthus altissima (Mill.) Swingle*	*Pinus densiflora Sieb. et Zucc.*	*Tilia tuan Szyszyl.*	*Pinus densiflora Sieb. et Zucc.*
Pinus densiflora Sieb. et Zucc.	*Ailanthus altissima (Mill.) Swingle*	*Robinia pseudoacacia Linn.*	*Ailanthus altissima (Mill.) Swingle*	*Pinus thunbergii Parlatore*	*Carpinus turczaninowii Hance*
Robinia pseudoacacia Linn.	*Robinia pseudoacacia Linn.*	*Quercus aliena Blume*	*Robinia pseudoacacia Linn.*	*Lespedeza bicolor Turcz.*	*Pinus armandii Franch.*
Kalopanax septemlobus (Thunb.) Koidz.	*Broussonetia kazinoki S. et Z.*	*Pinus armandii Franch.*	*Tilia tuan Szyszyl.*	*Sorbus pohuashanensis (Hance) Hedl.*	*Phellodendron amurense Rupr.*
Celtis koraiensis Nakai	*Albizia julibrissin Durazz.*	*Pistacia chinensis Bunge*	*Broussonetia kazinoki S. et Z.*	*Pinus armandii Franch.*	*Forsythia suspensa (Thunb.) Vahl*
Quercus serrata Murray var. brevipetiolata (A.DC.) Nakai	*Pinus thunbergii Parlatore*	*Diospyros lotus Linn.*	*Pinus thunbergii Parlatore*	*Alnus sibirica Fisch. ex Turcz*	*Albizia kalkora(Roxb．)Prain*
Tilia tuan Szyszyl.	*Quercus dentata Thunb.*	*Quercus acutissima Carr.*	*Pistacia chinensis Bunge*	*Larix kaempferi (Lambert) Carriere*	*Quercus variabilis Blume*
Carpinus turczaninowii Hance	*Cotinus coggygria Scop.*	*Pyrus pyrifolia (Burm. F.) Nakai*	*Vitex negundo Linn. var.*	*Malus baccata (Linn.) Borkh.*	*Acer saccharum Marsh.*
Quercus dentata Thunb.	*Koelreuteria paniculata Laxm.*	*Amygdalus davidiana (Carr.) C. de Vos*	*Diospyros lotus Linn.*	*Pinus tabulaeformis Carr.*	*Pinus tabulaeformis Carr.*
Sorbus pohuashanensis (Hance) Hedl.	*Quercus acutissima Carr.*	*Crataegus pinnatifida Bge.*	*Decaspermum gracilentum (Hance) Merr. et Perry*		
Tilia japonica Simonk.	*Pyrus pyrifolia (Burm. F.) Nakai*	*Quercus variabilis Blume*	*Quercus acutissima Carr.*		
Pinus armandii Franch.	*Albizia kalkora(Roxb．) Prain*		*Populus tomentosa Carr.*		
Phellodendron amurense Rupr.	*Quercus variabilis Blume*		*Morus mongolica (Bur.) Schneid.*		
Pistacia chinensis Bunge	*Populus alba Linn.*		*Albizia kalkora(Roxb．)Prain*		
Morus australis Poir.	*Pinus tabulaeformis Carr.*		*Quercus variabilis Blume*		
Vitex negundo Linn. var.	*Acer truncatum Bunge*		*Pinus tabulaeformis Carr.*		
Decaspermum gracilentum (Hance) Merr. et Perry			*Ulmus pumila Linn.*		
Quercus acutissima Carr.					
Larix kaempferi (Lambert) Carriere					

http://www.aloki.hu ● ISSN 1589 1623 (Print) ● ISSN1785 0037 (Online)
DOI: http://dx.doi.org/10.15666/aeer/1906_45154526

PT forest	PO forest	RP forest	PD forest	LK forest	PA forest
Albizia kalkora(Roxb．)Prain *Malus baccata (Linn.) Borkh* *Crataegus pinnatifida Bge.* *Pinus tabulaeformis Carr.*					

http://www.aloki.hu ● ISSN 1589 1623 (Print) ● ISSN1785 0037 (Online)
DOI: http://dx.doi.org/10.15666/aeer/1906_45154526

MAXENT MODELING THE CURRENT AND FUTURE DISTRIBUTION OF THE INVASIVE PEST, THE FALL ARMYWORM (*SPODOPTERA FRUGIPERDA*) (LEPIDOPTERA: NOCTUIDAE), UNDER CHANGING CLIMATIC CONDITIONS IN CHINA

CAI, P. M.[1,2,3#*] – MENG, F. H.[1#] – SONG, Y. Z.[1,2*] – MA, C. H.[1] – PENG, Y. W.[1] – WU, Q. F.[1] – LEI, S. Y.[1] – HONG, Y. C.[1] – HUO, D.[1] – LI, L.[1]

[1]*Department of Horticulture, College of Tea and Food Science, Wuyi University, Wuyishan 354300, China*

[2]*Biological Control Research Institute, College of Plant Protection, Fujian Agriculture and Forestry University, Fuzhou 350002, China*

[3]*Key Laboratory of Biopesticide and Chemical Biology, Ministry of Education, Fuzhou 350002, China*

[#]*These two authors made equal contributions to this work.*

[*]*Corresponding authors*
e-mail: caipumo@qq.com; phone: +86-150-8045-6908 (Cai, P. M.);
e-mail: 1023554932@qq.com; phone: +86-155-0690-0021 (Song, Y. Z.)

(Received 4th Jun 2021; accepted 4th Sep 2021)

Abstract. In this study we investigated the effects of climate change on the fall armyworm, *Spodoptera frugiperda* (Lepidoptera: Noctuidae). Based on the current distribution records of *S. frugiperda* and selected bioclimatic factors, we modelled its potential habitat suitability in China under four climate change scenarios using Maximum Entropy Models (MaxEnt) and Geographic Information Systems (GIS). Our results showed that: (1) the mean area under curve (AUC) values of both our initial and final models were greater than 0.978, indicating high accuracy in the predictions; (2) the dominant environmental factors regulating the habitat suitability of *S. frugiperda* were Precipitation of Warmest Quarter (bio18), Temperature Seasonality (bio4), Annual Mean Temperature (bio1) and Precipitation Seasonality (bio15); (3) the highly suitable areas for *S. frugiperda* were mainly distributed in Jiangsu, Anhui, Jiangxi, most parts of Henan and Guangxi, central and eastern Hubei, central and southern Shaanxi, and southeastern and northern Zhejiang, accounting for 17.6% of China's landmass; (4) from the present until the 2070s, the areas of the non-suitable regions will decrease as climate warming becomes more severe, and the geometric center of the highly and total suitable areas will displace to the north under all four climate change scenarios.
Keywords: *biological invasion, Maximum Entropy Models, climate change, bioclimatic variables, habitat suitability*

Introduction

Invasive species threaten ecosystems due to their impacts on native flora and fauna through predation and competition. They also threaten human-managed systems, such as those associated with agriculture, forestry and animal health (Simberloff et al., 2003). A considerable amount of evidence has indicated that their impact on new communities and ecosystems will be aggravated as a result of climate change (Ekesi et al., 2016), which is in itself one of the greatest threats to the global economy, agricultural production, animal health and biodiversity (Roy et al., 2011). Climate change will likely influence almost all

http://www.aloki.hu ● ISSN 1589 1623 (Print) ● ISSN1785 0037 (Online)
DOI: http://dx.doi.org/10.15666/aeer/1906_45274546

aspects of the life history traits and population dynamics of pests, including their growth and development, metabolic rate, survival, propagation, and distribution range (Battisti et al., 2005; Tobin et al., 2008; Faccoli, 2009). Due to the sensitivity of insects to climate conditions, global climate change has significantly broadened their distribution, enhanced generation and ecological adaptability variations, altered the structure, composition, function, and succession of insect communities within ecosystems, and subsequently influenced the interrelationship among pests, natural enemies and plants, resulting in outbreaks of some species (Kyrre et al., 2012; Celine et al., 2012). Therefore, being able to predict changes in their distribution as a result of climate change is an important baseline to prevent and manage the introduction and diffusion of invasive species. This, in turn, will provide a reference for risk assessments and integrated pest management (Massin et al., 2012).

Spodoptera frugiperda (J. E. Smith) (Lepidoptera: Noctuidae), commonly known as the fall armyworm (FAW), is a polyphagous moth pest that can feed on more than 350 host plant species, although it has a preference towards cultivated grasses such as rice, maize, cotton, sorghum and sugarcane (Montezano et al., 2018). Native to the tropical and subtropical areas of the Americas, *S. frugiperda* was not recorded elsewhere until 2015 (Wang et al., 2020). The literature indicates that *S. frugiperda* invaded Africa as a stowaway on a passenger flight via the agricultural trade and rapidly diffused to almost the whole of sub-Saharan Africa due to its prominent dispersal ability (Day et al., 2017). This resulted in a 20–50% decrease in maize production in the absence of management measures (Nagoshi, 2019). Since its introduction and establishment in Africa in 2016, *S. frugiperda* quickly spread to most of the maize production areas, leading to estimated financial losses between USD 2.48 and 6.19 billion every year (Day et al., 2017). Indeed, *S. frugiperda* has now invaded approximately 100 countries throughout the world and continues to search for new ecological niches, where it threatens agricultural production systems and potentially causes food insecurity (Center for Agriculture and Bioscience International, 2016).

In China, *S. frugiperda* was first recorded in Yunnan Province at the end of 2018, and in 2019 caused an estimated economic loss of CNY 29 billion to maize industries (Zhang et al., 2020). By 31st August 2020, it had been documented in 27 provinces/municipalities, encompassing 1338 counties, with a total damage area of 3.68 million hectares (National Agro-Tech Axtension and Service Center, 2020). Thus, it is very important to understand how climate change impacts its geographic distribution, to enable better detection, early warning, quarantine inspection and control.

Projecting the potential spatial distribution of pests is an important research area within quantitative pest risk analysis (Li et al., 2018). As statistical modeling has developed, ecological theories combined with geographic information system (GIS) technologies have been utilized to improve our ecological understanding, particularly for agricultural production and conservation biology (Brito et al., 2009). Species distribution models (SDMs), including the maximum entropy model (MaxEnt), Climex, GARP, DOMAIN and BIOCLIM, are important tools widely applied to determine the impacts of climate change (Zhu et al., 2013). Their main principle is to apply known occurrence data, related environmental factors and certain algorithms to evaluate the ecological demands and habitat suitability for a given species. They can then provide a projection of different spatial and temporal ranges in order to forecast future distribution patterns (Venette et al., 2010). The MaxEnt model is the most commonly used predictive tool for quantifying the future distributions of a species and has been widely applied in the areas of ecology,

http://www.aloki.hu ● ISSN 1589 1623 (Print) ● ISSN1785 0037 (Online)
DOI: http://dx.doi.org/10.15666/aeer/1906_45274546

conservation, biosafety and species evolution since it emerged in 2004 (Elith et al., 2006). The merits of the MaxEnt model are its high simulation precision with a small sample size, short operation time, convenient use, stable prediction results, and the ease with which results can be interpreted (Li et al., 2013). However, it inevitably has certain defects; for example, abiotic factors without biotic factors are considered in MaxEnt operation, and the forecast from this software only represents the greatest possibility of species distribution rather than 'real' distributions (Wang et al., 2017).

Due to the severe impacts caused by *S. frugiperda*, several attempts to understand its response to different climate change scenarios have been made (Valdez-Torres et al., 2012; Ramirez-Cabral et al., 2017; Wang et al., 2020; Liu et al., 2020). The biomechanical pathways of *S. frugiperda* invasion in maize fields were investigated by Valdez-Torres et al. (2012), while possible changes in habitat suitability in its native regions were estimated based on two global circulation models (GCM) and known occurrence records (Ramirez-Cabral et al., 2017). More recently, many research teams assessed the responses of *S. frugiperda* to different climatic variables within an invaded area (Baloch et al., 2020; Cokola et al., 2020; Fan et al., 2020; Wang et al., 2020), while Liu et al. (2020) determined its response to land use under current and future climate conditions. Additionally, Zacarias (2020) explored the potential implications of climate change on its global geographical distribution, as well as the interaction with its main economically-important host plants. Overall, the abovementioned research suggests that the invasive potential of *S. frugiperda* is largely attributed to factors related to temperature, rainfall and land use, with an immense potential for invasion in Africa (Ramirez-Cabral et al., 2017; Early et al., 2018; Cokala et al., 2020; Liu et al., 2020; Fan et al., 2020), South America (Ramirez-Cabral et al., 2017), central Asia (Baloch et al., 2020), and other areas of Asia such as China (Liu et al., 2020; Wang et al., 2020).

Due to the devastating impacts of *S. frugiperda* invasion on agricultural production, along with its excellent spread ability, projecting the potential distribution of this pest in relation to climate conditions and ascertaining the regulating factors are important tasks. They are particularly important in China, where diverse host plants of this pest are widely grown, and where this pest has already begun to proliferate. Such knowledge will be useful for developing strategies to prevent it from spreading and reduce the incidence of high-level infestations. In the present study, a MaxEnt model based on available occurrence data was chosen to estimate the distribution pattern and spread of *S. frugiperda* in China under different climate change scenarios. The main aims were as follows: (1) to confirm key climatic factors that restrict the potential distribution of *S. frugiperda*; (2) to forecast how its suitable habits will change under different emission scenarios; as well as (3) to provide a theoretical reference framework and data support for the comprehensive prevention and management of this pest in China.

Materials and Methods

Species occurrence data

Global presence records of *S. frugiperda* were compiled from three main sources: two online species distribution databases, the Global Biodiversity Information Facility (GBIF, https://www.gbif.org/) and the Centre for Agriculture and Bioscience International (CABI, https://www.cabi.org/), and a significant amount of published literature. Geographical coordinates for each data point were either referenced from information in the article or acquired from Google Earth. In strict conformity with the requirements of

http://www.aloki.hu ● ISSN 1589 1623 (Print) ● ISSN1785 0037 (Online)
DOI: http://dx.doi.org/10.15666/aeer/1906_45274546

MaxEnt, adjacent records, duplicate records, and fuzzy records were eliminated (Jiang et al., 2018), and data were manually inspected for accuracy. Ultimately, 375 validated records were used to establish the models (*Figure 1*). All filtered occurrence records were imported into Microsoft Excel and saved as ".csv" files (Wang et al., 2019).

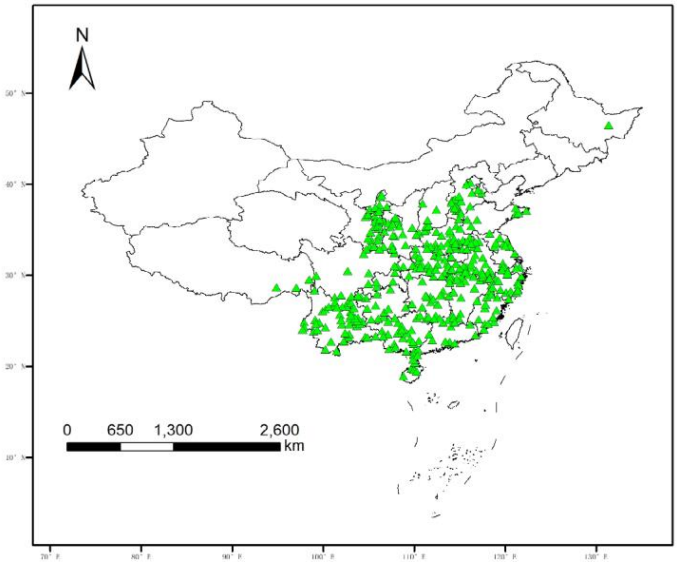

Figure 1. *Geographic distribution of S. frugiperda occurrence in China*

Environmental variables

To evaluate the climatic suitability regionalization of *S. frugiperda* in China, environmental variables that could characterize the ecological requirements of this pest were chosen as initial environmental factors. Data for 19 bioclimatic variables (*Table 1*) were downloaded from the WorldClim database (http://www.worldclim.org/) for current climatic conditions. These data included average, minimum and maximum ambient temperatures as well as precipitation values documented for the interval between 1950 and 2000. For assessing the impact of climate change on the future niche suitability of *S. frugiperda*, four representative CO_2 concentration pathways (RCPs) issued by the Intergovernmental Panel on Climate Change (IPCC) were applied as future climate change scenarios, namely RCP2.6, RCP4.5, RCP6.0 and RCP8.5, which indicate different levels of greenhouse gas emission (Dong and Gao, 2014). The future time intervals in consideration were the 2050s (2041–2060) and 2070s (2061–2080); predicted future environmental data were also obtained from the WorldClim database. All bioclimatic variables under current and future conditions had a spatial resolution of 2.5 arcminutes (about 9 km at the equator).

Environmental data for defining ecological niches

The MaxEnt model (version 3.3.3) applies environmental data and species distribution data to predict future distributions under a maximum entropy scenario. It is open source and available from http://www.cs.princeton.edu/. MaxEnt is an ideal predictive tool for simulating the geographical distribution of species and has spectacular merits (Wang et al., 2019), thus was chosen for application in the present research. The specific operational procedures for MaxEnt are described below.

http://www.aloki.hu ● ISSN 1589 1623 (Print) ● ISSN1785 0037 (Online)
DOI: http://dx.doi.org/10.15666/aeer/1906_45274546

Table 1. *Environmental variables used to predict the distribution of S. frugiperda in China*

Code	Bioclimatic variable	Unit
bio1	Annual Mean Temperature	°C
bio2	Mean Diurnal Range (Mean of monthly (max temp - min temp))	°C
bio3	Isothermality (BIO2/BIO7) (* 100)	-
bio4	Temperature Seasonality (standard deviation *100)	-
bio5	Max Temperature of Warmest Month	°C
bio6	Min Temperature of Coldest Month	°C
bio7	Temperature Annual Range (BIO5-BIO6)	°C
bio8	Mean Temperature of Wettest Quarter	°C
bio9	Mean Temperature of Driest Quarter	°C
bio10	Mean Temperature of Warmest Quarter	°C
bio11	Mean Temperature of Coldest Quarter	°C
bio12	Annual Precipitation	mm
bio13	Precipitation of Wettest Month	mm
bio14	Precipitation of Driest Month	mm
bio15	Precipitation Seasonality (Coefficient of Variation)	-
bio16	Precipitation of Wettest Quarter	mm
bio17	Precipitation of Driest Quarter	mm
bio18	Precipitation of Warmest Quarter	mm
bio19	Precipitation of Coldest Quarter	mm

Abbreviations: -, not applicable

To prevent collinearity between modeling variables influencing the prediction outcomes, the variables were screened in accordance with the following procedure (Wang et al., 2020). First, the initial model was created by importing the occurrence points of *S. frugiperda* and 19 bioclimatic variables into the MaxEnt software. Within the framework of the initial model, the 'Random test percentage' was set as 25, and 'Make pictures of predictions' and 'Do jackknife to determine factor importance' were selected; the other model values were set to default. Then, the percent contribution and permutation contribution of each variable to the initial simulation results were investigated by a Jackknife test to choose the main environmental factors for modeling. To avoid variable spatial autocorrelation, a Pearson correlation analysis was conducted on the filtered variables using SPSS v.22 (SPSS, Inc., Chicago, IL, USA). Based on the percent contribution of each variable in the initial model, bioclimatic variables with correlation coefficients > |0.8| (highly correlated) were filtered. Only one variable from each of such pairs, chosen based upon its relative importance in modeling the *S. frugiperda* distribution and its predictive power (such as percent contribution and jackknife training gain) was chosen for developing the model (Wei et al., 2017). After this screening step, 7 bioclimatic variables were chosen as the potential predictors of *S. frugiperda* habitat suitability, namely Annual Mean Temperature (bio1), Mean Diurnal Range (bio2), Temperature Seasonality (bio4), Max Temperature of Warmest Month (bio5), Precipitation Seasonality (bio15), Precipitation of Warmest Quarter (bio18) and Precipitation of Coldest Quarter (bio19).

http://www.aloki.hu ● ISSN 1589 1623 (Print) ● ISSN1785 0037 (Online)
DOI: http://dx.doi.org/10.15666/aeer/1906_45274546

Distribution modeling

The 7 selected bioclimatic variables, along with occurrence records, were applied to construct the relationship between the potential distribution of *S. frugiperda* and current climate conditions. This was then further processed to project the potential distribution under future climate conditions (Fand et al., 2014). The occurrence points of *S. frugiperda* and the 7 bioclimatic variables were imported into the MaxEnt model to simulate the distribution of *S. frugiperda* in China. In our model, 25% of the distribution points were applied for testing the model and 75% of the points were used for training. Moreover, the response curve for each climatic variable was used to determine the relationship between the probability distribution and the variable, ranging from highest suitability (value of 0) to lowest suitability (value of 1) (Khanum et al., 2013). In the final model, "Random seed" was selected. Model replicates were run 10 times to enhance model performance, and the other model settings were the same as for the initial model. The best model with the highest AUC (Area Under Curve) value was chosen to evaluate the probability distribution (Xu et al., 2019).

The ASCII-formatted file output from the MaxEnt model was imported into ArcGIS and converted into a raster format file using "Conversion Tools", which was used to classify and visualize the distribution region, and the "Extraction" function was used to produce a graphical representation of the distribution across China. Jenks' natural breaks were employed to reclassify the distribution threshold and divide the levels of habitat suitability into four categories: unsuitable area (no risk, $P < 0.10$), marginally suitable area (low risk, $0.10 < P < 0.31$), moderately suitable area (medium risk, $0.31 < P < 0.52$) and highly suitable area (high risk, $P > 0.52$), which were then displayed as different colors (Wang et al., 2018, 2019).

Model evaluation

The receiver operating characteristic curve (ROC) is an effective and widely used tool for assessing the discriminative power of a species distribution model (Wang et al., 2020). The area under a ROC curve (AUC), theoretically varying from 0.5 to 1.0, was taken as a measure of model accuracy, with a value close to 1 indicative of high simulation accuracy (Araujo et al., 2005). Specifically: for a value $0.5 \leq AUC < 0.5$, the assessment criteria suggest prediction failure (fail); $0.6 \leq AUC < 0.7$, poor prediction results (poor); $0.7 \leq AUC < 0.8$, generally fair prediction results (fair); $0.8 \leq AUC < 0.9$, good prediction results (good); and $0.9 \leq AUC < 1$, excellent prediction results (excellent) (Wang et al., 2020). For our model, the AUC values were generally found to be greater than 0.8, suggesting that it is superior to the random model (Swets, 1988).

Results

Screening of the main environmental variables

Based on the principle of climate similarity, MaxEnt is a mathematical model that can be used to investigate the correlation between geographical distribution and environmental factors. Selection of climatic factors is the main determinant for the precision of the results. The percent contribution for each bioclimatic variable on the distribution simulation model was calculated by the knife cutting method (*Table 2*), revealing that Precipitation of Warmest Quarter (bio18) made the largest contribution to the predicted distribution of *S. frugiperda* (43.9%), followed by Temperature Seasonality

http://www.aloki.hu ● ISSN 1589 1623 (Print) ● ISSN1785 0037 (Online)
DOI: http://dx.doi.org/10.15666/aeer/1906_45274546

(bio4), Annual Mean Temperature (bio1) and Precipitation Seasonality (bio15), with 21.1%, 15.6% and 11.6%, respectively. Notably, the variables Mean Diurnal Range (bio2), Precipitation of Coldest Quarter (bio19) and Max Temperature of Warmest Month (bio5) only had slight effects at 5.2%, 1.8% and 0.8%, respectively. Variables which did not show any contribution were removed from our model. Finally, a Pearson correlation coefficient analysis was used to confirm that the extracted variables had no co-correlation with each other (*Table 3*). On this basis, the final model of the habitat suitability of *S. frugiperda* in China was constructed, and the accuracy of the prediction results was assessed.

Table 2. *Relative percentage of bioclimatic factors imported into MaxEnt to predict the current and future distribution of S. frugiperda*

Environmental variable	Percent contribution (%)	Permutation importance (%)
Bio_18	43.9	7.1
Bio_4	21.1	33.8
Bio_1	15.6	39.2
Bio_15	11.6	8.4
Bio_2	5.2	7.0
Bio_19	1.8	1.9
Bio_5	0.8	2.5

Table 3. *Pearson correlation coefficient analysis of selected environmental variables used in the final model*

Variable	bio1	bio2	bio4	bio5	bio15	bio18
bio1						
bio2	-0.572					
bio4	-0.522	0.201				
bio5	0.625	-0.404	0.323			
bio15	-0.449	0.742	0.154	-0.380		
bio18	0.609	-0.370	-0.667	0.030	-0.211	
bio19	0.565	-0.687	-0.132	0.504	-0.782	0.378

Modeling performance

The MaxEnt model can directly draw ROC curves and calculate the AUC value of the model, which can be then used for result validation. The ROC curves of the initial model and the reconstruction model under present climatic conditions are displayed in *Figure 2*. The AUC values for the training data and the test data of the initial model were 0.98 and 0.975, respectively, and the average AUC value of 10 replicates of the reconstruction model was 0.977 (*Figure 2*). *Figure 3* shows the AUC values under future climatic conditions. Curve analysis revealed that the average AUC values of the training data were all higher than 0.978, which was much greater than the AUC value of the random simulation model (0.5), suggesting that the accuracy of the prediction results was "excellent". These results demonstrate that the model can be used for the potential habitat suitability of *S. frugiperda* in China.

http://www.aloki.hu ● ISSN 1589 1623 (Print) ● ISSN1785 0037 (Online)
DOI: http://dx.doi.org/10.15666/aeer/1906_45274546

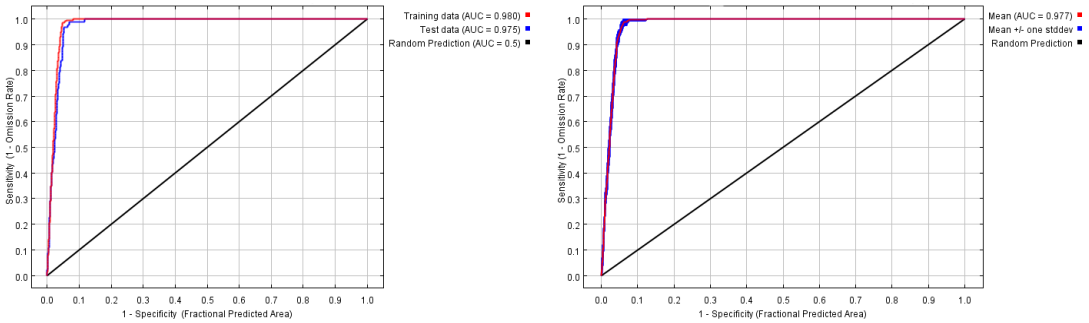

Figure 2. *ROC curve and AUC values for the initial model and the reconstructed model under current climatic conditions*

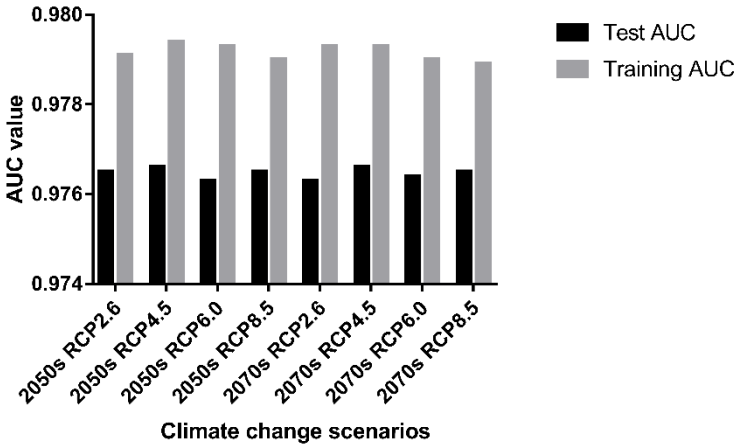

Figure 3. *ROC curves and AUC values of the final model for future scenarios*

Modeled current potential distribution

A graphical representation of the present potential distribution of *S. frugiperda* based on collected occurrence data and environmental variables modeled by the MaxEnt software was created using ArcGIS v10.7 software and is shown in *Figure 4*. The simulation results of the MaxEnt model suggested that the range of suitable habitats of *S. frugiperda* in China was very wide, and that unsuitable regions were mainly located in Qinghai-Tibet Plateau, Xinjiang, Jilin, Inner Mongolia, eastern Heilongjiang, and western Gansu. The highly suitable areas for *S. frugiperda* in China were mainly distributed in Jiangsu, Anhui, Jiangxi, most parts of Henan and Guangxi, central and eastern Hubei, central and southern Shaanxi, southeastern and northern Zhejiang, western Shandong, southern Hebei, northeastern Guizhou, eastern Sichuan, northwestern Hunan, western Chongqing, southeastern Fujian and northern Guangdong, spanning an area of 167.01×10^4 km^2. The moderately suitable areas were mainly concentrated in most parts of Fujian, western and eastern Guangdong, central and northern Yunnan, central and eastern Shandong, central and southeastern Beijing, western Guizhou, northern Hainan, southeastern Hunan, western Hubei, western Hebei, northern Taiwan, and sporadic areas of Zhejiang, spanning an area of 124.13×10^4 km^2. The total highly suitable, moderately suitable, marginally suitable and unsuitable areas comprised 17.6%, 13.08%, 8.88% and 60.43%, respectively, of the total Chinese landmass.

http://www.aloki.hu ● ISSN 1589 1623 (Print) ● ISSN1785 0037 (Online)
DOI: http://dx.doi.org/10.15666/aeer/1906_45274546

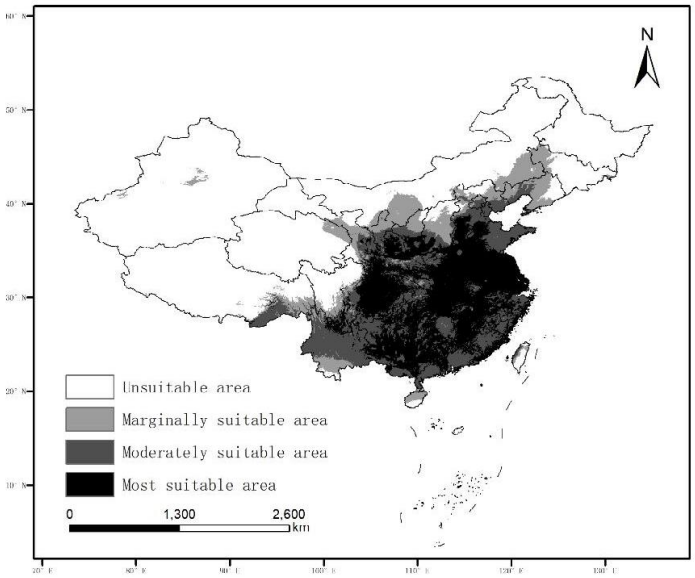

Figure 4. *Probability of the current potential distribution of S. frugiperda in China*

Response curves display the quantitative relationship between a bioclimatic variable and the logistic habitat suitability, helping us to better understand the ecological niche of a species. Responses curves for the effect of 7 bioclimatic variables on *S. frugiperda* are shown in *Figure 5*. Based on this analysis, the most contributing variable to high suitability was a precipitation of 386.41–923.07 mm for bio18. Other climate conditions also displayed a relationship with high probability of presence, namely 7321.84–9928.73 for bio4, 12.04–18.54 ℃ for bio1 and 53.08–92.65 for bio15. The results suggested that the maximum habitat suitability of *S. frugiperda* occurred when Precipitation of Warmest Quarter was 544.93 mm, Temperature Seasonality (standard deviation × 100) was 9064.27, Annual Mean Temperature was 15.26 ℃, Precipitation Seasonality (Coefficient of Variation) was 81.39, Mean Diurnal Range was 7.34 ℃, Precipitation of Coldest Quarter was 189.5 mm and Max Temperature of Warmest Month was 32.48 ℃.

Potential future distribution under different climatic conditions

The predicted distribution of *S. frugiperda* under four representative climate change scenarios for future intervals 2050s and 2070s are illustrated in *Figure 6* and *Table 4*. The results showed significant differences between the current suitable habitat and those predicted for future periods, with the risk-free area narrowing and risk area expanding continuously.

In the 2050s interval, the area of habitat unsuitable for *S. frugiperda* under RCP2.6, RCP4.5, RCP6.0 and RCP8.0 scenarios would reduce by 4.27%, 6.07%, 6.07% and 9.32%, respectively, whereas the marginally suitable area would increase by 17.54%, 12.60%, 6.88% and 12.06%. Moreover, the highly suitable habitats would decrease under RCP2.6 and RCP4.5 by 7.44% and 1.55%, respectively, but increase by 22.08% and 12.82% under RCP6.0 and RCP8.5. Except for the scenario of RCP 6.0, the moderately suitable area of *S. frugiperda* under would increase under the other scenarios, RCP2.6, RCP4.5 and RCP8.0, by 17.85%, 21.55% and 17.60%, respectively (*Table 4*).

http://www.aloki.hu ● ISSN 1589 1623 (Print) ● ISSN1785 0037 (Online)
DOI: http://dx.doi.org/10.15666/aeer/1906_45274546

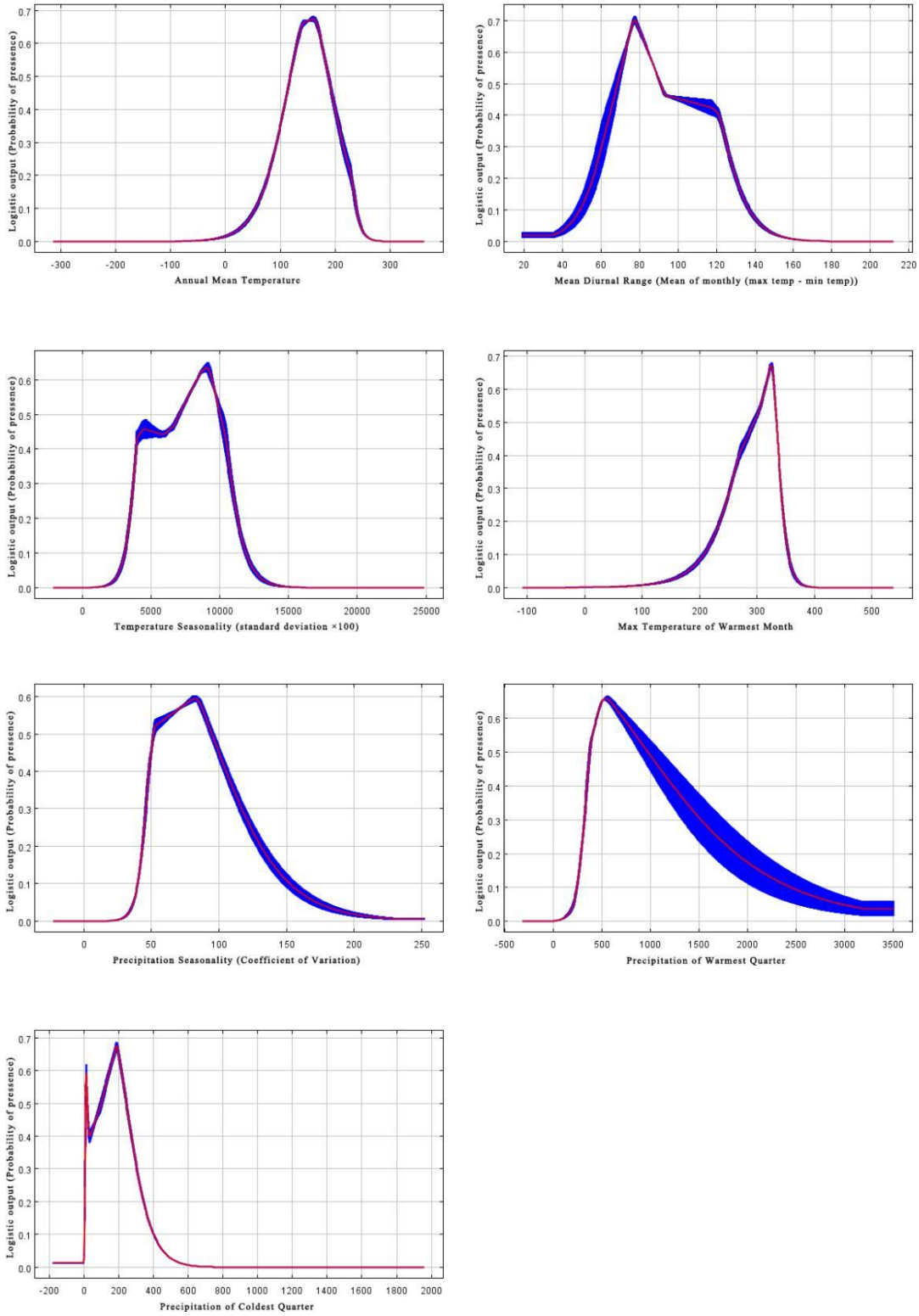

Figure 5. *Response curves of 7 environmental variables showing their relationship with the habitat suitability of S. frugiperda. The red line indicates the mean response and the blue areas are ± SD calculated over 10 replicates*

http://www.aloki.hu ● ISSN 1589 1623 (Print) ● ISSN1785 0037 (Online)
DOI: http://dx.doi.org/10.15666/aeer/1906_45274546

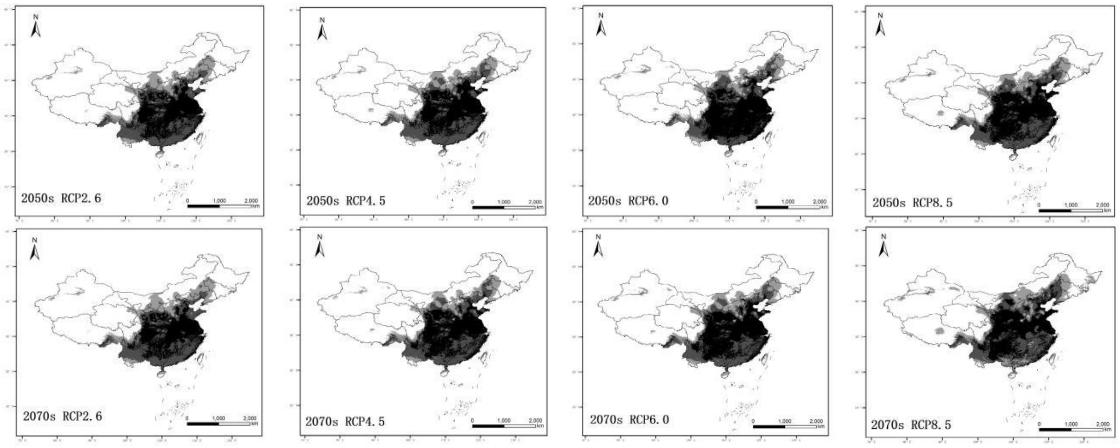

Figure 6. *Potential habitat suitability of S. frugiperda under different climate change scenarios. The white, light gray, dark gray, and black shading represent the unsuitable, marginally suitable, moderately suitable, and highly suitable areas, respectively*

Table 4. *Predicted suitable habitats for S. frugiperda under current and future climatic situations*

		Predicted area ($\times 10^4$ km^2)				Comparison with current distribution (%)			
Period	**Scenario**	**Unsuitable area**	**Marginally suitable area**	**Moderately suitable area**	**Highly suitable area**	**Unsuitable area**	**Marginally suitable area**	**Moderately suitable area**	**Highly suitable area**
Current	-	573.4	84.26	124.13	167.01	-	-	-	-
2050s	RCP2.6	548.89	99.04	146.29	154.58	-4.27	17.54	17.85	-7.44
	RCP4.5	538.62	94.88	150.88	164.42	-6.07	12.60	21.55	-1.55
	RCP6.0	538.6	90.06	116.26	203.88	-6.07	6.88	-6.34	22.08
	RCP8.5	519.98	94.42	145.98	188.42	-9.32	12.06	17.60	12.82
2070s	RCP2.6	551.13	100.71	147.77	149.18	-3.88	19.52	19.04	-10.68
	RCP4.5	492.9	119.46	159.37	177.05	-5.15	7.90	13.64	3.55
	RCP6.0	529.78	96.75	134.41	187.85	-7.61	14.82	8.28	12.48
	RCP8.5	492.91	119.46	159.37	177.05	-14.04	41.78	28.39	6.01

Abbreviations: -, not applicable

In the 2070s, the area of unsuitable habitats would reduce for all scenarios (RCP2.6, RCP4.5, RCP6.0 and RCP8.0) by 3.88%, 5.15%, 7.61% and 14.04%, respectively, while the areas of marginally suitable and moderately suitable habitats would increase by different amounts (*Table 4*). Regarding highly suitable habitats, scenario RCP2.6 resulted in the area reducing by 10.68%, but it would increase for RCP4.5, RCP6.0 and RCP8.5 by 6.01%, 12.48% and 6.01%, respectively.

The transposition pathway of the geometric center of S. frugiperda under future scenarios

To determine the effects of climate change on the habitat suitability of *S. frugiperda*, the spatial analysis function of AcrGIS was used to calculate the position of the geometric

http://www.aloki.hu ● ISSN 1589 1623 (Print) ● ISSN1785 0037 (Online)
DOI: http://dx.doi.org/10.15666/aeer/1906_45274546

center, migration distance and direction of *S. frugiperda* under different climatic scenarios in China. The results are shown in *Figure 7* and elaborated below.

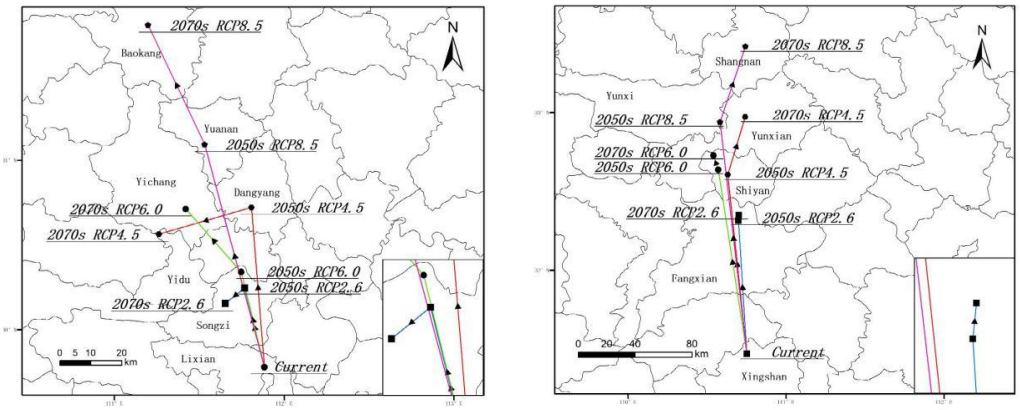

Figure 7. *Trajectory of the geometric center of highly suitable (A) and total suitable (B) areas under different climate change scenarios. "●", "■" and " " indicate the geometric center of suitable areas under each scenario, and "▲" indicates the direction of movement*

Under RCP2.6, the geometric center of highly suitable habitat for *S. frugiperda* will transpose 53.199 km northwest from Lixian (current) to Songzi (2050s), then 14.865 km southwest in Songzi (2070s). For the total suitable areas, the geometric center will move 94.068 km northwest from Xingshan (current) to Fangxian (2050s), then 3.711 km northeast in Fangxian (2070s).

Under RCP4.5, the geometric center of the highly suitable areas will move 105.068 km northwest from Lixian (current) to Dangyang (2050s), then 54.969 km southwest to Yidu (2070s). For total suitable areas, the center will transfer 126.547 km northwest from Xingshan (current) to Shiyan (2050s), then 41.907 km northeast to Yunxian (2070s).

Under RCP6.5, the geometric center of the highly suitable areas will move 63.67 km northwest from Lixian (current) to Songzi (2050s), then 51.899 km northwest to Yichang (2070s). For total suitable areas, center will move 130.762 km northwest from Xingshan (current) to Shiyan (2050s), then 10.422 km northwest in Shiyan (2070s).

Under RCP8.5, the geometric center of the highly suitable areas will move 149.944 km northwest from Lixian (current) to Yuanan (2050s), then 84.65 km northwest to Baokang (2070s). For total suitable areas, the center will move 164.008 km northwest from Xingshan (current) to Yunxi (2050s), then 53.315 km northeast to Shangnan (2070s).

Discussion

Spodoptera frugiperda is an important transboundary migratory insect pest, which has expanded its range to new areas, including China, forcing the Food and Agriculture Organization of the United Nations to issue alerts worldwide. The strain that has recently invaded China is considered the "maize strain" with some heterozygotes and at present threatens more than 50% of the maize crop producing areas in China, leading to huge economic loss and potentially influencing food security (da Silva et al., 2017; Huang et al., 2020). Recently, the Chinese government has launched the "three areas, three belts, and three lines of defense" policies to deal with this notorious pest. With the ever-

http://www.aloki.hu ● ISSN 1589 1623 (Print) ● ISSN1785 0037 (Online)
DOI: http://dx.doi.org/10.15666/aeer/1906_45274546

increasing impact of climate change and its related consequences, a raised incidence of reduced agricultural production and food insecurity are expected, particularly since climate change will negatively affect the agricultural suitability of some areas, enhance the risk of pest infestation, and even alter the distribution of some crops (Kukal and Irmak, 2018; Deutsch et al., 2018). Within this context, assessing the impact of climate change on agricultural production systems will help to mitigate its negative consequences.

From the viewpoint of niche conservation, high accuracy in predicting the geographical distribution of a species can be achieved using local occurrence data for a particular species (Phillips, 2007). However, accurately modeling its simulation results for other areas and predicting the probability of presence in this area is usually unstable. It is not recommended to use occurrence data from one region to project habitat suitability in another; therefore, for the present research, we used data relating solely to *S. frugiperda* in China.

In the present study, we used a MaxEnt model combined with ArcGIS to understand the effects of climate change on areas potentially suitable for *S. frugiperda* at a national level. Furthermore, we investigated how these changes could influence the geometric center of this pest at two different time points, the 2050s and 2070s, and under four different climate change scenarios. ROC curves were applied to estimate the accuracy of the prediction of the MaxEnt model; the results showed high AUC values, confirming excellent model performance. Seven bioclimatic variables were then selected as predictors in the reconstructed MaxEnt model. bio18 (Precipitation of Warmest Quarter) was found to have the strongest effect on the potential distribution of this pest and contributed more to the simulation than other variables (*Table 2*). Notably, the impact of precipitation on habitat suitability for *S. frugiperda* has already been documented. For instance, Du Plessis et al. (2018) mapped the habitat suitability of this pest and suggested that precipitation and irrigation scenarios were important factors in the distribution of *S. frugiperda*. Moreover, Day et al. (2017) reported that precipitation in the wettest month and the mean temperature of coldest quarter were important variables in the diffusion of this pest in Africa. Rainfall can directly and indirectly influence the distribution of *S. frugiperda*, with both positive and negative consequences. That is, precipitation can contribute to the proliferation of host plants, an important habitat and food resource, thereby generating favorable conditions for the *S. frugiperda* population; meanwhile, precipitation and irrigation can drown or wash them away, reducing their population (Nboyine et al., 2020). Additionally, Early et al. (2018) found that precipitation had a negative influence on the larvae of *S. frugiperda*, with fewer adult moths captured and the peaks of moth population were postponed during the dry season (Andrews, 1988).

Previous studies have also shown temperature to be a key environmental variable, influencing the development, reproduction and distribution of *S. frugiperda* (Hogg et al., 1982). Valdez-Torres et al. (2012) reported that the highest and lowest temperature thresholds for the growth of *S. frugiperda* under laboratory conditions were 39.8 and 8.7 ℃, respectively. In the present study, the existence probability of *S. frugiperda* was found to be higher when the mean annual temperature (bio1) was between 12.0 and 18.5 ℃, which is within the aforementioned temperature range. However, it is inconsistent with another previous study which suggested that the suitable mean annual temperature ranged from 19 to 23 ℃ (Wang et al., 2020). This difference is likely due to the difference in geographical location of the sample points and environmental factors in establishing the prediction model. In South and East China, which are considered highly and moderately suitable areas for *S. frugiperda*, the annual average temperature was about

http://www.aloki.hu ● ISSN 1589 1623 (Print) ● ISSN1785 0037 (Online)
DOI: http://dx.doi.org/10.15666/aeer/1906_45274546

15–18 ℃ (data from China Meteorological Administration), characterized by higher winter temperatures and a short duration of low temperature, which are good climatic conditions for the persistence of this pest. Hence, it was inferred that this pest could reproduce all year round in these areas and thus it may become the central location from which *S. frugiperda* can spread to other parts of China, such as the Yangtze River Basin and North China. Within a certain temperature range, the development rate of insects has been found to increase with increasing climatic temperature but reduces beyond a certain threshold (Wang et al., 2020). Similarly, a previous study indicated that the growth rate of *S. frugiperda* increases linearly with increasing temperature between the range of 18-30 ℃ (Du Plessis et al., 2018). Furthermore, based on the response curve of bio5, the occurrence probability of *S. frugiperda* reduced sharply when temperatures exceeded 32.5 ℃, indicating that a high temperature in the warmest quarter may be an important factor restricting the habitat suitability of this pest.

In summary, the occurrence and prevalence of *S. frugiperda* are closely associated with climatic conditions, such as temperature and rainfall (Ramirez-Cabral et al., 2017). This is supported by research in Africa by Cokola et al. (2020), who found that the incidence of *S. frugiperda* in South Kivu Province, DC Congo was also related to temperature and rainfall. However, the habitat suitability of *S. frugiperda* may be affected by other non-climatic factors, such as host plants, natural enemies, human activities, land use, soil traits and management intervention levels (Hijmans et al., 2005; Biber-Freudenberger et al., 2016). In a paper by Liu et al. (2020), the authors noted that land-use was more important than climate in regulating the distribution of *S. frugiperda*, according to the resource concentration hypothesis (Root, 1973). Whether these factors can exert a significant effect on the accuracy of our simulation results deserves to be investigated.

The results of the present study highlight the potential for climate change to increase the spread of pests. As conditions become more favorable for pest species, their ability to expand and damage crops grows, as elaborated by examples worldwide (Deutsch et al., 2018). Our future simulations were performed under four different CO_2 concentration pathways, whereby RCP2.6 represents the most optimistic scenario, RCP8.5 represents the most pessimistic, and RCP4.5 and RCP6.0 in between (IPCC, 2007). Our study confirmed that the total area of suitable habitats increased in line with the severity of greenhouse gases emissions (to different extents). This, therefore, indicates that climate change could extend the potential distribution of *S. frugiperda*, which is consistent with previous studies (Early et al., 2018). The alteration in habitat suitability caused by climate change could be explained by the biological traits of insects. Since they are temperature-sensitive, and have a strong spread ability, short life-cycles, and strong reproductive capacity, even slight alterations in temperature have the potential to bring about significant changes in abundance and distribution (Ayres and Lombardero, 2000). However, climate change has also been documented to have other impacts on insects, such as directly influencing their life history traits or indirectly through their natural enemies and hosts plants (Patterson et al., 1999; Bale et al., 2002), resulting in changes to the suitability of a particular insect for a given habitat. Ramirez-Cabral et al. (2017) has suggested that the low-risk area would increase 40% by 2050 and 23% by 2100 but medium- and high-risk areas would in fact reduce more than 50% by 2050 and more than 39% by 2100, compared with the present risk. As such, they concluded that that future climate scenarios (A2 Special Report on Emissions Scenarios, SRES) would result in a reduction of risk for *S. frugiperda* outbreaks (Ramirez-Cabral et al., 2017). However,

http://www.aloki.hu ● ISSN 1589 1623 (Print) ● ISSN1785 0037 (Online)
DOI: http://dx.doi.org/10.15666/aeer/1906_45274546

unlike in the present study, the authors used two general circulation models (GCM) including CRIRO MK3.0 and MIROC-H under the scenario of A2 SRES.

Additionally, the results of the present study highlighted that *S. frugiperda* is highly likely to migrate northward in China. The geometric center of both highly and total suitable areas was found to move northwards under all four climate scenarios. This can be clearly explained by the fact that polyphagous insects, such as *S. frugiperda*, are able to transfer to more favorable areas as conditions change (Kennedy and Storer, 2000). Therefore, rapid cross-region communication and collaboration in China will be key to effective management, especially in regions that are climatically low- or unsuitable for *S. frugiperda*. At present, *S. frugiperda* is a seasonal pest in most parts of China, and the warmer weather may enable this pest to persevere over a longer period, as highlighted by the future simulations (Xie et al., 2021). Furthermore, *S. frugiperda* may benefit from climate change since polyphagous insects are more adaptable to a changing environment due to their genotypic and phenotypic plasticity, and may even feed on lower-quality hosts when preferred hosts are unavailable (Bale et al., 2002). Moreover, climate change may accelerate the northward migration of multivoltine insects to higher and medium latitudes (Altermatt, 2010). Thus, those areas currently designated as either low- or unsuitable may ultimately become suitable for *S. frugiperda*. From another point of view, pest outbreaks and their risks, under future climate situations, may be more difficult to model due to enhanced climate variability and extreme climate events. Of note, the strong flight ability of adult *S. frugiperda* is yet another of their adaptative characteristics that enables them to translocate long distances (29.14 km/day in China, Ge et al., 2019), a key factor that has promoted the expansion of this pest. However, its ability in long-distance migration is only partly to blame and research has indicated that the movement of infested agricultural commodities also promoted its migration between regions (Wang et al., 2020). For example, Faulkner et al. (2017) speculated that the rapid diffusion of this pest throughout Africa was aided by intra-continental transportation links. Within China, this feature may make it more challenging to suppress outbreaks of *S. frugiperda* by managing any single location. Therefore, efforts need to be coordinated across areas and country borders.

The host plants of *S. frugiperda* are diverse, with major hosts extensively distributed around the world. Thus, the host plant may not be a significant factor in restricting their distribution. Currently, *S. frugiperda* can be divided into two haplotypes, namely maize strain and rice strain. Rice-strain *S. frugiperda* feed on rice and various pastures, whilst the maize-strain (which recently invaded China) feeds mainly on maize, sorghum and cotton (Dumas et al., 2015). In China, maize is one of the major grain crops, and is widely cultivated and distributed in the hilly maize area of South and Southwest China, irrigation maize area of Northwest China, spring maize area of East and North China, summer maize area of Huanghuaihai Plain, and maize area of Qinghai-Tibet Plateau (He and Zhou, 2011, 2012), with several of these production areas overlapping with the moderately and highly suitable areas for *S. frugiperda* in our results. At present, there has been little study into the differing climate tolerances between rice- and maize-strain *S. frugiperda* and there is insufficient information on their respective habitat suitability to model their distribution individually. At present, the two strains appear to substantially overlap in their distributions, thus we inferred that any difference in climate tolerance was unlikely to exert a significant influence on their geographic distribution, but has the potential affect their abundance. As such, further research is needed. According to previous records, no *S. frugiperda* have been detected in Qinghai-Tibet Plateau, Xinjiang,

http://www.aloki.hu ● ISSN 1589 1623 (Print) ● ISSN1785 0037 (Online)
DOI: http://dx.doi.org/10.15666/aeer/1906_45274546

Jilin, Heilongjiang or Gansu, which were identified as unsuitable areas for the pest. However, this does not imply that these areas will not be severely affected and can be ignored, given the ability of *S. frugiperda* to migrate long distances.

Finally, it is important to acknowledge some constraints with the present research. First, we only used climatic factors and did not investigate the effect of other biotic or abiotic factors which could significantly affect species distribution, such as host plant, natural enemies, land use or the application of pesticide and fertilizer, etc. Secondly, MaxEnt, as an occurrence-background approach, cannot adequately illustrate the spatial deviation of presence records (Shabani et al., 2019), and only evaluates the relative habitat suitability irrespective of how the background sample is specified (Guillera-Arroita et al., 2014).

Conclusion

Native to the Americas, *S. frugiperda* is one of the most economically destructive crop pests that has recently invaded both Asia and Africa. In general, pest management within agricultural systems may become more difficult under future climate change scenarios, particularly in terms of its variability. Understanding the effect of climate change on the habitat of this pest and responding with timely management measures are therefore essential to protect future crop production. The results of the present study show that the high-risk area is mainly distributed in Jiangsu, Anhui, Jiangxi, most parts of Henan and Guangxi, central and eastern Hubei, central and southern Shaanxi, southeastern and northern Zhejiang, western Shandong, southern Hebei, northeastern Guizhou, eastern Sichuan, northwestern Hunan, western Chongqing, southeastern Fujian and northern Guangdong, covering a total area of 167.01×10^4 km^2. From the present to the 2070s, the area of highly and moderately suitable areas will increase, with the distribution expanding toward northern China as the climate warms. The ROC curve test performed in the present study offers reliable evidence that the MaxEnt model is highly accurate in predicting the potential distribution of *S. frugiperda* in China. Moreover, the key environmental factors regulating the habitat suitability of this pest were Precipitation of Warmest Quarter, Temperature Seasonality, Annual Mean Temperature and Precipitation Seasonality.

As a next step, we recommend the use of ensembles of ecological niche models such as MaxEnt, Climex, BIOCLIM and GARP to estimate the future habitat suitability of *S. frugiperda*, its host plants and natural enemies in China, and integrate their interaction into the model simulation process. With this information, crop growers, the agricultural sector and policy makers could develop adaptation strategies, such as new techniques, new pest-resistant crop varieties and control practices, to overcome the climate change-induced effects of *S. frugiperda* on economically important crops. Further work is needed at a regional level to understand the factors affecting the development and life history traits of this pest.

Acknowledgements. This research was financially supported by Innovation and Entrepreneurship Training Program for College Students of Fujian Province (202110397033), Advanced Talents Introduction Project of Wuyi University (YJ201910), Education and Scientific Research Project for Young and Middle-aged Teachers in Fujian Province (JAT190801, JAT190805), Science & Technology Innovation Platform Construction Project of Fujian Province (2018N2004) and Scientific Research Team Jointly Build By Teachers and Students of Wuyi University (20200701-20230630).

http://www.aloki.hu ● ISSN 1589 1623 (Print) ● ISSN1785 0037 (Online)
DOI: http://dx.doi.org/10.15666/aeer/1906_45274546

Author Contributions. PC, FM: conceived and designed the experiments. YS, YP, QW, SL: collected the sample data. FM, YS, YP, QW, SL, CM, YH, DH and LL: performed the experiments. FM: carried out the data analysis. PC: drafted the manuscript.

Conflict of interests. The authors declare that they have no competing interests.

REFERENCES

[1] Altermatt, F. (2010): Climatic warming increases voltinism in European butterflies and moths. – Proceedings of the Royal Society B: Biological Sciences 277: 1281-1287.
[2] Andrews, K. L. (1988): Latin American research on *Spodoptera frugiperda* (Lepidoptera: Noctuidae). – Florida Entomologist 71: 630-653.
[3] Araujo, M. B., Pearson, R. G., Thuiller, W., Erhard, M. (2005): Validation of species–climate impact models under climate change. – Global Change Biology 11: 1504-1513.
[4] Ayres, M. P., Lombardero, M. J. (2000): Assessing the consequences of global change for forest disturbance from herbivores and pathogens. – Science of the Total Environment 262: 263-286.
[5] Bale, J. S., Masters, G. J., Hodkinson, I. D., Awmack, C., Bezemer, T. M., Brown, V. K., Butterfield, J., Buse, A., Coulson, J. C., Farrar, J., Good, J. E. G., Harrington, R., Hartley, S., Jones, T. H., Lindroth, R. L., Press, M. C., Symrnioudis, I., Watt, A. D., Whittaker, J. B. (2002): Herbivory in global climate change research: direct effects of rising temperature on insect herbivores. – Global Change Biology 8: 1-16.
[6] Baloch, M. N., Fan, J., Haseeb, M., Zhang, R. (2020): Mapping potential distribution of *Spodoptera frugiperda* (Lepidoptera: Noctuidae) in central Asia. – Insects 11(11): 1-10.
[7] Battisti, A., Stastny, M., Netherer, S., Robinet, C., Schopf, A., Roques, A., Larsson, S. (2005): Expansion of geographic range in the pine processionary moth caused by increased winter temperatures. – Journal of Applied Ecology 15: 2084-2096.
[8] Biber-Freudenberger, L., Ziemacki, J., Tonnang, H. E. Z., Borgemeister, C. (2016): Future risks of pest species under changing climatic conditions. – PLoS ONE 11(4): e0153237.
[9] Brito, J. C., Acosta, A. L., Alvares, F., Cuzin, F. (2009): Biogeography and conservation of taxa from remote regions: an application of ecological-niche based models and GIS to North-African Canids. – Biological Conservation 142: 3020-3029.
[10] Celine, B., Cleo, B., Paul, L., Wilfried, T., Franck, C. (2012): Impacts of climate change on the future of biodiversity. – Ecology Letters 15(4): 365-377.
[11] Center for Agriculture and Bioscience International. Datasheet. *Spodoptera frugiperda* (fall armyworm). (2016): Invasive Species Compendium. – Available online: http://www.cabi.orglisc/datasheet129810 (accessed on 5 June 2020).
[12] Cokola, M. C., Yannick, M., Noel, G., Espoir, B., David, B., Chuma, G., Adrien, B., Francis, F. (2020): Bioclimatic zonation and potential distribution of *Spodoptera frugiperda* (Lepidoptera: Noctuidae) in South Kivu Province, DR Congo. – BMC Ecology 20(66): 1-13.
[13] Da Silva, D. M., de Freitas Bueno, A., Andrade, K., dos Santos Stecca, C., Neves, P. M. O. J., de Oliveira, M. C. N. (2017): Biology and nutrition of *Spodoptera frugiperda* (Lepidoptera: Noctuidae) fed on different food sources. – Scientia Agricola 74: 18-31.
[14] Day, R., Abrahams, P., Bateman, M., Beale, T., Clottey, V., Cock, M., Colmenarez, Y., Corniani, N., Early, R., Godwin, J., Gomez, J., González-Moreno, P., Murphy, S. T., Oppong-Mensah, B., Phiri, N., Pratt, C., Silvestri, S., Witt, A. (2017): Fall Armyworm: impacts and implications for Africa. – Outlook Pest Management 28: 196-201.
[15] Deutsch, C. A., Tewksbury, J. J., Tigchelaar, M., Battisti, D. S., Merrill, S. C., Huey, R. B., Naylor R. L. (2018): Increase in crop losses to insect pests in a warming climate. – Science 361(6405): 916-919.

http://www.aloki.hu ● ISSN 1589 1623 (Print) ● ISSN1785 0037 (Online)
DOI: http://dx.doi.org/10.15666/aeer/1906_45274546

[16] Dong, S. Y., Gao, X. J. (2014): Long-term climate change: interpretation of IPCC fifth assessment report. – Progressus Inquisitiones de Mutatione Climatis 10: 56-59.
[17] Du Plessis, H., Van den Berg, J., Ota, N., Kriticos, D. J. (2018): *Spodoptera frugiperda*. – CSIRO - InSTePP Pest Geog: 1-7.
[18] Dumas, P., Legeai, F., Lemaitre, C., Scaon, E., Orsucci, M., Labadie, K., Gimenez, S., Clamens, A. L., Henri, H., Vavre, F., Aury, J. M., Fournier, P., Kergoat, G. J., d'Alençon, E. (2015): *Spodoptera frugiperda* (Lepidoptera: Noctuidae) host-plant variants: two host strains or two distinct species? – Genetica 143(3): 305-316.
[19] Early, R., González-Moreno, P., Murphy, S. T., Day, R. (2018): Forecasting the global extent of invasion of the cereal pest *Spodoptera frugiperda*, the fall armyworm. – NeoBiota 40: 25-50.
[20] Ekesi, S., Meyer, M. D., Mohamed, S. A., Virgilio, M., Borgemeister, C. (2016): Taxonomy, ecology, and management of native and exotic fruit fly species in Africa. – Annual Review of Entomology 61(1): 219-238.
[21] Elith, J., Graham, C. H., Anderson, R. P., Dudík, M., Ferrier, S., Guisan, A., Hijmans, R. J., Huettmann, F., Leathwick, J. R., Lehmann, A. (2006): Novel methods improve prediction of species' distributions from occurrence data. – Ecography 29: 129-151.
[22] Faccoli, M. (2009): Effect of weather on Ipstypographus (Coleoptera: Curculionidae) phenology, voltinism, and associated spruce mortality in the southeastern Alps. – Environment Entomology 38: 307-316.
[23] Fan, J., Wu, P., Tian, T., Ren, Q., Zhang, R. (2020): Potential distribution and niche differentiation of *Spodoptera frugiperda* in Africa. – Insects 11: 383.
[24] Fand, B. B., Kumar, M., Kamble, A. L. (2014): Predicting the potential geographic distribution of cotton mealybug *Phenacoccus solenopsis* (Hemiptera: Pseudococcidae) in India based on MAXENT ecological niche model. – Journal Environment Biology 35(5): 973-982.
[25] Faulkner, K. T., Hurley, B. P., Robertson, M. P., Rouget, M., Wilson, J. R. (2017): The balance of trade in alien species between South Africa and the rest of Africa. – Bothalia - African Biodiversity & Conservation 47(2): 1-16.
[26] Ge, S. S., He, L. M., He, W., Xu, R. B., Sun, X. T., Wu, K. M. (2019): Determination on moth flight capacity of *Spodoptera frugiperda*. – Plant Protection 45(4): 28-33.
[27] Guillera-Arroita, G., Lahoz-Monfort, J. J., Elith, J. (2014): Maxent is not a presence–absence method: a comment on Thibaud et al. – Methods in Ecology & Evolution 5(11): 1192-1197.
[28] He, Q. J., Zhou, G. S. (2011): Climatic suitability of potential summer maize planting zones in China. – Acta Geograph Sinica 66(11): 1443-1450.
[29] He, Q. J., Zhou, G. S. (2012): Climatic suitability of potential spring maize cultivation distribution in China. – Acta Ecologica Sinica 32(12): 3931-3939.
[30] Hijmans, R. J., Cameron, S. E., Parra, J. L., Jones, P. G., Jarvis, A. (2005): Very high resolution interpolated climate surfaces for global land areas. – International Journal of Climatology 25: 1965-78.
[31] Hogg, D. B., Pitre, H. N., Anderson, R. E. (1982): Assessment of early-season phenology of the fall armyworm (Lepidoptera: Noctuidae) in Mississippi. – Environment Entomology 11: 705-10.
[32] Huang, Y. R., Dong, Y. Y., Huang, W. J., Ren, B. Y., Deng, Q. Y., Shi, Y., Bai, J., Ren, Y., Geng, Y., Ma, H. Q. (2020): Overwintering distribution of fall armyworm (*Spodoptera frugiperda*) in Yunnan, China, and influencing environmental factors. – Insects 11(11): 805.
[33] IPCC (2007): Climate change 2007: the physical science basis. contribution of working group i to the fourth assessment report of the intergovernmental panel on climate change. – Avaibale on http://www.ipcc.ch/publications_and_data/publications ipcc_fourth assessment_report_wg1_report_the_physical_science_basis.htm.

http://www.aloki.hu ● ISSN 1589 1623 (Print) ● ISSN1785 0037 (Online)
DOI: http://dx.doi.org/10.15666/aeer/1906_45274546

[34] Jiang, D., Chen, S., Hao, M. M., Fu, J. Y., Ding, F. Y. (2018): Mapping the potential global codling moth (*Cydia pomonella* L.) distribution based on a machine learning method. – Scientifc Reports 8: 13093.
[35] Kennedy, G. G., Storer, N. P. (2000): Life systems of polyphagous arthropod pests in temporally unstable cropping systems. – Annual Review of Entomology 45: 467-493.
[36] Khanum, R., Mumtaz, A., Kumar, S. (2013): Predicting impacts of climate change on medicinal asclepiads of Pakistan using Maxent modeling. – Acta Oecologica 49: 23-31.
[37] Kukal, M. S., Irmak, S. (2018): Climate-driven crop yield and yield variability and climate change impacts on the U.S. Great Plains agricultural production. – Scientific Reports 8: 3450.
[38] Kyrre, K., Bjorn, O., Olav, S., Jean, C. G., Nadir, E., Nils, C. S. (2012): Population dynamics in changing environments: the case of an eruptive forest pest species. – Biological Reviews 87(1): 34-51.
[39] Li, G. Q., Liu, C. C., Liu, Y. G., Yang, J., Zhang, X. S., Guo, K. (2013): Advances in theoretical issues of species distribution models. – Acta Ecologica Sinica 33: 4827-4835.
[40] Li, Z. H., Qin, Y. J. (2018): Review on the quantitative assessment models for pest risk analysis and their comparison. – Plant Protection 44: 134-145.
[41] Liu, T., Wang, J., Hu, X., Feng, J. (2020): Land-use change drives present and future distributions of fall army worm, *Spodoptera frugiperda* (J. E. Smith) (Lepidoptera: Noctuidae). – The Science of Total Environment 706: 135872.
[42] Massin, M. B., Rome, Q., Muller, F., Perrard, A., Villemant, C., Jiguet, F. (2012): Climate change increases the risk of invasion by the yellow-legged hornet. – Biological Conservation 157: 4-10.
[43] Montezano, D. G., Specht, A., Sosa-Gomez, D. R., Roque-Specht, V. F., Sousa-Silva, J. C., Paula-Moraes, S. V., Peterson, J. A., Hunt, T. E. (2018): Host plants of *Spodoptera frugiperda* (Lepidoptera: Noctuidae) in the Americas. – African Entomology 26(2): 286e301.
[44] Nagoshi, R. N. (2019): Evidence that a major subpopulation of fall armyworm found in the Western Hemisphere is rare or absent in Africa, which may limit the range of crops at risk of infestation. – PLoS ONE 14: e0208966.
[45] National Agro-Tech Axtension and Service Center (2020): Occurrence trend of *Spodoptera frugiperda* in maize grassland on autumn. – https://www.natesc.org.cn/ (accessed on 3 September 2020).
[46] Nboyine, J. A., Kusi, F., Abudulai, M., Badii, B. K., Zakaria, M., Adu, G. B., Haruna, A., Seidu, A., Osei, V., Alhassan, S., Yahaya, A. (2020): A new pest, *Spodoptera frugiperda* (J.E. Smith), in tropical Africa: Its seasonal dynamics and damage in maize fields in northern Ghana. – Crop Protection 127: 104960.
[47] Patterson, D. T., Westbrook, J. K., Joyce, R. J. V., Lingren, P. D., Rogasik, J. (1999): Weeds, insects, and diseases. – Climatic Change 43: 711-27.
[48] Phillips, S. J. (2007): A Brief Tutorial on Maxent. – http://biodiversityinformatics.amnh.org/open_source/maxent/.
[49] Ramirez-Cabral, N. Y. Z., Kumar, L., Shabani, F. (2017): Future climate scenarios project a decrease in the risk of fall armyworm outbreaks. – The Journal of Agricultural 155(8): 1219-1238.
[50] Root, R. B. (1973): Organization of a plant–arthropod association in simple and diverse habitats: fauna of collards (*Brassica oleracea*). – Ecological Monographs 43: 95-120.
[51] Roy, H. E., De Clercq, P., Handley, L. J. L., Poland, R. L., Sloggett, J. J., Wajnberg, E. (2011): Alien arthropod predators and parasitoids: an ecological approach. – BioControl 56: 375-382.
[52] Shabani, F., Ahmadi, M., Peters, K. J., Haberle, S., Champreux, A., Saltre, F., Bradshaw, C. J. A. (2019): Climate-driven shifts in the distribution of koala-browse species from the Last Interglacial to the near future. – Ecography 42(9): 1587-1599.

http://www.aloki.hu ● ISSN 1589 1623 (Print) ● ISSN1785 0037 (Online)
DOI: http://dx.doi.org/10.15666/aeer/1906_45274546

[53] Simberloff, D., Martin, J. L., Genovesi, P., Maris, V., Wardle, D. A., Aronson, J., Courchamp, F., Galil, B., Garcia-Berthou, E., Pascal, M., Pysek, P., Sousa, R., Tabacchi, E., Vila, M. (2003): Impacts of biological invasions: what's what and the way forward. – Trends in Ecology and Evolution 28: 58-66.

[54] Swets, J. A. (1988): Measuring the accuracy of diagnostic systems. – Science 240: 1285-1293.

[55] Tobin, P. C., Nagarkatti, S., Loeb, G., Saunders, M. C. (2008): Historical and projected interactions between climate change and insect voltinism in a multivoltine species. – Global Change Biology 14: 951-957.

[56] Valdez-Torres, J. B., Soto-Landeros, F., Osuna-Enciso, T., Baez-Sanudo, M. A. (2012): Phenological prediction models for white corn (*Zea mays* L.) and fall armyworm (*Spodoptera frugiperda* J.E. Smith). – Agrociencia 46(4): 399-410.

[57] Venette, R. C., Kriticos, D. J., Magarey, R. D., Koch, F. H., Baker, R. H. A., Worner, S. P., Raboteaux, N. N. G., McKenney, D. W., Dobesberger, E. J., Yemshanov, D., Barro, P. J. D., Hutchison, W. D., Fowler, G., Kalaris, T. M., Pedlar, J. (2010): Pest risk maps for invasive alien species: A roadmap for improvement. – Bioscience 60: 349-362.

[58] Wang, R. L., Li, Q., Feng, C. H., Shi, C. P. (2017): Predicting potential ecological distribution of *Locusta migratoria tibetensis* in China using maxent ecological niche modeling. – Acta Ecologica Sinica 37(24): 8556-8566.

[59] Wang, R. L., Li, Q., He, S. S., Liu, Y., Wang, M. T., Jiang, G. (2018): Modeling and mapping the current and future distribution of *Pseudomonas syringae pv. actinidiae* under climate change in China. – PloS ONE 13: e0192153.

[60] Wang, R. L., Yang, H., Luo, W., Wang, M. T., Lu, X. L., Huang, T. T., Li, Q. (2019): Predicting the potential distribution of the Asian citrus psyllid, *Diaphorina citri* (Kuwayama), in China using the MaxEnt model. – PeerJ 7: e7323.

[61] Wang, R., Jiang, C., Guo, X., Chen, D., You, C., Zhang, Y., Wang, M., Li, Q. (2020): Potential distribution of *Spodoptera frugiperda* (J. E. Smith) in China and the major factors influencing distribution. – Global Ecology Conservation 21: e00865.

[62] Wei, J., Zhang, H., Zhao, W., Zhao, Q. (2017): Niche shifts and the potential distribution of *Phenacoccus solenopsis* (Hemiptera: Pseudococcidae) under climate change. – PLoS ONE 12(7): e0180913.

[63] Xie, D. J., Tang, J. H., Zhang, L., Cheng, Y. X., Jiang, X. F. (2021): Annual generation numbers prediction and division of fall armyworm, *Spodoptera frugiperda* in China. – Plant Protection 47(01): 61-67, 116.

[64] Xu, D. P., Wang, R. L., Ye, M., Pu, B. (2019): Modeling the distribution of *Zanthoxylum armatum* in China with MaxEnt modeling. – Global Ecology Conservation 19: e00691.

[65] Zacarias, D. A. (2020): Global bioclimatic suitability for the fall armyworm, *Spodoptera frugiperda* (Lepidoptera: Noctuidae), and potential co-occurrence with major host crops under climate change scenarios. – Climatic Change 161: 555-566.

[66] Zhang, Q., Zhao, L., He, P., Zheng, K. M., Wu, P. X., Fan, J. Y. (2020): The potential distribution analysis and economic loss assessment of *Spodoptera frugiperda* (Smith) in Qujing, Yunnan Province. – Journal of Yunnan University: Natural Sciences Edition 42(06): 1224-1229.

[67] Zhu, G. P., Liu, G. Q., Pu, W. J., Gao, B. Y. (2013): Ecological niche modeling and its applications in biodiversity conservation. – Biodiversity Science 21(1): 90-98.

http://www.aloki.hu ● ISSN 1589 1623 (Print) ● ISSN1785 0037 (Online)
DOI: http://dx.doi.org/10.15666/aeer/1906_45274546

ASSESSMENT OF INUNDATION AREA AND WATER LEVEL OF THE TONLE SAP LAKE USING MULTI-SOURCE REMOTE SENSING DATA BETWEEN 2008 AND 2018

YAN, Y.[1#] – HUANG, Y. Y.[2#] – ZHAO, Y. J.[1*] – TONG, K.[1] – LIANG, Y. L.[3]

[1]*Key Laboratory of Environment Change and Resources Use in Beibu Gulf, Nanning Normal University, Ministry of Education, Nanning 530001, China*
(phone: +86-132-9781-2623)

[2]*Natural Resources Information Center of Nanning, Nanning 530021, China*
(phone: +86-189-7882-9392)

[3]*School of Geography and Planning, Nanning Normal University, Nanning 530001, China*
(phone: +86-187-7675-6017)

**Corresponding author*
e-mail: yinjunzhao@nnnu.edu.cn; phone: +86-152-7713-3597

[#]*These authors contributed equally to this work*

(Received 11th Jun 2021; accepted 4th Sep 2021)

Abstract. As the largest freshwater lake located in the most controversial transboundary river in Asia, the Tonle Sap Lake is one of the most productive ecosystems in the world. However, uncertainty remains because of the inability to measure nonlinear inundation dynamics in remote lakes at fine spatial and temporal resolutions, let along the water levels. This research attempted to explore the reliability of radar altimetry data to detect the inland water level of inundation areas, like that of Tonle Sap Lake over the past decade. The results indicated that the Jason-2 and Jason-3 radar altimetry data were able to retrieve water level with high accuracy (R^2 = 0.9232 and confidence coefficient of 98%), and the composite index was proven to be the optimal method to identify inundation area of the Tonle Sap Lake compared to the single-band threshold method and modified normalized difference water index by applying Moderate Resolution Imaging Spectroradiometer Surface Reflectance products MOD09A1. The fluctuation trend of inundation area and water level were basically consistent with the precipitation, presenting a distinct lagging relationship. More important was the truth that the downstream water level had poor correlation with the upstream runoff both in flood period and non-flood periods (R^2 = 0.0542 and 0.2873, $p < 0.01$), which indicated that the upstream explorations over Lancang-Mekong River had little effects on the downstream water volume.
Keywords: *composite index, Jason-2 and Jason-3 radar altimetry, lagging relationship, variation tendency, flood pulse*

Introduction

As the most significant transnational river flowing through China, Laos, Burma, Thailand, Cambodia and Vietnam, the Lancang-Mekong River is also one of the most controversial transboundary rivers in the world. It contains the world's largest inland fishery and nourishes about a quarter of a billion people that lived in the river basin (Hecht et al., 2019). The river runs for approximately 4800 km and as it originates from the Qinghai-Tibet Plateau, so the elevation drop reaches up to 5000 m which makes it an abundant hydropower resource (Zhang et al., 2020). As a consequence, the exploitation of the river has led to international conflicts because different stakeholders competed for the allocation and utilization over the shared water resource (Li et al.,

http://www.aloki.hu ● ISSN 1589 1623 (Print) ● ISSN 1785 0037 (Online)
DOI: http://dx.doi.org/10.15666/aeer/1906_45474566

2019a). Especially the conflicts happened among upstream and downstream countries, which have attracted the attention of international community for a long time.

The Tonle Sap Lake, which is the largest freshwater lake and boundary lake of Lancang-Mekong River basin, is considered as the "heart of the Lower Mekong" due to the exceptional biodiversity and is also one of the most productive ecosystems in the world. It is a globally unique lake-floodplain system for its seasonal bi-directional hydrological characteristics, with the water inflows from Mekong River in rainy season and outflows during the dry season recurrently (Arias et al., 2014). So the water levels of Tonle Sap Lake vary from an average depth of less than 2 m in the dry season to over 10 m in the flood season being linked to the annual flood pulse governed by the flow of the Mekong River (Oeurng et al., 2019). Accordingly, the inundation area also varies significantly in both short-term (weeks to months) and long-term (years) scales (Kummu et al., 2014). Adding to this complexity is the rapid population growth, agricultural expansion and hydropower construction in the Mekong River basin (Arias et al., 2012; Larnberts and Koponen, 2008). Therefore, monitoring the current status of flood inundation and water levels in time and space accurately is important for local water resource management, ecological conservation and hydrological processes.

Whilst the regional significance of Tonle Sap Lake is undisputed, uncertainty remains because of an inability to measure or model nonlinear inundation dynamics in remote basins (for the vast and inaccessible nature of the Tonle Sap Lake) at fine spatial and temporal resolutions, let alone the water levels. The greatest challenge in addressing the problem is the lack of long-term in situ observation data, especially in transboundary basins where the data are not always shared publicly (Gleason and Hamdan, 2017). Remote sensing observations offer a unique opportunity to continuously monitor the large floodplain, although they could not replace in situ observations (Jahanbakhsh et al., 2017; Tangdamrongsub et al., 2016).

Abundant satellite images generated by various sensor types including visible/infrared (Amani et al., 2017; Schneider and Hook, 2010), SAR (Synthetic Aperture Radar) (Ding and Li, 2011; Millard and Richardson, 2013) are available for investigating inland water bodies. The free Landsat images which have a relatively high spatial resolution were extensively applied (Pekel et al., 2016). However, they are limited by the rather long 16 days repeat cycle and the frequent occurrence of cloud coverage. As microwave remote sensing data, SAR are able to detect the ground objects without been affected by clouds (Schlaffer et al., 2015). But as most SAR images are generated by commercial satellites, the researches were hindered by the data availability. And some free SAR data like Sentinel-1 are just available since 2014, which only cover a short span of time. In contrast, MODIS (Moderate Resolution Imaging Spectroradiometer) dataset with high-frequency measurements and medium resolution was particularly suitable to address both short- and long-term changes in inundation areas of moderate and large lakes (Feng et al., 2012). Previous studies have determined spatio-temporal flooding extent by applying a threshold approach to land surface reflectance, or spectral indexes from the MODIS image (Chen et al., 2013). A number of spectral indices have been explored including the Normalized Difference Vegetation Index (NDVI), Enhanced Vegetation Index (EVI), Land Surface Water Index (LSWI) and Normalized Difference Water Index (NDWI) and so on (Fan et al., 2020; Fayne et al., 2017). The results indicated that various derived indices presented different accuracy in regard to their ability to identify the inundation area (Kwak, 2017). In consequence, it is essential that the diverse indices must be evaluated on a case-by-

http://www.aloki.hu ● ISSN 1589 1623 (Print) ● ISSN 1785 0037 (Online)
DOI: http://dx.doi.org/10.15666/aeer/1906_45474566

case basis to determine the optimal method for further application, especially for the Tonle Sap Lake with periodic flooding.

Moreover, to better understand the hydrology of large river systems, information about the dynamics of inundation pattern alone is not sufficient, the water levels are also required. The satellite altimetry, which could provide long-term and repeated measurements nearly globally and operate under different weather conditions, was proved to be an effective technique to monitor inland water bodies although it was routinely monitor sea level changes over the global open ocean (Dubey et al., 2015). A number of past, present and planned satellite altimetry missions, such as European Remote Sensing (ERS-1/2) (1991-2000, 1995-2002), ENVIronmental SATellite (ENVISAT) (2002-2010), TOPEX/Poseidon(T/P) (1992-), JASON-1/2/3 (2001- , 2008-2016, 2016-present respectively) and CryoSat-2 (2010-present), are capable of monitoring inland water levels with different accuracy and space-time resolutions (Boergens et al., 2019; Breda et al., 2019; Maillard et al., 2015). However, the time span of these satellites varies considerably due to their launch time and working life, on account of which the application of long-term monitoring was confined.

Thanks to the uninterrupted succession of TOPEX/Poseidon, the Jason-1, Jason-2 and Jason-3 missions are on the same orbit (Kuo et al., 2015; Maiwald et al., 2016). The main advantages of using these continuous data records are not only the three missions on the same orbit comes from the "calibration phases", but also with same 10 days of orbit recurrence period which provide the highest temporal resolution (Huang et al., 2018). The consistently operating and short-repeat times make it possible to monitor both long-term and short-term water levels as they have been validated to have good data quality with accuracy on the order of decimeter (Wang et al., 2019). Although pioneering studies have attempted to document the changes of inland water levels (Biancamaria et al., 2018; Li et al., 2019b), the universality of the data for medium lakes and the usefulness of continuous altimetry techniques to retrieve water levels in Tonle Sap Lake are still need to be further explored. This study attempted to provide a comprehensive assessment of the variations of the inundation area as well as to explore water levels in the Tonle Sap Lake over the past decade, using various data sets delivered by remote sensing satellites.

Materials and methods

Study area

The Tonle Sap Lake is the largest freshwater lake in the Lancang-Mekong River basin and it is also the largest lake in Southeast Asia. The entire basin area is 85800 km^2, accounting for 11% of the total drainage area (*Fig. 1*). It provides favorable irrigation conditions for the thousands of farmlands in the ambient plain areas, and its fishery supports the livelihood and nutrition of millions of people in Cambodia (Hecht et al., 2019). The aquatic biodiversity of the Tonle Sap Lake has been listed as a World Biosphere Reserve by UNESCO (United Nations Educational, Scientific and Culture Organization).

Driven by the Asian monsoon, the Tonle Sap Lake presents distinct seasonal changes in precipitation varied from 1000 to 1500 mm between the dry and rainy season. It plays an important role as a natural regulator in the hydrological environment of Mekong Delta, because excessive water inflows to the lake during the rainy season (May to

http://www.aloki.hu ● ISSN 1589 1623 (Print) ● ISSN 1785 0037 (Online)
DOI: http://dx.doi.org/10.15666/aeer/1906_45474566

October) and discharge to the lower area during the dry season (November to April) with up to 8000 m^3/s out from the lake (Arias et al., 2014).

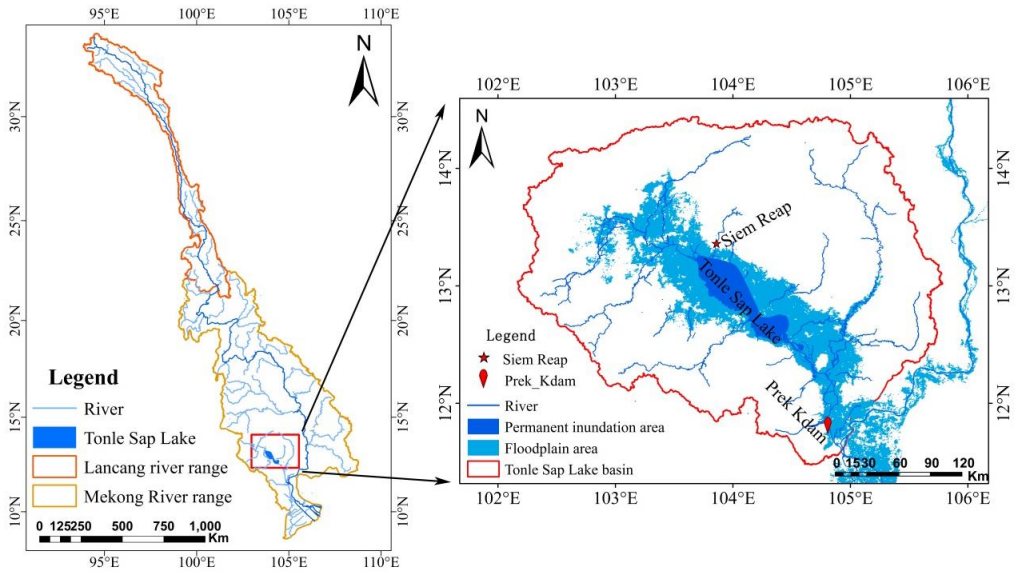

Figure 1. *Location of the Tonle Sap Lake*

This unique phenomenon causes the lake expands from 2500 km^2 to over 16000 km^2 and the water levels varies from less than 2 m in the dry season to more than 10 m in the rainy season. About 53.50% of the annual flow comes from the Mekong River and 12.50% from the precipitation (Kummu et al., 2014).

Data source

MODIS products

Launched as part of National Aeronautics and Space Administration (NASA)'s Earth Observation Sensor mission, MODIS is a multispectral instrument carried on two polar-orbiting satellites, Terra and Aqua. The MODIS surface reflectance product MOD09A1 with Bands 1-7 and spatial resolution of 500 m from 2008-2018 were selected (https://modis.gsfc.nasa.gov/) to extract the inundation area of Tonle Sap Lake. This product is obtained by combining the best surface reflectance data of every pixel acquired during an eight-day period and selecting pixels of the highest quality based on a combination of low view angle, the absence of clouds or cloud shadow, and aerosol loading. There are two scene images, h27v07 and h28v07, covering the study area with sinusoidal projection. The original images were processed to ensure a whole image per month that fitting the study area.

Radar altimetry data

As T/P-family altimeters provided continuous measurements with a time interval of 10 days and resolution of 20 Hz, Jason-2 (July 2008 - September 2016) and Jason-3 (February 2016 - August 2018) were selected in the study. To generate time series dataset of lake water levels, the geophysical data records (GDRs) from the Archiving,

http://www.aloki.hu ● ISSN 1589 1623 (Print) ● ISSN 1785 0037 (Online)
DOI: http://dx.doi.org/10.15666/aeer/1906_45474566

Validation and Interpretation of Satellite Oceanographic (AVISO) (https://www.aviso.altimetry.fr/) were acquired, which contained orbit heights, raw range measurements and geophysical corrections. As shown in *Figure 2*, there is one ground track of Jason family satellites passing over the Tonle Sap Lake.

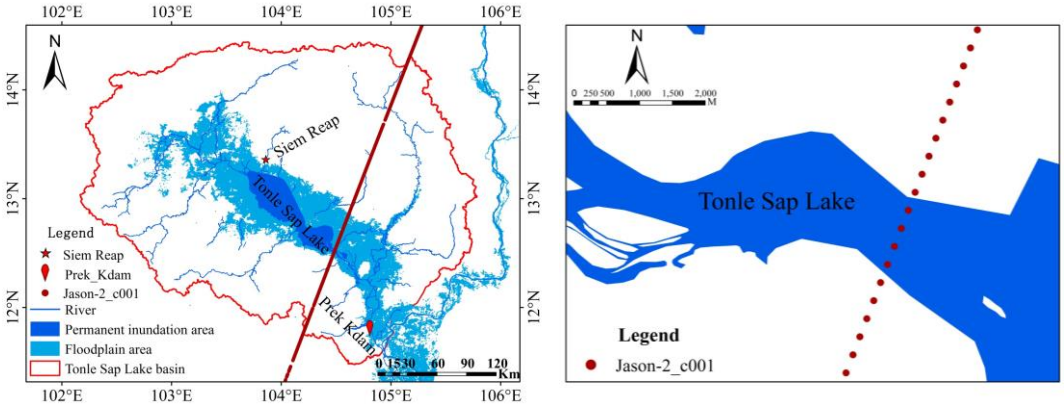

Figure 2. *The orbit of Jason-2 at the exit of the Tonle Sap Lake*

Daily precipitation data of TRMM 3B42

The Tropical Rainfall Measuring Mission (TRMM) is jointly mission of NASA and the Japan Aerospace Exploration Agency. The 3B42V7 is product of TRMM Multi-satellite Precipitation Analysis (TMPA) that takes input from several passive microwave sensors and has already been ground validated with the rain gauge data. The TRMM 3B42V7 Level 3 Product was provided by the Goddard Data Distribution Center of NASA (https://mirador.gsfc.nasa.gov/) with spatial resolution of 0.25° × 0.25° in gridded format. The daily precipitation data from 2008 to 2018 was composited in Arcgis10.6 software to obtain monthly precipitation data and annual precipitation data.

Meteorological data

The Mekong River Commission's official website (MRC) is the only intergovernmental organization that works directly with the governments of Cambodia, the Lao People's Democratic Republic, Thailand and Vietnam to manage the water resources and sustainable development of the Mekong River. The water level data of the Prek Kdam hydrological station from 2008 to 2018 (http://ffw.mrcmekong.org/reportflood.php) was obtained from the MRC, which was published by the Cambodian Meteorological Bureau, also including wind speed, wind direction, solar radiation, sunshine time, relative humidity, evaporation, temperature, pressure, flow and precipitation. The precipitation data from 2009 to 2018 of Siem Reap where the city Tonle Sap Lake located was obtained from the Word Weather website (https://www.worldweatheronline.com).

Methods

Inundation area extraction

As Tonle Sap Lake is featured with seasonal variation, three types of approaches were applied to extract the inundation area and the optimal method was determined.

http://www.aloki.hu ● ISSN 1589 1623 (Print) ● ISSN 1785 0037 (Online)
DOI: http://dx.doi.org/10.15666/aeer/1906_45474566

1. Single-band threshold method based on water body boundary

The spectral response in the short-wave infrared is mainly dominated by water absorption bands, which was proved to be directly sensitive to soil and vegetation moisture content (Frappart et al., 2018). The reflectance in the short-wave infrared is assumed to be zero for water surface, so it is well suited to distinguish water from other ground objects. As short-wave infrared band of MOD09A1 surface reflectance data is the sixth band, so this approach is defined as *Equation 1*.

$$\rho_{band6} < t \quad \text{(Eq.1)}$$

where ρ_{band6} refers to the surface reflectance value in the short-wave infrared band of MOD09A1 (1628-1652 nm, band 6), t is the threshold that segment the water and other ground objects. When the reflectance value below t, it will be defined as water body.

2. Composite index

Besides the above mentioned short-wave infrared band, the near infrared band is also sensitive to the surface object, especially the water and soil/vegetation. The reflectance in near infrared is low over water surface and high over vegetation, which is valuable to generate the efficient indices. This approach is based on the enhanced vegetation index (EVI), the land surface water index (LSWI) and the difference value between EVI (*Eq. 2*) and LSWI (DVEL) (*Eqs.3–4*), which was proved to be effective in quantifying the surface water extent (Normandin et al., 2018). The equations are as follows:

$$EVI = 2.5 \times (Band_{NIR} - Band_{Red}) / (Band_{NIR} + Band_{Red} \times 6 - Band_{Blue} \times 7.5 + 1) \quad \text{(Eq.2)}$$

$$LSWI = (Band_{NIR} - Band_{SWIR}) / (Band_{NIR} + Band_{SWIR}) \quad \text{(Eq.3)}$$

$$DVEL = EVI - LSWI \quad \text{(Eq.4)}$$

where for MODIS, $Band_{Red}$, $Band_{NIR}$, $Band_{Blue}$ and $Band_{SWIR}$ refer to surface reflectance value of band 1 (621-670 nm), band 2 (841-875 nm), band 3 (459-479 nm) and band 6 (1628-1652 nm) respectively. The water body was extracted when the threshold range was EVI < 0.3 and DVEL < 0.05.

3. Modified normalized difference water index

The modified normalized difference water index (MNDWI) was developed by replacing the near infrared band used in normalized difference water index (NDWI) with the shortwave infrared band, since the water body was proved to have stronger absorbability in the shortwave infrared band than in the near infrared band. And a number of peer research works have turned out that MNDWI could extract water body with greater accuracy than NDWI (Du et al., 2016; Li et al., 2013). The MNDWI was defined as *Equation 5:*

$$MNDWI = (Band_{Green} - Band_{SWIR}) / (Band_{Green} + Band_{SWIR}) \quad \text{(Eq.5)}$$

where $Band_{Green}$ refer to the surface reflectance value in the green band (545-565 nm, band 4) and $Band_{SWIR}$ is the reflectance in the short-wave infrared band (1628-1652 nm,

http://www.aloki.hu ● ISSN 1589 1623 (Print) ● ISSN 1785 0037 (Online)
DOI: http://dx.doi.org/10.15666/aeer/1906_45474566

band 6). The optimal threshold to segment water body is 0. When the reflectance greater than 0, the pixel was defined as water body.

Water level extraction

The altimeter measures water level by transmitting radar pulse to lake's surface and measuring the vertical distance between the satellite and the lake surface. The lake level is the difference between the satellite's ellipsoidal height and the range (*Eq. 6*).

$$H = H_{alt} - H_{ran} - H_{hei} - \Delta H_{cor} - 0.71 \quad \text{(Eq.6)}$$

where H is the corrected orthometric height; H_{alt} represents the satellite altitude with respect to reference ellipsoid, H_{ran} is the satellite measure range, H_{hei} refers to the height of geodetic datum to the reference ellipsoid, ΔH_{cor} represents the correction parameter and 0.71 is the vertical offset of the Topex ellipsoid to the WGS84 ellipsoid. H_{alt}, H_{ran} and H_{hei} were given by the downloaded GDRs with the file name of alt_20hz, ice_range_20hz_ku, geoid respectively.

The correction parameter ΔH_{cor} generally includes the range and geophysical corrections over the inland water bodies. For range correction, there are dry tropospheric correction, wet tropospheric correction and ionospheric correction. The geophysical corrections include earth tide and the pole tide corrections. The corrections are provided using mathematical formulas (*Eq. 7*):

$$\Delta H_{co} = I_{iono} + D_{dry} + W_{wet} + P_{pt} + S_{et} \quad \text{(Eq.7)}$$

where I_{iono}, D_{dry} and W_{wet} are the ionospheric correction, the dry tropospheric correction and the wet troposphere correction respectively and P_{pt} and S_{et} are the pole tide and earth tide correction respectively. All the parameters were offered by the GDRs files.

Differences between heights at individual spots and the mean height were computed based the above preliminary results. The heights with continuous sequence number and differences less than 0.3 m were retained as the most valid data. And a new mean height was computed from the outlier-free heights, which represent the height of the pass. All the data were processed in BRAT (Basic Radar Altimetry Toolbox) software (https://www.aviso.altimetry.fr/en/data/tools.html), which was provided by the official website of AVISO.

Mann–Kendall trend analysis

The Mann–Kendall rank correlation test is a nonparametric statistical test method, which was developed to test the non-linear trend and turning point. It has the advantage of not requiring a sample to obey a certain distribution, nor interfering with a few outliers, which is more suitable for typed variables and ordinal variables. When the test statistic $|Z| > Z1-\alpha/2$, it represents that the time series data has a significant ascending or descending trend at the confidence level α, and vice versa, the trend change is not significant. When the normalized statistic Z is positive, it indicates that the variables in the time series show an upward trend, with the negative values indicating a downward trend. When the absolute value of Z is equal or greater than 1.28, 1.64 or 2.32, demonstrating the significance tests were passed at the confidence coefficient of 90%, 95%, and 99% respectively.

http://www.aloki.hu ● ISSN 1589 1623 (Print) ● ISSN 1785 0037 (Online)
DOI: http://dx.doi.org/10.15666/aeer/1906_45474566

Results

Comparison of the inundation area

The inundation area of the Tonle Sap Lake in 2008-2018 was extracted by single-band threshold method, composite index and MNDWI respectively. Generally, the results of the three methods have presented similar variation trend and strong correlations (*Table 1*).

Table 1. *The correlation of three methods and measured water level*

Methods	Single-band threshold method	Composite index	MNDWI	Measured water level
Single-band threshold method	1	0.979	0.940	0.900
Composite index	0.979	1	0.964	0.929
MNDWI	0.940	0.964	1	0.900

The inundation area extracted by single-band threshold method was close to the composite index, while the result of MNDWI was obviously lower than the two methods, especially during the rainy season (*Fig. 3*). For example, the inundation area in September 2009 extracted by single-band threshold method, composite index and MNDWI was 17306.77 km^2, 18497.44 km^2 and 10131.21 km^2 respectively. However, the results of the three methods were close to each other in the dry season. The area of Tonle Sap Lake in rainy season is approximate six times larger than the dry season. In recent decade, the maximum inundation area of Tonle Sap Lake extended 5.9, 5.5 and 3.6 times extracted by the single-band threshold method, composite index and MNDWI respectively.

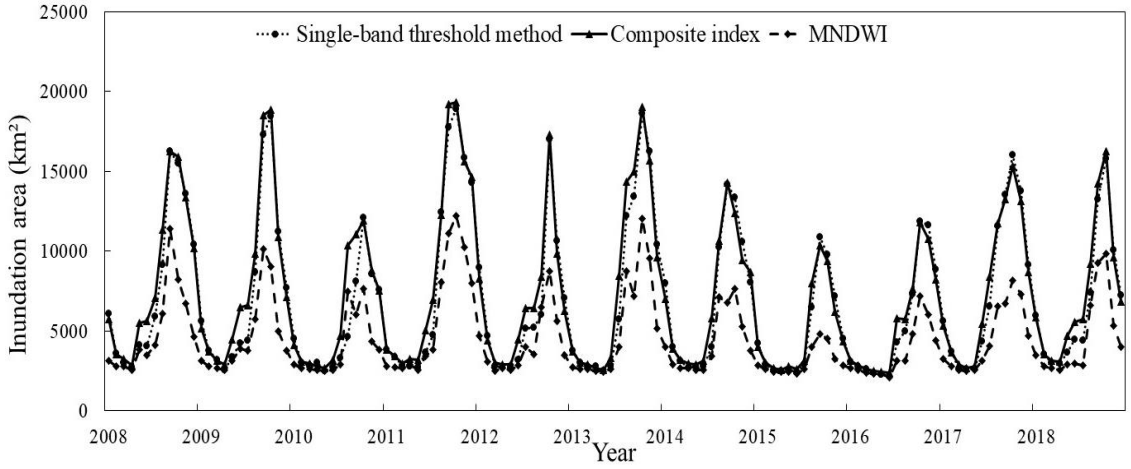

Figure 3. *Inundation area of Tonle Sap Lake from January 2008 to December 2018 with three methods*

The advantages and disadvantages of the three methods were quite different as can be observed from the spatial distribution of the extracted inundation area (*Fig. 4*). The composite index was able to extract water bodies with smaller area, such as the channel of Tonle River in the dry season (*Fig. 4a*), while the other two methods were incapable

http://www.aloki.hu ● ISSN 1589 1623 (Print) ● ISSN 1785 0037 (Online)
DOI: http://dx.doi.org/10.15666/aeer/1906_45474566

of identify the smaller water area. This could because the composite method combined the EVI and the LSWI, and the difference between them enhances the contrast between water and background objects, which made it better to distinguish the water body and extract with mixed pixels (Frappart et al., 2018; Normandin et al., 2018). The MNDWI enhanced the contrast between the water body and the building, which greatly reduced the confounding effect of ground buildings (Du et al., 2016). It was more appropriate to identify water body with clear boundaries. Although single-band threshold method was easy to implement and was insusceptible to the quality of the images, it had problem to distinguish the water body within mixed pixels.

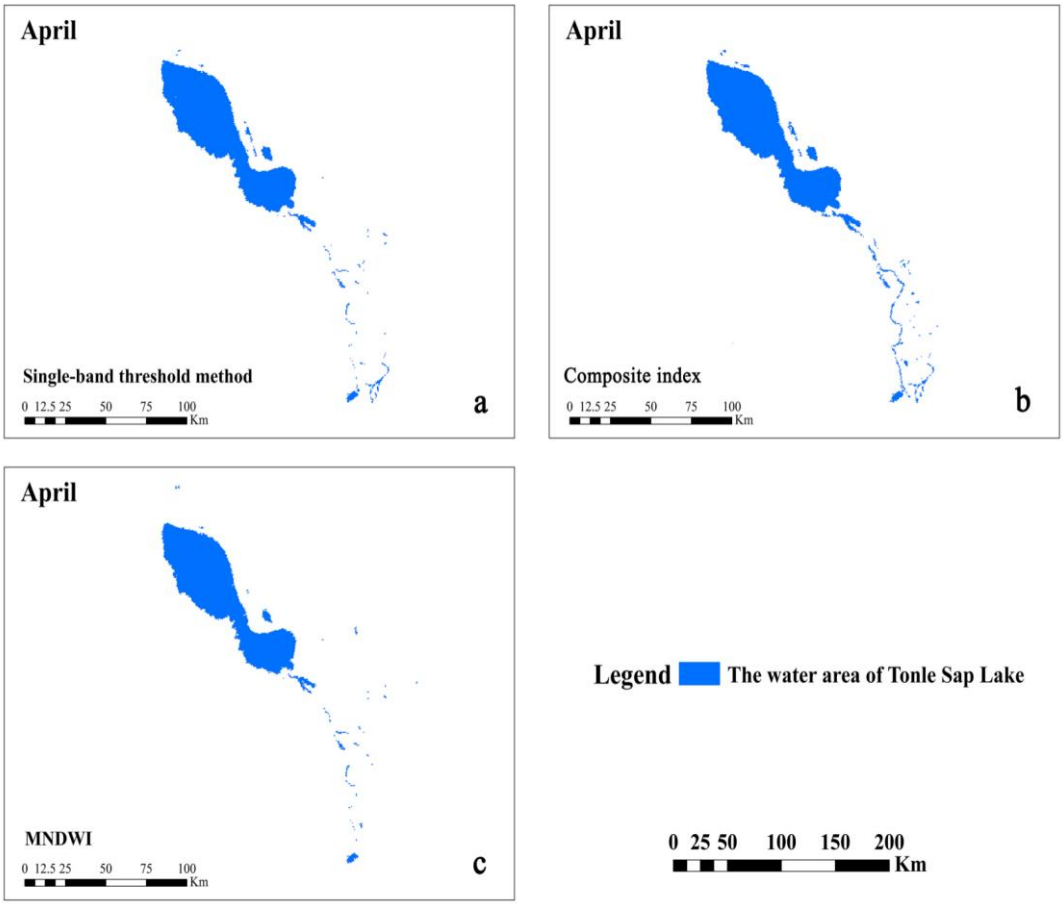

Figure 4. *Comparison of spatial distribution of water body in the Tonle Sap Lake*

Therefore, the composite index was the optimal method to identify the inundation area of the Tonle Sap Lake, followed by the single-band threshold method and MNDWI, in the case of the same spatial resolution.

Accuracy of altimetry water level

The data of the Prek Kdam hydrological station was downloaded from the official website of the MRC and was used as the measured data of the water level of the Tonle Sap Lake. The site is located on the Tonle Sap River, about 86 km away from the location where Jason-2 and Jason-3 radar altimeter monitored. Therefore, there were differences between measured data and satellite results due to gaps of the height datum,

http://www.aloki.hu ● ISSN 1589 1623 (Print) ● ISSN 1785 0037 (Online)
DOI: http://dx.doi.org/10.15666/aeer/1906_45474566

terrain and observation time. And as only part of the data was published to the public, about 100 measured water levels from 2008 to 2018 were obtained to verify the altimeter data. Compared to the in situ measured water levels, the water levels observed by Jason-2 and Jason-3 radar altimetry were a little bit higher (*Fig. 5*). Although there were differences between the two datasets, the variation trend was similar and extreme values were generally appeared in the same period of time.

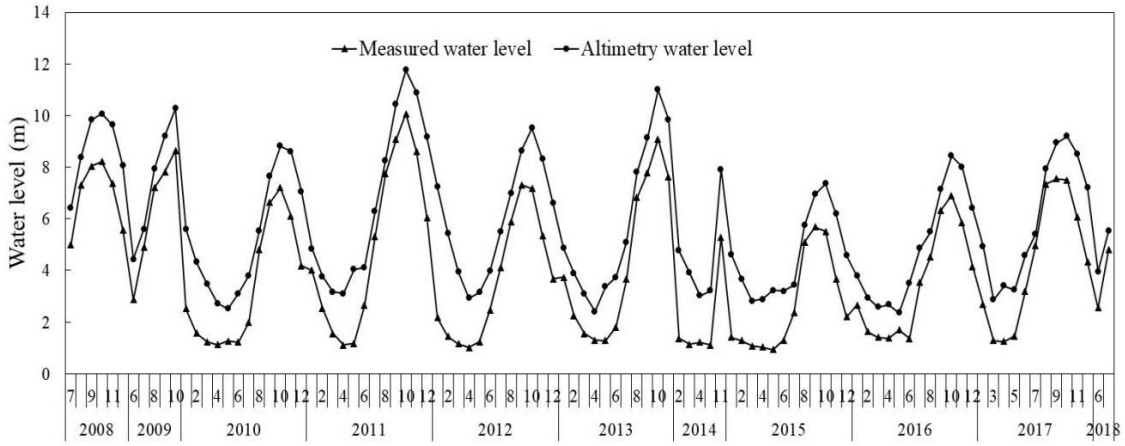

Figure 5. *Comparison of altimetry water level and measured water level in 2008-2018*

Linear correlation analysis indicated a significant positive correlation between measured water levels and the water levels observed by Jason-2 and Jason-3 radar altimetry with $R^2 = 0.9232$ and confidence coefficient of 98% (*Fig. 6*). It was demonstrated that the Jason-2 and Jason-3 radar altimetry data were reliable to detect the inland water level like Tonle Sap Lake with high accuracy.

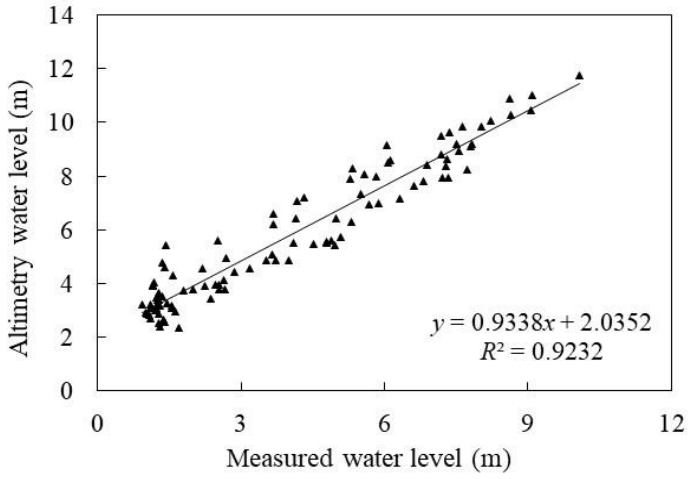

Figure 6. *Scatter plot of the altimetry water level and the measured water level*

Changing trend of inundation area and water level

Linear tendency estimation, moving average and Mann-Kendall trend analysis were applied to analyze the changing trend of inundation area and water level. The slope rates

http://www.aloki.hu ● ISSN 1589 1623 (Print) ● ISSN 1785 0037 (Online)
DOI: http://dx.doi.org/10.15666/aeer/1906_45474566

of linear equation for inundation area and water level were -151.96 and -0.11, with both of them presented decline trend. As well as the 3-year sliding average, the inundation area and water level appeared decreasing tendency with fairy fluctuation from 2008 to 2018 (*Fig. 7*).

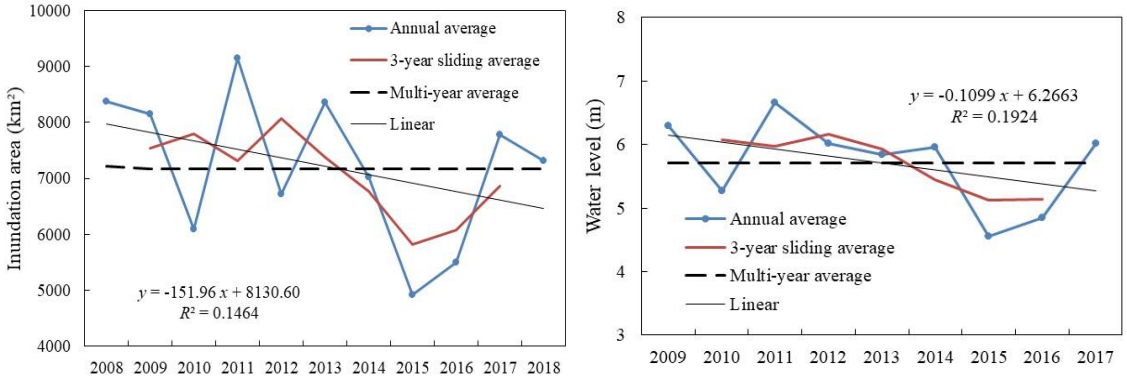

Figure 7. *Linear tendency and moving average of inundation area and water level in the study area*

The Z values of Mann-Kendall were -1.09 and -0.8 for inundation area and water level respectively, and both the absolute values were less than 1.96, which indicated that both the inundation area and water level shown the decline trend. In consequence, the inundation area of the Tonle Sap Lake shrinking gradually and the water level declined in the past decade.

Discussion

Variation of inundation area

As can be observed from the spatial distribution of the inundation area of the Tonle Sap Lake, the large inundation area was generally distributed along with the north and south tributaries, where the Ramsar wetland and Tonle Sap Biosphere Reserve located, and then expanded to northwest part (*Fig. 8*). This was consistent with the results of previous studies carried out by Kummu et al., which documented that the floods in the Tonle Sap Lake mostly occurred in the western part of the lake (Kummu et al., 2014).

The variation trend of the inundation area was similar on annual scale, but varied within the year with seasonal cycle (*Fig. 9*). The minimum inundation area always appeared in April or May, while the maximum area generally turned up during September and November. The characteristics were accordance with finding from previous studies (Arias et al., 2012, 2014). In the rainy season, followed by the increasing precipitation, the water level of the mainstream of Mekong River increased which forcing the water flows to Tonle Sap Lake through Tonle Sap River and resulting the inundation area expanded promptly. When the dry seasons came and the precipitation decreased, the water in Tonle Sap Lake flowed back to replenish the Mekong River and nourished the Mekong Delta. This was obvious in the northwestern part of the lake, where the inundation area decreased dramatically.

http://www.aloki.hu ● ISSN 1589 1623 (Print) ● ISSN 1785 0037 (Online)
DOI: http://dx.doi.org/10.15666/aeer/1906_45474566

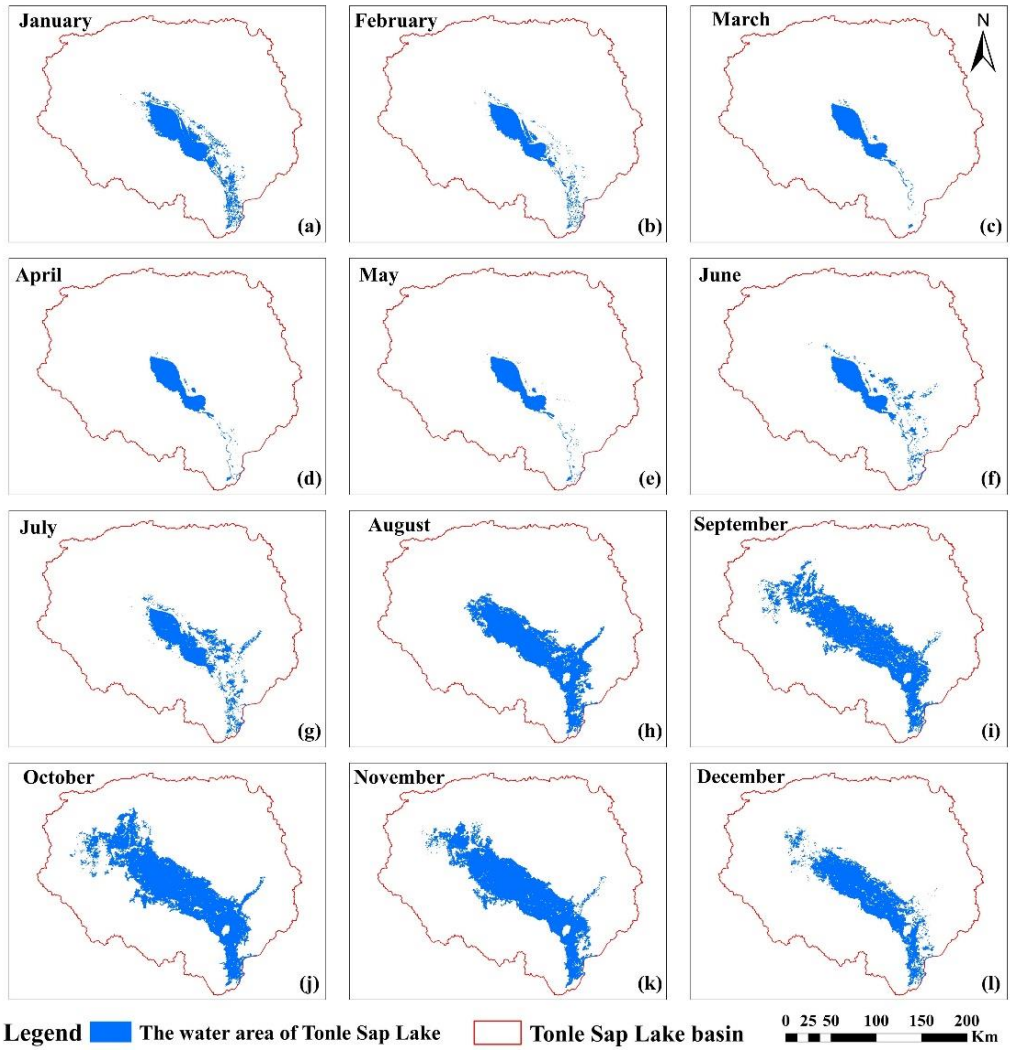

Figure 8. *Spatial distribution of inundation area in the Tonle Sap Lake in 2017*

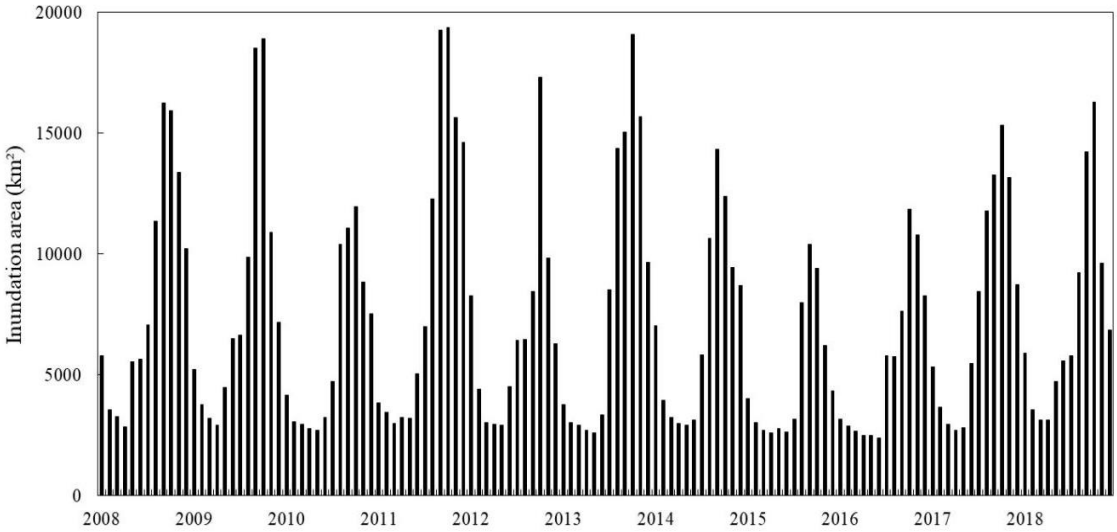

Figure 9. *Monthly average inundation area of the study area from 2008 to 2018*

http://www.aloki.hu ● ISSN 1589 1623 (Print) ● ISSN 1785 0037 (Online)
DOI: http://dx.doi.org/10.15666/aeer/1906_45474566

The minimum inundation area reached 2265.80 km^2 and 2736.79 km^2 in 2016 and 2009, which were both dry years, and presented relatively less inter-annual variations in dry seasons. Due to the impact of the El Niño happened at the end of 2014, the entire Mekong River Basin was suffered with severe drought, reduced precipitation and runoff (Frappart et al., 2018), which led to little water could be injected into the Tonle Sap Lake during the rainy season. However, the inundation area has shown significant inter-annual variations in rainy seasons, with the maximum inundation area varied from 10623.66 km^2 in September 2015 to 19144.58 km^2 in October 2011, when the catastrophic flood occurred in 2011 in the Tonle Sap Lake.

Variation of water level

The monthly water level of Tonle Sap Lake was monitored by the Jason-2 and Jason-3 radar altimetry from 2008 to 2018 (*Fig. 10*). In general, the lowest water level appeared in April or May and the highest water level appeared during September to November. April and May are the late stage of the dry season per year, the lake continued to evaporate without plenty precipitation to supply, the water level could reach the minimum of 2.36 m. Whereas during September to October, the late stage of rainy season, the water supply continued and led to the possibility to reach the highest water level during this period. The water level varied significant over the period of one year and steady trend was observed in the inter-annual scale.

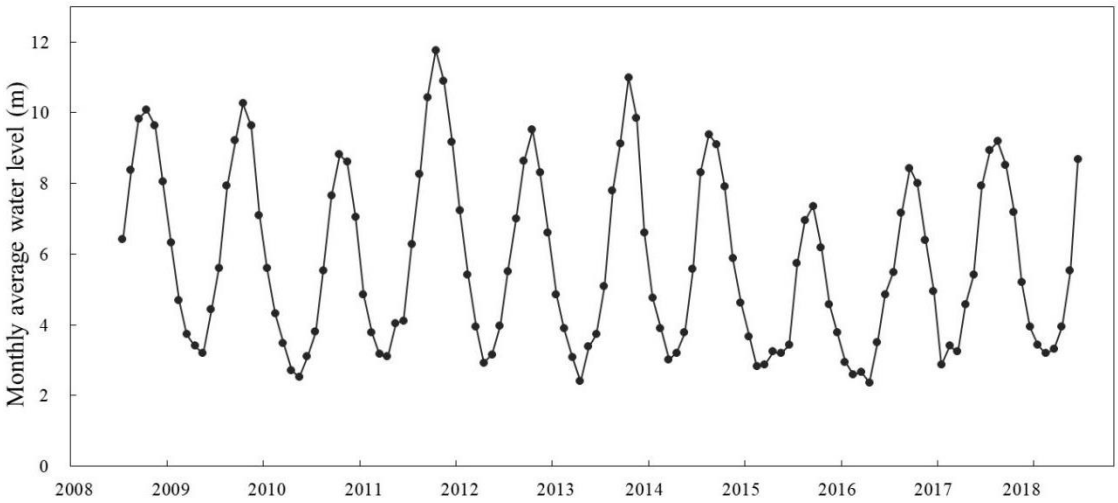

Figure 10. *Estimated monthly average water level of the Tonle Sap Lake from 2008 to 2018*

Take the water level of flood year 2011 and drought year 2015 as the example, the water level escalated from May to October and presented decline trend from November to May of next year (*Fig. 11*). The variation tendency of water level in flood year was fairly consistent with the drought year. During the rainy season from June to October, the differences of water level between flood year and drought year increased progressively and reached the highest value 4.42 m in October. The differences of water level showed relatively little change from January to April with water levels close to each other.

As the catastrophic flood occurred in 2011, the water level reached the maximum of 11.76 m in October. And due to the impact of El Niño from the end of 2014, the ambient countries all suffered from severe drought, especially downstream of the Mekong Delta.

http://www.aloki.hu ● ISSN 1589 1623 (Print) ● ISSN 1785 0037 (Online)
DOI: http://dx.doi.org/10.15666/aeer/1906_45474566

The water level of Tonle Sap Lake reached the minimum of 7.35 m in October 2015. The altimetry water level was able to derive reliable water levels which was quite consistence with the actual situation. The result was expected to provide a reference for the practice of deriving water level of medium water bodies by altimetry satellites.

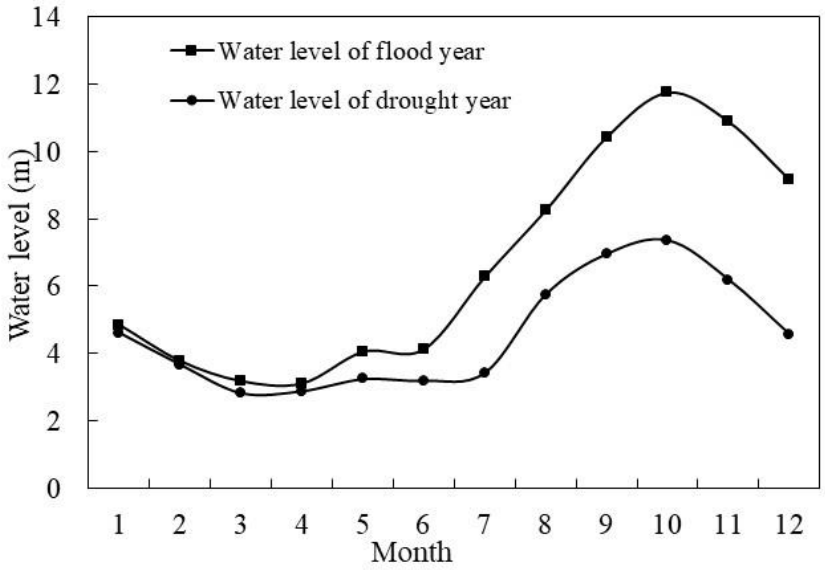

Figure 11. *Comparison of water level in drought year (2015) and flood year (2011)*

Response to precipitation

Combined with the monthly precipitation data from TRMM 3B42V7, the fluctuation trend of inundation area (*Fig. 12*) and water level (*Fig. 13*) were basically consistent with the precipitation. However, the time lags of the extremes (both the minimum and the maximum) between inundation area/water level and precipitation were approximate one month, which was a distinct lagging relationship. The findings of Kummu et al. demonstrated that more than half of the annual flow into the Tonle Sap came from Mekong River, 34% from the tributaries and 12.5% from precipitation (Kummu et al., 2014). And the runoff of Mekong River is mainly from precipitation. Therefore, the variation of inundation area and water level in the Tonle Sap Lake were closely related to the change of precipitation, which were driven by the monsoon flood in the Mekong River Basin.

In the past decade, both the precipitation of the Tonle Sap Lake Basin (*Fig. 14a*) and the Mekong River Basin (*Fig. 14b*) presented declined trend which were not significant. If the precipitation decreases, the runoff of the Mekong River will go down correspondingly. As a result, the discharge flows into Tonle Sap Lake in the rainy seasons will decrease and the water level will decline as well. These phenomena happened in 2015, after the El Niño phenomenon occurred in the Mekong River Basin with the sudden drop of precipitation and climate warming. The precipitation of Mekong River Basin in 2015 was only 1567.08 mm, which was 13.29% lower compared to the average annual precipitation. In consequence, the inundation area decreased 29.75% and water level declined 20.33% in comparison with the average annual values.

http://www.aloki.hu ● ISSN 1589 1623 (Print) ● ISSN 1785 0037 (Online)
DOI: http://dx.doi.org/10.15666/aeer/1906_45474566

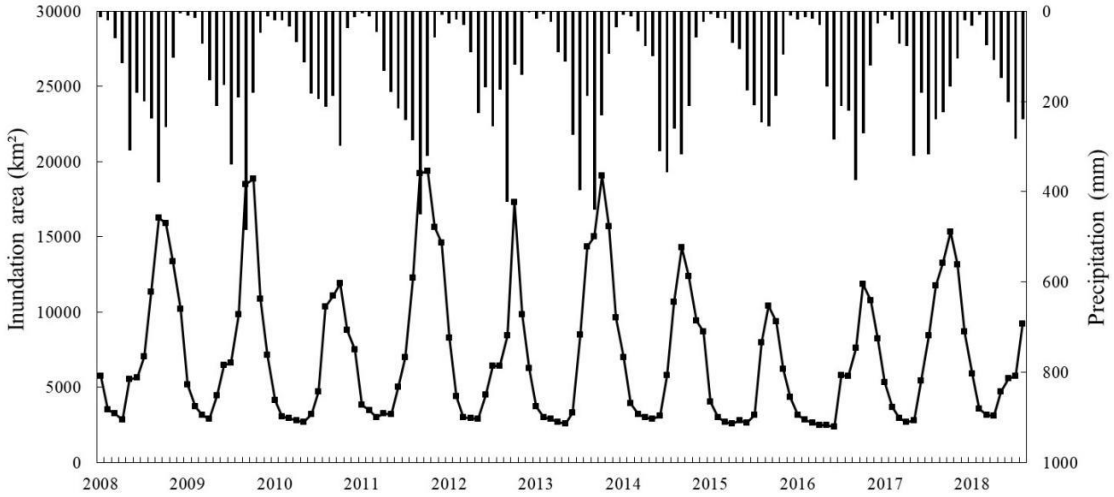

Figure 12. *Comparison of inundation area and precipitation*

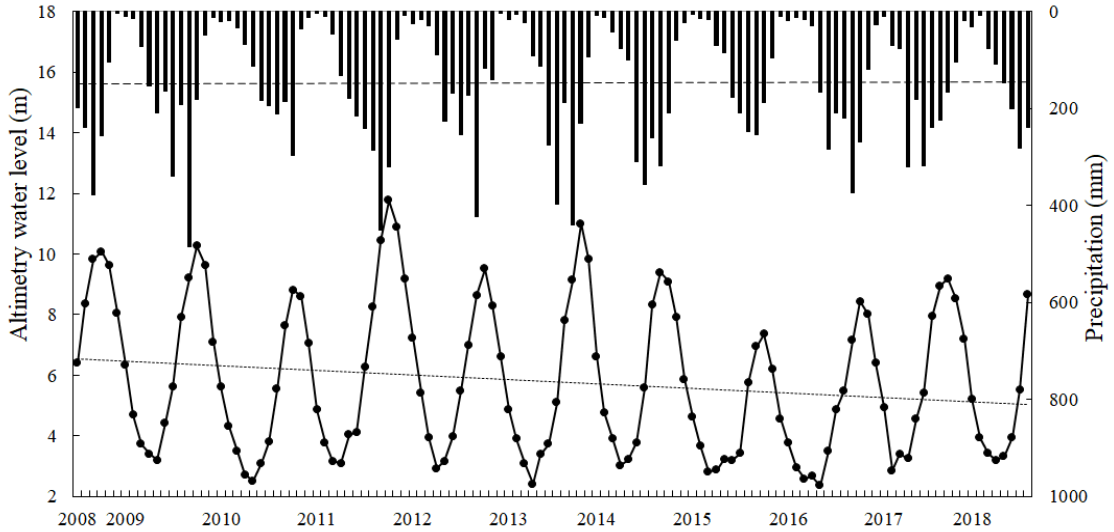

Figure 13. *Comparison of water level and precipitation*

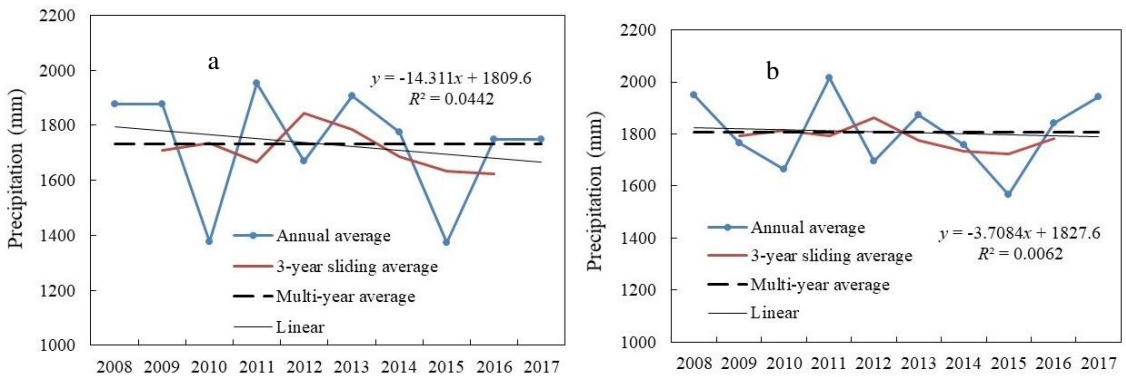

Figure 14. *Linear tendency and moving average of precipitation of Tonle Sap Lake basin and Mekong River basin*

http://www.aloki.hu ● ISSN 1589 1623 (Print) ● ISSN 1785 0037 (Online)
DOI: http://dx.doi.org/10.15666/aeer/1906_45474566

Moreover, plenty of sediments brought by the floods and the deforestation around the lake have caused massive deposit in the inundation area, which could give rise to the shrinking of the water body. The area already decreased at the speed of 30 km² per year. At the same time, construction of the dams on the tributary of Tonle Sap River reduced the surface water that flowed into Tonle Sap Lake (Arias et al., 2019).

Response to the upstream hydrology regime

Conflicts often arise over the Lancang-Mekong River, since it spread across the six riparian countries with more than 70 dams. Different stakeholders compete for the scarce water resources and limited reservoir storage capacity. As the largest boundary lake that regulates and stores the flood from this controversial transnational river, the water regime of the Tonle Sap Lake also attracted extensive attention worldwide.

Some international media reported that the decline of downstream water level was attributed to the exploration of the upstream countries, especially the dam construction over the Lancang River in China. The disputes of whether the upstream exploitation such as dam construction and hydropower station have definitely negative effects on downstream water resource utilization have been lasted for several decades (Lu et al., 2014).

However, our result demonstrated that the average water level derived from the radar altimeter did not follow the change of the average runoff from Jinghong hydrological station (100°47’ E, 22°02’ N) distinctly, which is the last control station that located in the upstream of the Lancang-Mekong river in China, both in flood period and non-flood periods (*Fig. 15*). Although, the Chinese government was requested to increase the discharge to alleviate the drought in the downstream since the El Niño event in 2014, the water level also declined slightly. This was also proved by other research, which found that the shrinking water area of Tonle Sap Lake was not attributed to the development of the Lancang cascade hydropower stations (Ji et al., 2018).

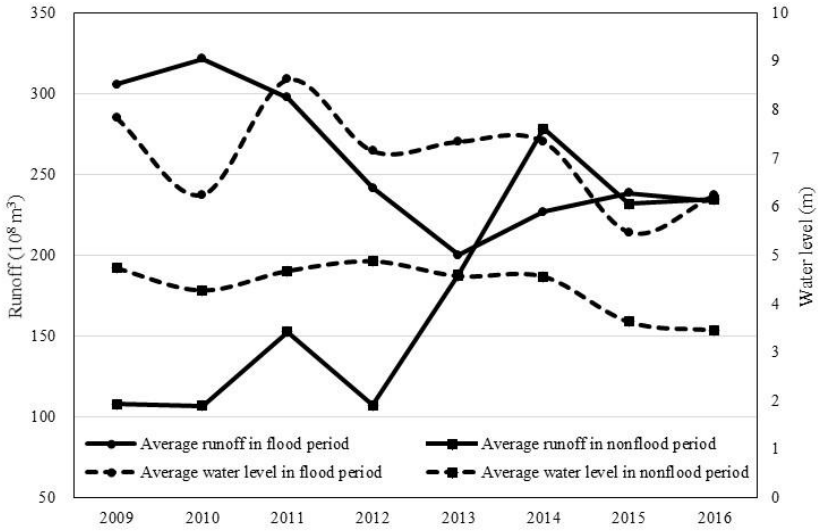

Figure 15. *Distribution of average runoff and water level in flood and non-flood periods*

The correlation coefficients between average water level and runoff in flood period and non-flood periods were 0.0542 and 0.2873 with $p < 0.01$ (*Fig. 16*), which presented the poor correlation between the downstream water level and the upstream runoff.

http://www.aloki.hu ● ISSN 1589 1623 (Print) ● ISSN 1785 0037 (Online)
DOI: http://dx.doi.org/10.15666/aeer/1906_45474566

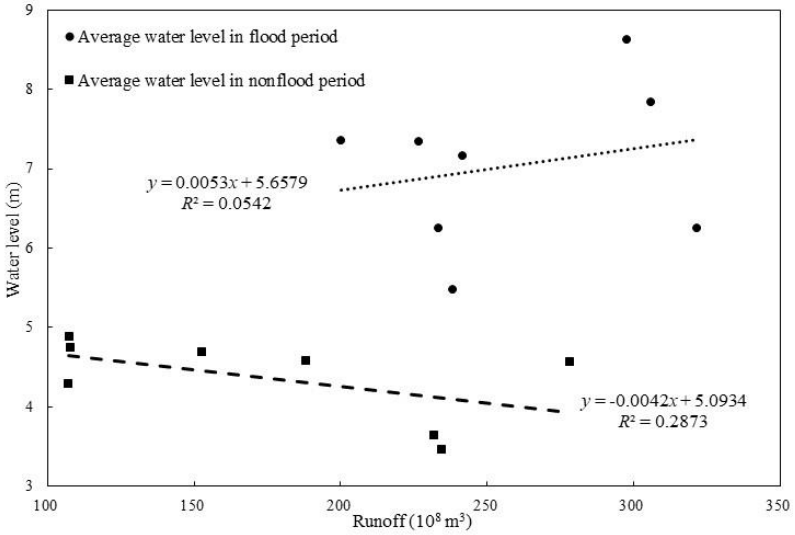

Figure 16. *Correlation between average runoff and water level in flood and non-flood periods*

Coincidentally, results from other researches also indicated no major difference in flows between the pre- and post-development of hydropower projects. And the inclusion of a few major dams resulted in decreased river streamflow of 6% to 15% possibly due to irrigation diversions and climate change (Fan et al., 2015; Lu et al., 2014; Sridhar et al., 2019).

Conclusions

Our study provided a comprehensive assessment of the variations of the inundation area as well as to explore water levels in the Tonle Sap Lake over the past decade, using various data sets delivered by remote sensing satellites. It was demonstrated that the Jason-2 and Jason-3 radar altimetry data were reliable to detect the inland water level like Tonle Sap Lake with high accuracy ($R^2 = 0.9232$ and confidence coefficient of 98%). And the composite index was the optimal method to identify inundation area of the Tonle Sap Lake, due to the difference between EVI and LSWI, which enhanced the contrast between water and background objects and made it better to distinguish the water body and extract with mixed pixels compared to the other two methods.

The fluctuation trend of inundation area and water level were basically consistent with the precipitation, presented a distinct lagging relationship. And the time lags of the extremes (both the minimum and the maximum) between inundation area/water level and precipitation were approximate one month. The variation of inundation area and water level in the Tonle Sap Lake were closely related to the change of precipitation. Moreover, the runoff from upstream hydropower station presented poor correlation with the downstream water level both in flood period and non-flood periods, which indicated that the upstream explorations over Lancang-Mekong River had little effects on the downstream water volume.

In the future, we would like to explore some other altimetry mission in order to obtain finer temporal and spatial resolution water levels, which were expected to provide more details. We will also apply the proposed technology to some other poorly gauged river basins to expand our knowledge of radar altimetry.

http://www.aloki.hu ● ISSN 1589 1623 (Print) ● ISSN 1785 0037 (Online)
DOI: http://dx.doi.org/10.15666/aeer/1906_45474566

Acknowledgments. This research was funded by National Natural Science Foundation of China (NO. 41661085, 41763004, 41461021), Guangxi Scientific Project (NO. AD19110140), Guangxi Scholarship Fund of Guangxi Education Department, "Specially Employed Expert" project of Guangxi Zhuang Autonomous Region.

REFERENCES

[1] Amani, M., Salehi, B., Mahdavi, S., Granger, J. E., Brisco, B., Hanson, A. (2017): Wetland classification using multi-source and multi-temporal optical remote sensing data in Newfoundland and Labrador, Canada. – Canadian Journal of Remote Sensing 43(4): 360-373.

[2] Arias, M. E., Cochrane, T. A., Piman, T., Kummu, M., Caruso, B. S., Killeen, T. J. (2012): Quantifying changes in flooding and habitats in the Tonle Sap Lake (Cambodia) caused by water infrastructure development and climate change in the Mekong Basin. – Journal of Environmental Management 112: 53-66.

[3] Arias, M. E., Cochrane, T. A., Kummu, M., Lauri, H., Holtgrieve, G. W., Koponen, J., Piman, T. (2014): Impacts of hydropower and climate change on drivers of ecological productivity of Southeast Asia's most important wetland. – Ecological Modelling 272: 252-263.

[4] Arias, M. E., Holtgrieve, G. W., Ngor, P. B., Dang, T. D., Piman, T. (2019): Maintaining perspective of ongoing environmental change in the Mekong floodplains. – Current Opinion in Environmental Sustainability 37: 1-7.

[5] Biancamaria, S., Schaedele, T., Blumstein, D., Frappart, F., Boy, F., Desjonqueres, J. D., Pottier, C., Blarel, F., Nino, F. (2018): Validation of Jason-3 tracking modes over French rivers. – Remote Sensing of Environment 209: 77-89.

[6] Boergens, E., Dettmering, D., Seitz, F. (2019): Observing water level extremes in the Mekong River Basin: The benefit of long-repeat orbit missions in a multi-mission satellite altimetry approach. – Journal of Hydrology 570: 463-472.

[7] Breda, J., Paiva, R. C. D., Bravo, J. M., Passaia, O. A., Moreira, D. M. (2019): Assimilation of satellite altimetry data for effective river bathymetry. – Water Resources Research 55(9): 7441-7463.

[8] Chen, Y., Huang, C., Ticehurst, C., Merrin, L., Thew, P. (2013): An evaluation of MODIS daily and 8-day composite products for floodplain and wetland inundation mapping. – Wetlands 33(5): 823-835.

[9] Ding, X. W., Li, X. F. (2011): Monitoring of the water-area variations of Lake Dongting in China with ENVISAT ASAR images. – International Journal of Applied Earth Observation and Geoinformation 13(6): 894-901.

[10] Du, Y., Zhang, Y. H., Ling, F., Wang, Q. M., Li, W. B., Li, X. D. (2016): Water bodies' mapping from Sentinel-2 imagery with modified normalized difference water index at 10-m spatial resolution produced by sharpening the SWIR band. – Remote Sensing 8(4): 1-19.

[11] Dubey, A. K., Gupta, P. K., Dutta, S., Singh, R. P. (2015): An improved methodology to estimate river stage and discharge using Jason-2 satellite data. – Journal of Hydrology 529: 1776-1787.

[12] Fan, H., He, D. M., Wang, H. L. (2015): Environmental consequences of damming the mainstream Lancang-Mekong River: a review. – Earth-Science Reviews 146: 77-91.

[13] Fan, X. W., Liu, Y. B., Wu, G. P., Zhao, X. S. (2020): Compositing the minimum NDVI for daily water surface mapping. – Remote Sensing 12(4): 700.

[14] Fayne, J. V., Bolten, J. D., Doyle, C. S., Fuhrmann, S., Rice, M. T., Houser, P. R., Lakshmi, V. (2017): Flood mapping in the lower Mekong River Basin using daily MODIS observations. – International Journal of Remote Sensing 38(6): 1737-1757.

http://www.aloki.hu ● ISSN 1589 1623 (Print) ● ISSN 1785 0037 (Online)
DOI: http://dx.doi.org/10.15666/aeer/1906_45474566

[15] Feng, L., Hu, C. M., Chen, X. L., Cai, X. B., Tian, L. Q., Gan, W. X. (2012): Assessment of inundation changes of Poyang Lake using MODIS observations between 2000 and 2010. – Remote Sensing of Environment 121: 80-92.
[16] Frappart, F., Biancamaria, S., Normandin, C., Blarel, F., Bourrel, L., Aumont, M., Azemar, P., Vu, P. L., Le Toan, T., Lubac, B., Darrozes, J. (2018): Influence of recent climatic events on the surface water storage of the Tonle Sap Lake. – Science of the Total Environment 636: 1520-1533.
[17] Gleason, C. J., Hamdan, A. N. (2017): Crossing the (watershed) divide: satellite data and the changing politics of international river basins. – Geographical Journal 183(1): 2-15.
[18] Hecht, J. S., Lacombe, G., Arias, M. E., Dang, T. D., Piman, T. (2019): Hydropower dams of the Mekong River basin: a review of their hydrological impacts. – Journal of Hydrology 568: 285-300.
[19] Huang, Q., Long, D., Du, M. D., Zeng, C., Li, X. D., Hou, A. Z., Hong, Y. (2018): An improved approach to monitoring Brahmaputra River water levels using retracked altimetry data. – Remote Sensing of Environment 211: 112-128.
[20] Jahanbakhsh, G., M., Khorasani, N., Morshedi, J., Danehkar, A., Naderi, M. (2017): An investigation on spatial changes of Parishan international wetland using remote sensing methods. – Applied Ecology and Environmental Research 15(3), 549-562.
[21] Ji, X., Li, Y. G., Luo, X., He, D. M. (2018): Changes in the lake area of Tonle Sap: possible linkage to runoff alterations in the Lancang River? – Remote Sensing 10: 866.
[22] Kummu, M., Tes, S., Yin, S., Adamson, P., Jozsa, J., Koponen, J., Richey, J., Sarkkula, J. (2014): Water balance analysis for the Tonle Sap Lake-floodplain system. – Hydrological Processes 28(4): 1722-1733.
[23] Kuo, C. Y., Cheng, Y. J., Lan, W. H., Kao, H. C. (2015): Monitoring vertical land motions in southwestern Taiwan with retracked Topex/Poseidon and Jason-2 satellite altimetry. – Remote Sensing 7(4): 3808-3825.
[24] Kwak, Y. J. (2017): Nationwide flood monitoring for disaster risk reduction using multiple satellite data. – ISPRS International Journal of Geo-Information 6(7): 203.
[25] Larnberts, D., and Koponen, J. (2008): Flood pulse alterations and productivity of the Tonle Sap ecosystem: a model for impact assessment. – Ambio 37(3): 178-184.
[26] Li, W. B., Du, Z. Q., Ling, F., Zhou, D. B., Wang, H. L., Gui, Y. M., Sun, B. Y., Zhang, X. M. (2013): A comparison of land surface water mapping using the normalized difference water index from TM, ETM plus and ALI. – Remote Sensing 5(11): 5530-5549.
[27] Li, D. N., Zhao, J. S., Govindaraju, R. S. (2019a): Water benefits sharing under transboundary cooperation in the Lancang-Mekong River Basin. – Journal of Hydrology 577: 1-13.
[28] Li, X. D., Long, D., Huang, Q., Han, P. F., Zhao, F. Y., Wada, Y. (2019b): High-temporal-resolution water level and storage change data sets for lakes on the Tibetan Plateau during 2000-2017 using multiple altimetric missions and Landsat-derived lake shoreline positions. – Earth System Science Data 11(4): 1603-1627.
[29] Lu, X. X., Li, S. Y., Kummu, M., Padawangi, R., Wang, J. J. (2014): Observed changes in the water flow at Chiang Saen in the lower Mekong: Impacts of Chinese dams? – Quaternary International 336: 145-157.
[30] Maillard, P., Bercher, N., Calmant, S. (2015): New processing approaches on the retrieval of water levels in Envisat and SARAL radar altimetry over rivers: A case study of the Sao Francisco River, Brazil. – Remote Sensing of Environment 156: 226-241.
[31] Maiwald, F., Montes, O., Padmanabhan, S., Michaels, D., Kitiyakara, A., Jarnot, R., Brown, S. T., Dawson, D., Wu, A., Hatch, W., Stek, P., Gaier, T. (2016): Reliable and stable radiometers for Jason-3. – IEEE Journal of Selected Topics in Applied Earth Observations and Remote Sensing 9(6): 2754-2762.

http://www.aloki.hu ● ISSN 1589 1623 (Print) ● ISSN 1785 0037 (Online)
DOI: http://dx.doi.org/10.15666/aeer/1906_45474566

[32] Millard, K., Richardson, M. (2013): Wetland mapping with LiDAR derivatives, SAR polarimetric decompositions, and LiDAR–SAR fusion using a random forest classifier. – Canadian Journal of Remote Sensing 39(4): 290-307.
[33] Normandin, C., Frappart, F., Lubac, B., Belanger, S., Marieu, V., Blarel, F., Robinet, A., Guiastrennec-Faugas, L. (2018): Quantification of surface water volume changes in the Mackenzie Delta using satellite multi-mission data. – Hydrology and Earth System Sciences 22(2): 1543-1561.
[34] Oeurng, C., Cochrane, T. A., Chung, S., Kondolf, M. G., Piman, T., Arias, M. E. (2019): Assessing climate change impacts on river flows in the Tonle Sap Lake Basin, Cambodia. – Water 11(3): 618.
[35] Pekel, J. F., Cottam, A., Gorelick, N., Belward, A. S. (2016): High-resolution mapping of global surface water and its long-term changes. – Nature 540(7633): 418-422.
[36] Schlaffer, S., Matgen, P., Hollaus, M., Wagner, W. (2015): Flood detection from multi-temporal SAR data using harmonic analysis and change detection. – International Journal of Applied Earth Observation and Geoinformation 38: 15-24.
[37] Schneider, P., Hook, S. J. (2010): Space observations of inland water bodies show rapid surface warming since 1985. – Geophysical Research Letters 37(22): L22405.
[38] Sridhar, V., Kang, H., Ali, S. A. (2019): Human-induced alterations to land use and climate and their responses for hydrology and water management in the Mekong River Basin. – Water 11(6): 1307.
[39] Tangdamrongsub, N., Ditmar, P. G., Steele-Dunne, S. C., Gunter, B. C., Sutanudjaja, E. H. (2016): Assessing total water storage and identifying flood events over Tonle Sap basin in Cambodia using GRACE and MODIS satellite observations combined with hydrological models. – Remote Sensing of Environment 181: 162-173.
[40] Wang, H. H., Chu, Y. H., Huang, Z. K., Hwang, C., Chao, N. F. (2019): Robust, long-term lake level change from multiple satellite altimeters in Tibet: observing the rapid rise of Ngangzi Co over a New Wetland. – Remote Sensing 11(5): 558.
[41] Zhang, X. J., Qu, Y. P., Ma, M. M., Liu, H., Su, Z. C., Lv, J., Peng, J., Leng, G. Y., He, X. G., Di, C. L. (2020): Satellite-based operational real-time drought monitoring in the transboundary Lancang-Mekong River Basin. – Remote Sensing 12(3): 376.

http://www.aloki.hu ● ISSN 1589 1623 (Print) ● ISSN 1785 0037 (Online)
DOI: http://dx.doi.org/10.15666/aeer/1906_45474566

GENETIC VARIATION OF ARCTIC STARFLOWR (*TRIENTALIS EUROPAEA* SUBSP. *ARCTICA* (FISCH. EX HOOK.) HULTÉN) (PRIMULACEAE), AN ENDANGERED HERB SPECIES OF SOUTH KOREA: IMPLICATIONS FOR CONSERVATION STRATEGIES

YEON, M. H. – LEE, S. H. – LEE, Y. E. – KIM, S. K.*

Department of Life Science, Chung-Ang University, 84 Heukseok-ro, Dongjak-gu, Seoul, Korea

**Corresponding author*
e-mail: skkimbio@cau.ac.kr; phone: +82-2-820-5210; fax: +82-2-825-5206

(Received 17th Jun 2021; accepted 3rd Sep 2021)

Abstract. *Trientalis europaea* subsp. *arctica* (Primulaceae) is an herb species that is distributed widely across the northern hemisphere but is endangered in South Korea. In this study, we investigated the genetic diversity and structure of *T. arctica* populations by using Random Amplification Polymorphic DNA (RAPD) markers. Ten RAPD primers were used to amplify 81 loci from 9 populations consisting of 270 individuals. *T. arctica* shows high genetic diversity at the species level, but low genetic diversity at the population level. The percentage of polymorphic bands (PPB) was 86.4% at the species level, but the average PPB at the population level was 7.1%. In addition, Nei's gene diversity (species level = 0.27; population level = 0.02) and Shannon's information index (species level = 0.41; population level = 0.04) indicated similar genetic structures. *T. arctica* showed a high degree of genetic differentiation (Φst = 0.96 and *Gst* = 0.911) between populations and limited gene flow (*Nm* = 0.01). These results may be attributed to the fact that *T. arctica* is a refugial species in South Korea and to its long-term isolation in alpine regions. Considering the extremely low genetic diversity and high genetic differentiation of *T. arctica* populations, both in situ and ex situ conservation should be carried out actively for this species.
Keywords: *genetic diversity, genetic differentiation, plant conservation, RAPD, northern plant*

Introduction

The genus *Trientalis* belongs to the Primulaceae family and is composed of boreal herb species that are distributed in the understory of woodlands. Plants of this genus appear widely throughout Northern Europe, East Asia, and North America in the northern hemisphere, have creeping rhizomes, and undergo vegetative reproduction by extending sideways near the soil surface (Hiirsalmi, 1969; Kovanda, 1995; Piqueras and Klimes, 1998; Piqueras, 1999; Piqueras et al., 1999). Two species, *T. europaea* L. and *T. europaea* subsp. *arctica* (Fisch. ex Hook.) Hultén, grow naturally in South Korea (Lee, 2003, 2006). However, *T. europaea* has been rarely reported in domestic research on flora and plant distribution, whereas almost all data report the distribution of *T. arctica* (Song et al., 2009; Shin et al., 2010; Park et al., 2011; Kim et al., 2012, 2015, 2017; Park and Kim, 2012; Li et al., 2014; Yoon et al., 2015; Sung et al., 2018) therefore, most *Trientalis* species in South Korea are considered to *be T. arctica.*

In South Korea, the distribution of *T. arctica* is limited to the alpine and sub-alpine regions of the Baekdu-daegan area in the north–south Korean Peninsular region. The Baekdu-daegan region on the Korean Peninsula is believed to have served as a major refugia for northern plants during the Quaternary Period (Chung et al., 2012, 2013, 2014; Lee et al., 2016). Therefore, the current distribution of *T. arctica*, a northern plant, is expected to have been greatly affected by climate change from the ice age to the present. During the ice age, the distribution of northern plants expanded to the south due to

http://www.aloki.hu ● ISSN 1589 1623 (Print) ● ISSN 1785 0037 (Online)
DOI: http://dx.doi.org/10.15666/aeer/1906_45674581

reduced temperatures; subsequently, these plants either retreated to the north or changed their habitats to the alpine regions, which had lower temperatures than the other areas after the interglacial period. Plants left in the alpine regions were blocked in by temperature barriers and isolated, and form the current distribution of plants with ecological characteristics similar to those of *T. arctica* in these alpine regions. Since *T. arctica* is threatened by its limited distribution and population decline through indiscriminate harvesting and habitat damage, it has been designated as an endangered wildlife class II species by the Ministry of Environment, South Korea. It is also designated as a vulnerable species (VU), an endangered species category on the Korean Red List (Korea National Arboretum, 2009).

Genetic variation is considered an important factor in determining the survival of a species in a changing environment and is a fundamental component of biodiversity (Pauls et al., 2013). In particular, the maintenance of genetic diversity is a major concern for conservation biologists involved in the conservation and management of endangered species with small numbers or a limited distribution. To establish an appropriate conservation strategy for endangered or rare species, knowledge on the level of genetic variation within and between populations is essential basic information (Jiménez et al., 2002; Jeong et al., 2010; Wang et al., 2012). However, despite the importance of research on the genetic variations of *T. arctica* in ensuring the protection and proper management of this species, few studies have evaluated this topic.

Molecular markers have been used to measure genetic diversity and to study the genetic structure of plants within populations. Among them, random amplification polymorphic DNA (RAPD) markers are DNA-based dominant markers (Williams et al., 1990). Since they are dominant markers, they cannot easily distinguish between homozygotes and heterozygotes, and may exhibit low reproducibility. Nevertheless, these markers have been frequently used in studies on genetic variation because they offer advantages such as random sampling of the genome, high polymorphism, and low cost, and the fact that they do not require genomic information of the target species (Singh et al., 2012). In addition, since analysis using these markers requires only a small amount of sample, it is suitable for research on endangered or rare species.

In this study, we attempted to determine the level and structure of genetic variation in nine natural populations of *T. arctica*, an endangered species in South Korea, by using RAPD markers. Our main goals were as follows: (1) to measure genetic diversity at the species and population levels, (2) to understand the genetic differentiation pattern and genetic structure between populations, and (3) to interpret our results to an effective conservation strategy.

Materials and methods

Study species and sampling

According to a previous study, *T. arctica* is a clonal plant that reproduces through rhizomes, has very low seed production and seedling settlement, and is believed to have physiological and ecological characteristics almost similar to those of *T. europaea* (Tikhodeyev, 2003). During its vegetative pseudo-annual life cycle, the mother ramet dies after producing several daughter ramets during the growing season. These daughter ramets remain dormant in the ground, before growing and continuing the cycle during the next growing period (Piqueras et al., 1999). Five to ten leaves are gathered on the upper part of the stem and their edges are flat. One or two white whole flowers hang at the end

http://www.aloki.hu ● ISSN 1589 1623 (Print) ● ISSN 1785 0037 (Online)
DOI: http://dx.doi.org/10.15666/aeer/1906_45674581

of the peduncle from the end of the stem, and they are deeply divided into seven petals. The seven calyx leaves are narrow and lanceolate, have a pointed end, are split deeply, and spread horizontally. Fruits mature in September and are spherical capsules with a diameter of 2.5 to 3 mm (National Institute of Biological Resources, https://species.nibr.go.kr/, *Fig. 1*).

Figure 1. *Morphological features of T. arctica in South Korea*

In South Korea, *T. arctica* is mainly distributed on the northern slopes at an altitude of more than 1,000 m (*Table 1, Fig. 2*). It is known to be distributed in five areas, including Yongneup, Mount (Mt.) Seorak, Mt. Gaya, and Mt. Jiri. Among these, Yongneup, the northernmost area, is an alpine wetland located around the summit of Mt. Daeam. The Yongneup population inhabits the peat moss layer on the wetland floor and occupies a more heterogeneous habitat than the other populations, which live in the herbaceous layers of forests. The Mt. Seorak population is divided into three subpopulations (SA1, SA2, and SA3) according to the peaks inhabited, which are several kilometers apart from each other, and show no continuous distribution. The Mt. Taebaek population is divided into two subpopulations, TB1 and TB2. The TB1 population inhabits the moss layer on the rocky area of the ridge, and the TB2 population lives in the lower herbaceous layer of the coniferous forest near the peak. The Mt. Gaya population inhabits the herbaceous layer on the mountain ridge and the moss layer above the rock. The Mt. Jiri population is divided into two subpopulations (JR1, JR2) that occupy the herbaceous layer on the northwestern slope of the ridge.

A total of 270 *T. arctica* samples were collected from nine natural populations in South Korea, with 30 samples collected per population. Sample collection within each population was conducted with consideration to the topography of the area and was carried out at certain intervals between individuals to minimize their genetic relationship. The samples were collected in a paper bag, placed in a plastic container along with a moisture absorbent, and moved to the laboratory. Plant samples were stored at -20 °C until DNA extraction.

http://www.aloki.hu ● ISSN 1589 1623 (Print) ● ISSN 1785 0037 (Online)
DOI: http://dx.doi.org/10.15666/aeer/1906_45674581

Table 1. *The location of T. arctica populations and sample size of surveyed populations in South Korea (N = sample size)*

No.	Population	Latitude	Longitude	Altitude (m)	Slope orientation	N
1	Yong-neup (YN)	38°12'46.4"	128°07'34.4"	1,186	-	30
2	Mt. Seolark (SA1)	38°08'08.4"	128°20'07.6"	1,206	NE	30
3	Mt. Seolark (SA2)	38°07'14.6"	128°23'23.3"	1,477	N	30
4	Mt. Seolark (SA3)	38°07'05.0"	128°27'50.3"	1,597	NE	30
5	Mt. Taebaek (TB1)	37°06'23.6"	128°54'38.9"	1,276	NW	30
6	Mt. Taebaek (TB2)	37°05'29.8"	128°56'31.3"	15,12	NW	30
7	Mt. Gaya (GY)	35°49'11.1"	128°07'27.6"	1,425	NE	30
8	Mt. Jiri (JR1)	35°20'52.9"	127°44'93.3"	1,586	NW	30
9	Mt. Jiri (JR2)	35°18'05.5"	127°41'18.7"	1,600	NW	30

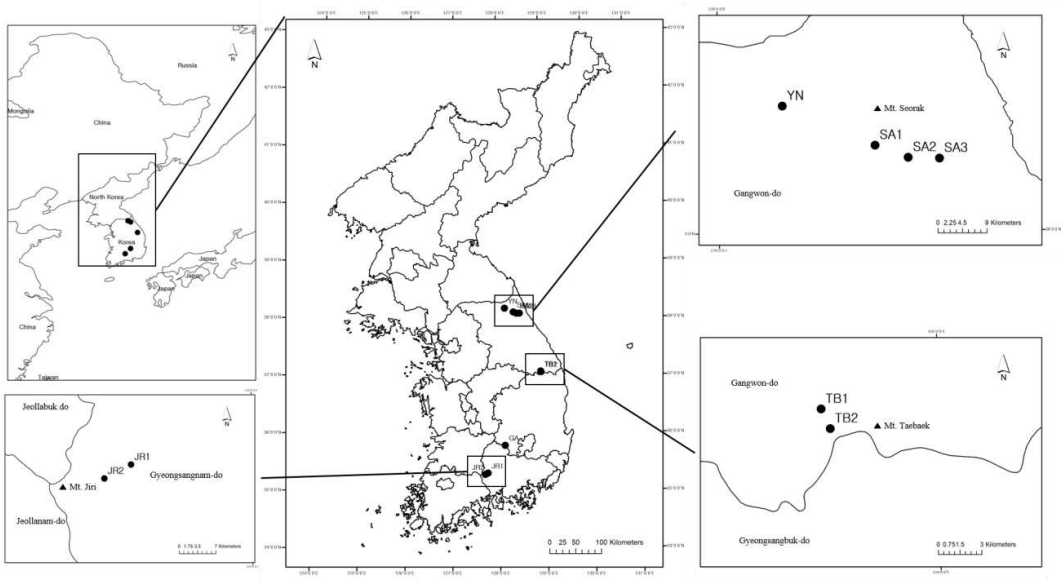

Figure 2. *Geographical distribution of T. arctica populatons in Korea (Population abbreviations are shown in Table 1.)*

DNA extraction and RAPD polymerase chain reaction (PCR)

Genomic DNA was extracted using the DNeasy® Plant mini kit (Qiagen Inc., Alameda, CA, USA). Leaf samples were frozen with liquid nitrogen and ground using a mortar and pestle. These ground samples were subjected to DNA extraction according to the manufacturer's instructions. The extracted DNA was diluted to a concentration of 25 ng/μL for RAPD PCR.

Ten random decamer primers from the A, N, O, P, and AF series were selected through screening (Qiagen Inc., Alameda, CA, USA) for RAPD analysis. Screening of the primers was performed in duplicate using two representatives from each of the nine populations and relied on the clarity and repeatability of the RAPD amplification bands.

We conducted RAPD amplification with a reaction volume of 20 μL, which contained 2.0 μL of 10X PCR buffer, 1 U Taq DNA polymerase (Takara Bio Inc., Shiga, Japan), 2.0 μL of primer (20 pmol), and 1.0 μL of deoxyribonucleotide triphosphate (dNTP)

http://www.aloki.hu ● ISSN 1589 1623 (Print) ● ISSN 1785 0037 (Online)
DOI: http://dx.doi.org/10.15666/aeer/1906_45674581

mixture (2.5 mM each). We performed PCR in the TProfessional basic thermocycler (Biometra, Göttingen, Germany) with initial denaturation at 94 °C for 2 min, followed by 36 cycles of 30 s at 94 °C (denaturation), 30 s at 36 °C (annealing), and 1 min at 72 °C (extension), and a final extension at 72 °C for 10 min. The PCR products were fractionated on 1.4% agarose gel in 0.5× tris-acetate-ethylenediaminetetraacetic acid (TAE) buffer for 30 min. After electrophoresis, gels were stained with ethidium bromide and viewed and photographed under a UV transilluminator using the Gel Doc 2000 (Bio-Rad Laboratories Inc., CA, USA) gel imaging system.

Data analysis

The binary data matrix was created by scoring the PCR-amplified band as "1," if present, or "0," if absent, for calculating the statistics of genetic variation. The data matrix was analyzed using POPGENE version 1.32 (Yeh et al., 1999) as follows: percentage of polymorphic bands (PPB), Nei's gene diversity (*H*), Shannon information index (*I*), observed number of alleles (*Ao*), effective number of alleles (*Ae*), coefficient of gene differentiation (*Gst*), and Nei's unbiased genetic identity and genetic distance.

To describe the partitioning of the genetic variance within and between populations, an analysis of molecular variance (AMOVA) was conducted using ARLEQUIN ver. 3.0 (Excoffier et al., 2005). The Φ statistics calculated from AMOVA and their significance were tested by 1000 permutations. The level of gene flow (*Nm*), which is the proportion of new immigrant genes moving into a population, was calculated from the Φst using the formula: Nm = 1/4 (1- Φst)/Φst (Slatkin and Barton, 1989). The relationships between the populations were displayed as a dendrogram through an unweighted pair-group method with arithmetic average (UPGMA) clustering method using POPGENE 1.32.

A principal coordinate analysis (PCoA) was carried out by plotting Euclidean distance in three-dimensional space, which was calculated on the basis of an RAPD binary matrix, to determine how individuals from all populations clustered together by using GenAlEx 6.5 (Peakall and Smouse, 2006) The correlation between geographic distance (km) and genetic distance among populations was calculated using the Mantel test (Mantel, 1967) and GenAlEx 6.5.

Results

Genetic diversity

The ten selected RAPD primers yielded 81 reliable bands across 270 individuals from nine *T. arctica* populations. The average number of bands and polymorphic bands per primer were 8.1 and 7, respectively (*Table 2*). The genetic variation parameters of the *T. arctica* populations based on RAPD markers are summarized in *Table 3*.

The genetic diversity indices of *T. arctica* were significantly higher at the species level than at the population level. The PPB was 86.4% at the species level but ranged from 18.52% to 1.26% at the population level, and the population mean was 7.1%. The *Ao* value was 1.864 at the species level, ranged from 1.185 to 1.012 at the population level, and the population mean was 1.071. The *Ae* value was 1.454 at the species level, ranged from 1.105 to 1.007 at the population level, and the population mean was 1.039. The *H* value was 0.271 at the species level, ranging from 0.065 to 0.005 at the population level, and the population mean was 0.024. The *I* value was 0.412 at the species level, ranging from 0.008 to 0.099 at the population level, and the population mean was 0.036.

http://www.aloki.hu ● ISSN 1589 1623 (Print) ● ISSN 1785 0037 (Online)
DOI: http://dx.doi.org/10.15666/aeer/1906_45674581

Table 2. *Random amplification polymorphic DNA (RAPD) primer sequences and amplified products for nine T. arctica populations in South Korea*

Primer	Sequence (3'-5')	No. of loci	No. of polymorphic loci
OPA-10	GTGATCGCAG	7	5
OPN-08	ACCTCAGCTC	6	6
OPN-11	TCGCCGCAAA	10	8
OPN-15	CAGCGACTGT	9	8
OPO-03	CTGTTGCTAC	8	8
OPP-05	CCCCGGTAAC	7	7
OPP-06	GTGGGCTGAC	7	5
OPAF-11	ACTGGGCCTC	8	6
OPAF-16	TCCCGGTGAG	10	10
OPAF-17	TGAACCGAGG	9	7
Mean		8.1	7

Table 3. *The genetic variations revealed through random amplification polymorphic DNA (RAPD) markers among populations of T. arctica in South Korea*

Populations	PPB	*Ao*	*Ae*	*H*	*I*
YN	2.5	1.024	1.017	0.010	0.015
SA1	1.2	1.012	1.011	0.006	0.008
SA2	4.9	1.049	1.016	0.012	0.019
SA3	9.9	1.099	1.049	0.032	0.050
TB1	18.5	1.185	1.105	0.065	0.099
TB2	3.7	1.037	1.007	0.005	0.009
GY	14.8	1.148	1.084	0.051	0.077
JR1	3.7	1.037	1.027	0.016	0.023
JR2	4.9	1.049	1.031	0.018	0.028
Average	7.1	1.071	1.039	0.024	0.036
Total	86.4	1.864	1.454	0.271	0.412

PPB=Percentage of polymorphic band; Ao=Observed number of alleles; Ae= Effective number of alleles; H=Nei's gene diversity; I=Shannon's information index; Population abbreviations are shown in *Table 1*

Among the nine populations, the population with the highest genetic diversity was the TB1 population, followed by the GY and SA3 populations. In comparison with the other populations, the SA1 population had the lowest genetic diversity in the PPB, *Ao*, *Ae*, and *I* indices, and the TB2 population in the *H* index. The genetic diversity of each population differed even for subpopulations distributed on the same mountain. In particular, the Mt. Taebaek subpopulations showed large differences in their genetic diversity.

Genetic structure

The coefficient of genetic differentiation between populations, derived from Nei's genetic diversity statistics, showed a significantly high value ($Gst = 0.911$). This indicates that each population is highly differentiated with a large genetic difference, similar to the results obtained from the AMOVA analysis. According to our AMOVA analysis, 96% of the total genetic variation was due to genetic differences between populations, and only the remaining 4% was due to variations within populations (*Table 4*). These results show that individuals within a population are nearly genetically homogeneous, while genetic differences between populations are quite large. This is also supported by the results of

http://www.aloki.hu ● ISSN 1589 1623 (Print) ● ISSN 1785 0037 (Online)
DOI: http://dx.doi.org/10.15666/aeer/1906_45674581

the PCoA analysis, which showed that each individual in a population was distributed independent from individuals in other populations to form their own populations (*Fig. 3*).

Table 4. *Analysis of molecular variance (AMOVA) for populations of T. arctica in South Korea*

Source of variance	d.f.	Variance components	% of total variance	*P*-value
Among Populations	8	2,760.489	96	< 0.001
Within Population	261	109.467	4	
Total	269	2,869.956	100	

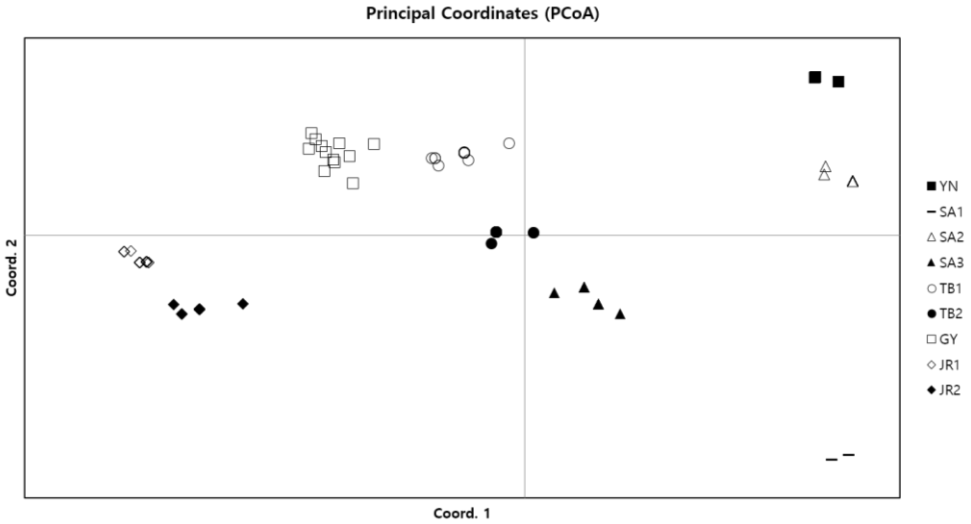

Figure 3. *Principal coordinates analysis (PCoA) plot for 270 individuals from nine T. arctica populations in South Korea based on Random Amplification Polymorphic DNA (RAPD) markers. Population abbreviations are shown in Table 1*

Genetic distances between individual populations ranged from 0.173 to 0.515, with significant differences between pairs of populations (*Table 5*). The genetic distance was the shortest between the two sub-populations on Mt. Taebaek, and the genetic distance between SA1 and JR1 was the farthest. Our results showed that SA3 and SA2, which are subpopulations on Mt. Seorak, showed relatively close genetic distance, but SA1 showed the greatest genetic distance from other populations.

Table 5. *Genetic identities (above diagonal) and Nei's genetic distance (below diagonal) between nine populations of T. arctica in South Korea*

Population	YN	SA1	SA2	SA3	TB1	TB2	GY	JR1	JR2
YN	-	0.656	0.793	0.703	0.680	0.651	0.694	0.606	0.615
SA1	0.422	-	0.725	0.733	0.633	0.686	0.630	0.598	0.609
SA2	0.232	0.322	-	0.828	0.772	0.752	0.715	0.630	0.632
SA3	0.352	0.311	0.189	-	0.760	0.791	0.736	0.744	0.763
TB1	0.386	0.458	0.259	0.274	-	0.841	0.800	0.719	0.730
TB2	0.430	0.378	0.285	0.235	0.173	-	0.758	0.725	0.715
GY	0.366	0.462	0.335	0.306	0.224	0.278	-	0.824	0.728
JR1	0.501	0.515	0.461	0.296	0.329	0.322	0.194	-	0.805
JR2	0.486	0.497	0.459	0.271	0.315	0.336	0.318	0.217	-

Population abbreviations are shown in *Table 1*

http://www.aloki.hu ● ISSN 1589 1623 (Print) ● ISSN 1785 0037 (Online)
DOI: http://dx.doi.org/10.15666/aeer/1906_45674581

The UPGMA dendrogram, which was constructed based on the genetic distance between each population, showed that populations were clustered according to geographic location with some exceptions (*Fig. 4*). The TB1 and TB2 populations were collected first, followed by SA2. Unlike the other two subpopulations on Mt. Seorak, SA1 showed the most distant relationship with all other populations. The YN population was the second-most distant, after SA1, from the rest of the populations. The two subpopulations of Mt. Jiri were not clustered closest to each other, but the JR1 and GY populations were collected first, after which the JR2 population was grouped.

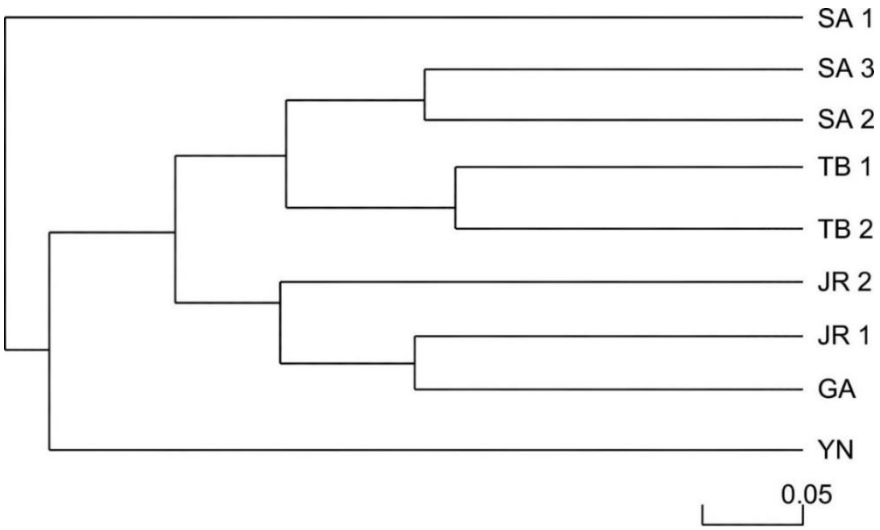

Figure 4. *The unweighted pair group method with arithmetic mean (UPGMA) dendrogram of the nine T. arctica populations in South Korea. The scale bar represents Nei's genetic distance. Population abbreviations are shown in Table 1*

The PCoA plot of the RAPD banding pattern of all *T. arctica* individuals showed that most individuals from a given population were inclined to cluster together (*Fig. 3*). Axis one and axis two explained 26.05% and 16.33% of the total genetic variation, respectively. The Mantel test showed no significant correlation between genetic and geographic distance ($r^2 = 0.03$, $p > 0.090$).

Discussion

Genetic diversity

T. arctica showed relatively high genetic diversity at the species level, but very low values at the population level. The genetic diversity at the species level was either higher or similar to that of other species of the same primula family (PPB = 86.4%, He = 0.27, I = 0.41). However, the genetic diversity at the population level was lower than that of other species (*Table 6*).

The high genetic diversity of *T. arctica* at the species level is likely influenced by past ancestral populations. The distribution of many existing plant species is known to be influenced by the quaternary glaciers (Hewitt, 2000). Northern plants expanded to the south during the ice age, retreated to the north after the Interglacial Period, and were trapped in the low-temperature highlands. *T. arctica*, which is a northern plant, is also

http://www.aloki.hu ● ISSN 1589 1623 (Print) ● ISSN 1785 0037 (Online)
DOI: http://dx.doi.org/10.15666/aeer/1906_45674581

believed to have undergone the same process. Considering the worldwide distribution of *T. arctica*, the genetic variation of *T. arctica* distributed throughout the Korean Peninsula during the ice age may have been abundant. Therefore, the high species-level genetic diversity at present is thought to have been inherited from the high genetic diversity of the ancestral populations (Comes and Kaderetit, 1998; Ge et al., 2005).

Table 6. *Comparison of the genetic diversity in T. arctica and literature data for other Primulaceae species*

Species	Marker	Status	PPB		*He*		*I*		*Φst*	*Gst*	*Fst*	References
			Pop.	Sp.	Pop.	Sp.	Pop.	Sp.				
T.arctica	RAPD	EN	7.1	86.4	0.024	0.271	0.036	0.412	0.96	0.911		This study
P.interjacens	ISSR	ED	59.75	75.47	0.2368	0.3205	0.3459	0.4618		0.2613		XUE et al., 2004
P.merrilliana	ISSR	EN,ED	44.28	79.56	0.12	0.25	0.19	0.38	0.494			Shao et al., 2009
P.farinosa	RAPD		82.3		0.21		0.33		0.17			Reisch et al., 2005
P.apennina	ISSR	ED	75.92	96.95	0.204	0.242	0.319	0.381	0.14	0.157		Crema et al., 2009
P.sikkimensis	ISSR						0.3211	0.5576		0.4127		Wang et al., 2005
	ISSR		79.3		0.268	0.4032	0.3211	0.5576				Wang et al., 2008
	CpSSR									0.697		
O.souliei	ISSR	EN	15.71	42.53			0.0701	0.1762		0.6038	0.6797	Huang et al., 2009

EN = Endangered species; ED = Endemic species; PPB = Percentage of Polymorphic Band; He = Expected Heterozygosity; I = Shannon's information index; Pop. = Population level; Sp. = Species level; RAPD =Rrandom Amplification Polymorphic DNA; ISSR = Inter Simple Sequence Repeat; CpSSR = Chloroplast Simple Sequence Repeat

At the population level, *T. arctica* showed low genetic diversity (*Table 6*). The genetic diversity of any species or population is a product of the combined effects of genealogical history and evolutionary processes (Comes and Kaderetit, 1998). The low genetic diversity of *T. arctica* at the population level can be explained by two causes: historical factors and the life history of *T. arctica*. First, the diversity of the *T. arctica* population was very low in comparison with the diversities of populations with similar life-history traits. It was lower than the average of perennial herbs and lower than those of self-fertilizing plants and clonal plants (Nybom, 2004). It was also lower than that of other Primulaceae species (*Table 6*). The main reason for the low population-level genetic diversity may have been the historical factors associated with this species. Long-term isolation and a reduction in population size may cause multiple genetic drifts, resulting in the loss of genetic variation and a decrease in genetic diversity within the population. Second, the low population-level genetic diversity of *T. arctica* is affected by the life history of *T. arctica*, which is known to reproduce primarily by its creeping roots in the ground (Tylor et al., 2002). These reproductive methods are advantageous in maintaining the survival of individuals but may be disadvantageous in terms of genetic diversity. When populations are divided or suffer local extinctions due to various reasons such as fire, feeding, and extreme weather, clonal plants have an advantage in increasing the number of individuals but, since all daughters have the same genotype, their genetic

http://www.aloki.hu ● ISSN 1589 1623 (Print) ● ISSN 1785 0037 (Online)
DOI: http://dx.doi.org/10.15666/aeer/1906_45674581

diversity decreases. Therefore, the low genetic diversity of *T. arctica* at the population level is due to the fact that the current population consists of individuals originating from a small number of individuals.

Genetic differentiation and gene flow among populations

The genetic structure of a plant population reflects the interaction of various factors such as long-term evolutionary history, genetic drift, mating system, gene flow, and selection (Hamrick and Godt, 1996; Nybom and Bartish, 2000; Nybom, 2004). The AMOVA analysis was performed to measure the degree of genetic differentiation among *T. arctica* populations, and it showed an *Φst* value of 0.96, indicating a very high level of inter-population genetic differentiation. This means that 96% of the total genetic variation is attributable to the genetic difference between populations and only the remaining 4% is due to the genetic variation within populations. In addition, *Nm*, which was calculated on the basis of the *Φst* value, showed a very low value of 0.01, indicating only 0.01 individuals between populations per generation move. Thus, each *T. arctica* population is composed of a small number of genetic traits that are very different from each other, and there is no exchange of genetic traits between them. These results showed a similar trend as that from the *Gst* value derived from Nei's genetic statistics, which was 0.911. In comparison, in studies using dominant markers RAPD and ISSR for other constituents of the same family, *Primula farinose*, *Primula interjacens*, *Primula merrilliana*, *Primula apennina*, and *Primula sikkimensis* had *Φst* or *Gst* values ranging from 0.14 to 0.49. The *Gst* value of *T. artica* in our study was very high in comparison with these values. In addition, *Omphalogramma souliei* showed a *Φst* value of 0.60 and an *Fst* value of 0.68, which was relatively high but lower than that of *T. arctica* (*Table 6*). A previous study by Nybom (2004), which summarizes the genetic variation indices reported in RAPD studies, shows that the genetic differentiation of plant species with life history traits such as annual life form (*Φst* = 0.62, *Gst* = 0.47), selfing breeding system (*Φst* = 0.65, *Gst* = 0.59), and attached seed dispersal mechanism (*Φst* = 0.46, *Gst* = 0.32) is higher than that of other forms. *T. arctica* showed significantly higher values (*Φst* = 0.96, *Gst* = 0.911) than these values, regardless of the corresponding life history traits. *T. arctica* shows an extremely high degree of genetic differentiation, and the main reason for this phenomenon is probably the low genetic diversity of populations as well as the decline in habitats due to climate change and long-term isolation of this species. This may be due to the historical process.

The genetic differentiation analysis suggested that *T. arctica* populations were very different from each other and were genetically independent, and PCoA analysis also showed that this trend was consistent. Individuals from individual populations did not mix with individuals from other populations, and there was no significant relationship among populations. The UPGMA dendrogram showed a form in which the geographic location and genetic distance did not completely match. Each subpopulation generally showed close correlation with each other, but there were also very heterogeneous populations, such as SA1. In addition, the Mantel test showed low significance and no correlation between geographic distance and genetic distance ($r^2 = 0.03$, $p > 0.09$). This is thought to be the result of genetic diversity within the population, even though the populations are geographically close and the gene flow between populations is very low (*Nm* = 0.01). The loss of common genotypes between populations is caused by a variety of reasons, such as habitat fractionation and genetic drift, whereas the fixation of

http://www.aloki.hu ● ISSN 1589 1623 (Print) ● ISSN 1785 0037 (Online)
DOI: http://dx.doi.org/10.15666/aeer/1906_45674581

population-specific traits is thought to increase genetic differences between populations because genetic commonality cannot be restored due to low gene flow.

Implications for conservation

Maintenance of genetic variation is one of the main objectives of conservation of endangered and threatened species, and knowledge of genetic variation within and between populations provides essential information for the proper conservation management (Hamrick and Godt, 1996). The results of this study show that the *T. arctica* population has low genetic diversity, high genetic differentiation, and very low gene flow. This information could be applied for conservation of *T. arctica*.

Since each population of *T. arctica* has low genetic diversity and exhibits an independent genetic trait, all populations should be subject to in situ conservation. Specific management options for in situ conservation should take into account the habitat and physiological and ecological characteristics of this species. First, the area where each population is located must be designated as a conservation area and protected, and the conservation of woody vegetation in the upper layer is necessary depending on the characteristics of species located in the herbaceous layer of forest vegetation. Since a large number of populations are located around the trails, damage caused by foot pressure by implementation of facilities such as fences or changes to the trails should be minimized. In addition, damage or loss of the soil around the habitat should be taken into account, considering the life history of the species, which breeds mainly by generating bulbs under the ground.

Considering the characteristics of species with high genetic differentiation, the collection of germplasms for ex situ conservation should be carried out in the maximum possible number of populations so as to allow segregation of as many genetic traits as possible. Since the level of genetic variation of the selectively neutral marker loci is mainly generated by mutation or genetic drift (Kimura, 2020), the level of variation detected by RAPD does not directly reflect the level of variation that determines the degree of adaptation or the individual's fitness (Booy et al., 2000). Therefore, samples from various habitats should be considered for conservation (Ge et al., 2005). When considering the restoration of habitats or the creation of alternative habitats, it is necessary to select an area with the ecological characteristics of the species habitats, such as relatively low temperatures (average temperature in July, below 15.6°C), high organic matter content in the soil, and relatively low soil pH (Taylor et al., 2002). For conservation of botanical or genetic resources, the genetic diversity of the population should be increased by introducing individuals from various populations, considering the low genetic diversity of a single population.

A representative example of successful conservation and restoration of alpine plants is *Potentilla robbinsiana* in Illinois, USA. Habitat protection through the relocation of hiking trails and designation of protected areas, long-term monitoring, and various research and restoration work on the habitats ensured the development of stable populations and eventually removing them from list of endangered species (Brumback et al., 2004). The case of this species may help the research and management groups in the protection and restoration of *T. arctica*.

http://www.aloki.hu ● ISSN 1589 1623 (Print) ● ISSN 1785 0037 (Online)
DOI: http://dx.doi.org/10.15666/aeer/1906_45674581

Conclusions

The aim was to study attempted to determine the level and structure of genetic variation in nine natural populations of *T. arctica*, an endangered species in South Korea, by using RAPD markers. In South Korea, these results were studied here first in natural populations of *T. arctica*.

T. arctica has high genetic diversity at the species level, but low genetic diversity at the population level. In addition, *T. arctica* showed a high degree of genetic differentiation between populations and limited gene flow. The genetic diversity and structure of *T. arctica* are thought to be influenced by the historical factor as an ice age species and life history traits, which are clonal plants.

Considering the genetic diversity and structure of this species, extremely low genetic diversity in population level and high genetic differentiation, both in situ and ex situ conservation should be carried out actively for this species.

Further studies using various markers, such as allozyme amplified fragment length polymorphism (AFLP), and chloroplast DNA (cpDNA) sequences may help to obtain more accurate information on the level and structure of genetic variation in the *T. arctica* population. Moreover, comparison with the samples derived from other regions of the Northern Hemisphere, such as Europe or northern China, is expected to broaden the perspectives on the genetic linkage and current status of *T. arctica* population in South Korea.

Acknowledgement. This research was supported by the Chung-Ang University Research Scholarship Grants in 2021.

REFERENCES

[1] Booy, G., Hendriks, R. J. J., Smulders, M. J. M., Van Groenendael, J. M., Vosman, B. (2000): Genetic diversity and the survival of populations. – Plant biology 2(4): 379-395.

[2] Brumback,W. E., Weihrauch, D. M., Kimball, K. D. (2004): Propagation and Transplanting of an Endangered Alpine Species, Robbins' Cinquefoil *Potentilla robbinsiana* (Rosaceae). – Native Plants Journal 5(1): 91-97.

[3] Chung, M. Y., López-Pujol, J., Maki, M., Kim, K. J., Chung, J. M., Sun, B. Y., Chung, M. G. (2012): Genetic diversity in the common terrestrial orchid *Oreorchis patens* and its rare congener *Oreorchis coreana*: inference of species evolutionary history and implications for conservation. – Journal of Heredity 103: 692-702.

[4] Chung, M. Y., Moon, M. O., López-Pujol, J., Chung, J. M., Chung, M. G. (2013): Genetic diversity in the two endangered endemic species *Kirengeshoma koreana* (Hydrangeaceae) and *Parasenecio pseudotaimingasa* (Asteraceae) from Korea: Insights into population history and implications for conservation. – Biochemical Systematics and Ecology 51: 60-69.

[5] Chung, M. Y., López-Pujol, J., Chung, M. G. (2014): Genetic homogeneity between Korean and Japanese populations of the broad-leaved evergreen tree *Machilus thunbergii* (Lauraceae): A massive post-glacial immigration through the Korean Strait or smoething else? – Biochemical Systematics and Ecology 53: 20-28.

[6] Comes, H. P., Kadereit, J. W. (1998): The effect of Quaternary climatic changes on plant distribution and evolution. – Trends in plant science 3: 432-438.

[7] Crema, S., Cristofolini, G., Rossi, M., Conte, L. (2009): High genetic diversity detected in the endemic *Primula apennina* Widmer (Primulaceae) using ISSR fingerprinting. – Plant Systematics and Evolution 280: 29-36.

http://www.aloki.hu ● ISSN 1589 1623 (Print) ● ISSN 1785 0037 (Online)
DOI: http://dx.doi.org/10.15666/aeer/1906_45674581

[8] Excoffier, L., Laval, G., Schneider, S. (2005): Arlequin (version 3.0): an integrated software package for population genetics data analysis. – Evolutionary Bioinformatics 1: 47-50.
[9] Ge, X. J., Zhang, L. B., Yuan, Y. M., Hao, G., Chiang, T. Y. (2005): Strong genetic differentiation of the East-Himalayan *Megacodon stylophorus* (Gentianaceae) detected by inter-simple sequence repeats (ISSR). – Biodiversity & Conservation 14(4): 849-861.
[10] Hamrick, J. L., Godt, M. J. W. (1996): Effects of life history traits on genetic diversity in plant species. – Philosophical Transactions of the Royal Society in Lodon, Series B 351: 1291-1298.
[11] Hewitt, G. (2000): The genetic legacy of the Quaternary ice ages. – Nature 405: 907-913.
[12] Hiirsalmi, H. (1969): *Trientalis europaea* L. A study of the reproductive biology, ecology and variation in Finland. – Annales Botanici Fennici 6: 119-173.
[13] Huang, Y., Zhang, C. Q., Li, D. Z. (2009): Low genetic diversity and high genetic differentiation in the critically endangered *Omphalogramma souliei* (Primulaceae): implications for its conservation. – Journal of Systematics and Evolution 47: 103-109.
[14] Jeong, J. H., Kim, E. H., Guo, W., Yoo, K. O., Jo, D. G., Kim, Z. S. (2010): Genetic diversity and structure of the endangered species *Megaleranthis saniculifolia* in Korea as revealed by allozyme and ISSR markers. – Plant systematics and evolution 289(1-2): 67-76.
[15] Jiménez, J. F., Sánchez-Gómez, P., Güemes, J., Werner, O., Rosselló, J. A. (2002): Genetic variability in a narrow endemic snapdragon (*Antirrhinum subbaeticum*, Scrophulariaceae) using RAPD markers. – Heredity 89: 387-393.
[16] Kim, B. D., Kang, S. G., Yu, S. T., Shin, H. T. (2012): A study on the plants for phenology of the Mt. Gaya National Park. – Journal of Climate Research 7: 174-186.
[17] Kim, Y. C., Chae, H. H., Oh, S. H., Choi, S. H., Hong, M. P., Nam, G. H., Choi, J. Y., Choi, H. S., Lee, K. S. (2015): Floristic characteristics of vascular plants and first distributional report of *Pseudostellaria baekdusanensis* M. Kim in Yongneup wetland protected area. – Korean Journal of Environment and Ecology 29: 132-159.
[18] Kim, Y. Y., Leem, H., Han, S., Ji, S. J., So, S. (2017): Conservation measures and distribution of vulnerable species for climate change in Gayasan National Park. – Korean Journal of Plant Resources 30: 167-175.
[19] Kimura, M. (2020): The neutral theory and molecular evolution. In My Thoughts on Biological Evolution. – Springer, Singapore, pp 119-138.
[20] Korea National Arboretum. (2009): Rare plants data book in Korea. – GeoBook Publishing Co. Seoul.
[21] Kovanda, M. (1995): Reproductive strategy and morphological variation in *Trientalis europea*. – Verhandlungen der Zoologisch-Botanischen Gesellschaft in Österreich 132: 251-264.
[22] Lee, T. B. (2003): Illustrated Flora of Korea. – Hyang-mun Pub. Co., Seoul.
[23] Lee, Y. N. (2006): New flora of Korea. – Kyo-Hak Pub. Co., Seoul.
[24] Lee, S. H., Yeon, M. H., Shim, J. K. (2016): Conservation implications of the genetic diversity of *Gymnospermium microrrhynchum* in Korea. – Genetics and molecular research: GMR 15.4.
[25] Li, L., Park, E. K., Park, M. O., Koo, B. H. (2014): Ecosystem Analysis for Little Yong-neup, Baby Yong-neup in Daeam-san in Korea. – Journal of the Korean Society of Environmental Restoration Technology 17: 43-56.
[26] Mantel, N. (1967): The detection of disease clustering and a generalized regression approach. – Cancer Research 27: 209-220.
[27] Nybom, H., Bartish, I. V. (2000): Effects of life history traits and sampling strategies on genetic diversity estimates obtained with RAPD markers in plants. – Perspectives in Plant Ecology, Evolution and Systematics 3(2): 93-114.
[28] Nybom, H. (2004): Comparison of different nuclear DNA markers for estimating intraspecific genetic diversity in plants. – Molecular ecology 13: 1143-1155.

http://www.aloki.hu ● ISSN 1589 1623 (Print) ● ISSN 1785 0037 (Online)
DOI: http://dx.doi.org/10.15666/aeer/1906_45674581

[29] Park, K. H., Son, J. I., Kwon, J. H. (2011): A Study on Vascular Plants around the Seobuk-Ridgeline of Seoraksan National Park. – Journal of National Park Research 2: 19-32.
[30] Park, J. H., Kim, J. G. (2012): Ecological Characteristics of *Pseudostellaria baekdusanensis* in Mt. Odae: 2. Conservation Area of Jilmoe-neup. – Journal of Wetlands Researh 14: 101-120.
[31] Pauls, S. U., Nowak, C., Bálint, M., Pfenninger, M. (2013): The impact of global climate change on genetic diversity within populations and species. – Molecular Ecology 22: 925-946.
[32] Peakall, R., Smouse, P. E. (2006): GENALEX 6 genetic analysis in Excel. Population genetic software for teaching and research. – Molecular Ecology Notes 6: 288-295.
[33] Piqueras, J., Klimes, L. (1998): Demography and modeling of clonal fragments in the pseudoannual plant *Trientalis europea* L. – Plant ecology 136: 213-227.
[34] Piqueras, J. (1999): Herbivory and ramet performance in the clonal herb *Trientalis europeae* L. – Journal of Ecology 87: 450-460.
[35] Piqueras, J., Klimes, L., Redbo-Torstensson, P. (1999): Modelling the morphological response to nutrient availability in the clonal plant *Trientalis europaea* L. – Plnat Ecology 141: 117-127.
[36] Reisch, C., Anke, A., Röhl, M. (2005): Molecular variation within and between ten populations of *Primula farinosa* (Primulaceae) along an altitudinal gradient in the northern Alps. – Basic and Applied Ecology 6: 35-45.
[37] Shao, J. W., Chen, W. L., Peng, Y. Q., Zhu, G. P., Zhang, X. P. (2009): Genetic diversity within and among populations of the endangered and endemic species *Primula merrilliana* in China. – Biochemical Systematics and Ecology 37: 699-706.
[38] Shin, H. T., Yi, M. H., Yoon, J. W., Yoo, J. H., Lee, B. C., Park, E. H. (2010): Distribution of rare plants and endemic plants in Jirisan national park. – Journal of Korean Nature 3: 219-222.
[39] Singh, S., Panda, M. K., Nayak, S. (2012): Evaluation of genetic diversity in turmeric (*Curcuma longa* L.) using RAPD and ISSR markers. – Industrial Crops and Products 37: 284-291.
[40] Slatkin, M., Barton, N. H. (1989): A comparison of three indirect methods for estimating average levels of gene flow. – Evolution 43: 1349-1368.
[41] Song, J. M., Choi, K. H., Lee, K. Y. (2009): Soil Properties and Vegetation Structure of Natural Habitat of Endangered Plant, *Trientalis europaea* L. – Journal of Korean Society of Forest Science Academic Symposium Annual Report, pp. 163-165.
[42] Sung, J. W., Kim, G. H. (2018): Changes of Flowering Time Affected by Climate Change in the Subalpine Region of Mt. Gaya. – Journal of Agriculture & Life Science 52: 13-23.
[43] Taylor, K., Havill, D. C., Pearson, J., Woodall, J. (2002): *Trientalis europaea* L. – Journal of Ecology 90(2): 404-418.
[44] Tikhodeyev, O. N., Neustroeva, M. A., Tikhodeyeva, M. Y. (2003): (+1) and (-1) deviations in development of floral meristems in *Trientalis europaea* L. – Wulfenia 10: 103-114.
[45] Wang, F. Y., Ge, X. J., Hao, G., Hu, Q. M. (2005): Genetic diversity and differentiation in *Primula sikkimensis* (Primulaceae) in Himalayan-hengduan mountains. – Journal of Tropical and Subtropical Botany 13: 149-153.
[46] Wang, F. Y., Ge, X. J., Gong, X., Hu, C. M., Hao, G. (2008): Strong genetic differentiation of *Primula sikkimensis* in the East Himalaya–Hengduan Mountains. – Biochemical Genetics 46: 75-87.
[47] Wang, Y., Qin, Y., Du, Z., Yan, G. (2012): Genetic diversity and differentiation of the endangered tree *Elaeagnus mollis* Diels (*Elaeagnus* L.) as revealed by Simple Sequence Repeat (SSR) Markers. – Biochemical Systematics and Ecology 40: 25-33.
[48] Williams, J. G., Kubelik, A. R., Livak, K. J., Rafalski, J. A., Tingey, S. V. (1990): DNA polymorphisms amplified by arbitrary primers are useful as genetic markers. – Nucleic acids research 18: 6531-6535.

http://www.aloki.hu ● ISSN 1589 1623 (Print) ● ISSN 1785 0037 (Online)
DOI: http://dx.doi.org/10.15666/aeer/1906_45674581

[49] Xue, D. W., Ge, X. J., Hao, G., Zhang, C. Q. (2004): High genetic diversity in a rare, narrowly endemic primrose species: *Primula interjacens* by ISSR analysis. – Acta Botanica Sinica (English edition) 46: 1163-1169.
[50] Yeh, F. C., Boyle, T., Yang, R. C. (1999): PopGene. – Microsoft Window-based freeware for population genetic analysis, version 1.31.
[51] Yoon, J. W., Shin, H. T., Kim, S. J., Heo, T. I., An, J. B., Kwon, Y. H. (2015): A Study on the Distribution of Rare and Endemic Plants in Eastern DMZ Region. – Korean Journal of Plant Resources Academic Symposium, p.27.

http://www.aloki.hu ● ISSN 1589 1623 (Print) ● ISSN 1785 0037 (Online)
DOI: http://dx.doi.org/10.15666/aeer/1906_45674581

VARIATION AND PREDICTION OF LANDSCAPE PATTERN AND HABITAT CONSERVATION BASED ON CA-MARKOV AND INVEST MODEL IN HAIHE SOURCE REGION, CHINA

WANG, J.[1] – WU, T.[1] – LI, Q.[2] – WANG, S.[1*]

[1]*School of Geographical Science, Shanxi Normal University, Taiyuan 030000, Shanxi Province, P. R. China*

[2]*Institute of Geographical Sciences, Hebei Academy of Sciences, Hebei Engineering Research Center for Geographic Information Application, Shijiazhuang 050011, Heibei Province, P. R. China*

**Corresponding author*
e-mail: wangsheng@sxnu.edu.cn

(Received 21st Jun 2021; accepted 3rd Sep 2021)

Abstract. The fragmentation of landscape caused by urbanization and over-exploitation of water resource could result in the degradation of ecosystem services in arid and semiarid regions. Dynamic monitoring of habitat variation is of great significance to maintain regional ecological security. Habitat quality decreased from 1990 to 2015, and the mean habitat quality decreased by 1.83% in the Zhanghe River Basin in China. The habitat degradation increased during the 1990-2010 period, then decreased in 2010-2015. The spatial pattern of habitat quality and land use type correlated: The highest values were mainly distributed in the northern hilly region with high vegetation coverage, while the lowest values were mainly located in the southern crop and construction lands. The highest habitat degradation level occurred mainly along the roads and the agricultural areas of the peri-urban fringe. The correlation analysis indicated that slope was the dominant factor ($r = 0.72$, $p < 0.01$) on habitat quality, followed by land use intensity ($r = -0.57$, $p < 0.01$). Furthermore, habitat quality was also affected by landscape pattern, and presented positive correlation with the Contagion Index, Shannon Diversity Index, Shannon Evenness Index, Landscape Shape Index and Mean Patch Size. These results could provide scientific basis for optimizing regional ecological environment and landscape management in arid and semiarid regions.
Keywords: *habitat variation, model simulation, correlation analysis, landscape pattern, Zhanghe River Basin*

Introduction

River areas, which provide many resources, such as fresh water, hydropower, fertile land, and support 10% of all known species (Carrizo et al., 2013), are the most productive ecosystems around the world. Unfortunately, 48% of river is facing moderate and severe fragmentation by increasingly intensive anthropogenic activities (e.g. dam construction) on a global basis (Grill et al., 2015), and causes drastic change of land use types in the basin, which could lead to biodiversity loss, habitat degradation, and produce important effect on watershed ecosystem services (Nelson et al., 2010; Seto et al., 2012). During the last decades, China has suffered the largest extinction of species, the watershed biodiversity in China continued to decline despite government efforts to alleviate threats, many precious species and habitat have lost (Liu et al., 2003). Thus, promoting the balance between habitat conservation and meeting development demands has become an increasingly urgent issue (He et al., 2017).

Habitat quality is used as an important indicator for biodiversity (Tallis et al., 2010), to some extent it can assess ecological environment change. Currently,

http://www.aloki.hu ● ISSN 1589 1623 (Print) ● ISSN 1785 0037 (Online)
DOI: http://dx.doi.org/10.15666/aeer/1906_45834597

researchers have effectively evaluated the variation of habitat quality and degradation at different scales, such as regional (Upadhaya et al., 2019), local (Sallustio et al., 2017), coastal zones (Zhang et al., 2020) and islands (Moreira et al., 2018). Traditional field surveys, ecological indicators and ecological model are three major methods to assess habitat quality change (Sun et al., 2019). Among these, the Integrated Valuation of Ecosystem Services and Tradeoffs (InVEST)-habitat quality (HQ) is widely used to calculate habitat quality and degradation based on land use and provides a visual tool which quantitatively evaluates biodiversity conservation, especially in areas with scarce data (Sharp et al., 2016). Sun et al. (2019) utilized InVEST model to monitor and analyze the dynamics and potential factors of habitat quality in the Nansihu Lake Basin from 1980 to 2015. Li et al. (2020) assessed the effects of urban expansion on habitat quality in the middle reaches of Heihe River from 2015 to 2030 by using the InVEST model and the slope, land use, exclusion, urban extent, transportation and hillshade (SLEUTH) model.

Land use change is the most important driver on habitat degradation (Upadhaya et al., 2019), in particular, agriculture expansion strongly affects habitat quality (FAO, 2016; Lambin et al., 2003), and this trend particularly amplifies in northern China. Previous studies have found that the newly reclaimed land and construction land in northern China kept increasing in recent 30 years (Zhao et al., 2014; Angel et al., 2011), which led to a huge loss of biodiversity. Thus, understanding the effect of land use change on habitat conservation and biodiversity is important for ecological conservation and management (Sun et al., 2019). The CA-Markov model is the most widely applied tool for simulation and predication of land use patterns, and it integrates the complex spatial systems analysis capabilities of the CA model with the long-term forecasting techniques of the Markov model (Batty and Xie., 1994; Luijten., 2003). A number of studies have effectively applied CA-Markov to simulate land use in different spatial and temporal scale, such as, Nourqolipour et al. (2015) used CA, multi-criteria evaluation (MCE), and Markov chain (MC) to simulate the expansion of oil palm in the Kuala Langat district, Malaysia. Chen et al. (2018) simulates the future landscape pattern in Hubei Section of Three Gorges Reservoir area in 2020. Cheng et al. (2020) utilized the CA-Markov model to simulate the evolution trend of the land to propose the ecological division of the main urban area of Jinzhong in Shanxi Province.

In this paper, the spatio-temporal change of habitat quality and degradation was analyzed in Zhanghe River Basin, which was an important water conservation source for local and downstream areas. Zhanghe River Basin has experienced rapid urban expansion and over-exploitation of mineral resources, facing severe water resource shortage and prominent water conflicts, which has resulted in serious ecological threats. Previous studies focused on assessing the change of water quality, runoff, and sediment under the climate change and land use change. However, few studies were concerned with dynamic monitoring habitat conservation change. Thus, this study aimed to (1) assess habitat quality and degradation from 1990 to 2030 in the Zhanghe River Basin; (2) explore the main impact factors on habitat quality; and (3) analyze the role of the landscape pattern indexes on affecting habitat quality. The research fills a knowledge gap about the impact of anthropogenic activities (especially landscape pattern) on biodiversity status by adopting an integrative approach. This paper is helpful to understand the importance of landscape structure and pattern on habitat quality, and guide habitat conservation and management in arid/semi-arid areas facing serious water conflicts.

http://www.aloki.hu ● ISSN 1589 1623 (Print) ● ISSN 1785 0037 (Online)
DOI: http://dx.doi.org/10.15666/aeer/1906_45834597

Materials and methods

The Zhanghe River Basin

Zhanghe River (112°~114°30'E, 35°30'~38°N) is an important water conservation source for local and downstream areas, which are located in the southwest of Haihe River Basin, China (*Fig. 1*). It spans a total length of 460 km and has a drainage area of about 17874 km^2. Cropland, forestland, grassland, construction land and water bodies occupy 40%, 23%, 33%, 3%, and 0.9% in 2015, respectively (Wang et al., 2021). The basin is species-rich, including 40 families and 117 genera of bird species, and 26 of them are classified in the first or second levels of national protected birds, and is the home for several threatened wildlife species, such as the leopard and the taiga musk deer. Additionally, there are two or three hundred years of natural forest communities, and some wild plants, such as the *Juglans mandshurica, Amur linden* and *Acanthopanax senticosus.* The basin is rich in mineral resources, including coal, iron, aluminum, and other mineral resources. In recent years, water resource and biodiversity face severe threats under the impact of intensive human activities.

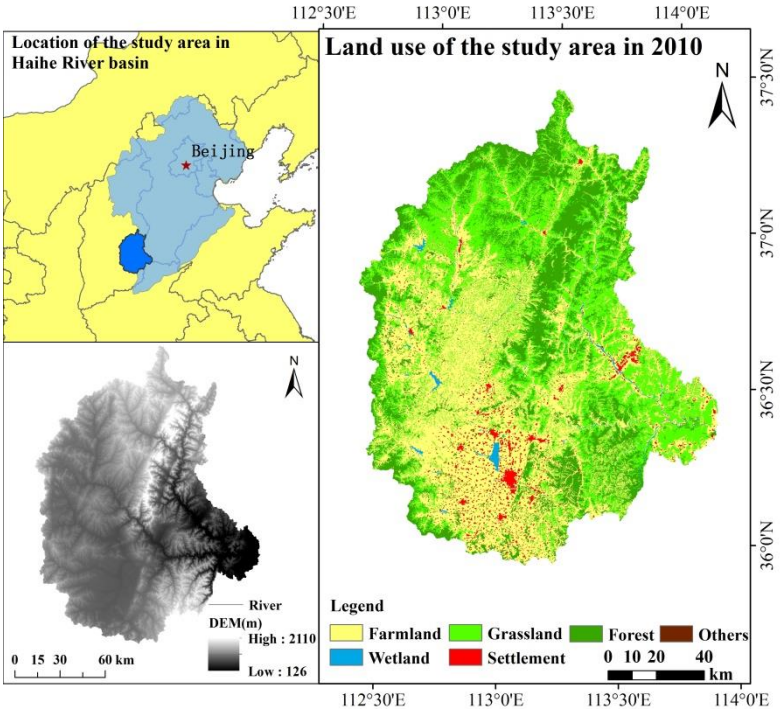

Figure 1. *Geographic location of Zhanghe River Basin of China*

Data collection

Land use data in 1990, 1995, 2000, 2005, 2010 and 2015 of Zhanghe River Basin were obtained from the Resource and Environmental Data Cloud Platform (http://www.resdc.cn/), with a spatial resolution of 1 km. The digital elevation model (DEM) data with 90 m resolution was downloaded from the Geospatial Data Cloud. A normalized difference vegetation index map (NDVI), a map of gross domestic product (GDP), and a population distribution map were collected by the Data Center for Resources and Environmental Sciences from the Chinese Academy of Sciences

http://www.aloki.hu ● ISSN 1589 1623 (Print) ● ISSN 1785 0037 (Online)
DOI: http://dx.doi.org/10.15666/aeer/1906_45834597

(RESDC) (http://www.resdc.cn). Main roads and railways were derived from the national fundamental geographic information system (http://nfgis.nsdi.gov.cn/).

Landscape pattern analysis

The effects of landscape patterns on ecological security are increasingly recognized. In this study, the landscape pattern indexes were used to assess the effect of LUCC on habitat quality in the Zhanghe River Basin by using FRAGSTATS version 4.2.1. Based on the relevant study (Han et al., 2019; Huang et al., 2020) and the scale of the study area, the variation of landscape pattern in Zhanghe River Basin was explored from two levels, including the class level and landscape level, and 8 indices were selected to describe landscape structure and patterns. At the class level, we chose the Number of Patches (NP), Patch Density (PD), Mean Patch Size (MPS), and Landscape Shape Index (LSI). At the landscape level, the Contagion Index (CONTAG), Shannon Diversity Index (SHDI), Shannon Evenness Index (SHEI), and Edge Density (ED) were calculated.

The InVEST-habitat quality module

InVEST-HQ module was used to assess the habitat quality and degradation degree of Zhanghe River Basin (Sharp et al., 2016). This model was developed at Stanford University, The Nature Conservancy and World-Wildlife Fund (Zhang et al., 2020), and was used to detect the impact of human activities on ecosystem based on suitability and threats and assumed that areas with high habitat quality would support more species (Terrado et al., 2016). The calculation method is as follows:

$$D_{xj} = \sum_{1}^{r}\sum_{1}^{y}\left(\frac{\omega_r}{\sum_{r=1}^{n}\omega_r}\right)\times r_y \times i_{rxy} \times \beta_x \times S_{jr} \quad \text{(Eq.1)}$$

$$i_{rxy} = \begin{cases} 1-\left(\dfrac{d_{xy}}{d_{r\max}}\right) \\ \exp\left[-\left(\dfrac{2.99}{d_{r\max}}\right)\times d_{xy}\right] \end{cases} \quad \text{(Eq.2)}$$

where r is the number of threats (r = 1,2,3…R); ω_r is the impact weight of threat *r*; r_y is the number of threat factors on each grid of land classification layers; i_{rxy} is the degradation decay function through distance, which can be expressed as the linear or exponential function of distance from threats to habitats; β_x is the accessibility level of pixel *x*; s_{jr} represents the sensitivity of habitat type *j* to threat *r*. d_{xy} is the linear distance between *x* and *y*; d_{rmax} is the maximum effective distance of threat *r*.

$$Q_{xj} = H_j\left[1-\left(\frac{D_{xj}^{z}}{D_{xj}^{z}+k_z}\right)\right] \quad \text{(Eq.3)}$$

where Q_{xj} is the habitat quality of raster *x* in land use type *j*; H_j is the habitat suitability of land use type *j*; D^z_{xj} is the threat level of raster *x* in land use type *j*; *K* and *Z* is the

http://www.aloki.hu ● ISSN 1589 1623 (Print) ● ISSN 1785 0037 (Online)
DOI: http://dx.doi.org/10.15666/aeer/1906_45834597

half-saturation constant and the scaling parameter to reflect the spatial heterogeneity, respectively.

The main data of the InVEST-HQ module include current LUCC, threats factor layers, index of threats and sensitivity, weight of threat factor, distance from threat (Zhang et al., 2020). For this study, we assumed that forest, grassland, and water provided better habitat conservation than agriculture and construction land (Upadhaya et al., 2019), so we set agriculture, construction land as the major threat factors. In addition, we also selected main roads and railways as threat factors (*Table 1*). The index of threats, sensitivity and other parameters were derived from cognate studies (Chen et al., 2020; Wu et al., 2015; Wang et al., 2019) (*Table 2*).

Table 1. *Maximum distance and weight of the threats affecting habitat quality*

Threat factor	Maximum effective distance	Weight	Decay
Agriculture	2	0.6	Linear
Construction land	8	1	Exponential
Main road	3	0.6	Exponential
Main railway	5	0.6	Exponential

Table 2. *The sensitivity of landscape types to each threat factor*

Land use type	Habitat	Agriculture	Construction land	Main road	Main railway
Agriculture	0.4	0.3	0.5	0.7	0.6
Forestland	1	0.6	0.8	0.7	0.8
Grassland	0.85	0.4	0.7	0.5	0.4
Water body	1	0.4	0.8	0.6	0.5
Construction land	0	0	0	0	0

The CA-Markov model

The CA-Markov model is an effective tool to predict LUCC. It considers spatial distribution of each land type and geographic directions (Mansour et al., 2020). We applied the CA-Markov module of IDRISI 17 to predict LUCC in 2030. To obtain the projected LUCC in 2030, we prepared suitability map for any land use type using Multi-Criteria-Evaluation (MCE). Under the background of fast urbanization and land use policy, it was assumed that current construction land and water remained unchanged, while the multiple ecological land was transformed into urban land. We have defined transition rules for any land use types considering a number of factors (e.g. elevation, slope, distance to road and railway, distance to city, population, and GDP).

In this paper, we set LUCC in 2000 as a starting year with the transition probability matrix of 1990-2000 and the suitability maps of each land use type to predict LUCC in 2010. The Kappa index was used to validate the accuracy of the projected LUCC in 2010 with the observed LUCC in 2010. The result (*Table 3*) showed the simulation generally matched well for each class type, so, the model could predict future land use in a reliable way. Therefore, based on the reliable simulation of LUCC in 2010, we used the transition probability matrix of 2000-2010 and the 2010 land use map to predict LUCC in 2030.

http://www.aloki.hu ● ISSN 1589 1623 (Print) ● ISSN 1785 0037 (Online)
DOI: http://dx.doi.org/10.15666/aeer/1906_45834597

Table 3. *Observed and simulated LUCC of Zhanghe River Basin in 2010*

Land use type	Agriculture	Forestland	Grassland	Water body	Construction land
Actual area	7213.07	4168.26	5829.49	160.43	497.37
Simulate area	7207.21	4047.70	5744.05	129.58	502.29
Kappa	0.96	0.92	0.99	0.80	0.75

Results

Landscape pattern indexes change

Extensive human activities in the Zhanghe River Basin have resulted in profound change in the size, number, and spatial distribution of landscape patterns, with the increase in habitat degradation (Han et al., 2019). Based on the statistical results (*Table 4*), NP, PD and ED increased by 3.58%, 2.75% and 1.38% from 1990 to 2010, respectively, then fell in 2015, which indicated that the watershed faced severe landscape fragmentation and heterogeneity during the 1990-2010 period, while slowed down in recent years. SHDI and SHEI showed an increasing tendency, and increased by 0.0891 and 0.0498, respectively. By contrast, CONTAG decreased continuously from 49.3957 to 46.5833, which reflected increased landscape diversity and heterogeneity in the last 25 years.

Table 4. *Landscape pattern indices of landscape level*

Year	NP	PD	ED	CONTAG	SHDI	SHEI
1990	16555	0.9295	36.4358	49.3957	1.1975	0.6683
2000	16584	0.9398	36.5753	49.2784	1.1999	0.6697
2005	16947	0.9516	36.8563	48.7547	1.2133	0.6772
2010	17114	0.9628	36.9402	48.6638	1.2153	0.6783
2015	17108	0.9567	36.5693	46.5833	1.2866	0.7181

At the class level (*Fig. 2*), the landscape with the highest NP, PD and LSI was grassland, the maximum appeared in 2010 and then decreased from 2010 to 2015, while MPS increased by 3.51%, demonstrating that landscape of grassland spatially centralized due to the GGP. NP and PD of agricultural land increased by 5.53% and 5.08%, while MPS decreased by 8.16%, which indicated that the degree of agriculture patches fragmentation increased in the past 25 years. NP and PD of forest land showed no obvious change, while MPS decreased, mainly manifested that forest land experienced fragmentation to a certain extent. NP and PD of construction land decreased, and MPS increased, which showed that construction land tended to expand and concentrate. Further analysis of the patch change based on LSI showed that construction land experienced large change. From 1990 to 2000, LSI of construction land showed no obvious change, while increased during 2005-2010 and then decreased in 2015.

Spatial distribution of habitat quality and degradation

The habitat quality value was between 0 and 1, and the closer to 1, the higher the habitat quality. Overall, the level of habitat quality was comparatively high since forestland and grassland accounted for about 58%, while decreased from 1990 to 2015 in

http://www.aloki.hu ● ISSN 1589 1623 (Print) ● ISSN 1785 0037 (Online)
DOI: http://dx.doi.org/10.15666/aeer/1906_45834597

the Zhanghe River Basin (*Fig. 3a*). The value of habitat quality showed slight decreasing trend during 1990-2010, with a rate of 0.15%, and then fell dramatically. The mean habitat quality decreased by 1.83% during 1990-2015. From the perspective of the spatial distribution pattern, the distribution of habitat quality was correlated with land use type. Specifically, the lowest habitat quality was mainly consistent with construction land and agricultural land, which was mainly distributed in the central and western plain, while the highest habitat quality was distributed in the northern and southeast mountain which were thickly forested and grassed (*Fig. 4*). Furthermore, based on the natural breaks method and cognate studies (He et al., 2017; Tang et al., 2020), we divided habitat quality into five classes: low quality (0-0.25), relatively low (0.26-0.65), medium (0.66-0.85), relatively high (0.86-0.95) and high quality (0.96-1.0). In 1990, the area with low and relatively low habitat quality accounted for 43.4%, while the high and relatively high accounted for only 24.2% of all habitats. In 2015, the area with low and relatively low habitat quality increased by 1%, while the high and relatively high habitat quality area decreased by 0.7%, and the medium grade decreased by 0.58%. This indicated that the habitat quality declined mainly due to the contraction of high and medium grades.

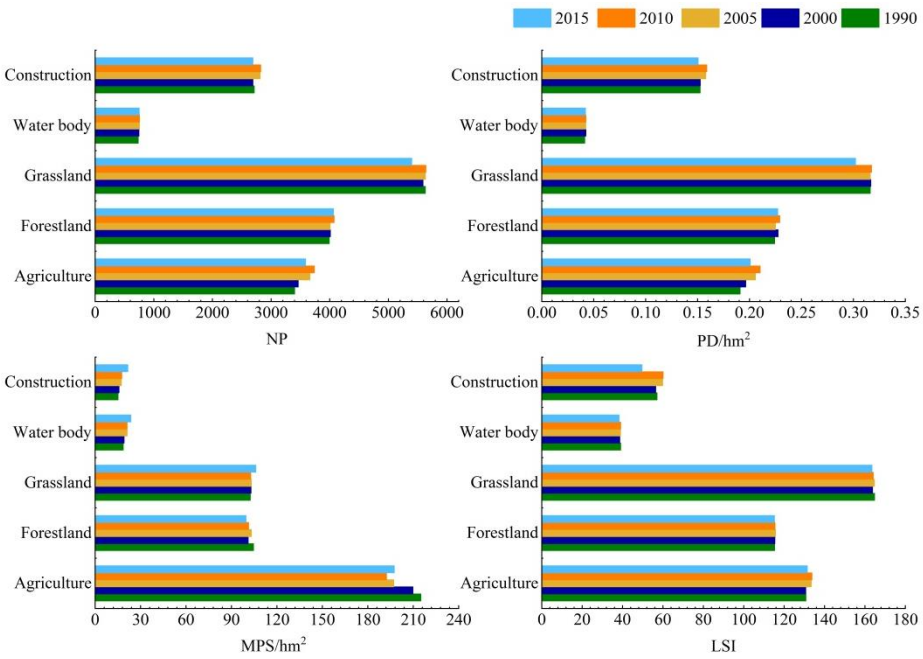

Figure 2. *Landscape indices of class metrics level*

The habitat degradation increased from 1990 to 2015, with the highest habitat degradation of 0.23 in the Zhanghe River Basin (*Figs. 3b* and *5*). The trend of habitat degradation increased in 1990-2010 and then decreased in 2010-2015, and the value of habitat degradation increased by 0.37% from 1990 to 2015. The main reason is that the agricultural land converted into grassland owing to the GGP, which alleviated habitat degradation. But the habitat quality of grassland was relatively low compared to forestland, and the habitat degradation increased during 1990-2015 in the Zhanghe River Basin. The spatial patterns manifested that the high and relatively high grades of habitat degradation were mainly concentrated in the roads and farmland of urban fringe, indicating the negative impact of anthropogenic activities on the ecosystem. The low

http://www.aloki.hu ● ISSN 1589 1623 (Print) ● ISSN 1785 0037 (Online)
DOI: http://dx.doi.org/10.15666/aeer/1906_45834597

grade was mainly located in the north and southeast owing to the mountainous terrain and implementation of the GGP. The median grade was mainly distributed in the central region, where the landscape types were dominated by agriculture. Based on the natural breaks method (He et al., 2017; Tang et al., 2020), the habitat degradation in Zhanghe River Basin was divided into five levels: low quality (0-0.02), relatively low (0.03-0.04), medium (0.05-0.08), relatively high (0.09-0.10) and high quality (0.11-0.23). From 1990 to 2015, the low grade increased by 37.8 km^2, the medium grade decreased by 198.67 km^2, while the high and relatively high grade increased by 169.49 km^2, which indicated that most medium grade converted to high and relatively high grade and caused the degradation of watershed habitat conservation. In other words, a number of agricultural lands replaced by urban land caused the watershed ecological environment deterioration.

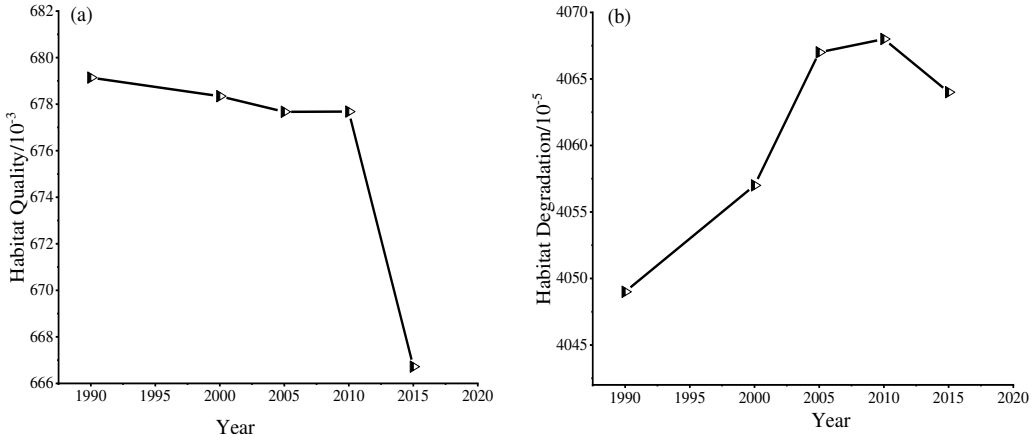

Figure 3. *The mean habitat quality and degradation from 1990 to 2015 in the Zhanghe River Basin*

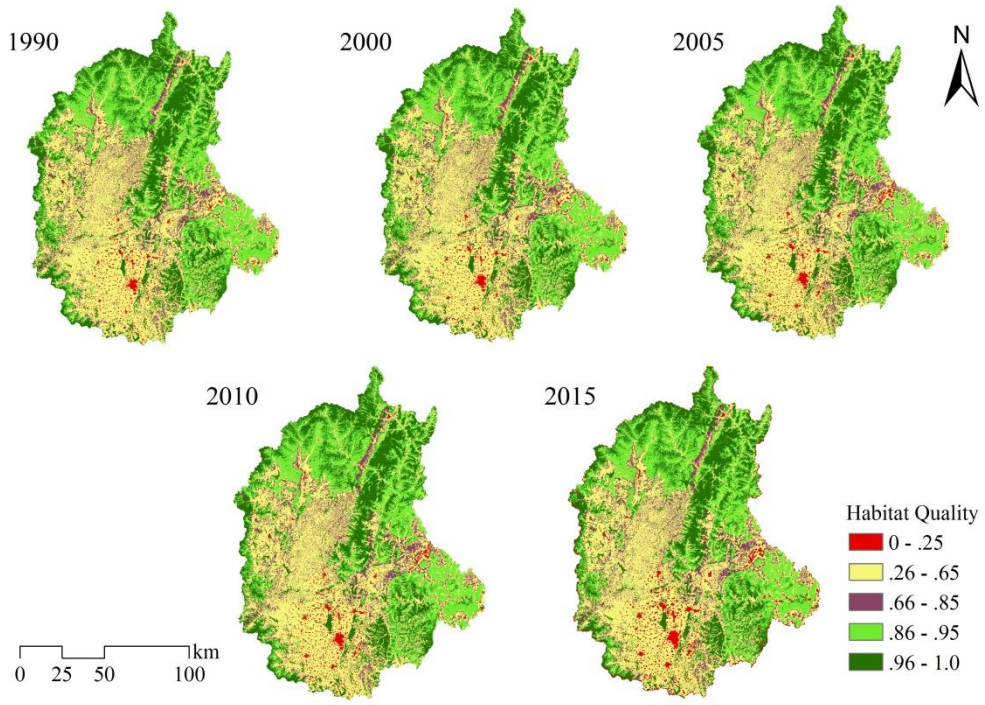

Figure 4. *The distribution pattern of habitat quality from 1990 to 2015*

http://www.aloki.hu ● ISSN 1589 1623 (Print) ● ISSN 1785 0037 (Online)
DOI: http://dx.doi.org/10.15666/aeer/1906_45834597

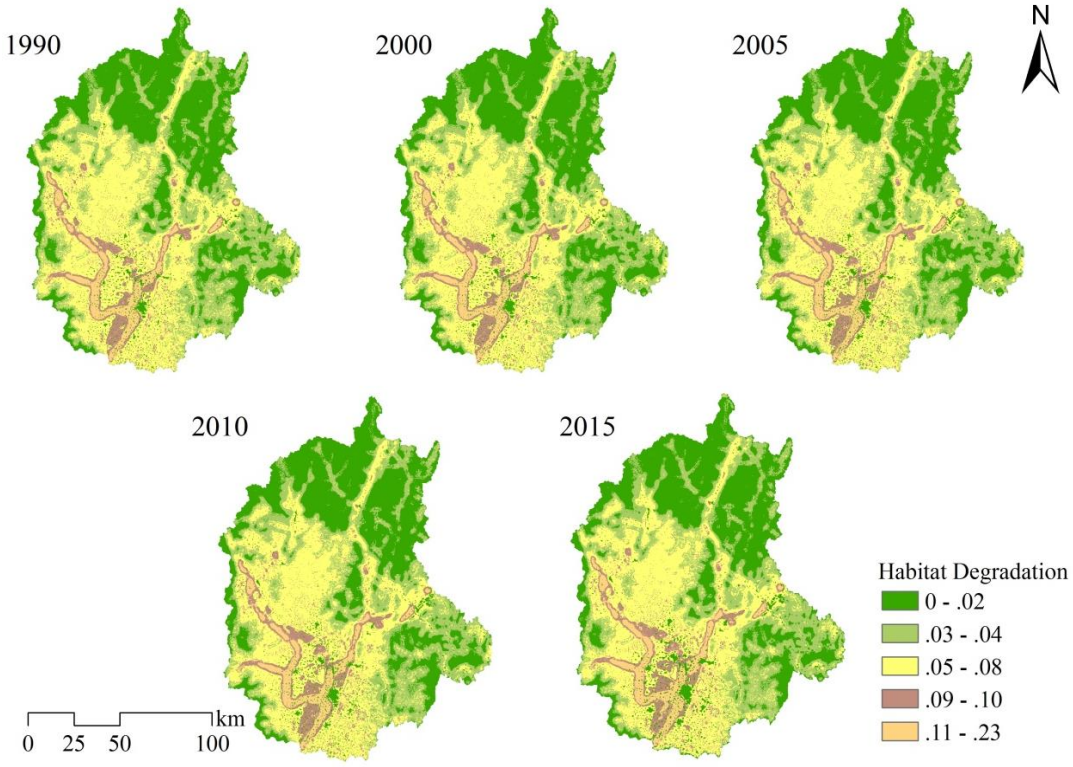

Figure 5. *The distribution pattern of habitat degradation from 1990 to 2015*

From the perspective of the spatial pattern, the decrease of habitat quality showed obvious spatial aggregation, and mainly concentrated in the peri-urban fringe and agricultural land (*Figs. 6* and *7*). Further analysis of the spatial change process was carried out based on Moran's *I* and LISA statistics, which showed that habitat loss in the Zhangehe River Basin from 1990 to 2015 mainly owed to the decline of agricultural land. The Moran's *I* of habitat quality decreased from 0.202 in 1990 to 0.191 in 2015, indicating that the spatial aggregation of habitat quality was poor and tended to be dispersed. The Moran's *I* of habitat degradation was more than 0.8 during 1990-2015, demonstrating that the spatial aggregation was significant, but there was a tendency of dispersion (the value decreased from 0.867 in 1990 to 0.840 in 2015). LISA statistics was used to identify local cluster. The high-high aggregation area of habitat quality was concentrated in the central forestland with mountain terrain and less human activities in 2015, while the low-low area was mainly located in the southwest with agricultural land. And most of the high-high aggregation area of habitat degradation was distributed in agricultural land, indicating that agricultural activities posed a great threat to the habitat conservation in Zhanghe river basin.

Forecast of landscape pattern and habitat status

Figure 8 showed the spatial distribution of LUCC, habitat quality and degradation in 2030. Based on land use policy and urban expansion, the agricultural land and construction land increased by 134.28 km^2 and 226.5 km^2, while forestland and grassland decreased by 160.42 km^2 and 531.91 km^2, respectively. Construction land was mainly converted from agricultural land, while forestland and grassland converted to agricultural land.

http://www.aloki.hu ● ISSN 1589 1623 (Print) ● ISSN 1785 0037 (Online)
DOI: http://dx.doi.org/10.15666/aeer/1906_45834597

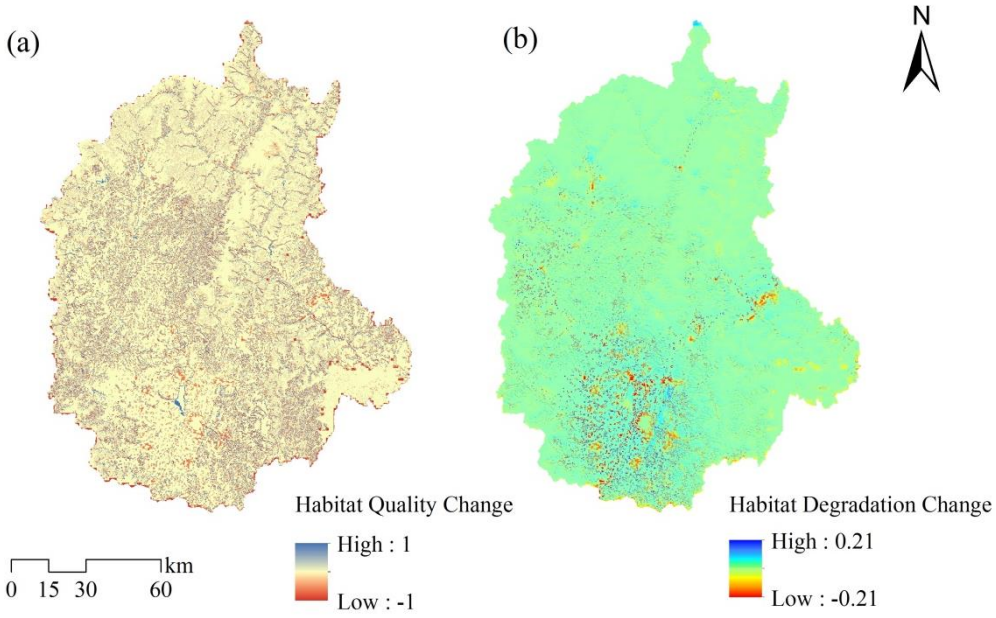

Figure 6. *The spatial change pattern for habitat quality and degradation in the Zhanghe River Basin*

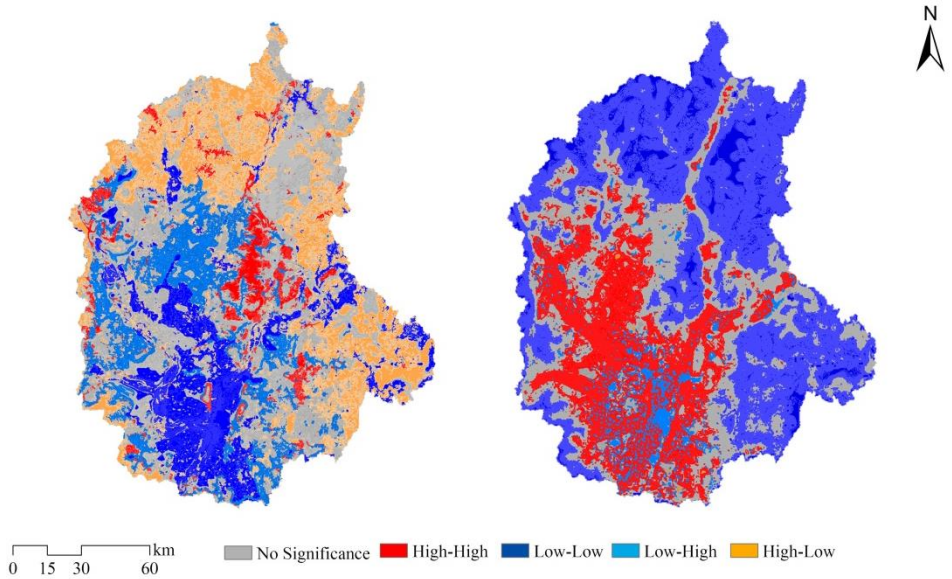

Figure 7. *LISA aggregation in 2015: (left) habitat quality, (right) habitat degradation*

The overall ecological environment continued to decline in 2030, and the mean value of habitat quality and degradation was 0.6535 and 0.0423, respectively (*Table 5*). Compared to 2015, the area with low and relatively low habitat quality increased by 342.62 km^2, but the area with medium value decreased by 410.23 km^2, and the area with high and relatively high habitat degradation increased by 314.42 km^2. The results indicated that the decline of ecological environment was mainly due to the conversion of medium grade to low grade. Thus, under current land use policy, we should do more effort to balance economic development and habitat conservation.

http://www.aloki.hu ● ISSN 1589 1623 (Print) ● ISSN 1785 0037 (Online)
DOI: http://dx.doi.org/10.15666/aeer/1906_45834597

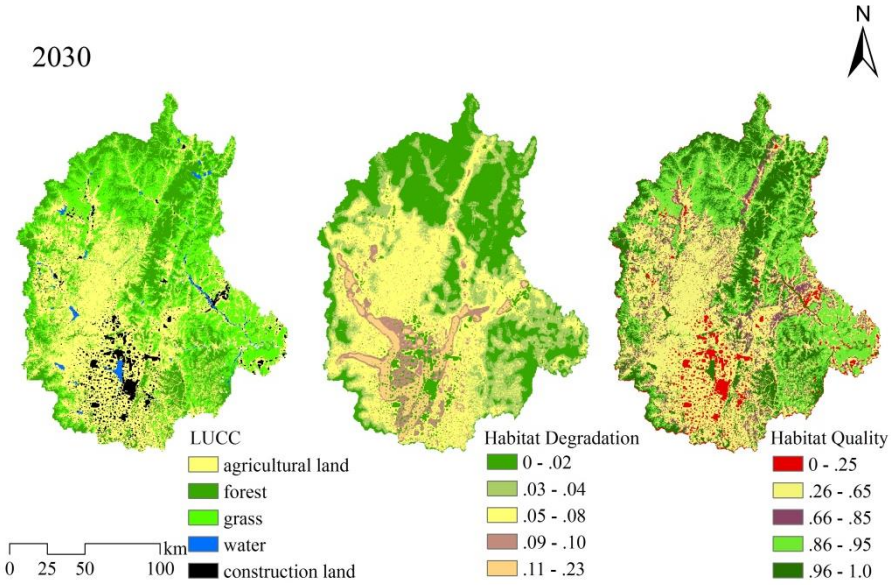

Figure 8. *Land use map, habitat quality and degradation for 2030*

Table 5. *Area of the landscape under different habitat quality and degradation classes in 2030 (km^2)*

	Low	Relatively low	Medium	Relatively high	High
Habitat quality	1051.89	7227.28	5347.78	40.1	4195.31
Habitat degradation	6940.69	3320.05	5702.95	1014.39	911.75

Discussion

Habitat quality could reflect regional change of biodiversity and is regarded as proxy, and the geographical factors and human activities are essential to understand the change of habitat quality and degradation (Sun et al., 2019). To investigate the potential impact factors on habitat quality, 6 typical impact factors were listed (*Table 6*). In this paper, we subdivided the watershed into Hydrological Response Units (HRUs) based on the SWAT model (Wang et al., 2021), and a total of 872 units were formed, then the correlations between the habitat quality and the impact factors were analyzed based on HRUs by using Pearson correlation coefficient. The results showed that habitat quality and the geographical factors (DEM, slope and NDVI) presented significant positive correlation, while habitat quality was significantly negative with human activities, such as GDP, population density and intensity of land use (*Table 6*). Slope was the dominant factor, followed by intensity of land use and NDVI. The flat terrain and steep slope regions were consistent with forestland and grassland regions with less human activities. Thus, habitat quality in mountains was better than in plain areas. Land use intensity (Hu et al., 2013) is an important index for the level of anthropogenic disturbance. Construction land and agricultural land distributed mainly in the plain and were greatly affected by human activities. Correspondingly, these regions presented dramatic habitat degradation. The related coefficient between habitat quality and other socio-economic factors (e.g. GDP and population density) further indicated that intensive human activities could cause habitat degradation in the basin (Sun et al., 2019).

http://www.aloki.hu ● ISSN 1589 1623 (Print) ● ISSN 1785 0037 (Online)
DOI: http://dx.doi.org/10.15666/aeer/1906_45834597

Table 6. *The related coefficient between distribution of habitat quality and impact factors in 2015*

Impact factors	DEM	Slope	NDVI	GDP	Population	Intensity of land use
Related coefficient	0.53**	0.72**	0.55**	-0.45**	-0.33**	-0.57**

**Correlation is significant at the 0.01 level

The landscape composition and configuration played an important role on exploring regional habitat quality variation. In this study, we further analyzed the correlation between landscape patterns and habitat quality (*Table 7*). Habitat quality presented a significant positive correlation with CONTAG, SHDI and SHEI, which indicated that habitat quality would increase with better landscape diversity, evenness, and contagion. The correlation between habitat quality and LSI, MPS was slight but obvious, which reflected that larger mean patch size, better habitat quality, and complexity of landscape shapes increased the heterogeneity of habitat quality. Agricultural land was the main land use type in the Zhanghe River Basin, but the increasing fragmentation of agricultural land caused the decline of ecological system function and habitat degradation. In addition, along with deforestation and urban expansion, the large patches of forestland became smaller, while the patches of construction land tended to expand, which led to the decline of habitat quality.

Table 7. *The correlation coefficient between distribution of habitat quality and impact factors*

At the landscape level						
Landscape metrics	NP	PD	ED	CONTAG	SHDI	SHEI
Related coefficient	-0.57	-0.44	0.19	0.98**	0.99**	0.99**
At the class level						
Landscape metrics	NP	PD	LSI	MPS		
Related coefficient	-0.01	-0.07	0.14**	0.11**		

**Correlation is significant at the 0.01 level

The Zhanghe River Basin has undergone habitat degradation and fragmentation during 1990-2015. Based on current land use policy and the urban expansion trend, LUCC would continue to fragment, and the habitat degradation would become more severe. Therefore, the balance between habitat conservation and urbanization was the key to socio-economic sustainable development. More effective habitat conservation policies and integrated landscape management strategies should be adopted in the future.

Conclusion

Habitat quality and degradation are important indicators for exploring watershed ecological status. In this study, Zhanghe River Basin, with severe water conflicts, was selected to investigate characteristics, prediction, and potential causes of habitat variation by using CA-Markov and the InVEST model.

http://www.aloki.hu ● ISSN 1589 1623 (Print) ● ISSN 1785 0037 (Online)
DOI: http://dx.doi.org/10.15666/aeer/1906_45834597

The results showed that Zhanghe River Basin has experienced landscape fragmentation and habitat loss during 1990-2015, and the area with habitat degradation existed in the peri-urban fringe and agricultural land. Specifically, the agriculture and forestland fragmentation increased, while grassland and construction land tended to expand and concentrate, and the mean habitat quality decreased by 1.83% from 1990 to 2015. The overall distribution pattern of habitat quality in the basin was significantly related to spatial distribution of land use types: the low grade of habitat quality was mainly consistent with construction land and agricultural land, while forestland and grassland with higher habitat quality were distributed in the northern mountainous area. The area with high grade habitat degradation was mainly existed in the roads and the agriculture in peri-urban fringe. The simulated LUCC and habitat quality/degradation map for 2030 indicated that the overall habitat quality continued to decline under current land use policy and urban expansion. The potential impact factors on habitat quality were further analyzed, which showed that terrain was the main factor, intensity of land use was the secondary factor, and other factors (e.g. NDVI, GDP, Population) also had an important impact on the habitat quality. From the perspective of landscape pattern, the CONTAG, SHDI, SHEI, LSI and MPS showed more significant correlation with habitat quality. If the land use policy and urban expansion do not change, the ecological environment will continue to deteriorate.

In the following research, we will use the InVEST model to further explore the ecosystem service functions such as soil conservation, carbon fixation and food production in the Zhanghe River Basin to provide feasible suggestions for ecological environment protection in the Zhanghe River Basin.

Acknowledgments. This research was funded by the National Key Research and Development Program of China (2020YFF0305905), the National Natural Science Foundation of China (No. 41801034; 41801007), Shanxi philosophy and social science planning project (2020YY069, 2020YY070), the Science and Technology program of Linfen City (2060499). We would like to extend special thanks to the editor and reviewers for insightful advice and comments on the manuscript.

REFERENCES

[1] Angel, S., Parent, J., Civco, D. L., Blei, A., Potere, D. (2011): The dimensions of global urban expansion: estimates and projections for all countries 2000–2050. – Progress in Planning 75: 53-107.

[2] Batty, M., Xie, Y. (1994): From cells to cities. – Environment and Planning B: Planning and Design 21: 31.

[3] Carrizo, S. F., Smith, K. G., Darwall, W. R. T. (2013): Progress towards a global assessment of the status of freshwater fishes (Pisces) for the IUCN Red List: application to conservation programs in zoos and aquariums. – International Zoo Yearbook 47: 46-64.

[4] Chen, Y. J., Zhao, L., Tao, J. Y., Zhang, P. T. (2020): Habitat quality evaluation before and after unused land development based on the InVEST model: a case study of Tang Country. – Chinese Journal of Eco-Agriculture 28(7): 1093-1102.

[5] Cheng, C. N., Hu, Y., Feng, Y., Zhao, M. (2020): Construction of urban ecological zones based on CA-Markov model: a case study of the main urban area of Jinzhong. – Acta Ecological Sinica 40(4): 1455-1462.

http://www.aloki.hu ● ISSN 1589 1623 (Print) ● ISSN 1785 0037 (Online)
DOI: http://dx.doi.org/10.15666/aeer/1906_45834597

[6] Chun, L., Sun, T., Wang, T., Li, Z., Cai, C. (2018): Evolution and prediction of landscape pattern and habitat quality based on CA-Markov and InVEST model in Hubei Section of Three Gorges Reservoir Area. – Sustainability 10: 3854.
[7] FAO (2016): Global Forest Resources Assessment 2015. – FAO Forestry Paper No. 1.
[8] Grill, G., Lehner, B., Lumsdon, A. E., MacDonald, G. K., Zarfl, C., Reidy, L. C. (2015): An index-based framework for assessing patterns and trends in river fragmentation and flow regulation by global dams at multiple scales. – Environmental Research Letters 10: 015001.
[9] Han, Y. W., Kang, W. M., Thorne, J., Song, Y. K. (2019): Modeling the effects of landscape patterns of current forests on the habitat quality of historical remnants in a highly urbanized area. – Urban Forestry and Urban Greening 41: 354-363.
[10] He, J. H., Huang, J. L., Li, C. (2017): The evaluation for the impact of land use change on habitat quality: a joint contribution of cellular automata scenario simulation and habitat quality assessment model. – Ecological Modelling 366: 58-67.
[11] Hu, H., Liu, H., Hao, J., An, J. (2013): Spatio-temporal variation in the value of ecosystem services and its response to land use intensity in an urbanized watershed. – Acta Ecologica Sinica 33 (8): 2565-2576.
[12] Huang, M. J., Yue, W. Z., Feng, S. R., Zhang, J. H. (2020): Spatial-temporal evolution of habitat quality and analysis of landscape patterns in Dabie Mountain area of west Anhui province based on InVEST model. – Acta Ecologica Sinica 40(9): 1-12.
[13] Lambin, E. F., Geist, H. J., Lepers, E. (2003): Dynamics of land-use and land-cover change in tropical regions. – Annual Review of Environment and Resources 28: 205-241.
[14] Li, S. G., Wang, L. C., Yan, C. X., Liu, H. Y. (2020): Simulation of urban spatial expansion in oasis towns based on habitat quality: a case study of the middle reaches of Heihe River. – Acta Ecologica Sinica 49(9): 1-12.
[15] Liu, J., Ouyang, Z., Pimm, S. L., Raven, P. H., Wang, X., Miao, H., Han, H. (2003): Ecology Protecting China's biodiversity. – Science (New York) 300(5623): 1240-1241.
[16] Luijten, J. C. (2003): A systematic method for generating landuse patterns using stochastic rules and basic landscape characteristics: results for a Colombian Hillside Watershed. – Agriculture Ecosystems & Environment 95(2-3): 427-441.
[17] Mansour, S., Al-Belushi, M., Al-Awadhi, T. (2020): Monitoring land use and land over changes in the mountainous cities of Oman using and CA-Markov modelling techniques. – Land Use Policy 91: 104414.
[18] Moreira, M., Fonseca, C., Vergilio, M., Calado, H., Gil, A. (2018): Spatial assessment of habitat conservation status in a Macaronesian island based on the InVEST model: a case study of Pico Island (Azores, Portugal). – Land Use Policy 78: 637-649.
[19] Nelson, E., Sander, H., Hawthorne, P., Conte, M., Ennaanay, D., Wolny, S., Manson, S., Polasky, S. (2010): Projecting global land-use change and its effect on ecosystem service provision and biodiversity with simple models. – PLoS One 5(12): e14327.
[20] Nourqolipour, R., Shariff, A. R. B. M., Balasundram, S. K., Ahmad, N. B., Sood, A. M. (2015): A GIS-based model to analyze the spatial and temporal development of oil palm land use in Kuala Langat district, Malaysia. – Environmental Earth Sciences 73(4): 1687-1700.
[21] Sallustio, L., De Toni, A., Strollo, A., Di Febbraro. M., Gissi, E., Casella, L., Geneletti, D., Munafo, M., Vizzarri, M., Marchetti, M. (2017): Assessing habitat quality in relation to the spatial distribution of protected areas in Italy. – Journal of Environmental Management 201: 129-137.
[22] Sharp, R., Chaplin-kramer, R.,Wood, S., Guerry, A., Tallis, H., Ricketts, T. (2016): InVEST User's Guide. – The Natural Capital Project, Stanford University, University of Minnesota, The Nature Conservancy, and Word Wildlife Fund, Minneapolis, MN.
[23] Seto, K. C., Guneralp, B., Hutyra, L. R. (2012): Global forecasts of urban expansion to 2030 and direct impacts on biodiversity and carbon pool. – PNAS 109(40): 16083-16088.

http://www.aloki.hu ● ISSN 1589 1623 (Print) ● ISSN 1785 0037 (Online)
DOI: http://dx.doi.org/10.15666/aeer/1906_45834597

[24] Sun, X. Y., Jiang, Z., Liu, F., Zhang, D. Z. (2019): Monitoring spatio-temporal dynamics of habitat quality in Nansihu Lake basin, eastern China, from 1980 to 2015. – Ecological Indicator 102: 716-723.
[25] Tallis, H. T., Ricketts, T., Nelson, E., Ennaanay, D., Wolny, S., Olwero, N., Vigerstol, P. D., Mendoza, G., Aukema, J., Foster, J., Forrest, J., Cameron, D., Lonsdorf, E., Kennedy, C. (2010): InVEST 1.005 beta User's Guide. – The Natural Capital Project, Stanford.
[26] Tang, F., Fu, M., Wang, L., Zhang, P. (2020): Land-use change in Changli County, China: predicting its spatio-temporal evolution in habitat quality. – Ecological Indicators 117: 106719.
[27] Terrado, M., Sabater, S., Chaplin-Kramer, B., Mandle, L., Ziv, G., Acuna, V. (2016): Model development for the assessment of terrestrial and aquatic habitat quality in conservation planning. – Science of Total Environment 540: 63-70.
[28] Upadhaya, S., Dwivedi, P. (2019): Conversion of forestlands to blueberries: assessing implications for habitat quality in Alabaha river watershed in Southeastern Georgia, United States. – Land Use Policy 89: 104229.
[29] Wang, H., Xu, Y. Q., Liu, C., Huang, A., Lu, L. H., Zheng, W. R. (2019): Response of habitat quality to land use change based on geographical weighted regression. – Acta Scientiarum Naturalium Universitatis Pekinensis 55(3): 509-518.
[30] Wang, J. F., Wu, T. L., Li, Q., Wang, S. (2021): Quantifying the effect of environmental drivers on water conservation variation in the eastern Loess Plateau, China. – Ecological Indicators 125: 107493.
[31] Wu, J. S., Cao, Q. W., Shi, S. Q., Huang, X. L., Lu, Z. Q. (2015): Spatio-temporal variability of habitat quality in Beijing-Tianjin-Hebei Area based on land use change. – Chinese Journal of Applied Ecology 26(11): 3457-3466.
[32] Zhang, Y. Z., Chen, R. S., Wang, Y. (2020): Tendency of land reclamation in coastal areas of Shanghai from 1998 to 2015. – Land Use Policy 91: 104370.
[33] Zhao, X. L., Zhang, Z. X., Wang, X., Zuo, L. J., Liu, B., Yi, L., Xu, J. Y., Wen, Q. K. (2014): Analysis of Chinese cultivated land's spatial-temporal changes and causes in recently 30 years. – Transactions of the Chinese Society of Agricultural Engineering 30(3): 1-11.

http://www.aloki.hu ● ISSN 1589 1623 (Print) ● ISSN 1785 0037 (Online)
DOI: http://dx.doi.org/10.15666/aeer/1906_45834597

THE EFFECT OF THE BACTERIUM *BACILLUS MEGATERIUM* VAR. *PHOSPHATICUM*, THE AMINO ACID L-ALPHA PROLINE AND MINERAL FERTILISATION WITH NITROGEN ON HEAVY METAL CONTENT IN SPRING WHEAT (*TRITICUM AESTIVUM* L.) GRAIN

PŁAZA, A.* – RZĄŻEWSKA, E.

Siedlce University of Natural Sciences and Humanities, Faculty of Agrobioengineering and Animal Husbandry, Siedlce, Poland

**Corresponding author*
e-mail: anna.plaza@uph.edu.pl

(Received 21st Jun 2021; accepted 3rd Sep 2021)

Abstract. The objective of the present work was to determine the effect of the bacterium *Bacillus megaterium var. phosphaticum*, the amino acid L-alpha proline and mineral fertilisation with nitrogen on heavy metal content in spring wheat (*Triticum aestivum* L.) grain destined for human consumption. Field research was conducted on a family-owned farm located in Krzymosze, Poland. Two factors were examined: factor I – biological products: control where no biological products were applied, *Bacillus megaterium var. phosphaticum*, L-alpha proline, *Bacillus megaterium var. phosphaticum* + L-alpha proline; factor II – mineral fertilisation with nitrogen: unfertilised control, 60 kg N∘ha^{-1}, 90 kg N∘ha^{-1}, and 120 kg N∘ha^{-1}. Grain samples were taken to determine Cu, Zn, Cd, Cr and Ni contents. The research demonstrated that weather conditions during the growing season had a significant influence on the heavy metal content of spring wheat grains. Increasing rates of mineral fertilisation with nitrogen contributed to an increase in the spring wheat grain content of heavy metals, an exception being zinc content in the grain of spring wheat fertilised with 120 kg N∘ha^{-1}. The lowest heavy metal content was recorded in the grain of spring wheat treated with the bacteria *Bacillus megaterium var. phosphaticum* + the amino acid L-alpha proline, regardless of whether the crop was unfertilised or fertilised with the rates of 60 and 90 kg N∘ha^{-1}.
Keywords: *phosphorus bacteria, mineral fertilisation, biostimulator, content in grain metal*

Introduction

Spring wheat grain is a raw material for the food industry so its content of heavy metals should be as low as possible. Some of these metals, e.g. Ni, Cu and Zn, are microelements necessary for biomolecules, and to maintain cell structure, function and proliferation (Khajeh et al., 2010). The metals are potentially toxic if present in excess in food. They may be the cause of genetic disorders (Zheng et al., 2008). Other metals, e.g. Cd, Pb and Cr are carcinogenic substances and they are responsible for the occurrence of conditions such as Alzheimer's disease, Parkinson's disease, multiple sclerosis and osteoporosis. Also, they negatively affect such organs as the heart, kidneys and lungs as well as the immune system (Jamova and Valko, 2011; Zakir et al., 2011; Pirsaheb et al., 2015). Numerous research have revealed excessive amounts of heavy metals in cereals and rice grown in various countries. This is due to the fact that currently harmful substances in the environment are pesticide residues and heavy metal compounds. Reducing the emission of heavy metal compounds is more difficult to achieve. Their main sources are the steel industry, energy, mining and transport. That is why it is of paramount importance to constantly monitor and check cereal grain for heavy metals. The value of guidance documents and safety standards as established by Food Safety Authorities (*Table 2*) around the world cannot be overstated in terms of protecting public health and providing

http://www.aloki.hu ● ISSN 1589 1623 (Print) ● ISSN1785 0037 (Online)
DOI: http://dx.doi.org/10.15666/aeer/1906_45994609

guidance and assistance to stakeholders, not least farmers and processors (Thielecke and Nugent, 2018). Refining grains will reduce the presence of many contaminants but it also removes 50 to 80% of phytonutrients from whole grains. The studies demonstrated that it is these phytonutrients, (vitamins, minerals and fibres) that may exert a potentially protective effect against toxic metals in particular (Thielecke and Nugent, 2018). Further, the consumer also has a choice in mitigating any risk from contaminants, and to do so best by continuing to eat a healthy balanced diet, rich in nutrient dense foods, and including whole grain foods (Thielecke and Nugent, 2018).

According to Shicheng et al. (2018), mineral fertilisation with nitrogen increases the wheat grain content of heavy metals. Jastrzębska and Kostrzewska (2019) have demonstrated that an application of the phosphorus-dissolving bacteria *Bacillus megaterium*, compared to mineral fertilisation of spring wheat, contributed to a decline in the soil content of heavy metals. In the research, the phosphorus-dissolving bacteria were applied with fertiliser as ash produced from sewage sludge, and they reduced heavy metal content in the soil as opposed to mineral fertilisation. Also Asfa et al. (2020) observed lower phytotoxicity of heavy metals after inclusion of microbiology in wheat cultivation. Apart from microorganisms, modern agriculture also recommends an application of biostimulants, including amino acids (Calvo et al., 2014). Biostimulants serve to control and enhance plant life processes, and thus they increase plant resistance to stress and stimulate the development of rooting (Du Jardin, 2015). In this respect, it is a novel approach to apply the bacteria *Bacillus megaterium var. phosphaticum* and the amino acid L-alpha proline which willhopefully contribute to a decline in heavy metal content in spring wheat grain. As there is no research into this issue, it was attempted to determine the impact of the bacteria *Bacillus megaterium var. phosphaticum*, the amino acid L-alpha proline and mineral fertilisation with nitrogen on heavy metal content in the grain of spring wheat destined for human consumption.

Materials and Methods

A field experiment was conducted on a family-owned farm in Krzymosze near Siedlce, Poland, in 2017-2019. The trial was set up on soil classified as Stagnic Luvisol and whose contents of available macroelements was as follows: P 8.2, K 18.7, and Mg 4.8 mg⊙100 g^{-1} soil. Other contents were as follows: Mn 131, Cu 4.9, Zn 5.5, Pb less than 16.2, Cd 0.14, Cr less than 12.3 and Ni 12.4 mg⊙kg^{-1} soil. Soil reaction was neutral and humus content was 1.88%. The experiment was a split-block arrangement with three replicates. The experimental factors were as follows: factor I – biological products: control where no biological products were applied, *Bacillus megaterium var. phosphaticum*1 l⊙ha^{-1}, L-alpha proline 2 g⊙ha^{-1}, *Bacillus megaterium var. phosphaticum*1 l⊙ha^{-1}+ L-alpha proline 2 g⊙ha^{-1}; factor II – mineral fertilisation with nitrogen: unfertilised control, 60 kg N⊙ha^{-1} (pre-plant), 90 kg N⊙ha^{-1} (60 kg N⊙ha^{-1} pre-plant + 30 kg N⊙ha^{-1} at the stem elongation stage), and 120 kg N⊙ha^{-1} (60 kg N⊙ha^{-1} pre-plant + 30 kg N⊙ha^{-1} at the stem elongation stage + 30 kg N⊙ha^{-1} as foliar application of 8% solution of urea at the early ear formation stage).

Spring wheat cv. Mandaryna was grown after maize. Phosphorus and potassium fertiliser rates were adjusted to soil contents of available forms of these elements and were as follows: P 30.8 kg⊙ha^{-1} and K 99.6 kg⊙ha^{-1}. Mineral fertilisation with nitrogen was applied as described for factor II above. Spring wheat was sown in early April at the amount of 500 grains per 1 m^2. Biological products were applied once at the stage of

http://www.aloki.hu ● ISSN 1589 1623 (Print) ● ISSN1785 0037 (Online)
DOI: http://dx.doi.org/10.15666/aeer/1906_45994609

spring wheat tillering. Spring wheat was harvested in early August. From each plot after the grain was harvested, a representative sample with a volume of 250 g was taken. Then it was ground and intended for chemical analysis. During harvest, grain samples were taken in each plot to determine microelements. Cu, Zn, Mn, Pb, Cd, Cr and Ni contents were determined by means of inductively coupled plasma optical emission spectrometry (ICP-OES) using an emission spectrometer Perkin Elmer Optima 8300.

The results for each trait tested were subjected to ANOVA suitable for the split-block design. When significant sources of variation were confirmed, their means were separated using Tukey test. Calculations were performed in MS Excel 12.0. The results for each characteristic were subjected to analysis of variance following the mathematical model: $y_{ijl}= n + a_i + g_i + e_{ij}^{(1)} + b_l + e_{jl}^{(2)} + ab_{il}+ e_{ijl}^{(3)}$, where a = 1.. 4; b = 1, 2, … 4; n = 1, 2, 3 (number of replicates); y_{ijl} – value of the examined characteristic; a_i – effect of i-th level of factor A; g_j– effect of replicates (blocks); $e_{ij}^{(1)}$ – error 1 resulting from the interaction: factor A × replicates; b_l – effect of l-th level of factor B; $e_{jl}^{(2)}$ – error 2 from the interaction: factor B × replicates; ab_{il} – effect of the interaction: factor A × factor B; $e_{ijl}^{(3)}$ – random error. The course of weather conditions in the years of the research was varied (*Table 1*).

Table 1. *Weather conditions in the growing season of spring wheat according to the Zawady Meteorological Station*

Years	Month					Mean
	IV	V	VI	VII	VIII	
Mean air temperature ºC						
2017	6.9	13.9	17.8	16.9	18.4	14.8
2018	13.1	17.0	18.3	20.4	20.6	17.9
2019	9.8	13.3	17.9	18.5	19.9	15.9
Long-term (50yr) mean	8.2	14.2	17.6	19.7	19.1	15.8
Rainfall sum, mm						
2017	59.6	49.5	57.9	23.6	54.7	245.3
2018	34.5	27.3	31.5	67.1	24.5	184.9
2019	5.9	59.8	35.9	29.7	43.9	175.2
Long-term (50yr) mean	37.4	47.1	48.1	65.5	43.5	241.6

The most favorable year for the cultivation of spring wheat was 2017, when the highest amount of rainfall was recorded. Worse weather conditions were recorded in 2018, with a lower total of precipitation and an average air temperature higher than the long-term average. The strongest rainfall shortage was recorded in 2019. The average air temperature oscillated around the long-term average.

Table 2 shows the regulatory autorities' permissible metal limits WHO/FAO.

Table 2. *Metal levels in food by WHO/FAO*

Metal	Concentrations (µg/g)
Cd	0.10
Cu	73.00
Cr	2.30
Pb	0.30
Zn	100.00

http://www.aloki.hu ● ISSN 1589 1623 (Print) ● ISSN1785 0037 (Online)
DOI: http://dx.doi.org/10.15666/aeer/1906_45994609

Results and Discussion

Heavy metal contents in spring wheat grain were significantly affected by weather conditions and their interaction with biological products (*Table 3*).

Table 3. *Spring wheat grain content of heavy metals according to biological products applied in 2017-2019, mg kg^{-1} DM*

Biological products (A)	Years (Y)		
	2017	2018	2019
Manganese			
Control	82.14c	79.49d	77.68d
Bacillus megaterium var. phosphaticum	72.32a	72.69b	71.07b
L-alpha proline	78.98b	76.34c	74.72c
Bacillus megaterium var. phosphaticum + L-alpha proline	71.14a	68.51a	66.89d
Means	76.15C	74.26B	72.59A
Zinc			
Control	18.59a	20.00a	20.65a
Bacillus megaterium var. phosphaticum	23.16c	24.57c	25.22c
L-alpha proline	21.59b	23.05b	23.71b
Bacillus megaterium var. phosphaticum + L-alpha proline	25.68d	27.08d	27.72d
Means	22.26A	23.68B	24.33C
Copper			
Control	6.24c	5.37b	5.01b
Bacillus megaterium var. phosphaticum	5.30a	4.43a	4.07a
L-alpha proline	5.49ab	4.62a	4.26a
Bacillus megaterium var. phosphaticum + L-alpha proline	5.08a	4.23a	3.87a
Means	5.53C	4.66B	4.30A
Nickel			
Control	0.769c	0.669c	0.638a
Bacillus megaterium var. phosphaticum	0.638b	0.538b	0.508b
L-alpha proline	0.671b	0.573b	0.543b
Bacillus megaterium var. phosphaticum + L-alpha proline	0.556a	0.458a	0.427a
Means	0.659B	0.560A	0.529A
Chromium			
Control	0.463c	0.378d	0.355c
Bacillus megaterium var. phosphaticum	0.310a	0.225b	0.203a
L-alpha proline	0.355b	0.271c	0.248b
Bacillus megaterium var. phosphaticum + L-alpha proline	0.319a	0.189a	0.181a
Means	0.362B	0.266A	0.247A

In 2017, characterised by the highest precipitation sum, there was recorded an increase in manganese, copper, nickel and chromium contents as well as a decline in zinc content in spring wheat grain compared with the dry years 2018 and 2019 whose precipitation

http://www.aloki.hu ● ISSN 1589 1623 (Print) ● ISSN1785 0037 (Online)
DOI: http://dx.doi.org/10.15666/aeer/1906_45994609

sums were much lower. Similarly, Radkowski et al. (2020a) reported a decline in microelements in the year with a higher precipitation sum compared with dry years. In the present study, an interaction was confirmed. The lowest manganese, copper, nickel and chromium contents and the highest zinc content were recorded in spring wheat grain in 2018-2019, when precipitation was lower, in the plot treated with the bacteria *Bacillus megaterium var. phosphaticum* + the amino acid L-alpha proline. By contrast, the highest heavy metal contents, excluding zinc, were found in the control plot, where no biological products had been applied, in 2017 characterised by the highest precipitation sum.

Statistical analysis demonstrated a significant influence of the experimental factors and their interaction on manganese content in spring wheat grain (*Table 4*).

Table 4. *Manganese content in spring wheat grain (means across 2017-2019), mg⊙kg^{-1} DM*

Biological products (A)	**Mineral fertilisation with nitrogen, kg N⊙ha^{-1} (B)**				**Means**
	Control	**60**	**90**	**120**	
Control	76.08d	78.50d	80.77d	83.24d	79.65D
Bacillus megaterium var. phosphaticum	71.32b	72.59b	73.86b	74.33b	73.03B
L-alpha proline	74.47c	75.74c	77.01c	79.48c	76.68C
Bacillus megaterium var. phosphaticum + L-alpha proline	66.14a	68.41a	69.68a	71.15a	68.85A
Means	72.00A	73.81B	75.33C	77.05D	-

Compared to control, biological products contributed to a decline in the spring wheat content of manganese. Also the study by Arhar and Ahmad (2018) showed that nitrogen-fixing bacteria reduced Mn uptake by wheat plants. In the present study, the lowest concentration of Mn was recorded in spring wheat grain following an application of the bacteria *Bacillus megaterium var. phosphaticum*and the amino acid L-alpha proline. Kandii et al. (2016) reported a decline in Mn content in wheat after amino acids had been applied in combination with mineral fertilisation with nitrogen. The same relationship was observed by Radkowski et al. (2020). In the present study, mineral fertilisation with nitrogen significantly influenced manganese content in spring wheat grain. Increasing rates of mineral nitrogen fertiliser contributed to a significant increase in Mn content in spring wheat grain. This finding corresponds with results reported by Hellal et al. (2012) and Radkowski et al. (2020a,b). In the experiment discussed here, an interaction was confirmed indicating that the lowest manganese content was found in the grain of spring wheat grown in plots treated with the bacteria *Bacillus megaterium var. phosphaticum*and the amino acid L-alpha proline and not fertilised with mineral nitrogen. By contrast, the highest values were found in units fertilised with 120 kg N⊙ha^{-1} and untreated with biological products. However, also in this case the spring wheat grain content of Mn was lower than the standards quoted by WHO/FAO, and was safe for humans (Adefarati et al., 2017).

Zinc content in spring wheat grain was significantly affected by the experimental factors and their interaction (*Table 5*).

Biological products significantly increased zinc content in spring wheat grain compared with control where no biological products were applied. Zinc plays an important role in plant metabolism. Both zinc excess and shortage considerably limit plant growth and development (Ociepa-Kubicka and Ociepa, 2012). It should be

http://www.aloki.hu ● ISSN 1589 1623 (Print) ● ISSN1785 0037 (Online)
DOI: http://dx.doi.org/10.15666/aeer/1906_45994609

mentioned that plants growing in a polluted environment may accumulate high concentrations of this microelement, which poses a serious threat to human health (Srinivas et al., 2002; Sharma et al., 2004; Luo et al., 2013). Research by Fytianos et al. (2001), Demirezen and Ahmet (2006), Muchuweti et al. (2006) as well as Mahamed et al. (2012) demonstrated a low zinc content in cereal grain. In the present study, the highest concentration of zinc was recorded in spring wheat grain following an application of the bacteria *Bacillus megaterium var. phosphaticum*and the amino acid L-alpha proline. Also Athar and Ahmad (2018) reported increased zinc contents in cereal grain due to an application of bacteria. Radkowski et al. (2020a) demonstrated that an application of amino acids increases Zn concentration in spring wheat grain as well. In the experiment reported here, mineral fertilisation with nitrogen increased Zn content in spring wheat grain up to the rate 90 kg N◎ha^{-1}. The highest rate, that is 120 kg N◎ha^{-1}, was followed by a significant decline in the spring wheat grain content of zinc. The same relationship was demonstrated in research by Kandii et al. (2016) and Radkowski et al. (2020a,b). In the present work, an interaction was confirmed indicating that the highest zinc content was present in spring wheat grain following an application of the bacteria *Bacillus megaterium var.phosphaticum*, the amino acid L-alpha proline and mineral fertilisation with nitrogen at the rate of either 60 or 90 kg N◎ha^{-1}, it being the lowest in the control unit where no biological products had been applied, at all the rates of mineral fertilisation with nitrogen.

Table 5. *Zinc content in spring wheat grain (means across 2017-2019), mg kg^{-1} DM*

Biological products (A))	Mineral fertilisation with nitrogen, kg N◎ha^{-1} (B)				Means
	Control	60	90	120	
Control	19.17a	20.65a	19.79a	19.37a	19.75A
Bacillus megaterium var. phosphaticum	23.05b	24.25b	26.44b	23.53b	24.32C
L-alpha proline	20.16a	23.53b	24.89b	22.54b	22.78B
Bacillus megaterium var. phosphaticum + L-alpha proline	25.54c	26.96c	28.60c	26.18c	26.82D
Means	21.98A	23.85B	24.93C	22.91B	-

Statistical analysis demonstrated a significant impact of the experimental factors and their interaction on copper content in spring wheat grain. Biological products used in the study contributed to a significant drop in copper content in spring wheat grain compared with control. The lowest concentration of copper was recorded in spring wheat grain following an application of the bacteria *Bacillus megaterium var. phosphaticum*and the amino acid L-alpha proline. Research by Garcia-Fraile et al. (2015) and Vejan et al. (2016) revealed that plant growth stimulating bacteria occur around roots and are responsible for nutrient mobilisation, heavy metal sequencing and break-down of toxic elements present in soil. Also Athar and Ahmad (2018) reported that *Azotobacter* reduces Cu content in wheat grain. A similar relationship was observed by Radkowski et al. (2020a) who applied amino acids while growing wheat. In the present study, increasing rates of mineral fertilisation with nitrogen were followed by an increase in copper content in spring wheat grain. However, the content associated with the highest rate of mineral fertilisation with nitrogen, that is 120 kg N◎ha^{-1}, was lower than the permissible standards set by the WHO/FAO and is not harmful to humans (Adefarati et al., 2017). In studies by

http://www.aloki.hu ● ISSN 1589 1623 (Print) ● ISSN1785 0037 (Online)
DOI: http://dx.doi.org/10.15666/aeer/1906_45994609

Hellal et al. (2012), Kandii et al. (2016) and Radkowski et al. (2020b), there was observed an increase in the spring wheat grain content of copper following increasing rates of mineral fertilisation with nitrogen. In the study reported here, there was confirmed an interaction which indicated that the lowest copper content was present in spring wheat grain after an application of the bacteria *Bacillus megaterium var. phosphaticum*, the amino acid L-alpha proline and mineral fertilisation with nitrogen at the rate of up to 90 kg N◎ha^{-1}. The highest copper content was determined in control grain produced without using biological products at the highest rate of mineral fertilisation with nitrogen, that is 120 kg N◎ha^{-1}.

Lead and cadmium contents in spring wheat grain were insignificantly affected by the experimental factors, and their concentration in spring wheat grain was too low to be detected by an emission spectrometer Perkin Elmer Optima 8300. This may be explained by the fact that the fields where the experiment was set up were located relatively far away from communication routes. Hence, spring wheat grain met standards the set by the WHO/FAO for lead and cadmium contents. Despite the low Cd and Pb contents in spring wheat grain, they must be constantly monitored and checked.

Statistical analysis demonstrated a significant influence of the experimental factors and their interaction on nickel content in spring wheat grain (*Table 6*).

Table 6. *Nickel content in spring wheat grain (means across 2017-2019), mg kg^{-1} DM*

Biological products (A)	Mineral fertilisation with nitrogen, kg N◎ha^{-1} (B)				Means
	Control	60	90	120	
Control	0.591c	0.683c	0.721c	0.772c	0.692C
Bacillus megaterium var. phosphaticum	0.493a	0.534b	0.575b	0.644b	0.562B
L-alpha proline	0.512b	0.576b	0.613b	0.681b	0.596B
Bacillus megaterium var. phosphaticum + L-alpha proline	0.427a	0.453a	0.494a	0.547a	0.480A
Means	0.506A	0.562A	0.601B	0.661B	-

The applied biological products significantly reduced the concentration of nickel in spring wheat grain compared with untreated control. In their work, Jastrzębska and Kostrzewska (2019) pointed to the fact that phosphorus-dissolving *Bacillus* bacteria contributed to reduction in nickel content in spring wheat grain. Similarly, Sarfaz et al. (2019) and Figueiredo et al. (2011) reported that also rhizobacterine limits heavy metal content in plants. Plant growth promoting rhizobacteria (PGPR) are responsible for stimulating plant growth, heavy metal sequencing and break-down of toxic elements present in soil (Garcia-Fraile et al., 2015). A similar relationship was reported by Athar and Ahmad (2018) who examined *Azotobacter*. Naveed et al. (2020) and Turan et al. (2018) demonstrated that an application of bacteria contributed to a decline in the spring wheat grain content of nickel. In the present work, also an application of the amino acid L-alpha proline was followed by a decline in nickel content in spring wheat grain, particularly when combined with the bacteria *Bacillus megaterium var. phosphaticum*. It was confirmed by Popko et al. (2018) who demonstrated that an application of biostimulants contributes to a decline in the spring wheat content of nickel. In the study reported here, increasing rates of mineral fertilisation with nitrogen, in particular the rate 120 kg N◎ha^{-1}, were followed by an increase in nickel content in spring wheat grain.

http://www.aloki.hu ● ISSN 1589 1623 (Print) ● ISSN1785 0037 (Online)
DOI: http://dx.doi.org/10.15666/aeer/1906_45994609

However, even in the case of the highest N rate, Ni content in spring wheat grain was low and did not exceed standards set by the WHO/FAO and was not harmful to humans (Adefarati et al., 2017). This finding was confirmed by Shicheng et al. (2018) in their research on an application of mineral fertilisation with NPK. In the experiment reported here, an interaction was found and it indicated that the lowest nickel content was present in spring wheat grain following an application of the bacteria *Bacillus megaterium var. phosphaticum*and the amino acid L-alpha proline and no mineral fertilisation with nitrogen, or an application of either 60 or 90 kg N◎ha^{-1}. By contrast, it was the highest for the untreated control where the rate of mineral fertilisation with nitrogen was either 90 or 120 kg N◎ha^{-1}.

Chromium content in spring wheat grain was significantly affected by the experimental factors and their interplay (*Table 7*).

Table 7. *Chromium content in spring wheat grain (means across 2017-2019), mg kg^{-1} DM*

Biological products (A)	**Mineral fertilisation with nitrogen, kg N◎ha^{-1} (B)**				**Means**
	Control	**60**	**90**	**120**	
Control	0.314b	0.362c	0.423c	0.495c	0.399C
Bacillus megaterium var. phosphaticum	0.186a	0.214a	0.261a	0.323a	0.246A
L-alpha proline	0.211a	0.261b	0.317b	0.376b	0.291B
Bacillus megaterium var. phosphaticum + L-alpha proline	0.158a	0.185a	0.223a	0.272a	0.210A
Means	0.217A	0.256A	0.306B	0.367C	-

Biological products significantly reduced chromium content in spring wheat grain compared with untreated control. Also Jastrzębska and Kostrzewska (2019) reported that the phosphorus-dissolving bacteria *Bacillus megaterium* reduced chromium concentration in spring wheat grain. Sarfaz et al. (2019), Figueiredo et al. (2011) and Rizvi et al. (2020) demonstrated that bacteria incorporated into soil reduce chromium content in wheat. Also in the present study, an application of the amino acid L-alpha proline contributed to a decline in chromium content in spring wheat grain compared with control. Similarly, Popko et al. (2018) found that biostimulants reduce heavy metals in wheat. In the experiment reported here, the lowest chromium content was recorded in spring wheat grain following an application of the bacteria *Bacillus megaterium var. phosphaticum*and the amino acid L-alpha proline. Mineral fertilisation with nitrogen affected chromium content in spring wheat grain, too. The highest chromium content was determined in spring wheat grain following the highest rate of mineral fertilisation with nitrogen, that is 120 kg N◎ha^{-1}. Despite this, the chromium content was low and did not exceed standards set by the WHO/FAO, and was safe for humans (Adefarati et al., 2017). Also research by Shicheng et al. (2018) demonstrated that mineral fertilisation is associated with an increase in the spring wheat grain content of chromium. An interaction was confirmed in the study reported here which indicated that the highest chromium content was present in spring wheat grain following an application of the bacteria *Bacillus megaterium var. Phosphaticum* and the amino acid L-alpha proline and no mineral fertilisation with nitrogen or at the rates of 60 or 90 kg N◎ha^{-1}.

http://www.aloki.hu ● ISSN 1589 1623 (Print) ● ISSN1785 0037 (Online)
DOI: http://dx.doi.org/10.15666/aeer/1906_45994609

Conclusions

1. Weather conditions during the growing season significantly affected heavy metal contents in spring wheat grain.
2. The examined biological products significantly reduced heavy metal contents in spring wheat grain, excluding zinc content.
3. Increasing rates of mineral fertilisation with nitrogen contributed to an increase in the spring wheat grain content of heavy metals. The only exception was zinc content determined in the grain of spring wheat fertilised with 120 kg N◎ha^{-1}.
4. The lowest heavy metal contents were recorded in the grain of spring wheat treated with the bacteria *Bacillus megaterium var. phosphaticum* + the amino acid L-alpha proline, whether the cereal was unfertilised or fertilised with 60 and 90 kg N◎ha^{-1}.
5. Research on the use of bacillus bacteria and biostimulants in spring wheat cultivation should be continued and the content of heavy metals in the grain should be constantly monitored.

REFERENCES

[1] Adefarati, O., Adedeji, P. O., Ajala, O. (2017): Determination of heavy metal levels in green pea (*Pisum sativum*) a case study of selected markets in Abuja, FCT. – American Journal of Innovative Research and Applied Sciences. www.american-jiras.com.

[2] Asfa, R., Almas, Z., Fuad, A., Bilal, A., Muneera, D. F., AlKahtani, F., Saghir, K. (2020): Heavy metal induced stress on wheat: phytotoxicity and microbiological management. – The Royal Society of Chemistry 10: 38379-38403.

[3] Athar, M. J., Ullah, S., Ahmad, I., Rauf, A., Nadeem, S. M., Khan, M. Y., Hussain, S., Bulgariu, L. (2018): Nickel phytoextraction through bacterial inoculation in *Raphanus sativus*. – Chemosphere 190: 234-242.

[4] Calvo, P., Nelson, L., Kloepper, J. W. (2014): Agricultural uses of plant biostimulants. – Plant Soil 383: 3-41.

[5] Demirezen, D., Ahmet, A. (2006): Heavy metal levels in vegetables in Turkey are within safe limits for Cu, Zn, Ni and exceeded for Cd and Pb. – Journal of Food Quality 29: 252-265.

[6] Du Jardin, P. (2015): Plant biostimulants: definition, concept, main categories and regulation. – Sci. Hort. 196: 3-14.

[7] Figueiredo, M. V. B., Selin, L., Araujo, F. F., Mariano, R. L. R. (2011): Plant growth promoting rhizobacteria: fundamentals and applications. – In: Maheshwari, D. K. (ed.) Plant growth and health promoting bacteria. Berlin: Springer-verlag, pp. 21-42.

[8] Fytianos, K., Katsianis, G., Triantafyllou, P., Zachariadis, G. (2001): Accumulation of heavy metals in vegetables grown in an industrial area in relation to soil. – Bulletin of Environment Contamination and Toxicology 67: 423-430.

[9] Garcia-Fraile, P., Menendez, E., Rivas, R. (2015): Role of bacterial biofertilizers in agriculture and forestry. – AIMS Bioengineering 2: 183-205.

[10] Hellal, F. A., Zeweny, R. M., Yassen, A. A. (2012): Evaluation of nitrogen and silicon application for enhancing yield production and nutrient uptake by wheat in clay soil. – J. Ap. Sci. Res. 8: 686-692.

[11] Jamova, K., Valko, M. (2011): Advances in metal-induced oxidative stress and human disease. – Toxicol. 283: 65-87.

[12] Jastrzębska, M., Kostrzewska, M. K. (2019): Using an environment-friendly fertiliser form sewage sludge ash with the addition of *Bacillus megaterium*. – Minerals 9: 423. doi:10.3390/min9070423.

http://www.aloki.hu ● ISSN 1589 1623 (Print) ● ISSN1785 0037 (Online)
DOI: http://dx.doi.org/10.15666/aeer/1906_45994609

[13] Kandii, A. A., Sharief, A. E. M., Sedh, S. E., Altai, D. S. K. (2016): Role of humic acid and amino acids in limiting loss of nitrogen fertilizer and increasing productivity of some wheat cultivars grown under newly reclaimed sandy soil. – Int. J. Adv. Res. Biol. Sci. 394: 123-136.
[14] Khajeh, M., Moghaddam, A. R. A., Sanchooli, E. (2010): Application of Doehlert design in the optimization of microwave-assisted extraction for determination of zinc and copper in cereals samples using FAAS. – Food Anal methods 3: 133-137.
[15] Luo, Y. W., Xie, W. H., Jin, X. X., Wang, Q., He, Y. J. (2013): Effects of germination on iron, zinc, calcium, manganese, and copper availability from cereals. – CyTA-Journal of Food 12(1): 22-26.
[16] Mahamed, H. H., Kaharia, M. (2012): Assessment of some heavy metals in vegetables, cereals and fruits in Saudi Arabian markets. – Egyptian Journal of Aquatic Research 38: 31-37.
[17] Muchuwenti, M., Birkett, J. W., Chinyanga, E., Zvauya, R., Scimshaw, M. D., Lester, J. N. (2006): Heavy metal content of vegetables irrigated with mixtures of wastewater and sewage sludge in Zimbabwe: Implications for human health. – Agriculture, Ecosystems and Environment 112: 41-48.
[18] Naveed, M., Bukhari, S. S., Mustafa, A., Ditta, A., Almri, S., El-Esawi, M. A., Rafique, M., Ashraf, S. (2020): Mitigation of nickel toxicity and growth promotion in sesame through the application of a bacterial endophyte and zeolite in nickel contaminated soil. – International Journal of Environmental Research and Public Health 17: 8859. doi:10.3390/ijerph17238859.
[19] Ociepa-Kubicka, A., Ociepa, E. (2012): Toxic effect of heavy metals on plants, animals and animals, Engineering and Environment 15(2): 169-180.
[20] Pirsaheb, M., Fattahi, N., Sharafi, K., Khamotian, R., Atafar, Z. (2015): Essential and toxic heavy metals in cereals and agricultural products marketed in Kermanshah, Iran, and human health risk assessment. – Food Additives and Contaminants Part B. doi: 10.1080/19393210.2015.1099570.
[21] Popko, M., Michalak, I., Wilk, R., Gramza, M., Chojnacka, K., Górecki, H. (2018): Effect on the new plant growth biostimulants based on amino acids on yield and grain quality of winter wheat. – Molecules 23: 470. doi:10.3390/molecules23020470.
[22] Radkowski, A., Radkowska, I., Bocianowski, J., Florkiewicz, A. (2020a): Synergistic effects of foliar application of amino acid and silicon on the content of micro- and macroelements in phytomass of grassland. – J. Elem. 25(3): 879-891.
[23] Radkowski, A., Radkowska, I., Bocianowski, J. (2020b): Effect of the fertilization of meadow sward with amino acids obtained from enzymatic hydrolysis on silage quality. – J. Elem. 25(1): 259-277.
[24] Rizvi, A., Zaidi, A., Ameen, F., Ahmed, B., AlKahtani, M. D. F., Khan, M. S. (2020): Heavy metal induced stress on wheat: phytotoxicity and microbiological management. – Royal Society of Chemistry 10: 38379-38403.
[25] Sarfaz, R., Hussain, A., Sabir, A., Ibtissem, B. F., Allah, D., Shihe, X. (2019): Role of biochar and plant growth promoting rhizobacteria to enhance soil carbon sequestration. – Environ. Monit. Assess. 191: 251. doi.org/10.1007/s10661-019-7400-9.
[26] Sharma, O. P., Bangar, K. S., Jain, R., Sharma, P. K. (2004): Heavy metals accumulation in soil irrigated by municipal and industrial effluent. – Journal of Environmental Science and Engineering 46(1): 65-73.
[27] Shicheng, Z., Shaoju, Q., Ping, H. (2018): Changes of heavy metals in soil and wheat grain under long-term environmental impact and fertilization practices in North China. – Journal of plant Nutrition 41(3): 1-10.
[28] Srinivas, N., Vinod Kumar, B., Suresh Kumar, K. (2002): Lead pollution in roadside plant in Visakhapatinam. – Journal of Environmental Studies and Pol. 5(1): 63-68.
[29] Thielecke, F., Nugent, A. P. (2018): Contaminants in Grain - A Major Risk for Whole Grain Safety? – Nutrients 10(9): 1213.

http://www.aloki.hu ● ISSN 1589 1623 (Print) ● ISSN1785 0037 (Online)
DOI: http://dx.doi.org/10.15666/aeer/1906_45994609

[30] Turan, V., Khan, S. A., Mahmood-ur-Rahman, Iqbal, M., Ramzani, P. M. A., Fatima, M. (2018): Promoting the productivity and quality of brinjal aligned with heavy metals immobilization in a wastewater irrigated heavy metal polluted soil with biochar and chitosan. – Ecotoxicol. Environ. Saf. 161: 409-419.
[31] Vejan, P., Abbullah, R., Khadiran, T., Ismail, S., Nasrulhaq, B. (2016): Role of plant growth promoting rhizobacteria in agricultural sustainability. – Molecules 12(5): 1-17.
[32] WHO. (2001): Food additives and contaminants. – Joint Codex Alimentarius Commission, FAO/WHO Food standards Programme, 2001; ALINORM 01/12A.
[33] Zakir, H., Brennan, J. D. (2011): β-galactosidase-based colorimetric paper sensor for determination of heavy metal. – Anal. Chem. 83: 772-8778.
[34] Zheng, Y., Li, X-K., Wang, Y., Cai, L. (2008): The role of zinc, copper and iron in the pathogenesis of diabetes and diabetic complications: therapeutic effects by chelators. – Hemoglobin 32: 135-145.

http://www.aloki.hu ● ISSN 1589 1623 (Print) ● ISSN1785 0037 (Online)
DOI: http://dx.doi.org/10.15666/aeer/1906_45994609

EFFECTS OF DIFFERENT FERTILIZATION TREATMENTS ON THE YIELD PERFORMANCE, YIELD PARAMETERS AND GRAIN QUALITY OF WINTER WHEAT GROWN ON VERTISOL SOIL TYPE

TMUŠIĆ, N.[1*] – ĆIRIĆ, S.[1] – NIKOLIĆ, K.[1] – KNEŽEVIĆ, J.[1] – RAJIČIĆ V.[2]

[1]*Faculty of Agriculture, University of Priština in Kosovska Mitrovica, Kosovska Mitrovica - Lešak, st Kopaonička bb, 38219 Lešak, Serbia*

[2]*Faculty of Agriculture, University of Niš, Kruševac, st Kosančićeva No 4, 37000 Kruševac, Serbia*

**Corresponding author*
e-mail: nadica.tmusic@pr.ac.rs

(Received 22nd Jun 2021; accepted 1st Oct 2021)

Abstract. Fertilization effects were performed in a stationary type of field trial, on a vertisol soil type, on the premises of the Small Grains Research Center in Kragujevac, central Serbia, over a three-year period (2010–2013). In addition to untreated control, the trial included six mineral nutrition treatments: (1) $N_0P_0K_0$; (2) $N_{80}P_0K_0$; (3) $N_{80}P_{60}K_{60}$; (4) $N_{80}P_{100}K_{60}$; (5) $N_{80}P_{60}K_0$; (6) $N_{80}P_{100}K_0$; (7) $N_{80}P_0K_{60}$. Individual fertilizers used in the trial were as follows: KAN (nitrogen fertilizer), super phosphate (phosphate fertilizer), and 60% of potassium salt (potassium fertilizer). Mineral nutrition treatments mentioned above were applied in the two winter wheat cultivars: Ana Morava and KG 100. Favorable physical properties of the soil are of major importance for efficient growth of wheat. In this regard, the aim of this study was to determine to what extent the different fertilizing treatments influence yield performance, yield parameters and grain quality of winter wheat cultivars grown on vertisol soil type. The highest yield of winter wheat over the three-year trial was obtained from the Ana Morava cultivar (6,276 kg ha^{-1}) in the treatment that involved the application of $N_{80}P_{60}K_{60}$. Variance analysis implied very highly significant individual effects of study year and fertilization on grain yield in the studied winter wheat cultivars, as well as very highly significant effect of interaction between year × fertilization.
Keywords: *wheat, vertisol, mineral nutrition, cultivars, grain yield*

Introduction

Wheat is the major product of crop and agricultural production and the most significant food source of the entire human population (Dixon et al., 2009; Todorovska et al., 2009; Nouri et al., 2011; Rizvan et al., 2016). As winter wheat uses large amounts of mineral elements during the growing period, it has high soil fertility requirements (Maleševic et al., 2008). The productivity of winter wheat grown on acidic soils such as vertisol is generally significantly reduced. Yield performance, yield parameters and grain quality are critical indicators of productivity of winter wheat plants. Yield, yield parameters (grain number and grain weight) and quality of winter wheat grain (1000-grain weight and hectoliter weight) are crucial to determining the correlation between plant, soil and mineral nutrition.

A universal method of fertilizing wheat grown on low pH soils is difficult to devise due to numerous nutrition and nutrition application specificities. The nutritional needs of plants grown on acid soils are somewhat difficult to specify due to the highly non-uniform physical and chemical properties of soil (Nemeth, 2006). As wheat cultivated on an acidic soil requires specific mineral nutrition, i.e. appropriately balanced nitrogen

http://www.aloki.hu ● ISSN 1589 1623 (Print) ● ISSN 1785 0037 (Online)
DOI: http://dx.doi.org/10.15666/aeer/1906_46114627

and phosphorus nutrition, the increased nutritive input of phosphorus is a must (Jevtić et al., 1988; Riley et al., 2001; Dolijanović, et al., 2019).

Low production capacity of vertisols is the result of poor physical and mechanical, and water and air properties (Malešević et al., 2008; Jaćimović et al., 2012). The use of fertilizers is based on soil fertility control, which infers preserving the existing favorable soil fertility or maintaining soil fertility improved with fertilizers. Fertilizers establish a balance between the total amount of nutrients ensuring high yields, on the one hand, and the amount of nutrients contained in the soil, on the other. In order to determine the optimal amount of mineral nutrients from a fertilizer, it is necessary to be acquainted with the specificities of nutrients uptake by plants, as well as with the fertilizer dynamics in the soil (Korchens (2006); Jelić et al., 2012; Djekić, et al., 2013).

Yield performance of winter wheat depends on a number of factors, primarily cultivar genotype, agro-environmental conditions (soil fertility, precipitation and air temperature) and the applied production technology (Fagam et al., 2006; Trethowan et al., 2007; Rashid et al., 2013). Also, studies performed so far suggest that yield performance of wheat depends on a number of yield components, i.e. number of plants, number of grains per spike, grain weight per spike, 1000-grain weight. Correlation among these parameters is highly complex, as the increase in the value of one parameter often results in a decrease in the value of another (Hristov et al., 2008).

Grain number and grain weight are considered as cultivar specificities however, they are generally affected by agro-environmental conditions and mineral nutrition (Savić et al., 2006).

Studies performed so far imply the necessity of continuously determining quantity and nutrients ratios of fertilizers as imposed by specific agro-environmental conditions. Under the agro-environmental conditions of Serbia most commonly applied amounts of N ensuring overall high yields range from 80–120 kg ha^{-1}, depending on the agrochemical properties of the soil.

Stationary field trials, such as ours, are of utmost importance (Cooke (1976); Ragasits et al., 2000; Malešević et al., 2008; Đekić et al., 2014b).

Newly developed wheat cultivars have substantially higher yield potential (Rajaram, 2001; Ogbonnaya et al., 2008; Denčić et al., 2010) however their mineral nutrition requirements are highly demanding consequently (Đekić et al., 2014a; Jelić et al., 2012).

The objective of this research was to examine the effects of different fertilization treatments on yield performance, yield parameters (number of grains per spike and grain weight per spike) and grain quality (1000-grain weight and hectoliter weight) in different winter wheat cultivars grown on a vertisol.

Materials and methods

The experiment was performed in a stationary type field trial (the experimental field of the Small Grains Research Center, Kragujevac (44°02'N, 20°56'E, altitude: 185 m a.s.l.), Republic of Serbia (central Serbia) (*Fig. 1*) involving fertilization over a long-term period (over 30). The study location of Kragujevac is approximately 113 km away from Belgrade. The study was performed over the three-year period, from 2010 to 2013.

The experiment was conducted on two winter wheat cultivars, 1) Ana Morava and 2) KG 100. In addition to an untreated control, the trial included six mineral nutrition

http://www.aloki.hu ● ISSN 1589 1623 (Print) ● ISSN 1785 0037 (Online)
DOI: http://dx.doi.org/10.15666/aeer/1906_46114627

treatments: 1) $N_0P_0K_0$; 2) $N_{80}P_0K_0$; 3) $N_{80}P_{60}K_{60}$; 4) $N_{80}P_{100}K_{60}$; 5) $N_{80}P_{60}K_0$; 6) $N_{80}P_{100}K_0$; 7) $N_{80}P_0K_{60}$.

The following fertilizers were used in the trial: KAN (nitrogen fertilizer), super phosphate (phosphate fertilizer), and 60% of potassium salt (potassium fertilizer).

The following parameters were examined: grain yield, hectoliter weight, 1000 grain weight, number of grains per spike and grain weight per spike.

The experiment was set up at an area of 50 m^2 following the random block design with five replications Conventional cultural practices were applied in the trial. The seeding rate in the cultivars studied was 600 germinated seeds per m^2. Statistical data processing was performed in the Analyst module of the SAS/STAT program (SAS Institute, 2000). The Descriptive Statistics and Analysis Variance was applied.

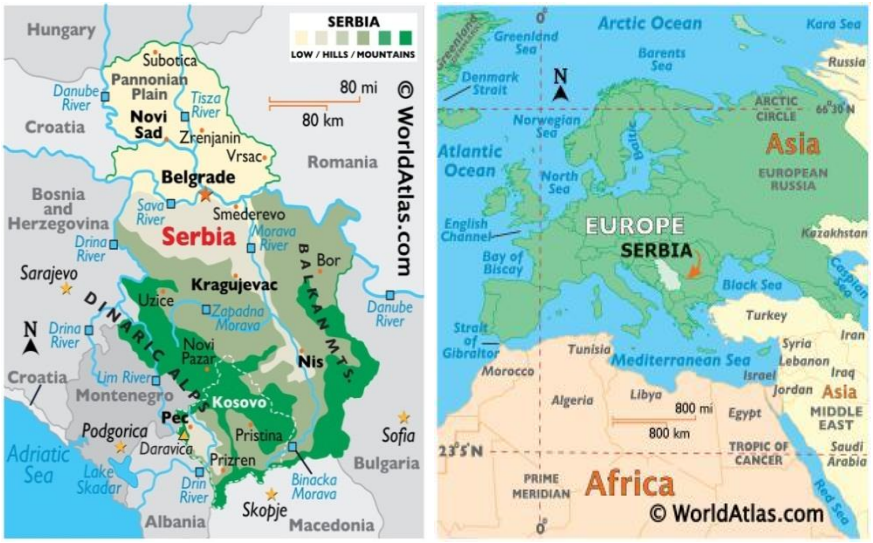

Figure 1. *Study area of (Central Serbia-Kragujevac) and Europe – Serbia*

Climatic conditions

Agricultural production greatly depends on climatic conditions of a production area. As an essential element of the climate, air temperature is crucial to successful wheat growth. In this regard, precipitation is a highly relevant factor, both in terms of its annual amounts and the distribution (Savić et al., 2006). Favorable soil humidity conditions have a stimulating effect on seed germination and sprouting, as well as on plant development.

The area of Kragujevac is located at an altitude of 186 m, in temperate climate zone.

Meteorological conditions, i.e. air temperature and precipitation rates over the 2011/2012 and 2012/2013 growing periods were relatively favorable, whereas the 2010/2011 growing period exhibited lower precipitation rates, as well as lower air temperatures over some periods in the season (Tahmasebi et al., 2014).

Mean monthly air temperatures (°C) and monthly precipitation sum (lm^{-1}) over the examination examined are given in *Table 1*.

In the first year of our study in the area of Kragujevac (2010/2011), the recorded precipitation during spring was 444.2 l m^{-1}, which is some 127.4 l m^{-1} lower than multi-year average, while mean air temperature over the same period was 10.41, or within the multi-year average. Precipitation recorded in March and April, 20.4 l m^{-1} and 20.8 l m^{-1}

http://www.aloki.hu ● ISSN 1589 1623 (Print) ● ISSN 1785 0037 (Online)
DOI: http://dx.doi.org/10.15666/aeer/1906_46114627

respectively, was lower by 20–30 l m^{-1} compared to the multi-year average. This lack of precipitation in the first year of study (2010/2011) affected growth and development of plants, especially clustering, rooting, leaf mass ratio, which consequently had an adverse effect on yield performance, yield parameters (grain number and grain weight) and grain quality (1000-grain weight and hectoliter weight).

Table 1. *Temperature and water in the course of the vegetation in 2010/2011, 2011/2012 and 2012/2013*

Month	Temperature (t °C)				Water (l m^{-1})			
	Year			Average	Year			Average
	2010/2011	2011/2012	2012/2013	1961/99	2010/2011	2011/2012	2012/2013	1961/99
October	10.2	10.4	13.5	11.3	86.9	33.3	56.2	42.8
November	11.4	3.1	9.5	6.5	27.9	1.3	17.7	46.4
December	2.4	4.6	1.7	1.1	50.1	43.3	16.4	46.8
January	0.9	0.7	2.9	-1.8	29.1	117.2	65.8	38.3
February	0.5	-3.7	4.0	3.0	48.5	60.1	84.4	35.7
March	7.2	8.1	6.5	6.5	20.4	5.7	102.9	40.4
April	12.0	12.9	13.4	11.3	20.8	74.5	41.2	53.1
May	15.8	16.1	18.2	16.3	65.8	83.3	70.8	66.7
Jun	20.9	23.0	19.9	19.0	32.3	57.8	85.4	80.3
July	22.8	25.8	21.9	21.1	62.4	35.4	60.6	70.6
(X – VII)	10.41	10.10	11.50	10.40	444.2	515.9	601.4	571.6

In the second year of the study (growing season 2011/2012), the recorded precipitation was 515.9 lm^{-1}, which is only 56 l m^{-1} lower compared to the multi-year average. The precipitation rate over the growing period was rather high and well distributed, accompanied with favorable air temperature average, all of which ensured proper development of plants. Favorable climatic conditions in June fostered the development of winter wheat plants, which resulted in high winter wheat grain yield.

Climatic conditions were the most favorable in the third study year (2012/2013), precipitation being 601.4 l m^{-1} and mean air temperature 11.50 °C.

Air temperatures were higher than average from January to March, which promoted plant growth. Precipitation rate in March, which amounted to 102.9 l m^{-1}, ensured good clustering of winter wheat plants. Mean monthly temperature in April was 13.4 °C, which was by 2.1 °C higher than the multi-year average. Favorable air temperatures in May (18.2 °C) and proper water balance (70.8 l m^{-1}) ensured good plant development and stimulated grain filling.

The values of mean monthly air temperatures (°C) and monthly precipitation sums (l m^{-1}) over the 2012/2013 examination period gave the highest grain yield and quality of winter wheat grain.

The data presented in *Table 1* (mean monthly temperatures and precipitation rates during the study) suggest that climatic conditions varied among the years of study. Weather conditions greatly affected the duration of specific phases of wheat plant

http://www.aloki.hu ● ISSN 1589 1623 (Print) ● ISSN 1785 0037 (Online)
DOI: http://dx.doi.org/10.15666/aeer/1906_46114627

development as well as the overall dynamics of plant growth and development over the growing periods (Savić et al., 2007; Paunović et al., 2010).

Favorable weather conditions confirmed over season 2012/2013 i.e. highest precipitations rate proper precipitations distribution by months and agreeable monthly air temperatures suggested optimal conditions for growing winter wheat on a vertisol especially during critical phases of plants development.

The 2011/2012 growing season was also favorable for growing winter wheat, while the most unfavorable climatic conditions for growing winter wheat were in the first study year (2010/2011).

Results and discussion

For the successful development, wheat requires fertile soils of favorable physical properties. The soil in the trial is a degrading smonica (vertisol), of an A-Bt-C profile. The upper part of the A horizon is gray, showing signs of substantial deficiencies in bases and humus due to leaching. The upper part of the A horizon is strongly acidic to acidic, the degree of base saturation being lower than 70%. In the deeper layers of this soil, there is a Bt horizon, which is strongly enriched with clay and poorly permeable. During wet periods, surface water is retained above this horizon, which leads to the formation of reddish brown Fe-hydroxide mottles as well as small grains of spodic materials (orstein). In addition to the heavy mechanical composition and rough, unstable structure, this soil is of poor porosity, which significantly deteriorates physical properties of this soil (Li et al., 2010; Meng et al., 2009).

Before the trial, in order to determine soil fertility, samples were taken and analyses were performed involving fertility parameters based on the fertilization treatments (*Table 2*).

Table 2. *Facts of soil fertility at experimental field*

Fertilizing variants	Profound (cm)	HUMUS (%)	pH		N overall (%)	P_2O_5	K_2O
			H_2O	KCl		mg/100 g soil	
$N_0P_0K_0$	0 - 20	2.13	5.85	4.37	0.12	2.60	18.67
$N_{80}P_0K_0$		2.10	5.83	4.26	0.14	2.20	17.60
$N_{80}P_{60}K_{60}$		2.39	5.58	4.27	0.15	8.17	27.47
$N_{80}P_{100}K_{60}$		2.25	5.72	4.28	0.14	9.83	24.00
$N_{80}P_{60}K_0$		2.34	5.63	4.15	0.15	9.00	17.40
$N_{80}P_0K_{60}$		2.24	5.73	4.22	0.16	2.83	23.53

The soil used in the experiment is strongly acidic (pH in Kcl < 4.5) with a moderate humus content. The highest replaceable acidity was observed in $N_{80}P_{60}K_0$ and $N_{80}P_0K_{60}$ fertilization treatments. Treatments which involved mineral nutrition had higher humus contents (on average) compared to the control. The highest humus content was observed in $N_{80}P_{60}K_{60}$ and $N_{80}P_{60}K_0$ fertilization treatments.

The total nitrogen content was moderate (according to the Wohltmann classification) with fertilizer treatments exhibiting higher total nitrogen content compared to the untreated control. The content of readily available phosphorus was low (2.20–9.83 mg/100 g of soil), while readily available potassium content was moderately high to high (17.40–27.47 mg/100 g of soil).

http://www.aloki.hu ● ISSN 1589 1623 (Print) ● ISSN 1785 0037 (Online)
DOI: http://dx.doi.org/10.15666/aeer/1906_46114627

Grain yield

Average grain yield in the studied winter wheat cultivars (‘Ana Morava’ and ‘KG 100’) grown in five replications over the three growing periods (2010/2011, 2011/2012 and 2012/2013) are presented in *Table 3*.

Grain yield is the most significant indicator of plant productivity. It is also the most reliable indicator of differences in productivity among cultivars and their mineral nutrition specificities, as yield is the final result of mutual actions, both external factors influencing plant growth and development, and bio-rhythmic dynamics of physiological and biochemical processes.

Average values of yield varied between the studied winter wheat cultivars over the three-year period on a vertisol as influenced by fertilization treatments and climatic conditions.

Table 3. *Grain yield (t ha^{-1}) - cultivars 1) Ana Morava and 2) KG 100*

Cult.	Fertilization	Years									Average		
		2010/2011			2011/2012			2012/2013					
		$\bar{x}$	S	Sx	$\bar{x}$	S	Sx	$\bar{x}$	S	Sx	$\bar{x}$	S	Sx
1	N0P0K0	0.819	0.122	0.071	1.605	0.345	0.199	1.335	0.422	0.255	1.253	0.449	0.150
	N80P0K0	2.448	0.442	0.255	3.931	0.739	0.427	4.491	1.900	1.091	3.623	1.387	0.463
	N80P60K60	3.403	1.147	0.662	4.928	0.711	0.410	6.276	0.130	0.075	4.896	1.417	0.472
	N80P100K60	3.994	0.440	0.254	4.156	1.146	0.662	5.723	0.654	0.377	4.625	1.080	0.360
	N80P60K0	2.898	0.616	0.355	4.050	1.023	0.591	4.195	0.780	0.450	3.714	0.942	0.314
	N80P100K0	3.190	0.421	0.243	3.969	0.685	0.395	4.116	1.018	0.587	3.758	0.778	0.259
	N80P0K60	2.491	0.455	0.263	3.563	1.018	0.588	4.210	0.960	0.544	3.421	1.052	0.351
2	N0P0K0	0.896	0.283	0.164	1.548	0.324	0.187	1.381	0.123	7.131	1.275	0.369	0.123
	N80P0K0	1.690	0.693	0.340	3.186	0.215	0.124	3.563	1.220	0.704	2.813	1.113	0.371
	N80P60K60	3.837	0.889	0.513	4.378	0.530	0.307	4.896	1.608	0.929	4.370	2.155	0.718
	N80P100K60	3.503	0.260	0.150	4.210	0.689	0.398	4.876	1.606	0.927	4.196	1.065	0.355
	N80P600K0	3.368	0.739	0.427	3.962	1.200	0.693	4.017	2.120	1.270	3.782	1.343	0.448
	N80P100K0	2.765	0.308	0.178	3.984	0.260	0.150	4.053	1.286	0.743	3.601	0.921	0.307
	N80P0K60	2.862	0.392	0.226	3.553	0.597	0.345	4.080	1.690	0.976	3.498	1.059	0.353

The lowest grain yield was obtained in untreated control in all study year, in both cultivars (‘Ana Morava’ and ‘KG 100’). Fertilization significantly increased grain yield of winter wheat (Kovačević (2005); Savić et al., 2005). In regard to grain yield, some differences were perceived between the examined winter wheat cultivars.

In the first experimental year, ‘Ana Morava’ fertilized with $N_{80}P_{100}K_{60}$ had the highest grain yield (3,994 kg ha^{-1}), while $N_{80}P_{60}K_{60}$ fertilization treatment gave the highest grain yield in ‘KG 100’ (3,837 kg ha^{-1}) in the same season.

In the second and third years of examination, both cultivars exhibited the best grain yield performance when fertilized with $N_{80}P_{60}K_{60}$. The application of NK fertilizers considerably reduced the grain yield of winter wheat compared to fertilization treatments involving phosphorus (both low and high rates of phosphorus) (Kostić et al., 1987; Tyrone et al., 2002; Bálint et al., 2008) over the entire study period. This confirms that the examined winter wheat cultivars grown on acidic soils (vertisol) had considerably higher productivity when fertilized with NPK compared to the yields obtained on non-acidic soils (Rehman et al., 2006; El-Lethy et al., 2013; Jelić et al., 2015).

http://www.aloki.hu ● ISSN 1589 1623 (Print) ● ISSN 1785 0037 (Online)
DOI: http://dx.doi.org/10.15666/aeer/1906_46114627

During the three-year period, average grain yield was slightly higher in 'Ana Morava' fertilized with $N_{80}P_{60}K_{60}$ (4,836 kg ha^{-1}) than 'KG 100' (4,370 kg ha^{-1}) under the same treatment.

N fertilization treatment gave the lowest grain yield in 'KG 100' (1,690 kg ha^{-1}) in the first study year.

The highest grain yield of winter wheat grown on a vertisol over the three-year period was obtained in 'Ana Morava' (6,276 kg ha^{-1}) fertilized with $N_{80}P_{60}K_{60}$.

'Ana Morava' and 'KG 100' had a considerably higher grain yield in the second and third years of examination, which confirms that favorable climatic conditions (average values of mean monthly air temperatures (°C) and monthly precipitation sums (lm^{-1}) are crucial to grain yield performance (Paunović et al., 2010). In conclusion, besides genotype, grain yield of winter wheat is governed to a great extent by the fertilization system, which, along with climatic, soil conditions and cultivar specificities, is a key factor in crop yield and quality (Jelic and et al., 2015).

Number of grains per spike

The number of grains per spike is a parameter of wheat yield closely correlated with number of spikelets per spike, number of flowers per spikelet as well as with successful fertilization and germination of grains (Borojević, 1978). As these parameters are greatly governed by agro-environmental conditions and the applied cultural practices, number of grains per spike is considered a highly variable trait (Milošev, 1996).

Average number of grains per spike in the studied winter wheat cultivars ('Ana Morava' and 'KG 100') grown in five replications over the three growing seasons (2010/2011, 2011/2012 and 2012/2013) are given in *Table 4*.

Table 4. *Number of grains per spike – cultivars 1) Ana Morava and 2) KG 100*

Cult.	Fertilization	Years									Average		
		2010/2011			2011/2012			2012/2013					
		$\bar{x}$	S	Sx	$\bar{x}$	S	Sx	$\bar{x}$	S	Sx	$\bar{x}$	S	Sx
1	N0P0K0	20.67	6.658	3.844	15.67	2.887	1.667	28.33	1.527	0.882	21.56	6.654	2.218
	N80P0K0	35.00	1.000	0.577	35.00	2.646	1.527	36.33	1.528	0.882	35.44	1.740	0.580
	N80P60K60	43.67	5.132	2.963	48.00	8.660	5.000	45.00	1.000	0.577	45.56	5.411	1.804
	N80P100K60	40.67	5.508	3.180	41.67	6.110	3.528	46.00	1.000	0.577	42.78	4.816	1.605
	N80P60K0	39.67	6.110	3.528	41.00	9.849	5.686	45.00	4000	2.309	41.89	6.585	2.195
	N80P100K0	38.33	2.082	1.202	39.67	5.508	3.180	40.33	0.577	0.333	39.44	3.087	1.029
	N80P0K60	37.67	2.082	1.202	36.67	8.327	4.807	39.67	1.528	0.882	38.00	4.555	1.518
2	N0P0K0	13.67	2.517	1.453	19.00	6.000	3.464	25.67	2.517	1.453	19.44	6.267	2.089
	N80P0K0	33.00	7.211	4.163	36.67	4.726	0.728	42.00	5.000	2.887	37.22	6.340	2.113
	N80P60K60	35.33	7.095	4.096	37.00	4.359	2.517	42.00	1.000	0.577	38.11	5.159	3.302
	N80P100K60	34.33	5.774	3.333	36.33	3.215	1.856	40.00	2.000	1.155	36.89	4.256	1.419
	N80P60K0	41.68	9.238	5.333	34.67	5.508	3.180	31.33	4.509	2.603	35.89	7.704	2.469
	N80P100K0	29.33	3.786	2.186	35.33	5.686	3.283	39.67	5.508	3.180	34.78	6.280	2.093
	N80P0K60	22.33	5.508	3.180	32.00	9.539	5.508	41.33	0.577	3.333	31.89	9.905	3.302

The results achieved over the entire study period showed that the smallest number of grains per spike was observed in the control, while the treatments involving mineral

http://www.aloki.hu ● ISSN 1589 1623 (Print) ● ISSN 1785 0037 (Online)
DOI: http://dx.doi.org/10.15666/aeer/1906_46114627

nutrition gave a significantly larger number of grains per spike. Compared to the untreated control, this increase in number of grains per spike was only due to the application of nitrogen over the entire study period (all the three study years) (Blandino et al., 2016; Litke et al., 2018; Terzić et al., 2018).

Under NP_1K treatment, average number of grains per spike over the three-year period was significantly higher in 'Ana Morava' (45.56) than in 'KG 100 (38.71).

The third year of study (2012/2013) resulted in the highest number of grains per spike in both cultivars ('Ana Morava' and 'KG 100') as this season provided the most favorable conditions for the wheat crop.

The smallest number of grains per spike was observed in cv. 'KG 100' (22.33) in the first study year (2010/2011) in the treatment under $N_{80}P_0K_{60}$ mineral nutrition.

The greatest number of grains per spike in all years was obtained by cv. 'Ana Morava' under $N_{80}P_{60}K_{60}$ treatment in the third study year (2012/2013).

Grain weight per spike

Average grain weight per spike in the studied winter wheat cultivars ('Ana Morava' and 'KG 100') grown in five replications over the three growing periods (2010/2011, 2011/2012 and 2012/2013) are shown in *Table 5*.

Grain weight per spike in wheat is considered a relevant indicator of yield quality in general. It depends on agro-environmental conditions and applied cultural practices, as well as on fertilization percentage and grain formation in flowers (Milošev, 2000).

Table 5. *Grain weight per spike (g) - cultivars 1) Ana Morava and 2) KG 100*

Cult.	Fertilization	Years									Average		
		2010/2011			2011/2012			2012/2013					
		$\bar{x}$	S	Sx	$\bar{x}$	S	Sx	$\bar{x}$	S	Sx	$\bar{x}$	S	Sx
1	N0P0K0	0.603	0.015	0.009	0.560	0.075	0.044	1.347	0.031	0.018	0.837	0.385	0.128
	N80P0K0	1.157	0.211	0.122	1.240	0.010	0.006	1.720	0.060	0.035	1.372	0.285	0.095
	N80P60K60	1.343	0.211	0.122	2.233	0.484	0.279	2.073	0.095	0.055	1.883	0.491	0.164
	N80P100K60	1.237	0.055	0.032	1.653	0.352	0.203	2.220	0.110	0.063	1.703	0.466	0.155
	N80P60K0	1.073	0.102	0.059	1.560	0.387	0.233	2.203	0.145	0.084	1.612	0.535	0.178
	N80P100K0	1.280	0.020	0.011	1.637	0.275	0.159	1.810	0.010	0.006	1.576	0.272	0.091
	N80P0K60	1.143	0.107	0.062	1.547	0.226	0.130	1.970	0.040	0.023	1.553	0.380	0.127
2	N0P0K0	0.597	0.075	0.043	0.513	0.100	0.058	1.260	0.060	0.035	0.790	0.361	0.120
	N80P0K0	1.213	0.115	0.066	1.417	0.239	0.138	1.817	0.165	0.095	1.482	0.308	0.103
	N80P60K60	1.203	0.050	0.029	1.517	0.293	0.169	1.983	0.097	0.056	1.568	0.374	0.125
	N80P100K60	1.283	0.247	0.142	1.463	0.294	0.169	1.757	0.275	0.159	1.501	0.314	0.105
	N80P60K0	1.323	0.071	0.041	1.273	0.273	0.158	1.777	0.285	0.165	1.458	0.313	0.104
	N80P100K0	1.200	0.050	0.029	1.673	0.281	0.162	1.483	0.215	0.124	1.452	0.273	0.091
	N80P0K60	1.167	0.153	0.088	1.495	0.220	0.129	1.495	0.220	0.129	1.386	0.518	0.173

The application of different fertilizers had a strong impact on grain weight per spike. In both cultivars studied ('Ana Morava' and 'KG 100') grain weight per spike was markedly higher over the second and third growing seasons compared to the season 2010/2011.

Compared to the untreated control and the other fertilization treatments, both cultivars exhibited the highest grain weight per spike under the fertilization treatment

http://www.aloki.hu ● ISSN 1589 1623 (Print) ● ISSN 1785 0037 (Online)
DOI: http://dx.doi.org/10.15666/aeer/1906_46114627

involving NPK, at both rates of phosphorus, which is in agreement with the results (Jelić et al., 2012; Djekić, et al., 2014b). Grain weight per spike varied between the winter wheat cultivars examined.

The highest grain weight per spike was obtained in 'Ana Morava' (2.233 g) under $N_{80}P_{60}K_{60}$ fertilization treatment in the third year of study, while 'KG 100' gave the lowest grain weight per spike (1.167 g) when fertilized with $N_{80}P_0K_{60}$, also in season 2012/2013. Weather conditions (precipitation and air temperature) during the seasons 2011/2012 and 2012/2013 were more favorable, as shown by the results of the study. Grain weight per spike was lower in the first study year, when precipitation and air temperatures were less favorable for wheat plant growth and development.

1000-grain weight

The average 1000-grain weight in the studied winter wheat cultivars ('Ana Morava' and 'KG 100') grown in five replications over the three growing periods (2010/2011, 2011/2012 and 2012/2013) are given in *Table 6*.

1000-grain weight is an important parameter of wheat grain quality which is governed by genotype, however it is largely influenced by agro-environmental conditions and cultural practices.

1000-grain weight varied considerably between the cultivars under the different mineral nutrition treatments. The data given in *Table 6* infer that 1000-grain weight was lowest in untreated control, as show in the results (Savić et al., 2005).

Table 6. *1000-grain weight (g) - cultivars 1) Ana Morava and 2) KG 100*

Cult.	Fertilization	Years									Average		
		2010/2011			2011/2012			2012/2013					
		$\bar{x}$	S	Sx	$\bar{x}$	S	Sx	$\bar{x}$	S	Sx	$\bar{x}$	S	Sx
1	N0P0K0	33.67	1.258	0.726	32.83	2.082	1.202	39.83	0.725	0.419	35.44	3.546	1.182
	N80P0K0	39.33	1.527	0.882	35.50	1.803	1.041	43.33	0.757	0.437	39.39	3.612	1.204
	N80P60K60	44.50	0.866	0.500	46.33	2.021	1.167	45.67	1.332	0.769	45.50	1.516	0.505
	N80P100K60	41.17	0.764	0.441	43.33	3.055	1.764	46.23	1.002	0.578	43.58	2.753	0.917
	N80P60K0	39.67	3.819	2.205	43.33	2.517	1.453	42.73	1.563	0.902	41.91	2.956	0.985
	N80P100K0	38.17	0.764	0.441	41.67	2.082	1.202	45.73	0.643	0.371	41.86	3.477	1.159
	N80P0K60	37.50	2.784	1.607	40.67	2.021	1.167	45.63	0.666	0.384	41.27	3.959	1.320
2	N0P0K0	32.50	2.179	1.258	32.17	0.577	0.333	40.38	0.520	0.300	35.02	4.190	1.397
	N80P0K0	38.50	1.803	1.041	42.17	1.041	0.601	41.33	0.379	0.219	40.70	1.986	0.662
	N80P60K60	40.67	2.566	0.481	42.00	3.464	2.000	43.47	3.449	1.991	42.04	3.015	1.005
	N80P100K60	40.33	1.528	0.882	43.00	2.000	1.150	42.73	0.462	0.267	42.02	1.804	0.601
	N80P60K0	39.83	1.258	0.726	42.83	0.577	0.333	42.73	1.501	0.867	41.80	1.794	0.598
	N80P100K0	41.83	1.756	1.014	41.17	5.008	2.892	41.73	1.724	0.996	41.58	2.807	0.936
	N80P0K60	38.33	1.527	0.882	38.33	1.893	1.093	43.00	0.346	0.200	39.96	2.726	0.909

Treatments that involved full NPK fertilization, at both rates of phosphorus, gave the highest 1000-grain weight, while mineral nutrition treatments that contained nitrogen fertilizer (Protić et al., 2007) only or $N_{80}P_0K_{60}$ treatments resulted in lower 1000-grain weights.

The lowest 1000-grain weight over the three years of examination was observed in 'KG 100' (38.33) treated with NK (the result of the first year of the study). This cultivar

http://www.aloki.hu ● ISSN 1589 1623 (Print) ● ISSN 1785 0037 (Online)
DOI: http://dx.doi.org/10.15666/aeer/1906_46114627

had the highest 1000-grain weight (43.47) when treated with $N_{80}P_{60}K_{60}$ (the result of the third study year).

The highest 1000-grain weight over the entire study period was obtained in 'Ana Morava' (46.33) under the fertilization treatment that involved $N_{80}P_{60}K_{60}$.

Higher 1000-grain weights in both cultivars were recorded in the 2011/2012 and 2012/2013 seasons, characterized by favorable weather conditions.

Hectoliter weight

Average values of hectoliter weight in the studied winter wheat cultivars ('Ana Morava' and 'KG 100') grown in five replications over the three growing periods (2010/2011, 2011/2012 and 2012/2013) are presented in *Table 7*.

Hectoliter weight is a parameter most commonly considered when assessing wheat grain quality.

Average hectoliter grain weight in the untreated control was lower than in the fertilized plants over the entire three-year examination period, which is in agreement with a results (Savić et al., 2005).

'Ana Morava' exhibited the best performance in terms of average hectoliter weight of grain across experimental years. As for 'KG 100', it recorded lower average hectoliter grain weight in all the three growing periods examined.

Based on the fertilization treatments, 'Ana Morava' treated with $N_{80}P_{60}K_{60}$ gave the highest hectoliter grain weight on average in all three study years (74.01hl $^{-1}$), while 'KG 100' had the highest hectoliter grain weight when treated with $N_{80}P_{100}K_{60}$ (71.83 hl^{-1}) over the entire study period.

Table 7. *Hectoliter weight (kg hl^{-1}) - cultivars 1) Ana Morava and 2) KG 100*

Cult.	Fertilization	Years									Average		
		2010/2011			2011/2012			2012/2013					
		$\bar{x}$	S	Sx	$\bar{x}$	S	Sx	$\bar{x}$	S	Sx	$\bar{x}$	S	Sx
1	N0P0K0	70.98	1.514	0.874	69.45	0.200	0.115	74.93	3.826	2.209	71.79	3.201	1.067
	N80P0K0	69.78	2.663	1.538	70.52	2.101	1.213	76.73	1.643	0.949	72.34	3.806	1.269
	N80P60K60	71.38	2.572	1.485	73.52	1.007	0.581	77.13	1.685	0.973	74.01	2.992	0.997
	N80P100K60	71.25	1.744	1.007	72.98	0.611	0.353	74.32	3.402	1.964	72.85	2.349	0.783
	N80P60K0	69.63	4.087	2.359	72.05	2.400	1.386	75.40	2.751	1.588	72.36	3.714	1.238
	N80P100K0	72.45	0.400	0.231	72.45	2.000	1.155	73.65	4.613	2.663	72.85	2.592	0.864
	N80P0K60	70.32	2.013	1.162	71.78	1.155	0.667	75.12	4.046	2.336	72.41	3.159	1.053
2	N0P0K0	66.42	2.462	1.421	69.12	2.948	1.702	74.98	1.847	1.067	70.17	4.351	1.450
	N80P0K0	66.83	1.087	0.627	70.45	1.058	0.611	73.78	1.155	0.667	70.36	3.158	1.052
	N80P60K60	67.50	0.953	0.550	68.83	2.646	1.528	77.00	1.314	0.759	71.11	4.717	1.572
	N80P100K60	69.65	0.800	0.462	70.32	1.007	0.581	75.52	2.411	1.392	71.83	3.099	1.033
	N80P60K0	67.37	1.249	0.721	70.18	0.231	0.133	75.12	2.444	1.411	70.89	3.666	1.222
	N80P100K0	67.57	1.184	0.683	68.52	2.026	1.170	75.20	2.433	1.405	70.44	4.002	1.334
	N80P0K60	67.92	0.462	0.267	68.70	3.866	2.232	74.85	1.442	0.833	70.49	3.889	1.296

The lowest hectoliter grain weight was recorded in 'KG 100' (66.83 hl^{-1}) under N treatment in the first study year on a vertisol.

The highest hectoliter grain weight was obtained by 'Ana Morava' (77.13 hl^{-1}) under $N_{80}P_{60}K_{60}$ fertilization treatment in the third growing period on a vertisol.

http://www.aloki.hu ● ISSN 1589 1623 (Print) ● ISSN 1785 0037 (Online)
DOI: http://dx.doi.org/10.15666/aeer/1906_46114627

Variance analysis

Variance analysis of individual effect of year, cultivar specificity, and fertilization on grain yield in the studied cultivars of winter wheat grown in five replications over the three growing periods (2010/2011, 2011/2012 and 2012/2013) is presented in *Table 8*.

Variance analysis implied very highly significant individual effects of year of the study and fertilization on grain yield in the studied winter wheat cultivars, as well as very highly significant effect of interaction between year × fertilization. The individual effect of cultivar specificity, along with the effects of interactions between year × cultivar, cultivar × fertilization, and year × cultivar × fertilization on grain yield in the investigated winter wheat cultivars was nonsignificant statistically.

Table 8. *Effect of year, cultivar specificity, and fertilization on grain yield (t ha $^{-1}$)*

Effect	df	Mean sqr effect	Mean sqr error	F	p-level
Year (A)	2, 123	21.050	2.169	9.703***	0.000
Cultivar (B)	2, 124	5.865	2.444	2.400^{ns}	0.234
Fertilization (C)	6, 119	19.983	1.589	12.579***	0.000
Year × Cultivar (AB)	2, 120	3.467	2.117	1.638^{ns}	0.469
Year × Fertilization (AC)	12, 105	3.097	1.045	2.962***	0.001
Cultivar × Fertilization (BC)	6, 112	1.913	1.533	1.248^{ns}	0.222
Year × Cultivar × Fertilization (ABC)	12, 84	0.739	0.912	0.810^{ns}	0.033

Variance analysis of individual effects of year, cultivar specificity, and fertilization on number of grains per spike in the investigated winter wheat cultivars grown in five replications over the three growing periods (2010/2011, 2011/2012, 2012/2013) are shown in *Table 9*.

Table 9. *Effects of year, cultivar specificity, and fertilization on number of grains per spike*

Effect	df	Mean sqr effect	Mean sqr error	F	p-level
Year (A)	2, 123	328.032	77.310	4.243*	0.016
Cultivar (B)	2, 124	595.841	77.172	7.721**	0.006
Fertilization (C)	6, 119	846.590	42.737	19.809***	0.000
Year × Cultivar (AB)	2, 120	51.460	73.420	0.701^{ns}	0.498
Year × Fertilization (AC)	12, 105	49.356	36.546	1.351^{ns}	0.202
Cultivar × Fertilization (BC)	6, 112	95.267	34.984	2.723*	0.017
Year × Cultivar × Fertilization (ABC)	12, 84	31.025	26.127	1.187^{ns}	0.305

The individual effect of fertilization on number of grains per spike in the examined winter wheat cultivars was statistically very highly significant. The individual effect of cultivar as well as the effect of interaction between cultivar × fertilization on number of grains per spike in the studied winter wheat cultivars was statistically highly significant. The effects of interactions between year × cultivar, year × fertilization, and year × cultivar × fertilization on number of grains per spike was statistically nonsignificant.

http://www.aloki.hu ● ISSN 1589 1623 (Print) ● ISSN 1785 0037 (Online)
DOI: http://dx.doi.org/10.15666/aeer/1906_46114627

Variance analysis of individual effects of year, cultivar, and fertilization on grain weight in the studied winter wheat cultivars grown in five replications over the three growing periods (2010/2011, 2011/2012, 2012/2013) are given in *Table 10*.

Variance analysis indicated very highly significant individual effects of year and fertilization on grain weight in the examined winter wheat cultivars, whereas the effects of interactions between year × fertilization, and year × cultivar × fertilization on grain weight was statistically highly significant in the studied winter wheat cultivars. The individual effect of cultivar specificity as well as the effects of interactions between year × cultivar and cultivar × fertilization on grain weight in the studied winter wheat cultivars was statistically nonsignificant.

Table 10. *Effects of year, cultivar, and fertilization on grain weight (g)*

Effect	df	Mean sqr effect	Mean sqr error	F	p-level
Year (A)	2, 123	5.122	0.137	37.424^{***}	0.000
Cultivar (B)	2, 124	0.517	0.214	2.413^{ns}	0.123
Fertilization (C)	6, 119	1.504	0.151	9.914^{***}	0.000
Year × Cultivar (AB)	2, 120	0.184	0.132	1.387^{ns}	0.254
Year × Fertilization (AC)	12, 105	0.155	0.057	2.728^{**}	0.003
Cultivar × Fertilization (BC)	6, 112	0.125	0.150	0.834^{ns}	0.546
Year × Cultivar × Fertilization (ABC)	12, 84	0.094	0.038	2.474^{**}	0.008

Variance analysis of individual effects of year, cultivar specificity, and fertilization on 1000-grain weight in the examined winter wheat cultivars grown in five replications over the three growing periods (2010/2011, 2011/2012 and 2012/2013) is shown in *Table 11*.

Table 11. *Effects of year, cultivar specificity, and fertilization on 1000-grain weight (g)*

Effect	df	Mean sqr effect	Mean sqr error	F	p-level
Year (A)	2, 123	192.809	12.404	15.544^{***}	0.000
Cultivar (B)	2, 124	21.833	15.238	1.433^{ns}	0.234
Fertilization (C)	6, 119	136.668	9.171	14.903^{***}	0.000
Year × Cultivar (AB)	2, 120	9.419	12.375	0.761^{ns}	0.469
Year × Fertilization (AC)	12, 105	15.056	5.000	3.011^{***}	0.001
Cultivar × Fertilization (BC)	6, 112	12.408	8.884	1.397^{ns}	0.222
Year × Cultivar × Fertilization (ABC)	12, 84	7.610	3.793	2.006^{*}	0.033

The individual effects of year and fertilization, as well as the effect of interaction between year × fertilization on thousand-grain weight in the examined winter wheat cultivars was very highly statistically significant. The effect of the interaction between cultivar × fertilization on thousand-grain weight in the examined winter wheat cultivars was statistically significant. Variance analysis indicated that the individual effect of cultivar specificity as well as the effects of interactions between year × cultivar and cultivar × fertilization on 1000-grain weight in the examined winter wheat cultivars was nonsignificant.

Variance analysis of individual effects of year, cultivar specificity, and fertilization on hectoliter weight in the studied winter wheat cultivars grown in five replications over the three growing periods (2010/2011, 2011/2012 and 2012/2013) are given in *Table 12*.

http://www.aloki.hu ● ISSN 1589 1623 (Print) ● ISSN 1785 0037 (Online)
DOI: http://dx.doi.org/10.15666/aeer/1906_46114627

Table 12. *Effects of year, cultivar specificity, and fertilization on hectoliter weight (kg hl $^{-1}$)*

Effect	df	Mean sqr effect	Mean sqr error	F	p-level
Year (A)	2, 123	401.788	6.135	65.489***	0.000
Cultivar (B)	2, 124	114.095	11.646	9.797**	0.002
Fertilization (C)	6, 119	3.013	12.942	0.233^{ns}	0.965
Year × Cultivar (AB)	2, 120	46.306	4.566	10.141***	0.000
Year × Fertilization (AC)	12, 105	3.283	6.640	0.494^{ns}	0.914
Cultivar × Fertilization (BC)	6, 112	4.296	12.502	0.344^{ns}	0.912
Year × Cultivar × Fertilization (ABC)	12, 84	3.886	4.977	0.780^{ns}	0.668

Variance analysis inferred very highly significant individual effect of the year as well as the effect of interaction between year × cultivar on hectoliter weight in the studied winter wheat cultivars. The individual effect of cultivar specificity on hectoliter weight in the examined winter wheat cultivars was statistically highly significant. The individual effect of fertilization and the effects of interactions between year × fertilization, cultivar × fertilization, and year × cultivar × fertilization on hectoliter weight in the studied winter wheat cultivars was statistically nonsignificant.

Conclusion

Productivity and grain quality of winter wheat depend on genotype, agro-environmental conditions and applied cultural practices. Acidic soils, such as vertisol, on which the trial was conducted, substantially reduce the productivity of winter wheat.

The results obtained in our study suggest that grain yield of winter wheat grown on a vertisol varied across fertilization treatments and cultivars. Given that the trial was set up on an unfavorable vertisol, grain yield of winter wheat was significantly higher in fertilization treatments involving NPK, both at low and high rates of phosphorus included.

The highest grain yield of winter wheat over the trial period was obtained in 'Ana Morava' (6,276 kg ha^{-1}) in $N_{80}P_{60}K_{60}$ fertilization treatment. Number of grains per spike and grain weight per spike produced by 'Ana Morava' correlated with the yield of 'Ana Morava' in our three-year trial, which is in agreement with the data of similar trials performed by other authors.

As regards quality of winter wheat, the highest thousand-grain weight in the first, second and third years of testing was recorded in 'Ana Morava', which also produced the highest hectoliter grain weight in all the three years of study.

Over the entire trial period, weather conditions influenced significantly all the parameters of winter wheat grown on a vertisol. Given that weather conditions were more favorable in the second and particularly the third year of study, the performance of both winter wheat cultivars ('Ana Morava' and 'KG 100') was higher in these years than in the first study year.

Based on the results obtained in our three-year examination, given all the parameters studied, 'Ana Morava' is highly recommended for cultivation both in our country and abroad.

Variance analysis indicated the existence of very highly significant individual effects of year and fertilization, as well as the effect of the interaction between year ×

http://www.aloki.hu ● ISSN 1589 1623 (Print) ● ISSN 1785 0037 (Online)
DOI: http://dx.doi.org/10.15666/aeer/1906_46114627

fertilization on grain weight and 1000-grain weight parameters in the studied winter wheat cultivars. The individual effect of year and the effect of interaction between year × cultivar on hectoliter weight in the examined winter wheat cultivars was also statistically very highly significant. The effect of cultivar specificity on hectoliter weight in the examined winter wheat cultivars was highly significant statistically.

Variance analysis suggested very highly significant individual effect of fertilization on both number of grains per spike and grain weight in the studied winter wheat cultivar. The analysis also points to a statistically highly significant individual effect of cultivar specificity and the effect of interaction between cultivar × fertilization in the investigated winter wheat cultivars. The effects of interactions between year × fertilization, and year × cultivar × fertilization on grain weight in the studied winter wheat cultivars was highly significant statistically.

Future studies will be focused on cultivars newly developed in Kragujevac as well as the application of different fertilization treatments involving higher nitrogen rates (N 120 kg ha^{-1}). The studies will be performed under identical environmental conditions (in the same region), and will include monitoring identical parameters. The above aims at yield increase of newly developed winter wheat cultivars and the selection based on significance of fertilization for growing this culture.

REFERENCES

[1] Bálint, A., Gyarmati, B., Hárshegyi, Z., Heltai, G. (2008): Effect of nitrogen fertilization on grain of winter wheat. – Cereal Research Communications 36: 1687-1690.

[2] Blandino, M., Marinaccio, F., Reyneri, A. (2016): Effect of late-season nitrogen ferilization on grain yield and on flour rheological quality and stability common wheat, under different production situations. – Italian Journal of Agronomy 11(745): 107-113.

[3] Borojević, S. (1978): Genetics. Contribution of genetics, environment interaction and modelling in plant selection. – Contemporary Agriculture 11-12: 5-27.

[4] Cooke, G., W. (1976): Long-term fertilizer experiments in England the significance of their rezults for agricultural science and for practical farming. – Annales Agronomiques 27(5-6): 503-536.

[5] Đekić, V., Staletić, M., Jelić, M., Popović, V., Branković, S. (2014a): The stability properties of wheat production on acid soil. – Proceedings, 4th International Symposium Agrosym 2013, 03-06. October, Jahorina, pp. 175-183.

[6] Đekić, V., Glamočlija, Đ., Jelić, M., Simić, D., Perišić, V., Perišić, V., Mitrović, M. (2014b): The effects of fertilization on yield performance of wheat. – Proceedings of Institute PKB, Belgrade 20(1-4): 79-86.

[7] Denčić, S., Kobeljski, B., Mladenović, G., Jestrović, Z., Štatkić, S., Pavlović, M., Orbović, B. (2010): Cultivar as a factor in wheat production. – Field and Vegetable Crops Research 47(1): 317-324.

[8] Dixon, J., Braun, H. J., Crouch, J. N. (2009): Overview Transitioning Wheat Research to Serve the Future Needs of the Developing World. – In: Dixon, J., Braun, H.-J., Kosina, P., Crouch, J., (eds). Wheat Facts and Futures. CIMMYT, Mexico.

[9] Dolijanović, Ž., Roljević Nikolić, S., Kovačević, D., Djurdjić, S., Miodragović, R., Jovanović Todorović, M., Popović Djordjević, J. (2019): Mineral profile of the winter wheat grain: effects of soil tillage systems and nitrogen fertilization. – Applied Ecology and Environmental Research 17(5): 11757-11771.

[10] El-Lethy, S. R., Abdelhamid, M. T., Reda, F. (2013): Effect of potassium application on wheat (*Triticum aestivum* L.) cultivars grow under salinity stress. – World Applied Sciences Journal 26(7): 840-850.

http://www.aloki.hu ● ISSN 1589 1623 (Print) ● ISSN 1785 0037 (Online)
DOI: http://dx.doi.org/10.15666/aeer/1906_46114627

[11] Fagam, A. S., Bununu, A., M., Buba, U. M (2006): Path coefficient analysis of the components of grain yield in wheat (*Triticum aestivum* L.). – International Journal of Natural and Applied Sciences 2(4): 336-340.
[12] Hristov, N., Mladenov, N., Špika, A. K., Štatkić, S., Kovačević, N (2008): Direct and indirect effects of some traits on yield performance of wheat grain. – Proceedings of Institute of Field and Vegetable Crops 45: 15-20.
[13] Jaćimović, G., Malešević, M., Aćin, V., Xristov, N., Marinković, B., Crnoborac, J., Latinović, Dragana (2012): Yield components and yield performance of winter wheat grown under different nitrogen, phosphorous and potassium rates. – Annals of Agronomy 36(1): 72-80.
[14] Jelić, M., Kastori, R., Dugalić, G., Knežević, D. (2008): Environmental and genetic influense of nutritional status of wheat grain. – Cereal Research Communications 36: 683-686.
[15] Jelić, M., Milivojević, J., Paunović, A., Biberdzic, M., Nikolić, O., Madić, M., Đekić, V. (2012): Response of wheat genotypes to liming and fertilization on pseudogley soil. – Proceedings 47th Croatian and 7th International Symposium on Agriculture, 13-17. Februar, Opatija, Croatia, pp. 488-491.
[16] Jelić, M., Milivojević, J., Nikolić, O., Djekić, V., Stamenković, S. (2015): Effect of long-term fertilization and soil amendments on yield, grain quality and nutrition optimization in winter wheat on an acidic pseudogley. – Romanian Agricultural Research 32: 165-174.
[17] Jevtić, S., Malešević, M. (1988): The effects of increasing nitrogen rates on yield performance of wheat grown on a chernozem under different growing conditions. – Contemporary Agriculture 36(3-4): 101-113.
[18] Kastori, R. et al. (2005): Nitrogen – Agro-chemical, Agro-technical, Physiological and Ecological Aspects. – Institute of Field and Vegetable Crops, Novi Sad.
[19] Korchens, M. (2006): The importance of long-term field experiments for soil science and environmental research. A review. – Plant Soil Environ. 52(Special Issue): 1-8.
[20] Kostić, M., Sarić, M., Jocić, V. (1987): Delovanje azota, fosfora i kalijuma na prinos pšenice u višegodišnjim ogledima na smonici i černozemu, Zbornik radova, Uslovi i mogućnost proizvodnje 6 miliona tona pšenice. – Novi Sad 177-188.
[21] Kovačević, V. (2005): Wheat yield variations among the years in the Eastern Croatia. – In: Kovačević, V., Jovanović, S. (eds.) Proceedings of the XL Croatian Symposium on Agriculture with International Participation 15-18 February 2005. Opatija, Croatia, pp. 453-454.
[22] Li, L., Wang, Y. X., Wang, W. B. (2010): Effects of mining subsidence on physical and chemical properties of soil in slope in hilly-gully region of Loess Plateau. – Chinese Journal of Soil Science 41(5): 1237-1240.
[23] Litke, L., Gaile, Z., Ruža, A. (2018): Effect of nitrogen fertilization on winter wheat yield quality. – Agronomy Research 16(2): 500-509.
[24] Malešević, M. (1989): Aspects of air temperature and precipitation in determining optimal nitrogen nutrition rates and their influence on winter wheat yield performance. – PhD dissertation, Faculty of Agriculture, Novi Sad.
[25] Malešević, M., Starčević, Lj., Jaćimović, G., Đurić, V., Šeremešić, S., Milošev, D. (2008): Grain yield performance in winter wheat as influenced by growing period conditions and incorporated nitrogen rates. – XIII Symposium on Biotechnology, Čačak, March 28-29, 2008, Proceedings 13(14): 135-141.
[26] Meng, Q. J., Feng, Q. Y., Wu, Q. Q., Meng, L., Cao, Z. Y. (2009): Distribution characteristics of nitrogen and phosphorus in mining induced subsidence wetland in Panbei coal mine, China. – Procedia Earth and Planetary Science 1: 1237-1241.
[27] Milošev, D (1996): Uticaj azota i temperature u fazi formiranja zrna na broj zrna po klasu ozime pšenice. – Zbornik radova Instituta za ratarstvo i povrtarstvo, Novi Sad 25: 379-385.

http://www.aloki.hu ● ISSN 1589 1623 (Print) ● ISSN 1785 0037 (Online)
DOI: http://dx.doi.org/10.15666/aeer/1906_46114627

[28] Milošev, D (2000): Izbor sistema ratarenja u proizvodnji pšenice. – Zaduzbina Andrejevic, Beograd.
[29] Nemeth, T (2006): Nitrogen in the soil-plant system, nitrogen balances. – Cereal Research Communications 34(1): 61-65.
[30] Nouri, A., Etminan, A., Teixeira da Silva, J. A., Mohammadi, R. (2011): Assessment of yield, yield-related traits and drought tolerance of durum wheat genotypes (*Triticum aestivum* var. durum Desf.). – Australian Journal Crop Science 5(1): 8-16.
[31] Ogbonnaya, F. C., Imtiaz, F. C., Bariana, H. S., McLean, M., Shankar, M. M. (2008): Mining synthetic hexaploids for multiple disease resistance to improve bread wheat. – Crop and Pasture Science 59: 421-431.
[32] Paunović, A., Kovačević, V., Milomirka Madić, Jelić, M., Iljkić, D. (2010): Yield performance of wheat as influenced by weather conditions over the 2000-2007 growing seasons. – XV Symposium on Technology, Čačak, 26-27, March, 2010, Proceedings 15(16): 29-36.
[33] Protić, R., Jovin, P., Protić, N., Janković, S., Jovanović, Ž. (2007): Mass of 1000 grains several winter wheat genotypes at different dates of sowing and rates of nitrogen fertilizer. – Romanian Agricultural Research No. 24: 39-42.
[34] Ragasits, I., Debreczeni, K., Berecz, K. (2000): Effect of long-term fertilization on grain yield, yield components and quality parameters of winter wheat. – Acta Agronomica Hungarica 48(2): 149-154.
[35] Rajaram, S. (2001): Prospects and promise of wheat breeding in the 21st century. – Euphytica 119: 3-15.
[36] Rashid, M. A. R., Khan, A. S., Iftikhan, R. (2013): Genetic studies for yield and yield related parameters in bread wheat. – Am. Eurasian J. Agric. Environ. Sci. 12(12): 1579-1583.
[37] Rehman, O., Zaka, M. A., Rafa, H. U., Hassan, N. M. (2006): Effect of balanced fertilization on yield and phosphorus uptake in wheat-rise rotation. – J. Agric. Res. 44(2): 105-115.
[38] Riley, J. W., Ortiz-Monasterio, I., Matson, P. A. (2001): Nitrogen leaching and soil nitrate, nitrite and ammonium levels under irrigated wheat in Northern Mexico. – Nutrient Cycling in Agroecosystems 61: 223-236.
[39] Rizwan, M., Ali, S., Abbas, T., Zia-ur-Rehman, M., Hnnan, F., Keller, C., Ok, Y. S. (2016): Cadmium minimization in wheat: a critical review. – Ecotoxicology and Environmental Safety 130: 43-53.
[40] Savić, N., Jelić, M., Nikolic, K. (2005): The influence of increased dose of nitrogen on yield grain and grain quality of various of cultivars of winter wheat. – Zemljište i biljka, Belgrade 54(2): 91-97.
[41] Savić, N., Biberdzić, M., Nikolić, K., Knežević, J. (2006): The effect of increasing nitrogen rates on productive elements of wheat spike. – XI Scientific Conference of Agronomists of the Republic of Srpska, Agro-Knowledge, Taslić 7(1): 5-12.
[42] Savić, N., Jelić, M., Knežević, B., Knežević, J. (2007): Productivity of wheat depending on weather conditions in district of Rasina. – Agroznanje 8(3): 105-110.
[43] Tahmaselbi, S., Heidari, B., Pakniyat, H., Kamali, J., Reza, M. (2014): Independent and combined effects of heat and drought stress in the Seri M82X Babax bread wheat population. – Plant Breeding 133: 702-711.
[44] Terzić, D., Đekić, V., Milivojević, J., Branković, S., Perišić, V., Perišić, V., Đokić, D. (2018): Yield components and yield of winter wheat in different years of research. – Biologica Nyssana 9(2): 119-131.
[45] Todorovska, E., Christov, N., Slavov, S., Christova, P., Vassilev, D. (2009): Biotic stress in wheat breeding and genomic selection implications. – Biotechnol Biotec Eq. 23(4): 1417-1426.
[46] Trethowan, R. M., Reynolds, M. P., Ortiz-Monasterio, J. I., Ortiz, R. (2007): The genetic basis of the green revolution in wheat production. – Plant Bread. Rev. 8: 39-58.

http://www.aloki.hu ● ISSN 1589 1623 (Print) ● ISSN 1785 0037 (Online)
DOI: http://dx.doi.org/10.15666/aeer/1906_46114627

[47] Tyrone, H., Lionel, M., Wal, A. (2002): Effects of nitrogen and phosphorus on the grain yield and quality of noodle wheat. – Crop Updates, 2002, Cereals Update, Perth, Australia, pp. 33-38.
[48] www.WorldAtlas.com.

http://www.aloki.hu ● ISSN 1589 1623 (Print) ● ISSN 1785 0037 (Online)
DOI: http://dx.doi.org/10.15666/aeer/1906_46114627

PERSIMMON (*DIOSPYROS KAKI* L.) AND JOHNSONGRASS [*SORGHUM HALEPENSE* (L.) PERS.] ARE NEW NATURAL HOSTS OF *PEACH LATENT MOSAIC VIROID*

OKSAL, H. D.[1*] – AYDIN, S.[1] – BARAN, M.[1] – EMIR, C.[1] – KARANFIL, A.[2] – BOZDOĞAN, O.[1] – SIPAHIOGLU, H. M.[1]

[1]*Department of Plant Protection, Faculty of Agriculture, Malatya Turgut Ozal University, Alacakapı Mahallesi Kırkgöz Caddesi No:70 P.K. 44210 Battalgazi, Malatya, Turkey (e-mail: songulaydin.aydin@gmail.com, mert.baran@tarimorman.gov.tr, canselemirr@gmail.com, olcay.bozdogan@ozal.edu.tr, murat.sipahioglu@ozal.edu.tr; phone: +90-422-846-1255; fax: +90-422-846-1225)*

[2]*Çanakkale Onsekiz Mart University, Faculty of Agriculture, Department of Plant Protection, Terzioğlu Yerleşkesi, 17100 Çanakkale, Turkey (e-mail: alikaranfil@comu.edu.tr; phone: +90-286-218-0018; fax: +90-286-218-0018)*

[*]*Corresponding author*
e-mail: digdem.oksal@ozal.edu.tr; phone: +90-422-846-1255; fax: +90-422-846-1225

(Received 24th Jun 2021; accepted 20th Sep 2021)

Abstract. *Peach latent mosaic viroid* (PLMVd) naturally infects stone fruits worldwide. Here, we report the first detection of PLMVd in persimmon (*Diospyros kaki* L.) and a weed Johnsongrass [*Sorghum halepense* (L.) Pers.]. Samples corresponding to 12 persimmon specimens and weeds nearby the persimmon trees were collected from a germplasm collection plot in Malatya (Turkey). Total RNAs were isolated using a silica-based method and the complete viroid genome was amplified by reverse transcriptase polymerase chain reaction (RT-PCR). From these samples, PLMVd was detected in 7 of the 12 persimmons and in Johnsongrass revealing 8 new sequence variants. Multiple alignment and phylogenetic analyses revealed that identified persimmon and Johnsongrass isolates clustered only with PLMVd-walnut isolates previously identified from same locality. The nucleotide sequences of PLMVd persimmon and Johnsongrass isolates showed 96.71-99.11% similarity with the PLMVd isolates detected in different fruit crops in the world. A single specific mutation identified in two PLMVd persimmon variants (-TH2 and -TH10) effectively changed the predicted secondary structure of the agent. The identification and the genetic analyses of PLMVd variants in persimmon and Johnsongrass confirm that the agent is a ubiquitous and genetically variable viroid that infects many cultivated fruit crops and weeds worldwide.
Keywords: *PLMVd, RT-PCR, Turkey, weed, persimmon, identification*

Introduction

Viroids are small, circular RNAs replicating autonomously in many cultivated and wild plant species. They are noncoding plant pathogenic RNA molecules of 246 to 401 nucleotides in length, however, they induce visible symptoms in susceptible host plants that resemble those associated with many plant viruses. The disease symptoms greatly depend on the host they infect and the viroid strain (Adkar-Purushothama and Perreault, 2019).

PLMVd was first detected in peaches in France. For many years, PLMVd was believed to be restricted to peach (*P. persica*) and peach hybrids (Desvignes, 1976, 1999). Later on, the pathogen has been reported to infect members of the *Rosaceae* family including Japanese plum (*Prunus salicina Lindl.*), apricot (*Prunus armeniaca* L.), sweet cherry (*Prunus avium* L.), European *plum* (*Prunus domestica* L.) and cultivated and wild pears

http://www.aloki.hu ● ISSN 1589 1623 (Print) ● ISSN 1785 0037 (Online)
DOI: http://dx.doi.org/10.15666/aeer/1906_46294639

(*Pyrus communis* L. and *P. amygdaliformis*, respetively) (Shamloul et al., 1995; Faggioli et al., 1997; Hadidi et al., 1997; Giunchedi et al., 1998, 2011; Osaki et al., 1999; Kyriakopoulou et al., 2001). The agent was reported in many stone fruit growing countries including US, Italy, Spain, Austria, Turkey, Greece, Yugoslavia, Romania, Morocco, Algeria, China, Japan, Chile, and in Australia (Desvignes, 1986; Flores and Llácer, 1988; Flores et al., 1990, 1992; Albanese et al., 1992; Shamloul et al., 1995; Di Serio and Ragozzino, 1995; Skrzeczkowski et al., 1996; Di Serio et al., 1999; Pelchat et al., 2000; Fiore et al., 2003; Torres et al., 2004; Sipahioglu et al., 2006; Gumus et al., 2007; Gazel et al., 2008). Although it remains latent for many years following the first infection, PLMVd causes mosaic, bud necrosis, vain banding, blotch and death of branches in peach trees (Desvignes, 1999).

There are few studies dealing with the natural and experimental host ranges for PLMVd (Flores et al., 2000). With the advancements in plant pathogen diagnosis methods, new viroids and their hosts in different geographic areas of the world, are constantly being reported (Adkar-Purushothama and Perreault, 2019). Recently in Turkey, for instance, isolates of PLMVd have been fully characterized infecting walnut trees (Tuncel et al., 2020). There is no report of any persimmon disease associated with a viroid so far. Here, we studied and characterized PLMVd isolates infecting persimmon and Johnsongrass plants. The full-length genome of PLMVd isolates were amplified and sequenced from seven field-collected persimmon and a weed nearby the infected trees expressing no symptoms. The sequence analyses revealed the presence of PLMVd in persimmon and Johnsongrass. To our knowledge, there have been no previous reports of PLMVd infecting these two hosts in the world.

Materials and Methods

Collecting plant material and total RNA extraction

In late summer of 2020, twelve asymptomatic leaf samples from persimmon trees and from the most common annual weeds around persimmon trees were collected from a fruit collection orchard in Malatya province (*Fig. 1*). The collected weeds were included: *Consolida regalis* Gray, *Sorghum halepense* (L.) Pers., *Carduus pycnocephalus* L., *Lactuca serriola* L., *Convovulus arvensis* L. and a weed from Apiaceae family. A sample from each weed species around the trees was collected and tested. No visual symptoms were observed either in persimmon or in weed samples except a persimmon tree which exhibited severe fruit deformation (*Fig. 2*). The all collected plant samples were shipped to laboratory in a cool chain for viroid testing. The leaf samples were rinsed in 70% ethanol for one minute and then rinsed twice with sterilized deionized water to eliminate the external microbial contaminants. Total RNA was extracted from fresh leaf tissues using a commercial genomic RNA purification kit (GeneJET Plant RNA Purification Kit). An isolate of PLMVd from a walnut tree identified positively from preliminary tests was used as positive control in diagnosis of the viroid. RNA from an asymptomatic persimmon tree was used as negative control.

Complementer DNA (cDNA) synthesis and amplification

A total of 3 µl of purified RNA was added to cDNA reaction mixture containing 1 µl 20 pmol/ml genome specific reverse primer (PLMVd-R-5'-CCCGATAGAAAGGCTAAGCACCTCG-3') (Loreti et al., 1999), 1 µl of 10 mM

http://www.aloki.hu ● ISSN 1589 1623 (Print) ● ISSN 1785 0037 (Online)
DOI: http://dx.doi.org/10.15666/aeer/1906_46294639

dNTP, 8 µl of RNAase free water to a total volume of 12 µl. The mixture was heated for 5 min at 65 °C then chilled on ice. Then, four microliters of 5x first-strand cDNA buffer (250 mM Tris-HCl, pH 8.3, 375 mM KCl, and 15 mM $MgCl_2$), 2 µl of DTT, and 1 µl of Moloney murine leukemia virus reverse transcriptase (Promega, Madison, WI, USA) was mixed to reaction mixture and incubated at 42 °C for 50 min. For the inactivation of reverse transcriptase enzyme, the reaction mixture was incubated at 70 °C for 15 minutes and stored at -20 °C until use. PCR assay was performed in a 25 µl reaction volume in a sterile microfuge tube containing 5 µl of 5X Go*Taq* Green Buffer (Promega, Madison, WI, USA), 1 µl of dNTP (20 mM each), 1 µl of each forward and reverse primer (100 mM each) (PLMVd-F-5'-AAC TGC AGT GCT CCG AAT AGG GCA C-3' PLMVd-R-5'-CCC GAT AGA AAG GCT AAG CAC CTC G-3') (Loreti et al., 1999), 1.5 µl of $MgCl_2$, 3 µl of cDNA template and 12.3 µl nuclease-free water. PCR was performed in a Thermo Scientific Arktik Thermal Cycler (Waltham, MA, USA) and the cycling parameters were as follows: initial denaturation at 94 ºC for 2 min followed by 35 cycles of denaturation at 94 ºC for 1 min, annealing at 56 ºC for 2 min, extension at 72 ºC for 1 min, and final extension at 72 ºC for 10 min. Fifteen µl of RT-PCR product of each amplification was electrophoresed on 2% agarose gel in 1x TAE buffer (40 mM Tris-acetate, 1 mM EDTA, pH 8.0) and stained with Pronasafe nucleic acid staining solution (CondaLab).

Figure 1. *Map of Turkey showing the Malatya province where persimmon and the weed samples were surveyed for the presence of Peach latent mosaic viroid*

Figure 2. *Severe fruit malformation in Peach latent mosaic viroid infected persimmon*

http://www.aloki.hu ● ISSN 1589 1623 (Print) ● ISSN 1785 0037 (Online)
DOI: http://dx.doi.org/10.15666/aeer/1906_46294639

Phylogenetic analyses and predicting the most stable secondary structure

Reverse transcription polymerase chain reaction (RT-PCR) amplicons were sequenced bidirectionally by a commercial firm (BM Labosis, Ankara/Turkey) and compared with different PLMVd isolates from the NCBI database online. Multiple alignments were initially aligned by the neighbour joining method and analyzed with the CLC Main workbench program (CLC Bio, Qiagen, Aarhus, Denmark). The relationships were assessed phylogenetically using maximum likelihood algorithm of CLC Main Workbench Software by 1000 bootstrap replicates. Secondary structure analyses were obtained with the mfold structure prediction package of CLC Workbench program.

Results

Symptoms in the field

To investigate the presence of PLMVd in persimmon trees and weed plants we selected randomly and from those plants various viroid-like symptoms, including fruit malformation, stunting, and mosaics. During the field observation, almost no visual symptoms were seen in persimmon trees except one tree which exhibited severe fruit deformation (*Fig. 2*). The symptomatic persimmon tree was found infected by PLMVd in molecular tests (*Fig. 3*). However, we did not observe distinct mosaic and stunting symptoms in field plants. Likewise, no visual symptoms were observed in weed samples.

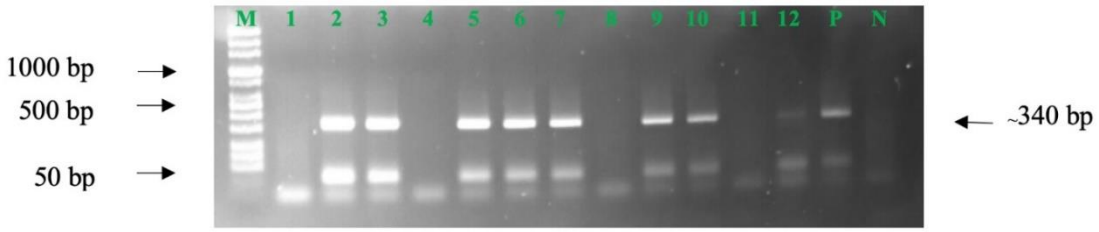

Figure 3. *Agarose gel showing the reverse-transcription polymerase chain reaction assay of persimmon and weed samples using Peach latent mosaic viroid genome specific primer pairs, expected amplicon size ~340 bp. Lanes 1–12 are the tested persimmon samples, lane 2, lane 3, lane 5, lane 6 lane 7, lane 9 and lane 10 (0.34 kb) are positively reacted samples, P: positive control, N: negative control, M: 3.000 bp molecular markers*

RT-PCR detection

In 2020, a total of 18 samples were collected from a persimmon orchard in Malatya province. Of these samples, 12 were from persimmon trees and remaining were various weed samples around the trees. PLMVd was detected in 7 persimmon samples and in one Johnsongrass plant (*Table 1*). Persimmon and Johnsongrass plant testing positive for PLMVd by RT-PCR were further sequenced. Among them, only the PLMVd-TH6 isolate was not registered in the gene bank because the poor sequence output. The results of RT-PCR assays and sequencing confirmed the presence of PLMVd infections in collected samples. PCR amplified products from viroid-infected samples were examined by agarose gel electrophoresis and typical bands specific to PLMVd from infected samples (approx. 0.34 kb) and the positive control were visualized in agarose gel (*Fig. 3*). No

http://www.aloki.hu ● ISSN 1589 1623 (Print) ● ISSN 1785 0037 (Online)
DOI: http://dx.doi.org/10.15666/aeer/1906_46294639

amplicon was observed when RNA from healthy plant was used as a template in the negative control.

Table 1. *PLMVd infection of persimmon and weed samples*

Sample short name	Sample	PLMVd Infection	Symptom observed	Accession No
TH1	Persimmon	–	No visual symptoms	NA
TH2	Persimmon	+	No visual symptoms	MZ289074
TH3	Persimmon	+	No visual symptoms	MZ289073
TH4	Persimmon	–	No visual symptoms	NA
TH5	Persimmon	+	Fruit deformation	MZ289072
TH6	Persimmon	+	No visual symptoms	NA
TH7	Persimmon	+	No visual symptoms	MZ289071
TH8	Persimmon	–	No visual symptoms	NA
TH9	Persimmon	+	No visual symptoms	MZ289070
TH10	Persimmon	+	No visual symptoms	MZ289069
TH11	Persimmon	–	No visual symptoms	NA
TH12	Persimmon	–	No visual symptoms	NA
G2	*Sorghum halepense* (L.) Pers., Johnson grass	+	No visual symptoms	MZ289068
T1	*Consolida regalis* Gray, field larkspur	–	No visual symptoms	NA
E1	*Carduus pycnocephalus* L., Italian thistle	–	No visual symptoms	NA
M1	*Lactuca serriola* L., prickly lettuce	–	No visual symptoms	NA
S1	*Convovulus arvensis* L., field bindweed	–	No visual symptoms	NA
A1	a weed from Apiaceae	–	No visual symptoms	NA

NA: Not applicable

The tested weeds were included: *C. regalis*, *S. halepense*, *C. pycnocephalus*, *L. serriola*, *C. arvensis* and an identified weed from Apiaceae family. Among these weeds, since PLMVd infection was detected only in Johnsongrass, it was thought that Johnsongrass may be the most important weed species to be a potential reservoir. However, no PLMVd was detected in other weed samples collected from persimmon orchard (*Table 1*).

The BLAST analyses of 7 complete PLMVd sequences did not reveal any hundred present identical hits to the currently available complete sequences of PLMVd in GenBank. Multiple alignment between the persimmon variants and all GenBank complete PLMVd sequences revealed that the 6 persimmon variants share 99.11–96.71% identity with available PLMVd sequences. The high level of nucleotide similarity with local isolates indicates that the agent might be spread from species to another by cross-infection due to use of contaminated pruning and grafting tools or by unknown insect vectors.

The full-length of the PLMVd variants identified in Malatya contains a few substitutions on their genomes. In the phylogenetic dendrogram, two major clusters (I and II) were observed. Majority of local PLMVd variants were clustered in branch-I,

http://www.aloki.hu ● ISSN 1589 1623 (Print) ● ISSN 1785 0037 (Online)
DOI: http://dx.doi.org/10.15666/aeer/1906_46294639

indicating a high level of genetic relatedness. With the exception of PLMVd-TH5, TH6 and TH7 variants, all local PLMVd variants were clustered into branch-I distantly from other Turkish and the world samples (*Fig. 4*). The PLMVd variant identified in *S. halepense* was clustered with local PLMVd walnut and the persimmon variants identified in this study. None of the PLMVd isolates, studied in this paper, were clustered with the similar sequences of the same species from other countries including Turkey.

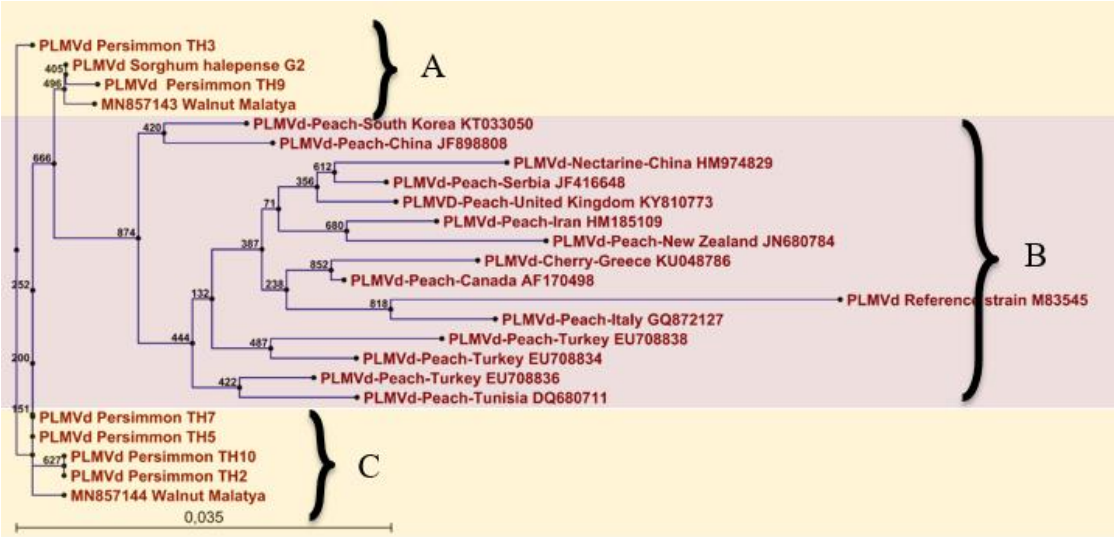

Figure 4. *Phylogenetic relationships of Peach latent mosaic viroid (PLMVd) persimmon and Sorghum halepense L. variants along with PLMVd-walnut isolates compared to 20 genetically-related species reconstructed from the full-length viroid genome. The tree was generated by the neighbor joining algorithm and the bootstrap values of 1000 are indicated at key nodes*

The minimum free energy of optimal secondary structure was modelled for seven PLMVd variants using their consensus sequences (MZ289068, MZ289069, MZ289070, MZ289071, MZ289072, MZ289073 and MZ289074). The nucleotide sequence of PLMVd isolates studied in this paper had a nucleotide sequence identical to that determined by our group in walnut (Tuncel et al., 2020). All changes found in the new PLMVd variants did not affect the most stable secondary structure, except for PLMVd-persimmon TH2 and TH10 variants where serious changes observed. A specific mutation at the nucleotide 63 (G in position 63 instead of U) has changed the secondary structure drastically. However, the mutation did not interfere with the hypothesized hammerhead-like structure of PLMVd (*Fig. 5*). This nucleotide change was detected only in PLMVd variants of TH2 and TH10 (*Fig. 6*). Comparative analysis suggests that this single nucleotide change is solely responsible for the secondary structure difference between the reference PLMVd and the two persimmon PLMVd variants (TH2 and TH10), eliminating the P6 and P7 branches and creating one new branch and two spherical centers for branching of the viroid structure (*Fig. 5*). In order to prove the phenomenon, the nucleotide 63 was manually converted from Guanine to Uracil and the secondary structure analysis was reanalyzed using the same software. The results confirmed that the secondary structure of PLMVd-TH2 and TH10 variants were formed as a classical branched sphere.

http://www.aloki.hu ● ISSN 1589 1623 (Print) ● ISSN 1785 0037 (Online)
DOI: http://dx.doi.org/10.15666/aeer/1906_46294639

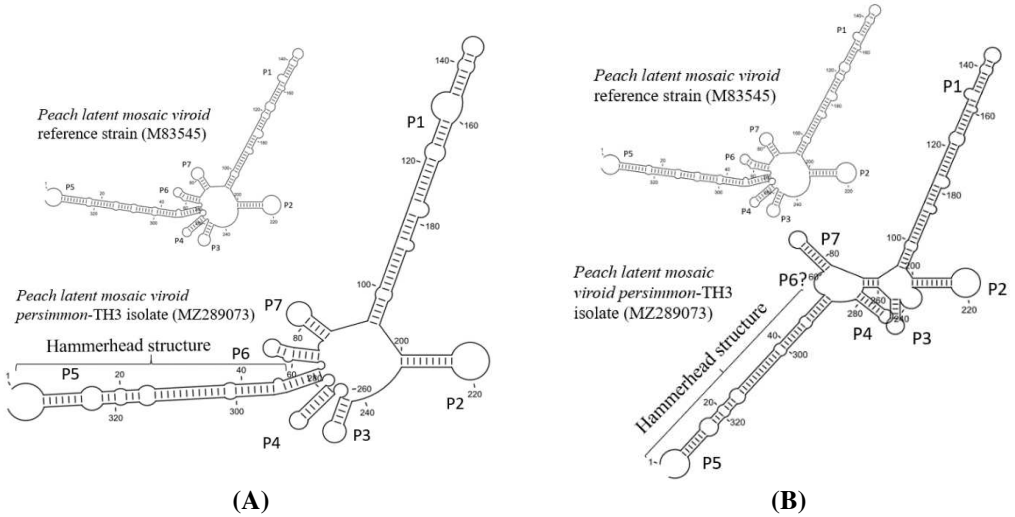

Figure 5. *The most stable secondary structure model for Peach latent mosaic viroid (PLMVd) sequences: (A) PLMVd- TH3, TH5, TH6, TH7, TH9 and G2 variants (MZ289073, MZ289072, MZ289071, MZ289070, MZ289068) and GenBank sequence (M83545), (B) PLMVd-TH2 and TH10 variants (MZ289074 AND MZ289069)*

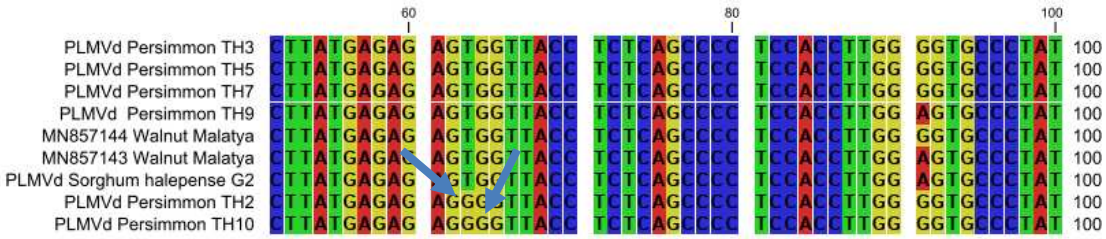

Figure 6. *The multiple alignment of 10 complete Peach latent mosaic viroid (PLMVd) sequences from Malatya province. Six of these sequences identified in persimmon (this study), one in Sorghum halepense L. (this study) and two in walnut (Tuncel et al., 2020) are shown. The difference on the nucleotide sequences on PLMVd-TH2 and TH10 variants are indicated by arrows. The nucleotide changes at 63 T>G is exclusively responsible for the changed the most stable secondary structure of these two variants*

Discussion

The present results indicate that a wide range of cultivated and weed plants may susceptible to PLMVd infections. PLMVd (genus *Pelamoviroid*, family *Avsunviroidae*) was first discovered in peach trees in France in 1976 and known to be latent in plum, apricot, cherry, apple, and pear varieties (Faggioli et al., 1997; El-Dougdoug, 1998; Fiore et al., 2000; Kyriakopoulou et al. 2001; Matic et al., 2005). PLMVd was recently reported for the first time on a crop outside of the *Prunus* genus as a widespread pathogen on walnut in Malatya province (Turkey) (Tuncel et al., 2020). In Turkey, this pathogen was reported previously in peach and nectarine (Sipahioglu et al., 1999; Gümüş et al., 2007; Gazel et al., 2008). Our work showed the existence of natural infections of PLMVd in persimmon trees and in Johnsongrass grown around the sampled trees. This is the first documented report of PLMVd infecting both species. Only one overt disease symptom of fruit malformation was observed in productive persimmon orchard, no other symptoms

http://www.aloki.hu ● ISSN 1589 1623 (Print) ● ISSN 1785 0037 (Online)
DOI: http://dx.doi.org/10.15666/aeer/1906_46294639

were recorded in the surveyed trees and weeds. However, it is still unknown whether the symptom of severe fruit deformation is caused by PLMVd. The identification of new natural hosts of PLMVd may help clarify the actual epidemiology of this pathogen in fruit crops. However, additional regional surveys both internationally and in Turkey are required to investigate the existence of PLMVd infections in other crops since it is occasionally latent in its hosts.

As a preliminary attempt to characterize PLMVd, the nucleic acid sequences of 6 isolates were examined at nucleotide level and analyzed phylogenetically. For the phylogenetic analysis, 20 previous PLMVd sequences deposited in GenBank (NCBI) database were aligned with the sequences reported in this work from persimmon and Johnsongrass. Two isolates of PLMVd identified in the same location in previous study in walnut (Tuncel et al., 2020) were also included to phylogenetic study. The analysis showed that PLMVd persimmon and Johnsongrass isolates reported in this study clustered with only PLMVd isolates reported from the same region from walnut. None of the local PLMVd-persimmon variants were clustered either with other Turkish PLMVd isolates from elsewhere or world isolates indicating a high diversity of genetic relatedness. BLAST analysis of full genomes of PLMVd isolates showed a sequence similarity ranging from 96.71% to 99.11% for persimmon isolates and from 97.01% to 99.10% for Johnsongrass isolate with similar sequences belonging to different geographical origins of the world. All local PLMVd isolates were clustered into two major lineages (A and C) distantly from world isolates. Both clades consisted of PLMVd walnut isolate, previously identified at the same region indicating their close relationships. Sequence and phylogenetic analysis confirmed that the PLMVd sequences obtained from persimmon and Johnsongrass were highly similar to those from PLMVd-walnut isolates identified at the same region. Cross-infection due to pruning and grafting or vector transmission may be the main spreading mechanisms of the agent. Further studies of the origin and possible intermediate hosts of PLMVd are required to understand the nature of possible cross-infection particularly from walnut trees to persimmon and vice versa, where the persimmon samples were collected (Elleuch et al., 2013).

In previous studies, using the mfold software, the secondary structures of lowest free energy were predicted for several PLMVd isolates (Zuker, 1989; Bussiere et al., 2000; Rodio et al., 2006). In these variants, the main secondary structure, involving branched core and several stems, was always obvious in the resulting topologies. However, in our study the occurrence of a significant amount of structural diversity was observed only in PLMVd-TH2 and TH10 variants (*Fig. 5*). The reason for this variance is the mutation that caused the Uracil base at number 63 converting it to the guanine base. It has been observed that a single base change at a specific point can lead to a serious change in the secondary structure of PLMVd. For instance, stems P6 and P7 were absent in each predicted structure, whereas the central core was divided into two cores forming a tween center and e new stem instead P6 and P7.

Sorghum halepense (Pers.) L. (Johnsongrass), in the Poaceae family, is a perennial graminoid plant species (Holm et al., 1997) and distributed over one-third of the total global area, causing significant losses to agriculture (Chirita et al., 2007). It harbors many plant viruses including *Maize dwarf mosaic virus* (Achon and Sobrepere, 2001), *Wheat dwarf virus*, *Sugarbeet yellow virus*, *Maize chlorotic mottle virus* and *Wheat streak mosaic* (Warwick and Black, 1983; Ikley et al., 2015; Achon et al., 2016; Parizipour et al., 2016). Control of Johnsongrass throughout the season will probably prevent its seed production and possible transmissions by unknown vectors.

http://www.aloki.hu ● ISSN 1589 1623 (Print) ● ISSN 1785 0037 (Online)
DOI: http://dx.doi.org/10.15666/aeer/1906_46294639

Since PLMVd is graft transmissible pathogen in many host plants there has been an increased risk of spread via propagation plant material. To evaluate its natural spread and to determine the actual prevalence, further survey studies are needed in fruit crop orchards in Turkey and in the world. Using clean propagation material will be a basic approach for the fruit crop industry to prevent the spread of this newly discovered viroid agent in fruit orchards. This will also provide the means for the long-term elimination of disease from productive orchards. By identifying persimmon and Johnsongrass as new natural hosts, here we report that PLMVd is a ubiquitous viroid that infects many different fruit trees cultivated worldwide and the weeds.

Conclusions

Very little is known about the possible origin of the viroid infections in crop plants. Here we present the natural infections, nucleotide sequences and several new features of PLMVd isolated from persimmon and Johnsongrass. This is the first description of PLMVd from its natural hosts. By identifying these two new natural hosts, it has been confirmed that PLMVd is a genetically variable viroid that infects numerous different cultivated fruit crops and weeds around the globe. Additional survey studies are needed on the occurrence and geographical distribution of PLMVd in other fruit crops and weed species.

REFERENCES

[1] Achon, M. A., Sobrepere, M. (2001): Incidence of potyvirus in commercial maize fields and their seasonal cycles in Spain. – Journal of Plant Diseases and Protection 108: 399-406.

[2] Achon, M. A., Serrano, L., Clemente, O. G., Sossai, S. (2016): First Report of Maize chlorotic mottle virus on a Perennial Host, Sorghum halepense, and Maize in Spain. – Plant Disease 101(2). 10.1094/PDIS-09-16-1261-PDN.

[3] Adkar-Purushothama, C. R., Perreault, J. P. (2019): Current overview on viroid–host interactions. – WIREs RNA.

[4] Albanese, G., Giunchedi, L., La Rosa, R., Poggi-Pollini, C. (1992): *Peach latent mosaic viroid* in Italy. – Acta Horticulturae 309: 331-338.

[5] Bussière, F., Ouellet, J., Coteou, E., Perreault, J. P. (2000): Mapping in solution shows the *Peach latent mosaic viroid* to possess a new pseudoknot in a complex, branched secondary structure. – Journal of Virology 74(6): 2647-54.

[6] Chirita, R., Grozea, I., Sarpe, N., Lauer, K. F. (2007): Control of *Sorghum halepense* (L.) species in western part of Romania Communications. – Agricultural and Applied Biological Sciences 73: 959-964.

[7] Desvignes, J. C. (1976): The virus diseases detected in greenhouse and in field by the peach seedling GF 305 indicator. – Acta Horticulturae 67: 315-323.

[8] Desvignes, J. C. (1986): *Peach latent mosaic* and its relation to peach mosaic and peach yellow mosaic virus diseases. – Acta Horticulturae 193: 51-58.

[9] Desvignes, J. C. (1999): Virus diseases of fruit trees. – Edition CTIFL Publication, Paris.

[10] Di Serio, F., Ragozzino, A. (1995): Indagini sulla presenza del viroide del mosaico latente del pesco (PLMVd) in Campania. – Informatore Fitopatologico 9: 57-61.

[11] Di Serio, F., Malfitano, M., Flores, R., Randles, J. W. (1999): Detection of PLMVd in Australia. – Australasian Plant Pathology 28: 80-81.

[12] El-Dougdoug, Kh. A. (1998): Occurrence of *Peach latent mosaic viroid* in apple (*Malus domestica*). – Annals of Agricultural Science (Cairo) 43(1): 21-30.

http://www.aloki.hu ● ISSN 1589 1623 (Print) ● ISSN 1785 0037 (Online)
DOI: http://dx.doi.org/10.15666/aeer/1906_46294639

[13] Elleuch, A., Hamdi, I., Ellouze, O., Ghrab, M., Fkahfakh, H., Drira, N. (2013): Pistachio (*Pistacia vera* L.) is a new natural host of *Hop stunt viroid*. – Virus Genes 47(2): 330-337.
[14] Faggioli, F., Loreti, S., Barba, M. (1997): Occurrence of *Peach latent mosaic viroid* (PLMVd) on plum in Italy. – Plant Disease 81(4): 423.
[15] Fiore, N., Aboughanem, N., Infante, R., Myrta, A., Pallás, V. (2000): Detection of Peach Latent Mosaic Viroid in Stone Fruits from Chile. – In: Myrta, A., Di Terlizzi, B., Savino V. (eds.) Virus and virus-like diseases of stone fruits, with particular reference to the Mediterranean region. Bari: CIHEAM, pp. 143-145.
[16] Flores, R., Llácer, G. (1988): Isolation of a viroid-like RNA associated with peach latent mosaic disease. – Acta Horticulturae 235: 325-332.
[17] Flores, R., Hernández, C., Desvignes, J. C., Llácer, G. (1990): Some properties of the viroid inducing the peach latent mosaic disease. – Research in Virology 141: 109-118.
[18] Flores, R., Hernández, C., Avinent, L., Hermoso, A., Llácer, G., Juárez, J., Arregui, J. M., Navarro, L., Desvignes, J. C. (1992): Studies on the detection, transmission and distribution of *Peach latent mosaic viroid* in peach trees. – Acta Horticulturae 309: 325-330.
[19] Flores, R., Daro`s, J. A., Hernández, C. (2000): The *Avsunviroidae* family: viroids with hammerhead ribozymes. – Advances in Virus Reseach 55: 271-323.
[20] Gazel, M., Ulubas Serce, C., Caglayan, K., Luigi, M., Faggioli, F. (2008): Incidence and genetic diversity of *Peach latent mosaic viroid* isolates in Turkey. – Journal of Plant Pathology 90: 495-503.
[21] Giunchedi, L., Gentit, P., Nemchinov, L., Poggi-Pollini, C., Hadidi, A. (1998): Plum spotted fruit: a disease associated with *peach latent mosaic viroid*. – Acta Horticulturae 472: 571-579.
[22] Giunchedi, L., Kyriakopoulou, P., Barba, M., Hadidi, A. (2011): *Peach latent mosaic viroid* in naturally infected temperate fruit trees. – In: Hadidi, A., Barba, M., Candresse, T., Jelkmann, W. (eds.) Virus and Virus-Like Diseases of Pome and Stone Fruits. St. Paul, MN, USA, The American Phytopathological Society Press, pp. 225-227.
[23] Gumus, M., Paylan, I. C., Matic, S., Myrta, A., Sipahioglu, H. M., Erkan, S. (2007): Occurrence and distribution of stone fruit viruses and viroids in commercial plantings of *Prunus* species in Western Anatolia, Turkey. – Journal of Plant Pathology 89(2): 255-258.
[24] Hadidi, A., Giunchedi, L., Shamloul, A. M., Poggi-Pollini, C., Amer, M. A. (1997): Occurrence of *Peach latent mosaic viroid* in stone fruits and its transmission with contaminated blades. – Plant Disease 81: 154-158.
[25] Holm, L. G., Plucknett, D. L., Pancho, J. V., Herberger, J. P. (1997): Sorghum halepense L. Pers. – In: Holm, L. G. (ed.) The world's worst weeds, distribution and biology. The University Press of Hawaii, Honolulu, pp. 54-61.
[26] Ikley, J. T., Wise, K. A., Johnson, W. G. (2015): Annual Ryegrass (*Lolium multiflorum*), Johnsongrass (*Sorghum halepense*), and Large Crabgrass (*Digitaria sanguinalis*) are alternative hosts for *Clavibacter michiganensis* subsp. *nebraskensis*, causal agent of Goss's wilt of corn. – Weed Science 63: 901-909.
[27] Kyriakopoulou, P., Giunchedi, L., Hadidi, A. (2001): Peach latent mosaic and pome fruit viroids in naturally infected cultivated pear *Pyrus communis* and wild pear *P. amygdaliformis*: implications on possible origin of these viroids in the Mediterranean region. – Journal of Plant Pathology 83: 51-62.
[28] Loreti, S., Faggioli, F., Cardini, M., Mordent, G., Bambini, A. R., Poggi-Pollini, C., Barba, M. (1999): Comparison of different diagnostic methods for detection of *Peach latent mosaic viroid*. – EPPO Bulletin 29: 433.
[29] Matic, S., Al Rwahnih, M., Arben, M. (2005): Occurrence of Stone Fruit Viroids in Bosnia and Herzegovina. – Phytopathologia Mediterranea 44: 285-290.
[30] Osaki, H., Yamamuchi, Y., Sato, Y., Tomita, Y., Kawai, Y., Miyamoto, Y., Ohtsu, Y. (1999): Peach latent mosaic isolated from stone fruits in Japan. – Annuals of Phytopathology Society of Japan 65: 3-8.

http://www.aloki.hu ● ISSN 1589 1623 (Print) ● ISSN 1785 0037 (Online)
DOI: http://dx.doi.org/10.15666/aeer/1906_46294639

[31] Parizipour, M. G., Behjatnia, S. A. A., Afsharifar, A., Izadpanah, K. (2016): Natural hosts and efficiency of leafhopper vector in transmission of *Wheat dwarf virus*. – Journal of Plant Pathology 98: 483-492.
[32] Pelchat, M., Levesque, D., Ouellet, J., Laurendeau, S., Levesque, S., Lehoux, J., Thompson, D. A., Eastwell, K. C., Skrzeczkowski, L. J., Perreault, J. P. (2000): Sequencing of *Peach latent mosaic viroid* variants from nine North American peach cultivars shows that this RNA folds into a complex secondary structure. – Virology 271: 37-45.
[33] Rodio, M. E., Delgado, S., Flores, R., Di Serio, F. (2006): Variants of *Peach latent mosaic viroid* inducing peach calico: uneven distribution in infected plants and requirements of the insertion containing the pathogenicity determinant. – Journal of General Virology 87: 231-240.
[34] Shamloul, A. M., Minafra, A., Hadidi, A., Giunchedi, L., Waterworth, H. E., Allam, E. K. (1995): *Peach latent mosaic viroid*: nucleotide sequence of an Italian isolate, sensitive detection using RT-PCR and geographic distribution. – Acta Horticulturae 386: 522-530.
[35] Sipahioglu, H. M., Myrta, A., Abou-Ghanem, N., Di Terlizzi, B., Savino, V. (1999): Sanitary Status of Stone Fruit Trees in East Anatolia (Turkey) with Particular Reference to Apricot. – Bulletin OEPP/EPPO Bulletin 29: 439-442.
[36] Sipahioğlu, H. M., Demir, S., Myrta, A., Al Rwahnih, M., Polat, B., Schena, L., Usta, M., Akkopru, A., Selcuk, M., Ippolito, A., Minafra, A. (2006): Viroid, phytoplasma and fungal diseases of stone fruits in Eastern Anatolia, Turkey. – New Zealand Journal of Crop and Horticultural Science 34: 1-6.
[37] Skrzeczkowski, L. J., Howell, W. E., Mink, G. I. (1996): Occurrence of *Peach latent mosaic viroid* in commercial peach and nectarine cultivars in the U.S. – Plant Disease 80: 823.
[38] Torres, H., Gómez, G., Pallás, V., Stamo, B., Shalaby, A., Aouane, B., Gavriel, I., Kominek, P., Caglayan, K., Sipahioglu, H. M. (2004): Detection by tissue printing of stone fruit viroids, from Europe, the Mediterranean and north and south America. – Acta Horticulturae 657: 379-383.
[39] Tuncel, F., Tekkaş, N., Türk, G., Oksal, H. D., Sipahioğlu, H. M. (2020): First Detection and Molecular Characterization of *Peach latent mosaic viroid* in a New Natural Host: Walnut (*Juglans regia* L.). – Alinteri Journal of Agriculture Sciences 35(2): 37-44.
[40] Warwick, S. I., Black, L. D. (1983): The biology of Canadian weeds. *Sorghum halepense* (L.) Pers. – Canadian Journal of Plant Sciences 63: 997-1014.
[41] Zuker, M. (1989): On finding all suboptimal foldings of an RNA molecule. – Science 244: 48-52.

http://www.aloki.hu ● ISSN 1589 1623 (Print) ● ISSN 1785 0037 (Online)
DOI: http://dx.doi.org/10.15666/aeer/1906_46294639

EVALUATION OF THE METALLIC TRACE ELEMENT CONTAMINATION OF COMMON SOLE (*SOLEA SOLEA*, L. 1758) BY THE WESTERN ALGERIAN COAST

TABECHE, A.[1*] – BELHOUCINE, F.[1] – BOUHADIBA, S.[2] – ALIOUA, A.[1] – BELHABIB, L.[1] – ROUABHI, Y. L.[3]

[1]*Laboratory Toxicology Environment and Health (LATES), Department of Life and the Environment, University of Sciences and Technology Oran-Mohamed Boudiaf USTO-MB, El Mnaouar, BP 1505, Bir El Djir 31000, Oran, Algeria*

[2]*Laboratory Toxicology Environment and Health (LATES), Higher School of Biological Sciences in Oran (ESSBO), BP 1042, Saim Mohamed 31003, Oran, Algeria*

[3]*Laboratory Network for Environmental Monitoring (LRSE), Department of Biology, University of Oran 1, Oran, Algeria*

**Corresponding author*
e-mail: ali.tabeche@univ-usto.dz

(Received 27th Jun 2021; accepted 1st Oct 2021)

Abstract. Metal contamination is one of the most worrying risks today. Our study is interested in the compartmentalisation of metallic trace elements in organs; gills, gonads and liver of common soles (*Solea solea*, L. 1758) from the western region of Algeria. The fish were collected seasonally between October 2018 and September 2019 in the two largest port areas of this region; Oran and Ghazaouet. Samples were compared by temperature, pH, salinity, dissolved oxygen and organic matter. The concentrations of four metallic trace elements: zinc (Zn), copper (Cu), lead (Pb) and cadmium (Cd) were analyzed by atomic absorption spectrophotometry. From a statistical point of view, according to (Anova, F value = 0.01, p value = 0.99), The results obtained from the average concentrations of the four metallic trace elements analyzed at the level of the organs showed no significant variation between the sampling sites and between the two sexes. On the other hand, for the three organs studied taken separately, we demonstrated a significant variation between the seasons for each of the metals studied. Pb concentrations were higher in sole organs collected from Oran Bay (2.02 ± 0.75 $\mu g.g^{-1}_{dw}$) than those from Ghazaouet Bay ($1.44 \pm 0.41 \mu g.g^{-1}_{dw}$). These results do not reveal the origin of the micropollutants but they focus on the existence of this pollution which requires wider monitoring.
Keywords: *metal pollution, atomic absorption spectrophotometry, physico-chemical parameters, Oran Bay, Ghazaouet Bay*

Introduction

Marine pollution is one of the most worrying problems today. It is often emitted as a result of anthropogenic activities, such as industrial activities, agriculture or even domestic activities and in different forms (e.g., pesticides, hydrocarbons, metallic trace elements, etc.) (Aydoğan and İncekara, 2017; Pal et al., 2018).

Aquatic ecosystems are the most affected by metal pollution (Rodrigue et al., 2016). This chemical contamination can represent a toxicological risk and affect marine life. Lead and cadmium are considered toxic elements in high concentrations, Cu and Zn are trace elements but can become dangerous if they exceed a certain threshold in the body (Borsali, 2015). By their resistance to biodegradation, their persistence and their toxicity, these elements can concentrate in the tissues of living organisms (Förstner and Wittmann, 1981; Boucheseiche et al., 2002). These organisms then enter the food chain. If the product is not

http://www.aloki.hu ● ISSN 1589 1623 (Print) ● ISSN 1785 0037 (Online)
DOI: http://dx.doi.org/10.15666/aeer/1906_46414664

degraded or eliminated, it will concentrate more and more at each level of the food chain. Indeed, heavy metals are poorly metabolized. They can therefore be transferred into the food web and accumulated in living matter (Duquesne, 1992).

In recent years, the monitoring of metallic contamination in the marine environment relied solely on the chemical analysis of the water (Lafabrie, 2007). In addition, this analytical technique does not provide information on the bioavailability of trace metal elements for organisms and does not allow to assess, or even predict, the impact of these substances on organisms or, on the ecosystem as a whole (Lagadic et al., 1998; Morillo et al., 2005). Fish have been shown to be vectors of trace metal contamination in humans, so some species are now used as biological tools for assessing trace metal pollution in water (Goldberg, 1975).

Various studies have shown that xenobiotics cause disturbances in the reproductive system, changes in behavior, disturbances in energy metabolism and the appearance of mutagenic or carcinogenic effects in aquatic species (Meyer, 2003). Pollution can have repercussions on all food chains, from primary producers to final consumers and, consequently, alter the functioning of ecosystems (Borsali, 2015). Chemical contaminants can have cascading effects on the growth and reproduction of organisms, leading to changes in higher biological organization, in populations and communities (Amiard-Triquet and Amiard, 2008).

Pollution in Algeria is mainly generated by discharges of untreated industrial and urban water (Taleb et al., 2007; Grimes et al., 2010). Petrochemical, chemical, steel and agrifood activities are mainly concentrated on the Algerian coastal strip (Grimes et al., 2010).

Our choice fell on the common sole (*Solea solea*, L. 1758), it is a fish that is widespread on the Algerian coasts and consumed by a large part of the population. According to Wessel (2010), this species is particularly sensitive to anthropogenic pressure. Indeed, due to its benthic way of life, it is constantly in contact with sediments, reservoirs of many contaminants including trace metals. It should be noted that at the level of the Algerian west coast, common sole has never been used as a bio indicator of metal pollution to date, hence the interest of its choice and in order to complement the various research projects relating to the installation of a monitoring network for marine pollution and fishery products in the same region.

Materials and methods

Study area

Algeria has a wide maritime frontage which is located in the heart of the Mediterranean. From an ecological point of view, its coastline is rich and diverse, and alternates between rocky shores, sandy beaches and wetlands (Benzohra and Millot, 1995). Two sites were selected for our study, Oran Bay and Ghazaouet Bay.

The bay of Oran with a latitude of 35°43’ North and a longitude of 00° 38’ West (*Fig. 1*) occupies the central part of the Oran coast (Belhoucine et al., 2014). The Oran coast is severely affected by the nuisances of the civilized world: industrial activities, intensive tourism and massive urbanization with an ever-increasing level of domestic pollution (Kerfouf et al., 2010).

The bay of Ghazaouet with a latitude of 35° 06’ North and a longitude of 1° 52’ West (*Fig. 1*) is located at the western end of Algeria. This area is subjected to industrial wastewater from the zinc electrolysis unit ALZINC (Algerian Zinc Company by abbreviation is a subsidiary of METANOF), these discharges loaded with metallic trace

http://www.aloki.hu ● ISSN 1589 1623 (Print) ● ISSN 1785 0037 (Online)
DOI: http://dx.doi.org/10.15666/aeer/1906_46414664

elements, contributed to the uncontrolled storage of leaching waste from zinc on the cliff overlooking the sea and the factory (DPRHT, 2004). This unit is currently the most important industrial activity center in the region, being the only producer of electrolytic zinc in the Arab world and the second in Africa after South Africa.

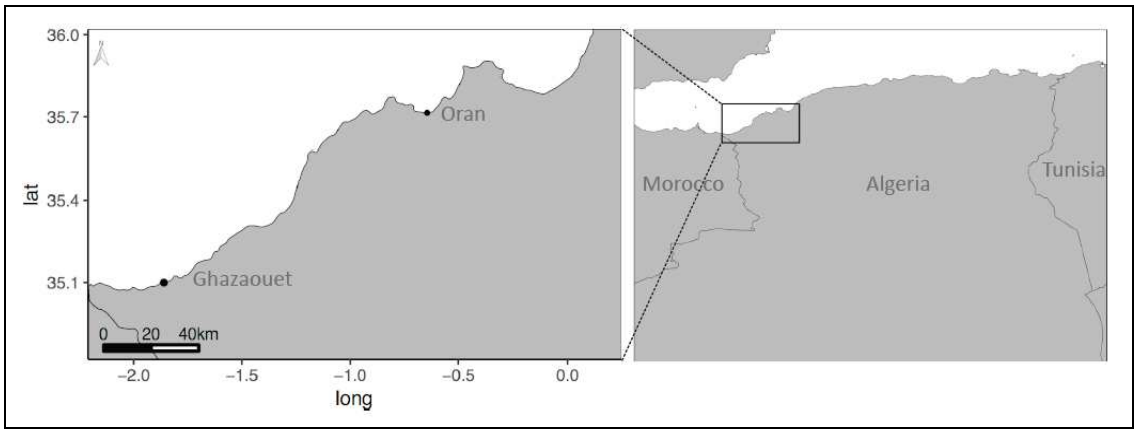

Figure 1. *Location of the study area: Oran bay and Ghazaouet bay*

Sample collection and processing

Sampling was carried out seasonally between October 2018 and September 2019 at the two sites (one day per month). In total, we collected 120 individuals of *Solea solea* (L. 1758) from the fishing ports. The samples were processed the same day at the laboratory level. After the biometric measurements, the fish were dissected in order to remove the liver, gills and gonads.

Sampling of fish was accompanied by sampling of seawater. A liter of water was taken from the surface, using polyethylene bottles, washed and rinsed with distilled water, then transported to the laboratory in the cooler to be stored at + 4 °C until analysis.

Temperature, pH, salinity, dissolved oxygen and organic matter were measured using the multi-parameter instrument (WTW Multi 340i).

Extraction and analysis of ETMs (Pb, Cu, Zn and Cd)

Before carrying out the analysis of the metals in the various organs studied, the samples studied had been mineralized (Chiffoleau et al., 2001). This step consists of the destruction of the organic matter by an acid attack (pure nitric acid HNO_3). The subsamples were dried in an oven at 60 °C until a constant weight was obtained (24 to 72 h), then crushed. 0.2 g of dried sample for each replica, had been mineralized in 4 ml of pure HNO_3 at room temperature overnight, then placed in an oven at 90 °C for 3 h. The mineralisates were then filtered with wattman filter paper. The determination of the ETMs had been carried out by a flame atomic absorbance spectrophotometer of the Perkin Elmer precisely AAnalyst 400 type.

The verification of the absence of possible contamination of the samples during the analysis was made using the test blanks. These negative controls were treated according to the same protocol as the other samples in order to verify the validity of the method by ensuring that the compounds detected in the samples did not come from contamination during the analysis.

http://www.aloki.hu ● ISSN 1589 1623 (Print) ● ISSN 1785 0037 (Online)
DOI: http://dx.doi.org/10.15666/aeer/1906_46414664

The reliability of the protocol described above was also validated using a homogenized standard sample known as the intercalibration sample provided by the International Atomic Energy Agency (IAEA, 1995). In our case, this is a fish sample coded 140/TM.

Statistical analyses

First, a study of distribution and homogeneity had been carried out. The variations between sites, seasons and organs were analyzed with a multi-parameter Anova test followed by a post-hoc Duncan test.

In order to study the distribution of the data a Spearman correlation matrix and PCA were used. The minimum level of significance for all analyzes was 0.05. The statistical analyzes were carried out in R version 3.4.2 (R Core Team, 2017), with the packages: RStudio v. 1.2.5033 (RStudio Team, 2019), ggplot2 (Wickham, 2016), corrgram (Wright, 2018), dplyr (Wickham et al., 2020), FSA (Ogle et al., 2020).

Results

The analysis (mean ± standard deviation (SD)) of the physico-chemical parameters of the seawater in each of the two bays (Oran bay and Ghazaouet bay), recorded during the different seasons, are grouped together in *Table 1*.

Table 1. *Averages the physico-chemical parameters of the coastal waters of the bay of Oran and the bay of Ghazaouet*

Parameter	Bay of Oran (mean ± SD)	Bay of Ghazaouet (mean ± SD)
T °C	21.25 ± 6.85	22.47 ± 6.79
pH	7.66 ± 0.18	7.75 ± 0.11
Salinity (PSU)	36.57 ± 0.67	36.84 ± 0.78
O_2 dissolved (mg L^{-1})	5.98 ± 1.90	6.39 ± 1.16
Organic matter (mg L^{-1})	15.14 ± 0.88	15.28 ± 0.33

Figure 2 represents the average concentrations of the targeted metal trace elements zinc, copper, lead and cadmium in common sole (*Solea solea*, L. 1758) fished in the bay of Oran and in the bay of Ghazaouet.

The results of base Anova for the comparison of the metallic elements in the organs of the common sole fished in the two bays: Oran bay and Ghazaouet bay, are grouped in *Table 2*.

Figure 3 shows the comparison of the average concentrations of heavy metals studied in the hepatic, gonadal and branchial tissues in common sole (Solea solea, L. 1758) fished in the bay of Oran and the bay of Ghazaouet.

Our results showed significant seasonal variations of the four metallic trace elements, in the three organs of common sole fished in the bay of Oran. For liver, Zn (Anova 2, F value = 95.69, p value < 0.001), Cu (Anova 2, F value = 99.54, p value < 0.001), Pb (Anova 2, F value = 44.12, p value < 0.001) and Cd (Anova 2, F value = 31.35, p value < 0.001) (*Tables 3* and *4*). For the gills, Zn (Anova 2, F value = 255.10, p value < 0.001), Cu (Anova 2, F value = 54.56, p value < 0.001), Pb (Anova 2, F value = 92.11, p value < 0.001) and Cd (Anova 2, F value = 26.62, p value < 0.001) (*Tables 3* and *5*). For the gonads, Zn (Anova 2, F value = 182.72, p value < 0.001), Cu

http://www.aloki.hu ● ISSN 1589 1623 (Print) ● ISSN 1785 0037 (Online)
DOI: http://dx.doi.org/10.15666/aeer/1906_46414664

(Anova 2, F value = 37.97, p value < 0.001), Pb (Anova 2, F value = 20.28, p value < 0.001) and Cd (Anova 2, F value = 13.40, p value < 0.001) (*Tables 3* and *6*).

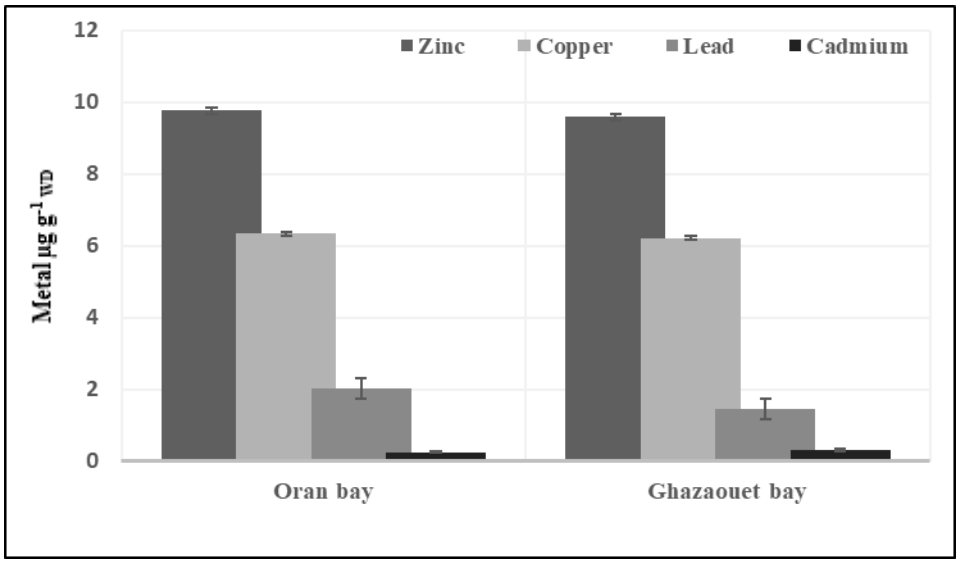

Figure 2. *Average levels of metallic trace elements (Zn, Cu, Pb and Cd) evaluated in sole fished in the two bays: Oran Bay and Ghazaouet Bay*

Table 2. *Anova base for the comparison of metallic elements in the organs of the common sole fished in the two bays: Oran Bay and Ghazaouet Bay*

Variable	Df	Sum of squares	Mean of squares	F value	p value
Organ	2	15.0	7.501	0.4751	0.6220893
Sex	1	11.6	11.593	0.7343	0.3918802
Site	1	6.1	6.111	0.3871	0.5341031
Saison	3	331.3	110.425	6.9945	< 0.001 ***
Organ: Sex	2	5.0	2.503	0.1586	0.8534093
Organ: Site	2	0.5	0.269	0.0170	0.9830978
Sex: Site	1	0.7	0.696	0.0441	0.8337577
Organ: Season	6	2.8	0.465	0.0275	0.9998912
Sex: Season	3	0.2	0.041	0.0026	0.9998184
Site: Season	3	14.5	4.842	0.3067	0.8205793
Organ: Sex: Site	2	0.4	0.196	0.0124	0.9876370
Organ: Sex: Season	6	0.1	0.018	0.0011	1.0000000
Organ: Site: Season	6	1.0	0.167	0.0106	0.9999948
Sex: Site: Season	3	0.2	0.073	0.0046	0.9995671
Organ: Sex: Site: Season	6	0.3	0.057	0.0036	0.9999998

Df: Degrees of freedom. Signif. codes: 0 '***' 0.001 '**' 0.01 '*' 0.05 '.' 0.1 ' ' 1

In Oran Bay, seasonal variations of metallic trace elements showed the highest average concentrations in the organs of fish collected mainly in summer, autumn and spring. The lowest concentrations were noted during the winter period (*Fig. 4*).

http://www.aloki.hu ● ISSN 1589 1623 (Print) ● ISSN 1785 0037 (Online)
DOI: http://dx.doi.org/10.15666/aeer/1906_46414664

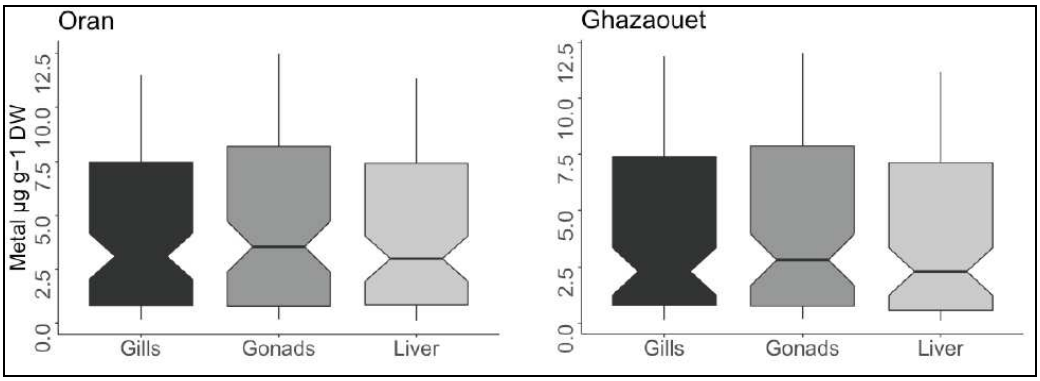

Figure 3. *Comparison between metal organs combined in the two bays: Oran Bay and Ghazaouet Bay*

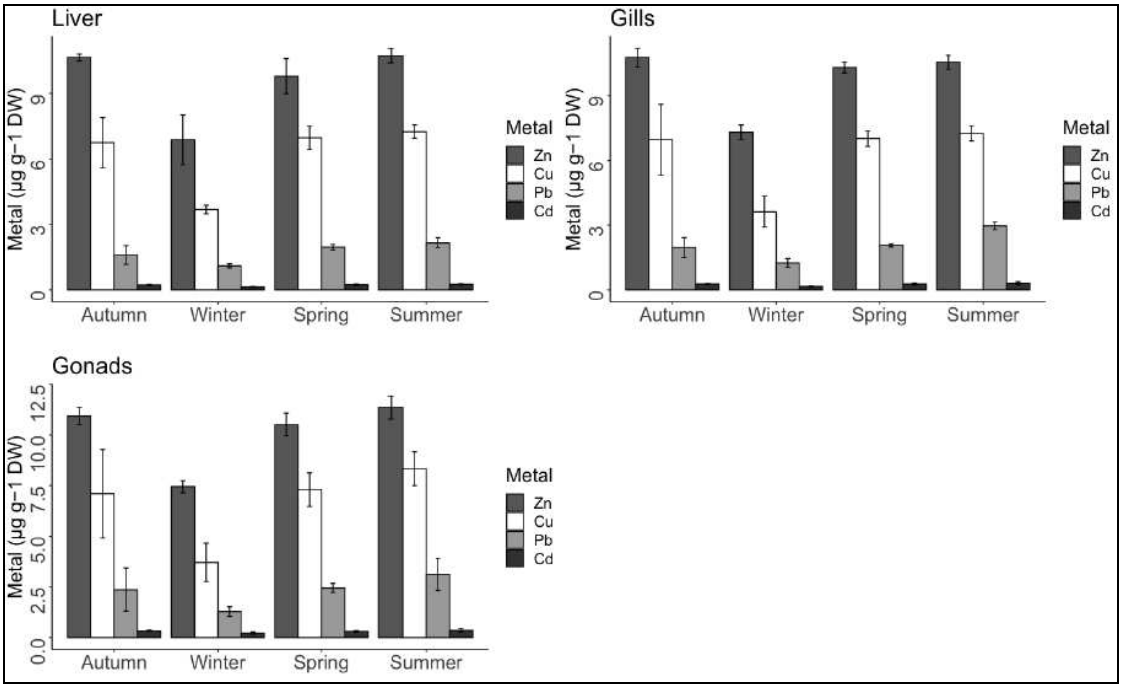

Figure 4. *Seasonal variations of metals (Zn, Cu, Pb and Cd) in organs at Oran bay*

In the liver, the average concentrations of heavy metals: Cd, Cu, Pb and Zn recorded in the summer season were respectively equal to 0.25 ± 0.03 $\mu g.g^{-1}_{dw}$, 7.25 ± 0.31 $\mu g.g^{-1}_{dw}$, 2.15 ± 0.24 $\mu g.g^{-1}_{dw}$, 10.74 ± 0.34 $\mu g.g^{-1}_{dw}$. In the winter season, their concentrations were 0.13 ± 0.02 $\mu g.g^{-1}_{dw}$, 3.68 ± 0.19 $\mu g.g^{-1}_{dw}$, 1.10 ± 0.09 $\mu g.g^{-1}_{dw}$, 6.87 ± 1.14 $\mu g.g^{-1}_{dw}$, respectively. In the gills, their mean concentrations in the summer season were 0.31 ± 0.06 $\mu g.g^{-1}_{dw}$, 7.25 ± 0.35 $\mu g.g^{-1}_{dw}$, 2.96 ± 0.17 $\mu g.g^{-1}_{dw}$, 10.56 ± 0.33 $\mu g.g^{-1}_{dw}$ respectively. In the winter season, they were respectively equal to 0.16 ± 0.02 µg.g-1dw, 3.62 ± 0.71 $\mu g.g^{-1}_{dw}$, 1.24 ± 0.20 $\mu g.g^{-1}_{dw}$, 7.31 ± 0.34 $\mu g.g^{-1}_{dw}$. In the gonads, their mean concentrations were respectively equal to 0.35 ± 0.08 $\mu g.g^{-1}_{dw}$, 8.34 ± 0.84 $\mu g.g^{-1}_{dw}$, 3.12 ± 0.79 $\mu g.g^{-1}_{dw}$, 11.36 ± 0.57 $\mu g.g^{-1}_{dw}$, in the summer period. During the winter, they reached 0.22 ± 0.05 $\mu g.g^{-1}_{dw}$, 3.71 ± 0.94 $\mu g.g^{-1}_{dw}$, 1.28 ± 0.24 $\mu g.g^{-1}_{dw}$, 7.45 ± 0.31 $\mu g.g^{-1}_{dw}$, respectively.

http://www.aloki.hu ● ISSN 1589 1623 (Print) ● ISSN 1785 0037 (Online)
DOI: http://dx.doi.org/10.15666/aeer/1906_46414664

Table 3. *Anova base for seasonal variations of the four metallic trace elements (Zn, Cu, Pb and Cd) in the liver, in the gills and in the gonads of common sole fished in the bay of Oran*

Organ	Metal	Df	Sum of squares	Mean of squares	F value	p value
Liver	Zn	3	49.282000	49.282000	95.692	< 0.001 ***
	Cu	3	42.333000	42.333000	99.540	< 0.001 ***
	Pb	3	3.121180	3.121180	44.125	< 0.001 ***
	Cd	3	0.044171	0.044171	31.348	< 0.001 ***
Gills	Zn	3	40.708000	40.708000	255.100	< 0.001 ***
	Cu	3	45.533000	45.533000	54.558	< 0.001 ***
	Pb	3	7.332600	7.332600	92.111	< 0.001 ***
	Cd	3	0.065307	0.065307	26.622	< 0.001 ***
Gonads	Zn	3	48.591600	48.591600	182.720	< 0.001 ***
	Cu	3	60.605000	60.605000	37.973	< 0.001 ***
	Pb	3	9.202600	9.202600	20.285	< 0.001 ***
	Cd	3	0.150060	0.050020	13.402	< 0.001 ***

Df: Degrees of freedom. Signif. codes: 0 '***' 0.001 '**' 0.01 '*' 0.05 '.' 0.1 ' ' 1

Table 4. *The results of the post hoc test (Duncan test) of the seasonal variations for the four metallic trace elements (Zn, Cu, Pb and Cd) in the liver of common sole fished in the bay of Oran*

Organ	Metal	Comparison	Z value
Liver	Zn	Autumn - Spring	2.21
		Autumn - Summer	- 0.39
		Spring - Summer	- 2.60
		Autumn - Winter	5.27
		Spring - Winter	3.06
		Summer - Winter	5.66
	Cu	Autumn - Spring	- 0.33
		Autumn - Summer	- 1.20
		Spring - Summer	- 0.87
		Autumn - Winter	4.19
		Spring - Winter	4.53
		Summer - Winter	5.39
	Pb	Autumn - Spring	- 1.66
		Autumn - Summer	- 3.06
		Spring - Summer	- 1.41
		Autumn - Winter	2.71
		Spring - Winter	4.37
		Summer - Winter	5.78
	Cd	Autumn - Spring	- 0.73
		Autumn - Summer	- 1.55
		Spring - Summer	- 0.82
		Autumn - Winter	3.73
		Spring - Winter	4.46
		Summer - Winter	5.28

http://www.aloki.hu ● ISSN 1589 1623 (Print) ● ISSN 1785 0037 (Online)
DOI: http://dx.doi.org/10.15666/aeer/1906_46414664

Table 5. *The results of the post hoc test (Duncan test) of the seasonal variations for the four metallic trace elements (Zn, Cu, Pb and Cd) in the gills of common sole fished in the bay of Oran*

Organ	Metal	Comparison	Z value
Gills	Zn	Autumn - Spring	2.25
		Autumn - Summer	1.08
		Spring - Summer	- 1.17
		Autumn - Winter	5.81
		Spring - Winter	3.56
		Summer - Winter	4.74
	Cu	Autumn - Spring	0.95
		Autumn - Summer	0.08
		Spring - Summer	- 0.87
		Autumn - Winter	4.98
		Spring - Winter	4.03
		Summer - Winter	4.90
	Pb	Autumn - Spring	- 0.56
		Autumn - Summer	- 3.89
		Spring - Summer	- 3.33
		Autumn - Winter	2.96
		Spring - Winter	3.52
		Summer - Winter	6.85
	Cd	Autumn - Spring	- 0.44
		Autumn - Summer	- 1.38
		Spring - Summer	- 0.94
		Autumn - Winter	3.99
		Spring - Winter	4.43
		Summer - Winter	5.37

Our results showed significant seasonal variations of the four metallic trace elements, in the three organs of common sole fished in the bay of Ghazaouet. For liver, Zn (Anova 2, F value = 57.24, p value < 0.001), Cu (Anova 2, F value = 68.23, p value < 0.001), Pb (Anova 2, F value = 51.69, p value < 0.001) and Cd (Anova 2, F value = 11.61, p value < 0.001) (*Tables 7* and *8*). For the gills, Zn (Anova 2, F value = 65.38, p value < 0.001), Cu (Anova 2, F value = 68.87, p value < 0.001), Pb (Anova 2, F value = 22.79, p value < 0.001) and Cd (Anova 2, F value = 59.87, p value < 0.001) (*Tables 7* and *9*). For the gonads, Zn (Anova 2, F value = 73.91, p value < 0.001), Cu (Anova 2, F value = 40.89, p value < 0.001), Pb (Anova 2, F value = 33.33, p value < 0.001) and Cd (Anova 2, F value = 25.90, p value < 0.001) (*Tables 7* and *10*).

http://www.aloki.hu ● ISSN 1589 1623 (Print) ● ISSN 1785 0037 (Online)
DOI: http://dx.doi.org/10.15666/aeer/1906_46414664

Table 6. *The results of the post hoc test (Duncan test) of the seasonal variations for the four metallic trace elements (Zn, Cu, Pb and Cd) in the gonads of common sole fished in the bay of Oran*

Organ	Metal	Comparison	Z value
Gonads	Zn	Autumn - Spring	1.43
		Autumn - Summer	- 1.09
		Spring - Summer	- 2.52
		Autumn - Winter	4.82
		Spring - Winter	3.39
		Summer - Winter	5.91
	Cu	Autumn - Spring	0.62
		Autumn - Summer	- 1.41
		Spring - Summer	- 2.03
		Autumn - Winter	4.18
		Spring - Winter	3.55
		Summer - Winter	5.59
	Pb	Autumn - Spring	- 0.79
		Autumn - Summer	- 2.50
		Spring - Summer	- 1.71
		Autumn - Winter	3.46
		Spring - Winter	4.26
		Summer - Winter	5.97
	Cd	Autumn - Spring	0.97
		Autumn - Summer	0.02
		Spring - Summer	- 0.95
		Autumn - Winter	4.20
		Spring - Winter	3.22
		Summer - Winter	4.18

Table 7. *Anova base for seasonal variations of the four metallic trace elements (Zn, Cu, Pb and Cd) in the liver, in the gills and in the gonads of common sole fished in the bay of Ghazaouet*

Organ	Metal	Df	Sum of squares	Mean of squares	F value	p value
Liver	Zn	3	73.021000	24.340200	57.245	< 0.001 ***
	Cu	3	64.248000	21.416100	68.232	< 0.001 ***
	Pb	3	7.931300	2.643770	51.691	< 0.001 ***
	Cd	3	0.124560	0.041522	11.614	< 0.001 ***
Gills	Zn	3	84.897000	28.299100	65.381	< 0.001 ***
	Cu	3	88.807000	29.602200	68.871	< 0.001 ***
	Pb	3	4.568400	1.522790	22.786	< 0.001 ***
	Cd	3	0.418330	0.139444	59.872	< 0.001 ***
Gonads	Zn	3	91.703000	30.567800	73.914	< 0.001 ***
	Cu	3	56.443000	18.814500	40.892	< 0.001 ***
	Pb	3	7.359500	2.453200	33.33	< 0.001 ***
	Cd	3	0.120684	0.068947	25.897	< 0.001 ***

Df: Degrees of freedom. Signif. codes: 0 '***' 0.001 '**' 0.01 '*' 0.05 '.' 0.1 ' ' 1

http://www.aloki.hu ● ISSN 1589 1623 (Print) ● ISSN 1785 0037 (Online)
DOI: http://dx.doi.org/10.15666/aeer/1906_46414664

Table 8. *The results of the post hoc test (Duncan test) of the seasonal variations for the four metallic trace elements (Zn, Cu, Pb and Cd) in the liver of common sole fished in the bay of Ghazaouet*

Organ	Metal	Comparison	Z value
Liver	Zn	Autumn - Spring	3.98
		Autumn - Summer	- 0.49
		Spring - Summer	- 4.47
		Autumn - Winter	4.77
		Spring - Winter	0.86
		Summer - Winter	5.26
	Cu	Autumn - Spring	1.73
		Autumn - Summer	- 0.52
		Spring - Summer	- 2.25
		Autumn - Winter	5.11
		Spring - Winter	3.38
		Summer - Winter	5.63
	Pb	Autumn - Spring	- 0.62
		Autumn - Summer	- 4.90
		Spring - Summer	- 4.28
		Autumn - Winter	0.04
		Spring - Winter	0.66
		Summer - Winter	4.94
	Cd	Autumn - Spring	- 0.23
		Autumn - Summer	- 0.92
		Spring - Summer	- 0.68
		Autumn - Winter	2.47
		Spring - Winter	2.71
		Summer - Winter	3.39

In Ghazaouet bay, seasonal variations of metallic trace elements showed the highest average concentrations were also noted in this region in summer, fall and spring. The lowest concentrations were noted in winter (*Fig. 5*).

In the liver of these fish, the mean concentrations of Cd, Cu, Pb and Zn were respectively equal to 0.33 ± 0.05 $\mu g.g^{-1}_{dw}$, 6.91 ± 0.50 $\mu g.g^{-1}_{dw}$, 1.95 ± 0.16 $\mu g.g^{-1}_{dw}$, 10.21 ± 0.80 $\mu g.g^{-1}_{dw}$. In winter, they were 0.21 ± 0.09 $\mu g.g^{-1}_{dw}$, 4.24 ± 0.96 $\mu g.g^{-1}_{dw}$, 1.06 ± 0.29 $\mu g.g^{-1}_{dw}$, 7.61 ± 0.77 $\mu g.g^{-1}_{dw}$ respectively. In the gills, their highest mean concentrations were reached in summer 0.38 ± 0.03 $\mu g.g^{-1}_{dw}$, 7.12 ± 0.32 $\mu g.g^{-1}_{dw}$, 1.92 ± 0.28 $\mu g.g^{-1}_{dw}$, 10.86 ± 0.91 $\mu g.g^{-1}_{dw}$ respectively. In winter, they were respectively equal to 0.17 ± 0.03 $\mu g.g^{-1}_{dw}$, 4.28 ± 1.11 $\mu g.g^{-1}_{dw}$, 1.25 ± 0.16 $\mu g.g^{-1}_{dw}$, 7.81 ± 0.84 $\mu g.g^{-1}_{dw}$. In the gonads, the maximum concentrations reached in summer were equal to 0.38 ± 0.04 $\mu g.g^{-1}_{dw}$, 7.52 ± 0.62 $\mu g.g^{-1}_{dw}$, 2.06 ± 0.19 $\mu g.g^{-1}_{dw}$, 11.30 ± 0.40 $\mu g.g^{-1}_{dw}$ and the minima reached in winter, were equal to 0.23 ± 0.05 $\mu g.g^{-1}_{dw}$, 4.71 ± 0.98 $\mu g.g^{-1}_{dw}$, 1.12 ± 0.16 $\mu g.g^{-1}_{dw}$, 7.96 ± 0.01 $\mu g.g^{-1}_{dw}$ respectively.

http://www.aloki.hu ● ISSN 1589 1623 (Print) ● ISSN 1785 0037 (Online)
DOI: http://dx.doi.org/10.15666/aeer/1906_46414664

Table 9. *The results of the post hoc test (Duncan test) of the seasonal variations for the four metallic trace elements (Zn, Cu, Pb and Cd) in the gills of common sole fished in the bay of Ghazaouet*

Organ	Metal	Comparison	Z value
Gills	Zn	Autumn - Spring	3.22
		Autumn - Summer	- 0.51
		Spring - Summer	- 3.73
		Autumn - Winter	5.52
		Spring - Winter	2.30
		Summer - Winter	6.03
	Cu	Autumn - Spring	0.17
		Autumn - Summer	- 0.86
		Spring - Summer	- 1.02
		Autumn - Winter	4.47
		Spring - Winter	4.31
		Summer - Winter	5.33
	Pb	Autumn - Spring	- 0.43
		Autumn - Summer	- 4.15
		Spring - Summer	- 3.72
		Autumn - Winter	1.05
		Spring - Winter	1.48
		Summer - Winter	5.20
	Cd	Autumn - Spring	- 0.81
		Autumn - Summer	- 1.49
		Spring - Summer	- 0.68
		Autumn - Winter	3.95
		Spring - Winter	4.75
		Summer - Winter	5.43

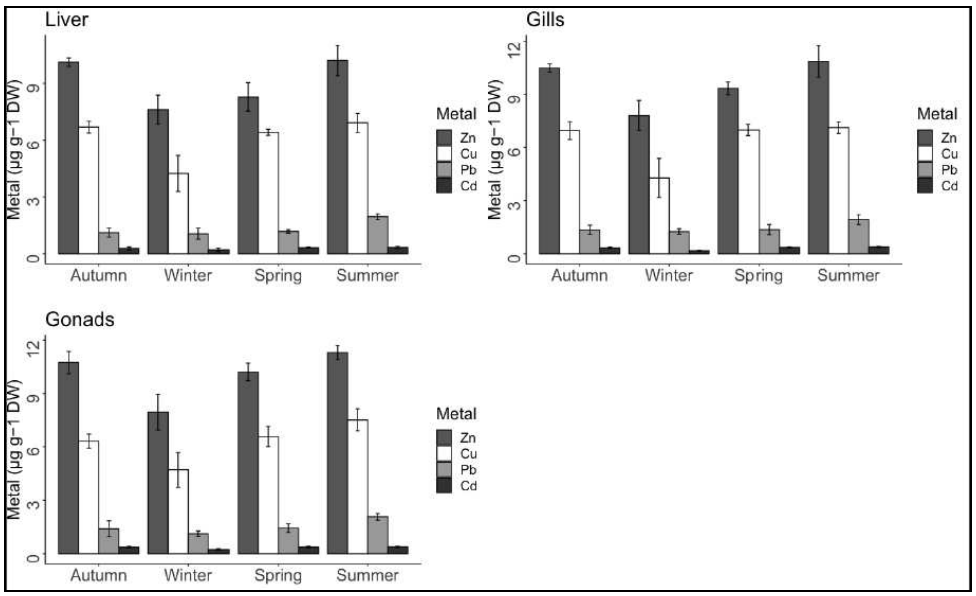

Figure 5. *Seasonal variations of metals (Zn, Cu, Pb and Cd) in organs at Ghazaouet bay.*

http://www.aloki.hu ● ISSN 1589 1623 (Print) ● ISSN 1785 0037 (Online)
DOI: http://dx.doi.org/10.15666/aeer/1906_46414664

Table 10. *The results of the post hoc test (Duncan test) of the seasonal variations for the four metallic trace elements (Zn, Cu, Pb and Cd) in the gonads of common sole fished in the bay of Ghazaouet.*

Organ	Metal	Comparison	Z value
Gonads	Zn	Autumn - Spring	2.21
		Autumn - Summer	- 1.37
		Spring - Summer	- 3.59
		Autumn - Winter	4.95
		Spring - Winter	2.74
		Summer - Winter	6.33
	Cu	Autumn - Spring	- 0.88
		Autumn - Summer	- 3.09
		Spring - Summer	- 2.21
		Autumn - Winter	3.16
		Spring - Winter	4.05
		Summer - Winter	6.26
	Pb	Autumn - Spring	- 0.27
		Autumn - Summer	- 4.03
		Spring - Summer	- 3.76
		Autumn - Winter	1.60
		Spring - Winter	1.87
		Summer - Winter	5.63
	Cd	Autumn - Spring	0.62
		Autumn - Summer	- 0.55
		Spring - Summer	- 1.17
		Autumn - Winter	4.49
		Spring - Winter	3.87
		Summer - Winter	5.04

The results of base Anova for metallic element variations (Zn, Cu, Pb and Cd) between the two sexes of common sole fished in the two bays: bay of Oran and bay of Ghazaouet, are regrouped in *Table 11*.

Table 11. *Anova base of metallic element variations (Zn, Cu, Pb and Cd) between the two sexes of common sole fished in the two bays: bay of Oran and bay of Ghazaouet.*

Bay	Metal	Df	Sum of squares	Mean of squares	F value	p value
Oran bay	Zn	1	3.836000	3.836000	13.3596	< 0.001 ***
	Cu	1	11.856000	11.856000	13.8375	< 0.001 ***
	Pb	1	0.176400	0.176400	0.6375	0.4276
	Cd	1	0.030013	0.030013	10.1797	< 0.05 *
Ghazaouet bay	Zn	1	5.202000	5.202000	8.7551	< 0.05 *
	Cu	1	0.933000	0.932800	2.1914	0.1437
	Pb	1	0.063500	0.063490	0.9444	0.3342
	Cd	1	0.018689	0.018689	6.4739	< 0.05 *

Df: Degrees of freedom. Signif. codes: 0 '***' 0.001 '**' 0.01 '*' 0.05 '.' 0.1 ' ' 1

http://www.aloki.hu ● ISSN 1589 1623 (Print) ● ISSN 1785 0037 (Online)
DOI: http://dx.doi.org/10.15666/aeer/1906_46414664

In terms of the inertias of the factorial axes of the PCA (*Fig. 6*), the Dim1 axis would explain 68% of the variance of the concentrations of metallic trace elements between the organs and the Dim2 axis would explain 14.5%.

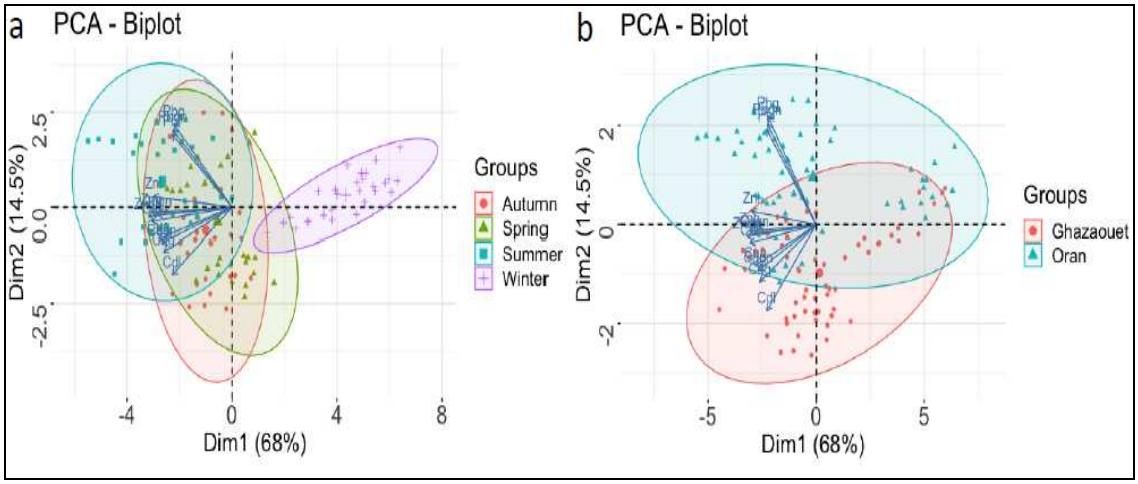

Figure 6. *Projection of heavy metals according to the seasons at the two bays: Oran Bay and Ghazaouet Bay. (a) Projection of heavy metals according to the seasons at the two sites studied. (b) Projection of heavy metals according to the sites studied.*

Discussion

The physicochemical results in *Table 1* of the water obtained generally comply with Algerian and European standards (JORA, 2006) whether for T °, pH, salinity or even the O_2 dissolved.

All of our results concerning temperature are comparable to those obtained by (Rouane-Hacene et al., 2018) (21.40 ± 1.41 °C) in the same region as well as those of (Dahel, 2009) (20.25 °C) and (Boucetta, 2017) (20.52 ± 5.37 °C) in the waters of the Algerian coast. According to Imasheva et al. (1997), temperature is considered to be an essential ecological factor in the control of various biological and physiological processes such as metabolism, reproduction, growth and biogeographic distribution of marine species, either directly or in correlation with other ecological factors.

The pH values in *Table 1* taken during the study period did not show significant spatio-temporal fluctuations. In general, for both berries the pH is slightly alkaline. Our results agree with other values found in previous studies carried out on the Algerian east coast (Boudelaa and Medjram, 2011; Hamdani, 2012; Rouidi et al., 2013) and on the Algerian west coast (Remili and Kerfouf, 2013; Rouane-Hacene et al., 2018; Rouabhi et al., 2019).

According to Boucetta (2017), pH is a fundamental ecological factor that plays an important role in the marine environment, as it can affect many physiological and biochemical processes. According to Blakeslee et al. (2013), pH also acts on certain chemical components which can become toxic.

The measured mean salinity value in *Table 1* is (36.57 ± 0.67) psu in the bay of Oran and (36.84) psu in the bay of Ghazaouet, these results agree with those obtained on the Algerian east coast, where the salinity varies between 35 and 38 psu (Sifi, 2009; Hamdani, 2012).

http://www.aloki.hu ● ISSN 1589 1623 (Print) ● ISSN 1785 0037 (Online)
DOI: http://dx.doi.org/10.15666/aeer/1906_46414664

Numerous studies had shown that species exposed to low levels of salinity increase their oxygen uptake and weaken energy metabolism. Low salinity results in high food consumption (Widmeyer and Bendell-Young, 2007; Mattozo et al., 2012; Rashida et al., 2015). Salinity largely controls biological processes, but also chemical processes in water, it also has an impact on the bioavailability of metals (Mouneyrac et al., 2009).

The dissolved oxygen level reaches its maximum in winter with (8.31 ± 0.24 mg L^{-1}) in the bay of Oran and 7.89 ± 0.10 mg L^{-1} in the bay of Ghazaouet. A gradual drop in its concentrations was observed in summer in both bays. This may be due to the increase in temperature and the impact of hydrodynamics (Florian, 2011). The same observations were made in the gulfs of Annaba and Skikda in the bay of Collo (Guemouda, 2015), in the bay of Algiers (Bachari et al., 2011), and in the bay of Oran (Rouane-Hacene, 2013). It is also noted that a low dissolved oxygen content may be associated with industrial releases and organic pollutants (Boucetta, 2017).

According to Belghiti et al. (2013), dissolved oxygen is one of the parameters most sensitive to pollution, and its concentration tells us about the level of pollution and therefore the degree of self-purification. Indeed, the alteration of the polluting material causes a drop in the dissolved oxygen content in the environment, causing a disturbance in the preservation and development of aquatic flora and fauna (Afri-Mehennaoui, 1998).

According to Karayücel and Karayücel (2000), the physicochemical factors (temperatures, salinity, dissolved oxygen, pH, etc.) of the medium play an important role since they act both on the physicochemical form of metals (adsorption-desorption on suspended metals) therefore on their bioavailability, but also on the metabolism of the species (respiration, reproduction, trophic activities, etc.), which partly influences the kinetics of accumulation and excretion of metals.

Statistical processing of variations in average trace metal contents evaluated in the common sole fished in the two sites (*Fig. 2*) indicate the presence of very heterogeneous values. Zn concentrations were highest with 9.77 ± 1.61 $\mu g.g^{-1}_{dw}$ in Oran and 9.58 ± 1.42 $\mu g.g^{-1}_{dw}$ in Ghazaouet, followed by that of Cu with 6.33 ± 1.84 $\mu g.g^{-1}_{dw}$ in Oran and 6.21 ± 1.25 $\mu g.g^{-1}_{dw}$ in Ghazaouet, Pb with 2.02 ± 0.75 $\mu g.g^{-1}_{dw}$ in Oran and 1.44 ± 0.41 $\mu g.g^{-1}_{dw}$ in Ghazaouet, and finally Cd with 0.25 ± 0.07 $\mu g.g^{-1}_{dw}$ in Oran and 0.31 ± 0.08 $\mu g.g^{-1}_{dw}$ in Ghazaouet. The same classification of the ETM accumulation gradient has often been observed in this region for different marine species (Borsali et al., 2014; Guendouzi et al., 2017; Rouabhi et al., 2019). It is clear that the process of bioaccumulation depends on the extent of the contamination of the medium. The accumulation of metallic trace elements in aquatic organisms results from the net balance of capture and excretion processes. According to Casas (2005), three mechanisms must be taken into account: metal capture, excretion and storage by the organism. According to Di Bella et al. (2006), Bodin et al. (2007) and Belhoucine et al. (2014), the bioaccumulation process is indeed influenced by the physicochemical properties of compounds but also by biological, physiological and specific ecological aspects of the exposed species, such as habitat, sex, age, reproduction, diet or the state of health of the animals. According to other authors, the level of heavy metals in different species depends mainly on eating habits (Mormede and Davies, 2001; Watanabe et al., 2003; Bouhadiba et al., 2017).

Amara et al. (2001) indicates that the common sole *S. solea* (L. 1758) is a benthic fish which with a diet, consisting of benthic and epi-benthic invertebrates (polychaetes, molluscs and crustaceans), shows variations qualitative and quantitative depending on

http://www.aloki.hu ● ISSN 1589 1623 (Print) ● ISSN 1785 0037 (Online)
DOI: http://dx.doi.org/10.15666/aeer/1906_46414664

the season, the area and the size of the individuals. Benthic fish generally accumulate higher concentrations of heavy metals than pelagic fish (Bustamante et al., 2003; Belhoucine et al., 2015; Bouhadiba et al., 2017).

The data recorded by (Kerfouf et al., 2010; Remili and Kerfouf, 2013) are practically similar to our results. The latter stressed that the bay of Oran is threatened by various forms of nuisance, industrial activities, intensive tourism and massive urbanization, which generates increasing pollution.

The results of this work also tend to support the observations of Benguedda et al. (2011) who point out the importance of the industrial unit ALZINC (Algerian Zinc Company) in the pollution of the Ghazaouet region. The purpose of this unit is the production and marketing of zinc and its alloys, sulfuric acid, cathodic copper (Benguedda et al., 2011). This plant uses seawater for cooling the sulfuric acid manufacturing facilities and some of the plant's thermal power plant (Bakalem, 1980). According to Belhoucine et al. (2014) anthropogenic inputs of zinc into the environment result mainly from mining activities, agricultural spraying and urban activities. They also assume that domestic wastewater inputs contain Zn. According to the work of (Casas, 2005), in port areas, zinc is introduced from the dissolution of anodes intended to protect boat hulls against corrosion, and is contained in certain anti-fouling paints. For copper, most of it comes from soil erosion by watercourses (68%) (Casas, 2005), contamination of copper sulphate (13%) and discharges of wastewater that still contains copper, even after treatment (Casas, 2005). According to Rouabhi (2020), the high lead concentrations in Oran Bay could be due to the proximity to the Arzew industrial zone responsible for processing and exporting hydrocarbons mainly to Europe. According to Belhoucine et al. (2014) its high concentrations could also be due to the combustion of automotive fuels. Regarding cadmium, according to Miramand et al. (2000) and Bosch et al. (2016), its presence in aquatic environments is mainly of atmospheric origin and also due to leaching of soils (phosphate fertilizers).

The results obtained from the average concentrations of the four metallic trace elements analyzed at the organ level showed no significant variation between the sampling sites and between the two sexes (Anova, F value = 0.01, p value = 0.99) (*Table 2*). However, the results recorded have made it possible to reveal that the three tissues chosen bioaccumulate all the micropollutants (Zn, Cu, Pb and Cd) and appear to have similar concentrations. No significant difference was noted between the three organs studied (Anova, F value = 0.47, p value = 0.62) (*Table 2*) regardless of the site of harvest. Ennouri et al. (2008), El Morhit et al. (2009) and Belhoucine et al. (2014) observed a different accumulation between organs which followed a decreasing scale: Gonads > gills > liver, in different species of fish.

The distribution, location and bioaccumulation of metallic elements in tissues do not depend on a single mechanism (Belhoucine et al., 2014). In fact, the quantity of metals transferred is influenced both by the irrigation of the organ considered and by the intracellular binding capacities (Boudou, 1982). According to this author, the relative importance of these two parameters determines the target organs of metallic bioaccumulation. Therefore, tolerance to such a form of pollution by marine organisms has been attributed to the presence of metallothionein, proteins involved in the processes of storage, bioaccumulation, transport and detoxification (immobilization of heavy metals in non-toxic form inside the cell) (Linde et al., 1999; Evoglu et al., 2005; Atli and Canli, 2008).

http://www.aloki.hu ● ISSN 1589 1623 (Print) ● ISSN 1785 0037 (Online)
DOI: http://dx.doi.org/10.15666/aeer/1906_46414664

The increase in the levels of metals, which for the most part are not lipophilic contaminants, is due to slower elimination; This may be explained by the role of the liver in detoxifying contaminants and the importance of the gonads in reproductive physiology (Zhang and Wang, 2007).

Numerous studies had shown a preferential organotropism of trace metals such as Cd, Cu and Zn for the liver in fish (De Boeck et al., 2004; Usero et al., 2004; Ribeiro et al., 2005). According to Rouabhi (2020), the gills reflect the bioavailability of contaminants in the medium and according to Capene and Vasak (1989), the liver is more efficient in biomonitoring studies using fish.

Bioaccumulation of toxic metals can affect the liver, gonads, gills and other tissues of fish, resulting in metabolic disruption and obstruction of fish growth and development (Junejo et al., 2019).

The same seasonal variations had been observed in the work of Miramand et al. (2000) for *Mullus barbatus* from French marine waters. The highest concentrations of metallic trace elements were also reached in the summer season.

Barhoumi et al. (2009) had underlined in their study that the gills are the main targets of direct contamination, because they play an important role in the absorption of metals, in the storage and possibly in the transfer to the internal compartments by the blood. Similar seasonal variations on the Algerian west coast were also observed in the sardine *Sardinella aurita* (Benamar et al., 2010), in the *hake Merluccius merluccius* (Belhoucine et al., 2014) and in the Mullets *Mugil cephalus* (Bouhadiba et al., 2017). According to Belhoucine et al. (2014), the Algerian coastal population increases considerably during the summer, which can increase direct discharges into water.

According to Bennett (1978), the increase in water temperature causes an increase in ventilation of the gills in response to the decrease in the concentration of oxygen in the water. Thus, increased metabolic rate during the summer could lead to increased absorption of bioavailable contaminants in water. In addition, temperature also has a strong influence on the properties of the metal by changing the effect of equilibrium between molecular and ionized forms (El Morhit et al., 2009). Storelli and Marcotrigiano, (2001) conclude in their work that the concentration of metals in fish tissue generally reflects the pollution profile.

On the other hand, it is possible that this difference in bioaccumulation is conditioned by the fluctuation of certain biological factors such as growth and reproduction. These factors contribute greatly to the variability of heavy metal bioaccumulation (Langston and Spence, 1995). Especially since this species spawns mainly in winter (Morat, 2011), which can induce an excretion of contaminants from the organism (Casas, 2005).

No significant difference was observed between the two sexes regardless of the organ studied (Anova, F value = 0.16, p value > 0.05) or the site of harvest (Anova, F value = 0.04, p value > 0.05) (*Table 2*). In Oran, there is a significant variation between the two sexes for Zn (Anova 3, F value = 13.36, p value < 0.001), Cu (Anova 3, F value = 13.84, p value < 0.001) and Cd (Anova 3, F value = 10.18, p value < 0.05) (*Table 11*). Concerning Ghazaouet bay, there is a significant variation between the two sexes for Zn (Anova 3, F value = 8.75, p value < 0.05), and Cd (Anova 3, F value = 6.47, p value < 0.05) (*Table 11*).

Different variations between the two sexes were noted by Belhoucine et al. (2014) in *M. merluccius* fished at the level of the Oran coastline and Bodiguel et al. (2008) in *M. merluccius* fished in the French Mediterranean (Golf du Lyon). Which can mean that

http://www.aloki.hu ● ISSN 1589 1623 (Print) ● ISSN 1785 0037 (Online)
DOI: http://dx.doi.org/10.15666/aeer/1906_46414664

gender can influence the accumulation of contaminants under certain conditions due to the difference in growth between males and females.

However, several studies had also shown that there was no difference between the accumulation of contaminants in organs between the two sexes (Lombardi, et al., 2010; Hosseini Alhashemi et al., 2012). This can be explained by the sedentary nature of the common sole (*Solea solea*, L. 1758) (De Serres, 1845; Wessel, 2010). In fact, males and females in this species have the same ecology and the same behavior, and are constantly in contact with sediments, a compartment that allows the capture of many contaminants such as, for example, metallic trace elements (Wessel, 2010).

The projection of the observations on the Dim1 axis (*Fig. 6*), shows that the seasonal aspect has a great influence on the distribution of the data. The winter season is the one that shows the most difference compared to the other seasons. Seasonality is one of the most influential factors in the build-up of contaminants. Numerous studies have shown its importance in the accumulation of metallic trace elements by marine species (Kaimoussi et al., 2000; Orban et al., 2002; Belhoucine et al., 2014).

The projection of the observations in relation to the sampling sites (*Fig. 6*) shows higher Pb concentrations in the organs of sole sampled in the bay of Oran (2.02 ± 0.75 µg g^{-1}_{wd}) than those of Ghazaouet bay (1.44 ± 0.41 µg g^{-1}_{wd}). These high Pb concentrations may be due to the presence of several important industrial zones in this region (Sonatrach, ammoniac industries and water treatment plants) (Grimes, 2010; Rouabhi, 2020). The concentrations of other metallic trace elements in the region of Ghazaouet mainly those of Zn may be due to the proximity of the company Alzinc (production and processing of Zn) in this region (Benguedda et al., 2011).

These concentrations of trace metal elements can also return to wastewater discharges without prior treatment (Taleb et al., 2007). In addition, this coast is also under the direct influence of maritime traffic which could be the source of trace metals (Belhoucine et al., 2015).

Conclusion

Marine pollution has been a very worrying universal problem for two decades now. Today, the threat is so great for all seas and oceans, and public concern is so great, that states are individually and collectively seeking the necessary instruments to curb it. Man being the last link in the food chain and the end consumer of marine products can be a victim at any time. The risks of bioavailability and toxicity of these trace metals are to be feared because they constitute permanent dangers for the entire food chain and threaten public health.

This present work, the interest of which we emphasize, allows us to take stock of the current situation of the bay of Oran and the bay of Ghazaouet in terms of coastal and marine environmental pollution.

Regarding the physico-chemical analysis of seawater, parameters: T°, pH, salinity, organic matter or even dissolved O_2, our results are in Algerian standards and coincide with previous studies in the same region.

Organs from common sole taken from the two contrasting sites showed the same process of bioaccumulation of metallic trace elements with the same proportions, implying the importance of the physiological role of each organ in the process of bioaccumulation. The average concentrations of metals measured in the tissues of the common sole collected in the two sampling sites, varied according to the seasons, in

http://www.aloki.hu ● ISSN 1589 1623 (Print) ● ISSN 1785 0037 (Online)
DOI: http://dx.doi.org/10.15666/aeer/1906_46414664

relation to the biology of the animals (growth, reproduction, etc.) and under the influence of certain parameters. environment, mainly temperature. This marked a seasonal variability mainly between the winter period and the summer period.

The results obtained show that the common sole of the Algerian west coast has great potential as a tool for evaluating metal pollution in the marine environment. This work allowed us to highlight the omnipresence of the four metallic trace elements in each target organ of this species. This contamination of fish is a risk factor not only for the life of these aquatic species, but also for humans. To further this study, it is important to carry out toxicological analyzes on the flesh of this fish in order to better assess the potential risks to human health linked to their consumption.

This study would also deserve in the future to extend well and be enriched by expanding the sampling network to the entire Algerian coastline and integrating other trace metals in particular mercury and evaluating organic pollutants such as hydrocarbons, pesticides. On the biological level, we must take into account the biological cycle and the behavior of the bioindicator with respect to contaminants. In addition, it would be very interesting to assess the contamination, distribution and speciation of these xenobiotics in the water column of the Algerian coast and to perform sequential extractions to better identify their mobility within a sediment in order to better correlate the potential toxicity of metallic trace elements in a sediment to the surrounding biological activity.

REFERENCES

[1] Afri-Mehennaoui, F. Z. (1998): Contribution à l'étude physico-chimique et biologique de l'oued Kebir Rhumel et de ses principaux affluents. – Mémoire de Magistère en écologie. Département de Biologie et Ecologie Végétale, Université de Constantine.

[2] Amara, R., Laffargue, P., Maryniak, C., Lagardere, F., Luzac, C. (2001): Feeding ecology and growth of O-group flatfish (sole, dab and plaice) on a nursery ground (Southern Bight of the North Sea). – Journal of Fish Biology 58(3): 788-803. DOI: 10.1111/j.1095-8649.2001.tb00531.x.

[3] Amiard-Triquet, C., Amiard, J. C. (2008): Les biomarqueurs dans l'évaluation de l'étatécologique des milieux aquatiques. – Tec & Doc, Paris.

[4] Atli, G., Canli, M. (2008): Reponses of metallothionein and reduced glutathione in a freshwater fish Oreochromis niloticus following metal exposures. – Environmental Toxicology and Pharmacologie 25: 33-38.

[5] Aydoğan, Z., İncekara, Ü. (2017): Heavy element pollution their meaning in literature and using organisms to monitor this pollution. – https://nbn-resolving.org/urn:nbn:de:101:1-201712292883 (accessed: 7 September 2020).

[6] Bachari, S., Houma, F., Bachouche, N., Kessar, A., Belkessa, R. (2011): Contribution to the assessment of pollution of marine water on the west coast of Algeria using satellite imagery. – Con Méd Côt & Mar. 2nde edition, pp. 339-344.

[7] Bakalem, A. (1980): Aménagement du littoral ouest: problème de pollution marine - étude préliminaire de la zone Arzew-mers el Hadjadj. – Cahiers géographiques de l'Ouest 5-6: 115-49

[8] Barhoumi, S., Messaoudi, I., Deli, T., Saïd, K., Kerkeni, A. (2009): Cadmium bioaccumulation in three benthic fish species, *Salaria basilisca*, *Zosterisessor ophiocephalus* and *Solea vulgaris* collected from the Gulf of Gabes in Tunisia. – Journal of Environmental Sciences 21(7): 980-984. DOI: 10.1016/S1001-0742(08)62371-2.

http://www.aloki.hu ● ISSN 1589 1623 (Print) ● ISSN 1785 0037 (Online)
DOI: http://dx.doi.org/10.15666/aeer/1906_46414664

[9] Belghiti, M. L., Chahlaoui, A., Bengoumi, A. (2013): Caractéristiques physico-chimique des eaux de certains puits utilisés comme source d'eau portable en milieu rural dans la région de Meknès (Maroc). – Larhyss Journal 46: 21-36.

[10] Belhoucine, F., Alioua, A., Bouhadiba, S., Boutiba, Z. (2014): Impact of some biotics and abiotics factors on the accumulation of heavy metals by a biological model Merluccius merluccius in the bay of Oran in Algeria. – Journal of Biodiversity and Environmental Sciences (JBES) 5(6): 33-44.

[11] Belhoucine, F., Habbar, C., Alioua, A., Bouahdiba, S., Mohamed Benkada, M., Benhabara, R., Boutiba, Z. (2015): Assessment of contamination by xenobiotics (lead and cadmium) in the muscle tissue of two teleost spotted weever (*Trachinus Araneus*, Cuvier, 1829) and the axillary seabream, (*Pagellus Acarne*, Risso, 1826) in the Algerian West coast. – International Journal of Scientific Research in Science and Technology. DOI: 10.32628/CIBA06.

[12] Benamar, N., Bouderbala, M., Boutiba, Z. (2010): Evaluation de la concentration en cadmium d'un poisson pélagique commun, *Sardinella aurita*, dans la baie d'Oran. – Journal des Sciences Halieutique et Aquatique 1: 16-20.

[13] Benguedda, W., Dali, Y. N., Amara, R. (2011): Trace metals in sediments, macroalgae and benthic species from the western part of Algerian coast. – Journal of Environmental Science and Engineering 15(2): 1604-1612.

[14] Bennett, A. F. (1978): Activity metabolism of the lower vertebrates. – Annual Review of Physiology 40(1): 447-469. DOI: 10.1146/annurev.ph.40.030178.002311.

[15] Benzohra, M., Millot, C. (1995): Characteristics and circulation of the surface intermediate water masses of Algeria. – Deep Sea Research Part I: Oceanographic Research Papers 10(42): 1803-1830.

[16] Blakeslee, C. J., Galbraith, H. S., Robertson, L. S., St John, W. B. (2013): The effects of salinity exposure on multiple life stages of a common freshwater mussel, Elliptio complanata: effects of salinity on Elliptio complanata. – Environmental Toxicology and Chemistry 32(12): 2849-2854. DOI: 10.1002/etc.2381.

[17] Bodiguel, X., Tronczyński, J., Loizeau, V., Munschy, C., Guiot, N., Le Guellec, A. M., Olivier, N., Roupsard, F., Mellon, C. (2008): Classical and novel organohalogen compounds (PCBs and PBDEs) in hake (*M. merluccius*, L.) from the Mediterranean and Atlantic coasts (France). – Environmental Toxicology. DOI: 10.2495/ETOX080171.

[18] Bodin, N., Caisey, X., Abarnou, A., Loizeau, V., Latrouite, D., Le Guellec, A., Guillou, M. (2007): Polychlorinated biphenyl contamination of the spider crab (*MAJA BRACHYDACTYLA*): Influence of physiological and ecological processes. – Environmental Toxicology and Chemistry 26(3): 454. DOI: 10.1897/06-076R.1.

[19] Borsali, S. (2015): Evaluation de la contamination métallique dans trois organes (foie, gonades et muscle) du Rouget de roche *Mullus surmuletus* (L.1758) par quatre métaux lourds (Zn, Cu, Cd, Pb) peché dans la baie d'Oran. – Thése de Doctorat. Université d'Oran, Oran.

[20] Borsali, S., Bouderbala, M., Boutiba, Z. (2014): Evaluation of metal contamination of mullet (Mullus surmuletus L. 1758) in the Bay of Oran. – Journal of Life Sciences 8(4): 344-350.

[21] Bosch, A. C., O'Neill, B., Sigge, G. O., Kerwath, S. E., Kerwath, L. C. (2016): Heavy metals in marine fish meat and consumer health: a review: heavy metals in marine fish meat. – Journal of the Science of Food and Agriculture 96(1): 32-48. DOI: 10.1002/jsfa.7360.

[22] Boucetta, S. (2017): Biosurveillance des eaux du littoral Est algérien à travers un mollusque gastropode : *Phorcus (=Osilinus) turbinatus* (BORN, 1780). – Thése de Doctorat es sciences. Départements des sciences de la Mer. Université Badji Mokhtar, Annaba.

http://www.aloki.hu ● ISSN 1589 1623 (Print) ● ISSN 1785 0037 (Online)
DOI: http://dx.doi.org/10.15666/aeer/1906_46414664

[23] Boucheseiche, C., Cremille, E., Pelte, T., Pojer, K. (2002): Bassin Rhône - Méditerranée - Corse. – Guide technique n°7, Pollution toxique et écotoxicologie: notion de base. Lyon, Agence de l'Eau Rhône - Méditerranée - Corse.

[24] Boudelaa, S., Medjram, M. S. (2011): Assessment of chemical and petrochemical effluent: case of hydrocarbon pole of skikda, Algeria. – European Journal of Scientific Research 4(63): 563-584.

[25] Boudou, A. (1982): Recherches en éco toxicologie expérimentale sur les processus de bioaccumulation et de transfert des dérivés du mercure. – Thèse de doctorat d'Etat. Université de Bordeaux 1, Bordeaux.

[26] Bouhadiba, S., Belhoucine, F., Belhadj, H., Alioua, A., Boutiba, Z. (2017): Quantification of two metallic elements in the Mullet, *Mugil cephalus* Linnaeus, 1758 (Perciformes Mugilidae), fished at the bay of Oran (NW Algeria). – Biodiversity Journal 8(3): 807-818.

[27] Bustamante, P., Bocher, P., Chérel, Y., Miramand, P., Caurant, F. (2003): Distribution of trace elements in the tissues of benthic and pelagic fish from the Kerguelen Islands. – Science of the Total Environment 313(1-3): 25-39. DOI: 10.1016/S0048-9697(03)00265-1.

[28] Capene, E., Vasak, M. (1989): Hepatic metallothionein from goldfish (*Carassius auratus*). – Comparative Biochemistry and Physiology 92(3): 463-468.

[29] Casas, S. (2005): Modélisation de la bioaccumulation des métaux traces (Hg, Cd, Pb, Cu et Zn) chez la moule, *mytulus galloprovincialis*, en milieu méditerranéen. – Doctorat de l'université du sud de Toulon Var. l'université du sud de Toulon Var.

[30] Chiffoleau, J. F., Claisse, D., Cossa, D., Ficht, A., Ganzalez, J. L., Guyot, T., Michel, P., Miramand, P., Oger, C., Petit, F. (2001): La contamination métallique. Programme Seine Aval, fascicule n°8, – Editions Ifremer, Plouzané (France).

[31] Dahel Zanat Amina-Tania. (2009): Analyse de la qualité bactériologique des eaux du littoral Nord-Est algérien à travers un bioindicateur la moule Perna perna. – Magister en Sciences de la Mer. Département des Sciences de la Mer. Université Badji-Mokhtar, Annaba.

[32] De Boeck, G., Petit, W., De Coen, W., Blust, R. (2004): Tissue-specific Cu bioaccumulation patterns and differences in sensitivity to waterborne Cu in three freshwater fish: rainbow trout (*Oncorhynchus mykiss*), common carp (*Cyprinus carpio*), and gibel carp (*Carassius auratus gibelio*). – Aquatic Toxicology (Amsterdam, Netherlands) 70(3): 179-188. DOI: 10.1016/j.aquatox.2004.07.001.

[33] De Serres, M. (1845): Des causes des migrations des animaux, et particulièrement des oiseaux et des poissons. Volume 1. – Lagny frères, Paris.

[34] Di Bella, G., Licata, P., Bruzzese, A., Naccari, C., Trombetta, D., Lo Turco, V., Dugo, G., Richetti, A., Naccari, F. (2006): Levels and congener pattern of polychlorinated biphenyl and organochlorine pesticide residues in bluefin tuna (*Thunnus thynnus*) from the Straits of Messina (Sicily, Italy). – Environment International 32(6): 705-710. DOI: 10.1016/j.envint.2006.02.001.

[35] DPRHT (2004): Le secteur de la pêche et de l'état environnemental du littoral de la Wilaya de Tlemcen, 41P. Direction de la Pêche et des Ressources Halieutiques de Tlémcen, Algérie.

[36] Dusquene, S. (1992): Bioaccumulation métallique et métallothioneines chez trois espèces de poissons du littoral Nord-Pas De Calais. – Thèse de Doctorat en Biologie et Santé. Université des Sciences et Techniques de Lille.

[37] El Morhit, M., Fekhaoui, M., Elie, P., Girard, P., Yahyaoui, A., El Abidi, A., Jbilou, M. (2009): Heavy metals in sediment, water and the european glass eel, *Anguilla anguilla* (Osteichthyes: Anguillidae), from Loukkos River estuary (Morocco, eastern Atlantic). – Cybium: International Journal of Ichthyology 33(3): 219-228. DOI: https://doi.org/10.26028/cybium/2009-333-005.

http://www.aloki.hu ● ISSN 1589 1623 (Print) ● ISSN 1785 0037 (Online)
DOI: http://dx.doi.org/10.15666/aeer/1906_46414664

[38] Ennouri, R., Chouba, L., Kraiem, M. M. (2008): Evaluation de la contamination chimique par les metaux traces (Cd, Pb, Hg et Zn) du zooplancton et de la sardinelle (*Sardinella aurita*) dans le golf de Tunis. – Bulletin de l'Institut National des Sciences et Technologies de la Mer,33.
[39] Evoglu, K., Atli, G., Canli, M. (2005): Effects of metal (Cd, Cu, Zn) interactions on the profiles of metallothionein-like proteins in the Nile fish *Oreochromis niloticus*. – Bulletin of Environmental Contamination and Toxicology 75(2): 309-399.
[40] Florian, G. (2011): Rôle des herbiers de zostères (*Zostera noltii*) sur la dynamique sédimentaire du Bassin d'Arcachon. Rôle des herbiers de zostères (*Zostera noltii*) sur la dynamique sédimentaire du Bassin d'Arcachon. – Thèse de Doctorat. Université de Bordeaux 1, Bordeaux.
[41] Förstner, U., Wittmann, G. T. W. (1981): Metal Pollution in the Aquatic Environment. 2nd Ed. – Springer, Berlin.
[42] Goldberg, E. D. (1975): The "Mussel Watch" Mar. – Pollut. Bull. 6: 111-113.
[43] Grimes, S. (2010): Peuplements benthiques des substrats meubles de la côte algérienne: Taxonomie, structure et statut écologique. – Thése de Doctorat es sciences. Université d'Oran, Oran.
[44] Grimes, S., Ruellet, T., Dauvin, J. C., Boutiba, Z. (2010): Ecological quality status of the soft-bottom communities on the algerian coast: general patterns and diagnosis. – Marine Pollution Bulletin 60(11): 1969-1977. DOI: 10.1016/j.marpolbul.2010.07.032.
[45] Guemouda, M. (2015): Impact de la pollution par les hydrocarbures sur *Perinereis cultrifera* (Annélides, Polychètes) dans le littoral Est-Algérien. – Thèse de doctorat. Département de Biologie. Université Badji Mokhtar. Annaba.
[46] Guendouzi, Y., Soualili, D. L., Boulahdid, M., Boudjellal, B. (2017): Biological indices and monitoring of trace metals in the mussel from the southwestern Mediterranean (Algeria): seasonal and geographical variations. – Thalass An Int J Mar Sci. 1(34): 103-112.
[47] Hamdani, A. (2012): La reproduction chez un mollusque bivalve *Donax trunculus* L. dans le golfe d'Annaba. Rapport entre les aspects cytologique et biochimique et la pollution. – Thèse de doctorat. Département de Biologie. Université Badji Mokhtar, Annaba.
[48] Hosseini Alhashemi, A., Karbassi, A., Hassanzadeh, K. B., Monavari, S. M., Sekhavatjou, M. (2012): Bioaccumulation of trace elements in different tissues of three commonly available fish species regarding their gender, gonadosomatic index, and condition factor in a wetland ecosystem. – Environmental Monitoring and Assessment 184(4): 1865-1878. DOI: 10.1007/s10661-011-2085-8.
[49] IAEA (1995): Echantillons pour comparaisons inter-oratoire, Matière de référence. Doc. Des Services de contrôle de la qualité des Analyses. 40p. International Atomic Energy Agency.
[50] Imasheva, A. G., Loeschcke, V., Zhivotovsky, L. A., Lazebny, O. E. (1997): Effects of extreme temperatures on phenotypic variation and developmental stability in Drosophila melanogaster and Drosophila buzzatii. – Biological Journal of the Linnean Society 61(1): 117-126. DOI: 10.1111/j.1095-8312.1997.tb01780.x.
[51] JORA (2006): Journal Officiel de la République Algérienne Et Populaire. – 46 executive decree n° 93-164, Directive 2006/7 / CE.
[52] Junejo, S. H. Baig, J. A., Kazi, T. J., Afridi, H. I. (2019): Cadmium and lead hazardous impact assessment of pond fish species. – Biological Trace Element Research 191(2): 502-511. DOI: 10.1007/s12011-018-1628-z.
[53] Kaimoussi, A., Chafik, A., Cheggour, M., Mouzdahir, A. F., Bakkas, S. (2000): Variations saisonnières des concentrations en métaux (Cd, Cu, Zn, Fe et Mn) chez la moule *Mytilus galloprovincialis* du littoral de la région d'El Jadida (Maroc). – Marine Life 10(1-2): 77-85.

http://www.aloki.hu ● ISSN 1589 1623 (Print) ● ISSN 1785 0037 (Online)
DOI: http://dx.doi.org/10.15666/aeer/1906_46414664

[54] Karayücel, S., Karayücel, I. (2000): The effect of environmental factors, depth and position on the growth and mortality of raft-cultured blue mussels (*Mytilus edulis L.*). – Aquaculture Research 31: 893-899.
[55] Kerfouf, A., Alaoui, F. Z., Djoudi, O., Mebarki, Z., Benyahia, M. (2010): Le dessalement de l'eau de mer dans la perspective d'une gestion intégrée et d'un développement durable: Cas de la station de dessalement d'Oran: Algérie Nord Occidentale. – European Journal of Scientific Research 96(2): 245-249.
[56] Lafabrie, C. (2007): Utilisation de *Posidonia oceanica* (L) Delile comme bio-indicateur de la contamination métallique. – Thèse de Doctorat en écologie marine. Univerité De Corse. Corse.
[57] Lagadic, L., Caquet, T., Amirad, J. O., Ramade, F. (1998): Utilisation de biomarqueurs pour la surveillance de la qualité de l'enviroimement. – Lavoisier, Paris.
[58] Langston, W. J., Spence, S. K. (1995): Biological Factors Involved in Metal Concentrations Observed in Aquatic Organisms. – In: Tessier, A., Turner, D. R. (eds.) Metal Speciation and Bioavailability in Aquatic Systems. John Wiley & Sons, London, pp. 407-478.
[59] Linde, A. R., Sánchez-Galán, S., Klein, D., Garcia-Vázquez, E., Summer, K. H. (1999): Metallothionein and heavy metals in brown trout (*Salmo trutta*) and European Eel (*Anguilla anguilla*): a comparative study. – Ecotoxicology and Environmental Safety 44: 168-173.
[60] Lombardi, P. E., Peri, S. I., Verrengia Guerrero, N. R. (2010): Trace metal levels in *Prochilodus lineatus* collected from the La Plata River, Argentina. – Environmental Monitoring and Assessment 160(1-4): 47-59. DOI: 10.1007/s10661-008-0656-0.
[61] Mattozo, V., Binelli, A., Parolini, M., Previato, M., Masiero, L., Finos, L. (2012): Biomarker responses in the clam *Ruditapes philippinarum* and contamination levels in sediments from seaward and landward sites in the Lagoon of Venice. – Ecological Indicators, (19): 191-205.
[62] Meyer, O. (2003): Testing and assessment strategies, including alternative and new approaches. – Toxicol. Lett 140-141: 21-30.
[63] Miramand, P., Guyot, T., Pigeot, J., Bustamante, P., Caurant, F., Ferchaud, R. (2000): Le cadmium dans les réseaux trophiques marins: de la source aux consommateurs. – Journal européen d'hydrologie 31(2): 127-143. DOI: 10.1051/water/20003102127.
[64] Morat, F. (2011): Influence des apports rhodaniens sur les traits d'histoire de vie de la sole commune (*Solea solea*): apports de l'analyse structurale et minéralogique des otolithes. – Thèse de doctorat. Université d'Aix Marseille II, Marseille.
[65] Morillo, J., Usero, J., Gracia, I. (2005): Biomonitoring of trace metals in a mine-polluted estuarine system (Spain). – Chémosphere 58: 1421-1430.
[66] Mormede, S., Davies, I. M. (2001): Heavy metal concentrations in commercial deep-sea fish from the Rockall Trough. – Continental Shelf Research 21(8-10): 899-916. DOI: 10.1016/S0278-4343(00)00118-7.
[67] Mouneyrac, C., Durou, C., Gillet, P., Hummel., H., Amiard, T. C. (2009): Linking Energy Metabolism, Reproduction, Abundance, and Structure of Nereis Diversicolor Populations. – In: Amiard-Triquet, C., Rainbow, P. S. (eds.) Environmental Assessment of Estuarine Ecosystems A Case Study. CRC, Boca Rarton, FL.
[68] Ogle, D., Wheeler, P., Dinno, A. (2020): Package « FSA » Title Simple Fisheries Stock Assessment Methods. – https://cran.r-project.org/.
[69] Orban, E., Di Lena, G., Nevigato, T., Casini, I., Marzetti, A., Caproni, R. (2002): Seasonal changes in meat content, condition index and chemical composition of mussels (*Mytilus galloprovincialis*) cultured in two different Italian sites. – Food Chemistry 77(1): 57-65. DOI: 10.1016/S0308-8146(01)00322-3.
[70] Pal, R., Dubey, R. K., Dubey, S. K., Singh, A. K., Nitant, A. K. (2018): Assessment of heavy metal and organic pollution in Yamuna river at Etawah district of Uttar Pradesh. – International Journal of Chemical Studies 6(1): 399-402.

http://www.aloki.hu ● ISSN 1589 1623 (Print) ● ISSN 1785 0037 (Online)
DOI: http://dx.doi.org/10.15666/aeer/1906_46414664

[71] R Core Team. (2017): The R Project for Statistical Computing. – https://www.r-project.org/.
[72] Rashida, Q., Olufemi, A., Rana., M., Rahim, A. A. (2015): Seasonal variation in occurrence of heavy metals in *Perna Viridis* from Manora Channel of Karachi, Arabian Sea. – International Journal of Marine Science 5(45): 1-13.
[73] Remili, S., Kerfouf, A. (2013): Évaluation de la qualité physico-chimique et du niveau de contamination métallique (Cd, Pb, Zn) des rejets d'eaux usées d'Oran et de Mostaganem (littoral Ouest algérien). – Physio-Géo 7: 165-182. DOI: 10.4000/physio-geo.3258.
[74] Ribeiro, C. A. O., Vollaire, Y., Sanchez, C. A., Roche, H. (2005): Bioaccumulation and the effects of organochlorine pesticides, PAH and heavy metals in the Eel (*Anguilla anguilla*) at the Camargue Nature Reserve, France. – Aquatic Toxicology (Amsterdam, Netherlands) 74(1): 53-69. DOI: 10.1016/j.aquatox.2005.04.008.
[75] Rodrigue, K. A., Yao, B., Trokourey, A., Kopoin, A. (2016): Assessment of heavy metals contamination in sediments of the Vridi Canal (Cote d'Ivoire). – Journal of Geoscience and Environment Protection 4(10): 65-73. DOI: 10.4236/gep.2016.410004.
[76] Rouabhi, Y. L. (2020): Étude comparative de la biologie et de la bioaccumulation des métaux traces chez deux Mytilidae: *Mytilus galloprovincialis* Lamarck, 1819 et *Perna perna* (Linnaeus, 1758) de la côte ouest algérienne. – Thèse de doctorat. Université de Mons, Belgique.
[77] Rouabhi, Y. L., Grosjean, P., Boutiba, Z., Rouane-Hacene, O., Richir, J. (2019): Reproductive cycle and follicle cleaning process of *Mytilus galloprovincialis* (Mollusca: Bivalvia) from a polluted coastal site in Algeria. – Invertebrate Reproduction & Development 63(4): 255-267. DOI: 10.1080/07924259.2019.1631221.
[78] Rouane-Hacene, O. (2013): Biosurveillance de la qualité des eaux côtières du littoral ccidental algérien, par le suivi des indices biologiques, de la biodisponibilité et la bioaccumulation des métaux lourds (Zn, Cu, Pb et Cd) chez la moule Mytilus galloprovincialis et l'oursin Paracentrotus lividu. – Thèse de doctorat. Département de Biologie. Université d'Oran, Oran.
[79] Rouane-Hacene, O., Boutiba, Z., Benaissa, M., Belhouari, B., Francour, P., Guibbolini, S. M., Faverney, C. R. (2018): Seasonal assessment of biological indices, bioaccumulation, and bioavailability of heavy metals in sea urchins *Paracentrotus lividus* from Algerian west coast, applied to environmental monitoring. – Environmental Science and Pollution Research 25(12): 11238-11251. DOI: 10.1007/s11356-017-8946-0.
[80] Rouidi, S., Hadjem, A., Asia, L., Mille, G., Tahar, A. (2013): Sources and distribution of hydrocarbons in surface sediments of saf-saf oued (Skikda city, northeastern Algeria). – Annals of Biological Research 4(4): 61-69.
[81] Sifi, K. (2009): Biosurveillance de la qualité des eaux du golfe d'Annaba: croissance, composition biochimique et dosage de biomarqueurs du stress environnemental chez Donax trunculus (Mollusque, Bivalve). – Thèse de Doctorat en Ecotoxicologie. Université de Badji Mokhtar, Annaba.
[82] Storelli, M. M. and Marcotrigiano, G. O. (2001): Heavy metal monitoring in fish, bivalve molluscs, water, and sediments from Varano Lagoon, Italy. – Bulletin of Environmental Contamination and Toxicology 66(3): 365-370. DOI: 10.1007/s001280014.
[83] Taleb, Z., Benghali, S., Kadour, A. S., Boutiba, Z. (2007): Monitoring the biological effects of pollution on the Algerian west coast using mussels *Mytilus galloprovincialis*. – Oceanologia 4(49).
[84] Usero, J., Izquierdo, C., Morillo, J., Gracia, I. (2004): Heavy metals in fish (*Solea vulgaris*, *Anguilla anguilla* and *Liza aurata*) from salt marshes on the southern Atlantic coast of Spain. – Environment International 29(7): 949-956. DOI: 10.1016/S0160-4120(03)00061-8.
[85] Watanabe, K., Desimone, F., Thiyagarajah, A., Hartley, W., Hindrichs, A. (2003): Fish tissue quality in the lower Mississippi River and health risks from fish consumption. –

http://www.aloki.hu ● ISSN 1589 1623 (Print) ● ISSN 1785 0037 (Online)
DOI: http://dx.doi.org/10.15666/aeer/1906_46414664

The Science of the Total Environment 302(1-3): 109-126. DOI: 10.1016/S0048-9697(02)00396-0.

[86] Wessel, N. (2010): Étude des voies de bioactivation du benzo[a]pyrène et du fluoranthène chez la sole commune (*Solea solea*): Profil métabolique et génotoxicité. – Université de Nantes, Nante.

[87] Wickham, H. (2016): ggplot2p. Chap. 2: Getting Started with ggplot2. – Springer, New York, pp. 11-31.

[88] Wickham, H., Romain, F., Kirill, M. (2020): CRAN - Package dplyr. – https://cran.r-project.org/web/packages/dplyr/index.html (accessed: 7 Sept 2020).

[89] Widmeyer, J. R., Bendell-Young, L. I. (2007): Influence of food quality and salinity on dietary cadmium availability in *Mytilus trossulus*. – Aquatic Toxicology 2(81): 144-151.

[90] Wright, K. (2018): Package « corrgram » Plot a Correlogram. – https://cran.r-project.org/.

[91] Zhang, L., Wang, W.-X. (2007): Waterborne cadmium and zinc uptake in a euryhaline teleost Acanthopagrus schlegeli acclimated to different salinities. – Aquatic Toxicology 84(2): 173-181. DOI: 10.1016/j.aquatox.2007.03.027.

http://www.aloki.hu ● ISSN 1589 1623 (Print) ● ISSN 1785 0037 (Online)
DOI: http://dx.doi.org/10.15666/aeer/1906_46414664

SPATIAL DISTRIBUTION AND INTERSPECIFIC ASSOCIATION PATTERNS BETWEEN *SHOREA ROXBURGHII* G. DON AND OTHER TREE SPECIES IN A SOUTH VIETNAM EVERGREEN FOREST

QUY, N. V.[1,2] – KANG, Y. X.[1*] – KHOT, C.[1] – HOP, N. V.[2,3] – TUAN, N. T.[2]

[1]*College of Forestry, Northwest A&F University, Yangling, Shaanxi 712100, China*

[2]*Vietnam National University of Forestry – Southern Campus, Trang Bom, Dong Nai 810000, Vietnam*

[3]*College of Forestry, Fujian A&F University, Fuzhou, Fujian 350000, China*

**Corresponding author*
e-mail: yxkang@nwsuaf.edu.cn; phone: +86-1522-930-8798

(Received 30th Jun 2021; accepted 20th Sep 2021)

Abstract. To understand the ecology and spatial distribution patterns of *Shorea roxburghii*, a vulnerable plant on the IUCN's Red List, this study was conducted in a Vietnamese evergreen forest. To collect data, a 100 m × 100 m plot was established in the Tan Phu protected forest, in South Vietnam. Relative density, relative basal area, and importance value index (IVI) were determined for each species. Individuals were categorized by juvenile (dbh < 5 cm), subadult (5 cm ≤ dbh < 10 cm) and adult (dbh ≥ 10 cm) life-history stages. We used Excel, Programita Noviembre 2018 and R to analyze data. Spatial analyses focused on overall univariate patterns, dispersion patterns, and hetero-specific association of the species. A total of 111 species was found. *Shorea roxburghii* has higher basal area, relative density, maximum dbh, IVI and lower median main neighbour. *Shorea roxburghii* has cluster distribution in the juvenile (5f) and subadult stage (5g), regular or clustered pattern in the adult stage (5h). However, the general trend is a regular pattern as the dbh increases. With the achieved results, this study contributes to the simulation method of forest species ecological characteristics, including distribution characteristics, intra and interspecific relationships in the space of *Shorea roxburghii*.
Keywords: *threatened species, life-history stages, ecological characteristics, interspecific relationships, conservation planning*

Introduction

Biodiversity management lies on the master of many ecological rules and mechanisms from local and global environmental and biotic variables. To efficiently manage and conserve wild resources, the understanding of their ecology, biology and behaviour is crucial (Cirimwami et al., 2019). Plant species communities are under the effect of deterministic factors albeit some stochastic forces cannot be ruled out (Amani and Lejoly, 2014). Fine-scale study of population successional dynamic, natural and human-driven threats acting on forest ecosystems, spatial distribution patterns… could also be important to efficiently manage plant resources worldwide (Getzin et al., 2006). The studies aiming at the understanding of spatial distribution patterns of tree species are very essential because these studies allow us to understand mechanisms of plant species competition and coexistence (Getzin et al., 2006; Guo et al., 2013), plant species diversity (Fibich et al., 2016), successional dynamics of species (Arévalo and Fernández-Palacios, 2003; Wédjangon et al., 2020), forest structure and composition change (Call et Nilsen, 2003) as well as species intraspecific and interspecific association patterns (Wédjangon et al., 2020).

http://www.aloki.hu ● ISSN 1589 1623 (Print) ● ISSN 1785 0037 (Online)
DOI: http://dx.doi.org/10.15666/aeer/1906_46654681

To understand these floristic parameters is important, for example, the competition is one of major ecological processes regulating forest communities (Nguyen et al., 2020a).

Shorea are a tropical genus counting approximately 196 species, most of them belonging to rainforest ecosystems. More than 75% of *Shorea* species (about 148 species) are present on the plant species Red List of IUCN; the majority of them are critically endangered. Despite this situation, many Shorea species are economically important timber trees (Raju et al., 2009). *Shorea roxburghii* G. Don (from the Dipterocarpaceae family) is classified as "Vulnerable" on the IUCN Red List due to many threats to which it is subjected. This species is found in the mixed dipterocarp forests in countries such as Cambodia, India, Lao Popular Democratic Republic, Peninsular Malaysia, Myanmar, Thailand and Viet Nam (Pooma et al., 2017). The species has an economic significance as it is used as valuable commercial timber and as 'white meranti' in many countries of the Southeastern Asia region. A population reduction of at least 30% in the last three centuries has resulted in overall population decline and potential future species decline. This being a consequence of agriculture practices and timber logging, these are the principal threats to the species *S. roxburghii* (Pooma et al., 2017; Mun et al., 2018).

The germination of *S. roxburghii* is not easy. In an experimental plot where many seeds were sown, Raju et al. (2011) obtained 8% of seed germination rate which also explains and increases the vulnerability of the species. By this difficulty in its germination, the plant could encounter a disequilibrium in its population structure, having many more mature individuals than sapling ones. Its adult trees may reach about 28 m in height. Although this species has a low rate of seed germination (Raju et al., 2011), seeds which succeed to germinate are supposed to have a high survival rate (Mun et al., 2018).

The species *S. roxburghii* is a fast-growing species (Mun, 2018). In good conditions, the adult individual of the species (six-year-old *S. roxburghii* with dbh and height of 23.6 cm and 16.6 m) achieve 4 cm per year for dbh and 3 m per year for height (Mun, 2018; Nguyen et al., 2020c). Being a semi-evergreen tree species, *S. roxburghii* is a brief leafless species especially during the dry season. *S. roxburghii* is usually found in combination with other species from Dipterocarpaceae, Myrtaceae and Euphorbiaceae families (Raju et al., 2011).

Assessments on the ecology and living strategies of a rare or an important species, is a way for managers, conservationists as well as planners to protect the species from many threats (Pham et al., 2020). Thus, understanding the spatial structure and association of this species *Shorea roxburghii* in its different life-history stages could help in the explanation of its ecology and population dynamics in the studied area as it was the case for other species from the northern evergreen forests of Vietnam (Nguyen et al., 2014, 2020a). The management of *S. roxburghii* in local forests and areas where it is located suggests the understanding of its ecology including the study of its population structure, dendrometric characteristics, the spatial distribution patterns and interspecific association patterns with its closer neighbours. The principal objective of this paper is to contribute to the improvement of the conservation status of *S. roxburghii* trees in South Vietnam evergreen forests. Four (4) main questions will be addressed: i) How are the population structure and dendrometric characteristics (Stem density, diameter, and importance value index) of *Shorea roxburghii* compared to its neighbours? ii) What are the spatial distribution patterns from juvenile stage to adult stage of *S. roxburghii*? iii) How does *S. roxburghii* coexist with its main neighbours tree species when comparing their spatial distribution patterns? iv) How do these interspecific association patterns change with life stages?

http://www.aloki.hu ● ISSN 1589 1623 (Print) ● ISSN 1785 0037 (Online)
DOI: http://dx.doi.org/10.15666/aeer/1906_46654681

Material and methods

Study area

This research study was conducted at Tan Phu protected forest, Dong Nai province, Southern Vietnam (11°7'36" N of latitude and 107°24'46" E of longitude). Tan Phu protected forest is a tropical moist evergreen forest, which covers 13 733.12 ha, in which forested land accounts for 89.76% (12 127.41 ha) of the total area (*Fig. 1*). This area has been reported as a species-rich ecosystem with many highly valuable plant species. The Tan Phu protected forest has a major economic role as it participates in the storing of carbon, the nourishing and protection of soil, and the water resources for Tri An hydroelectricity reservoir in the Dong Nai province. The average elevation of this area ranges from 60 to 120 m a.s.l. The annual mean temperature of the study area is 27.1 °C, while the annual mean humidity is 82% and the average annual rainfall is 2.140 mm year^{-1} (Nguyen et al., 2020b). This forest ecosystem was specifically selected to conduct the present study on the spatial distribution of *Shorea roxburghii*. The study was carried out from December 2020 to April 2021 with four field surveys at Tan Phu Protection Forest.

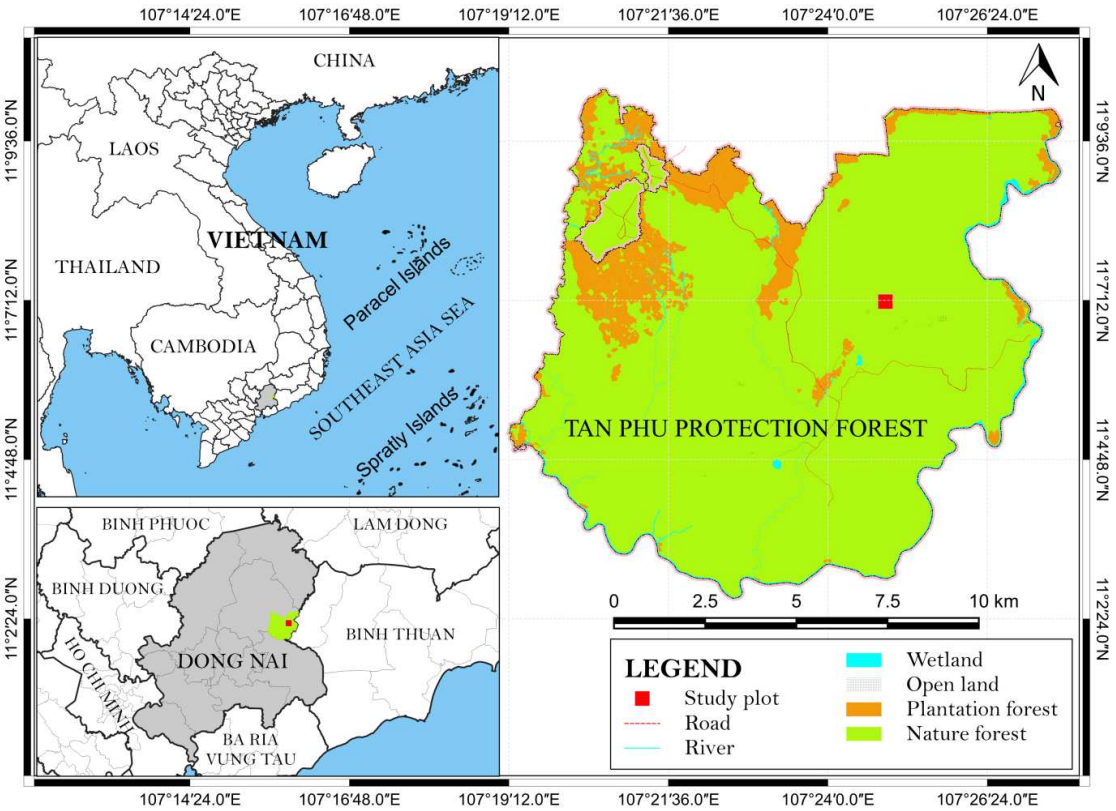

Figure 1. *Map of the study area*

Data collection

We selected a stand where *Shorea roxburghii* species distributed and predominated to establish the 1 ha (100 m × 100 m) study plot in the Tan Phu forest (11°7'7.97" N of latitude and 107°24'56.31" E of longitude). This plot continues to be broken down into

http://www.aloki.hu ● ISSN 1589 1623 (Print) ● ISSN 1785 0037 (Online)
DOI: http://dx.doi.org/10.15666/aeer/1906_46654681

100 subplots (10 m × 10 m) to facilitate the investigation, avoiding the omission of tree species. All woody plants with dbh (diameter at breast height) > 2.5 cm were tapped, numbered, tapped and measured in each plot. A wooden stick 1.3 m in length will be used to identify the location of 1.3 m, which will avoid mistakes regarding the correct measuring height. Moreover, climbers, vines, and loose bark must be removed before measuring to avoid mistakes in the measured process. The coordinates of all plots were marked by GPS meter.

All individual trees were allocated into one of the three basic life-history stages, namely, juvenile (dbh < 5 cm), subadult (5 cm ≤ dbh < 10 cm), or adult (dbh ≥ 10 cm). The identification of trees was done in the field during plot inventory. When some species were not identified in the field, voucher specimens were collected, prepared and subsequently identified by taxonomic specialists after the field work.

Data analysis

Different parameters were calculated as below:

$$\mathbf{d = \frac{n_i}{S}} \quad \text{(Eq.1)}$$

where d is the stem density of species i (the number of individual trees ha^{-1}), n_i is the total individual trees calculated for species i (the number of individual trees) and S is the study plot area (unit of area in ha) (Brower et al., 1997).

$$\mathbf{BA = \pi \times r^2 = \frac{3.142 \times dbh^2}{200^2}} \quad \text{(Eq.2)}$$

where BA is the tree basal area (m^2), r is the radius and dbh is the diameter at breast height (cm) (Brower et al., 1997)

$$\mathbf{IVI\ (\%) = \frac{RD + RBA}{2}} \quad \text{(Eq.3)}$$

where RD is the relative density and RBA is the relative basal area. The relative basal area is defined as total basal area of species i as a percent of the total basal area of all species. The ecological value of species in a forest stand is obtained by determining its importance value index (Curtis and Macintosh, 1951).

The data was analysed by using Excel 2013, Programita Noviembre 2018 and R 4.0.5 software. Excel was used to present the population structure and dendrometric characteristics. Point pattern analyses were performed using the Programita software (Wiegand and Moloney, 2004). The spatstat package implemented in R software was used for spatial distribution and interspecific association patterns (Baddeley et al., 2015). We used the spatstat package to make the distribution map of all species in the studied area, the pair-correlation function, Ripley's K functions, and L-function as it is explained by many researchers over the world (Dixon, 2002; Sotirios and Alan, 2005; Getzin et al., 2006; Bolibok, 2008; Nguyen, 2017; Wédjangon et al., 2020; Nguyen et al., 2021).

The Ripley's K-function is the expected number of points in the r distance of an arbitrary point which is divided by the intensity λ where λ is the intensity of the pattern in the study area (Ripley, 1976). According to the tree–tree distances, $g_{11}(r)$ (univariate

http://www.aloki.hu ● ISSN 1589 1623 (Print) ● ISSN 1785 0037 (Online)
DOI: http://dx.doi.org/10.15666/aeer/1906_46654681

pair-correlation function) describes the spatial distribution of trees at r radius using a standardized density. Consequently, when this parameter equals to 1 it means under complete spatial randomness, > 1 indicates aggregation and < 1 indicates regularity at distance r within trees of the pattern. The parameter $g_{12}(r)$ (bivariate pair-correlation function) was used to describe spatial association between two types of points. Function $g_{12}(r)$is the expected density of points of type 2 at r distance beginning from a randomly chosen point of type 1. Similarly to the univariate version, $g_{12}(r) = 1$ indicates independence, $g_{12}(r) < 1$ indicates repulsion and $g_{12}(r) > 1$ indicates attraction between two tree species at distance r (Nguyen et al., 2014).

Null models of random distribution, spatial independence and random labelling of trees were tested for null hypotheses related to ecological questions (Goreaud and Pelissier, 2003; Wiegand and Moloney, 2004; Illian et al., 2008). As it was done by other authors, the significant departure from the null models was evaluated using 999 Monte Carlo simulations. Approximately 99% confidence envelopes were built by 5th lowest and highest values of these simulations. Point pattern analyses were performed using the software Programita (Wiegand and Moloney, 2004). We used the null model complete spatial randomness to investigate whether the environmental heterogeneity restricted spatially the tree distribution based on the spatial distribution of all adult trees. The distribution of all adult trees at scales beyond direct tree–tree interaction should indicate environmental suitability for colonization and growth as well as allow capturing of environmental effects common to all species within the stand (Getzin et al., 2008). L-function and pair-correlation function allowed us to observe the change in tree density from both cumulative and non-cumulative perspectives at various scales. As mentioned by Wiegand et al. (2007), in plant communities, clumping at small scales generally indicated plant–plant interactions, while at large scales it showed the effect of environmental heterogeneity.

Analysis 1: Overall univariate patterns

The spatial distributions in size classes of all species, *S. roxburghii* and the remaining species were analyzed and compared using the univariate pair-correlation function. We tested the null hypothesis of a random univariate spatial distribution of trees in each life-history stage (juvenile, subadult and adult). If a random distribution of a life stage over the entire plot was confirmed, this meant that no strong interaction occurred between the trees within this size class. Comparisons of the spatial distributions of the whole plot with and without considering *S. roxburghii* allowed us to interpret the abundance effect of the species. Overall, we expected that spatial patterns of adult trees were more regular than those of earlier life-history stages, with the increase of tree size being evidence of self-thinning.

Analysis 2: Dispersion patterns of S. roxburghii

Using random labelling null model, we investigated whether or not a random structure of two labels occurred within the joined patterns. The g-functions are invariant under random thinning of the joined patterns 1 and 2 (Wiegand and Moloney, 2004). Thus, we expected $g_{12}(r) = g_{21}(r) = g_{11}(r) = g_{22}(r)$. In our case-control design, control was pattern 1 (adult trees) and case was pattern 2 (one of the early life-history stages). If the test statistic $g_{12}(r) - g_{11}(r) \approx 0$, it meant that individuals of pattern 2

http://www.aloki.hu ● ISSN 1589 1623 (Print) ● ISSN 1785 0037 (Online)
DOI: http://dx.doi.org/10.15666/aeer/1906_46654681

around individuals of pattern 1 at scale r were distributed in the same way as individuals of pattern 1 around themselves. Therefore, this would imply that both life-history stages exploit the natural resources at that scale in a similar way (Getzin et al., 2008). In addition, if the test statistic $g_{21}(r) - g_{22}(r) < < 0$, there were more individuals of cases than controls in proximity of case individuals, therefore we would expect an additional clustered pattern of cases independent of the controls (i.e. adult trees).

We used a case-control design to estimate mutual effects between early life-history stages (cases) and the adult stage (control) of *S. roxburghii*. Under the null hypothesis of random labelling, if the cases did not show any significant difference from the controls then they were a random subset of the joint pattern of both cases and controls. We expected a clustering of the cases reflecting regeneration mechanisms via independent clumping relative to the controls and, if clustering decreased with increasing size class, density-dependent thinning with increasing size class. For example, there may be an additional clustering of juveniles independently from adult trees that may be caused by canopy gaps with conditions suitable for survival and growth of juveniles. Details on spatial patterns statistics were developed and used by many authors (Bivand et al., 2008; Illian et al., 2008; Macron, 2010; Szmyt, 2014; Baddeley et al., 2015).

Analysis 3: Hetero-specific association of S. roxburghii

To describe the spatial association between adult trees of the remaining species (pattern 1) and the different life-history stages of *S. roxburghii* (pattern 2), we used the bivariate pair-correlation function. The null hypothesis of spatial independence was used to test for non- randomness in spatial arrangement between two patterns based on the assumption that the two patterns were generated by two independent processes. We kept the first pattern unchanged and then randomly shifted the second pattern relative to pattern 1 (Wiegand and Moloney, 2004). We hypothesized that *S. roxburghii* had gap-phase regeneration mode, i.e. the early stages of *S. roxburghii* were clustered independently of con-specific adults and simultaneously, they were repulsed by hetero-specific adults. Thus, we expected a negative association of pattern 2 (a life-history stage of *S. roxburghii*) relative to pattern 1 (adult trees of the remaining species).

Results

Dendrometric characteristics

In *Table 1* we compare *Shorea roxburghii*'s IVI (importance value index), stem density and basal area with its main local neighbours' tree species viz. *Aporosa planchoniana*, *Syzygium zeylanicum*, *Vatica odorata* and *Anisoptera costata*.

A total of 1371 individuals with dbh ≥ 2.5 cm were enumerated in the 1-ha study plot, 111 species were identified and belonged to 43 families while one species was not fully identified (Lauraceae). *Shorea roxburghii* (Dipterocarpaceae) was most abundant with 271 individuals ha^{-1} (*Table 1*), approximately 19.8% of the total. The four most abundant species following *Shorea roxburghii* species were *Aporosa planchoniana* (Phyllanthaceae), *Syzygium zeylanicum* (Myrtaceae), *Vatica odorata* (Dipterocarpaceae) and *Anisoptera costata* (Dipterocarpaceae), with respectively 117, 91, 62 and 61 trees ha^{-1}. The species *Shorea roxburghii* and its four main neighbours

http://www.aloki.hu ● ISSN 1589 1623 (Print) ● ISSN 1785 0037 (Online)
DOI: http://dx.doi.org/10.15666/aeer/1906_46654681

(*Aporosa planchoniana*, *Syzygium zeylanicum*, *Vatica odorata* and *Anisoptera costata*) account for 602 stems ha^{-1} in the studied area. *S. roxburghii* has more stems *per* ha than these four aforementioned species ($\chi = 253.28$, df = 4, p-value < 0.0001). This species has the higher value of total basal area, maximum dbh, important value index and lower median NN when compared to four main species in the study plot. When compared to the remaining species, the maximum dbh of Shorea roxburghii is too small (69.4 vs 106.6).

Table 1. *Dendrometric characteristics of Shorea roxburghii and its main neighbours tree species*

Species	Stem density (ha^{-1})	Basal area (m^2 ha^{-1})	Average dbh (cm)	Maximum dbh (cm)	Median NN (m)	Importance value index (%)
Shorea roxburghii	271	12.24	17.74 ± 16.17	69.4	2.93	29.48
Aporosa planchoniana	117	0.58	6.77 ± 4.22	39.5	4.82	5.20
Syzygium zeylanicum	91	1.76	12.59 ± 9.43	50.9	5.33	6.14
Vatica odorata	62	0.76	10.61 ± 6.71	39.5	6.19	3.48
Anisoptera costata	61	2.61	18.93 ± 13.79	53.5	6.03	6.40
Others (106 species)	769	13.26	10.58 ± 10.39	106.6	1.84	49.29
All	1371	31.21	12.17 ± 11.92	106.6	1.39	100

dbh: diameter at breast height; NN: nearest neighbour distance

Diameter class distribution

The comparison of diameter classes between *Shorea roxburghii* and the four neighbours species (*Aporosa planchoniana*, *Syzygium zeylanicum*, *Vatica odorata* and *Anisoptera costata*) as well as other remaining species (*Fig. 2*).

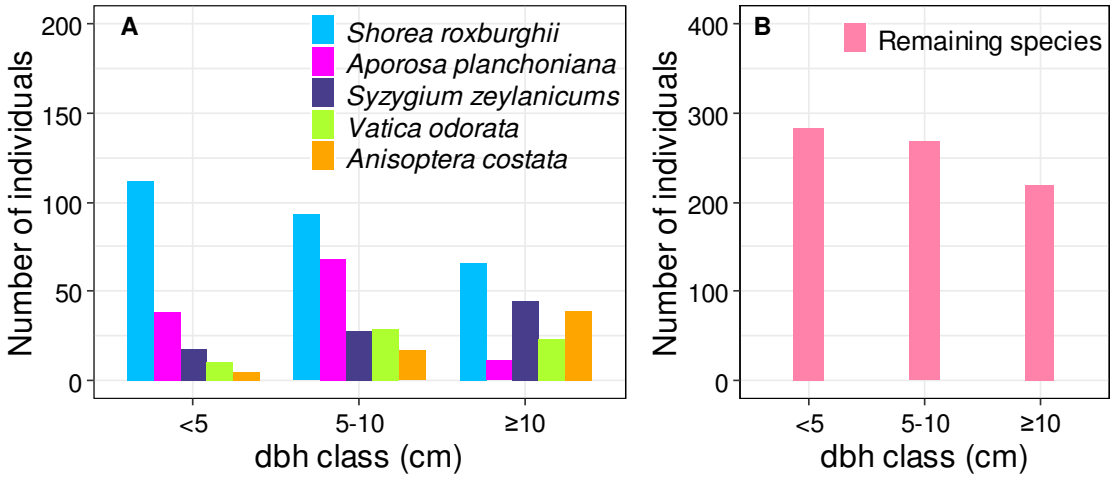

Figure 2. *Dbh class distribution of Shorea roxburghii and its main neighbours (A) and the remaining species (106 species) in the study plot (B)*

As shown in *Figure 2,* when compared to four main species in the study plot, *Shorea roxburghii* has more individuals than other species in any diameter class from juvenile

http://www.aloki.hu ● ISSN 1589 1623 (Print) ● ISSN 1785 0037 (Online)
DOI: http://dx.doi.org/10.15666/aeer/1906_46654681

tree class (dbh < 5 cm) to adult tree class (dbh ≥ 10 cm). In general, classes with many individuals are juvenile and subadult tree classes (5 cm ≤ dbh < 10 cm). This trend is also shaped by *Shorea roxburghii* with the number of juvenile and subadult individuals accounting for 75.6% of the total number of individuals of species. The dbh distribution characteristics showed that the forest status here is not stable. There will be changes at a future stage when the number of trees at small diameter classes is large.

Spatial patterns

Univariate patterns for all species

In *Figure 3,* we present the distribution map of all tree individuals according to their spatial patterns.

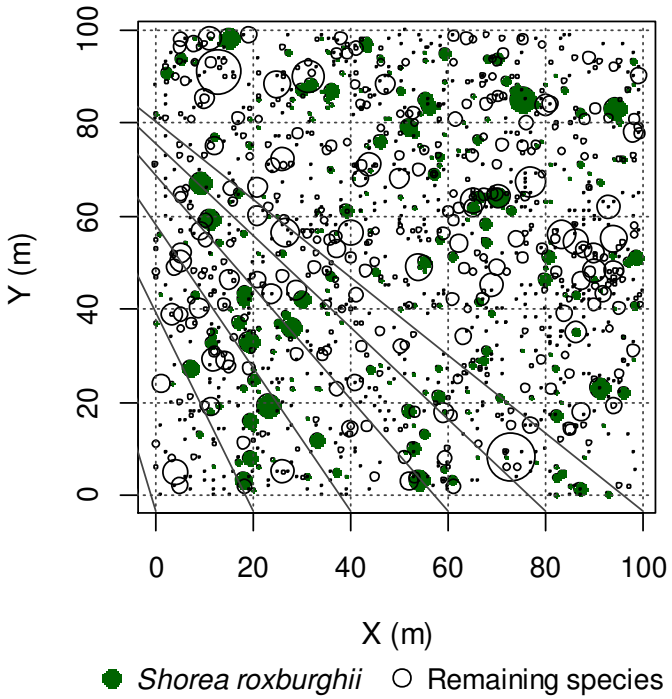

Figure 3. *Individuals' distribution map: Shorea roxburghii (darkgreen circles) and the remaining species (open circles). The size of symbols is related to the dbh of the individual*

The pattern drawn in *Figure 3* illustrates that in general case when considering all the collected species, *Shorea roxburghii* species do not have many bigger trees (in terms of the diameter at breast height: dbh) compared to other remaining species. The dbh stretches between 2.5 cm to 106.6 cm. However, the species *Shorea roxburghii* does not have very smaller individuals (according to its dbh sizes: radius of circles in *Fig. 3*) compared to the remaining species (110 species).

Figure 4 presents the univariate L-function (on the left) and pair-correlation function (on the right) for spatial distribution for all adult trees (dbh ≥ 10 cm). In the light of *Figure 4a,* according to the L-function, the drawn pattern is regular at low scale between 0 and 5 m and it becomes a clustered pattern as long as the scale increases (from 22 m and above). These patterns are shaped for all the species and individuals with ≥ 10 cm dbh. When considering *Figure 4b* (pair-correlation function), spatial

http://www.aloki.hu ● ISSN 1589 1623 (Print) ● ISSN 1785 0037 (Online)
DOI: http://dx.doi.org/10.15666/aeer/1906_46654681

pattern for all adult trees was regular distribution at scales up 2 m, and cluster distribution at a distance of 9-10 m, 12-13 m, 20-23 m.

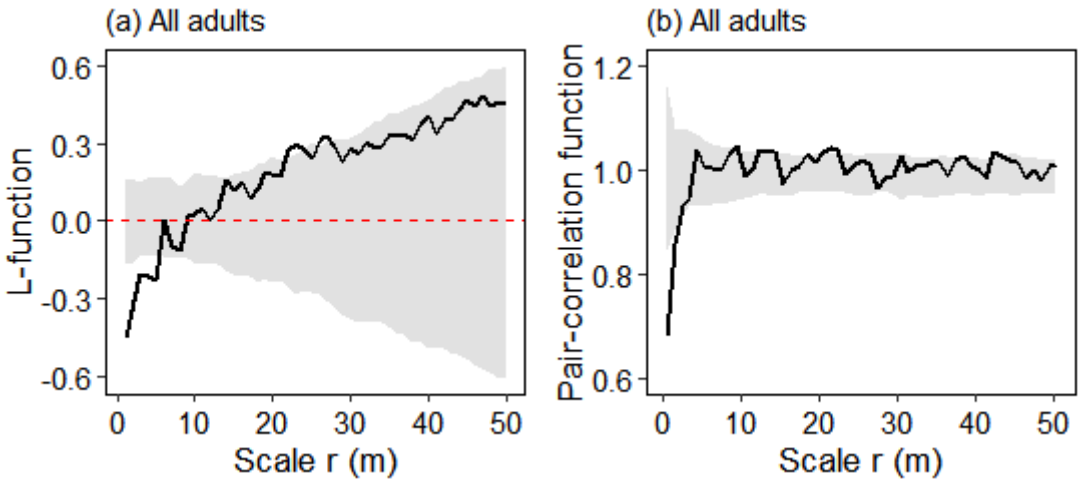

Figure 4. *Univariate L-function and pair-correlation function show spatial distributions of all adult trees (dbh ≥ 10 cm) at different scales. Dark line lying beyond the confidence envelope region (grey area) indicate significant departure from the null model of complete spatial randomness. The grey envelope region are the p = 0.05 confidence interval for Monte Carlo simulations around the red 0 dashed straight line (values < 0 indicate a regular pattern; values > 0 a clustered pattern)*

Variation of spatial distribution patterns considering all life stages

The spatial distribution patterns for juveniles, subadults and adults individuals are shown in *Figure 5*. From *Figure 5a* to *d* we present all species, from *Figure 5e* to *h* we present the spatial distribution patterns shaped by *Shorea roxburghii* at its all life stages and from *Figure 5i* to *5l* we represent the remaining species excluding *S. roxburghii.*

From *Figure 5b-d,* we noticed that concerning all species combined together, the spatial patterns of juveniles, subadults and adults passed from aggregation structure to regular pattern with the increasing of tree sizes from juveniles to adults. When gathered (juveniles + subadults + adults) in *Figure 5a,* regular patterns of all trees at scales up to 2 m is shaped. On one hand, the cluster distribution at a juveniles stage and subadults is partly due to the size of a small tree, thus competition between trees is not clear. On the other hand, the environment in the study plot is heterogeneous through the testing of g and L functions. When considering only the case of Shorea roxburghii species, the juveniles + subadults + adults of this species showed a general clustered spatial distribution pattern at scales up to 26 m (*Fig. 5e*). Shorea roxburghii has cluster distribution type in the juvenile (*Fig. 5f*) and subadult stage (*Fig. 5g*), regular pattern or clustered pattern in the adults stage (*Fig. 5h*). However, the general trend is regular pattern as the dbh of trees increases. Spatial distribution of all Shorea roxburghii tree (*Fig. 5e*) shows that it has cluster distribution at the distance up to 25 m. This is explained by its strong particle dispersion ability. Considering the ecological characteristics, the Shorea roxburghii tree has a winged fruit, this is an advantage in dispersing. There is no competition at the juveniles stage (*Fig. 5f*) and the subadults (*Fig. 5g*), but there is competition in the adults with a scales of 0-5 m (*Fig. 5h*).

http://www.aloki.hu ● ISSN 1589 1623 (Print) ● ISSN 1785 0037 (Online)
DOI: http://dx.doi.org/10.15666/aeer/1906_46654681

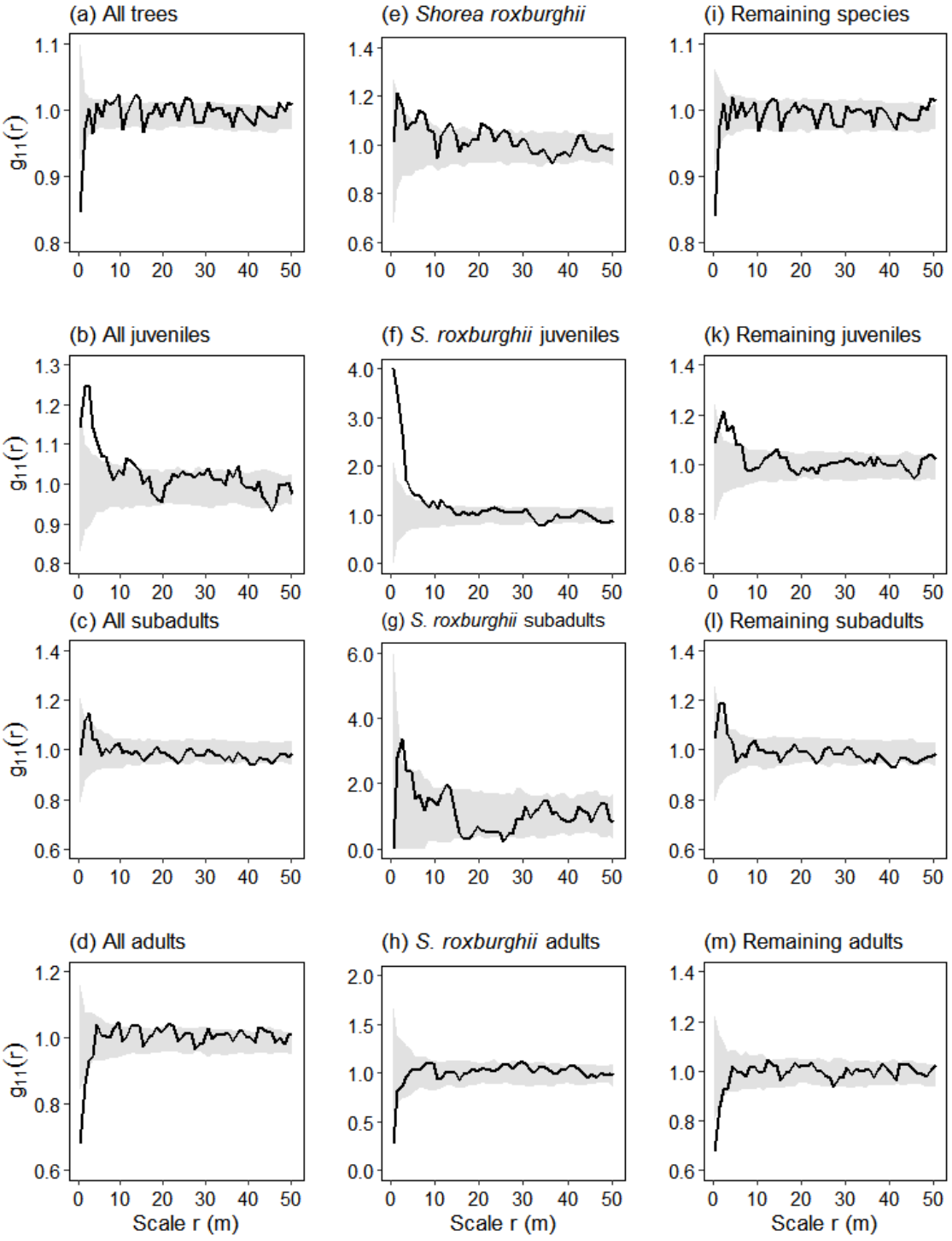

Figure 5. *Spatial distributions of all individuals and life-history stages of all species (a–d), Shorea roxburghii (e–h) and remaining species (i–l) are shown by the univariate pair-correlation function* $g_{11}(r)$

Dispersion patterns of the studied species Shorea roxburghii

In *Figure 6* we compare the spatial distribution patterns of adults and earlier life stages (juveniles and subadults) of the species *Shorea roxburghii* in the study area.

http://www.aloki.hu ● ISSN 1589 1623 (Print) ● ISSN 1785 0037 (Online)
DOI: http://dx.doi.org/10.15666/aeer/1906_46654681

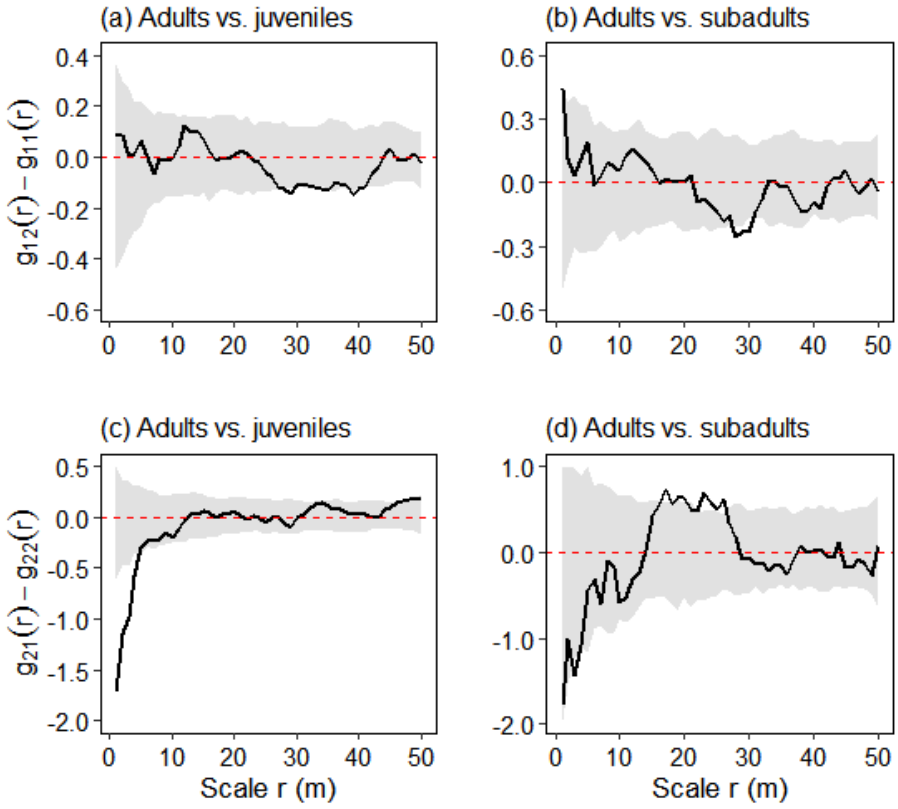

Figure 6. *Test statistics* $g_{11}(r) - g_{12}(r)$ *and* $g_{21}(r) - g_{22}(r)$ *showing spatial associations between adult stage and two early stages in the life-history of Shorea roxburghii*

According to the statistic test $g_{12}(r) - g_{11}(r)$ significant difference was found when comparing distributions of adult individuals of *Shorea roxburghii* and its juveniles (*Fig. 6a*) and its subadults (*Fig. 6b*). The statistic test $g_{12}(r) - g_{11}(r) < 0$ indicates a higher density of adults trees than juveniles around it at a scales of 29-30 m (*Fig. 6a*), and a density of mature trees is higher than a subadults at a scales of 28-30 m (*Fig. 6b*).

Test statistic $g_{21}(r) - g_{22}(r)$ showed significant differences from the null model of random for juveniles (*Fig. 6c*) but not for subadults (*Fig. 6d*). This test shows that juveniles have an independent cluster distribution compared to adults trees at a distance of 0-5 m. Results showed that there were strong additional clumping which were independent of adult individuals at earlier scales up to 5 m in the case of juveniles. For subadults, at scales 16 m, $g_{21}(r) - g_{22}(r) > 0$ meant that there were significantly less subadults surrounding adults compared with the adult–adult relationship (*Fig. 6d*).

Heterospecific association of Shorea roxburghii

The heterospecific association of *Shorea roxburghii* following its life stages is presented in *Figure 7.*

The juveniles individuals of *Shorea roxburghii* were independent of the heterospecific adults (*Fig. 7a*). However, the subadults of *S. roxburghii* were marginally repulsed by heterospecific adults at a scale of 27 to 28 m (*Fig. 7b*). Likewise, adults individuals were also attracted by heterospecific adults at a scale of 10-29 m (*Fig. 7c*). There is competition for different species at the scale of 0-5 m. Thus, there is strong

http://www.aloki.hu ● ISSN 1589 1623 (Print) ● ISSN 1785 0037 (Online)
DOI: http://dx.doi.org/10.15666/aeer/1906_46654681

evidence of interspecific repulsion existing between subadults and adults of *Shorea roxburghii* and its neighbours.

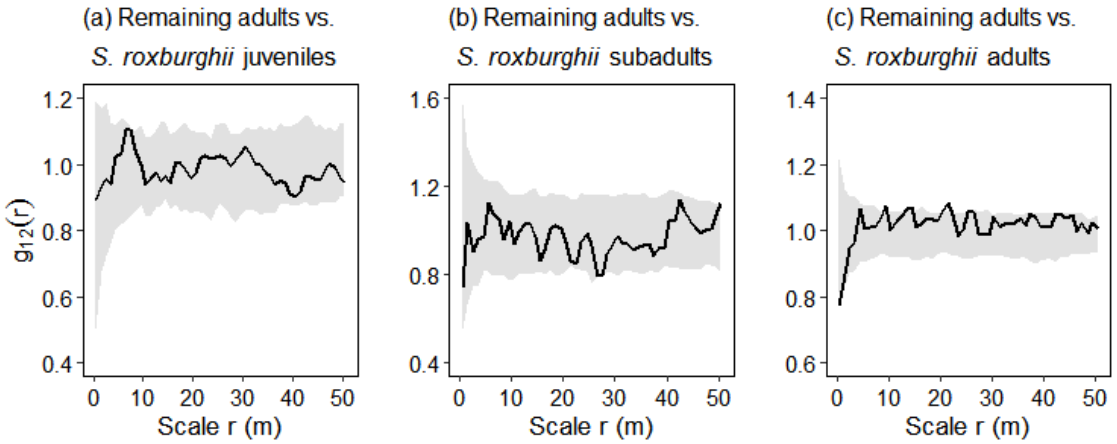

Figure 7. *The bivariate pair-correlation functions show association patterns between adults of remaining species and different life stages of Shorea roxburghii*

Discussion

Dendrometric characteristics and diameter class distribution

In the studied area, we found that the species *Shorea roxburghii* has the higher value of basal area, maximum dbh, important value index and lower median NN (nearest neighbour distance) when compared to four other dominant species (*Aporosa planchoniana*, *Syzygium zeylanicum*, *Vatica odorata* and *Anisoptera costata*). When it is compared to the remaining 106 species (except for four other dominant species), its maximum dbh value is very small. This can be explained by the fact that the species is threatened and logged as commercial timber and "white meranti" in many southern Asia countries where it is located including in South Vietnam (Pooma et al., 2017; Mun et al., 2018). Logically, when people exploit a species for timber of plank production, they mainly focus their attention on individuals with bigger diameter than smaller ones. This could also be an explanation of why the species does not have many representatives in high diameter classes above 50 cm of dbh (*Fig. 2*). As found by Dupuy (1998) in tropical Africa forests and by Hoang (2010) and Pham et al. (2020) in Vietnam evergreen forests, threatened species are usually represented by smaller trees (in terms of dbh) in forest stands where they occur. But also, the reverse J-shaped distribution size structure of *S. roxburghii* (presence of many individuals in lower diameter classes) can suggest continuous population regeneration and environmental suitability for establishment and survival of seedlings (Dupuy, 1998; Nguyen et al., 2014). Thus, in Dipterocarpaceae forests where *S. roxburghii* is a dominant tree species, the similarity coefficient of value between mature individuals and regenerating individuals is high, 96.4% for the study conducted by Long et al. (2018) in the Tan Phu area of Dong Nai Province in Vietnam.

Spatial patterns of Shorea roxburghii

In the light of *Figure 4a, b* there exists strong competition within all adults individuals at scales ≤ 2 m. When the aggregation of individuals is observed at scales smaller than 20 m, it means that there is seed dispersal limitation or seed facilitation

http://www.aloki.hu ● ISSN 1589 1623 (Print) ● ISSN 1785 0037 (Online)
DOI: http://dx.doi.org/10.15666/aeer/1906_46654681

(Hubbell et al., 2001; Nguyen et al., 2014). At larger scales, this aggregation may be obscured by the environmental heterogeneity (Nguyen et al., 2014) because local environment plays an important role in the spatial distribution patterns of tree species (John et al., 2007). One of possible explanations for the aggregated patterns of most species is the effect of dispersal facilized by the ability of pioneer species to establish their seed in the forest stand as they are to the proximity of parent trees (Dalling et al., 2002; Fibich et al., 2016).

The different life-history stages of *Shorea roxburghii* do not have the same spatial distribution patterns (*Fig. 5f-h*). Its juveniles and subadults showed clustered spatial distribution patterns at lower scales (*Fig. 5f, g*) while its adults showed regular or clustered patterns. The adults individuals were overdispersed at 1 m scale and random between 1-50 m scale. These different spatial patterns in the life-history of the species suggest dynamic changes in its population and existence of self-thinning process resulting from competition for natural resources (Nguyen et al., 2014) and confirm the fact that habitat heterogeneity can cause individual aggregation (Wang et al., 2020). This can be explained by the species' light requirement at different stages (Nguyen et al., 2014; Cirimwami et al., 2017), its successional dynamics (Wédjangon et al., 2020), its crown spatial patterns (Blanchard et al., 2016) and the intensity of competition at each level of growth (Getzin et al., 2006; Guo et al., 2013). The density of *Shorea roxburghii* has a cluster distribution and decreases as the distance and age of the tree increases (dbh increases, from juveniles to subadults, adults) and changes to evenly distributed in adults trees. This is a clear sign of competition for nutrient space between plants and plants during growth.

The cluster pattern distribution of forest tree individuals at distances less than 20 m which is often interpreted as seed dispersal limitation or facilitation (Hubbell et al., 2001; Uriarte et al., 2004) while at larger scales, it may be obscured by environmental heterogeneity, e.g. rock outcrops, slope or soil nutrients (Harms et al., 2001; John et al., 2007). The test results of the univariate L-function and the pair-correlation function showed that the environmental heterogeneity played a big role in the structuration of the vegetation in the study plot. Environmental heterogeneity in the same study plot in tropical rainforest subject is a fairly common phenomenon, it has been proven in many previously published studies, with cumulative density of all adult trees changed from regularity or random distribution to cluster distribution at distances over 20 m (Wiegand et al., 2007).

In the spatial relationship between the life stages of forest trees, two important mechanisms, density-dependent mortality and gap-phase regeneration mode regulate the relationships of the life stages (Nguyen et al., 2014). *Figure 6a* and *b* also show that the density of subadults of *S. roxburghii* and juveniles around the adults is lower than that of the adult's trees around it, the juveniles and subadults are distributed around the adults with similar density. This may be due to the density-dependent mortality rate, in particular governed by natural thinning that resulted in a decrease in the density around the parent plant (Wright, 2002). In addition, juveniles have an independent cluster distribution from adults trees (larger diameter size). Another mechanism could be the gap-phase regeneration mode (Hamill and Wright, 1986; Condit et al., 1992), however, considering the ecological characteristics of the species, previous studies on regeneration of *S. roxburghii* can see that it is a shade tolerant plant, so when it is young it needs to live under the mother tree or larger trees. So there is no gap-phase regeneration.

http://www.aloki.hu ● ISSN 1589 1623 (Print) ● ISSN 1785 0037 (Online)
DOI: http://dx.doi.org/10.15666/aeer/1906_46654681

Conclusion

This study conducted in rich southern evergreen forests of Vietnam aimed the understanding of population structure and spatial distribution patterns of *Shorea roxburghii*. This species is a Dipterocarpaceae threatened species from south Asia, classified as "Vulnerable" on the IUCN red list.

In the broadleaf secondary forest in the study area, *Shorea roxburghii* is a shade tolerant tree species living in the lower layer. Its dbh size is small but densely populated, and with 4 dominant tree species, it can form the dominant tree species group. In terms of the IVI index, it accounts for the highest percentage, making it an important plant species in the stand. *Shorea roxburghii* has both regular patterns and a cluster pattern at small distances, but the general trend is to have cluster type distribution at a scale up to 25 m, the density decreases as the distance increases. This species has a cluster type distribution in the juveniles tree and subadults tree stage, evenly distributed or clustered in the adults tree stage. However, the general trend is evenly distributed as the age of the trees increases. *Shorea roxburghii* juveniles were found to have a cluster distribution independent of mature trees at a distance less than 10 m.

For this species (*Shorea roxburghii*), there is competition for different species and the same species at the scale of 0-5 m in adult stage. In the juveniles and subadults stage, the competition is not clear because the size of the small trees and the environment in the study plot is heterogeneous. Natural thinning and strong dispersal (winged fruit) are the mechanisms that govern the spatial distribution pattern of *Shorea roxburghii* species. In addition, the competition for the same species at the distance of 0-5 m of mature trees should be considered when planting pure forest with this tree to expand the area of distribution of tree species. These findings are key resource for the conservation of this species and the forests in which it occurs.

We recommend carrying out study to the influence of environmental factors (soil, altitude, topography, and climate) on the distribution characteristics of *Shorea roxburghii* species in future studies; on that basis the ecological information about this plant will be more complete.

Acknowledgement. The authors would like to thank Prof. Dr. Kang Yong Yong-Xiang, Dr. Nguyen Hong Hai, Dr. Nguyen Thanh Tuan, and the research team of Northwest A&F University, China for their valuable assistance during the preparation of the manuscript.

REFERENCES

[1] Amani, I. A. C., Lejoly, J. (2014): Floristic patterns and impact of edaphic heterogeneity on species assemblages within woody forests layers in semi-deciduous forests from the Congo Basin. – Greener Journal of Agronomy, Forestry and Horticulture 2(3): 62.

[2] Arévalo, J. R., Fernández-Palacios, J. M. (2003): Spatial patterns of tree and juveniles in a laurel forest of Tenerife, Canary Islands. – Plant Ecology 165(1): 0.

[3] Baddeley, A., Rubak, E., Turner, R. (2015): Spatial Point Patterns: Methodology and Applications with R. – Chapman and Hall/CRC Press, London.

[4] Bivand, R. S., Pebesma, E. J., Gómez-Rubio, V. (2008): Applied Spatial Data Analysis with R. – Springer Science. Business Media, LLC, Berlin.

[5] Blanchard, E., Birnbaum, P., Ibanez, T., Boutreux, T., Antin, C., Ploton, P., Vincent, G., Pouteau, R., Vendroit, H., Hequet, V., Barbier, N., Droissart, V., Sonké, B., Texier, N.,

http://www.aloki.hu ● ISSN 1589 1623 (Print) ● ISSN 1785 0037 (Online)
DOI: http://dx.doi.org/10.15666/aeer/1906_46654681

Kamdem, N. G., Zebaze, D., Libalah, M., Couteron, P. (2016): Contrasted allometries between stem diameter, crown area, and tree height in five tropical biogeographic areas. – Trees 30: 195968.

[6] Bolibok, L. (2008): Limitations of Ripley's K(t) function use in the analysis of spatial patterns of tree stands with heterogeneous structure. – Acta Sci. Pol. Silv. Colendar. Rat. Ind. Lignar. 7(1).

[7] Brower, J. E., Jerold, H. Z., Von Ende, C. (1997): Field and Laboratory Methods for General Ecology. – McGraw-Hill Education, New York.

[8] Call, L. J., Nilsen, E. T. (2003): Analysis of spatial association between the invasive Tree-of-Heaven (Ailanthus altissima) and the Native Black Locust (Robinia pseudoacacia). – The American Midland Naturalist 1(150): 1-14.

[9] Cirimwami, L., Gourlet-Fleury, S., Gonmadje, C., Kahindo, J-M., Doumenge, C., Gonmadje, C., Amani, C. (2017): Does the altitude affect the stability of montane forests? A study in the Kahuzi-Biega National Park (Democratic Republic of the Congo). – Applied Ecology and Environmental Research 15(4): 169713.

[10] Cirimwami, L., Kahindo, J-M., Doumenge, C., Amani, C. (2019): The effect of elevation on species richness in tropical forests depends on the considered lifeform: results from an East African mountain forest. – Tropical Ecology 60(4): 4784.

[11] Condit, R., Hubbell, S. P., Lafrankie, J. V., Sukumar, R., Manokaran, N., Foster, N. B., Ashton, P. S. (1996): Species-area and species-individual relationships for tropical trees: a comparison of three 50-ha plots. – Journal of Ecology 84(4): 549-562.

[12] Curtis, J. T., Macintosh, R. P. (1951): An upland forest continuum in the prairie - forest border region of Wisconsin. – Ecology 32(3): 4796.

[13] Dalling, J. W., Muller-Landau, H. C., Wright, S. J., Hubbell, S. P. (2002): Role of dispersal in the recruitment limitation of neotropical pioneer species. – Journal of Ecology 90(4): 714-727.

[14] Dixon, P. M. (2002): Ripley's K function. – Encyclopedia of Environmetrics 3: 1796-1803.

[15] Dupuy, B. (1998): Bases pour une sylviculture en forêt dense tropicale humide africaine. – Série FORAFRI Document 4, CIRAD-Forêt.

[16] Fibich, P., Lepš, J., Novotný, V., Klimeš, P., Těšitel, J., Molem, K., Damas, K., Weiblen, G. (2016): Spatial patterns of tree species distribution in New Guinea primary and secondary lowland rain forest. – Journal of Vegetation Sciences 27(2): 3239.

[17] Getzin, S., Dean, C., He, F., Trofymow, J. A., Wiegand, K., Wiegand, T. (2006): Spatial patterns and competition of tree species in a Douglas-fir chronosequence on Vancouver Island. – Ecography 29(5): 6782.

[18] Getzin, S., Wiegand, T., Wiegand, K., He, F. (2008): Heterogeneity influences spatial patterns and demographics in forest stands. – Journal of Ecology 96: 8020.

[19] Guo, Y., Lu, J., Franklin, S. B., Wang, Q., Xu, Y., Zhang, K., Bao, D., Qiao, X., Huang, H., Lu, Z., Jiang, M. (2013): Spatial distribution of tree species in a species-rich subtropical mountain forest in Central China. – Can. J. For. Res. 43(9): 8235.

[20] Hamil, D. N., Wright, S. J. (1986): Testing the dispersion of juveniles relative to adults: a new analytic method. – Ecology 67(4): 9557.

[21] Harms, E. K., Condit, R., Hubbell, S. P., Foster, R. B. (2001): Habitat associations of trees and shrubs in a 50-ha neotropical forest plot. – Journal of Ecology 89: 9459.

[22] Hoang, V. H. (2010): Evaluation of the Conservation Status and Risks for Some Endangered Plant Species in Ba Be National Park, Backan Province, Vietnam. – University of Technology, Sydney.

[23] Hubbell, S. P. (2001): The Unified Neutral Theory of Biodiversity and Biogeography. – Princeton University Press, United Kingdom.

[24] Illian, J., Penttinen, A., Stoyan, H., Stoyan, D. (2008): Statistical Analysis and Modelling of Spatial Point Patterns. – John Wiley and Sons, Chichester.

http://www.aloki.hu ● ISSN 1589 1623 (Print) ● ISSN 1785 0037 (Online)
DOI: http://dx.doi.org/10.15666/aeer/1906_46654681

[25] John, R., Dalling, J. W., Harms, K. E., Yavitt, J. B., Stallard, R. F., Mirabello, M., Hubbell, S. P., Valencia, R., Navarrete, H., Vallejo, M., Foster, R. (2007): Soil nutrients influence spatial distributions of tropical tree species. – PNAS 104(3): 8669.
[26] Long, L. V., Tuyen, P. T., Toan, L. B., Quy, P. X. (2018): Natural regeneration characteristics of tropical evergreen moist close forest in Tan Phu area of Dong Nai Province. – Journal of Forestry Sciences and Technology 5(11): 32.
[27] Marcon, E. (2010): Statistiques spatiales avec applications à l'écologie et à l'économie. – Biodiversité et Ecologie. Ph.D. Thesis, AgroParisTech, Paris.
[28] Mun, H. W. (2018): Assessment of growth and biomass of *Shorea roxburghii* G. Don in selected areas of peninsular Malaysia. – International Journal of Agriculture, Forestry and Plantation 7: 45.
[29] Nguyen, H. H. (2017): Methods of spatial point pattern analysis applied in forest ecology. – National Scientific Conference on Ecology and Biological Resources 7: 160617.
[30] Nguyen, H., Wiegand, K., Getzin, S. (2014): Spatial patterns and demographics of Streblus macrophyllus in a tropical evergreen forest, Vietnam. – Journal of Tropical Forest Science 26(3): 3019.
[31] Nguyen, H. H., Erfanifard, Y., Bao, T. Q., Petritan, A. M., Mai, T. H., Petritan, I. C. (2020a): Phylogenetic community and rearest neighbor structure of disturbed tropical rain forests encroached by Streblus macrophyllus. – Forests 11(7): 722.
[32] Nguyen, V. H., Le Hong, V., Tran, Q. B., Nguyen, T. L. (2020b): Woody plant diversity and aboveground carbon stocks of (*Shorea roxburghii*) dominant forests in Tan Phu, Dong Nai province. – Journal of Forestry Science and Technology 10: 66-76.
[33] Nguyen, T. T., Tran, T. C., Tran, Q. B. (2020c): Individual tree diameter increment and mortality models for medium and rich forest in Dong Nai Culture and Nature Reserve. – Vietnam Journal of Forest Science 3: 73-86.
[34] Nguyen, H. H., Erfanifard, Y., Bui, V. B., Mai, T. H., Petritan, A. M., Petritan, I. C. (2021): Topographic effects on the spatial species associations in diverse heterogeneous tropical evergreen forests. – Sustainability 13(5): 2468.
[35] Pham, V. V., Ammer, C., Annighöfer, P. (2020): The presence of IUCN Red list tree species in dependence of site characteristics in the Vietnamese Cat Ba National Park. – Sustanability12(3): 104.
[36] Pooma, R., Newman, M., Barstow, M. (2017): *Shorea roxburghii*. – The IUCN Red List of Threatened Species 2017.
[37] Raju, A. J. S., Ramana, K. V., Jonathan, K. H. (2009): Anemophily, anemochory, seed predation and seedling ecology of Shorea tumbuggaia Roxb. (Dipterocarpaceae), an endemic and globally endangered red listed semi-evergreen tree species. – Current Science 96(6): 827-833.
[38] Raju, A. J. S., Ramana, K. V., Chandra, P. H. (2011): Reproductive ecology of *Shorea roxburghii* G. Don (Dipterocarpaceae), an endangered semievergreen tree species of peninsular India. – Journal of Threatened Taxa 3(9): 206070.
[39] Ripley, B. D. (1976): The second-order analysis of stationary point processes. – Journal of Applied Probability 13(2): 255-266.
[40] Sotirios, K., Alan, B. G. (2005): Spatial relationships between tree species and gap characteristics in broad-leaved deciduous woodland. – Journal of Vegetation Science 16(5): 5896.
[41] Szmyt, J. (2014): Spatial statistics in ecological analysis: from indices to functions. – Silva Fennica 48(1): 31.
[42] Uriarte, M., Condit, R., Canham, C. D., Hubbell. S. P. (2004): A spatially explicit model of sapling growth in a tropical forest: does the identity of neighbours matter? – Journal of Ecology 92(2): 3460.
[43] Wang, X., Jiang, C., Jia, C., Tai, Y., Hou, Y., Zhang, W. (2020): A new digital method of data collection for spatial point pattern analysis in grassland communities. – Ecology and Evolution 10(14): 785860.

http://www.aloki.hu ● ISSN 1589 1623 (Print) ● ISSN 1785 0037 (Online)
DOI: http://dx.doi.org/10.15666/aeer/1906_46654681

[44] Wédjangon, A. A., Kuiga, N. B. S., Houêtchétgnon, T., Ouinsavi, C. A. I. N. (2020): Spatial ditribution and interspecific association patterns between Mansonia altissima A. Chev., Ceiba pentandra (L.) Gaertn and Triplochiton scleroxylon K. Schum. in a moist semi-deciduous forest. – Annals of Forest Sciences 77(1): 6.
[45] Wiegand, T., Moloney, K. A. (2004): Rings, circles, and null models for point pattern analysis in ecology. – Oikos 104(2): 2029.
[46] Wiegand, T., Gunatilleke, C. V. S., Gunatilleke, I. A. U. N. (2007): Species associations in a heterogeneous Sri Lankan dipterocarp forest. – The American Naturalist 170(4): 75.
[47] Wright, S. J. (2002): Plant diversity in tropical forests: a review of mechanisms of species coexistence. – Oecologia 130(1): 1-14.

http://www.aloki.hu ● ISSN 1589 1623 (Print) ● ISSN 1785 0037 (Online)
DOI: http://dx.doi.org/10.15666/aeer/1906_46654681

FISH FUNCTIONAL GROUP DIVERSITY AND ANALYSIS OF INFLUENCING FACTORS IN THE MULING RIVER BASIN IN NORTHEAST CHINA

SUN, X.[1,2#] – CHAI, Y. H.[3#] – WANG, Y.[1,2] – YU, H. X.[4] – CHAI, F. Y.[5*] – WANG, W.[1,2*]

[1]*College of Fisheries and Life Science, Dalian Ocean University, Dalian 116023, China*

[2]*Key Laboratory of Applied Biology and aquaculture of northern fishes in Liaoning Province, Dalian 116023, China*

[3]*Aulin College, Northeast Forestry University, Harbin 150020, China*

[4]*College of Wildlife and Protected Area, Northeast Forestry University, Harbin 150040, China*

[5]*School of Management, Heilongjiang University of Science and Technology, Harbin 150020, China*

[#]*Co-first authors*
These authors contributed to the work equally.

[*]*Corresponding authors*
e-mail: chaifangying@126.com (Chai, F. Y.); wangwei@dlou.edu.cn (Wang, W.)

(Received 6th Jul 2021; accepted 20th Sep 2021)

Abstract. In order to understand fish fauna in the Muling river in Northeast China, an experiment was carried out in May, July and October 2015. This survey set up 28 sampling sites where 348 fishes were identified in total belonging to 4 orders, 5 families, and 22 species. The dominant species were *Cobitis granoci, Rostrogobio amurensisi, Cobitis lutheri, Pseudorasbora parva, Phoxinus lagowskii, Perccottus glehni, Carassius auratus gibelio, Aristichthys nobilis* in the Muling River basin. The diversity of species was analysed by the Shannon-Weaver and Pielou methods, which indicated few differences between sampling site of these two methods. Muling River showed an average Shannon-Weaver index of 1.97, an average Pielou index of 0.36, and an average Maralef index of 1.16. According to feeding habits, catchment fishes of the Muling river were divided into 7 functional groups: herbivores, insectivores, phytoplanktivore, zooplanktivores, benthivores, omnivores, piscivores. Canonical Correlation Analysis (CCA) found that, water environmental factors influencing fish functional groups varied between different seasons. In spring, the factors were total nitrogen (TN), oxidation-reduction potential (ORP), pH value (pH), water transparency (SD), conductivity (COND). In summer, the factors were total nitrogen (TN), oxidation-reduction potential (ORP), pH value (pH), dissolved iron (Fe), water temperature (WT), total dissolved solids (TD). In autumn, the factors were the same as that of in summer.
Keywords: *fish, freshwater, wetland, correlation, environmental variables*

Introduction

Fish has an important position in the aquatic ecosystem, which distributed in various water bodies around the world (Holmlund and Hammer, 1999). Fish is the most biologically diverse group of vertebrates, accounting for more than half of the number of vertebrate species on Earth, and 40% of fish live in freshwater. There are nearly 1,000 species of freshwater fishes in China, which are widely distributed in major water systems in our country. In the process of the evolution of various organisms, fish have gradually acquired more and more extensive habitats, which promotes them to have a

http://www.aloki.hu ● ISSN 1589 1623 (Print) ● ISSN1785 0037 (Online)
DOI: http://dx.doi.org/10.15666/aeer/1906_46834697

variety of physiological and ecological characteristics. Since the 1990s, countries around the world have gradually realized the importance of fish resource management. The continuous development of high technology such as fish investigation and monitoring, sustainable development and utilization of fish resources, and fishery product processing has improved water protection. The environment and fish species diversity have been recognized by major countries with fisheries (Wang et al., 2006). Moreover, because of the important economic position of fisheries in human society, when fish ecology research came out, it has achieved rapid development. Its scientific research results can not only provide scientific basis for water environment assessment and fish resource development and utilization, but also provide scientific basis for fish protection and aquatic product production.

Humans can use the characteristics of fish to adapt to water bodies and regard them as a type of indicator organisms when evaluating the health of river ecosystems (Karr, 1981). It is used to diagnose the degree of accumulation of chemical, physical and biological pollutants in the water body, thereby reflecting the quality of the water environment (Simon, 1999). In addition, as a tool for evaluating and monitoring water quality, fish has many unique conveniences. With a long life history, acceptance and long-term effects of biological conditions, it has a wider habitat range compared with smaller plankton and benthic animals, thus possesses a certain versatility. As an evaluation element, fish have larger biological individuals, which are more intuitive and easy to identify and identify during monitoring, and fish classification work is relatively complete, and the relevant scientific research results are accumulated, which makes the fish easy to capture and the data easy to measure and analyze (Xia et al., 2009). Biodiversity not only reflects the diversification and variability of organisms and the complexity of the ecological conditions of species habitats, it also reflects the diversity of biological organisms on Earth (Ma, 1994). Fish are important indicators of the water environment. Fish occupy an important position in the ecosystem. In recent years, human activities have had a huge impact on fish diversity, leading to the decline of species diversity, endangerment and extinction of species, miniaturization of fish, and changes to the structure and function of aquatic ecosystems (Chen, 1990; Sarkar et al., 2012). Regarding the above issues related to fish diversity, humans use different targeted survey methods to monitor different water bodies. The "Handbook of Biodiversity Methods" (Giles et al., 2005) has detailed and specific descriptions of fish monitoring methods. These methods include traditional fishing gear, such as gill nets (Yang, 2012), trawl nets (Mao et al., 2016), various trapping nets including fixed nets (Shi et al., 2015), ground cages, shrimp cages (Xiao et al., 2015), etc., as well as modern fish hunters. Under different water environment conditions, hydroacoustic equipment such as instrument can be used as a reference when used for different purposes (Liu et al., 2016). The rational use of fishing tools can not only improve the ecological environment and contribute to scientific research, but also promote the harmonious coexistence of humans and organisms (Chen, 2014).

In the history of the Muling River basin, fishery resources were very rich. The ancestors mostly lived on fishing. However, due to overfishing and environmental pollution and other factors, fishery resources have declined sharply in the past 30 years. With the intensification of human activities and the construction of water conservancy projects, the ecological environment of Muling River has undergone tremendous changes, and the structure of fish communities has also changed. In this study, by monitoring the fish diversity of the Muling River basin and measuring the water quality,

http://www.aloki.hu ● ISSN 1589 1623 (Print) ● ISSN1785 0037 (Online)
DOI: http://dx.doi.org/10.15666/aeer/1906_46834697

the status of fish resources was investigated and monitored, and the factors affecting the diversity of fish species were found. The evaluation provides a scientific basis for the restoration of fish diversity and watershed management in the Muling River bBasin.

Materials and methods

Study area

Muling River has a total length of 834 km and a drainage area of 18427 km^2. It is the largest tributary on the left bank of the Wusuli River, a border river in the northeast of China. The Muling River Basin belongs to the temperate semi-humid monsoon climate. The annual average temperature is 3.2℃, the average temperature in January is -19℃, the average temperature in July is 21.3℃, the average annual precipitation is 532 mm, and the frost-free period is 148 d. The Muling River is a mountainous river with a total river drop of 699 m and an average annual runoff of 2.35 billion m^3. It is rich in hydropower resources.

The Muling River Basin is divided into upper, middle and lower reaches according to geographical location. Most areas in the upper reaches of the mountain are mountainous and have a temperate continental climate. The winter is not only long and cold, but the summer is short but dry. The annual average rainfall is 531 mm. The rainfall is mostly in July, August and September. Floods mostly occur in late June and July and August. The upstream is not only the center of heavy rain, but also the source of flooding. The middle reaches are located in Mishan City, with the Wanda Mountains in the north, the Changbai Mountains in the south, and the Muling River alluvial plain in the middle, with Xingkai Lake, which is the largest boundary lake in the country. The downstream is located in the border city of Northeast China-Hulin City, located at the southern foot of Wanda Mountain, in the Muling River-Xingkai Lake Plain Area of the Sanjiang Plain. It belongs to a temperate continental monsoon climate, and it is a mild and humid climate zone in the Sanjiang Plain.

Field sampling and laboratory analysis

In May, July and October 2015, a three-season fish sampling survey was conducted in the Muling River basin. According to the characteristics of fish distribution, a total of 28 sampling sites were set up from upstream, midstream to downstream. Three parallels were set for each sampling sites (*Fig. 1, Table 1*).

The survey method is in accordance with the principles and requirements of the "Inland Water Fishery Natural Resources Survey Manual" (Zhang and He, 1993), and the identification of fish samples refers to the "Heilongjiang Province Fish History" (Zhang, 1995). Gillnet (40 m, 3-7 cm mesh) and electric fish device (2000W, 650V) for fish specimen collection. Some fish species cannot be accurately identified at the scene, and the specimens are marked, photographed and kept on file, and taken back to the laboratory for further processing. While sampling, local residents and fishermen were visited to learn more about the current status of the Muling River fish resources.

According to the requirements of "Water and Wastewater Monitoring Method" (Fourth Edition) (MEP, 2002) and the needs of on-site investigation, the following environmental factors are measured: conductivity (COND), dissolved oxygen (DO), pH value (pH), water temperature (WT), oxidation-reduction potential (ORP), total nitrogen (TN), total phosphorus (TP), total dissolved solids (TD), nitrate nitrogen (NO_2-N),

http://www.aloki.hu ● ISSN 1589 1623 (Print) ● ISSN1785 0037 (Online)
DOI: http://dx.doi.org/10.15666/aeer/1906_46834697

ammonium nitrogen (NH_4-N), nitrate (NO_3-N), chemical oxygen demand (COD), dissolved iron (Fe) and dissolved copper (Cu) and water transparency (SD).

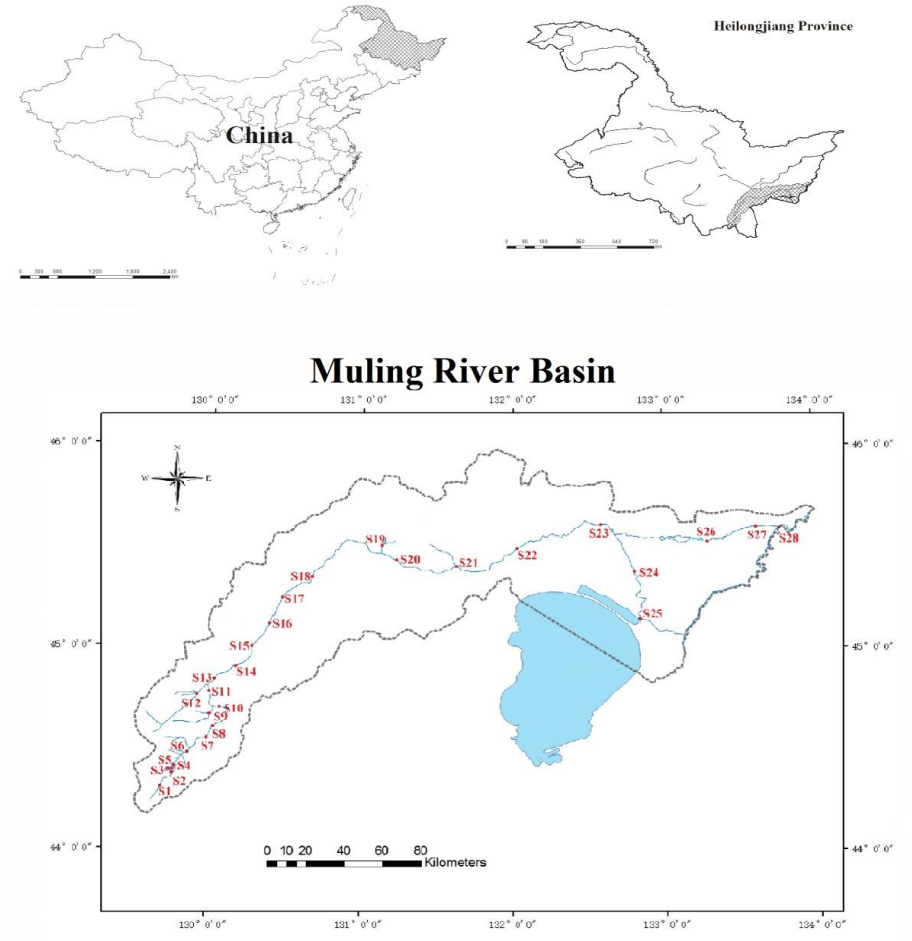

Figure 1. *Location of sampling sites in the Muling River basin*

Table 1. *The sampling stations and coordinates in the Muling River basin*

Sampling sites	Coordination	Sampling sites	Coordination
S1	44°01′48″N, 130°11′24″E	S15	44°40′12″N, 130°26′24″E
S2	44°03′36″N, 130°10′48″E	S16	44°53′24″N, 130°30′36″E
S3	44°03′00″N, 130°09′36″E	S17	45°00′00″N, 130°32′24″E
S4	44°04′12″N, 130°10′48″E	S18	45°04′48″N, 130°40′12″E
S5	44°04′48″N, 130°10′48″E	S19	45°18′00″N, 131°00′36″E
S6	44°11′24″N, 130°15′36″E	S20	45°18′00″N, 131°03′36″E
S7	44°13′12″N, 130°15′00″E	S21	45°20′24″N, 131°31′48″E
S8	44°13′48″N, 130°15′36″E	S22	45°27′00″N, 131°52′12″E
S9	44°21′36″N, 130°16′48″E	S23	45°42′00″N, 132°25′12″E
S10	44°24′36″N, 130°19′12″E	S24	45°35′24″N, 132°36′36″E
S11	44°28′12″N, 130°14′24″E	S25	45°19′48″N, 132°48′36″E
S12	44°28′12″N, 130°12′36″E	S26	45°44′24″N, 132°57′00″E
S13	44°29′24″N, 130°13′48″E	S27	45°45′36″N, 133°06′00″E
S14	44°34′48″N, 130°19′48″E	S28	45°58′12″N, 133°40′12″E

http://www.aloki.hu ● ISSN 1589 1623 (Print) ● ISSN1785 0037 (Online)
DOI: http://dx.doi.org/10.15666/aeer/1906_46834697

Data analysis

For data analysis the following indices were calculated:

Pinkas index (*IRI*):

$$IRI = (N\%+W\%)\times F\% \quad \text{(Eq.1)}$$

where, *N%* is the percentage of a certain fish's tail to the total, *W%* is the percentage of a certain fish's mass to the total mass, *F%* is the percentage of the number of sampling points that a certain fish appears in the total number of sampling sites.

Shannon-Weaver index (*H'*):

$$H' = -\sum_{i=1}^{s} P_i \log_2 P_i \quad \text{(Eq.2)}$$

where, P_i is the percentage of the total number of *i*-th individuals to the total number of individuals.

Pielou index (*J'*):

$$J' = H' / \ln S \quad \text{(Eq.3)}$$

where, *H'* is the Shannon-Wiener index, and *S* is the total number of species.

Margalef index (*D*):

$$D = \frac{S-1}{\ln N} \quad \text{(Eq.4)}$$

where, *S* is the total number of species, and *N* is the total number of all individuals.

For the correlation analysis of fish functional groups in Muling River, CANOCO 4.5 software is used to perform canonical correspondence analysis (referred to as CCA analysis) on fish species data and water environmental factor data. Before the analysis, in order to reduce the influence of extreme data, each data matrix (except pH value) is transformed by lg(x+1), and the sorting result is represented by a double sequence graph.

Results

Environmental factors

The seasonal variations of environmental factors (mean ± standard error) values among the sampling sites in different seasons were presented in *Fig. 2*. We found that COND, pH, NO_2-N, COD_{Mn} and SD showed the lowest values in summer. On the contrary, DO, WT, ORP, TN, TP, NH_4-N, NO3-N, Fe and Cu showed the highest values in the same season. TD showing a continuous growth trend, and COD_{Mn} seasonal variation fluctuates little.

Fish community structure

A total of 348 individual catchment fish belongs to 4 orders, 5 families, 16 genera, 22 species (*Table 2*). The Cypriniformes are the most numerous, with 19 species

http://www.aloki.hu ● ISSN 1589 1623 (Print) ● ISSN1785 0037 (Online)
DOI: http://dx.doi.org/10.15666/aeer/1906_46834697

(86.36%), and each of the remaining three orders (4.55%). At the family level, Cyprinids are also the most numerous, with 14 species (63.64%), followed by Loach, with 5 species (22.73%), Lamprey, Siluriaceae, and Channaidae family containing only one species each, accounting for 4.55% each.

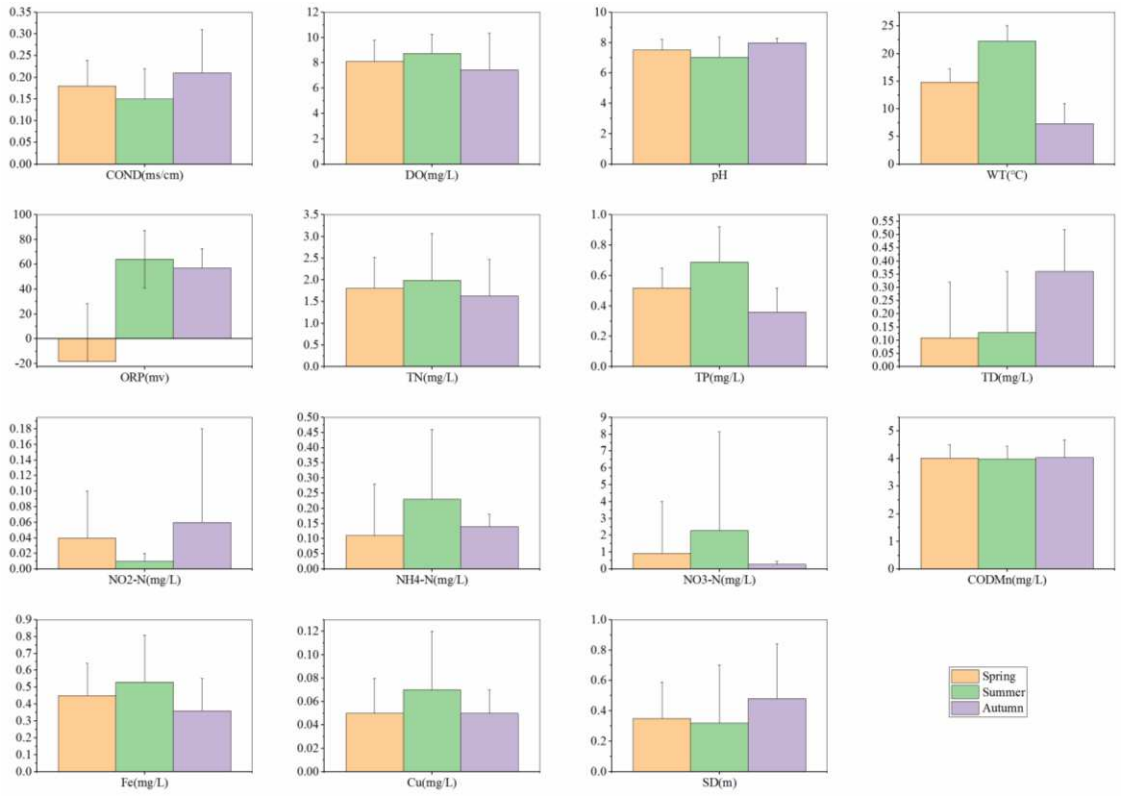

Figure 2. *The seasonal variations of environmental factors (means ± standard error): conductivity (COND), dissolved oxygen (DO), pH value (pH), water temperature (WT), oxidation-reduction potential (ORP), total nitrogen (TN), total phosphorus (TP), total dissolved solids (TD), nitrate nitrogen (NO_2-N), ammonium nitrogen (NH_4-N), nitrate (NO_3-N), chemical oxygen demand (COD_{Mn}), dissolved iron (Fe) and dissolved copper (Cu) and water transparency (SD)*

Variation of fish diversity index

The annual mean of Shannon-Weaver index is 1.97 (*Fig. 3*) in the Muling River Basin, the mean of Pielou index is 2.94 (*Fig. 4*), and the mean of Maralef index is 1.16 (*Fig. 5*). The three indices fluctuate little with the seasons throughout the year, and their changing trends are roughly the same. This shows that the fish species in the Muling River Basin are relatively stable.

In spring, the mean of Shannon-Weaver index at each sampling site is 1.92, and the fluctuation range is 0.7~3.99, the mean of Pielou index is 0.36, and the fluctuation range is 0.16~0.8, the mean of Maralef index is 1.14, the fluctuation range is 0.28~2.68.

In summer, the mean of Shannon-Weaver index at each sampling site is 2.02, and the fluctuation range is 0.92~4.02, the mean of Pielou index is 0.37, and the fluctuation range is 0.2~0.58, the mean of Maralef index is 1.16, the fluctuation range is 0.35~2.75.

http://www.aloki.hu ● ISSN 1589 1623 (Print) ● ISSN1785 0037 (Online)
DOI: http://dx.doi.org/10.15666/aeer/1906_46834697

In autumn, the mean of Shannon-Weaver index at each sampling site is 1.97, and the fluctuation range is 0.70~4.09, the mean of Pielou index is 0.36, and the fluctuation range is 0.17~0.55, the mean of Maralef index is 1.18, the fluctuation range is 0.49~2.83.

Table 2. *List of catchment fish of Muling River basin*

Order	Family	Genus	Species	*IRI*
Cypriniformes	Cyprinidae	*Ctenopharyngodon*	*Ctenopharyngodon idellus*	45.76
		Phoxinus	*Phoxinus phoxinus*	7.2
			Phoxinus percnurus	69.55
			Phoxinus czekanowskii	52.91
			Phoxinus lagowskii	9
		Hemiculter	*Hemiculter leucisclus*	187.95
		Pseudorasbora	*Pseudorasbora parva*	19.88
		Abbottina	*Abbottina rivularis*	241.65
		Rostrogobio	*Rostrogobio amurensisi*	31.95
		Saurogobio	*Saurogobio dabryi*	326.04
		Cyprinus	*Cyprinus carpio haematopterus*	4.32
		Carassius	*Carassius auratus gibelio*	84.24
		Aristichthys	*Aristichthys nobilis*	151.94
		Hypophthalmichthys	*Hypophthalmichthys molitrix*	133.92
	Cobitidae	*Lefua*	*Lefua costata*	46.08
		Cobitis	*Cobitis lutheri*	24.65
			Cobitis granoci	256.8
		Misgurnus	*Misgurnus mohoity*	831.39
			Misgurnus bipartitus	67.21
Petromyzoniformes	Petromyzonidae	*Lampetra*	*Lampetra reissneri*	53.25
Siluriformes	Siluridae	*Silurus*	*Silurus asotus*	97.5
Perciformes	Eleotridae	*Perccottus*	*Perccottus glehni*	136.04

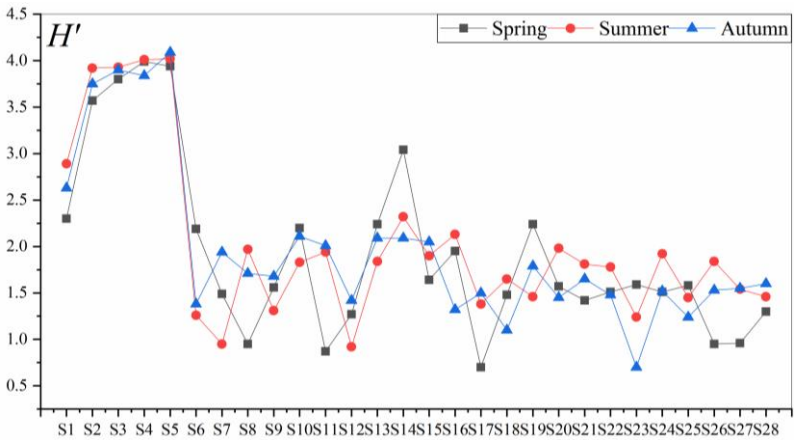

Figure 3. *Shannon-Weaver index (H') of different sampling sites*

http://www.aloki.hu ● ISSN 1589 1623 (Print) ● ISSN1785 0037 (Online)
DOI: http://dx.doi.org/10.15666/aeer/1906_46834697

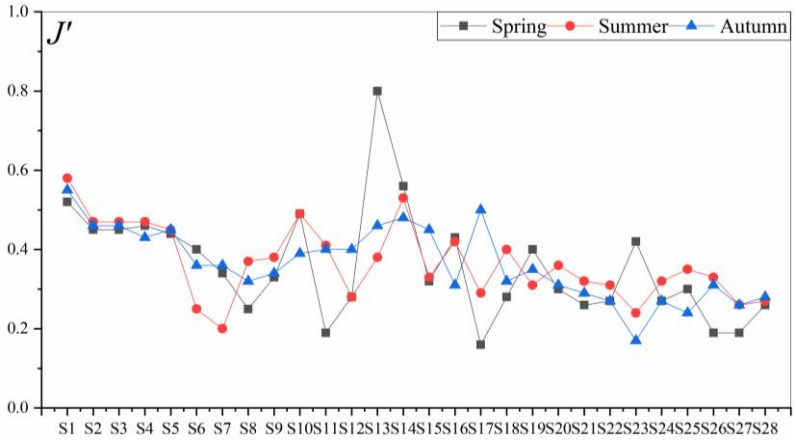

Figure 4. *Pielou index (J') of different sampling sites*

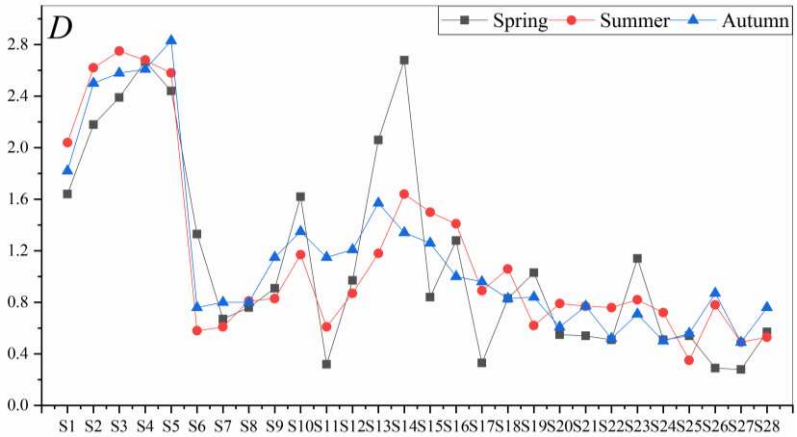

Figure 5. *Margalef index (D) of different sampling sites*

Correlation analysis of fish functional groups and water environment factors

According to the food habit of the fish caught in the Muling River, especially the omnivorous fish, it is further refined according to the main source of food. For fish that do not have clear references to determine their feeding habits, they are inferred based on their close relatives and the structure of their feeding organs (Ding and Liu, 2011). The fish caught in the Muling River are mainly divided into seven types of functional groups: aquatic plant feeding (herbivores), aquatic insect feeding (insectivores), phytoplankton feeding (phytoplanktivores), zooplankton feeding (zooplanktivores), benthic animal feeding habits (benthivores), omnivores (omnivores), and carnivorous (piscivores). The coding of each functional group is shown in *Table 3*, and the data of different seasons and environmental factors of the catch were analyzed by Canonical Correlation Analysis (CCA) in CANOCO for Windows 4.5 software.

In spring (*Fig. 6*), pH, TD, WT, DO negatively correlated with axis 1, NH_4-N, NO_2-N, Cu positively correlated with axis 1. SD negatively correlated with axis 2, TN, ORP, COND, Fe, TP, NO_3-N, and COD positively correlated with axis 2, NO_3-N, COD, and DO relatively weakly correlated. From the perspective of vector length, SD, pH, TN, ORP, and COND are the environmental factors that mainly affect the functional groups

http://www.aloki.hu ● ISSN 1589 1623 (Print) ● ISSN1785 0037 (Online)
DOI: http://dx.doi.org/10.15666/aeer/1906_46834697

of the Muling River fish in spring. Function group FG1, FG2, FG3, and FG4 are distributed on the left side of axis 1 and below axis 2, and are mainly affected by hydrological factors (SD, pH, TD, WT). FG5 is distributed on the right side of axis 1, which is mainly affected by the concentration of nutrients (NH_4-N, NO_2-N, TN, TP) and hydrological factors (COND, ORP). FG7 is mainly affected by Cu and FG6 is not greatly affected by water environmental factors.

Table 3. *Catchment fish functional group composition and codes in Muling River basin*

Codes	FGs	Catchment
FG1	herbivores	*Ctenopharyngodon idellus*, *Phoxinus phoxinus*, *Phoxinus lagowskii*
FG2	insectivores	*Phoxinus percnurus*, *Lefua costata*, *Misgurnus bipartitus*
FG3	phytoplanktivores	*Phoxinus czekanowskii*, *Rostrogobio amurensisi*, *Hypophthalmichthys molitrix*
FG4	zooplanktivores	*Aristichthys nobilis*
FG5	benthivores	*Hemiculter leucisclus*, *Pseudorasbora parva*, *Abbottina rivularis*, *Saurogobio dabryi*, *Cobitis lutheri*, *Cobitis granoci*, *Misgurnus mohoity*
FG6	omnivores	*Cyprinus carpio haematopterus*, *Carassius auratus gibelio*
FG7	piscivores	*Silurus asotus*, *Perccottus glehni*, *Lampetra reissneri*

Fish functional groups: aquatic plant feeding (FG1, herbivores), aquatic insect feeding (FG2, insectivores), phytoplankton feeding (FG3, phytoplanktivores), zooplankton feeding (FG4, zooplanktivores), benthic animal feeding habits (FG5, benthivores), omnivores (FG6, omnivores), carnivorous (FG7, piscivores)

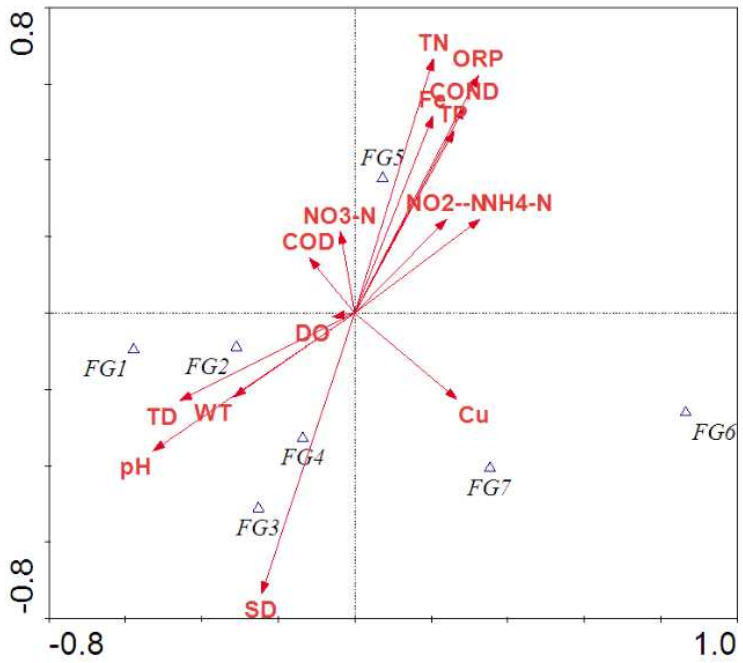

Figure 6. *CCA tri-plot of fish functional groups and environmental factors in spring. Environmental factors: conductivity (COND), dissolved oxygen (DO), pH value (pH), water temperature (WT), oxidation-reduction potential (ORP), total nitrogen (TN), total phosphorus (TP), total dissolved solids (TD), nitrate nitrogen (NO_2-N), ammonium nitrogen (NH_4-N), nitrate (NO_3-N), chemical oxygen demand (COD), dissolved iron (Fe) and dissolved copper (Cu) and water transparency (SD). Fish functional group: herbivores (FG1), insectivores (FG2), phytoplanktivores (FG3), zooplanktivores (FG4), benthivores (FG5), omnivores (FG6), piscivores (FG7)*

http://www.aloki.hu ● ISSN 1589 1623 (Print) ● ISSN1785 0037 (Online)
DOI: http://dx.doi.org/10.15666/aeer/1906_46834697

In summer (*Fig. 7*), Cu and SD negatively correlated with axis 1, while COD, NO_3-N, ORP positively correlated with axis 1. Meanwhile, TD and pH negatively correlated with axis 2, while TN, WT, Fe, DO, COND, NO_2-N, TP, NH_4-N positively correlated with axis 2. The correlation between COD, NO_3-N, TP, NO_2-N, NH_4-N, SD, and Cu was weak. From the perspective of vector length, TN, Fe, WT, ORP, TD, and pH are the environmental factors that mainly affect the functional groups of the Muling River fish in summer. Functional group FG3 and FG6 are distributed on the left side of axis 1 and below axis 2, and are mainly affected by hydrological factors (hardness, pH), other functional groups are less affected by water environment factors.

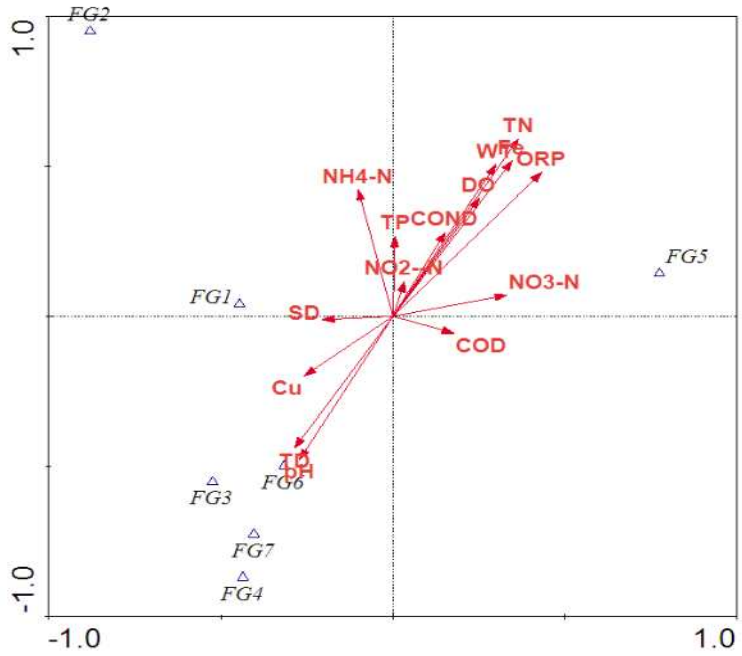

Figure 7. *CCA tri-plot of fish functional groups and environmental factors in summer. Environmental factors: conductivity (COND), dissolved oxygen (DO), pH value (pH), water temperature (WT), oxidation-reduction potential (ORP), total nitrogen (TN), total phosphorus (TP), total dissolved solids (TD), nitrate nitrogen (NO_2-N), ammonium nitrogen (NH_4-N), nitrate (NO_3-N), chemical oxygen demand (COD), dissolved iron (Fe) and dissolved copper (Cu) and water transparency (SD). Fish functional group: herbivores (FG1), insectivores (FG2), phytoplanktivores (FG3), zooplanktivores (FG4), benthivores (FG5), omnivores (FG6), piscivores (FG7)*

In autumn (*Fig. 8*), WT and COD negatively correlated with axis 1, while pH, NO_3-N, COND and ORP positively with axis 2. Meanwhile, SD, DO, Fe and TP negatively correlated with axis 2. While, Cu, TN, NO_2-N, NH_4-N and TD positively correlated with axis 2. The correlation between SD and Fe was weak. From the perspective of vector length, NO_3-N, NO_2-N, Cu and DO are the environmental factors that mainly affect the functional groups of the Muling River fish in autumn. Functional group FG3 and FG7 are distributed on the left side of axis 1 and above axis 2, mainly affected by WT and COD. FG2 is distributed on the upper side of axis 1 on the right side of axis 2, and is mainly affected by hydrological factors (COND, ORP) and nitrogen salt concentration (NO_3-N, TN), FG5 is mainly affected by Fe and TP. The others are not greatly affected by water environmental factors.

http://www.aloki.hu ● ISSN 1589 1623 (Print) ● ISSN1785 0037 (Online)
DOI: http://dx.doi.org/10.15666/aeer/1906_46834697

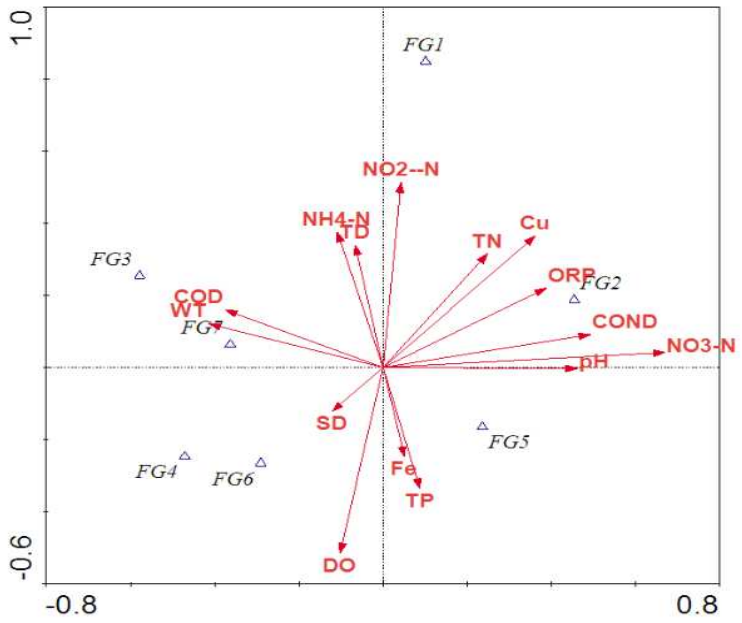

Figure 8. *CCA tri-plot of fish functional groups and environmental factors in autumn. Environmental factors: conductivity (COND), dissolved oxygen (DO), pH value (pH), water temperature (WT), oxidation-reduction potential (ORP), total nitrogen (TN), total phosphorus (TP), total dissolved solids (TD), nitrate nitrogen (NO_2-N), ammonium nitrogen (NH_4-N), nitrate (NO_3-N), chemical oxygen demand (COD), dissolved iron (Fe) and dissolved copper (Cu) and water transparency (SD). Fish functional group: herbivores (FG1), insectivores (FG2), phytoplanktivores (FG3), zooplanktivores (FG4), benthivores (FG5), omnivores (FG6), piscivores (FG7)*

Discussion

According to records, no relevant fish surveys have been conducted in the Muling River Basin, and the data available for reference is very limited. However, it is certain that due to external factors, the fish composition and distribution of the Muling River Basin have undergone obvious changes. Under the strong interference of human activities, the pressure of human activities has become an important factor affecting fish, which is reflected in the greater damage to the living environment of fish (Li et al., 2012). The biological basis of fish bait, changes in fish community structure and biological characteristics all need in-depth investigation and research. Only a comprehensive investigation can formulate reasonable and effective protection measures. In addition, a monitoring system for fish and its ecological environment should be established to discover changes and development trends of the ecological environment in a timely manner through dynamic monitoring, understand the temporal and spatial laws of changes in the aquatic organisms' ecological environment in related areas, predict adverse trends and issue early warnings in time.

In a few areas of the Muling River Basin, fish resources have not been strictly managed, and random fishing still exists, and the use of nets is denser, which makes juvenile fish repeatedly caught and reduces the number of replenishments. With the growth of residents on both sides of the Muling River Basin in recent years, the catch has continued to increase. Illegal fishing activities such as electric fish poisoning have brought great damage to the fish resources of the Muling River Basin. In order to ensure

http://www.aloki.hu ● ISSN 1589 1623 (Print) ● ISSN1785 0037 (Online)
DOI: http://dx.doi.org/10.15666/aeer/1906_46834697

the proliferation of fish resources, net meshes may be restricted to 10-15 cm in the future, the reproduction protection objects may be clearly defined, fishing licenses shall be implemented and fishing prohibited areas may be designated. It is hoped that the fishery department will strengthen management, resolutely implement the protection regulations and relevant laws and regulations, ban harmful fishing gear and fishing methods, and effectively protect juvenile fish resources (Liu and Cao, 1992). There are 44 water pollution sources in the basin, and the total wastewater discharge of key industrial enterprises is 30,501,600 m^3/a, accounting for 65.02% of the whole basin. Non-point source pollution occurred in the agricultural land, and a large amount of residual pesticides and fertilizers were lost to the river. Industrial enterprises along the Muling River Basin should strictly abide by the wastewater discharge indicators and do a good job of treatment before discharge. The abuse of pesticides and fertilizers is prohibited to reduce the amount of pesticides and fertilizers entering rivers in natural processes, and timely treatment measures should be taken for river sections with more serious pollution.

In the upper reaches of Muling River, there are Tuanjie Reservoir, Chengzi River Irrigation District, Liumao Irrigation District, Lishu Irrigation District and other water storage projects and irrigation projects. There are 27 dams in the whole water area. Due to changes in hydrological conditions, the habitats of some fish have been greatly reduced, such as benthic species (such as loach) that are accustomed to living in rapids. Not only will the original habitat be lost, but also the source of bait will be lost, which directly leads to the loss of some fish breeding conditions. The construction of water conservancy projects has reduced the living space of fish, which has led to a decrease in population and genetic diversity (Li and Xie, 2004; Yang et al., 2011). In order to coordinate the contradiction between the construction of water conservancy projects in the Muling River Basin and the protection of fish resources, and to make up for the damage caused to the fish habitat by the construction of water conservancy projects, according to the characteristics of different habitats in the upper, middle and lower reaches of the Muling River, suitable river sections should be selected to establish fish nature reserves to ensure that most fish will not become extinct, especially endemic species. The principle of nature reserves is to maintain the original natural appearance of the ecosystem. Therefore, water conservancy projects should not be built in the upper reaches of the rivers selected as nature reserves, and industrial and mining wastewater should be controlled to minimize the interference of human activities. Also, the ideological awareness of the protection of fish resources should further be strengthened for the managers of the protected area and the local residents, so that they can more deeply realize the importance of protection.

Fish functional groups are mainly classified according to their biological characteristics such as differences in feeding habits (Figuerola et al., 2012). By dividing functional groups, it is not only convenient to study the structure of fish communities, but also greatly simplifies the food web, which also opens up new ideas for scientific research (Bulman et al., 2001). The study of fish functional groups is mostly found in various sea areas. Hu et al. (2016) studied fish in the Qixing Islands Marine Special Reserve in Zhejiang Province, and Zhang et al. (2012) fish functional groups in the Bohai Sea and the East China Sea (Zhang et al., 2007). They also use the same functional species clusters to study the seasonal changes of fish, such as Li et al. (2014) on Laizhou Bay fish, and Lv et al. (2012) on the spring and autumn fish diversity in the Shandong waters of the Yellow Sea. The study of fish functional groups in freshwater

http://www.aloki.hu ● ISSN 1589 1623 (Print) ● ISSN1785 0037 (Online)
DOI: http://dx.doi.org/10.15666/aeer/1906_46834697

river basins only found in rivers in the transitional region between the warm temperate zone and subtropical zone in the south (Yan, 2013) and lakes in subtropical regions (Wang, 2014). The Muling River is located in the northern alpine region. Compared with the ocean, the salinity and pH value of the water body are different, which leads to different plankton community composition (Chapman, 1973). The increase in the concentration of nutrient salts (nitrogen and phosphorus) in the water body will promote the synthesis of chlorophyll a, and the density of phytoplankton will increase, thereby promoting the growth of zooplankton (Li and Yu, 2002), which will directly affect the phytoplankton feeding functional groups of fish and phytoplankton. Feeding functional group of zooplankton fish.

The development of cold-water fish farming in the corresponding section of the Muling River has great resource potential, and it is possible to select and breed chickfish and tequila as the main economic fish for promotion. Both fish are suitable for breeding in cold spring water and mountain streams. In rich areas, the prospects for artificial breeding are promising (Cheng, 2015). While protecting fish resources, it can also increase people's income and improve people's livelihood. Artificial reproduction and release are common practices in countries all over the world to restore fish resources. It can supplement the size of fish populations and reserve a sufficient number of broodstock reserve groups. It can also preserve fish germplasm resources and maintain the species diversity of local indigenous fish (Yang et al., 2013). It is recommended that artificial breeding and releasing stations be established in suitable sections of the Muling River Basin, and artificial reproduction and releasing can be carried out in a planned way. While promoting the recovery of fish species, it can also increase fishery resources and increase residents' income.

Conclusion

A total of 22 species of fish caught in the Muling River Basin were identified in this investigation, belonging to 4 orders, 5 families and 16 genera. The three fish diversity indices do not fluctuate greatly with the seasons throughout the year, and their changing trends are roughly the same. It can be seen that the fish species of the Muling River are relatively stable. The fish caught in the Muling River are mainly divided into seven types of functional groups. The environmental factors affecting the functional groups of fish are slightly different from season to season. Spring is TN, pH, ORP, SD, COND, summer is TN, pH, Fe, ORP, WT, TD, and autumn is the same as summer. These environmental factors should be taken into account for future fish population restoration.

Acknowledgements. The study was supported by the central government supports the reform and development fund projects of local colleges and universities “Research on integrated technology innovation of sustainable utilization of cold water fish resources industrialization” (2020GSP14), and Key research topics of economic and social development in Heilongjiang Province (20309), and the major special projects of science and technology in Liaoning Province (2020JH1/10200002), Dalian Science and Technology Innovation Fund Project (2019J12SN64), and Agricultural finance special project "Investigation of fishery resources and environment in key waters of Northeast China".

http://www.aloki.hu ● ISSN 1589 1623 (Print) ● ISSN1785 0037 (Online)
DOI: http://dx.doi.org/10.15666/aeer/1906_46834697

REFERENCES

[1] Bulman, C., Althaus, F., He, X., Bax, N. J., Williams, A. (2001): Diets and trophic guilds of demersal fishes of the southeastern Australian shelf. – Marine and Freshwater Research 52: 537-548.
[2] Chapman, D. J. (1973): Biliproteins and bile pigments. – London: Blackwell Scientific Publications.
[3] Chen, Y. Y. (1990): Several biodiversity issues in freshwater ecosystems. – Chinese Bulletin of Life Sciences 5: 197-200. (in Chinese with English abstract).
[4] Chen, X. J. (2014): Impacts of operation of hydropower projects on aquatic organisms and mitigation measures. – Yangtze River 15: 7-13. (in Chinese with English abstract).
[5] Cheng, Z. Y. (2015): Species and prospects of cold-water fish breeding in Heilongjiang Province. – Northern Chinese Fisheries 6: 9-11. (in Chinese).
[6] Ding, B. Q., Liu, H. Z. (2011): Analysis of fish feeding guild composition in the Yangtze River. – Sichuan Journal of Zoology 1: 31-35. (in Chinese with English abstract).
[7] Figuerola, B., Maceda-Veiga, A., De, S. A. (2012): Assessing the effects of sewage effluents in a Mediterranean creek: fish population features and biotic indices. – Hydrobiologia 694(1): 75-86.
[8] Giles, N., Sands, R., Fasham, M. (2005): Fish. – In: Hill, D., Fasham, M., Tucker, G., Shewry, M., Shaw, P. (eds.) Handbook of Biodiversity Methods: Survey, Evaluation and Monitoring. Cambridge University Press, Cambridge, pp. 368-386.
[9] Holmlund, C. M., Hammer, M. (1999): Ecosystem services generated by fish populations. – Ecological Economic 29: 253-268.
[10] Hu, C. Y., Shui, Y. Y., Tian, K., Li, L., Qin, H. L., Zhang, C. C., Ji, M. M., Shui, B. N. (2016): Functional group classification and niche identification of major fish species in the Qixing Islands Marine Reserve, Zhejiang Province. – Biodiversity Science 2: 175-184. (in Chinese with English abstract).
[11] Karr, J. R. (1981): Assessment of biotic integrity using fish communities. – Fisheries 6: 21-27.
[12] Li, G. G., Yu, Z. M. (2002): Community Structure of Zooplankton in Lake Qiandaohu. – Acta Ecologica Sinica 22(2): 156-162. (in Chinese with English abstract).
[13] Li, H. J., Xie, C. X. (2004): Fauna Composition and Resources Protection of Freshwater Fish in Forest Streams in the Central North of Guangxi Province. – Journal of Northeast Forestry University 32(1): 89-92. (in Chinese with English abstract).
[14] Li, J., Li, X. H., Jia, X. P., Tan, X. C., Wang, C., Li, Y. F., Shao, X. F. (2012): Relationship between fish community diversity and environmental factors in the Lianjiang River, Guangdong, China. – Acta Ecologica Sinica 18: 5795-5805. (in Chinese with English abstract).
[15] Li, F., Xu, B. Q., Ma, Y. Q., Lv, Z. B., Wang, T. T. (2014): Seasonal changes of functional guilds of fish community in Laizhou Bay, East China. – Acta Ecologica Sinica 34(7): 1736-1745. (in Chinese with English abstract).
[16] Liu, J. K., Cao, W. X. (1992): Fish resources of the Yangtze River basin and the tactics for their conservation. – Resources and Environment in the Yangtze Valley 1(1): 17-23. (in Chinese with English abstract).
[17] Liu, H. Z., Yang, J. X., Liu, S. W., Gao, X., Chen, Y. S., Zhang, C. G., Zhao, K., Li, X. H., Liu, W. (2016): Theory and methods on fish diversity monitoring with an introduction to the inland water fish diversity observation in China. – Biodiversity Science 11: 1227-1233. (in Chinese with English abstract).
[18] Lv, Z. B., Li, F., Xu, B. Q., Wang, B. (2012): Fish community diversity during spring and autumn in the Yellow Sea off the coast of Shandong. – Biodiversity Science 20(2): 207-214. (in Chinese with English abstract).
[19] Ma, K. P. (1994): Methods of Measuring the Diversity of Biological Community. – Chinese Biodiversity 2(3): 162-168. (in Chinese with English abstract).

http://www.aloki.hu ● ISSN 1589 1623 (Print) ● ISSN1785 0037 (Online)
DOI: http://dx.doi.org/10.15666/aeer/1906_46834697

[20] Mao, Z. G., Gu, X. H., Zeng, Q. F. (2016): The structure of fish community and changes of fishery resources in Lake Hulun. – Journal of Lake Science 2: 387-394. (in Chinese with English abstract).
[21] MEP. (2002): Water and Wastewater Monitoring Method (Fourth Edition). – Beijing: China Environmental Science Press. (in Chinese).
[22] Sarkar, U. K., Pathak, A. K., Sinha, R. K., Sivakumar, K., Pandian, A. K., Pandey, A., Dubey, V. K., Lakra, W. S. (2012): Freshwater fish biodiversity in the River Ganga (India): changing pattern, threats and conservation perspectives. – Reviews in Fish Biology and Fisheries 22: 251-272.
[23] Shi, R. D., Wu, Z. Q., Huang, L. L., Feng, W. L., Zhu, Z. J., Ding, Y., Hu, Y. X. (2015): Fish species diversity of the upper Xiangjiang River in North Guangxi Province. – Journal of Guangxi Normal University: Natural Science Edition 4: 127-136. (in Chinese with English abstract).
[24] Simon, T. P. (1999): Assessing the sustainability and biological integrity of water resources using fish communities. – New York: CRC Press 6-7.
[25] Wang, S. B., Song, Z., Li, P. (2006): Current situation of China fishery resources and countermeasures for the sustainable development. – Chinese Fisheries Economics 1: 24-27. (in Chinese with English abstract).
[26] Wang, W. J. (2014): Spatial pattern in the structure and diversity of the taxonomic and functional organizations of stream fish in the mountains of southern Anhui. – Anhui Normal University. (in Chinese with English abstract).
[27] Xia, J. H., Lu, J. F., Zhou, B. C., Tan, H. Z. (2009): A preliminary study on fish communities in Suzhou Creek, Shanghai. – Journal of Lake Sciences 04: 538-546. (in Chinese with English abstract).
[28] Xiao, Q., Yang, Z., Tang, H. Y., Duan, P. X., Wang, X. Q., Xiao, T. Y., Liu, X. Y. (2015): Species diversity of fish and its conservation in the mainstream of the lower reaches of Wu River. – Biodiversity Science 4: 499-506. (in Chinese with English abstract).
[29] Yan, L. L. (2013): Longitudinal patterns in taxonomic and functional organizations of fish assemblages of the headwater streams within the Qingyi River. – Anhui Normal University. (in Chinese with English abstract).
[30] Yang, Y. H., Yang, J. X., Pan, X. B., Zhou, W., Yang, M. L. (2011): Fishery resource protection by artificial propagation in hydroelectric development: Lixianjiang River drainage in Yunnan as an example. – Zoological Research 32(2): 188-195. (in Chinese with English abstract).
[31] Yang, C. Y. (2012): Diversity of fishery resources of the Yuanshui River. – Central South University of Forestry & Technology 48-56. (in Chinese with English abstract).
[32] Yang, J. X., Pan, X. B., Chen, X. Y., Wang, X. A., Zhao, Y. P., Li, J. Y., Li, Z. Y. (2013): Overview of the artificial enhancement and release of endemic freshwater fish in China. – Zoological Research 34(4): 267-280. (in Chinese with English abstract).
[33] Zhang, J. M., He, Z. H. (1993): Neilu Shuiyu Yuye Ziran Ziyuan Shouce. – Beijing: Science Press. (in Chinese).
[34] Zhang, J. M. (1995): Fish History of Heilongjiang Province. – Harbin: Heilongjiang Science and Technology Press. (in Chinese).
[35] Zhang, B., Tang, Q. S., Jin, X. S. (2007): Functional groups of fish assemblages and their major species at high trophic level in the East China Sea. – Journal of Fishery Science of China 6: 939-949. (in Chinese with English abstract).
[36] Zhang, B., Li, Z. Y., Jin, X. S. (2012): Functional groups of fish assemblages and their major species in the Bohai Sea. – Journal of Fisheries of China 1: 64-72. (in Chinese with English abstract).

http://www.aloki.hu ● ISSN 1589 1623 (Print) ● ISSN1785 0037 (Online)
DOI: http://dx.doi.org/10.15666/aeer/1906_46834697

A GIBBERELLIN, ABSCISIC ACID, AND *DELAY OF GERMINATION 1* INTERACTION NETWORK REGULATES CRITICAL DEVELOPMENTAL TRANSITIONS IN MODEL PLANT *ARABIDOPSIS THALIANA* – A REVIEW

GUAN, S. X.[1,2] – LI, Y. S.[2] – ZENG, W. Q.[2] – LIN, J. W.[3] – ZHAN, H.[1,2] – HAN, X. Y.[2] – ZHANG, X. L.[2] – LU, X. J.[2*]

[1]*College of Horticulture, Shenyang Agricultural University, Shenyang 110866, Liaoning, China*

[2]*College of Forestry, Shenyang Agricultural University, Shenyang 110866, Liaoning, China*

[3]*College of Bioscience and Biotechnology, Shenyang Agricultural University, Shenyang 110866, Liaoning, China*

[*]*Corresponding author*
e-mail: lxjsyau@syau.edu.cn

(Received 24th Jul 2021; accepted 20th Sep 2021)

Abstract. Seed germination and flowering are two critical developmental transitions in the life cycles of plants. These transitions are coordinately regulated by exogenous environmental cues and endogenous hormonal signals to match plant establishment and reproduction to the appropriate seasons. The phytohormones, abscisic acid (ABA) and gibberellins (GAs), are the key players that antagonistically regulate seed dormancy and germination; ABA positively modulates dormancy induction and maintenance, while GA stimulates germination. For the control of flowering time, GA has been shown to have a positive role in the modulation of floral transition, whereas both positive and negative roles have been recorded for ABA in this process. *DELAY OF GERMINATION 1* (*DOG1*) delays floral transition and functions in dormancy induction and maintenance, acting in parallel with ABA and/or GA. However, DOG1 is also involved in ABA and GA antagonism through affecting hormone biosynthesis and/or signal transduction pathways. Moreover, the expression of *DOG1* is directly regulated by ABA. In this review, we summarize recent developments in seed dormancy and flowering research on the model plant *Arabidopsis thaliana*, focusing on the crosstalk between ABA, GA, and DOG1. Finally, the open questions and remaining challenges in this field are presented.
Keywords: *seed dormancy, flowering, phytohormone, DOG1, crosstalk*

Abbreviations: 13ox: GA 13-oxidase, 2ox: GA 2-oxidase, 20ox: GA 20-oxidase, 3ox: GA 3-oxidase, AAO3: abscisic aldehyde oxidase, ABA: abscisic acid, ABA2: ABA deficient 2 (short chain alcohol dehydrogenase), ABI: ABA INSENSITIVE, ABRE: ABA responsive element, AGL24: AGAMOUS LIKE 24, AP1: APETALA1, AREB/ABF: ABRE-binding protein/ABRE-binding factor, BRs: brassinosteroids, CE1: coupling element 1, CHD3: chromodomain-helicase-DNA-binding domain, CO: CONSTANS, CPS: ent-copalyl diphosphate synthase, CTKs: cytokinins, Cvi: Cape Verde Islands, CYP707A: ABA 8'-hydroxylase, DOG1: DELAY OF GERMINATION 1, DPA: dihydrophaseic acid, ent-CDP: ent-copalyl diphosphate, ET: ethylene, FLC: FLOWERING LOCUS C, FT: FLOWERING LOCUS T, FUL: FRUITFULL, GAs: gibberellins, GGDP: geranylgeranyl diphosphate, GID1: GIBBERELLIN INSENSITIVE DWARF1, JA: jasmonic acid, KAO: ent-kaurenoic acid oxidase, KO: ent-kaurene oxidase, KS: ent-kaurene synthase, Ler: Landsberg erecta, LFY: LEAFY, miRNAs: microRNAs, NCEDs: 9-cis-epoxycarotenoid dioxygenases, NSY: neoxanthin synthase, PA: phaseic acid, PKL: PICKLE, PP2Cs: protein phosphatases type 2C, PRC2: Polycom Repressive Complex 2, PYL: pyrabactin-like, PYR: pyrabactin resistance, RCAR: regulatory components of ABA receptors, RY/Sph: RY/Sph element, SA: salicylic acid, SAM: shoot apical meristem, SCF: Skp1-cullin-F-box, SLs: strigolactones, SMZ: SCHLAFMUTZE, SnRK2s: Snf1-related protein kinases type 2, SNZ: SCHNARCHZAPFEN, SOC1: SUPPRESSOR OF OVEREXPRESSION OF CONSTANS 1, SPL: SQUAMOSA PROMOTER BINDING PROTEIN-LIKE, TOE: TARGET OF EAT, TSF: TWIN SISTER OF FT, Ub: ubiquitin, ZEP: zeaxanthin epoxidase

http://www.aloki.hu ● ISSN 1589 1623 (Print) ● ISSN 1785 0037 (Online)
DOI: http://dx.doi.org/10.15666/aeer/1906_46994720

Introduction

As sessile organisms, plants cannot actively determine where they establish themselves, but they can adapt to environmental changes through several specific mechanisms. Annual plants acclimatize to their environment by precisely matching their life cycles, especially seed germination and flowering, to seasonal conditions (Huo et al., 2016). Seed dormancy, which has been described as 'the incapacity of a viable seed to germinate under favorable conditions', is an important adaptive trait determining plant survival (Bewley, 1997; Finch-Savage and Leubner-Metzger, 2006). Seed dormancy is induced during seed maturation, preventing or delaying germination of maturated seeds until conditions are conducive to the beginning of a new life cycle (Baskin and Baskin, 2004; Bewley et al., 2013). Flowering is another important adaptive trait for plant species and the correct timing of the transition to flowering is pivotal for the reproductive success of all flowering plants as its timing must match the right conditions for fertilization and seed dispersal (Huijser and Schmid, 2011; Yamaguchi and Abe, 2012). Recent studies have suggested that classic genes modulating flowering, such as *FLOWERING LOCUS C* (*FLC*) and *FLOWERING LOCUS T* (*FT*), also participate in the transition from seed dormancy to germination (Chiang et al., 2009; Chen et al., 2014; Zhao et al., 2015), indicating that seed dormancy and flowering may be coordinately modulated via overlapping molecular pathways (Huo et al., 2016). It is increasingly clear that germination cannot be considered in isolation from flowering since these two processes can have cascading effects on each other (Post et al., 2008; Huo et al., 2016), with consequences for life-cycle expression (Burghardt et al., 2015; Springthorpe and Penfield, 2015) and potentially also for adaptation (Chiang et al., 2013).

Germination and flowering time are triggered and regulated by both exogenous environmental cues and endogenous hormonal signals (Huijser and Schmid, 2011; Conti, 2017; Buijs et al., 2018). The status of germination and flowering depends on the balance between abscisic acid (ABA) and the gibberellins (GAs) (Finkelstein et al., 2008; Holdsworth et al., 2008; Lee et al., 2015; Shu et al., 2017). Abscisic acid is needed for dormancy induction and maintenance (Finch-Savage and Leubner-Metzger, 2006; Finkelstein et al., 2008; North et al., 2010; Dekkers and Bentsink, 2015), whereas GA is required for germination (Karssen and Lacka, 1986; Finch-Savage et al., 2007; Holdsworth et al., 2008; Née et al., 2017b). Gibberellin has a positive effect on floral transition (Ding et al., 2013; Hyun et al., 2016), while both positive and negative effects of ABA on flowering have been reported (Riboni et al., 2013; Wang et al., 2013). *DELAY OF GERMINATION 1* (*DOG1*) delays floral transition and is a crucial player in dormancy induction and maintenance (Nakabayashi et al., 2012; Huo et al., 2016; Li et al., 2019). The DOG1-mediated regulatory pathway is distinct from those of ABA and/or GA (Huo et al., 2016; Shu et al., 2016b). However, DOG1 can carry out functions, central to ABA and GA antagonism, that influence hormone biosynthesis and/or signal transduction pathways (Tuan et al., 2018). Moreover, *DOG1* expression is controlled directly by ABA (Graeber et al., 2010, 2013).

In this review, we summarize recent advances, mainly in the case of the model plant *Arabidopsis thaliana*, associated with the modulation of seed dormancy and flowering, focusing on the three crucial players, ABA, GA, and *DOG1*. Finally, unanswered questions and future directions for research in this area will be discussed.

http://www.aloki.hu ● ISSN 1589 1623 (Print) ● ISSN 1785 0037 (Online)
DOI: http://dx.doi.org/10.15666/aeer/1906_46994720

The roles of ABA metabolism and signaling in modulating seed dormancy induction and maintenance

The phytohormone ABA is a master inducer and protector of seed dormancy (Vaistij et al., 2013), and both ABA content and related sensitivity have been shown to be important for these processes (Bewley et al., 2013; Finkelstein, 2013; Dekkers and Bentsink, 2015). The role of ABA in seed dormancy is conserved among different species (Dekkers and Bentsink, 2015). Evidence for the role of ABA in dormancy is provided by the dormancy variability observed among Arabidopsis seeds with altered ABA biogenesis or signaling genes. Seeds that lose the ability to produce ABA (Frey et al., 2011) or transduce the ABA signal (Ma et al., 2009; Park et al., 2009) have reduced seed dormancy levels. In contrast, seeds that accumulate high ABA levels, or those that possess an ABA hypersensitive phenotype, show increased seed dormancy (Cutler et al., 1996; Matakiadis et al., 2009; Martinez-Andujar et al., 2011; Nonogaki et al., 2014). Similar results were also reported for other species. An increase in ABA content resulted in an enhanced degree of seed dormancy in wheat (Chono et al., 2013). In tomato, defective ABA signaling resulted in nondormant seeds (Groot and Karssen, 1992) whereas higher ABA content increased seed dormancy levels (Thompson et al., 2000). Moreover, active ABA biogenesis is essential for the maintenance of dormancy in imbibed Arabidopsis and *Nicotiana plumbaginifolia* seeds (Grappin et al., 2000; Ali-Rachedi et al., 2004). Maintenance of seed dormancy is also determined by seed sensitivity to ABA (Tuan et al., 2018). Enhanced ABA sensitivity is necessary to maintain dormancy during imbibition of both wheat and Arabidopsis seeds (Barrero et al., 2010; Tuttle et al., 2015). These studies highlighted the important roles that ABA plays in seed dormancy.

ABA metabolism

The cellular level of ABA is modulated by its biosynthesis and catabolism (Nambara and Marion-Poll, 2005; Nambara et al., 2010; Tuan et al., 2018) (*Fig. 1*). Nine-*cis*-epoxycarotenoid dioxygenases (NCEDs) catalyze the cleavage of 9-*cis*-violaxanthin and 9'-*cis*-neoxanthin, which is the rate-limiting step in ABA biosynthesis (Schwartz et al., 2003). Abscisic acid is inactivated either by hydroxylation or conjugation with a sugar. The catabolism of ABA occurs primarily through 8′-hydroxylation via the activity of ABA 8′-hydroxylase (ABA8′OH) (Nambara and Marion-Poll, 2005; Finkelstein, 2013) which is encoded by the *CYP707A* genes (Kushiro et al., 2004; Saito et al., 2004). All plant species identified to date have *NCED* and *CYP707A* as multigene families, indicating that the expression of these factors is important for the regulation of seed ABA levels and, consequently, dormancy and germination.

ABA signaling

The core ABA signaling pathway contains three master components: pyrabactin resistance (PYR)/pyrabactin-like (PYL)/regulatory components of ABA receptors (RCAR) family members, protein phosphatases type 2C (PP2Cs), and Snf1-related protein kinases type 2 (SnRK2s) (Cutler et al., 2010; Dekkers and Bentsink, 2015; Vishwakarma et al., 2017) (*Fig. 2*). A recent significant finding was the identification of the ABA receptors PYR/PYL/RCAR that have a major role in seed responsiveness to ABA (Ma et al., 2009; Park et al., 2009). Fourteen members of this protein family (PYR1, PYL1-13) are encoded in the Arabidopsis genome, with the *pyr1 prl1 prl2 prl4* quadruple mutant displaying a strong ABA-insensitive germination phenotype (Park et al., 2009).

http://www.aloki.hu ● ISSN 1589 1623 (Print) ● ISSN 1785 0037 (Online)
DOI: http://dx.doi.org/10.15666/aeer/1906_46994720

Members of the PP2C gene family, including *ABA INSENSITIVE 1* (*ABI1*) and *ABI2*, are prominent regulators. Mutations in these genes result in ABA hypersensitivity (Koornneef et al., 1984; Gosti et al., 1999), suggesting that they are negative regulators of ABA signaling (Yoshida et al., 2015). A member of SnRK2 is a critical positive regulator of ABA signaling (Yoshida et al., 2015). Three Arabidopsis SnRK2 protein kinases (SnRK2.2, SnRK2.3, and SnRK2.6) have been indicated to function redundantly in ABA signal transduction (Nambara et al., 2010). The triple mutant of these kinases is almost completely insensitive to ABA and germinates precociously under conditions of high humidity (Nakashima et al., 2009). In the absence of ABA, PP2Cs repress SnRK2 activity via dephosphorylation of its kinase activation loop; meanwhile, the ABA receptors PYR/PYL/RCAR form a complex with PP2C, which results in the repression of PP2C phosphatase activity and thereby activating SnRK2 in the presence of ABA (Finkelstein, 2013; Ng et al., 2014; Yang et al., 2017). The targets of active SnRK2 have been shown to be ABRE-binding protein/ABRE-binding factor (AREB/ABF) transcription factors, which induce the onset of ABA-responsive gene transcription (Ng et al., 2014). Among the AREB/ABF transcription factors, ABI5 (bZIP type) plays an important role in modulating seed ABA-responsive genes (Nambara et al., 2010; Finkelstein, 2013; Yu et al., 2015).

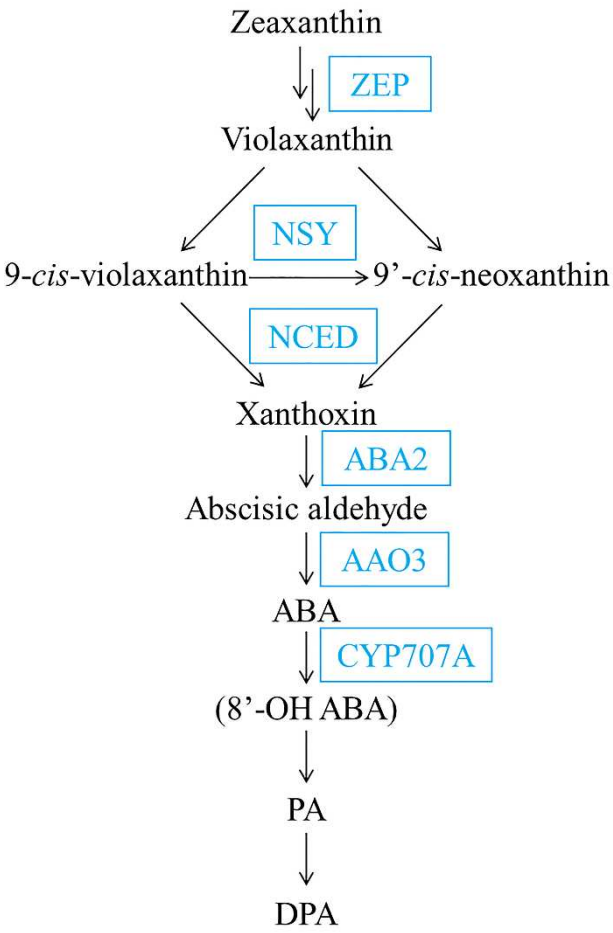

Figure 1. *The ABA metabolism pathway. Each box represents an enzyme. ZEP, zeaxanthin epoxidase; NSY, neoxanthin synthase; NCED, 9-cis-epoxycarotenoid dioxygenase; ABA2, ABA deficient 2 (short chain alcohol dehydrogenase); AAO3, abscisic aldehyde oxidase; CYP707A, ABA 8'-hydroxylase. PA, phaseic acid; DPA, dihydrophaseic acid*

http://www.aloki.hu ● ISSN 1589 1623 (Print) ● ISSN 1785 0037 (Online)
DOI: http://dx.doi.org/10.15666/aeer/1906_46994720

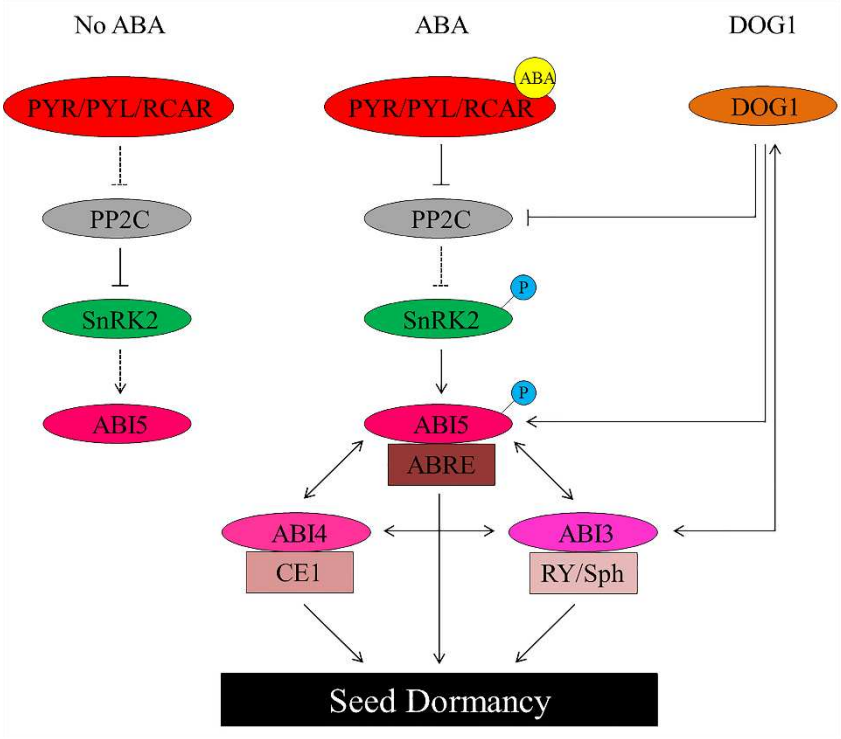

Figure 2. *ABA and DOG1 influence seed dormancy via independent pathways. Solid lines denote the valid pathway and dashed lines denote the invalid pathway. Arrows represent positive regulatory role, while bars represent negative regulatory role. PYR/PYL/RCAR, pyrabactin resistance1/pyrabactin-like/regulatory components of ABA receptors; PP2C, protein phosphatase 2C; SnRK2, SNF1-related protein kinase 2; ABI3, ABA insensitive 3; ABI4, ABA insensitive 4; ABI5, ABA insensitive 5. RY/Sph, RY/Sph element; CE1, coupling element 1; ABRE, ABA responsive element*

Transcription is a key step in seed ABA responsiveness. In addition to ABI5, other transcription factor types, including ABI3 (B3 type) and ABI4 (AP2 type), are critical for ABA responsiveness in seeds (Finkelstein et al., 2002; Dekkers and Bentsink, 2015; Shu et al., 2018b). One pioneering study has revealed that *abi3*, *abi4*, and *abi5* mutants exhibit an ABA-resistant germination phenotype and that these transcription factors seem to interact extensively (Söderman et al., 2000). These transcription factors appear to be conserved among different plant species and corresponding Arabidopsis orthologues are also present in monocots (Nambara et al., 2010). The ABI5/TRAB1, ABI4/*Zm*ABI4 and ABI3/VP1 transcription factors target the ABA-responsive element (ABRE), coupling element 1 (CE1), and RY/Sph repeat element (Nambara et al., 2010), respectively, which act together to activate ABA-mediated transcription and consequently control seed dormancy and germination (*Fig. 2*).

DOG1 functions independently of ABA in modulating the induction and maintenance of seed dormancy

The *DOG1* gene was first identified as a master quantitative trait locus for seed dormancy using recombinant inbred lines from a cross between the weakly dormant Arabidopsis ecotype Landsberg *erecta* (L*er*) and the strongly dormant Arabidopsis

http://www.aloki.hu ● ISSN 1589 1623 (Print) ● ISSN 1785 0037 (Online)
DOI: http://dx.doi.org/10.15666/aeer/1906_46994720

ecotype Cvi from the Cape Verde Islands (Alonso-Blanco et al., 2003). Both DOG1 and ABA have been found to modulate dormancy through independent pathways, although they have common downstream targets (Dekkers et al., 2016; Née et al., 2017a; Nishimura et al., 2018) (*Fig. 2*). In addition, DOG1 can control seed dormancy by an influence on microRNAs (miRNAs) miR156 and miR172 levels (Huo et al., 2016). Like the phytohormone ABA, DOG1 is essential for dormancy induction (Née et al., 2017a; Li et al., 2019); *dog1* mutants are thoroughly nondormant and do not display any obvious pleiotropic phenotypes, except for reduced seed longevity (Bentsink et al., 2006). The effects of a lack of either DOG1 or ABA cannot be rescued by increasing the contents of the other (Nakabayashi et al., 2012). The *DOG1* gene encodes a protein lacking domains with any known function and is localized in the nucleus (Bentsink et al., 2006; Nakabayashi et al., 2012; Dekkers and Bentsink, 2015). Importantly, it is expressed only in seeds and its expression increases during seed maturation (Bentsink et al., 2006).

The *DOG1* gene is highly conserved in the plant kingdom and homologs in diverse species have been shown to control seed dormancy (Ashikawa et al., 2014; Huo et al., 2016). *DOG1* genes have been described in dicots, including *Brassica rapa*, *Lepidium sativum*, and *Sisymbrium officinale* (Graeber et al., 2010, 2014; Carrillo-Barral et al., 2015). Increased *DOG1* expression was reported for ABA-treated *L. sativum* seeds, suggesting that *DOG1* acts in germination timing in this species (Graeber et al., 2010). In *S. officinale*, *SoDOG1* expression peaked at the onset of silique maturation, identical to that reported for Arabidopsis (Bentsink et al., 2006; Carrillo-Barral et al., 2015). In addition, *DOG1*-like genes have also been reported in monocots like *Oryza sativa*, *Triticum aestivum*, and *Hordeum vulgare* (Ashikawa et al., 2010; Sugimoto et al., 2010). Overexpression of a wheat *DOG1*-like gene increases the dormancy level in this species (Ashikawa et al., 2014). Interestingly, ectopic expression of *DOG1*-like genes from rice, wheat, and barley increases dormancy when expressed in Arabidopsis (Ashikawa et al., 2013). Moreover, high *DOG1* transcript levels during maturation may be involved in dormancy maintenance in imbibed *S. officinale* and Arabidopsis seeds (Nakabayashi et al., 2012; Carrillo-Barral et al., 2015). Hence, like ABA, DOG1 is also a key regulator of seed dormancy.

The roles of GA metabolism and signaling in modulating seed germination

The GAs stimulate seed germination in numerous plant species. Both GA content and sensitivity to GA are important for seed germination (Karssen and Lacka, 1986; Derkx and Karssen, 1993; Yamaguchi and Kamiya, 2002; Yamauchi et al., 2004; Ariizumi et al., 2013; Tuttle et al., 2015). The GA-deficient Arabidopsis mutant is non-germinating (Koornneef and Van der Veen, 1980). In agreement with this, GA deficiency in tomato results in non-germinating seeds (Koornneef et al., 1990). Semidominant *gai* mutants exhibit a GA-insensitive phenotype with reduced germination ability in both Arabidopsis (Koornneef et al., 1985; Derkx and Karssen, 1993) and grape (Boss and Thomas, 2002). Furthermore, imbibition leads to increased GA content as well as sensitivity to GA in both Arabidopsis and wheat seeds (Derkx and Karssen, 1993; Izydorczyk et al., 2017), indicating that increased GA content and sensitivity to GA are necessary for promoting seed germination. Therefore, the role of GA in seed germination appears to be conserved among plant species.

http://www.aloki.hu ● ISSN 1589 1623 (Print) ● ISSN 1785 0037 (Online)
DOI: http://dx.doi.org/10.15666/aeer/1906_46994720

GA metabolism

Gibberellin is the master plant hormone with a vital role in the regulation of seed dormancy and germination (Finch-Savage and Leubner-Metzger, 2006). The content of bioactive GAs in plant tissues is controlled by the equilibrium between its biosynthesis and inactivation (Yamaguchi, 2008; Tuan et al., 2018). The biosynthesis of GA is modulated primarily via reactions catalyzed by both GA 20-oxidase (GA20ox) and GA 3-oxidase (GA3ox), while GA inactivation is mainly regulated via reactions catalyzed by GA 2-oxidase (GA2ox) (Yamauchi et al., 2004; Yamaguchi, 2006; Tuan et al., 2018) (*Fig. 3*). All plant species examined to date have *GA20ox*, *GA3ox*, and *GA2ox* as multigene families, indicating that these genes play significant roles in controlling seed GA levels and, consequently, dormancy and germination.

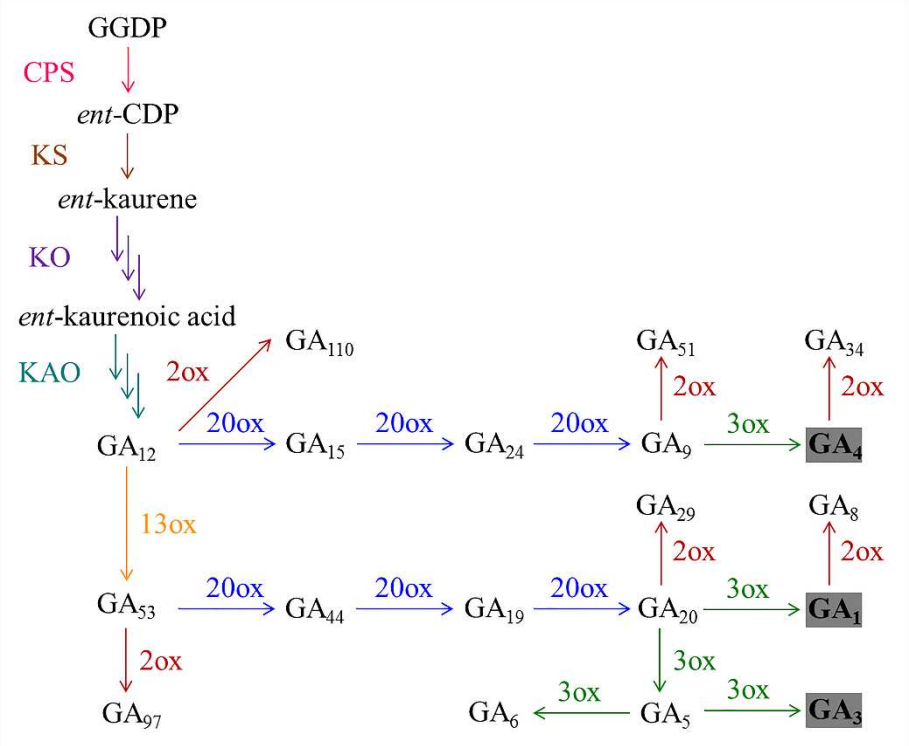

Figure 3. *The GA metabolism pathway. Bioactive GAs discovered in various plant species (highlighted dark grey) are exhibited (GA4 is considered to be the major bioactive form in Arabidopsis). GGDP, geranylgeranyl diphosphate; ent-CDP, ent-copalyl diphosphate; CPS, ent-copalyl diphosphate synthase; KS, ent-kaurene synthase; KO, ent-kaurene oxidase; KAO, ent-kaurenoic acid oxidase; 2ox, GA 2-oxidase; 3ox, GA 3-oxidase; 13ox, GA 13-oxidase; 20ox, GA 20-oxidase*

GA signaling

Gibberellin signaling is activated as soon as biologically active GA is perceived via its receptor GIBBERELLIN INSENSITIVE DWARF1 (GID1) (Nakajima et al., 2006) (*Fig. 4*). The GID1 receptor is triggered upon GA binding, permitting recognition of DELLA proteins. Responses to GA, including induction of seed germination, require GA-induced degradation of DELLA proteins, which function as negative GA signaling regulators (Salazar-Cerezo et al., 2018). Binding of GA to GID1 stimulates GA-GID1-

http://www.aloki.hu ● ISSN 1589 1623 (Print) ● ISSN 1785 0037 (Online)
DOI: http://dx.doi.org/10.15666/aeer/1906_46994720

DELLA complex formation (Murase et al., 2008), after which the complex is targeted for polyubiquitination through the F-box component of a Skp1-cullin-F-box (SCF) ubiquitin ligase, followed by DELLA degradation via the 26S proteasome (Dill et al., 2004; Fleet and Sun, 2005; Harberd et al., 2009; Gao et al., 2011; Wallner et al., 2016).

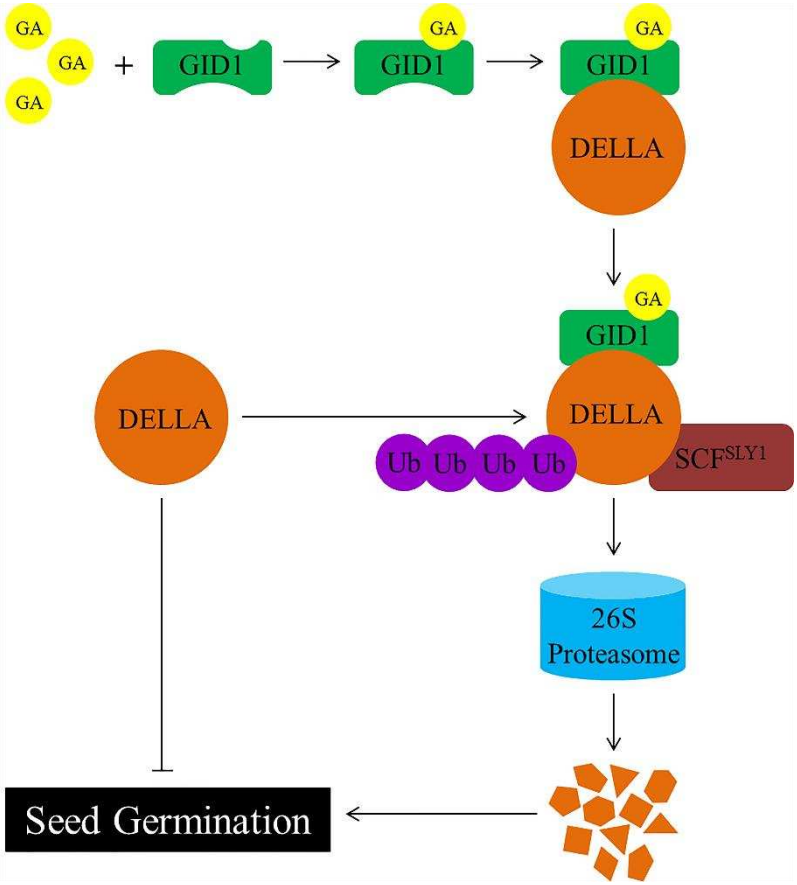

Figure 4. *The GA signaling pathway. A relief of inhibition induces seed germination. DELLA protein will be polyubiquitinated and then degraded through the ubiquitin-proteasome pathway. The arrows and bars denote the positive and negative regulation, respectively. GID1, gibberellin insensitive dwarf1; SCF(SLY1), Skp1-cullin-F-box; Ub, ubiquitin*

GA, ABA, and DOG1: focusing on the regulation of flowering time

Accurate time of flowering is pivotal and significant for the growth and survival of plants under various environmental conditions. ABA has been implicated in the control of flowering time (Riboni et al., 2013; Wang et al., 2013). Nevertheless, the contribution of ABA to the regulation of flowering time remains controversial since both positive and negative effects have been documented (Riboni et al., 2016; Shu et al., 2016a). ABA acts as a positive regulator of flowering by activating *FT* and *TWIN SISTER OF FT* (*TSF*) genes during long days (Riboni et al., 2013, 2016). Mutants of *ABA1* or *ABA2* are deficient in ABA production and either do not flower under short days, or display a late flowering phenotype under long days (Riboni et al., 2013, 2016). ABA promotes floral transition upstream of the *CONSTANS* (*CO*) transcriptional activation (Koops et al., 2011; Yoshida et al., 2014; Riboni et al., 2016). The ABA-mediated *FT* activation requires CO and repressing ABA signaling remarkably reduces *FT* expression with little impact on the

http://www.aloki.hu ● ISSN 1589 1623 (Print) ● ISSN 1785 0037 (Online)
DOI: http://dx.doi.org/10.15666/aeer/1906_46994720

accumulation of *CO* transcript (Riboni et al., 2016). ABA signaling thus influences CO activity and/or function rather than its transcript level (Riboni et al., 2016). ABI3 may have an effect on the expression of *FT* by inhibiting the CO activity via binding to the CCT domain (Kurup et al., 2000; Zhang et al., 2005). ABA negatively modulates ABI3 through causing the ubiquitination and consequent proteasome-dependent degradation (Zhang et al., 2005). It is likely that ABA might promote the accumulation of *FT* via CO, partly by the degradation of ABI3 (Conti, 2017). Interestingly, it is also found that the physical interaction between ABI3 and CO might enhance the CO function, and further facilitate *FT* upregulation (Tiwari et al., 2010). ABA positively regulates *ABI3* by promoting its transcription (Finkelstein, 2013). These results demonstrate that ABA might trigger ABI3 accumulation, and thereby stimulate *FT* expression by CO. The precise mechanism underlying the role of ABI3 in regulation of CO activity in the leaf warrants further exploration.

On the other hand, ABA is also implicated in modulating floral transition downstream of *FT*, but through a negative way. In coincidence with this, loss of function mutants of positive modulators for ABA signaling pathway, *abi3*, *abi4* and *abi5*, facilitate the floral transition, while overexpressing transgenic plants carrying these genes (*ABI3*, *ABI4* and *ABI5*) exhibit late flowering phenotypes (Kurup et al., 2000; Zhang et al., 2005; Foyer et al., 2012; Wang et al., 2013; Shu et al., 2016a). These phenotypes may possibly result from a different action mode of ABA in the shoot apical meristem (SAM). It is suggested that the negative effect of ABA on floral transition is played by *SUPPRESSOR OF OVEREXPRESSION OF CONSTANS 1* (*SOC1*) (Riboni et al., 2016). Numerous studies show that ABA directly activates *FLC* by *ABI3*, *ABI4* and *ABI5* (Wang et al., 2013; Shu et al., 2016a, 2018a). Consequently, ABA might reduce the *SOC1* levels through activating *FLC*, leading to a delay in flowering. It is *ABI4* and perhaps *ABI3* that might contribute to the modulation of *FLC* and *SOC1* during short days for *ABI5* does not play a role in floral transition during these conditions (Wang et al., 2013; Shu et al., 2016a, 2018a). Shu et al. (2018a) have proposed a working model for the effect of ABA on flowering. A moderate level of environmental stress (e.g., moderate drought), resulting in ABA accumulation, delays flowering until the stress abates, while a serious level of environmental stress (e.g., serious drought), eliciting marked ABA accumulation, stimulates floral transition to maximize reproductive success. Endogenous ABA accumulation (e.g., through transgene expression) also delayed flowering (Shu et al., 2018a).

The *DOG1* gene has been found to influence both germination and flowering time (Chiang et al., 2013; Huo et al., 2016). In Arabidopsis *dog1-3* mutants, there are no effects on flowering times under short- or long-day conditions (Huo et al., 2016). In contrast, suppression of expression of *DOG1* leads to early flowering in lettuce (Huo et al., 2016), as also occurs in wheat (Ashikawa et al., 2014). *DOG1* delays flowering time through indirectly inhibiting expression of *FT* in leaves and of *SOC1* in apical meristems (Huijser and Schmid, 2011; Spanudakis and Jackson, 2014; Huo et al., 2016). Recent studies delineate a regulatory mechanism between DOG1 and ABA in the context of seed dormancy. DOG1 increases ABA signaling possibly through modulating the transcription of *ABI5* and binding to ABI3 (Dekkers et al., 2016). It is obscure whether this pathway also operates in the SAM, and contributes to transcriptional inhibition of *SOC1* via *FLC* activation.

Gibberellin can regulate plant flowering time (Zhu et al., 2016; Gong et al., 2017; Shu et al., 2018b) and the positive effect of GA on floral transition has been extensively

http://www.aloki.hu ● ISSN 1589 1623 (Print) ● ISSN 1785 0037 (Online)
DOI: http://dx.doi.org/10.15666/aeer/1906_46994720

investigated and documented (Srikanth and Schmid, 2011; Ding et al., 2013; Hyun et al., 2016; Brambilla et al., 2017; Conti, 2017; Sawettalake et al., 2017). The lack of activity of any of the GA biosynthesis and signaling components can elicit defects in flowering (Wilson et al., 1992; Sun and Kamiya, 1994; Iuchi et al., 2007). Mutants defective in GA biosynthesis (*ga1*) display a moderate delay in flowering time during long days but never flower during short day conditions (Wilson et al., 1992). In agreement with the role of GA signaling in flowering, mutants impaired in GA perception (*gid1*), DELLA ubiquitination (*sly1*), or mutants with a dominant, non-degradable DELLA protein GAI (*gai*) show similar flowering phenotypes to the above-mentioned *ga1* biosynthetic mutants (Griffiths et al., 2006; Willige et al., 2007; Galvão et al., 2012; Porri et al., 2012). Conversely, mutants with loss of function alleles in *DELLA* genes, show early flowering phenotypes (Galvão et al., 2012). Increasing levels of GA facilitate DELLA degradation (Harberd, 2003; Fu et al., 2004), while reduced GA levels increase DELLA accumulation (King et al., 2001; Silverstone et al., 2001). DELLA proteins interact with FLC, which inhibits floral transition by directly repressing the transcriptional activation of floral genes *FT* and *SOC1* in the leaf and SAM, respectively (Li et al., 2016; Conti, 2017). In Arabidopsis, *PICKLE* (*PKL*) codes for an ATP-dependent chromodomain-helicase-DNA-binding domain (CHD3) chromatin remodeling enzyme (Zhang et al., 2008). PKL is essential for GA-promoted floral transition and plays a positive role in modulating GA signaling (Park et al., 2017). PKL recruits the Polycom Repressive Complex 2 (PRC2), which elevates histone mark H3K27me3 levels in *FLC*, thus contributing to the expression of *FT* and *SOC1* (Campos-Rivero et al., 2017). Floral transition is inhibited via DELLA and activated via PKL (Park et al., 2017). PKL is still needed to facilitate flowering in the lack of any functional DELLA (Park et al., 2017). Furthermore, DELLA opposes PKL function through direct protein-protein interaction (Zhang et al., 2014). Nevertheless, further studies are required to elucidate the detailed molecular mechanisms by which ABA, GA, and DOG1 modulate floral transition.

An interaction web consisting of GA, ABA, and DOG1 is implicated in the control of seed dormancy and flowering time

Recent studies have indicated that DOG1 stimulates the conversion of *MIR156* and *MIR172* transcripts to miR156 and miR172 through DOG1-stimulated expression of DICER complex components (Huo et al., 2016). miR156 binds specifically to SQUAMOSA PROMOTER BINDING PROTEIN-LIKE (SPL) transcripts and elicits their degradation, which delays or inhibits flowering (Huijser and Schmid, 2011; Spanudakis and Jackson, 2014). SPL3/4/5/9/15 have been shown to target and induce FT expression in leaves and SOC1, AGAMOUS LIKE 24 (AGL24), FRUITFULL (FUL), LEAFY (LFY), and APETALA1 (AP1) expression in apical meristems (Huijser and Schmid, 2011; Spanudakis and Jackson, 2014). SPL9/10/15 can increase miR172 levels by stimulating *MIR172* expression (Wang et al., 2009; Wu et al., 2009). miR172 promotes floral transition by inhibiting *AP2*-like floral repressor genes including *AP2*, *TARGET OF EAT1* (*TOE1*), *TOE2*, *TOE3*, *SCHLAFMUTZE* (*SMZ*), and *SCHNARCHZAPFEN* (*SNZ*) (Wu et al., 2009; Zhu and Helliwell, 2011) and can also stimulate seed germination (Huo et al., 2016). However, how miR172 achieves this regulatory role is still unclear.

The role of DOG1 in dormancy maintenance was found to be partially mediated via the regulation of GA metabolism through temperature-dependent changes in the expression of GA biosynthetic and inactivation genes (Kendall et al., 2011; Graeber et

http://www.aloki.hu ● ISSN 1589 1623 (Print) ● ISSN 1785 0037 (Online)
DOI: http://dx.doi.org/10.15666/aeer/1906_46994720

al., 2014). The lower levels of FT and TSF in *gid1agid1bgid1c* triple mutants conferred a late-flowering phenotype in long days (Galvão et al., 2012). The decreased *FT* and *TSF* expression results from the inhibition of *SPL3* expression by DELLA proteins in leaves and *SPL3*, *SPL4*, and *SPL5* in the shoot apex (Galvão et al., 2012; Yu et al., 2012). The DOG1 content is positively correlated with the degree of seed dormancy partly due to the effect of DOG1 on ABA levels in the maturation stage (Chiang et al., 2011; Nakabayashi et al., 2012). In addition, *DOG1* expression is directly modulated by ABA (Graeber et al., 2010, 2013). Several studies have demonstrated that DOG1 enhances ABA signaling and, consequently, seed dormancy, through its interaction with PP2C (Née et al., 2017a; Nishimura et al., 2018) and likely also by regulating *ABI5* expression and genetically interacting with *ABI3* (Dekkers et al., 2016); this suggests that the role of DOG1 in modulating seed dormancy is coordinated with ABA (Nakabayashi et al., 2012). Both ABI4 and ABI5 negatively modulate floral transition by directly promoting *FLC* transcription (Wang et al., 2013; Shu et al., 2016a), while FLC further inhibits the expression of the florigen gene, *FT* (Shu et al., 2018a). In addition, ABI4 negatively regulates GA biogenesis, which represses the floral transition (Blazquez et al., 1998; Achard et al., 2004; Shu et al., 2013). Similarly, both ABI5-GA-flowering and ABI3-FLC-FT-flowering cascades are proposed (Shu et al., 2018a). Furthermore, the ABI3-GA-flowering cascade is valuable hypothesis to identify (*Fig. 5*).

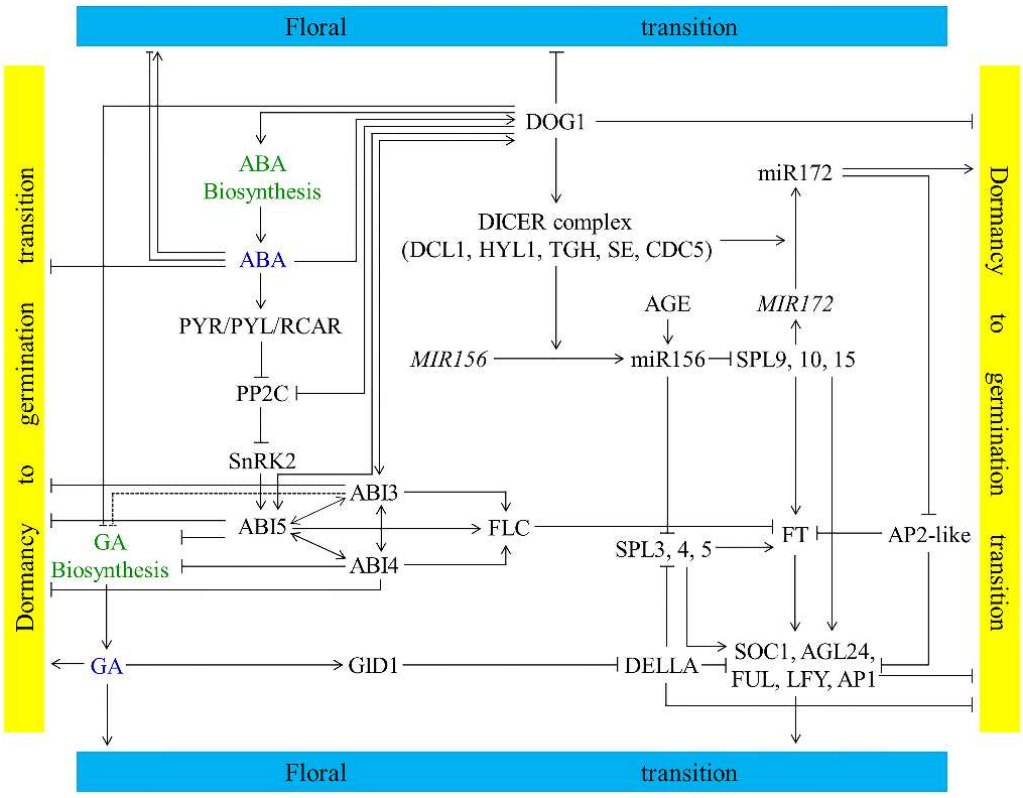

Figure 5. *Underlying interactions between GA, ABA and DOG1 in the control of seed dormancy and flowering time. Seed dormancy and flowering are strongly regulated by the content and signaling balance between ABA and GA. DOG1 impinges on this balance and functions in largely parallel to it, and common downstream targets exist between both pathways. ABA in turn directly promotes the expression of DOG1. Solid lines indicate the documented pathway, while dashed lines are proposed from current studies and require further exploration. Arrows represent positive regulation and bars represent negative regulation*

http://www.aloki.hu ● ISSN 1589 1623 (Print) ● ISSN 1785 0037 (Online)
DOI: http://dx.doi.org/10.15666/aeer/1906_46994720

In the flowering pathway, *FLC* inhibits the genes *FT* and *SOC1*, eliciting low *AP1* level and thereby impeding flowering (Chiang et al., 2009). The master flowering time gene *FLC* stimulates seed germination as well (Blair et al., 2017; Auge et al., 2018). Shared pathways of germination and flowering emerge, with *FLC*-mediated germination acting by *FT*, *SOC1*, and *AP1*, similar to what emerges in *FLC*-mediation of flowering (Chiang et al., 2009). *FLC* modulation of germination subsequently acts by the pathway of ABA catabolism (via *CYP707A2*) and GA anabolism (via *GA20ox1*) in germinating seeds (Chiang et al., 2009). Vital components in the same pathway are shared between germination and flowering modulation, but downstream difference may arise. More research on the shared pathways between germination and flowering is clearly required.

In summary, pleiotropy exists in the regulation of germination and flowering. Three important integrators for the modulation of floral transition, *FLC*, *FT*, and *SOC1*, also influence seed germination (Chiang et al., 2009; Chen et al., 2014; Blair et al., 2017). Hence, the three integrators are versatile genes that regulate both seed germination and floral transition. An interaction network consisting of ABA, GA, and DOG1 regulates the transition from seed dormancy to germination. In addition, the ABA, GA, and DOG1 interaction network further extends and converges on the *FLC*, *FT*, and *SOC1* integrator genes, which confers the function for the regulation of floral transition and seed germination. The three integrator genes are essential for the interaction network in the control of flowering and germination. Consequently, the ABA, GA, and DOG1 interaction network regulates not only floral transition but also the transition from seed dormancy to germination.

The influence of the environment on seed dormancy and flowering

Various environmental cues determine the proper timing for germination and flowering. Temperature is a particularly important environmental factor influencing seed dormancy. Low temperatures during seed maturation increase seed dormancy levels by increasing the expression of the ABA anabolic gene, *NCED4*, as well as the expression of *GA2ox6*, a GA catabolic gene (Kendall et al., 2011). The expression of *DOG1* is elevated and dormancy levels are enhanced under low temperatures during seed maturation (Chiang et al., 2011; Nakabayashi et al., 2012; Née et al., 2017b). Seed dormancy increases during the winter as soil temperature declines, while the expression of the *DOG1*, *NCED6* (ABA synthesis), and *GA2ox2* (GA catabolism) genes increases (Footitt et al., 2011). Thus, temperature affects seed dormancy both during seed maturation and in the soil via regulation of the ABA, GA, and DOG1 interaction network.

Light is another environmental factor that positively affects seed germination, inducing increased transcription of the GA biosynthetic genes, *GA3ox1* and *GA3ox2*, and enhancing the transcription of *CYP707A2*, an ABA catabolism gene (Cho et al., 2012). Previous studies have shown that blue light inhibits seed germination by promoting the expression of ABA synthesis genes and downregulating the transcription of GA anabolic genes (Gubler et al., 2008; Barrero et al., 2014). Red light and far-red light both control seed germination through changes in the levels of ABA and GA (Seo et al., 2006, 2009). Together, these observations imply that light affects seed germination at least partly by regulating the balance between ABA and GA. Whether light also influences *DOG1* expression and thereby seed germination is a worthwhile project for future investigation.

Temperature and light can also affect flowering time (Srikanth and Schmid, 2011; Cho et al., 2017). This poses the interesting question as to whether the same regulators control

http://www.aloki.hu ● ISSN 1589 1623 (Print) ● ISSN 1785 0037 (Online)
DOI: http://dx.doi.org/10.15666/aeer/1906_46994720

the ABA, GA, and DOG1 interaction network to modulate seed dormancy and flowering when temperature and light function as environmental factors.

Conclusion and outlook

The crosstalk between ABA, GA, and DOG1 in the regulation of seed dormancy and flowering is an interesting research area in plant molecular biology. Great advances have been made in our understanding of the molecular mechanisms involved in these processes using the model plant *Arabidopsis thaliana*. However, several open questions remain to be addressed.

First, plant hormones, including ethylene (ET), brassinosteroids (BRs), jasmonic acid (JA), salicylic acid (SA), cytokinins (CTKs), and strigolactones (SLs), modulate seed dormancy and flowering, most likely by regulating the balance between ABA and GA. Nevertheless, the underlying mechanisms involved in this hormonal balance remain largely unclear. Consequently, it would be worthwhile to establish a metabolic and signaling network for these phytohormones to further elucidate the mechanisms regulating the ABA/GA balance as well as the crosstalk between ABA, GA, and DOG1.

Second, it is necessary to obtain temporal and spatial expression information for the distinct parameters and factors that regulate seed dormancy and/or flowering through their effects on the interaction between ABA, GA, and DOG1, as only this type of information can be used to model the regulation of seed dormancy and/or flowering. However, we still know little about these parameters or the expression pattern of these factors, including those of NCED, CYP707A, GA20ox, GA3ox, GA2ox, DOG1, ABI, FLC, FT, SOC1, and AP1 (*Figs. 1, 3* and *5*), that act as the central components in the interaction between ABA, GA, and DOG1 and have a crucial function in seed germination and/or flowering.

Third, although ABA has been indicated to control floral transition in both a positive and negative manner, the detailed mechanisms involved, particularly the distinction at the origin of ABA increases caused by moderate or serious environmental stresses and genetic changes, require further study. In addition, ABA and GA act synergistically to positively modulate flowering when ABA plays a positive role in floral transition. However, understanding of the crosstalk between ABA, GA, and DOG1 under this condition is also largely elusive.

Finally, the genes implicated in other phase transitions may also be involved in controlling the transition from dormancy to germination, and genes acting at the seed stage can also regulate subsequent life stages. Consequently, it is possible that the pathway involved in the transition from dormancy to germination is shared with other phase transitions. The identification of a common regulatory web based on ABA, GA, and DOG1 would be a very worthwhile project. Altogether, these remaining scientific questions associated with ABA, GA, and DOG1 are worthy of further investigation.

Acknowledgements. This work was supported by the funding from National Natural Science Foundation of China (No. 31971647 and 31570621). We are grateful to Zhifu Guo and members of our lab for valuable discussion about, and anonymous reviewers for highly constructive comments on, the manuscript.

http://www.aloki.hu ● ISSN 1589 1623 (Print) ● ISSN 1785 0037 (Online)
DOI: http://dx.doi.org/10.15666/aeer/1906_46994720

REFERENCES

[1] Achard, P., Herr, A., Baulcombe, D. C., Harberd, N. P. (2004): Modulation of floral development by a gibberellin-regulated microRNA. – Development 131: 3357-3365.
[2] Ali-Rachedi, S., Bouinot, D., Wagner, M. H., Bonnet, M., Sotta, B., Grappin, P., Jullien, M. (2004): Changes in endogenous abscisic acid levels during dormancy release and maintenance of mature seeds: Studies with the Cape Verde Islands ecotype, the dormant model of *Arabidopsis thaliana*. – Planta 219: 479-488.
[3] Alonso-Blanco, C., Bentsink, L., Hanhart, C. J., Blankestijn-de Vries, H., Koornneef, M. (2003): Analysis of natural allelic variation at seed dormancy loci of *Arabidopsis thaliana*. – Genetics 164: 711-729.
[4] Ariizumi, T., Hauvermale, A. L., Nelson, S. K., Hanada, A., Yamaguchi, S., Steber, C. M. (2013): Lifting DELLA repression of Arabidopsis seed germination by nonproteolytic gibberellin signalling. – Plant Physiol. 162: 2125-2139.
[5] Ashikawa, I., Abe, F., Nakamura, S. (2010): Ectopic expression of wheat and barley DOG1-like genes promotes seed dormancy in Arabidopsis. – Plant Sci. 179: 536-542.
[6] Ashikawa, I., Abe, F., Nakamura, S. (2013): *DOG1*-like genes in cereals: investigation of their function by means of ectopic expression in Arabidopsis. – Plant Sci. 208: 1-9.
[7] Ashikawa, I., Mori, M., Nakamura, S., Abe, F. (2014): A transgenic approach to controlling wheat seed dormancy level by using Triticeae DOG1-like genes. – Transgenic Res. 23: 621-629.
[8] Auge, G. A., Blair, L. K., Karediya, A., Donohue, K. (2018): The autonomous flowering-time pathway pleiotropically regulates seed germination in *Arabidopsis thaliana*. – Ann. Bot. 121: 183-191.
[9] Barrero, J. M., Millar, A. A., Griffiths, J., Czechowski, T., Scheible, W. R., Udvardi, M., Reid, J. B., Ross, J. J., Jacobsen, J. V., Gubler, F. (2010): Gene expression profiling identifies two regulatory genes controlling dormancy and ABA sensitivity in Arabidopsis seeds. – Plant J. 61: 611-622.
[10] Barrero, J. M., Downie, A. B., Xu, Q., Gubler, F. (2014): A role for barley CRYPTOCHROME1 in light regulation of grain dormancy and germination. – Plant Cell 26: 1094-1104.
[11] Baskin, J. M., Baskin, C. C. (2004): A classifcation system for seed dormancy. – Seed Sci. Res. 14: 1-16.
[12] Bentsink, L., Jowett, J., Hanhart, C. J., Koornneef, M. (2006): Cloning of DOG1, a quantitative trait locus controlling seed dormancy in Arabidopsis. – Proc. Natl. Acad. Sci. USA 103: 17042-17047.
[13] Bewley, J. D. (1997): Seed germination and dormancy. – Plant Cell 9: 1055-1066.
[14] Bewley, J. D., Bradford, K. J., Hilhorst, H. W., Nonogaki, H. (2013): Seeds: Physiology of development, germination and dormancy. – 3rd ed., Springer, New York.
[15] Blair, L., Auge, G., Donohue, K. (2017): Effect of *FLOWERING LOCUS C* on seed germination depends on dormancy. – Funct. Plant Biol. 44: 493-506.
[16] Blazquez, M. A., Green, R., Nilsson, O., Sussman, M. R., Weigel, D. (1998): Gibberellins promote flowering of Arabidopsis by activating the LEAFY promoter. – Plant Cell 10: 791-800.
[17] Boss, P. K., Thomas, M. R. (2002): Association of dwarfism and floral induction with a grape 'green revolution' mutation. – Nature 416: 847-850.
[18] Brambilla, V., Gomez-Ariza, J., Cerise, M., Fornara, F. (2017): The importance of being on time: regulatory networks controlling photoperiodic flowering in cereals. – Front. Plant Sci. 8: 665.
[19] Buijs, G., Kodde, J., Groot, S. P., Bentsink, L. (2018): Seed dormancy release accelerated by elevated partial pressure of oxygen is associated with *DOG* loci. – J. Exp. Bot. 69: 3601-3608.

http://www.aloki.hu ● ISSN 1589 1623 (Print) ● ISSN 1785 0037 (Online)
DOI: http://dx.doi.org/10.15666/aeer/1906_46994720

[20] Burghardt, L. T., Metcalf, C. J., Wilczek, A. M., Schmitt, J., Donohue, K. (2015): Modeling the influence of genetic and environmental variation on the expression of plant life cycles across landscapes. – Am. Nat. 185: 212-227.
[21] Campos-Rivero, G., Osorio-Montalvo, P., Sánchez-Borges, R., Us-Camas, R., Duarte-Aké, F., De-la-Peña, C. (2017): Plant hormone signaling in flowering: An epigenetic point of view. – J. Plant Physiol. 214: 16-27.
[22] Carrillo-Barral, N., Matilla, A. J., García-Ramas, C., Rodríguez-Gacio Mdel, C. (2015): ABA-stimulated *SoDOG1* expression is after-ripening inhibited during early imbibition of germinating *Sisymbrium officinale* seeds. – Physiol. Plant. 155: 457-471.
[23] Chen, M., MacGregor, D. R., Dave, A., Florance, H., Moore, K., Paszkiewicz, K., Smirnoff, N., Graham, I. A., Penfield, S. (2014): Maternal temperature history activates Flowering Locus T in fruits to control progeny dormancy according to time of year. – Proc. Natl. Acad. Sci. USA 111: 18787-18792.
[24] Chiang, G. C., Barua, D., Kramer, E. M., Amasino, R. M., Donohue, K. (2009): Major flowering time gene, *FLOWERING LOCUS C*, regulates seed germination in *Arabidopsis thaliana*. – Proc. Natl. Acad. Sci. USA 106: 11661-11666.
[25] Chiang, G. C., Bartsch, M., Barua, D., Nakabayashi, K., Debieu, M., Kronholm, I., Koornneef, M., Soppe, W. J., Donohue, K., De Meaux, J. (2011): DOG1 expression is predicted by the seed-maturation environment and contributes to geographical variation in germination in *Arabidopsis thaliana*. – Mol. Ecol. 20: 3336-3349.
[26] Chiang, G. C., Barua, D., Dittmar, E., Kramer, E. M., de Casas, R. R., Donohue, K. (2013): Pleiotropy in the wild: the dormancy gene *DOG1* exerts cascading control on life cycles. – Evolution 67: 883-893.
[27] Cho, J. N., Ryu, J. Y., Jeong, Y. M., Park, J., Song, J. J., Amasino, R. M., Noh, B., Noh, Y. S. (2012): Control of seed germination by lightinduced histone arginine demethylation activity. – Dev. Cell 22: 736-748.
[28] Cho, L. H., Yoon, J., An, G. (2017): The control of flowering time by environmental factors. – Plant J. 90: 708-719.
[29] Chono, M., Matsunaka, H., Seki, M., Fujita, M., Kiribuchi-Otobe, C., Oda, S., Kojima, H., Kobayashi, D., Kawakami, N. (2013): Isolation of a wheat (*Triticum aestivum* L.) mutant in ABA 8'-hydroxylase gene: effect of reduced ABA catabolism on germination inhibition under field condition. – Breed. Sci. 63: 104-115.
[30] Conti, L. (2017): Hormonal control of the floral transition: can one catch them all. – Dev. Biol. 430: 288-301.
[31] Cutler, S., Ghassemian, M., Bonetta, D., Cooney, S., McCourt, P. (1996): A protein farnesyl transferase involved in abscisic acid signal transduction in *Arabidopsis*. – Science 273: 1239-1241.
[32] Cutler, S. R., Rodriguez, P. L., Finkelstein, R. R., Abrams, S. R. (2010): Abscisic acid: emergence of a core signaling network. – Annu. Rev. Plant Biol. 61: 651-679.
[33] Dekkers, B. J., Bentsink, L. (2015): Regulation of seed dormancy by abscisic acid and *DELAY OF GERMINATION 1*. – Seed Sci. Res. 25: 82-98.
[34] Dekkers, B. J., He, H., Hanson, J., Willems, L. A., Jamar, D. C., Cueff, G., Rajjou, L., Hilhorst, H. W., Bentsink, L. (2016): The Arabidopsis *DELAY OF GERMINATION 1* gene affects *ABSCISIC ACID INSENSITIVE 5 (ABI5)* expression and genetically interacts with ABI3 during Arabidopsis seed development. – Plant J. 85: 451-465.
[35] Derkx, M. P., Karssen, C. M. (1993): Effects of light and temperature on seed dormancy and gibberellin-stimulated germination in *Arabidopsis thaliana*: studies with gibberellin-deficient and -insensitive mutants. – Physiol. Plant. 89: 360-368.
[36] Dill, A., Thomas, S. G., Hu, J., Steber, C. M., Sun, T. P. (2004): The Arabidopsis F-box protein SLEEPY1 targets gibberellin signaling repressors for gibberellin-induced degradation. – Plant Cell 16: 1392-1405.

http://www.aloki.hu ● ISSN 1589 1623 (Print) ● ISSN 1785 0037 (Online)
DOI: http://dx.doi.org/10.15666/aeer/1906_46994720

[37] Ding, L., Wang, Y., Yu, H. (2013): Overexpression of *DOSOC1*, an ortholog of Arabidopsis *SOC1*, promotes flowering in the orchid *Dendrobium* Chao Parya Smile. – Plant Cell Physiol. 54: 595-608.
[38] Finch-Savage, W. E., Leubner-Metzger, G. (2006): Seed dormancy and the control of germination. – New Phytol. 171: 501-523.
[39] Finch-Savage, W. E., Cadman, C. S., Toorop, P. E., Lynn, J. R., Hilhorst, H. W. (2007): Seed dormancy release in Arabidopsis Cvi by dry after-ripening, low temperature, nitrate and light shows common quantitative patterns of gene expression directed by environmentally specific sensing. – Plant J. 51: 60-78.
[40] Finkelstein, R. (2013): Abscisic acid synthesis and response. – Arabidopsis Book 11: e0166.
[41] Finkelstein, R. R., Gampala, S. S., Rock, C. D. (2002): ABA signaling in seeds and seedlings. – Plant Cell 14: S15-S45.
[42] Finkelstein, R., Reeves, W., Ariizumi, T., Steber, C. (2008): Molecular aspects of seed dormancy. – Annu. Rev. Plant Biol. 59: 387-415.
[43] Fleet, C. M., Sun, T. P. (2005): A DELLAcate balance: the role of gibberellin in plant morphogenesis. – Curr. Opin. Plant Biol. 8: 77-85.
[44] Footitt, S., Douterelo-Soler, I., Clay, H., Finch-Savage, W. E. (2011): Dormancy cycling in *Arabidopsis* seeds is controlled by seasonally distinct hormone-signaling pathways. – Proc. Natl. Acad. Sci. USA 108: 20236-20241.
[45] Foyer, C. H., Kerchev, P. I., Hancock, R. D. (2012): The ABA-INSENSITIVE-4 (ABI4) transcription factor links redox, hormone and sugar signaling pathways. – Plant Signal. Behav. 7: 276-281.
[46] Frey, A., Effroy, D., Lefebvre, V., Seo, M., Perreau, F., Berger, A., Sechet, J., To, A., North, H. M., Marion-Poll, A. (2011): Epoxycarotenoid cleavage by NCED5 fine-tunes ABA accumulation and affects seed dormancy and drought tolerance with other NCED family members. – Plant J. 70: 501-512.
[47] Fu, X., Richards, D. E., Fleck, B., Xie, D., Burton, N., Harberd, N. P. (2004): The Arabidopsis mutant sleepy1gar2-1 protein promotes plant growth by increasing the affinity of the SCFSLY1 E3 ubiquitin ligase for DELLA protein substrates. – Plant Cell 16: 1406-1418.
[48] Galvão, V. C., Horrer, D., Küttner, F., Schmid, M. (2012): Spatial control of flowering by DELLA proteins in *Arabidopsis thaliana*. – Development 139: 4072-4082.
[49] Gao, X. H., Xiao, S. L., Yao, Q. F., Wang, Y. J., Fu, X. D. (2011): An updated GA signaling 'relief of repression' regulatory model. – Mol. Plant 4: 601-606.
[50] Gong, X., Shen, L., Peng, Y. Z., Gan, Y., Yu, H. (2017): DNA topoisomerase Ialpha affects the floral transition. – Plant Physiol. 173: 642-654.
[51] Gosti, F., Beaudoin, N., Serizet, C., Webb, A. A., Vartanian, N., Giraudat, J. (1999): ABI1 protein phosphatase 2C is a negative regulator of abscisic acid signaling. – Plant Cell 11: 1897-1909.
[52] Graeber, K., Linkies, A., Müller, K., Wunchova, A., Rott, A., Leubner-Metzger, G. (2010): Cross-species approaches to seed dormancy and germination: conservation and biodiversity of ABA-regulated mechanism and the Brassicaceae DOG1 gene. – Plant Mol. Biol. 73: 67-87.
[53] Graeber, K., Voegele, A., Büttner-Mainik, A., Sperber, K., Mummenhoff, K., Leubner-Metzger, G. (2013): Spatiotemporal seed development analysis provides insight into primary dormancy induction and evolution of the *Lepidium DELAY OF GERMINATION1* genes. – Plant Physiol. 161: 1903-1917.
[54] Graeber, K., Linkies, A., Steinbrecher, T., Mummenhoff, K., Tarkowská, D., Turečková, V., Ignatz, M., Sperber, K., Voegele, A., De Jong, H., Urbanová, T., Strnad, M., Leubner-Metzger, G. (2014): *DELAY OF GERMINATION 1* mediates a conserved coat-dormancy mechanism for the temperature- and gibberellin-dependent control of seed germination. – Proc. Natl. Acad. Sci. USA 111: E3571-E3580.

http://www.aloki.hu ● ISSN 1589 1623 (Print) ● ISSN 1785 0037 (Online)
DOI: http://dx.doi.org/10.15666/aeer/1906_46994720

[55] Grappin, P., Bouinot, D., Sotta, B., Miginiac, E., Jullien, M. (2000): Control of seed dormancy in *Nicotiana plumbaginifolia*: post-imbibition abscisic acid synthesis imposes dormancy maintenance. – Planta 210: 279-285.
[56] Griffiths, J., Murase, K., Rieu, I., Zentella, R., Zhang, Z. L., Powers, S. J., Gong, F., Phillips, A. L., Hedden, P., Sun, T. P., Thomas, S. G. (2006): Genetic characterization and functional analysis of the GID1 gibberellin receptors in Arabidopsis. – Plant Cell 18: 3399-3414.
[57] Groot, S. P., Karssen, C. M. (1992): Dormancy and germination of abscisic acid-deficient tomato seeds studies with the *sitiens* mutant. – Plant Physiol. 99: 952-958.
[58] Gubler, F., Hughes, T., Waterhouse, P., Jacobsen, J. (2008): Regulation of dormancy in barley by blue light and after-ripening: effects on abscisic acid and gibberellin metabolism. – Plant Physiol. 147: 886-896.
[59] Harberd, N. P. (2003): Relieving DELLA restraint. – Science 299: 1853-1854.
[60] Harberd, N. P., Belfield, E., Yasumura, Y. (2009): The angiosperm gibberellin-GID1-DELLA growth regulatory mechanism: how an "inhibitor of an inhibitor" enables flexible response to fluctuating environments. – Plant Cell 21: 1328-1339.
[61] Holdsworth, M. J., Bentsink, L., Soppe, W. J. (2008): Molecular networks regulating Arabidopsis seed maturation, after-ripening, dormancy and germination. – New Phytol. 179: 33-54.
[62] Huijser, P., Schmid, M. (2011): The control of developmental phase transitions in plants. – Development 138: 4117-4129.
[63] Huo, H., Wei, S., Bradford, K. J. (2016): *DELAY OF GERMINATION1* (*DOG1*) regulates both seed dormancy and flowering time through microRNA pathways. – Proc. Natl. Acad. Sci. USA 113: E2199-E2206.
[64] Hyun, Y., Richter, R., Vincent, C., Martinez-Gallegos, R., Porri, A., Coupland, G. (2016): Multi-layered regulation of SPL15 and cooperation with SOC1 integrate endogenous flowering pathways at the *Arabidopsis* shoot meristem. – Dev. Cell 37: 254-266.
[65] Iuchi, S., Suzuki, H., Kim, Y. C., Iuchi, A., Kuromori, T., Ueguchi-Tanaka, M., Asami, T., Yamaguchi, I., Matsuoka, M., Kobayashi, M., Nakajima, M. (2007): Multiple loss-of-function of *Arabidopsis* gibberellin receptor AtGID1s completely shuts down a gibberellin signal. – Plant J. 50: 958-966.
[66] Izydorczyk, C., Nguyen, T. N., Jo, S., Son, S., Tuan, P. A., Ayele, B. T. (2017): Spatiotemporal modulation of abscisic acid and gibberellin metabolism and signaling mediates the effects of suboptimal and supraoptimal temperatures on seed germination in wheat (*Triticum aestivum* L.). – Plant Cell Environ. 41: 1022-1037.
[67] Karssen, C. M., Lacka, E. (1986): A revision of the hormone balance theory of seed dormancy. – In: Bopp, M. (ed.) Plant growth substances. Springer-Verlag, Berlin, pp. 315-323.
[68] Kendall, S. L., Hellwege, A., Marriot, P., Whalley, C., Graham, I. A., Penfield, S. (2011): Induction of dormancy in *Arabidopsis* summer annuals requires parallel regulation of *DOG1* and hormone metabolism by low temperature and CBF transcription factors. – Plant Cell 23: 2568-2580.
[69] King, K. E., Moritz, T., Harberd, N. P. (2001): Gibberellins are not required for normal stem growth in *Arabidopsis thaliana* in the absence of GAI and RGA. – Genetics 159: 767-776.
[70] Koops, P., Pelser, S., Ignatz, M., Klose, C., Marrocco-Selden, K., Kretsch, T. (2011): EDL3 is an F-box protein involved in the regulation of abscisic acid signalling in Arabidopsis thaliana. – J. Exp. Bot. 62: 5547-5560.
[71] Koornneef, M., Van der Veen, J. H. (1980): Induction and analysis of gibberellin-sensitive mutants in *Arabidopsis thaliana* (L) Heynh. – Theor. Appl. Genet. 58: 257-263.
[72] Koornneef, M., Reuling, G., Karssen, C. M. (1984): The isolation and characterization of abscisic acid insensitive mutants of Arabidopsis thaliana. – Physiol. Plant. 61: 377-383.

http://www.aloki.hu ● ISSN 1589 1623 (Print) ● ISSN 1785 0037 (Online)
DOI: http://dx.doi.org/10.15666/aeer/1906_46994720

[73] Koornneef, M., Eigersma, A., Hanhart, C. J., Van loenen-Martinet, E. P., Van Rijn, L., Zeevaart, J. A. (1985): A gibberellin insensitive mutant of *Arabidopsis thaliana*. – Physiol. Plant. 65: 33-39.
[74] Koornneef, M., Bosma, T. D., Hanhart, C. J., Van der Veen, J. H., Zeevaart, J. A. (1990): The isolation and characterization of gibberellin-deficient mutants in tomato. – Theor. Appl. Genet. 80: 852-857.
[75] Kurup, S., Jones, H. D., Holdsworth, M. J. (2000): Interactions of the developmental regulator ABI3 with proteins identified from developing Arabidopsis seeds. – Plant J. 21: 143-155.
[76] Kushiro, T., Okamoto, M., Nakabayashi, K., Yamagishi, K., Kitamura, S., Asami, T., Hirai, N., Koshiba, T., Kamiya, Y., Nambara, E. (2004): The *Arabidopsis* cytochrome P450 CYP707A encodes ABA 8'-hydroxylases: key enzymes in ABA catabolism. – EMBO J. 23: 1647-1656.
[77] Lee, H. G., Lee, K., Seo, P. J. (2015): The *Arabidopsis* MYB96 transcription factor plays a role in seed dormancy. – Plant Mol. Biol. 87: 371-381.
[78] Li, M., An, F., Li, W., Ma, M., Feng, Y., Zhang, X., Guo, H. (2016): DELLA proteins interact with FLC to repress flowering transition. – J. Integr. Plant Biol. 58: 642-655.
[79] Li, X. Y., Chen, T. T., Li, Y., Wang, Z., Cao, H., Chen, F. Y., Li, Y., Soppe, W. J., Li, W. L., Liu, Y. X. (2019): ETR1/RDO3 regulates seed dormancy by relieving the inhibitory effect of the ERF12-TPL complex on *DELAY OF GERMINATION 1* expression. – Plant Cell 31: 832-847.
[80] Ma, Y., Szostkiewicz, I., Korte, A., Moes, D., Yang, Y., Christmann, A., Grill, E. (2009): Regulators of PP2C phosphatase activity function as abscisic acid sensors. – Science 324: 1064-1068.
[81] Martinez-Andujar, C., Ordiz, M. I., Huang, Z., Nonogaki, M., Beachy, R. N., Nonogaki, H. (2011): Induction of 9-cis-epoxycarotenoid dioxygenase in *Arabidopsis thaliana* seeds enhances seed dormancy. – Proc. Natl. Acad. Sci. USA 108: 17225-17229.
[82] Matakiadis, T., Alboresi, A., Jikumaru, Y., Tatematsu, K., Pichon, O., Renou, J. P., Kamiya, Y., Nambara, E., Truong, H. N. (2009): The Arabidopsis abscisic acid catabolic gene CYP707A2 plays a key role in nitrate control of seed dormancy. – Plant Physiol. 149: 949-960.
[83] Murase, K., Hirano, Y., Sun, T. P., Hakoshima, T. (2008): Gibberellin-induced DELLA recognition by the gibberellin receptor GID1. – Nature 456: 459-463.
[84] Nakabayashi, K., Bartsch, M., Xiang, Y., Miatton, E., Pellengahr, S., Yano, R., Seo, M., Soppe, W. J. (2012): The time required for dormancy release in *Arabidopsis* is determined by DELAY OF GERMINATION1 protein levels in freshly harvested seeds. – Plant Cell 24: 2826-2838.
[85] Nakajima, M., Shimada, A., Takashi, Y., Kim, Y. C., Park, S. H., Ueguchi-Tanaka, M., Suzuki, H., Katoh, E., Iuchi, S., Kobayashi, M., Maeda, T., Matsuoka, M., Yamaguchi, I. (2006): Identification and characterization of Arabidopsis gibberellin receptors. – Plant J. 46: 880-889.
[86] Nakashima, K., Fujita, Y., Kanamori, N., Katagiri, T., Umezawa, T., Kidokoro, S., Maruyama, K., Yoshida, T., Ishiyama, K., Kobayashi, M., Shinozaki, K., Yamaguchi-Shinozaki, K. (2009): Three Arabidopsis SnRK2 protein kinases, SRK2D/SnRK2.2, SRK2E/SnRK2.6/OST1 and SRK2I/SnRK2.3, involved in ABA signaling are essential for the control of seed development and dormancy. – Plant Cell Physiol. 50: 1345-1363.
[87] Nambara, E., Marion-Poll, A. (2005): Abscisic acid biosynthesis and catabolism. – Annu. Rev. Plant Biol. 56: 165-185.
[88] Nambara, E., Okamoto, M., Tatematsu, K., Yano, R., Seo, M., Kamiya, Y. (2010): Abscisic acid and the control of seed dormancy and germination. – Seed Sci. Res. 20: 55-67.
[89] Née, G., Kramer, K., Nakabayashi, K., Yuan, B., Xiang, Y., Miatton, E., Finkemeier, I., Soppe, W. J. (2017a): DELAY OF GERMINATION1 requires PP2C phosphatases of the ABA signalling pathway to control seed dormancy. – Nat. Commun. 8: 72.

http://www.aloki.hu ● ISSN 1589 1623 (Print) ● ISSN 1785 0037 (Online)
DOI: http://dx.doi.org/10.15666/aeer/1906_46994720

[90] Née, G., Xiang, Y., Soppe, W. J. (2017b): The release of dormancy, a wake-up call for seeds to germinate. – Curr. Opin. Plant Biol. 35: 8-14.
[91] Ng, L. M., Melcher, K., Teh, B. T., Xu, H. E. (2014): Abscisic acid perception and signaling: structural mechanisms and applications. – Acta Pharmacol. Sin. 35: 567-584.
[92] Nishimura, N., Tsuchiya, W., Moresco, J. J., Hayashi, Y., Satoh, K., Kaiwa, N., Irisa, T., Kinoshita, T., Schroeder, J. I., Yates, J. R., Hirayama, T., Yamazaki, T. (2018): Control of seed dormancy and germination by DOG1-AHG1 PP2C phosphatase complex via binding to heme. – Nat. Commun. 9: 2132.
[93] Nonogaki, M., Sall, K., Nambara, E., Nonogaki, H. (2014): Amplification of ABA biosynthesis and signaling through a positive feedback mechanism in seeds. – Plant J. 78: 527-539.
[94] North, H., Baud, S., Debeaujon, I., Dubos, C., Dubreucq, B., Grappin, P., Jullien, M., Lepiniec, L., Marion-Poll, A., Miquel, M., Rajjou, L., Routaboul, J. M., Caboche, M. (2010): Arabidopsis seed secrets unravelled after a decade of genetic and omics-driven research. – Plant J. 61: 971-981.
[95] Park, S. Y., Fung, P., Nishimura, N., Jensen, D. R., Fujii, H., Zhao, Y., Lumba, S., Santiago, J., Rodrigues, A., Chow, T. F., Alfred, S. E., Bonetta, D., Finkelstein, R., Provart, N. J., Desveaux, D., Rodriguez, P. L., McCourt, P., Zhu, J. K., Schroeder, J. I., Volkman, B. F., Cutler, S. R. (2009): Abscisic acid inhibits type 2C protein phosphatases via the PYR/PYL family of START proteins. – Science 324: 1068-1071.
[96] Park, J., Oh, D. H., Dassanayake, M., Nguyen, K. T., Ogas, J., Choi, G., Sun, T. P. (2017): Gibberellin signaling requires chromatin remodeler PICKLE to promote vegetative growth and phase transitions. – Plant Physiol. 173: 1463-1474.
[97] Porri, A., Torti, S., Romera-Branchat, M., Coupland, G. (2012): Spatially distinct regulatory roles for gibberellins in the promotion of flowering of Arabidopsis under long photoperiods. – Development 139: 2198-2209.
[98] Post, E. S., Pedersen, C., Wilmers, C. C., Forchhammer, M. C. (2008): Phenological sequences reveal aggregate life-history response to climatic warming. – Ecology 89: 363-370.
[99] Riboni, M., Galbiati, M., Tonelli, C., Conti, L. (2013): GIGANTEA enables drought escape response via abscisic acid-dependent activation of the florigens and SUPPRESSOR OF OVEREXPRESSION OF CONSTANS1. – Plant Physiol. 162: 1706-1719.
[100] Riboni, M., Test, A. R., Galbiati, M., Tonelli, C., Conti, L. (2016): ABA-dependent control of *GIGANTEA* signalling enables drought escape via up-regulation of *FLOWERING LOCUS T* in *Arabidopsis thaliana*. – J. Exp. Bot. 67: 6309-6322.
[101] Saito, S., Hirai, N., Matsumoto, C., Ohigashi, H., Ohta, D., Sakata, K., Mizutani, M. (2004): Arabidopsis *CYP707As* encode (+)-abscisic acid 8'-hydroxylase, a key enzyme in the oxidative catabolism of abscisic acid. – Plant Physiol. 134: 1439-1449.
[102] Salazar-Cerezo, S., Martínez-Montiel, N., García-Sánchez, J., Pérez-Y-Terrón, R., Martínez-Contreras, R. D. (2018): Gibberellin biosynthesis and metabolism: A convergent route for plants, fungi and bacteria. – Microbiol. Res. 208: 85-98.
[103] Sawettalake, N., Bunnag, S., Wang, Y., Shen, L., Yu, H. (2017): DOAP1 promotes flowering in the orchid *Dendrobium* Chao Praya Smile. – Front. Plant Sci. 8: 400.
[104] Schwartz, S. H., Qin, X., Zeevaart, J. A. (2003): Elucidation of the indirect pathway of abscisic acid biosynthesis by mutants, genes, and enzymes. – Plant Physiol. 131: 1591-1601.
[105] Seo, M., Hanada, A., Kuwahara, A., Endo, A., Okamoto, M., Yamauchi, Y., North, H., Marion-Poll, A., Sun, T. P., Koshiba, T., Kamiya, Y., Yamaguchi, S., Nambara, E. (2006): Regulation of hormone metabolism in Arabidopsis seeds: phytochrome regulation of abscisic acid metabolism and abscisic acid regulation of gibberellin metabolism. – Plant J. 48: 354-366.
[106] Seo, M., Nambara, E., Choi, G., Yamaguchi, S. (2009): Interaction of light and hormone signals in germinating seeds. – Plant Mol. Biol. 69: 463-472.

http://www.aloki.hu ● ISSN 1589 1623 (Print) ● ISSN 1785 0037 (Online)
DOI: http://dx.doi.org/10.15666/aeer/1906_46994720

[107] Shu, K., Zhang, H., Wang, S., Chen, M., Wu, Y., Tang, S., Liu, C., Feng, Y., Cao, X., Xie, Q. (2013): ABI4 regulates primary seed dormancy by regulating the biogenesis of abscisic acid and gibberellins in Arabidopsis. – PLoS Genet. 9: e1003577.
[108] Shu, K., Chen, Q., Wu, Y., Liu, R., Zhang, H., Wang, S., Tang, S., Yang, W., Xie, Q. (2016a): ABSCISIC ACID-INSENSITIVE 4 negatively regulates flowering through directly promoting Arabidopsis *FLOWERING LOCUS C* transcription. – J. Exp. Bot. 67: 195-205.
[109] Shu, K., Liu, X. D., Xie, Q., He, Z. H. (2016b): Two Faces of One Seed: Hormonal Regulation of Dormancy and Germination. – Mol. Plant 9: 34-45.
[110] Shu, K., Zhou, W. G., Yang, W. Y. (2017): APETALA 2-domain-containing transcription factors: focusing on abscisic acid and gibberellins antagonism. – New Phytol. 217: 977-983.
[111] Shu, K., Luo, X. F., Meng, Y. J., Yang, W. Y. (2018a): Toward a molecular understanding of abscisic acid actions in floral transition. – Plant Cell Physiol. 59: 215-221.
[112] Shu, K., Zhou, W. G., Chen, F., Luo, X. F., Yang, W. Y. (2018b): Abscisic Acid and Gibberellins Antagonistically Mediate Plant Development and Abiotic Stress Responses. – Front. Plant Sci. 9: 416.
[113] Silverstone, A. L., Jung, H. S., Dill, A., Kawaide, H., Kamiya, Y., Sun, T. P. (2001): Repressing a repressor: gibberellin-induced rapid reduction of the RGA protein in Arabidopsis. – Plant Cell 13: 1555-1566.
[114] Söderman, E. M., Brocard, I. M., Lynch, T. J., Finkelstein, R. R. (2000): Regulation and function of the Arabidopsis ABA-*insensitive4* gene in seed and abscisic acid response signaling networks. – Plant Physiol. 124: 1752-1765.
[115] Spanudakis, E., Jackson, S. (2014): The role of microRNAs in the control of flowering time. – J. Exp. Bot. 65: 365-380.
[116] Springthorpe, V., Penfield, S. (2015): Flowering time and seed dormancy control use external coincidence to generate life history strategy. – eLife 4: e05557.
[117] Srikanth, A., Schmid, M. (2011): Regulation of flowering time: all roads lead to Rome. – Cell. Mol. Life Sci. 68: 2013-2037.
[118] Sugimoto, K., Takeuchi, Y., Ebana, K., Miyao, A., Hirochika, H., Hara, N., Ishiyama, K., Kobayashi, M., Ban, Y., Hattori, T., Yano, M. (2010): Molecular cloning of *Sdr4*, a regulator involved in seed dormancy and domestication of rice. – Proc. Natl. Acad. Sci. USA 107: 5792-5797.
[119] Sun, T., Kamiya, Y. (1994): The Arabidopsis GA1 locus encodes the cyclase ent-kaurene synthetase A of gibberellin biosynthesis. – Plant Cell 6: 1509-1518.
[120] Thompson, A. J., Jackson, A. C., Symonds, R. C., Mulholland, B. J., Dadswell, A. R., Blake, P. S., Burbidge, A., Taylor, I. B. (2000): Ectopic expression of a tomato 9-*cis*-epoxycarotenoid dioxygenase gene causes over-production of abscisic acid. – Plant J. 23: 363-374.
[121] Tiwari, S. B., Shen, Y., Chang, H. C., Hou, Y., Harris, A., Ma, S. F., McPartland, M., Hymus, G. J., Adam, L., Marion, C., Belachew, A., Repetti, P. P., Reuber, T. L., Ratcliffe, O. J. (2010): The flowering time regulator CONSTANS is recruited to the FLOWERING LOCUS T promoter via a unique cis-element. – New Phytol. 187: 57-66.
[122] Tuan, P. A., Kumar, R., Rehal, P. K., Toora, P. K., Ayele, B. T. (2018): Molecular Mechanisms Underlying Abscisic Acid/Gibberellin Balance in the Control of Seed Dormancy and Germination in Cereals. – Front. Plant Sci. 9: 668.
[123] Tuttle, K. M., Martinez, S. A., Schramm, E. C., Takebayashi, Y., Seo, M., Steber, C. M. (2015): Grain dormancy loss is associated with changes in ABA and GA sensitivity and hormone accumulation in bread wheat, *Triticum aestivum* (L.). – Seed Sci. Res. 25: 179-193.
[124] Vaistij, F. E., Gan, Y., Penfield, S., Gilday, A. D., Dave, A., He, Z., Josse, E. M., Choi, G., Halliday, K. J., Graham, I. A. (2013): Differential control of seed primary dormancy in

http://www.aloki.hu ● ISSN 1589 1623 (Print) ● ISSN 1785 0037 (Online)
DOI: http://dx.doi.org/10.15666/aeer/1906_46994720

Arabidopsis ecotypes by the transcription factor SPATULA. – Proc. Natl. Acad. Sci. USA 110: 10866-10871.
[125] Vishwakarma, K., Upadhyay, N., Kumar, N., Yadav, G., Singh, J., Mishra, R. K., Kumar, V., Verma, R., Upadhyay, R. G., Pandey, M., Sharma, S. (2017): Abscisic Acid Signaling and Abiotic Stress Tolerance in Plants: A Review on Current Knowledge and Future Prospects. – Front. Plant Sci. 8: 161.
[126] Wallner, E. S., López-Salmerón, V., Greb, T. (2016): Strigolactone versus gibberellin signaling: reemerging concepts. – Planta 243: 1339-1350.
[127] Wang, J. W., Czech, B., Weigel, D. (2009): miR156-regulated SPL transcription factors define an endogenous flowering pathway in *Arabidopsis thaliana*. – Cell 138: 738-749.
[128] Wang, Y., Li, L., Ye, T., Lu, Y., Chen, X., Wu, Y. (2013): The inhibitory effect of ABA on floral transition is mediated by ABI5 in *Arabidopsis*. – J. Exp. Bot. 64: 675-684.
[129] Willige, B. C., Ghosh, S., Nill, C., Zourelidou, M., Dohmann, E. M. N., Maier, A., Schwechheimer, C. (2007): The DELLA domain of GA INSENSITIVE mediates the interaction with the GA INSENSITIVE DWARF1A gibberellin receptor of *Arabidopsis*. – Plant Cell 19: 1209-1220.
[130] Wilson, R. N., Heckman, J. W., Somerville, C. R. (1992): Gibberellin is required for flowering in *Arabidopsis thaliana* under short days. – Plant Physiol. 100: 403-408.
[131] Wu, G., Park, M. Y., Conway, S. R., Wang, J. W., Weigel, D., Poethig, R. S. (2009): The sequential action of miR156 and miR172 regulates developmental timing in *Arabidopsis*. – Cell 138: 750-759.
[132] Yamaguchi, S., Kamiya, Y. (2002): Gibberellins and light-stimulated seed germination. – J. Plant Growth Regul. 20: 369-376.
[133] Yamaguchi, S. (2006): Gibberellin biosynthesis in *Arabidopsis*. – Phytochem. Rev. 5: 39-47.
[134] Yamaguchi, S. (2008): Gibberellin metabolism and its regulation. – Annu. Rev. Plant Biol. 59: 225-251.
[135] Yamaguchi, A., Abe, M. (2012): Regulation of reproductive development by non-coding RNA in *Arabidopsis*: to flower or not to flower. – J. Plant Res. 125: 693-704.
[136] Yamauchi, Y., Ogawa, M., Kuwahara, A., Hanada, A., Kamiya, Y., Yamaguchi, S. (2004): Activation of gibberellin biosynthesis and response pathways by low temperature during imbibition of *Arabidopsis thaliana* seeds. – Plant Cell 16: 367-378.
[137] Yang, W., Zhang, W., Wang, X. (2017): Post-translational control of ABA signalling: the roles of protein phosphorylation and ubiquitination. – Plant Biotechnol. J. 15: 4-14.
[138] Yoshida, T., Fujita, Y., Maruyama, K., Mogami, J., Todaka, D., Shinozaki, K., Yamaguchi-Shinozaki, K. (2014): Four *Arabidopsis* AREB/ABF transcription factors function predominantly in gene expression downstream of SnRK2 kinases in abscisic acid signalling in response to osmotic stress. – Plant Cell Environ. 38: 35-49.
[139] Yoshida, T., Mogami, J., Yamaguchi-Shinozaki, K. (2015): Omics Approaches Toward Defining the Comprehensive Abscisic Acid Signaling Network in Plants. – Plant Cell Physiol. 56: 1043-1052.
[140] Yu, S., Galvão, V. C., Zhang, Y. C., Horrer, D., Zhang, T. Q., Hao, Y. H., Feng, Y. Q., Wang, S., Schmid, M., Wang, J. W. (2012): Gibberellin regulates the Arabidopsis floral transition through miR156-targeted SQUAMOSA PROMOTER BINDING-LIKE transcription factors. – Plant Cell 24: 3320-3332.
[141] Yu, F., Wu, Y., Xie, Q. (2015): Precise protein post-translational modifications modulate ABI5 activity. – Trends Plant Sci. 20: 569-575.
[142] Zhang, X., Garreton, V., Chua, N. H. (2005): The AIP2 E3 ligase acts as a novel negative regulator of ABA signaling by promoting ABI3 degradation. – Genes Dev. 19: 1532-1543.
[143] Zhang, H., Rider, S. D., Henderson, J. T., Fountain, M., Chuang, K., Kandachar, V., Simons, A., Edenberg, H. J., Romero-Severson, J., Muir, W. M., Ogas, J. (2008): The CHD3 remodeler PICKLE promotes trimethylation of histone H3 lysine 27. – J. Biol. Chem. 283: 22637-22648.

http://www.aloki.hu ● ISSN 1589 1623 (Print) ● ISSN 1785 0037 (Online)
DOI: http://dx.doi.org/10.15666/aeer/1906_46994720

[144] Zhang, D., Jing, Y., Jiang, Z., Lin, R. (2014): The chromatin-remodeling factor PICKLE integrates brassinosteroid and gibberellin signaling during skotomorphogenic growth in *Arabidopsis*. – Plant Cell 26: 2472-2485.
[145] Zhao, M., Yang, S., Liu, X., Wu, K. (2015): *Arabidopsis* histone demethylases LDL1 and LDL2 control primary seed dormancy by regulating *DELAY OF GERMINATION 1* and ABA signaling-related genes. – Front. Plant Sci. 6: 159.
[146] Zhu, Q. H., Helliwell, C. A. (2011): Regulation of flowering time and floral patterning by miR172. – J. Exp. Bot. 62: 487-495.
[147] Zhu, Y., Liu, L., Shen, L., Yu, H. (2016): NaKR1 regulates long-distance movement of FLOWERING LOCUS T in *Arabidopsis*. – Nat. Plants 2: 16075.

http://www.aloki.hu ● ISSN 1589 1623 (Print) ● ISSN 1785 0037 (Online)
DOI: http://dx.doi.org/10.15666/aeer/1906_46994720

CELLULAR IMPACT OF METAL TRACE ELEMENTS ON THE LICHEN *LOBARIA PULMONARIA* (L.) HOFFM. (1796), A BIO INDICATOR OF ATMOSPHERIC POLLUTION AND IDENTIFICATION OF ITS ANTIOXIDANT RESPONSE

KOUADRIA, N.* – ALIOUA BERREBBAH, A. – BELHOUCINE, F. – BOUREDJA, N. – AITKACI, M.

Laboratoire de Toxicologie Environnement et Santé (LATES), Faculté des sciences de la nature et de la vie, Université des Sciences et de la Technologie d'Oran Mohamed Boudiaf USTO-MB, BP 1505, el M'naouer, 31000 Oran, Algérie
(phone: +213-699-135-342)

**Corresponding author*
e-mail: Nawel.kouadria@univ-usto.dz

(Received 5th Aug 2021; accepted 1st Oct 2021)

Abstract. We used the bioindicator *Lobaria pulmonaria* (L.) Hoffm. to assess air pollution, particularly induced by heavy metals, in urban and peri urban regions in the city of Oran (N-W of Algeria) and evaluated their environmental impact. For this purpose, we adopted the active biomonitoring technique to monitor lead (Pb), Cadmium (Cd) and Chromium (Cr) bioaccumulation in transplanted *Lobaria pulmonaria* thalli and assessed the detoxification enzyme's activity: Catalase (CAT), Ascorbate peroxidase (APX), and Guaiacol peroxidase (GPX) to examine the antioxidant system's response to heavy metal-induced stress. This study, revealed significant bioaccumulation of Pb, Cd and Cr in the following order Pb > Cr > Cd, increasing significantly in time reaching 301.83 mg/kg with the highest concentrations recorded in the urban regions indicating high metallic pollution levels. Additionally, heavy metal concentrations were proven to be significantly correlated with the over expression of detoxification enzymes. The response of *Lobaria pulmonaria* to air quality, along with its bio-accumulative capacity, confirmed that it is indeed a good bio-indicator of atmospheric pollution, especially that induced by heavy metals.
Keywords: *ecotoxicology, bio monitoring, xenobiotic, bioaccumulation, bioindication, air pollution*

Introduction

Air pollution is a significant ecological issue worldwide, which, as per the World Health Organization, influences the majority of the world's population (WHO, 2018). Some activities generating progress and modernity in the urban communities, notably economic activities, industrialization and expansions in street traffic, in addition to the population growth, have caused a significant increase in air pollution levels, affecting humans and the ecosystem (Bouteraa, 2014; Rahal et al., 2018; Jiang et al., 2018). Indeed, previous studied found that pollutants of road emission origin are the most ubiquitous group of pollutants detected in plants tissues (Akomolafe et al., 2019).

Air pollution incorporates a range of pollutants emitted frequently into the air, among which heavy metals (HMs), essentially resulting from road traffic, represent an important group (Belhadj, 2015). The danger of these non-biodegradable hazardous materials results from the fact that once in the atmosphere, they can travel several kilometers away from emission sources upon wind direction (Shahid et al., 2017), and are capable to remain in nature through biomagnification, affecting thus human and environment even in areas far from contamination sources (Mahapatra et al., 2019).

http://www.aloki.hu ● ISSN 1589 1623 (Print) ● ISSN 1785 0037 (Online)
DOI: http://dx.doi.org/10.15666/aeer/1906_47214738

The deterioration of air quality has severe consequences on human health. According to Çomaklı and Bingöl (2021), the exposure of humans to important heavy metals contents often causes serious health problems. Moreover, a lot of papers have also highlighted air pollution's impact on the environment including lichens, and proved that heavy metal are responsible for altering physiological and morphological characteristics of these plants since lichens are sensitive to atmospheric changes and micro-climatic conditions (Akomolafe et al., 2019; Ilondu, 2019). Indeed, the impact of these hazardous depends on their concentration, their chemical properties, and on the resistance or the sensibility of the contaminated species (Kaur et al., 2021). However, even if heavy metal combinations are common in nature, their combined effects have not been extensively studied (Tkalec et al., 2014).

As in many countries in the world, Algerian urban population continues to rise. In the western region, the city of Oran in particular, the regional metropolis and the country's second-largest city, has known over the last decade a strong urbanization, reflected in a vast urban territory and numerous extensions, which has led to more and longer trips, mostly made by individual motorized transport. This, in addition to its industrial infrastructure, has led to an increase in atmospheric emissions (Kadri and Madani, 2015; Rahal et al., 2018) In addition, some topographical, geographical and climatic characteristics like humidity and dominant wind speed lead to a considerable increase in pollution levels in the various ecosystems, and more particularly in air (Stankevich et al., 2015).

Due to a lack of appropriate instrumentation for monitoring air quality in Oran region, it became necessary to develop a bio monitoring system based on an alternative method of air quality assessment, involving bio-indicators. This use is based on their integrative nature regarding environmental factors. Indeed, "living beings are a reflection of the environment in which they evolve and their observations at the various levels of biological organization can provide indications of the quality of this environment" (Guelorget et al., 1986). Biomonitoring includes the use of different matrices among which lichens are the most used over the last years, because of their morphological properties since they get their nutriment directly from ambient air due to the absence of root and cuticle layer. In addition, lichens are very sensitive to environmental conditions which allows them reacting to ecological changes reflecting thus the environmental conditions, and also have an important bioaccumulation capabilities allowing them indicating the concentrations of atmospheric bio accumulated pollutants, as well as their spatial distribution (Deruelle, 1978, 1983; Tyler, 1989; Alioua, 1995; Alioua, 2001; Alioua et al., 2008; Garrec and Van Haluwyn, 2002; Yemets et al., 2014; Kłos et al., 2018; Jiang et al., 2018; Ramade, 2007; Rola, 2020).

In Algeria, bio-monitoring studies using lichens were conducted largely in the central and eastern regions (Rahali, 2002; Semadi and Deruelle, 1993; Alioua, 2001; Alioua et al., 2008; Belhadj, 2015). However, according to the Oran's Directorate of Environment, no atmospheric biomonitoring study has ever been conducted in this region (DOE, 2018).

The aim of this work is to investigate atmospheric heavy metal contents using the bio indicator *Lobaria pulmonaria* (L.) Hoffm. in the region of Oran, as an alternative approach in air quality assessment, and to assess the impact of these heavy metals on the studied species through examining the response of the plant's antioxidant system to these stressors.

http://www.aloki.hu ● ISSN 1589 1623 (Print) ● ISSN 1785 0037 (Online)
DOI: http://dx.doi.org/10.15666/aeer/1906_47214738

Materials and methods

Study area

The study region is located in the southwest of the Mediterranean (north-west of Algeria 35°42 N and 00°36 W). This region belongs to the semi-arid Mediterranean bio climatic zone with a six-month dry season (April to October with rare rainfall exceeding barely 30 mm) and abundant rainfall in winter. In addition, winds blow mainly from the north (19%) at 12 m/s and from the west (18%) at more than 17 m/s, with three other directions: southwest (14%), northeast (10%) and east (7%) reaching a maximum speed of 8 m/s. 30% of the time, the wind is calm (<1 m/s). (Bendaikha and Hadjadj-Aoul, 2016). Moreover, the region of Oran is characterized by an important car fleet estimated at 357,988 in 2017, mainly in the Oran agglomeration, where the majority were vehicles in use for more than 20 years (OTD, 2018).

This study has been conducted in twelve different sites in Oran covering both urban and peri urban region (*Fig. 1; Table 1*).

Transplantation and sampling

In this study we adopted the transplantation technique developed by (Brodo, 1961), which consists in introducing bio-indicators taken from a control site into the study sites (*Fig. 2*). We chose a foliaceous species, *Lobaria pulmonaria* (L.) Hoffm. an epiphytic lichen resulting from the symbiosis of a green algae and a cyanobacterium, while the fungus (Ascomycetes) provides protection against dehydration, the green algae (*Dictyochloropsis reticulata*) produces the carbohydrates necessary for the organism, and the cyanobacterium (Nostoc) allows the capture of atmospheric nitrogen necessary for growth (Carlsson and Nilsson, 2009).

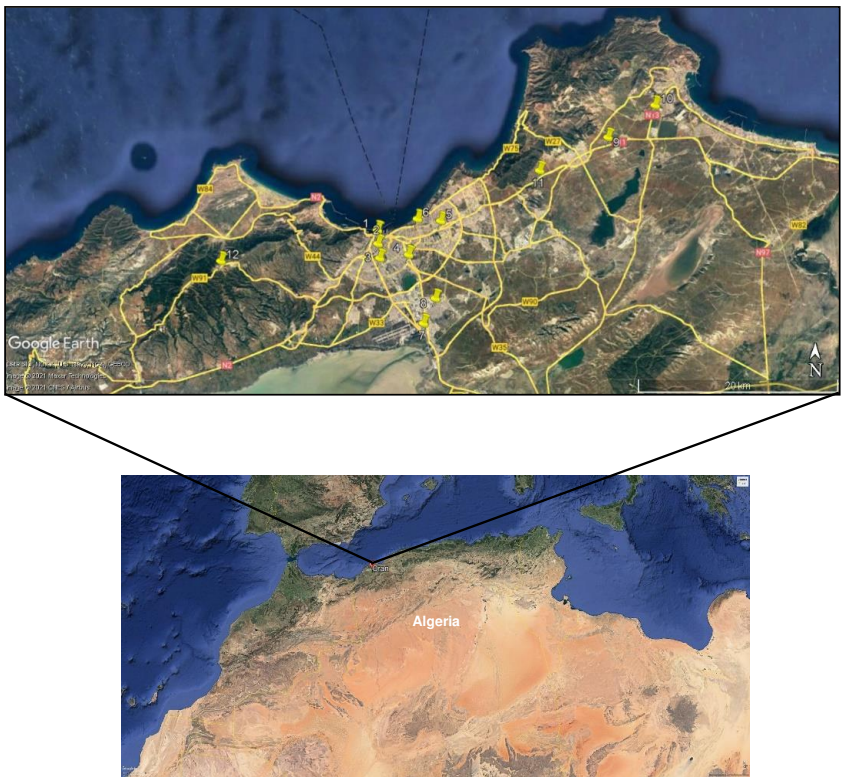

Figure 1. *Geographical location of the study sites*

http://www.aloki.hu ● ISSN 1589 1623 (Print) ● ISSN 1785 0037 (Online)
DOI: http://dx.doi.org/10.15666/aeer/1906_47214738

Table 1. *Description and geographical location of the study sites*

Site No.	Site description	Longitude/E	Latitude/N	Altitude (m)
1	An urban site located in the center of Oran next to the Pasteur high school, 20 m from the ALN boulevard on the seafront overlooking the port of Oran, and 20 m from a bus stop, this site is exposed to heavy road traffic and pedestrian traffic	0°38'44.62"	35°42'18.64"	60
2	An urban site located in the center of Oran, next to the largest popular market in the city with a high pedestrian traffic during the day. This site is located 39.78 m from the 1st November 1950 roundabout with a huge road traffic as it leads to one of the biggest hospitals in Oran	0°38'41.47"	35°41'34.52"	110
3	An urban site characterized by a high density as it is located next to a middle school, and intense road traffic since it is situated at 72 m from the second peripheral highway and at 155.35 m from the ANP roundabout	0°38'32.93"	35°40'48.35"	102
4	An urban site located in the center of the city at 20.30 m from one of the largest roundabouts characterized by heavy road traffic, especially since it provides transportation to and from the main bus station which is 480.59 m away this site located near two service stations (at 383 m and 329 m)	0°36'39.30"	35°41'2.23"	90
5	an urban site located 10 m from a big roundabout, characterized by heavy traffic due to the presence of a bus station that considerably disturbs the traffic	0°34'35.89"	35°42'53.12"	147
6	An urban site located 21 m from a large roundabout, it is located in the middle of a built-up area near several intersections. This site has physical and aesthetic characteristics suitable for high traffic and high density	0°36'7.39"	35°42'57.59"	161
7	A peri-urban site located in the middle of a roundabout. This site is near to Oran's airport and is located at 692.46 m from the national road N4, and 2.95 km from the Es Senia industrial zone	0°35'33.13"	35°37'23.42"	89
8	A peri-urban site located in the center of the industrial zone of Es Senia, and at 886.04 m from the national road N4	0°34'49.07"	35°38'44.55"	90
9	A peri-urban site located in the east of the Oran on the edge of the national road N11 linking the industrial zone of Arzew to the town of Oran, which is characterized by heavy traffic, especially during rush hours. This site is located 1.6 km from a gas station and 5.7 km from the industrial zone of ARZEW	0°23'41.52"	35°47'34.31"	152
10	A peri-urban site located in the east of Oran on the edge of the national road N13 at 69.69 m from the industrial pole of Arzew. The site is located 1.85 km from the Arzew refinery, 2.18 km from the power station and 1.41 km from the Sorfert company known for its toxic emissions	0°20'37.72"	35°49'20.91"	82
11	A peri-urban site located in the east of Oran on the edge of the national highway N11 and at 13.42 km from the industrial zone of Arzew	0°28'9.19"	35°45'42.36"	124
12	A peri-urban site located in the middle of the forest of Msila in the West of Oran, however this region is the favorite destination of Oranese to make outings, camping and picnik during which they opt for the combustion to prepare their meals	0°49'1.09"	35°40'25.06"	507

http://www.aloki.hu ● ISSN 1589 1623 (Print) ● ISSN 1785 0037 (Online)
DOI: http://dx.doi.org/10.15666/aeer/1906_47214738

Figure 2. *Habitat of the lichen Lobaria pulmonaria and the followed transplantation technique. (a) habitat, (b) lichenic thalli transplnated in the urban site (1), (c) the peri-urban site (7)*

The thallus of *Lobaria pulmonaria* were collected with their phorophytes from a control site, located in the Seraidi forest 36° 55 N and 7° 40 E in northeastern Algeria, located far from major sources of pollution, and then transplanted to the study sites (*Fig. 1*), at a height varying from 1.5 m to 2 m (*Fig. 2b*). We carried monthly sampling during seven months from December 2018 to June 2019 in order to perform the various measurements.

Analysis and measurement

Heavy metal analysis

We followed Deruelle (1978) technique for samples digestion. After drying samples for 72 h at 105 °C, they were crushed, placed in pill boxes and treated with 30% pure RP Norma hydrogen peroxide H_2O_2 until complete digestion. The digestion took place in an oven set at 90 °C for 72 h. Lead (Pb), chromium (Cr) and cadmium (Cd) analysis were performed using the ICP-OES Thermo Scientific iCAP 7000 (France). HM analysis include the HM particles deposited on lichen surface. For each heavy metal and for each site three replicates were carried out.

Enzyme assays

The investigation of enzymatic activity was proceeded in two stages. First, we prepared the enzyme extract from collected transplants and from the control site following the protocol of Loggini et al. (1999). The enzyme extract is used to prepare the reaction mixture respective for each enzyme CAT, APX and GPX.

The catalase optical density is obtained at 240 nm following (Cakmaki, 1991) technique, the Ascorbate-peroxidase's optical density is obtained at 290 nm following (Nakano and Asada, 1987) technique and the Guaiacol peroxidase's optical density is obtained at 470 nm following (Fielding and Hall, 1978) technique. The

http://www.aloki.hu ● ISSN 1589 1623 (Print) ● ISSN 1785 0037 (Online)
DOI: http://dx.doi.org/10.15666/aeer/1906_47214738

spectrophotometer used is a UV-VIS spectrophotometer (190-1000 nm) - JENWAY (France). For each enzyme and for each site three replicates were carried out (*Fig. 3*).

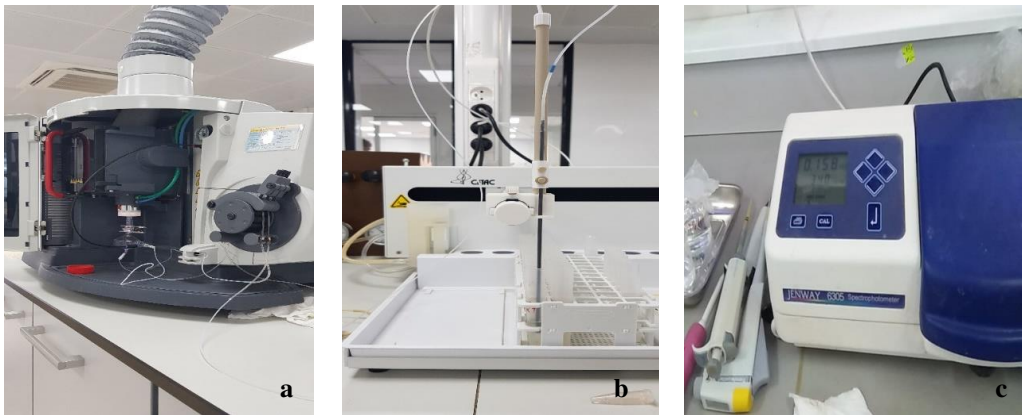

Figure 1. *Analysis and dosages in laboratory (a and b) HMs analysis by ICP-OES, (c) enzymatic activity analysis by UV-VIS spectrophotometer*

Statistical analysis

The obtained data were subjected to a statistical analysis:

- The two ways ANOVA is conducted for Pb, Cd, Cr, APX, GPX and CAT in order to study the significance of the spatio-temporal variation of each parameter.
- We carried out a two-way ANOVA with co-variates for the three enzymes in order to investigate the influence of heavy metal accumulation on the spatio-temporal variation of the enzymatic activity.
- Post Hoc tests were carried out, notably the Tukey test to determine the significance between homogeneous group means and the Dunnett test to determine the significance between homogeneous group means and the control mean.
- The correlation analyses between Pb, Cd, Cr concentrations and APX, CAT, GPX activities were conducted using a bivariate correlation test with Pearson's correlation coefficient.

XLstat and Minitab software packages were used to conduct the statistical analysis.

Results and discussion

Heavy metals results

In general, the spatio-temporal variations in HM concentrations show that for the three metals Pb, Cd and Cr, the concentrations tend to increase from the first sampling comparing to control, regardless of the site in the following order Pb > Cr > Cd (*Fig. 4*). These concentrations varies depending on the study sites and continue to increase significantly ($p = 0.000^{***}$) to reach a maximum of 301.83 mg/kg of Pb at site 5 during the last sampling of June. Moreover, results show a significant increase in Cd concentrations ($p = 0.000^{***}$) with a predominance in sites 1, 4, 6 and 10 where we record close highest concentrations during the month of June.

http://www.aloki.hu ● ISSN 1589 1623 (Print) ● ISSN 1785 0037 (Online)
DOI: http://dx.doi.org/10.15666/aeer/1906_47214738

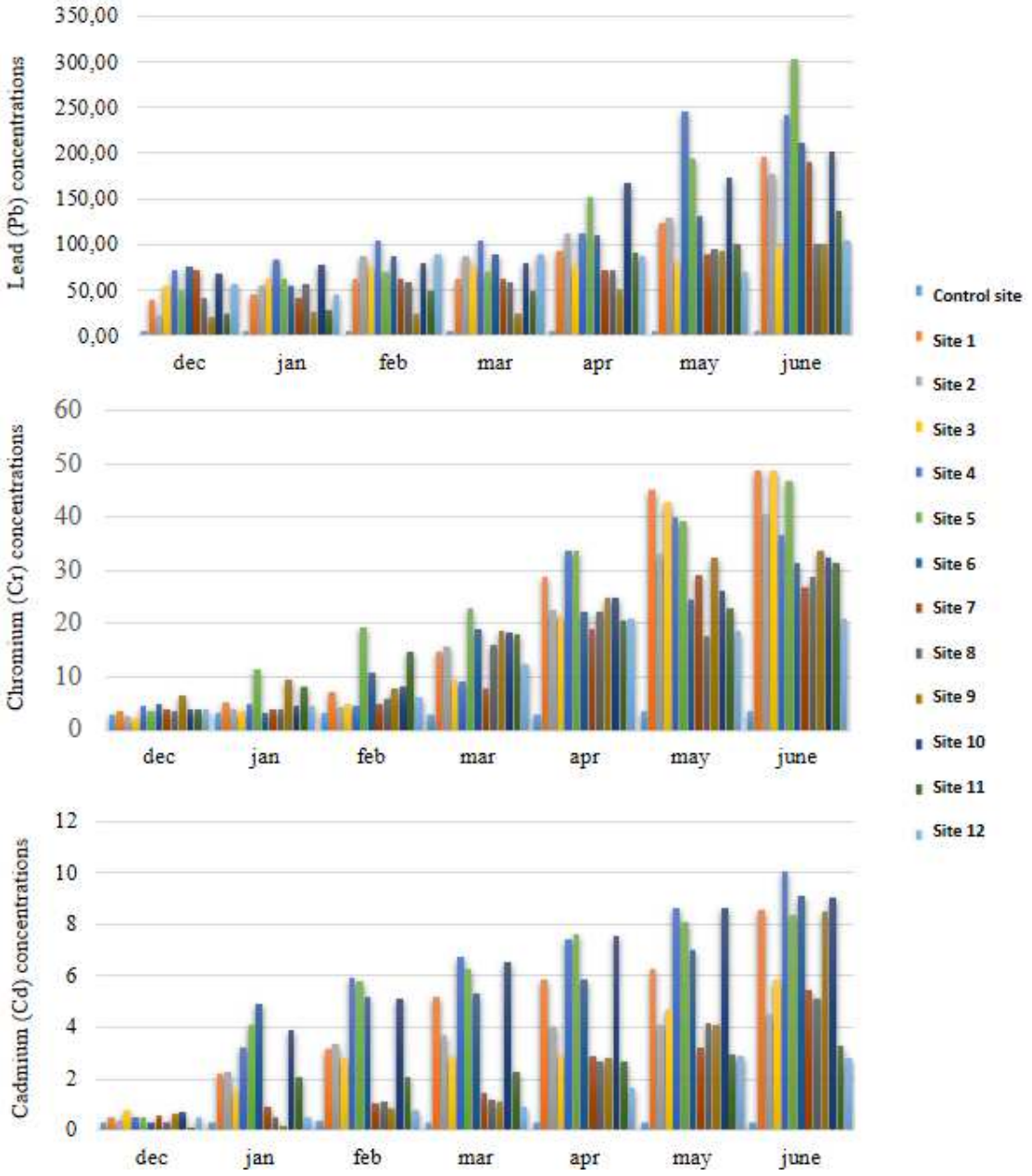

Figure 4. *Spatio-temporal heavy metal (lead (Pb), Cadmium (Cd), Chromium (Cr)) concentrations (mg/kg DW) bioaccumulated in thallus of Lobaria pulmonaria*

The results of post hoc tests for spatio-temporal heavy metal concentrations are shown in (*Fig. 5*). These results allow identifying site-specific and month-specific fluctuations in bioaccumulated heavy metal concentrations. In space, according to Tukey test the highest averages of Pb, Cd and Cr are recorded in site four. Averages of site four are significantly different from the control according to Dunnet test. However, in time, according to Tukey test, averages of Pb, Cd and Cr increase to reach maximum averages in the last month, these averages are significantly different from the control according to Dunnet test. The spatial variation of obtained HM concentrations made it possible to locate the most contaminated sites, since the bioavailability of these elements allows their bioaccumulation (Rola, 2020).

http://www.aloki.hu ● ISSN 1589 1623 (Print) ● ISSN 1785 0037 (Online)
DOI: http://dx.doi.org/10.15666/aeer/1906_47214738

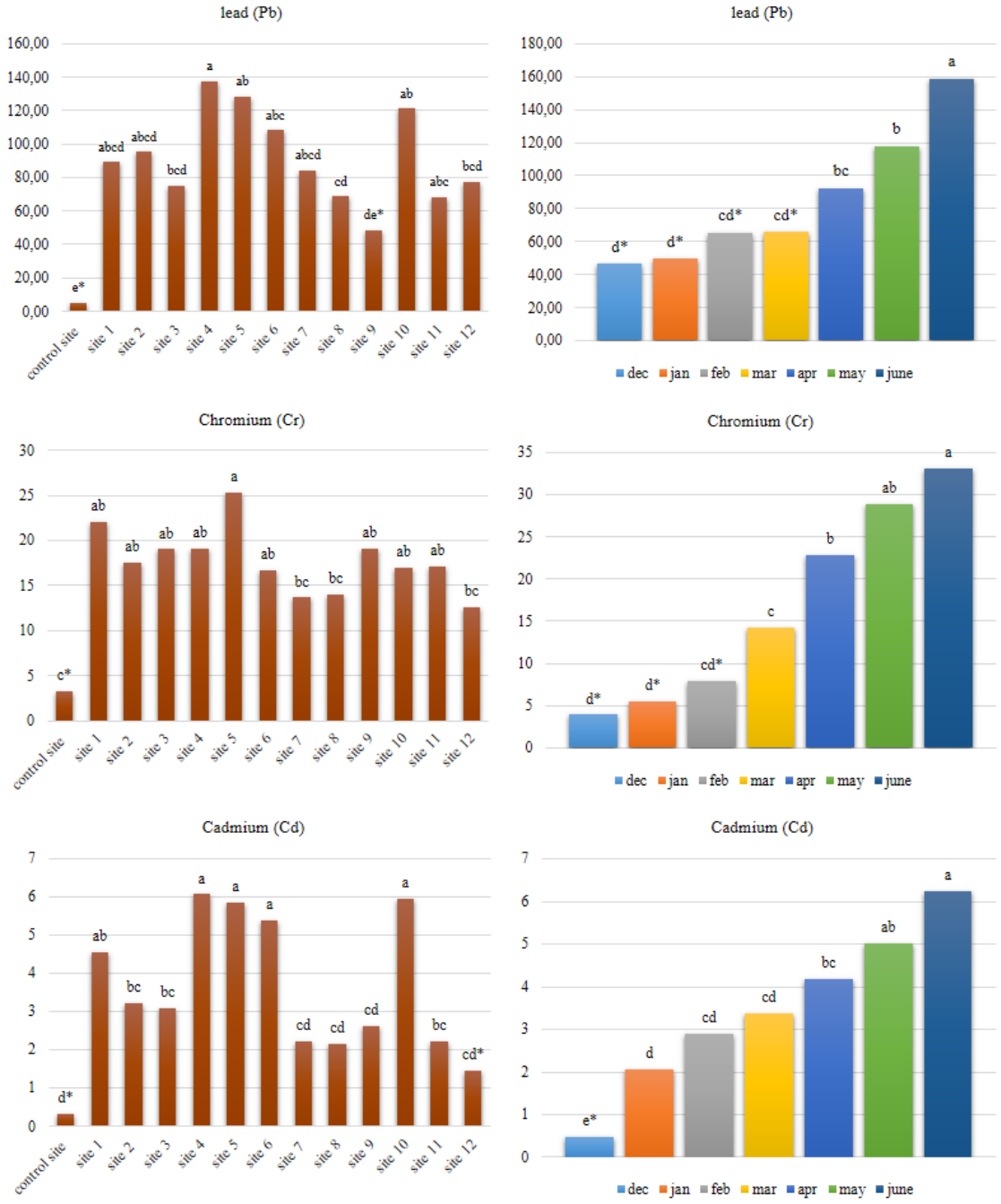

***Figure 5**. Heavy metal means recorded in space and in time in Lobaria pulmonaria thallus. The different letters show significant differences according to Tukey's HSD ($p < 0.05$). Means not marked with a (*) are significantly different from the control site's mean according to Dunnet ($p < 0.05$)*

Indeed, the concentrations of Pb, Cd and Cr bio-accumulated by transplants increase the closer they get to urban sites, in particular sites 1, 2, 4, 5 and 6, since urban sites are characterized by dense automobile traffic and high population concentration (Hamutoğlu et al., 2017; Kaur et al., 2021; Çomaklı and Bingöl, 2021). In fact, many studies reported a significant correlation between road traffic and the accumulation of HMs like, Pb, such as Belhadj (2015), Maizi and Alioua (2015), Rahali (2002) and

http://www.aloki.hu ● ISSN 1589 1623 (Print) ● ISSN 1785 0037 (Online)
DOI: http://dx.doi.org/10.15666/aeer/1906_47214738

Semadi and Deruelle (1993) in Algeria, Tkalec et al. (2014) in Finland, and Abas et al. (2019) in Malaysia. Other factors, such as topographic variations, may also have an impact on HMs rated in the environment, especially in lichens. According to the work of Belhadj (2015), atmospheric particle concentrations are higher in low altitude areas than on slopes and mountains; this topographic factor explains the relatively low concentrations of HMs recorded in site 12 which is located in a mountainous region. These factors are in addition to lichens complex accumulation mechanisms, which are influenced by a variety of factors such as age, thallus size, and species-specific characteristics (Alami et al., 2014). According to Rahma et al. (2014), HM presence in the thallus of transplants is essentially associated with the lichen's accumulative potential, which is attributable to the physiological properties of lichens allowing them to maintain pollutants in their tissues. Moreover, due to the lack of surface protective barriers, the thallus of lichens are highly permeable to airborne pollutants, especially heavy metals, considered as a major component of air pollution (Álvarez et al., 2015; Hamutoğlu et al., 2017). According to Garty et al. (1998) and Belhadj (2015), the capacity of lichens to absorb metals is directly related to their morphological and anatomical structures since lichens accumulate more HMs as their surface area increases.

In addition, Angold (1997) reported that atmospheric pollutants from traffic origin are likely to contaminate natural vegetation located 80 m to 200 m from the road, while Viskari and Kärenlampi (2000) reported in a study conducted on snow samples and moss bags, collected 30 to 60 m from the road, a distance-dependent decrease in the deposition of inorganic air pollutants (Yemets et al., 2014), which explains the results we recorded in site 10 of our study, which recorded significant concentrations of Pb, Cd and Cr, although it is located far from the agglomeration. Indeed, this site is located on the side of the street that connects the agglomeration of Oran to the largest industrial zone of the country "Arzew", which has an important road traffic, especially at peak hours, in addition to industrial discharges, considered as an important emissions source of HMs (Yemets et al., 2014). Furthermore, according to the obtained results, in the peri-urban sites located far from the city, notably sites 3, 7, 8 and 9, recorded HM concentrations are relatively low compared to the urban sites. These results are consistent with those of many authors who have studied the deposition of road pollutants according to distance from the road (Agnan et al., 2017; Kłos et al., 2018; McAdam et al., 2011; Pagotto et al., 2001; Škrbić et al., 2012). In particular, Yemets et al. (2014) found that the accumulation of Cr, Pb and Cd decreases with increasing distance from the source of pollution.

Furthermore, the temporal variation of concentrations bioaccumulated by transplants over time shows the increasing of the levels of Pb, Cd and Cr, indeed, the literature usually reports on the temporal rises and decreases of the HMs accumulated by lichens. In fact, our experiment was conducted over two seasons, a winter season including the first three months, for which statistical analysis recorded the lowest concentrations of HMs, and a spring-summer season with higher concentrations of HMs, which is consistent with the results of Belhadj (2015), Maizi and Alioua (2015) and Abas et al. (2019). This temporal variation can be correlated with the environmental conditions that may influence the bioaccumulation of HMs (Agnan et al., 2017). In general, the wet season is marked by an important rainfall and a relatively high frequency of winds, as in the case of Oran, with rainfall up to 513 mm, and a dominant wind direction from North to West (18%) at 12 m/s and from South-East to East at a speed of 17 m/s (Bendaikha

http://www.aloki.hu ● ISSN 1589 1623 (Print) ● ISSN 1785 0037 (Online)
DOI: http://dx.doi.org/10.15666/aeer/1906_47214738

and Hadjadj-Aoul, 2016). According to Alami et al. (2014) rainfall causes atmospheric purification and contributes to the leaching of pollutants from lichen thallus. Moreover, the impact of winds on atmospheric pollutant's travelling seems to have a great influence on the accumulation of the pollutant (Semadi and Deruelle, 1993; Belhadj, 2015).

In addition, high concentrations of HMs during the summer period may also be correlated with the increase in pollution rates, due to the increase in road traffic intensity, and also to other factors such as: the effect of slope, long periods of drought, and the unequal distribution of road traffic which is reflected in the high concentrations of pollutants that remain in the atmosphere for a relatively long period (Belhadj, 2015). In addition, many papers reported that the concentrations of HMs absorbed in lichen samples are also influenced by exposure time (Garty et al., 1998; Yemets et al., 2014; Nimis et al., 2002). Hamutoğlu et al. (2017) also found significant accumulation of HMs after 6 months of transplantation along a highway, while Agnan et al. (2017) found that bioaccumulated amounts of HMs reached 964 mg/kg after 3 years of exposure.

Enzyme assay results

The spatio-temporal variation of the three enzymes CAT, APX and GPX shown in (*Fig. 6*) follows the same tendency as HMs. CAT variation is very highly important in space, according to the two-way ANOVA ($p = 0.000$***) and highly significant in time ($p = 0.003$**). CAT levels tend to increase to reach a maximum of $3.93.\ 10^8$ nmol/min/mg recorded in site 2 during the sampling of June. In addition, APX rates increase gradually to reach a maximum value of $901.67.\ 10^8$ nmol/min/mg in site 2 during the sampling of June. Based on the two ways ANOVA, variation in APX is not significant in space ($p = 0.432$) and very highly significant in time ($p = 0.000$***). Moreover, maximum GPX activity reaches $23.47.10^{-8}$ nmol/min/mg at site 4 in June. Variation in GPX activity is very highly significant in space and time ($p = 0.000$***). The results of post hoc tests for spatio- temporal enzymatic activity (*Fig. 7*) allows identifying site-specific and month-specific fluctuations in enzymatic response. According to Tukey's test, the monthly averages of the APX increase significantly from the sixth month. While monthly averages of CAT increase significantly from the 5^{th} month of exposure, these monthly averages are significantly different from control according Dunnet test. However, For GPX, Tukey's test shows that monthly concentrations increase significantly from the first month of sampling. Regarding spatial averages of enzymatic activity, results show that averages of APX, GPX and CAT recorded in site 4, 5 and 6 are significantly the highest according Tukey test. These spatial averages are significantly different from the control at ($p < 0.05$) according to Dunnet test.

Furthermore, results of the two ways ANOVA with covariates (*Table 2*) shows that GPX variation is very highly significant with bio accumulated Pb, highly significant with Cd ($p = 0.001$**) and significant with Cr ($p = 0.047$*).

In addition, CAT and APX variations are significant with Pb ($p = 0.011$* and $p = 0.002$** respectively), very highly significant with Cr ($p = 0.000$***). However, the variation of the two enzymes is not significant with Cd concentrations. Lichens react quickly to deteriorating air quality and are extremely sensitive to other types of environmental changes (Agnan et al., 2017; Belhadj, 2015). In nature, lichens are exposed to a variety of stressors including HMs (Ilondu, 2019; Paoli et al., 2018; Yemets et al., 2014).

http://www.aloki.hu ● ISSN 1589 1623 (Print) ● ISSN 1785 0037 (Online)
DOI: http://dx.doi.org/10.15666/aeer/1906_47214738

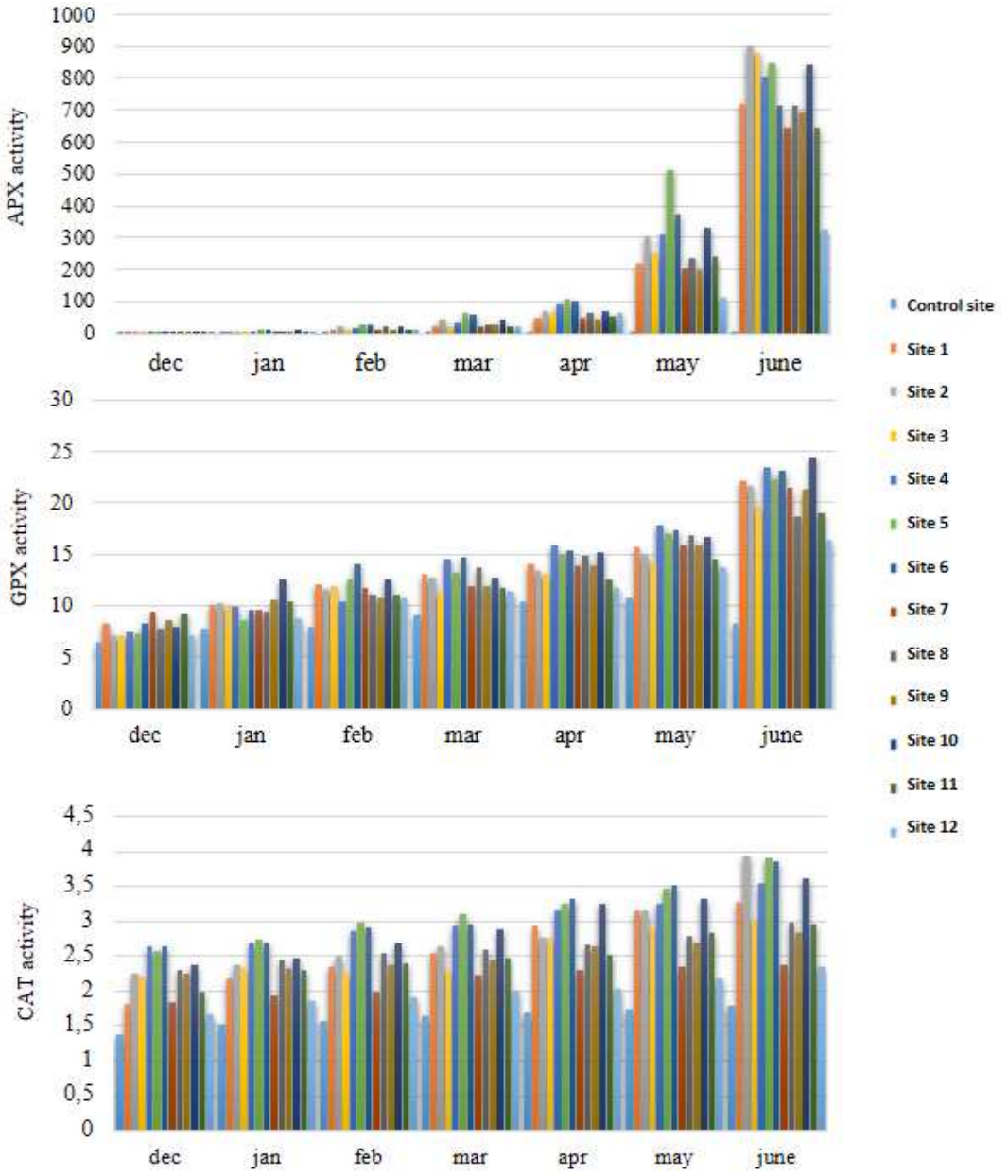

Figure 6. *Spatio-temporal activity of Catalase (CAT), Ascorbate peroxidase (APX) and Guaiacol peroxidase (GPX) (in nmol/min/mg of protein ×10-8) in collected Lobaria pulmonaria thallus*

Table 2. *Two ways ANOVA with covariates. Variation of APX, GPX, and CAT activity according to the variation of heavy metal concentrations*

Sources	DL	APX		GPX		CAT	
		F value	P value	F value	P value	F value	P value
Cd	1	1.31	0.256	13.09	**0.001**	0.41	0.522
Cr	1	16.25	**0.000**	4.08	**0.047**	17.88	**0.000**
Pb	1	10.27	**0.002**	16.46	**0.000**	6.90	**0.011**
Sites	12	1.03	0.432	4.09	0.000	23.03	0.000
Months	6	35.01	0.000	12.22	0.000	3.72	0.003

http://www.aloki.hu ● ISSN 1589 1623 (Print) ● ISSN 1785 0037 (Online)
DOI: http://dx.doi.org/10.15666/aeer/1906_47214738

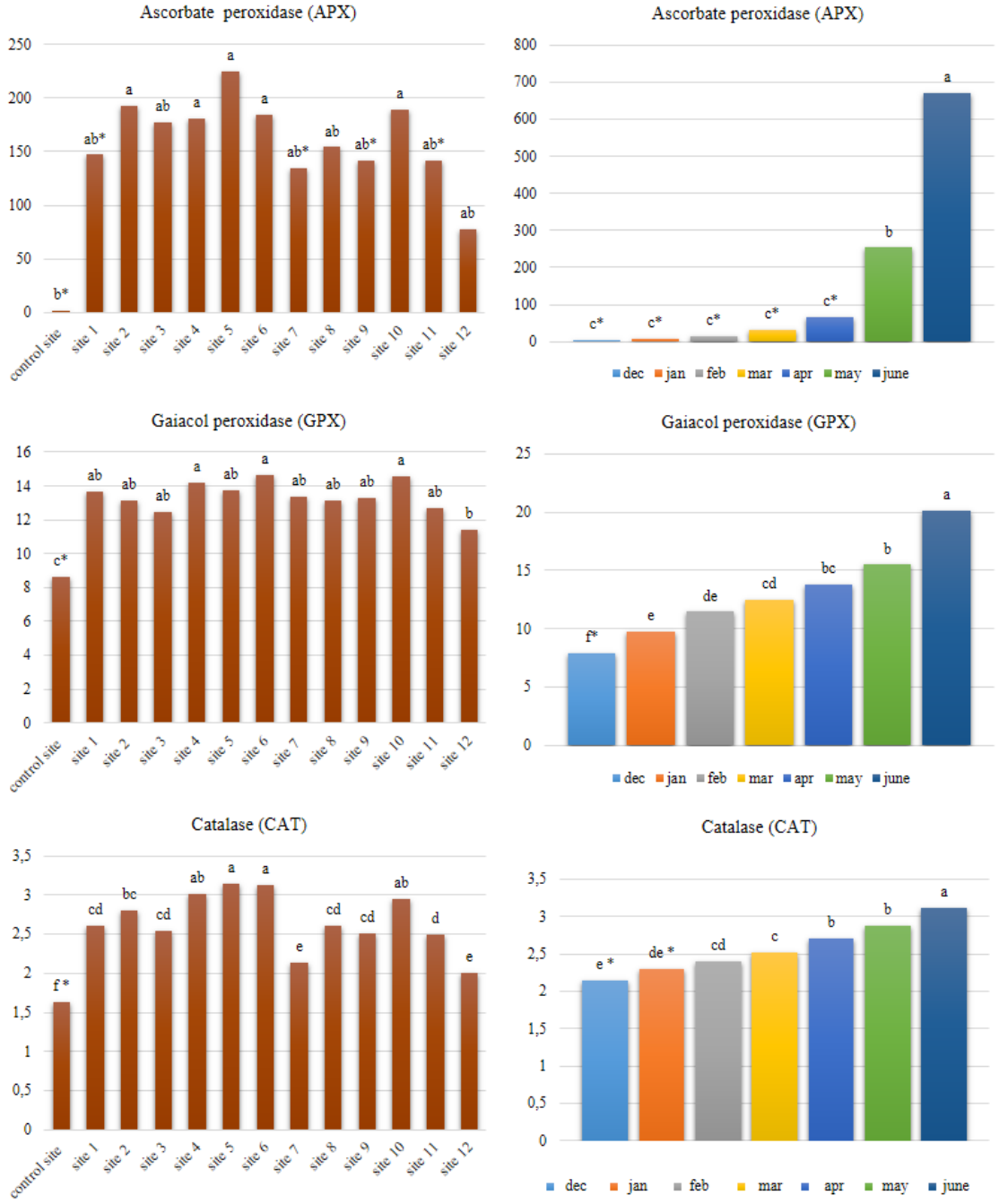

Figure 7. *Means of enzymatic activity recorded in space and in time in Lobaria pulmonaria thallus. The different letters show significant differences according to Tukey's HSD ($p < 0.05$). Means not marked with a (*) are significantly different from the control site's mean according to Dunnet ($p < 0.05$)*

Our results reveal a highly significant spatio-temporal increase in activity of GPX and CAT, and a significant temporal increase in APX in *Lobaria pulmonaria* transplants. This increase is most likely due to increased antioxidant activity in cells because of reactive oxygen species formation (ROS).

http://www.aloki.hu ● ISSN 1589 1623 (Print) ● ISSN 1785 0037 (Online)
DOI: http://dx.doi.org/10.15666/aeer/1906_47214738

In general, at the cellular level, ROS can be produced by normal metabolisms, like photosynthesis in chlorophyll cells; the ROS production in cells is low (240 μM s^{-1} 0^{2-} and 0.5 μM H_20_2 in chloroplast according to Polle (2001)). Several forms of stress, however, disrupt cell homeostasis and increase ROS production (240- 720 μM s^{-1} 0^{2-} and 5-15 μM H_20_2) (Bouziane, 2006; Chirva et al., 2019). At low concentrations, ROS are involved in cell signaling and defense responses, stimulating cells to develop strategies that involve an important antioxidant system including non-enzymatic and enzymatic components that protect them from destructive oxidative reactions (Serradj-Ali Ahmed et al., 2014). Among these enzymes, catalase, APX and GPX belong to the primary defense mechanism against ROS by catalyzing the conversion of H_2O_2 to H_2O, however, an increased level of antioxidant components is often correlated with increased stress (Chance et al., 1979; Jaskulak et al., 2019; Serradj-Ali Ahmed et al., 2014).

Indeed, according to Cui et al. (2022) the increase in H_2O_2 and $O2^{\bullet-}$ levels may be correlated with stress induced by heavy metals. In fact, the increase in the three enzymes activity: APX, GPX and catalase fluctuates according to accumulated HMs concentrations, which is shown in correlation matrices (*Fig. 8*). significant positive correlations between bioaccumulated heavy metal concentrations and enzymatic activity, which is consistent with the results of several authors (Álvarez et al., 2015; Jaskulak et al., 2019; Serradj-Ali Ahmed et al., 2014; Cui et al., 2022). In fact, it has been proven that the heavy metals are responsible for the detoxification enzymes's activation and the increase of the expression of the gene coding for certain enzyme. However, antioxidant response in plan cells varies depending on the plant species, the type of metal ion, the metal concentration and the duration of exposure (Cui et al., 2022).

The most cytotoxic effects of HMs are indirect, through the stimulation of the production of reactive oxygen species (ROS) that alter the antioxidant defenses and generate oxidative stress (Cui et al., 2022). Indeed, many authors reported that the intracellular accumulation of HMs constitutes a potential metabolic risk for lichens, as HMs are recognized as being able to generate oxidative stress in living organisms, leading to the formation of ROS such as hydrogen peroxide (H_2O_2) superoxide ions ($O_2^{\bullet-}$) and hydroxyl radicals ($^{\bullet}OH$) via Fenton or Haber-Weiss reactions (Álvarez et al., 2015; Assad, 2017).

The study of Bolan et al. (2014) in particular, confirms that the exposure to heavy metals affects redox homeostasis and leads to oxidative stress, while Cui et al. (2022) assumes that the increase in the superoxide anion levels is caused by the heavy metals accumulated by the plant. Other works shows that HMs have many toxic effects that can affect different metabolic pathways such as photosynthesis, respiration, etc. (Chiboub et al., 2019; Nash III, 2008; Vitali et al., 2019). Once inside the cell the non-essential heavy metal's response can be represented by the bell curve with only the second and third phase: tolerance and toxicity involving detoxification enzymes.

According to the statistical analysis of our results, APX levels are the highest compared to GPX and CAT, with non-significant correlations between APX and Cr, and between CAT and Cd. Indeed, the differences in affinity of APX (of the order of μM) and catalase (of the order of mM) for H_2O_2, produced in the presence of HMs makes the two enzymes react differently to this radical. In fact, APX acts as a messenger to activate defense systems, while catalase eliminates excess H_20_2 during stress (Bouziane, 2006).

http://www.aloki.hu ● ISSN 1589 1623 (Print) ● ISSN 1785 0037 (Online)
DOI: http://dx.doi.org/10.15666/aeer/1906_47214738

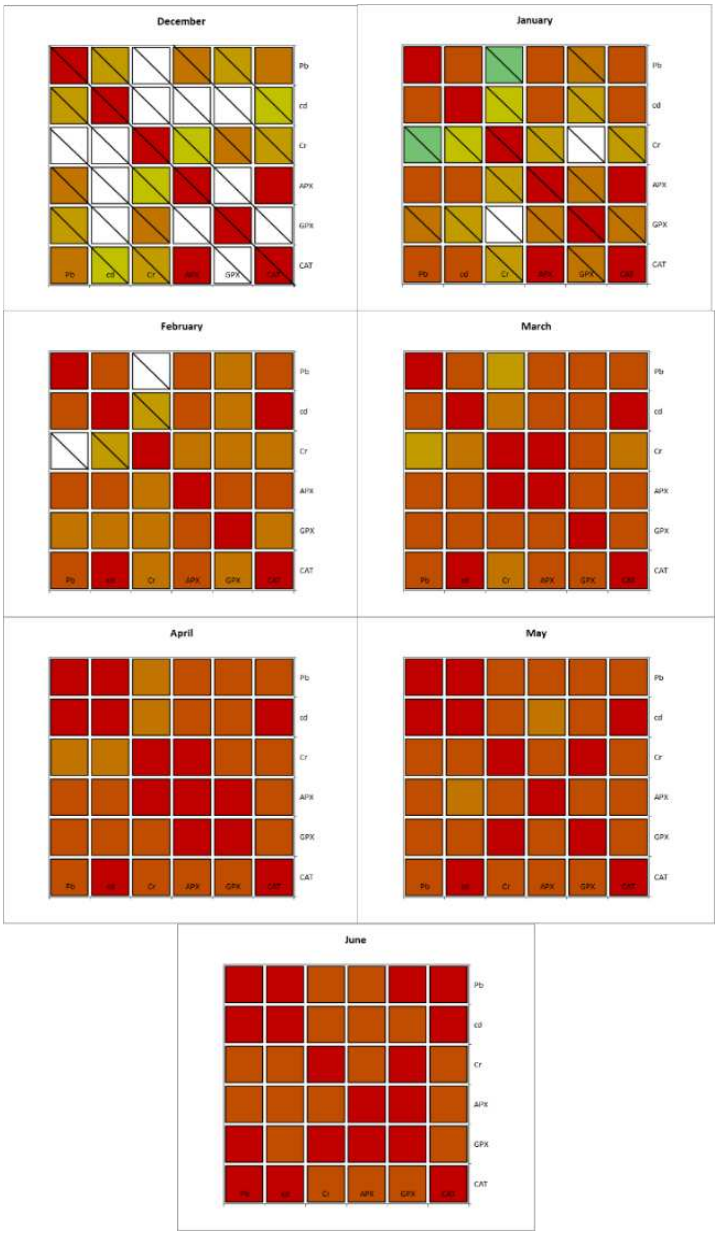

Figure 8. *Correlation between heavy metal concentrations and enzyme activity. Based on a color scale from blue to red (cold-hot scale) to display correlations. The blue color corresponds to a negative correlation close to -1 and the red color corresponds to a positive correlation close to 1, the crossed boxes represent non-significant correlations*

Conclusion

The active bio-monitoring of air quality in the Oran region, the first study of its kind to be conducted in this region, using the foliaceous lichen *Lobaria pulmonaria* has made it possible, on the one hand, to assess and locate air pollution in the region through the interpretation of the concentrations of HMs bio-accumulated by the transplants, which testifies to the bio-accumulative power of the studied bio-indicators. And at the same time, to understand the impact of air pollution in the studied region on the physiological parameters of the lichen *Lobaria pulmonaria*, the focus of our study, notably through the activation of the detoxification enzyme system, notably APX, GPX

http://www.aloki.hu ● ISSN 1589 1623 (Print) ● ISSN 1785 0037 (Online)
DOI: http://dx.doi.org/10.15666/aeer/1906_47214738

and CAT. The study area lacks air quality bio monitoring studies as well as the air quality monitoring systems, the current research serves valuable information about air quality in this region which should be taken into consideration by the authorities, and which in particular can be used as a reference for long-term monitoring of pollution in the same region. Future studies should focus on the measurement of heavy metal concentration in the atmosphere in parallel with the detection of their concentration in lichens, and should focus also as on the study of the impact of air pollution on climate change.

Acknowledgements. We would like to thank the DGRSDT for sponsoring this project.

REFERENCES

[1] Abas, A., Sulaiman, N., Adnan, N. R., Aziz, S. A., Nawang, W. N. S. W. (2019): Using lichen (dirinaria sp.) as bio-indicator for airborne heavy metal at selected industrial areas in malaysia. – Environment Asia 12(3): 85-90.

[2] Agnan, Y., Probst, A., Séjalon-Delmas, N. (2017): Evaluation of lichen species resistance to atmospheric metal pollution by coupling diversity and bioaccumulation approaches: a new bioindication scale for French forested areas. – Ecological Indicators 72: 99-110.

[3] Akomolafe, G., David, O., Nkemdy, A. (2019): Comparative anatomical studies of responses of some roadside plants to highway automobile exhausts. – Journal of Research in Forestry, Wildlife 11(3): 246-255.

[4] Alami, F. O., Elabidi, A., Mouhir, L., Fekhaoui, M. (2014): Utilisation des lichens comme bio-indicateurs de la pollution atmosphérique par le plomb, cadmium et zinc de la région de Rabat-Sale-Zemmour-Zaêr (Maroc). – Afrique Science: Revue Internationale des Sciences et Technologie 10(3): 89-106.

[5] Alioua, A. (1995): Détection de la pollution mercurielle dans la région de Azzaba (Algérie orientale) à l'aide de bioaccumulateurs (Xanthoria parietina, Olea europea, Cupressus sempervirens, Casuarina equisetifolia et Triticum durum). – Magister thesis in ecotoxicology, Université Badji Mokhtar Annaba, Algeria.

[6] Alioua, A. (2001): Détection de la pollution plombique d'origine automobile à l'aide de bio-accumulateurs végétaux dans l'agglomération de Skikda (NE Algérie). – Doctoral thesis in ecotoxicology, Université Joseph Fourier (Grenoble), Greboble, France.

[7] Alioua, A., Maizi, N., Maizi, L., Tahar, A. (2008): Caractérisation de la pollution par le NO2 à l'aide d'un couplage de technique biologique et physico-chimique dans la région d'Annaba (Algérie). – Pollution Atmosphérique 50(200): 325-332.

[8] Álvarez, R., Del Hoyo, A., Díaz-Rodríguez, C., Coello, A. J., Del Campo, E., Barreno, E., Catalá, M., Casano, L. M. (2015): Lichen rehydration in heavy metal-polluted environments: Pb modulates the oxidative response of both Ramalina farinacea thalli and its isolated microalgae. – Microbial Ecology 69(3): 698-709.

[9] Angold, P. G. (1997): The impact of a road upon adjacent heathland vegetation: effects on plant species composition. – Journal of Applied Ecology 34(2): 409-417.

[10] Assad, M. (2017): Transfert des éléments traces métalliques vers les végétaux: mécanismes et évaluations des risques dans des environnements exposés à des activités anthropiques. – Doctoral thesis école doctorale environnement et santé, Université Bourgogne Franche-Comté, Franche-Comté.

[11] Belhadj, H. (2015): Détection de la pollution atmosphérique à l'aide du lichen Xanthoria parietina (L.) bio-accumulateur d'éléments traces métalliques dans le centre urbain de la ville de Sidi Bel Abbés (Algérie occidentale). – Doctoral thesis in science, sciences de l'environnement, Université Djillali Liabes de SBA, Algeria.

http://www.aloki.hu ● ISSN 1589 1623 (Print) ● ISSN 1785 0037 (Online)
DOI: http://dx.doi.org/10.15666/aeer/1906_47214738

[12] Bendaikha, Y., Hadjadj-Aoul, S. (2016): Diversity of lichens flora in Oran area (north-western Algeria). – Advances in Environmental Biology 10(7): 180-191.
[13] Bolan, N., Kunhikrishnan, A., Thangarajan, R., Kumpiene, J., Park, J., Makino, T. (2014): Remediação de solos contaminados com metais pesados (em movimento)-Mobilizar ou imobilizar. – Hazard Mater 266: 141-166.
[14] Bouteraa, M. (2014): Utilisation des végétaux pour l'évaluation de la pollution atmosphérique le long de l'autoroute Est-Ouest dans la région de Constantine. – Magister thesis, Département de biologie végétale et écologie, Université Constantine 1, constantine, Algeria.
[15] Bouziane, M. (2006): Étude physico-chimique de l'accumulation de métaux lourds par les lichens: impacts sur les voies de biosynthèse et interprétation du mécanisme de tolérance chez Diploschistes muscorum. – Doctoral thesis, Ecole Doctorale des Sciences pour l'Ingénieur de Lille, Université des Sciences et Technologies de Lille, France.
[16] Brodo, I. M. (1961): Transplant experiments with corticolous lichens using a new technique. – Ecology 42(4): 838-841.
[17] Cakmaki, H. (1991): Effect of aluminium on lipid peroxidation, superoxide dismutase, catalase, and peroxide activities in root tips of soybean. – PhysiolPlant 83(3): 463-468.
[18] Carlsson, R., Nilsson, K. (2009): Status of the red-listed lichen *Lobaria pulmonaria* on the Åland Islands, SW Finland. – Annales Botanici Fennici, BioOne, 549-554.
[19] Chance, B., Sies, H., Boveris, A. (1979): Hydroperoxide metabolism in mammalian organs. – Physiological Reviews 59(3): 527-605.
[20] Chiboub, M., Jebara, S. H., Abid, G., Jebara, M. (2019): Co-inoculation effects of Rhizobium sullae and Pseudomonas sp. on growth, antioxidant status, and expression pattern of genes associated with heavy metal tolerance and accumulation of cadmium in Sulla coronaria. – Journal of Plant Growth Regulation 39: 1-13.
[21] Chirva, O. V., Nikerova, K. M., Androsova, V. I., Ignatenko, R. V. (2019): Activity of catalase and superoxide dismutase in *Lobaria pulmonaria* from forest communities of middle and northernmost boreal zone (NW Russia). – Czech Polar Reports 9(2): 228-242.
[22] Çomaklı, E., Bingöl, M. S. (2021): Heavy metal accumulation of urban Scots pine (Pinus sylvestris L.) plantation. – Environmental Monitoring Assessment 193(4): 1-13.
[23] Cui, N., Qu, L., Wu, G. J. J. O. E. S. (2022): Heavy metal accumulation characteristics and physiological response of Sabina chinensis and Platycladus orientalis to atmospheric pollution. – Journal of Environmental Sciences 112: 192-201.
[24] Deruelle, S. (1978): Etude comparee de la sensibilite de trois methodes d'estimation de la pollution atmospherique, en utilisant les lichens comme indicateurs biologiques, dans la region de Mantes (Yvelines). – Rev. Bryol. Lichenol 44(4): 429-441.
[25] Déruelle, S. (1983): Les Lichens Témoins De La Pollution. – Vuibert, Paris.
[26] DOE (2018): Directorate of Environment of Oran city. – DOE, Oran.
[27] Fielding, J. L., Hall, J. (1978): A biochemical and cytochemical study of peroxidase activity in roots of Pisum sativum: II. Distribution of enzymes in relation to root development. – Journal of Experimental Botany 29(4): 983-991.
[28] Garrec, J., Van Haluwyn, C. (2002): Biosurveillance végétale de la qualité de l'air e Concepts, méthodes et applications (Air Quality Biomonitoring with Plants e Concepts, Methods and Applications). – Lavoisier, Paris.
[29] Garty, J., Kloog, N., Cohen, Y. (1998): Integrity of lichen cell membranes in relation to concentration of airborne elements. – Archives of Environmental Contamination Toxicology 34(2): 136-144.
[30] Guelorget, O., Frisoni, G., Monti, D., Perthuisot, J. (1986): Contribution à l'étude écologique des lagunes septentrionales de la baie d'Amvrakia (Grèce). – Oceanologica Acta 9(1): 9-17.
[31] Hamutoğlu, R., Aslan, A., Aras, S., Cansaran-Duman, D. (2017): Environmental risk assessment under the pollutants exposure with using four lichen species and molecular assay in cement plant, Aşkale-Erzurum (Turkey). – Cancer 73(3): 253-266.

http://www.aloki.hu ● ISSN 1589 1623 (Print) ● ISSN 1785 0037 (Online)
DOI: http://dx.doi.org/10.15666/aeer/1906_47214738

[32] Ilondu, E. (2019): Occurrence and diversity of Lichens in Abraka and its environs, Delta State, Nigeria. – Journal of Applied Sciences Environmental Management 23(5): 947-951.
[33] Jaskulak, M., Rorat, A., Grobelak, A., Chaabene, Z., Kacprzak, M., Vandenbulcke, F. (2019): Bioaccumulation, antioxidative response, and metallothionein expression in Lupinus luteus L. exposed to heavy metals and silver nanoparticles. – Environmental Science Pollution Research 26(16): 16040-16052.
[34] Jiang, Y., Fan, M., Hu, R., Zhao, J., Wu, Y. (2018): Mosses are better than leaves of vascular plants in monitoring atmospheric heavy metal pollution in urban areas. – International Journal of Environmental Research 15(6): 1-13.
[35] Kadri, Y., Madani, M. (2015): L'agglomération oranaise (Algérie) entre instruments d'urbanisme et processus d'urbanisation. – EchoGéo 34: 1-20.
[36] Kaur, M., Bhatti, S. S., Katnoria, J. K., Nagpal, A. K. (2021): Investigation of metal concentrations in roadside soils and plants in urban areas of Amritsar, Punjab, India, under different traffic densities. – Environmental Monitoring Assessment 193(4): 1-20.
[37] Kłos, A., Ziembik, Z., Rajfur, M., Dołhańczuk-Śródka, A., Bochenek, Z., Bjerke, J. W., Tømmervik, H., Zagajewski, B., Ziółkowski, D., Jerz, D. (2018): Using moss and lichens in biomonitoring of heavy-metal contamination of forest areas in southern and north-eastern Poland. – Science of the Total Environment 627: 438-449.
[38] Loggini, B., Scartazza, A., Brugnoli, E., Navari-Izzo, F. (1999): Antioxidative defense system, pigment composition, and photosynthetic efficiency in two wheat cultivars subjected to drought. – Plant Physiology 119(3): 1091-1100.
[39] Mahapatra, B., Dhal, N. K., Dash, A. K., Panda, B. P., Panigrahi, K. C. S., Pradhan, A. (2019): Perspective of mitigating atmospheric heavy metal pollution: using mosses as biomonitoring and indicator organism. – Journal Environmental Science Pollution Research 26(29): 29620-29638.
[40] Maizi, N., Alioua, A. (2015): Evaluation of levels of lead pollution from automobiles near Highway using phanerogamic and cryptogamic species in the city of Annaba (Algeria). – IJSRST 1(6): 33-43.
[41] Mcadam, K., Steer, P., Perrotta, K. (2011): Using continuous sampling to examine the distribution of traffic related air pollution in proximity to a major road. – Atmospheric Environment 45(12): 2080-2086.
[42] Nakano, Y., Asada, K. (1987): Purification of ascorbate peroxidase in spinach chloroplasts; its inactivation in ascorbate-depleted medium and reactivation by monodehydroascorbate radical. – Plant Cell Physiology 28(1): 131-140.
[43] Nash Iii, T. H. 2008. Lichen Sensitivity to Air Pollution. – In: Nash, T., III (ed.) Lichen Biology. 2nd Ed. Cambridge University Press, Cambridge, UK.
[44] Nimis, P. L., Scheidegger, C., Wolseley, P. A. (2002): Monitoring with Lichens—Monitoring Lichens. – Springer, Dordrecht.
[45] OTD (2018): Oran Transport Direction. – OTD, Oran.
[46] Pagotto, C., Remy, N., Legret, M., Le Cloirec, P. (2001): Heavy metal pollution of road dust and roadside soil near a major rural highway. – Environmental Technology 22(3): 307-319.
[47] Paoli, L., Vannini, A., Fačkovcová, Z., Guarnieri, M., Bačkor, M., Loppi, S. (2018): One year of transplant: is it enough for lichens to reflect the new atmospheric conditions? – Ecological Indicators 88: 495-502.
[48] Polle, A. J. P. P. (2001): Dissecting the superoxide dismutase-ascorbate-glutathione-pathway in chloroplasts by metabolic modeling. Computer simulations as a step towards flux analysis. – Plant Physiology 126(1): 445-462.
[49] Rahal, F., Hadjou, Z., Blond, N., Aguejdad, R. J. C. E. J. O. G. (2018): Croissance urbaine, mobilité et émissions de polluants atmosphériques dans la région d'Oran, Algérie. – Cybergeo. https://doi.org/10.4000/cybergeo.29111

http://www.aloki.hu ● ISSN 1589 1623 (Print) ● ISSN 1785 0037 (Online)
DOI: http://dx.doi.org/10.15666/aeer/1906_47214738

[50] Rahali, M. (2002): Mapping of lead pollution in Algiers area with a lichen (Xanthoria parietina) as indicator. – Pollution Atmosphérique 44(175): 421-432.
[51] Rahma, K., Aminata, O. E. H.-K., Belkeir, D., Francisc, C.-H., Marie-André, E. (2014): EFFET DE LA Pollution Atmospherique Par Les Hydrocarbures Sur Le Lichen Xanthoria Parietina (L.) Th (Teloschistaceae) Dans La Zone De Hassi Messaoud (Sahara Septentrional Est Algerien). – Algerian Journal of Arid Environment "AJAE" 4(2): 98-106.
[52] Ramade, F. (2007): Introduction à l'écotoxicologie: fondements et applications. – Tec & Doc, Paris.
[53] Rola, K. (2020): Insight into the pattern of heavy-metal accumulation in lichen thalli. – Journal of Trace Elements in Medicine 61: 126512.
[54] Semadi, A., Deruelle, S. (1993): Détection de la pollution plombique à l'aide de transplants lichéniques dans la région de Annaba (Algérie). – Pollution Atmosphérique 86: 86-102.
[55] Serradj-Ali Ahmed, M., Boumedris, Z., Djebar, M., Tahar, A. (2014): Responses of antioxidants in Flavoparmelia caperata (L.) Hale to the atmospheric pollution air at two urban and semi-urban areas in the region of Annaba (East of Algeria). – Pollution Atmosphérique 221. https://doi.org/10.4267/pollution-atmospherique.2674.
[56] Shahid, M., Dumat, C., Khalid, S., Schreck, E., Xiong, T., Niazi, N. K. (2017): Foliar heavy metal uptake, toxicity and detoxification in plants: a comparison of foliar and root metal uptake. – Journal of Hazardous Materials 325: 36-58.
[57] Škrbić, B., Milovac, S., Matavulj, M. (2012): Multielement profiles of soil, road dust, tree bark and wood-rotten fungi collected at various distances from high-frequency road in urban area. – Ecological Indicators 13(1): 168-177.
[58] Stankevich, S., Titarenko, O., Kharytonov, M., Benselhoub, A., Bounouala, M., Chaabia, R., Boukeloul, M.-L. (2015): Mapping of urban atmospheric pollution in the northern part of Algeria with nitrogen dioxide using satellite and ground-truth data. – Studia Universitatis "Vasile Goldis" Arad. Seria Stiintele Vietii 25(2): 87-92.
[59] Tkalec, M., Štefanić, P. P., Cvjetko, P., Šikić, S., Pavlica, M., Balen, B. (2014): The effects of cadmium-zinc interactions on biochemical responses in tobacco seedlings and adult plants. – Plos One 9(1): e87582.
[60] Tyler, G. (1989): Uptake, retention and toxicity of heavy metals in Lichens. – Water, Air, Soil Pollution 47(3): 321-333.
[61] Viskari, E.-L., Kärenlampi, L. (2000): Roadside Scots pine as an indicator of deicing salt use–a comparative study from two consecutive winters. – Water, Air, Soil Pollution 122(3): 405-419.
[62] Vitali, M., Antonucci, A., Owczarek, M., Guidotti, M., Astolfi, M. L., Manigrasso, M., Avino, P., Bhattacharya, B., Protano, C. (2019): Air quality assessment in different environmental scenarios by the determination of typical heavy metals and Persistent Organic Pollutants in native lichen Xanthoria parietina. – Environmental Pollution 254(part A): 113013.
[63] WHO (2018): Ambient Outdoor Air Pollution. – World Health Organisation, Geneva.
[64] Yemets, O. A., Solhaug, K. A., Gauslaa, Y. J. T. L. (2014): Spatial dispersal of airborne pollutants and their effects on growth and viability of lichen transplants along a rural highway in Norway. – The Lichenologist 46(6): 809-823.

http://www.aloki.hu ● ISSN 1589 1623 (Print) ● ISSN 1785 0037 (Online)
DOI: http://dx.doi.org/10.15666/aeer/1906_47214738

ANALYSIS OF LAND USE AND LAND COVER DYNAMICS USING REMOTE SENSING AND GIS IN THE UPPER TAMIRAPARANI WATERSHED OF TAMIL NADU, INDIA

SANTHANAKRISHNAN, P. T.* – AMBUJAM, N. K. – NARAYANAN, M.

Centre for Water Resources, Anna University, Chennai, Tamil Nadu 600025, India

**Corresponding author*
e-mail: santhanakrishnan.pt@gmail.com

(Received 31st Mar 2020; accepted 10th Jun 2021)

Abstract. Analysing the land use and land cover change along with its cause and consequence on the livelihood of people as well as on the environment is important for sustainable development and management of natural resources. The present study focuses on analysis of land use and land cover dynamics using Landsat images with 30 m spatial resolution for upper Tamiraparani watershed located in Tamil Nadu state in India. ArcGIS 10.3 and ERDAS Imagine 14 have been used for the image processing to produce five land use and land cover classes in the watershed. The results after classification indicates that over the past 17 years, expansion of urban built-up and agricultural land have increased at a rate of 195.2 ha/year and 37.1 ha/year respectively and contrary to this the share of forest land, barren land and water bodies shrunk with the rate of 118.2 ha/year, 96.6 ha/year and 17.6 ha/year respectively. It is understood that the urban built-up has intensively expanded at the expense of other land use and land cover without significant conservation measure. In particular, integrated approach with community participation is required in the watershed development for management of natural resources and sustainable development.
Keywords: *image processing, ecosystem conservation, environment, urban sprawl, ArcGIS and ERDAS*

Introduction

Land use and land cover dynamics have become a major concern in the twenty first century, with remarkable implications for human survival. Land cover change refers to the change in the physical and biological characteristics of land on account of the modification of natural environments into built environments such as settlements or farm land for agricultural activities (Prakasam, 2010; Dezso et al., 2005). Recently, the research on land use and land cover change has drawn the attention of the researchers since these dynamics affect the hydrological cycle, natural biodiversity, land productivity and sustainability of the natural ecosystem (Nurelegn and Amare, 2014; Minale and Rao, 2012). This land use dynamics in recent years plays a wide role as driving force in alternating the global environment (Bae and Ryu, 2014).

Land use and land cover change detection is essential for better understanding of landscape dynamic during a known period of time having sustainable management (Praveen Kumar and Sreenivasula Reddy, 2013). According to Abbas et al. (2010) alteration in land use and land cover significantly aggravates the phenomenon like soil erosion, land degradation, increased surface runoff, siltation, sedimentation, drought, migration, desertification with loss of biodiversity, decrease in productivity and famine. Though we have many controversies on the factors affecting land cover dynamics, few research studies states that demographic factor intensively hasten the land use dynamics (Abate, 2011). Increase in rate of population, insecure land use right and lack of credit facilities are some of the socio-economic factors which facilitates for the change of land

http://www.aloki.hu ● ISSN 1589 1623 (Print) ● ISSN 1785 0037 (Online)
DOI: http://dx.doi.org/10.15666/aeer/1906_47394749

use and land cover. For the poor those are living under subsistence farming has no other option other than exploiting available natural resource. In major parts of the world, particularly in developing countries agriculture is the major livelihood of people, but primarily the most driver of land use change (Shiferaw, 2011). Relationship between various socio-economic conditions of the society, population pressure and physiographic feature, the land use type has resulted in land use change. Therefore, land use and land cover classification is used to analyse the interaction between socio-economic and land use, which is contributed for the dynamics of land use and land cover change resulted from diversified and intensified agriculture and urbanization.

Understanding the changes in landscape patterns and their interactions with human activities and natural phenomenon are very essential for proper land management and decision improvement. Today, the data available from earth resource satellites are very applicable and useful for land use and land cover change detection studies (Song et al., 2011). With the aid of remote sensing and Geographical Information System (GIS) techniques, land use and land cover mapping has given a useful and detailed way to improve the selection of areas designed to agricultural, urban or industrial areas of a region (Deng et al., 2013; Dessie and Kleman, 2007). Application of remotely sensed data helps to determine the alterations in land cover in less time, at low cost and with better accuracy (NRSC and ISRO, 2011; FAO, 2004). Recent developments in GIS techniques provides suitable platform for data analysis, update and retrieval.

Although there have been extensive reports of current researches, there is still much unknown about the impacts of regional land use change on ecosystem management. Though various studies have under taken about the extent and status of clearing of forest, land cover change and soil erosion in many parts of Tamil Nadu, these studies feebly recognized the land cover dynamics and its driving force. Therefore, the prime objective of the study was to analyse and identify the land use and land cover dynamics and its driving force in upper Tamiraparani watershed in the past 17 years.

Study area

The watershed considered for the study is upper Tamiraparani which is located in the upper reach of Tamiraparani river basin, a region located in southern part of Tamil Nadu in India with a geographic location of 80 33’ 01” N and 80 48’ 24” N latitude and 770 10’ 16” E and 770 32’ 02” E longitude. The upper Tamiraparani watershed covers an area of about 514.33 square kilometers holding a population density of 621 persons per square kilometer covering the major portions Tirunelveli district with agriculture as main economic activity of the people. The river Tamiraparani originates from Agasthiya malai on the eastern slopes of Western Ghats of India and confluences with Bay of Bengal near Palaya kayal as shown in *Figure 1*. The upper Tamiraparani watershed occupies the head reach of river Tamiraparani and comprises of two reservoirs namely Papanasam reservoir and Servalar reservoir the major portion of the watershed is covered by forest land which ranged densely vegetated trees (natural forest), plantations, shrubs and bushes. The watershed is characterized with diverse topographic conditions like mountainous, dissected terrain with moderate and steep slopes. The upper Tamiraparani watershed lies within the tropical monsoon zone. Based on the hydro-meteorological features the monsoon period is Southwest monsoon period spanning from June to September and Northeast monsoon period spanning from October to December with an annual average rainfall of the basin is about 1526 mm.

http://www.aloki.hu ● ISSN 1589 1623 (Print) ● ISSN 1785 0037 (Online)
DOI: http://dx.doi.org/10.15666/aeer/1906_47394749

The major crops cultivated in the watershed are paddy, banana, sugarcane, pulses, fruits and vegetables. The educational levels of farmers are favorable to adopt modern water management practices and cropping pattern.

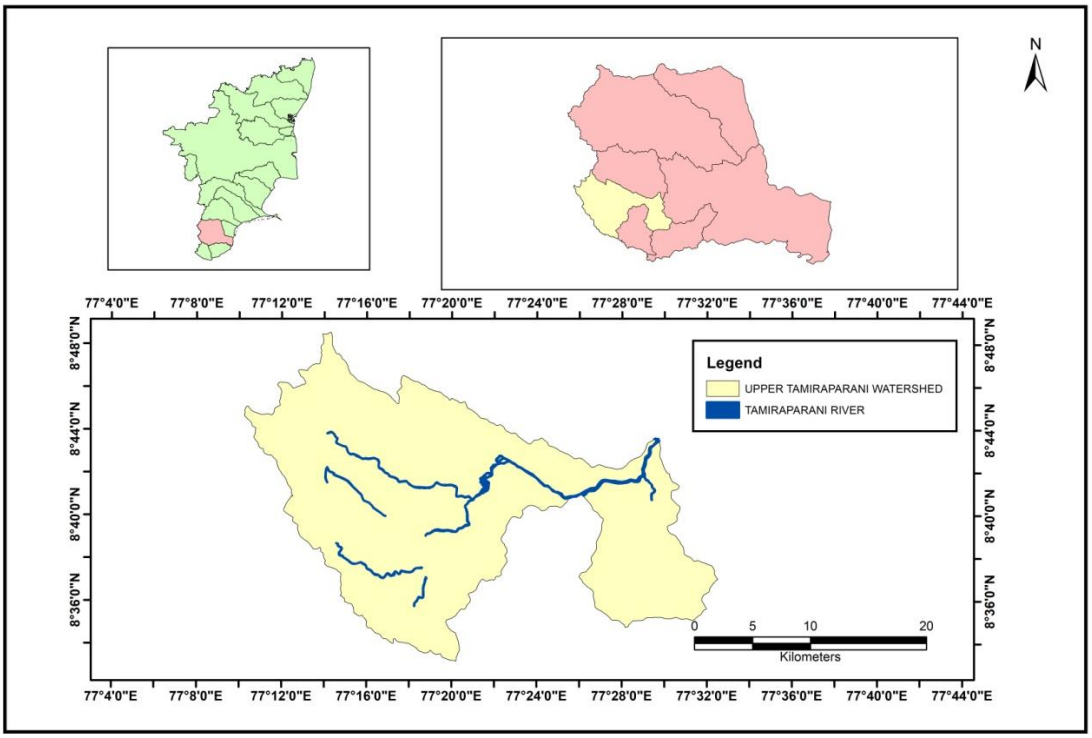

Figure 1. *Index map of upper Tamiraparani watershed*

Data source and analysis method

For the land cover and land use dynamics analysis the Landsat imagery was download from https://earthexplorer.usgs.gov/. The imagery was processes using ArcGIS 10.3 and classified with ERDAS IMAGE14 software. The details of the satellite data is presented in *Table 1*. Landsat 7 and Landsat 8 in path/row of 143/54 with spatial resolution of 30 m were taken for the study (Meshesha et al., 2016; Clevers et al., 2004). The land use and land cover change detection of the watershed under the study was analyzed for last 17 years. Supervised classification was carried out to classify the Landsat images (Carlson and Sanchez-Azofeifa, 1999; Baulies and Szejwach, 1998).

The parameters of the watershed like slope, slope length, slope width and stream network was obtained from the Digital Elevation Models (DEM) and the topography of the study area was defined by DEM which is used to describe the elevation of points for the given area at a spatial resolution of 30 m × 30 m. Finally about five land use and land cover were identified for the watershed. The five classes of use and land cover are given in *Table 2*. In order to get further information about the long term understanding of land use and land cover change practice in the watershed under study, focus group discussion have been conducted. For the discussion and in-depth interview elder peoples were selected as they assumed to have better local ecological information about the trend of land use and land cover change.

http://www.aloki.hu ● ISSN 1589 1623 (Print) ● ISSN 1785 0037 (Online)
DOI: http://dx.doi.org/10.15666/aeer/1906_47394749

Table 1. *Materials and their source used for the analysis*

S. No	Images	Resolution (m)	Sensor	Path	Row	Date (dd-mm-yyyy)
1	Landsat 7	30 × 30	TM	143	54	04-09-2001
2	Landsat 7	30 × 30	TM	143	54	15-10-2013
3	Landsat 8	30 × 30	TM	143	54	03-03-2018

Table 2. *Description of land use and land cover class*

S. No.	Land use and land cover class	Description
1	Forest land (FL)	Region covered with thick natural forest, plantation forest and riparian forest
2	Agricultural land (AL)	Land allotted for cultivation of crops in seasonal, annual and perennial
3	Urban built-up (UB)	Settlements closely associated with cultivated land, urban settlements, industrial and commercial buildings and transportation regions
4	Barren land (BL)	Area with very little or no vegetation cover on land surface, vulnerable soil to erosion and degradation. It also includes bedrock which is unable to support cultivation
5	Water body (WB)	Is having surface water. It includes reservoirs, rivers, streams, ponds, lakes, Irrigation tanks and marsh lands

After the classification process the geographical extent of the land use and land cover in terms of hectare was calculated for each mentioned time periods and the extent of the change in land use type between the periods and within the periods was compared. The land use and land cover class has been performed using both ArcGIS10.3 and ERDAS IMAGINE14 and using the following formula necessary calculation has been engaged to know the rate of change in land use and land cover in hectare/year and percentage share of each class has studied in the time periods.

$$\Delta A\ (\%) = \frac{At2 - At1}{At1} \times 100 \qquad \text{(Eq.1)}$$

where ΔA (%) = change in area of land use and land cover class between the time interval At1 and At2 in percentage. At1 = area of land use and land cover type at initial time. At2 = area of land use and land cover type at final time.

The rate of change of land use and land cover type was calculated by the following formula:

$$\Delta R \left(\frac{ha}{year}\right) = \frac{Z - X}{W} \qquad \text{(Eq.2)}$$

where ΔR = rate of change in hectare per year, Z = recent area of land use and land cover type in hectare, X = previous area of land use and land cover type in hectare, W = the time interval that lapsed between Z and X in years.

http://www.aloki.hu ● ISSN 1589 1623 (Print) ● ISSN 1785 0037 (Online)
DOI: http://dx.doi.org/10.15666/aeer/1906_47394749

Results and discussion

Land use and land cover map

Combinations of red, green and blue bands were adopted to display the layer stacked image in the standard color composite. In order to carry out the analysis false color composite bands 2, 3 and 4 used.

In order to meet the basic requirements of the increasing human population, agricultural land and urban and has increased in all parts of the world at the expense of other land use class such as forest, barren land and water bodies particularly in the developing countries where the greater part of inhabitants are depending on urban for their survival (Asres et al., 2016; Ayele et al., 2016). In the present study similar trend in the watershed has been found where agricultural land and settlement area have increased over time in all the time period of analysis. A considerable land use change has been observed in the study region since 1990s. To illustrate this substantial change through over time due to various uses and the overall change was presented in the year 2001, 2013 and 2018.

Land use and land cover dynamics

In the present study five classes of land use and land cover were presented namely forest land, agriculture land, urban land, barren land and water body. The land use and land cover dynamics is discussed in the following sections.

Forest land

The most prevailing land use cover class of the study catchment was forest resources which ranged densely vegetated trees (natural forest), plantations, shrubs and bushes. Thus in the study area, forest land occupies the major share of land cover class and the area covered by such forest could be deciduous, semi deciduous forest and mixed forest land. From the total area of the watershed in 2001 the share of the forest cover was 75%, in contrast the coverage slightly decreased to 69.7% in the year 2013. It is evident that the decrease in forest cover corresponds to increase in the population and expansion of agricultural land. However, in 2018 the forest cover has regenerated by 1.4%. The decrease of forest in the initial periods between 2001 and 2013 was around 2717.1 ha (5.3% lost), this is a considerable reduction in the forest cover given the expansion of built up area and agricultural fields and it is contradicted from the expectations. However, in the next period between 2013 and 2018 the share of the forest cover has increased by 1.4%. Therefore, over the period of 17 years in between 2001 and 2018 the share has decreased by 3.9%. On the basis of local ecological knowledge from interview and group discussion, factors like private and community level tree plantation helped in increasing the share of forest cover in later periods by 1.4% (between 2013 and 2018).

Agricultural land

Agricultural land is the region for crop cultivation for both annual and perennial crops. In the region under the study agriculture occupies a considerable land cover class (4.1, 7.7 and 5.3% in 2001, 2013 and 2018 respectively). This implies that the agricultural land cover has been increased at the expense of forest land. This is due to rise in demand on account of population growth, additional farm land required to meet

http://www.aloki.hu ● ISSN 1589 1623 (Print) ● ISSN 1785 0037 (Online)
DOI: http://dx.doi.org/10.15666/aeer/1906_47394749

the food demand. Due to ever increase in cultivated land, farmer's exerted pressure on forest land and other barren land. This further hastened the erosion and degradation of soil and similar studies elsewhere states that alarming population rates resulted for the change of land cover class through time.

Urban built-up

The urban settlements in the study watershed have shown a persistent increase in the time period of analysis. The total area of the watershed covered by settlement has increased by 3.7% from 2001 to 2013, 2.8% from 2013 to 2018 (*Figs. 2, 3, 4; Table 3*). Unlike other types of land use systems, the growth rate of both rural and urban settlements took the largest share by covering other land use types for instance forest, bushes, water bodies, agriculture and barren land. In the time period of study (2001–2018) there has been 6.5% increase of settlement land within the last 17 years. This is because of continuous increase in population number they need addition land for settlement area, which costs 3319.11 ha of other land use type.

Table 3. *Land use and land cover area of upper Tamiraparani watershed*

LULC classes	Land use and land cover area (ha) and percentage share					
	2001		2013		2018	
	Area (ha)	%	Area (ha)	%	Area (ha)	%
Forest land	38615.7	75.0	35898.6	69.7	36606.2	71.1
Agricultural land	2097.1	4.1	3972.9	7.7	2727.6	5.3
Urban built-up	1414.9	2.7	3311.3	6.4	4734.0	9.2
Barren land	8501.0	16.5	7518.8	14.6	6859.4	13.3
Water body	872.7	1.7	799.8	1.6	574.1	1.1
Total	51501.3	100	51501.3	100	51501.3	100

Barren land

This type of land use within the stated years has shown continuously decreasing trend from 16.5% in 2001 to 14.6%, 13.3% in 2013 and 2018 respectively. With a declining trends in the first periods from 2001 to 2013 by 1.9% and further in the second periods from 2013 to 2018 further declined by 1.3%. That is for the last 17 years; about 3.2% of barren land was changed into other type of land cover classes. This is due to ease of use of fixed plot of farm land in collaboration with alarming population rate growth negatively contributed for the decline of barren land.

Water bodies

This land use type includes reservoirs, ponds, lakes, streams and rivers within the watershed. In the study area water bodies covered only 1.7% in 2001 decreased to 1.6% in 2013 and further reduced to 1.1% in 2018 (*Figs. 5, 6; Table 4*). It is understood that this fluctuation water bodies in the analysis period (2001–2018) is that water harvesting habit of local people was low, though there is an increase in the rainfall trend within the watershed.

http://www.aloki.hu ● ISSN 1589 1623 (Print) ● ISSN 1785 0037 (Online)
DOI: http://dx.doi.org/10.15666/aeer/1906_47394749

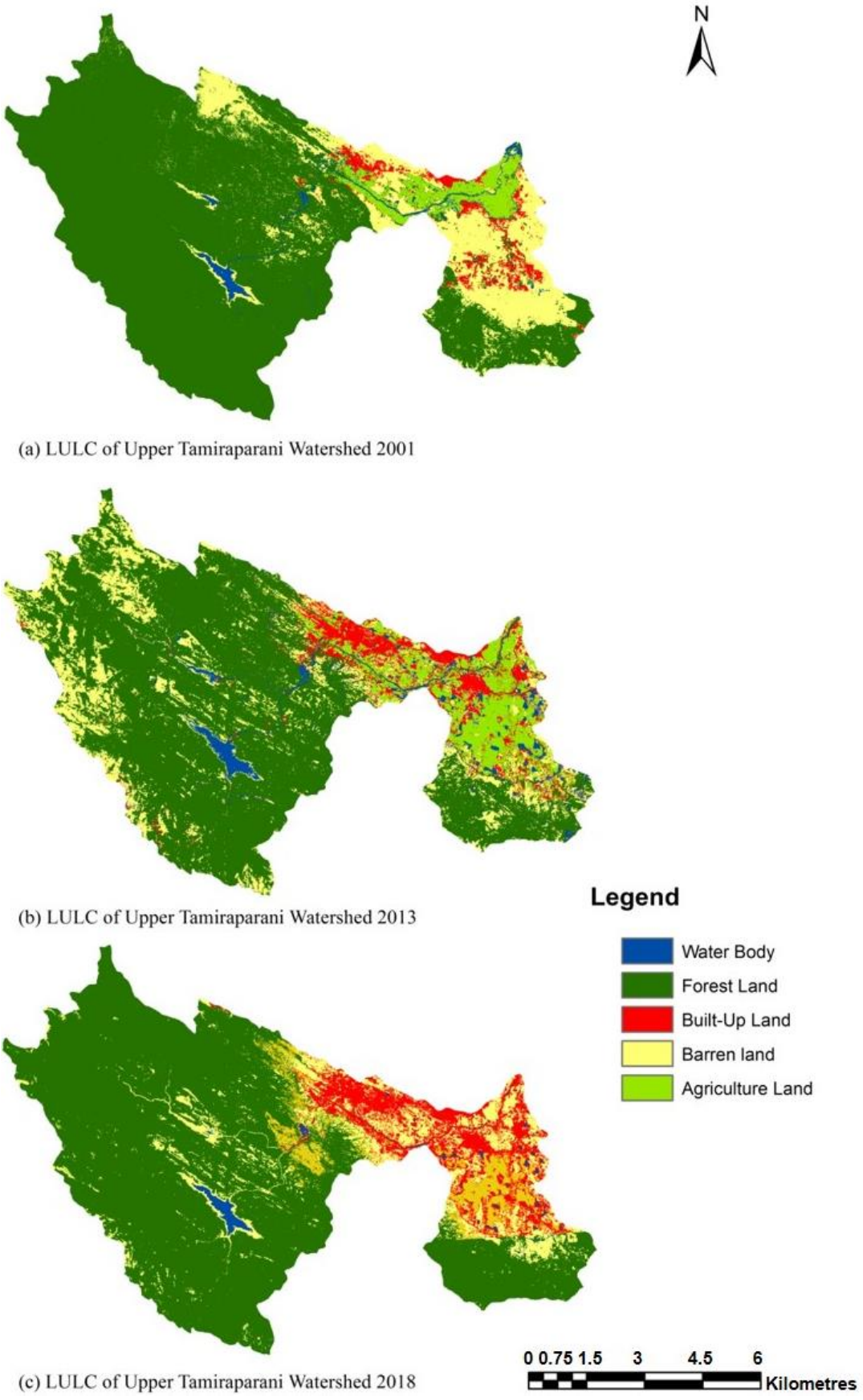

Figure 2. *Land use and land cover map of upper Tamiraparani watershed*

http://www.aloki.hu ● ISSN 1589 1623 (Print) ● ISSN 1785 0037 (Online)
DOI: http://dx.doi.org/10.15666/aeer/1906_47394749

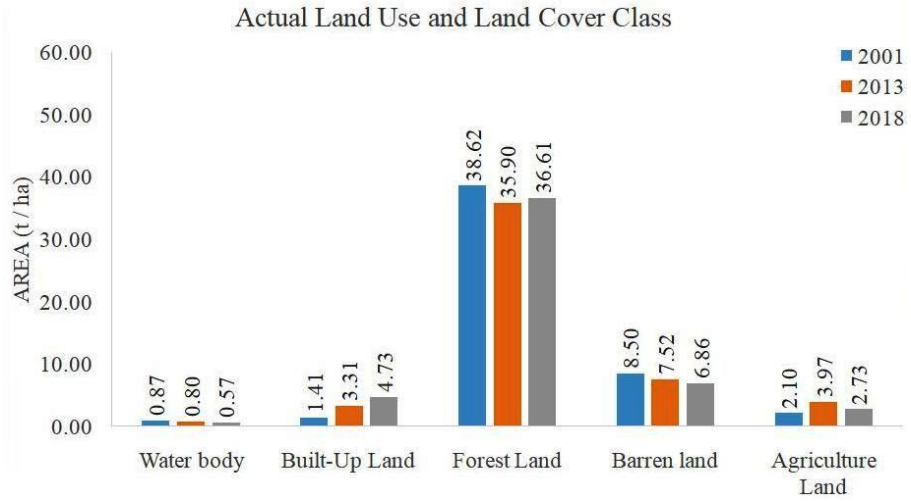

Figure 3. *Land use and land cover type and area of upper Tamiraparani watershed in hectare*

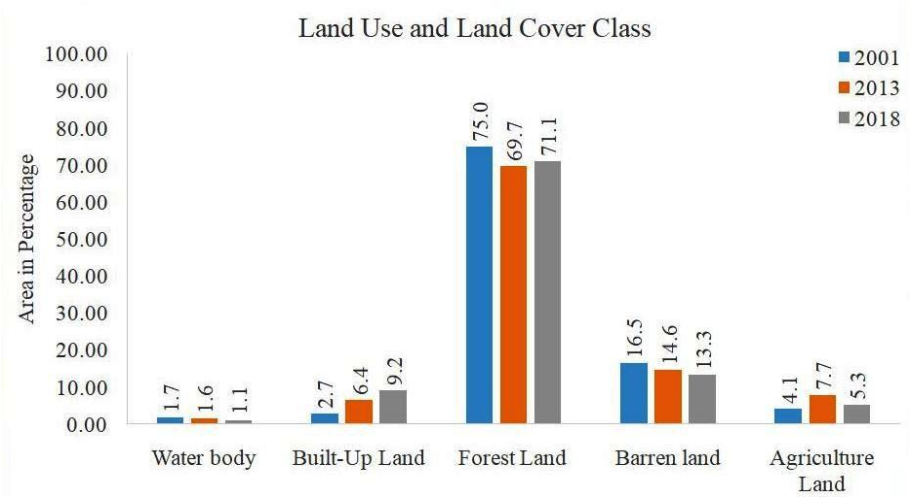

Figure 4. *Percentage share of land use and land cover of upper Tamiraparani watershed*

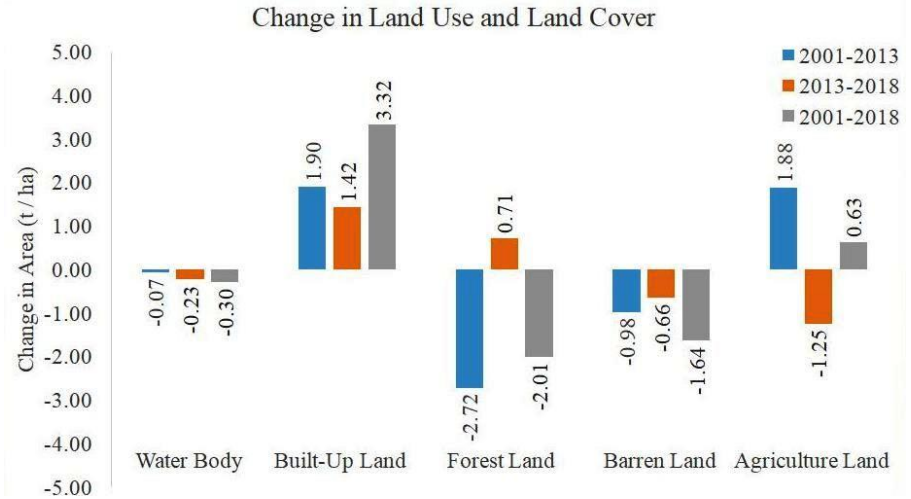

Figure 5. *Change in land use and land cover of upper Tamiraparani watershed in hectare*

http://www.aloki.hu ● ISSN 1589 1623 (Print) ● ISSN 1785 0037 (Online)
DOI: http://dx.doi.org/10.15666/aeer/1906_47394749

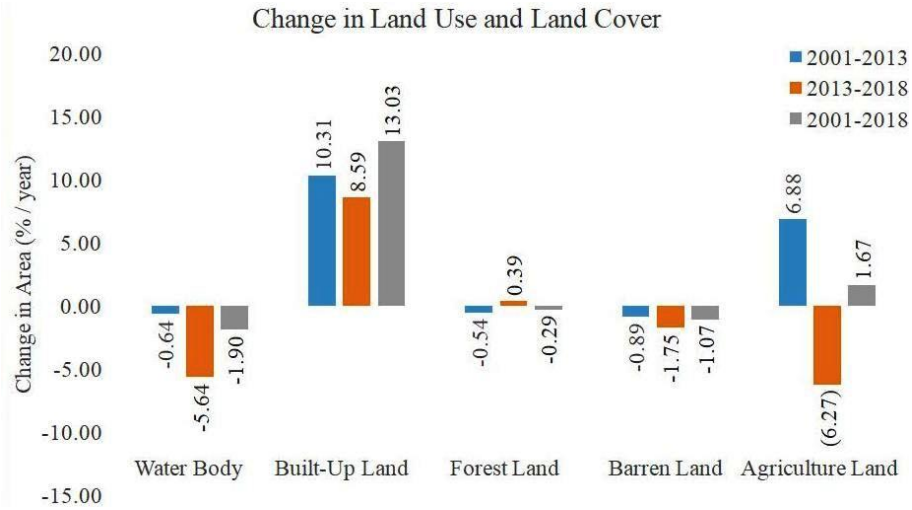

Figure 6. *Percentage change of land use and land cover of upper Tamiraparani watershed*

Table 4. *Change in Land use and land cover of upper Tamiraparani watershed*

LULC classes	Change in land use and land cover (ha) and percentage share					
	2001–2013		2013–2018		2001–2018	
	Area (ha)	%	Area (ha)	%	Area (ha)	%
Forest land	-2717.1	-5.3	+ 707.7	+ 1.4	-2009.4	-3.9
Agricultural land	+ 1875.8	+ 3.6	-1245.2	-2.4	+ 630.5	+ 1.2
Urban built-up	+ 1896.4	+ 3.7	+ 1422.7	+ 2.8	+ 3319.1	+ 6.4
Barren land	-982.2	-1.9	-659.4	-1.3	-1641.6	-3.2
Water body	-72.9	-0.1	-225.7	-0.4	-298.6	-0.6

Rate of land use and land cover change dynamics

The rate of change of forest land, agricultural land, built-up land, barren land and water bodies of Upper Tamiraparani watershed is presented in *Table 5*. This results states that though the resource is fixed, there exist various rate of change in different land cover types. However, the change rate of different land cover types has slightly variable among themselves.

The analysis indicates that between 2001 and 2013, agriculture land and built-up area has increased with the rate of 156.3 ha/year and 158 ha/year respectively caused for the outflow of other remaining land use classes. In the same period forest land, barren land and water body areas have decreased at the rate of 226.4 ha/year, 81.8 ha/year and 6.1 ha/year respectively. But, between the periods 2013 and 2018 expansion of urban built-up persistently increased with a rate of 284.5 ha/year and in this period, in the forest land there exist an increment in rate of forest cover as 141.5 ha/year. Unlike the previous period, unexpectedly with the increasing rate of urban built-up, the forest land has increased with a rate of 141.5 ha/year which is understood from the local investigation that the conservation of forest land has gained the importance within the watershed. However, agricultural land, barren land and water bodies rapidly decreased at the rate of 249 ha/year, 131.9 ha/year and 45.1 ha/year in between 2013 and 2018. Over the last 17 years expansion of agriculture land and urban built-up area increased

http://www.aloki.hu ● ISSN 1589 1623 (Print) ● ISSN 1785 0037 (Online)
DOI: http://dx.doi.org/10.15666/aeer/1906_47394749

with a rate of 37.1 ha/year and 195.2 ha/year respectively and contrary to this the share of forest land, barren land and water bodies shrunk with the respective rate of 118.2 ha/year, 96.6 ha/year and 17.6 ha/year. The result of the finding is particularly urban built-up have intensively expanded at the expense of other land use and land cover without significant conservation measure.

Table 5. *Rate of change in LULC of upper Tamiraparani watershed*

LULC classes	Rate of change (ha/year)		
	2001–2013	**2013–2018**	**2001–2018**
Forest land	-226.4	141.5	-118.2
Agricultural land	156.3	-249.0	37.1
Urban built-up	158.0	284.5	195.2
Barren land	-81.8	-131.9	-96.6
Water body	-6.1	-45.1	-17.6

Conclusion

In the last 17 years land use and land cover dynamics have undergone a considerable change in the upper Tamiraparani watershed. The observations in the land use and land cover dynamics showed the expansion of urban built-up and agricultural land as leading. On the other hand the forest land, water body and barren land declined. Though there exist overall decline in forest land, in recent five year (2013 to 2018) observation the trend of forest cover was increasing and this was possible because of the initiative of the local communities and government in conservation of the forest land. Similarly necessary action ought to be considered such that the water bodies within the watershed are also conserved with necessary rain water harvesting technologies. The increase in forest cover promotes the surrounding environmental condition because massive soil erosion and land degradation would be reduced. This could be possible only by proper integrated approach in conservation activities within the watershed considering both the upstream and downstream of the water bodies along with the forest cover. There should be appropriate land management activities in the barren lands such that the land cover in this region is conserved. Proper control should be maintained in the urban sprawl within the watershed, since this is in the upper reach of river Tamiraparani. In addition to this conservation of the riparian zones near the water bodies is highly essential to promote and maintain the health of the ecosystem within the watershed. In general, site-specific community-based awareness should be created among the community within the watershed for appropriate utilization of the available resources as well as the conservation of the scarce resources such that rehabilitation of environment is proved to be very effective.

REFERENCES

[1] Abate, S (2011): Evaluating the land use and land cover dynamics in Borena Woreda of South Wollo Highlands, Ethiopia. – J Sustainable Dev Afr 13(1): 1520-5509.

[2] Abbas, I. I., Muazu, K. M., Ukoje, J. A. (2010): Mapping land use-land cover and change detection in Kafur local government, Katsina, Nigeria (1995-2008) using remote sensing and GIS. – Res J Environ Earth Sci 2(1): 6-12.

http://www.aloki.hu ● ISSN 1589 1623 (Print) ● ISSN 1785 0037 (Online)
DOI: http://dx.doi.org/10.15666/aeer/1906_47394749

[3] Asres, R. S., Tilahun, S. A., Ayele, G. T., Melesse, A. M. (2016): Analyses of Land Use/Land Cover Change Dynamics in the Upland Watersheds of Upper Blue Nile Basin. – In: Melesse, A. M., Abtew, W. (eds.) Landscape Dynamics, Soils and Hydrological Processes in Varied Climates. Springer, Berlin, pp. 73-91.

[4] Ayele, G. T., Demessie, S. S., Mengistu, K. T., Tilahun, S. A., Melesse, A. M. (2016): Multitemporal Land Use/Land Cover Change Detection for the Batena Watershed, Rift Valley Lakes Basin, Ethiopia. – In: Melesse, A. M., Abtew, W. (eds.) Landscape Dynamics, Soils and Hydrological Processes in Varied Climates. Springer, Berlin, pp. 51-72.

[5] Bae, J., Ryu, Y. (2014): Land use and land cover changes explain spatial and temporal variations of the soil organic carbon stocks in a constructed urban park. – Landscape and Urban Planning 136: 57-67.

[6] Baulies, X., Szejwach, G (eds.) (1998): LUCC Data Requirements Workshop: Survey of Needs, Gaps and Priorities on Data for Land-Use/Land-Cover Change Research, Barcelona, 11-14 Nov 1997. – Institut Cartografic de Catalunya, Barcelona.

[7] Carlson, T. N., Sanchez-Azofeifa, G. A. (1999): Satellite remote sensing of land use changes in and around San Jose, Costa Rica. – Remote Sens Environ 70(3): 247-256.

[8] Clevers, J., Bartholomeus, H., Mucher, S., De Wit, A. (2004): Land cover classification with the medium resolution imaging spectrometer (MERIS). – EARSeL eProc 3(3): 354-362.

[9] Deng, X. Z., Liu, J. Y., Lin, Y. Z., Shi, C. C. (2013): A framework for the land use change dynamics model compatible with RCMs. – Advances in Meteorology. https://doi.org/10.1155/2013/658941.

[10] Dessie, G., Kleman, J. (2007): Pattern and magnitude of deforestation in the South Central Rift Valley Region of Ethiopia. – Mt Res Dev 27(2): 162-168.

[11] Dezso, Z., Bartholy, J., Pongracz, R., Barcza, Z. (2005): Analysis of land- use/land-cover change in the Carpathian region based on remote sensing techniques. – Phys Chem Earth, Parts A/B/C 30(1): 109-115.

[12] FAO (2004): Methodological Framework for Land Degradation Assessment in Dry Lands (LADA). – Food and Agriculture Organization (FAO), Rome.

[13] Meshesha, T. W., Tripathi, S. K., Khare, D. (2016): Analyses of land use and land cover change dynamics using GIS and remote sensing during 1984 and 2015 in the Beressa Watershed Northern Central Highland of Ethiopia. – Model. Earth Syst. Environ. 2: 1-12. https://doi.org/10.1007/s40808-016-0233-4.

[14] Minale, A. S., Rao, K. K. (2012): Impacts of land cover/use dynamics of Gilgel Abbay catchment of Lake Tana on climate variability, Northwestern Ethiopia. – Appl Geomat 4(3): 155-162.

[15] NRSC, ISRO (2011): Manual on "Preparation of Geo Spatial Layers Using High Resolution (Cartosat-1 Pan + LISS-IV Mx) Orthorectified Satellite Imagery". – Space Based Information Support for Decentralized Planning (SIS-DP), Remote Sensing and GIS Applications Area National Remote Sensing Centre, Indian Space Research Organisation (ISRO), Department of Space, Government of India, Hyderabad.

[16] Nurelegn, M., Amare, S. (2014): Land use/cover dynamics in Ribb watershed, North Western, Ethiopia. – J Nat Sci 4(16): 9-16.

[17] Prakasam, C. (2010): Land use and land cover change detection through remote sensing approach: a case study of Kodaikanal taluk, Tamil Nadu. – Int J Geomat Geosci 1(2): 150.

[18] Praveen Kumar, M., Sreenivasula Reddy, J. R. (2013): Analysis of land use/land cover changes using remote sensing data and GIS at an urban area, Tirupati, India. – The Scientific World Journal. https://doi.org/10.1155/2013/268623.

[19] Shiferaw A. (2011): Evaluating the land use and land cover dynamics in Borena Woreda of South Wollo highlands, Ethiopia. – J Sustain Dev Afr 13(1): 87-107.

[20] Song, K. S., Wang, Z. M., Liu, Q. F., Liu, D. W., Ermoshin, V. V., Ganzei, S. S., Zhang, B., Ren, C. Y., Zeng, L. H., Du, J. (2011): Land use/land cover (LULC) classification with MODIS time series data and validation in the Amur River basin. – Geography and Natural Resources 32: 9-15.

http://www.aloki.hu ● ISSN 1589 1623 (Print) ● ISSN 1785 0037 (Online)
DOI: http://dx.doi.org/10.15666/aeer/1906_47394749

EFFECT OF TENDING AND THINNING ON SPATIAL AND CARBON DISTRIBUTION PATTERNS OF NATURAL MIXED BROADLESF-CONIFER SECONDARY FOREST IN XIAOXING'AN MOUNTAINS, PR CHINA

WANG, Z. C. – LI, Y. X.* – MENG, Y. B. – WANG, C.

College of Engineering and Technology, Northeast Forestry University, Harbin 150040, PR China

**Corresponding author*
e-mail: yaoxiangli@nefu.edu.cn; phone: +86-136-4450-5681

(Received 17th Jan 2021; accepted 1st Oct 2021)

Abstract. Four 0.25-ha natural mixed broadleaf-conifer secondary forest plots (CK, T_{15}, T_{25}, T_{35}) were established in Xiaoxing'an Mountains, PR China. The spatial pattern of plant community was studied by using O-ring statistical analysis method and field survey was carried out to estimate the carbon storage of trees. The research was done in order to explore the effects of different thinning intensities on the spatial and carbon distribution patterns of natural secondary forests in order to provide a reasonable forest management method. We described three main findings. (1) The spatial patterns of either the whole forest or the dominant tree species almost took on a random distribution. Thinning changed the distribution patterns of forest at ≤ 4 m scales, and the distribution changed from random distribution to cluster distribution. (2) It also altered the distribution of dominant tree species, the spatial correlation between dominant species changed from partial negative associations to independence or partial positive associations, and the negative associations in T_{35} plot were the lowest. (3) The carbon storage in the T_{15} plot was significantly lower than that in the other plots at ≥ 10 m scales. The carbon storage in the T_{35} plot was higher than that in the CK plot at almost all scales. In conclusion, the T_{35} plot optimized the forest structure and it was more beneficial to the carbon storage of natural mixed broadleaf-conifer secondary forests in Xiaoxing'an Mountains after 8 years thinning.
Keywords: *thinning intensity, O-ring statistical analysis, spatial pattern, spatial correlation, carbon storage*

Introduction

Natural disturbance and anthropogenic disturbance work in parallel with competition to shape the spatial pattern of vegetation in boreal ecosystems (Felinks and Wiegand, 2008; Gray and He, 2009). In natural ecosystems, altitude factors, climate factors, precipitation factors and soil factors worked together on the spatial distribution pattern of trees (Moeur, 1993). Among human factors, tending thinning was an important part of forest managements which changed the forest spatial structure and spatial distribution pattern, so the spatial correlation among different species and biomass distributions are also affected (Li et al., 2011; Duan et al., 2019). At present, most of the existing studies were about the effect of selective cutting on natural forest or tending thinning on plantation forest in population structures and distribution patterns (Shen et al.,2013; Wu et al., 2015). However, few scholars have studied the impact of tending thinning on nature secondary forest distribution patterns.

A powerful tool to characterize the spatial pattern and spatial correlation is point patterns analysis, individual is regarded as a point with coordinate figure in a two-dimensional space plane. The dominant tree species constitute a point set, and then, it will be drawn as a point graph. The spatial pattern and inter-specific association at

http://www.aloki.hu ● ISSN 1589 1623 (Print) ● ISSN 1785 0037 (Online)
DOI: http://dx.doi.org/10.15666/aeer/1906_47514764

different scales are described on the basis of point graph (Diggle, 2003; Illian et al., 2008; Law et al., 2009). This method is more rigorous in data requirements and it can maximize the use of spatial information. On the one hand, the point pattern analysis can judge the distribution state of population. On the other hand, it can describe diverse intra- and interspecies relationships at different scales (Yao, et al., 2020). As most inter-tree interactions are expected to occur within 10 m scales (Stoyan and Penttinen, 2000; Getzin et al., 2008), so plots < 1 ha have been widely used to investigate tree spatial patterns in different environments (Svoboda et al., 2010; Aakala et al., 2012; Petritan et al.,2014; Sanatan and Bradley, 2018). However, some researchers have analyzed the spatial pattern of dominant tree species at different scales in plots < 1 ha but drew different conclusions. For example, Yang and Li (1985) reported that *Tilia amurensis* were randomly distributed in several 10 m × 10 m plots, while the results of Du (2012) suggested that *Tilia amurensis* showed a significant cluster distribution in a small scale of 0.16 ha permanent plot. These studies drew different conclusions because they had different scales, different analysis methods, and different natural and human factors.

A large number of primary forests have been converted into secondary forests due to the degradation of top plant communities. More than 50% of China's forest areas are secondary forests (Du et al., 2013), and natural mixed broadleaf-conifer secondary forests are typical forest types in Northeast China. Xiaoxing'an Mountains are the main natural forest areas in Northeast China. It is significant to explore the effects of different tending and thinning intensities on the spatial and carbon distribution patterns of natural mixed broadleaf-conifer secondary forests. It is very important for reasonable management forests and the development of forestry carbon sinks. In this study, the sites after 8 years tending thinning (thinning intensities were about 0, 15%, 25% and 35%) in Xiaoxing'an Mountains were selected, and analyzed the spatial distribution pattern and carbon distribution pattern of these plots through sample plot investigation. Using the spatial point pattern analysis method, the spatial distribution patterns and associations of dominant tree species of different tending and thinning intensities were analyzed. It provides the basis for further scientific management of natural secondary forests of Xiaoxing'an Mountains. The O-ring statistic was used for point pattern analysis at various scales (Hao et al., 2007). In this study, it was used to analyze the spatial patterns and the spatial correlations between different dominant tree species.

In order to evaluate the tending and thinning effects of natural secondary forest in Xiaoxing'an Mountains comprehensively, the spatial structure and carbon storage of stands at different scales were used as indicators to explore the optimal intensity after thinning for 8 years.

Materials and methods

Study sites

We conducted this study in natural mixed broadleaf-conifer secondary forest located in Dongfanghong Forest Farm, Yichun City, Heilongjiang province, Northeast China, with latitude 128°37′46″ - 129°17′50″ and longitude 46°50′8″ - 47°21′32″ (*Fig. 1*). The average elevation of this area is 600 m above sea level, the average slope is 14° in the northwest direction. The average annual precipitation is 661 mm, mainly concentrates in July and August. The top climatic community in the study area is mixed broadleaf-conifer secondary forest, and the dominant tree species are *Picea asperata*, *Abies fabric, Acer mono, Acer tegmentosum*, *Fraxinus mandshurica* Rupr, *Pinus koraiensis* Sieb. et

http://www.aloki.hu ● ISSN 1589 1623 (Print) ● ISSN 1785 0037 (Online)
DOI: http://dx.doi.org/10.15666/aeer/1906_47514764

Zucc and *Tilia tuan* Szyszyl. The types of shrubs include *Acanthopanax senticosus* (Rupr. Maxim.) Harms, *Spodiopogon cotulife*r (Thunb) and so on.

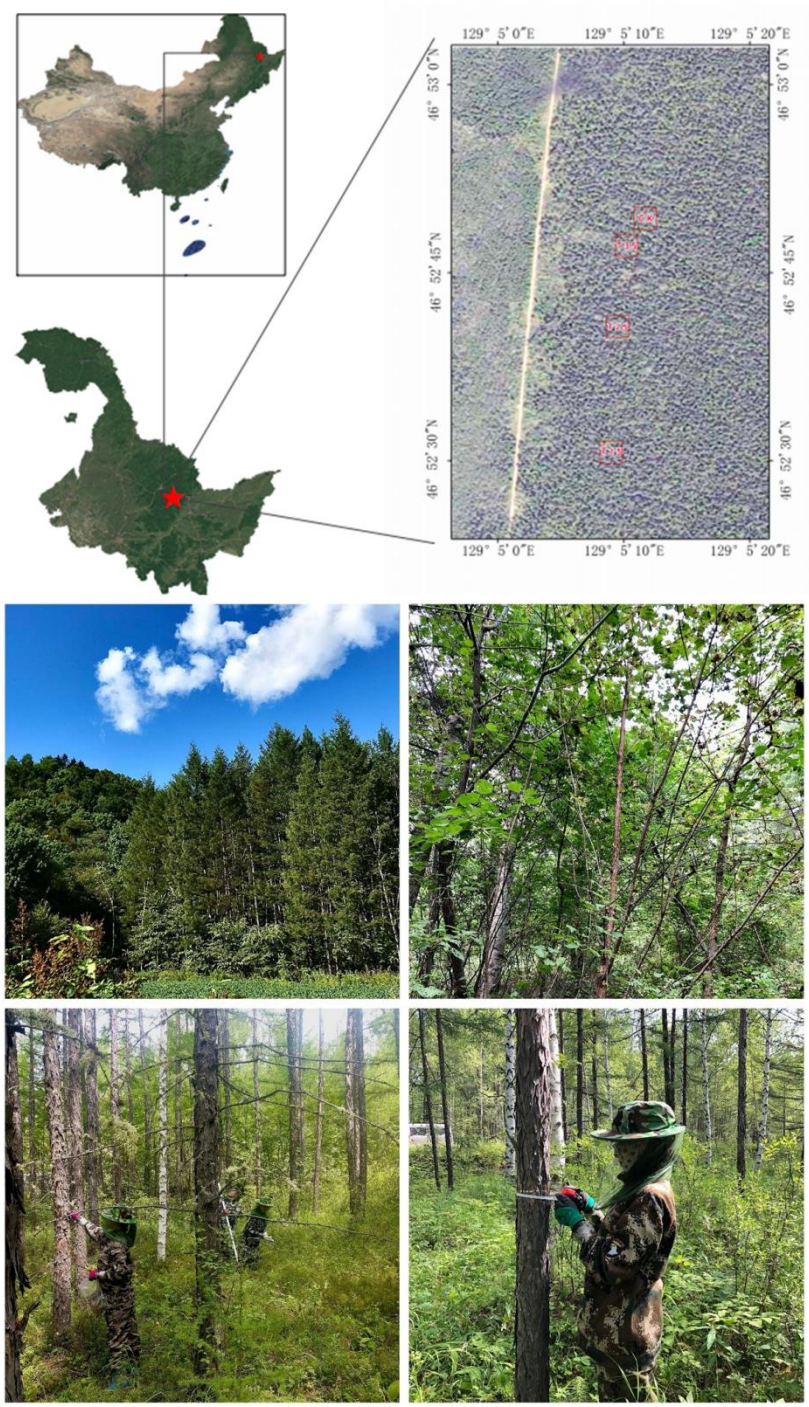

Figure 1. *The Research area of Xiaoxing'an Mountains*

Data collection

In 2012, the experimental sites with relatively consistent stand conditions were selected for tending thinning. At the same time, repair planting was carried out in the

http://www.aloki.hu ● ISSN 1589 1623 (Print) ● ISSN 1785 0037 (Online)
DOI: http://dx.doi.org/10.15666/aeer/1906_47514764

thinning sites, the replanting trees included *Pinus koraiensis Sieb*. et Zucc., Picea asperata, and *Larix* gmelinii. These experimental sites were surveyed repeatedly in August 2019. In these sites, we established four 0.25-ha (50 m × 50 m) plots, which marked as CK (control area, non-thinning), T_{15} (thinning intensity was about 15%), T_{25} (thinning intensity was about 25%), T_{35} (thinning intensity was about 35%). Each plot was divided into one hundred 5 m × 5 m quadrates. Our survey was based on these 5 m × 5 m quadrates. All free-standing tree stems ≥ 5 cm diameter at breast height (DBH, 1.3 m above the ground) have been measured. The measuring contents include tree species, coordinate position, DBH, height, tree crown, branch height and so on. *Table 1* shows the basic status of thinned forests.

Table 1. *Basic status of thinning stand (mean ± SD)*

Thinning treatment	Elevation (m)	Diameter at breast height (cm)	Tree height (m)	Basal area at breast height ($m^2 \cdot hm^{-2}$)	Stand density ($plant \cdot hm^{-2}$)	Canopy density (%)
CK	457~492	16.62±4.62	11.69±3.06	2.59±0.67	958	90
T_{15}	504~509	13.53±2.97	9.69±2.03	2.38±0.53	1183	92
T_{25}	487~540	15.96±3.45	11.48±2.77	1.96±0.46	925	81
T_{35}	468~499	16.31±3.98	11.09±2.43	2.12±0.63	733	76

Data analysis

Ripley's K or L function have been used frequently in point pattern analysis (Rozas, 2006; Fajardo et al., 2006). Ripley's K or L function is used to analyze the spatial patterns of species in a circle of radius r centered at one point. When the space scale increases, the Ripley's K or L function have the problem of small-scale accumulation, because the results include all information in the circle. Therefore, O-ring statistical analysis is developed on the basis of Ripley's K or L function and Mark function (Stoyan and Stoyan, 1994). The O-ring statistical analysis replaces the circles with rings, so cumulative effects on small scales are eliminated. The O-ring statistical analysis gives an intuitive interpretation of a neighborhood density and is especially sensitive to small-scale effects (Wiegand and Moloney, 2004; Illian et al., 2008).

The O-ring statistics includes both univariate and bivariate statistics (Getzin et al.,2006). The univariate statistics are used to analyze the spatial pattern of one object, while the bivariate statistics are used to analyze the spatial association of two objects (pattern 1 and pattern 2). The choice of null models is very important to ensure the accuracy of data analysis in O-ring statistical analysis (Zhao et al., 2011). In this study, univariate O-ring statistics was used to analyze the distribution pattern of each dominant tree species in the sample plot. Bivariate O-ring statistics were used to analyze the spatial correlation between dominant tree species in the sample plot. For the univariate O-ring statistic, analyze the spatial distribution of dominant tree species in each thinning plot, if there are no strong aggregation phenomena, complete spatial randomness (CSR) is chosen as the null model. If there are obvious indication of strong aggregation, the heterogeneous Poisson process was adopted. The confidence intervals of dominant tree species of spatial distributions were simulated by Monte Carlo. Departure from a given null model was tested by comparing the pair correlation

http://www.aloki.hu ● ISSN 1589 1623 (Print) ● ISSN 1785 0037 (Online)
DOI: http://dx.doi.org/10.15666/aeer/1906_47514764

function of point data with the 5th lowest and 5th highest value of 99 Monte Carlo simulation to generate an approximately 99% simulation envelope. If the point was above the upper envelope, it indicated clumped. If the points between the envelopes, it indicated random. If the points under the lower envelopes, it indicated regular. For the bivariate O-ring statistic, the spatial correlation between two dominant species in the experimental plots was compared using the CSR. According to Monte Carlo simulation results, in these analyses, points above the upper envelope indicated positive associations, points between the envelopes indicate spatial independence, and points below the lower envelope indicate negative associations. All point pattern analyses were conducted using Programita software (Wiegand and Moloney, 2004) and Spatstat library (Baddeley and Turner, 2005) in R (3.6.3). Details on the estimators of the summary statistics and edge correction used in Programita can be found in Wiegand and Moloney (2014).

Cumulative carbon reserve estimation

The biomass estimation of *P. asperata* and *A. fabric* were based on the biomass equations, which were established by Hu in this area (Hu et al., 2015). The biomass estimations of *A. mono* and *A. tegmentosum* were carried out by using the ten biomass models in Northeast China which established by Wang (2005). In each plot, 2~3 standard trees of dominant tree species were selected in order to avoid different carbon content which caused by different thinning intensities, different tree species and so on. Samples were taken from trunk, branches, leaves and skins of dominant tree species. And then the carbon content were determined by potassium dichromate oxidation-external heating method in the laboratory.

The product of individual biomass and carbon content was the individual carbon storage, and cumulative carbon storages were obtained by accumulating the individual carbon storage of quadrats. To consider that the quadrats had various tree species, spatial distributions and growth states, so the cumulative carbon storages did not grow in a straight line on different spatial spaces. Therefore, ten quadrats of 5 m × 5 m, 10 m × 10 m, 15 m × 15 m, 20 m × 20 m, 25 m × 25 m, 30 m × 30 m were generated randomly in the plots (Duan et al., 2015). It was used to analyze the partial characteristics of cumulative carbon reserves under different spatial patterns.

Results

Stand structure

There were 539 living trees of four dominant species with the DBH ≥ 5 cm in four experimental plots (*Fig. 2*). The number of dominant tree species in the CK, T_{15}, T_{25} and T_{35} plots were 141, 158, 114 and 126. In the CK plot, the DBH class distribution curves of *A. fabric* and *A. mono* were shifted to the right. It showed that *A. fabric* and *A. mono* had larger DBH in the CK plot. There were large numbers of *A. tegmentosum* whose DBH was from 6 cm to 10 cm in the T_{15} plot. In the T_{25} plot, the number of four dominant tree species was smaller than in the other plots, whose DBH was from 16 cm to 20 cm. In the T_{35} plot, the number of *A. fabric* was the largest, and the number of *P. asperata* was significantly less than other dominant species. In four experimental plots, the length of *A. fabric* step curve was the largest, it suggested that the individual differentiation of *A. fabric* was obvious.

http://www.aloki.hu ● ISSN 1589 1623 (Print) ● ISSN 1785 0037 (Online)
DOI: http://dx.doi.org/10.15666/aeer/1906_47514764

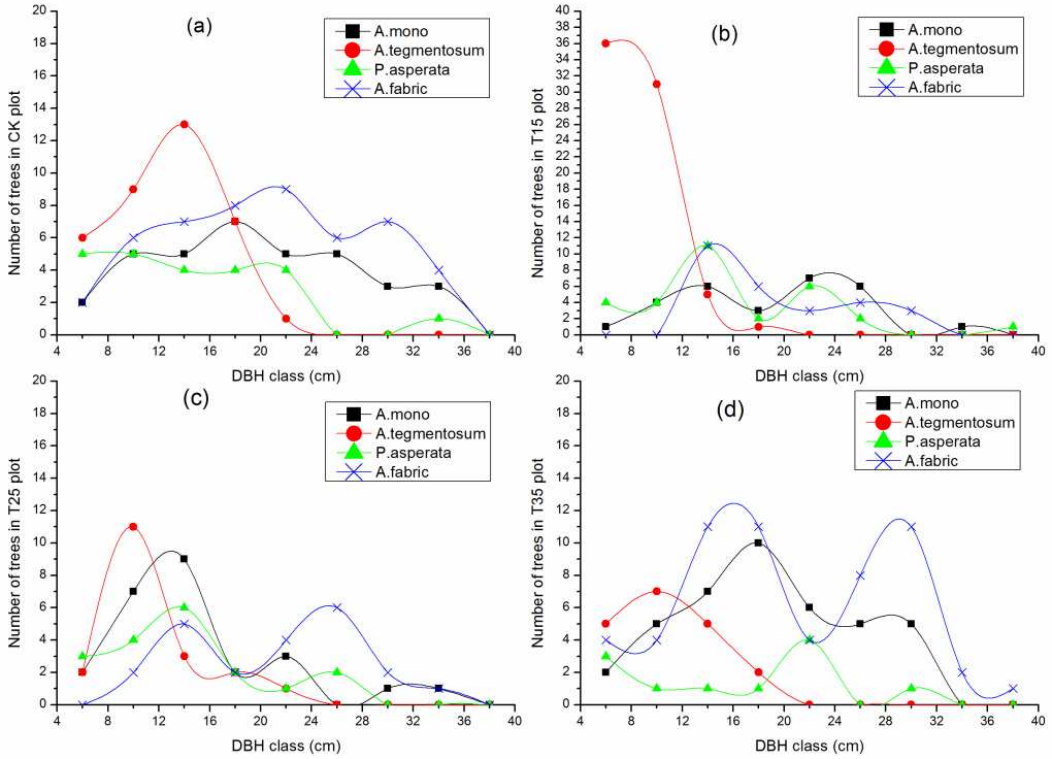

Figure 2. *The DBH class distributions of four dominant tree species in the 0.25-ha forest plot. (a) CK plot (b) T15 plot (c) T25 plot (d) T35 plot*

The structure of DBH size class of dominant trees in three thinning plots was significantly different from that in the CK plot. The test of normality for DBH of dominant tree species in four experimental plots showed that thinning caused the distribution curve changed from normal distribution to non-normal distribution. ($P < 0.05$) (*Table 2*).

Table 2. *Test for normality in different DBH of all dominant tree species*

Test	CK	T_{15}	T_{25}	T_{35}
Skewness	0.223	0.918	0.530	0.272
Kurtosis	-0.197	0.561	-0.444	-0.887
Shapiro-Wilk to check *P*	0.148	0.002	0.004	0.007

$P > 0.05$, the diameter order curve conforms to the normal distribution

Spatial patterns of dominant tree species under different thinning intensity

According to the distribution of dominant tree species in the CK plot and three thinning plots (*Fig. 3*), it could be seen that: Tending thinning did not change the distribution status of forests in all plots, but it changed the distribution ratio of dominant tree species. There were great differences in the densities of different tree species in some local areas, and the densities of the dominant tree species varied greatly with the changing spatial positions. It could be seen from (*Figs. 2* and *3*) that there were obviously more juvenile *A. tegmentosum* in the T_{15} plot than other plots, and in this plot,

http://www.aloki.hu ● ISSN 1589 1623 (Print) ● ISSN 1785 0037 (Online)
DOI: http://dx.doi.org/10.15666/aeer/1906_47514764

A. tegmentosum had many initiation distribution and rosette distribution, it was very consistent with the characteristics of secondary forests.

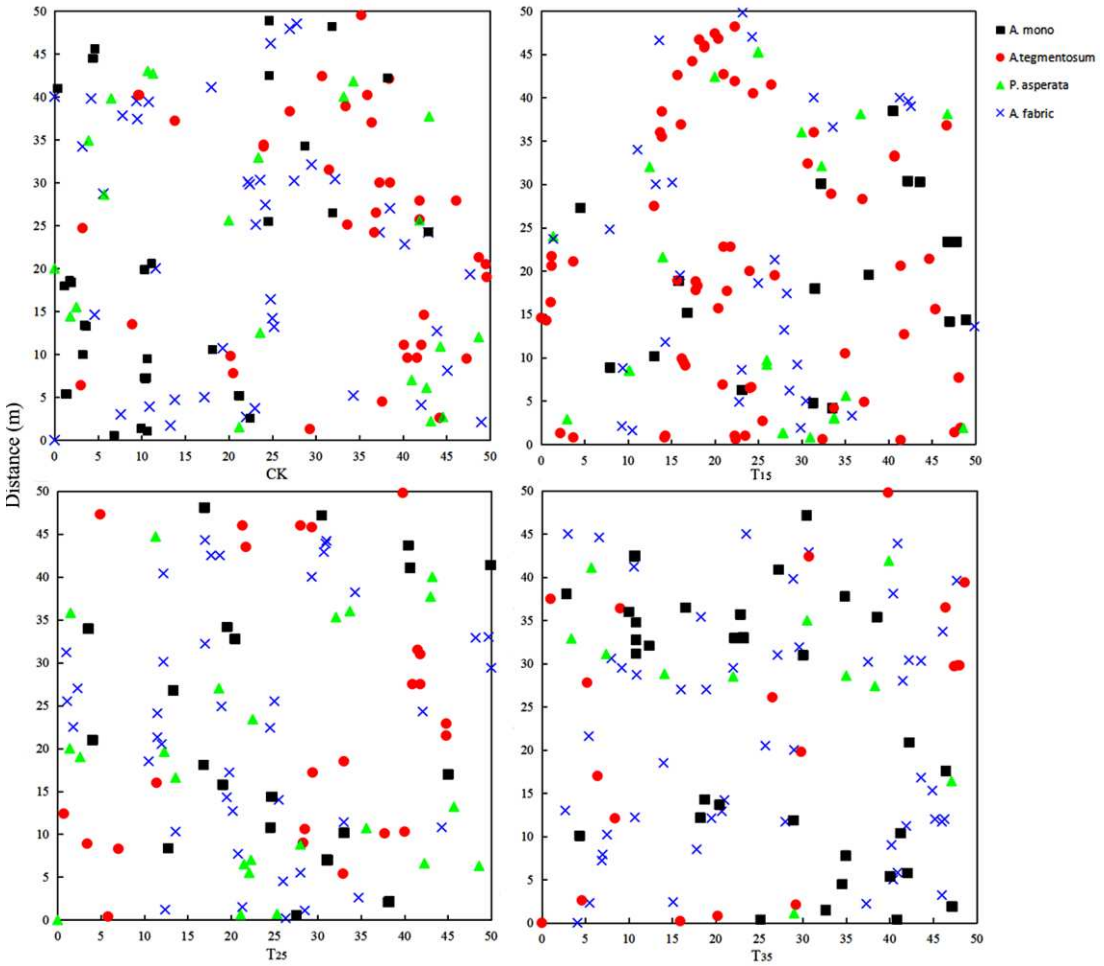

Figure 3. *Spatial distribution of dominant tree species in various plots*

When the four dominant tree species were analyzed together (*Fig. 4*), (a) was randomly distributed at scales ≤ 25 m, while (b), (c) and (d) were clustered at smaller scales. (b) was also significantly aggregated at 20 m scale. (c) and (d) showed regular distributions at some scales, such as 12 m, 17 m and 21 m scales in (c) and 9 m, 18~19 m scales in (d).

A. mono showed significant clustering when the spatial scales were 1 m and 8-9 m, but showed regular at 16~17 m scales in the CK plot. Meanwhile, in the 3 thinning plots, as the intensity of thinning increases, the clustered distribution of *A. mono* were more, such as: the scale at 10 m in the T_{15} plot, 8-10 m in the T_{25} plot and 0-1 m, 7-8 m, 17 m in the T_{35} plot. *A. tegmentosum* were randomly distributed at almost all scales, while, at the scale of 0~3 m in the T_{15} plot and 21 m in the T_{35} plot, the clusters were appeared. *P. asperata* were only clustered at small scales of the CK plot and the T_{15} plot, and randomly distributed at larger scales. At different scales, *A. fabric* showed random distribution basically, however, at some scales, they were clustered, such as 2 m in the CK plot, 9 m in the T_{15} plot, 3 m and 8-9 m in the T_{25} plot, respectively (*Fig. 5*).

http://www.aloki.hu ● ISSN 1589 1623 (Print) ● ISSN 1785 0037 (Online)
DOI: http://dx.doi.org/10.15666/aeer/1906_47514764

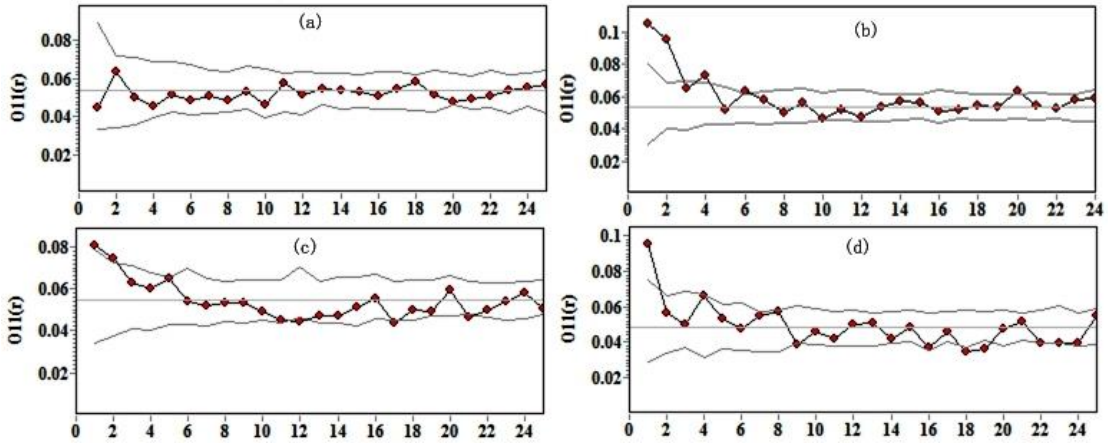

Figure 4. *The spatial distribution pattern of four dominant tree species. (a) CK plot. (b) T_{15} plot. (c) T_{25} plot. (d) T_{35} plot. Solid lines indicate ring statistics O11(r). Dotted lines indicate the upper and lower limits of the 99% simulation envelope. Points above the upper envelope indicate clumped, points between the envelopes indicate random, and points below the lower envelope indicate regular*

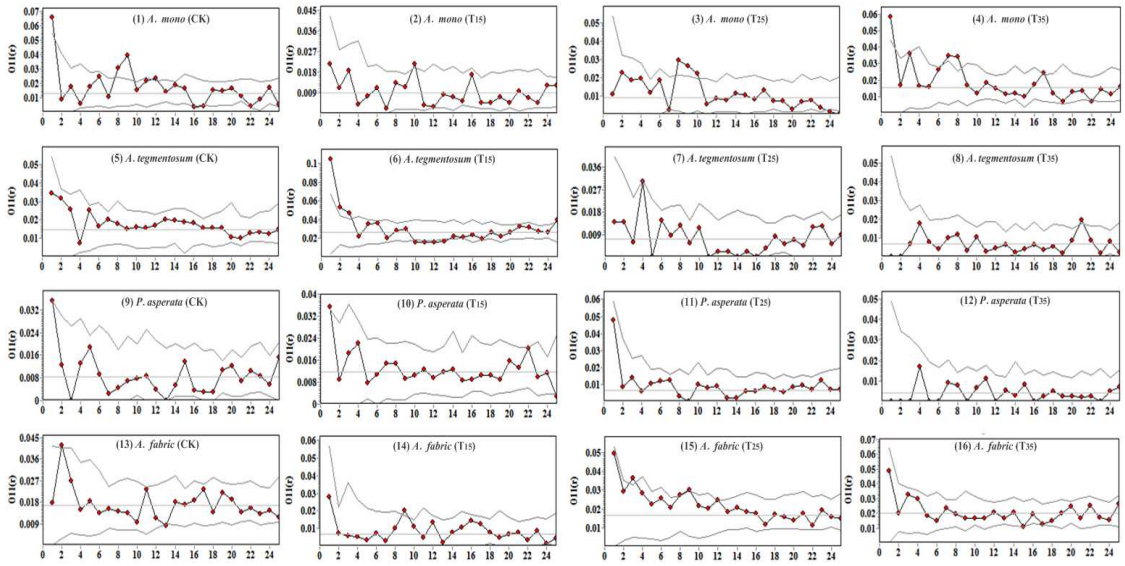

Figure 5. *Univariate O-ring statistics of four dominant tree species under different thinning intensity*

Interspecies spatial associations of dominant tree species under different thinning intensities

A. mono showed a slight positive correlation to *A. tegmentosum* at some scales in the CK plot, while the relationship between *A. mono* and *A. tegmentosum* was independent at almost all scales in 3 thinning plots (*Fig. 6(1-4)*). *A. mono* was dominated by inhibition to *P. asperata* and *A. fabric* at scales ≥ 12 m in the CK plot. However, in 3 thinning plots, *A. mono* was spatially independent of *P. asperata* and *A. fabric* at almost all scales and showed a slight positive correlation at some scales (*Fig. 6(5-12)*). *A. tegmentosum* and *P. asperata* were not correlated at all scales in all plots (*Fig. 6(13-*

http://www.aloki.hu ● ISSN 1589 1623 (Print) ● ISSN 1785 0037 (Online)
DOI: http://dx.doi.org/10.15666/aeer/1906_47514764

16)). The relationship of A. tegmentosum and *A. fabric* showed 3 different patterns (*Fig. 6(17-20*), (1) In the CK plot, *A. tegmentosum* was spatially independent of *A. fabric* at all scales. (2) In the T_{15} plot, *A. tegmentosum* was significantly positive correlation to *A. fabric* at scales was 2 m. (3) Yet, in the T_{25} and T_{35} plots, *A. tegmentosum* was spatially independent of *A. fabric* at scales ≤ 12 m, yet slight inhibition at scales greater than 12 m. *P. asperata* was dominated by inhibition to *A. fabric*, such as at 3 m, 4-5 m, 12 m, 17 m and 21-23 m scales in the CK plot, while, in 3 thinning plots, it showed a slight positive correlation at ≥ 4 m scales.

The spatial associations between dominant tree species showed that the spatial associations of dominant tree species were mainly independent of different thinning intensities. In the CK plot, *A. mono* showed slight inhibition to *A. tegmentosum*, while it showed a slight positive correlation to *P. asperata* and *A. fabric* at different scales. Particularly, *P. asperata* showed strong negative correlation at many scales in response to *A. fabric* in the CK plot.

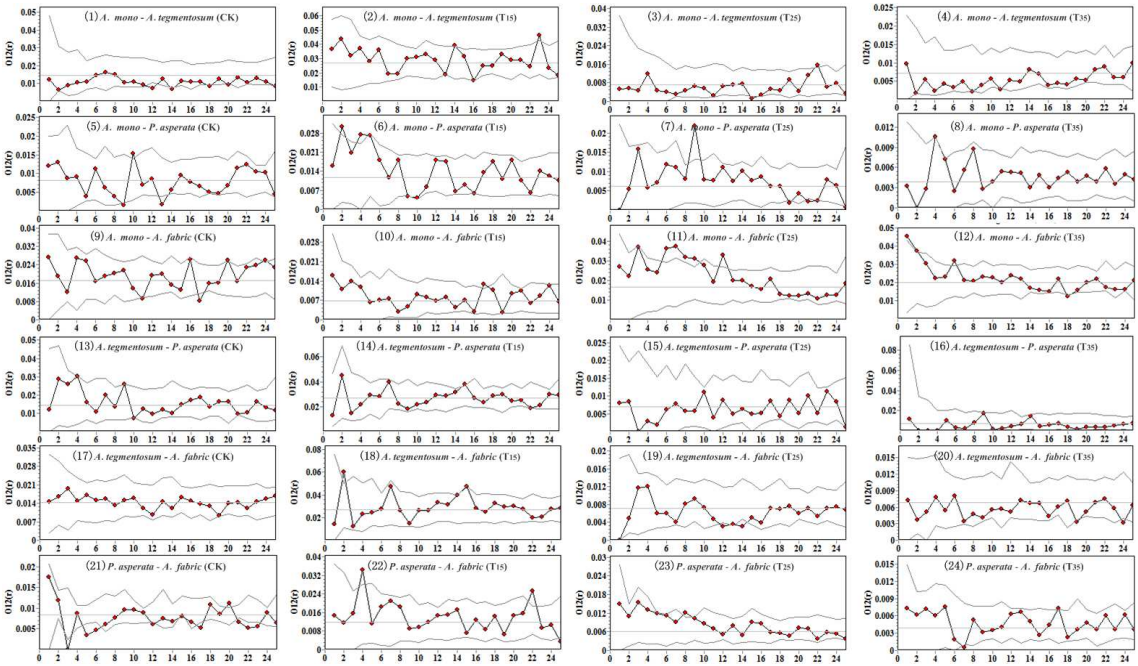

Figure 6. *O12(r) values of spatial associations between different tree spices under different thinning intensity. Solid lines indicate ring statistics O12(r); Dotted lines indicate the upper and lower limits of the 99% simulation envelope of the CSR. Points above the upper envelope indicate positive associations, points between the envelopes indicate spatial independence, and points below the lower envelope indicate negative associations*

Spatial patterns of carbon reserves of dominant tree species under different thinning intensities

It can be seen from *Table 3* that the accumulative carbon storages in different thinning plots were different at the same scales. There was no difference in the cumulative carbon storages of dominant tree species between the CK plot and 3 thinning plots at 0-10 m scales. When the scales at 15 m, 20 m, 25 m, 30 m, the cumulative carbon storage in the T_{15} plot was significantly different from those in the CK, T_{25} and T_{35} plots. Compared with the CK plot, the cumulative carbon storages in

http://www.aloki.hu ● ISSN 1589 1623 (Print) ● ISSN 1785 0037 (Online)
DOI: http://dx.doi.org/10.15666/aeer/1906_47514764

the T_{15} plot were reduced by 38.67%, 44.04%, 41.86% and 41.38% at the 15 m, 20 m, 25 m and 30 m scales, respectively. The carbon storage at 5 m, 10 m, 15 m and 20 m scales of the T_{25} plot was slightly lower than that of the CK plot, while the carbon storage at 25 m and 30 m scales was slightly higher than that of the CK plot, but there was no significant difference at all scales. However, in the T_{35} plot, the cumulative carbon reserves at all scales were greater than those in the CK plot, but no significant difference.

Table 3. *Cumulative carbon storage of dominant tree species at different scales*

Thinning treatment	Cumulative carbon storage at different scales (t)					
	5 m	**10 m**	**15 m**	**20 m**	**25 m**	**30 m**
CK	0.05a	0.23a	0.75a	1.09a	1.72a	2.61a
T_{15}	0.03a	0.23a	0.46b	0.61b	1.00b	1.53b
T_{25}	0.03a	0.19a	0.68a	0.97a	1.75a	2.71a
T_{35}	0.05a	0.26a	0.76a	1.12a	1.88a	2.76a

Discussion

The study site was a natural secondary forest with complicated stand structure in Xiaoxing'an Mountains (*Table 1, Figs. 2* and *3*). Normally, the DBH class distribution of natural secondary forest is normal distribution. That means most of the individuals are middle DBH, while individuals with large and small DBH are fewer (Wang, et al., 2017; Duan et al., 2019). Thinning changed the DBH class distribution of trees (Hu et al., 2011). In this experiment, the DBH of dominant tree species in the CK plot was normal distribution, while thinning caused the distribution curve to deviate from the normal. The average DBH of dominant tree species in the T_{35} plot was significantly higher than other thinning plots. We could infer that thinning also release the pressure of competition among reserved trees and promote the growth of natural secondary forests. This was the same as Hu's conclusion (Hu et al., 2011).

Four experimental plots have different gaps, different soil nutrient conditions and different light intensity, which caused the difference of spatial and carbon patterns. Meanwhile, these factors will cause uneven distribution of forest resources (He and Duncan, 2000; Boyden et al., 2005; Druckenbrod et al., 2005). With the thinning intensity increasing, the aggregation phenomena of *A. mono* increased. The reasons were that it had weak positive biological characteristics and responses to the gaps. Evenly distributed gaps and upper canopy gaps provided space and opportunity for the growth of *A. mono* (Huang et al., 2004). The aggregation phenomena of *A. tegmentosum* could also be explained by the above content. *A. fabric* were aggregated around their parent trees under smaller thinning intensities (*Figs. 5(10)* and *5(13-15)*). Limited seed dispersal ability provided seed sources for seedling and sapling recruitment, while shade-tolerant characteristics ensured that seedlings and saplings could grow well under the canopy of parent trees (Hou et al., 2004). *P. asperata* and *A. fabric* mainly showed significant clustering at small scales. As the scale increased, the aggregation of trees began to decrease and showed random distribution gradually, which was similar to the results reported in the literature (Liu et al., 2005). The scale variability of the forest spatial patterns is restricted by many factors. On one hand, at small scales, different spatial patterns may be caused by varying degrees of intra- and interspecies competitions, restriction of seed dispersal, etc. On the other hand, at large scales, different spatial patterns may be determined by the

http://www.aloki.hu ● ISSN 1589 1623 (Print) ● ISSN 1785 0037 (Online)
DOI: http://dx.doi.org/10.15666/aeer/1906_47514764

heterogeneity or plaque-type of species distribution and the nonbiological environments (topography, soil moisture, soil pH, soil nutrients, etc.) (He et al., 1997; Harms et al., 2000; Zhang et al., 2008; Wang et al., 2008).

Spatial correlation is used to describe the static relationship of dominant tree species in spatial distribution. The dominant tree species showed mainly independent at different scales in four experimental plots, this was the important reason for the stable distribution of dominant tree species for a long time (Shen et al., 2013). *A. mono* and *A. tegmentosum* have similar ecological habits. In the CK plot, *A. mono* showed spatial independence at small scales, and were negatively associated at larger scales to *A. tegmentosum*. *P. asperata* also showed strong negative correlation at many scales in response to *A. fabric* in the CK plot, Because they had similar ecological habits. However, thinning changed the distributions of dominant tree species and the correlation of dominant tree species tended to positive correlations or independent, which were more conducive to the growth of the forest. *A. tegmentosum* and *A. fabric* were positively correlated at some scales and negatively correlated at some scales, because this study neglected the law of spatial correlation between two dominant tree species of different DBH classes.

Particularly, the cumulative carbon storages depend on the species of trees, the number of trees and the carbon storage of individual tree at this scale. In our study, the accumulative carbon storages at different spatial scales were different under different thinning intensities. When the scale ≤ 10 m, there was no significant difference in carbon storage between the CK plot and 3 thinning plots. At > 10 m scales, the accumulative carbon storages in the T_{15} plot was significantly smaller than those in other plots. It indicates that 15% thinning intensity was not conducive to the accumulation of carbon reserves. Ding (2016) and Han (2015) have shown that thinning could removing part of trees that would reduce carbon reserves. However, Duan (2019) suggested that carbon storage would recover after a period of time. Shen (2013) believed that thinning released competitive pressure of trees, which was conducive to the increase of carbon storage. In this experiment, the cumulative carbon storages in the T_{25} and T_{35} plots were not significantly different from those in the CK plot at all scales, particularly, the cumulative carbon storages in the T_{35} plot was larger than that in the CK plot at all scales, indicating that reasonable thinning would not reduce carbon storages. It was consistent with the research results of Duan (2019), Shen (2013), etc.

Conclusion

Our results clearly showed that the competition pressure of natural mixed broadleaf-conifer secondary forest in Xiaoxing'an Mountains was released after 8 years of thinning, and the stand structure was optimized, so that the reserved trees could grow better. Through the analysis of spatial point patterns, the spatial distribution feature points were found, which had guiding significance for forest management. For example, thinning should be reduced in areas with few trees, and should be appropriately increased in tree gathering areas to release competition pressure among trees. Evenly distributed forests can help plants make better use of light and make plants grow better. The cumulative carbon storages of the forest in the T_{35} plot were almost higher than those in the CK plot at all scales. And the results showed that the cutting intensity of 35% could promote the optimization of the stand structure and it was beneficial to the carbon sink of natural mixed broadleaf-conifer secondary forest in Xiaoxing'an Mountains.

http://www.aloki.hu ● ISSN 1589 1623 (Print) ● ISSN 1785 0037 (Online)
DOI: http://dx.doi.org/10.15666/aeer/1906_47514764

The stand structure characteristics of natural secondary forests are very complex, and the sample plots set in Xiaoxing'an Mountains could only represent the growth status of the stand in this range, which had some limitations, other representative stands should be added to make the data more comprehensive. Forest structure is a dynamic process of long-term change, and it should be observed and analyzed for a longer period of time by extending restoration period. On the basis of this study, the effects of different tending and thinning intensities on the spatial and carbon distribution patterns of shrubs and herbs can be explored to form different hierarchical relationships and network structures. Finally, combine the research results of various aspects to better determine the ideal thinning intensity.

Acknowledgements. This study was financially supported by the Research and development plan of Applied Technology in Heilongjiang Province of China (GA19C006). And the data source was supported by field investigation in 2019.

REFERENCES

[1] Aakala, T., Fraver, S., Palik, B. J., D'Amato, A. W. (2012): Spatially random mortality in old-growth red pine forests of northern Minnesota. – Can. J. For. Res 42: 899-907.
[2] Baddeley, A., Turner, R. (2005): Spatstat: an R package for analyzing spatial point patterns. – J. Stat. Software 12: 1-42.
[3] Boyden, S., Binkley, D., Shepperd, W. (2005): Spatial and temporal patterns in structure, regeneration, and mortality of an old-growth ponderosa pine forest in the Colorado Front Range. – For. Ecol. Manage 219: 43-55.
[4] Diggle, P. J. (2003): Statistical Analysis of Spatial Point Patterns. – Arnold, London.
[5] Ding, B., Ding, G. J., Li, X. Z., Yang, Y. Z. (2016): Effects of short-term thinning on the carbon storage in Cunninghamia lanceolata plantation ecosystem. – Journal of Central South University of Forestry & Technology 36(08): 66-71.
[6] Druckenbrod, D. L., Shugart, H. H., Davies, I. (2005): Spatial pattern and process in forest stands within the Virginia piedmont. – J. Veg. Sci 16(1): 37-48.
[7] Du, Z., Kang, X. G., Bao, Y. J., Yang, X. X. (2012): Spatial distribution patterns and associations of tree species during different succession stages in spruce-fir forests of Changbai Mountains, northeastern China. – Journal of Beijing Forestry University 34(02): 14-19.
[8] Du, Z., Kang, X. G., Meng, J., H., Kong, L., Guo, W. W., Yue, G. (2013): Spatial distribution patterns and associations of dominant tree species in poplar birch secondary forest stand in Changbai Mountains. – Journal of Northeast Forestry University 41(04): 36-42.
[9] Duan, M. C., Wang, G. L., Shi, J. Y., Zhou, H. X. (2019): Effects of thinning on structure and spatial pattern of dominant populations in Pinus tabuliformis plantations. – Chinese Journal of Ecology 38(01): 1-10.
[10] Fajardo, A., Goodburn, J. M., Graham, J. (2006): Spatial patterns of regeneration in managed uneven-aged ponderosa pine/Douglas-fir forests of Western Montana, USA. – For. Ecol. Manage 223(1-3): 255-266.
[11] Felinks, B., Wiegand, T. (2008): Exploring spatiotemporal patterns in early stages of primary succession on former lignite mining sites. – J. Veg. Sci 19: 267-276.
[12] Getzin, S., Dean, C., He, F., Trofymow, J. A., Wiegand, K., Wiegand, T. (2006): Spatial patterns and competition of tree species in a Douglas-fir chronosequence on Vancouver Island. – Ecography 29: 671-682.

http://www.aloki.hu ● ISSN 1589 1623 (Print) ● ISSN 1785 0037 (Online)
DOI: http://dx.doi.org/10.15666/aeer/1906_47514764

[13] Gray, L., He, F. (2009): Spatial point-pattern analysis for detecting density-dependent competition in a boreal chrono sequence of Alberta. – For. Ecol. Manag. 259: 98-106.
[14] Han, F. L., Tian, X. L., Dang, S. L., Cao, T. J. (2015): Impact of thinning on carbon storage for *Pinus tabuliformis* stands in Shaanxi Qiaoshan. – Journal of Northwest Forestry University 30(04): 184-191.
[15] Hao, Z. Q., Zhang, J., Song, B., Ye, J., Li, B. H. (2007): Vertical structure and spatial associations of dominant tree species in an old-growth temperate forest. – For. Ecol. Manage 252: 1-11.
[16] Harms, K. E., Wright, S. J., Calderón, O., Hernóndez, A., Herre, E. (2000): Pervasive density-dependent recruitment enhances seedling diversity in a tropical forest. – Nature 404: 493-495.
[17] He, F., Duncan, R. P. (2000): Density-dependent effects on tree survival in an old growth Douglas fir forest. – J. Ecol 88: 676-688.
[18] He, F., Legendre, P. L., Frankie, J. V. (1997): Distribution patterns of tree species in a Malaysian tropical rain forest. – Journal of Vegetation Science 8: 105-114.
[19] Hou, J., Mi, X., Liu, C., Ma, K. (2004): Spatial patterns and associations in a Quercus-Betula forest in northern China. – J. Veg. Sci 15(3): 407-414.
[20] Hu, Y. Y., Min, Z. Q., Gao, Y., Feng, Q. X. (2011): Effects of selective cutting on stand growth and structure for natural mixed spruce (Picea koraiensis) fir (Abies nephrolepis) forests. – Scientia Silvae Sinicae 47(02): 15-24.
[21] Hu, H. Q., Luo, B. Z., Wei, S. J., Sun, L., Luo, S. S., Ma, H. B. (2015): Biomass carbon density and carbon sequestration capacity in seven typical forest types of the Xiaoxing'an Mountains, China. – Chinese Journal of Plant Ecology 39(02): 140-158.
[22] Huang, X. F., Kang, X. G. (2004): A review on the study of regeneration of natural spruce-fir mixed stand of coniferous and broad-leaved trees in China. – World Forestry Research 5: 34-38.
[23] Illian, J., Penttinen, A., Stoyan, H., Stoyan, D. (2008): Statistical Analysis and Modelling of Spatial Point Patterns. – John Wiley & Sons, Chichester, UK.
[24] Law, R., Illian, J., Burslem, D. F. R. P., Gratzer, G., Gunatilleke, C. V. S., Gunatilleke, I. A. U. N. (2009): Ecological information from spatial patterns of plants: insights from point process theory. – Journal of Ecology 97: 616-628.
[25] Li, R., Zhang, W. H., He, J. F., Zhou, J. Y. (2011): Effect of thinning on natural regeneration and growth of Quercus wutaishanica saplings. – Journal of Northwest A & F University (Natural Science Edition) 39(01): 52-60 + 68.
[26] Liu, Z. G., Li, Z. Q. (2005): Perspectives on small-scale spatial structure of plant species in plant communities. – Acta Phytoecologica Sinica 29(6): 1020-1028.
[27] Moeur, M. (1993): Characterizing spatial patterns of trees using stem-mapped data. – Forest Science 4(39): 756-775.
[28] Petritan, I. C., Marzano, R., Petritan, A. M., Lingua, E. (2014): Overstory succession in a mixed Quercus petraea–Fagus sylvatica old growth forest revealed through the spatial pattern of competition and mortality. – Forest Ecology & Management 326: 9-17.
[29] Rozas, V. (2006): Structural heterogeneity and tree spatial patterns in an old-growth deciduous lowland forest in Cantabria, northern Spain. – Plant Ecology (185): 57-72.
[30] Sanatan, D. G., Bradley, D. P. (2018): Spatial patterns and competition in trees in early successional reclaimed and natural boreal forests. – Acta Oecologica 92: 138-147.
[31] Shen, L., Yang, H., Kang, X. G., Yue, G. (2013): Effects of selective cutting intensity on spatial distribution pattern of natural spruce-fir forests. – Journal of Central South University of Forestry & Technology 33(01): 68-74.
[32] Stoyan, D., Penttinen, A. (2000): Recent applications of point process methods in forestry statistics. – Statistical Science 15(1).
[33] Stoyan, D., Stoyan, H. (1994): Fractals, Random Shapes and Point Fields. – Wiley, Chichester.

http://www.aloki.hu ● ISSN 1589 1623 (Print) ● ISSN 1785 0037 (Online)
DOI: http://dx.doi.org/10.15666/aeer/1906_47514764

[34] Svoboda, M., Fraver, S., Janda, P., Bače, R., Zenáhlíková, J. (2010): Natural development and regeneration of a Central European montane spruce forest. – Forest Ecology & Management 260: 707-714.
[35] Wang, C. K. (2005): Biomass allometric equations for 10 co-occurring tree species in Chinese temperate forests. – Forest Ecology and Management 222(1).
[36] Wang, X. G., Hao, Z. Q., Ye, J., Zhang, J., Li, B. H., Yao, X. L. (2008): Relationships between species abundance and spatial distribution pattern of broad-leaved Korean pine (Pinus koraiensis) mixed forest in Changbai Mountains of China. – Chinese Journal of Ecology 27(2): 145-150.
[37] Wang, Y., Bi, R. C., Xu, Q. (2017): Community characteristics and spatial distribution of mixed conifer and broad-leaved forest in South Taiyue Mountain, Shanxi Province of China. – Guihaia 37(07): 901-911.
[38] Wiegand, T., Moloney, K. A. (2004): Rings, circles, and null-models for point pattern analysis in ecology. – Oikos 104: 209-229.
[39] Wiegand, T., Moloney, K. A. (2014): A Handbook of Spatial Point Pattern Analysis in Ecology. – Chapman and Hall/CRC Press, Boca Raton, FL.
[40] Wu, J. Q., Wang, Y. X., Yang, Y., Zhu, T. T., Zhu, X. D. (2015): Effects of crop tree release on stand growth and stand structure of Cunninghamia lanceolata plantation. – Chinese Journal of Applied Ecology 26(02): 340-348.
[41] Yang, H., Li, D. (1985): Distribution patterns of dominant tree species on northern slope of Changbai Mountain. – Research Forest. Ecosyst. 5: 1-14.
[42] Yao, H. F., Wang, C., Lu, J. (2020): Survey of research on spatial distribution pattern of plant population. – Agricultural Development & Equipment (10): 113-115.
[43] Zhang, C. Y., Zhao, X. H., Xia, F. C. (2008): Spatial distribution of tree species and environmental interpretations of secondary forest in Changbai Mountains. – Scientia Silvae Sinicae 44(8): 1-8.
[44] Zhao, Z. H., Hui, G. Y., Hu, Y. B., Zhou, H. M., Zhang, L. J. (2011): Spatial distribution patterns and associations of dominate population in two types of broadleaved Korean pine mixed forest. – Forest Research 24(05): 554-562.

http://www.aloki.hu ● ISSN 1589 1623 (Print) ● ISSN 1785 0037 (Online)
DOI: http://dx.doi.org/10.15666/aeer/1906_47514764

SIMULTANEOUS IMMOBILIZATION OF SOIL ARSENIC AND CADMIUM WITH REDUCED ACCUMULATION IN CABBAGE (*BRASSICA OLERACEA* L.) USING FE MODIFIED BIOCHAR

JIANG, P.[1,2] – LIU, J.[2,3] – JIANG, W.[2] – YU, G.[2,4*] – ZHANG, X.[2,3] – ZHU, Z.[2] – YOU, S.[2,3] – LIN, F.[4]

[1]*Key Laboratory of Ecology of Rare and Endangered Species and Environmental Protection (Guangxi Normal University), Ministry of Education, Guilin, China*

[2]*College of Environmental Science and Engineering, Guilin University of Technology, Guilin, China*

[3]*Technical Innovation Center of Mine Geological Environmental Restoration Engineering in Southern Karst Area, MNR, Nanning, China*

[4]*Third Institute of Oceanography, Ministry of Natural Resources, Xiamen, China*

**Corresponding author*
e-mail: yguo2020@163.com; phone: +86-773-253-7332; fax: +86-773-589-5330

Key Laboratory of Ecology of Rare and Endangered Species and Environmental Protection (Guangxi Normal University), Ministry of Education and Guilin University of Technology contributed equally to this work

(Received 5th Feb 2021; accepted 9th Apr 2021)

Abstract. Biochar (BC) has been widely studied as a soil amendment for immobilizing heavy metals in contaminated soil. However, the effect of modified biochar on arsenic (As) and cadmium (Cd) immobilization in soils and plant uptake rates are still unclear due to complex environmental interactions. To assess the effects of Fe_2O_3, BC and iron (Fe)-modified biochar (FMB) on the bioavailability of As and Cd in soil and their accumulation in cabbages (*Brassica oleracea* L.), these values were investigated. The results indicated that the addition of 0.5% amendment to the soil significantly reduced the mobility of As/Cd in soil. Of the three soil amendments, FMB significantly reduced As and Cd accumulation in the cabbages by 27.4% and 30.1%, respectively. This is achieved possibly by reducing the mobility of soil As/Cd, and as a result the available As/Cd were reduced by 12.3% and 7.94%, respectively. The chemical forms of soil As/Cd may change from the available fraction to less available fractions, while the residual As/Cd increased by 16.3% and 353% compared to control, respectively. In summary, FMB demonstrated great potential in stabilizing As/Cd in the soil and in reducing the accumulation of As/Cd in plants.
Keywords: *Fe-modified biochar, heavy metal, immobilization, accumulation, bioavailability*

Introduction

Heavy metal contamination in paddy soils is threatening human health in many parts of the world (Zhao et al., 2015). Co-contamination of As and Cd has raised public concern, especially in Southern China (Yu et al., 2016a; Qiao et al., 2018a). Both metals have great mobility and can accumulate in the human body through the food chain. The bioavailability of heavy metals in soils is directly related to their toxicity and the amount of accumulation in crops (Li et al., 2017; Kumarathilaka et al., 2018). In recent years, numerous methods have been investigated to reduce the soil bioavailability of As and Cd, such as excavation, soil washing, and electrokinetics. However, these methods are prohibitively expensive and usually require intensive labor. Therefore, it is

http://www.aloki.hu ● ISSN 1589 1623 (Print) ● ISSN 1785 0037 (Online)
DOI: http://dx.doi.org/10.15666/aeer/1906_47654780

important to look for a cost-effective and environmentally friendly method to simultaneously immobilize As and Cd in the soil.

The application of biochar in remediating heavy metal contaminated soils has attracted much attention (Sneath et al., 2013). Biochar is a porous and fine-grained substance that is produced by the combustion of biomass under limited oxygen conditions. It has great adsorption abilities due to its porous structures, large specific surface area, high alkalinity, and special functional groups (Zhang et al., 2020). The results of previous studies have shown that the supplement of biochar significantly immobilized metals such as Cd in the soil through surface complexation, cation exchange, and metal precipitation (Venegas et al., 2016; Liang et al., 2017). For instance, the Cd accumulation in Indian mustard significantly decreased with biochar supplement (Park et al., 2011). As and Cd have almost opposite chemical behaviours in the soil (Al-Abed et al., 2007). Biochar addition in the soil can enhance the mobility of As, as it has a rich mineral ash content and increases the soil pH. In addition, biochar enhances the formation of oxy-anions and thus promotes the mobility of As (Rocco et al., 2018). To increase the adsorption of As by the biochar, iron (Fe) modified biochar was suggested. Studies have proven that Fe oxides, including goethite, hematite, ferrous, and Fe(II), influenced the bioavailability of As and Cd (Yu et al., 2017, 2016b). Fe-amendments reduce the bioavailability of As and increase the crystalline/crystalline Fe oxide-bound As through adsorption/desorption and co-precipitation with metal oxide (Yu et al., 2016b; Wen et al., 2020; Irshad et al., 2020). In addition, a reactive Fe (III) species is formed during the oxidation of Fe (II) to goethite. The reactive Fe (III) species is then able to interact with Fe-oxides and serve as the electron transfer from Fe (II) to goethite to form a reactive Fe (III) species as a reactive intermediate phase, which can interact with As (III) and lead to As (III) oxidation. Besides, Fe minerals and bacteriogenic Fe oxides produced by Fe(III)-reducing bacteria and Fe(II)-oxidizing microorganisms, respectively, can enhance the immobilization of Cd (Qiao et al., 2018b). Cabbage (*Brassica chinensis* L.) is an important vegetable in Asia, especially in China. Cabbage tends to absorb Cd from the soil, which poses a great risk for human health (Bashir et al., 2018). In general, Fe-amendment can reduce the bioavailability of As in the soil. Supplementation with biochar enhances As mobility but reduces Cd mobility. The immobilization effects of Fe-modified biochar (FMB) in As and Cd co-contaminated soil still remain largely unknown. Therefore, in order to obtain materials with the characteristics of both Fe-oxides and biochar, we modified the biochar (FMB) by covering the surface with Fe-oxides to study its effect on As and Cd bioavailability in As and Cd co-contaminated soil. Additionally, we compared the effects of FMB to Fe_2O_3 and biochar. Our aims were to (1) determine the best soil amendment concentrations by using a column experiment in As and Cd co-contaminated soil and (2) to identify the most suitable soil amendments by reducing the mobility of As and Cd in soils and reducing the accumulation of As and Cd in cabbages.

Materials and methods

FMB preparation

Bamboo (*Phyllostachys pubescens*) individuals were collected from the Yanshan campus of Guilin University of Technology, Guangxi, China. The bamboo stalks were cut into sizes of 30 × 10 × 3 mm^3. The samples were heated in dilute ammonia (NH_3)

http://www.aloki.hu ● ISSN 1589 1623 (Print) ● ISSN 1785 0037 (Online)
DOI: http://dx.doi.org/10.15666/aeer/1906_47654780

solution (5%) for 6 h to enhance the connectivity between the pores and cellular materials. The treated bamboo stalks were washed with deionized water three times and then dried at 80 °C for 24 h. The dried samples were roasted at 600 °C for 3 h. The samples were ground into power after cooling to room temperature. The dried samples were then soaked in a solution of iron (III) nitrate ($Fe(NO_3)_3$) (1.2 mol•L^{-1}) for 5 d. The $Fe(NO_3)_3$ solvent constituted a mixture of ethanol and ultra-pure water (1:1, v/v) (Zhu et al., 2018). To ensure that all samples were soaked in the solution, we added some additional ethanol solution. The bamboo stalks were then dried at 80 °C for 24 h. We repeated the process of soaking and drying for three times. Lastly, the samples were placed into a muffle device at 600 °C for 3 h, following which we obtained the BC material.

Characterization of FMB and BC

We obtained the phase recognition of the BC and FMB by X-ray diffraction (XRD). The XRD analysis was carried out with copper Kα radiation at 40 kv and 150 mA. The morphological characters and chemical compositions of the BC and FMB were observed using scanning electron microscopy (SEM) and energy dispersive X-ray (EDS) spectroscopy, respectively (SEM-EDS, JEM-6380LV, JEOL, Tokyo, Japan). The tests of cyclic voltammetry (CV) and electrochemical impedance spectroscopy (EIS) were measured at the electrochemical workstation (CHI660E, Shanghai Chenhua Company, Shanghai, China). For CV, we scanned the potential from -1.6 V to 0.8 V at a scan rate of 100, 300, and 500 mV/s in o.1 M degassed PBSS. We recorded impedance spectra in 0.1 M phosphate-buffered saline (PBS) at 25 °C within a frequency range from 10^{-2} to 10^{5} Hz with perturbation amplitude of 5 mV.

Soil properties and plant preparation

Two soils (soil 1 and soil 2) used in this study were collected from the topsoil (0–20 cm) of different farmlands next to a smelter in Hechi, Guangxi. The soil properties have been influenced by smelting, wastewater irrigation, and open-pit mining, resulting in the soils being polluted in different degrees (Yu et al., 2020). The soils were placed in a room to air-dry at room temperature and then ground and sieved through 20- and 100-mesh sieves before further use.

Cabbage seeds were purchased from the Yanshan Farmers Market, Guilin, Guangxi. The seeds were soaked for one night and then surface sterilized with a 10% H_2O_2 solution for 10 min. The seeds were sown into seedbeds filled with nutrient soil after rinsing with deionized water. The seedbeds were placed in a greenhouse, which the temperatures of the greenhouse were maintained at 25 °C/day and 18 °C/night. The relative humidity was about 75% with a 14 h photoperiod. We added deionized water to the soil to maintain the soil moisture content (about 50%). After the seeds had germinated, we selected seedlings 6–8 cm high and with 2–3 fronds for soil pot experiment 2.

Pot experiment

Pot experiment 1: The effect of Fe_2O_3, BC, and FMB on As and Cd mobility were studied in actual As/Cd-contaminated soil (soil 1). Fe_2O_3, BC, and FMB were mixed completely with the soil samples. The mixed soil was placed into 2 L polypropylene pots (1.5 kg soil). We added Fe_2O_3, BC, and FMB at concentrations of 0 (control),

http://www.aloki.hu ● ISSN 1589 1623 (Print) ● ISSN 1785 0037 (Online)
DOI: http://dx.doi.org/10.15666/aeer/1906_47654780

0.2%, 0.5%, and 1% (w/w). The pots were then incubated in the greenhouse (described in the plant preparation section). To maintain the soil moisture (70%) at field capacity, the soils were watered with As/Cd-free tap water. Then, the soil samples were collected and incubated for 5 d, 30 d, and 90 d. The soil pH and available As/Cd as well as residual As/Cd were analysis.

Pot experiment 2: To study the accumulation of As and Cd in cabbages planted in the soil (soil 2), the soils were treated with Fe_2O_3, BC, and FMB. Based on the results of pot experiment 1, we selected 0.5% as the experimental concentration. After 10 days of cultivation, the seedlings were transferred into 22-cm-diameter round plastic pots (5 kg soil). Each treatment had three replications, and the seedlings were in similar sizes. One group was replicated for three times as a control group without any soil amendment supplement. In total, there were 12 pots in the greenhouse (described in the plant preparation section). To maintain 50% soil moisture, the plants were sprayed with tap water daily. The plants were harvested after 30 d of cultivation. We determined the flesh weight (FW), dry weight (DW), and the contents of total Cd and total As.

Chemical analysis of soil and plant samples

All the chemicals were reagent grade in this study. The soil pH, ammonium N, available P, and available K of soil 1 and soil 2 were determined by using routine analytical methods (Liu et al., 2018). Soil samples (about 0.25 g) were digested with 12 mL of HCl: HNO_3 (4:1, *v/v*). The concentration of pseudo-total Cd was measured by using the atomic absorption spectrophotometry method (ICP, PE-AA700, USA). Soil pseudo-total (Aqua regia) As was determined by hydride generation-atomic fluorescence (SA-20). The concentrations of soil available Cd and available As were extracted with 0.005 M DTPA + 0.01 M $CaCl_2$ + 0.1 M TEA) and 0.5 M $NaHCO_3$ (pH 8.5) + 0.5 M (NaH_2PO_4) + 0.1 M HCl, respectively. The soil homogenate of Cd was shaken at 5000 × *g* for 20 min, and then the supernatant was tested by ICP-OES (PE-AA700). The suspension of As was shaken at 250 × *g* for 1 h, and then the supernatant was determined by hydride generation atomic fluorescence spectrometry (HG-AFS, SA-20, China).

The measured soil properties of soil 1 and soil 2 are summarized in *Table 1*. We extracted soil residual As and soil residual Cd in pot experiment 1 according to the five-step sequential extraction scheme based on the procedures described by Wenzel et al. (2001) and Tessier et al. (1979). Then we determined the residual As and residual Cd by HG-AFS (SA-20) and ICP-OES (PE-AA700), respectively. The measurement methods of the other soil properties in pot experiment 1 and experiment 2 were the same as in soil 1 and soil 2.

The harvested plants were washed with water. The moisture on the plant surface was absorbed by paper, and then we determined the fresh weight (FW). The plants were separated into roots, stems, and leaves and then dried (65 °C) until a constant weight to determine the dry weight (DW). The dry shoots were digested with a mixture of HNO_3 and $HClO_4$ (9:1, *v/v*). We determined the Cd concentration by ICP-OES. The dry shoot was digested with $HClO_4$:H_2SO_4:HNO_3 (1:1.5:4, v/v) at 110–130 °C (Qiao et al., 2018a). We measured the total As concentration by HG-AFS (SA-20). To ensure quality control, certified standard reference materials were addressed (soil Cd: GBW(E)07429, plant Cd: GBW(E)10023; soil As: GBW(E)070008, plant As: GBW(E)10014).

http://www.aloki.hu ● ISSN 1589 1623 (Print) ● ISSN 1785 0037 (Online)
DOI: http://dx.doi.org/10.15666/aeer/1906_47654780

Table 1. *The physicochemical properties of the tested soil*

	pH	Ammonium nitrogen (mg•kg^{-1})	Available P (mg•kg^{-1})	Available K (mg•kg^{-1})	Total Cd (mg•kg^{-1})	Total As (mg•kg^{-1})	Available Cd (mg•kg^{-1})	Available As (mg•kg^{-1})
Soil 1	6.46	12.4	8.53	3.10	19.54	332.91	5.41	9.2
Soil 2	5.62	27.3	17.4	13.5	5.19	133.54	1.23	0.77

Statistical analyses

The mean and standard deviation (SD) of the experimental data were analyzed in Microsoft Office Excel 2010 (Microsoft Corporation, Redmond, WA, USA). Two-way analysis of variances (ANONA) were performed with SPSS 18.0 software (IBM Corporation, Armonk, USA). Duncan's multiple range tests as a multiple compassion procedure at significant levels of $P < 0.05$. Figures were plotted using Origin 2020b (OriginLab, Northampton, Massachusetts, USA).

Results

Characterization of biochar and Fe-modified biochar

XRD was used to characterize the crystalline structure of the BC and FMB. As shown in *Figure 1,* magnetite, hematite, and carbon were presented on the surfaces of the FMB. Only one carbon was on the surface of the BC. The location and intensity of the XRD peaks in the FMB matched the two reference peaks. The peaks at 2θ of 30.09°, 35.44°, 43.07°, 56.96°, and 62.54° corresponded to Fe_3O_4 (reference code 01-089-3854), and the peaks at 2θ of 24.13°, 33.14°, 35.63°, 49.52°, 54.06°, 57.66°, and 62.42° were identified as Fe_2O_3 (reference code 01-079-1741), respectively. The peaks of biochar at 2θ of 23.36° and 43.33° belonged to amorphous carbon.

The SEM results showed that there was a hierarchical porous framework in the bamboo woods of the biochar (*Fig. 2*). The diameters of the parenchyma cells and fibres were about 10–40 μm and < 1 μm, respectively. The surfaces of the FMB were filled with particles, even in the pores. To determine the ingredients of the particles on the surfaces of the FMB, we performed an EDS analysis. The results illustrated that the Fe ion was associated with the FMB surface (*Fig. 3*).

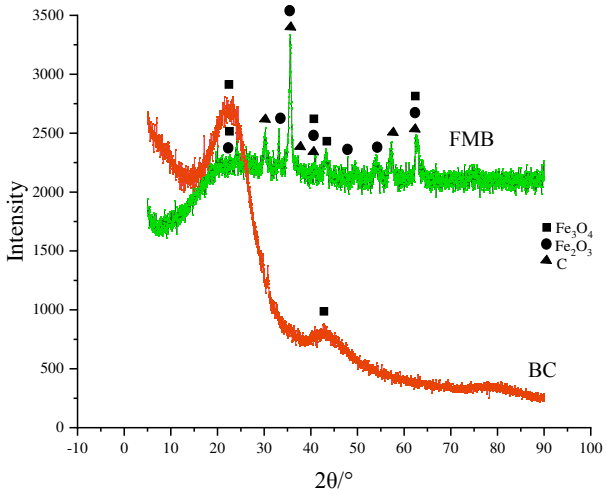

Figure 1. *XRD patterns of the BC and FMB*

http://www.aloki.hu ● ISSN 1589 1623 (Print) ● ISSN 1785 0037 (Online)
DOI: http://dx.doi.org/10.15666/aeer/1906_47654780

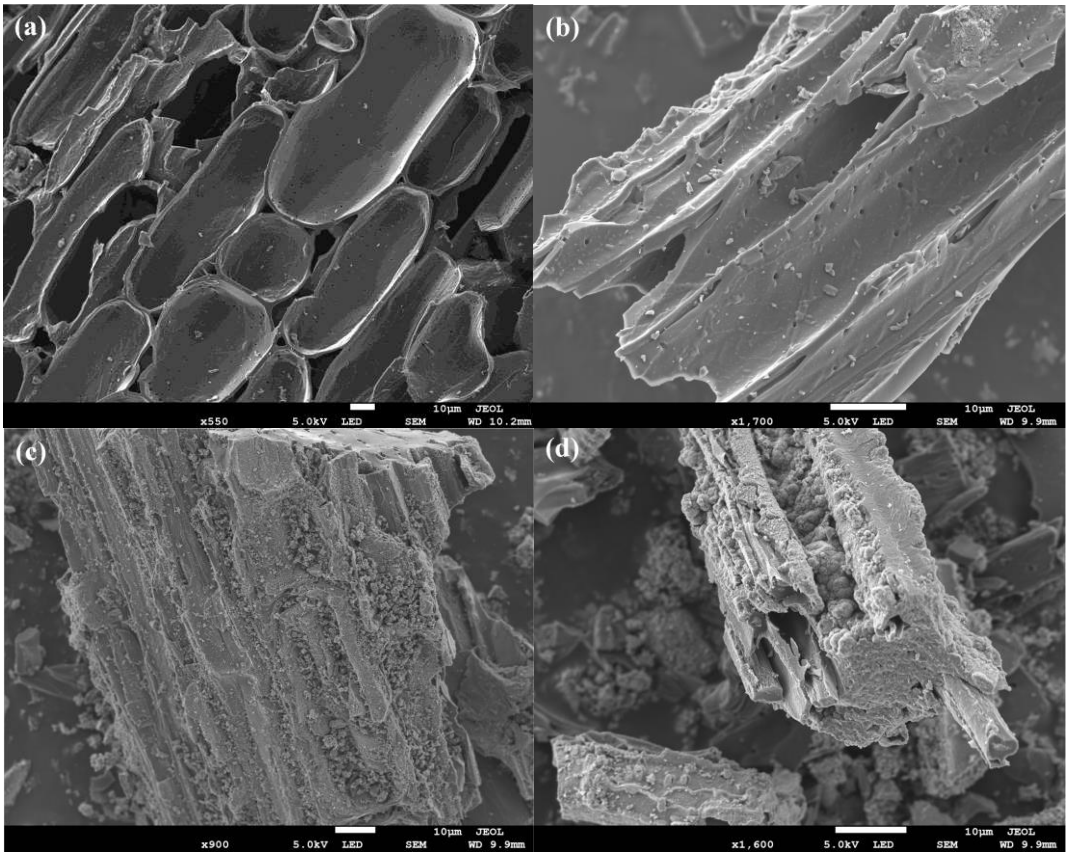

Figure 2. *SEM images of BC and FMB: (a, b) SEM images of BC, and (c, d) SEM images of FMB*

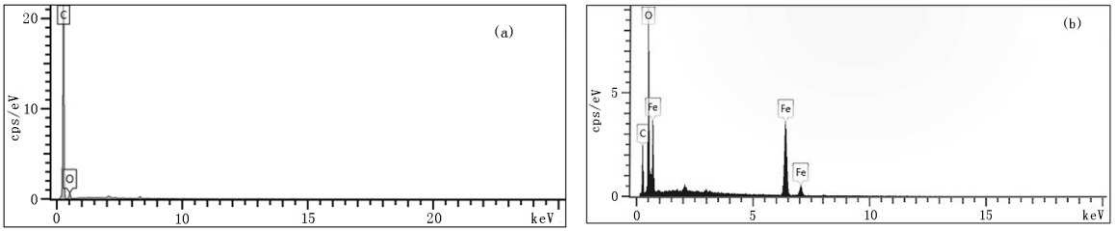

Figure 3. *EDS spectrum of BC and FMB: (a was the BC and b was the FMB)*

Electrochemical detection of BC and FMB

We used the CV patterns in this study to analyze the electro-oxidation mechanism of the biochar and FMB. There were no oxidation peaks and reduction peaks in the CV of the BC (*Fig. 4*) at 100, 300, and 500 mV. The CV pattern of the FMB presented redox and oxidation peaks. Furthermore, the peak was more obvious at 500 mV than at 100 and 300 mV. The redox peak and oxidation peak were positioned at -0.63 V and -1.11 V, respectively. The EIS of the BC and FMB showed a semicircle line and an almost straight line in the high- and low-frequency range, respectively (*Fig. 5*). The EIS of Fe_2O_3, however, presented a line in all frequency ranges. In the high-frequency range, the data fitted from the semicircle indicated that the FMB electrode had a lower CD resistance of 15000 Ω than the BC.

http://www.aloki.hu ● ISSN 1589 1623 (Print) ● ISSN 1785 0037 (Online)
DOI: http://dx.doi.org/10.15666/aeer/1906_47654780

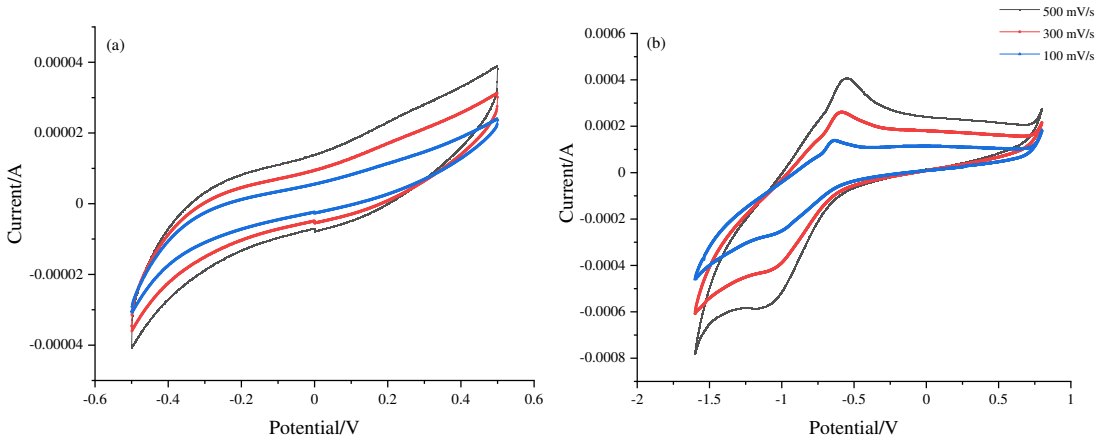

Figure 4. *Cyclic voltammeter curves after BC and FMB addition*

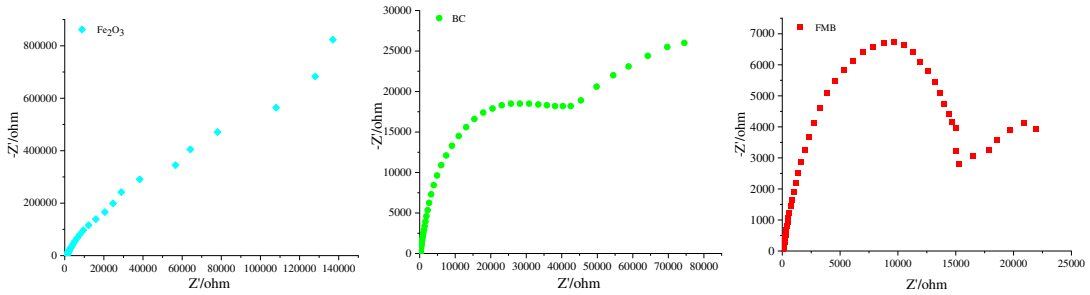

Figure 5. *EIS patterns of the electrodes in the different treatments*

Soil-column experiment at different treatment times

The result of soil-column experiment showed that the pH of the Fe_2O_3 treatment was not significantly different from the control at the different treatment concentrations (*Table 2*). On the fifth day, the pH of the BC and FMB was significantly higher than the control at three addition concentrations. The pH reached the maximum in the two materials at a concentration of 1%, namely, 6.63 ± 0.01 (BC) and 6.70 ± 0.03 (FMB). On the 90th day, the pH in the three treatment concentrations of Fe_2O_3 was higher than that in the control group. There was no significant difference between the three BC treatment concentrations, but they were all higher than the control. The addition of different concentrations of FMB had enhanced the pH in comparison to the control group.

The concentrations of available As and available Cd in the soil-column experiment were determined on the fifth, 30th, and 90th days, respectively. The data were presented using the ratio of the experimental group and the control group (*Fig. 6*). As shown in *Figure 6,* the ratios of As reached the lowest values on the 30th day in the different material treatments. In particular, the As ratio in the BC and FMB on the 30th day was significantly lower than under the other treatment durations. The As ratio decreased with increased concentrations of Fe_2O_3 and FMB, whereas the addition of BC showed the opposite trend. When the concentration was 0.2%, the As ratios in the Fe_2O_3, BC, and FMB were 78%, 44%, and 50%, respectively. When the addition concentration was 0.5%, the corresponding values were 75%, 49%, and 46%, respectively. The addition of Fe_2O_3 and FMB had the lowest values at a concentration of 1%, which were 62% and

http://www.aloki.hu ● ISSN 1589 1623 (Print) ● ISSN 1785 0037 (Online)
DOI: http://dx.doi.org/10.15666/aeer/1906_47654780

44%, respectively. The As ratio was 53% with 1% BC addition. The results illustrated that 0.5% and 1% concentrations had no significantly different effects on the As ratio, except under Fe_2O_3 addition. On the fifth day, the three materials showed differing trends with increased concentration addition. The lowest As ratios of Fe_2O_3, BC, and FMB were 76%, 75%, and 68%, respectively. On the 90th day, the trends in Fe_2O_3, BC, and FMB were similar to those on the 30th day. The lowest As ratios in the Fe_2O_3, BC, and FMB treatments were 72%, 75%, and 60%, respectively.

Table 2. *Soil pH at different treatment durations*

Time/d	Addition concentration	Fe_2O_3	BC	FMB
5	0%	6.46 ± 0.05a	6.46 ± 0.05d	6.46 ± 0.05c
	0.2%	6.60 ± 0.04a	6.60 ± 0.01b	6.61 ± 0.01b
	0.5%	6.73 ± 0.01a	6.54 ± 0.03c	6.61 ± 0.02b
	1%	6.50 ± 0.01a	6.63 ± 0.01a	6.70 ± 0.03a
30	0%	6.46 ± 0.05a	6.46 ± 0.05a	6.46 ± 0.05a
	0.2%	6.51 ± 0.12a	6.47 ± 0.03a	6.50 ± 0.06a
	0.5%	6.48 ± 0.03a	6.53 ± 0.10a	6.51 ± 0.06a
	1%	6.56 ± 0.22a	6.53 ± 0.04a	6.54 ± 0.04a
90	0%	6.46 ± 0.05c	6.46 ± 0.05b	6.46 ± 0.05c
	0.2%	6.60 ± 0.07bc	6.69 ± 0.08a	6.76 ± 0.10a
	0.5%	6.65 ± 0.05ab	6.70 ± 0.10a	6.72 ± 0.12a
	1%	6.68 ± 0.03a	6.63 ± 0.03a	6.68 ± 0.02b

Results are means ± SD (n = 3). Means within the same column are not significantly different according to the LSD test ($p < 0.05$)

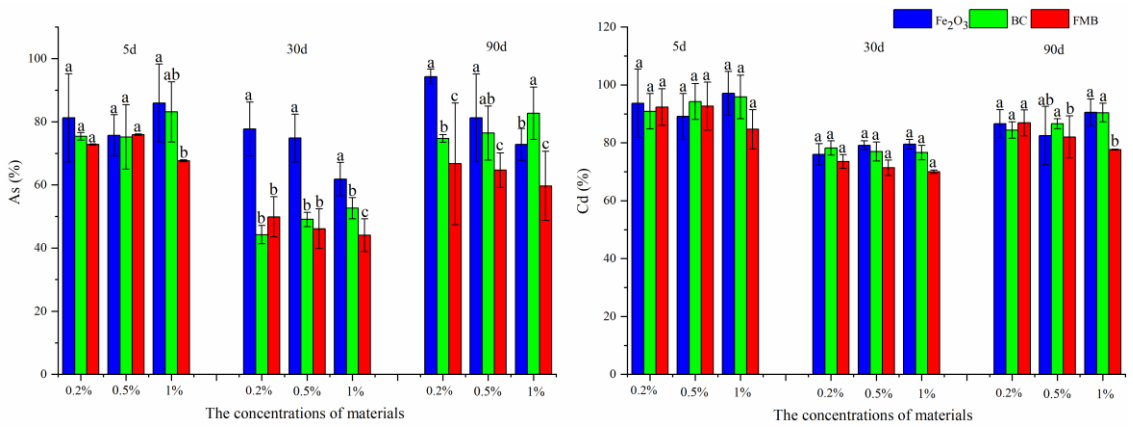

Figure 6. *Reduction rates of available Cd/As in the different treatments*

The Cd ratios of Fe_2O_3, BC, and FMB on the 30th day were all lower than the other treatment durations at different concentrations (*Fig. 6*). The trends in Cd ratios in the biochar and FMB were similar and decreased with increased concentration. The addition of Fe_2O_3, however, showed the opposite trend. The lowest Cd ratio in the FMB was at a concentration of 1% (70%). It was only slightly lower than the concentration of 0.5% (71%). Under 0.5% and 1% addition, the BC had the same Cd ratio (77%), which was lower than under 0.2% addition. The addition of Fe_2O_3 had the lowest Cd ratio (76%) at a concentration of 0.2%, which was slightly higher than the concentration of

http://www.aloki.hu ● ISSN 1589 1623 (Print) ● ISSN 1785 0037 (Online)
DOI: http://dx.doi.org/10.15666/aeer/1906_47654780

0.5% (79%). On the fifth day, the lowest Cd ratios in the Fe_2O_3, BC, and FMB treatments were 89%, 91%, and 85%, respectively. On the 90th day, the corresponding values were 82%, 84%, and 82%, respectively.

Chemical forms of soil As and Cd after harvesting

Based on the results of the soil-column experiment, the concentrations of soil available As and available Cd exhibited the lowest values on the thirtieth day. When the treatment concentration was 1%, the BC and FMB had lower available As and available Cd concentrations compared with the other two concentrations. Fe_2O_3 had the lowest available As and available Cd concentrations at a concentration of 0.2%. However, three soil amendments all had better treatment effects on the soil Cd and As when the addition concentration was 0.5%. Therefore, we selected a concentration of 0.5% for further experiments according to the economy and efficiency.

Soil available As concentrations in the Fe_2O_3, BC, and FMB treatments differed significantly (*Fig. 7*). The soil available As concentration in the BC treatment (0.92 ± 0.17 mg•kg^{-1}) was higher than in the control group (0.81 ± 0.04 mg•kg^{-1}). Conversely, the concentration in the FMB treatment (0.71 ± 0.01 mg•kg^{-1}) was lower than in the control group. The addition of Fe_2O_3 resulted in the highest available Cd concentration (1.39 ± 0.16 mg•kg^{-1}), followed by BC and FMB at 1.19 ± 0.07 mg•kg^{-1} and 1.16 ± 0.08 mg•kg^{-1}, respectively.

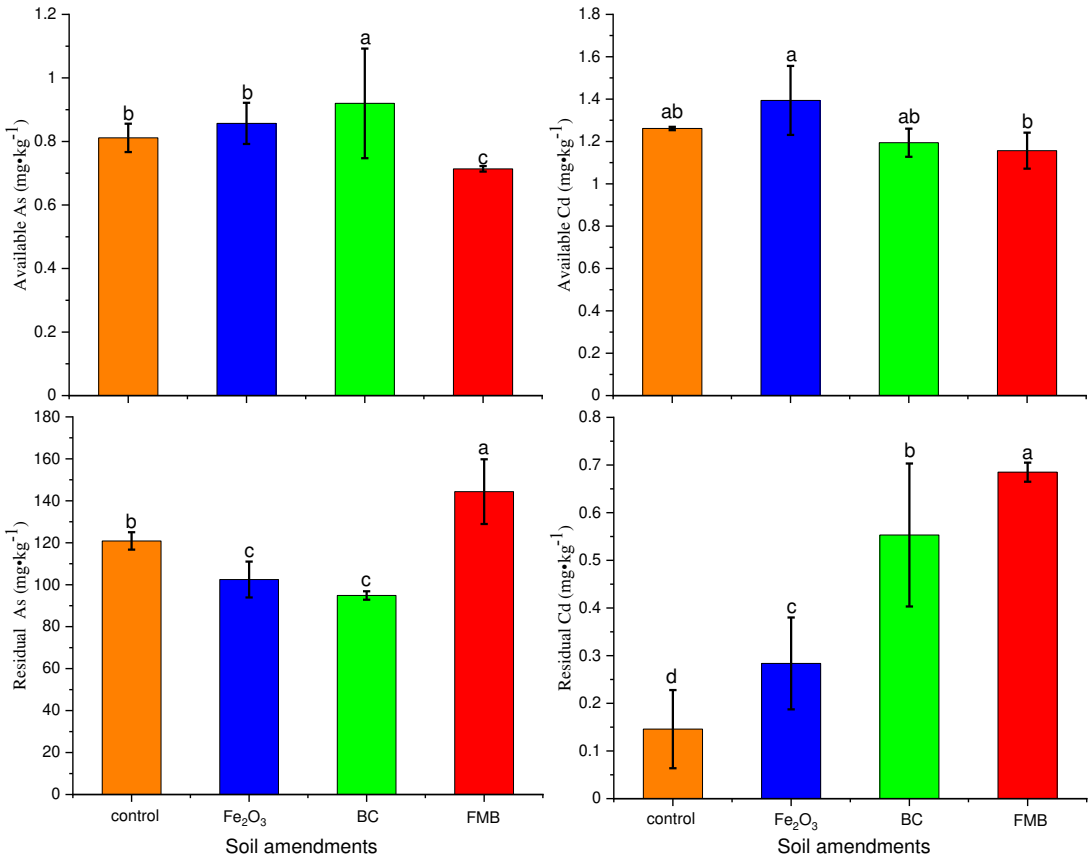

Figure 7. *The chemical format of Cd/As after harvesting. Results are means ± SD (n = 3). Means within the same column are not significantly different according to the LSD test ($p < 0.05$)*

http://www.aloki.hu ● ISSN 1589 1623 (Print) ● ISSN 1785 0037 (Online)
DOI: http://dx.doi.org/10.15666/aeer/1906_47654780

Supplementation with FMB significantly increased the residual As concentration compared with the control group (*Fig. 7*). The addition of Fe_2O_3 and BC, however, presented an opposite trend. The concentrations of residual As in Fe_2O_3 and BC were 102 ± 8.56 mg•kg^{-1} and 94.9 ± 2.00 mg•kg^{-1}, respectively, which were lower than in the control group. The residual Cd concentrations in the three materials were significantly increased in comparison to the control group. The concentrations of residual Cd in the control, Fe_2O_3, BC, and FMB were 0.15 ± 0.08 mg•kg^{-1}, 0.28 ± 0.10 mg•kg^{-1}, 0.55 ± 0.15 mg•kg^{-1}, and 0.68 ± 0.02 mg•kg^{-1}, respectively.

Cabbage biomass and As/Cd accumulation under the different treatments

BC and FMB increased the FW of cabbages compared to control and Fe_2O_3 (*Fig. 8*). The FW in the soil under BC addition had the highest value of 17.5 ± 0.85 mg•kg^{-1}, followed by FMB (15.2 ± 1.58 mg•kg^{-1}) and Fe_2O_3 (13.3 ± 1.15 mg•kg^{-1}). Compared with the control group, the addition of different materials had no significant impact on the DW of the cabbages. The DWs of the cabbages in the control, Fe_2O_3, BC and FMB treatments were 0.27 ± 0.01 mg•kg^{-1}, 0.24 ± 0.04 mg•kg^{-1}, 0.30 ± 0.08 mg•kg^{-1} and 0.24 ± 0.03 mg•kg^{-1}, respectively.

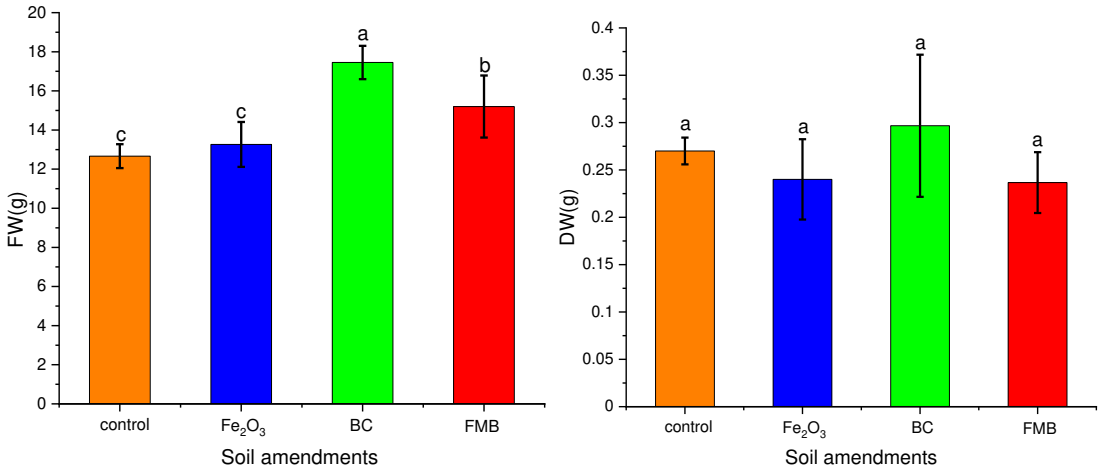

Figure 8. *Cabbage biomass of the different treatments. Results are means ± SD (n = 3). Means within the same column are not significantly different according to the LSD test ($p < 0.05$)*

The As concentrations of the cabbages were significantly lower than in the control group under treatment with the different materials (*Fig. 9*), being 3.14 ± 0.33 mg•kg^{-1}, 2.87 ± 0.33 mg•kg^{-1}, 2.15 ± 0.20 mg•kg^{-1}, and 2.28 ± 0.19 mg•kg^{-1} in the control, Fe_2O_3, BC, and FMB treatments, respectively. The Cd concentrations of the cabbages presented different trends as As. Only FMB significantly reduced the Cd concentrations in the cabbages. The Cd concentrations of the cabbages in the control, Fe_2O_3, BC, and FMB treatments were 15.9 ± 0.11 mg•kg-1, 14.6 ± 0.77 mg•kg^{-1}, 13.7 ± 3.67 mg•kg^{-1}, and 11.1 ± 1.23 mg•kg^{-1}, respectively.

Discussion

The total concentrations of Cd in the cabbages decreased under the three soil amendment treatments compared with the control group (*Fig. 9*). BC increased the

http://www.aloki.hu ● ISSN 1589 1623 (Print) ● ISSN 1785 0037 (Online)
DOI: http://dx.doi.org/10.15666/aeer/1906_47654780

residual Cd concentration, indicating that BC may have the ability to reduce the Cd mobility in the soil. Some studies indicated that the immobilization of Cd by biochar may be related to specific adsorption, which specifically occurs with organic matter (Zhang et al., 2020). The soil Cd was immobilized by forming ionic, covalent, or hydrogen bonds on the surface of the biochar (Bian et al., 2014). Compared with the BC, the FMB was better at reducing the soil Cd mobility (*Fig. 7*) and Cd accumulation in cabbages (*Fig. 9*). The FMB had the ability to adsorb Cd on its surface to form unlabile chemical forms, thus reducing the mobility of Cd. In addition, it indicated that the Fe could reduce the Cd uptake by plants. The rice cultured in Fe-deficient medium absorbed more Cd than rice cultured in Fe-sufficient medium (Nakanishi et al., 2006). Therefore, Cd and Fe may have the same uptake pathway in the plant. Supplementation with Fe could reduce the Cd uptake into the cabbage, as they may be in competition for the same heavy metal transporters. Yin et al. (2017) reported that Fe ions could inhibit the uptake and accumulation of Cd in plants. Therefore, FMB has the advantages of both biochar and Fe oxides, and it can promote the stabilization of soil Cd and thus reduce Cd accumulation in the cabbages.

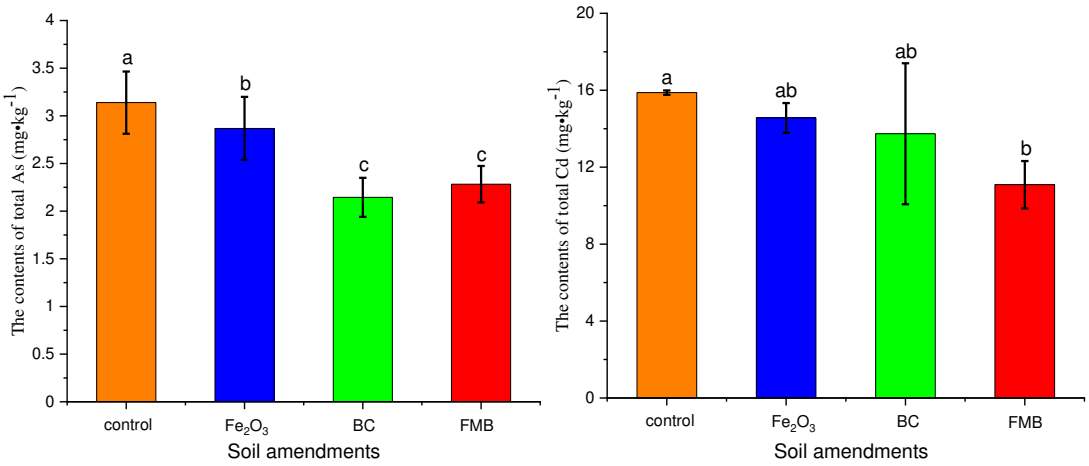

Figure 9. *Total content of Cd/As in cabbage. Results are means ± SD (n = 3). Means within the same column are not significantly different according to the LSD test (p < 0.05)*

FMB significantly decreased the soil As mobility (*Fig. 7*) and its accumulation in the cabbage (*Fig. 9*). Arsenic has been shown to have a high affinity for iron oxide surfaces (Wen et al., 2020). As and Fe can form the amorphous iron (III) arsenate ($FeAsO_4 \cdot H_2O$) and scorodite ($FeAsO_4 \cdot 2H_2O$) to influence As immobilization and bioavailability in the soil (Mladenov et al., 2010; Pedersen et al., 2006). The surface of the FMB was covered with Fe_2O_3 and Fe_3O_4 (*Figs. 1-3*). Fe oxides such as goethite, hematite, and lepidocrocite are related to soil chemical stabilization, especially As stability. The adsorption of As by natural iron oxides (hematite, magnetite, and goethite) can be fitted with a noncompetitive Langmuir isotherm (Mladenov et al., 2010). In addition, previous studies showed that Fe contents of iron plaques increased with the addition of Fe compound in the soil and thus limited the As uptake into the plant roots (Wen et al., 2020; Irshad et al., 2020; Yin et al., 2017). Therefore, FMB reduced the accumulation of As in the cabbages by reducing the As uptake. Fe_2O_3 reduced the total As accumulation in the cabbage compared with the control group (*Fig. 9*), but the

http://www.aloki.hu ● ISSN 1589 1623 (Print) ● ISSN 1785 0037 (Online)
DOI: http://dx.doi.org/10.15666/aeer/1906_47654780

accumulation of As in the cabbages was significantly higher than in the BC and FMB treatments. The Cd accumulation in the cabbage showed the same trend as As. This indicated that Fe_2O_3 is not suitable for the treatment of As/Cd -contaminated soil. BC could promote the mobility of As in the soil (*Fig. 7*). This was proved by the results of Beesley et al. (2013), Wu et al. (2015) and Yin et al. (2017), they found that biochar increased the As desorption from the soil solid phased by ligand exchange. The transfer electrons of BC and FMB may be another important factor, as they influence the As bioavailability in the environment. Biochar contains a variety of functional groups, such as quinones, furans, and phenols, giving it the ability to store and transfer electrons. Qiao et al. (2018b) discovered that biochar at the cell surface of Fe(III)-/As(V)-reducing bacteria could serve as electron shuttles between the outer-membrane reductases from dissimilatory Fe(III)-/As(V)-reducing bacteria and the terminal electron acceptor Fe(III)/As(V). There are two steps between metal-reducing bacteria and As (V) when biochar serves as the electron shuttle: biochar reduction by the Fe(III)/As (V)-reducing bacteria, followed by the reduction of abiotic As (V) by the microbial reduced biochar (Qiao et al., 2018b). Therefore, biochar facilitates the release of As (V) into the soil. The CVs of the BC showed no obvious current peaks (*Fig. 4*) and were similar to natural organic matter. This indicated that the BC in this study had the slow electron transfer and low reduction potentials of redox-active moieties (Sun et al., 2017). Ryu et al. (2015) found no obvious redox peaks in the CV curves of biochar. FMB had an oxidation peak and reduction peak in the CV curves (*Fig. 4*), which indicated that the FMB had higher electron transfer ability than the BC. The result of EIS also showed that the FMB had better electrolyte infiltration and charge-transport capability than biochar (*Fig. 5*). In addition, the electron transfer from Fe (II) to goethite formed a reactive Fe (III) species as a reactive intermediate phase, which could interact with As (III) by ternary complex formation, leading to As (III) oxidation (Amstaetter et al., 2010). The toxicity and mobility of As (V) species were less than those of As (III) in the soil (Xu et al., 2017), and the As (V) tended was more easily adsorbed by Fe-oxides (Wu et al., 2018). Therefore, the FMB could promote the oxidation of As (III) to As (V) by electron transfer and then reduce the As mobility in the soil. This is one of the main mechanisms by which FMB has a better effect on stabilizing soil As than BC. However, the total As content in the cabbage was reduced by the BC addition compared with the control group (*Fig. 9*). This may have been influenced by As soil-plant transfer coefficients. In Kloke et al. (1984), the As soil-plant transfer coefficients ranged between 0.01 and 0.1, whereas the results of Warren et al. (2003) reported that the transfer coefficients ranged between 0.0007 and 0.032. The transfer coefficient is influenced by soil texture. The content of sand in the soil increases the transfer coefficient, whereas the content of clay decreases the transfer coefficient (Warren et al., 2003). Therefore, the uptake of As is relatively higher in sands and sandy loams than in clays. In this study, the soil collected from the farmlands was mainly composed of clay, and thus the As transfer coefficient of the soil to plant was lower. This may be the main reason for the low As accumulation in the cabbages under BC addition.

Excepting the obvious effect of FMB in reducing the As and Cd accumulation in cabbage in comparison to BC and Fe_2O_3, we did not find a significant difference in the dry weight of the cabbages among the three amendments (*Fig. 8*). BC and FMB significantly increased the fresh weight of the cabbages. Dong et al. (2016) found that when the addition concentration of biochar was 20 g/kg, it could significantly enhance the biomass of cabbage. Biochar is rich in organic matter and nutrients (N, P, and K),

http://www.aloki.hu ● ISSN 1589 1623 (Print) ● ISSN 1785 0037 (Online)
DOI: http://dx.doi.org/10.15666/aeer/1906_47654780

which could increase the contents of organic matter, available N, available P, and available K in the soil, thus promoting cabbage growth (Glaser et al., 2002). The effects of biochar on cabbage growth, however, are influenced by the soil physical and chemical properties. Thus, the effects of biochar on the biomass of plants may present different trends. Park et al. (2011) discovered that biochar would not increase the dry weight of plants. Fe oxides could alter the physiological functions of plants and cause iron poisoning, thus reducing the plant biomass (Xiao et al., 2012). This process is also controlled by the Fe concentration. Dong et al. (2016) found that the concentration of Fe-modified biochar addition could enhance the biomass of cabbages. In this study, however, the dry weight of the cabbage was not influenced by Fe-modified biochar supplementation. In addition, biochar contains a porous structure that can adsorb more water and prevent the loss of nutrients needed for plant growth in the soil (Dong et al., 2016). This could explain why the fresh weight of the cabbages increased when they were treated with BC and FMB addition. In summary, FMB concentrations of 0.5% for the three amendments were suitable for cabbage growth in As/Cd-contaminated soil and did not cause iron poisoning.

Conclusions

The results of column experiment indicated that the addition concentration of 0.5% in the three soil amendments was most suitable for As and Cd co-contaminated soils based on characteristics of economy and efficiency. The total As and Cd concentrations in the cabbages were significantly lower under FMB addition than in the control group. Additionally, FMB significantly increased the residual As and Cd concentrations in the soil, indicating that the FMB had the best effect on the immobilization of As and Cd in the soil. Furthermore, FMB had no ill effect on cabbage growth under the experimental concentration. Therefore, 0.5% FMB demonstrated great potential application in the treatment of As/Cd-contaminated soil. FMB as a soil amendment is one of the development directions of soil remediation or soil stabilization, and its cost and process safety need to be further evaluated and studied.

Funding. This research was sponsored by the National Science Foundation of China (41867022; 21707024), the Special Funds of Guangxi Distinguished Experts, and Program for High Level Innovation Team and Outstanding Scholar of Universities in Guangxi (GuiCaiJiaoHan[2018]319), Guilin Science and Technology Development Program (20190219-3), Key Laboratory of Ecology of Rare and Endangered Species and Environmental Protection (Guangxi Normal University), Ministry of Education, China (ERESEP2018K03).

REFERENCES

[1] Al-Abed, S. R., Jegadeesan, G., Purandare, J., Allen, D. (2007): Arsenic release from iron rich mineral processing waste: influence of pH and redox potential. – Chemosphere 66: 775-782.

[2] Amstaetter, K., Borch, T., Casanova, P. L., Kappler, R. (2010): Redox transformation of arsenic by Fe(II)-activated goethite (α-FeOOh). – Environ. Sci. Technol. 44: 102-108.

[3] Bashir, S., Hussain, Q., Shaaban, M., Hu, H. Q. (2018): Efficiency and surface characterization of different plant derived biochar for cadmium (Cd) mobility, bioaccessibility and bioavailability to Chinese cabbage in highly contaminated soil. – Chemosphere 211: 632-639.

http://www.aloki.hu ● ISSN 1589 1623 (Print) ● ISSN 1785 0037 (Online)
DOI: http://dx.doi.org/10.15666/aeer/1906_47654780

[4] Beesley, L., Marmiroli, M., Pagano, L., Pigoni, V., Fellet, G., Fresno, T., Vamerali, T., Bandiera, M., Marmiroli, N. (2013): Biochar addition to an arsenic contaminated soil increases arsenic concentrations in the pore water but reduces uptake to tomato plants (Solanum lycopersicum L.). – Sci. Total. Environ. 454-455: 698-603.

[5] Bian, R. J., Joseph, S., Cui, L. Q., Pan, G. X., Li, L. Q., Liu, X. Y., Zhang, A., Rutlidge, H., Wong, S. W., Chia, C., Marjo, C., Gong, B., Munroe, P., Donne, S. (2014): A three-year experiment confirms continuous immobilization of cadmium and lead in contaminated paddy field with biochar amendment. – J. Hazard. Mater. 272: 121-128.

[6] Dong, S. K., Xu, W. L., Wu, F. F., Yan, C. X., Li, D. P., Jia, H. T. (2016): Fe-modified biochar improving transformation of arsenic form in soil and inhibiting its adsorption of plant. – Transaction of the Chinese Society of Agricultural Engineering 32(15): 204-212.

[7] Glaser, B., Lehmann, J., Zech, W. (2002): Ameliorating physical and chemical properties of highly weathered soils in the tropics with charcoal: a review. – Biol. Fert. Soils 35(4): 219-230.

[8] Irshad, M. K., Noman, A., Alhaithloul, H. A. S., Adeel, M., Rui, Y., Shah, T., Zhu, S., Shang, J. (2020): Goethite-modified biochar ameliorates the growth of rice (Oryza sativa L.) plants by suppressing Cd and As-induced oxidative stress in Cd and As co-contaminated paddy soil. – Sci. Total. Environ. 717.

[9] Kloke, A., Sauerbeck, D. R., Vetter, H. (1984): The Contamination of Plants and Soils with Heavy Metals and the Transport of Metals in Terrestrial Food Chains. – In: Nriagu, J. (ed.) Changing Metal Cycles and Human Health. Springer, Berlin, pp. 113-141.

[10] Kumarathilaka, P., Seneweera, S., Meharg, A., Bundschuh, J. (2018): Arsenic speciation dynamics in paddy rice soil-water environment: sources, physico-chemical, and biological factors-A review. – Water Res.140: 403-414.

[11] Li, H., Li, Y. W., Cai, Q. Y., Li, H. Y., Mo, C. H., Wong, M. H. (2017): Cadmium in rice: transport mechanisms, influencing factors, and minimizing measures. – Environ. Pollut. 224: 622-630.

[12] Liang, J., Yang, Z. X., Tang, L., Zeng, G. M., Yu, M., Li, X. D., Wu, H. P., Qian, Y. Y., Li, X. M., Luo, Y. (2017): Changes in heavy metal mobility and availability from contaminated wetland soil remediated with combined biochar-compost. – Chemosphere 181: 281-288.

[13] Liu, J., Mo, L. Y., Zhang, X. H., Yao, S. Y., Wang, Y. X. (2018): Simultaneous hyperaccumulation of cadmium and manganese in *Celosia argentea* Linn. – Int J Phytoremediat 20(11): 1106-1112.

[14] Mladenov, N., Zheng, Y., Miller, M. P., Nemergut, D. R., Legg, T., Simone, B., Hageman, C., Rahman, M. M., Ahmed, K. M., Mchnight, D. M. (2010): Dissolved organic matter sources and consequences for iron and arsenic mobilization in Bangladesh aquifer. – Environ. Sci. Technol. 44(1): 123-128.

[15] Nakanishi, H., Ogawa, I., Ishimaru, Y., Mori, S., Nishizawa, N. K. (2006): Iron deficiency enhances cadmium uptake and translocation mediated by the Fe^{2+} transporters OsIRT1 and OsIRT2 in rice. – Soil Sci. Plant Nutr. 52: 464-469.

[16] Park, J. H., Choppala, G. K., Bolan, N. S., Chung, J. W., Chuasacathi, T. (2011): Biochar reduces the bioavailability and phytotoxicity of heavy metals. – Plant Soil 348: 439-451.

[17] Pedersen, H. D., Postma, D., Jakobsen, R. (2006): Release of arsenic associated with the reduction and transformation of iron oxides. – Geochim. Cosmochim. Ac. 70(16): 4116-4129.

[18] Qiao, J. T., Liu, T. X., Wang, X. Q., Li, F. B., Lv, Y. H., Cui, J. H., Zeng, X. D., Yuan, Y. Z., Liu, C. P. (2018a): Simultaneous alleviation of cadmium and arsenic accumulation in rice by applying zero-valent iron and biochar to contaminated paddy soils. – Chemosphere 195: 260-271.

[19] Qiao, J. T., Li, X. M., Hu, M., Li, F. B., Young, L. Y., Sun, W. M., Huang, W. L., Cui, J. H. (2018b): Transcriptional activity of arsenic-reducing bacteria and genes regulated by

http://www.aloki.hu ● ISSN 1589 1623 (Print) ● ISSN 1785 0037 (Online)
DOI: http://dx.doi.org/10.15666/aeer/1906_47654780

lactate and biochar during arsenic transformation in flooded paddy soil. – Environ. Sci. Technol. 52: 61-70.

[20] Rocco, C., Seshadri, B., Adamo, P., Bolan, N. S., Mbene, K., Naidu, R. (2018): Impact of waste-derived organic and inorganic amendments on the mobility and bioavailability of arsenic and cadmium in alkaline and acid soils. – Environ. Sci. Pollut. R. 25: 25896-25905.

[21] Ryu, D. J., Oh, R. G., Seo, Y. D., Oh, S. Y., Ryu, K. S. (2015): Recovery and electrochemical performance in lithium secondary batteries of biochar derived from rice straw. – Environ. Sci. Pollut. Res. 22: 10405-10412.

[22] Sneath, H. E., Hutchings, T. R., de Leij, F. A. A. M. (2013): Assessment of biochar and iron filing amendments for the remediation of a metal, arsenic and phenanthrene co-contaminated spoil. – Environ. Pollut. 178: 361-366.

[23] Sun, T., Levin, B. D. A., Guzman, J. J. L., Enders, A., Muller, D. A., Angenent, L. T., Lehmann, J. (2017): Rapid electron transfer by the carbon matrix in natural pyrogenic carbon. – Nat. Commun. 14873.

[24] Tessier, A., Campbell, P. G. C., Bisson, M. (1979): Sequential extraction procedure for the speciation of particulate trace metals. – Anal. Chem. 51(7): 844-851.

[25] Venegas, A., Rigol, A., Vidal, M. (2016): Changes in heavy metal extractability from contaminated soils remediated with organic waste or biochar. – Geoderma 279(1): 132-140.

[26] Warren, G. P., Alloway, B. J., Lepp, N. W., Singh, B., Bochereau, F. J. M., Penny, C. (2003): Field trials to assess the uptake of arsenic by vegetables from contaminated soils and soil remediation with iron oxides. – Sci. Total. Environ. 311: 19-33.

[27] Wen, E., Yang, X., Chen, H., Shaheen, S. M., Sarkar, B., Xu, S., Song, H., Liang, Y., Rinklebe, J., Hou, D., Li, Y., Wu, F., Pohorely, M., Wong, J. W. C., Wang, H. (2020): Iron-modified biochar and water management regime-induced changes in plant growth, enzyme activities, and phytoavailability of arsenic, cadmium and lead in a paddy soil. – J. Hazard. Mater. 124344.

[28] Wenzel, W. W., Kirchbaumer, N., Prohaska, T., Stingeder, G., Lombi, E., Adriano, D. C. (2001): Arsenic fraction in soils using an improved sequential extraction procedure. – Anal. Chim. Acta. 436: 309-323.

[29] Wu, S. X., Wang, X., Chen, C., Bo. P., Tan, C. Y., Zhang, F., Xu, Y. Q., Zhuang, Y. J. (2015): Characterization of biochar derived from water hyacinth, rice straw and sewage sludge and their environmental implications. – Acta Sci. Circum. 35.

[30] Wu, Y., Kukkadapu, R. K., Livi, K. J. T., Xu, W. Q., Li, W. (2018): Iron and arsenic speciation during As(III) oxidation by manganese oxides in the presence of Fe(II): molecular-level characterization using XAFS, Mössbauer, and TEM analysis. – Acs Earth Space Chem. 2: 256-268.

[31] Xiao, Y. K., Yu, H. Y., Li, J. M., Zhang, Y. P. (2012): Effect of concentration of iron element in aeroponic cultivation on photosynthesis and yield of potato minituber. – Transactions of the Chinese Society for Agriculture Machinery 43(10): 195-199.

[32] Xu, X. W., Chen, C., Wang, P., Kretzschmar, R., Zhao, F. J. (2017): Control of arsenic mobilization in paddy soils by manganese and iron oxides. – Environ. Pollut. 231: 37-47.

[33] Yin, D. X., Wang, X., Peng, B., Tan, C. Y., Ma, L. Q. (2017): Effect of biochar and Fe-biochar on Cd and As mobility and transfer in soil-rice system. – Chemosphere 186: 928-937.

[34] Yu, H. Y., Liu, C. P., Zhu, J. S., Li, F. B., Deng, D. M., Wang, Q., Liu, C. S. (2016a): Cadmium availability in rice paddy fields a mining area: the effects of soil properties highlighting iron fractions and pH value. – Environ. Pollut. 209: 38-45.

[35] Yu, H. Y., Liu, C. S., Huang, W., Liu, T. X., Yu, W. M. (2016b): Chapter five- iron redox cycling coupled to transformation and immobilization of heavy metals: implications for paddy rice safety I the red soil of south China. – Adv Agron. 137: 279-317.

http://www.aloki.hu ● ISSN 1589 1623 (Print) ● ISSN 1785 0037 (Online)
DOI: http://dx.doi.org/10.15666/aeer/1906_47654780

[36] Yu, H. Y., Wang, X. Q., Li, F. B., Li, B., Liu, C. P., Wang, Q., Lei, J. (2017): Arsenic mobility and bioavailability in paddy soil under iron compound amendments at different growth stages of rice. – Environ. Pollut. 224: 136-147.
[37] Yu, G., Long, Y. M., Chen, Z., Sunahara, G. I., Jiang, P. P., You, S. H., Lin, H., Xiao, H. (2020): Phytoextraction of cadmium-contaminated soils: comparison of plant species and low molecular weight organic acids. – Int. J. Phytoremediat. 22(4): 383-391.
[38] Zhang, H., Shao, J., Zhang, S., Zhang, X., Chen, H. (2020): Effect of phosphorus-modified biochars on immobilization of Cu (II), Cd (II), and As (V) in paddy soil. – J. Hazard. Mater. 390.
[39] Zhao, F. J., Ma, Y. B., Zhu, Y. G., Tang, Z., McGrath, S. (2015): Soil contamination in China: current status and mitigation strategies. – Environ. Sci. Technol. 49: 750-759.
[40] Zhu, Z. Q., Huang, C. P., Zhu, Y. Q., Wei, W. H., Qin, H. (2018): A hierarchical porous adsorbent of nano-α-Fe_2O_3/Fe_3O_4 on bamboo biochar (HPA-Fe/C-B) for the removal of phosphate from water. – J. Water Process Eng. 25: 96-104.

http://www.aloki.hu ● ISSN 1589 1623 (Print) ● ISSN 1785 0037 (Online)
DOI: http://dx.doi.org/10.15666/aeer/1906_47654780

ALGICIDAL EFFECT OF EXTRACTS FROM A GREEN MACROLAGAE (*CHARA VULGARIS)* ON THE GROWTH OF THE POTENTIALLY TOXIC CYANOBACTERIUM (*MICROCYSTIS AERUGINOSA)*

DOUMA, M.[1*] – TAZART, Z.[2] – TEBAA, L.[2] – EL BOUAIDI, W.[2] – HAKKOUM, Z.[2] – MINAOUI, F.[2] – LAZRAK, K.[2] – MANAUT, N.[3] – MOUHRI, K.[2] – LOUDIKI, M.[2]

[1]*Natural Resources Engineering and Environmental Impacts Team, Multidisciplinary Research and Innovation Laboratory, Polydisciplinary Faculty of Khouribga (FPK), Sultan Moulay Slimane University, Beni-Mellal 23000, Morocco*

[2]*Water, Biodiversity and Climate Change Laboratory; Phycology, Biotechnology and Environmental Toxicology Research Unit; Faculty of Sciences Semlalia, Cadi Ayyad University, Av. Prince My Abdellah P.O. Box 2390, Marrakech 40000, Morocco*

[3]*Cadi Ayyad University, Faculty of Sciences Semlalia, Laboratory of Microbial Biotechnology, Agrosciences and Environment, 40000 Marrakesh, Morocco*

[*]*Corresponding author*
e-mail: douma_mountasser@yahoo.fr; phone: +212-(061)-967-057

(Received 1st May 2021; accepted 30th Aug 2021)

Abstract. The extracts of *Chara vulgaris* (a green macroalgae) were tested to explore its algicidal potential on *Microcystis aeruginosa* growth. Firstly, the anticyanobacterial effect of both macroalgae aqueous (MAA) and macroalgae etyl acetate (MEA) extracts against *M. aeruginosa* was assessed using both the paper disc diffusion and microdilution methods. Minimum inhibitory concentrations (MIC) and minimum algicidal concentrations (MAC) were evaluated. Secondly, the growth of *M. aeruginosa* in response to the MEA extracts was investigated in an experimental bioassay. To reveal the potential allelochemicals, total phenols (TPs), total flavonoids (TFs), tannins (TTs) were analyzed in both MAA and MEA extracts. The identification of the phenolic compounds in MEA extracts was performed by high-performance liquid chromatography (HPLC). The results from the bioassay demonstrated that MEA extracts inhibit the growth of *M. aeruginosa* in a concentration dependent way. The highest inhibition rate (IR) exceeds 83% on day (d) 4 of experimentation, and achieved (97.98%) on 7-d. HPLC analysis revealed seven phenolic compounds known as effective allelochemicals. Overall, the obtained results demonstrate that MEA extracts might be proposed as a potential allelochemicals, and it can be considered as an ecofriendly alternative algaecide to control *Microcystis* blooms in the eutrophic water bodies.
Keywords: *Chara vulgaris, natural algaecides, allelochemicals, M. aeruginosa, inhibitory effect*

Introduction

Harmful algal blooms (HABs) constitute a major human health risk and an environmental problem worldwide. Cyanobacterial blooms have occurred extensively in superficial eutrophic freshwater bodies used for recreational purposes and drinking water sources (De Figueiredo et al., 2004). *Microcystis spp.* are the most common bloom-forming cyanobacteria in eutrophic freshwaters (Douma et al., 2016). *Microcystis* blooms occurrences are frequently toxic and are able to produce hepatotoxins (Microcystins) which are responsible for the contamination of drinking water, and for the intoxication of many vegetal and animal organisms (Douma et al., 2017).

http://www.aloki.hu ● ISSN 1589 1623 (Print) ● ISSN1785 0037 (Online)
DOI: http://dx.doi.org/10.15666/aeer/1906_47814794

In order to control the proliferation of toxic cyanobacteria, several solutions have been used. The classical approaches recommended to reduce algal proliferation were often chemical and physical methods (eg; algaecide addition, centrifugation, filtration, flocculation); however, these measures induce secondary pollution (Li et al., 2016). Biological control approaches using aquatic plants have emerged as economic and ecofriendly alternatives. Various aquatic macrophytes have been used to inhibit several kinds of cyanobacteria and green algae such as *Myriophyllum spicatum* ,*Ceratophyllum demersum*, *Najas marina, Najas minor* (Zhang et al., 2014), *Elodea spp. Eichhornia crassipes*, *Nymphaea tetragona*, *Typha orientalis*, *Nelumbo nucifera,* and *Irris wilsonii* (Chen et al., 2012), *Sagittaria trifolia* (Li et al., 2016). However, among the submerged aquatic macrophytes, freshwater and brackish water macrolagae are little studied (Zhang et al., 2009).

Phytochemical characterization of macrophytes indicated that the revealed constituents are allelechemical products. The most important of these bioactive constituents are flavonoids, tannins, alkaloids, fatty acids and several phenolic compounds (Li and Hu, 2005; Chen et al., 2012; Zhang et al., 2014; Canton et al., 2019). More specific allelochemicals on the inhibition of *Microcystis spp.* were previously identified and purified from aquatic plants. The most effective allelochemicals were Ethyl 2-Methyl Acetoacetate (EMA), N-phenyl-2-naphthylamine and Pyrogallol acid (Li and Hu, 2005; Pei et al., 2018).

Hydrophyte flora is very common in Mediterranean area such as Morocco, which is known by high biodiversity. Several invasive and/or native aquatic plants proliferate intensively in several wetlands. Among these, freshwater and brakish water macroalgae that belongs to Characeae family. *Chara vulgaris* is a freshwater species, generally developing in very shallow waters, in temporary ponds, rivers, thermal springs or seepages of inundated meadows, with high resistance to eutrophication (Zouaïdia et al., 2015; Muller et al., 2017). The Characeae family had known an important interest in many pharmacological uses, with antimicrobial activities (Cai et al., 2013). Also, some species belonging to this family have been recognized in algicidal activities against various microalgae including *Microsytis spp* (Kurashov et al., 2021; Zhu et al., 2021).

Our hypothesis is that allelochemicals from *Chara vulgaris var. vulgaris* have antialgal potential and could inhibit the growth of *M. aeruginosa*. The aim of this study was to assess the algicidal effects of *Chara vulgaris* on *M. aeruginosa*; with regard to growth inhibition, photosynthetic comportment, and characterization of the potential allelochemicals.

Materials and methods

Biological materials

M. aeruginosa was isolated from eutrophic Lalla Takerkoust reservoir, Morocco, (31°21'36" N; 8°7'48" W) in October 2015, and was grown in laboratory cultures at 26 °C ± 2 °C under light intensity of 65 µE/m^2/S, with a light/dark cycle of 15h/9h.

Biological material of the macroalgae was collected in April 2016 from an urban pond in Marrakesh city, and identified as *Chara vulgaris var. vulgaris*. The whole plant was rinsed several times with distilled water to remove debris, and conserved for farther use.

http://www.aloki.hu ● ISSN 1589 1623 (Print) ● ISSN1785 0037 (Online)
DOI: http://dx.doi.org/10.15666/aeer/1906_47814794

Preparation of macroalgae Aqueous (MAA) and ethyl acetate *(MEA) extracts*

20 g of fresh *biomass* was cut into small pieces in 300 mL of distilled water under agitation for 48h at room temperature. The solution was filtered through glass fiber papers (Whatman GF/C, 0.22 µm). The filtrate was collected as an aqueous extract for the biological test and for further fractionations. The aqueous extract was fractionated according to Wang et al. (2010) and Tazart et al. (2020a). Briefly, the filtrate was adjusted to pH 12 with 2M NaOH. The alkaline extract was centrifuged at 6000 rpm for 10 min. The supernatant was transferred to a separating funnel and washed three times with 200 mL hexane. The aqueous fraction was acidified to pH 5 with 2 M HCl and then extracted three times with 100 mL ethyl acetate. The ethyl acetate extracts were first dried with anhydrous sodium sulfate and then evaporated to dryness by rotary evaporator at 39 ºC. The ethyl acetate extracts were stored at 4 ºC until used for biological assay.

Total phenols (TPs), total flavonoids (TFs), tannins (TTs) concentrations determination in LA extracts

TPs concentration was determined with the Folin–Ciocalteu method (Singleton et al., 1965). Briefly, 0.5 ml of the extract was added to 0.5 ml of Folin-Ciocalteu reagent (Sigma-Aldrich) in water, and then 0.5 ml sodium carbonate solution (20% w/v) was added. The mixture was left for 1 h at room temperature and absorbance was measured at 760 nm. TFs content concentration was determined by the method described by Kim (2003). Briefly, 500 µl of aqueous extract was mixed with 500 µl distilled water. Then 150 µl sodium nitrite solution (5%) was added, followed by 150 µl aluminum chloride solution (10%) after 5 min. Test tubes were incubated for 11 min at ambient temperature, and then 500 µl sodium hydroxide (1 M) was added. The mixture was vortexed and absorbance was determined at 510 nm. TTs content was determined with Folin-Denis test described by Salunkhe and Chavan (1989). Briefly, 1 ml of the aqueous extract was added to 75 ml distilled water, and then 5 ml Folin Denis reactif (Sigma-Aldrich) solution and 10 ml sodium carbonate solution was added. The mixture was vortexed and absorbance was determined after 30 mn at 760 nm.

Minimal inhibitory concentration (MIC) and minimal algicidal concentration (MAC) determinations

The MIC preventing visible algal growth was measured by the broth dilution method developed by the Clinical and Laboratory Standards Institute (CLSI) using 96-well microplates (Hammer et al., 1996; Joshi et al., 2016). The MAA and MEA concentrations were ranged from 0.78 to 100 mg/L. The MEA were prepared by dissolution in 0.1% dimetyl sulfoxyde (DMSO). Subsequently in each well of 96 well plates, 100 µl of plant extracts concentrations were added to 100 µl of test microalgae of 3.10^6 Cells/mL (exponential growth phase). Inoculated microplate were incubated after careful mixing under controlled conditions in a culture room at 26 ± 2 °C, illuminated in 15h/9h light-dark cycle with fluorescent tubes (65 µE/m^2/S). The MIC of each extract was defined as the lowest concentration which inhibited either microalgal growth. The MAC was determined by subculture on microplate under the same controlled conditions of clear wells, which did not show any visible growth after incubation during the test. Copper sulphate was used as algicidal positive controls with the concentrations ranged from 0.001 to 0.1 mg/L.

http://www.aloki.hu ● ISSN 1589 1623 (Print) ● ISSN1785 0037 (Online)
DOI: http://dx.doi.org/10.15666/aeer/1906_47814794

Disc diffusion assay

M. aeruginosa was used for susceptibility-screening tests using the disc diffusion method (Kil et al., 2009). Sterilized filter paper discs of 9 mm were saturated with 20 µl of MAA or MEA extracts prepared in the Z8 medium with 0.1% of DMSO. Copper sulphate with a concentration of 10 µg were used as positive controls and (0.1%) of DMSO was used as negative control. Anticyanobacterial activity was measured by the formation of inhibition zones (in mm) around the discs where the extracts tested were applied.

Algicidal activity bioassay

The bioassay was conducted according to Tazart et al. (2019, 2020b), with some modifications. 6 groups of Erlenmeyer flasks (500 ml) containing Z8 medium (Kotai, 1972) to a final volume (300 ml) were used. Each flask was inoculated by a volume of *M. aeruginosa,* in exponential growth phase, to make an initial density (11-12 x 10^5 cell/ml). The macrophyte ethyl acetate (MEA) extracts were dissolved in dimethyl sulfoxide (DMSO) 0.1% (v/v) and added to 300 ml of *M. aeruginosa* cultures to obtain final concentrations (0 (control), 25, 50, 75, 100; mg/l). An untreated equal volume of cyanobacterial culture with 0.1% of DMSO was used as negative control. Flasks were incubated under controlled conditions in a culture room at 26 ± 2 °C, illuminated in 15h/9h light-dark cycle with fluorescent tubes (65 µE/m2/S) within 7-d. All the experiments were conducted in triplicate. *M. aeruginosa* growth under different treatments was quantified daily using Malassez hemocytometer. Inhibitory rate (IR) of *M. aeruginosa* growth was determined according to the following *Eq.1*:

$$IR\ (\%) = \frac{N0 - N}{N0} \times 100 \qquad \text{(Eq.1)}$$

where No and N are the cell density (cells/ml)in the treatment and control cultures, respectively.

Pigments determination

Chlorophyll-a and Carotenoids pigments were calculated according to Lichtenthaler and Wellburn (1983). They extracted with Ethanol 95% at 4 °C for 48 h, and then determined using a UV-Spectrophotometer (Carré 50 Scan) at 470, 649, 665 nm. The following formulas were used to calculate the concentrations as mentioned in the *Eq.2* and *Eq.3*:

$$[\text{Chlorophylle a}] = (13.95 * DO665) - (6.88 * DO649) \qquad \text{(Eq.2)}$$

$$[\text{Caroténoïdes}] = \frac{[(1000 * DO470) - (2.05 chla)]}{229} \qquad \text{(Eq.3)}$$

where Chla and Carot. represent the concentration of chlorophyll-a and Carotenoids (µg/ml) respectively; OD470, OD649 and OD665 are wavelengths absorbance (nm).

http://www.aloki.hu ● ISSN 1589 1623 (Print) ● ISSN1785 0037 (Online)
DOI: http://dx.doi.org/10.15666/aeer/1906_47814794

Identification and quantification of phenolic compounds by HPLC

In order to identify the phenolic compounds in MEA extracts, the samples were filtered first through Whatman filter paper N°42 and then through 0.22 mm membrane filters (Millipore). Phenolic compounds were separated using HPLC with a 250 mm x 4.6 mm, 5.0 µm reversed- phase (RP-18) column (Agilent Technologies) and a 10 mm× 4.6 mm RP-18 pre-column (Agilent Technologies). The two columns were placed into a column furnace at 25 °C. The HPLC system consists of an automated injector (Shimadu SCL-10A series pumping system, SIL-10AD) coupled to a SPD 10A UV-visible detector (set to start at 200 nm and end at 700 nm). Data collection and analysis were performed using the Shimadu LC Solution chromatography data station software. Two solvents were used in a constant flow rate of 0.1 ml/min, with an injection volume of 10 µl. Solvent A consisted of acetonitrile (5%) and water (95%), solvent B is a phosphate buffer solution in water (pH=2.6). All solvents employed were HPLC-grade. The following proportions of solvent B were used for the elution program. Standards were run on the machine first, followed by plant extracts and then samples. Phenolic compounds were identified by comparing their retention times to those of the standards.

Statistical analysis

Data with three replicates were statistically analyzed by two-way analysis of variance (ANOVA) with Tukey´s test to assess differences between exposure concentrations and those untreated (control) at different concentrations and over the time at $p = 0.05$. Correlation coefficients were calculated between cellular density and PTs, FTs, TTs concentrations in the end of experimentation.

Results

Anticyanobacterial activity assessment

The anti-cyanobacterial activity of the extracts was evaluated qualitatively using the disk diffusion methods and quantitatively by the broth microdilution methods in 96 wells. The results were presented in *Figure 1* and *Table 1*. The results indicate that the MIC and MAC had equal concentrations values for each extract. For the macroalgae extracts, the most important activity against *M. aeruginosa* was observed under MEA extract with (31 ± 1 mm; MIC = MAC = 25 mg/l), followed by the MAA extract with (16.67 ± 0.58 mm; MIC = MAC = 50 mg/L). The Copper sulphate as a positive control showed the greatest effectiveness with the MIC and MAC = 3.12 mg/l. Thus, the tested MEA extracts appear to have a more pronounced anti-cyanobacterial activity (*Table 1*).

Effects on M. aeruginosa growth

Based on their relative stronger inhibitory effects, the MEA extracts were chosen to conduct a bioassay. As shown in *Figure 2*, it can be seen that MEA extracts may inhibit the growth of *M. aeruginosa* and exhibited a concentration dependent trend. In control group, the cell densities remained between 11.86 x 10^5 and 133.63 x 10^5 cell/mL over the test period. Conversely, the cell densities of *M. aeruginosa* at tested concentrations (25, 50, 75 and 100 mg/l) were reduced during the 7-d test period. The detailed data on the IRs through the test period was listed in *Table 2*. Indeed, *Microcystis* growths appeared significantly reduced ($p<0.05$) by the tested concentrations; with an overall

http://www.aloki.hu ● ISSN 1589 1623 (Print) ● ISSN1785 0037 (Online)
DOI: http://dx.doi.org/10.15666/aeer/1906_47814794

inhibition rates (IRs) exceeding globally 50% after 4-d at the 50 mg/l concentration (*Fig. 2, Table 2*). Under the highest concentration (100 mg/l) of MEA extracts, the inhibition rate (IR) exceeds 83% on 4-d of experimentation; and it was achieved (97.98%) on 7-d.

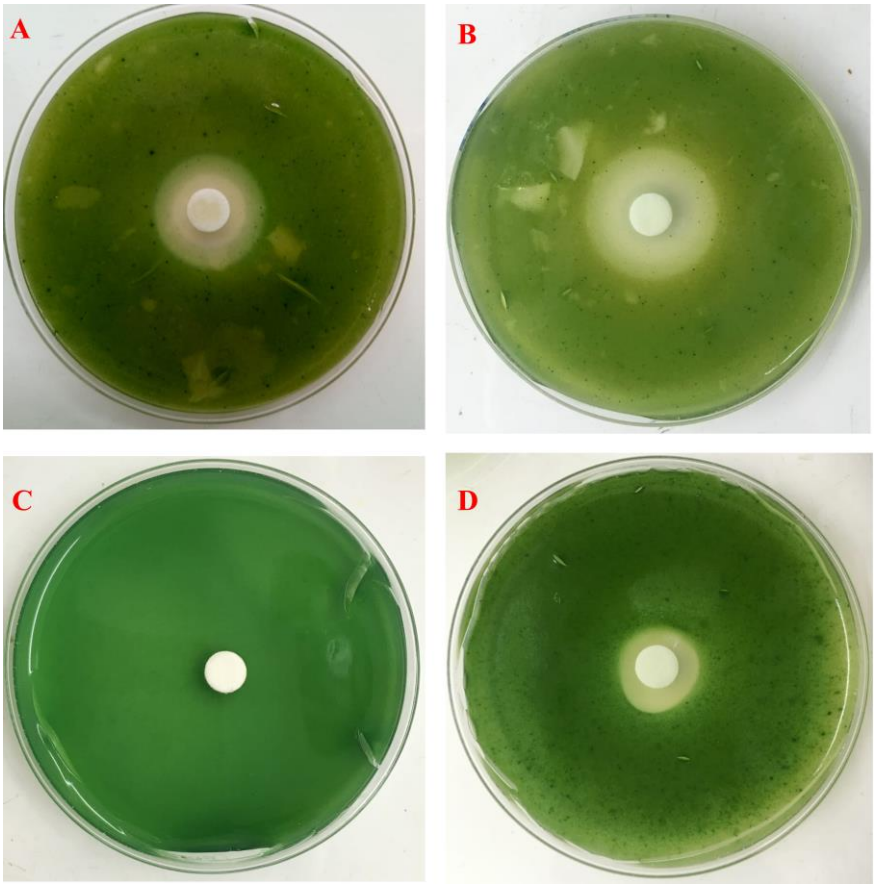

Figure 1. *Antialgal activity: aqueous (A) and (B) Ethyl acetate extracts; DMSO (C) and Copper sulphate (D)*

Table 1. *Results of Anticyanobacterial activity assessment using the disk diffusion and microdilution methods*

	Test on solid media		**Microdilution methods**			
	Inhibition zone diameter on *Microcystis aeruginosa* (mm)		Minimal inhibitory concentration (MIC) (mg/l)		Minimal bactericidal concentration (MAC) (mg/l)	
Chara Extracts	Aqueous	Ethyl acetat	Aqueous	Ethyl acetat	Aqueous	Ethyl acetat
Means	16.67±0,58	**31.00**±1	50	**25**	50	**25**
Copper sulphate	14.67 ± 1.15		3.12±1.15			
DMSO	0.00					

*: Similar values indicate here the standard deviation *(n=3)*

http://www.aloki.hu ● ISSN 1589 1623 (Print) ● ISSN1785 0037 (Online)
DOI: http://dx.doi.org/10.15666/aeer/1906_47814794

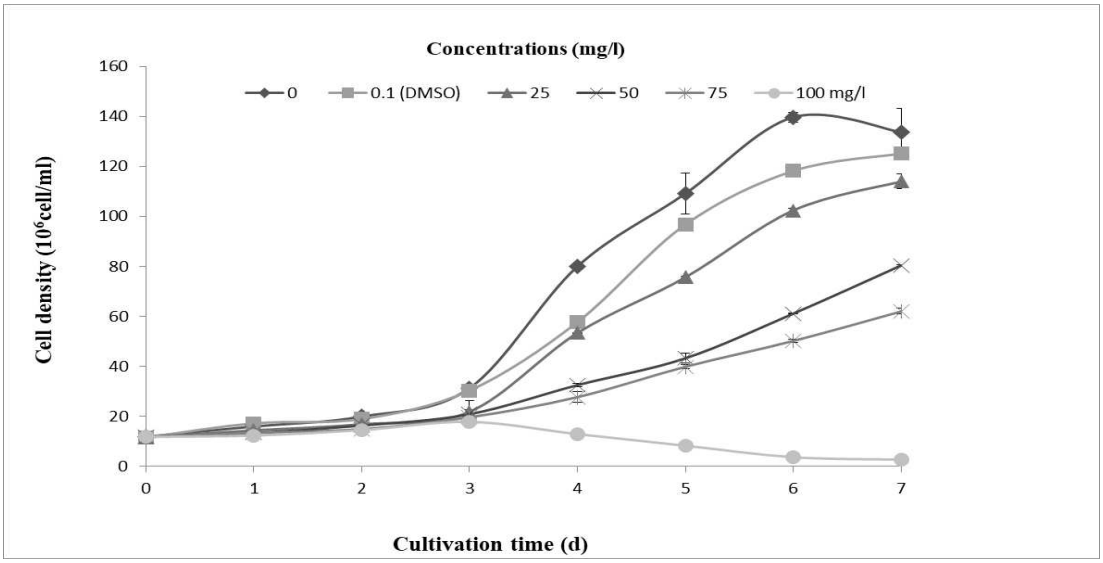

Figure 2. *Effects of the different concentrations of MEA extracts on M. aeruginosa growth. Errors bars represent the standard deviation (n=3). *<0.05 indicate significant differences compared to the untreated culture (ANOVA tow-way)*

Table 2. *The inhibitory effects expressed as inhibitory rate (%) of MEA extracts on M. aeruginosa growth*

Treatements (mg/L)	0	1	2	3	4	5	6	7
0.1	2.39 ± 0	-7.73 ± 1	4.86 ± 2	3.09 ± 3	27.85 ± 4	11.34 ± 5	15.39 ± 6	6.41 ± 7
25	1.97 ± 2.54	9.82 ± 15.63	15.42 ± 2.32	30.25 ± 4.88	33.27 ± 0.07	30.69 ± 0.05	26.71 ± 0.29	14.74 ± 1.88
50	0.98 ± 2.54	16.5 ± 7.78	17.93 ± 3.03	33.34 ± 18.98	**59.36 ± 0.22**	**60.38 ± 0.36**	**56.26 ± 0.79**	39.86 ± 2.94
75	1.12 ± 1.99	16.5 ± 11.04	25.13 ± 4.03	37.28 ± 7.95	**65.37 ± 1.23**	**63.49 ± 2.28**	**64.08 ± 0.29**	**53.63 ± 0.26**
100	0.7 ± 2.74	22.77 ± 11.04	27.14 ± 16.15	43.14 ± 4.52	**83.88 ± 3.29**	**92.43 ± 1.09**	**97.38 ± 0.62**	**97.98 ± 1.1**

*: Similar values indicate here the standard deviation *(n=3)*

Effects on photosynthetic pigments

In order to assess the physiological modification, two photosynthetic pigments were measured (Chl-a and carotenoids). Under control treatment, the Chl-a and carotenoids concentrations increase as a function of tested concentrations (*Fig. 3A,B*). By contrast, in treatments they decrease negatively with the augmentation of extract concentrations. The content pigment concentrations are appearing to be strongly inhibited at the all treatments since 5-d. The significant differences between the concentration in treatment and controls groups were remarquably observed for Chl-a ($p < 0.05$) and carotenoids after 5-d and 7-d, respectively (*Fig. 3A,B*).

http://www.aloki.hu ● ISSN 1589 1623 (Print) ● ISSN1785 0037 (Online)
DOI: http://dx.doi.org/10.15666/aeer/1906_47814794

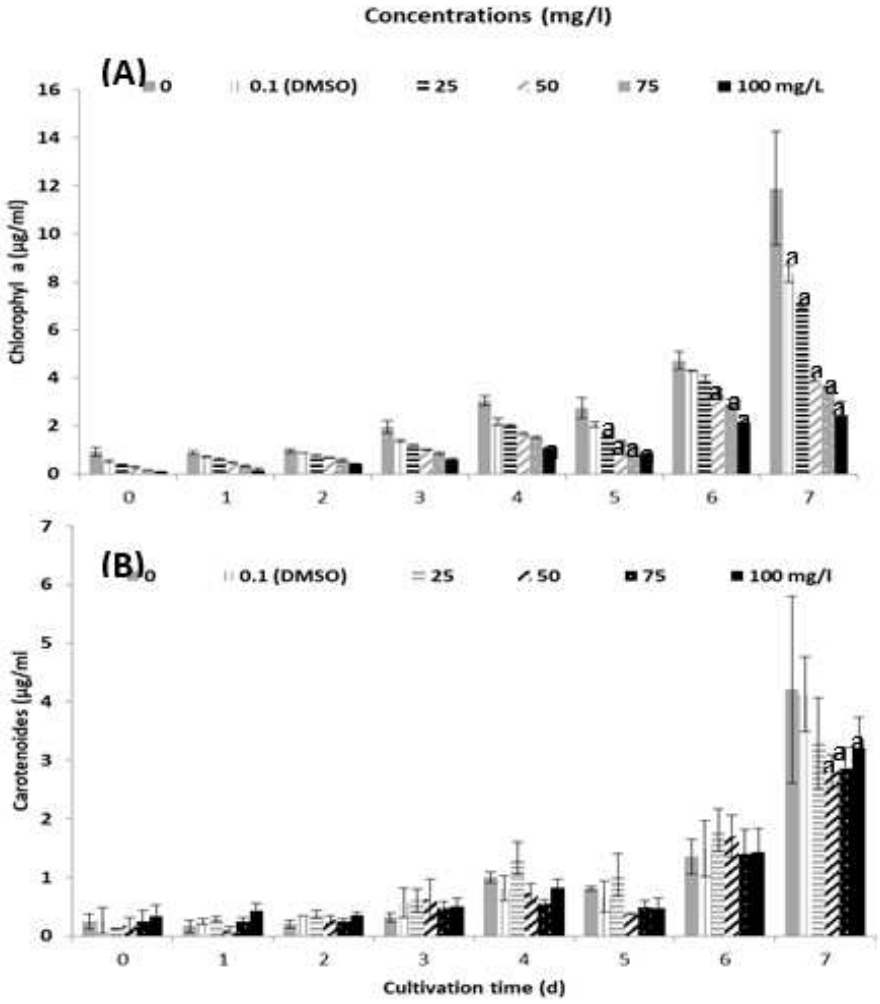

Figure 3. *Effects of Chara sp. ethyl acetate extract on Chl-a (A) and carotenoides (B) in M. aeruginosa cultures, respectively. Each value is the mean ± SD of three replicates, a indicate significant differences compared to the untreated culture (ANOVA tow-way) at $p < 0.05$*

Phytochemical characterization

The results of the phytochemical characterization are shown in *Table 3*. MEA extract exhibited important values on TPs, TFs, and TTs. As well, a high significant correlation (0.97) have been well obtained between the IRs of the three high concentrations of TPs (50, 75, 100 mg/l) in the end of the experiment.

Table 3. *Total phenolic (TPs), Total flavonoids (TFs), Total tannins (TTs) amounts in MEA extracts; and correlations between all amounts and IRs of the three high after 7 days of exposure*

	TPs [1]	**TFs [2]**	**TTs [3]**
Concentrations	124.35	101.02	0,08
Coefficient of correlation	**0.97**	0.75	0.93

([1]): µg Gallic acide quivalent /mL extract, ([2]): µg catechin equivalent/mL extract, ([3]): µg tannic acid equivalents /mL extract

http://www.aloki.hu ● ISSN 1589 1623 (Print) ● ISSN1785 0037 (Online)
DOI: http://dx.doi.org/10.15666/aeer/1906_47814794

HPLC technique was used to identify and quantify the major phenolic compounds in MEA extracts. From the HPLC chromatogram (*Fig. 4* and *Table 4*), 7 different chemicals were identified from the three MEA extracts. Characterization of major phenolic components from MEA extract was dominated by p-coumaric acid (36.58%) of the total identified compounds, followed by caffeic acid (25.78%), Catechic acid (23.37%), tanic acid (21.03%), sorbic acid (6.06%) and rutic acid (4.47%), and furulic acid (1.36%).

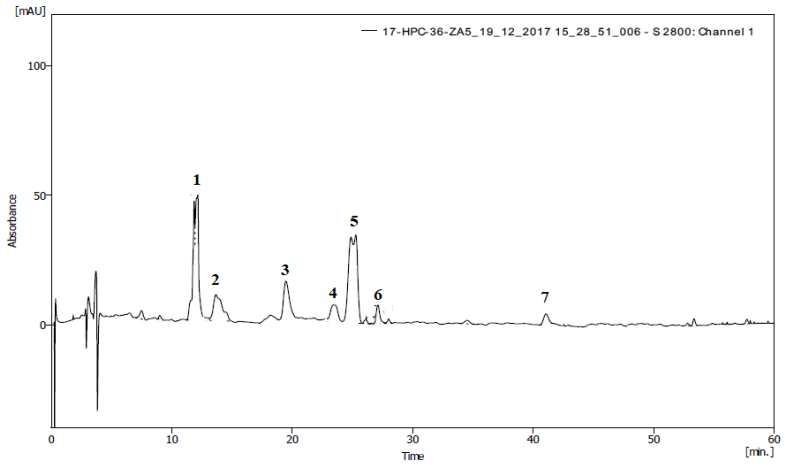

Figure 4. *HPLC chromatogram recorded at 280 nm for the main phenolic compounds identified in the Chara sp. ethyl-acetate extracts: 1) catechic acid, 2) tanic acid, 3) cafféic acid, 4) ferrulic acid, 5) p-coumaric acid, 6) sorbic acid and 7) rutic Acid*

Table 4. *Concentrations of the main phenolic compounds identified in the Chara sp. ethyl acetate extracts expressed in mg EGA/ g DM*

Compound Nº	Retention Time [min]	Area [mAU.s]	Compound	Concentrations (mg EGA /g DM)	% of Compounds
1	11.9	581.353	Catechic acid	23.37	20%
2	13.7	522.861	Tanic acid	21.03	18%
3	19.5	641.564	Cafféic acid	25.78	22%
4	23.4	31.106	Ferrulic acid	1.36	1%
5	24.9	911.536	p-coumaric acid	36.58	31%
6	27.1	148.454	Sorbic acid	6.06	5%
7	41.1	108.862	Rutic Acid	4.47	4%

Discussion

In search of an ecofriendly algaecide to control cyanoHABs, several bioactive compounds from macrophytes were screened and characterized which may be important sources of allelochemicals. In the present study, the antialgal activities of the MAA and MEA extracts were assessed qualitatively and quantitatively in both solid and liquid medium. Based on their relative stronger inhibitory effect, the MEA extracts were used to conduct an experimental bioassay.

http://www.aloki.hu ● ISSN 1589 1623 (Print) ● ISSN1785 0037 (Online)
DOI: http://dx.doi.org/10.15666/aeer/1906_47814794

The obtained results confirmed that the MEA extracts act negatively on the *M. aeruginosa* growth in a dose dependent manner. For the MEA extract, the highest inhibition rate (IR) exceeds 83% on day 4 of experimentation; and it was achieved (97.98%) on 7-d. These results remain globally similar to those observed in other previous works that studied macrophyte aqueous and etyl acetat extracts on *Microcystis* spp. Tazart et al. (2019, 2020a,b) showed that the growth of *M. aeruginosa* was effectively inhibited by macrophyte aqueous and ethyl acetate extracts, with strongest inhibition rates (IR values between 95 and 100%) for *Ranunculus aquatilis*, *Nasturtium officinale* and *Potamogeton natans*.

Similar results were observed with the use of other macrophytes aqueous extracts such as *Spartina alterniflora* with IR= 99.4% (Yuan et al., 2020), both *Cyperus alternifolius* and *Canna generalis* with more than IR= 99.6% (Zhou et al., 2019). These strong inhibitions demonstrated the relative high algicidal potential of macrophyte extracts compared to those of certain terrestrial plants: *Ailanthus altissima* (66.3-91.8%) on 5 d (Meng et al., 2015), *S. trifolia* (70%) after 6 d (Li et al., 2016), *Thalia dealbata* (92.7%) on 7-d (Zhang et al., 2011), *N. tetragona, T. orientalis, N. nucifera* and *I. wilsonii* (75-82%) during 19 d (Chen et al., 2012), *Achillea ageratum, Origanum compactum* (88-95) after 8 d (Tebaa et al., 2017; 2018).

Although many aquatic and terrestrial plants, and marine algae have been tested to control *Microcystis* harmful blooms; freshwater macroalgae are very little studied. To our knowledge, the freshwater *Chara* genus is the most recognized in bioassays that have tested the algaecide effect on *Microcystis spp* (Berger and Schagerl, 2004).

In our experimental study, the growth inhibition is well confirmed by the decrease of the two photosynthetic pigments (Chl-a and carotenoids) in treatments groups. The growth inhibition accompanied by photosynthetic pigments reduction and morphological changes of *M. aeruginosa*, were mainly indicators of physiological alterations under a stress environment in several works (Meng et al., 2015; Li et al., 2016). Also, some studies showed specially the negative effect of the extracts on Chl-a content (Ni et al., 2012; Meng et al., 2015). Their decrease shows the disturbance of the photosynthesis affecting the growth and reproduction of *M. aeruginosa* (Li et al., 2016). Zhu et al. (2010) demonstrated that polyphenols, pyrogallic acid and gallic acid produced by *M. spicatum* decreased the photosynthetic activity of the cyanobacterium species by inhibiting the activity of PSII.

This inhibitory effect might be related to potential allelochemicals released by *Chara vulgaris*. From the obtained results, it seems that TPs participate more in the inhibitory activity (*Tables 3 and 4*). These results agreed with previous works showing the effect of PTs, in the *M. aeruginosa* inhibition (Chen et al., 2012). In fact, the phytochemical investigation of extracts allowed the identification of several other compounds. They are mainly flavonoids, glycosides, terpenoids, saponins and several phenolic acids (Li and Hu, 2005; Chen et al., 2012; Li et al., 2016). However, plant-derived polyphenolics were the most common allelochemicals in HABs control (Zhu et al., 2021).

In the only study devoted to the characterization of allelochemicals of *Chara vulgaris*, Zhang et al. (2009) reported three phenolic coumpounds (The (Z, Z)-9,12-octadecadienoic, tetradecanoic and hexadecanoic acides) as the potent allelochemicals for *Chara vulgaris* L. against the toxic *M. aeruginosa*. In our study, the characterization of major phenolic components from MEA extracts of the Moroccan *Chara vulgaris var. vulgaris*, showed the dominance of p-coumaric acid (36.58%), caffeic acid (25.78%), Catechic acid (23.37%), tanic acid (21.03%) over the other identified compounds:

http://www.aloki.hu ● ISSN 1589 1623 (Print) ● ISSN1785 0037 (Online)
DOI: http://dx.doi.org/10.15666/aeer/1906_47814794

sorbic acid (6.06%) and rutic acid (4.47%), and furulic acid (1.36%) (*Table 4*). Among the 3 major phenolic compounds, p-coumaric acid is recognized as an effective allelochemical on *M. aeruginosa* (Wang et al., 2010). However, it is rarely identified from macrophytes (Agnihotri et al., 2008). In the other hand, caffeic acid and Catechic acid, are often repeated as effective allelochemicals (Gao and Xie, 2011; Gao et al., 2015; Zhu et al., 2021).

It is well known that the allelochemical compounds inhibited the growth of the cell through the perturbation of the cellular structure as and the physiological statute (Gigova and Ivanova, 2014). Phenolic acids exhibit cell-permeability features due to their amphiphilic and lipophilic nature (Lan et al., 2020). Wang et al. (2016) found that p-coumaric acid and ferulic acid disrupted the cell membrane integrity of *M. aeruginosa.* Furthermore, under stress conditions, the Reactive Oxygen Species (ROS) act on cell membranes through the degradation of unsaturated phospholipids (Meng et al., 2015), allowing to the increased of their permeability. Thus, the perturbations of antioxidant defense system leading to the inhibition of photosynthesis and oxygen evolution through interactions with components of photosystem II (PS II) (Einhellig, 1995), and finally to induce the cell death (Zhang et al., 2011).

Conclusion

This study demonstrates the inhibitory effect of the MEA extracts of *Chara macroalgae* on the *M. aeruginosa* growth. This effect is dose-dependent. TPs characterized might be the main responsible allelochemicals. MEA extracts might be recommend as a potential allechemicals, and it can be considered as an ecofriendly alternative algaecide to control *Microcystis* blooms. Other future approaches will be necessary to assess its potential effects in mesocosms and in field studies, and against non-target organisms.

Acknowledgements. This work was supported by the Laboratory of Water, Biodiversity and Climate Change Laboratory; Phycology, Biotechnology and Environmental Toxicology Research Unit. The useful comments of anonymous reviewers are also acknowledged.

Conflict of interests. The authors declare no conflict of interests.

REFERENCES

[1] Agnihotri, V. K., Elsohly, H. N., Khan, S. I., Smillie, T. J., Khan, I. A., Walker, L. A. (2008): Antioxidant constituents of Nymphaea caerulea flowers. – Phytochemistry 69: 2061-2066.

[2] Berger, J., Schagerl, M. (2004): Allelopathic activity of Characeae. – Biologia, Bratislava 59(1): 9-15.

[3] Cai, J., Xie, S., Feng, J. (2013): Antimicrobial activities of Nitellopsis obtusa (Desvaux) Groves and Chara vulgaris L. – Journal of Applied Botany and Food Quality 86: 24-32.

[4] Canton, M. C., Holguin, F. O., Boeing, W. J. (2019): Alkaloid gramine to control algal invaders: Algae inhibition and gramine persistence. – Bioresour Technol Reports 7: 100304.

[5] Chen, J. Z., Zhang, H. Y., Han, Z. P., Ye, J. Y., Liu, Z. (2012): The influence of aquatic macrophytes on Microcystis aeruginosa growth. – Ecological Engineering 42: 130-133. doi: 10.1016/j.ecoleng.2012.02.021.

http://www.aloki.hu ● ISSN 1589 1623 (Print) ● ISSN1785 0037 (Online)
DOI: http://dx.doi.org/10.15666/aeer/1906_47814794

[6] De Figueiredo, D. R., Azeiteiro, U. M., Esteves, S. M., Goncalves, F. J. M., Pereira, M. J. (2004): Microcystin-producing blooms - a serious global public health issue. – Ecotoxicology and Environmental Safety 59: 151-163.

[7] Douma, M., Manaut, N., Oudra, B., Loudiki, M. (2016): First report of cyanobacterial diversity and microcystins in a Microcystis strain from a Mediterranean coastal lagoon (Sidi Boughaba, Morocco). – African Journal of Aquatic Science 41(4): 445-452.

[8] Douma, M., Ouahid, Y., Loudiki, M., del Campo, F. F., Oudra, B. (2017): The first detection of potentially toxic *Microcystis* strains in two Middle Atlas Mountains natural lakes (Morocco). – Environmental Monitoring and Assessment 189: 1-9. doi: 10.1007/s10661-016-5753-x.

[9] Einhellig, F. A. (1995): Mechanism of action of allelochemicals in allelopathy. – In: Inderjit Einhellig, F. A., Dakshini, K. M. M. (eds.) Allelopathy: Organisms, Processes, and Applications. American Chemical Society, Washington DC.

[10] Gao, Y., Liu, B., Dong, X., Zhou, Q., Hu, C., Ge, F., Zhang, L., Wu, Z. (2011): Phenolic Compounds Exuded from Two Submerged Freshwater Macrophytes and Their Allelopathic Effects on Microcystis aeruginosa. – Polish Journal of Environmental Studies 20(5): 1153-1159.

[11] Gao, Y., Liu, B., Ge, F., He, Y., Lu, Z., Zhou, Q., Zhang, Y., Wu, Z. (2015): Joint effects ofallelochemical nonanoic acid, N-phenyl-1-naphtylamine and caffeic acid on the growth of Microcystis aeruginosa. – Allelopathy Journal 35(2): 249-257.

[12] Gigova, L., Ivanova, N. (2014): Reponses of Symploca sp. (Cyanobacteria) to Nitrogen depletion during culturing. – Comptes rendus de l'Academie bulgare des Sciences 67(1): 43-48.

[13] Hammer, K. A., Carson, C. F., Riley, T. V. (1996): Susceptibility of transient and commensal skin flora to the essential oil of Melaleuca alternifolia (tea tree oil). – American Journal of Infection Control 24: 186-189. doi: 10.1016/S0196-6553(96)90011-5.

[14] Joshi, A., Prasad, S. K., Joshi, V. K., Hemalatha, S. (2016): Phytochemical standardization, antioxidant, and antibacterial evaluations of Leea macrophylla: A wild edible plant. – Journal of Food and Drug Analysis 24: 324-331. doi: 10.1016/J.JFDA.2015.10.010.

[15] Kil, H., Seong, E., Ghimire, B., Chung, I., Kwon, S., Goh, E., Heo, K., Kim, M., Lim, J., Lee, D., Yu, C. (2009): Antioxidant and antimicrobial activities of crude sorghum extract. – Food Chemistry 115: 1234-1239.

[16] Kim, U-K. (2003): Positional Cloning of the Human Quantitative Trait Locus Underlying Taste Sensitivity to Phenylthiocarbamide. – Science 299: 1221-1225. doi: 10.1126/science.1080190.

[17] Kotai, J. (1972): Instructions for preparation of modified nutrient solution Z8 for algae. – Oslo: Norwegian Institute for Water Research Publication B-11/69, Blindem.

[18] Kurashov, E., Krylova, J., Protopopova, E. (2021): The Use of Allelochemicals of Aquatic Macrophytes to Suppress the Development of Cyanobacterial "Blooms". – In: Plankton Communities. IntechOpen edition, doi: 10.5772/intechopen.95609.

[19] Lan, Y., Chen, Q., Gou, T., Sun, K., Zhang, J., Sun, D., Duan, S. (2020): Algicidal Activity of Cyperus rotundus Aqueous Extracts Reflected by Photosynthetic Efficiency and Cell Integrity of Harmful Algae Phaeocystis globosa. – Water 12: 3256. https://doi.org/10.3390/w12113256.

[20] Li, F. M., Hu, H. Y. (2005): Isolation and characterization of a novel antialgal allelochemical from Phragmites communis. – Applied and Environmental Microbiology 71: 6545-6553. doi: 10.1128/AEM.71.11.6545-6553.2005.

[21] Li, J., Liu, Y., Zhang, P., Zeng, G., Cai, X., Liu, S., Yin, Y., Hu, X., Hu, X., Tan, X. (2016): Growth inhibition and oxidative damage of Microcystis aeruginosa induced by crude extract of Sagittaria trifolia tubers. – Journal of environmental sciences 43: 40-47.

http://www.aloki.hu ● ISSN 1589 1623 (Print) ● ISSN1785 0037 (Online)
DOI: http://dx.doi.org/10.15666/aeer/1906_47814794

[22] Lichtenthaler, H., Wellburn, A. (1983): Determinations of total carotenoids and chlorophylls b of leaf extracts in different solvents. – Biochem Soc Trans 11: 591-592. doi: 10.1042/bst0110591.

[23] Meng, P., Pei, H., Hu, W., Liu, Z., Li, X., Xu, H. (2015): Allelopathic effects of *Ailanthus altissima* extracts on *Microcystis aeruginosa* growth, physiological changes and microcystins release. – Chemosphere 141: 219-226. doi: 10.1016/j.chemosphere.2015.07.057.

[24] Muller, S. D., Rhazi, L., Soulie-Märsche, I., Benslama, M., Bottollier-Curtet, M., Daoud-Bouattour, A., De Belair, G., Ghrabi-Gammar, Z., Grillas, P., Paradis, L., Zouaïdia-Abdelkassa, H. (2017): Diversity and distribution of Characeae in the Maghreb (Algeria, Morocco, Tunisia). – Cryptogamie Algologie 38(3): 201-251.

[25] Ni, L., Acharya, K., Hao, X., Li, S. (2012): Isolation and identification of an anti-algal compound from Artemisia annua and mechanisms of inhibitory effect on algae. – Chemosphere 88: 1051-1057. doi: 10.1016/j.chemosphere.2012.05.009.

[26] Pei, Y., Liu, L., Hilt, S., Xu, R., Wang, B., Li, C., Chang, X. (2018): Root exudated algicide of Eichhornia crassipes enhances allelopathic effects of cyanobacteria Microcystis aeruginosa on green algae. – Hydrobiologia 823: 67-77.

[27] Salunkhe, D. K., Chavan, J. K. (1989): Dietary tannins: consequences and remedies. – Boca Raton, Fla. CRC Press.

[28] Singleton, V. L., Rossi, J. A. (1965): Colorimetry of Total Phenolics with Phosphomolybdic-Phosphotungstic Acid Reagents. – American Journal of Enology and Viticulture 16: 144-158. doi: 10.12691/ijebb-2-1-5.

[29] Tazart, Z., Douma, M., Tebaa, L., Loudiki, M. (2019): Use of macrophytes allelopathy in the biocontrol of harmful microcystis aeruginosa blooms. – Water Supply 19: 245-253. doi: 10.2166/ws.2018.072.

[30] Tazart, Z., Caldeira, A. T., Douma, M., Salvador, C., Loudiki, M. (2020a): Inhibitory effect and mechanism of three macrophytes extract on Microcystis aeruginosa growth and physiology. – Water and Environment Journal 35(2): 580-592. doi: 10.1111/wej.12653.

[31] Tazart, Z., Douma, M., Caldeira, A. T., Tebaa, L., Mouhri, K., Loudiki, M. (2020b): Highlighting of the antialgal activity of organic extracts of Moroccan macrophytes: potential use in cyanobacteria blooms control. – Environmental Science and Pollution Research 27: 19630-19637. doi: 10.1007/s11356-020-08440-w.

[32] Tebaa, L., Douma, M., Tazart, Z., Manaut, N., Mouhri, K., Loudiki, M. (2017): Algicidal effects of *Achillea ageratum* L. and Origanum compactum benth. plant extracts on growth of Microcystis aeruginosa. – Applied Ecology and Environmental Research 15: 719-728. doi: 10.15666/aeer/1504_719728.

[33] Tebaa, L., Douma, M., Tazart, Z., Manaut, N., Mouhri, K., Loudiki, M. (2018): Assessment of the potentially algicidal effects of Thymus satureioides Coss. and *Artemisia herba alba* L. against Microcystis aeruginosa. – Applied Ecology and Environmental Research 16: 903-912. doi: 10.15666/aeer/1601_903912.

[34] Wang, H., Cheng, S., Zhang, S., He, F., Liang, W., Zhang, L., Hu, C., Ge, F., Wu, Z. (2010): Chemical Composition in Aqueous Extracts of Potamogeton malaianus and Potamogeton maackianus and their Allelopathic Effects on Microcystis aeruginosa. – Polish Journal of Environmental Studies 19: 213-218.

[35] Wang, R., Hua, M., Yu, Y., Zhang, M., Xian, Q., Yin, D. (2016): Evaluating the effects of allelochemical ferulic acid on Microcystis aeruginosa by pulse-amplitude-modulated (PAM) fluorometry and flow cytometry. – Chemosphere 147: 264-71.

[36] Yuan, R., Li, Y., Li, J., Ji, S., Wang, S., Kong, F. (2019): The allelopathic effects of aqueous extracts from Spartina alterniflora on controlling the Microcystis aeruginosa blooms. – The Science of the total environment 712: 136332.

[37] Zhang, T. T., He, M., Wu, A. P., Nie, L. W. (2009): Allelopathic effects of submerged macrophyte Charo vulgaris on toxic Microcystis aeruginosa. – Allelopathy Journal 23(2): 391-401.

http://www.aloki.hu ● ISSN 1589 1623 (Print) ● ISSN1785 0037 (Online)
DOI: http://dx.doi.org/10.15666/aeer/1906_47814794

[38] Zhang, T., Wang, L., He, Z., Zhang, D. (2011): Growth inhibition and biochemical changes of cyanobacteria induced by emergent macrophyte Thalia dealbata roots. – Biochemical Systematics and Ecology 39: 88-94.
[39] Zhang, T., Lu, L., Yang, X., Zhang, S., Xia, W., Li, C. (2014): Allelopathic control of freshwater phytoplankton by the submerged macrophyte Najas minor All. – Acta Ecologica Sinica 34: 351-355.
[40] Zhou, L., Chen, G., Cui, N., Pan, Q., Song, X., Zou, G. (2018): Allelopathic Effects on Microcystis aeruginosa and Allelochemical Identification in the Cuture Solutions of Typical Artificial Floating-Bed Plants. – Bulletin of Environmental Contamination and Toxicology 102: 115-121.
[41] Zhu, J., Liu, B., Wang, J., Gao, Y., Wu, Z. (2010): Study on the mechanism of allelopathic influence on cyanobacteria and chlorophytes by submerged macrophyte (Myriophyllum spicatum) and its secretion. – Aquatic toxicology 98(2): 196-203.
[42] Zhu, X., Dao, G., Tao, Y., Zhan, X., Hu, H. (2020): A review on control of harmful algal blooms by plant-derived allelochemicals. – Journal of hazardous materials 401: 123403.
[43] Zouaïdia, H., Bélair, G., Benslama, M., Soulié-Märsch, I., Muller, S. (2015): Intérêt des Characeae comme bioindicateurs de la qualité des eaux: le cas des zones humides de Numidie (Nord-Est algérien). – Revue d'écologie (Terre et vie) 70: 121-134.

http://www.aloki.hu ● ISSN 1589 1623 (Print) ● ISSN1785 0037 (Online)
DOI: http://dx.doi.org/10.15666/aeer/1906_47814794

BIOGAS HARVESTING FROM ANAEROBICALLY DIGESTED FOOD WASTE: A REVIEW

SABIANI, N. H. M.[1*] – TAJARUDIN, H. A.[2]

[1]*School of Civil Engineering, Universiti Sains Malaysia, 14300 Nibong Tebal, Pulau Pinang, Malaysia*

[2]*School of Industrial Technology, Universiti Sains Malaysia, 11800 USM, Penang, Malaysia (phone: +60-46-536-194; fax: +60-46-536-375)*

[*]*Corresponding author*
e-mail: cenoor@usm.my; phone: +60-45-996-228; fax: +60-45-996-906

(Received 3rd May 2021; accepted 20th Sep 2021)

Abstract. Food waste (FW) is the largest and most problematic organic waste component in the solid waste management system around the world including Malaysia. In promoting renewable energy production, FW has enormous potential and is one of the most promising sources as it can be converted into energy due to high organic matter content found in this source. Improper handling of FW has adverse effects on humans and the environment. FW that ends up in landfills is capable of producing greenhouse gases such as methane and carbon dioxide which can lead to increased atmospheric temperature, climate change, and global warming as well as causing serious health hazards. Compared to landfilling, incineration, and composting, anaerobic digestion (AD) is considered the best treatment alternative in FW management. This paper reviews the efficacy of using FW AD for energy production, focusing on the critical factors influencing the digestion process, the characteristics of the FW and their impact on the AD process, and the method of anaerobic conversion of FW (batch or continuous) to methane. To enhance the AD of FW, the co-digestion and pretreatment method will also be discussed further in this review paper.
Keywords: *anaerobic digestion, food waste, energy, methane, co-digestion, pretreatment, factors influencing anaerobic digestion process*

Introduction

Food waste (FW), which is known as a complex heterogeneous organic material consisting of highly recalcitrant material up to extremely biodegradable compounds has become a major global problem. In the United States, the generation of FW has reached 188 kg/capita per year with total losses reaching $165.6 billion at consumer and retail levels (Abd Ghafar, 2017). According to Liu et al. (2021), the annual food loss per capita in North America and Europe is 280–300 kg. Furthermore, approximately 33% of food is wasted in Southeast Asia (Yang et al., 2016). According to Kamaruddin et al. (2017), Malaysia presently produces around 1.1 kg/capita/day of municipal solid waste (MSW) where about 40% of MSW consists of FW. The remaining 60% is comprised of inorganic waste such as plastics, papers, diapers/napkins, textile, metal, glass, rubber and leather, garden or yard waste, and others (SWCorp, 2016). Approximately, 77% of the FW produced consists of cooked rice, noodles, bread, and pastries (carbohydrate group) produced by cafeterias, commercial restaurants, meat, and market industries (Tanimu et al., 2014). Most of the polymeric carbohydrates and proteins are present in solid form, for example, rice, bread, noodles, vegetables, and meat. The composition of FW discarded from the households and foodservice level comprising restaurants, canteens, and others can be varied. In countries like Europe and Asia, the largest composition of FW produced is vegetables and fruits with a percentage of 40% and 56%, respectively. The rest consists

http://www.aloki.hu ● ISSN 1589 1623 (Print) ● ISSN 1785 0037 (Online)
DOI: http://dx.doi.org/10.15666/aeer/1906_47954847

of pasta and bread, rice, dairy products, meat, and fish. In general, the FW generated comprises 41-62% of degradable carbohydrate, 15-25% protein, and followed by 13-30% of lipids (Braguglia et al., 2018). In addition, for many countries in Southeast Asian continent such as Malaysia and Thailand, the largest composition of FW is dominated by carbohydrates groups such as cooked or uneaten rice, noodles, and bread. Meanwhile, proteins and lipids are typically derived from FW comprising meat, fish, eggs, and oily gravy.

Ineffective FW disposal will contribute to severe environmental problems including odour emission, leachate production, greenhouse gas emissions (GHG), and groundwater pollution (Zhou et al., 2018). Landfilling, incineration, and aerobic composting are some of the traditional approaches that are often taken into consideration in FW management in Malaysia. Several factors make these three methods unfavourable to dispose of FW, namely the tendency to create environmental problems, space constraints, and characteristics of FW. In FW management, anaerobic digestion (AD) is considered the best alternative of treatment compared to landfilling, incineration, and composting. Limited environmental impacts and a high potential for energy recovery make this technology best suited for treating FW (Ariunbaatar et al., 2014) as well as having great potential in reaching 40 to 60% of waste reduction. Anaerobic digestion is a biological process that takes place in the absence of oxygen and results in the destruction and stabilization of organic waste (Negri et al., 2020), involving 4 stages of processes namely hydrolysis, acidogenesis, acetogenesis, and methanogenesis (Zhou et al., 2018; Negri et al., 2020). This method offers several environmental benefits over other forms of treatment technology, for example, it reduces greenhouse gas emission (methane and carbon dioxide), reduces odors, and produces sanitized nutrient-rich fertilizer (Seruga, 2021).

This paper will discuss the anaerobic conversion of FW for energy production, particularly methane. The focus will be given to the critical factors influencing the digestion process, the characteristics of the FW, and their impact on the AD process. Further explanation will be given to the anaerobic conversion of FW into methane either by batch or continuous AD method. Methods to enhance the AD of FW such as co-digestion and pretreatment will also be evaluated further.

Anaerobic digestion

Biogas is the most important product in the anaerobic digestion process. Biogas is a combustible gas, and the quality is defined by its composition. The main composition of biogas consists of CH_4 and CO_2. In addition, small quantities of other gas components are also present in the biogas produced through the anaerobic digestion process which includes nitrogen (N_2), hydrogen (H_2), hydrogen sulfide (H_2S), ammonia (NH_3), oxygen (O_2), and water vapour (H_2O). According to Bharathiraja et al. (2018), biogas is largely made up of methane (CH_4) (40-75%) and carbon dioxide (CO_2) (15-60%), with minor amounts of hydrogen (H_2), nitrogen (N_2) (0-5%), hydrogen sulfide (H_2S) (0-5000 ppm), oxygen (O_2) (2%), water (H_2O) (1-5%), and saturated hydrocarbons (i.e. ethane, propane). Furthermore, the anaerobic digestion process is becoming popular nowadays because of its methane recovery potential, and the nutrient-rich solids produced following digestion (digestate) can be utilized as fertilizer. Waste stabilization is demonstrated by the generation of methane and carbon dioxide at the end of the anaerobic digestion process.

http://www.aloki.hu ● ISSN 1589 1623 (Print) ● ISSN 1785 0037 (Online)
DOI: http://dx.doi.org/10.15666/aeer/1906_47954847

The anaerobic process begins with hydrolysis where complex organic materials will be hydrolyzed to a smaller size and soluble organic substrate. Meanwhile, in acidogenesis stage, amino acids, simple sugars, and long-chain fatty acids have been broken down into short-chain fatty acids. In the third stage (acetogenesis), the simple molecules from acidogenesis are further digested to produce carbon dioxide, hydrogen, and mainly acetic acid. Then, methanogenesis stage will take place in which the carbon dioxide and hydrogen are converted into methane gas.

Critical factors influencing anaerobic digestion

In order to ensure the operation of the anaerobic digestion process occurs in optimum conditions, there are a few parameters that should be taken into consideration and controlled. Therefore, any drastic changes in the parameters involved in the anaerobic digestion system will affect the chain reaction that ultimately inhibits the digestion process. Complete microbial metabolic processes, which entail intricate interactions of various types of bacteria, must be in continual equilibrium to ensure the digester remains stable. Physiology, nutritional needs, growth kinetics, and sensitivity to environmental conditions are the important characteristics that distinguish between the acid-forming and methane-forming microorganisms in the anaerobic digestion system. The instability of an anaerobic digester is caused by the failure to ensure a balance between these two groups of microorganisms (Li et al., 2018). Thus, parameters such as temperature, pH and alkalinity, volatile fatty acids (VFA), mixing, hydraulic retention time (HRT), and organic loading rate (OLR) must be observed and maintained within the permitted range to enhance microbial activity and thus boost the efficiency of the anaerobic decomposition of organic matter in the system.

Temperature

Anaerobic digestion (AD) can function over a large range of temperatures. Temperature is one of the important operating parameters in determining the performance of AD reactor to ensure the survival and optimum development of microbial consortium. Bacteria have two optimum temperature ranges known as mesophilic and thermophilic although they can survive in a wide range of temperatures. Anaerobic digesters are discovered to be operated at temperatures ranging from 20 ^{o}C to 60 ^{o}C. Mesophilic (20-40 ^{o}C) and thermophilic (50-65 ^{o}C) temperature ranges are responsible for methane generation, with optimum temperatures of 35 ^{o}C and 55 ^{o}C, respectively (Panigrahi and Dubey, 2019). The value of the optimum temperature for the anaerobic digestion process is different and it depends on the composition of the feedstock and type of digester used. Since the rate of digestion is greatly affected by temperature, it is considered a critical parameter that must be maintained in the desired range. Anaerobic bacteria can survive in a wide temperature range, from low temperatures (freezing point) until reaching a temperature of 70 °C. However, the most significant development is in the two ranges of temperature from 25 °C to 40 °C (mesophilic) and from 50 °C to 65 °C (thermophilic). The active microbial community structure is different at both optimum temperatures. The temperature range had a significant influence on the transition of the reactor's methanogenic activity from mesophilic to thermophilic, as evidenced by the sudden performance deterioration and complete cessation of methane recovery when the temperature range was increased from mesophilic to thermophilic (Kim and Lee, 2016).

The optimum temperature setting (35 ^{o}C) during mesophilic anaerobic digestion of FW has successfully produced a high methane yield. This is evidenced through a study

http://www.aloki.hu ● ISSN 1589 1623 (Print) ● ISSN 1785 0037 (Online)
DOI: http://dx.doi.org/10.15666/aeer/1906_47954847

conducted by Wang et al. (2014), Gou et al. (2014), Dai et al. (2013), Shen et al. (2013), Ratanatamskul and Manpetch (2016), Drennan and Di Stefano (2014), Wu et al. (2016) and Paudel et al. (2017). The range of methane yield recorded through their study was between 153-620 L CH_4/kgVS. In addition, the setting of the optimum temperature (55 ^oC) during thermophilic anaerobic digestion of FW also produced a high methane yield. Some researchers such as Castrillon et al. (2013), Gou et al. (2014), Yang et al. (2015), Nagao et al. (2012), and Qiang et al. (2013) have recorded high methane yield production (178–475 L CH_4 / kgVS). However, the increase in methane yield produced does not only depend on the setting of the optimum temperature during the process alone. Factors such as pH and co-digestion of the FW with other substrates also contributed to the increase in methane yield.

In comparison to mesophilic digestion, thermophilic digestion results in a greater reduction of pathogens in the digested substrate, a higher specific growth rate of microorganisms, a shorter hydraulic retention time (HRT), and a faster rate of biogas production (Fernandez-Rodriguez et al., 2013; Cavinato et al., 2013). According to the Arrhenius equation, increasing the reaction temperature by 10 ^oC doubles the rate of many chemical processes (Panigrahi and Dubey, 2019). The specific gas production and gas production rate rose from 0.34 to 0.49 m^3/kgVS and 0.53 - 0.78 m^3/m^3 day, respectively, as the temperature climbed from 37 to 55 ^oC (Cavinato et al., 2013). In the thermophilic process, on the other hand, the high rate of acidogenesis leads to an buildup of propionic acid in the digester, which may limit methanogen activity. Another issue with thermophilic AD is its greater energy demand and process instability, both of which can have a negative impact on energy balance and the entire digestion process (Beevi et al., 2015). The benefits of thermophilic (increased hydrolysis and conversion rates) and mesophilic (elevated process stability, better effluent quality) conditions were combined to develop temperature phased AD (TPAD) (Fuess et al., 2018). TPAD consists of two stages: a shorter thermophilic pretreatment phase and a subsequent mesophilic phase with a longer retention duration. The thermophilic stage accelerates hydrolysis and acidogenesis, which seem to be the rate-limiting processes in anaerobic digestion whereas the mesophilic stage maintains constant conditions for syntrophic acetogenesis and methanogenesis owing to methanogens' superior resistance to inhibitory or toxic chemicals (Borowski, 2015). According to Borowski (2015) and Akgul et al. (2017), TPAD can improve volatile solids and total coliform degradation, enhance methane production and organic loading rates (OLR), increase operational stability and effluent quality in terms of volatile fatty acids (VFA) and soluble chemical oxygen demand (SCOD), and lowering hydraulic retention times (HRT) for total coliform degradation. It has the same potential as single-stage thermophilic anaerobic digestion, but it is much more efficient than single-stage mesophilic anaerobic digestion. The TPAD has been used to digest sewage sludge, FW, the organic fraction of municipal solid waste (OFMSW), as well as a solid residue from olive mills. The TPAD of FW is capable of producing high methane yields as reported by Ventura et al. (2014), Yeshanew et al. (2016), Wu et al. (2016), and Li et al. (2020). Ventura et al. (2014) have conducted TPAD of FW from a recycling company using a combination of mesophilic-thermophilic (10L: 30L) and thermophilic-mesophilic (10L: 30L) reactors. They found that the methane yields obtained were 440 and 370 L CH_4/kg VS_{added}, respectively using a combination of mesophilic-thermophilic and thermophilic-mesophilic reactors. Yeshanew et al. (2016) reported that approximately 334.7 L CH_4/kg $COD_{removed}$ of methane yield was produced through the TPAD process of synthetic FW using a combination of continuously stirred

http://www.aloki.hu ● ISSN 1589 1623 (Print) ● ISSN 1785 0037 (Online)
DOI: http://dx.doi.org/10.15666/aeer/1906_47954847

tank reactor (CSTR) and anaerobic baffled reactor (ABR) with recirculation. Wu et al. (2016) used a combination of the thermophilic-mesophilic reactor with a capacity of 10L to digest food waste with de-oiled grease trap waste and found that a total of 520 L CH_4/kg VS_{added} of methane yield was produced. Li et al. (2020) reported that two temperature-phased anaerobic digestion (TPAD) systems, non-recirculation temperature-phased anaerobic digestion (NR-TPAD) and recirculation temperature-phased anaerobic digestion (R-TPAD), were operated in parallel for the co-digestion of FW and paper waste (55 °C in the first reactor and 35 °C in the second reactor). The range of methane content obtained through these two systems is between 53.99-59.23% and 56.14-60.28% respectively, using NR-TPAD and R-TPAD. Recirculation had a big impact on the microbial population's composition and variations. Recirculation promotes phase separation in the R-TPAD system, converting lactic acid to hydrogen in the first reactor, and has been shown to enhance co-digestion of food waste and paper waste, resulting in methane production. However, the utilization of the TPAD system does not all produce the expected results. For example; Xiao et al. (2018) found methane yield produced through the TPAD system was lower (454 L CH4/kg VSadded) compared to single mesophilic AD (477 L CH_4/kg VS_{added}) and single thermophilic AD system (461 L CH_4/kg VS_{added}). The TPAD employed in the test resulted in a lower biogas and methane production rate and yield, but a greater biogas and methane recovery rate than the two single-stage anaerobic digestion systems. The methane recovery rate for TPAD, single mesophilic AD, and single thermophilic AD systems is 577, 574, and 564 L CH_4/kg $VS_{degraded}$, respectively.

pH and alkalinity

For optimum growth, each group of anaerobic microorganisms involved in the anaerobic digestion process has a specific optimum pH, therefore AD is strongly dependent on the pH of the system. In order to ensure the success of the operation and stability of an anaerobic digester, this parameter must be monitored and maintained. According to Parawira (2004), the utilization of carbon and energy sources, efficiency of substrate dissimilation, synthesis of protein and various types of storage material, and release of metabolic products of cells are among a few aspects that are influenced by pH. Since fermentative microorganism is less sensitive to changes, then it can work in a wider pH range. The acetogenesis phase necessitates a pH of 6.5–7, which is near neutral to acidic. A slightly acidic and basic pH of 6 and 7.5 are essential for hydrolysis and methanogenesis, respectively (Leung and Wang, 2016). The literature has indicated a range of pH values (6.5-8.5) for anaerobic digestion, although the ideal pH for an efficient anaerobic digestion process is about 7 (Kumar and Samadder, 2020). A decline in pH (below 6) significantly reduces the activity of the methanogens more than that of the acidogens and causes volatile fatty acids (VFAs) formation (Panigrahi and Dubey, 2019), which could inhibit the whole process and contributed to digester instability (Kumar and Samadder, 2020). Alkalinity can be defined as a measurement of the chemical buffering capacity of an aqueous solution. Agbalakwe (2011) states that to ensure the operation of an anaerobic digester is in stable condition, the digester needs to provide adequate buffering capacity to maintain the pH of the system to be in the range of 6.7 to 7.4 by neutralizing the VFA which may present in the system. The presence and concentration of buffering compounds are influenced by the composition of the total organic load and substrate. Several compounds provide significant buffering capacity in the anaerobic digestion process such as hydrogen sulfide (H_2S), ammonia (NH_3), bicarbonate (H_2CO_3),

http://www.aloki.hu ● ISSN 1589 1623 (Print) ● ISSN 1785 0037 (Online)
DOI: http://dx.doi.org/10.15666/aeer/1906_47954847

and di-hydrogen phosphate. An anaerobic treatment system has its buffering capacity against pH drop. Alkalinity in the form of CO_2, NH_3, and H_2CO_3 is produced by methanogenic bacteria. According to Appels et al. (2008), the concentration of CO_2 in the gaseous state and bicarbonate (H_2CO_3) alkalinity in the liquid state play a huge role in controlling the pH system. The addition of bicarbonate alkalinity (in the liquid phase) will increase the pH if the concentration of CO_2 (in the gas phase) is constant.

According to Zamri et al. (2021), the optimum pH ranges for acidogenesis and methanogenesis are 5.5 to 6.5 and 6.5 to 8.2, respectively. Optimum pH values for high methane yield recovery in AD have been discovered in several studies. According to Liu et al. (2008), the optimum pH range for OFMSW biogas yield in AD is 6.5–7.5. The optimal pH range for methanogenesis utilizing Korean FW leachate was 6.5–8.2 (Lee et al., 2009). Meanwhile, when anaerobic digestion was performed on FW obtained from the hostel mess of the National Institute of Technology Calicut, Kerala, India, Jayaraj et al. (2014) discovered that biogas yield and degradation efficiency were significantly higher for the substrate of pH 7 compared to other pH values. The methane content of biogas produced at pH 7 was found to be 60.8% (v/v). The cumulative biogas production over a 30-day retention period at the same pH was measured at 5655 mL. The results, however, vary depending on the characteristics of the OFMSW and the acid conditions. Alkali-based chemicals such as sodium bicarbonate ($NaHCO_3$), sodium carbonate (Na_2CO_3), calcium hydroxide ($Ca(OH)_2$), and sodium hydroxide (NaOH) were added to the reactor during the start-up period to maintain the pH stability for the continuous process, and NaOH is most efficacious in enhancing the AD process (Kondusamy and Kalamdhad, 2014; Jain et al., 2015). Before the reactors are fed, neutralization is required if the anaerobic digestion feedstock has a very high or low pH (Kouzi et al., 2020; Zamri et al., 2021). According to Zhang et al. (2009), hydrolysis and pH have also been found to have a strong positive correlation ($P= 0.01$). Therefore, the hydrolysis rate constant is inferred to depend on the pH. Both methanogenic and acidogenic microorganisms have optimum pH levels, which should be highlighted. pH 6.5–8.2 is optimum for methanogenesis, while 7.0 is the most efficient pH (Lee et al., 2009). Methanogens' growth rate is considerably lowered at pH values below 6.6, and methanogenic bacteria's activity is inhibited at higher or lower pH levels (Mao et al., 2015). Because the optimal pH for acidogenesis was between 5.5 and 6.5, a two-stage AD process splitting the hydrolysis-acidification and acetogenesis-methanogenesis processes is the recommended mode of operation (Mao et al., 2015).

The equilibrium of CO_2 and bicarbonate ions is known as buffering capacity. Direct pH measurement is less reliable than buffering capacity in determining digester imbalance. VFAs are formed during the acidogenesis phase, and the pH inside the digester is decreased. Methanogens, which produce alkalinity in the form of CO_2 and bicarbonate, counteract this pH drop. The concentration of CO_2 in the gas phase and the bicarbonate in the liquid phase govern the pH inside the digester. Lowering the OLR, applying salts to turn CO_2 to bicarbonate, or simply adding bicarbonate can all help with inadequate buffering capacity (Panigrahi and Dubey, 2019). The food/microorganism (F/M) ratio also can be altered to adjust for insufficient buffer capacity. It is typically recommended that alkalinity be kept around 1000 and 5000 mg $CaCO_3$/L to maximize methane production (Tchobanoglous et al., 2003).

http://www.aloki.hu ● ISSN 1589 1623 (Print) ● ISSN 1785 0037 (Online)
DOI: http://dx.doi.org/10.15666/aeer/1906_47954847

Volatile fatty acids (VFA)

In an anaerobic digestion monitoring process, volatile fatty acids (VFA) concentration is one of the parameters that play an important role that causes toxicity and reactor failure. VFA consisting of acetic, propionic, butyric and valeric acid is an intermediate compound produced during the acidogenesis stage. The presence of VFA in the anaerobic digestion process can reduce the production of methane gas. The effect of fermentation digestion can be seen as a result of an increase in acid concentration in the system. In case of uncontrolled accumulation of acid, hydrogen exists in the anaerobic digestion process will play an important role in preventing the formation of methane gas. According to Mao et al. (2015) and Jin et al. (2021), methanogenesis inhibition can occur in anaerobic digestion if the VFA produced has a high concentration. The dissociated form of VFA is dominant at elevated pH, while at low pH the undissociated VFAs (free volatile fatty acids) are dominant (Forgacs, 2012). According to Deublein and Steinhauser (2008), the ability of undissociated VFAs to diffuse into cells and denatured the proteins can cause inhibiting effect. The best indicator of the most sensitive metabolic group of microbial groups in the anaerobic system usually refers to the concentration of acetic, propionic, and butyric acids (Lee et al., 2015). In anaerobic digestion, acetic acid normally presents in much higher concentrations than the other types of fatty acids (Lee et al., 2015). Sabri et al. (2018) explain that the conversion rate of VFA to methane varies according to the sequence of acetic acid > ethanol> butyric acid> propionic acid. Lactic acid is an undesirable terminal fermentation product and this acid has the potential to be converted into propionic acid. Propionic acid which accumulates during anaerobic digestion will lead to failure in the production of methane gas (Mamimin et al., 2017).

VFAs regulate pH, which is one of the most critical factors in AD. Fermentative bacteria require a pH range of 4.0–8.5, whereas methanogens prefer a limiting pH range of 6.5–7.2 (Zhang et al., 2014). Previous studies have shown that the pH of anaerobic digesters has a substantial impact on VFAs: at low pH, acetic and butyric acids are the predominant VFAs, but at pH 8.0, acetic and propionic acids play a prominent role (Appels et al., 2011). Furthermore, pH control can influence both the type and amount of acid-producing bacteria (Horiuchi et al., 2002). The generation and accumulation of volatile fatty acids (VFAs) have been found to impede and harm the digestion process, resulting in delayed biogas production (Labatut et al., 2011; Vijayaraghavan et al., 2012). According to Paritosh et al. (2017), the inhibition of VFAs on methanogen activity is produced by a pH drop, which may result in acid-sensitive enzyme activity loss. Macromolecules can be destroyed by large amounts of undissociated acids that can penetrate cellular membranes. Solid-state food waste anaerobic digestion might produce VFA concentrations of up to 20,000 mg/L, which is significantly greater than a wastewater anaerobic process. VFAs vary from 2000 to 3000 mg/L in the optimal conditions for metabolic activity (Paritosh et al., 2017). According to Lee et al. (2015), VFA concentrations in field anaerobic digestion facilities processing FW leachate should be kept below 4,000 mg/L to achieve the Korean guideline of 65% VS removal rate. The concentrations of VFA should be employed as a key operational parameter for controlling and managing the anaerobic digestion process. To ensure the success of anaerobic digestion processes in which high methane yields can be produced as well as prevent inhibition from occurring, the VFA content must be controlled to be within the optimal range. The pH control needs to be done throughout the digestion process.

http://www.aloki.hu ● ISSN 1589 1623 (Print) ● ISSN 1785 0037 (Online)
DOI: http://dx.doi.org/10.15666/aeer/1906_47954847

Mixing strategy

Mixing is one of the important factors in the production of biogas during the AD process. Increasing the contact between substrate and microorganisms is the main objective to carry out the mixing process in the digester. Mixing will uniformly distribute heat and bacteria in the digester to prevent the formation of scum and the occurrence of temperature gradients in the digester. In addition to maintaining a more uniform temperature in the digester, mixing can also help to release the resulting biogas during the AD process. Substrates that have been introduced into the digester should be mixed at regular intervals to prevent settling as well as maintaining contact between bacteria and substrate. Mixing aids in achieving substrate homogeneity and uniform distribution of nutrients, pH, and temperature in the digester, as well as assisting in the release of trapped biogas in the digestate (Singh et al., 2020).

A slow or minimal mixing process is preferable rather than vigorous and excessive mixing. Vigorous continuous mixing process will disrupt the structure of microbial flocs, which consequently interfere with the syntrophic relationships between microorganisms in the digester which will ultimately affect the reactor performance (Singh et al., 2020). When compared to vigorous continuous mixing, Lindmark et al. (2014) found that minimal mixing intensities boosted biogas production rate and overall volume produced. Kariyama et al. (2018) reported that excellent performance is achieved (high biogas production rates and specific gas production) when minimal mixing is used in the digestion of livestock manure. Mechanical mixers, recirculation of digester contents, or recirculation of the produced biogas to the bottom of the digester using pumps are a few methods used to mix the organic material in the digester during the AD process (Mao et al., 2019). To ensure that the solids are in suspension, mechanical or gas mixers can be used for mixing the organic material in the digester. One of the inexpensive methods to enhance the movement of organic materials in the digester is by bubbling the biogas through the chamber. Recirculation of waste is another mixing method in which the digestate produced at the end of the AD process will be removed and only certain percentages will be fed into the digester along with the fresh substrate. This action aims to inoculate the fresh substrate fed into the digester with the bacteria and thus increase the movement in the digester and avoid the formation of the scum layer.

Mixing is a major difficulty in attaining good digestion performance, especially in dry AD (TS>10%), because a thick slurry like food waste slurry requires more energy input to homogenize the feedstock. Mechanical mixing outperforms gas circulation and pumped circulation, according to a comparison of the three mixing methods (Panigrahi and Dubey, 2019). During startup and shock loads in combination with higher mixing intensities, instabilities in the anaerobic digestion process, the buildup of volatile fatty acids (VFAs), and decreased gas generation were detected (Lindmark et al., 2014). Shear stress is caused by high mixing intensity, which can decrease and disintegrate flock formations, as well as reduce biogas generation. Higher mixing intensities also impact the microbial community's composition by boosting VFA concentrations during startup and shock loads, hence increasing the relative competitiveness of certain acetate-degrading bacteria (Lindmark et al., 2014). Lowering the mixing intensity can aid in digester stabilization. Biogas yield has been demonstrated to increase during mixing in contrast to unmixed digesters for greater organic loadings and TS concentrations, whereas mixing is less significant at lower loadings (Karim et al., 2005). Changing from a continuous to an intermittent mixing regime can also help enhance biogas production (Kaparaju et al., 2008).

http://www.aloki.hu ● ISSN 1589 1623 (Print) ● ISSN 1785 0037 (Online)
DOI: http://dx.doi.org/10.15666/aeer/1906_47954847

Lindmark et al. (2014) compared three different mixing intensities for a fresh substrate of the organic fraction of municipal solid waste (OFMSW), i.e. 150 rpm and 25 rpm continuous mixing and minimally intermittent mixing, to the effect of mixing intensity on biogas production and energy efficiency of the biogas plant (OFMSW). The results show that a lower mixing intensity leads to a higher biogas production rate and higher total biogas production in both cases. After process stability, 25 rpm continuous mixing and minimally intermittent mixing produced equivalent amounts of biogas, however, 150 rpm continuous mixing produced lesser biogas throughout the trial. During digestion, cumulative biogas generation was 295±2.9, 317±1.9, and 304±2.8 NmL/g VS_{added} until day 31. In addition to improving gas generation, optimal mixing can increase the anaerobic digestion process' energy efficiency.

Hydraulic retention time (HRT)

One of the most important design parameters that affect the economics of anaerobic digestion is hydraulic retention time (HRT) (Ta et al., 2020). A shorter HRT reduces the size of the digester for a given waste volume, thus reducing the capital cost. Depending on the substrate types and process parameters, the HRT of a digester can range from a few days to months. A longer retention duration typically results in higher cumulative methane production as well as a lower total VS reduction. Microbes can adapt to toxic compositions by having a lengthy retention duration. For a longer HRT, a large digester volume would be required, as a short retention period could result in the microbial washout, leading to a low methane yield (Panigrahi and Dubey, 2019). The rate of microbe loss may outweigh the rate of bacterial growth in the case of a short HRT, causing the anaerobic digestion process to fail. A short HRT also caused VFAs to build up in the digester (Pan et al., 2021). HRT measures the time taken by the substrate or feedstock to stay in the digester. HRT can be calculated using *Equation 1*.

$$\mathrm{HRT} = \frac{V}{Q} \qquad \text{(Eq.1)}$$

where, HRT denotes the hydraulic retention time (days), V denotes the working volume (m^3), and Q denotes the flow rate (m^3/day).

Several researchers agree that the HRT for mesophilic digesters is longer (15-30 days) (Mao et al., 2015) compared to the thermophilic digesters with a shorter HRT range between 12-14 days (Arsova, 2010). Though, some AD process requires longer HRT. For example, as reported by Owamah and Izinyon (2015) and Bhatia et al. (2021), the HRT between 50-100 days was required to decompose the solid waste generated from the feedstock from fibers and lignocellulose-containing plants. Owamah and Izinyon (2015) reported that the HRT for anaerobic digestion process of food waste and maize husk is 68 days and produces cumulative methane production of about 400 LCH_4/kgVS. Meanwhile, Bhatia et al. (2021) recorded an HRT of 120 days to decompose a lignin-rich plant (*Ludwigia grandiflora*) and produced an average biogas yield of 265 LCH_4/kgVS. Meanwhile, Arsova (2010) points out that longer HRT can be observed in AD processes using high solid content systems or dry digestion compared to low solid content systems or also known as wet digestion. Normally, the HRT range for dry digestion is between 14-30 days, while the HRT range is as low as 3 days for wet digestion. The decomposition of organic material inside the digester will become more complete if the substrate is allowed to have a longer HRT. The substrate in the reactor that has uniform HRT can be

http://www.aloki.hu ● ISSN 1589 1623 (Print) ● ISSN 1785 0037 (Online)
DOI: http://dx.doi.org/10.15666/aeer/1906_47954847

observed in a continuously mixed digester. Different microbial communities that grow in the digesters function according to their respective HRT. In a continuously mixed digester, the minimum HRT is determined by the growth rate of the slowest growing, an important microorganism in the anaerobic bacterial community. Nevertheless, the reaction rate will decrease with HRT. This suggests that there is an optimum retention time that will allow the AD process to completely occur while reducing operational costs. The HRT has been identified as a significant parameter that may influence bacteriological ecology (Siddique et al., 2016). The HRT must be optimized for each waste mixture introduced into the system (Anggarini et al., 2015).

There are several examples of studies involving the influence of HRT on biogas production during anaerobic digestion of food waste as conducted by Kim et al. (2006), and Liu et al. (2018). The effects of temperature and hydraulic retention time (HRT) on methanogenesis were investigated by Kim et al. (2006). The operating temperature was varied between 30 °C and 55 °C, with HRTs ranging from 8 to 12 days. Thermophilic digesters were shown to remove more sCOD from liquid food waste than mesophilic digesters. Regardless of HRT, the rates of biogas and methane production in thermophilic digesters were higher than those in mesophilic digesters. Although a 10-day HRT produced the most biogas, a 12-day HRT yielded the most methane (223 LCH_4/kg $sCOD_{degraded}$) in the reactor. This suggests that longer HRTs can produce more biogas. Nevertheless, when 8-day HRT was used, digestion stability showed a decrease. By varying process parameters such as hydraulic retention time (HRT) and organic loading rate (OLR), Liu et al. (2018) observed the biogasification performance of food waste. Using a continuously stirred tank reactor (CSTR), they experimented with two operating conditions: R1 (fixed HRT and OLR) and R2 (varying HRT and OLR) for 116 and 92 days, respectively. They discovered that food waste was anaerobically digested with CSTR under two distinct circumstances, producing the highest biogas generation of 787 mL/g.day achieved at 2.25 g/L.day with a fixed HRT of 30 days. OFMSW (including food waste) comprises a high concentration of carbohydrate, cellulose, protein, lipid, and fat components, necessitating a longer HRT (Zamri et al., 2021). Longer HRTs can result in higher biogas production. The shorter HRT is advantageous because it directly corresponds to production costs and process efficiency improvements (Shi et al., 2017).

Organic loading rate (OLR)

Organic loading rate (OLR) can be defined as the quantity of organic matter fed per unit volume of reactor per unit of time. This parameter plays a significant role in the AD process that serves to evaluate the performance of a reactor (Panigrahi and Dubey, 2019). The OLR values are usually associated with the HRT. If the concentration of the organic matter in the substrate is relatively constant, high OLR will be attained from short HRT. Instead, the OLR will vary at the same HRT if there are variations in the concentration of organic matter in the substrate. Generally, OLR of liquid substrates or slurry refers to organic matter expressed as kg COD/m^3.day, while the OLR of solid feedstock refers to volatile solids denoted as kg VS/m^3.day. OLR can be computed by using *Equation 2*.

$$\text{OLR (kg COD/m}^3\text{.day)} = \frac{Q \; x \; S_o}{V} \qquad \text{(Eq.2)}$$

where Q denotes the flow rate (m^3/day), S_o denotes COD or VS concentration (kg COD/m^3 or kg VS/m^3), and V denotes the working volume (m^3).

http://www.aloki.hu ● ISSN 1589 1623 (Print) ● ISSN 1785 0037 (Online)
DOI: http://dx.doi.org/10.15666/aeer/1906_47954847

The overloading system (high OLR) tends to result in the accumulation of inhibiting substances such as VFAs which will cause low biogas production and thereby causing a process termination or reactor failure. Meanwhile, reactors operating on low OLR are uneconomical because they are not fully utilized (Forgacs, 2012). Optimum OLR to dispersed growth digesters have been reported to be 1-4 kg VS/m^3.day and 1-6 kg COD/m^3.day, 1-15 kgCOD/m^3.day for attached growth digesters, and 5-30 kg COD/m^3.day for anaerobic filters and upflow sludge blanket digesters, respectively (Polprasert, 2007). In a biological system, OLR can be added to a degree of starvation of microorganisms where too low OLR leads to starvation, whereas high OLR leads to intoxication (subjected to fast microbial growth). The system will fail if it is not prepared because high OLR will require more bacterial to decompose the organic material found in the reactor. Acidogenic bacteria, which act early in the degradation process and multiply rapidly if given sufficient substrates, will reproduce and be able to generate acids quickly. This is one of the issues of OLR if it is not monitored since the beginning of the AD process. On the other hand, methanogenic bacteria that take a longer time to escalate their population will not be able to utilize acid at the same rate. As a result, the pH of the system will drop and this will kill more methanogenic bacteria, stop the digestion process and ultimately lead to reactor failure. Low biogas production is an indication that the system has experienced a drop in pH (Charalambous and Vyrides, 2021).

The OLR ranges from 1.2 to 12 kg VS/m^3/day or 2.2-33.7 kG COD/m^3/day in organic digestion (Qiao et al., 2013; Guo et al., 2014). Nonetheless, the OLR behavior is influenced by substrate features, temperature conditions, and the HRT of the AD operation (Zamri et al., 2021). According to Panigrahi and Dubey (2019), many anaerobic digesters treating actual OFMSW operated at an OLR of 4.4-22 kgVS/m^3/day. There are several examples of studies involving the influence of OLR on biogas production during the anaerobic digestion of food waste. Nagao et al. (2012) found that as OLR climbed to 3.7, 5.5, 7.4, and 9.2 kgVS/m^3/day, the volumetric biogas production rate has risen to roughly 2.7, 4.2, 5.8, and 6.6 L/L/day, respectively, and remained constant. The volumetric gas production rate fell below the gas production rate at OLR of 7.4 kgVS/m^3/day at the greatest OLR (12.9 kgVS/m^3/day). Tampio et al. (2014) investigated autoclaved and untreated food waste and discovered that the maximum methane yield was produced for untreated food waste at an organic loading rate of 3 kgVS/m^3/day and for autoclaved food waste at a rate of 4 kgVS/m^3/day. The experiment was carried out at 2, 3, 4, and 6 kgVS/ m^3/day. Agyeman and Tao (2014) co-digested food waste with dairy manure anaerobically at various OLRs and found that when OLR was increased from 1 to 2 gVS/L/day, biogas generation rate rose by 101-116%, but only by 25-38% when OLR was increased from 2 to 3 gVS/L/day. In the digesters using fine and medium-sized food waste, specific methane yield reached an OLR of 2 gVS/L/day. In an experiment conducted by Dhar et al. (2016), 3 distinct OLRs were introduced into a lab-scale batch anaerobic digester processing OFMSW. At OLRs of 5.1, 10.4, and 15.2 g/L COD, methane yields of 84.3, 101.0, and 168.4 mg/$gVS_{removed}$ were recorded; the optimum OLR was discovered to be 15.2 g/L COD for a HRT of 27 days and temperature of 38 ^oC. Furthermore, OLR affects bacterial populations. *Firmicutes* are the most common bacteria at low OLR, while *Gammaproteobacteria, Actinobacteria, Bacteroidetes*, and *Deferribacteria* have been found at high OLR (Mao et al., 2015).

http://www.aloki.hu ● ISSN 1589 1623 (Print) ● ISSN 1785 0037 (Online)
DOI: http://dx.doi.org/10.15666/aeer/1906_47954847

Anaerobic digestion of food waste

As reported by the Food and Agriculture Organization of the United Nation in 2011, about one-third of all food produced for human consumption is wasted as much as 1.3 billion tonnes per year (Kondusamy and Kalamdhad, 2014). Of this amount, the rest of the food produced will be distributed equally between industrialized countries and developing countries. Approximately, 40% of FW is produced at retail and consumer levels of consumption in industrialized countries (Kondusamy and Kalamdhad, 2014). Some amount of energy can be recovered when FW is anaerobically digested. This method has a great potential to generate 367 m^3 of biogas per dry tone of FW at about 65% of CH_4 with an energy content of 6.025 x 10^{-9} TWh/m^3 (Kondusamy and Kalamdhad, 2014). Sen et al. (2016) agree that the selection of FW as a feedstock to run the AD process is a well-established process for the production of sustainable energy. The method is capable to produce carrier materials for biofertilizers (Kuruti et al., 2017), producing restricted environmental tracks (Capson-Tojo et al., 2016), and has a great prospective for energy recovery (Zhang et al., 2014; Zamanzadeh et al., 2016; Kuruti et al., 2017). Therefore, AD has been selected as one of the alternative methods that are environmentally friendly to treat the FW generated daily.

The composition and characteristics of FW

The results from the previous studies conducted worldwide by several researchers found that the composition of FW generated greatly influences the physicochemical characteristics of the FW. According to Fisgativa et al. (2016a), the value of moisture content, volatile solid fraction, and pH that are commonly reported worldwide are 74-90%, 85 ± 5%, and 5.1 ± 0.7, respectively, are the general characteristics of FW. The characteristics of FW which include moisture content (MC), total solids (TS), volatile solids (VS), VS/TS ratio, pH, and C: N are summarized in *Table 1*. Previous studies conducted in the countries in Southeast Asian continent (Malaysia and Thailand) on FW have shown that the value of moisture content varies from 70-98% (Ibrahim et al., 2010; Cheerawit et al., 2012; Tanimu et al., 2014). Since it has a relatively high moisture content, thus the FW contained sufficient moisture for AD. Moreover, Zhang et al. (2011, 2015, 2017, 2018, 2020), Tanimu et al. (2014), Nguyen et al. (2017), Hegde and Trabold (2019), and Chuenchart et al. (2020) found that the TS of FW sample obtained in their characterization work was in the range between 15-33%. Meanwhile, the VS recorded was between 13-31% in the FW sample tested. High VS indicates that the FW is rich in organic solid content which can be converted to biogas during the anaerobic digestion process. The volatile fraction of total solids of the FW (VS/TS ratio) was greater than 0.90, indicating that the FW contained more digestible organic matters which favours anaerobic conversion (Zhang et al., 2011). In anaerobic digestion of FW, the pH value of the feedstock or substrate is considered a pivotal factor as the methanogenic bacteria are very sensitive to acidic conditions. An acidic environment may impede methane production and retard the growth of bacteria. *Table 1* shows that the pH value of the FW produced is within the acidic pH range between 4.06-6.50 (Ibrahim et al., 2010; Zhang et al., 2011, 2015, 2017, 2018, 2020; Cheerawit et al., 2012; Tanimu et al., 2014; Nguyen et al., 2017; Hegde and Trabold, 2019; Chuenchart et al., 2020). In the anaerobic digestion process, constant pH is important in the start-up stage because the fresh FW to be fed into the digester has to go through the hydrolysis and acidogenesis stage before methane formation (methanogenesis stage), which will lower the pH. To maintain the value of pH

http://www.aloki.hu ● ISSN 1589 1623 (Print) ● ISSN 1785 0037 (Online)
DOI: http://dx.doi.org/10.15666/aeer/1906_47954847

in equilibrium, a buffer such as sodium hydroxide, calcium carbonate or lime, has to be added into the digester. As shown in *Table 1*, FW is reported to have a C: N ratio of 13.2-28.2 (Ibrahim et al., 2010; Zhang et al., 2011, 2015, 2017, 2020; Cheerawit et al., 2012; Tanimu et al., 2014; Nguyen et al., 2017; Hegde and Trabold, 2019; Chuenchart et al., 2020).The optimum C: N ratio is 20-30:1, which is a suitable range used in the AD process as reported in many pieces of literature (Esposito et al., 2012). In the AD process, carbon is generally used 20-35 times faster than nitrogen by the bacteria. Thus, at optimum C: N ratio, the digester is anticipated to function at an optimum level to produce methane. Nitrogen is transformed to ammonium at a faster rate than can be assimilated by methanogenic bacteria at a minimum C: N ratio. Meanwhile, a high C: N ratio will inhibit methane production due to the increase in acid formation in the digester.

Table 1. *The characteristics of FW as reported in the literatures*

Parameter	Ibrahim et al. (2010)	Zhang et al. (2011)	Cheerawit et al. (2012)	Tanimu et al. (2014)	Zhang et al. (2015)	Nguyen et al. (2017)	Zhang et al. (2017)	Zhang et al. (2018)	Hedge and Trabold (2019)	Chuenchart et al. (2020)	Zhang et al. (2020)
Moisture (%)	70.88-74.68	-	72.31	97.43	-	-	-	-	-	85.11	-
TS (%)	-	18.1	-	29.57	18.9	23.02	22.1	32.70	23.8	14.89	30.57
VS (%)	-	-	-	-	17.5	20.55	20.4	30.99	22.9	13.89	29.10
VS/TS	-	0.94	-	-	0.93	0.92	0.92	0.95	0.91	0.93	0.95
pH	4.59-4.90	6.5	5.5	4.25	5.2	4.91	5.92	-	4.2	4.06	-
C:N	-	13.2	20.24	16.5	21.3	14.58-22.00	28.2	16.46-17.67	15.8	21.20	16.07

There are various types of macronutrients and micronutrients (Ni, Zn, Cu, Pb, Fe, Mn, Cd, Al, M, P, and K) present in the FW with varying concentrations. These nutrients are required by methanogenic bacteria for robust growth which plays an important role in the production of methane gas. To ensure proper bacterial metabolism and a stable AD process, these nutrients must be present in the feedstock in correct ratios and concentrations. According to Zhang et al. (2013b) and Fisgativa et al. (2016a), the characteristics of the feedstock or substrate will greatly affect the performances of the AD process. The basic features such as high carbohydrate content, extensive obtainability, and extremely decomposable organic fractions causing FW to be a very attractive source for AD substrates as well as economical for energy production.

The implementation of batch or continuous method in the AD of FW

There are two methods or systems to be described in this section, namely the batch and continuous systems. In a batch system, the feedstock will be fed into the digester and completed until the methane gas production ceases. There are several advantages of the batch system which include minimum operating costs, shorter digestion time and less complicated technical problems to be solved. Meanwhile, in the continuous system, the feedstock will be fed continuously into the digester until the steady-state condition is achieved with a constant methane yield. Compared to a batch system, continuous reactors are capable to maintain and allow the microorganisms to adapt to the system and thus

http://www.aloki.hu ● ISSN 1589 1623 (Print) ● ISSN 1785 0037 (Online)
DOI: http://dx.doi.org/10.15666/aeer/1906_47954847

avoiding lag time accompanied by the growth of microorganisms. However, the methane yield generated from the anaerobic conversion of organic feedstock in the continuous digester is highly dependent on the OLR and HRT.

In the batch method, Biochemical Methane Potential (BMP) test is a popular method that is often used to determine the feasibility of a substrate or feedstock in the AD process. In this BMP test, the organic materials that have been mixed with anaerobic bacteria will be incubated in the incubator under controlled conditions (e.g. temperature, mixing), and monitoring is performed on the production of methane gas. A comprehensive protocol for BMP determination has been suggested as the BMP for organic matter is extremely vital in the design, fitting, and conducting of an anaerobic reactor (Holliger et al., 2016).

Table 2 summarizes the generation of methane yield from batch anaerobic digestion of FW as reported in the literatures. Several researchers have reported that the BMP value recorded was between 400-530 L CH_4/kgVS_{added} when the AD process of FW was conducted at mesophilic temperature (35-37 ^oC) (Izumi et al., 2010; Lu et al., 2012; Browne and Murphy, 2013; Facchin et al., 2013; Zhang et al., 2013a; Kawai et al., 2014; Ariunbaatar et al., 2014). Meanwhile, Nathao et al. (2013) and Yang et al. (2015) reported that a relatively low methane yield between 90-180 L CH_4/kg VS_{added} was recorded when the batch AD process was performed at both temperatures. Low methane yield is usually associated with the acidification process that occurs during digestion.

The substrate to inoculum ratio (S/I) is a significant aspect influencing the performance of batch reactors. In order to prevent the accumulation of VFAs in inoculum particles beyond their assimilative methanogenic ability, batch reactors play a significant role. According to Kawai et al. (2014), to overcome the irreversible acidification during the start-up stage, the amount of inoculum fed into the digester has been increased to prevent the accumulation of VFAs. Based on previous studies, it is found that acidification can be prevented when the AD process is conducted at S/I ratio below 1.0. *Table 2* shows that the values of methane yield between 417-529 L CH_4/kg VS_{added} can be achieved from a single mesophilic batch-test performed using the S/I ratio of ≤ 0.5 (Browne and Murphy, 2013; Facchin et al., 2013; Kawai et al., 2014; Ariunbaatar et al., 2015a). This indicates that the stability of the process has been achieved in the AD process. Nathao et al. (2013) has conducted the AD process on synthetic FW and found that methane yield less than 100 L CH_4/kg VS_{added} was obtained when the high S/I ratio (greater than 1.0) was used and the AD process was performed within a shorter time (100 hours). Instead, Lu et al. (2012) obtained methane yield exceeding 400 L CH_4/kg VS_{added} although using a S/I ratio ≥ 1.0 (18.9). This may be due to the application of double-stage batch reactors that can separate acidogenic and methanogenic phases and a longer digestion period (55 days).

The production of methane yield in the batch AD system is also influenced by other factors such as the impact of process temperature, addition of micronutrients or trace elements, and inoculum acclimatization. The effect of temperature (mesophilic or thermophilic) on the batch AD system plays a significant role in the production of methane. However, only a couple of studies, such as those carried out by Algapani et al. (2017), Jiang et al. (2018) and Yang et al. (2015) have concentrated on thermophilic AD. High risk of ammonia inhibition and a greater degree of imbalance are two important things that need to be considered in the implementation of thermophilic AD. At thermophilic temperature, Algapani et al. (2017) and Jiang et al. (2018) obtained higher methane yields between 531-591 L CH_4/ kgVS_{added}, but a lower methane yield value (178 L CH_4/ kgVS_{added}) was achieved by Yang et al. (2015). It is due to the S/I ratio > 1.0 used and the difference in the characteristics of the FW based on the source of the FW.

http://www.aloki.hu ● ISSN 1589 1623 (Print) ● ISSN 1785 0037 (Online)
DOI: http://dx.doi.org/10.15666/aeer/1906_47954847

Table 2. *Methane yield from batch anaerobic digestion of FW*

Substrate	Anaerobic digestion conditions	S/I	Methane yield L CH_4/kg VS_{added}	References
Disposer ground standard FW	Volume = 1L Temperature = Mesophilic Digestion period = 16 days	N.R	417	Izumi et al. (2010)
Standard FW	Volume = 2L Temperature = Mesophilic Digestion period = 45 days	0.33	435	Kawai et.al (2014)
Canteen FW	Volume = 1L Temperature = Mesophilic Digestion period = 28 days	8g VS/L	410	Zhang et al. (2013a)
Synthetic FW	Volume = 1L Temperature = Mesophilic Digestion period = 25 days	0.5	469 ± 6.8	Ariunbaatar et al. (2015a)
Canteen FW	Volume = 0.5L Temperature = Thermophilic Digestion period = 29 days	20.12 g VS/L	591± 30	Jiang et al. (2018)
Synthetic FW	Volume = 0.5 L each (Double stage) Temperature = Mesophilic Digestion period = 100 hours	7.5	94	Nathao et al. (2013)
Canteen FW	Volume = 0.5L Temperature = Thermophilic Digestion period = 28 days	1.5	178	Yang et al. (2015)
Canteen FW	Volume = 0.12L Temperature = Thermophilic Digestion period = 55 days	N.R	531	Algapani et al. (2017)
Vegetable waste from the supermarket	Volume = 1L (Double stage) Temperature = Mesophilic Digestion period = 55 days	18.9	445	Lu et al. (2012)
Canteen FW	Volume = 0.5L Temperature = Mesophilic Digestion period = 25 days	0.33	529	Browne and Murphy (2013)
Source segregated FW	Volume = N.R Temperature = Mesophilic Digestion period = 40 days	0.3-0.4	434±40 (inoculum A) 338 ±30 (inoculum B)	Facchin et al. (2013)

Batch anaerobic digestion was carried out using 0.12-2.0 L screw cap bottles and glass reactors, N.R= not reported

Several studies on the addition of micronutrients were conducted during AD of FW. Micronutrients such as Na, Ni, Co, Fe, Zn, Mg, Ca, K, W, and Mo help the methanogens to grow. High methane yields (45-65%) have been achieved when micronutrients such as Co, Mo, Ni, Se, and W were added to the FW during the digestion process (Facchin et al., 2013). The addition of Se and Mo with a concentration of 10 mg/kg and 3-12 mg/kg dry matter, respectively, will enhance the production of methane up to 30-40%. The study

http://www.aloki.hu ● ISSN 1589 1623 (Print) ● ISSN 1785 0037 (Online)
DOI: http://dx.doi.org/10.15666/aeer/1906_47954847

on the effects of the use of an acclimatized inoculum in the BMP test to promote the production of methane was conducted by some previous researchers. Browne and Murphy (2013) emphasize that for precise BMP evaluation, inoculums must be obtained from the AD process that has achieved stability and is acclimatized to their substrate. However, Holliger et al. (2016) argue that the inoculum to be used in the AD process does not need to be acclimatized first with the feedstock to be tested. This is based on the comparisons of the latest methodologies used in different laboratories. Facchin et al. (2013) also studied the effect of inoculum source and found that high methane yield (434 L CH_4/kg VS_{added}) was produced in the AD process when the inoculum from anaerobic digester co-digesting FW and waste activated sludge was used rather than consuming the inoculum obtained from anaerobic digester handling only FW (338 L CH_4/kg VS_{added}).

Two limits influence the effectiveness of methane gas production from a semi-continuous digester that processes FW, i.e solubilization of organic matters and acidogenesis stage. According to Capson-Tojo et al. (2016), to ensure the success of biogas production, two critical factors should be given special attention which is microbial communities and the quality of inoculum to be applied in the digester start-up process. Long acclimatization duration and operational changes that occur gradually in the semi-continuous digester are caused by slower growth of methanogens than acidogens. The semi-continuous test requires a longer period. The digestion process is considered to have reached stability when parameters such as pH, VS content, and specific methane production recorded an average value of around 10% consistently for a minimum duration of one HRT.

The performance for a single and two-stage for the semi-continuous AD system that has been reported by some previous researchers is shown in *Table 3*. In the semi-continuous AD system, parameters such as OLR and HRT greatly affect the stability of the digester and methane gas production. It can be inferred from *Table 3* that equilibrium has been achieved in the AD of FW when OLR is less than 4.5 gVS/L.day and HRT range between 16-40 days. The range of methane yield obtained is between 316-544 LCH_4/kg VS_{added} (Shen et al., 2013; Ventura et al., 2014; Grimberg et al., 2015; Zhang et al., 2015; Voelklein et al., 2016; Zamanzadeh et al., 2016). According to Ariunbaatar et al. (2015a), the AD can operate at high OLR and subsequently produces high methane yield without decreasing the pH when the AD system has high buffering capacity due to the production of total ammoniacal nitrogen (TAN). The literature has indicated a wide range of inhibitory (TAN) concentrations (1700–14000 mg/L). Unacclimated microorganisms are hazardous at TAN concentrations of 1700–2000 mg/L, whereas acclimated methanogens can be inhibited at concentrations of 12,000–14,000 mg/L (Ariunbaatar et al., 2015a). However, this depends on the operating parameters, source of inoculum, and feedstock applied. The addition of micronutrients in a small quantity in the FW plays a significant role in the AD process. According to Yirong et al. (2015), the addition of micronutrients such as selenium (Se) into the digester can restore the digester that experiences propionic acid accumulation due to the increase in the concentrations of ammonia. The addition of cobalt is required in the digester which operates at high OLR.

The two-stage AD system separates between acidogenesis and methanogenesis phases that optimize the reactor condition for different microbes performing their functions. In the acidogenesis (first stage), lower pH and shorter HRT (2-3 days) lead to the washout of acidogenic bacteria. Meanwhile, methanogenesis (second stage) which occurs in the pH range of 6-8 and HRT of 20-30 days provides a suitable environment for the development of slow-growing methanogens. Grimberg et al. (2015) have made

http://www.aloki.hu ● ISSN 1589 1623 (Print) ● ISSN 1785 0037 (Online)
DOI: http://dx.doi.org/10.15666/aeer/1906_47954847

comparisons in methane yields between single-stage and two-stage anaerobic digesters processing kitchen waste with a capacity of 5 m^3 in mesophilic conditions. Two-stage digesters produced higher methane yield (446 LCH_4/kg VS_{added}) compared to single-stage digester (380 LCH_4/kg VS_{added}). It is found that OLR used for the single-stage digester was much higher than the two-stage digester. At the same time, the fermentation reactor can maintain stability with pH 5.2 despite operating under very low OLR (0.78 kg COD/m^3d). Ventura et al. (2014) treated FW from an FW recycling company using an alternating mesophilic and thermophilic two-stage AD process involving three different temperature combinations (mesophilic: mesophilic, mesophilic: thermophilic, thermophilic: mesophilic) and found that the highest methane yield was recorded (440 L CH_4/kgVS_{added}) when the FW was treated using a combination of mesophilic: thermophilic two-stage AD process. Due to higher temperatures in the second digester, the process was found to be less stable than the first digester. The use of higher OLR and the combination of thermophilic: thermophilic two-stage AD by Micolucci et al. (2014) produced higher methane yields of 476 L CH_4/kg VS_{added}. By optimizing OLRs and HRTs using methanogenic sludge recirculation, this combination will prevent inhibition from happening in the digesters. Additionally, Chu et al. (2012) used the same combination of two-stage AD to treat the same waste without sludge recirculation and thereby achieved low methane yield (364 L CH_4/kg VS_{added}) with low TS content in the feedstock. Shen et al. (2013) conducted a study on the FW mixed with vegetable and fruit waste using a two-stage anaerobic digester. They found that this digester was able to produce a higher methane yield (546 L CH_4/ kg VS_{added}) because it is less susceptible to overloading systems due to the increase in methanogenic activity.

During the AD process in a single-stage digester, all four AD stages in the biochemical pathway including hydrolysis, acidogenesis, acetogenesis, and methanogenesis occur in the same digester in which polymeric organic compounds converted to CH_4, H_2S, NH_3, and CO_2 are also taken place in the same digester (Kondusamy and Kalamdhad, 2014). The use of a single-stage digester to treat complex FW has been proposed by Shen et al. (2013), Zhang et al. (2014), and Tran (2017). Up to 38% more methane is obtained when the AD process is performed in a single-stage digester than a two-stage digester (Nagao et al., 2012). The use of a single-stage digester in AD of FW also exhibits an increase in methane yield as shown in *Table 3*. Tampio et al. (2014) reported that about 483 ± 13 LCH_4/kg VS_{added} of methane yield was obtained when treating source segregated domestic FW using 1 L single-stage digester at the mesophilic condition with an OLR of 3 g VS/L.d, where the VS removal obtained was 77.7%. A comparison has been made by Zamanzadeh et al. (2016) in methane yield produced by two 10 L single-stage digesters operating at two different conditions, i.e. mesophilic and thermophilic, but at the same OLR and HRT (3 gVS/L.day, 20 days) with digestate recirculation. The resulting methane yield was higher (480 ± 33 LCH_4/kg VS_{added}) in the mesophilic single-stage digester than thermophilic single-stage digester (448 ± 44 LCH_4/kg VS_{added}). It also shows that the recirculation of digestate worked very well under mesophilic conditions. Zhang et al. (2015a) have investigated the effect of micronutrients on the anaerobic digestion of campus restaurant FW in a single-stage digester operating at OLRs ranging from 1.0 to 5.5 g VS/L.d in mesophilic conditions. A high methane yield (465.4 L CH_4/kgVS_{added}) was obtained. In the digester containing micronutrients, there was no substantial buildup of VFA. These data suggest that introducing micronutrients to the AD of FW has a significant influence on its stability.

http://www.aloki.hu ● ISSN 1589 1623 (Print) ● ISSN 1785 0037 (Online)
DOI: http://dx.doi.org/10.15666/aeer/1906_47954847

Table 3. *The performance of semi-continuous AD involving single and double stage digesters*

Type of FW/source	Single/double stage digesters/type of reactor (volume)	Process temperature / condition	HRT (days)	Digestion period	OLR (g VS/L.d; kg VS/m^3.day)	Methane yield (LCH_4/kg VS_{added})	References
FW + fruit and vegetable waste	Single (8L) Double (5L: 8L) CSTR	Mesophilic Mesophilic: Mesophilic	30 days 10 days:10 days	210 days 210 days	1-3.5 First stage: 2.0-10 Second stage : 1.0-5.0	328-544 198-546	Shen et al. (2013)
Local waste management company	Double (5L:5L) Single (5 L) CSTR	Mesophilic: Mesophilic Mesophilic	4 days: 12 days 16 days	N.R N.R	15:5 4	389.2 ± 31.8 316.4 ± 17.9	Voelklein et al. (2016)
Source segregated FW (with micronutrients)	Single (5L) CSTR	Thermophilic	N.R	50 days	2	400	Yirong et al. (2015)
Pasteurized FW	Single (10L) Single (10L) CSTR	Mesophilic Thermophilic	20 days 20 days	152 days 152 days	3 3	480±33 448±44	Zamanzadeh et al. (2016)
Campus restaurant (with TEs)	Single (6L) Semi continuous fed digester	Mesophilic	40 days	-	4.5	465.4	Zhang et al. (2015a)
Source segregated domestic FW	Single (11 L) SCSTR	Mesophilic	78 days	100 days	3	483±13	Tampio et al. (2014)
Kitchen	Single ($5m^3$) Double ($5m^3$: $5m^3$) CSTR	Mesophilic Mesophilic: Mesophilic	N.R N.R	6 months 400 days	3.79 0.78	380 446	Grimberg et al. (2015)
Incoming FW at the WWTP	Double (200 L : 380L) CSTR	Thermophilic : Thermophilic	3.3 days : 12.6 days	140 days	18.4 : 4.8	476	Micolucci et al. (2014)
Kitchen garbage	Double (1L : 5 L) CSTR	Thermophilic : Thermophilic	2 days : 10 days	60 days	N.R	364	Chu et al. (2012)
Food waste recycling company	Double (10L : 30L) Double (10L : 30L) Double (10L : 30L) CSTR	Mesophilic: Mesophilic Mesophilic: Thermophilic Thermophilic : Mesophilic	5 days: 15 days 5 days: 15 days 5 days: 15 days	195 days 109 days 43 days	3.2 4.4 4.0	380 440 370	Ventura et al. (2014)

Methods for improving the AD of FW

Food waste (FW) is a complex organic material that consists of highly recalcitrant substances up to biodegradable compounds. Therefore, to enhance the performance of AD of FW, two main strategies can be utilized: 1) co-digestion the FW with the different

http://www.aloki.hu ● ISSN 1589 1623 (Print) ● ISSN 1785 0037 (Online)
DOI: http://dx.doi.org/10.15666/aeer/1906_47954847

substrate to stabilize the entire process and 2) conducting the pretreatment on the feedstock to increase the solubilization of organic matter in the AD process.

a, Co-digestion of FW with other substrates

Siddique and Wahid (2018) have considered co-digestion as the instantaneous digestion of two or more substrate and co-substrate mixtures. Co-digestion of FW with organic substrates is getting more attention from researchers who have conducted researches related to the AD of FW. The ability to increase the number of major nutrients, stabilize the digestate produced, dilute toxic chemicals, balance the nutrients, and take full advantage of the synergistic effect of microorganisms to enhance biogas and methane production for an efficient AD process are all advantages of the co-digestion strategy (Nghiem et al., 2017; Chen et al., 2020). According to Mata-Alvarez et al. (2014), green waste and agricultural waste, sewage sludge and animal dungs are among the organic wastes that are often used to co-digest with the FW to increase the biogas and methane yields. *Table 4* shows a summary of anaerobic digestion of FW with different co-substrates involving green/agricultural waste, sewage sludge, and animal dungs obtained from the previous literatures.

Due to a very low cost associated with their collection, agricultural waste and green waste can be considered as the potential co-substrate to be mixed with FW besides animal dungs and sewage sludge (Chen et al., 2014). According to Gianico et al. (2013), conducting AD processes on agricultural waste and green waste will face various challenges. Besides having high lignin and cellulose content, these wastes are not suitable for single digestion because of several reasons such as low nutrient content, long retention time, and have a great potential to produce inhibitory compounds. The biodegradable rate of FW can be reduced when co-digesting the FW with agricultural waste or green waste to prevent the accumulation of VFAs in the digester. Yong et al. (2015) reported that an increase in methane yields from 171 to 313 LCH_4/kg VS_{added} were observed when the FW ratio was increased during mesophilic batch co-digestion (35 ^oC with the initial loading of 5 gVS/L.d) with straw. Owamah and Izinyon (2015) achieved an increase in methane yields of up to 482 L CH_4/kg VS_{added} with the removal of approximately 74.3-80.7% of VS when co-digesting FW with maize husk (MH). Ratanatamskul and Manpetch (2016) have attempted to co-digest the FW with rain tree leaf using a pilot-scale single-stage (2500 L) and two-stage (1000 L: 2500 L) digesters and found that the VS removal was higher than 80%, but the resulting methane yield was lower:153 L CH_4/kg VS_{added} (single-stage) and 283 L CH_4/kg VS_{added} (two-stage). Jabeen et al. (2015) co-digested FW with rice husk (RH) with C: N ratio of 28 using an 80 L pilot-scale plug flow reactor at 37 ^oC. When the OLR was raised from 5 gVS/L.d to 9 gVS/L.d, it was found that there was a reduction in the reactor stability, VS removal efficiency (a decline from 82.4% to 35.4%), and biogas production (from 446 L biogas/kg VS to 215 L biogas/kg VS). Tanimu et al. (2014) co-digested FW mixture (C: N ratio 17) with meat, fruits, and vegetable wastes to achieve a C: N ratio of 26 and 30. From their work, it can be seen that the increase in methane yield is 48.2% from 0.352 to 0.679 L/gVS_{added} and at the same time recording the methane composition by 85%. COD removal showed an increase from 69% to 85% at C: N ratio of 30. While at C:N ratio of 26, the increase in methane yield is 21.3% from 0.352 to 0.447 L/gVS_{added} and recorded 54% and 74% of VS and COD removal, respectively. Panigrahi et al. (2020) used mesophilic conditions to co-digest FW (rice, cooked vegetables, bread, meat) with pretreated YW (grass-33% w/w; dry leaves-65% w/w; wood chips-2% w/w). They discovered that anaerobic co-digestion of FW with

http://www.aloki.hu ● ISSN 1589 1623 (Print) ● ISSN 1785 0037 (Online)
DOI: http://dx.doi.org/10.15666/aeer/1906_47954847

pretreated YW at F/M ratio of 1.5 improved biogas generation to 431 mL/g VS_{added}, with VS removal of 62%. Tayyab et al. (2019) have conducted anaerobic co-digestion of catering food waste (CFW) and pretreated parthenium weed (PPW) to assess the potential of these plants for biogas production. The investigation involved different mixing ratios (0: 100, 20:80, 60:40, 40:60, 80:20, and 100: 0 TS basis) using laboratory-scale bioreactors under mesophilic conditions (30 ± 1 °C). The results showed that in the co-digestion reactor, where 60% CFW and 40% PPW were employed, the maximum biogas production rate (559 mL/L.day) and accumulative biogas (5532 mL/L) were attained.

Sewage sludge is another co-substrate for FW which is often used by researchers in studies related to anaerobic co-digestion. Sewage sludge has a low C: N ratio and organic content. These two characteristics can help to balance C: N ratio, reduce the intermediate accumulation such as ammonia and increase the microbial activity (Liu et al., 2013). Dai et al. (2013) co-digested the FW with dewatered sludge and found that the stability has been achieved and produced high methane yield (258-380 $LCH_4/kgVS_{added}$) with VS removal of 46-67%. Meanwhile, Gou et al. (2014) conducted anaerobic co-digestion of FW and WAS using a mixing ratio of 33: 67 with increased temperature and increased HRT using 2 L CSTR. The increased process temperature up to the thermophilic condition was found to result in higher methane yields from 250 LCH_4/kg VS to 370 LCH_4/kg VS, but the VS removal decreased from 62-58%. The co-digestion between FW and WAS resulted in a significant reduction in volatile solids in a single-stage and two-stage CSTR up to 48% and a significant increase in biogas yields, i.e. 960 L biogas/kg VS (single-stage) and 440 L biogas/kg VS (two-stage) (Zhang et al., 2013b).

The use of biochar to AD processes improves the removal of COD and lowers the lag phase of methanogenesis, resulting in increased methane generation (Kumar et al., 2021). Li et al. (2018) utilized biochar in batch tests to increase stable and efficient methane generation from thermophilic co-digestion of food waste (FW) and waste activated sludge (WAS) at F/S ratios of 0.25, 0.75, 1.5, 2.25, and 3. The addition of biochar significantly reduced the lag time of methane production and enhanced the rate of methane production with increased organic loading, according to the findings. Microorganism growth and adaptation to VFA accumulation were aided by biochar's increased buffer capacity and large specific surface area.

Features such as the low C: N ratio and a wide range of macronutrients and micronutrients needed by anaerobic bacteria have resulted in the combination of animal waste with FW to encourage higher methane yields through the AD process as an excellent co-substrate. The results from the co-digestion of fine and coarse ground FW particle and dairy manure showed that the highest specific methane yield (630 LCH_4/kg VS_{added}) was obtained in the fine ground FW while the lowest methane yield (470 LCH_4/ kg VS_{added}) was obtained in the coarse ground food co-digested with dairy manure (Agyeman and Tao, 2014). Wang et al. (2014) used chicken manure as a co-substrate to study the possibility of increasing methane yield from the co-digestion of FW with chicken manure in CSTR using alternate feeding mode (FW and chicken manure were fed into the reactor alternately) at OLR 2.50 gVS/L.day. A higher methane yield of 508 mL/gVS was obtained from the co-digestion process. Zhang et al. (2012) conducted a study using a continuously stirred tank reactor (CSTR) with the capacity of 75 L to co-digest FW with cattle slurry (CS) with a ratio of 20:80 (FW: CS). Greater stability was achieved when operating at OLR 2 $kgVS/m^3$.day with the methane yield of 220 L $CH_4/kgVS_{added}$. According to Naran et al. (2016), when mono-digestion was conducted on the FW, it produces a lot of VFAs together with substances containing ammonium,

http://www.aloki.hu ● ISSN 1589 1623 (Print) ● ISSN 1785 0037 (Online)
DOI: http://dx.doi.org/10.15666/aeer/1906_47954847

which impede microbial activity and digestion rate. When FW is digested at organic loadings of more than 2.5 g VS/L/d and at predominantly thermophilic conditions, the AD process can become more extreme and even fail completely (Oladejo et al., 2020). To address this issue, FW is frequently co-digested with animal dung, lignocelluloses, and sewage sludge, which assist to dilute harmful chemicals, improve nutritional balance, and accelerate microbial activities (Zhang et al., 2014). In the production of biogas, cow dung (CD) is a significant organic feedstock (Franco et al., 2018). Due to its poor biogas output, it is frequently co-digested with other biodegradable organic feedstock in order to boost biogas yield (Ormaechea et al., 2018). According to Dhamodharan et al. (2015), although co-digested of FW with the CD is revealed to generate the highest methane compared to other livestock manure, Gaur and Suthar (2017) noted that the combination of a few types of animal manure in anaerobic co-digestion with FW will increase biogas production. As a result, Oladejo et al. (2020) have used automated batch anaerobic reactors to examine the production of biogas from co-digestion of FW with 2 types of animal manure namely cow dung (CD) and piggery dung (PD). The major goal of their research is to see how substrate mixing affects the overall reactor and biogas production. Although biogas was generated by mono-digesting each of the substrates, nutritional balance and gas output were severely limited. From the observation, after 30 days, the digestion of FW + CD + PD produced the maximum cumulative biogas yield of 0.67 L. The digestion of FW + PD yielded the highest methane level of 64.6%, while digestion of FW alone yielded the lowest (54.0%). Overall, the four digestion regimes of cumulative biogas production can be stated in the following order: FW + CD + PD, FW + PD, FW + CD, and FW only.

Apart from the utilization of agricultural waste or green waste, sewage sludge, and animal manures as co-substrate in the AD of FW, researchers have carried out extensive research on other co-substrates such as fresh leachate (Zhang et al., 2015b), brown wastewater (Paudel et al., 2017) and grease trap waste (Wu et al., 2016) which can help to increase higher methane production and reactor stability. In conclusion, anaerobic co-digestion has been identified as an efficient, low-cost, and adaptable method for minimizing process constraints and improving digestion and biodegradation rates, the quantity of biogas, and methane yield. There are various types of co-substrates commonly used in the anaerobic co-digestion of organic waste including the organic fraction of MSW, fat, oil, and grease (FOG), lipid-rich industrial effluent, agricultural waste (including animal manure), sewage sludge, and wood waste. Agricultural waste/green waste, sewage sludge, and animal manure are among the potential co-substrate that are often used in anaerobic co-digestion of FW. The agricultural plant residues consist of rice husks, sugar cane fiber, coconut husks and shells, groundnut shells, wheat straws, and other crop residues. Animal manures usually comprise cattle, chicken, and pig manure. HRT, OLR, operating temperature (mesophilic and thermophilic), C: N ratio, particle size, and feeding method can all affect co-digestion with different substrates. Although co-digestion can offer essential nutrients, the features and components of the substrates must be thoroughly examined to guarantee that the anaerobic co-digestion process produces good outcomes. To prevent the inhibition and optimize the production of methane gas, the mixture ratio between FW and selected co-substrate should provide positive interactions based on proper nutrient selection and moisture balance. If the selection of the combination between FW and the co-substrate is not appropriate, negative results will be achieved such as low methane yield and digester instability.

http://www.aloki.hu ● ISSN 1589 1623 (Print) ● ISSN 1785 0037 (Online)
DOI: http://dx.doi.org/10.15666/aeer/1906_47954847

Table 4. *Anaerobic co-digestion of FW with other substrates*

Types of co-substrate	Types of co-digestion	Types of reactor	Process temperature/ condition	HRT	OLR or S/I	Duration (days)	VS removal (%)	CH_4 yield (LCH_4/kg VS)	References
Agricultural waste / green waste	FW + pretreated yard waste (PYW)	Batch	Mesophilic (30 °C)	NR	1.0 1.5 2.0 2.5	30 30 30 30	62 ± 0.4	394 431 419 338	Panigrahi et al. (2020)
	Catering FW + pretreated parthenium weed (PPW)	Batch (2.5 L)	Mesophilic (30 ± 1 °C)	NR	NR	60	62.2	559 mL/L.d (maximum biogas production rate)	Tayyab et al. (2019)
	FW + maize husk (MH) (w/w) 75:25	CSTR (5L)	Mesophilic (37 °C)	68 27 19 15	1 gVS/L.d 2.5 gVS/L.d 3.5 gVS/L.d 4.5 gVS/L.d	120 120 120 120	80.7 % 76.5 % 74.3 % 78.3 %	400 408 447 482	Owamah and Izinyon (2015)
	FW + straw (w/w) 20:80 60:40 80:20	Batch (1L)	Mesophilic (35 °C)	-	Initial loading = 5g VS/L	NR	NR	171 299 313	Yong et al., (2015)
	FW + fruit and vegetable waste +meat C:N ratio = 17, 26, 30	Batch (1L)	Mesophilic (35 oC)	N.R	Initial loading = 3.5gVS/L	30	38% 54% 71%	0.352 0.447 0.679	Tanimu et al., (2014)
	FW + rain tree leaf (RTL) (w/w) 95:5	Pilot scale one stage (2500L) Pilot scale two stage (1000 L + 2500L)	Mesophilic (35 °C)	30 30	6.8 g VS/L.d 9.5 gVS/L.d	112	80.4 % 89.2 %	153 283	Ratanatamskul and Manptech (2016)

http://www.aloki.hu ● ISSN 1589 1623 (Print) ● ISSN 1785 0037 (Online)
DOI: http://dx.doi.org/10.15666/aeer/1906_47954847

Types of co-substrate	Types of co-digestion	Types of reactor	Process temperature/ condition	HRT	OLR or S/I	Duration (days)	VS removal (%)	CH_4 yield (LCH_4/kg VS)	References
	FW + rice husk (RH) Mixed to obtain a C:N = 28	Pilot scale plug flow (80L)	Mesophilic (37 °C)	26 25 14	5 gVS/L.d 6 gVS/L.d 9 gVS/L.d	27 52 30	82.4 % 73.1 % 35.4 %	446 L_{biogas}/kg VS 399 L_{biogas}/kg VS 215 L_{biogas}/kg VS	Jabeen et al., (2015)
Sewage sludge	FW + dewatered sludge (DS) FW : DS (VS ratio) 30:70 50:50 70:30	CSTR (6L)	Mesophilic (35 °C)	20 days	6.3 gVS/L.d 7.2 gVS/L.d 7.6 gVS/L.d	NR	46 % 58 % 67%	258 332 380	Dai et al., (2013)
	FW + WAS (TS ratio) 33.3:66.6 33.3:66.6 33.3:66.6	CSTR (2L)	35 45 55	16.7 days	2 gVS/L.d	160 178 188	62 % 60 % 58%	250 290 370	Gou et al., (2014)
	FW + WAS (VS ratio) 16.5 : 83.5 FW + WAS (VS ratio) 16.5 : 83.5	Single stage pilot CSTR (20 tonnes) Two stage pilot CSTR (4.5 + 15.5 tonnes)	Mesophilic (35 °C) Mesophilic (35 °C)	20 NR	0.85 g VS/L.d NR	350 350	46 % 48 %	960 L_{biogas}/kg VS 440 L_{biogas}/kg VS	Zhang et al., (2013b)
	Synthetic FW + waste activated sludge (WAS) (addition of biochar)	Batch (0.12 L)	Thermophilic (55 °C)	NR	0.25 0.75 1.5 2.25 3.0	20	NR	20 50 90 150 200 (cumulative methane production, mL)	Li et al. (2018)

http://www.aloki.hu ● ISSN 1589 1623 (Print) ● ISSN 1785 0037 (Online)
DOI: http://dx.doi.org/10.15666/aeer/1906_47954847

Types of co-substrate	Types of co-digestion	Types of reactor	Process temperature/ condition	HRT	OLR or S/I	Duration (days)	VS removal (%)	CH_4 yield (LCH_4/kg VS)	References
Animal manures/dung	FW + cattle slurry (CS) (VS ratio = 20:80)	CSTR (75 L)	Mesophilic (36°C)	30 days	2 gVS/L.day	308	NR	220	Zhang et al., (2012)
	FW + dairy manure (DM) (VS ratio = 50:50)	CSTR (2 L)	Mesophilic (36°C)	80 days	2 gVS/L.day	180	NR	630 (fine), 560 (medium), 470 (coarse)	Agyeman and Tao (2014)
	FW + chicken manure	CSTR (3.5 L)	Mesophilic (35°C)	35 days	2.5 gVS/L.day	225	NR	508	Wang et al., (2014)
	FW + cow dung (CD) + piggery dung (PD) (1:2:2)	CSTR (10 L)	Mesophilic	NR	NR	30	NR	FW+CD+PD : 0.67 L FW+CD: 0.62L FW+PD : 0.58L FW only : 0.49L	Oladejo et al. (2020)

NR = not reported

http://www.aloki.hu ● ISSN 1589 1623 (Print) ● ISSN 1785 0037 (Online)
DOI: http://dx.doi.org/10.15666/aeer/1906_47954847

b, FW pretreatment

Pretreatment and other in-situ procedures (such as co-digestion and addition of additives) are two methods that have been studied to enhance the hydrolysis rate (Panigrahi and Dubey, 2019). Pretreatment is required to convert complex structures such as cellulose, hemicellulose, and lignin, which are difficult for microbes to degrade, into biodegradable substances that can be digested by microbes (Siddique and Wahid, 2018). This method is used to boost methane production by increasing chemical oxygen demand and releasing the substrates' intracellular nutrients (Neshat et al., 2017). As a pretreatment stage happens early in the digestion process, it can minimize the level of difficulty in the hydrolysis stage, resulting in a more efficient digestion process. An effective pretreatment should be able to: (i) maintain organic components in biomass; ii) promote hydrolysis progress; iii) prevent the development of hazardous and/or inhibitory compounds; iv) be environmentally friendly, and v) be economically feasible (Derman et al., 2018; Choi et al., 2019). There are various effective pretreatment methods to increase biogas production especially methane through the anaerobic digestion process. These include physical, chemical, biological, and combination of these methods.

Mechanical, freezing/thawing, ultrasonic, microwave, and thermal/hydrothermal treatment are examples of physical pretreatment procedures. The purpose of physical treatments is to alter the morphological structure of substances in order to improve the solubilization and hydrolysis of solid organic materials (Ma et al., 2018). The application of the mechanical pretreatment method can help to boost the effectiveness of the anaerobic digestion process and increase biogas production especially methane. This method has the potential to reduce the size of the substrate particles and increase the surface area of the substrate to be exposed to anaerobic bacterial activity. As reported by Panigrahi and Dubey (2019), Braguglia et al. (2018), and Ariunbaatar et al. (2014), several mechanical methods are often used to pretreat the substrate before introduction into the anaerobic digester. These include grinding, bead milling, high-pressure homogenizer (HPH), stirred ball mills, ultrasonic, and the jetting and colliding method. The mechanical pretreatment method is a physical process that does not involve the addition of chemical substances. Mechanical pretreatment improves the kinetics of biological processes by altering the chemical composition, reducing particle size, crystallinity, polymerization, the release of dissolved organic matter (Panigrahi and Dubey, 2019), as well as improving the substrate's surface area to volume ratio and pore volume (Jain et al., 2015). A larger surface area allows for better contact between the substrate and the anaerobic bacteria, which improves the AD process. Ultrasonic (Rasapoor et al., 2016; Menon et al., 2016; Deepanraj et al., 2017), mechanical grinding (Izumi et al., 2010; Agyeman and Tao, 2014), and freezing/thawing are some of the physical pretreatment procedures employed on FW (Stabnikova et al., 2008).

Thermal pretreatment enhances the AD process by disinfecting by sterilization (Li and Jin, 2015), deflocculating macromolecules, and enhancing dewaterability (Jin et al., 2016), solubilizing refractory particles (Ariunbaatar et al., 2015b), and lowering exogenous pollution, but it also inactivates methanogenic bacteria in the raw material. Thermal pretreatment is often evaluated in terms of soluble COD, VFA, and biogas generation. The existence of oil in OFMSW, on the other hand, necessitates the examination of both physical and chemical properties following thermal pretreatment (Jin et al., 2016) The primary affecting parameters in the thermal pretreatment method are treatment temperature, treatment time, and heat transfer mode, but treatment temperature is more essential than the duration of treatment (Panigrahi and Dubey, 2019). Thermal

http://www.aloki.hu ● ISSN 1589 1623 (Print) ● ISSN 1785 0037 (Online)
DOI: http://dx.doi.org/10.15666/aeer/1906_47954847

pretreatment (the only temperature is regulated, for example in a hot air oven, microwave, or hot water bath) and hydrothermal pretreatment (both temperature and pressure are regulated such as autoclave pretreatment) are the two types of thermal pretreatment methods. Microwave pretreatment for organic solid waste is more successful than autoclave pretreatment in terms of methane production (Tampio et al., 2014; Pecorini et al., 2016). Various studies related to thermal pretreatment have been carried out at temperatures ranging from 50 to 250 ^{o}C. According to Ariunbaatar et al. (2014), the effects of thermal pretreatment are dependent on the kind of substrate or feedstock used and the temperature range involved. Although the degree of solubilization shows a significant effect when higher temperatures (>110 ^{o}C) and longer retention times are applied to the substrate during thermal pretreatment, it cannot be directly attributed to the final energy yield (Braguglia et al., 2018). In some cases, higher solubilization can also be achieved at a low temperature (<110 ^{o}C) but requires a longer retention time. According to Ariunbaatar et al. (2014), many studies related to thermal pretreatment performed at low temperatures (<110 ^{o}C) i.e 70 ^{o}C. This is based on EU Regulation EC1772/2002 which requires organic solid waste to be pretreated at 70 ^{o}C at least 1 hour. Thermal pretreatment on FW has been carried out by several previous researchers such as Gnaoui et al. (2020), Li et al. (2017), Li and Jin (2015), and Tampio et al. (2014).

In chemical pretreatment, chemicals such as strong acids, alkalis, or oxidants have been used as pretreatment methods to break down the organic constituents by hydrolyzing the cell walls and membranes resulting in higher solubility of organic matter in the cells. To solve problems related to sludge solubilization efficiently with little or no energy demand, acid and alkali pretreatment become the appropriate option in addition to producing pathogen-free digestate. According to Sarto et al. (2019), acid pretreatment aims to weaken covalent hydrogen bonds and van der Waals forces in order to solubilize hemicellulose, break down cellulose, and hydrolyze hemicellulose into monosaccharides. Dilute acid was chosen for this pretreatment because it is less poisonous, less corrosive, and less costly, as well as requiring fewer neutralizing reagents and involving cheaper reactor construction material costs. The lignocellulosic substrates such as agricultural wastes, wood chips, crop waste, and paper waste have all been subjected to the dilute acid pretreatment approach. Various types of lignocellulosic fractions of MSW have been treated with dilute sulfuric acid (H_2SO_4), dilute nitric acid (HNO_3), dilute hydrochloric acid (HCl), dilute phosphoric acid (H_3PO_4), dilute glycolic acid ($C_2H_4O_3$), and dilute oxalic acid ($C_2H_2O_4$), however, because of its inexpensive cost, dilute H_2SO_4 is the most often used (Panigrahi and Dubey, 2019). During alkaline pretreatment, acetyl groups are removed and uronic acid is substituted, making cellulose and hemicellulose more accessible to hydrolytic enzymes. Pretreatment with alkaline improves the internal surface area, degrades lignin, and destroys the lignin-carbohydrate bond. Alkaline reagents such as NaOH, KOH, $Mg(OH)_2$, $Ca(OH)_2$, and NH_4OH have been employed in previous investigations (Bazargan et al., 2015). In terms of COD solubilization, NaOH is the most effective of these chemicals, followed by KOH, $Mg(OH)_2$, and $Ca(OH)_2$ (Panigrahi and Dubey, 2019). By increasing the internal surface area of biomass, NaOH has the maximum ability to reduce crystallinity and degree of polymerization, as well as boost biomass degradability. Because part of the chemicals is used by the biomass during alkaline pretreatment, a larger chemical dosage is required. However, it has been noted that using NaOH can raise the cost of pretreatment and that a high concentration of Na^+ can impede the AD process. When comparing NaOH to $Ca(OH)_2$, $Ca(OH)_2$ is preferable since it is less expensive, safer, and easier to extract from aqueous solutions using CO_2.

http://www.aloki.hu ● ISSN 1589 1623 (Print) ● ISSN 1785 0037 (Online)
DOI: http://dx.doi.org/10.15666/aeer/1906_47954847

Apart from acid and alkaline pretreatment, the oxidation process is one of the pretreatment methods found in chemical pretreatment. This method includes ozonation, peroxidation, and peracetic acid. Ozonation and peroxidation pretreatment methods are very useful in sludge stabilization. The use of ozone will cause cellular disruption, flocs disintegration, and high COD solubilization (Salihu and Alam, 2016). There are some disadvantages of this pretreatment method which require high capital. In addition, higher ozonation will cause the formation of soluble compounds that will have a damaging effect when released into the environment. The use of the peroxidation method is also limited due to the factors such as low pH, requiring proper handling, and special equipment and corrosion problems (Salihu and Alam, 2016). Therefore, most researchers prefer acid and alkaline pretreatment methods to treat organic waste that will be used as a feedstock for the anaerobic digestion process because both methods are easier with little or no energy demand. There are several researchers such as Junoh et al. (2015), Naran et al. (2016), Jang et al. (2015), and Yue et al. (2020) who used chemical methods (acid, alkaline, and ozonation) to perform FW pretreatment to increase biogas production during AD process (refer *Table 5*).

According to Panigrahi and Dubey (2019), the major objective of biological pretreatment is to improve the digestibility of complex waste by eliminating covalent cross-linkages and non-covalent interactions between hemicelluloses and lignin, as well as increasing particle surface area. Various types of feedstocks such as wood and grass, waste office paper, lignocellulosic substrate, agricultural residues, hardwood, FW, and MSW are suitable for biological pretreatment before the AD process. Biological pretreatment is an environmentally friendly process but time-consuming and that requires a longer retention time. During the pretreatment process, the microbes utilize free and easily accessible carbohydrates as their primary carbon source. Because the microbes compete with the native microorganisms during the pretreatment process, maintaining a pure culture of bacteria and optimizing their growth conditions for an FW pretreatment can be difficult (Banu et al., 2020). In biological pretreatment, the primary affecting parameters are incubation temperature and time, moisture content, type of biological pretreatment, pH of the medium, and substrate particle size. Aeration of FW is another biological pretreatment option that can boost hydrolysis rates. Aeration changes the biomass community in the FW and slows the build-up of volatile fatty acids, as well as hydrolyzing resistant substrates by mobilizing enzymes. Not limited to microbial systems alone, the biological pretreatment also involves enzymes such as amylase, lipase, protease, and cellulase which works to accelerate hydrolysis through enzymatic catalysis and further promote methane production through an anaerobic digestion process. The utilization of enzymes in biological pretreatment promotes the solubilization process that occurs earlier within the system than in the microbial process which requires an acclimatization period. Enzymatic pretreatment is one of the most promising biological pretreatment methods in which the rate of hydrolysis for organic residues can be improved further before anaerobic digestion. Before the digestion process, enzymes may be introduced to the substrate as a pretreatment or directly added to the digester. According to Carrere et al. (2016), the addition of enzymes directly into the digester is a common procedure in the full-scale scenario. Although enzymatic pretreatment requires less input energy than mechanical and thermal pretreatment methods without involving the addition of chemicals, other factors as the main issues would be the price, enzyme selection (lipase or glucoamylase), and process efficiency.

http://www.aloki.hu ● ISSN 1589 1623 (Print) ● ISSN 1785 0037 (Online)
DOI: http://dx.doi.org/10.15666/aeer/1906_47954847

Table 5. *Summary for some of the pretreatment studies involving mechanical, chemical, thermal, biological and combination of various pretreatment methods reported on FW*

Type of organic waste	Pretreatment conditions	Type of AD system	Impact of pretreatment	Anaerobic digestion performance	References
Food waste (FW)	MECHANICAL Grinding	Mesophilic (semi-continuous)	• reduction in the average size of FW particles to 2.5, 4 and 8 mm	• the range of methane yield produced for particle sizes of 2.5, 4, and 8 mm is in the range between 510-630, 470-560 and 460-470 mL CH_4/g VS.	Agyeman and Tao (2014)
Food waste (FW)	MECHANICAL Bead milling (1000 rpm)	Mesophilic (batch)	• the mean particle size of the FW decreased from 0.843 to 0.391 mm. • substrate solubilization has increased by 40 % of the total COD.	• methane yield has increased by 28 %	Izumi et al., (2010)
Food waste (FW)	MECHANICAL High voltage pulse discharge (HVPD) Voltage = 40 kV Electrode distance = 5 mm Pulse frequency = 400 Hz Duration = 30 min	Mesophilic (batch)	• the COD removal rate of FW pretreated with HVPD was over 100%, significantly greater than the control. • more VFAs would be neutralized due to the greater ammonia content in the reactor after HVPD pretreatment.	• the methane yield increased by 34.6% from 234 mL $CH_4/gCOD_{removed}$ to 315 mL $CH_4/gCOD_{removed}$.	Zou et al. (2016)
Food waste (FW)	MECHANICAL Microwave Temperature = 100 °C Power = 600W	Mesophilic (batch)	• Proteins and polysaccharides were degraded by *Proteiniborus* and *Parabacteroides,* respectively. • *Bacteroides* was the only bacteria that dominated in the co-digestion system. • At the active methane generation phase, *Methanosphaera* predominated in microwave pretreated FW.	• There was an increase in methane yield from 297 mL CH_4/g VS_{added} to 316 mL CH_4/g VS_{added}.	Zhang et al. (2016)
FW from the campus cafeteria	MECHANICAL Ultrasonic	Mesophilic (batch)	• There was an increase of 7 % in SCOD.	• Produce 149 mL H_2/gVS_{added} (sonicated) and 85 mL H_2/gVS_{added} (non-sonicated)	Gadhe et al., (2014)

http://www.aloki.hu ● ISSN 1589 1623 (Print) ● ISSN 1785 0037 (Online)
DOI: http://dx.doi.org/10.15666/aeer/1906_47954847

Type of organic waste	Pretreatment conditions	Type of AD system	Impact of pretreatment	Anaerobic digestion performance	References
(rice, vegetables, fruit peels, other residues)	Power = 1200 W Ultrasonic density = 1.5 W/mL SE = varied depends on sonication duration and TS Frequency = 20 kHz Sonication duration = 15 min			• The biogas production has been enhanced with a 75.3 % increase in hydrogen content.	
FW co-digested with poultry manure	MECHANICAL Ultrasonic Power = 130 W SE = N.R Frequency = 20kHz Sonication duration = 30 min	Thermophilic (batch)	• TS, VS and COD removal efficiency recorded 61.83%, 65.21% and 54.66%, respectively.	• Produce maximum cumulative biogas of 9926 mL with methane composition of 62.47 %	Deepanraj et al., (2017)
Kitchen waste	MECHANICAL Ultrasonic UD =0.2-0.6 W/L SE = 5000-10000 kJ/kg TS Frequency = 20kHz Sonication duration = 10-30 min Power = N.R	Mesophilic (batch)	• There was an increase about 93%, 83% and 37% in TVFA when the kitchen waste with TS of 6%, 8% and 10% was sonicated for 30 min, respectively.	The maximum biogas yield produced after 72 h of digestion ranged between 220-440 mL/gVS at this condition :5000 kJ/kg TS-10,000 kJ/kg TS, 6 % TS.	Rasapoor et al. (2016)
Canteen FW	MECHANICAL Ultrasonic Power = 100 W SE = N.R Frequency = 20kHz	Thermophilic (batch)	• Reduction of processing time to 38h from the 60-80h needed in normal operation. • No significant improvement in either SCOD or VFA production	• There was an increase in total biogas production with 52 % H_2 and 47 % CO_2.	Menon et al. (2016)

http://www.aloki.hu ● ISSN 1589 1623 (Print) ● ISSN 1785 0037 (Online)
DOI: http://dx.doi.org/10.15666/aeer/1906_47954847

Type of organic waste	Pretreatment conditions	Type of AD system	Impact of pretreatment	Anaerobic digestion performance	References
	Sonication duration = 15 -45min				
Food waste (FW)	CHEMICAL Alkaline pretreatment (40-190 meq/L $Ca(OH)_2$, 1-6 hours)	Mesophilic (batch)	• COD solubilization was optimum at 166.98 meq/L (equivalent to 6.1 g $Ca(OH)_2$/L) for 1 hour.	• the methane production of 864.19 mL/g $VS_{destructed}$ was obtained with an increase of 20% compared to untreated FW.	Junoh et al. (2016)
Food waste	CHEMICAL Alkaline pretreatment Alkali concentration= 0.4N NaOH pH = 12.7 Duration= 1 hour	Mesophilic (batch)	• better VS and COD solubilization was obtained, which increased CH4 recovery.	• there was an increase in methane yield (25%) from 271.7 to 339.2 mL CH_4/g$VS_{removed}$ when alkaline pretreatment was performed on FW.	Naran et al. (2016)
Food waste (FW)	CHEMICAL Alkaline pretreatment Alkali concentration = 0.4N NaOH pH = 12.0 Duration= 30 hours	Mesophilic (batch)	• the VS reduction recorded after alkaline pretreatment was 51 ± 4.0 %.	• the resulting hydrogen yield was 162 mL H_2/g VS_{added}.	Jang et al. (2016)
Food waste (FW)	CHEMICAL Ozone pretreatment Flow rate = 30 mL/min Ozone concentrations = 0, 0.02, 0.05, 0.2 and 0.8 g-O3/g-TVS. Pretreatment time = 0, 1.5, 3.75, 15, 60 min	Mesophilic (batch)	• When the ozone content in the pretreatment was increased to 0.8 g-O3/g-TVS, the decomposition rate of glycerol trioleate into hexadecanoic acid and tetradecanoic acid increased to 78.6%. • After ozonation pretreatment, the coating of methanogens by lipids during the anaerobic digestion process was significantly reduced. • When food waste (carbohydrate 45.7 %, protein 21.4 %, lipid 28.1%) and	• At a concentration of 0.8 g-O3/g-TVS, the methane yield from glycerol trioleate increased by 81.9 % to 946.5 mL/g TVS after dark hydrogen fermentation. • Because ozone oxidization damaged most small-molecular carbohydrates and a portion of proteins, excessive ozone pretreatment (0.05 g-O3/g-TVS) lowered not only hydrogen yield but also methane yield.	Yue et al. (2020)

http://www.aloki.hu ● ISSN 1589 1623 (Print) ● ISSN 1785 0037 (Online)
DOI: http://dx.doi.org/10.15666/aeer/1906_47954847

Type of organic waste	Pretreatment conditions	Type of AD system	Impact of pretreatment	Anaerobic digestion performance	References
			glycerol trioleate were combined with a total volatile solids (TVS) ratio of 1:1, an ozonation pretreatment of 0.02 g-O3/g-TVS resulted in the maximum energy conversion efficiency of 78.7% through two-stage dark hydrogen fermentation and anaerobic digestion.		
Food waste (FW)	THERMAL Autoclave at 160 ºC, 6.2 bar	Mesophilic (semi-continuous)	• increase soluble COD by 16.4 % • slight increase in pH from 4.96 to 5.01 • most parameters show a decline after the autoclave pretreatment such as TS, VS, VFA, and density.	• the methane yields at all OLR for autoclaved FW were lower than untreated FW. • lower ammonium and hydrogen sulphide concentrations, due to reduced protein hydrolysis as a result of the formation of Maillard compounds where the substrate cannot be biodegraded.	Tampio et al. (2014)
Kitchen waste (KW)	THERMAL Pretreatment condition = 70 min at 55-90 ºC and 50 min at 120-160 ºC.	Mesophilic (batch)	• improve the breakdown efficiency of crude protein (CP), fat, oil and grease (FOG), volatile solid (VS), and volatile fatty acids (VFA), according to the kinetics results. • had no effect on the ultimate protein content, but it did reduce the FOG degradation potential (7-36%) and lengthened the lag phase for protein and FOG degradation by 35-65 % and 11-82 %, respectively, as compared to untreated KW. • the reduction in CP rose tremendously with the efficiency of FOG removal.	• The removal efficiency of VS and other organics (CP and FOG) enhanced cumulative biogas yield in a linear and exponential way.	Li et al. (2017)
Food waste (FW)	THERMAL Temperatures = 60, 80, and 100 ◦C	Mesophilic (semi-continuous)	• Soluble COD was raised as a result of temperature and time treatment, reaching 68.54 ± 2.4 mg/L at (100 ºC, 30 min), which was 43.41 % greater than the control.	• Anaerobic (AD) digestion of thermally pretreated FW at 100 ºC for 30 min produced 382.82 mL STP CH_4/g VS of	Gnaoui et al. (2020)

http://www.aloki.hu ● ISSN 1589 1623 (Print) ● ISSN 1785 0037 (Online)
DOI: http://dx.doi.org/10.15666/aeer/1906_47954847

Type of organic waste	Pretreatment conditions	Type of AD system	Impact of pretreatment	Anaerobic digestion performance	References
	Duration = 15, 30 and 45 min		• Thermal pretreatment reduced the percentage of VS as compared to raw FW.	methane which was 23.68 % higher than untreated FW. • Biodegradability was improved by 9.8% from 83.23% to 91.44%.	
Kitchen waste (KW)	THERMAL Temperature = 55, 70, 90, 120, 140 and 160 °C	Mesophilic (batch)	• the increase in TS and VS solubilization rate at 55-120 °C (26.63% and 49.21%, respectively) but decreased when the temperature increased to 140-160 °C during acidification.	• reduce the retention time required for anaerobic acidification by 5 days. • at temperatures ranging from 50-70 °C and 140-160 °C, the organic removal rate and biogas production for subsequent anaerobic digestion showed a slight reduction. • at a temperature of 90 and 120 °C, a better result was achieved.	Li and Jin (2015)
Food waste (FW)	BIOLOGICAL Aeration Aeration in 10 L reactor Temperature = 40 °C Flow rate = 50 L/h Oxygen concentration = 21% O_2 Duration = 2, 4 days	Mesophilic (batch)	• After 4 days of aeration, there were up to 10% VS losses, as well as a reduction in VFA, simple sugars, and low-weight organic molecules. • The bacterial community became more diverse as a result of the aerobic circumstances. • Because of the high excretion of exoenzymes, the Proteobacteria phylum may have a superior capacity to hydrolyze less easily biodegradable compounds.	• The methane potential of pretreatment waste was maintained (500 NLCH4/kg VS), but after a long period of aeration, the methane potential was reduced to the starting amount of waste.	Fisgativa et al. (2016b)
Food waste (FW)	BIOLOGICAL Enzymatic pretreatment	Mesophilic (semi-continuous)	• COD removal rates were 96.7 ± 1.5%, 92.1 ± 3.4%, 88 ± 2.3%, 84.1 ± 2.3%, 88.4 ± 3.2% when OLRs of 12, 14, 16, 18, and 20 g COD/Ld were utilized, respectively. • The COD removal rate declined slightly as the OLR increased.	• The biogas production rate had increased to 5.2 ± 0.3, 5.7 ± 0.3, 6.4 ± 0.2, 6.9 ± 0.2 and 7.8 ± 0.1 L/L.d when the OLR was increased from 12 mgCOD/Ld to 14, 16, 18 and 20 mgCOD/L.d, respectively. • The resulting methane yields were 0.30, 0.28, 0.28, 0.26, 0.27 m3 CH4/ kg $COD_{removed}$, respectively.	Zhang et al. (2020)

http://www.aloki.hu ● ISSN 1589 1623 (Print) ● ISSN 1785 0037 (Online)
DOI: http://dx.doi.org/10.15666/aeer/1906_47954847

Type of organic waste	Pretreatment conditions	Type of AD system	Impact of pretreatment	Anaerobic digestion performance	References
				• Methane concentrations were typically between 60 – 64 %, showing that the digestion process was stable.	
Food waste (FW)	BIOLOGICAL Fungal mass	Mesophilic (batch)	• about 89.1 g/L glucose, 2.4 g/L free amino nitrogen and 165 g/L SCOD were produced • 64% reduction in VS within 24 hours.	• the methane yield and methane production rate were 2.3 and 3.5 times higher than untreated FW. • The percentage of VS of about 80.4 ± 3.5% was achieved.	Kiran et al., (2015)
Food waste (FW)	BIOLOGICAL Fungal mash (concentration: 2 g/L)	Mesophilic (batch)	• a total of 19.1% reduction in VS was achieved. • the SCOD concentrations increased to 6853.8 ± 223.7 mg/L after 24 h of hydrolysis with the fungal mash, higher than untreated FW. • the FAN concentration increased to 74.1 ± 13.9 mg/L after 24 hours pretreatment • The glucose concentration increased to 3598.8 ± 128.3 mg/L after 24 hours pretreatment.	• the methane yield increased from 610.3 to 817.0 mL CH_4/gVS (25.3%).	Yin et al., (2016)
Kitchen waste (KW)	COMBINATION PRETREATMENT Combined mechanical-ultrasonic pretreatment (CMUP) Mechanical pretreatment (MP): Size reduction using kitchen blender Ultrasonic pretreatment (UP): Frequency= 40 kHz Time = 24 min	Mesophilic (batch)	• The biodegradability of MP (control) and CMUP is 72 % and 86 %, respectively, in both trials.	• The control (MP) and CMUP experiments produced 382 mL CH_4/gVS and 493 mL $CH4/_gVS$ of methane, respectively. • This clearly reveals that the CMUP improves methane generation and biodegradability, implying that the hydrolysis and methanogenesis phases of the process are improved by this combined pretreatment.	Karouach et al. (2020)

http://www.aloki.hu ● ISSN 1589 1623 (Print) ● ISSN 1785 0037 (Online)
DOI: http://dx.doi.org/10.15666/aeer/1906_47954847

Type of organic waste	Pretreatment conditions	Type of AD system	Impact of pretreatment	Anaerobic digestion performance	References
Kitchen waste (KW)	COMBINATION PRETREATMENT Microwave-hydrogen peroxide pretreatment H_2O_2 added = 0.38 g/gTS at 30% (v/v); Contact time = 1 h; Microwave frequency = 2450 MHz T_{max} = 85 °C; Ramp time = 40 min Retention time = 1 min	Mesophilic (batch)	• Pretreatment of kitchen waste (KW) (from Canadian OFMSW) at 115°C and 145°C improved biogas production by 4–7% compared to untreated KW (control). • Biogas production was reduced when pretreated at 175 °C due to the development of refractory chemicals, which inhibited digestion. • The effect of pretreatment on cumulative biogas production (CBP) for the liquid component of KW was more obvious for SWA20 at 145 °C, with a 26% increase in biogas production after 8 days of digestion compared to the control. • The enhanced substrate availability in the liquid fraction following MW pretreatment resulted in a 78 % increase in biogas generation compared to the control.	• The combination of MW and H_2O_2 modalities had no effect on KW stabilization or increased biogas generation. • All H_2O_2-pretreated samples had a considerable lag phase, and the CBP was typically lower than MW irradiated only samples.	Shahriari et al. (2012)
Food waste (FW)	COMBINATION PRETREATMENT Ultrasonic with acid (UA) (SE= 79 kJ/kg TS, pH 3 with 1N HCl, 24 h). Ultrasonic with base (UB) SE= 79 kJ/kg TS, pH 11 with NaOH , 24 h).	Mesophilic (batch)	• UB preatreatment showed the highest increase in soluble COD and soluble protein by 33% and 40%, respectively. • the highest increase in soluble carbohydrate by 31% was indicated by UA pretreatment.	• UA pretreatment achieved the highest hydrogen yield of 118 mL/g $VS_{initial}$. • UB pretreatment produced a hydrogen yield of 67 mL/g $VS_{initial}$ which was slightly higher than that was observed in untreated FW (42 mL/g $VS_{initial}$).	Elbeshbishy et al., (2011)

http://www.aloki.hu ● ISSN 1589 1623 (Print) ● ISSN 1785 0037 (Online)
DOI: http://dx.doi.org/10.15666/aeer/1906_47954847

Type of organic waste	Pretreatment conditions	Type of AD system	Impact of pretreatment	Anaerobic digestion performance	References
Kitchen waste (from OFMSW)	COMBINATION PRETREATMENT Thermo-acid pretreatment 1.12% HCl for 94 min or 1017% HCl for 86 min Temperature = 100 °C		• Chemical pretreatment of KW using either 1.12 % HCl for 94 minutes or 1.17 % HCl for 86 minutes (at 100 ºC) raised soluble sugars concentration by 120 % compared to untreated KW.	• The mono-sugars glucose and fructose were primarily responsible for the rise in soluble sugars.	Vavouraki et al. (2013)

http://www.aloki.hu ● ISSN 1589 1623 (Print) ● ISSN 1785 0037 (Online)
DOI: http://dx.doi.org/10.15666/aeer/1906_47954847

In addition, longer contact time requirements (at least 24 hours) cause this pretreatment method is not appropriate to be performed on a full scale even though the batch test indicates high methane production (Braguglia et al., 2018). In addition to numerous modes of action depending on distinct FW components, Ma et al. (2018) showed that enzymatic pretreatment may be used quickly and effectively in FW hydrolysis. Amylase, protease, and lipase are enzymes that may break down macromolecular starches, proteins, and lipids into glucose, free amino acids (FAN), and long-chain fatty acids (LCFA), correspondingly. Despite the fact that enzymatic pretreatment of FW resulted in high-efficiency hydrolysis with a VSS removal rate of 60% and a methane yield and generation rate roughly double that of the control, it is still not extensively used in AD processes due to the high cost of commercial enzymes. Biological pretreatment methods of food waste consisting of microbial reactions, enzyme reactions, and aeration have been investigated by several researchers such as Kiran et al. (2015), Yin et al. (2016), Fisgativa et al. (2016b), and Zhang et al. (2020).

The combination of various pretreatment methods involves the utilization of more than one pretreatment method in which the combined effect produces better substrate solubilization which in turn produces higher biogas production and faster AD kinetic processes (Ariunbaatar et al., 2014; Salihu and Alam, 2016). Combination pretreatment can reduce inhibition, formation of recalcitrant products, long retention time, enzyme specialization as well as energy costs. Combination pretreatment is also used when a single pretreatment is insufficient to achieve the desired outcome due to its unique mechanism of action (Braguglia et al., 2018). There are two major combinations of pretreatment methods, namely thermo-chemical pretreatment and thermo-mechanical pretreatment. Thermo-chemical pretreatment is a combination of two methods, namely thermal pretreatment and chemical pretreatment. The chemicals that are commonly added to these pretreatment combinations are sodium hydroxide (NaOH), calcium oxide (CaO), or lime and hydrogen peroxide (H_2O_2). Several studies have been conducted and reported regarding the thermo-chemical pretreatment method to improve the anaerobic biodegradability of organic wastes such as sludge (Tong et al., 2018), animal manure (Khan and Ahring, 2021), organic fraction of municipal solid waste (OFMSW) (Bala et al., 2019), and FW (Junoh et al., 2015). Thermo-mechanical pretreatment is a combination of two methods: thermal and mechanical pretreatment. Combination of microwave-ultrasonic and thermo-pressure pretreatment are the two methods that are available under the thermo-mechanical pretreatment. Most studies involving thermo-mechanical pretreatment are performed on sludge. In addition, there is a combination of other pretreatment methods that are also used to pretreat the organic waste i.e physical-chemical pretreatment (ultrasonic-alkaline, ultrasonic-acid) and electro-chemical pretreatment. *Table 5* demonstrates the summary for some of the pretreatment studies involving mechanical, chemical, thermal, biological, and combination of various pretreatment methods reported on FW.

Inoculum and microbial communities in AD of FW

The AD of FW is a complicated process. Numerous inhibitors, such as ammonia buildup and VFAs, cause poor performance and then even system malfunction (Dai et al., 2013; Agyeman and Tao, 2014; Owamah and Izinyon, 2015). The digesters are typically run at a low organic loading rate (OLR) to ensure a steady operation (Tampio et al., 2014). The majority of prior studies focused on process monitoring and control to increase

http://www.aloki.hu ● ISSN 1589 1623 (Print) ● ISSN 1785 0037 (Online)
DOI: http://dx.doi.org/10.15666/aeer/1906_47954847

process stability and efficiency (Li et al., 2014). AD is a multi-stage biochemical process that involves complex organic molecules going through hydrolysis, acidogenesis, acetogenesis, and methanogenesis in order. In the process of producing methane by AD of FW, the microbial communities differ at different stages of hydrolysis and acidification, hydrogen synthesis, and methane production (Wang et al., 2018). Because AD is a biochemical process involving a wide range of microbial groups, microorganisms form the foundation of the digesters. Bacteria and archaea are the two types of microorganisms that participate in anaerobic digestion. Bacteria degrade complicated substrates to produce VFA, CO_2, and H_2, while archaea produce methane (Ren et al., 2018). Seon et al. (2014) and Yamada et al. (2006) pointed out that *Clostridium, Bacteroides, Bifidobacterium, Butyrivibrio, Proteobacteria, Pseudomonas, Bacillus, Streptococcus, Eubacterium*, and other bacteria are involved in the hydrolysis and acidogenesis processes. Methanogens are archaea, and there have been 65 species discovered so far, divided into 3 orders, 7 families, and 19 genera. Imachi et al. (2007), Nielsen et al. (2007), and Sousa et al. (2007) reveal that the primary bacteria that produce methane include *Methanobacterium, Methanococcus, Methanobrevibacter, Methanomicrobium, Methanosarcina, and Methanosaeta.*

To enhance the AD of organic waste, inoculum has been employed as a microbial booster. Fresh manure and anaerobically digested sludge from numerous wastewater treatment plants (WTPs) and manure treatment AD plants are typical inoculum sources, as the bacteria are more acclimated to anaerobic environments (Bong et al., 2017). According to Gu et al. (2014), some organic waste cannot be digested on its own, necessitating the use of additional methane-producing bacteria to commence the digestion process. Active microbial communities are required for anaerobic digestion, and inoculums should contain these communities. A good inoculum can speed up digestion, boost biogas production, reduce startup time, and make the digestion process more stable (Gu et al, 2014). Many trace elements could be found in the inoculum, which could aid in the activity of anaerobic microbes. Sufficient trace elements in the seeded inoculum, such as Ni and Mo, could have a good impact on the AD of FW, enhancing methane production and hydrolysis rate while also decreasing the lag phase (Sawatdeenarunat et al., 2021). The majority of studies examining the impacts of different inoculums in biomass digestion have concentrated on substrate breakdown and biogas production, rather than the inoculums themselves, such as enzyme activity and nutrient content. Inoculum micronutrients can boost enzyme activity and biogas output (Zhang et al., 2011).

The use of inoculum from various sources in the mono-digestion of FW has been practiced by several researchers such as Lim et al. (2020), Zhang et al. (2017), Wu et al. (2016), Li et al. (2015), Jang et al. (2015) and many more. Lim et al. (2020) compared two techniques of converting mesophilic to thermophilic consortia and evaluated the effect of inoculum on the start-up of thermophilic anaerobic digestion (AD) of FW. The use of inoculum was crucial during the start-up process, and a one-step temperature increase was the favored method. The inoculum employed in their investigation came from two places: anaerobic sludge obtained from a digester treating activated sludge from a wastewater reclamation plant in Singapore and anaerobic sludge taken from a laboratory pilot-scale 1000 L digester treating FW for more than three months at 35 ^{o}C. When the temperature approached 50 ^{o}C, there were symptoms of instability and failure, according to observations made during the investigation. For step-wise temperature increase reactors, a large increase in absolute abundance of bacteria but a decrease in archaea likely

http://www.aloki.hu ● ISSN 1589 1623 (Print) ● ISSN 1785 0037 (Online)
DOI: http://dx.doi.org/10.15666/aeer/1906_47954847

resulted in an excess of AD intermediates that were not digested by methanogens in time, generating reactor sourness. At this point, there will be an accumulation of VFA as well as an initial decrease in biogas. However, the one-step temperature increase reactor recovered from VFA accumulation and poor biogas generation after 10 days attributed to the successful adaptation of thermophilic bacteria such as *Thermotogae, Thermoanaerobacterales*, and *Thermoanaerobacterium*, as well as *Methanosarcina*. Microbial consortia for thermophilic AD were successfully generated using the one-step temperature increase technique and a suitable inoculum, which assisted the start-up of thermophilic AD of FW. Zhang et al. (2017) evaluated the efficacy of a three-stage anaerobic digester (TSAD) in treating FW, as well as the synergistic effect of microorganisms in the TSAD. The inoculum employed in this investigation was waste-activated sludge (WAS) from a large-scale anaerobic digester at Singapore's Ulu Pandan Water Reclamation Plant (UPWRP). TSAD exhibited a 24-54% higher methane yield at a high organic loading rate of 10 g VS/L when compared to standard one-stage and two-stage anaerobic digesters. TSAD also obtained a greater volatile solid reduction rate of 83.5 ± 1.3%. When the one-stage and two-stage digesters had already soured and failed, TSAD showed a strong buffering ability even at high organic loading. According to the pyrosequencing study, the bacterial community in TSAD is more diversified than in control digesters. Multi-function methanogens like *Methanosarcina*, as well as some dominant populations with acetogenesis, amino-acid consumption, and symbiotic functions, have been discovered to selectively enrich TSAD. Wu et al. (2016) used high-throughput sequencing of 16S rRNA genes to investigate the microbial community during the start-up stage of a thermophilic AD treating FW with sludge sourced from secondary sedimentation basin from the Jinhai Municipal Wastewater Treatment Plant in Chengdu. They discovered that thermophilic AD that treated FW could be started up fast and successfully. At the end of the start-up, bacterial groups involved in hydrolysis, fermentation, acetogenesis, and syntrophic oxidation were dominating, and a steady hydrogenotrophic/acetoclastic methanogen ratio was critical for methanogenesis. These modifications represented microbial communities' adaptation to AD environments in enhancing AD performance. The fast start-up of the AD process was likely aided by the cooperation of bacterial and methanogenic populations, as well as the thermophilic environment. During the start-up phase of this study, many thermophilic *Firmicutes, Bacteroidetes*, and *Thermotogae* with hydrolytic, acidogenic, and acetogenic activities became predominant. Li et al. (2015) utilized organic loading rate (OLR) disturbances in a mesophilic anaerobic digester to produce stable and deteriorative phases in FW inoculated with anaerobic sludge collected from a rural household biogas digester operated at ambient temperature. 454-pyrosequencing was used to look at the microbial community of each phase. At the deteriorative phase, the relative abundance of acid-producing bacteria and syntrophic volatile fatty acid (VFA) oxidizers grew considerably, but the dominant methanogens (*Methanosaeta*) remained acetoclastic. The mismatch between bacteria and methanogens could be contributing to the deterioration of the process.

One of the most important drivers of anaerobic bioconversion of various feedstocks in AD processes is the AD microbial community. As various microorganisms are regularly introduced through co-feedstocks, co-digestion systems tend to support microbial communities with greater variety than mono-digestion systems (Karki et al., 2021). Co-digestion of FW with other organic substrates is gaining popularity because it improves AD efficiency, increases biogas generation, and enhances microorganism synergy

http://www.aloki.hu ● ISSN 1589 1623 (Print) ● ISSN 1785 0037 (Online)
DOI: http://dx.doi.org/10.15666/aeer/1906_47954847

(Braguglia et al., 2018). *Firmicutes, Chloroflexi, Bacteroidetes, Proteobacteria*, and *Actinobacteria* are the most common bacteria found in traditional AD (Dai et al., 2016; Zamanzadeh et al., 2017). The type of feedstock has a significant impact on the structure of microbial communities. Animal dungs and sewage sludge are the most common organic waste streams explored for co-digesting FW for biogas production. *Firmicutes* (40.8%), *Bacteroidetes* (23.9%), *Proteobacteria* (5.9%), and *Chloroflexi* (1.1%) constitute the composition of bacterial communities found in sewage sludge-fed AD systems, while the percentage of bacterial communities consisting of *Chloroflexi* (52.9%), *Firmicutes* (20.6%), *Bacteroidetes* (6.6%), and *Proteobacteria* (6.3%) are found in manure-fed reactor systems (Dai et al., 2016). The microbial community structure is also influenced by the ratio of different feedstocks and their biodegradability (Karki et al., 2021).

Co-digestion of FW with other substrates such as animal manure and sewage sludge has been practiced by several researchers such as Muratcobanoglu et al. (2020), Chan et al. (2019), Kim et al. (2019), Wang et al. (2020), Lim et al. (2013) and many more. Muratcobanoglu et al. (2020) used batch tests in mesophilic conditions to explore the effects of graphite on the anaerobic digestion of food waste (FW), cow dung (CM), and their mixture (FW/CM). Graphite was employed as a conductive material in the anaerobic digestion of CW, FW, and the mixture of FW+CW in their investigation. Carbon allotrope graphite has a huge surface area and a strong conductivity. The maximum biogas generation with graphite addition is 1128.46, 829.6, and 1471.1 mL/gVS for FW + 1 g/L, CM + 1.5 g/L, and FW/CM + 0.75 g/L, respectively. Muratcobanoglu and his co-workers also studied the relationship between microbial community structure and biogas production when graphite is added. They found that *Aminiphilus* (13–14%), *Actinobaculum* (13–15%), and *Clostridium* (12–18%) were the most common bacterial genera in graphite-added FW, CM, and FW/CM reactors, according to 16S rRNA gene amplicon sequencing results. In this anaerobic digestion configuration, abundances of *Clostridium* along with co-digestion impact FW/CM biogas generation synergistically. In the graphite-added digesters, *Methanosaeta* was the most common methanogen; however, the relative abundance of these groups differed. Chan et al. (2019) supplemented copper (such as $CuSO_4$ and $CuCl_2$) at 10, 30, and 50 mg/L Cu^{2+} to boost anaerobic co-digestion of food waste and domestic wastewater. They reported that copper supplementation enhanced high methane production (0.260 – 0.325 L CH_4/g $COD_{removed}$) compared to control (0.175 L CH_4/g $COD_{removed}$), in addition to a COD removal efficiency of more than 90%. When 10 mg/L of Cu^{2+} was added to the mixture, the cumulative methane production increased by 94.1%. They also found that copper as a cofactor of several microbial enzymes and coenzymes involved in methane synthesis enhanced methane production as well as COD removal efficiency. However, microbial community analysis confirmed that copper supplementation had a considerable impact on bacterial populations, but only a little impact on archaea diversity. When compared to the control, there was a significant change in the microbial populations following copper supplementation. *Bacteroidetes* (37.2%) were the most common phylum followed by *Firmicutes* (20.7%), *Thermotogae* (17.3%), and *Synergistetes* (6.9%) after copper supplementation. Kim et al. (2019) investigated the impact of food waste (FW) co-digestion with wastewater biosolids (WWB) on microbial communities by running thirteen lab-scale digesters for 100 days under various operational conditions, including OLR (2 and 4 kg COD/m^3.day), feed types (WWB and FW), and FW content (10%, 90%, 100%). FW co-digestion increased biogas generation by 13% and COD degradation rates

http://www.aloki.hu ● ISSN 1589 1623 (Print) ● ISSN 1785 0037 (Online)
DOI: http://dx.doi.org/10.15666/aeer/1906_47954847

by up to 101% when compared to mono-digestion of WWB. From the microbial analysis, *Syntrophomonas* was the dominating genus among fermentative bacteria/acetogens in FW digesters, whereas *Clostridium* was prominent in WWB digesters. *Methanosarcina* and *Methanosaeta* are the dominant methanogens in FW digesters and WWB digesters, respectively. The *Bacteroidetes* population was shown to be highly associated with COD breakdown rates and methane production. *Clostridium* was shown to be highly associated with methane production rate in FW digesters, syntrophs in WWB digesters, and acetoclastic methanogens in both digesters. Wang et al. (2020) investigated the methane output from the digesters that co-digest pig manure (PM) and food waste (FW) at various TS concentrations (R1, TS 5%; R2, TS 10%; R3, TS 15%; and R4, TS 20%). They reported that the increase in TS concentrations from 5% to 15% did not have a significant effect on specific methane yield (278.8-291.7 NmL/g VS_{added}) and even decreased (259.8 NmL/g VS_{added}) when TS concentration was increased to 20% TS. There was a general shifting from the acetoclastic pathway to the mixotrophic pathway and hydrogenotrophic pathway in dry AD (20% TS), with mixotrophic and hydrogenotrophic methanogens predominant. *Firmicutes, Proteobacteria*, and *Chloroflexi* were the most prevalent bacteria in the samples. *Firmicutes, Proteobacteria*, and *Chloroflexi* all had relative abundances of 33.9%, 19.5%, and 11.4%, respectively, within the mixture. Lim et al. (2013) examined the microbial community and reactor performance in single and two-phase continuously stirred tank reactors (CSTRs) for the anaerobic co-digestion of brown water and food waste. After 150 days of reactor operation, the bacterial and archaeal populations were investigated. Methane generation in two-phase CSTR was found to be 23% greater than in single-phase CSTR. The abundance of *Firmicutes* and increased bacterial variety in two-phase CSTR, and the scarcity of *Firmicutes* in single-phase CSTR, might explain these observations. Both CSTRs had high amounts of *Methanosaeta*, which was associated with low acetate levels in their effluent.

Conclusions

To be known as substrate containing high organic matter and high moisture content as well as the highest contributor in the MSW composition, FW has enormous potential and is one of the most promising substrates to produce biogas and methane using biological treatment method, i.e. anaerobic digestion (AD). The concept of waste recovery is important in the present context in order to reduce waste and produce renewable energy due to the abundance of FW. This review shows the progress and changes in the field of research related to FW conversion to energy. From the reviews conducted, FW is a complicated substrate with different degrees of decomposability. The success of the biodegradation process also depends on several parameters such as temperature, pH and alkalinity, mixing strategy, hydraulic retention time (HRT) and organic loading rate (OLR). As a result, the biogas produced through the AD process can vary significantly when FW is processed either by batch, continuous or semi-continuous method. In FW-related research studies, pretreatment and co-digestion are among the issues that have been frequently highlighted over the last 20 years. The implementation of pretreatment can improve the degree of anaerobic biodegradability of FW which in turn increases the production of biogas and methane yield. Pretreatment technology is introduced in AD of FW aims to improve the solubilization of organic matter and reduces the size of organic compounds before decomposed by anaerobic bacteria, enhance the hydrolysis rate and improve the biodegradability of organic matter to support a more efficient hydrolysis

http://www.aloki.hu ● ISSN 1589 1623 (Print) ● ISSN 1785 0037 (Online)
DOI: http://dx.doi.org/10.15666/aeer/1906_47954847

process. However, adverse effects such as VFA accumulation during the hydrolysis stage may interfere in the AD process due to excessive pretreatment. Co-digestion of FW with organic substrates such as green waste or agricultural waste, sewage sludge and animal manures is getting more attention in the research field related to AD of FW. This strategy succeeded in increasing the number of major nutrients, stabilizing the digestate produced and increasing the biogas and methane production. Although many studies on AD of FW produced encouraging findings regarding the advances in the design and optimization process, but further studies related to cost savings in the construction of bioreactor and monitoring processes still need to be implemented.

Acknowledgment. The authors would like to thank Universiti Sains Malaysia for the financial support through USM Short Term Grant (304/PAWAM/60313043) and technical support to complete this study.

REFERENCES

[1] Abd Ghafar, S. W. (2017): Food waste in Malaysia: Trends, current practices and key challenges. – FFTC-AP 19582: 1-12.

[2] Agbalakwe, E. (2011): Anaerobic treatment of glycol contaminated wastewater for methane production. – Master Thesis, University of Stavanger, Retrieved from https://uis.brage.unit.no/uisxmlui/bitstream/handle/11250/182464/Agbalakwe%2c Ekene.pdf.

[3] Agyeman, F. O., Tao, W. (2014): Anaerobic co-digestion of food waste and dairy manure: effects of food waste particle size and organic loading rate. – Journal of Environmental Management 133: 268-274.

[4] Akgul, D., Cella, M. A., Eskicioglu, C. (2017): Influences of low-energy input microwave and ultrasonic pretreatments on single-stage and temperature-phased anaerobic digestion (TPAD) of municipal wastewater sludge. – Energy 123: 271-282.

[5] Algapani, D. E., Wang, J., Qiao, W., Su, M., Goglio, A., Wandera, S. M., Jiang, M., Pan, X., Adani, F., Dong, R. (2017): Improving methane production and anaerobic digestion stability of food waste by extracting lipids and mixing it with sewage sludge. – Bioresource Technology 244: 996-1005.

[6] Angelidaki, I., Ahring, B. K. (2000): Methods for increasing the biogas potential from the recalcitrant organic matter contained in manure. – Water Science and Technology 41(3): 189-194.

[7] Anggarini, S., Hidayat, N., Sunyoto, N. M. S., Wulandari, P. S. (2015): Optimization of hydraulic retention time (HRT) and inoculums addition in wastewater treatment using anaerobic digestion system. – Agriculture and Agricultural Science Procedia 3: 95-101.

[8] Appels, L., Baeyens, J., Degreve, J., Dewil, R. (2008): Principles and potential of the anaerobic digestion of waste-activated sludge. – Progress in Energy and Combustion Science 34: 755-781.

[9] Appels, L., Assche, A. V., Willems, K., Degrève, J., Impe, J. V., Dewil, R. (2011): Peracetic acid oxidation as an alternative pre-treatment for the anaerobic digestion of waste activated sludge. – Bioresource Technology 102: 4124-4130.

[10] Ariunbaatar, J., Panico, A., Esposito, G., Pirozzi, F., Lens, P. N. L. (2014): Pretreatment methods to enhance anaerobic digestion of organic solid waste. – Applied Energy 123: 143-156.

[11] Ariunbaatar, J., Di Perta, E. S., Panico, A., Frunzo, L., Esposito, G., Lens, P. N. L., Pirozzi, F. (2015a): Effect of ammoniacal nitrogen on one-stage and two-stage anaerobic digestion of food waste. – Waste Management 38: 388-398.

http://www.aloki.hu ● ISSN 1589 1623 (Print) ● ISSN 1785 0037 (Online)
DOI: http://dx.doi.org/10.15666/aeer/1906_47954847

[12] Ariunbaatar, J., Panico, A., Yeh, D. H., Pirozzi, F., Lens, P. N. L., Esposito, G. (2015b): Enhanced mesophilic anaerobic digestion of food waste by thermal pretreatment: substrate versus digestate heating. – Waste Management 46: 176-181.
[13] Arsova, L. (2010): Anaerobic digestion of food waste: Current status, problems and an alternative product. – Master Thesis, Columbia University.
[14] Bala, R., Gautam, V., Mondal, M. K. (2019): Improved biogas yield from organic fraction of municipal solid waste as preliminary step for fuel cell technology and hydrogen generation. – International Journal of Hydrogen Energy 44(1): 164-173.
[15] Banu, J. R., Merrylin, J., Mohamed Usman, T. M., Yukesh Kannah, R., Gunasekaran, M., Kim, S. H., Kumar, G. (2020): Impact of pretreatment on food waste for biohydrogen production: A review. – International Journal of Hydrogen Energy 45: 18211-18225.
[16] Bazargan, A., Bazargan, M., McKay, G. (2015): Optimization of rice husk pretreatment for energy production. – Renewable Energy 77: 512-520.
[17] Beevi, B. S., Madhu, G., Sahoo, D. K. (2015): Performance and kinetic study of semi-dry thermophilic anaerobic digestion of organic fraction of municipal solid waste. – Waste Management 36: 93-97.
[18] Bharathirajaa, B., Sudharsana, T., Jayamuthunagai, J., Praveenkumar, R., Chozhavendhan, S., Iyyappan, J. (2018): Biogas production - A review on composition, fuel properties, feed stock, and principles of anaerobic digestion. – Renewable and Sustainable Energy Reviews 90: 570-582.
[19] Bhatia, P., Fujiwara, M., Salangsang, M. C. D., Qian, J., Liu, X., Ban, S., Myojin, M., Toda, T. (2021): Effect of semi-continuous anaerobic digestion on the substrate solubilisation of lignin-rich steam-exploded *Ludwigia grandiflora*. – Applied Sciences 11: 4452.
[20] Bong, C. P. C., Lee, C. T., Ho, W. S., Hashim, H., Klemesc, J. J., Ho, C. S. (2017): Mini-review on substrate and inoculum loadings for anaerobic co-digestion of food waste. – Chemical Engineering Transactions 56: 493-498.
[21] Borowski, S. (2015): Temperature-phased anaerobic digestion of the hydromechanically separated organic fraction of municipal solid waste with sewage sludge. – International Biodeterioration and Biodegradation 105: 106-113.
[22] Braguglia, C. M., Gallipoli, A., Gianico, A., Pagliaccia, P. (2018): Anaerobic bioconversion of food waste into energy: A critical review. – Bioresource Technology 248: 37-56.
[23] Browne, J. D., Murphy, J. D. (2013): Assessment of the resource associated with biomethane from food waste. – Applied Energy 104: 170-177.
[24] Capson-Tojo, G., Rouez, M., Crest, M., Steyer, J.-P., Delgenès, J.-P., Escudié, R. (2016): Food waste valorization via anaerobic processes: A review. – Reviews in Environmental Science and Bio/Technology 15(3): 499-547.
[25] Carrere, H., Antonopoulou, G., Affes, R., Passos, F., Battimelli, A., Lyberatos, G., Ferrer, I. (2016): Review of feedstock pretreatment strategies for improved anaerobic digestion: from lab-scale research to full-scale application. – Bioresource Technology 199: 386-397.
[26] Castrillon, L., Maranon, E., Fernandez-Nava, Y., Ormaechea, P., Quiroga, G. (2013): Thermophilic co-digestion of cattle manure and food waste supplemented with crude glycerin in induced bed reactor (IBR). – Bioresource Technology 136: 73-77.
[27] Cavinato, C., Bolzonella, D., Pavan, P., Fatone, F., Cecchi, F. (2013): Mesophilic and thermophilic anaerobic co-digestion of waste activated sludge and source sorted biowaste in pilot-and full-scale reactors. – Renewable Energy 55: 260-265.
[28] Chan, P. C., Lu, Q., de Toledo, R. A., Gu, J. D., Shima, H. (2019): Improved anaerobic co-digestion of food waste and domestic wastewater by copper supplementation - Microbial community change and enhanced effluent quality. – Science of the Total Environment 670: 337-344.
[29] Charalambous, P., Vyrides, I. (2021): In situ biogas upgrading and enhancement of anaerobic digestion of cheese whey by addition of scrap or powder zero-valent iron (ZVI). – Journal of Environmental Management 280: 111651.

http://www.aloki.hu ● ISSN 1589 1623 (Print) ● ISSN 1785 0037 (Online)
DOI: http://dx.doi.org/10.15666/aeer/1906_47954847

[30] Cheerawit, R., Thunwadee, T. S., Duangporn, K., Tanawat, R., Wichuda, K. (2012): Biogas production from co-digestion of domestic wastewater and food waste. – Health and the Environment Journal 3(2): 1-9.
[31] Chen, X., Yan, W., Sheng, K., Sanati, M. (2014): Comparison of high solids to liquid anaerobic co-digestion of food waste and green waste. – Bioresource Technology 154: 215-221.
[32] Chen, S., Tao, Z., Yao, F., Wu, B., He, L., Hou, K., Pi, Z., Fu, J.,Yin, H., Huang, Q., Liu, Y., Wang, D., Li, X.,Yang, Q. (2020): Enhanced anaerobic co-digestion of waste activated sludge and food waste by sulfidated microscale zerovalent iron: Insights indirect interspecies electron transfer mechanism. – Bioresource Technology 316: 123901.
[33] Choi, J. H., Jang, S. K., Kim, J. H., Park, S. Y., Kim, J. C., Jeong, H., Kim, H. Y., Choi, I. G. (2019): Simultaneous production of glucose, furfural, and ethanol organosolv lignin for total utilization of high recalcitrant biomass by organosolv pretreatment. – Renewable Energy 130: 952-960.
[34] Chu, C. F., Xu, K. Q., Li, Y. Y., Inamori, Y. (2012): Hydrogen and methane potential based on the nature of food waste materials in a two-stage thermophilic fermentation process. – International Journal of Hydrogen Energy 37(14): 10611-10618.
[35] Chuenchart, W., Logan, M., Leelayouthayotin, C., Visvanathan, C. (2020): Enhancement of food waste thermophilic anaerobic digestion through synergistic effect with chicken manure. – Biomass and Bioenergy 136: 105541.
[36] Dai, X., Duan, N., Dong, B., Dai, L. (2013): High-solids anaerobic co-digestion of sewage sludge and food waste in comparison with mono digestions: Stability and performance. – Waste Management 33(2): 308-316.
[37] Dai, X., Chen, Y., Zhang, D., Yi, J. (2016): High-solid anaerobic co-digestion of sewage sludge and cattle manure: the effects of volatile solid ratio and pH. – Scientific Reports 6: 4-13.
[38] Deepanraj, B., Sivasubramanian, B., Jayaraj, S. (2017): Effect of substrate pretreatment on biogas production through anaerobic digestion of food waste. – International Journal of Hydrogen Energy 42(42): 26522-26528.
[39] Derman, E., Abdulla, R., Marbawi, H., Sabullah, M. K. (2018): Oil palm empty fruit bunches as a promising feedstock for bioethanol production in Malaysia. – Renewable Energy 129: 285-298.
[40] Dhamodharan, K., Kumar, V., Kalamdhad, A. S. (2015): Effect of different livestock dungs as inoculum on food waste anaerobic digestion and its kinetics. – Bioresource Technology 180: 237-241.
[41] Dhar, H., Kumar, P., Kumar, S., Mukherjee, S., Vaidya, A. N. (2016): Effect of organic loading rate during anaerobic digestion of municipal solid waste. – Bioresource Technology 217: 56-61.
[42] Drennan, M. F., Di Stefano, T. D. (2014): High solids co-digestion of food and landscape waste and the potential for ammonia toxicity. – Waste Management 34: 1289-1298.
[43] Elbeshbishy, E., Hafez, H., Dhar, B. R., Nakhla, G. (2011): Single and combined effect of various pretreatment methods for biohydrogen production from food waste. – International Journal of Hydrogen Energy 36(17): 11379-11387.
[44] Esposito, G., Frunzo, L., Giordano, A., Liotta, F., Panico, A., Pirozzi, F. (2012): Anaerobic co-digestion of organic wastes. – Reviews in Environmental Science and Bio/Technology 11(4): 325-341.
[45] Facchin, V., Cavinato, C., Fatone, F., Pavan, P., Cecchi, F., Bolzonella, D. (2013): Effect of trace element supplementation on the mesophilic anaerobic digestion of food waste in batch trials: the influence of inoculum origin. – Biochemical Engineering Journal 70: 71-77.
[46] Fernandez-Rodriguez, J., Perez, M., Romero, L. I. (2013): Comparison of mesophilic and thermophilic dry anaerobic digestion of OFMSW: kinetic analysis. – Chemical Engineering Journal 232: 59-64.

http://www.aloki.hu ● ISSN 1589 1623 (Print) ● ISSN 1785 0037 (Online)
DOI: http://dx.doi.org/10.15666/aeer/1906_47954847

[47] Fisgativa, H., Tremier, A., Dabert, P. (2016a): Characterizing the variability of food waste quality: a need for efficient valorization through anaerobic digestion. – Waste Management 50: 264-274.
[48] Fisgativa, H., Saoudi, M., Tremier, A. (2016b): Impact of an aerobic pretreatment on anaerobic biodegradability of food waste. – 6th international Conference on Engineering for Waste and biomass Valorization, May 23-26 2016, Albi, France.
[49] Forgacs, G. (2012): Biogas production from citrus wastes and chicken feather: pretreatment and co-digestion. – PhD Tesis. Chalmers University of Technology, Sweden.
[50] Franco, R. T., Buffiere, P., Bayard, R. (2018): Co-ensiling of cattle manure before biogas production: effects of fermentation stimulants and inhibitors on biomass and methane preservation. – Renewable Energy 121: 315-323.
[51] Fuess, L. T., Klein, B. C., Chagas, M. F., Rezende, M. C. A. F., Garcia, M. L., Bonomi, A., Zaiat, M. (2018): Diversifying the technological strategies for recovering bioenergy from the two-phase anaerobic digestion of sugarcane vinasse: an integrated techno-economic and environmental approach. – Renewable Energy 122: 674-687.
[52] Gadhe, A., Sonawane, S. S., Varma, M. N. (2014): Ultrasonic pretreatment for an enhancement of biohydrogen production from complex food waste. – International Journal of Hydrogen Energy 39(15): 7721-7729.
[53] Garrone, P., Melacini, M., Perego, A. (2014): Opening the black box of food waste reduction. – Journal of Food Policy 46: 129-139.
[54] Gaur, R. Z., Suthar, S. (2017): Anaerobic digestion of activated sludge, anaerobic granular sludge, and cow dung with food waste for enhanced methane production. – Journal of Cleaner Production 164: 557-566.
[55] Gianico, A., Braguglia, C. M., Mescia, D., Mininni, G. (2013): Ultrasonic and thermal pretreatments to enhance the anaerobic bioconversion of olive husks. – Bioresource Technology 147: 623-626.
[56] Gnaoui, Y. E., Karouach, F., Bakraoui, M., Barzb, M., Bari, H. E. (2020): Mesophilic anaerobic digestion of food waste: Effect of thermal pretreatment on improvement of anaerobic digestion process. – Energy Reports 6: 417-422.
[57] Gou, C., Yang, Z., Huang, J., Wang, H., Xu, H., Wang, L. (2014): Effects of temperature and organic loading rate on the performance and microbial community of anaerobic co-digestion of waste activated sludge and food waste. – Chemosphere 105: 146-151.
[58] Grimberg, S. J., Hilderbrandt, D., Kinnunen, M., Rogers, S. (2015): Anaerobic digestion of food waste through the operation of a mesophilic two-phase pilot scale digester - assessment of variable loadings on system performance. – Bioresource Technology 178: 226-229.
[59] Gu, Y., Chen, X., Liu, X., Zhou, X., Zhang, Y. (2014): Effect of inoculum sources on the anaerobic digestion of rice straw. – Bioresource Technology 158: 149-155.
[60] Guo, J., Wang, W., Liu, X., Lian, S., Zheng, L. (2014): Effects of thermal pre-treatment on anaerobic co-digestion of municipal biowastes at high organic loading rate. – Chemosphere 101: 66-70.
[61] Gupta, P., Singh, R. S., Sachan, A., Vidyarthi, A. S., Gupta, A. (2012): A re-appraisal on intensification of biogas production. – Renewable Sustainable Energy Reviews 16: 4908-4916.
[62] Hamdi Muratçobanoglu, H., Gokceka, O. B., Merta, R. A., Zanb, R., Demirel, S. (2020): Simultaneous synergistic effects of graphite addition and co-digestion of food waste and cow manure: Biogas production and microbial community. – Bioresource Technology 309: 123365.
[63] Hasegawa, S., Shiota, N., Katsura, K., Akashi, A. (2000): Solubilization of organic sludge by thermophilic aerobic bacteria as a pretreatment for anaerobic digestion. – Water Science and Technology 41(3): 163-169.

http://www.aloki.hu ● ISSN 1589 1623 (Print) ● ISSN 1785 0037 (Online)
DOI: http://dx.doi.org/10.15666/aeer/1906_47954847

[64] Hegde, S., Trabold, T. A. (2019): Anaerobic digestion of food waste with unconventional co-substrates for stable biogas production at high organic loading rates. – Sustainability 11: 1-15.
[65] Holliger, C., Alves, M., Andrade, D., Angelidaki, I., Astals, S., Baier, U., Bougrier, C. (2016): Towards a standardization of biomethane potential tests. – Water Science Technology 74(11): 2515-2522.
[66] Horiuchi, J. I., Shimizu, T., Tada, K., Kanno, T., Kobayashi, M. (2002): Selective production of organic acids in anaerobic acid reactor by pH control. – Bioresource Technology 82: 209-213.
[67] Ibrahim, N., Yusoff, M. S., Aziz, H. A. (2010): Food waste characteristics after autoclaving treatment. – Proceedings 2nd International Conference on Biotechnology and Food Science (IPCBEE), Singapore.
[68] Imachi, H., Sakai, S., Ohashi, A., Harada, H., Hanada, S., Kamagata, Y., Sekiguchi, Y. (2007): Pelotomaculum propionicicum sp. nov., an anaerobic, mesophilic, obligately syntrophic, propionate-oxidizing bacterium. – International Journal of Systematic and Evolutionary Microbiology 57(Pt7): 1487-1492.
[69] Izumi, K., Okishio, Y., Nagao, N., Niwa, C., Yamamoto, S., Toda, T. (2010): Effects of particle size on anaerobic digestion of food waste. – International Biodeterioration & Biodegradation 64(7): 601-608.
[70] Jabeen, M., Zeshan Yousaf, S., Rizwan Haider, M., Malik, R. N. (2015): High-solids anaerobic co-digestion of food waste and rice husk at different organic loading rates. – International Biodeterioration & Biodegradation 102: 149-153.
[71] Jain, S., Jain, S., Wolf, I. T., Lee, J., Tong, Y. W. (2015): A comprehensive review on operating parameters and different pretreatment methodologies for anaerobic digestion of municipal solid waste. – Renewable and Sustainable Energy Reviews 52: 142-154.
[72] Jang, H. M., Ha, J. H., Park, J. M., Kim, M. S., Sommer, S. G. (2015): Comprehensive microbial analysis of combined mesophilic anaerobicethermophilic aerobic process treating high-strength food wastewater. – Water Research 73: 291-303.
[73] Jang, S., Kim, D. H., Yun, Y. M., Lee, M. K., Moon, C., Kang, W. S., Kwak, S. S., Kim, M. S. (2015): Hydrogen fermentation of food waste by alkali shock pretreatment: microbial community analysis and limitation of continuous operation. – Bioresource Technology 186: 215-222.
[74] Jayaraj, S., Deepanraj, B., Sivasubramanian, V. (2014): Study on the effect of ph on biogas production from food waste by anaerobic digestion. – 9th Annual Green Energy Conference in (IGEC-IX), Tianjin China, May 2014.
[75] Jiang, J., Li, L., Cui, M., Zhang, F., Liu, Y., Liu, Y., Long, J., Guo, Y. (2018): Anaerobic digestion of kitchen waste: The effects of source, concentration, and temperature. – Biochemical Engineering Journal 135: 91-97.
[76] Jin, Y., Li, Y., Li, J. (2016): Influence of thermal pretreatment on physical and chemical properties of kitchen waste and the efficiency of anaerobic digestion. – Journal of Environmental Management 180: 291-300.
[77] Jin, C., Sun, S., Yang, D., Sheng, W., Ma, Y., He, W., Li, G. (2021): Anaerobic digestion: An alternative resource treatment option for food waste in China. – Science of the Total Environment 779: 146397.
[78] Jung, K. K., Baek, R. O., Young, N. C., Si, W. K. (2006): Effects of temperature and hydraulic retention time on anaerobic digestion of food waste. – Journal of Bioscience and Bioengineering 102(4): 328-332.
[79] Junoh, H., Yip, C. H., Kumaran, P. (2016): Effect on Ca $(OH)_2$ pretreatment to enhance biogas production of organic food waste. – IOP Conf. Series: Earth and Environmental Science 32: 012013.
[80] Kamaruddin, M. A., Yusoff, M. S., Rui, L. M., Isa, A. M., Zawawi, M. H., Alrozi, R. (2017): An overview of municipal solid waste management and landfill leachate treatment:

http://www.aloki.hu ● ISSN 1589 1623 (Print) ● ISSN 1785 0037 (Online)
DOI: http://dx.doi.org/10.15666/aeer/1906_47954847

Malaysia and Asian perspectives. – Environmental Science and Pollution Research 24(35): 26988-27020.

[81] Kaparaju, P., Buendia, I., Ellegaard, L., Angelidaki, I. (2008): Effects of mixing on methane production during thermophilic anaerobic digestion of manure: lab-scale and pilot-scale studies. – Bioresource Technology 99: 4919-4928.

[82] Karim, K., Hoffmann, R., Klasson, K. T., Al-Dahhan, M. H. (2005): Anaerobic digestion of animal waste: effect of mode of mixing. – Water Research 39: 3597-3606.

[83] Kariyama, I. D., Zhai, X., Wu, B. (2018): Influence of mixing on anaerobic digestion efficiency in stirred tank digesters: A review. – Water Research 143: 503-517.

[84] Karki, R., Chuenchart, W., Surendra, K. C., Shrestha, S., Raskin, L., Sung, S., Hashimoto, A., Khanal, S. K. (2021): Anaerobic co-digestion: Current status and perspectives. – Bioresource Technology 330: 125001.

[85] Karouach, F., Bakraoui, M., Gnaoui, Y. E., Lahboubi, N., Bari, H. E. (2020): Effect of combined mechanical–ultrasonic pretreatment on mesophilic anaerobic digestion of household organic waste fraction in Morocco. – Energy Reports 6: 310-314.

[86] Karthikeyan, O. P., Nguyen Hao, H. T., Razaghi, A., Heimann, K. (2018): Recycling of food waste for fuel precursors using an integrated bio-refinery approach. – Bioresource Technology 248: 194-198.

[87] Kawai, M., Nagao, N., Tajima, N., Niwa, C., Matsuyama, T., Toda, T. (2014): The effect of the labile organic fraction in food waste and the substrate/inoculum ratio on anaerobic digestion for a reliable methane yield. – Bioresource Technology 157: 174-180.

[88] Khan, M. U., Ahring, B. K. (2021): Improving the biogas yield of manure: Effect of pretreatment on anaerobic digestion of the recalcitrant fraction of manure. – Bioresource Technology 321: 124427.

[89] Kim, J., Lee, C. (2016): Response of a continuous anaerobic digester to temperature transitions: A critical range for restructuring the microbial community structure and function. – Water Research 89: 241-251.

[90] Kim, M., Abdulazeez, M., Haroun, B. M., Nakhlaa, G., Kelemanc, M. (2019): Microbial communities in co-digestion of food wastes and wastewater Biosolids. – Bioresource Technology 289: 121580.

[91] Kiran, E. U., Trzcinski, A. P., Liu, Y. (2015): Enhancing the hydrolysis and methane production potential of mixed food waste by an effective enzymatic pretreatment. – Bioresource Technology 183: 47-52.

[92] Kondusamy, D., Kalamdhad, A. S. (2014): Pretreatment and anaerobic digestion of food waste for high rate methane production - A review. – Journal of Environmental Chemical Engineering 2(3): 1821-1830.

[93] Kouzi, A. I., Puranen, M., Kontro, M. H. (2020): Evaluation of the factors limiting biogas production in full-scale processes and increasing the biogas production efficiency. – Environmental Science and Pollution Research 27: 28155-28168.

[94] Kumar, A., Samadder, S. R. (2020): Performance evaluation of anaerobic digestion technology for energy recovery from organic fraction of municipal solid waste: A review. – Energy 197: 117253.

[95] Kumar, M., Dutta, S., You, S., Luo, G., Zhang, S., Show, P. L., Sawarkar, A. D., Singh, Tsang, D. C. W. (2021): A critical review on biochar for enhancing biogas production from anaerobic digestion of food waste and sludge. – Journal of Cleaner Production 305: 127143.

[96] Kuruti, K., Begum, S., Ahuja, S., Rao Anupoju, G., Juntupally, S., Gandu, B., Kumar Ahuja, D. (2017): Exploitation of rapid acidification phenomena of food waste in reducing the hydraulic retention time (HRT) of high rate anaerobic digester without conceding on biogas yield. – Bioresource Technology 226: 65-72.

[97] Labatut, R. A., Angenent, L. T., Scott, N. R. (2011): Biochemical methane potential and biodegradability of complex organic substrates. – Bioresource Technology 102(3): 2255-2264.

http://www.aloki.hu ● ISSN 1589 1623 (Print) ● ISSN 1785 0037 (Online)
DOI: http://dx.doi.org/10.15666/aeer/1906_47954847

[98] Lee, D. H., Behera, S. K., Kim, J. W., Park, H. S. (2009): Methane production potential of leachate generated from Korean food waste recycling facilities: a lab-scale study. – Waste Management 29(2): 876-882.
[99] Lee, D. J., Lee, S. Y., Bae, J. S., Kang, J. G., Kim, K. H., Rhee, S. S., Park, J. H., Cho, J. S., Chung, J., Seo, D. C. (2015): Effect of volatile fatty acid concentration on anaerobic degradation rate from field anaerobic digestion facilities treating food waste leachate in South Korea. – Journal of Chemistry: 640717.
[100] Leung, D. Y. C., Wang, J. (2016): An overview on biogas generation from anaerobic digestion of food waste. – International Journal of Green Energy 13: 119-131.
[101] Li, L., He, Q., Wei, Y., He, Q., Peng, X. (2014): Early warning indicators for monitoring the process failure of anaerobic digestion system of food waste. – Bioresource Technology 171: 491-494.
[102] Li, L., He, Q., Ma, Y., Wang, X., Peng, X. (2015): Dynamics of microbial community in a mesophilic anaerobic digester treating food waste: Relationship between community structure and process stability. – Bioresource Technology 189: 113-120.
[103] Li, Y. Y., Jin, Y. Y. (2015): Effects of thermal pretreatment on acidification phase during two-phase batch anaerobic digestion of kitchen waste. – Renewable Energy 77: 550-557.
[104] Li, Y., Jin, Y., Li, J. (2016): Enhanced split-phase resource utilization of kitchen waste by thermal pre-treatment. – Energy 98: 155-167.
[105] Li, Y., Jin, Y., Li, J., Li, H., Yu, Z., Nie, Y. (2017): Effects of thermal pretreatment on degradation kinetics of organics during kitchen waste anaerobic digestion. – Energy 118: 377-386.
[106] Li, L., Peng, X., Wang, X., Wu, D. (2018): Anaerobic digestion of food waste: A review focusing on process stability. – Bioresource Technology 248: 20-28.
[107] Li, Q., Xu, M., Wang, G., Chen, R., Qiao, W., Wang, X. (2018): Biochar assisted thermophilic co-digestion of food waste and waste activated sludge under high feedstock to seed sludge ratio in batch experiment. – Bioresource Technology 249: 1009-1016.
[108] Li, L., Kong, Z., Qin, Y., Wu, J., Zhu, A., Xiao, B., Ni, J., Kubota, K., Li, Y. Y. (2020): Temperature-phased anaerobic co-digestion of food waste and paper waste with and without recirculation: Biogas production and microbial structure. – Science of the Total Environment 724: 138168.
[109] Lim, J. W., Chen, C. L., Ho, I. J. R., Wang, J. Y. (2013): Study of microbial community and biodegradation efficiency for single and two-phase anaerobic co-digestion of brown water and food waste. – Bioresource Technology 147: 193-201.
[110] Lim, J. W., Wen, S., Wong, K., Dai, Y., Tong, Y. W. (2020): Effect of seed sludge source and start-up strategy on the performance and microbial communities of thermophilic anaerobic digestion of food waste. – Energy 203: 117922.
[111] Lindmark, J., Eriksson, P., Thorin, E. (2014): The effects of different mixing intensities during anaerobic digestion of the organic fraction of municipal solid waste. – Waste Management 34: 1391-1397.
[112] Liu, C. F., Yuan, X. Z., Zeng, G. M., Li, W. W., Li, J. (2008): Prediction of methane yield at optimum pH for anaerobic digestion of organic fraction of municipal solid waste. – Bioresource Technology 99: 882-888.
[113] Liu, X., Li, R., Ji, M., Han, L. (2013): Hydrogen and methane production by co-digestion of waste activated sludge and food waste in the two-stage fermentation process: substrate conversion and energy yield. – Bioresource Technology 146: 317-323.
[114] Liu, X., Khalid, H., Amin, F. R., Ma, X., Li, X., Chen, C., Liu, G. (2018): Effects of hydraulic retention time on anaerobic digestion performance of food waste to produce methane as a biofuel. – Environmental Technology & Innovation 11: 348-357.
[115] Liu, J., Wang, D., Yu, C., Jiang, J., Guo, M., Hantoko, D., Yana, M. (2021): A two-step process for energy-efficient conversion of food waste via supercritical water gasification: Process design, products analysis, and electricity evaluation. – Science of the Total Environment 752: 142331.

http://www.aloki.hu ● ISSN 1589 1623 (Print) ● ISSN 1785 0037 (Online)
DOI: http://dx.doi.org/10.15666/aeer/1906_47954847

[116] Lu, F., Hao, L., Zhu, M., Shao, L., He, P. (2012): Initiating methanogenesis of vegetable waste at low inoculum to substrate ratio: Importance of spatial separation. – Bioresource Technology 105: 169-173.
[117] Ma, C., Liu, J., Ye, M., Zou, L., Qian, G., Li, Y. Y. (2018): Towards utmost bioenergy conversion efficiency of food waste: Pretreatment, co-digestion, and reactor type. – Renewable and Sustainable Energy Reviews 90: 700-709.
[118] Mamimin, C., Prasertsan, P., Kongjan, P., O-Thong, S. (2017): Effects of volatile fatty acids in biohydrogen effluent on biohythane production from palm oil mill effluent under thermophilic condition. – Electronic Journal of Biotechnology 29: 78-85.
[119] Mao, C., Feng, Y., Wang, X., Ren, G. (2015): Review on research achievements of biogas from anaerobic digestion. – Renewable and Sustainable Energy Reviews 45: 540-555.
[120] Mao, L., Zhang, J., Dai, Y., Tong, Y. W. (2019): Effects of mixing time on methane production from anaerobic co-digestion of food waste and chicken manure: Experimental studies and CFD analysis. – Bioresource Technology 294: 122177.
[121] Mata-Alvarez, J., Dosta, J., Romero-Güiza, M. S., Fonoll, X., Peces, M., Astals, S. (2014): A critical review on anaerobic co-digestion achievements between 2010 and 2013. – Renewable & Sustainable Energy Reviews 36: 412-427.
[122] Menon, A., Ren, F., Wang, J. Y., Giannis, A. (2016): Effect of pretreatment techniques on food waste solubilisation and biogas production during thermophilic batch anaerobic digestion. – Journal Material Cycles Waste Management 18: 222-230.
[123] Micolucci, F., Gottardo, M., Bolzonella, D., Pavan, P. (2014): Automatic process control for stable bio-hythane production in two-phase thermophilic anaerobic digestion of food waste. – International Journal of Hydrogen Energy 39(31): 17563-17572.
[124] Nagao, N., Tajima, N., Kawai, M., Niwa, C., Kurosawa, N., Matsuyama, T., Yusoff, F. M., Toda, T. (2012): Maximum organic loading rate for the single-stage wet anaerobic digestion of food waste. – Bioresource Technology 118: 210-218.
[125] Naran, E., Toor, U. A., Kim, D. (2016): Effect of pretreatment and anaerobic co-digestion of food waste and waste activated sludge on stabilization and methane production. – International Biodegradation and Biodeterioration 113: 17-21.
[126] Nathao, C., Sirisukpoka, U., Pisutpaisal, N. (2013): Production of hydrogen and methane by one and two stage fermentation of food waste. – International Journal of Hydrogen Energy 38(35): 15764-15769.
[127] Negri, C., Ricci, M., Zilio, M., D'Imporzano, G., Qiao, W., Dong, R., Adani, F. (2020): Anaerobic digestion of food waste for bio-energy production in China and Southeast Asia: A review. – Renewable and Sustainable Energy Reviews 133: 110138.
[128] Neshat, S. A., Mohammadi, M., Najafpour, G. D., Lahijani, P. (2017): Anaerobic co-digestion of animal manures and lignocellulosic residues as a potent approach for sustainable biogas production. – Renewable and Sustainable Energy Reviews 79: 308-322.
[129] Nghiem, L. D., Koch, K., Bolzonella, D., Drewes, J. E. (2017): Full scale co-digestion of wastewater sludge and food waste: Bottlenecks and possibilities. – Renewable and Sustainable Energy Reviews 72: 354-362.
[130] Nguyen, D. C., Yeop, J. S., Choi, J., Kim, S., Chang, S. W., Jeon, B. H., Guo, W., Ngo, H. H. (2017): A new approach for concurrently improving performance of South Korean food waste valorization and renewable energy recovery via dry anaerobic digestion under mesophilic and thermophilic conditions. – Waste Management 66: 161-168.
[131] Nielsen, H., Uellendahl, H., Ahring, B. (2007): Regulation and optimization of the biogas process: propionate as a key parameter. – Biomass Bioenergy 31(11-12): 820-830.
[132] Noyola, A., Tinajero, A. (2005): Effect of biological additives and micronutrients on the anaerobic digestion of physicochemical sludge. – Water Science and Technology 52(1-2): 275-281.
[133] Oladejo, O. S., Dahunsi, S. O., Adesulu-Dahunsi, A. T., Ojo, S. O., Lawal, A. I., Idowu, E. O., Olanipekun, A. A., Ibikunle, R. A., Osueke, C. O., Ajayi, O. E., Osueke, N.,

http://www.aloki.hu ● ISSN 1589 1623 (Print) ● ISSN 1785 0037 (Online)
DOI: http://dx.doi.org/10.15666/aeer/1906_47954847

Evbuomwan, I. (2020): Energy generation from anaerobic co-digestion of food waste, cow dung and piggery dung. – Bioresource Technology 313: 123694.
[134] Ormaechea, P., Castrillon, L., Suarez-Pena, B., Megido, L., Fernandez-Nava, Y., Negral, L., Maranon, E., Rodriguez-Iglesias, J. (2018): Enhancement of biogas production from cattle manure pretreated and/or co-digested at pilot-plant scale, characterization by SEM. – Renewable Energy 126: 897-904.
[135] Owamah, H. I., Izinyon, O. C. (2015): The effect of organic loading rates (OLRs) on the performances of food wastes and maize husks anaerobic co-digestion in continuous mode. – Sustainable Energy Technologies and Assessments 11: 71-76.
[136] Pagliaccia, P., Gallipoli, A., Gianico, A., Montecchio, D., Braguglia, C. M. (2016): Single stage anaerobic bioconversion of food waste in mono and co-digestion with olive husks: impact of thermal pretreatment on hydrogen and methane production. – International Journal of Hydrogen Energy 41(2): 905-915.
[137] Pan, S. Y., Tsai, C. Y., Liu, C. W., Wang, S. W., Kim, H., Fan, C. (2021): Anaerobic co-digestion of agricultural wastes toward circular bio-economy. – iScience 24: 102704.
[138] Panigrahi, S., Dubey, B. K. (2019): A critical review on operating parameters and strategies to improve the biogas yield from anaerobic digestion of organic fraction of municipal solid waste. – Renewable Energy 143: 779-797.
[139] Panigrahi, S., Sharma, H. B., Dubey, B. K. (2020): Anaerobic co-digestion of food waste with pretreated yard waste: A comparative study of methane production, kinetic modeling and energy balance. – Journal of Cleaner Production 243: 118480.
[140] Parawira, W. (2004): Anaerobic treatment of agricultural residues and wastewater - application of high- rate reactors. – PhD Thesis, Lund University. Retrieved from ttps://lup.lub.lu.se/search/ws/files/5606523/1472236.pdf.
[141] Paritosh, K., Kushwaha, S. K., Yadav, M., Pareek, N., Chawade, A., Vivekanand, V. (2017): Food waste to energy: an overview of sustainable approaches for food waste management and nutrient recycling. – BioMed Research International, Article ID: 2370927.
[142] Paudel, S., Kang, Y., Yoo, Y.-S., Seo, G. T. (2017): Effect of volumetric organic loading rate (OLR) on H_2 and CH_4 production by two-stage anaerobic co-digestion of food waste and brown water. – Waste Management 61: 484-493.
[143] Pecorini, I. Baldi, F., Carnevale, E. A., Corti, A. (2016): Biochemical methane potential tests of different autoclaved and microwaved lignocellulosic organic fractions of municipal solid waste. – Waste Management 56: 143-150.
[144] Pleissner, D., Kwan, T. H., Lin, C. S. (2014): Fungal hydrolysis in submerged fermentation for food waste treatment and fermentation feedstock preparation. – Bioresource Technology 158: 48-54.
[145] Polprasert, C. (2007): Organic Waste Recycling - Technology and Management. – 3rd Edition. IWA Publishing.
[146] Qiang, H., Niu, Q., Chi, Y., Li, Y. (2013): Trace metals requirements for continuous thermophilic methane fermentation of high solid food waste. – Chemical Engineering Journal 222: 330-336.
[147] Qiao, W., Takayanagi, K., Niu, Q., Shofie, M., Li, Y. Y. (2013): Long-term stability of thermophilic co-digestion submerged anaerobic membrane reactor encountering high organic loading rate, persistent propionate and detectable hydrogen in biogas. – Bioresource Technology 149: 92-102.
[148] Rasapoor, M., Ajabshirchi, Y., Adl, M., Abdi, R., Gharibi, A. (2016): The effect of ultrasonic pretreatment on biogas generation yield from organic fraction of municipal solid waste under medium solids concentration circumstance. – Energy Conversion and Management 119: 444-452.
[149] Ratanatamskul, C., Manpetch, P. (2016): Comparative assessment of prototype digester configuration for biogas recovery from anaerobic co-digestion of food waste and rain tree leaf as feedstock. – International Biodeterioration & Biodegradation 113: 367-374.

http://www.aloki.hu ● ISSN 1589 1623 (Print) ● ISSN 1785 0037 (Online)
DOI: http://dx.doi.org/10.15666/aeer/1906_47954847

[150] Ren, Y., Yu, M., Wu, C., Wang, Q., Gao, M., Huang, Q., Liu, Y. (2018): A comprehensive review on food waste anaerobic digestion: Research updates and tendencies. – Bioresource Technology 247: 1069-1076.
[151] Sabri, R. M., Jahim, J. M., Takriff, M. S., Yunus, N., Trisakti, B. (2018): Comparison of methane production utilizing raw and acidogenic effluent coming from sago starch processing in anaerobic sequencing batch reactor (ASBR). – Jurnal Kejuruteraan SI 1(7): 27-36.
[152] Salihu, A., Alam, Z. (2016): Pretreatment methods of organic wastes for biogas production. – Journal of Applied Science 16(3): 124-137.
[153] Sarto, S., Hildayati, R., Syaichurrozi, I. (2019): Effect of chemical pretreatment using sulfuric acid on biogas production from water hyacinth and kinetics. – Renewable Energy 132: 335-350.
[154] Sawatdeenarunat, C., Saipa, S., Suaisom, P. (2021): Methane recovery from cassava starch wastewater via anaerobic digestion: Effect of inoculum source and kinetic study. – Asia-Pacific Journal of Science and Technology 26(2): 1-9.
[155] Sen, B., Aravind, J., Kanmani, P., Lay, C. H. (2016): State of the art and future concept of food waste fermentation to bioenergy. – Renewable and Sustainable Energy Reviews 53: 547-557.
[156] Seon, J. Y., Lee, T., Lee, S. C., Pham, H. D., Woo, H. C., Song, M. (2014): Bacterial community structure in maximum volatile fatty acidsproduction from alginate in acidogenesis. – Bioresource Technology 157(1): 22-27.
[157] Seruga, P. (2021): The municipal solid waste management system with anaerobic digestion. – Energies 14: 2067.
[158] Shahriari, H., Warith, M., Hamoda, M., Kennedy, K. J. (2012): Anaerobic digestion of organic fraction of municipal solid waste combining two pretreatment modalities, high temperature microwave and hydrogen peroxide. – Waste Management 32: 41-52.
[159] Shen, F., Yuan, H., Pang, Y., Chen, S., Zhu, B., Zou, D., Liu, Y., Ma, J., Yu, L., Li, X. (2013): Performances of anaerobic co-digestion of fruit & vegetable waste (FVW) and food waste (FW): single-phase vs. two-phase. – Bioresource Technology 144: 80-85.
[160] Shi, X. S., Dong, J. J., Yu, J. H., Yin, H., Hu, S. M., Huang, S. X. (2017): Effect of hydraulic retention time on anaerobic digestion of wheat straw in the semicontinuous continuous stirred-tank reactors. – BioMed Research International 2017: 2457805.
[161] Siddique, M. N. I., Abdul Munaim, M. S., Wahid, Z. (2016): Role of hydraulic retention time in enhancing bioenergy generation from petrochemical wastewater. – Journal of Cleaner Production 133: 504-510.
[162] Siddique, M. N. I., Wahid, Z. A. (2018): Achievements and perspectives of anaerobic co-digestion: A review. – Journal of Cleaner Production 194: 359-371.
[163] Singh, B., Szamosi, Z., Simenfalvi, Z. (2020): Impact of mixing intensity and duration on biogas production in an anaerobic digester: A review. – Critical Reviews in Biotechnology 40(4): 508-521.
[164] Sousa, D. Z., Smidt, H., Alves, M. M., Stams, A. J. M. (2007): Syntrophomonas zehnderi sp. nov., an anaerobe that degrades long-chain fatty acids in co-culture with Methanobacterium formicicum. – International Journal of Systematic and Evolutionary Microbiology 57(Pt3): 609-615.
[165] Stabnikova, O., Liu, X. Y., Wang, J. Y. (2008): Digestion of frozen/thawed food waste in the hybrid anaerobic solid-liquid system. – Waste Management 28: 1654-1659.
[166] SWCorp News (2016): http://www.swcorp.gov.my/swcorpnews/2016/SWCorpNews-7.pdf. – Accessed on 20/8/2016.
[167] Ta, D. T., Lin, C. Y., Ngoc Ta, T. M., Chu, C. Y. (2020): Biohythane production via single-stage fermentation using gel-entrapped anaerobic microorganisms: Effect of hydraulic retention time. – Bioresource Technology 317: 123986.
[168] Tampio, E., Ervasti, S., Paavola, T. (2014): Anaerobic digestion of autoclaved and untreated food waste. – Waste Management 34: 370-377.

http://www.aloki.hu ● ISSN 1589 1623 (Print) ● ISSN 1785 0037 (Online)
DOI: http://dx.doi.org/10.15666/aeer/1906_47954847

[169] Tanimu, I. M., Ghazi, T. I. M., Harun, M. R., Idris, A. (2014): Effect of carbon to nitrogen ratio of food waste on biogas methane production in a batch mesophilic anaerobic digester. – International Journal of Innovation, Management and Technology 5(2): 116-119.
[170] Tayyab, A., Ahmad, Z., Mahmood, T., Khalid, A., Qadeer, S., Mahmood, S., Andleeb, S., Anjum, M. (2019): Anaerobic co-digestion of catering food waste utilizing *Parthenium hysterophorus* as co-substrate for biogas production. – Biomass and Bioenergy 124: 74-82.
[171] Tchobanoglous, G., Burton, F. L., Stensel, H. D. (2003): Wastewater Engineering Treatment and Reuse. – 4th Edition, Tata Mc Graw-Hill. New Delhi, India.
[172] Tong, J., Lu, X., Zhang, J., Angelidaki, I., Wei, Y. (2018): Factors influencing the fate of antibiotic resistance genes during thermochemical pretreatment and anaerobic digestion of pharmaceutical waste sludge. – Environmental Pollution 243: 1403-1413.
[173] Tran, D. (2017): Hydrodynamic cavitation applied to food waste anaerobic digestion. – Master Thesis. Linkoping University. Retrieved from http://www.diva-portal.org/smash/get/diva2:930482/fulltext01.pdf.
[174] Vavouraki, A. I., Angelis, E. M., Kornaros, M. (2013): Optimization of thermo-chemical hydrolysis of kitchen wastes. – Waste Management 33: 740-745.
[175] Ventura, J. R. S., Lee, J., Jahng, D. (2014): A comparative study on the alternating mesophilic and thermophilic two-stage anaerobic digestion of food waste. – Journal of Environmental Sciences 26(6): 1274-1283.
[176] Verma, S. (2002): Anaerobic digestion of biodegradable organics in municipal solid wastes. – Master Thesis. Columbia University. Retrieved from https://secureservercdn.net/198.71.233.199/epm.300.myftpupload.com/wp-content/uploads/2020/10/Verma_thesis.pdf.
[177] Vijayaraghavan, K., Varma, V. S., Kamala Nalini, S. P. (2012): Hydrogen generation from biological solid waste of milk processing effluent treatment plant. – International Journal of Current Trends and Resources 1: 17-23.
[178] Voelklein, M. A., Jacob, A., O'Shea, R., Murphy, J. D. (2016): Assessment of increasing loading rate on two-stage digestion of food waste. – Bioresource Technology 202: 172-180.
[179] Wang, M., Sun, X., Li, P., Yin, L., Liu, D., Zhang, Y., Li, W., Zheng, G. (2014): A novel alternate feeding mode for semi-continuous anaerobic co-digestion of food waste with chicken manure. – Bioresource Technology 164: 309-314.
[180] Wang, P., Wang, H., Qiu, Y., Ren, L., Jiang, B. (2018): Microbial characteristics in anaerobic digestion process of food waste for methane production–A review. – Bioresource Technology 248: 29-36.
[181] Wang, Z., Jiang, Y., Wang, S., Zhang, Y., Hu, Y., Hue, Z., Wu, G., Zhan, X. (2020): Impact of total solids content on anaerobic co-digestion of pig manure and food waste: Insights into shifting of the methanogenic pathway. – Waste Management 114: 96-106.
[182] Wu, B., Wang, X., Deng, Y. Y., He, X. L., Li, Z. W., Li, Q., Qin, H., Chen, J. T., He, M. X., Zhang, M., Hu, G. Q., Yin, X. B. (2016): Adaption of microbial community during the start-up stage of a thermophilic anaerobic digester treating food waste. – Bioscience, Biotechnology, and Biochemistry 80(10): 2025-2032.
[183] Wu, L.-J., Kobayashi, T., Kuramochi, H., Li, Y.-Y., Xu, K.-Q. (2016): Improved biogas production from food waste by co-digestion with de-oiled grease trap waste. – Bioresource Technology 201: 237-244.
[184] Xiao, B., Qin, Y., Zhang, W., Wu, J., Qiang, H., Liu, J., Li, Y. Y. (2018): Temperature-phased anaerobic digestion of food waste: A comparison with single-stage digestions based on performance and energy balance. – Bioresource Technology 249: 826-834.
[185] Yamada, T., Sekiguchi, Y., Hanada, S. (2006): Anaerolinea thermolimosa sp. nov., Levilinea saccharolytica gen. nov., sp. nov. and Leptolinea tardivitalis gen. nov., sp. nov., novel filamentous anaerobes, and description of the new classes Anaerolineae classis nov. and Caldilineae classis nov. in the bacterial phylum Chloroflexi. – International Journal of Systematic and Evolutionary Microbiology 56: 1331-1340.

http://www.aloki.hu ● ISSN 1589 1623 (Print) ● ISSN 1785 0037 (Online)
DOI: http://dx.doi.org/10.15666/aeer/1906_47954847

[186] Yang, L., Huang, Y., Zhao, M. (2015): Enhancing biogas generation performance from food wastes by high-solids thermophilic anaerobic digestion: effect of pH adjustment. – International Biodeterioration and Biodegradation 105: 153-159.
[187] Yang, Z., Koh, S. K., Ng, W. C., Lim, R. C. J., Tan, H. T. W., Tong, Y. W., Wang, C. H. (2016): Potential application of gasification to recycle food waste and rehabilitate acidic soil from secondary forests on degraded land in Southeast Asia. – Journal of Environmental Management 172: 40-48.
[188] Yeshanew, M. M., Frunzo, L., Pirozzi, F., Lens, P. N. L., Esposito, G. (2016): Production of biohythane from food waste via an integrated system of continuously stirred tank and anaerobic fixed bed reactors. – Bioresource Technology 220: 312-322.
[189] Yin, Y., Liu, Y., Meng, S., Kiran, E. U., Liu, Y. (2016): Enzymatic pretreatment of activated sludge, food waste and their mixture for enhanced bioenergy recovery and waste volume reduction via anaerobic digestion. – Applied Energy 179: 1131-1137.
[190] Yirong, C., Heaven, S., Banks, C. J. (2015): Effect of a trace element addition strategy on volatile fatty acid accumulation in thermophilic anaerobic digestion of food waste. – Waste Biomass Valorization 6(1): 1-12.
[191] Yong, Z., Dong, Y., Zhang, X., Tan, T. (2015): Anaerobic co-digestion of food waste and straw for biogas production. – Renewable Energy 78: 527-530.
[192] Zaher, U., Cheong, D. Y., Wu, B., Chen, S. (2007): Producing energy and fertilizer from organic municipal solid wastes. – Olympia, WA: Department of Biological Systems Engineering, WSU. http://www.ecy.wa.gov/programs/ swfa/solidwastedata/.
[193] Zamanzadeh, M., Hagen, L. H., Svensson, K., Linjordet, R., Horn, S. J. (2016): Anaerobic digestion of food waste - effect of recirculation and temperature on performance and microbiology. – Water Research 96: 246-254.
[194] Zamanzadeh, M., Hagen, L. H., Svensson, K., Linjordet, R., Horn, S. J. (2017): Biogas production from food waste via co-digestion and digestion- effects on performance and microbial ecology. – Scientific Reports 7: 1-12.
[195] Zamri, M. F. M. A., Hasmady, S., Akhiar, A., Ideris, F., Shamsuddin, A. H., Mofijur, M., Fattah, I. M. R., Mahlia, T. M. I. (2021): A comprehensive review on anaerobic digestion of organic fraction of municipal solid waste. – Renewable and Sustainable Energy Reviews 137: 110637.
[196] Zhang, P., Chen, Y., Zhou, Q. (2009): Waste activated sludge hydrolysis and short-chain fatty acids accumulation under mesophilic and thermophilic conditions: effect of pH. – Water Research 43: 3735-3742.
[197] Zhang, L., Lee, Y. W., Jahng, D. (2011): Anaerobic co-digestion of food waste and piggery wastewater: focusing on the role of trace elements. – Bioresource Technology 102(8): 5048-5059.
[198] Zhang, C., Su, H., Tan, T. (2013a): Batch and semi-continuous anaerobic digestion of food waste in a dual solid–liquid system. – Bioresource Technology 145: 10-16.
[199] Zhang, Z. L., Zhang, L., Zhou, Y. L., Chen, J. C., Liang, Y. M., Wei, L. (2013b): Pilot scale operation of enhanced anaerobic digestion of nutrient-deficient municipal sludge by ultrasonic pretreatment and co-digestion of kitchen garbage. – Journal of Environmental Chemical Engineering 1(1-2): 73-78.
[200] Zhang, C., Su, H., Baeyens, J., Tan, T. (2014): Reviewing the anaerobic digestion of food waste for biogas production. – Renewable and Sustainable Energy Reviews 38: 383-392.
[201] Zhang, C., Su, H., Wang, Z., Tan, T., Qin, P. (2015): Biogas by semi-continuous anaerobic digestion of food waste. – Applied Biochemical Biotechnology 175: 3901-3914.
[202] Zhang, W., Wu, S., Guo, J., Zhou, J., Dong, R. (2015a): Performance and kinetic evaluation of semi-continuously fed anaerobic digesters treating food waste: role of trace elements. – Bioresource Technology 178: 297-305.
[203] Zhang, W., Zhang, L., Li, A. (2015b): Anaerobic co-digestion of food waste with MSW incineration plant fresh leachate: process performance and synergistic effects. – Chemical Engineering Journal 259: 795-805.

http://www.aloki.hu ● ISSN 1589 1623 (Print) ● ISSN 1785 0037 (Online)
DOI: http://dx.doi.org/10.15666/aeer/1906_47954847

[204] Zhang, J., Lv, C., Tong, J., Liu, J., Liu, J., Yu, D., Wang, Y., Chen, M., Wei, Y. (2016): Optimization and microbial community analysis of anaerobic co-digestion of food waste and sewage sludge based on microwave pretreatment. – Bioresource Technology 200: 253-261.
[205] Zhang, W., Lang, Q., Fang, M., Li, X., Bah, H., Dong, H., Dong, R. (2017): Combined effect of crude fat content and initial substrate concentration on batch anaerobic digestion characteristics of food waste. – Bioresource Technology 232: 304-312.
[206] Zhang, J., Loh, K. C., Li, W., Lim, J. W., Dai, Y., Tong, Y. W. (2017): Three-stage anaerobic digester for food waste. – Applied Energy 194: 287-295.
[207] Zhang, L., Loh, K. C., Zhang, J. (2018): Food waste enhanced anaerobic digestion of biologically pretreated yard waste: Analysis of cellulose crystallinity and microbial communities. – Waste Management 79: 109-119.
[208] Zhang, J., Hu, Q., Qu, Y., Dai, Y., He, Y., Wang, C. H., Tong, Y. W. (2020): Integrating food waste sorting system with anaerobic digestion and gasification for hydrogen and methane co-production. – Applied Energy 257: 113988.
[209] Zhang, S., Zou, L., Wan, Y., Ye, M., Ye, J., Li, Y. Y., Liu, J. (2020): Using an expended granular sludge bed reactor for advanced anaerobic digestion of food waste pretreated with enzyme: The feasibility and its performance. – Bioresource Technology 311: 123504.
[210] Zhou, M., Yan, B., Wong, J. W. C., Zhang, Y. (2018): Enhanced volatile fatty acids production from anaerobic fermentation of food waste: A mini-review focusing on acidogenic metabolic pathways. – Bioresource Technology 248: 68-78.
[211] Zou, L., Ma, C., Liu, J., Li, M., Ye, M., Qian, G. (2016): Pretreatment of food waste with high voltage pulse discharge towards methane production enhancement. – Bioresource Technology 222: 82-88.

http://www.aloki.hu ● ISSN 1589 1623 (Print) ● ISSN 1785 0037 (Online)
DOI: http://dx.doi.org/10.15666/aeer/1906_47954847

COMPARATIVE ANALYSIS OF POTENTIAL EVAPOTRANSPIRATION CALCULATION METHODS WITH ERA-REANALYSIS CLIMATE MODELS' PROJECTIONS IN WESTERN ASIA, JORDAN

AL-SHIBLI, F. M.[1*] – OTTOM, M. A.[2] – SAOUB, H.[3] – AL-WESHAH, R.[4]

[1]*Land, Water and environment Department, School of Agriculture, University of Jordan, 11942 Amman, Jordan*

[2]*Department of Information Systems, Yarmouk University, 21163 Irbid, Jordan*

[3]*Department of Horticulture and Crop Science, School of Agriculture, University of Jordan, 11942 Amman, Jordan*

[4]*Department of Civil Engineering, School of Engineering, University of Jordan, 11942 Amman, Jordan*

[*]*Corresponding author*
e-mail: f.shibli@ju.edu.jo

(Received 21st May 2021; accepted 3rd Sep 2021)

Abstract. Evapotranspiration calculations are essential in quantifying available water, hydrological modelling, monitoring, and planning for drought occurrence and predicting its indices. Where observations are sparse and data quality is questionable; the need for simplified algorithm is urged. Thirteen models were used to calculate potential evapotranspiration (ET_p) on daily and monthly time series meteorological data in Central Jordan-Amman City. Temperature-based, Class A-Pan evaporation (1970-2013), and solar radiation-based methods (1986-1999) were elaborated to estimate the reference ET. Evaluation and benchmarking were performed based on regression algorithm of linearity assumption against the climate models ETs projections of CMIP5-RCP 2.6, CLM-ERAi, Penman Monteith ERA Interim, and Priestley Taylor ERA-CLM. All methods to estimate ET ratify significant trends to the state of local climate. The analysis showed asymmetry between both CMIP5-RCP 2.6 and CLM-ERAi outputs and calculated ETs but inconsistent with Penman Monteith ERA Interim and Priestley Taylor ERA-CLM. Penman Monteith ERA-Interim demonstrates the literature values that vary from 51 to 280 mm/month. Blaney Criddle and Hargreaves temperature and solar based formulas prototyped the potential evapotranspiration (R^2 = 0.99-0.97) followed by Makkink and Jensen-Haise radiation-based formulas (R^2 = 0.97-0.96). The remaining models need to be calibrated under the local conditions due to its limitation in the current constants.
Keywords: *temperature-based, solar radiation-based ET, Pan evaporation, Amman - Jordan, CMIP5, ECMWF reanalysis*

Introduction

Evapotranspiration is a main grouping of water balance since it includes the plant water uptake and evaporation and direct evaporation from soil. It can be defined as the maximum rate of evaporation and transpiration from fully covered crops with enough water applied to a field (Xu and Singh, 2001). Hence, many equations have developed over years to estimate the potential evapotranspiration based on the dependent variables that is mostly climatological quantities. Potential evapotranspiration is usually calculated as main input to hydrological models and simulated by climate models. Generally,

http://www.aloki.hu ● ISSN 1589 1623 (Print) ● ISSN 1785 0037 (Online)
DOI: http://dx.doi.org/10.15666/aeer/1906_48494879

temperature-based methods, solar radiation methods, class A-pan evaporation equation and aerodynamic and mass transfer-based methods are used.

The occurrence of climate extremes has increased as indices of climate change and variability which cause less available water to all sectors (Dingre and Gorantiwar, 2020). The most consumptive uses go to municipal and agricultural sectors (Al-Shibli et al., 2017) which urge to manage use in watering crops by unbiased evapotranspiration calculations. The importance of evapotranspiration calculations reflects the available water content after each precipitation event. The difference of rainfall and ET reflects the available water (Comair et al., 2012) diagnoses the drought, flood events and the trends of each rate. Particularly in limited water resources lands, ET calculations are essential for predicting drought and its indices.

Many studies use Penman method to calculate crop water requirement under semi-arid conditions (Dingre and Gorantiwar, 2020). Shahin (2007) has reported Jordan Rift evaporation by using three methods: Penman, Wartena and Neumann formulas. The yearly evaporation found by the three methods were; 2042 mm, 1685 mm, 1708 mm, respectively (Wartena, 1959). Another study by Al-Mahamid (2005) demonstrated long-term seasonal ET values which vary from 65 to 170 mm/month during winter months and vary from 129 to 250 mm/month during summer over Amman-Zarqa Basin using Penman-Monteith method. According to the same study, ET reaches 640-680 mm/month in some parts of the basin. Human induced-climate change and natural climate variability have contributed to drier dry seasons globally according to recent reconstruction studies (Padrón et al., 2020). The study reanalyzed the climate models to show the effects of climate change on the available water. It revealed the reason behind this dryness was the increasing of evapotranspiration inconsistently with the decreasing in precipitation over decades (Padrón et al., 2020). Regarding actual evapotranspiration, a new algorithm was developed by Guerschman et al. (2009) based on MODIS-Terra data images and calibrated using actual reading from seven stations across Australia then compared to average yearly difference between precipitation and runoff. The model showed promising approach since the actual ET values were fit with the runoff outputs especially in dry lands of study sites. The study elaborated a list of methods from each dependent variable-based equation excluding micrometeorological variables estimating the potential evapotranspiration.

Due to scarce data recordings and being as raw measures, it is required to specify the best method to calculate ET for hydro-meteorological modelling use and to quantify the available water remaining after each precipitation event. The study has investigated the trends of each based method with respect to climate models. The study compares the different potential evapotranspiration models in the middle of Jordan for the period from 1970 to 2013 using temperature-based, solar-based and pan evaporation methods. The comparison concluded the resemble trends in calculated methods' quality to represent the variations in weather and climates.

Data and Methods

Study area

Due to the scarce data, the study has focused on the most informative weather stations that have recorded most climate variables needed for the aim of the study sourced from Jordan Meteorological Department (JMD). The highest quality available observations are recorded in Amman Civil Airport Station. Missing data were filled from the neighbouring

http://www.aloki.hu ● ISSN 1589 1623 (Print) ● ISSN 1785 0037 (Online)
DOI: http://dx.doi.org/10.15666/aeer/1906_48494879

weather stations: Madaba, Salt and Queen Alia International Airport which distributed across the study area across the centre of Jordan-Amman as shown in (*Fig. 1*).

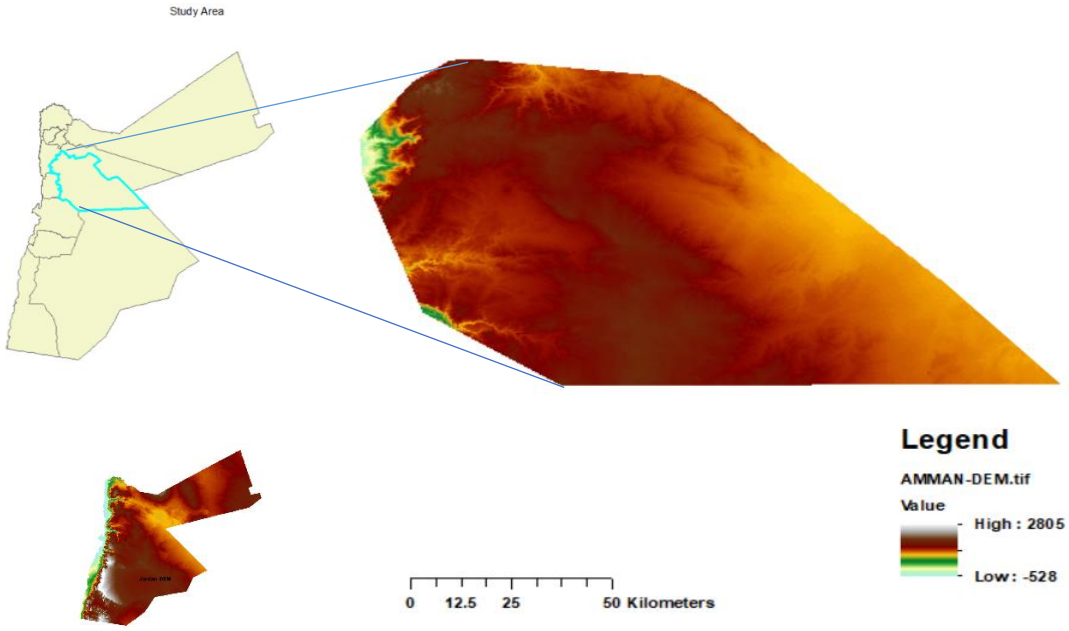

Figure 1. *Study area in the center of Jordan. Digital Elevation Model (DEM) is retrieved from SRTM Data – CGIAR-CSI SRTM and modified for cropping purposes*

ET Calculations

Thirteen formulas were used to calculate potential evapotranspiration on daily and monthly time series of meteorological data in Central Jordan-Amman. Temperature-, solar radiation-based methods and Class A-Pan evaporation were elaborated to estimate the potential evapotranspiration. Pre-whitening of observations datasets were avoided since the slope of trend is high and the sample size is large (Bayazit and Önöz, 2007).

Temperature-based and Pan methods calculated ET_p from Jan 1979 to Dec 2013 since the available ERA reanalysis data is only during this period. The analysis emphasized on (Jan 1979-Jan 1999) time slice comparing with Penman Monteith-ERA Interim, and (Jan 1979-Dec 2013) time slice comparing with Priestley Taylor ERA-CLM.

Solar radiation-based methods calculated ET_p from April 1986 to Dec 1999 since the available radiation readings are only during this period. Therefore, the analysis emphasized on (April 1986-Jan 1999) time slice comparing with Penman Monteith-ERA Interim, and (April 1986-Dec 1999) time slice with Priestley Taylor ERA-CLM.

Air Temperature-based Potential Evapotranspiration

By availability of air maximum and minimum temperatures as daily recorded, temperatures-based equations can be used to calculate potential evapotranspiration. The following methods are discussed and used in this study.

- Hargreaves Method

http://www.aloki.hu ● ISSN 1589 1623 (Print) ● ISSN 1785 0037 (Online)
DOI: http://dx.doi.org/10.15666/aeer/1906_48494879

Hargreaves' first equation is written as in *Eq. 1* (Hargreaves et al., 1985):

$$ET\circ = 0.0023\ Ra\sqrt{TD}\ (T_a + 17.8) \quad \text{(Eq.1)}$$

where; $ET\circ$ is the potential Evapotranspiration in mm/day; TD is the temperature difference (°C); T_a is mean air temperature (°C); and Ra is the water equivalent of extra-terrestrial radiation (mm/day). The equation has been modified many times (like: Allen et al., 1998; Trajkovic and Kolakovic, 2009) under different climate conditions where Talaee (2014) found that the best performance of the original Hargreaves method was in humid climate. A simple modification to Hargreaves equation in semi-arid and windy regions might require only precipitation daily measures (Talaee, 2014).

- Kharrufa Method

$$ET\circ = 0.34\ p\ Ta^{1.3} \quad \text{(Eq.2)}$$

This method is used in arid and semi-arid climates by using another variable which is the mean daily percentage of annual daytime hours (p) (Kharrufa, 1985); where $ET\circ$ is Kharrufa potential evapotranspiration. A study for Xu and Singh (2001) found that Kharrufa *Eq. 2* has seasonal bias especially in humid climate.

- Blaney-Criddle Method

Blaney and Criddle method (Blaney, 1952) and its modified formula below (*Eq. 3*) estimated the reference evapotranspiration ET from a reference crop since it included the monthly consumptive use coefficient k which depends on vegetation type, location and season (Blaney and Criddle, 1962). For the study, the study has estimated ET/k avoiding crop specification.

$$ET/k = p\ *(0.46Ta + 8.13) \quad \text{(Eq.3)}$$

where; p is the percentage of total daytime hours for the period used out of total daytime hours of the year (Xu and Singh, 2001) and can be calculated using site information for latitude and Julian day (Rahimikhoob and Hosseinzadeh, 2014) and Ta as mentioned earlier. This method has been used as alternative equation to NOAA images for irrigated agriculture in a semi-arid region estimating $ET\circ$.

- Romanenko Method

Romanenko method is derived from the relation between monthly evapotranspiration and both variables mean air temperature Ta and mean monthly relative humidity Rh (Romanenko, 1961).

$$ET = 0.0018(25 + Ta)^2(100 - Rh) \quad \text{(Eq.4)}$$

Romanenko original constants were recalibrated by many studies and concluded that the constant (0.002) might be used to estimate evapotranspiration in the Romanenko (*Eq. 4*) for many areas such as Sasireka and Xu studies (Xu and Singh, 2001; Sasireka et al., 2017) since the calculated ET by Romanenko was the most consistent results.

- Thornthwaite Method

It is an empirical method to estimate potential ET based on climate data such as radiation where this method works better in rainy seasons (Bautista et al., 2009). To

http://www.aloki.hu ● ISSN 1589 1623 (Print) ● ISSN 1785 0037 (Online)
DOI: http://dx.doi.org/10.15666/aeer/1906_48494879

calculate potential evapotranspiration ET' (*Eq. 5*), it requires (Thornthwaite, 1948) the average daily or monthly temperature Ta in °C, the annual heat index I which is the summation *Eq. 6* of 12 monthly indices i which can be estimated again by Ta (*Eq. 7*), then to the power (a) of cubic phrase (written below in *Eq. 8*) of annual heat index I and the constant 16 (Xu and Singh, 2001).

$$ET' = 16\left(\frac{10Ta}{I}\right)^{a} \quad \text{(Eq.5)}$$

$$I = \sum_{j=1}^{12} ij \quad \text{(Eq.6)}$$

$$i = \left(\frac{Ta}{5}\right)^{1.51} \quad \text{(Eq.7)}$$

$$a = 67.5 * 10^{-8} * I^3 - 77.1 * 10^{-6} * I^2 + 0.0179 * I + 0.492 \quad \text{(Eq.8)}$$

Although using the original constants in Thornthwaite method could result large error as in Sasireka and Xu (Xu and Singh, 2001; Sasireka et al., 2017) used 25.69 instead of 16, it did not provide the best performance among temperature-based ET methods in semiarid climates (Akhavan et al., 2019). Since each month differs in average daylight hours d and number of days in the month N, the adjusted evapotranspiration ET as obtained in (*Eq. 9*) is calculated according to site latitude and season.

$$ET = ET'\left(\frac{d}{12}\right) * \left(\frac{N}{30}\right) \quad \text{(Eq.9)}$$

Despite Thornthwaite, as temperature decisive method, is suitable to assess drought (Ogunrinde et al., 2020), it worsens the results in arid regions (Zhou et al., 2020) due to rapid warming up recently (Duffy et al., 2021).

- Hamon Method

Hamon potential ET formula (*Eq. 10*) depends on daylight hours for a given day D^2, and basically on determining the saturated water vapor density Pt which calculated through exponential formula (*Eq. 11*) of air temperature Ta (Hamon, 1963).

$$ET = 0.55\, D^2 * Pt \quad \text{(Eq.10)}$$

$$Pt = 4.95 * e^{(0.062\, Ta)}/100 \quad \text{(Eq.11)}$$

The use of original constants in the algorithm underestimated ET (Xu and Singh, 2001) whereas Zhou et al. (2020) found increasing dryness trend of PET in arid regions with least correlation but estimated severe drought in semi-arid and semi humid land.

Solar radiation-based potential evapotranspiration

- Jensen-Haise Method

Jensen-Haise estimated evapotranspiration in semi-arid and arid climate by recorded mean temperature *Ta* which required to calculate latent heat of vaporization λ in cal/cm^3 as in *Eq. 12* (Jensen and Haise, 1963).

http://www.aloki.hu ● ISSN 1589 1623 (Print) ● ISSN 1785 0037 (Online)
DOI: http://dx.doi.org/10.15666/aeer/1906_48494879

$$\lambda\,(cal/g) = 595 - (0.51 * Ta) \quad \text{(Eq.12)}$$

The main algorithm (*Eq. 13*) uses daily total solar radiation *Rs* (cal/cm^2) that suitable for light to moderate windy Mediterranean climates where daily maximum temperature is not available (Samaras et al., 2014). Radiation based methods work better than the temperature-based methods especially for rainfall-runoff modelling studies (Bormann, 2011).

$$ET = 0.025\,(Ta - (-3)) * Rs/\lambda \quad \text{(Eq.13)}$$

- Hargreaves method

The same inputs parameters that used in Jensen-Haise method are the same as in Hargreaves radiation formula shown in *Eq. 14* (Hargreaves, 1994; Hargreaves and Allen, 2003) where Ct is empirical coefficient equals 17.8 (Hargreaves, 1994).

$$ET = 0.0135(Ta + Ct)Rs/\lambda \quad \text{(Eq.14)}$$

Since complex calibration of Hargreaves formula by using the real Rs and large number of variables led to less accuracy, the simplest (Allen, 1995) linear regression approach produced higher accuracy instead (Gomariz-Castillo et al., 2018).

- Abtew Method

This method (*Eq. 16*) is better used in warm humid to semi-humid climates with given solar radiation Rs in MJ/m^2/day and λ is in MJ/Kg (Abtew, 1996; Xu, 2002) and can be calculated as in *Eq. 16*, further to some studies, Abtew formula performed better in semiarid area (Akhavan et al., 2019).

$$\lambda = 2.501 - (2.361 * 10^{-3})\,Ta \quad \text{(Eq.15)}$$

K is the linear regression dimensionless coefficient equals 0.15. In regard to winds, the conditions should not exceed moderate conditions (Samaras et al., 2014).

$$ET = K * Rs/\lambda \quad \text{(Eq.16)}$$

- Makkink Method

The method (Makkink, 1957) performed better in cool humid and light-windy conditions (Samaras et al., 2014). The *Eq. 17* requires (Hansen, 1984) the slope of saturation vapor pressure curve Δ by temperature showing in *Eq. 18*:

$$ET = 0.61\,\frac{\Delta}{\Delta+\boldsymbol{\gamma}}\frac{Rs}{58.5} - 0.012 \quad \text{(Eq.17)}$$

$$\Delta = 33.8639[0.05904 * (0.00738Ta + 0.8072)\text{^}7) - 0.0000342] \quad \text{(Eq.18)}$$

P is an atmospheric pressure in mbar at elevation above sea level in metres where assumed the average of Amman with maximum 1100 m and minimum 700 m elevation equals 900 m, so P is around 918.05 mbar calculated by *Eq. 19*. γ is the psychometric constant (in mbar/°C) can be calculated by *Eq. 20* from the pressure and humidity

http://www.aloki.hu ● ISSN 1589 1623 (Print) ● ISSN 1785 0037 (Online)
DOI: http://dx.doi.org/10.15666/aeer/1906_48494879

dependent variable Cp which ranging from (0.2397 to 0.26 cal/g/°C), and assumed here in the study as 0.242 (Xu, 2002).

$$\gamma = \frac{Cp * P}{0.622\lambda} \quad \text{(Eq.19)}$$

$$P = 1013 - 0.1055 * EL \quad \text{(Eq.20)}$$

The latent heat λ is calculated by temperature °C as mentioned earlier, and then ET estimates by the *Eq. 17*. Sabziparvar and Tabari (2010) reported that Hargreaves method was the best performed radiation-based ET among other methods in arid and semi-arid climates.

- Doorenbos and Pruitt Method

Another recommended radiation method which used different climate parameteres is Doorenbos and Pruitt method *Eq. 21* (Doorenbos, 1977). It required data of wind speed Ud (m/sec), relative humidity RH (%) to calculate adjustment coefficient a as in *Eq. 22*:

$$ET = a\left[\frac{\Delta}{\Delta+\gamma} Rs\right] + b \quad \text{(Eq.21)}$$

$$a = 1.066 - 0.13 * 10^{-2} RH + 0.045 Ud - 0.20 * 10^{-3} RH * Ud - 0.315 * 10^{-4} RH^2 - 0.11 * 10^{-2} Ud^2 \quad \text{(Eq.22)}$$

In Doorenbos and Pruitt method, Rs is in mm/day, b equals (-0.3) (Xu, 2002) and the remaining notations are all as same as in Makkink method. Fernández et al. (2010) found that Doorenbos and Pruitt calibrated radiation method was one of the most suitable approaches to estimate ET under standard conditions in Mediterranean climates.

Pan Evaporation Method

The evaporation Ep from a Pan with specific dimensions is an uncomplicated tool to estimate reference evapotranspiration (*Eq. 23*) under different climate conditions by determining pan coefficient Kp.

$$ET = Ep * Kp \quad \text{(Eq.23)}$$

Different algorithms are used to calculate pan coefficient. In this study, two methods were applied to estimate the coefficient by given data (Tabari et al., 2013) of wind speed at 2.0 m height $U2$, relative humidity, and the natural logarithm of fetch upwind distance F (100 m acquiring for the maximum ET estimates) which are:

- Orange Kpan

Orang (1998) has concluded the linear logarithm (*Eq. 24*) of fetch upwind distance with wind speed and relative humidity.

$$Kpan = 0.51206 - (0.000321 * U2) + (0.002889 * RH) + \left(0.03188 * ln(F)\right) - (0.000107 * RH * \ln(F)) \quad \text{(Eq.24)}$$

http://www.aloki.hu ● ISSN 1589 1623 (Print) ● ISSN 1785 0037 (Online)
DOI: http://dx.doi.org/10.15666/aeer/1906_48494879

- Allen Kpan

Allen et al. (1998) has computed the coefficient (*Eq. 25*) by the quadratic natural log of F comparing the evaporation from the pan with values of reference ET from different crops under different growth stages.

$$Kpan = 0.108 - (0.0286 * U2) + 0.0422 * ln(F) + 0.1434 * \ln(RH) - 0.000631 * [\ln(F)]^2 * \ln(RH) \quad \text{(Eq.25)}$$

Climate models

There are wide range of climate simulations that illustrate the history and future climate using wide range of systematic algorithms and theories called climate models projections. Each model represents range of possible future scenarios of climate parameters and range of carbon emission scenarios (RCPs) based on historical baselines vary with time and place. Coupled Model Intercomparison Project Phase 5 (CMIP5) is an ensemble representing of 34 models, which predict 1.8 ± 0.6 °C the increase of transient climate response in temperature (Flato et al., 2013; Nahar et al., 2020; Dosio et al., 2021). If the carbon emission concentration releases 2.2 watt/m^2 of effective radiative forcing (this scenario which represents RCP 2.6 (shortened to RCP26)), the peak emission years will be around (2010-2020) and the increasing of global surface temperature will be 0.4-1.6 ± 0.4°C to 0.3-1.7 ± 0.3°C during the period (2046-2065) and (2081-2100) respectively (Flato et al., 2013; Stocker et al., 2013). The projections outputs of CMIP5-RCP26 are evaluated in this study. All climate models datasets retrieved from (http://climexp.knmi.nl), according to the instructions of Trouet (Trouet and Van Oldenborgh, 2013). The climate models' datasets details are illustrated in *Table 1*.

Table 1. *List of climate models conducted in the study, its grid box coordinates, and the data time series period used in the analysis*

Model experiment	Horizontal Resolution (Long x Lat)	Interpolating points				Time scale	
		Long extent in degrees (E)		Lat extent in degrees (N)		Start	End
multi-model mean CMIP5 ET - rcp26	2.5° x 2.5°	33.750	36.250	31.250	33.750	Jan 1970	Dec 2013
Mean ET-CLM-ERAi	1.0° x 0.9°	35.000	36.000	31.571	32.513	Jan 1979	Dec 2013
Penman Monteith ET_p - ERA-Interim	0.7° x 0.7°	35.859	36.563	32.632	31.930	Jan 1979	Jan 1999
Priestley Taylor ET_p- ERA-CLM	1.25° x 0.9°	35.625	36.875	31.099	32.042	Jan 1979	Dec 2013
Weather Station	-	35.985 (X)		31.968056 (Y)		Jan 1970	Dec 2013

Another product from the European Centre for Medium Range Weather Forecast (ECMWF) Interim Reanalysis (ERA-Interim) data are used in this study. The product improved model physics of climate parameters including evaporation. Also, it varied satellite radiance data with faster radiative transfer model particularly a new humidity analysis and better representation of atmospheric physics (de Lima and Alcântara, 2019). The reanalysis of Interim gridded datasets quality were validated to observations and fitted to systematic hydrologic measures globally (Uppala et al., 2008). Most studies have

http://www.aloki.hu ● ISSN 1589 1623 (Print) ● ISSN 1785 0037 (Online)
DOI: http://dx.doi.org/10.15666/aeer/1906_48494879

analyzed one variable on specific region to validate the ERA datasets with observations such as Wang et al. (2015) and Simmons et al. (2004) and concluded the ERA capability to perform better in the region of interest despite some errors that may be adjusted using best algorithms (de Lima and Alcântara, 2019). Hence it provides robust improvement in temporal consistency datasets and more sensible representation of observations (Dee et al., 2011), this study has selected the ERA-Interim as benchmark to validate the calculated reference evapotranspiration. The study has elaborated the monthly frequency ERA-interim where the horizontal grid spacing is around 83 km (0.75° x 0.75°) and the grid boundaries have interpolated points.

Penman Monteith ET_p - ERA-Interim input data obtained from the Pre-Processor for LISFLOOD model estimated by Penman-Monteith combined approach (Monteith, 1965) using Angot radiation to calculate net-longwave radiation (Burek et al., 2013). Penman-Monteith equation is widely used in literature, and shortly, it calculates land surface evaporation by combining the sensible heat and latent heat with energy balance giving the *Eq. 26*.

$$\lambda ET = \frac{\varepsilon A + \left(\frac{\rho Cp}{\gamma}\right) DaGa}{\varepsilon + 1 + \frac{Ga}{Gs}} \quad \text{(Eq.26)}$$

where λ is measured in (MJ/kg), the γ psychometric constant is measured here in (kPa/°C), ε is (s/γ), the available energy A estimated from net radiation and G soil heat flux density (MJ/m^2/d), Ga and Gs are aerodynamic and surface conductances (m/sec), Da is vapor pressure deficit of air (kPa), air density ρ in g/m^3, and Cp is the specific heat of air at constant pressure (J/g/°C). Penman-Monteith model proved its reliability to estimate, at catchmnet scale, the short-term and long-term evaporation (Zhang et al., 2008).

Priestley Taylor ET_p-ERA-CLM (Szilagyi et al., 2014; Philip et al., 2020) that obtained from the ERA-Interim reanalysis data calculates potential ET using Priestley Taylor equation (Priestley and Taylor, 1972) that depend on ECMWF heat fluxes. All variables in Priestly-Taylor Equation have the same meanings and units as those in Penman-Monteith method. Priestly Taylor used a calibration constant α = 1.26; Δ is the slope of saturation vapor pressure-temperature curve (kPa/°C); Rn the net radiation in (MJ/m^2/day) which can be derived from solar radiation and extraterrestrial radiation; and G is the heat flux density to the ground (MJ/m^2/day), see *Eq. 27* (Lu et al., 2005).

$$\lambda ET = \alpha \frac{\Delta}{\Delta + \gamma} (Rn - G) \quad \text{(Eq.27)}$$

ERA-Interim assimilation methodology, model, and observations are detailed in Dee's research (Dee et al., 2011) and evaluated by Kunz's article (Kunz et al., 2014) using high quality airborne water vapor measurements dataset rather than the satellite data that unable to accurately track down gas distributions.

Models evaluation

In order to choose the best fit calculated ET_p among all based meteorological variables and equations, the study used regression model evaluation represented in *Eq. 28* to describe the relationship between the benchmark climate models ET projections for the

http://www.aloki.hu ● ISSN 1589 1623 (Print) ● ISSN 1785 0037 (Online)
DOI: http://dx.doi.org/10.15666/aeer/1906_48494879

baseline period and the different calculation methods. The analysis conducted RStudio coding to summarize linear regression test and graphing.

$$\gamma = \beta 1 + \beta 2x + \varepsilon \quad \text{(Eq.28)}$$

where; β_1 is the intercept, β_2 is the slope and ε is the error term. The metrics used for model's evaluation are in the following *Eqs. 29 to 34* (Ahmad, 2013; Wickham and Grolemund, 2016):

$$t - Statistic = \frac{\beta - coefficients}{Std.Error} \quad \text{(Eq.29)}$$

$$\text{Multiple R-squared} = R^2 = 1 - \frac{\sum_i^n (yi - \hat{y}i)^2}{\sum_i^n (yi - \bar{y}i)^2} \quad \text{(Eq.30)}$$

$$\text{Adjusted R-squared} = R^2_{adj} = 1 - \left(\frac{(1-R^2)(n-1)}{n-q}\right) \quad \text{(Eq.31)}$$

$$Std.Error = \sqrt{MSE} = \sqrt{\frac{SSE}{n-q}} \quad \text{(Eq.32)}$$

$$F - Statistic = \frac{MSR}{MSE} \quad \text{(Eq.33)}$$

$$MSR = \frac{\sum_i^n (\hat{y} - \bar{y})^2}{q-1} \quad \text{(Eq.34)}$$

where; $\hat{y}i$ is the fitted value for observations, $\bar{y}i$ is the mean of y, n is the number of observations, q is the number of coefficients in the model, SSE is the summation of squared errors, MSE is a mean squared error, and MSR is the mean squared regression.

Results

Running RStudio for evaluating the model between calculated ETs and climate models projections ETs, illustrated through plots and descriptive statics. Here the study divided the analysis into daily and monthly statistics. The resemblance methods were analysed with regression algorithm to measure the quality of the evapotranspiration methods as surrogates of modelled ETs. It evaluates the fitted model in order to be elaborated later in future water availability studies.

The results showed how changes in climatic conditions will change evapotranspiration estimates. The ET trends showed the sensitivity of evapotranspiration to temperature and radiation through the year. Through the temporal comparison with long-term ET_p values, CMIP5-RCP26 and CLM-ERAi showed a performance in the projections that might change as a function of the state of climate. *Fig. 2* illustrated the trends of ET that are lower in winter months and higher during warm month matching with Penman Monteith-ERA-Interim and Priestley Taylor-ERA-CLM ET_p, whereas, CMIP5-RCP26 and CLM-ERAi ETs are the opposite of such trends. Therefore, CMIP5-RCP26 and CLM-ERAi are excluded from models evaluations analysis.

http://www.aloki.hu ● ISSN 1589 1623 (Print) ● ISSN 1785 0037 (Online)
DOI: http://dx.doi.org/10.15666/aeer/1906_48494879

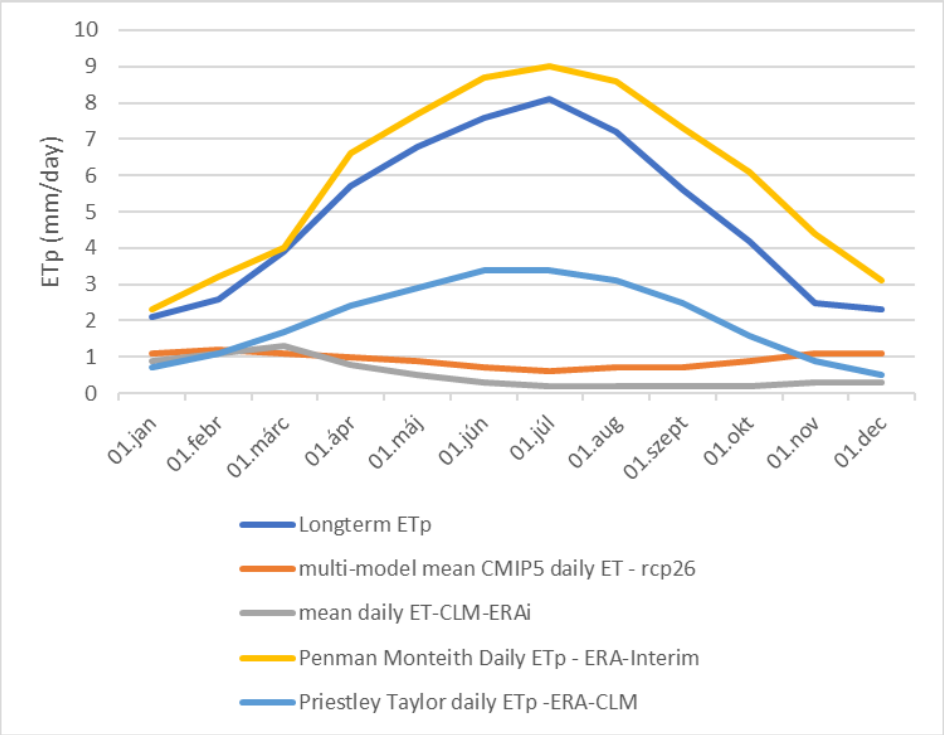

Figure 2. *Temporal change of ET_p through climate models projections comparing with long-term values in Amman*

Regression analysis

Calculated temperature-based daily ET methods

The aggregate plots (*Fig. 3*) instantly show the relationship of all variables; the calculated temp-based daily ET methods, Hargreaves, Karrufa and Blaney-Criddle equations, are correlated positively as strongly linear, wherein the RCP26-CMIP5 mean daily evaporation is negatively correlated to all calculated temperature-based daily ET methods. Mean daily ET-CLM-ERAi is positively correlated with CMIP5 and vector negatively with temperature-based daily ET_p methods. By looking merely at the scatterplots, Penman Monteith- ERA-Interim daily ET_p and Priestley Taylor-ERA-CLM daily ET_p are in positive relation with temperature-based daily ET_p methods but stronger linear relation to Penman ET_p. On the contrary, Penman ET_p is moderately inverse proportional to mean monthly CLM-ERAi and ensemble RCP26-CMIP5 evaporation estimations whereas the latter is clustering negative correlation with Priestly daily ET_p.

The descriptive analysis (*Table 2*) detected statistically the variant range of potential evapotranspiration calculating by observations of daily climatic data. Hargreaves method ranged from 1.2 mm to 6.6 mm maximum while Blaney-Criddle from 2.4 mm to 6.7 mm. Karrufa exceeded the maximum values over all methods as it reached 8.3 mm during the 528 months. Penman Monteith is more closely to Blaney-Criddle values. The daily temp-based ET_p means and 3rd quartiles are nearly the same, in comparison to the approximate 1st quartile Penman and maximum Priestly values, further to the 5.7 mm 3rd quartiles of temp-based ET_p's equal the mean of Penman ET_p through the study period.

http://www.aloki.hu ● ISSN 1589 1623 (Print) ● ISSN 1785 0037 (Online)
DOI: http://dx.doi.org/10.15666/aeer/1906_48494879

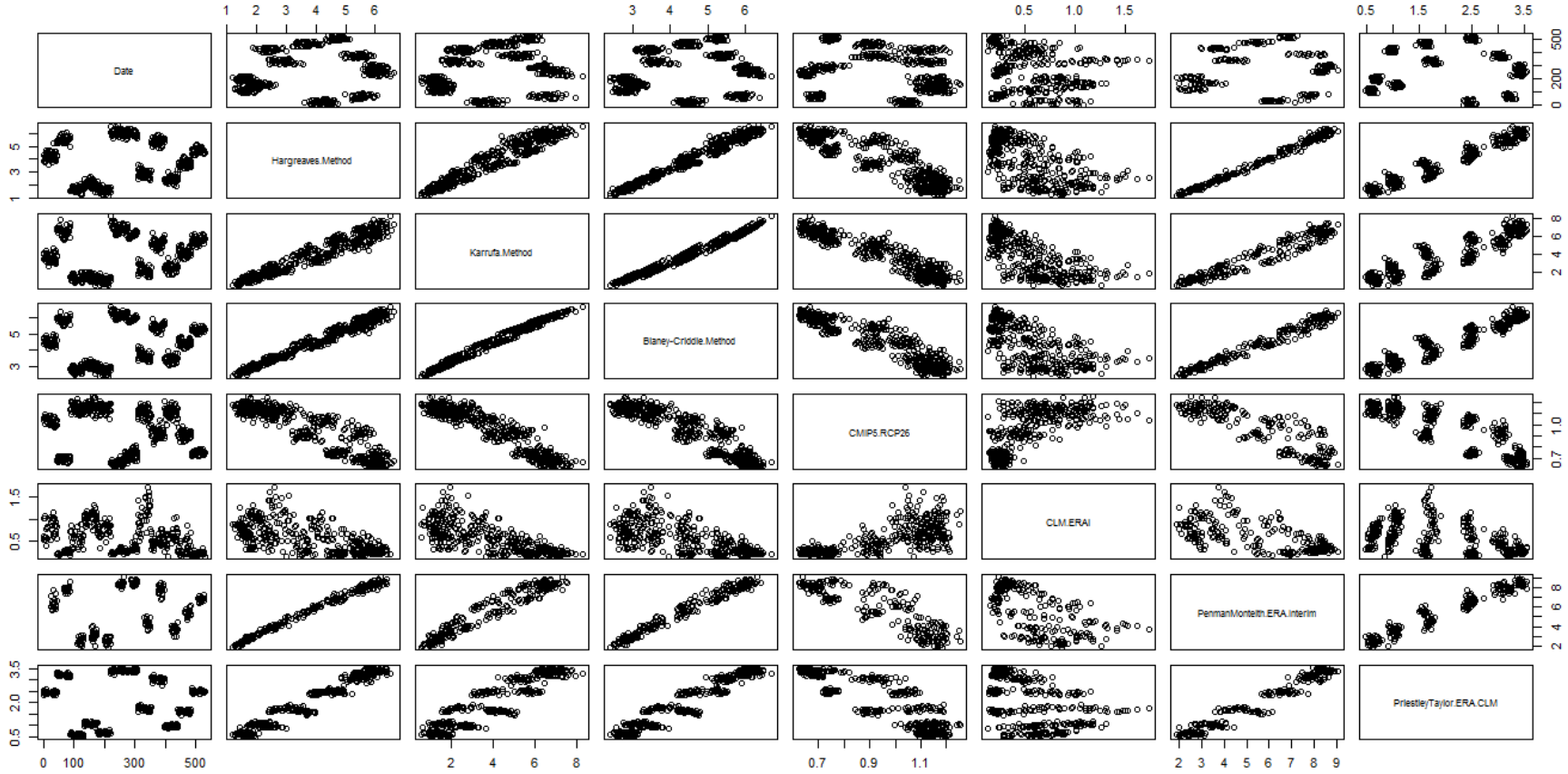

Figure 3. *Plotting Hargreaves, Karrufa and Blaney-Criddle daily ETs against RCP26-CMIP5, ET-CLM-ERAi, Penman Monteith- ERA-Interim daily ET_p and Priestley Taylor-ERA-CLM daily ET_p, where ETs in mm*

http://www.aloki.hu ● ISSN 1589 1623 (Print) ● ISSN 1785 0037 (Online)
DOI: http://dx.doi.org/10.15666/aeer/1906_48494879

Table 2. *Descriptive stats: Temperature-based Daily ET_p methods covering 528 months of observations in comparison to Climate Models and projections (ET in mm)*

Method / Metrics	Hargreaves Method	Karrufa Method	Blaney-Criddle Method	CMIP5-RCP26	CLM-ERAi	Penman Monteith ERA-Interim	Priestley Taylor ERA-CLM
Min.	1.186	0.5661	2.415	0.6257	0.1406	1.926	0.4863
1st Qu.	2.257	1.8635	3.237	0.7373	0.2601	3.483	1.0231
Median	3.915	3.9396	4.448	0.9881	0.489	5.782	2.1195
Mean	3.858	3.9502	4.437	0.9467	0.554	5.6	2.0525
3rd Qu.	5.499	5.9028	5.598	1.1234	0.7823	7.812	3.1381
Max.	6.614	8.2653	6.685	1.2532	1.7394	9.39	3.5407

Calculated temperature-based monthly ET methods

The analysis in *Table 3* detected statistically the variant range of potential evapotranspiration calculating by observations of monthly climatic data. Romanenko method ranged from 25.3 mm to 290.5 mm maximum while Thornthwaite from 2.09 mm to 150 mm. Hamon exceeded the maximum values over all methods as it reached 540 mm during the study period. Penman Monteith is more closely to Romanenko values whereas Priestly Taylor ERA-CLM is approximate to Thornthwaite in third quartile.

Table 3. *Descriptive stats: Temperature-based monthly ET_p methods covering 528 months of observations in comparison to Climate Models and projections (ET in mm)*

Method / Metrics	Romanenko Method	Thornthwaite Method	Hamon Method	CMIP5. RCP26	CLM. ERAi	PenmanMonteith-ERA.Interim	PriestleyTaylor-ERA.CLM
Min.	25.27	2.086	6.954	19.40	4.219	51.4	15.07
1st Qu	76.71	16.132	66.283	22.19	8.028	101.3	29.58
Median	144.85	52.269	165.589	30.00	14.884	177.3	64.54
Mean	143.14	56.891	204.539	28.76	16.761	170.6	62.59
3rd Qu	204.04	94.651	328.721	33.94	23.824	242.2	97.28
Max.	290.54	150.139	539.844	38.10	53.921	280.2	109.76
NA's	Nil	Nil	Nil	Nil	108	287	108

The plots in *Fig. 4* instantly show the relationship of all variables; the calculated ET methods are correlated positively wherein the RCP26-CMIP5 mean monthly evaporation is negatively correlated to all calculated temperature-based monthly ET methods. Mean monthly ET-CLM-ERAi is positively correlated with CMIP5 and vector negatively with temperature-based monthly ET_p methods. By looking merely at the scatterplots, Penman Monteith- ERA-Interim monthly sum of ET_p and Priestley Taylor-ERA-CLM monthly ET_p are in positive relation with temperature-based monthly ET_p methods, on the contrary, both are inversely proportional to Mean monthly CLM-ERAi and ensemble RCP26-CMIP5 evaporation estimations.

http://www.aloki.hu ● ISSN 1589 1623 (Print) ● ISSN 1785 0037 (Online)
DOI: http://dx.doi.org/10.15666/aeer/1906_48494879

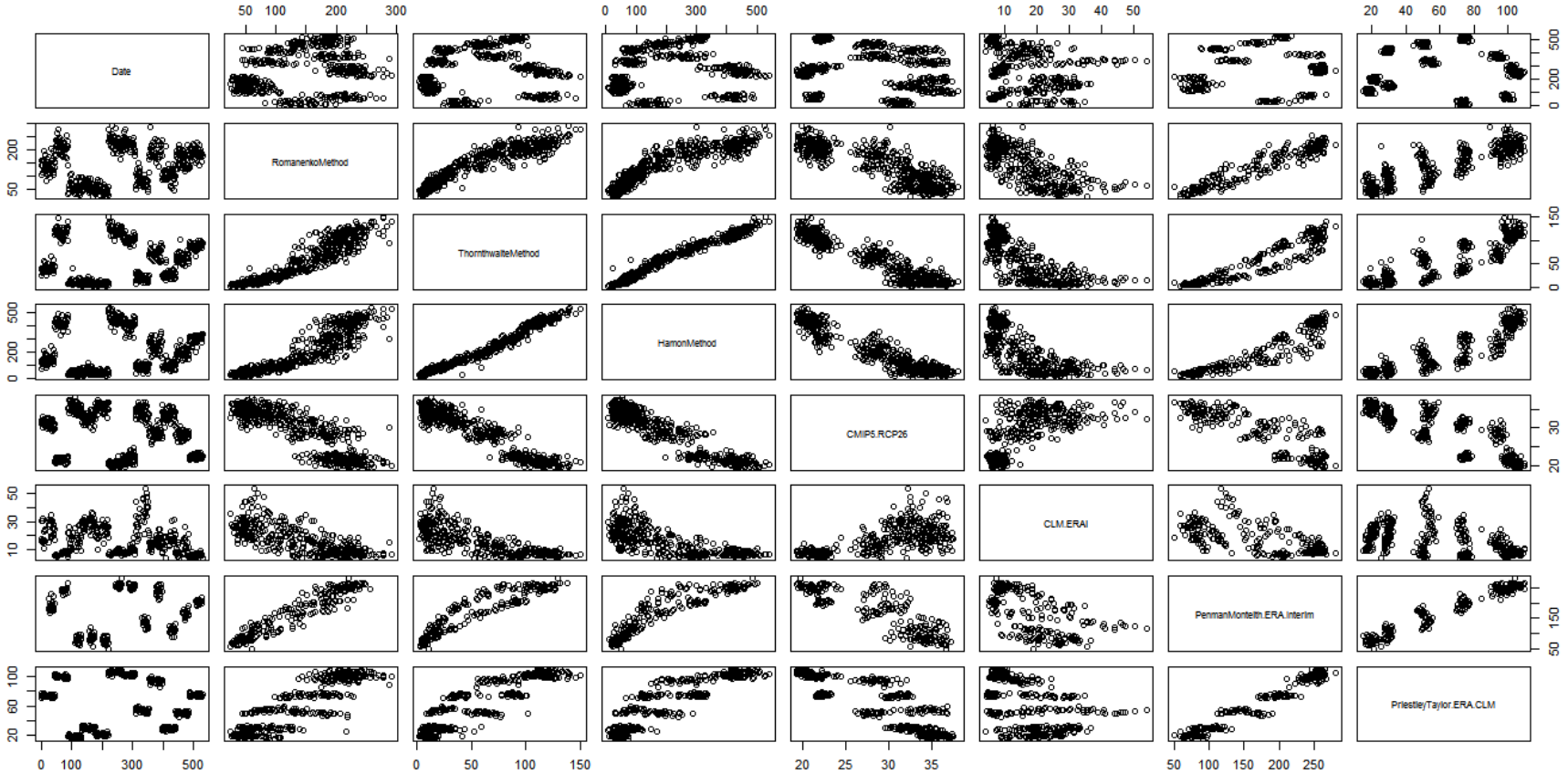

Figure 4. *Plotting Romanenko, Thornthwaite and Hamon monthly ETs against RCP26-CMIP5, ET-CLM-ERAi, Penman Monteith- ERA-Interim monthly ET_p and Priestley Taylor-ERA-CLM monthly ET_p, where ETs in mm*

http://www.aloki.hu ● ISSN 1589 1623 (Print) ● ISSN 1785 0037 (Online)
DOI: http://dx.doi.org/10.15666/aeer/1906_48494879

Class A-Pan method

The plots instantly showed in *Fig. 5* the strong positive linear correlation between both Class A-Pan methods of, Orange Kp and Allen Kp, and moderate correlation with Penman Monteith- ERA-Interim monthly sum of ET_p detecting continuous dots. On the other hand, Priestley Taylor-ERA-CLM monthly ET_p correlated positively in clusters (closed sets of points) within wider range versus Orange Kp and Allen Kp ET values. On the contrary, Priestley Taylor-ERA-CLM monthly ETp scatter plot formed distinct clusters but narrow range against Penman Monteith- ERA-Interim ET_p.

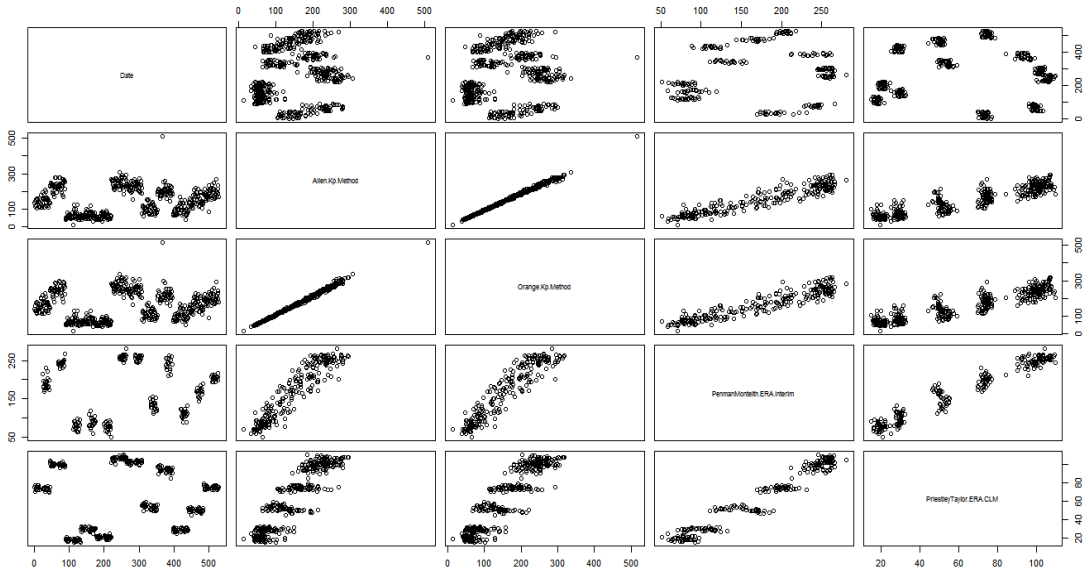

Figure 5. *Correlation between Class A-Pan methods of, Orange Kp and Allen Kp with Penman Monteith- ERA-Interim monthly ET_p and Priestley Taylor-ERA-CLM monthly ET_p*

Evapotranspiration calculated values by using Orange Kp and Allen Kp resembled to Penman Monteith- ERA-Interim ET_p in median, mean, 1st and 3rd quartiles; whereas Priestley Taylor-ERA-CLM monthly ET_p minimum value has a unique approximate to Orange Kp and Allen Kp evapotranspiration, stats are detailed in *Table 4*.

Table 4. *Descriptive stats: Class A-Pan monthly ET methods covering 528 months of observations in comparison with ERA projections (ET in mm)*

Method / Metrics	Orange Kp Method	Allen Kp Method	Penman Monteith-Monthly ERA Interim	Priestley Taylor-Monthly ERA.CLM
Min.	13.64	14.99	51.4	15.07
1st Qu	78.02	83.94	101.3	29.58
Median	145.87	154.74	177.3	64.54
Mean	148.41	158.16	170.6	62.59
3rd Qu	211.4	225.83	242.2	97.28
Max.	507.78	515.37	280.2	109.76
NA's	Nil	Nil	287	108

http://www.aloki.hu ● ISSN 1589 1623 (Print) ● ISSN 1785 0037 (Online)
DOI: http://dx.doi.org/10.15666/aeer/1906_48494879

Solar-based monthly evapotranspiration

The plots (in *Fig. 6a*) instantly showed the roughly to moderate positive linear correlation between Doorenbos & Pruitt Method and Penman-Monteith-Monthly Sum-ERA-Interim. A positive clustering with Priestley Taylor Monthly ET_p-ERA-CLM is detecting ascending dots and smoothing fit-line curve (see the plots in *Fig. 6b*). On the contrary, Priestley Taylor-ERA-CLM monthly ET_p scatter plot formed distinct clusters but narrow range against Penman Monteith- ERA-Interim ET_p.

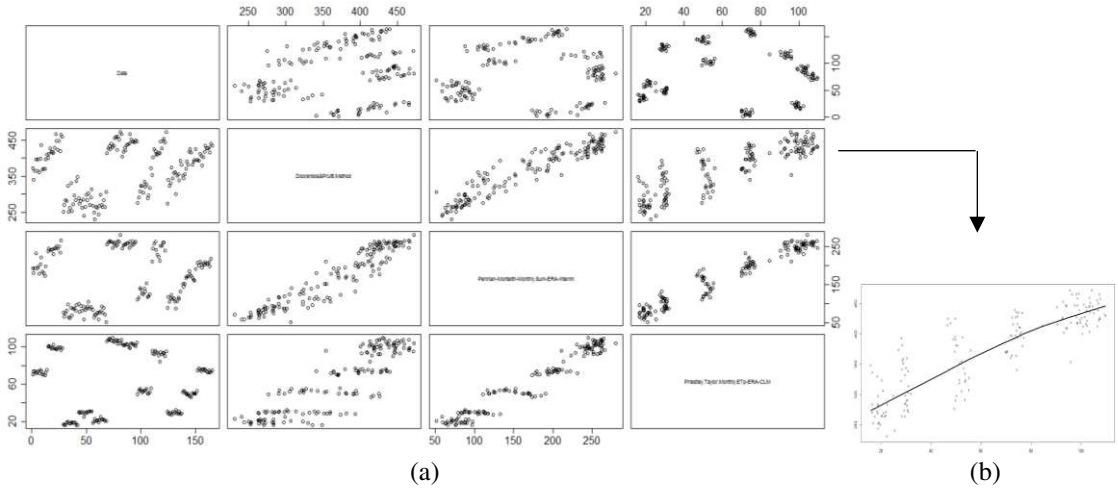

(a) (b)

Figure 6. *(a) Doorenbos & Pruitt Method against Penman-Monteith-Monthly Sum-ERA-Interim; and (b) ascending fit-line with Priestley Taylor Monthly ET_p-ERA-CLM*

Despite the correlation between Doorenbos & Pruitt ET_p solar-based method and the climate projection month-long methods, the values are varied. The maximum values of Priestly ET_p is approximate to 1st quartile Penman ET_p whereas the maximum Penman ET_p is about the 1st quartile of Doorenbos ET_p, the latter exceeded 470.0 mm monthly evapotranspiration (see *Table 5*).

Table 5. *Descriptive stats: Solar-Based Monthly Doorenbos & Pruitt ET_p Method covering 165 months of observations in comparison to Penman-Monteith ERA-Interim and Priestley-Taylor ERA-CLM monthly sum projections (ET in mm)*

Method / Metrics	**Doorenbos &Pruitt Method**	**Penman-Monteith-Monthly Sum-ERA-Interim**	**Priestley Taylor Monthly ET_p - ERA-CLM**
Min.	230.8	51.4	15.96
1st Qu	306.1	101.3	29.8
Median	390.8	179.6	69.99
Mean	369.7	171.6	62.93
3rd Qu	426.2	244.4	96.35
Max.	472.5	280.2	109.76
NA's	Nil	11	Nil

http://www.aloki.hu ● ISSN 1589 1623 (Print) ● ISSN 1785 0037 (Online)
DOI: http://dx.doi.org/10.15666/aeer/1906_48494879

Solar-based daily ET_p methods

Looking at the plots as representing in *Fig. 7*, simply it showed the strong and linear pattern between Jensen-Haise, Hargreaves and Makkink evapotranspiration values over 165 months. Abtew ET values were interpreted as positive strong correlation against Makkink, and Hargreaves methods but moderately linear. Wherein versus Jensen-Haise evapotranspiration values, Abtew ETs associate strongly in positive non-linear over-plotting data. While CLM-ERAi and ensemble RCP26-CMIP5 evaporation estimations have negative relationship with calculated ET methods, it shows clusters vs RCP26-CMIP5 and outliers vs CLM.ERAi at the end of the study period.

Solar-based ET_p values correlated moderately with Penman Monteith- ERA-Interim monthly sum of ET_p detecting continuous dots. On the other hand, Priestley Taylor-ERA-CLM monthly ET_p correlated positively in clusters (closed sets of points) within wider range versus Orange Kp and Allen Kp ET values. On the contrary, Priestley Taylor-ERA-CLM monthly ET_p scatter plot formed distinct clusters but narrow range against Penman Monteith- ERA-Interim ET_p. No relations were shown between CLM.ERAi and both Penman Monteith- ERA-Interim and Priestley Taylor-ERA-CLM monthly ET_p estimations. Clusters with gaps were vector the negative correlation between CMIP5 and both Penman Monteith- ERA-Interim and Priestley Taylor-ERA-CLM monthly ET_p values.

The metrics in descriptive stat in *Table 6* showed the narrow range of daily evapotranspiration values between calculated solar-based equations and climate projections. Priestley-Taylor ERA-CLM projections are more similar to Jensen-Haise Method and Hargreaves Method while Abtew Method is more analogous to Penman-Monteith-ERA-Interim. One of the calculated methods, Makkink equation, ranged out of the distributions of other variables from 4.6 to 24.0 mm per day.

Models' evaluation

The previous scatter plots show the linear regression between variables varied from strong to weak relation and meet the assumption for performing the regression analysis to linearity.

Calculated temperature-based Methods

The residuals between Hargreaves, Karrufa and Blaney Criddle equations with both Penman Monteith and Priestley Taylor daily ET are mostly approximate but not completely exact. The coefficients of linear relations showed, for example, the value of Y intercept 0.533 and the estimated effect of Penman relation on Hargreaves ET (1.32). All calculated methods meet the null hypothesis (here it is less than 2e-16, or almost zero and indicate that the model fits the data well).

From *Table 7* results, we can say that there is strong significant positive relationship between daily Penman Monteith and daily Hargreaves equation (R^2=0.99) and with Blaney-Criddle equation (R^2=0.97) followed by Priestly Taylor and Hargreaves (R^2=0.96) and with Blaney Criddle (R^2=0.93). Furthermore, p-Value consider a linear model to be statistically significance level when both the model p-Value and of the variables less than 0.05 which all met here in the summary statistics of daily calculated Temp-based methods. Karrufa equation performed better with Penman Monteith (R^2=0.92) rather than with Priestley Taylor (R^2=0.85). As expected, t-value is the highest among Temp-based calculation methods for Hargreaves method. Pr(>|t|) for all methods are low, therefore, the coefficients are significant, and our model is statistically significant.

http://www.aloki.hu ● ISSN 1589 1623 (Print) ● ISSN 1785 0037 (Online)
DOI: http://dx.doi.org/10.15666/aeer/1906_48494879

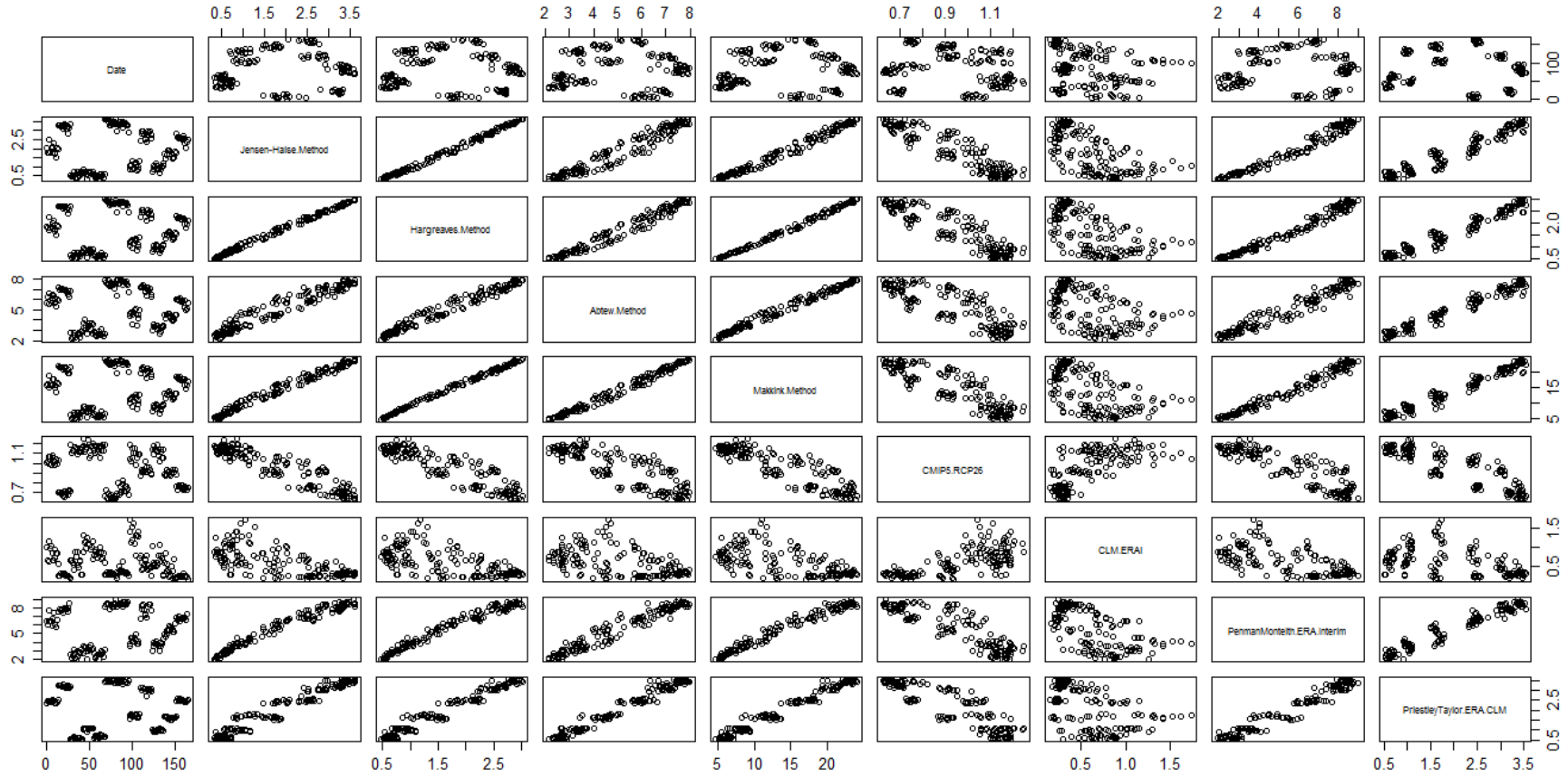

Figure 7. *Jensen-Haise, Hargreaves, Makkink and Abtew evapotranspiration values over 165 months are plotted against RCP26-CMIP5, ET-CLM-ERAi, Penman Monteith- ERA-Interim daily ET_p and Priestley Taylor-ERA-CLM daily ET_p, where ETs in mm*

http://www.aloki.hu ● ISSN 1589 1623 (Print) ● ISSN 1785 0037 (Online)
DOI: http://dx.doi.org/10.15666/aeer/1906_48494879

Table 6. *Descriptive stats: Solar-Based Daily ET_p Methods covering 165 months of observations in comparison to RCP26-CMIP5, CLM-ERAi, Penman-Monteith ERA-Interim and Priestley-Taylor ERA-CLM projections (ET in mm)*

Method / Metrics	Jensen-Haise Method	Hargreaves Method	Abtew Method	Makkink Method	CMIP5. RCP26	CLM ERAi	PenmanMonteith ERA.Interim	PriestleyTaylor ERA.CLM
Min.	0.3167	0.4783	2.133	4.681	0.6257	0.1518	1.926	0.515
1st Qu	0.7591	0.8858	3.405	8.213	0.7462	0.2939	3.484	1.031
Median	1.7908	1.6677	5.109	14.638	0.9542	0.5408	5.977	2.333
Mean	1.8926	1.7081	5.136	14.370	0.9408	0.5979	5.635	2.064
3rd Qu	2.9441	2.5375	6.899	20.732	1.1156	0.8370	7.892	3.18
Max.	3.6240	3.0134	7.978	24.034	1.2475	1.7394	9.039	3.541
NA's	Nil	Nil	Nil	Nil	Nil	Nil	11	Nil

Table 7. *Regression evaluation and validation: Calculated Temperature-Based Daily ET Methods vs. Climate Projections Daily ET*

Climate Model Projections		**Penman Monteith-ERA Interim Daily ET (Jan 1979-Jan 1999)**			**PriestleyTaylor.ERA.CLM (Jan 1979-Dec 2013)**		
Calculated Methods / Metrics		**Hargreaves Method**	**Karrufa Method**	**Blaney-Criddle Method**	**Hargreaves Method**	**Karrufa Method**	**Blaney-Criddle Method**
Min		-0.77551	-1.277	-0.86892	-0.7162	-1.06247	-0.84988
1Q		-0.15005	-0.4846	-0.25141	-0.132	-0.3045	-0.19236
Median		0.00624	-0.1831	-0.05159	0.0024	0.01292	0.02027
3Q		0.15916	0.5081	0.22534	0.1541	0.29793	0.20047
Max		0.78705	1.4569	1.17636	0.4891	0.94618	0.64411
Coefficients	Intercept Estimate	0.533191	1.65984	-2.2124	-0.30481	0.265235	-1.51964
	Intercept Std. Error	0.037633	0.0834	0.09066	0.026747	0.041306	0.05072
	Intercept t value	14.17	19.9	-24.4	-11.4	6.421	-29.96
	Intercept Pr(>|t|)	<2e-16	<2e-16	<2e-16	<2e-16	3.68e-10	< 2e-16
	Method Estimate	1.323232	1.00954	1.77034	0.61551	0.444624	0.79973
	Method Std. Error	0.009008	0.01878	0.01978	0.006418	0.009065	0.01094
	Method t value	146.9	53.74	89.5	95.9	49.05	73.11
	Method Pr(>|t|)	<2e-16	<2e-16	<2e-16	<2e-16	< 2e-16	< 2e-16
Degree of Freedom (months)		239	239	239	418	418	418
Residual standard error		0.2337	0.6174	0.3801	0.2161	0.3987	0.2791
Multiple R-squared		0.989	0.9236	0.971	0.9565	0.852	0.9275
Adjusted R-squared		0.989	0.9233	0.9709	0.9564	0.8516	0.9273
F-statistic		2.158e+04	2888	8010	9197	2406	5345
p-value (of the linear model)		< 2.2e-16	< 2.2e-16	< 2.2e-16	< 2.2e-16	< 2.2e-16	< 2.2e-16

http://www.aloki.hu ● ISSN 1589 1623 (Print) ● ISSN 1785 0037 (Online)
DOI: http://dx.doi.org/10.15666/aeer/1906_48494879

On monthly basis, the temp-based monthly methods showed that the residuals between Hamon, Remanenko and Thornthwaite equations with Priestley Taylor monthly ET are close in values, whereas against Penman Monteith monthly ET, the residuals have wider range. All calculated methods meet the null hypothesis (here it is less than 2e-16 indicating that the model fits the data well. The highest significant positive relationship between monthly Penman Monteith were against monthly Romanenko equation (R^2=0.90) and Thornthwaite equation (R^2=0.86) followed by Hamon method (R^2=0.84). Despite p-Values are considered in statistically significance level (less than 0.05), all monthly calculated Temp-based methods were ($R^2 \leq 0.80$) against Priestley & Taylor ERA-CLM monthly ET. t-values are greater than the standard level (1.96), furthermore, the standard error for all equations is close to zero. The best performance was for Romanenko method and Penman Monteith monthly ETs over 239 months with the highest F-statistic (see *Table 8*).

Table 8. *Models Evaluation: Calculated Temperature-Based Monthly ET Methods vs. Climate Projections monthly ET*

Climate Model Projections		**Penman Monteith-ERA Interim Monthly ET (Jan 1979-Jan 1999)**			**PriestleyTaylor.ERA.CLM (Jan 1979-Dec 2013)**		
Calculated Methods / Metrics		**Romanenko Method**	**Thornthwaite Method**	**Hamon Method**	**Romanenko Method**	**Thornthwaite Method**	**Hamon Method**
Min		-62.417	-49.524	-55.447	-67.177	-42.998	-30.978
1Q		-12.699	-18.934	-20.701	-9.113	-10.594	-10.211
Median		-0.618	-9.913	-7.642	1.105	-2.515	-3.981
3Q		14.193	16.74	12.241	10.2	11.41	9.489
Max		57.836	68.51	90.839	36.991	34.318	37.919
Coefficients	Intercept Estimate	40.62229	84.78962	86.57268	5.38105	24.38735	24.741960
	Intercept Std. Error	3.06934	2.76806	2.94851	1.71361	1.180	1.127674
	Intercept t value	13.23	30.63	29.36	3.14	20.66	21.94
	Intercept Pr(>|t|)	<2e-16	<2e-16	<2e-16	0.00181	<2e-16	< 2e-16
	Method Estimate	0.94796	1.53454	0.41632	0.40016	0.66487	0.184507
	Method Std. Error	0.01999	0.03969	0.01168	0.01077	0.016	0.004382
	Method t value	47.41	38.66	35.66	37.15	40.35	42.11
	Method Pr(>|t|)	<2e-16	<2e-16	<2e-16	<2e-16	< 2e-16	< 2e-16
Degree of Freedom		239	239	239	418	418	418
Residual standard error		21.44	25.68	27.52	15.41	14.44	13.96
Multiple R-squared		0.9039	0.8621	0.8418	0.7675	0.7957	0.8092
Adjusted R-squared		0.9035	0.8616	0.8411	0.767	0.7952	0.8088
F-statistic		2248	1495	1271	1380	1628	1773
Model p-value		< 2.2e-16	< 2.2e-16	< 2.2e-16	< 2.2e-16	< 2.2e-16	< 2.2e-16

http://www.aloki.hu ● ISSN 1589 1623 (Print) ● ISSN 1785 0037 (Online)
DOI: http://dx.doi.org/10.15666/aeer/1906_48494879

Calculated class-A Pan methods

There is a stronger significant relationship between both Orange and Allen Kp methods ET against Penman Monteith ERA-Interim ET than against Priestley Taylor ERA-CLM ET values (R^2= 0.88 ± 0.01997, 0.87 ± 0.0217, 0.84 ± 0.00879 and 0.84 ± 0.00797, respectively), see *Table 9*. All calculated class-A Pan methods' t-Values and p-values met the standard levels, further to standard error are close to zero as illustrated in *Table 9*. The residuals metrics are approximate between both Orange and Allen Kp methods against Penman and Priestely ET's.

Table 9. *Models Evaluation: Calculated Class A Pan ET Methods vs Climate Projections monthly ET*

Climate Model Projections			**Penman Monteith-ERA Interim ET (Jan 1979-Jan 1999)**		**PriestleyTaylor.ERA.CLM (Jan 1979-Dec 2013)**	
Calculated Methods / Metrics			**Allen Kp. Method**	**Orange Kp Method**	**Allen Kp Method**	**Orange Kp Method**
Min			-72.677	-76	-39.496	-40.08
1Q			-16.506	-16.6	-7.68	-7.455
Median			-0.767	-0.4	0.016	0.248
3Q			14.285	15.11	8.344	8.178
Max			58.481	59.6	31.673	29.231
Coeffecients	Intercept	Estimate	37.27940	37.74438	3.363588	3.454618
		Std. Error	3.64443	3.59304	1.428525	1.384011
		t value	10.23	10.51	2.355	2.496
		Pr(>|t|)	0.00181	<2e-16	0.019	0.0129
	Method	Estimate	0.88115	0.82066	0.406294	0.380216
		Std. Error	0.02169	0.01997	0.008793	0.007974
		t value	40.62	41.10	46.208	47.682
		Pr(>|t|)	<2e-16	< 2e-16	<2e-16	<2e-16
Degree of Freedom			239	239	418	418
Residual standard error			24.6	24.35	12.93	12.59
Multiple R-squared			0.8735	0.876	0.8363	0.8447
Adjusted R-squared			0.873	0.8755	0.8359	0.8443
F-statistic			1650	1689	2135	2274
p-value			< 2.2e-16	< 2.2e-16	< 2.2e-16	< 2.2e-16

Calculated solar ET methods

Although disparity changing over time among the solar ET methods, the regression model met the significant linearity correlation between Doorenbos method and both Penman Monteith and Priestley Taylor ERA evapotranspiration (*Table 10*); R^2= 0.89 ± 0.028 and 0.75 ± 0.019, respectively. The t-values are greater than the

http://www.aloki.hu ● ISSN 1589 1623 (Print) ● ISSN 1785 0037 (Online)
DOI: http://dx.doi.org/10.15666/aeer/1906_48494879

standard level furthermore to the lowest p-value < 2.2e-16. The best performance was for Doorenbos method with Penman Monteith ETs over 163 months with the highest F-statistic.

Table 10. *Model Evaluation: Doorenbos Monthly ET vs Climate Models Projections ET*

Climate Model Projections			**Penman Monteith-ERA Interim ET (April 1986-Jan 1999)**	**Priestley Taylor ERA.CLM (April 1986-Dec 1999)**
Calculated Methods / Metrics			**Doorenbos & Pruitt Method**	**Doorenbos & Pruitt Method**
Min			-64.74	-44.496
1Q			-10.191	-8.319
Median			2.798	2.155
3Q			14.707	10.777
Max			52.889	39.654
Coefficients	Intercept	Estimate	-190.2695	-90.30525
		Std. Error	10.4452	7.01201
		t value	-18.22	-12.88
		Pr(>|t|)	<2e-16	<2e-16
	Method	Estimate	0.9862	0.41446
		Std. Error	0.0280	0.01866
		t value	35.21	22.21
		Pr(>|t|)	<2e-16	< 2e-16
Degree of Freedom			152	163
Residual standard error			23.28	16.01
Multiple R-squared			0.8908	0.7516
Adjusted R-squared			0.8901	0.7501
F-statistic			1240	493.2
p-value			< 2.2e-16	< 2.2e-16

On daily basis, the solar-based ET methods showed in *Table 11* the best performance of overall calculated methods ($R^2 \geq 0.94$). Jensen-Haise, Hargreaves and Makkink equations with Penman Monteith ET are close in minimum residual values, whereas against daily Priestley Taylor ET, the minimum and 1st quartile residuals were approximately the same. All calculated methods meet the null hypothesis (here it is less than 2e-16 indicating that the model fits the data well. The highest significant positive relationship between daily climate projections were against Makkink equation (R^2=0.97) and Hargreaves equation ($R^2 \geq 0.96$) followed by Abtew and Jensen-Haise methods ($R^2 \geq 0.94$). Further to p-Values are considered in statistically significance level (less than 0.05), all daily solar calculated ETs had the lower standard errors (≤ 0.03) but the lowest with Makkink and Abtew methods against Priestley Taylor (≤ 0.008). The best performance was for Makkink method and Penman Monteith and Priestly Taylor ETs over 152 months with the highest F-statistic (> 5100).

http://www.aloki.hu ● ISSN 1589 1623 (Print) ● ISSN 1785 0037 (Online)
DOI: http://dx.doi.org/10.15666/aeer/1906_48494879

Table 11. *Models Evaluation: Solar-Based Daily ET Methods vs Penman Monteith-ERA Interim and Priestley Taylor.ERA.CLM evapotranspiration values*

Climate Model Projections			**Penman Monteith-ERA Interim Monthly ET (April 1986-Jan 1999)**				**PriestleyTaylor.ERA.CLM (April 1986-Dec 1999)**			
Calculated Methods / Metrics			**Jensen-Haise Method**	**Hargreaves Method**	**Abtew Method**	**Makkink Method**	**Jensen-Haise Method**	**Hargreaves Method**	**Abtew Method**	**Makkink Method**
Min			-0.8635	-0.85795	-1.2626	-0.79449	-0.52263	-0.44514	-0.50917	-0.3997
1Q			-0.3493	-0.25148	-0.33113	-0.24999	-0.18776	-0.12476	-0.13366	-0.10961
Median			-0.0758	-0.06105	-0.00107	-0.07696	-0.04631	-0.02944	-0.02323	-0.00655
3Q			0.3219	0.23482	0.29344	0.19681	0.15095	0.11441	0.10599	0.08775
Max			0.994	0.96988	1.65621	1.20678	0.64032	0.61355	0.74275	0.59853
Coefficients	Intercept	Estimate	1.88334	1.1398	-0.40943	0.613019	0.34135	-0.01519	-0.78236	-0.27023
		Std. Error	0.0694	0.07016	0.12937	0.076557	0.04019	0.03658	0.043747	0.03507
		t value	27.14	16.25	-3.165	8.007	8.494	-0.415	-17.88	-7.705
		Pr(>|t|)	<2e-16	<2e-16	0.00187	2.83e13	1.19E-14	0.678	<2e-16	1.2e-12
	Method	Estimate	1.98913	2.63713	1.17675	0.349923	0.90995	1.217	0.55408	0.162403
		Std. Error	0.03169	0.03689	0.02368	0.004878	0.01835	0.01924	0.008019	0.002236
		t value	62.76	71.48	49.692	71.738	49.591	63.245	69.09	72.625
		Pr(>|t|)	<2e-16	<2e-16	< 2e-16	< 2e-16	<2e-16	<2e-16	<2e-16	<2e-16
Degree of Freedom			152	152	152	152	163	163	163	163
Residual standard error			0.4378	0.3861	0.547	0.3847	0.2598	0.2062	0.1893	0.1804
Multiple R-squared			0.9628	0.9711	0.942	0.9713	0.9378	0.9608	0.967	0.97
Adjusted R-squared			0.9626	0.9709	0.9416	0.9711	0.9375	0.9606	0.9668	0.9698
F-statistic			3939	5109	2469	5146	2459	4000	4774	5274
p-value			< 2.2e-16	< 2.2e-16	< 2.2e-16	< 2.2e-16	< 2.2e-16	< 2.2e-16	< 2.2e-16	< 2.2e-16

http://www.aloki.hu ● ISSN 1589 1623 (Print) ● ISSN 1785 0037 (Online)
DOI: http://dx.doi.org/10.15666/aeer/1906_48494879

Data Distribution

To compare the distributions of data groups, daily and monthly boxplots are representing in *Fig. 8* and showed the most common data values and change over time among models. Regarding comparison, the solar-based ET, the ends of the daily boxplots outlined the similarity between Penman Monteith and Abtew methods as well as between Jensen-Haise and Hargreaves ETs, in addition to the central 50% of the data are almost the same for these models whereas the spread of data for Makkink was different. Jensen-Haise and Hargreaves vs Priestley Taylor ET values showed the approximate ends of daily boxplot, however, the same central 50% of its data. The ends of the daily boxplots, as well as the central 50% of the data, outlined the difference between Makkink and Abtew methods against Priestley Taylor ERA projections (see *Fig. 8a*).

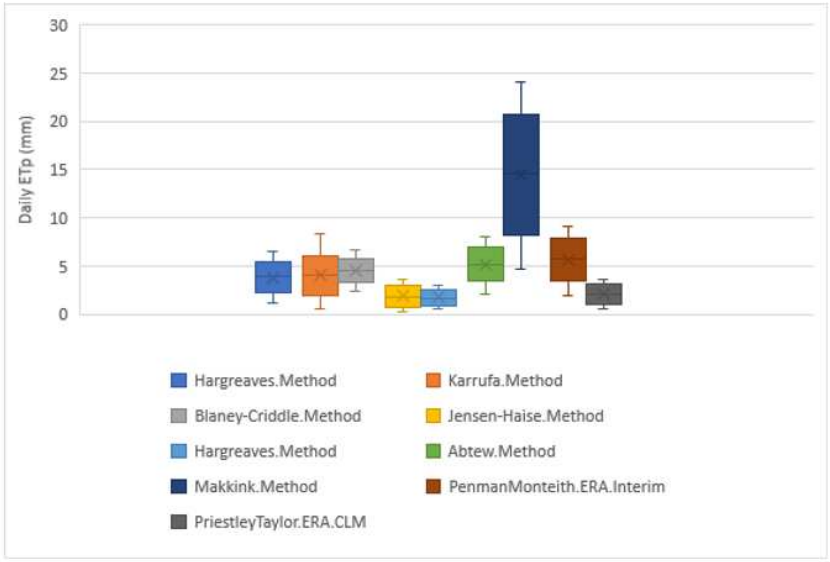

(a)

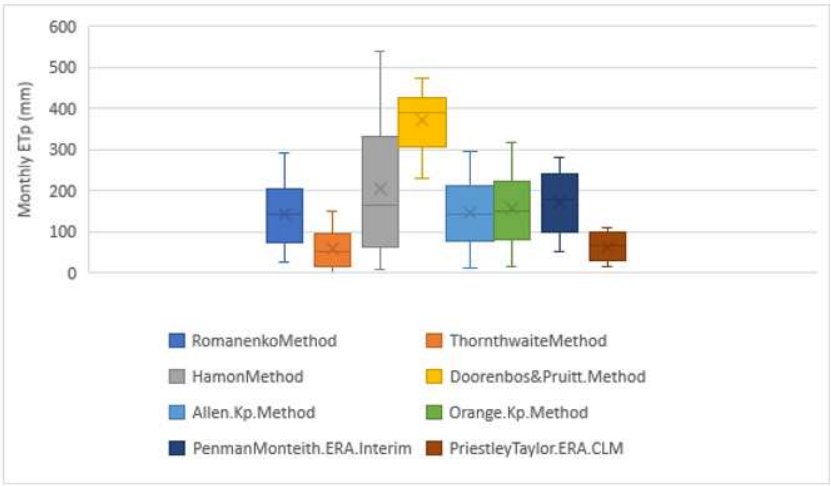

(b)

Figure 8. *(a) Boxplot's data distribution over time for temperature-based, solar-based and Class-A Pan methods on monthly basis with respect to Penman Monteith and Priestley Taylor climate models projections of Ets. (b) Boxplot's data distribution over time for temperature-based, and solar-based methods on daily basis with respect to Penman Monteith and Priestley Taylor climate models projections of ETs*

http://www.aloki.hu ● ISSN 1589 1623 (Print) ● ISSN 1785 0037 (Online)
DOI: http://dx.doi.org/10.15666/aeer/1906_48494879

On monthly basis in *Fig. 8b*, the ends of the monthly box outlined the similarity between Penman Monteith and Romanenko methods but shorter maximum ending for Thornthwaite method. The central 50% of the data are almost the same for Romanenko, Hamon and Penman Monteith methods. Whereas the spread of data for Priestly Taylor and Thornthwaite showed the approximate ends of monthly boxplot, however, the same central 50% of Romanenko and Hamon data with different maximum ends. The results characterized the difference in range and the central 50% of the data between Doorenbos and Pruitt method against climate models ET values during more than 150 months.

The ends of the Kp Pan methods box outlined the similarity between Orange Kp and Allen Kp evapotranspiration methods but shorter maximum and minimum endings for Penman method. The central 50% of the data are almost the same for Orange Kp, Allen Kp and Penman Monteith methods, whereas very narrower spread of data for Priestly Taylor, as shown in *Fig. 8b*.

Discussion

Since ET_p is difficult to estimate accurately, rigorous calculations should be considered because of its importance for estimating actual water loss from natural systems as well in hydrological studies. This study gave wide range of values and suggested the ET_p variations among 13 calculation models across the study area in the middle of Jordan-Amman. The study adopted four climate models projections as benchmark due to unavailable actual ET values.

ERA-Interim data are used for 20 years of measurements flights which extended regionally and covered the study area (Kunz et al., 2014; Philip et al., 2020). The selection of ERA-Interim as benchmark data was based on previous studies and its emphasis on terrestrial ET. Bai and Liu (2018), for example, concluded the best performance of ERA-interim with observations as one of the most consistent global high-resolution ET products. This was due to the effect of soil water stress on ET depend on soil moisture balance model (Martens et al., 2016) which made ERA-Interim ET product is an asset to benefit regional water users (Baik et al., 2018; Wang et al., 2019). Not to mention the good agreement between ERA-Interim and the high quality water vapor dataset is evaluated by Kunz's experiment (Kunz et al., 2014).

This study showed how changes in climatic conditions will change evapotranspiration. Through all the scatter plots and descriptive stats, CMIP5-RCP26 and CLM-ERAi showed a performance in the projections that might change as a function of the state of climate. Climate models CMIP5-RCP26 (Al-Shibli, 2018) and CLM-ERAi did not weight the evaporation in proportion to the season, as ET estimates are overestimated in winter and underestimated in summer months. This can be justified by the combined effect of soil moisture content and evapotranspiration on temperature and cloud cover. The latent heat flux incorporated with evaporation causes decreasing of land net radiation. Simply put, while ET decreases, the temperature rises (Mueller and Seneviratne, 2014; Dosio et al., 2021). Another explanation to the reversal effect of greenhouse gases concentrations that boost the changes in hydrological cycle, it decreases the precipitation and evapotranspiration due to the increasing weight of aerosols (Roeckner et al., 1999; Calanca et al., 2006).

Calculation methods showed that benchmarking ET_p of Penman-Monteith ERA Interim come close to previous studies. Al Mahamid (2005) calculated the long-term average of ET_p for the period from 1970 to 2001 Amman-Zarqa Basin, according to

http://www.aloki.hu ● ISSN 1589 1623 (Print) ● ISSN 1785 0037 (Online)
DOI: http://dx.doi.org/10.15666/aeer/1906_48494879

Penman-Monteith equation, between (65-170) mm/month during winter (173.00 mm/month for ERA Interim) and (129-250) mm/month during summer (264.5 mm/month for ERA Interim). As Doorenbos (1977) and Al Mahamid (2005) found the high correlation between actual ET and class A-pan evaporation ET, this study proved 75 percentile of Allen and Orange potential pan ET pan values are approximate to Doorenbos & Pruitt minimum ETs while the latter maximum ETs are similar to maximum Allen ET_p. Since Penman-Monteith equation was adopted even under missing data conditions, the reliability of Penman-Monteith method was verified at site and catchment scales in humid and semi-humid conditions but showed less reliable in semi-arid region as it is overly controlled by precipitation (Zhang et al., 2008). Alternative methods such as Hargreaves, Abtew, and Jensen-Haise could be used in semi-arid dry land as being reported by Djaman et al. (2019) and Hargreaves ET results under aridity conditions are better across Mediterranean region (Todorovic et al., 2013). The ET sharing component in water balance, however, was calculated also by using Shuttleworth-Wallace equation for the lower part of Jordan river basin, it was 72% of the rain as 269 mm/year during 2002-2003 (Gunkel and Lange, 2012). The minimum values of ET_p in Priestley Taylor ERA-CLM projections during short period from April 1986 to Dec 1999 showed higher ET than the values during the longer time slice from Jan 1979 to Dec 2013 as the lowest value is not overlapping within the short time slice comparison.

In our study, ET exceeds the total precipitation since no water body available in the study area except small dams and streams. Thornthwaite and Mather method was used to estimate potential ET in the northern parts of Jordan (Almagbile et al., 2019), where the study found the correlation that the higher ET the lower observed soil moisture. The solar radiation methods to calculate ET showed the best performance, among others. This analysis recommended as same as Valle Júnior's research (Valle Júnior et al., 2020) which recommended investing in radiation research for ET estimation simpler than using more data inputs for Penman-Monteith formula.

Conclusion and Recommendations

Clearly, some models to estimate ET_p evidence significant trends to climate parameters aligned with the direction of the change whether changing in temperature degrees or radiation energy. The study showed that ET_p estimation method' accurecy and applicability is likely to be site-specific.

Linear regression analysis between the standard ETs of climate models' outputs and the modelled potential ETs were performed. The analysis showed asymmetry between both CMIP5-RCP 2.6 and CLM-ERAi outputs and calculated ETs but inconsistent with Penman Monteith ERA Interim and Priestley Taylor ERA-CLM. Climate models CMIP5-RCP26 and CLM-ERAi did not weight the evapotranspiration in proportion to the season and showing inverse proportional to the trend of ETs which might be because of the combined effects of soil moisture content and ET on temperature and heat fluxes.

Penman Monteith ERA-Interim demonstrates the literature values that vary from 51 to 280 mm/month. Blaney Criddle and Hargreaves temperature-based and solar based methods prototyped the potential evapotranspiration (R^2 = 0.99-0.97) followed by Makkink and Jensen-Haise radiation-based formulas (R^2 = 0.97-0.96) which showed the best fitted with ERA climate models evapotranspiration. The remaining models need to be calibrated under the local conditions due to its limitation in the current constants. These results help to decide which method to estimate ET_p depending on the availability of data

http://www.aloki.hu ● ISSN 1589 1623 (Print) ● ISSN 1785 0037 (Online)
DOI: http://dx.doi.org/10.15666/aeer/1906_48494879

required per each equation. Radiation-based methods like Hargreaves, Makkink and Jensen-Haise equations are recommended if temperature and radiation data is available. Otherwise, temperature-based methods like Blaney Criddle and Hargreaves are recommended if temperature data is the only available observations. ERA-reanalysis proved capability to perform better in the study area with temporal consistency since it relies on ECMWF heat fluxes. Therefore, Penman Monteith- ERA-Interim and Priestley Taylor-ERA-CLM ET_p, however, could be used instead for ET_p estimation in hydro-meteorological modelling and actual water loss studies.

The ET trends showed the sensitivity of evapotranspiration to temperature and radiation more than the remaining meteorological parameters. Further work is needed for GCM/RCM models which cropped large grids and transferable coupling of its projections to a particular site should be considered and tested in the absence of reference values of models' parameters in sub-grid studies.

Funding. This research received fund from Australian Government - Direct Aid Program (DAP)-Department of Foreign Affairs and Trade and The Scientific Research Council -University of Jordan.

Data Availability Statement. Datasets will be provided upon request.

Acknowledgments. I appreciate the climate modelling groups for making their models outputs available: CMIP5-RCP 2.6, CLM-ERAi, ERA Interim, and ERA-CLM.

Conflicts of Interests. The authors declare no conflict of interests.

REFERENCES

[1] Abtew, W. (1996): Evapotranspiration measurements and modeling for three wetland systems in South Florida. – JAWRA J. Am. Water Resour. Assoc. 32(3): 465-473.
[2] Ahmad, M. A. B. (2013): Mining Health Data for Breast Cancer Diagnosis Using Machine Learning. – Doctoral thesis, Univ. of Canberra.
[3] Akhavan, S., Kanani, E., Dehghanisanij, H. (2019): Assessment of different reference evapotranspiration models to estimate the actual evapotranspiration of corn (*Zea mays* L.) in a semiarid region (case study, Karaj, Iran). – Theor. Appl. Climatol. 137: 1403-1419.
[4] Al Mahamid, J. (2005): Integration of water resources of the upper aquifer in Amman-Zarqa basin based on mathematical modeling and GIS, Jordan. – Inst. für Geologie.
[5] Al-Shibli, F. M., Maher, W. A., Thompson, R. M. (2017): The Need for a Quantitative Analysis of Risk and Reliability for Formulation of Water Budget in Jordan. – JJEES, Jordan J. Earth Environ. Sci. 8: 77-89.
[6] Al-Shibli, F. M. (2018): Modelling a Future Water Budget in the Amman-Zarqa Basin, Jordan: Evaluation of the Major Stressors Affecting Water Availability. – University of Canberra.
[7] Allen, R. G. (1995): Evaluation of procedures for estimating mean monthly solar radiation from air temperature. – AGRIS, Food and Agriculture Organization of the United Nations.
[8] Allen, R. G., Pereira, L. S., Raes, D., Smith, M. (1998): Crop evapotranspiration - Guidelines for computing crop water requirements. – FAO Irrigation and drainage paper 56. FAO, Rome 300, D05109.
[9] Almagbile, A., Zeitoun, M., Hazaymeh, K., Sammour, H. A., Sababha, N. (2019): Statistical analysis of estimated and observed soil moisture in sub-humid climate in north-western Jordan. – Environ. Monit. Assess. 191: 96.
[10] Bai, P., Liu, X. (2018): Intercomparison and evaluation of three global high-resolution

http://www.aloki.hu ● ISSN 1589 1623 (Print) ● ISSN 1785 0037 (Online)
DOI: http://dx.doi.org/10.15666/aeer/1906_48494879

evapotranspiration products across China. – J. Hydrol. 566: 743-755.
[11] Baik, J., Liaqat, U. W., Choi, M. (2018): Assessment of satellite-and reanalysis-based evapotranspiration products with two blending approaches over the complex landscapes and climates of Australia. – Agric. For. Meteorol. 263: 388-398.
[12] Bautista, F., Bautista, D., Delgado-Carranza, C. (2009): Calibration of the equations of Hargreaves and Thornthwaite to estimate the potential evapotranspiration in semi-arid and subhumid tropical climates for regional applications. – Atmósfera 22: 331-348.
[13] Bayazit, M., Önöz, B. (2007): To prewhiten or not to prewhiten in trend analysis? – Hydrol. Sci. J. 52: 611-624.
[14] Blaney, H. F. (1952): Determining water requirements in irrigated areas from climatological and irrigation data. – AGRIS, Food and Agriculture Organization of the United Nations.
[15] Blaney, H. F., Criddle, W. D. (1962): Determining consumptive use and irrigation water requirements. – US Department of Agriculture.
[16] Bormann, H. (2011): Sensitivity analysis of 18 different potential evapotranspiration models to observed climatic change at German climate stations. – Clim. Change 104: 729-753.
[17] Burek, P., van der Knijff, J., Ntegeka, V. (2013): LISVAP evaporation pre-processor for the LISFLOOD water balance and flood simulation model. – User Manual.
[18] Calanca, P., Roesch, A., Jasper, K., Wild, M. (2006): Global warming and the summertime evapotranspiration regime of the Alpine region. – Clim. Change 79: 65-78.
[19] Comair, G. F., McKinney, D. C., Siegel, D. (2012): Hydrology of the Jordan River Basin: Watershed delineation, precipitation and evapotranspiration. – Water Resour. Manag. 26: 4281-4293.
[20] de Lima, J. A. G., Alcântara, C. R. (2019): Comparison between ERA Interim/ECMWF, CFSR, NCEP/NCAR reanalysis, and observational datasets over the eastern part of the Brazilian Northeast Region. – Theor. Appl. Climatol. 138: 2021-2041.
[21] Dee, D. P., Uppala, S. M., Simmons, A. J., Berrisford, P., Poli, P., Kobayashi, S., Andrae, U., Balmaseda, M. A., Balsamo, G., Bauer, P. (2011): The ERA-Interim reanalysis: Configuration and performance of the data assimilation system. – Q. J. R. Meteorol. Soc. 137(656): 553-597.
[22] Dingre, S. K., Gorantiwar, S. D. (2020): Determination of the water requirement and crop coefficient values of sugarcane by field water balance method in semiarid region. – Agric. water Manag. 232: 106042.
[23] Djaman, K., O'Neill, M., Diop, L., Bodian, A., Allen, S., Koudahe, K., Lombard, K. (2019): Evaluation of the Penman-Monteith and other 34 reference evapotranspiration equations under limited data in a semiarid dry climate. – Theor. Appl. Climatol. 137: 729-743.
[24] Doorenbos, J. (1977): Guidelines for predicting crop water requirements. – FAO Irrig. Drain. Pap. 24: 1-179.
[25] Dosio, A., Jury, M. W., Almazroui, M., Ashfaq, M., Diallo, I., Engelbrecht, F. A., Klutse, N. A. B., Lennard, C., Pinto, I., Sylla, M. B., Tamoffo, A. T. (2021): Projected future daily characteristics of African precipitation based on global (CMIP5, CMIP6) and regional (CORDEX, CORDEX-CORE) climate models. – Clim. Dyn. 57: 3135-3158.
[26] Duffy, K. A., Schwalm, C. R., Arcus, V. L., Koch, G. W., Liang, L. L., Schipper, L. A. (2021): How close are we to the temperature tipping point of the terrestrial biosphere? – Sci. Adv. 7: eaay1052.
[27] Fernández, M. D., Bonachela, S., Orgaz, F., Thompson, R., López, J. C., Granados, M. R., Gallardo, M., Fereres, E. (2010): Measurement and estimation of plastic greenhouse reference evapotranspiration in a Mediterranean climate. – Irrig. Sci. 28: 497-509.
[28] Flato, G., Marotzke, J., Abiodun, B., Braconnot, P., Chou, S. C., Collins, W. J., Cox, P., Driouech, F., Emori, S., Eyring, V. (2013): Evaluation of climate models. – In: Climate Change 2013: The physical science basis. Contribution of working group I to the fifth

http://www.aloki.hu ● ISSN 1589 1623 (Print) ● ISSN 1785 0037 (Online)
DOI: http://dx.doi.org/10.15666/aeer/1906_48494879

assessment report of the intergovernmental panel on climate change. Clim. Chang. 2013 5: 741-866.
[29] Gomariz-Castillo, F., Alonso-Sarria, F., Cabezas-Calvo-Rubio, F. (2018): Calibration and spatial modelling of daily ET 0 in semiarid areas using Hargreaves equation. – Earth Sci. Informatics 11: 325-340.
[30] Guerschman, J. P., Van Dijk, A.I.J.M., Mattersdorf, G., Beringer, J., Hutley, L.B., Leuning, R., Pipunic, R.C., Sherman, B. S. (2009): Scaling of potential evapotranspiration with MODIS data reproduces flux observations and catchment water balance observations across Australia. – J. Hydrol. 369: 107-119.
[31] Gunkel, A., Lange, J. (2012): New insights into the natural variability of water resources in the Lower Jordan River Basin. – Water Resour. Manag. 26: 963-980.
[32] Hamon, W. R. (1963): Computation of direct runoff amounts from storm rainfall. – Int. Assoc. Sci. Hydrol. Publ. 63: 52-62.
[33] Hansen, S. (1984): Estimation of Potential and Actual Evapotranspiration: Paper presented at the Nordic Hydrological Conference (Nyborg, Denmark, August-1984). – Hydrol. Res. 15: 205-212.
[34] Hargreaves, G. L., Hargreaves, G. H., Riley, J. P. (1985): Agricultural benefits for Senegal River basin. – J. Irrig. Drain. Eng. 111: 113-124.
[35] Hargreaves, G. H. (1994): Defining and using reference evapotranspiration. – J. Irrig. Drain. Eng. 120: 1132-1139.
[36] Hargreaves, G. H., Allen, R. G. (2003): History and evaluation of Hargreaves evapotranspiration equation. – J. Irrig. Drain. Eng. 129: 53-63.
[37] Jensen, M. E., Haise, H. R. (1963): Estimating evapotranspiration from solar radiation. – Proc. Am. Soc. Civ. Eng. J. Irrig. Drain. Div. 89: 15-41.
[38] Kharrufa, N. S. (1985): Simplified equation for evapotranspiration in arid regions. – Beiträge zur Hydrol. 5: 39-47.
[39] Kunz, A., Spelten, N., Konopka, P., Müller, R., Forbes, R. M., Wernli, H. (2014): Comparison of Fast in situ Stratospheric Hygrometer (FISH) measurements of water vapor in the upper troposphere and lower stratosphere (UTLS) with ECMWF (re) analysis data. – Atmos. Chem. Phys. 14: 10803-10822.
[40] Lu, J., Sun, G., McNulty, S. G., Amatya, D. M. (2005): A Comparison of Six Potential Evapotranspiration Methods for Regional Use in the Southeastern United States. – JAWRA J. Am. Water Resour. Assoc. 41: 621-633.
[41] Makkink, G. F. (1957): Testing the Penman formula by means of lysimeters. – J. Inst. Water Eng. 11: 277-288.
[42] Martens, B., Miralles, D. G., Lievens, H., van der Schalie, R., de Jeu, R. A. M., Fernández-Prieto, D., Beck, H. E., Dorigo, W. A., Verhoest, N. E. C. (2016): GLEAM v3: Satellite-based evaporation and root-zone soil moisture. – Geosci. Model Dev. Discuss. 10: 1903-1925.
[43] Monteith, J. L. (1965): Evaporation and environment. – Symposia of the Society for Experimental Biology, pp. 205-234.
[44] Mueller, B., Seneviratne, S. I. (2014): Systematic land climate and evapotranspiration biases in CMIP5 simulations. – Geophys. Res. Lett. 41: 128-134.
[45] Nahar, K. M. O., Ottom, M. A., Alshibli, F., Shquier, M. M. A. (2020): Air Quality Index Using Machine Learning--A Jordan Case Study. – Compusoft 9: 3831-3840.
[46] Ogunrinde, A. T., Olasehinde, D. A., Olotu, Y. (2020): Assessing the sensitivity of standardized precipitation evapotranspiration index to three potential evapotranspiration models in Nigeria. – Sci. African 8: e00431.
[47] Orang, M. (1998): Potential accuracy of the popular non-linear regression equations for estimating pan coefficient values in the original and FAO-24 tables. – Unpubl. Rep., Calif. Dept. Water Resour. Sacramento.
[48] Padrón, R. S., Gudmundsson, L., Decharme, B., Ducharne, A., Lawrence, D. M., Mao, J., Peano, D., Krinner, G., Kim, H., Seneviratne, S. I. (2020): Observed changes in dry-season

http://www.aloki.hu ● ISSN 1589 1623 (Print) ● ISSN 1785 0037 (Online)
DOI: http://dx.doi.org/10.15666/aeer/1906_48494879

water availability attributed to human-induced climate change. – Nat. Geosci. 13: 477-481.
[49] Philip, S. Y., Kew, S. F., van der Wiel, K., Wanders, N., van Oldenborgh, G. J. (2020): Regional differentiation in climate change induced drought trends in the Netherlands. – Environ. Res. Lett. 15: 94081.
[50] Priestley, C. H. B., Taylor, R. J. (1972): On the assessment of surface heat flux and evaporation using large-scale parameters. – Mon. Weather Rev. 100: 81-92.
[51] Rahimikhoob, A., Hosseinzadeh, M. (2014): Assessment of Blaney-Criddle equation for calculating reference evapotranspiration with NOAA/AVHRR data. – Water Resour. Manag. 28: 3365-3375.
[52] Roeckner, E., Bengtsson, L., Feichter, J., Lelieveld, J., Rodhe, H. (1999): Transient climate change simulations with a coupled atmosphere--ocean GCM including the tropospheric sulfur cycle. – J. Clim. 12: 3004-3032.
[53] Romanenko, V. A. (1961): Computation of the autumn soil moisture using a universal relationship for a large area. – Proc. Ukr. Hydrometeorol. Res. Inst. 3: 12-25.
[54] Sabziparvar, A.-A., Tabari, H. (2010): Regional estimation of reference evapotranspiration in arid and semiarid regions. – J. Irrig. Drain. Eng. 136: 724-731.
[55] Samaras, D. A., Reif, A., Theodoropoulos, K. (2014): Evaluation of radiation-based reference evapotranspiration models under different Mediterranean climates in central Greece. – Water Resour. Manag. 28: 207-225.
[56] Sasireka, K., Reddy, C. J. M., Reddy, C. C., Ramakrishnan, K. (2017): Evaluation and Recalibration of Empirical Constant for Estimation of Reference Crop Evapotranspiration against the Modified Penman Method. – In: IOP Conference Series: Earth and Environmental Science. IOP Publishing.
[57] Shahin, M. (2007): Water resources and hydrometeorology of the Arab region. – Springer Science & Business Media.
[58] Simmons, A. J., Jones, P. D., da Costa Bechtold, V., Beljaars, A. C. M., Kållberg, P. W., Saarinen, S., Uppala, S. M., Viterbo, P., Wedi, N. (2004): Comparison of trends and low-frequency variability in CRU, ERA-40, and NCEP/NCAR analyses of surface air temperature. – J. Geophys. Res. Atmos. 109(D24).
[59] Stocker, T. F., Qin, D., Plattner, G. K., Tignor, M., Allen, S. K., Boschung, J., Nauels, A., Xia, Y., Bex, B., Midgley, B. M. (2013): IPCC, 2013: Climate Change 2013: the physical science basis. – Contribution of working group I to the fifth assessment report of the intergovernmental panel on climate change.
[60] Szilagyi, J., Parlange, M. B., Katul, G. G. (2014): Assessment of the Priestley-Taylor parameter value from ERA-Interim global reanalysis data. – J. Hydrol. Environ. Res 2: 1-7.
[61] Tabari, H., Grismer, M. E., Trajkovic, S. (2013): Comparative analysis of 31 reference evapotranspiration methods under humid conditions. – Irrig. Sci. 31: 107-117.
[62] Talaee, P. H. (2014): Performance evaluation of modified versions of Hargreaves equation across a wide range of Iranian climates. – Meteorol. Atmos. Phys. 126: 65-70.
[63] Thornthwaite, C. W. (1948): An approach toward a rational classification of climate. – Geogr. Rev. 38: 55-94.
[64] Todorovic, M., Karic, B., Pereira, L. S. (2013): Reference evapotranspiration estimate with limited weather data across a range of Mediterranean climates. – J. Hydrol. 481: 166-176.
[65] Trajkovic, S., Kolakovic, S. (2009): Evaluation of reference evapotranspiration equations under humid conditions. – Water Resour. Manag. 23: 3057.
[66] Trouet, V., Van Oldenborgh, G. J. (2013): KNMI Climate Explorer: a web-based research tool for high-resolution paleoclimatology. – Tree-Ring Res. 69: 3-13.
[67] Uppala, S., Dee, D., Kobayashi, S., Berrisford, P., Simmons, A. (2008): Towards a climate data assimilation system: Status update of ERA-Interim. – ECMWF Newsl. 115: 12-18.
[68] Valle Júnior, L. C. G., Ventura, T. M., Gomes, R. S. R., de S. Nogueira, J., de A. Lobo, F., Vourlitis, G. L., Rodrigues, T. R. (2020): Comparative assessment of modelled and empirical reference evapotranspiration methods for a Brazilian savanna. – Agric. Water

http://www.aloki.hu ● ISSN 1589 1623 (Print) ● ISSN 1785 0037 (Online)
DOI: http://dx.doi.org/10.15666/aeer/1906_48494879

Manag. 232: 106040.
[69] Wang, S., Zhang, M., Sun, M., Wang, B., Huang, X., Wang, Q., Feng, F. (2015): Comparison of surface air temperature derived from NCEP/DOE R2, ERA-Interim, and observations in the arid northwestern China: a consideration of altitude errors. – Theor. Appl. Climatol. 119: 99-111.
[70] Wang, Y., Li, R., Min, Q., Fu, Y., Wang, Y., Zhong, L., Fu, Y. (2019): A three-source satellite algorithm for retrieving all-sky evapotranspiration rate using combined optical and microwave vegetation index at twenty AsiaFlux sites. – Remote Sens. Environ. 235: 111463.
[71] Wartena, L. (1959): The climate and the evaporation from a lake in central Iraq. – Meded. van Landbouwhogesch. 59: 1-59.
[72] Wickham, H., Grolemund, G. (2016): R for data science: import, tidy, transform, visualize, and model data. – O'Reilly Media, Inc.
[73] Xu, C. (2002): Hydrologic models. – Textb. Uppsala Univ. Dep. Earth Sci. Hydrol.
[74] Xu, C., Singh, V. P. (2001): Evaluation and generalization of temperature-based methods for calculating evaporation. – Hydrol. Process. 15: 305-319.
[75] Zhang, Y. Q., Chiew, F. H. S., Zhang, L., Leuning, R., Cleugh, H. A. (2008): Estimating catchment evaporation and runoff using MODIS leaf area index and the Penman-Monteith equation. – Water Resour. Res. 44.
[76] Zhou, J., Wang, Y., Su, B., Wang, A., Tao, H., Zhai, J., Kundzewicz, Z. W., Jiang, T. (2020): Choice of potential evapotranspiration formulas influences drought assessment: A case study in China. – Atmos. Res. 242: 104979.

http://www.aloki.hu ● ISSN 1589 1623 (Print) ● ISSN 1785 0037 (Online)
DOI: http://dx.doi.org/10.15666/aeer/1906_48494879

MODELING THE DETERMINANTS OF SUSTAINABLE GREEN GROWTH IN THE MENAT REGION: USING THE DCCE-MG APPROACH

ODUGBESAN, J. A.[1*] – AGHAZADEH, S.[2] – RJOUB, H.[3] – DANTAS, R. M.[4] – CORREIA, A. B.[4] – RITA, J. X.[4] – MATA, M. N.[4]

[1]*Department of Business Administration, Cyprus West University, North Cyprus, Mersin 10, Turkey*

[2]*Department of Economics, Final International University, North Cyprus, Mersin 10, Turkey*

[3]*Department of Accounting and Finance, Cyprus International University, North Cyprus, Mersin 10, Turkey*

[4]*Instituto Superior de Contabilidade e Administração de Lisboa, Instituto Politécnico de Lisboa, Avenida Miguel Bombarda 20, 1069-035 Lisbon, Portugal*

**Corresponding author*
e-mail: odugbesanadetola@gmail.com

(Received 22nd May 2021; accepted 20th Sep 2021)

Abstract. The attempt of ensuring that economic growth is becoming greener with additional efficient use of natural capital which is captured in green growth has gained the interest of researchers, but studies in this regard on MENAT countries are scant. Thus, this study attempted to model the determinant factors of green growth in the MENAT countries using data from 1990 to 2019 and employed the Westerlund and Edgerton (2008) panel cointegration test to examine the cointegration among the variables of interest, and employed DCCE-MG technique to establish the significance of the determinant factors, while FMOLS and DOLS were utilized for robustness check. The result from the panel cointegration test revealed an existence of cointegration relationship between the variables in cases of "cross-sectional dependency" and structural breaks, which suggests that the variables move together in the long-run. Moreover, the findings from DCCE-MG estimates revealed that foreign direct investment, economic growth, renewable energy and institutional quality drives sustainable green growth in the MENAT countries, while population was found to exert negative impact on sustainable green growth. The study provides some information that will assist the policymakers in the MENAT countries to balance sustainable green growth, economic growth, internationalization, institutional quality, environmental cost, and population.

Keywords: *sustainable development, environmental quality, economic development, environmental regulation, energy use*

Introduction

Middle Eastern and North African countries including Turkey (MENAT) constitute heterogeneous traits in natural resources, geography, income levels, political and social structures (FAO, 2015; UNICEF, 2021), as well as common context of environmental challenges and trans-boundary conflicts (Abumoghli and Goncalves, 2021). According to Abumoghli and Goncalves (2021), environmental stresses have been one of the notable features in the history of the region and have shown an increasing trend in relation to development patterns in the present time. The environmental stresses among which environmental pollution is expected to exacerbate owing to developments could possibly heighten the climate change (Abumoghli and Goncalves, 2021; De Châtel,

http://www.aloki.hu ● ISSN 1589 1623 (Print) ● ISSN 1785 0037 (Online)
DOI: http://dx.doi.org/10.15666/aeer/1906_48814901

2014; Hungate and Koch, 2015), especially given that the region is one with high vulnerability to its impacts (IPCC, 2013). Meanwhile, this challenge of rising temperature and its attendant implication on livelihoods around the globe have put "sustainable development" (SD) as the top priority in international discourse (IPCC, 2018). The search for ways to tackle this challenge has been on the priority list of most countries and regions and stakeholders which became evident in the renewed actions towards a better environment by the Paris Agreement and 2030 Sustainable Development Agenda (OECD, 2020), with the suggestion that the agenda is for all nations. Meanwhile, even though almost all nations are committed to the agenda, significant variations are observed in the level at which nations are going in the direction of sustainable green growth. For instance, Australia and Belgium are the countries among OECD members that are experiencing a significant increase, while Portugal and Turkey are not showing significant efforts in this regard.

The consideration of the significant role of green growth in the preamble of sustainable development has been of interest to various stakeholders. The green growth in scope is more than the environment as it concerns the development of the economy. A substantial amount of importance in the economic growth paradigm is captured in the "green growth" phenomenon. Samad and Manzoor (2015) described green growth "as a process of greening the conventional economic system and as a strategy to arrive at green economy" (p. 2). This definition is congruent with the position of OECD (2011) which defines green growth as "fostering economic growth and development while ensuring that natural assets continue to provide resources and environmental services on which the intergenerational well-being of humankind relies". Given the multi-dimensional characteristic of environmental issues and the fact that these issues cannot be addressed with "one size fit all" strategy in this time of increasing economic activities, this present study investigates different set of factors that could drive green growth in the MENAT region. According to OECD (2020), green growth is about ensuring that economic growth is becoming greener with additional efficient use of natural capital. The indicator for green growth monitors progress towards a sustainable greener economy, and achievement of this implies the utilization of natural assets for economic growth in a sustainable manner, with the aim of moving in the direction of an economy that results in human well-being and decrease inequalities among people in the long-run without the exposure of unborn generations to environmental risk (OECD, 2018).

Despite the significant role of green growth towards green economy, its determinant factors have not been exhaustively investigated, especially within the MENAT region. Hence, the questions remain that: (i) what are the factors that could drive the sustainable green growth within the MENAT region? (ii) is there cointegration among these variables? These are the questions to be answered in this present study which constitute the study objectives. The MENAT region is one of the regions in the world that has experienced one of the fastest population growths (Lange, 2019). The region in 2019 accounted for a total population of 540 million (World Bank, 2021), with US$9,200 average GDP per capita, which was though below the global average of US$10,900 it is projected to reach about US$22,900 by 2050. These are indications that the region is experiencing development which could possibly increase their energy demand. Energy consumption is noted in the literature as one of the significant contributors to carbon emissions which results to greenhouse gas emissions (Adebayo et al., 2021; Odugbesan & Aghazadeh, 2021; Rjoub et al., 2021a, b, c). The MENAT countries are noted for

http://www.aloki.hu ● ISSN 1589 1623 (Print) ● ISSN 1785 0037 (Online)
DOI: http://dx.doi.org/10.15666/aeer/1906_48814901

accommodating 60% of the world oil reserves and 45% of natural resources which are used for production resulting to carbon emissions (Muhammad, 2019). In addition, according to IEA (2019), the energy-related CO_2 emissions per capita in 2018 were 5.7 t CO_2/capita which is projected to reach 5.97 t CO_2/capita by 2050. This current study would be helpful to make appropriate policy direction for the achievement of sustainable green growth which will ensure the economic growth and reduction in carbon emission shifting the MENAT countries towards green economy.

To the best knowledge of the authors, no comprehensive study has been conducted within the context of the MENAT region to address the determinant factors of sustainable green growth in the long-run, therefore this study will address the gap and thus constitute the motivation of this study. This study will address this gap by modeling carbon productivity (the ration between GDP and the quantity of CO_2 emissions) as dependent variable, and variables like economic factor, internationalization factor, energy-related factor, and institutional quality in reference to previous studies were employed as independent variables (Cosbey, 2011; OECD, 2011, 2012; Tawiah et al., 2021) with the use of "Dynamic Common Correlated Effects-Mean Group" (DCCE-MG). This technique has several advantages among which are: the ability to account for both heterogeneous and homogeneous coefficients; it supports instrumental variable regressions; it controls for "cross-sectional dependence"; appropriate in case of unbalanced panels; utilized "Jack-knife correction method" and "recursive mean adjustment"; and, has the potential of correcting for small sample bias. In order to ensure the robustness of our findings, "Dynamic Ordinary Least Square" (DOLS) regression and "Modified Ordinary Least Square" techniques were employed. The main contribution of this study lies in the novelty of the subject, the choice of estimation techniques and the area of study (MENAT region). Therefore, this present study is aimed at filling the gap in the environmental sustainability literature by investigating the significance of foreign direct investment, economic growth, renewable energy, institutional quality and population as a determinant of sustainable green growth in the MENAT countries with the aid of a novel dynamic panel data estimator which has the capability of addressing the cross-dependency issue in panel data estimation. The remainder of the paper is structured as follows: The "Literature Review" section presents the review of relevant studies capturing green growth determinants. The "Materials and Methods" section presents data description, sources and econometric model, while the estimation methods and findings are presented in the "Estimation Procedures" and "Results" sections, respectively, with important recommendations suggested in the "Conclusion" section.

Literature review

This study aims to empirically investigate the significance of economic development, foreign direct investment, renewable energy, and the institutional quality as a determinant factor for sustainable green growth in the context of the MENAT region, where population was utilized as the control variable. The pairwise nexus among the main study variables will be discussed on the basis of the following strands.

Economic growth and environment

The causal link between the environment and economic development was addressed with the "Environment Kuznet Curve" (EKC) developed by Grossman and Krueger

http://www.aloki.hu ● ISSN 1589 1623 (Print) ● ISSN 1785 0037 (Online)
DOI: http://dx.doi.org/10.15666/aeer/1906_48814901

(1995) which considered it to be an "inverted hum-shaped curve". The study posited that the increase of the environmental deterioration is proportional to income, while it starts decreasing when the curve gets to a plateau of the income threshold. This claim was sustained in some studies who argued that economic growth below the turning point has effect on CO_2 emissions, but when the turning point is crossed by economic growth, the environment quality is improved (Ardakani and Seyedaliakbar, 2019; Chen et al., 2019; Odugbesan & Aghazadeh, 2021; Xie and Liu, 2019). Another study by Wang (2011) examined the causal implication of economic growth on CO_2 emissions for 138 nations using a data from 1971 to 2007 and employed "error correction model", and a "feedback hypothesis" is supported in the study. This finding was similar to another panel study involving 25 OECD countries to examine long-run two-way causalities between per capita CO_2 emissions and GDP between the period from 1980 to 2010 (Jebli et al., 2016). Similar study by Peng et al. (2016) used a sample data from 16 Chinese provinces across three regions between the periods from 1985 to 2012 to examine the impact of GDP on CO_2 emissions. The study revealed that GDP granger cause CO_2 emissions in 15 of the 16 provinces studies, as well as finding a feedback relationship between GDP and CO_2 emissions for one of the provinces. In addition, the evidence of the devastating impact of economic growth on the environment was demonstrated in some previous studies (Adebayo et al., 2021; Adedoyin et al., 2020; Cai et al., 2018; Odugbesan et al., 2020; Pata, 2018; Shahbaz et al., 2013). Meanwhile, some studies demonstrated that increase in economic growth sustains the environment by decreasing CO_2 emissions (Alam and Kabir, 2013; Rahman et al., 2020). For instance, a joint contribution of investment and economic growth on environmental quality was demonstrated in the study of Wang et al. (2019), and the study opined that "emission mitigation policies that encompass the efficient use of energy, clean technology investment, and promotion of labor standard will cut down the rising emissions". Similar study by Mikayilov et al. (2018) showed a significant positive relationship between economic growth and a sustainable environment in Azerbaijan, which corroborates the position of Chang and Hao (2017) who found a positive interaction between environmental performance and economic growth in OECD and non-OECD countries. Though, the empirical studies on green growth is scant, a recent study by Tawiah et al. (2021) that investigated the determinants of green growth in developed and developing countries demonstrated a significant positive impact of economic growth on green growth and concluded that the result differs between developed and developing countries. Besides, literature suggests that several studies which are country-specific and panel studies presents support and opposing evidences on the EKC hypotheses.

Foreign direct investment and environment

From the literature, the impact of "foreign direct investment" (FDI) on environment seems to be heterogeneous, and the impact sometimes could be indirect. For instance, the study of Li et al. (2019) opined that "market-seeking FDI" reacts to market size, while the "efficiency-seeking FDI" reacts to technical endowment. This position was evident in the study of Pao and Tsai (2011) who demonstrated that FDI has a positive effect on productivity while exerts negative influence on the environment. The impact of FDI on the environment is mainly dualistic. For instance, the study of Asghari (2013) and Al-Mulali and Tang (2013) opined that the entrance of FDI into a country comes with consequence like environmental pollution to the host countries; while on the other

http://www.aloki.hu ● ISSN 1589 1623 (Print) ● ISSN 1785 0037 (Online)
DOI: http://dx.doi.org/10.15666/aeer/1906_48814901

hand, the entrance can bring cleaner technologies, stimulate productivity, transfer of technologies and appropriate management practices that will contribute to the environmental quality improvement of the host countries (Abdouli and Hammami, 2018; Al-Mulali and Tang, 2013; Hettige et al., 1996; Omri, 2014). From another perspective, the impact of FDI on environment may be different between developed and developing countries, owing to the fact that advanced level of technology evolution has already being achieved in developed countries. In addition, the stringent environmental regulations in developed countries typically enable the utilization of cleaner technologies, as well as advanced "environmental-management systems" for the optimization of their FDI activities. Meanwhile, this stage is yet to be achieved in the developing countries. The introduction of FDI into some developing countries is often accompanied with environmental pollution owing to the relaxed environmental regulations, which is congruent with the "pollution haven hypothesis" (Baek, 2016; Seker et al. 2015; Shahbaz et al., 2015). Meanwhile, some studies that validates "pollution halo hypothesis" believes that FDI exerts positive effect on environment through the introduction of eco-friendly techniques of production (Al-Mulali and Tang, 2013; Seker et al., 2015), and substantial environmental performance is possible for developing countries as suggested by Cole (2008) through the entrance of FDI with more advanced technologies and development of "environmental-management systems". Moreover, while Ayamba et al. (2019), Li et al. (2019), and Tawiah et al. (2021) found no significant effect of FDI on environmental performance in their respective studies, the study of Awodumi (2020) demonstrated that FDI inflows into West African countries hampers environmental efficiency.

Renewable energy and environment

Studies abound on the relationship between renewable energy and environment. While some studies demonstrate a positive influence of renewable energy on the environment (Akella et al., 2009; Apergis et al., 2010; Farhani and Shahbaz, 2014; Jebli and Youssef, 2017; Majeed and Luni, 2019), as well as ensuring sustainability (Prandecki, 2014), some studies argued that renewable energy exerts negative impact on the environment (Al-Mulali et al., 2016; Belaid and Youseef, 2017; Bilgili et al., 2016; Dogan and Ozturk, 2017; Ito, 2017; Jebli and Youssef, 2017; Kahia et al., 2019; Sharif et al., 2019; Sulaiman et al., 2013; Zoundi, 2017). Meanwhile, insignificance impact of renewable energy on emissions was reported in the study of Al-Mulali et al. (2015), as well as its significant positive effect on green growth was reported by Tawiah, Zakari, Adedoyin (2021). The argument of the studies that believes in the positive influence of renewable energy on the environment is that renewable energy does not emit pollutants; has a "substitution effect"; not prone to depletion unlike fossil fuel; and, with renewable energy, thermal pollution which is caused by conventional sources of energy production can be avoided. In spite of the significant positive effects of renewable energy on the environment, some studies argued that it has a potential of exerting negative effect on the environment. Among the concerns of studies in this category is that combustible renewables and waste for instance are not clean energy use. Jebli and Youssef (2017) opined that if these types of energy use constitute major share in the sources of renewable energy, then there could be increase in emissions. In addition, biofuels, solar, wind geothermal energy for instance require large expanse of land and water, and with the limited land and water availability, the ecological footprint will increase as a result of the renewable energy resources which will in turn contribute to environmental degradation (Al-Mulali et al., 2016). The review of studies on

http://www.aloki.hu ● ISSN 1589 1623 (Print) ● ISSN 1785 0037 (Online)
DOI: http://dx.doi.org/10.15666/aeer/1906_48814901

the relationship between renewable energy and environmental quality showed mixed results and were inconclusive. Meanwhile, renewable energy as a determinant of sustainable green growth is less explored in the literature.

Institutional quality and environment

The institutional quality according to Odugbesan and Rjoub (2019) and Rjoub et al. (2021c) includes rule of law, control of corruption, regulatory quality, political stability, government effectiveness, and voice and accountability have the potential of promoting or retarding green growth. According to Salman et al. (2019), an economic activity will be promoted with a well-established institutional quality while it can as well reduce CO_2 emissions (Sarkodie and Adams, 2018). Similarly, Ibrahim and Law (2016) opined that "high institutional quality is more beneficial in improving a sustainable environment through the effect of trade than in low institutional quality". In addition, the compliance of firms with environmental laws is possible with quality institutions. However, some studies argued that growth of firms could be hindered with stringent environmental regulations enforcement. For instance, Nguyen et al. (2018) observed that a strong enforcement could result to a less innovation and creativity towards environmental improvement. Similarly, some studies opined that environmental protection regulations could be counterproductive to economic growth and development (De Angelis et al., 2019; Wolde-Rufael and Weldemeskel, 2020). Meanwhile, the evidence in this regard is fragile. For instance, the study of Abid (2017) demonstrates the significant negative effects of government effectiveness and democracy on the environment and argued that "democratic institution paves way for foreign investment at the expense of the environment". This position corroborates the study of Kinda (2011) who observed that environmental regulations are being avoided by foreign investors, which motivates them to invest in a country where such policies are not in place and thus increase the pollution. Meanwhile, an insignificant effect of institutional quality on green growth was demonstrated in the study of Tawiah et al. (2021).

Materials and methods

Data

This study employed data from 1990 to 2019 in Middle East and North African countries including Turkey. This study started with the 21 countries mostly recognized under this category (FAO, 2015; UNICEF, 2021). Meanwhile, 8 countries were dropped owing data unavailability, as well as having variables with more than three years consecutive missing values. The final sample of this study covers 13 countries which are: Algeria, Egypt, Iran, Iraq, Jordan, Lebanon, Libya, Morocco, Saudi Arabia, Tunisia, Turkey, United Arab Emirate and Yemen. This study utilized carbon productivity as a proxy for green growth which is the dependent variable and in congruent with the literature (Cigu et al., 2020; Hu and Liu, 2016; Tawiah et al., 2021). Carbon productivity according to OECD (2020) is established as an inclusion in the assessment of economic growth of environment "consumption", being the "ratio between GDP and the quantity of CO_2 emissions". The GDP per capita was included as a determinant factor and a proxy for measuring the effect of economic development on green growth. FDI was used as a proxy to measure how the international activities drives green growth and it measured by the "net inflow of foreign direct investment as a percentage of GDP". Moreover, renewable

http://www.aloki.hu ● ISSN 1589 1623 (Print) ● ISSN 1785 0037 (Online)
DOI: http://dx.doi.org/10.15666/aeer/1906_48814901

energy was used to determine the type of energy consumption effect on the green growth, while institutional quality index was developed using principal component analysis method to examine the effect of institutional quality effect on sustainable green growth. The six institutional quality indicators (rule of law, control of corruption, regulatory quality, political stability, government effectiveness, and voice and accountability) developed by Kaufmann and Kraay (2018) is the most widely used proxy for measuring institutional quality (Odugbesan and Rjoub, 2019; Tawiah et al., 2021; Tunyi et al., 2020). As for the control variable, population was used to control the effect of human activities on green growth in line with the position of Aller et al. (2015) who opined that large population exerts significant impact on the environment. The data for green growth was sourced from OECD database, while the data for FDI, GDP per capita, renewable energy and total population were sourced from World Development Indicators, and institutional quality data were sourced from World Governance Indicator.

From the descriptive statistics presented in *Table 1,* maximum carbon productivity is 6.37 USD/kg, with the minimum of 0.687 USD/kg, while the mean value of 3.413 USD/kg with a standard deviation of 1.213 does not suggest a wide dispersion from the mean by the countries in the sample. Statistics on FDI shows a mean value of 2.654% of GDP, the highest and lowest values among the country being 23.537% and -4.337% of GDP respectively with a standard deviation of 3.606 which indicate a moderate dispersion from the mean by the countries in the sample. The standard deviation of 6.067 indicates a wide dispersion from the sample mean which is 5.078, while the highest and lowest renewable energy are 23.05% and 0.006% of the total final energy consumption of the sampled countries. On average, the intuitional quality index of the sampled countries is -0.019, where the maximum and minimum values are 1.960 and -2.329 respectively with a standard deviation of 0.972 which indicate no wide dispersion from the sample mean. The group statistic for per capita GDP of the sampled countries revealed a mean value of US$9386.55, with a US$64864.72 and US$785 maximum and minimum, respectively with a standard deviation of 13234.96 which suggest a wide dispersion from the sample mean. Finally, the group statistic for population shows an average value of 29 million, while the maximum and minimum population was around 92 million and 25 million with a standard deviation value of 25 million which indicate a wide dispersion from the mean value. The variations in the number of observations as presented in *Table 1* shows the unbalanced nature of the sample data.

Table 1. *Descriptive statistic*

Variable	Mean	Max.	Min.	Std. dev.	Obs
Carbon productivity	3.413	6.37	0.687	1.213	383
Foreign direct investment	2.654	23.537	-4.337	3.606	389
Renewable energy	5.078	23.505	0.006	6.067	338
Institutional quality index	-0.019	1.960	-2.329	0.972	312
GDP per capita	9386.547	64864.72	785.34	13234.96	381
Total population	29931641	92442547	2539126	25455447	390

Model specification

The modeling of determinant factors of sustainable green growth within the context of 13 selected MENAT countries was performed in this present study from 1990 to 2019, and the empirical model is stated as follows:

http://www.aloki.hu ● ISSN 1589 1623 (Print) ● ISSN 1785 0037 (Online)
DOI: http://dx.doi.org/10.15666/aeer/1906_48814901

$$\text{Green growth} = f(\text{Determinants}_{it} + \text{Control variable}_{it}) \quad \text{(Eq.1)}$$

where green growth is the carbon productivity (*CO_2_Prod*); determinants are GDP per capita (*GDP_PC*), foreign direct investment (*FDI*), renewable energy (*RE*), institutional quality index (*IQI*); and control variable is total population (*TP*). In its explicit form, *Equation 1* is expressed in *Equation 2* with the conversion of variable that could create bias due to outliers to natural logarithm. Thus, *Equation 2* is expressed as:

$$CO_{2_{Prod}} + \alpha_0 + \beta_1 FDI_{it} + \beta_2 RE_{it} + \beta_3 IQI_{it} + \beta_4 lnGDP\_PC_{it} + \beta_5 lnPOP_{it} + \varepsilon_{it} \quad \text{(Eq.2)}$$

where α represent intercept, natural logarithm is denoted with *ln*, *i* and *t* denotes the number of countries and time dimension, while represent the parameters to be estimated and ε is the error term.

Estimation procedures

In order to address the study objectives as expressed in *Equation 2,* series of procedures were followed and blend of analytical techniques which has been used in previous studies (Pala, 2020; Rahman, 2020) were deployed to ensure consistency of the estimates.

Cross-sectional dependency (CSD) test

First, the CSD test was applied to determine the appropriate method to be applied. According to Ditzen (2016) and Odugbesan and Rjoub (2020), panel data analysis has some advantages that range from suitable degree of freedom, high efficiency of estimates, and the low occurrence of multicollinearity among the variables. But, owing to the close proximities of the countries and given the likelihood of sharing common characteristics, the risk of "cross-sectionally dependent" panel is very high. Pesaran (2004) opined that biased results and inferences could happen where the data has "cross-sectional dependence" (CSD). This issue can be addressed with the use of Pesaran (2004, 2007) test for "cross-sectional dependency" which is applicable to both small and large panels. In reference to Pesaran (2004, 2007), the H_0 of no CSD which can be rejected at 1%, 5%, and 10% levels is stated as:

$$CD = \sqrt{\frac{2T}{N(N-1)}} \left(\sum_{i=1}^{N-1} \sum_{k=i+1}^{N} \hat{\rho}_{i,k} \right) \quad \text{(Eq.3)}$$

Slope homogeneity test

Moreover, the validity of con-constancy of slope homogeneity in the parameters among the units which according to Gunduz (2017) instigates the significance of "slope heterogeneity" was performed using "slope homogeneity test" developed by Pesaran and Yamagata (2008). This test is an extension of the $\tilde{\Delta}$ test (Swamy, 1970) which is applicable to "a cross-section that is relatively small to the time dimension", while the one by Pesaran and Yamagata (2008) is applicable to "panels with relatively large/small cross-section (*N*) to the time dimension (*T*). Meanwhile, the test can be applied to both unbalanced and balanced data, and the standardized statistics is given as:

http://www.aloki.hu ● ISSN 1589 1623 (Print) ● ISSN 1785 0037 (Online)
DOI: http://dx.doi.org/10.15666/aeer/1906_48814901

$$\tilde{\Delta} = \frac{1}{N}\sum_{i=1}^{N}\left(\frac{\hat{d}_i - k}{\sqrt{2k}}\right) \quad \text{(Eq.4)}$$

The test is asymptotically Δ~N (0,1) with a H_0 of slope homogeneity, d_1 denotes difference between *N* estimator and the pooled estimator $\left(\left(\hat{\beta}_I - \hat{\beta}_{WFE}\right)' \frac{X_{it} M_{ti} X_i}{\hat{\sigma}^2}\left(\hat{\beta}_I - \hat{\beta}_{WFE}\right)\right)$, and the test can be expressed in terms of normally distributed errors utilizing "mean-variance bias-adjusted $\tilde{\Delta}$" (Bersvendsen and Ditzen, 2020) as:

$$\tilde{\Delta}_{adj} = \sqrt{N}\left(\frac{N^{-1}\sum_{i=1}^{N}\hat{d}_i - K}{\sqrt{Var(\hat{z}_i T)}}\right) \quad \text{(Eq.5)}$$

where $Var(\hat{z}_i T) = \frac{2k(T-K-1)}{(T-K+1)}$.

Panel unit root tests

The "cross-sectional augmented Im, Pesaran, and Shin (CIPS)" (Im et al., 2003) and "cross-sectional augmented Dickey–Fuller (CADF)" tests developed by Pesaran (2007) were applied in this study, owing to the presence of "cross-sectional dependence", hence, the data is subjected to second-generation unit root test. In reference to Pesaran (2007), these tests are capable of accounting for "cross-sectional dependence" among the units in the panel, and the equation for CADF is expressed as follows:

$$\Delta y_{it} = \alpha_i + d_i y_{i,t-1} + c_i \Delta\bar{y}_{t-1} + b_i \Delta\bar{y}_t + u_{i,t} \quad \text{(Eq.6)}$$

where the variable being tested is denoted with z_{it}.

The augmented variant of Im et al. (2003) unit root test (CIPS) is stated as:

$$CIPS(N,T) = \bar{T} = N^{-1}\sum_{i=1}^{N} t_i(N,T) \quad \text{(Eq.7)}$$

where the numbers of units and years are represented with *N* and *T* respectively. The unit root test for heterogeneous panels is presented at the left-hand side of *Equation 7,* while term t_i is the "Ordinary least squares (OLS)", *t-ratios* employed in cross-sectional averaged "augmented Dickey-Fuller (ADF) regression is presented in the right-hand side of *Equation 7.*

Panel cointegration tests

This present study employed panel cointegration test developed by Westerlund and Edgerton (2008) which allowed for cross-sectional dependence, serially correlated errors, and structural breaks in both intercept and slope. The test was developed based on the study of Gregory and Hansen (1996). Hence two LM based statistics are defined by Westerlund and Edgerton (2008) which are stated as follows:

http://www.aloki.hu ● ISSN 1589 1623 (Print) ● ISSN 1785 0037 (Online)
DOI: http://dx.doi.org/10.15666/aeer/1906_48814901

$$LM_{\varphi}(i) = T\hat{\varphi}_i \left(\frac{\hat{\omega}_i}{\hat{\sigma}_i}\right) \quad \text{(Eq.8)}$$

$$LM_{\tau}(i) = \frac{\hat{\varphi}_i}{SE(\hat{\varphi}_i)} \quad \text{(Eq.9)}$$

where the least square estimate of φ_i with $\hat{\sigma}_i$ as its estimated standard error is denoted with $\hat{\varphi}_i$, while the estimated long-run variance of Δv_{it} is denoted with $\hat{\omega}_i^2$, and the estimated standard error of $\hat{\varphi}_i$ is represented with $SE(\hat{\varphi}_i)$.

Dynamic common correlated effects-mean group (DCCE-MG)

This study employed DCCE-MG proposed by Ditzen (2016, 2018) to test for the long-run relationship among the variables in this study. According to Ditzen, DCCE-MG has several advantages among which are: the ability to account for both heterogeneous and homogeneous coefficients; it supports instrumental variable regressions; it controls for "cross-sectional dependence"; appropriate in case of unbalanced panels; utilized "Jack-knife correction method" and "recursive mean adjustment"; and, has the potential of correcting for small sample bias. The equation for DCCE-MG is stated as:

$$y_{i,t} = \theta_i y_{i,t-1} + \beta_i x_{i,t} + \sum_{I=0}^{PT} \delta'_{i,I} \bar{Z}_{t-I} + \varepsilon_{i,t} \quad \text{(Eq.10)}$$

where $\bar{Z}_t = (\bar{y}_t \bar{y}_{t-1} \bar{x}_t)$. Therefore, the MG estimates are: $\hat{\pi}_{MG} = \frac{1}{N}\sum_{i=1}^{N} \hat{\pi}_i = (\hat{\theta}_i \hat{\beta}_i)$.

Dynamic OLS and fully modified OLS

The DOLS and FMOLS techniques were employed in the study to test for the robustness of our estimates. The former is "parametric approach in which lags and leads are introduced to cope with the challenges of cross-sectional dependence irrespective of the order of integration and the existence or absence of cointegration," while the latter is "a non-parametric approach that is utilized to deal with serial correlation". The extension of DOLS techniques to panel data analysis is in line with the study of Kao and Chiang (2001), and the model specification is expressed as:

$$y_{i,t} = \beta'_i x_{i,t} + \sum_{j=-q}^{q} \delta_{ij} \Delta x_{i,t+j} + \gamma li' Dl_i + \varepsilon_{i,t} \quad \text{(Eq.11)}$$

where q represents the lags, number chosen using a suitable information criterion. This study finds this technique suitable owing to its potential of providing a robust correction of endogeneity in the independent variables. Similar to DOLS, the use of FMOLS is in reference to Pedroni (2001) which opined that the technique gives consistent estimates of the parameters in small sample data, and it also controls for possible endogeneity of the independent variables and serial autocorrelation. Hence, FMOLS for the *i*-th units is expressed as:

http://www.aloki.hu ● ISSN 1589 1623 (Print) ● ISSN 1785 0037 (Online)
DOI: http://dx.doi.org/10.15666/aeer/1906_48814901

$$\beta_i^* = (X_i' X_i)^{-1}(X_i' y_i^* - T\delta) \quad \text{(Eq.12)}$$

where y^* represent the transformed endogenous variables, the parameter for autocorrelation adjustment is denoted with δ while T represent the years.

Results

CSD test result

The results presented in *Table 2* reveal the rejection of H_0 of no cross-sectional dependency at less than 1% for carbon productivity, FDI, renewable energy, GDP per capita, and total population, while it was rejected at less than 10% for institutional quality index. This outcome implies that any shock in one of the 13 selected MENAT countries may be transmitted to other countries in the panel.

Table 2. *CD test*

Variable	CD-test	*p*-value
Carbon productivity	31.79	.0000
Foreign direct investment	18.33	.0000
Renewable energy	7.07	.0000
Institutional quality index	1.85	.064
GDP per capita, log	14.17	.0000
Total population, log	47.89	.0000

Slope homogeneity test result

The results from the slope homogeneity test presented in *Table 3* shows that the H_0 of homogeneity slope is rejected at less than 1%. This indicates the existence of heterogeneity across the sample countries and as such a heterogeneous panel technique like DCCE-MG is appropriate.

Table 3. *Pesaran and Yamagata (2008) slope homogeneity test*

	Delta	*p*-value
$\tilde{\Delta}$	10.72*	0.0000
$\tilde{\Delta}_{adj}$	12.81*	0.0000

Panel unit root tests results

The results from both the CADF and CIPS are presented in *Table 4* which shows that the null hypothesis of unit root is rejected for almost all the variables at first difference except GDP_PC that is failed to reject the null hypothesis of unit root for CADF. In summary, all the variables are integrated of order 1.

http://www.aloki.hu ● ISSN 1589 1623 (Print) ● ISSN 1785 0037 (Online)
DOI: http://dx.doi.org/10.15666/aeer/1906_48814901

Table 4. *Panel unit root test*

	Level		1st Difference	
Variables	CADF	CIPS	CADF	CIPS
Carbon_Prod	0.450	-1.409	-4.323**	-6.962**
FDI	1.421	-1.605	-2.410*	-8.303**
RE	1..210	-1.350	-3.260**	-7.906**
IQI	0.210	-0.903	-4.308**	-7.109**
lnGDP_pc	-3.210**	-1.768	-	-4.321**
lnPOP	2.001	-1.382	-3.337*	-8.021**

Carbon_Prod = carbon productivity, FDI = foreign direct investment, RE = renewable energy, IQI = institutional quality index, lnGDP_PC = logarithm of gross domestic product per capita, lnPOP = logarithm of total population. *, ** denotes 10% and 5% significance level.

Panel cointegration result

The results from Westerlund and Edgerton (2008) panel cointegration test as presented in *Table 5* shows that the test statistics are significant at 5% significance level which indicate rejection of H_0 of no cointegration, except $Z_t(N)$ statistic for level shift. The outcomes imply the existence of cointegration relationship between the variables in cases of "cross-sectional dependency" and structural breaks, which suggests that the variables move together in the long-run.

Table 5. *Westerlund and Edgerton (2008) cointegration test*

Model	$Z_{\varphi}(N)$	$Z_{\tau}(N)$
No break	-4.520**	-10.112**
Level shift	-3.048**	-0.789
Regime shift	-3.522**	-3.445**

**5% significance level

DCCE-MG result

From the estimates of DCCE-MG presented in *Table 6,* the main determinants without control variable is presented in column 1 and 2, while the full results that includes control variable is presented in column 3 and 4. The FDI is positive and significant at 5% confidence level, indicating a positive effect of FDI on green growth in the long-run. The coefficient and sign for FDI remain unchanged in column 3 when population is added as control variable. This implies that increase in FDI in MENAT countries promotes green growth in the long-run. The finding is congruent with the assumption of "pollution halo hypothesis" which believes that entrance of FDI into a country can bring cleaner technologies, stimulate productivity, transfer of technologies and appropriate management practices that will contribute to the environmental quality improvement of the host countries. In addition, the finding is congruent with the positions of some studies that demonstrated similar finding in their studies (Abdouli and Hammami, 2018; Al-Mulali and Tang, 2013; Omri, 2014; Seker et al., 2015). Meanwhile, the finding contrasts the finding of Baek (2016), Seker et al. (2015), and

http://www.aloki.hu ● ISSN 1589 1623 (Print) ● ISSN 1785 0037 (Online)
DOI: http://dx.doi.org/10.15666/aeer/1906_48814901

Shahbaz et al. (2015); as well as those studies that showed an insignificant effect of FDI on the environmental quality (Ayamba et al., 2019; Tawiah et al., 2021).

The result from the estimation of renewable energy as a determinant of green growth as presented in *Table 6* shows renewable energy as a significant determinant of green growth at 5% confidence level. Meanwhile, the variable becomes insignificant when population is added to the model. The result implies that an increase in renewable energy in MENAT countries with regulated population will promote green growth in the long run. This finding is consistent with previous studies (Jebli and Youssef, 2017; Majeed and Luni, 2019; Tawiah et al., 2021) who argued that renewable energy is more beneficial to the environment. Meanwhile, the finding is in contrast with some studies (Al-Mulali et al., 2016; Belaid and Youssef, 2017; Kahia et al., 2019; Sharif et al., 2019) who argued that renewable energy has potential of exerting negative influence on environmental quality because it requires large expanse of resources like land and water that are limited in supply, and this can increase ecological footprint with attendant effect on the environment.

Table 6. *DCCE-MG results*

	(1)		(2)	
Variables	**Coefficient**	**t-statistics**	**Coefficient**	**t-statistics**
FDI	0.079	2.770**	0.060***	8.357
RE	0.271	2.948**	-0.019	-0.583
IQI	0.026	0.367	0.827***	7.017
lnGDP_pc	2.558	5.923**	5.409***	9.501
lnPOP			-0.019***	5.29

Carbon_Prod = carbon productivity, FDI = foreign direct investment, RE = renewable energy, IQI = institutional quality index, lnGDP_PC = logarithm of gross domestic product per capita, lnPOP = logarithm of total population. ** and *** denote 5% and 1% significance level

The output from the investigation of institutional quality as a determinant of green growth reveals non-significance of the coefficient, but when the control variable is added, it becomes positive and significant at 1% confidence level. This finding indicates that institutional quality promotes green growth in MENAT countries in the long run when population is controlled. This is consistent with the study of Ibrahim and Law (2016) and Sarkodie and Adams (2018) who argued in their respective study that a well-established institutional quality can reduce CO_2 emissions, but in contrast to the studies of De Angeli et al. (2019), Nguyen et al. (2018), and Wolde-Rufael and Weldemesle (2020), who suggest strong environmental regulations could result to less innovation and creativity towards environmental improvement, which can as well be counterproductive to development; as well as the study of Tawiah et al. (2021) who showed insignificant relationship between institutional quality and green growth.

As expected, the finding from the estimation of GDP per capita as a determinant of green growth as presented in *Table 6* reveal to be positive and significant. This is an indication that GDP per capita promotes green growth in MENAT countries in the long run at 5% confidence level. The sign of the parameter remains unchanged in column 3 when population is controlled. The finding is congruent with some previous studies (Ardakani and Seyedaliakbar, 2019; Chen et al., 2019; Mikayilov et al., 2018; Rahman et al., 2020; Wang et al., 2019; Xie and Liu, 2019), but contrasts to some studies

http://www.aloki.hu ● ISSN 1589 1623 (Print) ● ISSN 1785 0037 (Online)
DOI: http://dx.doi.org/10.15666/aeer/1906_48814901

(Adebayo et al., 2021; Adedoyin et al., 2020; Cai et al., 2018; Pata, 2018; Tawiah et al., 2018) who opined that increase in economic development has a devastating effect on the environment. Finally, the estimates for the control variable as presented in *Table 6* shows that population is a significant determinant of green growth. The negative and significant coefficient of the variable indicates that a percentage change in population will reduce the green growth of MENAT countries by 0.019% at less than 1% confidence level. This finding supports the position of Aller et al. (2015) who opined that large population exerts significant impact on environment, as well as the study of Tawiah et al. (2021) who established similar finding in their study.

Robustness check

The results from the FMOLS and DOLS techniques as presented in *Table 7* indicate that foreign direct investment, renewable energy, economic development promotes green growth in MENAT countries in the long run, while population exerts negative impact on the green growth of the sample countries in the long run. Generally, the estimates from FMOLS and DOLS estimations are in tandem with those of DCCE-MG, except for institutional quality that is not significant. The insignificance of the variable in the estimations of FMOLS and DOLS could be because the dependence among the sample countries has been controlled by the DCCE-MG technique. Thus, solely reliance on estimates from FMOLS and DOLS techniques could lead to a flawed outcome and bias inference.

Table 7. *FMOLS and DOLS results*

	FMOLS		**DOLS**	
Variables	(1)	(2)	(1)	(2)
FDI	0.067*	0.049**	0.190**	0.273**
RE	0.096*	0.065*	0.149***	0.225**
IQI	0.077	0.109	-0.084	0.078
lnGDP_pc	1.744**	1.881***	1.252**	9.795**
lnPOP		-1.368***		-3.803***

NCarbon_Prod = carbon productivity, FDI = foreign direct investment, RE = renewable energy, IQI = institutional quality index, lnGDP_PC = logarithm of gross domestic product per capita, lnPOP = logarithm of total population. *, ** and *** denotes 10%, 5% and 1% significance level respectively

Conclusion

This study investigates the significance of foreign direct investment, economic development, institutional quality, and renewable energy as determinant factor for green growth using an unbalanced panel data of 13 selected MENAT countries over the period 1990-2019. We used an innovative panel data estimator (DCCE-MG) that addresses cross-sectional dependency issue among the sample countries, as well as FMOLS and DOLS to ensure robustness of our estimates. Our findings provide sufficient evidence to address the study objectives which are: (i) to determine the significance of determinant factor for green growth in MENAT countries, and (ii) to examine the cointegration among the variables. The results from the Westerlund and Edgerton (2008) test show a cointegration relationship between green growth, foreign direct investment, economic

http://www.aloki.hu ● ISSN 1589 1623 (Print) ● ISSN 1785 0037 (Online)
DOI: http://dx.doi.org/10.15666/aeer/1906_48814901

development, renewable energy, institutional quality and population in cases of cross-sectional dependency and structural breaks. These findings address second objective of this study, and then conclude that the variables have potential of moving together in the long run. Moreover, the estimate from DCCE-MG addresses the first objective of this study which intends to examine the determinants factors of green growth in MENAT countries. The findings show that foreign direct investment, renewable energy, institutional quality, and GDP per capita promotes green growth, while population exerts a devastating effect on green growth in MENAT countries. This suggests that foreign direct investment, GDP per capita, renewable energy, institutional quality, and population are significant determinants of green growth in MENAT countries. In view of these, it becomes imperative for the countries in the region to pay more attention to inflow of foreign direct investment into their countries, implementation of institutional quality, the economic growth, as well the control of population, because of the heterogeneous nature of the countries (FAO, 2015; UNICEF, 2021); but as a region, owing to their common context of environmental challenges and trans-boundary conflicts (Abumoghli and Goncalves, 2021), especially as noted by Odugbesan and Rjoub (2019, 2020) sustainable development goes beyond a boundary.

An important policy implication in line with the findings from this study is that the results above do not provide concerted information for policy makers in these countries alone, but also individual details for each country's stakeholders since the result of heterogeneity implies that each countries country in the panel of the MENAT region may develop its green growth policies. Moreover, the government of the sample countries and policymakers should tread carefully in choosing international business policies towards green growth by ensuring that the entrance of such investment into their country is beneficial and not detrimental to the host country environment which could create pollution. Against this backdrop, employment of minimal foreign investment with stringent supervision is suggested, so as not to give room for foreign investors' exploitation. In reference to the finding on GDP per capital as a significant determinant, the sample countries should maintain high level of GDP per capita as this will drive the sustainability of green growth in the respective country through the purchase of eco-friendly products. Another policy implication on the renewable energy as a determinant factor is that policy makers should promote renewable energy through grant offers and loans to investors in this industry, as well as tax holiday which would give leverage to the investors and thus contribute to the reduction of emissions, and consequently achieve sustainable green growth. In reference to the institutional quality, policy makers should ensure that a well-established institutional quality is in place but not too strict to avoid the trap of being counterproductive to economic growth and development (De Angelis et al., 2019; Wolde-Rufael and Weldemeskel, 2020). Finally, the policy makers should put in place a policy that will address the geometrical growth of population in the MENAT countries which showed in this study to have a devastating effect on achieving green growth. Therefore, we encourage the government and policymakers to ensure that the population is checked in order to achieve sustainable green growth in the region.

Though, this study contributes significantly to the debates on investigating the determinants of green growth, meanwhile it is not devoid of limitation. The limitation lies in the number of determinant variables and control variable. Future studies can expand the model and add more variables, and also disaggregate the institutional quality to ascertain which of the six dimensions actually contribute to sustainable green growth.

http://www.aloki.hu ● ISSN 1589 1623 (Print) ● ISSN 1785 0037 (Online)
DOI: http://dx.doi.org/10.15666/aeer/1906_48814901

The investigation of more possible determinants of sustainable green growth is to avoid the omitted variable bias that could arise from the limited number of variables used in this study. Nevertheless, this study can help policy makers to balance sustainable green growth, economic growth, internationalization, institutional quality, environmental cost, and population.

REFERENCES

[1] Abdouli, M., Hammami, S. (2018): The dynamic links between environmental quality, foreign direct investment, and economic growth in the Middle Eastern and North African countries (MENA region). – Journal of the Knowledge Economy 9(3): 833-853.
[2] Abid, M. (2017): Does economic, financial and institutional developments matter for environmental quality? A comparative analysis of EU and MEA countries. – Journal of Environmental Management 188: 183-194.
[3] Abumoghli, I., Goncalves, A. (2021): Environmental challenges in the Mena region. – http://www.indiaenvironmentportal.org.in/files/file/Environmental-challenges-in-theMENA-region.pdf (accessed: 25th April 2021).
[4] Adebayo, T. S., Awosusi, A. A., Odugbesan, J. A., Akinsola, G. D., Wong, W. K., Rjoub, H. (2021): Sustainability of energy-induced growth nexus in Brazil: do carbon emissions and urbanization matter? – Sustainability 13(8): 4371.
[5] Adedoyin, F. F., Bekun, F. V., Alola, A. A. (2020): Growth impact of transition from non-renewable to renewable energy in the EU: the role of research and development expenditure. – Renewable Energy 159: 1139-1145.
[6] Akella, A. K., Saini, R. P., Sharma, M. P. (2009): Social, economical and environmental impacts of renewable energy systems. – Renewable Energy 34: 390-396.
[7] Alam, M. S., Kabir, N. (2013): Economic growth and environmental sustainability: empirical evidence from East and South-East Asia. – International Journal of Economics and Finance 5(2).
[8] Aller, C., Ductor, L., Herrerias, M. J. (2015): The world trade network and the environment. – Energy Economics 52:55-68.
[9] Al-Mulali, U., Tang, C. F. (2013): Investigating the validity of pollution haven hypothesis in the gulf cooperation council (GCC) countries. – Energy Policy 60: 813-819.
[10] Al-Mulali, U., Saboori, B., Ozturk, I. (2015): Investigating the environmental Kuznets curve hypothesis in Vietnam. – Energy Policy 76: 123-131.
[11] Al-Mulali, U., Solarin, S. A., Sheau-Ting, L., Ozturk, I. (2016): Does moving towards renewable energy cause water and land inefficiency? An empirical investigation. – Energy Policy 93: 303-314.
[12] Apergis, N., Payne, J. E., Menyah, K., Wolde-Rufael, Y. (2010): On the causal dynamics between emissions, nuclear energy, renewable energy, and economic growth. – Ecological Economics 69(11): 2255-2260.
[13] Ardakani, M. K., Seyedaliakbar, S. M. (2019): Impact of energy consumption and economic growth on CO_2 emission using multivariate regression. – Energy Strategy Reviews 26: 100428.
[14] Asghari, M. (2013): Does FDI promote MENA region's environment quality? Pollution halo or pollution haven hypothesis. – Int J Sci Res Environ Sci 1(6): 92-100.
[15] Awodumi, O. B. (2020): Does foreign direct investment promote environmental efficiency in developing economies? Evidence from Economic Community of West African States. – Business Strategy & Development. DOI: 10.1002/bsd2.137.
[16] Ayamba, E. C., Haibo, C., Ibn Musah, A.-A., Ruth, A., Osei-Agyemang, A. (2019): An empirical model on the impact of foreign direct investment on China's environmental

http://www.aloki.hu ● ISSN 1589 1623 (Print) ● ISSN 1785 0037 (Online)
DOI: http://dx.doi.org/10.15666/aeer/1906_48814901

pollution: analysis based on simultaneous equations. – Environmental Science and Pollution Research 26(16):16239-16248.
[17] Baek, J. (2016): A new look at the FDI–income–energy–environment nexus: dynamic panel data analysis of ASEAN. – Energy Policy 91: 22-27.
[18] Belaid, F., Youssef, M. (2017): Environmental degradation, renewable and nonrenewable electricity consumption, and economic growth: assessing the evidence from Algeria. – Energy Policy 102: 277-287.
[19] Bersvendsen, T., Ditzen, J. (2020): Xthst: Testing for Slope Homogeneity in Stata. – Centre for Energy Research and Policy, Working Paper No 11.
[20] Bilgili, F., Koçak, E., Bulut, U. (2016): The dynamic impact of renewable energy consumption on CO2 emissions: a revisited environmental Kuznets curve approach. – Renewable and Sustainable Energy Reviews 54: 838-845.
[21] Cai, Y., Sam, C. Y., Chang, T. (2018): Nexus between clean energy consumption, economic growth and CO2 emissions. – Journal of Cleaner Production 182: 1001-1011.
[22] Chang CP, Hao Y (2017): Environmental performance, corruption, and economic growth: global evidence using a new data set. – Applied Economics 49:498-514.
[23] Chen, Y., Zhao, J., Lai, Z., Wang, Z., Xia H (2019): Exploring the effects of economic growth, and renewable and non-renewable energy consumption on China's CO2 emissions: evidence from a regional panel analysis. – Renewable Energy 140:341-353.
[24] Cigu, E., Petrișor, M. B., Nuță, A. C., Nuță, F. M., Bostan, I. (2020): The Nexus between Financial Regulation and Green Sustainable Economy. – Sustainability 12(21): 8778.
[25] Cole, M. A., Elliott, R. J., Strobl, E. (2008): The environmental performance of firms: the role of foreign ownership, training, and experience. – Ecological Economics 65(3): 538-546.
[26] Cosbey A (2011): Trade, Sustainable Development and a Green Economy: Benefits, Challenges and Risks. – In: UN-DESA, UNEP, UNCTAD (eds.) The Transition to a Green Economy: Benefits, Challenges and Risks from a Sustainable Development Perspective. UNDESA, New York. http://www.uncsd2012.org/rio20/content/documents/Green%20Economy_full%20report.pdf.
[27] De Angelis, E. M., Di Giacomo, M., Vannoni, D. (2019): Climate change and economic growth: the role of environmental policy stringency. – Sustainability 11:2273.
[28] De Châtel, F. (2014): The role of drought and climate change in the Syrian uprising: untangling the triggers of the revolution. – Middle Eastern Studies 50(4): 521-535.
[29] Ditzen, J. (2016): xtdcce2: Estimating Dynamic Common Correlated Effects in Stata. – SEEC Discussion Papers 1601, Spatial Economics and Econometrics Centre, Heriot Watt University Edinburgh.
[30] Ditzen, J. (2018): Estimating dynamic commom-correlated effects in stata. – The Stata Journal 18(30): 585-617. DOI: 10.1177/1536867X0600600403.
[31] Dogan, E., Ozturk, I. (2017): The influence of renewable and non-renewable energy consumption and real income on CO2 emissions in the USA: evidence from structural break tests. – Environmental Science and Pollution Research 24(11): 10846-10854.
[32] FAO (2015): Egypt, Jordan, Morocco and Tunisia: Key Trends in the Agrifood Sector. – http://www.fao.org/3/i4897e/i4897e.pdf.
[33] Farhani, S., Shahbaz, M. (2014): What role of renewable and non-renewable electricity consumption and output is needed to initially mitigate CO2 emissions in MENA region? – Renewable and Sustainable Energy Reviews 40: 80-90.
[34] Gregory, A. W., Hansen, B. E. (1996): Residual-based tests for cointegration in models with regime shifts. – Journal of Econometrics 70(1): 99-126.
[35] Grossman, G. M., Krueger, A. B. (1995): Economic growth and the environment. – The Quarterly Journal of Economics 110(2): 353-377.
[36] Gunduz, H. I. (2017): Testing for Slope homogeneity in dynamic panel using the wild bootstrap test. – Ekonometric ve Istatistik Sayi 26: 53-59.

http://www.aloki.hu ● ISSN 1589 1623 (Print) ● ISSN 1785 0037 (Online)
DOI: http://dx.doi.org/10.15666/aeer/1906_48814901

[37] Hettige, H., Huq, M., Pargal, S., Wheeler, D. (1996): Determinants of pollution abatement in developing countries: evidence from South and Southeast Asia. – World Development 24(12): 1891-1904.
[38] Hu, X.; Liu, C. (2016): Carbon productivity: a case study in the Australian construction industry. – Journal of Cleaner Production 112: 2354-2362.
[39] Hungate, B. A., Koch, G. W. (2015): Global Change - Biospheric Impacts and Feedbacks. – In: North, G. R., Pyle, J., Zhang, F. (eds.) Encyclopedia of Atmospheric Science. Second Ed. Academic Press, London, pp. 132-140.
[40] Ibrahim, M. H., Law, S. H. (2016): Institutional quality and CO2 emission–trade relations: evidence from Sub-Saharan Africa. – South African Journal of Economics 84(2): 323-340.
[41] IEA (2019): IEA Beyond 20/20. 2019 Ed. – International Energy Agency, Paris.
[42] Im, K. S., Pesaran, M. H., Shin, Y. (2003): Testing for unit roots in heterogeneous panels. – Econometrics 115(1): 53-74.
[43] International Panel on Climate Change [IPCC] (2013): Climate Change 2013: The Physical Science Basis. – In: Stocker, T. F., Qin, D., Plattner, G.-K., Tignor, M., Allen, S. K., Boschung, J., Nauels, A., Xia, Y., Bex, V., Midgley, P. M. (eds.) Contribution of Working Group I to the Fifth Assessment Report of the Intergovernmental Panel on Climate Change. Cambridge University Press, Cambridge, United Kingdom and New York.
[44] IPCC (2018): Global warming of 1.5 °C. An IPCC special report on the impacts of global warming of 1.5 °C above pre-industrial levels and related global greenhouse gas emission pathways in the context of strengthening the global response to the threat of climate change. – https://www.ipcc.ch/sr15/.
[45] Ito, K. (2017): CO2 emissions, renewable, and non-renewable energy consumption, and economic growth: evidence from panel data for developing countries. – International Economics 151: 1-6.
[46] Jebli, M. B., Youssef, S. B. (2017): The role of renewable energy and agriculture in reducing CO2 emissions: evidence for North Africa countries. – Ecological Indicators 74: 295-301.
[47] Jebli, M. B., Youssef, S. B., Ozturk, I. (2016): Testing environmental Kuznets curve hypothesis: the role of renewable and non-renewable energy consumption and trade in OECD countries. – Ecological Indicators 60: 824-831.
[48] Kahia, M., Jebli, M. B., Belloumi, M. (2019): Analysis of the impact of renewable energy consumption and economic growth on carbon dioxide emissions in 12 MENA countries. – Clean Technologies and Environmental Policy 1-15.
[49] Kao, C., Chiang, M. H. (2001): On the Estimation and Inference of a Cointegrated Regression in Panel Data. – In: Baltagi, B. H. et al. (eds.) Nonstationary Panels, Panel Cointegration, and Dynamic Panels. Emerald Group Publishing Limited, Bingley.
[50] Kaufmann, D., Kraay, A. (2018): The Worldwide Governance Indicators. – The World Bank. https://info.worldbank.org/governance/wgi/.
[51] Kinda S (2011): Democratic institutions and environmental quality: effects and transmission channels. – SSRN 2714300.
[52] Lange, M. A. (2019): Impacts of climate change on the Eastern Mediterranean and the Middle East and North Africa region and the water–energy nexus. – Atmosphere 10(8): 455.
[53] Li, Z., Huang, Z., Dong, H. (2019): The influential factors on outward foreign direct investment: evidence from the "The Belt and Road". – Emerging Markets Finance and Trade 55(14): 3211-3226.
[54] Majeed, M. T., Luni, T. (2019): Renewable energy, water, and environmental degradation: a global panel data approach. – Pakistan Journal of Commerce and Social Sciences (PJCSS): 13(3): 749-778.

http://www.aloki.hu ● ISSN 1589 1623 (Print) ● ISSN 1785 0037 (Online)
DOI: http://dx.doi.org/10.15666/aeer/1906_48814901

[55] Mikayilov, J. I., Galeotti, M., Hasanov, F. J. (2018): The impact of economic growth on CO2 emissions in Azerbaijan. – Journal of Cleaner Production. 197:1558-1572.
[56] Muhammad, B. (2019): Energy consumption, CO2 emissions and economic growth in developed, emerging and Middle East and North Africa countries. – Energy 179: 232-245.
[57] Nguyen, C. P., Nguyen, N. A., Schinckus, C., Su, T. D. (2018): The ambivalent role of institutions in the CO2 emissions: the case of emerging countries. – International Journal of Energy Economics and Policy 8(5): 7.
[58] Odugbesan, J. A., Rjoub, H. (2019a): Relationship among HIV/AIDS prevalence, human capital, good governance, and sustainable development: empirical evidence from Sub-Saharan Africa. – Sustainability 11(5): 1348.
[59] ODUGBESAN, J. A. & Rjoub, H. (2019b). THE CAUSAL RELATIONSHIP BETWEEN ECONOMIC GROWTH AND REMITTANCE IN MINT COUNTRIES: AN ARDL BOUNDS TESTING APPROACH TO COINTEGRATION. *Journal of Academic Research in Economics*, *11*(2).
[60] Odugbesan, J. A., Rjoub, H. (2020): Evaluating HIV/Aids prevalence and sustainable development in sub-Saharan Africa: the role of health expenditure. – African Health Sciences 20(2): 568-578.
[61] Odugbesan, J. A., Ike, G., Olowu, G., Adeleye, B. N. (2020): Investigating the causality between financial inclusion, financial development and sustainable development in Sub-Saharan Africa economies: the mediating role of foreign direct investment. – Journal of Public Affairs, e2569.
[62] Odugbesan, J. A., & Aghazadeh, S. (2021). Environmental Pollution and Disaggregated Economic Policy Uncertainty: Evidence from Japan. *Pollution*, *7*(4), 749-767.
[63] OECD (2011): Tools for delivering on green growth. – http://www.oecd.org/dataoecd/32/48/48012326.pdf.
[64] OECD (2018): What is green growth, and how can it help deliver sustainable development? – – http://www.oecd.org/greengrowth/whatisgreengrowthandhowcanithelpdeliversustainabledevelopment.htm.
[65] OECD (2020): OECD work on green growth. – https://issuu.com/oecd.publishing/docs/gg_brochure_2019_web.
[66] OECD, World Bank, UN (2012): Incorporating green growth and sustainable development policies into structural reform agendas. – Prepared for the G20 Summit (Los Cabos, 18-19 June). OECD, Paris. http://www.oecd.org/eco/economicpoliciestofostergreengrowth/G20_report_on_GG_and_SD_final.pdf.
[67] Omri, A. (2014): The nexus among foreign investment, domestic capital and economic growth: empirical evidence from the MENA region. – Research in Economics 68(3): 257-263.
[68] Pala, A. (2020): Energy and economic growth in G20 countries: panel cointegration analysis. – Economics and Business Letters 9(2): 56-72.
[69] Pao, H. T., Tsai, C. M. (2011): Modeling and forecasting the CO2 emissions, energy consumption, and economic growth in Brazil. – Energy 36(5): 2450-2458.
[70] Pata, U. K. (2018): Renewable energy consumption, urbanization, financial development, income and CO2 emissions in Turkey: testing EKC hypothesis with structural breaks. – Journal of Cleaner Production 187: 770-779.
[71] Pedroni, P. (2001): Fully Modified OLS for Heterogeneous Cointegrated Panels. – In: Baltagi, B. H. et al. (eds.) Nonstationary Panels, Panel Cointegration, and Dynamic Panels. Emerald Group Publishing Limited, Bingley.
[72] Peng, H.; Tan, X.; Li, Y.; Hu, L. (2016): Economic growth, foreign direct investment and co2 emissions in China: a panel granger causality analysis. – Sustainability 8: 233.

http://www.aloki.hu ● ISSN 1589 1623 (Print) ● ISSN 1785 0037 (Online)
DOI: http://dx.doi.org/10.15666/aeer/1906_48814901

[73] Pesaran, M. H. (2004): General Diagnostic Tests for Cross Section Dependence in Panels. – Working Papers in Economics, No. 0435. University of Cambridge, Faculty of Economics, Cambridge.
[74] Pesaran, M. H. (2007): A simple unit root test in the presence of cross-section dependence. – Journal of Applied Economics 22: 265-312.
[75] Pesaran, M. H., Yamagata, T. (2008): Testing slope homogeneity in large panels. – Journal of Econometrics 142(2008): 50-93.
[76] Prandecki, K. (2014): Theoretical aspects of sustainable energy. – Energy and Environmental Engineering 2(4): 83-90.
[77] Rahman, M. M., Saidi, K., Mbarek, M. B. (2020): Economic growth in South Asia: the role of CO2 emissions, population density, and trade openness. – Heliyon 6:03903.
[78] Rjoub, H., Odugbesan, J. A., Adebayo, T. S., Wong, W. K. (2021a): Sustainability of the moderating role of financial development in the determinants of environmental degradation: evidence from Turkey. – Sustainability 13(4): 1844.
[79] Rjoub, H., Odugbesan, J. A., Adebayo, T. S., Wong, W. K. (2021b): Investigating the causal relationships among carbon emissions, economic growth, and life expectancy in Turkey: evidence from time and frequency domain causality techniques. – Sustainability 13(5): 2924.
[80] Rjoub, H., Ifediora, C. U., Odugbesan, J. A., Iloka, B. C., Xavier Rita, J., Dantas, R. M., ... & Martins, J. M. (2021). Implications of Governance, Natural Resources, and Security Threats on Economic Development: Evidence from Sub-Saharan Africa. *International Journal of Environmental Research and Public Health*, *18*(12), 6236.
[81] Salman, M., Long, X., Dauda, L., Mensah, C. N. (2019): The impact of institutional quality on economic growth and carbon emissions: evidence from Indonesia, South Korea, and Thailand. – Journal of Cleaner Production 241: 118331.
[82] Samad, G., Manzoor, R. (2015): Green growth: important determinants. – The Singapore Economic Review 60(02): 1550014.
[83] Sarkodie, S. A., Adams, S. (2018): Renewable energy, nuclear energy, and environmental pollution: accounting for political institutional quality in South Africa. – Science of the Total Environment 643: 1590-1601.
[84] Seker, F., Ertugrul, H. M., Cetin, M. (2015): The impact of foreign direct investment on environmental quality: a bounds testing and causality analysis for Turkey. – Renewable and Sustainable Energy Reviews 52: 347-356.
[85] Shahbaz, M., Ozturk, I., Afza, T., Ali, A. (2013): Revisiting the environmental Kuznets curve in a global economy. – Renewable and Sustainable Energy Reviews 25: 494-502.
[86] Shahbaz, M.; Nasreen, S.; Abbas, F.; Anis, O. (2015): Does foreign direct investment impede environmental quality in high-, middle-, and low-income countries? – Energy Economics 51: 275-287.
[87] Sharif, A., Raza, S. A., Ozturk, I., Afshan, S. (2019): The dynamic relationship of renewable and nonrenewable energy consumption with carbon emission: a global study with the application of heterogeneous panel estimations. – Renewable Energy 133: 685-691.
[88] Sulaiman, J., Azman, A., Saboori, B. (2013): The potential of renewable energy: using the Environmental Kuznets curve model. – American Journal of Environmental Sciences 9(2): 103-112.
[89] Swamy, P. A. (1970): Efficient inference in a random coefficient regression model. – Journal of the Econometric Society 38(2): 311-323.
[90] Tawiah, V., Zakari, A., Adedoyin, F. F. (2021): Determinants of green growth in developed and developing countries. – Environmental Science and Pollution Research. DOI: 10.1007/s11356-021-13429-0.
[91] Tunyi, A. A., Ehalaiye, D., Gyapong, E., Ntim, C. G. (2020): The value of discretion in Africa: evidence from acquired intangible assets under IFRS 3. – The International Journal of Accounting 55(02): 2050008.

http://www.aloki.hu ● ISSN 1589 1623 (Print) ● ISSN 1785 0037 (Online)
DOI: http://dx.doi.org/10.15666/aeer/1906_48814901

[92] UNICEF (2021): https://www.unicef.org/infobycountry/northafrica.html. – UNICEF, New York.
[93] Wang, K. M. (2011): Health care expenditure and economic growth: quantile panel-type analysis. – Economic Modelling 28(4): 1536-1549.
[94] Wang, Q., Jiang, X. T., Ge, S., Jiang, R. (2019): Is economic growth compatible with a reduction in CO2 emissions? Empirical analysis of the United States. – Resources, Conservation and Recycling 151: 104443.
[95] Westerlund, J., and Edgerton, D. (2008): A simple test for cointegration in dependent panels with structural breaks. – Oxford Bulletin of Economics and Statistics 70(5): 665-704.
[96] Wolde-Rufael, Y., Weldemeskel, E. M. (2020): Environmental policy stringency, renewable energy consumption and CO2 emissions: panel cointegration analysis for BRIICTS countries. – International Journal of Green Energy 17(10): 568-582.
[97] World Bank (2021): World Bank Development Indicators. – https://data.worldbank.org/.
[98] Xie, Q., Liu, J. (2019): Combined nonlinear effects of economic growth and urbanization on CO2 emissions in China: evidence from a panel data partially linear additive model. – Energy 186: 115868.
[99] Zoundi, Z. (2017): CO2 emissions, renewable energy, and the environmental Kuznets curve, a panel cointegration approach. – Renewable and Sustainable Energy Reviews 72: 1067-1075.

http://www.aloki.hu ● ISSN 1589 1623 (Print) ● ISSN 1785 0037 (Online)
DOI: http://dx.doi.org/10.15666/aeer/1906_48814901

PATTERNS OF BIRD RELATIVE ABUNDANCE, DIVERSITY INDICES AND CONSERVATION STATUS IN SHEIKH BADIN NATIONAL PARK, D. I. KHAN, PAKISTAN

ULLAH, I.[1] – SUN, X. Y.[1] – WU, Q.-M.[1*] – XU, Z.[1,2] – KHAN, M. S.[3] – RAJPAR, M. N.[4] – KHAN, T. U.[5] – PUSWAL, S. M.[6]

[1]*College of Wildlife and Protected Areas, Northeast Forestry University, No 26, Hexing Road, Harbin 150040, P. R. China*

[2]*Heilongjiang Zhalong National Nature Reserve, Qiqihar 161000, P. R. China*

[3]*Research Center for Eco-Environmental Sciences, University of Chinese Academy of Sciences, P. R. China*

[4]*Department of Forestry, Faculty of Life Sciences, Shaheed Benazir Bhutto University, Sheringal Dir Upper 18050, Pakistan*

[5]*School of Nature Conservation, Beijing Forestry University, Beijing 100083, P. R. China*

[6]*Instutute of Technical Biology & Agricultural Engineering, Hefei Institute of Physical Sciences, Chinese Academy of Sciences, 350 Shushanhu, Road Hefei, Anhui 230031, P. R. China*

**Corresponding author*
e-mail: qingmingwu@126.com; phone: +86-159-4568-5507

(Received 30th May 2021; accepted 3rd Sep 2021)

Abstract. Determining the bird assemblages is utmost important to identify the adequacy and efficiency of habitats. The line transect method was used to determine patterns of bird relative abundance, diversity indices, and conservation status in Sheikh Badin National Park from November 2017 to December 2019. In total, 7,919 individuals (2,592 migrants and 5,327 inhabitants) representing 42 species and 25 families were enlisted. Of 42 species, 27 were native (i.e., 67.26%) utilizing the study area throughout the year, while the remaining 15 species were migrant (e.g., 32.73%) that used the study area during the winter. *Passer domesticus* (0.06%), *Merops persicus* (0.05%), *Tachymarptis melba*, and *Ploceus philippinus* (each 0.04%) were the overwhelming bird species. In contrast, *Francolinus francolinus* (0.02%), *Falco tinnunculus* (0.008%), and *Alectoris chukar* (0.005%) were the rarest bird species. All species were identified as "Least Concern" based on IUCN RedList. Diversity results showed birds were assorted a diverse, i.e. H' = 3.608 (resident birds; H' = 3.608 and migratory birds; H' = 2.543), rich; i.e. D = 0.031 (resident birds; D = 0.046 and migratory birds D = 0.093) and evenly distributed J = 0.965 (resident birds, J = 0.967 and migratory birds, J = 0.939). The perceptions of local inhabitants and personnel observation shown that bird species are facing confronting threats due to human endeavor, such as illegal hunting, habitat loss due deforestation, and uncontrolled grazing.
Keywords: *bird, diversity, richness, conservation status, Sheikh Badin, distribution*

Introduction

Birds are vital components of the biosphere (Abbas et al., 2019), i.e. they provide ample services for the well beings and survival of human beings (Lepczyk and Warren, 2012) and are bioindicators of dwelling habitats (Drever et al., 2008; Fraixedas et al., 2020; Nelson et al., 2020). The occurrence and distribution of the bird species within a specific zone reflects the local biodiversity resources. Birds are of critical importance to

http://www.aloki.hu ● ISSN 1589 1623 (Print) ● ISSN 1785 0037 (Online)
DOI: http://dx.doi.org/10.15666/aeer/1906_49034921

the ecological functions and fundamental components of biodiversity that play a critical role in ecosystem functions. Birds are closely associated with vegetation structure (Cueto and Casenave, 1999; Lomolino, 2001) and habitat productivity (food resources, especially amphibians, reptiles, small mammals and invertebrates). They are an integral part of the food chain and food web, and this balances the ecosystem through dispersing seeds (Gracia et al., 2010; Martinez-Lopenz et al., 2019), pollinating plants (Mistry et al., 2008), bioindicator of the human footprint and climate change (Sharma, 1982; Amano et al., 2010) and environmental pollution (Gole, 1984; Talukdar, 1997; Radhouani et al., 2012; Pollack et al., 2017).

In an ecosystem, bird species plays a critical role in sustaining its health (Briggs, 2017; Law, 2019). Birds occupy a wonderful place among other species, since they are much appreciated by humans. They play a vital role in contributing to the consideration of the public with respect to natural habitats (Gascon et al., 2015; Donazar et al., 2016). Avian species are considered barometers of an ecosystem. Recent studies have shown that many bird populations are declining worldwide, while some are locally extinct due to degradation and fragmentation (Hewson et al., 2007).

Sibley and Monroe (1990) indicated that there are approximately 9702 avian species belonging to 1800 genera worldwide, including 1300 bird species in the Indian region (Manakadan and Pittie. 2001). Pakistan hosts 742 bird species that belongs to three zoogeographic areas, namely, Ethiopian, Palaeartic and Asian (Mirza and Wasiq, 2007; Lepage, 2014). The Indus (Green Migration Route) of which Pakistan is a part supports millions of migratory birds from northern latitudes in winter and from southern altitudes to breeding (summer visitors). The Indus flyway (green migratory route) of which Pakistan is a part supports millions of migratory birds from northern altitudes to overwinter and from southern altitudes to breed (summer visitors).

The population of bird species in Pakistan has declined as a result of the loss and degradation of habitat, illegal hunting and trapping, water pollution, food scarcity, inter–specific interactions and global warming (Kushlan, 1993; Hetrick and Sieving, 2012). Some of them have become threatened, vulnerable, endangered, critically endangered, or even extinct (Birdlife International, 2004; Yasué and Dearden, 2006). As such, information on the bird population structure (diversity, density, and conservation status) is essential to improve the future conservation and management of Sheikh Badin National Park. Thus, determining bird diversity, distribution, and conservation status is of critical importance to understanding productivity, threats. Therefore, important measures should be taken to protect and conserve the biodiversity especially bird population. As a result, this study looked at bird populations and habitat structure in Sheikh Badin National Park in Dera Ismail Khan, Pakistan.

Materials and methods

Study area

The Sheikh Badin National Park (NP) Dera Ismail Khan is located within 32.297534°N, 70.805227°E in the southern part of Khyber Pakhtunkhwa (KP), Pakistan (*Fig. 1*). The National Park is surrounded by Sheikh Badin Hills, an eastern extension of Sulaimon Mountains at an elevation of 1400 m above mean sea level and ranged from 300 m to 1400 m. The NP covers an area of 15,540 ha. The vegetation of Shaikh Badin national park is comprised of trees (Phulai – *Acacia modesta,* Indian olive – *Olea ferruginea*, Gum Arabic tree – *Vachellia nilotiea*, Athel tamarisk – *Tamarix aphylla*, Ghaf

http://www.aloki.hu ● ISSN 1589 1623 (Print) ● ISSN 1785 0037 (Online)
DOI: http://dx.doi.org/10.15666/aeer/1906_49034921

– *Prosopis cineraria,* Tree of heaven – *Ailanthus altissima,* Rohida – *Tecomella undulata* and Indian jujube – *Ziziphus mauritiana*), shrubs (Karira – *Capparis decidua*, Apple of sodom – *Calotropis procera,* Mazari palm – *Nannorrhops ritchiana*, Kannada – *Periploca aphylla*, Dwarf shrub – *Rhazya stricta*, Royle's spike thorn – *Maytenus royleana*) bushes and grasses (Kapok bush – *Aerva javanica,* Slender amaranth – *Amaranthus viridis,* wild sunflower – *Carthamus oxyacantha,* European milkvetch – *Astragalus hamosus,* red hogweed – *Boerhavia procumbens* and needle grass – *Aristida adscensionis*).

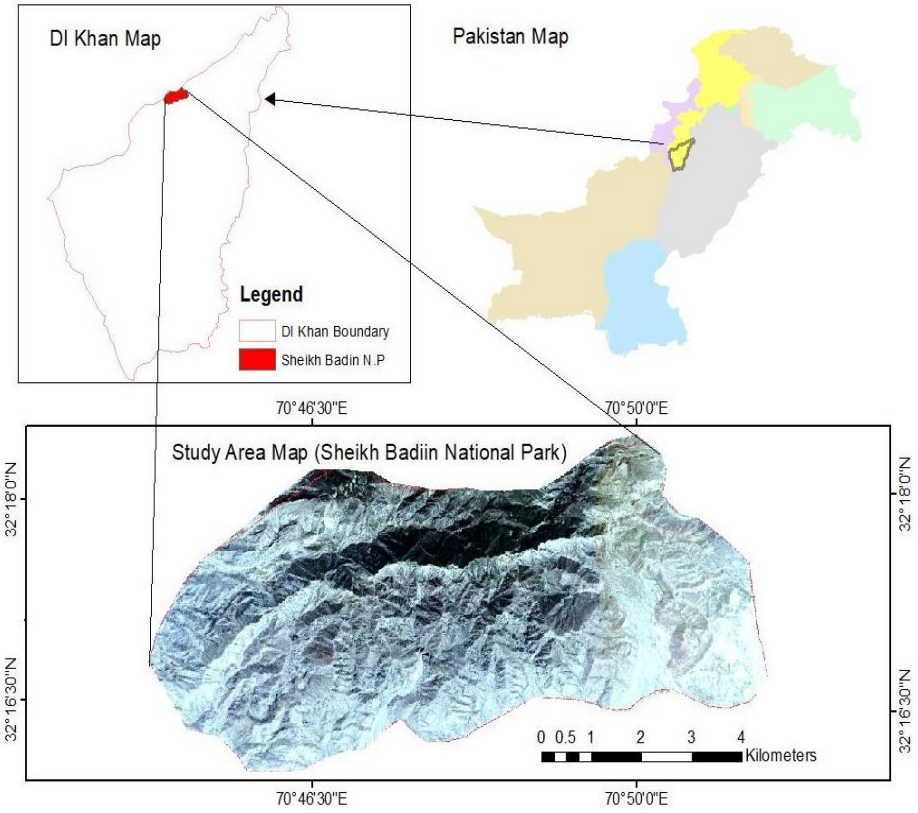

Figure 1. *A GIS-based map showing the location of the study area*

Precipitation at Sheikh Badin National Park ranged from 200 mm to 280 mm/year. The rainy season has a duration of 3.9 months. Most rainfall occurs during the monsoon season between June and September (*Fig. 2*). The winter is severe cold (a certain freezing weather) and the summer is warm 44.6 °C. The winter season lasts 2.9 months (December to February) and hottest season lasts 4.4 months (April to September). The average temperature may vary between 6.1 °C and 40.6 °C (*Fig. 3*). Its topography is hilly, hilly and mountainous.

Bird survey

Distance sampling line transect method was used for the detection of avian species for 26 consecutive months, from November 2017 to December 2019. The birds were recorded from 07:00–09:00 and 17:00–19:00 when they were most active in multiple activities. The birds were observed using binoculars (42 × 10 mm) to confirm the identity

http://www.aloki.hu ● ISSN 1589 1623 (Print) ● ISSN 1785 0037 (Online)
DOI: http://dx.doi.org/10.15666/aeer/1906_49034921

of the species and occasionally photographed with the Nikon D7200 (Sigma lens 150–600 mm). Overall, 100 point count stations were established randomly to avoide the double counting of the same bird individuals The methodology was followed according to Buckland et al. (2004).

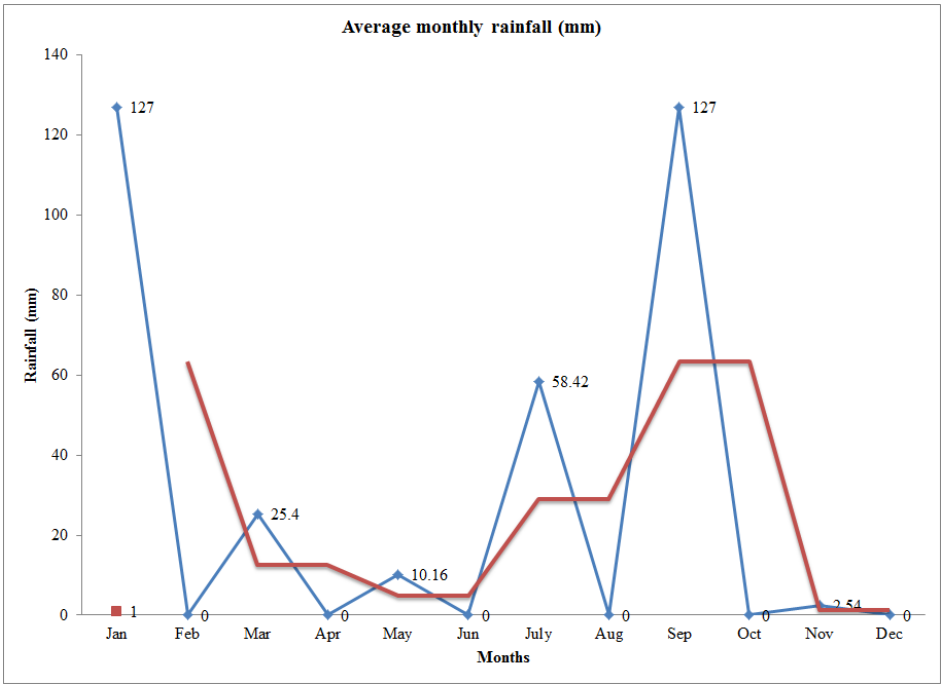

Figure 2. *Precipitation pattern throughout the year. (Source: https://weatherspark.com/y/148960/Average-Weather-at-Dera-Ismail-Khan-Year-Round)*

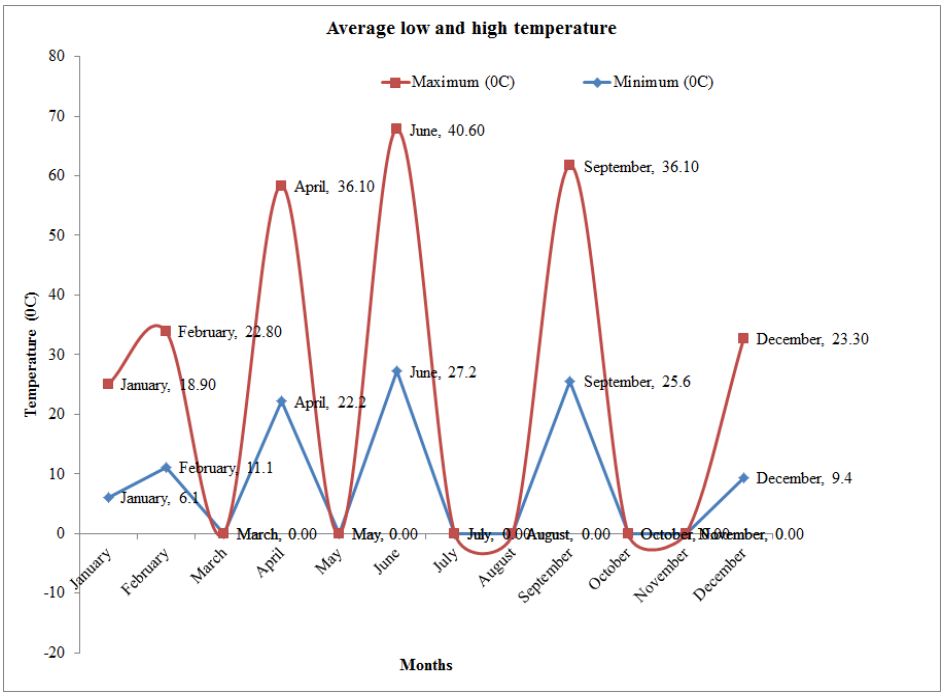

Figure 3. *Average low and high temperature throughout the year. (Source: https://weatherspark.com/y/148960/Average-Weather-at-Dera-Ismail-Khan-Year-Round)*

http://www.aloki.hu ● ISSN 1589 1623 (Print) ● ISSN 1785 0037 (Online)
DOI: http://dx.doi.org/10.15666/aeer/1906_49034921

Vegetation survey

The vegetation of the Sheikh Badin National Park was surveyed employing quadrant method (10 × 10 m for trees, 5 × 5 m for shrubs and 1 × 1 m for grasses) to identify the existing native flora to understand the habitat suitability, food resources and foraging sites for wide range of bird species. In total, 100 sampling sites were selected randomly at the simultaneously at same locations where bird species were documented. During vegetation inventory, the flora was divided into trees, shrubs and grasses. These sampling sites represented the entire area of the national park. The methodology was followed as described by Gandiwa and Kativu (2009), Zeh et al. (2019), Luna-Kamyshev et al. (2020).

Data analysis

Relative abundance

Relative abundance of bird species of the area was determined using *Equation 1:*

$$R.A = n/N \quad \text{(Eq.1)}$$

where: R.A: Relative Abundance, n = total number of individuals of a bird species and N = total number of individuals sighted of all bird species recorded during the surveys.

Diversity indices

Diversity reflects the heterogeneity of bird species in Sheikh Badin National Park. Diversity is an index that integrates the number of bird species found within a given habitat and the relative abundance that provides information on the scarcity and triviality of bird species. The Community Analysis Package Version 4.0 (Henderson and Seaby, 2007) has been used to determine diversity indices, i.e. species diversity, wealth and homogeneity in Sheikh Badin National Park.

Bird diversity

Shannon-Weiner Index (H′) was calculated in order to know the species diversity based on species abundance using *Equation 2* as given below:

$$H' = \sum[(pi) \times \ln(pi)] \quad \text{(Eq.2)}$$

where: H' designates diversity, S indicates the number of species, *i* specifies the abundance of species, *N* is the total number of all individuals, p_i is the relative abundance of each species, and ln is the natural logarithm.

In this study, the *Simpson Diversity Index* is a measure of bird diversity that takes into account the number of species occupied the national park, as well as the relative abundance of each particular species. The Simpson Diversity Index was calculated using *Equation 3* given below:

$$D = \Sigma n(n - 1) / N(N - 1) \quad \text{(Eq.3)}$$

where: n = the total number of individuals of a particular bird species and N = the total number of bird individuals detected in the national park of all species.

http://www.aloki.hu ● ISSN 1589 1623 (Print) ● ISSN 1785 0037 (Online)
DOI: http://dx.doi.org/10.15666/aeer/1906_49034921

Bird species evenness

Evenness is the distribution aspect of bird species in a Sheikh Badin National Park. How bird species have occupied the National Park was calculated using *Equation 4:*

$$J = H' / H_{max} \quad \text{(Eq.4)}$$

where: H' = diversity index and H_{max} = natural log of the total number of all bird species.

Comparison of feeding guilds among bird species

All enlisted bird species were divided into different feeding groups based on similar foraging behavior, food consumptions and habitat preferences. The methodology was followed as described (Lopez de Casenave et al., 2008; Liordos, 2010; Zakaria and Rajpar, 2010; Parajapati and Parajapati, 2013; Ding et al., 2019).

Results

Bird species composition and relative abundance

In total, 7,919 individuals representing 42 species encompassing 15 migratory species (2,574 individuals; 32.504%) and 27 resident species (5,345 individuals; 67.496%) of 10 orders and 23 families were detected between November 2017 to December 2019 within the National Park (*Table 1; Fig. 4a* and *b*).

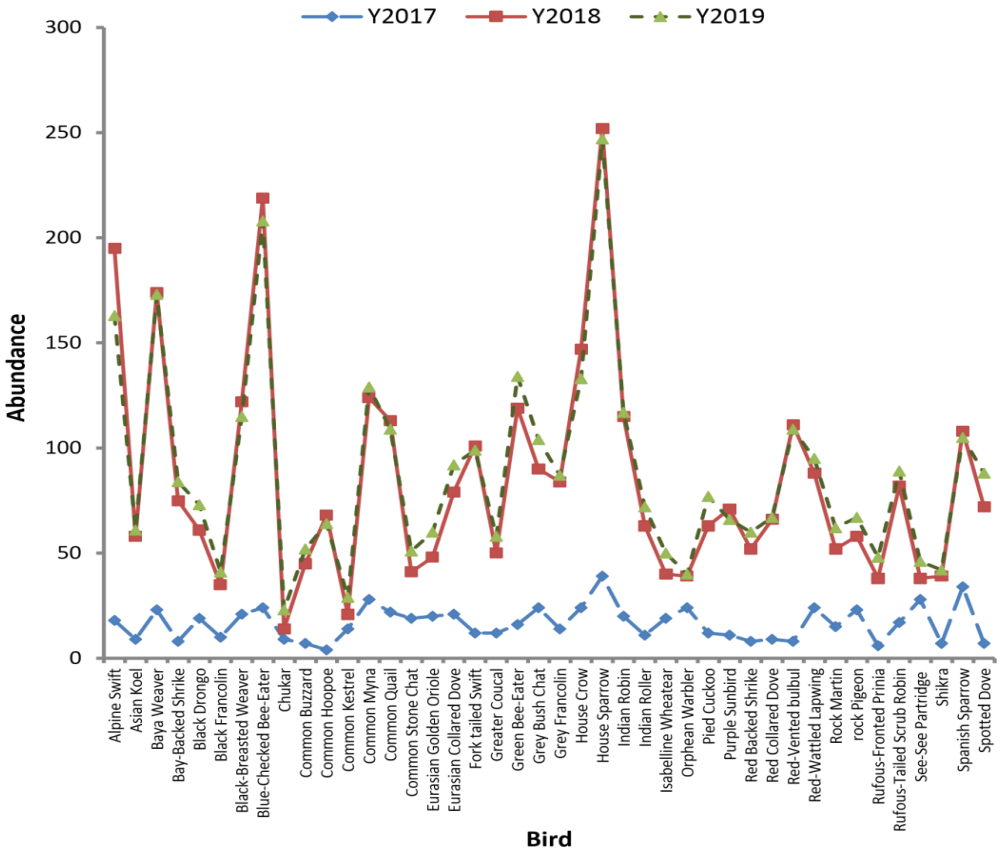

Figure 4a. *Bird relative abundance from 2017–2019*

http://www.aloki.hu ● ISSN 1589 1623 (Print) ● ISSN 1785 0037 (Online)
DOI: http://dx.doi.org/10.15666/aeer/1906_49034921

Muscicapidae (11.087%) and Meropidae (9.092%) were the leading families with five and two species respectively. By contrast, Cisticolidae (1.111%) and Falconidae (0.818%) were the rarest families to be found. Blue-cheeked flycatchers (5.695%) and Alpine Swifts (4.748%) were the two most abundant migratory bird species. House sparrow (6.794%) and Baya's weaver (4.672%) were the most plentiful resident bird species. The Chukor (0.581%) was the rarest residing bird. All bird species have been classified as Least Concern (*Table 1*).

Table 1. *Relative abundance of bird species detected in the Sheikh Badin National Park*

Family	Scientific name	Common name	National status	Total detections	%	IUCN status
Meropidae	*Merops persicus*	Blue-cheeked Bee-eater	M	451	5.695	LC
Apodidae	*Tachymarptis melba*	Alpine Swift	M	376	4.748	LC
Passeridae	*Passer hispaniolensis*	Spanish Sparrow	M	247	3.119	LC
Phasianidae	*Coturnix coturnix*	Common Quail	M	244	3.081	LC
Laniidae	*Lanius vittatus*	Bay-backed Shrike	M	167	2.109	LC
Cuculidae	*Clamator jacobinus*	Pied Cuckoo	M	152	1.919	LC
Hirundinidae	*Ptyonoprogne fuligula*	Rock Martin	M	129	1.629	LC
Oriolidae	*Oriolus oriolus*	Eurasian Golden Oriole	M	128	1.616	LC
Laniidae	*Lanius collurio*	Red-backed Shrike	M	120	1.515	LC
Muscicapidae	*Oenanthe isabellina*	Isabelline Wheatear	M	109	1.376	LC
Accipitridae	*Buteo buteo*	Common Buzzard	M	104	1.313	LC
Sylviidae	*Sylvia hortensis*	Orphean Warbler	M	103	1.301	LC
Cisticolidae	*Prinia buchanani*	Rufous-fronted Prinia	M	92	1.162	LC
Accipitridae	*Accipiter badius*	Shikra	M	88	1.111	LC
Falconidae	*Falco tinnunculus*	Common Kestrel	M	64	0.808	LC
Passeridae	*Passer domesticus*	House Sparrow	R	538	6.794	LC
Ploceidae	*Ploceus philippinus*	Baya Weaver	R	370	4.672	LC
Corvidae	*Orvus splendens*	House Crow	R	304	3.839	LC
Sturnidae	*Acridotheres tristis*	Common Myna	R	281	3.548	LC
Meropidae	*Merops orientalis*	Green Bee-eater	R	269	3.397	LC
Ploceidae	*Ploceus benghalensis*	Black-breasted Weaver	R	258	3.260	LC
Muscicapidae	*Copsychus fulicatus*	Indian Robin	R	252	3.182	LC
Pycnonotidae	*Pycnonotus cafer*	Red-vented Bulbul	R	228	3.637	LC
Muscicapidae	*Saxicola ferreus*	Grey Bush Chat	R	218	2.753	LC
Apodidae	*Apus pacificus*	Fork-tailed Swift	R	212	2.677	LC
Charadriidae	*Vanellus indicus*	Red-wattled Lapwing	R	207	2.614	LC
Columbidae	*Streptopelia decaocto*	Eurasian Collared Dove	R	192	2.425	LC
Muscicapidae	*Cercotrichas galactotes*	Rufous-tailed Scrub Robin	R	188	2.374	LC
Phasianidae	*Francolinus pondicerianus*	Grey Francolin	R	185	2.336	LC
Columbidae	*Spilopelia chinensis*	Spotted Dove	R	167	2.109	LC
Dicruridae	*Dicrurus macrocercus*	Black Drongo	R	153	1.932	LC
Nectariniidae	*Cinnyris asiaticus*	Purple Sunbird	R	148	1.869	LC
Columbidae	*Columba livia*	Rock Pigeon	R	148	1.869	LC
Coraciidae	*Coracias benghalensis*	Indian Roller	R	146	1.845	LC
Columbidae	*Streptopelia tranquebarica*	Red-collared Dove	R	142	1.793	LC
Upupidae	*Upupa epops*	Common Hoopoe	R	136	1.717	LC
Cuculidae	*Eudynamys scolopacea*	Asian Koel	R	128	1.616	LC
Cuculidae	*Centropus sinensis*	Greater Coucal	R	120	1.515	LC
Phasianidae	*Ammoperdix griseogularis*	See-see Partridge	R	112	1.414	LC
Muscicapidae	*Saxicola rubicola*	Common Stone Chat	R	111	1.402	LC
Phasianidae	*Francolinus francolinus*	Black Francolin	R	86	1.086	LC
Phasianidae	*Alectoris chukar*	Chukor	R	46	0.581	LC
		TOTAL		**7919**		

R = Resident, M = Migrant, LC = Least concerned

http://www.aloki.hu ● ISSN 1589 1623 (Print) ● ISSN 1785 0037 (Online)
DOI: http://dx.doi.org/10.15666/aeer/1906_49034921

The results of Wards Method indicated that branch lengths and topological changes of dendrogram revealed that bird diversity overall, resident and migrant species may vary in Sheikh Badin National Park (*Fig. 4b; A, B, C*).

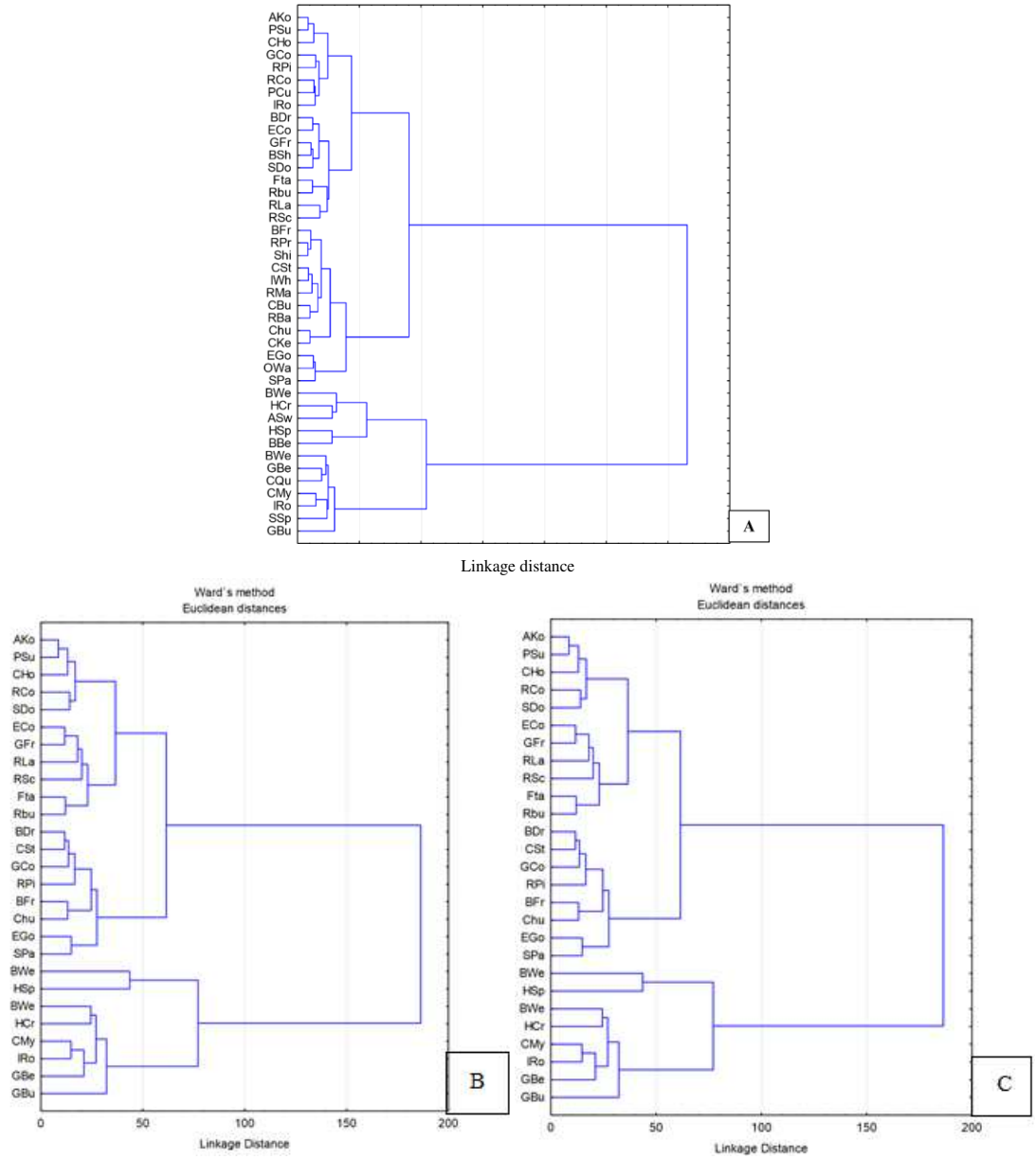

Figure 4b. *Dendrogram reflecting (A) the overall bird diversity, (B) resident bird diversity and (C) migrant bird diversity in Sheikh Badin National Park*

Bird species diversity indices

The overall Shannon Diversity Index (H' = 3.608) and Simpsons abundance (D = 0.031) have been recorded. Additionally, the Shannon Diversity Index (H' = 3.186) and Simpsons Diversity Index (D = 0.031) were related to resident birds and (H' = 2.543 and (D = 0.093) to migratory birds. Overall, the homogeneity of the species (H/In S = 0.965) was found in the study area. The species' homogeneity was found in resident

http://www.aloki.hu ● ISSN 1589 1623 (Print) ● ISSN 1785 0037 (Online)
DOI: http://dx.doi.org/10.15666/aeer/1906_49034921

birds E = 0.967 and E = 0.940 in migratory birds (*Tables 2* and 3). In *Figure 5* (A) graphically has shown richness S, in 2 (B) Shannon diversity index, 2 (C) Lambda (Simpsons index, l) and in 2 (D) Evenness.

Table 2. *Comparison of resident and migratory bird diversity indices from 2017 to 2019 detected in the Sheikh Badin National Park*

Diversity	Year	Resident birds	Migratory birds	Total
Shannon index = H'	2017	3.1915	2.5803	3.6236
	2018	3.1580	2.4866	3.5712
	2019	3.1886	2.5566	3.6138
	2017 – 2019	**3.1859**	**2.5426**	**3.6076**
Simpsons diversity index = D	2017	0.0446	0.0843	0.0292
	2018	0.082	0.1021	0.0327
	2019	0.0458	0.0901	0.03041
	2017 – 2019	**0.04614**	**0.09262**	**0.03080**
Evenness index = J	2017	0.9683	0.9528	0.9695
	2018	0.958	0.9182	0.9555
	2019	0.9675	0.9441	0.9669
	2017 – 2019	**0.9666**	**0.9389**	**0.9652**

Table 3*. Comparison of species composition, relative abundance, and diversity indices of resident and migratory birds from 2017 to 2019*

Year	Status	No of bird species	Total detection of bird individuals	Shannon diversity index	t-value	P-value
2017	Resident species	27	471	3.1915	16.72**	0.0000
	Migratory species	15	229	2.5803		
2018	Resident species	27	2368	3.1589	30.36**	0.0000
	Migratory species	15	1162	2.4866		
2019	Resident species	27	2488	3.1886	34.27**	0.0000
	Migratory species	15	1201	2.5566		
2017-19	Resident species	27	5327	3.1859	49.09**	0.0000
	Migratory species	15	2592	2.5426		

**Highly significant (P < 0.01)

Scatter plots of the bird species encountered

The purpose of the dispersion diagram is to show the distribution of different species according to their frequency and variance covariance matrices. The dispersal diagram of the bird species observed showed that most of the bird species were grouped, which clearly distinguishes them from others. Nine different bird species that distinguished themselves during the study were Domestic Sparrow (HSp), Baya's Weaver (BWe), Grey Brush Cat (GBu) and Partridge (Spa). Additionally, (BBe) Blue-cheeked Bee Feeder, (ASw) Alpine Swift, (SSp) Spanish Sparrow, (CQu) Common Quail and (OWa) Orpheus Warbler of Migratory Birds (*Fig. 6A-I*).

http://www.aloki.hu ● ISSN 1589 1623 (Print) ● ISSN 1785 0037 (Online)
DOI: http://dx.doi.org/10.15666/aeer/1906_49034921

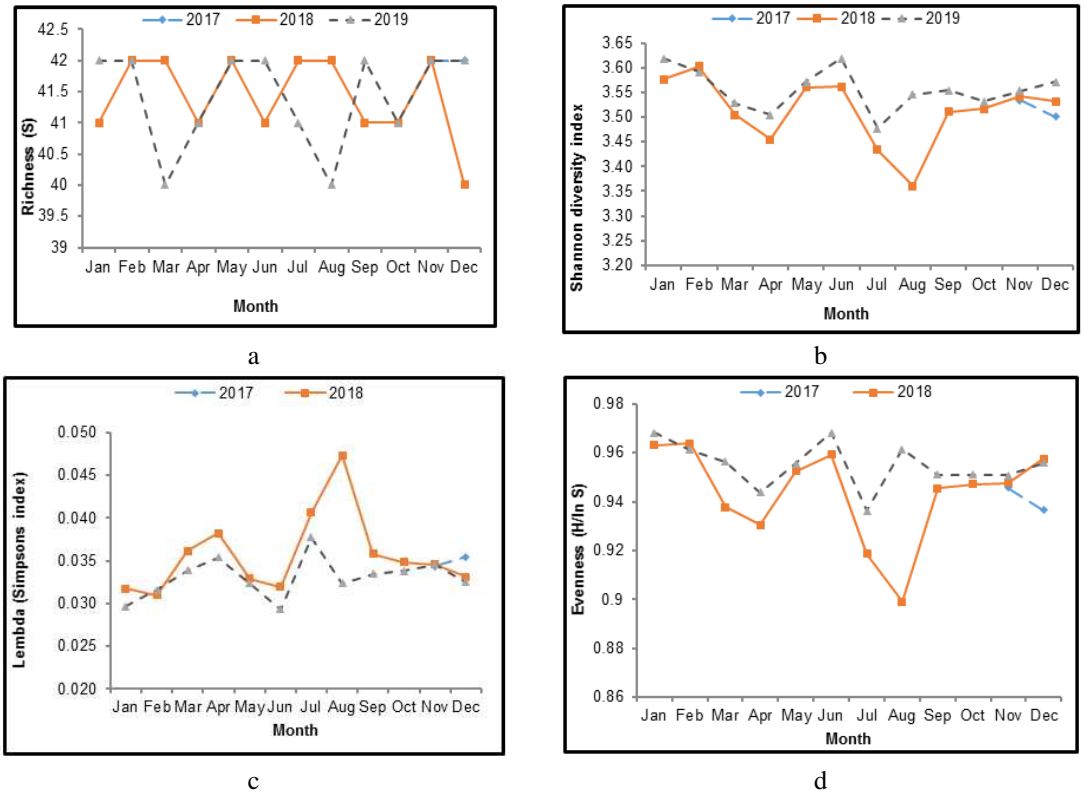

Figure 5. *Graphically showing (a) richness S, (b) Shannon variety index, (c) Lambda (Simpsons index, λ) and (d) regularity of birds*

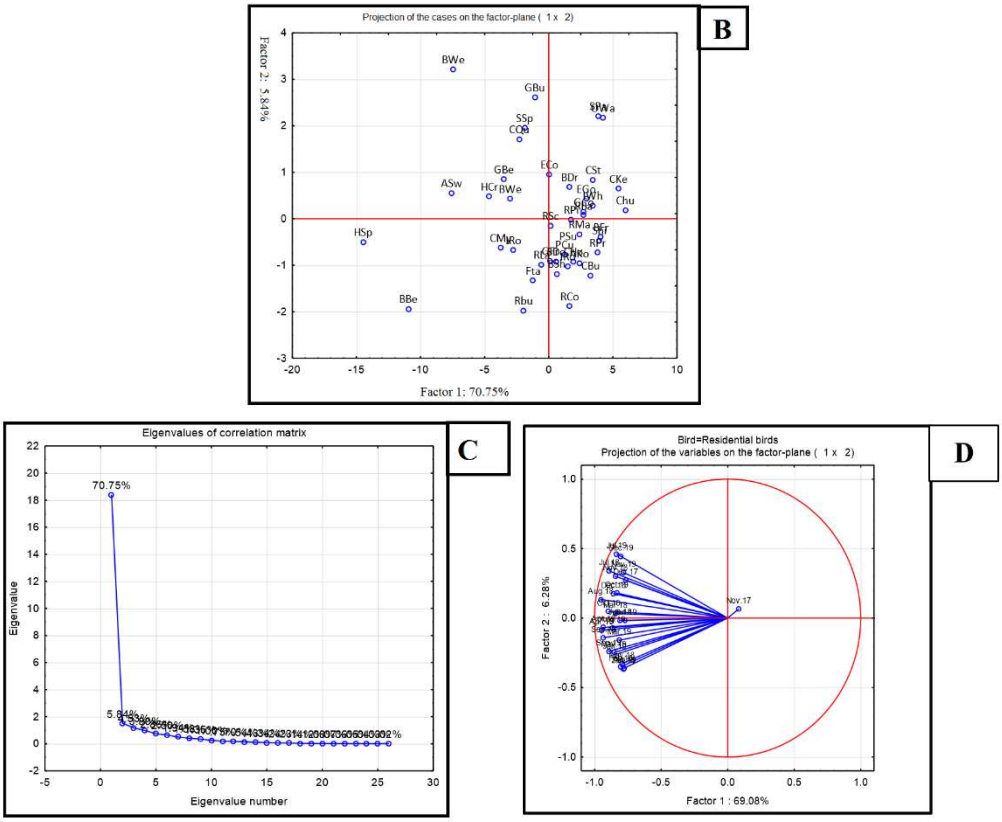

http://www.aloki.hu ● ISSN 1589 1623 (Print) ● ISSN 1785 0037 (Online)
DOI: http://dx.doi.org/10.15666/aeer/1906_49034921

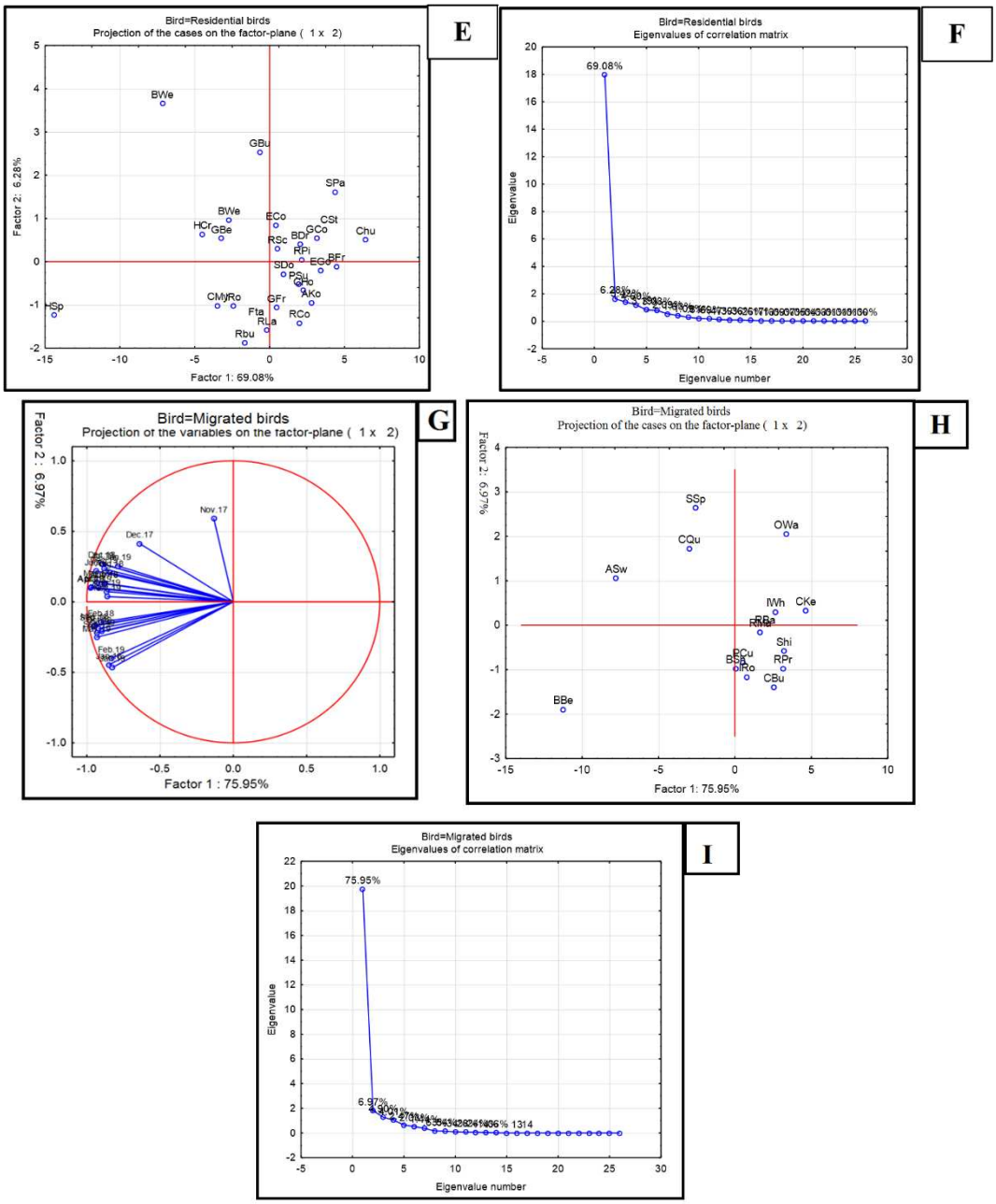

Figure 6. *Scatter plots of the bird species encountered in the study area (A-I)*

Vegetation structure and avian species composition in Sheikh Badin National Park

Vegetation of Sheikh Badin National Park is diverse and encompasses trees, shrubs, herbs, grasses, bushes and climbers. A total of 20 tree species (13 families), 21 shrub species (17 families), 36 herb species (21 families), 3 species of bushes (3 families) and 3 species of climbers (3 families) (*Table 4*).

Feeding guilds

The bird species were divided into nine feedings guilds. Insectivore (44.879%) was the most abundant guild based on number of detections and Frugivore (1.616%) was

http://www.aloki.hu ● ISSN 1589 1623 (Print) ● ISSN 1785 0037 (Online)
DOI: http://dx.doi.org/10.15666/aeer/1906_49034921

the rarest guild in the study area. In comparison between resident and migrant bird species, it was observed that Insectivore (24.801%) and Granivore/Insectivore (23.020%) were two most dominant resident bird species and Insectivore (20.078%) was the foremost abundant migrant bird species. However, no feeding guilds of resident carnivore and four guilds, namely; Carnivore/Insectivore, Frugivore, Nectarivore/Insectivore and Omnivore of migrant bird species were did not detected in the national park (*Table 5*).

Table 4. *Vegetation structure and composition of study area*

Family name	Scientific name	Common name
Trees		
Anacardiaceae	*Pistacia chinensis*	Chinese Pistachio
Arecaceae	*Phoenix dactylifera*	Date Palm
Bignoniaceae	*Tecomella undulata*	Roheda
Boragingaceae	*Cordia myxa*	Assyrian Plum
Fabaceae	*Prosopis juliflora*	Mesquite
	Acacia modesta	Phulai
	Vachella nilotica	Gum Arabic Tree
	Dalbergia sissoo	Shisham
	Prosopis cineraria	Jand or Ghaf
Meliaceae	*Melia azedarach*	Chinaberry
Moraceae	*Ficus carica*	Common Fig
	Ficus palmata	Wild Himalayan Fig
	Morus alba	White Mulberry
	Morus nigra	Black Mulberry
Myrtaceae	*Eucalyptus lanceolatus*	River Red Gum
Oleaceae	*Olea ferruginea*	Kahu
Rhamnaceae	*Ziziphus mauritiana*	Indian Jujube
Salvadoraceae	*Salvadora oleoides*	Vann, Peelu
Simaroubaceae	*Ailanthus altissima*	Tree of Heaven
Tamaricaceae	*Tamarix aphylla*	Ghaz, Athel Tamarisk
Shrubs		
Apocynaceae	*Calotropis procera*	Aak, Apple of Sodom
	Nerium oleander	Oleander
	Periploca aphylla	Kannada
	Rhazya stricta	Rhazya
Arecaceae	*Nannorrhops ritchiana*	Mazari Palm
Asparagaceae	*Agave sisalana*	Sisal
Boragingaceae	*Ehretia obtusifolia*	Stamper wood
Capparaceae	*Capparis decidua*	Karira
Celastraceae	*Maytenus royleana*	Royle's Spike Thorn
Euphorbiaceae	*Ricinus communis*	Caster Bean
Fabaceae	*Sophora mollis*	Soft Sophora
Lamiaceae	*Isodon rugosus*	Codd
	Otostegia limbata	Koi Booi
Lythraceae	*Punica granatum*	Pomegranate
Malvaceae	*Grewia optiva*	Bhimal or Bihul
Rhamnaceae	*Ziziphus nummularia*	Jhar Beri
Rosaceae	*Cotoneaster nummularius*	Coinwort Cotoneaster

http://www.aloki.hu ● ISSN 1589 1623 (Print) ● ISSN 1785 0037 (Online)
DOI: http://dx.doi.org/10.15666/aeer/1906_49034921

Sapindaceae	*Dodonaea viscoa*	Sanatha
Sapotaceae	*Monotheca buxifolia*	Gurguri
Solanaceae	*Datura metel*	Devil's Trumpet
Zygophyllaceae	*Tribulus terrestris*	Harmal Bindii
Herbs		
Amaranthaceae	*Amaranthus viridis*	Selender Amarantha
	Chenopodium album	Pig Weed
Amaryllidaceae	*Allium griffithianum*	Wild Onion
Asparagaceae	*Asparagus capitatus*	Blue Dicks
Asphodelaceae	*Aloe vera*	Indian Aloe
Asteraceae	*Carthamus oxyacantha*	Wild Safflower
	Conyza stricta	Horse Weed
	Echinops echinatus	Indian Globe Thistle
	Filago hurdwarica	Cud Weed
	Launaea procumbens	Creeping Launaea
	Saussurea heteromalla	Saw wort Kaliziri
Boragingaceae	*Heliotropium strigosum*	Bristly Heliotrope
Brassicaceae	*Eruca sativa*	Argula plant
Convolvulaceae	*Convolvulus arvensis*	Field Bindweed
Euphorbiaceae	*Euphorbia helioscopia*	Sun Spurge
	Euphorbia prostrata	Prostate Sandmat
Fabaceae	*Trigonella monantha*	Medick
Geraniaceae	*Erodium cicutarium*	Red Stem Filaree
Lamiaceae	*Mentha sylvestris*	Wild Mint
	Phlomis stewartii	Jerusalem Sage
	Withania coagulans	Paneer
	Withania somnifera	Winter Cherry
Zygophyllaceae	*Fagonia indica*	Indian Fagona
Grasses		
Asphodelaceae	*Asphodelus tenuifolius*	White Asphodel
Brassica	*Farsetia jacquemontii*	Boan
	Sisymbrium irio	London Rocket
Cannabaceae	*Cannabis sativa*	Hemp
Cyperaceae	*Cyperus rotundus*	Nut Grass
Fabaceae	*Astragalus hamosus*	European Milkvetch
Lamiaceae	*Lallemantia royleana*	Balangu
Poaceae	*Aristida adsensionsis*	Common Needle Grass
	Bromus japonicus	Japanese Brome
	Cenchrus ciliaris	Buffel-grass
	Cymbopogon jwarancusa	Khawi Oil Grass
	Cynodon dactylon	Khabbal Scuth Grass
	Eragrostis minor	Lesser Love Grass
	Saccharum bengalense	Kana Munj or Sweet cane
Bushes		
Amaranthaceae	*Aerva javanica*	Kapok Bush
Apocynaceae	*Caralluma edulis*	Pimpa
Fabaceae	*Alhagi maurorum*	Camel Thorn
Climbers		
Cucurbitaceae	*Citrullus colocynthis*	Bitter Apple
Fabaceae	*Vicia hirsuta*	Tiny Vetch
Solanaceae	*Solanum surattense*	Yellow-fruit Nightshade

http://www.aloki.hu ● ISSN 1589 1623 (Print) ● ISSN 1785 0037 (Online)
DOI: http://dx.doi.org/10.15666/aeer/1906_49034921

Table 5. *Comparison of feeding guilds of bird species recorded in Sheikh Badin National Park*

Guild name	Overall		Resident bird species		migrant bird species	
	N	%	N	%	N	%
Carnivore	256	3.232	0	0	256	3.232
Carnivore/insectivore	327	4.129	327	4.129	0	0
Frugivore	128	1.616	128	1.616	0	0
Frugivore/insectivore	356	4.495	228	2.879	128	1.616
Granivore	581	7.336	142	1.793	247	3.119
Granivore/insectivore	1984	25.053	1823	23.020	353	4.457
Insectivore	3554	44.879	1964	24.801	1590	20.078
Nectarnivore/insectivore	448	5.657	148	1.868	0	0
Omnivore	585	7.387	585	7.387	0	0
Grand total	7919		5,345		2,574	

N = total number of bird individuals

Discussion

It is of the utmost important to determine and understand the habitat avian community parameters in habitat relevance and productivity that a better plan can be made to enhance population and conserve their habitat. As habitat loss and degradation is a major anthropogenic factor, the bird population has decreased. The detection of 42 species representing 25 families reveals that Sheikh Badin National Park is a suitable and productive habitat for wide range of bird species. The indicated that vegetation structure and composition significantly attracted a wide array of bird species to utilize this productive habitat in order perform multiple activities.

Notably, 83 floral species, including 20 tree species, 21 shrub species, 36 grass species, and b climber species were recorded from Sheikh Badin National Park. This demonstrated that national park is rich and diverse in vegetation structure and composition. Previously, 107 plant species (26 trees, 20 shrubs, 53 herbs and 8 grasses) were also enlisted by Ullah et al. (2016). We recorded little bit less flora as compared to previous study. The reason might be application of different survey method or higher number of sample plots. The diversity of flora has created multilayered vegetation strata that established heterogeneous habitats and make this national park as a productive habitat (rich in food resources). Mengesha and Bekele (2008) stated that floral diversity and richness of food resources are the primary drivers that harbored a wide array of avian species. Likewise, Hanzelka and Reif (2016) reported that vegetation heterogeneity significantly enhances bird diversity. Furthermore, Kiros et al. (2018) also illustrated that vegetation composition is the key factor affecting chick survival, distribution of food sources and providing shelter from weather and predators. In the end, has an impact on feeding behavior, habitat preference, predation rate and population structure.

Strikingly, recording of migrant bird species revealed that the Sheikh Badin National Park is not only suitable habitat for resident birds, but also for migrant visitors. The reason is that, this national park fulfills the basic needs (i.e. living place, food, shlter, and breeding grounds) of avian species. The migrant bird species used this national park as refuge until weather conditions in northern/southern latitudes become favorable for them.

The feeding guild results showed that insect eating bird, i.e. bee-eater, swiftlets, shrikes, hoopoes, rollers, drongos, bushchats, robins, prinias, etc had densely occupied the national

http://www.aloki.hu ● ISSN 1589 1623 (Print) ● ISSN 1785 0037 (Online)
DOI: http://dx.doi.org/10.15666/aeer/1906_49034921

park. The occupation of higher number of insect eating bird could be richness and diversity of insect species. The occurring of wide range insect could be due to availability of wide array of floral species that bears flowers and fruits that had attracted them to utilize this habitat. However, the feeding guilds of resident and migrant species varied. It has been reported that environmental factors and land use changes significantly effects on vegetation characteristics that may influence on bird food selection (Tharme et al., 2001; Pearce-Higgins and Grant. 2006). Previously, such types of findings also have been reported by De Bonilla et al. (2012) and Panda et al. (2021).

Diversity indices suggest that bird species in Sheikh Badin National Park are diversified, rich and uniformly distributed. The results of this study are nearly identical to those of (Ali et al., 2011) at the Taunsa Dam, a wildlife sanctuary in Punjab, Pakistan. They stated that the Shannon Weiner Diversity Index values are typically between 1.5 and 3.5; however, under rare circumstances, it may exceed 4.5. The presence of a variety of avian species could be richness and diversity of food resources (insects, fruits, flowers, amphibians, reptiles, and small passerine birds for raptors) and heterogeneous vegetation layers that constituted multiple microhabitats. Thus, proving an ideal, productive and less disturb habitat that provides shelter from harsh weather and predators, offer suitable foraging and breeding grounds for a wide array of avian species.

Threats to avian species

Identifying the human footprint of wildlife and its habitat can provide a strong foundation for a better understanding of ecological models and processes. The results of this study identified the following major threats in Sheikh Buddin National Park to avifauna (*Fig. 7*).

Illegal hunting and trapping

Illegal hunting is the key factor that can cause bird species to decline or disperse. Bird species in the study area are illegally hunted by rifles and trapped by nets, resulting in a declining bird population every day. In addition, the breeding areas has also been disturbed by intensive livestock grazing on key breeding areas. Similar findings were also reported by Khan and Ali (2015).

Habitat loss and degradation

The second most serious threat identified was habitat loss and degradation as a result of land-use change. Habitat loss and degradation can cause the removal of vegetation and make it less productive and suitable for avian use. As a result of habitat loss and degradation, bird species migrate to less productive areas in the vicinity. e.g., agricultural fields for food, shelter and reproduction, where they are hunted by local people and easily preyed by predators due visibility. In addition, some bird species become victim of pesticides, die or become less productive. In addition, some bird species become victim of pesticides, die or become less productive.

Uncontrolled grazing

Livestock grazing is a major issue in this area, i.e. destruction of eggs and nesting sites by cattle hooves. Livestock roaming in basic habitat poses a major threat to bird breeding and the survival of avian species Khan and Ali (2015).

http://www.aloki.hu ● ISSN 1589 1623 (Print) ● ISSN 1785 0037 (Online)
DOI: http://dx.doi.org/10.15666/aeer/1906_49034921

Figure 7. *Threats to avifauna at Sheikh Badin National Park*

Conclusion

Sheikh Badin National Park is an attractive habitat for a broad range of avian species. However, low management, altered land use, illegal hunting, trapping, and grazing pose a serious threat to bird species. Based on the results, it is highly recommended that the relevant concerned department take immediate action to control illegal activities in the study area and strictly enforce the legislation. We also recommend that detailed future research be undertaken to explore biodiversity resources to improve future conservation and management measures. The Wildlife Department should coordinate with universities for research and training purposes. Local community awareness campaigns should also be conducted to highlight the importance of natural resource conservation.

Acknowledgements. We are very thankful to Shubana Luqman (M.Phil. Zoology), Miss Zarnab Gul (BS Botany), Raheem Ullah (BS Zoology) and Luqman Amin (BS Zoology) for their help during data collection and compiling the data. Also thankful to Dr Amjad for his help in data analysis and write-up.

Funding. The Fundamental Research Funds for the Central Universities (2572019BE04) and the National Natural Science Foundation of China (31401978) supported this paper.

REFERENCES

[1] Abbas, S., Hussain, E., Abbas, H., Hussain, S., Tabassum, R., Khan, M. Z., Nabi, M. (2019): Species diversity, feeding habits and conservation status of birds in Qurumber National Park, Gilgit-Baltistan, Pakistan. – Intern. J. Zoolo. Investig. 5(2): 108-117.

[2] Ali, Z., Bibi. F., Shelly, S. Y., Qazi, A., Khan, A. M. (2011): Comparative avian faunal diversity of Jiwani coastal wetlands and Taunsa barrage wildlife sanctuary, Pakistan. – J. Anim. Plan. Sci. 21(2): 381-387.

http://www.aloki.hu ● ISSN 1589 1623 (Print) ● ISSN 1785 0037 (Online)
DOI: http://dx.doi.org/10.15666/aeer/1906_49034921

[3] Amano, T., Székely, T., Koyama, K., Amano, H., Sutherland, W. J. (2010): A framework for monitoring the status of populations: an example from wader populations in the East Asian–Australasian Flyway. – Biol Conserv. 143: 2238-2247.
[4] Attaullah, N. K., Muhammad, Z. 2016: Tree communities analysis of Sheikh Buddin National Park, District Dera Ismail Khan, Pakistan. – Science 35: 67-74.
[5] Bird Life International (2004): State of the World's Birds 2004: Indicators for Our Changing World. – Bird Life International, Cambridge, UK.
[6] Briggs, L. (2017): Scientists highlight the critical role of birds in forest regeneration. Ecological information by nature. – www.https://theecologist.org/2017/jan/16/scientists-highlight-critical-role-birds-f (accessed on 30/05.2021).
[7] Buckland, S. T., Anderson, D. R., Burnhan, K. P., Lake, J. L., Borchers, D. L., Thomas, L. (2004): Advance Distance Sampling; Estimating Abundance of Biological Populations. – Oxford University Press, Oxford, pp. 141-172.
[8] Cueto, V. R., de Casenave, J. L. (1999): Determinants of bird species richness: role of climate and vegetation structure at a regional scale. – Journal of Biogeography 26: 487-492.
[9] De Bonilla, E., Leon-Cortes, J., Rangel-Slazar, J. (2012): Diversity of bird feeding guilds in relation to habitat heterogeneity and land-use cover in a human-modified landscape in southern Mexico. – Journal of Tropical Ecology 28(4): 369-376.
[10] Ding, Z., Liang, J., Hu, Y., Zhou, Z., Sun, H., Liu, H., Hu, H., Si, X. (2019): Different responses of avian feeding guilds to spatial and environmental factors across an elevation gradient in the central Himalaya. – Ecol. Evol. 1(7): 1-13.
[11] Donazar, J. A., Cortes–Avizanda, A., Fargallo, J. A., Margalida, A., Moleon, M., Morales–Reyes, Z., Moreno–Opo, R., Perez–Garcia, J. M., Sanchez–Zapata, J. A., Zuberogoitia, I., Serrano, D. (2016): Roles of Raptors in a Changing World: from flagship to providers of key ecosystem. – Ardeola 63(1): 181-234.
[12] Drever, M. C., Aitken, K. E. H., Norris, A. R., Martin, K. (2008): Woodpeckers are reliable indicators of bird richness, forest health and harvest. – Biological Conservation 141(3): 624-634.
[13] Fraixedas, S., Lindenc, A., Pihad, M., Cabezaa, M., Greygorye, R., Lehikoinen, A. (2020): State–of–the–art review on birds as indicators of biodiversity: advances, challenges and future directions. – Ecological Indicators 118: 106728.
[14] Gandiwa, E., Kativu, S. (2009): Influence of fire frequency on *Colophospermum mopane* and *Combretum apiculatum* woodland structure and composition in northern Gonarezhou national park, Zimbabwe. – Koedoe 51(1): a 685.
[15] Gascon, C., Brooks, T. M., Contreras–MacBeath, T., Heard, N., Konstant, W., Lamoreux, J., Launay, F., Maunder, M., Mittermeir, A. G. J., Molur, S., Al Mubarak, R.K., Parr, M. J., Rhodin, A. G. J., Rylands, A. B., Soorae, P., Anderson, J. G., Vie, J–C. (2015): The importance and benefits of species. – Current Biology 25: 431-438.
[16] Gole, P. (1984): Birds of a polluted river. – J Bombay Nat. Hist. Soc. 81: 613-625.
[17] Gracia, D., Zamora, R., Amico, G. C. (2010): Birds as supplier of seed dispersal in temperate ecosystems: conservation guidelines from real-world landscape. – Conserv. Biol. 24: 1070-1079.
[18] Hanzelka, J., Reif, J. (2016): Effects of vegetation structure on the diversity of breeding bird communities in forest stands of non-native black pine (*Pinus nigra* A.) and black locust (*Robinia pseudoacacia* L.) in the Czech Republic. – Fore. Ecol. Manag. 379: 102-113.
[19] Henderson, P. A., Seaby, R. M. H. (2007): Community Analysis Package 4.0. – Pisces Conservation Ltd, Lymington, UK.
[20] Hetrick, S. A., Sieving, K. E. (2012): Antipredator calls of tufted titmice and interspecific transfer of encoded threat information. – Behav Ecol. 23: 83-92.
[21] Hewson, C. M., Amar, A., Lindsell, J. A., Thewlis, R. M., Butler, S., Smith, K., Fuller, R. J. (2007): Recent changes in bird populations in British broadleaved woodland. – Ibis 149: 14-28.

http://www.aloki.hu ● ISSN 1589 1623 (Print) ● ISSN 1785 0037 (Online)
DOI: http://dx.doi.org/10.15666/aeer/1906_49034921

[22] Khan, B. N. and Ali, Z. (2015): Assessment of birds' fauna, Occurrence status, diversity indices and ecological threats at Mangla Dam, AJK. – J. Anim. Pl. Sci. 25(Suppl-2): 397-403.
[23] Kiros, S., Afework, B., Legese, K. (2018): A preliminary study on bird diversity and abundance from Wabe fragmented forests around Gubre subcity and Wolkite town, southwestern Ethiopia. – Internat. J. Avian & Wildl. Biol. 3(5): 333-340.
[24] Kushlan, J. A. (1993): Colonial water birds as bioindicators of environmental change. – Colonial Waterbirds 16(2): 223-251.
[25] Law, J. (2019): Hy we need birds (far more than they need us). – BirdLife International Organization. www. https://www.birdlife.org/worldwide/news/why-we-need-birds-far-more-they-need-us (accessed on 30/05.2021).
[26] Lepage, D. (2014): Avibase–bird checklist of the world Pakistan. – BirdLife International. https://avibase.bsc-eoc.org/checklist.jsp?region=PK&list=howardmoore& region=PK& list=howardmoore, (accessed on 1 April, 2019).
[27] Lepczyk, C. A., Warren, P. S. (2012): Urban Bird Ecology and Conservation. – University of California Press, Berkeley.
[28] Liordos, V. (2010): Foraging guilds of waterbirds wintering in a Mediterranean coastal wetland. – Zoological Studies 49(3): 311-323.
[29] Lomolino, M. V. (2001): Elevation gradients of species-density: historical and prospective views. – Global Ecol Biogeogr. 10: 3-13.
[30] Lopez de Casenave, J., Cueto, V. R., Marone, L. (2008): Seasonal dynamics of guild structure in bird assemblages of the central Monte desert. – Basic Appl. Ecol. 9: 78-90.
[31] Luna-Kamyshev, N., Lopez-Martmez, J. O., Vargas-Larreta, B., Islebe, G. A., Villalobos-Guerrero, T. F., Vazquez de la Rosa, A., Reyes-Mendoza, O. F., Trevino-Garza, E. (2020): Floristic composition, diversity, and biomass of a protected tropical evergreen forest Belize. – Tropical Conservation Science 13: 1-13.
[32] Manakadan, R., Pittie, A. (2001): Standardized common and scientific names of the birds of the Indian subcontinent. – Buceros. 6: 1-37.
[33] Martinez-Lopenz, V., Zapata, V., De la Rua, P., Robledano, F. (2019): Uncovering mechanisms of bird seed dispersal in semiarid environments to help to restore them. – Ecosphere 10(4): e02673.
[34] Mengesha, G., Bekele, A. (2008): Diversity and relative abundance of birds of Alatish National Park, North Gondar, Ethiopia. – Internat. J. Ecol. Environ. Sci. 34: 215-222.
[35] Mirza, Z. B., Wasiq, H. (2007): Field Guide to Birds of Pakistan. – WWF-Pakistan, Bookland, Lahore.
[36] Mistry, J., Berardi, A., Simpson, M. (2008): Birds as indicators of the wetland status and change in the North Rupununi, Guyana. – Biodiversity and Conservation 17(10): 2383-2409.
[37] Nelson, B. R., Mamat, M. A., Cheeho, W., Shahi, S. (2020): Forest birds as diversity indicator in suburban and residential areas. – Ecofeminism and Climate Change 1(1): 57-62.
[38] Panda, B. P., Prusty, B. A. K., Panda, B., Pradhan, A., Parida, S. P. (2021): Habitat heterogeneity influences avian feeding guild composition in urban landscape: evidence from Bhubaneswar, India. – Ecological Processes10(31): 1-10.
[39] Pearce–Higgins, J. W., Grant, M. C. (2006): Relationships between bird abundance and the composition and structure of moorland vegetation. – Bird Study 53: 112-125.
[40] Pollack, L., Naomi, R., Ondrasek, N. R., Calisi, R. (2017): Urban health and ecology: the promoise of an avian biomonitoring tool. – Current Zoology 63(2): 205-212.
[41] Prajapati, S. H., Prajapati, R. P. (2013): Classified guilds in avian community with respect to food and feeding behavior. – Indian J. Sci. Res. Technol. 1: 1-7.
[42] Radhouani, H., Poeta, P., Goncalves, A., Pacheco, R., Sargo, R., Igrejas, G. (2012): Wild birds as biological indicators of environmental pollution antimicrobial resistence patters of

http://www.aloki.hu ● ISSN 1589 1623 (Print) ● ISSN 1785 0037 (Online)
DOI: http://dx.doi.org/10.15666/aeer/1906_49034921

Escherichia coli and enterococci isolated from common buzzards (*Buteo buteo*). – J. Med. Microbiol. 61(6): 837-843.

[43] Sharma, I. K. (1982): Adverse effects of air, water and soil pollutions on flora and fauna of towns and villages of Western Rajasthan. – Symposium on Environment Consciousness, Problems of Pollution and Conservation in Rajasthan.

[44] Sibley, C. G., Monroe, B. L. (1990): Distribution and Taxonomy of Birds of the World. – Yale University Press, New Haven, CT.

[45] Talukdar, B. K. (1997): Water birds of Dibru–saikhowa wildlife sanctuary. – Assam J. Nat. Cons. 9: 243-250.

[46] Tharme, A. P., Green, R. E., Baines, D., Bainbridge, I. P., O'brien, M. (2001): The effect of management for red grouse shooting on the population density of breeding birds on heather-dominated moorland. – J. App. Ecol. 38: 439-457.

[47] Ullah, A., Khan, N., Muhammad, Z. (2016): A check list of angiospermic plants of Sheikh Buddin National Park, District Dera Ismail Khan, Khyber Pakhtunkhwa, Pakistan. – S. Asian J. Life Sci. 4(1): 18-24.

[48] Yasué, M., Dearden, P. (2006): The potential impact of tourism development on habitat availability and productivity of Malaysian plovers *Charadrius peronii*. – J. App. Ecol. 43: 978-989.

[49] Zakaria, M., Rajpar, M. N. (2010): Bird species composition and feeding guilds based on point count and mist-netting methods at Paya Indah Wetland Reserve, Peninsular Malaysia. – Tropical Life Sciences Research 21(2): 7-26.

[50] Zeh, A. F., Fuashi, N. A., Maurice, M. E. (2019): Flora composition, structure and diversity in the Kimbi Fungom National Park west region, Cameron. – J. Ecol. Nat. Environ. 11(1): 1-13.

http://www.aloki.hu ● ISSN 1589 1623 (Print) ● ISSN 1785 0037 (Online)
DOI: http://dx.doi.org/10.15666/aeer/1906_49034921

ALLEVIATION OF SALT-STRESS ON SUGAR BEET (*BETA VULGARIS* L.) USING MOLASSES, HUMIC, AND NANO-CACO$_3$

SOROUR, S. GH. R.[1] – MOSALEM, M. E.[1] – ABOTALEB, A. A. N.[1] – GHARIEB, A. S.[2*]

[1]*Agronomy Department, Faculty of Agriculture, Kafrelsheikh University, Kafr El-Sheikh, Egypt*

[2]*Rice Research and Training Center, Field Crops Research Institute, Agricultural Research Center, Kafr El-Sheikh, Egypt*

**Corresponding author*
e-mail: abdelfatah_sobhy@yahoo.com

(Received 2nd Jun 2021; accepted 1st Oct 2021)

Abstract. The impact of soil application (control (C), molasses (M) and humic acid (HA)) and foliar applicllation treatments (C, HA, M and lithovit Boron (LB)) on sugar beet (*Beta vulgaris* L.) growth, yield, and quality under saline conditions were studied. A field experiment was conducted in Oct. 2017 and 2018 at Tamrfayah village (31°22' N, 31°12' E), Kafr El-Shiekh Governorate, Egypt. Soil or foliar application treatments increased leaf area index (LAI), dry weight plant^{-1}, root weight, length and diameter, root yield (t/ha), gross sugar%, extractable white sugar%, juice purity%, and sugar yield (t/ha) of sugar beet compared to C. The inverse was true in K, Na, K + Na, α-amino nitrogen (meq/100 g), loss sugar (%), and quality for root juice. Adding M to soil along with foliar spraying with LB produced the maximum average increase of two season at about leaf area 53.67%, dry weight 18.56%, root diameter 7.88%, root weight (g plant^{-1}) 23.89%, root yield (t/ha) 29.8%, gross sugar (%) 9.29%, extractable white sugar (%) 14.97%, Juice purity (%) 4.93%, sugar yield (t/ha) 47.55 compared to C (Soil application) × C (Foliar application) treatment. The highest values of K 6.84 and 7.33, Na 2.47 and 2.53, and K + Na 9.32 and 9.85 meg/100 g of sugar beet were obtained with the C (Soil application) × C (Foliar application) treatment.
Keywords: *biofertilizer, lithovit, fulvic, salinity, Nano fertilizer,*

Introduction

Sugar beet (*Beta vulgaris* L) has become a prospective crop for sugar production in Egypt. The annual output reaches 11 million tons from a cultivated area 219 thousand hectares (FAO, 2018).

Abiotic stress, such as salinity, can be considered a limit factor for increasing crop yield. The alleviated adverse effect of salt stress on crop physiology and growth through nano-fertilizer (Sassine et al., 2020), molasses (El-Tokhy et al., 2018), and humic acid (Khaled and Fawy, 2011) are practical approaches.

The industrial process of sugar production results in by-products like molasses, a dark brown viscous liquid. Molasses contains varying humic, fulvic, and amino acids, which promote nutrient uptake efficiency and soil biological activity (Samavat and Samavat, 2014). Srivastava et al. (2012) found that beet molasses is high in mineral elements such as N, P, K, Ca, and micronutrients. It increases the abundance of nutrients and organic matter in the soil (Li et al., 2020). Soil and foliar applications of molasses increased beet root yield and sugar content (%) (Şanli et al., 2015). (Li et al., 2020) indicated that foliar application of molasses soluble increased the seed of rapeseed yields up to 20% compared to chemical fertilizer only treatment.

Humic substances, including humate potassium and fulvic acid, have a stimulating effect on plant growth and microbial activities (Canellas and Olivares, 2014). The

http://www.aloki.hu ● ISSN 1589 1623 (Print) ● ISSN 1785 0037 (Online)
DOI: http://dx.doi.org/10.15666/aeer/1906_49234939

humic soil application (12% of humic acids, 3% of fulvic acids) induced more intensive growth and a positive influence on beetroot and sugar content yield than the control (Wilczewski et al., 2017). The humic treatment application exceeded the control treatment in sucrose, refined sugar, root yield, and sugar yield (Rassam et al., 2015).

Nano-fertilizers, such as Lithovit® (Boron 05), contain nano-CaCO3, a carbonate that decomposes in the leaf stomata to calcium oxide (CaO) and carbon dioxide (CO2), increasing photosynthesis rate (Beinșan et al., 2014). The product contains boron, which is necessary for plant development through the structural integrity of the cell wall, sugar translocation, physiological functions such as carbohydrates and nitrogen metabolism, the formation of amino acid, and plant hormones (Marschner, 2012; Nyomora et al., 2000; Rawashdeh and Sala, 2013). Besides, iron is essential for electron transport systems of mitochondria and chloroplasts (Rochaix, 2011) and many vital enzymes in the photosynthetic system (Rout and Sahoo, 2015). Lithovit® contains magnesium, the central core of the chlorophyll molecule (Nawaz et al., 2020); silica plays a vital role in increased tolerance in plants against abiotic stress like deficit and salinity stresses balancing nutrients uptake (Alsaeedi et al., 2019). Lithovit foliar application improves the growth and yield of cotton (Attia et al., 2016), maize (Gigel and Florin, 2017), barley (Szczepanek, 2017), and stevia (Soliman et al., 2018).

The study aimed to evaluate the effect of soil application (control, molasses, and humic acid) and foliar application (humic, molasses and lithovit) treatments in combinations on sugar beet growth, yield, and quality under salinity soil and water conditions.

Material and methods

An experiment was established on 6 Oct. 2017 and 10 Oct. 2018 at the field of Qaryah_No. 1 at Tarfayah village (31°22’ N, 31°12’ E), Kafr El-Shiekh Governorate, in Northern Egypt. Rice was the previous crop.

Table 1 shows the chemical study of the experimental soil (0-30 cm) using (Black et al., 1965). Clay was the soil texture. The soil salinity level was mild to high (Abrol et al., 1988).

Table 1. *Chemical analysis of the experimental soil (0-30 cm) in 2017/18 and 2018/19 seasons*

Seasons	PH (2.5:1)	EC (dS.m-1)	OM (%)	(meq. L^{-1})							Available (ppm)		
				Ca++	Mg++	K+	Na+	HCO3	CL-	SO4-	Fe	Zn	Mn
2017/18	8.6	8.8	1.1	6.5	6.4	0.4	68	8.7	69.3	6.33	5.4	0.68	3.9
2018/19	8.2	7.9	0.98	6.2	7.3	0.6	79	8.2	65.3	5.33	4.9	0.76	3.2

*pH determined in soil suspension 1:2.5
**Ec determined in soil paste extract

The water source was drainage effluent mixed with canal water before application. The irrigation water was EC 2.01 dS m^{-1}, and SAR 5.5 (mmol L^{-1})$^{1/2}$, whereas the classification of degree of restriction on use was slight to moderate (Ayers and Westcot, 1985).

The trial was a split-plot arrangement with three soil application substances as main plots, 0 (control), humic acid (12 kg ha^{-1}) and beet molasses (60 kg ha^{-1}), and four foliar

http://www.aloki.hu ● ISSN 1589 1623 (Print) ● ISSN 1785 0037 (Online)
DOI: http://dx.doi.org/10.15666/aeer/1906_49234939

application substances in sub-plot 0 (control), humic, molasses and Nano-boron. The experimental units were in three replications. As a foliar application, humic acid in 1 g/l, molasses 20 cm^3/l, and lithovit in 0.4 g/l were sprayed twice at 45 and 60 days after sowing (DAS).

Molasses level of the soil and foliar applications was determined as Şanli et al. (2015). Lithovit and humic acid levels were used as company products recommend.

A humic substance contains 85% humate potassium, 10% soluble potassium, and 5% fulvic acids. The source of molasses was *Daqahlia* Sugar & Refining Company Kalabshou – Zayan – Belkas/Daqahlia Governorate, Egypt. Chemical and physical analysis of sugar beet molasses was Brix 81%, Total sugar 47%, purity 58%, unfermentable sugar 0.43%, specific gravity 1.42 gm/cm^3, pH 8.2, and Ash 10.56% (Analyzed by Daqahlia Manufacturing Co.). Some mineral analysis for molasses was N 1.3%, P 0.25%, K 3.2%, Ca 0.6%, Mg 0.19%, Na 1.3% and S 0.4%. Lithovit® (Boron 05) is a natural fertilizer; dolomite is tribodynamically activated and micronized to levels of 10-20 microns. Lithovit® (Boron 05) contains 50% (CaCO3) calcium carbonate, 28% (CaO) calcium oxide, 9% SiO_2 silicon dioxide, 15.0% B boron, 1.8% MgO magnesia, 1.0% Fe iron and 0.02% Mn manganese. The source is Agrolink Agricultural Co., Egypt, manufactured in Germany by (Tribodyn, 2020).

Nitrogen fertilizer with a rate of 214 N ha^{-1} in the form of Urea (46% N) was top-dressed in two equal splits at 35 and 70 days after sowing (DAS).

Supplying water to experiments was furrow irrigation. Light irrigation was given after ten days from sowing to ensure high seed emergence. Then, irrigation was carried out when 50 to 60% of the available soil moisture was depleted at 0-30 cm soil depth and was done at intervals of approximately 15 to 21 days depending on weather conditions and the amount of the effective rainfall. The seasonal water applied (irrigation water and effective rain) from sowing to harvesting were 5426 m^3 and 5595 m^3 in the first and second seasons.

The plot was 18 m^2 (3 × 6 m). Each plot had six ridges that were 50 cm apart and 6 m long. Seeds of the multigerm sugar beet cultivar "Cleopatra" were sown at 2-3 seeds per hill in hills 20 cm apart on one side of the ridge. Plants were hand thinned 35 days after sowing to one stable plant $hill^{-1}$. Plants were thinned by hand after thirty-five days from sowing to one healthy plant $hill^{-1}$. All plots received 119 Kg. ha^{-1} super phosphate triple (46% P_2o_5) before second ploughing and sulfate potassium (48% K_2O) after thinning in one dose at 60 Kg. ha^{-1}.

Beto 27.4% EC (a.i. Phenmedipham + ethofumesate + desmedipham) was applied at the rate of 1L/fed applied after 21 DAS for annual broad-leaved weed control. Select super 12.5% EC (a.i. Clethodim) was used at 1.19 L ha^{-1} on 24 DAS for annual grassy weed control.

At 180 DAS, five guarded plants were selected randomly from each plot to determine leaf area and dry weight of root and top $plant^{-1}$. The different plant fractions (leaf blade, petiole, and bulb) were oven-dried to a constant weight at 60 ° C. Leaf area (blades area) was measured by Portable Area Meter (Model LI-3000A). Leaf area of sample plants divided into a ground area of the sample to calculate the Leaf area index (LAI).

At harvest (210 DAS), the central area of three rows 9.5 m^2 avoids the border effect for top and root yield (Ton ha^{-1}). Ten guarded plants were taken randomly and screened for root and top yields/plant, root diameter (cm), and root length (cm).

http://www.aloki.hu ● ISSN 1589 1623 (Print) ● ISSN 1785 0037 (Online)
DOI: http://dx.doi.org/10.15666/aeer/1906_49234939

Gross sugar (total Sugar content%), K, Na, and α-amino-N in roots were analyzed using Daqahlia Sugar Co laboratory methods. Determination of the sugar content% (Pol%) in the juice was determined using an automatic saccharimeter on lead acetate, according to Le Docte (1927). A flame photometer measured the soluble non-sugar content, K and Na, in meq/100 g of beet according to Brown and Lilleland (1946). α-amino-N according was estimated by a spectrophotometer according to Cooke and Scott (1993).

$$\text{Alkalinity coefficient} = \frac{k+Na}{\alpha-\text{amino}-\text{N}} \quad \text{(Reinfeld et al., 1974)}$$

$$\text{Extractable white sugar} = Z_B = \text{Pol} - [0.343\ (K + Na) + 0.094\ N_{BI} + 0.29]$$

according to Harvey and Dutton (1993), where: Z_B = corrected sugar content (white sugar%), Pol = Gross sugar (total Sugar content%) and N_{BI} = α-amino-N determined by the "blue number" method. Loss sugar% = (Gross sugar − Extractable white sugar). Juice purity% was calculated by (Z_B/Pol).

Results

Leaf area, dry weight, root length, and root diameter of sugar beet were affected significantly by soil, foliar, and soil × foliar application interaction (*Table 2*). M (Soil application) treatment had the highest leaf area for 2017 and 2018 at about 3.56 and 5.35, respectively. The differences between M and HA treatments are not significant for LAI in 2017 (*Table 2*).

In terms of dry weight (g plant^{-1}), root length (Cm), and root diameter (Cm), M (Soil application) treatment had the highest values with insignificant differences with HA (Soil application) treatment compared to control (*Table 2*).

Data in *Table 2* show the foliar application of LB can significantly increase leaf area for first and second seasons at about 3.85 and 5.56, Dry weight 353.8 and 353.8 (g plant^{-1}), root length 30.03 and 31.24 cm, and root diameter 13.72 and 13.81 cm, respectively to the highest value compare with other treatments. In contrast, the control gave the lowest values.

LB (Foliar application) with M (Soil application) treatments gave the highest leaf area (*Fig. 1A*), dry weight (*Fig. 1B*), and root diameter (*Fig. 1D*) with an increase (50 and 57.34, 19.22 and 18.09 and 8.14 and 7.62%) in 2017 and 2018 seasons compared to C (Soil application) × C (Foliar application) treatment, respectively. HA (Soil application) and HA (Foliar application) combination caused the highest increase in root length of 24.39% in the first year and LB (Foliar application) with M (Soil application) treatments an increase of 16.54% in the second season in comparison with control C (Soil application) × C (Foliar application) treatment.

Similarly, Şanli et al. (2015) and Priyadarshani (2019) reported molasses increased leaf area, fresh plant weight, and root diameter and root weight of sugar beet. The results are in harmony with Badawi et al. (2013) and Nemeat-Alla et al. (2021), who reported that humic acid increased leaf area, root dry weight, length, and diameter of sugar beet.

A positive effect of lithovit on leaf area, chlorophyll, dry matter of tomato were reported by Sajyan et al. (2019).

http://www.aloki.hu ● ISSN 1589 1623 (Print) ● ISSN 1785 0037 (Online)
DOI: http://dx.doi.org/10.15666/aeer/1906_49234939

Table 2. *Leaf area index (LAI), dry weight, root length, and root diameter of sugar beet as affected by soil and foliar substances application in 2017 and 2018 seasons*

Treatments	LAI		Dry weight (g plant^{-1})		Root length (cm)		Root diameter (cm)	
	2017	2018	2017	2018	2017	2018	2017	2018
Soil application	0.005**	0.00**	0.044*	0.004**	0.00**	0.001 **	0.03*	0.02*
Molasses (M)	3.56 a	5.35 a	360 a	365.3 a	30.19 a	31.65 a	13.72 a	13.85 a
Humic (HA)	3.50 a	4.82 b	350.6 a	355.2 a	28.88 a	31.44 a	13.58 a	13.7 a
Control (C)	3.27 b	4.61 c	309.2 b	321.2 b	27.8 b	28.54 b	13.28 b	13.18 b
Foliar application	0.000**	0.00**	0.00**	0.00**	0.00**	0.00**	0.00**	0.00**
Control (C)	2.86 d	4.19 c	319.4 b	331.8 c	27.36 b	29.73 c	13.14 c	13.27 c
Humic (HA)	3.45 c	4.61 b	342.3 a	357 a	30.01 a	30.68 b	13.59 b	13.53 b
Molasses (M)	3.63 b	5.34 a	344.2 a	346 b	29.75 a	30.53 b	13.68 ab	13.71 a
Lithovit (LB)	3.85 a	5.56 a	353.8 a	354.3 a	30.03 a	31.24 a	13.72 a	13.81 a
Interaction	0.018*	0.001*	0.049*	0.04 *	0.03 *	0.047 *	0.033*	0.049*

*, ** and NS indicate $P < 0.05$, $P < 0.01$, and not significant, respectively. Means of each factor designated by the same letter are not significantly different at the 5% level using Duncan's Multiple Range Test

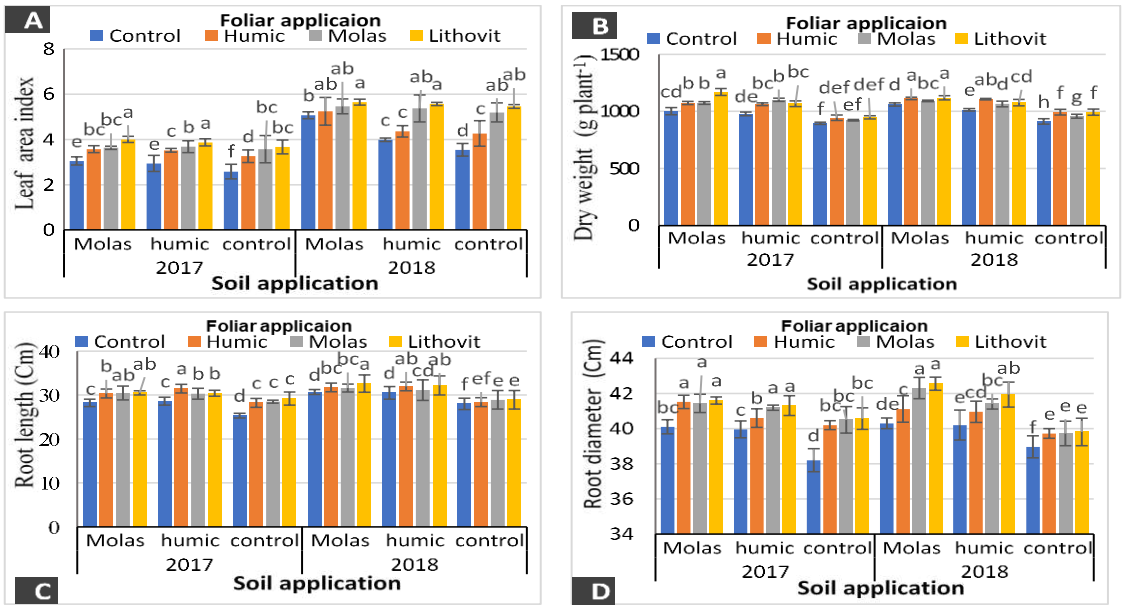

Figure 1. *Leaf area index (A), dry weight (g plant^{-1}) (B), root length (cm) (C), and root diameter (D) of sugar beet as affected by the interaction between soil and foliar application treatments in the 2017 and 2018 seasons*

As observed in *Table 3,* the soil application of M or HA increased the root weight (g plant^{-1}) significantly, top weight (g plant^{-1}), root yield (t/ha), and top yield (t/ha) of sugar beet compared to control. The maximum increase in root weight and root weight (T/ha) treated M (Soil application). There was an insignificant effect between M (Soil application) and HA (Soil application) in top weight (g plant^{-1}) and Top yield (T/ha).

http://www.aloki.hu ● ISSN 1589 1623 (Print) ● ISSN 1785 0037 (Online)
DOI: http://dx.doi.org/10.15666/aeer/1906_49234939

Data in *Table 3* showed that foliar application treatments had a significant effect on the root weight (g plant^{-1}), top weight (g plant^{-1}), root yield (t/ha), and top yield (t/ha). The root yield (t/ha) and top yield (t/ha) were higher on LB (Foliar application) treatment in both years. LB (Foliar application) gave the maximum root weight (g plant^{-1}) in 2018 and top weight (g plant^{-1}) in 2017. At the same time, there were insignificant differences between HA, LB, and M treatments for root weight in 2017 and top weight in 2018.

Under M (Soil application) treatment, LB (Foliar application) produced a maximum increase at about root weight (g plant-1) (21.34 and 26.45%), top weight (g plant^{-1}) (28.89 and 17.06%), root yield (t/ha) (28.36 and 31.25%) and top yield (t/ha) (28 and 25.15%) in 2017 and 2018, respectively more than C (Soil application) with C (Foliar application) (*Fig. 2A, B, C* and *D*).

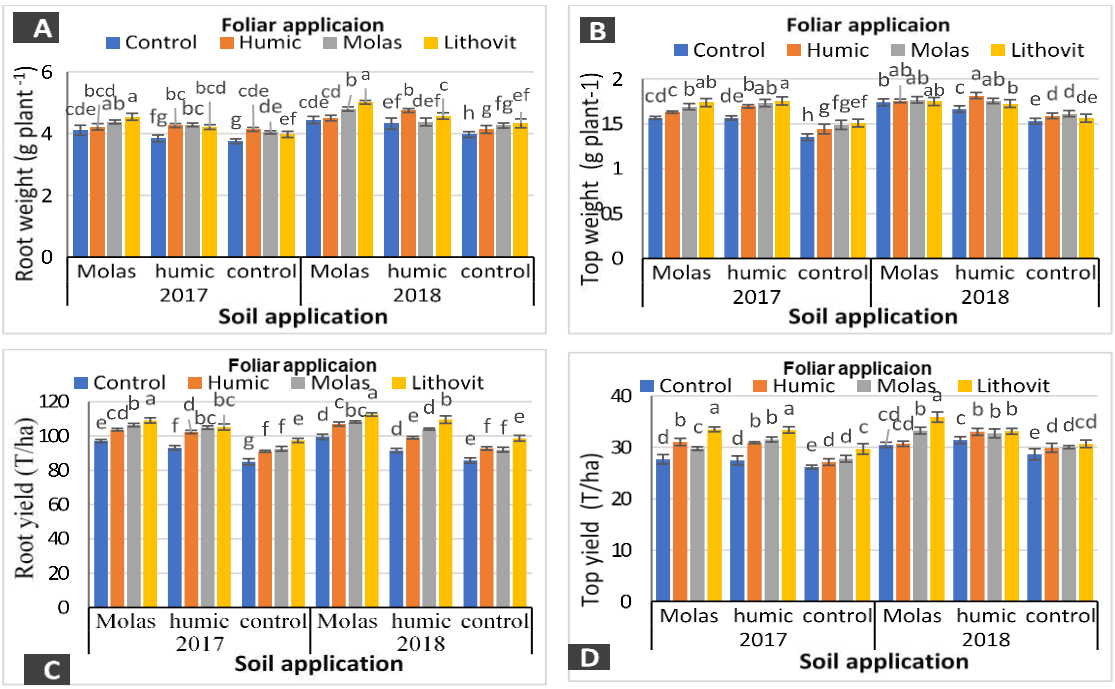

Figure 2. *Root weight (g plant^{-1}) (A), top weight (g plant^{-1}) (B), root yield (T/ha) (C), and top yield (T/ha) (D) of sugar beet as affected by the interaction between soil and foliar application treatments in the 2017 and 2018 seasons*

Such findings had also been pointed out by Priyadarshani (2019); Şanli et al. (2015) for molasses application in sugar beet. Similarly, Rehab et al. (2019) and Nemeat-Alla et al. (2021) for the effect of humic in sugar beet yield. These results are in coincidence with that reported by Artyszak et al. (2014) nano-caco$_3$ in sugar beet, Farouk (2015) lithovit in potato, and Sajyan et al. (2020) in pepper.

Gross sugar (%), Potassium (K) (meq/100 g), sodium (Na) (meq/100 g), K + Na (meg/100 g), α-amino nitrogen (meq/100 g), Alkalinity coefficient were significantly were affected by soil and foliar application in 2017 and 2018 (*Table 4*), except gross sugar (%) in 2017.

M (Soil application) gave the highest gross sugar (%) at 19.84 and 19.2% in the 2017 and 2018 seasons, respectively, which insignificant difference with HA (Soil

http://www.aloki.hu ● ISSN 1589 1623 (Print) ● ISSN 1785 0037 (Online)
DOI: http://dx.doi.org/10.15666/aeer/1906_49234939

application) treatment. The control (Soil application) treatment had the minimum gross sugar (%) of 18.42 in 2017 (*Table 4*). The control was 18.42% in 2018, with an insignificant difference with HA treatment.

Table 3. *Root weight (g plant-1), top weight (g plant-1), root yield (t/ha), and top yield (t/ha) of sugar beet as affected by soil and foliar substances application in 2017 and 2018 seasons*

Treatments	Root weight (g plant^{-1})		Top weight (g plant^{-1})		Root yield (T/ha)		Top yield (T/ha)	
	2017	2018	2017	2018	2017	2018	2017	2018
Soil application	0.00 **	0.00 **	0.00**	0.00**	0.00**	0.00**	0.00**	0.00**
Molasses (M)	1.43 a	1.56 a	0.552a	0.588a	82.56a	84.7a	24.18a	25.85a
Humic (HA)	1.38 b	1.50 b	0.563a	0.582a	80.42b	80.16b	24.44a	25.82a
Control (C)	1.32 c	1.39 c	0.483b	0.524b	72.57c	73.21c	21.97b	23.66b
Foliar application	0.00 *	0.00 **	0.01*	0.00**	0.00**	0.00**	0.00**	0.00**
Control (C)	1.30 b	1.41 c	0.498d	0.549b	72.78d	73.19d	21.52c	23.94d
Humic (HA)	1.40 a	1.48 b	0.529c	0.574a	78.54c	79.02c	23.54b	24.75c
Molasses (M)	1.41 a	1.49 b	0.546b	0.571a	80.35b	80.42b	23.54b	25.39b
Lithovit (LB)	1.42 a	1.54 a	0.557a	0.564a	82.42a	84.8a	25.54a	26.37a
Interaction	0.018 *	0.00 **	0.00 **	0.03*	0.04*	0.00**	0.00**	0.00**

*, ** and NS indicate P < 0.05, P < 0.01, and not significant, respectively. Means of each factor designated by the same letter are not significantly different at the 5% level using Duncan's Multiple Range Test

Table 4. *Gross sugar (%), Potassium (K) (meq/100 g), sodium (Na) (meq/100 g), K + Na (meg/100 g), α-amino nitrogen (meq/100 g), Alkalinity coefficient of sugar beet as affected by soil and foliar substances application in 2017 and 2018 seasons*

Treatments	Gross sugar (%)		K (meq/100 g)		Na (meq/100 g)		K + Na (meg/100 g)		α-amino nitrogen (meq/100 g)		Alkalinity coefficient	
	2017	2018	2017	2018	2017	2018	2017	2018	2017	2018	2017	2018
Soil application	0.00 **	0.00 **	0.00**	0.00**	0.00**	0.00**	0.00**	0.00**	0.00 **	0.00 **	0.00**	0.00**
Molasses (M)	19.84a	19.2a	6.59b	6.9b	2.16b	1.94b	8.75b	8.83b	2.82b	2.08b	3.11b	4.31a
Humic (HA)	19.63a	18.92ab	6.45c	6.93b	2.14b	1.55c	8.59b	8.48b	2.7b	2.08b	3.18a	4.13b
Control (C)	19.1b	18.42b	6.73a	7.02a	2.43a	2.43a	9.2a	9.46a	3.21a	2.33a	2.86c	4.12b
Foliar application	0.00 *	0.00 **	0.01*	0.00**	0.00**	0.00**	0.00**	0.00**	0.00 *	0.00 **	0.01*	0.00**
Control (C)	19.11c	18.58c	6.7a	7.26a	2.31a	2.08a	9.02a	9.32a	2.99a	2.56a	3.03bc	3.65c
Humic (HA)	19.61b	18.72b	6.68a	6.75c	2.21c	1.97b	8.89b	8.75c	2.9b	2.22b	3.07ab	3.94b
Molasses (M)	19.46b	18.75b	6.45b	7.04b	2.18c	1.94bc	8.64c	8.99b	2.88bc	1.96c	3.01c	4.6a
Lithovit (LB)	19.91a	19.33a	6.52b	6.75c	2.26b	1.9c	8.84b	8.63d	2.86c	1.91c	3.08a	4.55a
Interaction	0.17 NS	0.00 **	0.00**	0.00**	0.00**	0.00**	0.00**	0.00**	0.00 *	0.01*	0.00**	0.00**

*, ** and NS. Indicate P < 0.05, P < 0.01, and not significant, respectively. Means of each factor designated by the same letter are not significantly different at the 5% level using Duncan's Multiple Range Test

The control (Soil application) treatment accounted for the highest potassium (k) (meq/100 g), sodium (Na) (meq/100 g) and K + Na (meg/100 g) of sugar beet among soil application for 2017 and 2018 at about 6.73 and 7.02 (meq/100 g), 2.43 and 2.43 (meq/100 g) and 9.2 and 9.46 (meg/100 g), respectively. C (Soil application) treatment obtained the highest α-amino nitrogen in 2017 and 2018 with (3.21 and 2.33 meq/100 g, respectively). In contrast, C (Soil application) treatments recorded the lowest alkalinity of 2.86 and 4.12 in the first and second seasons, while the difference between C and HA was non-significant in 2018 (*Table 4*).

http://www.aloki.hu ● ISSN 1589 1623 (Print) ● ISSN 1785 0037 (Online)
DOI: http://dx.doi.org/10.15666/aeer/1906_49234939

Data in *Table 4* showed that the highest gross sugar (%) among the foliar treatments for 2017 and 2018 was recorded in the M (Foliar application) with 19.91 and 19.33%, respectively. C (Foliar application) treatment significantly exceeded other spray treatments in 2017 and 2018 at potassium (k) 6.7 and 7.26 meq/100 g, sodium (Na) 2.31 and 2.08 meq/100 g, and K + Na 9.02 and 9.32 meg/100 g of sugar beet.

C (Soil application) treatment obtained the highest α-amino nitrogen in 2017 and 2018 with 2.99 and 2.56 meq/100 g, respectively. In contrast, C (Soil application) treatments recorded the lowest alkalinity of 3.03 and 3.65 in the first and second seasons.

The Alkalinity coefficient was higher in LB (Foliar application) treatment 3.08 in 2017 and M (Foliar application) 4.55 in 2018.

The data in *Figure 3A* show that the Foliar application and Soil application treatments' interaction was insignificant on gross sugar (%) in 2017. The highest gross sugar (%) values, 19.86%, were obtained with M (Soil application) × LB (Foliar application) treatment in 2018. In *Figure 3B, C, D,* the maximum values of potassium (k) 6.84 and 7.33 meq/100 g, sodium (Na) 2.47 and 2.53 meq/100 g, and K + Na 9.32 and 9.85 meg/100 g of sugar beet in 2017 and 2018 were obtained with the C (soil application) × C (Foliar application) treatment.

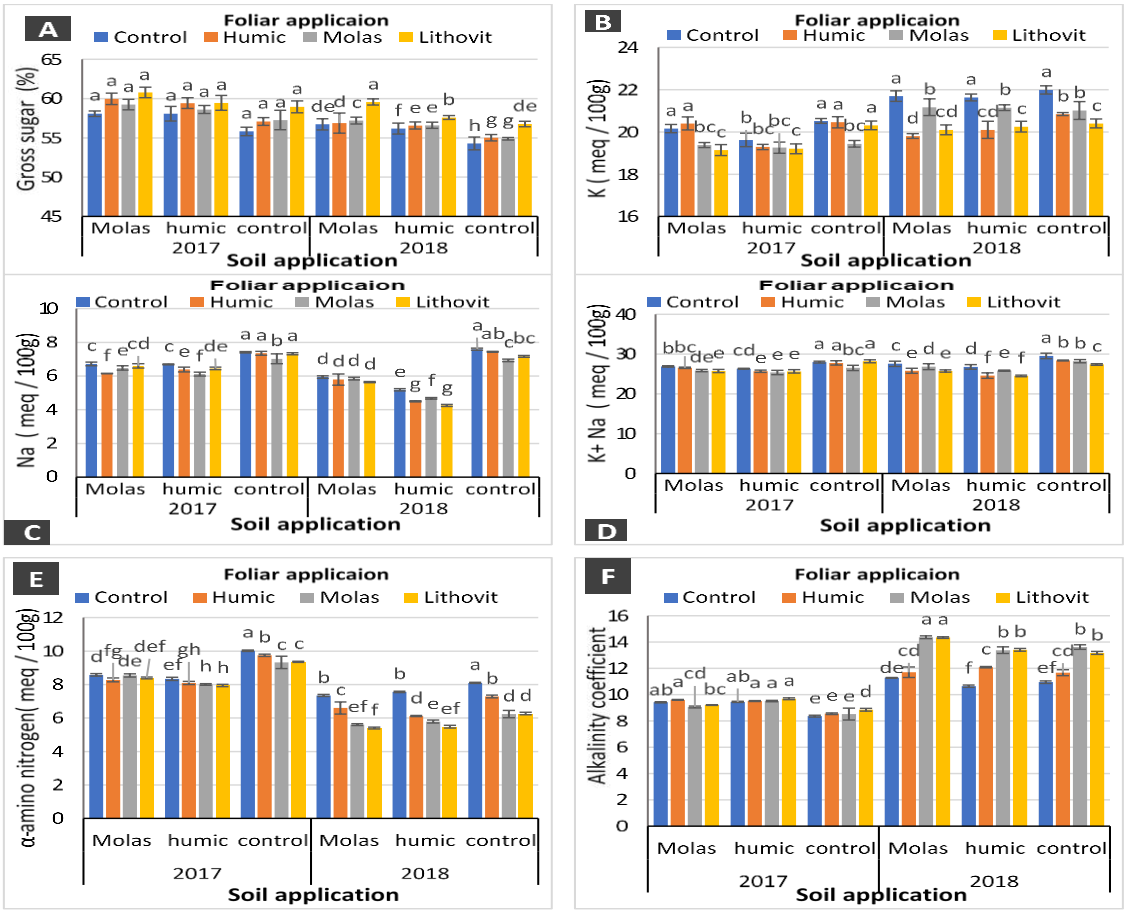

Figure 3. *Gross sugar (%) (A), K (meq/100 g) (B), Na (meq/100 g) (C) and K + Na (meg/100 g) (D), α-amino nitrogen (meq/100 g) (E), Alkalinity coefficient (F) of sugar beet as affected by the interaction between soil and foliar application treatments in the 2017 and 2018 seasons*

http://www.aloki.hu ● ISSN 1589 1623 (Print) ● ISSN 1785 0037 (Online)
DOI: http://dx.doi.org/10.15666/aeer/1906_49234939

Figure 3E shows the highest values of α-amino nitrogen was obtained by C (soil application) × C (Foliar application) in 2017 and 2018. HA (Soil application) × M (Foliar application) treatment gave the lowest values of α-amino nitrogen in 2017, while M (Soil application) × LB (Foliar application) for α-amino nitrogen in 2018 gave the minimum values.

Under HA (Soil application) with LB (Foliar application) in *Figure 3F,* the alkalinity coefficient had the highest values in 2017, while M (Soil application) × M (Foliar application) treatments gave the maximum value in 2018. C (Soil application) × C (Foliar application) showed the lowest value of alkalinity coefficient in 2017 and HA (Soil application) × C (Foliar application) in 2018. At M (Soil application) × LB (Foliar application) treatment gave the maximum value of extractable white sugar in 2017 and 2018.

The results also agree with (Rahimi et al., 2020; Rassam et al., 2015); Rehab et al. (2019), who use humic acid in sugar beet. Also, molasses improve the chemical and quality of tomato (El-Tokhy et al., 2018); and onion (Mahmoud et al., 2020). Similar results for nano caco$_3$ in sugar beet (Artyszak et al., 2014).

Loss sugar (%), Extractable white sugar (%) and Juice purity (%), and Sugar yield (t/ha) were significantly were affected by soil and foliar application in 2017 and 2018 (*Table 5*).

Data in *Table 5* showed that C (Soil application) treatment obtained the highest sugar loss (%) in 2017 and 2018 with 3.73%. In contrast, C (Soil application) treatments recorded the lowest extractable white sugar (%), 80.45 and 79.82%, Juice purity (%) 15.36 and 14.85%, and Sugar yield (t/ha) 11.43 and 10.91 in the first and second seasons.

Table 5. *Loss sugar (%), extractable white sugar (%) and juice purity (%) and Sugar yield (t/ha) of sugar beet as affected by soil and foliar substances application in 2017 and 2018 seasons*

Treatments	Loss sugar (%)		Extractable white sugar (%)		Juice purity (%)		Sugar yield (t/ha)	
	2017	2018	2017	2018	2017	2018	2017	2018
Soil application	0.00**	0.00**	0.00 **	0.00 **	0.00**	0.00**	0.00**	0.00**
Molasses (M)	3.56b	3.52b	82.12a	81.67 a	16.36a	15.68a	13.59a	13.24a
Humic (HA)	3.49c	3.39b	82.23a	82.09 a	16.15a	15.54a	13.45a	12.86a
Control ©	3.73a	3.73a	80.45b	79.82 b	15.36b	14.85b	11.43b	10.91b
Foliar application	0.00**	0.00**	0.00 *	0.00 **	0.00**	0.00**	0.01*	0.00**
Control (C)	3.67a	3.74a	80.81d	80.02 d	15.44c	14.91c	11.56c	11.05d
Humic (HA)	3.61b	3.49b	81.56c	81.36 b	16b	15.31b	13.08b	12.73b
Molasses (M)	3.52d	3.52b	81.89b	81.05 c	15.94b	15.25b	13.16b	12.47c
Lithovit (LB)	3.57c	3.44c	82.15a	82.34 a	16.45a	15.96a	13.5a	13.11a
Interaction	0.00**	0.00**	0.00 **	0.00 **	0.00**	0.00**	0.02*	0.00**

*, ** and NS. Indicate $P < 0.05$, $P < 0.01$, and not significant, respectively. Means of each factor designated by the same letter are not significantly different at the 5% level using Duncan's Multiple Range Test

Extractable white sugar (%) was the highest with HA (Soil application) treatment, while M (Soil application) gave the highest Juice purity (%) and Sugar yield (t/ha). The M and HA treatments were static par in Extractable white sugar (%), Juice purity (%) and Sugar yield (t/ha).

http://www.aloki.hu ● ISSN 1589 1623 (Print) ● ISSN 1785 0037 (Online)
DOI: http://dx.doi.org/10.15666/aeer/1906_49234939

The loss of sugar% was higher in values of 3.67 and 3.74% in C (Foliar application) in 2017 and 2018. LB (Foliar application) treatment gave the maximum value of extractable white sugar (%) 82.15 and 82.34%, Juice purity (%) 16.45 and 15.96%, and Sugar yield (t/ha) 13.5 and 13.11% in the first and second seasons (*Table 5*).

As shown in *Figure 4A,* the highest loss sugar values were obtained by C (Soil application × C (Foliar application) in 2017 and 2018. HA (Soil application) × M (Foliar application) treatment gave the lowest values of loss sugar in 2017, while HA (Soil application) × LB (Foliar application) for loss sugar in 2018 gave the minimum values.

Data in *Figure 4B* showed that at M (Soil application) × LB (Foliar application) treatment gave the maximum value of extractable white sugar in 2017 and 2018. LB (Foliar application) with M (Soil application) treatments gave the highest Juice purity (%) and Sugar yield (t/ha) in the 2017 and 2018 seasons (*Fig. 4C* and *D*). C (Soil application) × C (Foliar application)) the combination caused the lowest Juice purity (%) and Sugar yield (t/ha) in the 2017 and 2018 seasons.

These results are in agreement with Şanli et al. (2015) for molasses application in sugar beet. Similar, humic acid treatment in sugar beet (Rahimi et al., 2020; Rassam et al., 2015); Rehab et al. (2019.

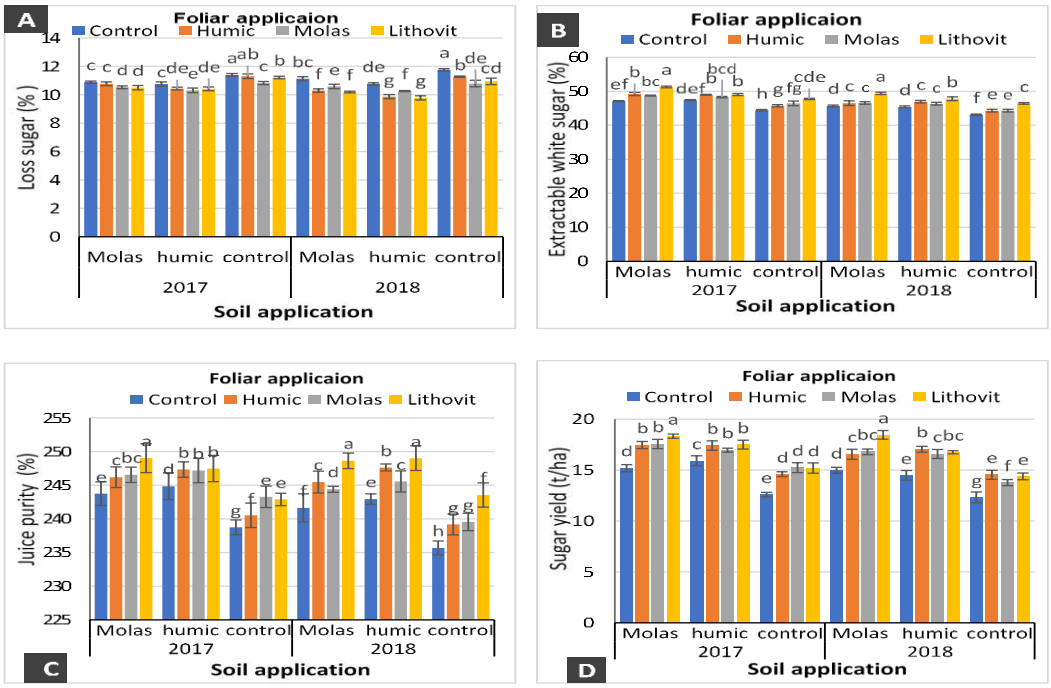

Figure 4. *Loss sugar (%) (A), Extractable white sugar (%) (B), Juice purity (%) (C), and Sugar yield (t/ha) (D) of sugar beet as affected by the interaction between soil and foliar application treatments in the 2017 and 2018 seasons*

Discussion

High salt stress showed an inhibitory effect on the growth and yield of sugar beet (Khorshid et al., 2018; Tahjib-UI-Arif et al., 2019). In the field experiments conducted to observe the soil application treatments (C, M, and HA) in combination with the foliar application (C, HA, M, and LB) for improving growth and yield of sugar beet and alleviate the harmful effects of saline water irrigation and soil.

http://www.aloki.hu ● ISSN 1589 1623 (Print) ● ISSN 1785 0037 (Online)
DOI: http://dx.doi.org/10.15666/aeer/1906_49234939

LAI, dry weight (g plant-1), root length (Cm), and root diameter (Cm) were enormously improved by M foliar or soil application compared to C treatment. Molasses contains large amounts of mineral elements K, N, P, Ca, Mg, Na, and S necessary for plant growth and development from the chemical composition of M in material and methods. Molasses include humic, fulvic, and amino acids, enhancing physical and chemical properties, biological activity, and soil fertility (Samavat and Samavat, 2014). Şanli et al. (2015) reported that molasses increased by 25% average root weight than control. Molasses soil application was higher than foliar application. Priyadarshani (2019) indicated that leaf area, fresh plant weight, and root diameter were increased in treatment contain molasses amended by soil. (Ramana et al., 2002) found that molasses increased total chlorophyll content, crop growth rate, total dry matter of groundnut. Li et al. (2020) concluded that molasses could encourage the root system, vigor, and nutrient usage in rapeseed planting. The increased weight and yield of the top and root plants was linked with improved LAI plant parameters, dry weight (g plant^{-1}), root length and root diameter. Şanli et al. (2015) recorded a noticeable improvement in root weight, root yield, and biological yield for foliar molasses.

In sugar beet, humic acid applied to the soil or foliar had a significant impact on LAI, dry weight (g plant^{-1}), root length (Cm), and root diameter (Cm) as compared to the control treatment. The humic compound contains organic matter and fulvic acid increase soil physicochemical properties and biological structure (Alsaeedi et al., 2019), enhances nutrients uptake (Gharib et al., 2011), improves cell membrane permeability of plants (Khaleda et al., 2017). Humic has the hormone-like activity response that may stimulate cell division and differentiation that enhance growth under salinity stress (Ouni et al., 2014), regulate the photosynthetic rate and cell elongation, and improve the water use efficiency (Zhang et al., 2013). Ali et al. (2020) indicated that HA increased root length, total dry weight, shoot length of sorghum in salinity soil. The HA foliar applications enhanced chlorophyll content and leaf area index (Khodadadi et al., 2020). Exogeneous fulvic acid on sugar beet gave the most outstanding root length values, root diameter, and root weight (Kandil et al., 2020). Kandil et al. (2020) in sugar beet that fluvic acid gave the maximum root weight (g)/plant, root yield (t/fed), and Top yield (t/fed), and Khodadadi et al. (2020) indicate that humic increased root yield (T/ha) of sugar beet. Rehab et al. (2019) found that humic acid foliar application gave the highest root and top yield (T/ha) of sugar beet. In past studies, foliar application of humic increased root yield (T/ha) of sugar beet (Rassam et al., 2015).

The foliar application of lithovit improved the growth and yield of sugar beet. Lithovit increases CO2 level inside the leaf intercellular, thereby improving photosynthesis (Bilal, 2010). It contains Mg, Ca, Fe, and Si, promoting effect through increased chlorophyll and carotenoid pigments. This compound improved weight and water content of plant parts cause better water movements in plants under salinity stress (Issa et al., 2020). In the previous study, nano-calcium had the promoting effect on plant growth, such as leaf area and plant dry weight of green bean plants and Ca and Si, mitigated salinity's negative impact (Gomaa et al., 2017). Lithovit enhanced chlorophyll content, leaf area, and dry matter of tomato in saline soil (Sajyan et al., 2019).

Lithovit@B is rich in boron. B foliar significantly increased the leaf area, root weight, length, and diameter of sugar beet (Kandil et al., 2020; Pirzad et al., 2019). The foliar application treatments with LB effectively enhanced root weight (g plant-1), root yield (t/ha), and top yield (t/ha) because of improving growth parameters like LAI, dry weight (g plant-1), root length, and root diameter. The positive effects of LB foliar

http://www.aloki.hu ● ISSN 1589 1623 (Print) ● ISSN 1785 0037 (Online)
DOI: http://dx.doi.org/10.15666/aeer/1906_49234939

application on root and shoot dry weight and pepper yield inform Sajyan et al. (2020). The mean yield of tomato is superior under the LB foliar application (Becherescu et al., 2017). The micronized marine calcite (CaCO3) compound increases the leaves and root yield of sugar beet (Artyszak et al., 2014).

Excessive Na in the salinity soil has detrimental effects on plant growth and physiology. Low gross sugar in control compared to other soil and foliar application treatments in saline soil may be ascribed to the dilution of sucrose in root through increased water content and also, gave low quality (high K meq/100 g, Na meq/100 g, and K + Na meg/100 g cause the high Na concentration (Tsialtas and Maslaris, 2009). The high a-amino-N compounds may be found as impurities in plants' storage roots under saline conditions, resulting from osmotic adjustment (Brown et al., 1987). The lowest value in control treatment may be due to the more significant amounts of a-amino-nitrogen than other treatments.

The highest value of loss sugar and the lowest means Extractable white sugar (%) and Juice purity (%) and Sugar yield (t/ha) for control compared to other soil application or foliar application treatments. It might be due to increasing K, Na, and α-amino nitrogen in juice roots, which causes troubles during juice purification and crystallization and, in turn, decreased purity and decreased extraction of white sugar (%).

Molasses has elements like K, P, S, Ca, and Mg. Molasses also contains different amounts of humic and fulvic acids and amino acids exhibiting hormone-like activity (Samavat and Samavat, 2014). molasses containing glycine betaine material are compatible solutes in osmotic adjustment and increased the net photosynthesis of water-stressed tomato plants (El-Tokhy et al., 2018). Şanli et al. (2015) concluded that foliar or soil application of molasses increased sugar content (%). Molasses treatments increased sugar yield by 2.9 t/ha compared to control (Şanli et al., 2015).

HA increased the uptake of P, K, Mg, Na, Cu, and Zn, so mitigate the saline's negative effect (Khaled and Fawy, 2011). (Rahimi et al., 2020; Rassam et al., 2015); Rehab et al. (2019) reported that humic application gave greater white sugar (%) than control while humic treatment was lower in α-amino nitrogen% and sodium% than control. (Rehab et al., 2019). El-Hassanin et al. (2016) reported that foliar application of humic acid increased extractable white sugar, purity, and sugar beet yield. Applying humic acid improved the percentage of sucrose and refined sugar compared with the control (Rassam et al., 2015). Fulvic foliar application increased the sugar yield and the portions of sucrose, TSS, and purity of the sugar beet plants (Kandil et al., 2020).

Lithovit® (Boron 05) contains nano-$CaCO_3$, 15.0% B boron, 9% SiO2, and other nutrients like Fe, Mg, and Mn. In a past study, the positive effects of marine calcite (containing CaCO3 and silicon mainly) foliar fertilization in lower Na and K, on the other hand, gave higher sugar beet content (Artyszak et al., 2014). Lithovit treatments gave the lowest sodium contents and recorded the highest sugar content (%) in the tomato fruits compared to control (Sajyan et al., 2018; Tantawy et al., 2014). (Rehab et al., 2019) indicated that foliar application of boron improved sugar and reduced Na and K. Lithovit improved the total soluble solids and soluble sugar concentrations compared to control in potato tubers (Farouk, 2015). The marine calcite (containing CaCO3 and silicon mainly) foliar resulted in increased content of refined sugar (%) and technological sugar yield (t/ha) (Artyszak et al., 2014). (Shallan et al., 2016) indicated that lithovit increased the total Soluble Sugars in leaves of cotton.

The integration of M (Soil application) treatment with LB (Foliar application) produced a maximum increase at LAI, root weight (g plant-1), top weight (g plant^{-1}),

http://www.aloki.hu ● ISSN 1589 1623 (Print) ● ISSN 1785 0037 (Online)
DOI: http://dx.doi.org/10.15666/aeer/1906_49234939

root yield (t/ha) and top yield (t/ha). Jiang et al. (2012) indicated that increased tillering, chlorophyll and yield relative to traditional fertilization through the amendment of condensed molasses soluble (CMS) in sugarcane resulted in enhanced physical and chemical soil characteristics. CMS application benefits crop productivity and physical soil structure enhancement and a rise in the biological activity of beneficial microorganisms (Wynne and Meyer, 2002). The CMS enhanced plant biomass, root vigour, and the superoxide dismutase function of the rapeseed shoot (Li et al., 2020). Molasses are rich in mineral elements and used as K sources due to their elevated levels. It also has critical other advantages, such as soil organic growth and nitrification-related microbial behaviour (Turner et al., 2002). According to Pujar (1995), foliar application of molasses improved Zn, Cu, Fe, and Mn uptake in corn and wheat.

LITHOVIT® or nano-CaCO3 is a carbon foliar fertilizer (Bilal, 2010), which increases CO2 concentration and stimulates light-saturated photosynthesis in C3 plants (Ainsworth and Rogers, 2007). Maswada and Abd El-Rahman (2014) demonstrated that using lithovit on wheat under natural or salinity stress significantly increased growth parameters, photosynthetic pigments, ion contents, yield, and components. Under salinity stress, Lithovit increased leaf area, dry matter, and total chlorophyll content of tomato (Sajyan et al., 2019). Lithovit foliar application greatly improved potato growth parameters (i.e. plant height, branch number per plant, shot fresh and dry weights, and leaf area per plant), potato tuber number and overall tuber yield per plant (Farouk, 2015).

Lithovit product contains B, silica, and Fe. Compared to the control treatment, foliar fertilization with marine calcite (Calcium carbonate (CaCO3) and silicon) improved root yield, leaf yield, and biological sugar output of sugar beet. Simultaneously, a beneficial influence on the technical quality of the roots was discovered. It resulted in a substantial decrease in alpha-amino-nitrogen content, as well as a reduction of potassium and sodium content (Artyszak et al., 2014). Pirzad et al. (2019) found that boron foliar application resulted in the highest yield of the root, sugar, and white sugar contents but decreased impurities (Na, K, and -amino-N) and molasses sugar percentage.

Conclusions

M could enhance the growth, yield, and quality of sugar beet under saline water and soil. Lithovit demonstrated the most significant advantages for biological and technical sugar yields. As a result, LB may be used as an agricultural fertilizer in the cultivation of sugar beet. In summary, the findings indicated that using an environmentally friendly Nano Caco3 foliar fertilizer (lithovit) and molasses soil fertilizer (by-products industrial process of sugar production) is beneficial for sugar beet development in saline soil and water. A long-term study for molasses and lithovit is needed to clarify product efficiency, optimal doses, application time and the methods used to improve the efficiency of the used product for different crops.

REFERENCES

[1] Abrol, I., Yadav, J. S. P., Massoud, F. (1988): Salt-Affected Soils and Their Management. – Soil Resources, Management and Conservation Service, FAO Land and Water Development Division, Rome.

http://www.aloki.hu ● ISSN 1589 1623 (Print) ● ISSN 1785 0037 (Online)
DOI: http://dx.doi.org/10.15666/aeer/1906_49234939

[2] Ainsworth, E. A., Rogers, A. (2007): The response of photosynthesis and stomatal conductance to rising [CO2]: mechanisms and environmental interactions. – Plant, Cell & Environment 30: 258-270.
[3] Ali, A. Y. A., Ibrahim, M. E. H., Zhou, G., Nimir, N. E. A., Jiao, X., Zhu, G., Elsiddig, A. M. I., Suliman, M. S. E., Elradi, S. B. M., Yue, W. (2020): Exogenous jasmonic acid and humic acid increased salinity tolerance of sorghum. – Agronomy Journal 112: 871-884.
[4] Alsaeedi, A., El-Ramady, H., Alshaal, T., El-Garawany, M., Elhawat, N., Al-Otaibi, A. (2019): Silica nanoparticles boost growth and productivity of cucumber under water deficit and salinity stresses by balancing nutrients uptake. – Plant Physiology and Biochemistry 139: 1-10.
[5] Artyszak, A., Gozdowski, D., Kucińska, K. (2014): The effect of foliar fertilization with marine calcite in sugar beet. – Plant, Soil and Environment 60: 413-417.
[6] Attia, A., El-Hendi, M., Hamoda, S., El-Sayed, O. (2016): Effect of nano-fertilizer (lithovit) and potassium on leaves chemical composition of Egyptian cotton under different planting dates. – Journal of Plant Production 7: 935-942.
[7] Ayers, R. S., Westcot, D. W. (1985): Water Quality for Agriculture. – Food and Agriculture Organization of the United Nations, Rome.
[8] Badawi, M., Attia, A., EL-Moursy, S., Seadh, S., Hamada, A. (2013): Effect of compost, humic acid and nitrogen fertilizer rates on: 1-growth of sugar beet crop. – Journal of Plant Production 4: 705-719.
[9] Becherescu, A., Horgoș, A., Dinu, M., Popa, D., Drăgunescu, A. (2017): Photosynthetic stimulation and its influence on the productive output increase in tomato hybrids. – Journal of Horticulture, Forestry and Biotechnology 21: 146-153.
[10] Beinşan, C., Şumălan, R., Gâdea, Ş., Vâtcă, S. (2014): Physiological indicators study involved in productivity increasing in tomato. – ProEnvironment 7: 218-224.
[11] Bilal, B. (2010): Lithovit: an innovative fertilizer. – The 3rd e-Conference on Agricultural Biosciences (IeCAB 2010), 1st-15th June 2010. http://www.slideserve.com/madison/lithovitan-innovative-fertilizer.
[12] Black, C., Evans, D., White, J., Ensminger, L., Clark, F. (1965): Methods of Soil Analysis. Part 2. Chemical and microbial properties. – American Society of Agronomy, Madison, WI.
[13] Brown, J., Lilleland, O. (1946): Rapid determination of potassium and sodium in plant materials and soil extracts by flame photometry. – In: Proceedings of the American Society for Horticultural Science 48: 341-346.
[14] Brown, K. F., McGowan, M., Armstrong, M. (1987): Response of the components of sugar beet leaf water potential to a drying soil profile. – The Journal of Agricultural Science 109: 437-444.
[15] Canellas, L. P., Olivares, F. L. (2014): Physiological responses to humic substances as plant growth promoter. – Chemical and Biological Technologies in Agriculture 1: 3.
[16] Cooke, D., Scott, R. (1993): The Sugar Beet Crop. Science into Practice. – Chapman and Hall, London.
[17] El-Hassanin, A. S., Samak, M. R., Moustafa, N., Shafika, A., Khalifa, N., Ibrahim Inas, M. (2016): Effect of foliar application with humic acid substances under nitrogen fertilization levels on quality and yields of sugar beet plant. – International Journal of Current Microbiology and Applied Sciences 5: 668-680.
[18] El-Tokhy, F. K., Tantawy, A., El-Shinawy, M., Abou-Hadid, A. (2018): Effect of sugar beet molasses and fe-edhha on tomato plants grown under saline water irrigation condition. – Arab Universities Journal of Agricultural Sciences 26: 2297-2310.
[19] FAO (2018): Food Agriculture Organization of the United Nations. FAOSTAT statistical database. – http://www.fao.org/faostat/en/#data/QC.

http://www.aloki.hu ● ISSN 1589 1623 (Print) ● ISSN 1785 0037 (Online)
DOI: http://dx.doi.org/10.15666/aeer/1906_49234939

[20] Farouk, S. (2015): Improving growth and productivity of potato (*Solanum tuberosum* L.) by some biostimulants and lithovit with or without boron. – Journal of Plant Production Mansoura University 6: 2187-2206.
[21] Gharib, H. S., Metwally, T., Naeem, S., Gewaily, E. (2011): Influence of some stimulating compounds and nitrogen fertilizer levels on growth and yield of hybrid rice. – Zagazig Journal of Agricultural Research 38: 1-21.
[22] Gigel, P., Florin, S. (2017): Response model of vegetation parameters and yield in maize under the influence of Lithovit fertilizer. – AIP Conference Proceedings 1863: 430005. AIP Publishing LLC, Melville, NY.
[23] Gomaa, R., Tantawy, A., El-Behairy, U., El-Shinawy, M. (2017): Effect of nano-calcium and nano-silicon compounds on salinity tolerance for green bean plants. – In: Twelfth International Dryland Development Conference, 'Sustainable Development of Drylands in the Post 2015 World', Alexandria, Egypt, 21-24 August 2016. International Dryland Development Commission (IDDC), pp. 252-263.
[24] Harvey, C. W., Dutton, J. V. (1993): Root Quality and Processing. – In: Cooke, D. A., Scott, R. K. (eds.) The Sugar Beet Crop. Springer Netherlands, Dordrecht, pp. 571-617.
[25] Issa, D., Alturki, S., Sajyan, T., Sassine, Y. (2020): Sorbitol and lithovit-guano25 mitigates the adverse effects of salinity on eggplant grown in pot experiment. – Agronomy Research 18: 113-126.
[26] Jiang, Z.-P., Li, Y.-R., Wei, G.-P., Liao, Q., Su, T.-M., Meng, Y.-C., Zhang, H.-Y., Lu, C.-Y. (2012): Effect of Long-Term Vinasse Application on Physico-chemical Properties of Sugarcane Field Soils. – Sugar Tech 14: 412-417.
[27] Kandil, E. E., Abdelsalam, N. R., EL Aziz, A. A. A., Ali, H. M., Siddiqui, M. H. (2020): Efficacy of nanofertilizer, fulvic acid and boron fertilizer on sugar beet (*Beta vulgaris* L.) yield and quality. – Sugar Tech 22: 782-791.
[28] Khaled, H., Fawy, H. A. (2011): Effect of different levels of humic acids on the nutrient content, plant growth, and soil properties under conditions of salinity. – Soil and Water Research 6: 21-29.
[29] Khaleda, L., Park, H. J., Yun, D.-J., Jeon, J.-R., Kim, M. G., Cha, J.-Y., Kim, W.-Y. (2017): Humic acid confers high-affinity K+ transporter 1-mediated salinity stress tolerance in Arabidopsis. – Molecules and Cells 40: 966.
[30] Khodadadi, S., Chegini, M. A., Soltani, A., Ajam Norouzi, H., Sadeghzadeh Hemayati, S. (2020): Influence of foliar-applied humic acid and some key growth regulators on sugar beet (*Beta vulgaris* l.) under drought stress: antioxidant defense system, photosynthetic characteristics and sugar yield. – Sugar Tech 22: 765-772.
[31] Khorshid, A., Moghadam, F., Bernousi, I., Khayamim, S., Rajabi, A. (2018): Comparison of some physiological responses to salinity and normal conditions in Sugar Beet. – Indian Journal of Agricultural Research 52: 362-367.
[32] Le Docte, A. (1927): Commercial determination of sugar in the beet root using the Sacks Le-Docte process. – International Sugar Journal 29: 488-492.
[33] Li, S., Zhao, X., Ye, X., Zhang, L., Shi, L., Xu, F., Ding, G. (2020): The Effects of condensed molasses soluble on the growth and development of rapeseed through seed germination, hydroponics and field trials. – Agriculture 10: 260.
[34] Mahmoud, S., El-Tanahy, A., Fawzy, Z. (2020): The effects of exogenous application of some bio stimulant substances on growth, physical parameters and endogenous components of onion plants. – International Journal of Agriculture and Earth Science 6: 1-13.
[35] Marschner, H. (2012): Mineral Nutrition of Higher Plants. – Academic Press LimitedHarcourt Brace and Company, London, pp. 347-364.
[36] Maswada, H., Abd El-Rahman, L. A. (2014): Inducing salinity tolerance in wheat plants by hydrogen peroxide and lithovit: a nano-$CaCO_3$ fertilizer. – Journal of Agricultural Research Kafrelsheikh University 40: 696-719.

http://www.aloki.hu ● ISSN 1589 1623 (Print) ● ISSN 1785 0037 (Online)
DOI: http://dx.doi.org/10.15666/aeer/1906_49234939

[37] Nawaz, F., Shehzad, M. A., Majeed, S., Ahmad, K. S., Aqib, M., Usmani, M. M., Shabbir, R. N. (2020): Role of Mineral Nutrition in Improving Drought and Salinity Tolerance in Field Crops. – In: Hasanuzzaman, M. (ed.) Agronomic Crops. Vol. 3: Stress Responses and Tolerance. Springer, Singapore, pp. 129-147.
[38] Nemeat-Alla, H. E., El-Gamal, I. S., El-Safy, N. K. (2021): Effect of potassium humate and boron fertilization levels on yield and quality of sugar beet in sandy soil. – Alexandria Science Exchange Journal 42: 395-405.
[39] Nyomora, A., Brown, P., Pinney, K., Polito, V. (2000): Foliar application of boron to almond trees affects pollen quality. – Journal of the American Society for Horticultural Science 125: 265-270.
[40] Ouni, Y., Ghnaya, T., Montemurro, F., Abdelly, C., Lakhdar, A. (2014): The role of humic substances in mitigating the harmful effects of soil salinity and improve plant productivity. – International Journal of Plant Production 8: 353-374.
[41] Pirzad, A., Mamyandi, M. M., Khalilzadeh, R. (2019): Physiological and morphological responses of sugar beet (*Beta vulgaris* L.) subjected to nano-boron oxide at different growth stages. – Acta Biologica Szegediensis 63: 103-111.
[42] Priyadarshani, W. M. N. (2019): Effect of goat manure and sugarcane molasses on growth and yield of beetroot (*Beta vulgaris* L.). – MSc thesis, Fac. of Agri., Eastern Univ., Sri Lanka.
[43] Pujar, S. (1995): Effect of distillery effluent irrigation on growth, yield and quality of crops. – M. Sc. (Agri.) thesis, University of Agricultural Sciences, Dharwad, India.
[44] Rahimi, A., Kiralan, M., Ahmadi, F. (2020): Effect of humic acid application on quantitative parameters of sugar beet (*Beta vulgaris* L.) Cv. Shirin. – Alexandria Science Exchange Journal 41: 85-91.
[45] Ramana, S., Biswas, A. K., Singh, A. B., Yadava, R. B. R. (2002): Relative efficacy of different distillery effluents on growth, nitrogen fixation and yield of groundnut. – Bioresource Technology 81: 117-121.
[46] Rassam, G., Dadkhah, A., Yazdi, A. K., Dashti, M. (2015): Impact of humic acid on yield and quality of sugar beet (*Beta vulgaris* L.) grown on calcareous soil. – Notulae Scientia Biologicae 7: 367-371.
[47] Rawashdeh, H., Sala, F. (2013): Effect of different levels of boron and iron foliar application on growth parameters of wheat seedlings. – African Crop Science Conference Proceedings 11: 861-864.
[48] Rehab, I., El Maghraby, S. S., Kandil, E., Ibrahim, N. Y. (2019): Productivity and quality of sugar beet in relation to humic acid and boron fertilization under Nubaria conditions. – Alexandria Science Exchange Journal 40: 115-126.
[49] Reinfeld, E., Emmerich, A., Baumgarten, G., Winner, C., Beiss, U. (1974): Zur Voraussage des Melassezuckers aus Rübenanalysen. – Zucker 27: 2-15.
[50] Rochaix, J.-D. (2011): Regulation of photosynthetic electron transport. – Biochimica et Biophysica Acta (BBA) - Bioenergetics 1807: 375-383.
[51] Rout, G. R., Sahoo, S. (2015): Role of iron in plant growth and metabolism. – Reviews in Agricultural Science 3: 1-24.
[52] Sajyan, T., Naim, L., Sebaaly, Z., Rizkallah, J., Shaban, N., Sassine, Y. (2018): Alleviating the adverse effects of salinity stress on tomato crop (*Solanum lycopersicum*) using nano-fertilizer as foliar application. – In: XXX International Horticultural Congress IHC2018: International Symposium on Water and Nutrient Relations and Management of 1253, pp. 33-40.
[53] Sajyan, T. K., Shaban, N., Rizkallah, J., Sassine, Y. N. (2019): Performance of salt-stressed tomato crop as affected by nano-caco 3, glycine betaine, MKP fertilizer and aspirin application. – Poljoprivreda i Sumarstvo 65: 19-27.
[54] Sajyan, T. K., Alturki, S. M., Sassine, Y. N. (2020): nano-fertilizers and their impact on vegetables: contribution of nano-chelate super plus ZFM and lithovit®-standard to improve salt-tolerance of pepper. – Annals of Agricultural Sciences 65: 200-208.

http://www.aloki.hu ● ISSN 1589 1623 (Print) ● ISSN 1785 0037 (Online)
DOI: http://dx.doi.org/10.15666/aeer/1906_49234939

[55] Samavat, S., Samavat, S. (2014): The effects of fulvic acid and sugar cane molasses on yield and qualities of tomato. – International Research Journal of Applied and Basic Sciences 8: 266-268.
[56] Şanli, A., Karadoğan, T., Tosun, B. (2015): The effects of sugar beet molasses applications on root yield and sugar content of sugar beet (*Beta vulgaris* L.). – Tarla Bitkileri Merkez Araştırma Enstitüsü Dergisi 24: 103-108.
[57] Sassine, Y. N., Alturki, S. M., Germanos, M., Shaban, N., Sattar, M. N., Sajyan, T. K. (2020): Mitigation of salt stress on tomato crop by using foliar spraying or fertigation of various products. – Journal of Plant Nutrition 43. https://doi.org/10.1080/01904167.2020.1771587.
[58] Shallan, M., Hassan, H., Namich, A. A., Ibrahim, A. A. (2016): The influence of lithovit fertilizer on the chemical constituents and yield characteristics of cotton plant under drought stress. – International Journal of ChemTech Research 9: 1-11.
[59] Soliman, A. M., Awad, A., Gendy, A., Abdelkader, M. (2018): Influence of foliar application of Fe, Zn, Mo and lithovit on growth and productivity of stevia plant (*Stevia rebaudiana*, Bert.). – Zagazig Journal of Agricultural Research 45: 1901-1912.
[60] Srivastava, P. C., Singh, R. K., Srivastava, P., Shrivastava, M. (2012): Utilization of molasses based distillery effluent for fertigation of sugarcane. – Biodegradation 23: 897-905.
[61] Szczepanek, M. (2017): Effect of biostimulant application in cultivation of spring barley. – Acta Scientiarum Polonorum Agricultura 16: 77-85.
[62] Tahjib-UI-Arif, M., Sohag, A. A. M., Afrin, S., Bashar, K. K., Afrin, T., Mahamud, A. G. M. S. U., Polash, M. A. S., Hossain, M. T., Sohel, M. A. T., Brestic, M., Murata, Y. (2019): Differential response of sugar beet to long-term mild to severe salinity in a soil–pot culture. – Agriculture 9: 223.
[63] Tantawy, A., Salama, Y., Abdel-Mawgoud, A. M. R., Ghoname ElSayed, A. (2014): Comparison of chelated calcium with nano calcium on alleviation of salinity negative effects on tomato plants. – Middle East Journal of Agriculture Research 3: 912-916.
[64] Tribodyn (2020): Lithovit® Boron 05 product. – Tribodyn AG CO., Germany. https://tribodyn.de/en/products/classic/bor-05.
[65] Tsialtas, J., Maslaris, N. (2009): Selective absorption of K over Na in sugar beet cultivars and its relationship with yield and quality in two contrasting environments of central Greece. – Journal of Agronomy and Crop Science 195: 384-392.
[66] Turner, P., Meyer, J., King, A. (2002): Field evaluation of concentrated molasses stillage as a nutrient source for sugarcane in Swaziland. – In: Proceedings of the Annual Congress-South African Sugar Technologists' Association. South African Sugar Technologists' Association, pp. 61-70.
[67] Wilczewski, E., Szczepanek, M., Wenda-Piesik, A. (2017): Response of sugar beet to humic substances and foliar fertilization with potassium. – Journal of central European agriculture 19: 153-165.
[68] Wynne, A., Meyer, J. (2002): An economic assessment of using molasses and condensed molasses solids as a fertilizer in the South African sugar industry. – Proceedings South African Sugar Technologists Association 76: 71-78.
[69] Zhang, L., Gao, M., Zhang, L., Li, B., Han, M., Alva, A. K., Ashraf, M. (2013): Role of exogenous glycinebetaine and humic acid in mitigating drought stress-induced adverse effects in Malus robusta seedlings. – Turkish Journal of Botany 37: 920-929.

http://www.aloki.hu ● ISSN 1589 1623 (Print) ● ISSN 1785 0037 (Online)
DOI: http://dx.doi.org/10.15666/aeer/1906_49234939

RESEARCH TREND AND STATUS OF FORESTRY BASED ON ESSENTIAL SCIENCE INDICATORS DURING 2010–2020: A BIBLIOMETRIC ANALYSIS

YUAN, B. Z.[1*] – SUN, J.[2]

[1]*College of Plant Science and Technology, Huazhong Agricultural University, Wuhan City, 430070 Hubei Province, PR China*

[2]*Library of Huazhong Agricultural Universillty, Wuhan City, 430070 Hubei Province, PR China*

**Corresponding author*
e-mail: yuanbz@mail.hzau.edu.cn

(Received 8th Jun 2021; accepted 20th Sep 2021)

Abstract. This study analyzed 302 top papers in the subject category of Forestry from 2010 to 2020, which include 300 highly cited papers and 3 hot papers. All papers were written in English, belonging to 1,567 authors, 694 organizations and 74 countries/territories, published in 35 journals and book series. The top five Journals were Agricultural and Forest Meteorology, Forest Ecology and Management, Forests, Tree Physiology and Forest Policy and Economics. Top five countries and regions were USA, Germany, Canada, France and Peoples R China. Top five organizations were US Forest Serv, Chinese Acad Sci, INRA, Swedish Univ Agr Sci and Univ Freiburg. Among the all authors, Bauhus, Juergen from Univ Freiburg of Germany provided the highest number in 6 papers. All keywords were separated into seven clusters for different research topics. Visualizations offered exploratory information on the current state in a scientific field or discipline as well as indicated possible developments in the future.
Keywords: *forestry category, top papers, visualization, VOSviewer*

Introduction

According to the category description for Forestry in Scope Notes of Science Citation Index Expanded, it covers resources concerning the science and technology involved in establishing, maintaining and managing forests for various uses, including wood production, water resource management, wildlife conservation and recreation (Clarivate, 2021. InCites Journal Citation Reports).

Bibliometrics technique has been adopted analyzing the forestry category on Web of Science (WoS) which included the following subjects, bibliometric analysis of forestry and forest research (Polinko and Coupland, 2021), assessing the scientific productivity of Italian forest researchers (Chirici, 2012), models for temperate forest management (Ordoñez and Galicia, 2020), evaluation of the status of Picea research and research hotspots (Duan et al., 2020), community forestry research in Canada (Bullock and Lawler, 2015), ecological restoration in Brazilian biomes (Guerra et al., 2020), wood modification and environmental impact assessment (Burnard et al., 2017), forest ecosystem services (Aznar-Sanchez et al., 2018), first decade bibliometric analysis of journal of Forests (Uribe-Toril et al., 2019), remote sensing applied in forest management to optimize ecosystem services (Abad-Segura et al., 2020), spatiotemporal analysis of forest modeling in Mexico (Martínez-Santiago et al., 2017), evaluation of the research on common forest management (Romanelli and Boschi, 2019), trees and parks as "the lungs of cities" (Xing and Brimblecombe, 2020).

http://www.aloki.hu ● ISSN 1589 1623 (Print) ● ISSN 1785 0037 (Online)
DOI: http://dx.doi.org/10.15666/aeer/1906_49414957

Bibliometrics technique has analyzed other WoS category documents, such as, classic publications in WoS category of orthopedics (Li et al., 2019), emergency medicine (Ho, 2021), materials science (Ho, 2014), horticulture (Kolle et al., 2017), dentistry, oral surgery and medicine from 2007 to 2016 (Yeung and Leung, 2018), dance (Ho and Ho, 2015), water resources (Chuang et al., 2011), environmental sciences (Khan and Ho, 2012), education and educational research (Ivanović and Ho, 2019).

Top papers are the sum of hot papers and highly cited papers, based on Clarivate Analytics' Essential Science Indicators (ESI). The ESI database is widely used to assess scientific outputs. Highly cited paper is a paper that belongs to the top 1% of papers in a research field published in a specified year. The 1% is determined by the highly cited threshold calculated for the research field in the specified year. Hot paper is a paper published in the past two years that received a number of citations in the most recent two-month period that places it in the top 0.1% of papers in the same field. Some papers focused on as Economics and Business (Zhang et al., 2018), operations research and management science (Liao et al., 2019), environmental sciences (Ma et al., 2020), macro-level collaboration network analysis and visualization (Yang et al., 2020). Sun and Yuan have analyzed the top papers in the world rice research (Sun and Yuan, 2020a), library and information science (Sun and Yuan, 2020b), water Resources (Sun and Yuan, 2020c), agronomy category (Sun and Yuan, 2021), green and sustainable science and technology (Yuan and Sun, 2019) and scientific research on maize or corn (Yuan and Sun, 2020a, b).

The purpose of this paper was to use bibliometric methods to analyze the top papers in the subject category of Forestry during 11 years period from 2010 to 2020 through publication year, category, author, affiliations, country, journals, all keywords and other key features. Co-authorship network visualization of author, organizations and countries, co-occurrence network visualization of all keywords were done by VOSviewer. Special attention will be dedicated to research topics and research fronts.

Materials and methods

Essential science indicators (ESI)

Essential science indicators (ESI) is a unique compilation of performance statistics and trends extrapolated from counts of articles published in scholarly journals and the citations to those articles. ESI is an analytical tool that helps you identify top-performing research in Web of Science (WoS) Core Collection. Article counts for ESI are derived from journals indexed in WoS Core Collection (SCIE and SSCI only) over a 11-year period. Citation counts for these articles are derived from journals indexed in WoS Core Collection (SCIE, SSCI and Arts and Humanities Citation Index). Each journal is assigned to one of 22 research fields. In ESI a journal can be assigned to only one field. Journals such as Science and Nature are categorized as multidisciplinary since they publish research in many different fields. As a result, papers published in these multidisciplinary journals are assigned to a field based on the representation of the cited journals. For example, if the majority of cited references in the paper are to neuroscience journals, the paper is then categorized as neuroscience (Clarivate, Version 3.0, Essential Science Indicators Help, 2021).

Here, the Essential Science Indicators database has been updated as of March 25, 2021, to cover an 11-year period from January 1, 2010 to December 31, 2020. Papers are defined as regular scientific articles and review articles.

http://www.aloki.hu ● ISSN 1589 1623 (Print) ● ISSN 1785 0037 (Online)
DOI: http://dx.doi.org/10.15666/aeer/1906_49414957

Data collection

Data collection was completed on the single day on May 1, 2021 to avoid the bias. We first conducted an advanced search in the WoS category (WC) of Forestry and publication year (PY) from 2010 to 2020. The query as following: (WC = Forestry) AND (PY 2010-2020).

The results were used to identify the top papers of the highly cited papers and hot papers in field. There are 302 top papers from WoS Core Collection. Full record and cited references of the included papers were extracted and imported into VOSviewer (Leiden University, Leiden, the Netherlands) for further citation analysis. The impact factors (IF 2019 and IF 5year) were taken from the Journal Citation Report (JCR 2019) published in 2020, which had the latest data available.

VOSviewer

VOSviewer were used to show the international collaboration between the authors, organizations, countries and the research trends through all keywords (Van Eck and Waltman, 2010). Visualizations (network and overlay) using program VOSviewer are conducted on WoS data in order to determine co-occurrence and clusters of connected publications, country input and author collaboration (co-authorship) as well as clusters of interrelated research topics (text data). In this paper, default parameters values of the VOSviewer are usually used in the analysis. Items are represented by a label and a circle. The size of circles reflects the weight of an item. Some items are not displayed in avoidance of overlapping. The colors in network visualization (text maps) represent clusters of similar items as calculated by the program. Distance between the items indicates the strength of relationships.

Results and discussion

Document type and language of publication

Based on Clarivate Analytics's WoS Index, there were total 302 top papers of the Forestry category during the period from January, 2010 to December, 2020. All of 302 top papers were identified in SCIE (302), SSCI (36), and CPCI-S (6). The document types of all 302 top papers were articles (213, 70.53%), reviews (89, 29.47%) and proceedings papers (6, 1.987%). Among the all 302 top papers, there were 3 hot papers and 300 the highly cited papers that means 2 papers were both the hot papers and the highly cited papers. All papers were published in English. The English was dominating language from the WoS, and scholars tended to publish their articles in English as they want them to be widely accepted (Khan et al., 2020).

Publication output

With the aim of knowing the research status and trend, *Figure 1* showed the top paper of Forestry category between 2010 and 2020. The mean publication was 27.45 each year, and the highest value was 40 in 2020. An increase in the number of cited references indicated that there are more citing or cited publications. The number of citations to a paper is considered a good quantitative measure of a paper's impact. The *h*-index was initially proposed as a measure of a researcher's scientific output based on counting the number of publications (N) by that researcher cited N or more times

http://www.aloki.hu ● ISSN 1589 1623 (Print) ● ISSN 1785 0037 (Online)
DOI: http://dx.doi.org/10.15666/aeer/1906_49414957

(Hirsch, 2005). For the total 302 papers, the *h*-index was 140, and the average citation per item was 153.61.

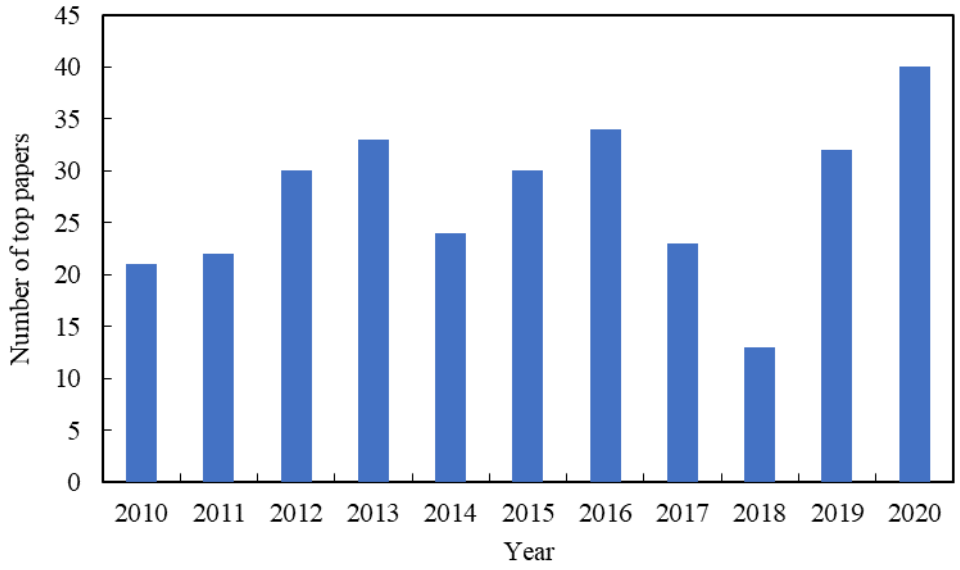

Figure 1. *Number of published top papers of Forestry category from 2010 to 2020*

Web of Science categories and research areas

Each paper indexed by the WoS belongs to one or more subject categories. There were total 14 WoS subject categories and 11 research areas including Forestry categories (*Table 1*). Among these, the top six categories included Forestry (302 papers, 100% of 302 papers), Agronomy (69, 22.848%), Meteorology Atmospheric Sciences (66, 21.854%), Plant Sciences (31, 10.265%), Ecology (23, 7.616%) and Environmental Studies (23, 7.616%). The top six research areas included Forestry (302 papers, 100% of 302 papers), Agriculture (73, 24.172%), Meteorology Atmospheric Sciences (66, 21.854%), Environmental Sciences Ecology (46, 15.232%), Plant Sciences (31, 10.265%) and Business Economics (31, 10.265%). Journals or papers may be classified into two or more categories in the WoS, showed the multidisciplinary character of this research field (Elango and Ho, 2018). In WoS, publications were also mapped to WoS categories which were more detailed than areas (Stopar et al., 2021).

Core journals

Based on JCR 2019 data (published in 2020), there were 68 journals of the WoS categories for Forestry. All the 302 publications were published in 35 journals and book series. The top 20 core journals were displayed in *Table 2* with total articles each more than four top papers, Journal impact factor as IF 2019 and IF 5 year, rank and Quartile in Forestry category.

The top 5 journals, top 10 journals, top 15 journals and top 20 journals published about 61.589%, 75.497%, 85.101% and 91.726% of the total top papers, respectively. The top five Journals are Agricultural and Forest Meteorology (66, 21.854%), Forest Ecology and Management (65, 21.523%), Forests (23, 7.616%), Tree Physiology (17, 5.629%) and Forest Policy and Economics (15, 4.967%), each published more than 15

http://www.aloki.hu ● ISSN 1589 1623 (Print) ● ISSN 1785 0037 (Online)
DOI: http://dx.doi.org/10.15666/aeer/1906_49414957

papers. Based on results of *Table 2,* among the top 20 journals, fourteen journals were in Quartile 1, six journals were in Quartile 2. White-Gibson et al. (2019) had also demonstrated the importance of publishing articles in the English language in a high IF journals.

Table 1. *WoS categories and research areas for forestry category during 2010-2020*

Rank	WoS categories			Research areas		
	Categories	No. papers	% Total papers	Areas	No. papers	% Total papers
1	Forestry	302	100	Forestry	302	100
2	Agronomy	69	22.848	Agriculture	73	24.172
3	Meteorology atmospheric sciences	66	21.854	Meteorology atmospheric sciences	66	21.854
4	Plant sciences	31	10.265	Environmental sciences ecology	46	15.232
5	Ecology	23	7.616	Plant sciences	31	10.265
6	Environmental studies	23	7.616	Business economics	15	4.967
7	Economics	15	4.967	Urban studies	8	2.649
8	Urban studies	8	2.649	Materials science	6	1.987
9	Materials science paper wood	6	1.987	Genetics heredity	4	1.325
10	Genetics heredity	4	1.325	Physical geography	3	0.993
11	Horticulture	4	1.325	Zoology	1	0.331
12	Geography physical	3	0.993			
13	Materials science textiles	1	0.331			
14	Zoology	1	0.331			

Table 2. *Top 20 core journals on forestry category research indexed in the WoS*

Rank	Journal	TP	Ratio	IF 2019	IF 5year	QC	QR
1	Agricultural and Forest Meteorology	66	21.854	4.651	5.142	Q1	2
2	Forest Ecology and Management	65	21.523	3.17	3.581	Q1	5
3	Forests	23	7.616	2.221	2.484	Q1	17
4	Tree Physiology	17	5.629	3.655	4.33	Q1	4
5	Forest Policy and Economics	15	4.967	3.139	3.085	Q1	6
6	Journal of Vegetation Science	12	3.974	2.698	3.177	Q1	7
7	Canadian Journal of Forest Research	8	2.649	1.812	2.162	Q2	25
8	Urban Forestry Urban Greening	8	2.649	4.021	4.468	Q1	3
9	Current Forestry Reports	7	2.318	4.972	5.115	Q1	1
10	European Journal of Forest Research	7	2.318	2.451	2.581	Q1	12
11	Forestry	7	2.318	2.293	3.036	Q1	14
12	Journal of Forestry Research	6	1.987	1.689	1.475	Q2	31
13	Journal of Plant Ecology	6	1.987	1.833	2.299	Q2	23
14	Annals of Forest Science	5	1.656	2.033	2.758	Q2	21
15	International Journal of Wildland Fire	5	1.656	2.627	2.939	Q1	9
16	Applied Vegetation Science	4	1.325	2.574	2.903	Q1	10
17	IAWA Journal	4	1.325	1.627	1.966	Q2	34
18	Journal of Forestry	4	1.325	2.342	2.681	Q1	13
19	New Forests	4	1.325	2.24	2.631	Q1	16
20	Tree Genetics Genomes	4	1.325	2.081	2.262	Q2	20

TP: Total publications; Ratio: Ratio of 302 (%); IF 2019: journal impact factor in 2019; IF5 year: journal impact factor of 5 years; QC: Quartile in Category; QR: Quartile rank of 68 journals in Forestry

http://www.aloki.hu ● ISSN 1589 1623 (Print) ● ISSN 1785 0037 (Online)
DOI: http://dx.doi.org/10.15666/aeer/1906_49414957

According to the publication data in the citation of 35 journals, they all meet the thresholds of one publication, but only 23 journals were connected to each other. The network of citation in the field of Forestry category based on WoS was shown seven clusters with different colors in *Figure 2,* the size of circles reflected a total number of journal publication records. Journals in the same cluster usually suggested that they published the similar content papers and had close relations with each other.

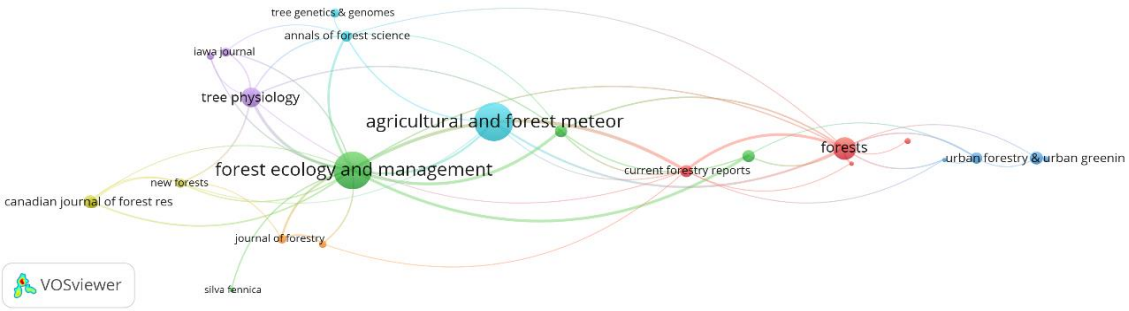

Figure 2. *Network visualization maps of citation journals in the field of Forestry category based on WoS with 23 nodes and 7 clusters*

Authors co-authorship analysis

In general, internationally collaborative articles had the highest visibility and scientific impact, followed by inter-institutional collaborative articles, single-country articles and single-author articles, respectively. A total of 1,567 authors had the 302 publications, and 127 authors met the thresholds of two publications, but only 23 authors were connected with each other. The network of authorship in the field of Forestry category based on WoS represented in *Figure 3,* the size of circles reflected a total number of records. Authors in the same cluster usually suggested that they studied in a similar field or worked at same institute or had close cooperation with each other.

The detail of author information published articles in the field of Forestry category from 2010 to 2020 along with citation, average citations, organization-enhanced and countries were provided in *Table 3*. The top eight authors published more than four papers. Though we combined the same author with the different spell, but the total number of authors were calculated separately. Among the all authors, Bauhus, Juergen from Univ Freiburg of Germany gave the most 6 papers.

The organization of the author was the latest institute. There were three authors from USA, the organizations were Colorado State Univ, Univ Washington and USDA FS; two authors from Germany, the organizations were Univ Freiburg and Tech Univ Munich; one author was from the Swiss Fed Inst Forest Snow and Landscape Res WSL of Switzerland; one author was from University of Kurdistan of Iran; one author was from Universidade Estadual Paulista of Brazil. The five authors with the higher average citations per paper were Forrester, David I., Pretzsch, Hans, Franklin, Bauhus, Juergen and Hessburg, Paul F., et al.

Countries/regions co-authorship analysis

There were 74 countries or regions that contributed 302 papers in the field of Forestry category from 2010 to 2020. *Table 4* represented the top 20 countries or regions that published more than 10 papers, and the cluster, total link strength,

http://www.aloki.hu ● ISSN 1589 1623 (Print) ● ISSN 1785 0037 (Online)
DOI: http://dx.doi.org/10.15666/aeer/1906_49414957

citations and average citations. Among the 20 countries, USA, Germany, Canada, France and Peoples R China were the major article contributors. In case of average citations, Spain, Italy, Switzerland, France and Australia showed the higher citations per paper.

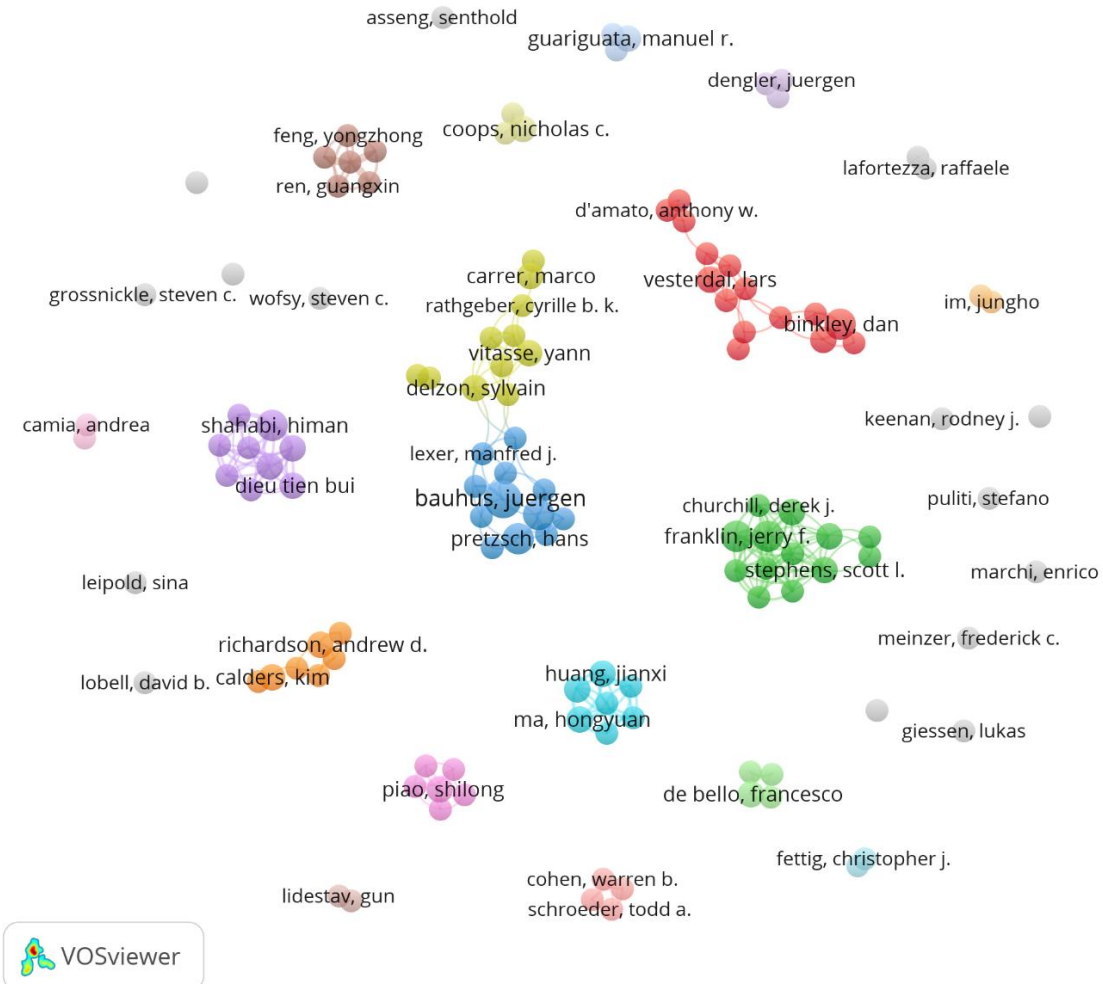

Figure 3. *Network visualization map of top authors in Forestry category from 2010 to 2020. Cooperation based on co-authorship between authors. Network visualization map of authors with minimum productivity of two publications in the studied field and exist within a collaborative research group*

Table 3. *The top eight most prolific authors published papers in the field of Forestry category from 2010 to 2020*

Rank	Author	Papers	Citations	Average citations	Organizations	Country
1	Bauhus, Juergen	6	751	125.17	Univ Freiburg	Germany
2	Binkley, Dan	4	319	79.75	Colorado State Univ	USA
3	Forrester, David I.	4	698	174.50	Swiss Fed Inst Forest Snow and Landscape Res WSL	Switzerland
4	Franklin, Jerry F.	4	572	143.00	Univ Washington	USA
5	Hessburg, Paul F.	4	497	124.25	USDA FS	USA
6	Pretzsch, Hans	4	575	143.75	Tech Univ Munich	Germany
7	Shahabi, Himan	4	195	48.75	University of Kurdistan	Iran
8	Stape, Jose L.	4	319	79.75	Universidade Estadual Paulista	Brazil

http://www.aloki.hu ● ISSN 1589 1623 (Print) ● ISSN 1785 0037 (Online)
DOI: http://dx.doi.org/10.15666/aeer/1906_49414957

Table 4. *Top 20 countries/regions publishing top papers in the field of Forestry category from 2010 to 2020*

Rank	Countries/regions	Records	Cluster	Total link strength	Citations	Average citations
1	USA	122	2	223	23822	195.26
2	Germany	55	1	223	7669	139.44
3	Canada	47	2	117	10399	221.26
4	France	45	3	181	10811	240.24
5	Peoples R China	44	2	69	8921	202.75
6	Australia	41	3	137	9748	237.76
7	Italy	40	4	167	10443	261.08
8	Switzerland	33	1	172	7957	241.12
9	England	28	3	133	3799	135.68
10	Spain	26	1	157	6963	267.81
11	Austria	24	1	163	4302	179.25
12	Sweden	23	1	111	2635	114.57
13	Netherlands	20	3	119	3896	194.80
14	Finland	19	4	66	2953	155.42
15	Brazil	18	3	49	2611	145.06
16	Czech Republic	18	1	86	2386	132.56
17	Japan	15	2	61	2095	139.67
18	Scotland	14	1	71	1953	139.50
19	Denmark	10	1	47	1359	135.90
20	Norway	10	2	39	948	94.80

There were 32 countries or regions that met the requirement threshold as five. The size of circles in *Figure 4* reflected a total number of records and the distance between the countries indicated the strength of relationships. The VOSviewer divided these circles into four clusters. The different colors group represented the different clusters formed by sets of countries.

According to *Figure 4,* the first cluster consisted of fourteen countries or regions (red colour) including Russia, Spain, Switzerland, Austria, Portugal, Ireland, Scotland, Germany, Denmark, Poland, Czech Republic, Slovenia, Sweden and Belgium. The second cluster consisted of eight countries or regions (green colour) including South Korea, Canada, Peoples R China, USA, Japan, Norway, Iran and Malaysia. The third cluster consisted of seven countries (blue colour) including France, Australia, Netherlands, New Zealand, Estonia, Brazil and England. The fourth cluster consisted of three countries and regions (yellow colour) including Italy, Finland and Mexico. More cooperation could bring more advanced achievements in scientific research. Nowadays, increasing concept of international exchanges have promoted academic communications (Tang et al., 2018).

Organizations co-authorship analysis

A total of 694 organizations had the all 302 publications. Organization co-authorship analysis reflected the degree of communication between institutions as well as the influential institutions in this field (Reyes-Gonzalez, 2016). *Table 5* represented the top twelve organizations and institutions ranked by the number of total publications (more than nine papers), the total link strength, citations, average citations and country.

http://www.aloki.hu ● ISSN 1589 1623 (Print) ● ISSN 1785 0037 (Online)
DOI: http://dx.doi.org/10.15666/aeer/1906_49414957

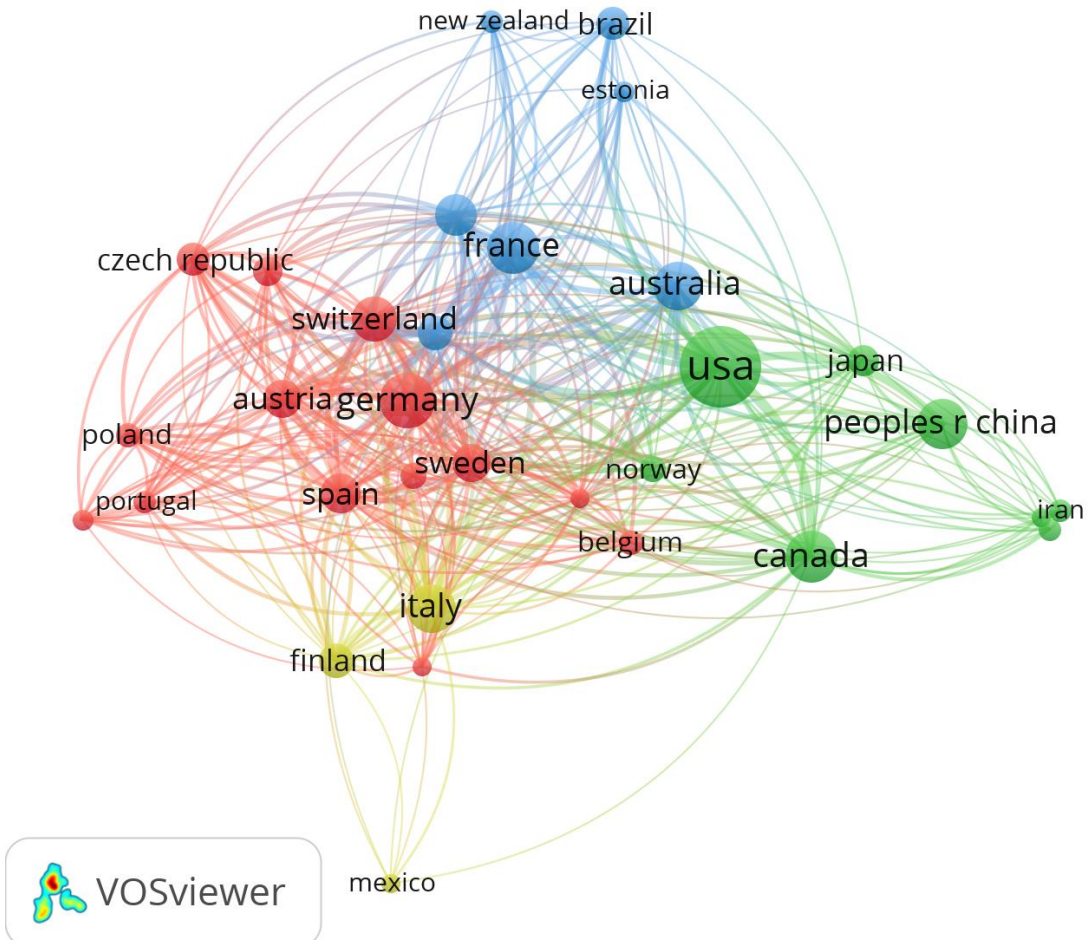

Figure 4. *The country co-authorship network of Forestry related top papers from 2010 to 2020. The country co-authorship network map with 32 nodes and 4 clusters, the bigger nodes represented the more influential countries in this field. The distance and thickness of links represented the degree of cooperation among countries*

Table 5. *Top 12 organizations published papers in the field of Forestry category from 2010 to 2020*

Rank	Organizations	Records	Total link strength	Citations	Average citations	Country
1	US Forest Serv	28	22	4537	162.04	USA
2	Chinese Acad Sci	17	7	2218	130.47	China
3	INRA	14	14	3679	262.79	France
4	Swedish Univ Agr Sci	14	19	1372	98.00	Sweden
5	Univ Freiburg	14	14	1757	125.50	Germany
6	Oregon State Univ	13	30	5413	416.38	USA
7	Univ British Columbia	13	9	1444	111.08	Canada
8	Univ Calif Berkeley	11	19	4930	448.18	USA
9	Nat Resources Canada	10	8	1058	105.80	Canada
10	Tech Univ Munich	9	13	1187	131.89	Germany
11	Univ Copenhagen	9	12	1100	122.22	Denmark
12	Univ Maryland	9	13	1015	112.78	USA

http://www.aloki.hu ● ISSN 1589 1623 (Print) ● ISSN 1785 0037 (Online)
DOI: http://dx.doi.org/10.15666/aeer/1906_49414957

These twelve organizations were mainly based in USA (four organizations), Germany (two organization), Canada (two organizations), China (1 organization), and France (1 organization), Sweden (1 organization) and Denmark (1 organization). Furthermore, top five organizations of US Forest Serv, Chinese Acad Sci, INRA, Swedish Univ Agr Sci and Univ Freiburg were popular based on contribution of articles more than 14 papers each. Similarly, in case of citation, the top five organizations of Univ Calif Berkeley, Oregon State Univ, INRA, US Forest Serv and Tech Univ Munich showed the higher average citations more than 131.89 times per paper.

Among the total 694 organizations, there were 29 organizations met the minimum thresholds of five, and connected to each other (*Fig. 5*). The VOSviewer software divided these 29 institutes into four clusters with different colors. Geographical localization is an important factor for partnership and joint venture.

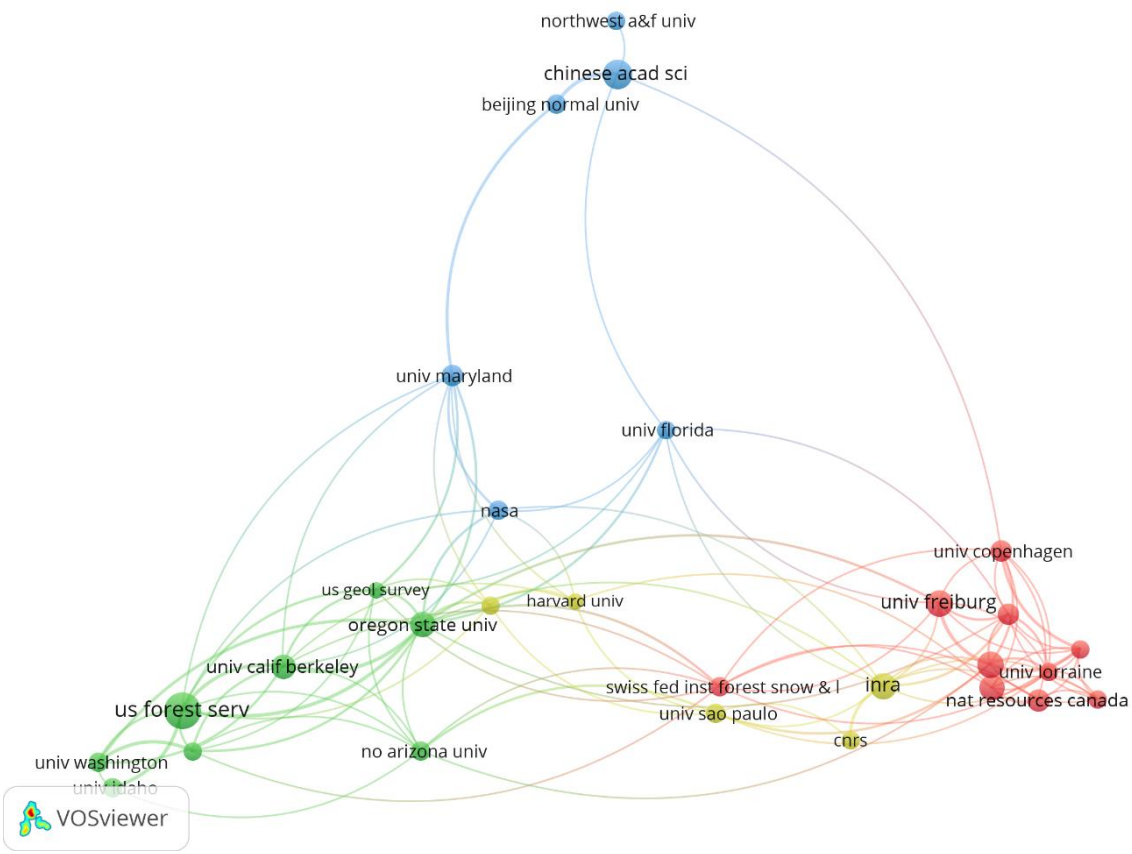

Figure 5. *The organizations co-authorship network of Forestry related publications from 2010 to 2020. The institutions co-authorship network map with 29 nodes and 4 clusters, the bigger nodes represented the more influential institution in this field. The distance and thickness of links represented the degree of cooperation among organizations*

All keywords co-occurrence analysis

Figure 6 showed the network map that links the all keywords to the entire sample of the articles analyzed. Among all 2,776 keywords, only 115 keywords met the threshold level of more than five times included in the map. There were seven main clusters that represented different viewpoints on Forestry category research topics (*Fig. 6*). The top twenty co-occurrence keywords more than eleven times were climate-change, climate

http://www.aloki.hu ● ISSN 1589 1623 (Print) ● ISSN 1785 0037 (Online)
DOI: http://dx.doi.org/10.15666/aeer/1906_49414957

change, drought, temperature, biodiversity, forest, growth, climate, model, remote sensing, vegetation, management, Scots pine, variability, diversity, Norway spruce, wildfire, area, biomass, conservation, Fagus sylvatica L., stomatal conductance, etc.

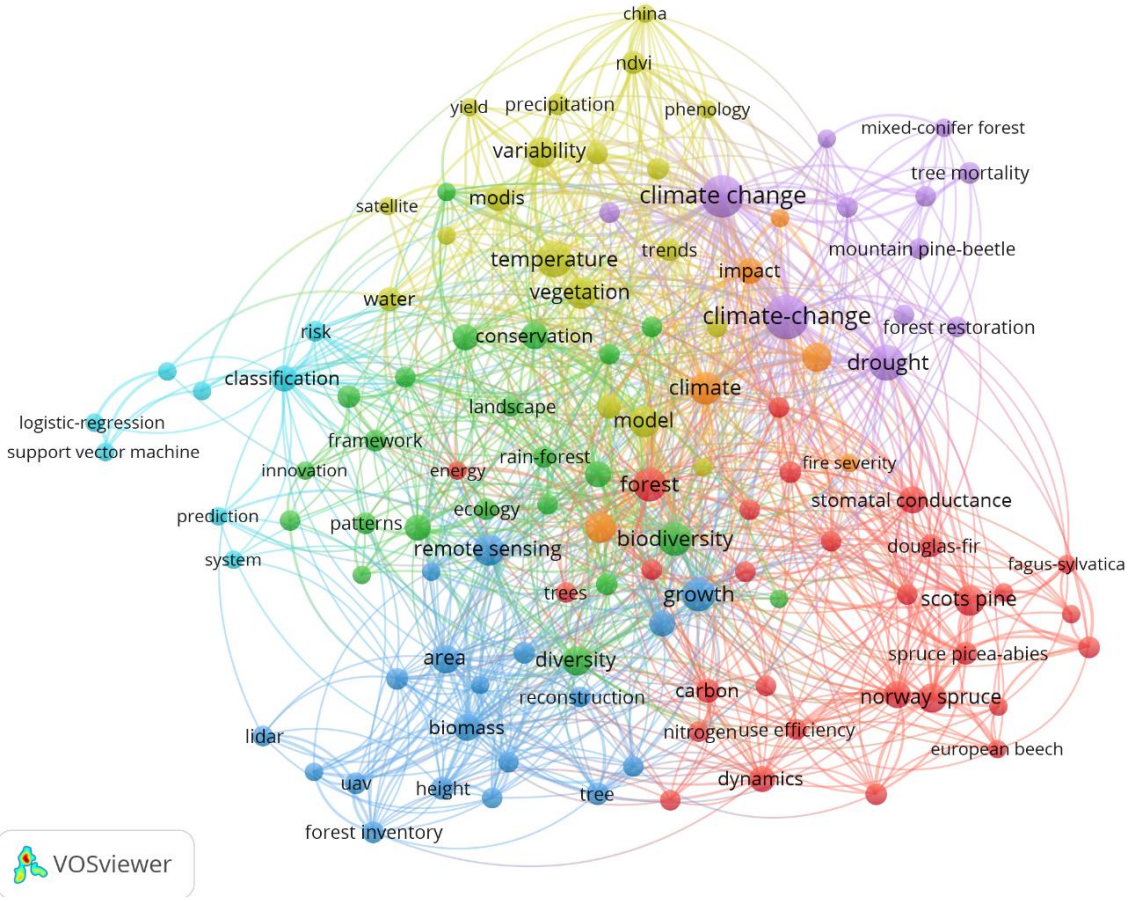

Figure 6. *VOSviewer co-occurrence network visualization mapping of most frequent all keywords (minimum of 5 occurrences) in Forestry. Co-occurrence network of all keywords included author keywords and keywords plus. Of the all 2,776 keywords, there were only 115 keywords meet the threshold more than 5 times included in the map. After keywords analyzed, there were 7 main clusters that represent 7 different viewpoints on Forestry*

The same data were then arranged by a period of Forestry category research as overlay map (*Fig. 7*). Blue colors indicated earlier research topics, whereas, yellow and green colors indicated more recent topics of interest. The blue-colored topics did not indicate no longer research work on that topics. It usually indicated that, on average, this topic was intensely investigated earlier and now more attention had shifted towards other topics. Yellow and green circles presented those research fronts.

Visualizations conducted on large datasets (big data) offer exploratory information on the current state in a scientific field or discipline as well as indicated possible developments in the future. Here, the keywords were list and ranked in each cluster based on *Figure 6*.

The first cluster (Red) focused on dynamics and production of different forests, and included keywords as forest, Scots pine, Norway spruce, Fagus-sylvatica L., stomatal conductance, dynamics, carbon, Douglas-fir, spruce Picea-abies, net primary

http://www.aloki.hu ● ISSN 1589 1623 (Print) ● ISSN 1785 0037 (Online)
DOI: http://dx.doi.org/10.15666/aeer/1906_49414957

production, temperate forests, water-use efficiency, beech Fagus-sylvatica, carbon sequestration, eddy covariance, elevated CO2, evaporation, nitrogen, photosynthesis, productivity, transpiration, trees, use efficiency, energy, European beech, Fagus-sylvatica, long-term, Picea-abies, Pinus-sylvestris, etc.

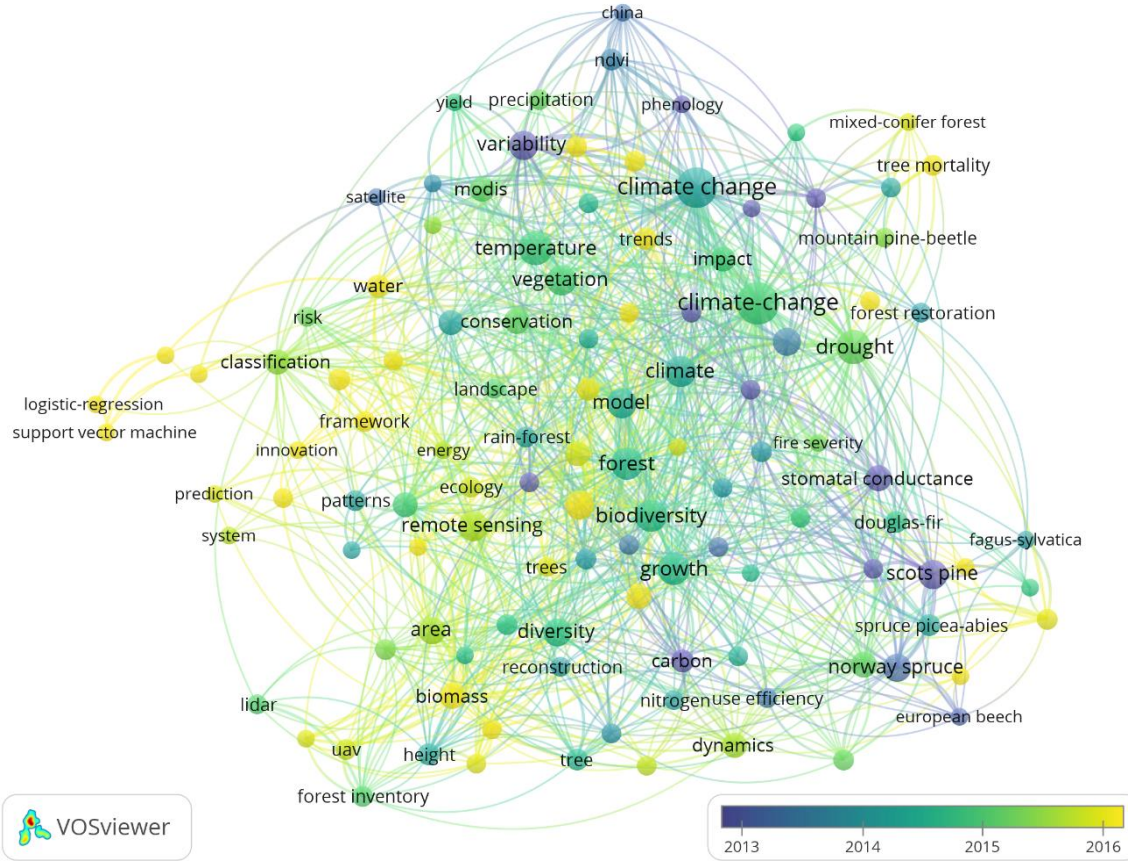

Figure 7. *VOSviewer co-occurrence overlay visualization mapping of most frequent all keywords (minimum of five occurrences) in Forestry research from 2010 to 2020*

The second cluster (Green) represented the biodiversity of forests and forest management, and included keywords as biodiversity, diversity, conservation, ecosystem services, forests, impacts, policy, ecology, framework, patterns, rain-forest, tropical forest, bioeconomy, decision-making, forest management, landscape, responses, united-states, adaptation, innovation, land-use change, species richness, etc.

The third cluster (blue) focused on remote sensing for forest growth, and included keywords as growth, remote sensing, area, biomass, boreal forest, height, tree, forest inventory, forestry, models, UAV, aboveground biomass, airborne lidar, eucalyptus, lidar, reconstruction, cover, density, inventory, etc.

The fourth cluster (yellow) represented temperature and vegetation model, and keywords included as temperature, model, vegetation, variability, modis, land-use, water, NDVI, trends, loess plateau, precipitation, time-series, carbon-dioxide, agriculture, China, leaf area index, phenology, satellite, yield, etc.

The fifth cluster (violet) focused on climate change on forest, and included keywords as climate-change, climate change, drought, tree mortality, ecological restoration, forest

http://www.aloki.hu ● ISSN 1589 1623 (Print) ● ISSN 1785 0037 (Online)
DOI: http://dx.doi.org/10.15666/aeer/1906_49414957

restoration, mountain pine-beetle, ponderosa pine forests, restoration, soil-moisture, mixed-conifer forest, spatial-patterns, etc.

The sixth cluster (shallow blue) focused on risk classification, keywords were ranked as classification, risk, logistic-regression, machine learning, prediction, random forest, support vector machine, system, etc.

The seventh cluster (orange) focused on the climate management, and keywords were climate, management, wildfire, impact, fire severity, weather, et al.

The most frequently cited articles

Citation analysis has been employed as a supplementary index to determine the impact of scientific studies, and to identify studies, researchers and the most renowned institutions dealing with the theme. Although a great many articles have been published, a relatively small number of individuals account for a large proportion of the citations within the period. The annual citations of the eight papers showed an increasing trend after year of publication (*Fig. 8*). The most citations eight papers were written by Allen et al. (2010), Lindner et al. (2010), Colwell et al. (2012), Richardson et al. (2013), Keenan et al. (2015), Rosenzweig et al. (2013), Way and Oren (2010), Sala et al. (2012). Here, the total citations for the most frequently cited articles were more than 417 times. The time dependence of a single paper is called its history. In the beginning year (zero year here), generally the articles have lower citation because of same year of publication.

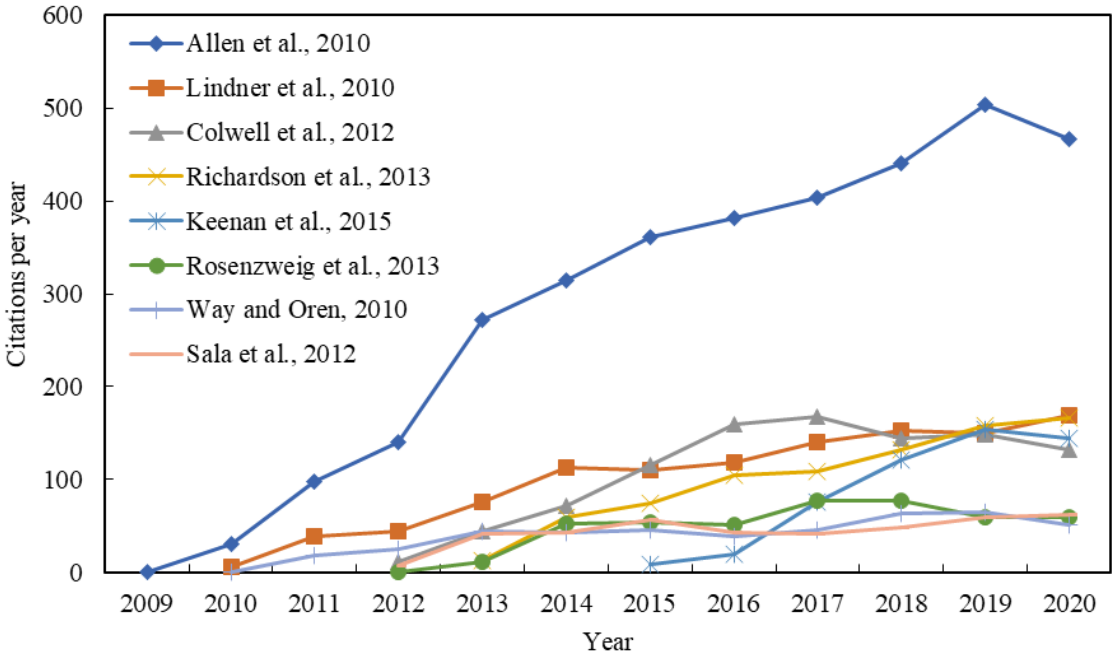

Figure 8. *Comparison of the citations per year of the most eight papers from their initial publications to May 1, 2021*

From the publication year to May 1, 2021, the average citation per year of the most citation eight papers were 296.92, 97, 102.6, 95.89, 82.29, 51.33, 37.92, and 41.7 times, respectively. From *Figure 8,* it can be found that the citation per year of the papers

http://www.aloki.hu ● ISSN 1589 1623 (Print) ● ISSN 1785 0037 (Online)
DOI: http://dx.doi.org/10.15666/aeer/1906_49414957

increased till to 2020, but the increase rate was different each year. Among the eight articles, the highest average citation per year (296.92-blue color) was observed for article of Allen et al. (2010) published in Forest Ecology and Management (*Fig. 8*).

Conclusions

This study analyzed 302 top papers in the subject category of Forestry from 2010 to 2020, which included 300 highly cited papers and 3 hot papers in the field. All papers were written in English, from 1,567 authors, 694 organizations and 74 countries or territories, published in 35 journals and book series in the field. The top five Journals were *Agricultural and Forest Meteorology, Forest Ecology and Management, Forests, Tree Physiology and Forest Policy and Economics*. The top five countries and regions were USA, Germany, Canada, France and Peoples R China. The top five organizations of US Forest Serv, Chinese Acad Sci, INRA, Swedish Univ Agr Sci and Univ Freiburg. Among the all authors, Bauhus, Juergen from Univ Freiburg of Germany gave the most 6 papers. All keywords were separated seven clusters for different research topics. This work is also useful for student identifying graduate schools and researchers selecting journals.

Acknowledgements. This research was supported by the Research Fund Program of Hubei Academic Library Committee (2019-YB-04).

REFERENCES

[1] Abad-Segura, E., Gonzalez-Zamar, M. D., Vazquez-Cano, E., Lopez-Meneses, E. (2020): Remote sensing applied in forest management to optimize ecosystem services: advances in research. – Forests 11(9): 969. https://doi.org/10.3390/f11090969.

[2] Allen, C. D., Macalady, A. K., Chenchouni, H., Bachelet, D., Mcdowell, N., Vennetier, M., Kitzberger, T., Rigling, A., Breshears, D. D., Hogg, E. H., Gonzalez, P., Fensham, R., Zhang, Z., Castro, J., Demidova, N., Lim, J. H., Allard, G., Running, S. W., Semerci, A., Cobb, N. (2010): A global overview of drought and heat-induced tree mortality reveals emerging climate change risks for forests. – Forest Ecology and Management 259(4 SI): 660-684. https://doi.org/10.1016/j.foreco.2009.09.001.

[3] Aznar-Sanchez, J. A., Belmonte-Urena, L. J., Lopez-Serrano, M. J., Velasco-Munoz, J. F. (2018): Forest ecosystem services: an analysis of worldwide research. – Forests 9(8): 453. https://doi.org/10.3390/f9080453.

[4] Bullock, R., Lawler, J. (2015): Community forestry research in Canada: a bibliometric perspective. – Forest Policy and Economics 59: 47-55. http://dx.doi.org/10.1016/j.forpol.2015.05.009.

[5] Burnard, M., Posavčević, M., Kegel, E. (2017): Examining the evolution and convergence of wood modification and environmental impact assessment in research. – iForest 10: 879-885. https://doi.org/10.3832/ifor2390-010.

[6] Chirici, G. (2012): Assessing the scientific productivity of Italian forest researchers using the Web of Science, SCOPUS and SCIMAGO databases. – iForest 5: 101-107. https://doi.org/10.3832/ifor0613-005.

[7] Chuang, K. Y., Wang, M. H., Ho, Y. S. (2011): High-impact papers presented in the subject category of water resources in the Essential Science Indicators database of the Institute for Scientific Information. – Scientometrics 87: 551-562. https://doi.org/10.1007/s11192-011-0365-2.

http://www.aloki.hu ● ISSN 1589 1623 (Print) ● ISSN 1785 0037 (Online)
DOI: http://dx.doi.org/10.15666/aeer/1906_49414957

[8] Clarivate (2021): Essential Science Indicators Help: About Essential Science Indicators. – http://esi.help.clarivate.com/Content/home.htm.
[9] Clarivate (2021): InCites journal citation reports. – https://jcr.clarivate.com/JCRLandingPageAction.action.
[10] Colwell, R. K., Chao, A., Gotelli, N. J., Lin, S. Y., Mao, C. X., Chazdon, R. L., Longino, J. T. (2012): Models and estimators linking individual-based and sample-based rarefaction, extrapolation and comparison of assemblages. – Journal of Plant Ecology 5(1): SI 3-21. https://doi.org/10.1093/jpe/rtr044.
[11] Duan, G. Z., Bai, Y., Ye, D. M., Lin, T., Peng, P., Liu, M., Bai, S. L. (2020): Bibliometric evaluation of the status of *Picea* research and research hotspots: comparison of China to other countries. – Journal of Forestry Research 31(4): 1103-1114. https://doi.org/10.1007/s11676-018-0861-9.
[12] Elango, B., Ho, Y. S. (2018): Top-cited articles in the field of tribology: a bibliometric analysis. – COLLNET Journal of Scientometrics and Information Management 12(2): 289-307. https://doi.org/10.1080/09737766.2018.1529125.
[13] Guerra, A., Reis, L. K., Borges, F. L. G., Ojeda, P. T. A., Pineda, D. A. M., Miranda, C. O., Maidana, D. P. F. D., Dos, S. T., Shibuya, P. S., Marques, M. C. M., Laurance, S. G. W., Garcia, L. C. (2020): Ecological restoration in Brazilian biomes: identifying advances and gaps. – Forest Ecology and Management 458: 117802. https://doi.org/10.1016/j.foreco.2019.117802.
[14] Hirsch, J. E. (2005): An index to quantify an individual's scientific research output. – Proc. Natl. Acad. Sci. U.S.A. 102(46): 16569-16572. https://doi.org/10.1073/pnas.0507655102.
[15] Ho, H. C., Ho, Y. S. (2015): Publications in dance field in Arts and Humanities Citation Index: a bibliometric analysis. – Scientometrics 105: 1031-1040. https://doi.org/10.1007/s11192-015-1716-1.
[16] Ho, Y. S. (2014): A bibliometric analysis of highly cited articles in materials science. – Current Science 107: 1565-1572.
[17] Ho, Y. S. (2021): A bibliometric analysis of highly cited publications in Web of Science category of emergency medicine. – Signa Vitae 17(1): 11-19. https://doi.org/10.22514/sv.2020.16.0091.
[18] Ivanovic, L., Ho, Y. S. (2019): Highly cited articles in the Education and Educational Research category in the Social Science Citation Index: a bibliometric analysis. – Educational Review 71(3): 277-286. https://doi.org/ 10.1080/00131911.2017.1415297.
[19] Keenan, R. J., Reams, G. A., Achard, F., De Freitas, J. V., Grainger, A., Lindquist, E. (2015): Dynamics of global forest area: results from the FAO Global Forest Resources Assessment 2015. – Forest Ecology and Management 352: 9-20. https://doi.org/10.1016/j.foreco.2015.06.014.
[20] Khan, M. A., Ho, Y. S. (2012): Top-cited articles in environmental sciences: merits and demerits of citation analysis. – Science of the Total Environment 431: 122-127. https://doi.org/10.1016/j.scitotenv.2012.05.035.
[21] Khan, A., Khan, D., Akbar, F. (2020): Bibliometric analysis of publications on research into cotton leaf curl disease. – Discoveries 8(2): e109. https://doi.org/10.15190/d.2020.6.
[22] Kolle, S. R., Shankarappa, T. H., Ho, Y. S. (2017): Highly cited articles in Science Citation Index Expanded - subject category of horticulture: a bibliometric analysis. – Erwerbs-Obstbau 59: 133-145. https://doi.org/10.1007/s10341-016-0308-4.
[23] Li, Y. Z., Xu, G., Long, X., Ho, Y. S. (2019): A bibliometric analysis of classic publications in web of science category of orthopedics. – Journal of Orthopaedic Surgery and Research 14: 227. https://doi.org/10.1186/s13018-019-1247-1.
[24] Liao, H. C., Tang, M., Li, Z. M., Lev, B. (2019): Bibliometric analysis for highly cited papers in operations research and management science from 2008 to 2017 based on Essential Science Indicators. – Omega-International Journal of Management Science 88: 223-236. https://doi.org/10.1016/j.omega.2018.11.005.

http://www.aloki.hu ● ISSN 1589 1623 (Print) ● ISSN 1785 0037 (Online)
DOI: http://dx.doi.org/10.15666/aeer/1906_49414957

[25] Lindner, M., Maroschek, M., Netherer, S., Kremer, A., Barbati, A., Garcia-Gonzalo, J., Seidl, R., Delzon, S., Corona, P., Kolstrom, M., Lexer, M. J., Marchetti, M. (2010): Climate change impacts, adaptive capacity, and vulnerability of European forest ecosystems. – Forest Ecology and Management 259(4): 698-709. https://doi.org/10.1016/j.foreco.2009.09.023.

[26] Ma, Q., Li, Y. D., Zhang, Y. (2020): Informetric analysis of highly cited papers in environmental sciences based on essential science indicators. – International Journal of Environmental Research and Public Health 17(11): 3781. https://doi.org/10.3390/ijerph17113781.

[27] Martínez-Santiago, S. Y., Alvarado-Segura, A. A., Zamudio-Sánchez, F. J., Cristóbal-Acevedo, D. (2017): Spatio-temporal analysis of forest modeling in Mexico. – Revista Chapingo Serie Ciencias Forestales y del Ambiente 23(1): 5-22. https://doi.org/10.5154/r.rchscfa.2016.01.003.

[28] Ordoñez, M. C., Galicia, L. (2020): Bibliometric analysis of models for temperate forest management: a global perspective on sustainable forest management tools. – Revista Chapingo Serie Ciencias Forestales y del Ambiente 26(3): 357-372. http://dx.doi.org/10.5154/r.rchscfa.2019.11.079.

[29] Polinko, A. D., Coupland, K. (2021): Paradigm shifts in forestry and forest research: a bibliometric analysis. – Canadian Journal of Forest Research 51(2): 154-162. https://doi.org/10.1139/cjfr-2020-0311.

[30] Reyes-Gonzalez, L., Gonzalez-Brambila, C. N., Veloso, F. (2016): Using coauthorship and citation analysis to identify research groups: a new way to assess performance. – Scientometrics 108: 1171-1191. https://doi.org/10.1007/s11192-016-2029-8.

[31] Richardson, A. D., Keenan, T. F., Migliavacca, M., Ryu, Y., Sonnentag, O., Toomey, M. (2013): Climate change, phenology, and phenological control of vegetation feedbacks to the climate system. – Agricultural and Forest Meteorology 169: 156-173. https://doi.org/10.1016/j.agrformet.2012.09.012.

[32] Romanelli, J. P., Boschi, R. S. (2019): The legacy of elinor ostrom on common forests research assessed through bibliometric analysis. – CERNE 25(4): 332-346. https://doi.org/10.1590/01047760201925042658.

[33] Rosenzweig, C., Jones, J. W., Hatfield, J. L., Ruane, A. C., Boote, K. J., Thorburn, P., Antle, J. M., Nelson, G. C., Porter, C., Janssen, S., Asseng, S., Basso, B., Ewert, F., Wallach, D., Baigorria, G., Winter, J. M. (2013): The agricultural model intercomparison and improvement project (AgMIP): protocols and pilot studies. – Agricultural and Forest Meteorology 170: 166-182. https://doi.org/10.1016/j.agrformet.2012.09.011.

[34] Sala, A., Woodruff, D. R., Meinzer, F. C. (2012): Carbon dynamics in trees: feast or famine? – Tree Physiology 32(6): 764-775. https://doi.org/10.1093/treephys/tpr143.

[35] Stopar, K., Mackiewicz-Talarczyk, M., Bartol, T. (2021): Cotton fiber in web of science and scopus: mapping and visualization of research topics and publishing patterns. – Journal of Natural Fibers 18(4): 547-558. https://doi.org/10.1080/15440478.2019.1636742.

[36] Sun, J., Yuan, B. Z. (2020a): Mapping of the world rice research: a bibliometric analysis of top papers during 2008–2018. – Annals of Library and Information Studies 67(1): 56-66.

[37] Sun, J., Yuan, B. Z. (2020b): Bibliometric mapping of top papers in Library and Information Science based on the Essential Science Indicators Database. – Malaysian Journal of Library and Information Science 25(2): 61-76. https://doi.org/10.22452/mjlis.vol25no2.4.

[38] Sun, J., Yuan, B. Z. (2020c): Mapping of top papers in the subject category of Water Resources based on the Essential Science Indicators. – Annals of Library and Information Studies 67(2): 90-102.

http://www.aloki.hu ● ISSN 1589 1623 (Print) ● ISSN 1785 0037 (Online)
DOI: http://dx.doi.org/10.15666/aeer/1906_49414957

[39] Sun, J., Yuan, B. Z. (2021): Trend and research status of Agronomy based on the Essential Science Indicators during 2009–2019. – Agronomy Journal 113(2): 2184-2194. https://doi.org/10.1002/agj220628.20628.
[40] Tang, M., Liao, H. C., Wan, Z. J., Herrera-Viedma, E., Rosen, M. A. (2018): Ten years of Sustainability (2009 to 2018): a bibliometric overview. – Sustainability 10(5): 1655. https://doi.org/10.3390/su10051655.
[41] Uribe-Toril, J., Ruiz-Real, J. L., Haba-Osca, J., Valenciano, J. D. (2019): Forests' first decade: a bibliometric analysis overview. – Forests 10(1): 72. https://doi.org/10.3390/f10010072.
[42] Van Eck, N. J., Waltman, L. (2010): Software survey: VOSviewer, a computer program for bibliometric mapping. – Scientometrics 84: 523-538. https://doi.org/10.1007/s11192-009-0146-3.
[43] Way, D. A., Oren, R. (2010): Differential responses to changes in growth temperature between trees from different functional groups and biomes: a review and synthesis of data. – Tree Physiology 30(6): 669-688. https://doi.org/10.1093/treephys/tpq015.
[44] White-Gibson, A., O'Neill, B., Cooper, D., Leonard, M., O'daly, B. (2019): Levels of evidence in pelvic trauma: a bibliometric analysis of the top 50 cited papers. – Irish Journal of Medical Science 188: 155-159. https://doi.org/10.1007/s11845-018-1818-x.
[45] Xing, Y., Brimblecombe, P. (2020): Trees and parks as "the lungs of cities". – Urban Forestry and Urban Greening 48: 126552. https://doi.org/10.1016/j.ufug.2019.126552.
[46] Yang, D. H., Wang, Y., Yu, T., Liu, X. Y. (2020): Macro-level collaboration network analysis and visualization with Essential Science Indicators: a case of social sciences. – Malaysian Journal of Library and Information Science 25(1): 121-138. https://doi.org/10.22452/mjlis.vol25no1.7.
[47] Yeung, A. W. K., Leung, W. K. (2018): Citation network analysis of dental implant literature from 2007 to 2016. – International Journal of Oral and Maxillofacial Implants 33(6): 1240-1246. https://doi.org/10.11607/jomi.6727.
[48] Yuan, B. Z., Sun, J. (2019): Bibliometric and mapping of top papers in the subject category of green and sustainable science and technology based on ESI. – COLLNET Journal of Scientometrics and Information Management 13(2): 269-289. https://doi.org/10.1080/09737766.2020.1716643.
[49] Yuan, B. Z., Sun, J. (2020a): Bibliometric analysis of research on the maize based on top papers during 2009–2019. – COLLNET Journal of Scientometrics and Information Management 14(1): 75-92. https://doi.org/10.1080/09737766.2020.1787110.
[50] Yuan, B. Z., Sun, J. (2020b): Mapping the scientific research on maize or corn: a bibliometric analysis of top papers during 2008–2018. – Maydica 65(2): M17.
[51] Zhang, N., Wan, S. S., Wang, P. L., Zhang, P., Wu, Q. (2018): A bibliometric analysis of highly cited papers in the field of Economics and Business based on the Essential Science Indicators database. – Scientometrics 116: 1039-1053. https://doi.org/10.1007/s11192-018-2786-7.

http://www.aloki.hu ● ISSN 1589 1623 (Print) ● ISSN 1785 0037 (Online)
DOI: http://dx.doi.org/10.15666/aeer/1906_49414957

MEASUREMENT OF CABBAGE (*BRASSICA OLERACEA* L.) ROOT TREATED WITH BENEFICIAL MICROBIAL CONSORTIA THROUGH COMPUTER VISION TECHNOLOGY

COBOS-TORRES, J. C.[1*] – ALVAREZ-VERA, M.[2] – FLORES-VASQUEZ, C.[3]

[1]*Postgraduate Leadership, Electrical Engineering Career, Research Group in Visible Radiation and Prototyping GIRVyP and Research Group in Embedded Systems and Artificial Vision in Architectural, Agricultural, Environmental and Automatic Sciences (SEVA4CA), Catholic University of Cuenca, Cuenca, Ecuador*

[2]*Postgraduate Leadership, Environmental Engineering Career, Research Group in Embedded Systems and Artificial Vision in Architectural, Agricultural, Environmental and Automatic Sciences (SEVA4CA), Catholic University of Cuenca, Cuenca, Ecuador*

[3]*Electrical Engineering Career, Research Group in Visible Radiation and Prototyping (GIRVyP), Catholic University of Cuenca, Cuenca, Ecuador*

**Corresponding author*
e-mail: juan.cobos@ucacue.edu.ec; phone: +593-96-263-5040

(Received 8th Jun 2021; accepted 4th Sep 2021)

Abstract. This study aimed to measure the root length and surface area of cabbage plants *(Brassica oleracea* L.*)* by using computer vision technology (RGB Camera). This investigation was conducted by a transdisciplinary team made up of researchers from the agronomy, environmental, electronic, and computer vision fields. Researchers from the first two fields were responsible for obtaining biofertilizers by applying beneficial microbial consortia to household organic waste; in addition, to planting cabbage seeds with different amounts of biofertilizer. The last two fields were responsible for developing a system that would measure root length and root surface area by using image analysis. As a result, plants enriched with 20% and 25% of biofertilizers showed better performance in root length. In comparison, these plants, compared to the control group had 63% more surface area root and were 61% longer root. These results show that biofertilizers should be applied in adequate amounts to obtain higher root length and surface area. This is important since plant roots absorb water and nutrients for plant development and these functions depend on the length of roots and fine roots. In addition, it should be emphasized that conventional root measurement techniques are time-consuming and provide inaccurate data. This research presents a methodology where computer vision technology is applied to optimize the measurement process, providing accurate data in less time.
Keywords: *biofertilizers, root length, root surface area, beneficial soil microorganisms, camera*

Introduction

Due to global population growth, efforts to increase food production are imperative in order to meet constant food demand. Though the roots of plants – which absorb water and soil nutrients needed for plant development and crop performance – play a fundamental role in agricultural production, they are sometimes undervalued. Although even today there are different criteria about roots measurement, Novoplansky (2019) affirms that until recently the study of roots has been neglected, despite its importance for plant life.

Roots secrete metabolites into the rhizosphere (the soil zone around the roots, which is also known to reserve microorganisms (Gouda et al., 2018) that fulfill primary functions in plant nutrition) intervening in several processes (Vives-Peris et al., 2019).

http://www.aloki.hu ● ISSN 1589 1623 (Print) ● ISSN 1785 0037 (Online)
DOI: http://dx.doi.org/10.15666/aeer/1906_49594975

Chemical fertilizers are used to improve plant development and performance; however, their permanent use represents an important economic outlay, and their indiscriminate use affects the soil and the environment.

To replace chemical fertilizers, one of the greatest gifts that nature offers are biofertilizers; they are composed of microorganisms that benefit the supply of nutritional elements to plants, therefore, contributing to improve their development and regulate their physiology (Kumar et al., 2018). Microbial biofertilizers are considered an alternative to chemical fertilizers, due to their high potential to enhance agricultural production (Mahanty et al., 2017) and preserve crop productivity, by efficiently using fertilizers without affecting the environment, which is key to agricultural systems (Paungfoo-Lonhienne et al., 2019) and sustainable development

The application of bioinoculants, with fertilizing properties, to soil has attracted great interest in recent times due to the environmental and economic advantages they provide and also due to their impact on the rhizosphere. Biofertilizers arise as potentially eco-friendly products that benefit agricultural crop production. They are applied in seeds or to the soil, improving nutrient availability, thus enhancing the growth and yield of cultivated plants (Bisht et al., 2016).

Automation and computer vision technology are viable options to be used in agriculture for studying the phenology of plants and crop yield precisely, as well as for time and resource optimization. Root size measurements have varied over the last decades, each quantification method has evolved in measurement reliabilities and the variation between results (Judd et al., 2015). Basic methods as drawing roots (Weaver et al., 1922), window (Böhm, 1979) trench (Schuurman and Goedewaagen, 1965), and currently in the last four decades using cameras (Ottman and Timm, 1984; Villordon et al., 2012; Wang et al., 2019) have made it possible to facilitate and improve the quantification of roots. Quantification using cameras, despite reducing the time required for measurement and avoiding human subjectivism, still takes considerable time when it comes to quantifying studies with repetitions. It is necessary to automate the process so that several measurements can be executed serially, reducing the measurements time. In addition, it is important to reduce costs by using Opensource software and low-cost hardware.

Cabbage (*Brassica oleracea* L.), an important element in people's diet, is part of a wide variety of vegetable plants that are cultivated locally. However, there is not enough research that focuses on the study of cabbage roots. Traditional methods applied have provided inaccurate data due to manual registration systems. The accuracy in measuring the characteristics of the root system is important for plant phenotyping (Van Dusschoten et al., 2016). Roots are responsible for water and nutrient absorption: processes required for photosynthesis and agricultural production (Tracy et al., 2020).

By means of technology, agriculture can be enhanced through automation for small field farming, allowing to achieve high precision, efficiency, and low costs (Tian et al., 2020). In agriculture, artificial intelligence becomes a key technique for solving different problems (Bannerjee et al., 2018); it is considered to be a feasible solution to increase food production for a constantly growing population (Zha, 2020). It is possible to improve the growth and performance of plants by mixing biofertilizers. Therefore, it is important for farmers to know the synergistic effects of these bioinoculants (Agarwal et al., 2018), relying on modern measurement and quantification techniques.

This research aimed to determine the length of roots of cabbage plants, by means of digital cameras, in order to know the effect of biofertilizers on root growth.

http://www.aloki.hu ● ISSN 1589 1623 (Print) ● ISSN 1785 0037 (Online)
DOI: http://dx.doi.org/10.15666/aeer/1906_49594975

Materials and methods

This research was carried out in four stages: (i) producing biofertilizers with household organic waste by applying beneficial microbial consortia, (ii) planting cabbage seeds with different amounts of fertilizer; iii) developing a system for measuring root length and surface area by means of images and iv) measuring root of cabbage plants.

In the first stage, beneficial microorganisms were obtained from the phyllosphere of the lemon verbena plant (*Aloysia citrodora*). All samples were obtained from the aerial region of the plant. Beneficial microbial consortia were obtained from the parts of the plants collected, through a fermentation process. At the same time, household organic food waste was collected, that is, vegetable waste. Organic waste was composted by applying beneficial microorganisms. Likewise, vermicompost of organic waste was carried out by applying beneficial microorganisms and using Red Californian Earthworms. Polystyrene boxes of 0.40 m × 0.30 m × 0.32 m were used in both processes. In the particular process of vermicomposting, 1 kg of earthworms was added to organic waste and vermicompost was obtained after 90 days. In addition, beneficial microbial consortia were applied, once a week, during the process. In contrast, composting was carried out under aerobic conditions, controlling humidity and temperature, for a period of 90 days as well. Beneficial microbial consortia were applied once every 15 days to moisten the substrate. The resulting material from both processes was black and smelled like petrichor. Finally, 5 kg of compost and 5 kg of vermicompost were mixed in a thoroughly cleaned container, in equal proportions, obtaining the desired biofertilizer. *Figure 1* shows the entire process.

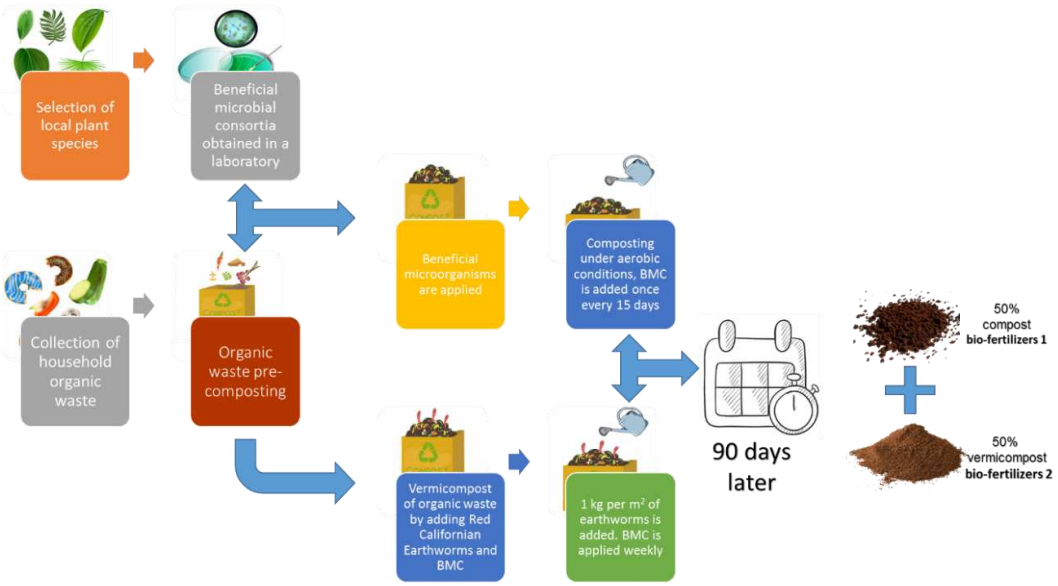

Figure 1. *Process for biofertilizer production*

In the second stage, cabbage seeds (this plant type was selected because it is a traditional crop in our environment) were planted in seedbeds made with cups. In each cup, 100 g of commercial peat (material used for rooting) and different concentrations of biofertilizer were added. These cups were holes in the bottom to ensure adequate drainage. Biofertilizer was not applied to one treatment for control purposes. A

http://www.aloki.hu ● ISSN 1589 1623 (Print) ● ISSN 1785 0037 (Online)
DOI: http://dx.doi.org/10.15666/aeer/1906_49594975

randomized complete block design was applied. Seven treatments and four repetitions were carried out. *Table 1* shows the different treatments and the percentage of biofertilizer added.

Table 1. *Treatment details*

Treatment	Biofertilizer percentage %
T1	0
T2	5
T3	10
T4	15
T5	20
T6	25
T7	30

The seeds were sown in the city of Gualaceo, Ecuador (2°53'10.4"S 78°46'45.2"W). Planting schematization and climatic factors can be seen in *Figure 2*.

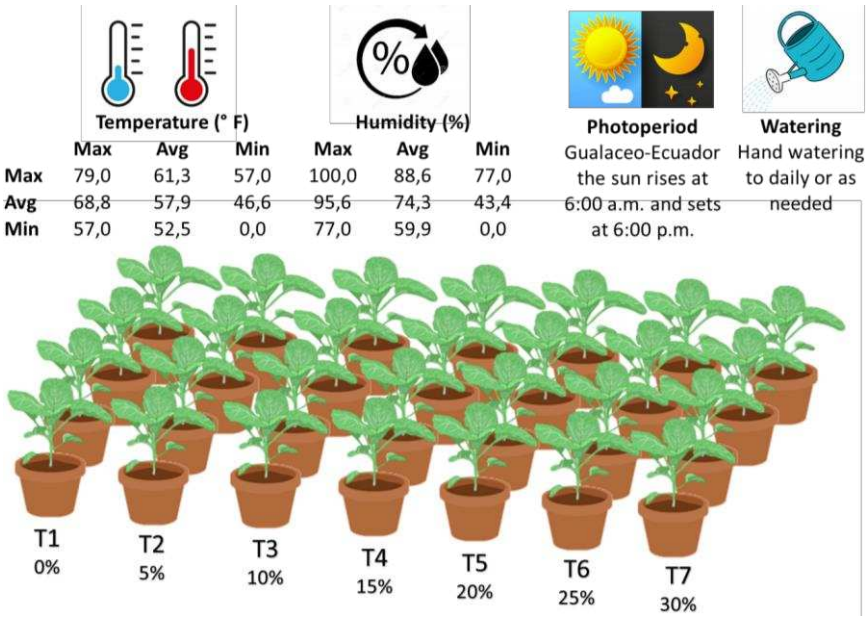

Figure 2. *Treatments performed with different amounts of biofertilizer*

For developing the measurement system, the third stage was divided into three sub-stages: (a) defining a methodology for taking photographs of cabbage roots; (b) developing an aberration correction algorithm; (c) developing root length and surface area measurement algorithm using digital cameras.

a) The system was composed of a Samsung Galaxy S7 Edge cellphone with a digital camera, with a 12 MP (f1.7) resolution and optical image stabilization. The phone was placed over a desk using a cellphone holder, aiming to position the phone in such a way that the image would be framed within a black construction paper, in order to reduce perspective distortion. This system can be seen in *Figure 3*.

http://www.aloki.hu ● ISSN 1589 1623 (Print) ● ISSN 1785 0037 (Online)
DOI: http://dx.doi.org/10.15666/aeer/1906_49594975

In this stage, the roots were cleaned and exposed. The plants were grown in disposable plastic cups, which allowed for their easy extraction. The plants – and soil– were soaked in a bucket filled with water for one day; any traces of soil in fine roots were washed. Once the fine roots were clean, they were placed over black construction paper for measuring.

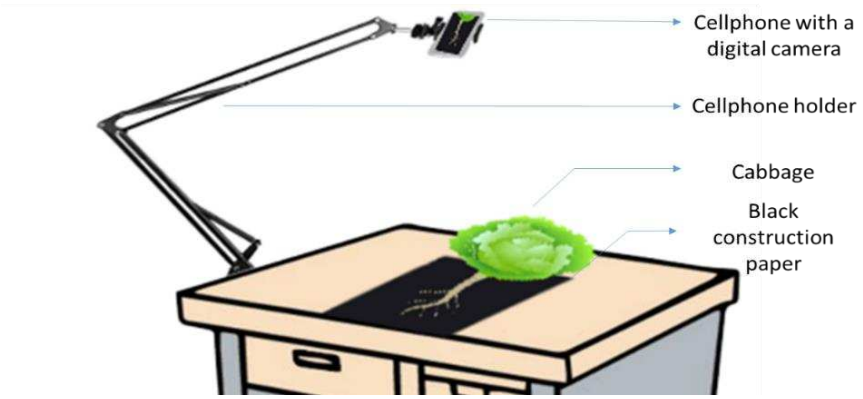

Figure 3. *Methodology outline for photographing*

b) The development of the algorithm for cabbage root length and surface area calculation was divided into five stages: first, obtaining the images in an RGB format by means of a camera; second, correcting perspective distortion; third, selecting pixels that correspond to the roots, by means of thresholding; fourth, counting the number of pixels of the region of interest; and fifth, calibrating the pixel/cm ratio to determine the perimeter and surface area. The outline proposed can be observed in *Figure 4*.

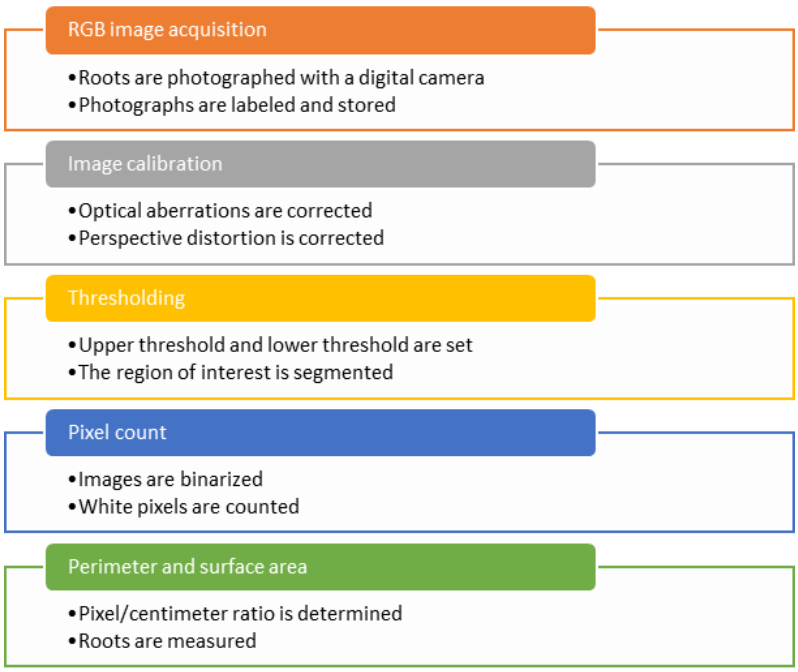

Figure 4. *Schematization of the development of an algorithm used for cabbage root size quantification*

http://www.aloki.hu ● ISSN 1589 1623 (Print) ● ISSN 1785 0037 (Online)
DOI: http://dx.doi.org/10.15666/aeer/1906_49594975

c) For this process, a ratio that could quantify the pixels per a given metric, within the image, was defined. This is known as pixels per metric ratio. It should be noted that first, the imaging (knowledge of its intrinsic and extrinsic parameters) and distortion correction systems were pre-calibrated. After pre-calibration, calibration was carried out using a reference object: size A4, black, construction paper. This reference object had all the required attributes: its dimensions (width and length) were known in centimeters and it could be easily identified by its shape.

For the statistical analysis, the graphical method proposed by (Tukey, 1977) called box-and-whisker graph will be used. This shows a statistical summary of median, quartiles, range, and possibly extreme values. Additionally, the variation proposed by (Altman, 1990) (McGill et al., 1978) will be calculated including confidence intervals for the median is provided by means of notches surrounding the medians. Finally, through moving average trend lines of consecutive observations, fluctuations in the data can be smoothed to see the pattern or trend more clearly.

Results

As previously detailed in the materials and methods section, this research was developed in four stages, which were carried out to successfully achieve the proposed objective. The results of each stage are detailed in the following subsections.

Biofertilizers production

The lemon verbena plant (*Aloysia citrodora*), cultivated in our environment, was used to obtain beneficial microbial consortia. The concentration of microorganisms in colony-forming units per milliliter of solution (CFU/mL), is presented in *Table 2*.

Table 2. *Composition of beneficial microbial consortia*

N°	Microorganism	CFU/mL
1	*Acinetobacter sp.*	0.34298
2	*Aeromonas sp.*	129.475
3	*Alcaligenes sp.*	28.472
4	*Bacillus cereus*	202.941
5	*Bacillus subtilis*	121.231
6	*Candida sp.*	0.98246
7	*Clostridium sp.*	190.928
8	*Lactobacillus spp.*	0.39875
9	*Listeria monocytogenes*	0.45922
10	*Micrococcus sp.*	213.476
11	*Pseudomonas aeruginosa*	0.6439
12	*Pseudomonas fluorescens*	0.27424
13	*Pseudomonas putida*	162.572
14	*Saccharomyces cerevisiae*	274.925
15	*Salmonella sp.*	0.29289
16	*Yarrowia lipolytica*	123.827

http://www.aloki.hu ● ISSN 1589 1623 (Print) ● ISSN 1785 0037 (Online)
DOI: http://dx.doi.org/10.15666/aeer/1906_49594975

The process began by cutting off the leaves of the plant. This can be seen in *Figure 5a*. The leaves were taken to the laboratory of the Postgraduate Leadership of the Catholic University of Cuenca to obtain beneficial microbial consortia by anaerobic fermentation. The final product can be seen in *Figure 5b*. At the same time, researchers collected organic waste from their homes. By a visual inspection, it was determined that most of the waste consisted of food waste. Once 20 kg of organic waste were collected, compost was prepared by inoculating it with previously obtained beneficial microorganisms. This can be seen in *Figure 5c*. Similarly, in a separate box, vermicompost was made by applying 1 kg of Red Californian Earthworms (*Eisenia foetida*) to the waste and inoculating it with beneficial microorganisms. As already detailed in the previous section, both composts were prepared in polystyrene boxes of 0.40 m × 0.30 m × 0.32 m. This can be seen in *Figure 5d* and *e*. Both processes were performed in ninety days. The composting process was checked and inoculated every 8 days with a liquid substrate enriched with beneficial microorganisms, which helped the process and kept the substrate moist. In contrast, the vermicomposting process was checked and inoculated every 7 days with the same liquid substrate, enriched with beneficial microorganisms. This can be seen in *Figure 5f* and *g*. The resulting material was black, smelled like petrichor, and met the stability characteristics. Finally, a biofertilizer was produced by mixing compost and vermicompost, in a 5 kg of compost and 5 kg of vermicompost ratio. *Figure 5h* shows the final result.

Seed planting in different treatments

Cabbage seeds were planted in seedbeds made with disposable plastic cups. Such containers were selected to facilitate plant removal. Each cup contained 100 g of commercial soil with different concentrations of biofertilizer (see *Table 1*). Plants in their seedbeds can be seen in *Figure 6*.

(a)

(b)

(c)

(d)

http://www.aloki.hu ● ISSN 1589 1623 (Print) ● ISSN 1785 0037 (Online)
DOI: http://dx.doi.org/10.15666/aeer/1906_49594975

(e) (f)

(g) (h)

Figure 5. *Stages in biofertilizer production: (a) Selection of phyllosphere microorganisms; (b) Liquid solution with beneficial microorganisms; (c) Organic waste in the composting process; (d) Vermicomposting with earthworms; (e) Compost under aerobic conditions; (f) Vermicompost; (g) Inoculation with beneficial microorganisms; (h) Biofertilizer*

(a) (b)

Figure 6. *Cabbage seedbeds: (a) One week after planting; (b) Four weeks after planting*

Measurement system

In this stage, the plants were removed from their seedbeds and soaked in a bucket filled with water, for one day. Once the soil was loose, any remaining soil was washed, cleaning the roots completely, leaving white fine roots exposed. Next, photographs were

http://www.aloki.hu ● ISSN 1589 1623 (Print) ● ISSN 1785 0037 (Online)
DOI: http://dx.doi.org/10.15666/aeer/1906_49594975

taken; fitting the image within the black construction paper, providing high color contrast. This was useful for the segmentation of the photographed roots performed in the following stage. This can be seen in *Figure 7*.

(a) (b)

Figure 7. *Preparation and cleaning of cabbage roots: (a) Plant removed from its seedbed; (b) Plant exposing its roots after being washed*

Root measuring

The development of the algorithm for calculating the root length and surface area of cabbage plants was carried out by using the Python programming language and the OpenCV library. The first step was analyzing the RGB images, which were previously labeled according to the treatment. Once the analysis was completed, perspective distortion was corrected and the thresholding technique was applied to select the pixels that corresponded to the roots. The stem and leaves were removed from the image for they had white shades. This task was easily performed by means of a visual assessment that allowed to identify the parts. This can be seen in *Figure 8*.

(a) (b)

Figure 8. *Image processing: (a) Perspective distortion correction; (b) Root selection by thresholding*

http://www.aloki.hu ● ISSN 1589 1623 (Print) ● ISSN 1785 0037 (Online)
DOI: http://dx.doi.org/10.15666/aeer/1906_49594975

The pixels of the selection are quantified. The extract is the total area of the background image and the exact root surface area has to be calculated. With a scale of 136.678 pixels/cm and a root pixel count of 437,878 pixels, the root surface area is 23.439 cm^2.

Measurement results can be analyzed by multiple comparisons, which would allow to visualize differences between subgroups of the percentage of added biofertilizer and measurements obtained. This can be seen in *Figure 9a* and *b*. Likewise, this information is presented in *Table 3*.

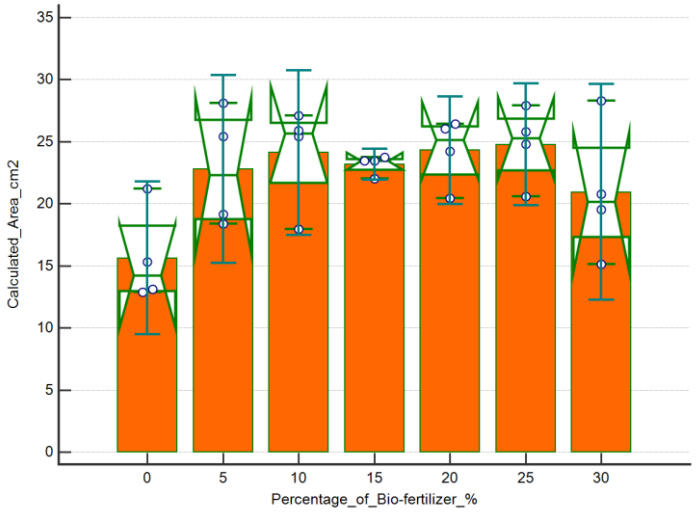

(a)

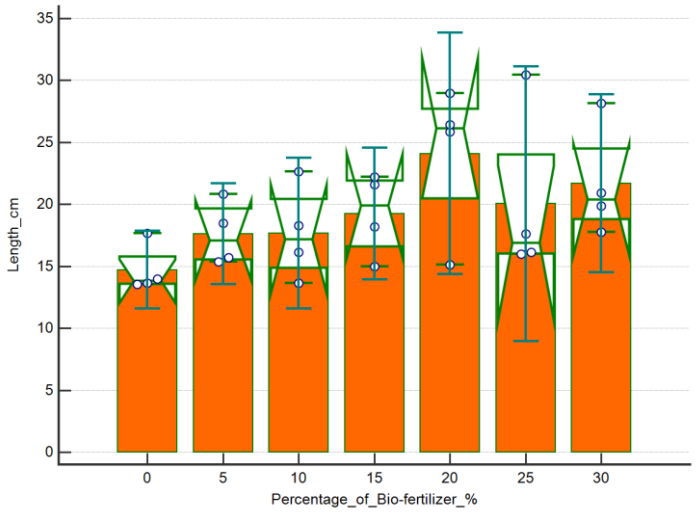

(b)

Figure 9. *Root length and surface area comparison between plant samples with different contents of biofertilizer using notched box plots: (a) Surface area and (b) Perimeter*

Finally, an analysis is presented in *Figure 10* showing consecutive observations of both measured variables. A moving average trendline has been traced, for each variable, to smooth out the fluctuations in data, allowing for the pattern or trend to be observed more clearly.

http://www.aloki.hu ● ISSN 1589 1623 (Print) ● ISSN 1785 0037 (Online)
DOI: http://dx.doi.org/10.15666/aeer/1906_49594975

Table 3. *Treatment measurements*

Treatment	n	Surface area cm^2		Length cm	
		Mean	Median	Mean	Median
(T1) 0%	4	15.62	14.22	14.71	13.82
(T2) 5%	4	22.78	22.31	17.60	17.11
(T3) 10%	4	24.11	25.68	17.67	17.21
(T4) 15%	4	23.18	23.46	19.25	19.91
(T5) 20%	4	24.30	25.16	24.10	26.15
(T6) 25%	4	24.78	25.29	20.04	16.88
(T7) 30%	4	20.94	20.16	21.67	20.39

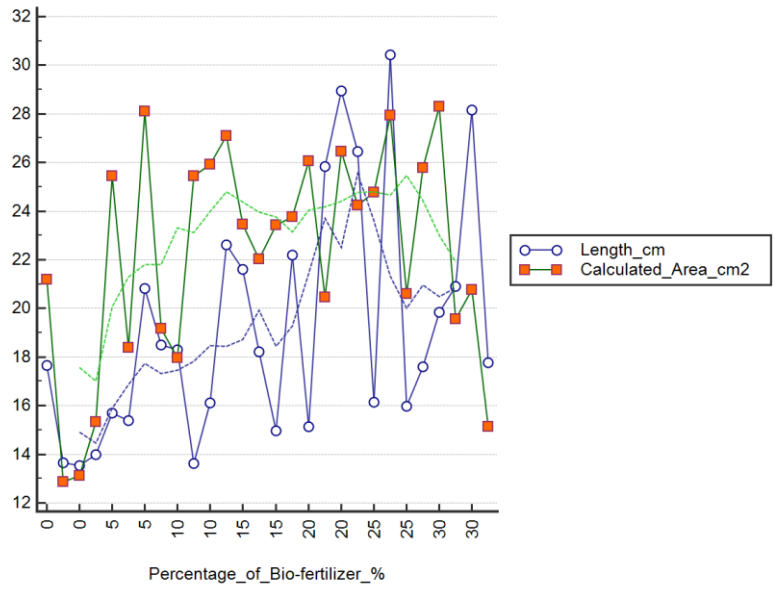

Figure 10. *Root length and surface area comparison between plant samples with different contents of biofertilizer using a multiple trendline graph*

Measurements comparison

In order to verify the measurements using the proposed method, these measurements were compared with the measurements made using the imageJ program (image processing program designed for scientific images). Image processing time was longer with this software but it allowed us to observe the accuracy of our measurements. For this, the Bland-Altman method quantifies the mean difference between both methods, see *Figure 11*.

The differences between estimates both methods were plotted against the averages of both systems for length and area, *Figure 11a* and *b,* respectively. Means are represented by dotted lines; 95% limits of agreement (±1.96 SD) are represented by dashed lines on the plots. Specifically, the mean biases were 0.001 cm with 95% limits of agreement -0.015 to 0.0017 cm for the length and 0.001 cm with 95% limits of agreement -0.013 to 0.015 cm for the area. The standard deviation of the residuals is 0.008 cm for length and 0.007 cm for area.

http://www.aloki.hu ● ISSN 1589 1623 (Print) ● ISSN 1785 0037 (Online)
DOI: http://dx.doi.org/10.15666/aeer/1906_49594975

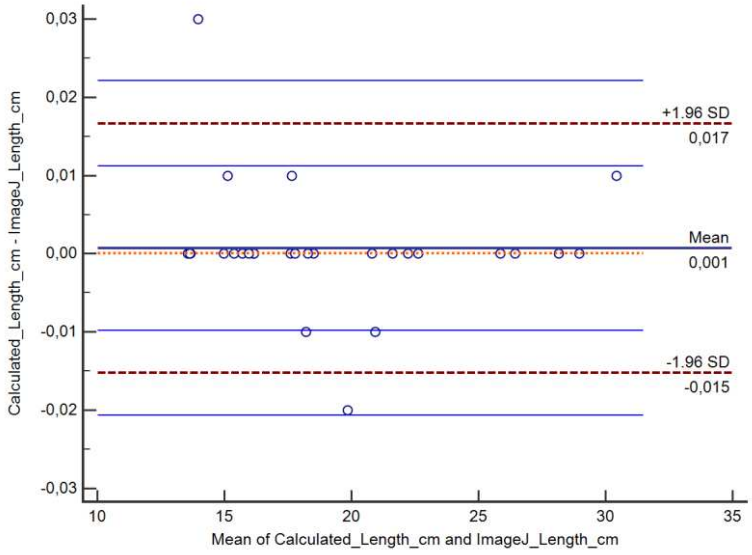

(a)

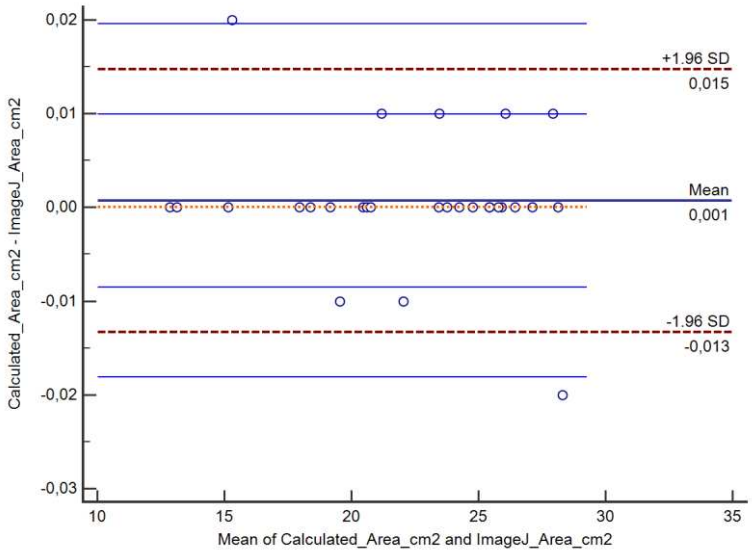

(b)

Figure 11. *Bland-Altman plot showing the level of agreement between proposed method and imageJ Software: (a) length measurement and, (b) area measurement*

Discussion

The application of biofertilizers benefits the root growth of crops. Several studies have previously determined benefits in the morphological characteristics of plants by using conventional measuring methods such as counting the number of leaves, measuring stem length and diameter, and measuring root length manually; thus, requiring a considerable amount of work and time, and yielding inaccurate results. This study seeks to provide a different approach: establishing a framework for measuring root length and surface area by means of technology. Applying and improving the proposal for the semi-automatic quantification of root growth of seedlings growing directly in agar plates (Betegón-Putze et al., 2018) as a reference for performing measurements outside a laboratory. This research aimed to quantify the root growth of

http://www.aloki.hu ● ISSN 1589 1623 (Print) ● ISSN 1785 0037 (Online)
DOI: http://dx.doi.org/10.15666/aeer/1906_49594975

seedlings, yielding accurate and rapid results on root development of plants that have been rooted in substrates with different contents of biofertilizer. Thus, the perimeter, surface area, and length of fine roots were obtained by means of image analysis.

Today, biofertilizers are used by farmers to enhance nitrogen fixation capacity. Several studies highlight that vermicompost can improve soil fertility physically, chemically, and biologically (Lim et al., 2014; Chatterjee and Debnath, 2020). It is also stated that vermicompost benefits crop growth and yield (Chatterjee R., Debnath A., 2020), increasing soil quality and plant performance (Zuo et al., 2018). Based on all these scientific statements, this research demonstrates, in a precise manner and by using software as a measuring tool, that biofertilizer application improves root length and root surface area of plants.

It is important to note that all plants inoculated with biofertilizers showed higher root growth compared with the control group. Thus, showing a larger root surface area: 45.8% (T2 vs T1), 54.4% (T3 vs T1), 48.4% (T4 vs T1), 55.6% (T5 vs T1), 58.6% (T6 vs T1) and 34.1% (T7 vs T1). Similarly, plants with biofertilizers showed longer roots: 19.6% (T2 vs T1), 20.1% (T3 vs T1), 30.9% (T4 vs T1), 63.8% (T5 vs T1), 36.2% (T6 vs T1) and 47.3% (T7 vs T1). This can be seen in *Figure 9a* and *b*, where highly significant differences between treatments are evident. The application of compost and vermicompost substantially improves soil health, microorganism diversity, nutrient availability (Goswami et al., 2017), root growth, and organ development in plants. In addition, the inoculation with microorganisms fulfills fundamental functions in the rhizosphere. One study showed that bagasse compost, prepared with microorganisms, significantly improved the morphological characteristics of sorghum plants (Gopalakrishnan et al., 2019). These results are consistent with (Nascente et al., 2017), who claims that microorganisms enhance yield, promoting plant development by increasing phytomass, photosynthesis, and nutrient absorption. It is also important to highlight several particularities found in this study. First, the amount of biofertilizer seems to have a different influence on root length. Although plant containers were 10 cm high, the roots of plants inoculated with 20% of biofertilizer reached an average length of 24.10 cm and a median of 26.15 cm; followed by plants inoculated with 30%, 25%, and 15% of biofertilizer, where the roots reached an average length of 21.67 cm and a median of 20.39 cm in the first case; an average length of 20.04 cm and a median of 16.88 cm in the second case; and an average length of 19.25 cm and a median of 19.91 cm in the third case. While it might seem confusing, it is important to analyze *Figure 9b* where it can be observed that plants inoculated with 15% of biofertilizer have a higher grouping in the upper quartiles, thus the notches define an upper trend. This would affirm that, in order to obtain better plant yield, the concentration of vermicompost must be applied in moderation (Lim et al., 2014). The second particularity observed is how the amount of biofertilizer influences root surface area. Plants inoculated with 25% of biofertilizer reached an average surface area of 24.78 cm^2 and a median of 25.29 cm^2; followed by plants inoculated with 20%, 10%, and 15% of biofertilizer, where the roots reached an average surface area of 24.30 cm^2 and a median of 25.16 cm^2 in the first case; an average area of 24.11 cm^2 and a median of 25.68 cm^2 in the second case; and an average area of 23.18 cm^2 and a median of 23.46 cm^2 in the third case. Vermicompost improves soil water retention as well as plant growth regulator production (Gupta et al., 2019), which influence root development. It can be seen in *Figure 9a* that the notches define a higher trend for all these cases.

http://www.aloki.hu ● ISSN 1589 1623 (Print) ● ISSN 1785 0037 (Online)
DOI: http://dx.doi.org/10.15666/aeer/1906_49594975

It could be stated that biofertilizer content between 15% and 25% is important. This can be observed in *Figure 10,* where trend lines of both length and surface area show an upward tendency in the range defined above. While this does not fully agree with Ahmadpour and Armand (2020), the results are similar. They recommend the application of compost and vermicompost in a ratio of 30% of the total soil weight to improve the physiological and morphological characteristics of tomato plants under greenhouse conditions. First, it is a different crop and the methodology they used may differ in results, since in the cleaning stage there was an involuntary loss or separation of root segments. In addition, these involuntary losses could also have occurred in the drying stage. In addition, they produce biofertilizers with a discretization of more than 0%, 10%, 20%, and 30%. In the present study, the amount of biofertilizer is discretized in 5% increments. In any case, it is clear that an adequate addition of biofertilizer increases root length and fine roots. It would be important to further demonstrate that the appropriate proportion of vermicompost allows for the development of thicker roots as Esteves et al. (2020) claim. This is planned to be developed with another type of plant in a future investigation. The use of artificial intelligence in agriculture changes the way it is currently practiced (Dharmaraj and Vijayanand, 2018).

Finally, in *Figure 12,* a table with photographs of plants before soil removal can be observed. This analysis was not included in the results since, initially, it was not intended to measure visible fine roots for they were attached to the walls of the seedbed. Nevertheless, it is important to observe that the results visually agree with the projections estimated in *Figure 10*. The next research will be carried out with a larger sample and each plant will be photographed four times, every 90 degrees, in order to measure, with computer vision technology, the number of fine roots visible once they are removed from their seedbeds.

				(T1) 0%
				(T2) 5%
				(T3) 10%
				(T4) 15%
				(T5) 20%

http://www.aloki.hu ● ISSN 1589 1623 (Print) ● ISSN 1785 0037 (Online)
DOI: http://dx.doi.org/10.15666/aeer/1906_49594975

Figure 12. *Root growth comparison between plant samples with different contents of biofertilizer before removing the soil*

Conclusions

Microbial load fulfills essential functions in the rhizosphere. In order to achieve better root and root surface area development, it is important to add adequate amounts of biofertilizer; adding more than what is needed does not guarantee better development. The application of biofertilizers, enriched with beneficial microorganisms, benefits root development and plant growth. In addition, it improves soil characteristics, moisture retention, and nutrient availability. Vermicompost and compost together play an important role in water retention, nutrient supply, and soil characteristics. Mixing both materials with beneficial microorganisms (biofertilization) favors root length and root surface area. This research shows highly-accurate measurement results obtained by using computer vision technology. This also demonstrates that Python and OpenCV library are tools that can be used by the research community within the field of agricultural engineering to carry out high-performance experiments in less time. The use of non-destructive methods in real-time are the future research works, as detailed previously, in the discussion section on the visible roots attached to the walls of the seedbed. Additionally, this methodology is being tested in other crops in the study region, such as corn, wheat, among others.

Acknowledgements. This research has received funding from the Smart University 2.0 program, funded by "Tratamiento de residuos del faenamiento de aves, con aplicación de microorganismos benéficos."

REFERENCES

[1] Agarwal, P., Gupta, R., Gill, I. K. (2018): Importance of biofertilizers in agriculture biotechnology. – Sch. Res. Libr. 9: 1-3.
[2] Ahmadpour, R., Armand, N. (2020): Effect of ecophysiological characteristics of tomato (Lycopersicon esculentum L.) in response to organic fertilizers (compost and vermicompost). – Not. Bot. Horti Agrobot. Cluj-Napoca 48: 1248-1259.
[3] Altman, D. G. (1990): Practical Statistics for Medical Research. – Chapman & Hall, London.
[4] Bannerjee, G., Sarkar, U., Das, S., Ghosh, I. (2018): Artificial intelligence in agriculture: a literature survey. – Int. J. Sci. Res. Comput. Sci. Appl. Manag. Stud. 7: 1-6.
[5] Betegón-Putze, I., González, A., Sevillano, X., Blasco-Escámez, D., Caño-Delgado, A. I. (2018): MyROOT: A novel method and software for the semi-automatic measurement of plant root length. – bioRxiv 1-23.

http://www.aloki.hu ● ISSN 1589 1623 (Print) ● ISSN 1785 0037 (Online)
DOI: http://dx.doi.org/10.15666/aeer/1906_49594975

[6] Bisht, J. K., Meena, V. S., Mishra, P. K., Pattanayak, A. (2016): Role of Biofertilizers in Conservation Agriculture. – In: Bisht J., Meena V., Mishra P., P. A. (eds.), Conservation Agriculture. Springer, Singapore, pp. 113-134.
[7] Böhm, W. (1979): Methods of Studying Root Systems. – Springer, Berlin.
[8] Chatterjee, R., Debnath, A., M. S. (2020): Soil Health. Soil Biology. – In: Giri, B., Varma, A. (eds.) Soil Health. Springer, Cham, pp. 69-88.
[9] Dharmaraj, V., Vijayanand, C. (2018): Artificial intelligence (AI) in Agriculture. – Int. J. Curr. Microbiol. Appl. Sci. 7: 2122-2128.
[10] Esteves, G. de F., de Souza, K. R. D., Bressanin, L. A., Andrade, P. C. C., Veroneze Júnior, V., dos Reis, P. E., da Silva, A. B., Mantovani, J. R., Magalhães, P. C., Pasqual, M., de Souza, T. C. (2020): Vermicompost improves maize, millet and sorghum growth in iron mine tailings. – J. Environ. Manage. 264: 1-11.
[11] Gopalakrishnan, S., Srinivas, V., Kumar, A. A., Umakanth, A. V., Addepally, U., Rao, P. S. (2019): Composting of sweet sorghum bagasse and its impact on plant growth promotion. – Sugar Tech 22: 143-156.
[12] Goswami, L., Nath, A., Sutradhar, S., Bhattacharya, S. S., Kalamdhad, A., Vellingiri, K., Kim, K.-H. (2017): Application of drum compost and vermicompost to improve soil health, growth, and yield parameters for tomato and cabbage plants. – J. Environ. Manage. 200: 243-252.
[13] Gouda, S., Kerry, R. G., Das, G., Paramithiotis, S., Shin, H.-S., Patra, J. K. (2018): Revitalization of plant growth promoting rhizobacteria for sustainable development in agriculture. – Microbiol. Res. 206: 131-140.
[14] Gupta, C., Prakash, D., Gupta, S., Nazareno, M. A. (2019): Role of Vermicomposting in Agricultural Waste Management. – In: Shah, S., Venkatramanan, V., Prasad, R. (eds.) Sustainable Green Technologies for Environmental Management. Springer, Singapore, pp. 283-295.
[15] Judd, L. A., Jackson, B. E., Fonteno, W. C. (2015): Advancements in root growth measurement technologies and observation capabilities for container-grown plants. – Plants 4: 369-392.
[16] Kumar, S. M., Reddy, C. G., Phogat, M., Korav, S. (2018): Role of biofertilizers towards sustainable agricultural development: a review. – J. Pharmacogn. Phytochem. 7: 1915-1921.
[17] Lim, S. L., Wu, T. Y., Lim, P. N., Shak, K. P. Y. (2014): The use of vermicompost in organic farming: overview, effects on soil and economics. – J. Sci. Food Agric. 95: 1143-1156.
[18] Mahanty, T., Bhattacharjee, S., Goswami, M., Bhattacharyya, P., Das, B., Ghosh, A., Tribedi, P. (2017): Biofertilizers: a potential approach for sustainable agriculture development. – Environ. Sci. Pollut. Res. 24: 3315-3335.
[19] Nascente, A. S., De Filippi, M. C. C., Lanna, A. C., De Sousa, T. P., De Souza, A. C. A., Lobo, V. L. da S., Da Silva, G. B. (2017): Effects of beneficial microorganisms on lowland rice development. – Environ. Sci. Pollut. Res. 24: 25233-25242.
[20] Novoplansky, A. (2019): What plant roots know? Semin. – Cell Dev. Biol. 92: 126-133.
[21] Ottman, Timm (1984): Measurement of viable plant roots with the image analyzing computer. – Agron. J. 76.
[22] Paungfoo-Lonhienne, C., Redding, M., Pratt, C., Wang, W. (2019): Plant growth promoting rhizobacteria increase the efficiency of fertilisers while reducing nitrogen loss. – J. Environ. Manage. 233: 337-341.
[23] Schuurman, Goedewaagen (1965): Methods for the examination of root systems and roots. – Wageningen Cent. Agric. Publ. Doc. 37-41.
[24] Tian, H., Wang, T., Liu, Y., Qiao, X., Li, Y. (2020): Computer vision technology in agricultural automation–a review. – Inf. Process. Agric. 7: 1-19.

http://www.aloki.hu ● ISSN 1589 1623 (Print) ● ISSN 1785 0037 (Online)
DOI: http://dx.doi.org/10.15666/aeer/1906_49594975

[25] Tracy, S. R., Nagel, K. A., Postma, J. A., Fassbender, H., Wasson, A., Watt, M. (2020): Crop improvement from phenotyping roots: highlights reveal expanding opportunities. – Trends Plant Sci. 25: 105-118.
[26] Tukey, J. W. (1977): Exploratory Data Analysis. – Pearson, London, pp. 131-160.
[27] Van Dusschoten, D., Metzner, R., Kochs, J., Postma, J. A., Pflugfelder, D., Bühler, J., Schurr, U., Jahnke, S. (2016): Quantitative 3D analysis of plant roots growing in soil using magnetic resonance imaging. – Plant Physiol. 170: 1176-1188.
[28] Villordon, A., LaBonte, D., Solis, J., Firon, N. (2012): Characterization of lateral root development at the onset of storage root initiation in 'Beauregard' sweetpotato adventitious roots. – HortScience 47: 961-968.
[29] Vives-Peris, V., De Ollas, C., Gómez-Cadenas, A., Pérez-Clemente, R. M. (2019): Root exudates: from plant to rhizosphere and beyond. – Plant Cell Rep. 39: 3-17.
[30] Wang, T., Rostamza, M., Song, Z., Wang, L., McNickle, G., Iyer-Pascuzzi, A. S., Qiu, Z., Jin, J. (2019): SegRoot: a high throughput segmentation method for root image analysis. – Comput. Electron. Agric. 162: 845-854.
[31] Weaver, J. E., Jean, F. C., Crist, J. W. (1922): Development and Activities of Roots of Crop Plants; a Study in Crop Ecology. – Carnegie Inst., Washington.
[32] Zha, J. (2020): Artificial intelligence in agriculture. – J. Phys. Conf. Ser. 1693: 1-6.
[33] Zuo, Y., Zhang, J., Zhao, R., Dai, H., Zhang, Z. (2018): Application of vermicompost improves strawberry growth and quality through increased photosynthesis rate, free radical scavenging and soil enzymatic activity. – Sci. Hortic. (Amsterdam) 233: 132-140.

http://www.aloki.hu ● ISSN 1589 1623 (Print) ● ISSN 1785 0037 (Online)
DOI: http://dx.doi.org/10.15666/aeer/1906_49594975

ASSESSMENT OF MICROPLASTICS CONTAMINATION IN COMMERICIAL CLAMS IN THE COASTAL ZONE OF VIETNAM

HUE, H. T. T.[1,2*] – DONG, L. K.[3] – HIEN, T. T.[4] – NGUYEN, T. N.[4] – PRADIT, S.[1,5*]

[1] *Faculty of Environmental Management, Prince of Songkla University, Songkhla 90110, Thailand*

[2]*Central Institute for Natural Resources and Environmental Studies, Vietnam National University, Ha Noi, Vietnam*

[3]*Pu Hu Nature Reserve, Department of Agriculture&Rural Development, Thanh Hoa, Vietnam*

[4]*University of Nature and Science, Vietnam National University, Ho Chi Minh, Vietnam*

[5]*Coastal Oceanography and Climate Change Research Center, Prince of Songkla University, Hat Yai, Songkhla 90110, Thailand*

[*]*Corresponding authors*
e-mail: hathithuhue2001@yahoo.com (Hue, H. T. T.), siriporn.pra@psu.ac.th (Pradit, S.)

(Received 10th Jun 2021; accepted 1st Oct 2021)

Abstract. Microplastics (MPs) present in aquaculture farms represent a big issue globally due to their effect on human health. Both vertebrates and invertebrates have been found to ingest microplastics in coastal areas. However, in Vietnam, the impact of microplastics on aquaculture farms is not yet well understood because there has been no research on the presence of microplastics in local clam species even though they are a common food safety concern. This study aimed to understand the ingestion of microplastic contamination in local clam samples of two species (*Meretrix lyrata and Tapes dorsatus)* from household aquaculture farms. In this study, a total of 182 particles consisting of fibers (67%) was separated and the EVA (18%) was identified. Furthermore, the number of MPs was correlated with the clam's weight and soft tissues during the sample taking. In terms of the distribution of the MPs, efficient management of environmental pollution should be considered in the coastal areas as it is so crucial for human seafood consumption in the long-term future.
Keyword: *aquaculture, coastal areas, farming, local clam, species*

Introduction

In the marine environment, microplastics of all types are rapidly proliferating. At the same time, society makes ever-increasing demands on the aquatic environment, such that the environmental resource management practices of the past need to be reconsidered (Narmatha Sathish et al., 2020a., Strady et al., 2020., Groesbeck et al., 2014). The effect of the persistent plastic contamination on the environment cannot simply be ignored (Hall et al., 2015). A growing body of research shows plastic is ubiquitous globally (McNeish et al., 2018) and plastic contamination in the marine environment has gained intensive consideration (Wu et al., 2020). There is no doubt that microplastic is potentially harmful to all marine life forms that ingest it. Many researches into microplastic ingestion run short-term investigations in areas where plastic pollution has exponentially grown (Azad et al., 2018; Beer et al., 2018; Pradit et al., 2020, 2021). Furthermore, during the MPs progress of marine species, these particles can enter the cycling of the food web (Bergmann, 2009). Furthermore, marine plastic contamination also affects the society, economy (Wu et al., 2020), ecology, and biology (McNeish et al., 2018; Botterell et al.,

http://www.aloki.hu ● ISSN 1589 1623 (Print) ● ISSN 1785 0037 (Online)
DOI: http://dx.doi.org/10.15666/aeer/1906_49774991

2019; Wu et al., 2020). Marine organisms like the clam species are greatly exposed to microplastic pollution even though they have constituted an important part of the everyday seafood produce sold in local and international markets from ancient times, today the clam species are contaminated because of their exposure to microplastic pollution from phytoplankton that have attached to minute particles of plastic found throughout the world's oceans. It may affect on human health when they eat polluted clams (Botterell et al., 2019).

Microplastics are widely scattered in all marine environments (Rillig et al., 2017; Wu et al., 2020). The size of microplastic particles is from 5 mm to 0.1 μm (Lippiatt et al., 2013; Rillig et al., 2017). Furthermore, plastics of different sizes enter the marine environment as particles up to 5 mm in length (Arthur et al., 2009) with larger pieces broken up through physical and mechanical fragmentation (Li et al., 2020). Microplastic debris proliferates, migrates, and accumulates in natural habitats and is scattered on the ocean surface (Ivar and Costa, 2014; McNeish et al., 2018). For instance, fish can transfer microplastic particles to greater trophic levels and humans from zooplankton and phytoplankton (Wu et al., 2020). Even, some inedible parts of fish used in aquaculture or pig raising could be used as feed material for other animals. As a result, the microplastic particles could be continually spread through food as a health hazard (Botterell et al., 2019).

Carpenter et al. (1972) predicted that microplastic contamination would influence several forms of ecosystems and organisms. The microplastic particles are easily broken down by many marine organisms through the ingestion process (Botterell et al., 2019). Therefore, there is a speedily developing awareness of general marine and plastic pollution (Beer et al., 2018). There has been some research on microplastic contamination in the digestive tracts of commercial fish (McNeish et al., 2018; Wu et al., 2020), earthworms in soil (Rillig et al., 2017), Pacific Oyster Larvae (Cole and Galloway, 2015), Zooplankton in the Northeast Pacific Ocean (Desforges et al., 2015), seafood (Chen et al., 2020), and the mussel, Mytilus edulis (Browne et al., 2008). Recently, some researchers have also expressed concern about the clam gardens on the northwest coast (Groesbeck et al., 2014). However, up to now, there have been few studies on microplastics in Vietnam. Furthermore, as yet, none of the studies have focussed on microplastic contamination in clams (*Meretrix lyrata and Tapes dorsatus*) anywhere.

There are two clam species: the *Meretrix lyrata* species in Nam Dinh province and the *Tapes dorsatus* species in Quang Ninh province on intertidal beaches along the coastal waters of North Vietnam (Baechler et al., 2020). Vietnamese government has issued many policies to encourage clam aquaculture based on the situation of coastal zones.

The clam species is not only valued as a chief traditional food value and popular seafood (Li et al., 2015), but is also valued as an essential form of income for the coastal communities. Historically, these species are the main traditional food and an essential source of income for aquacultural farming members (Crosman et al., 2019).

To better understand the pollution in farming (clam species), the objective of this study is to perceive the occurrence of microplastics in clam species from coastal commercial aquaculture. Furthermore, the relationships between different kinds of plastic particles in the tissues of and biological features of clam will be examined.

http://www.aloki.hu ● ISSN 1589 1623 (Print) ● ISSN 1785 0037 (Online)
DOI: http://dx.doi.org/10.15666/aeer/1906_49774991

Materials and methods

Study area

The study was implemented on one oceanic region in Ban Sen commune (latitude 20°58' N and longitude 107°27''E), Van Don district, located on the edge of Quang Ninh province in the northeast of Vietnam, near the world heritage area of Ha Long Bay (*Fig. 1*). Ban Sen commune has access to diverse aquatic life such as a variety of pelagic fish and clams. It also has other aquacultural resources. Recently, aquaculture has mainly focused on clam production as the main source of income for this area. There are around 150 households with 2.600.000 clam cages. In the last year, the production of aquatic products (clams and oysters) in the commune was estimated at 2.250 tons.

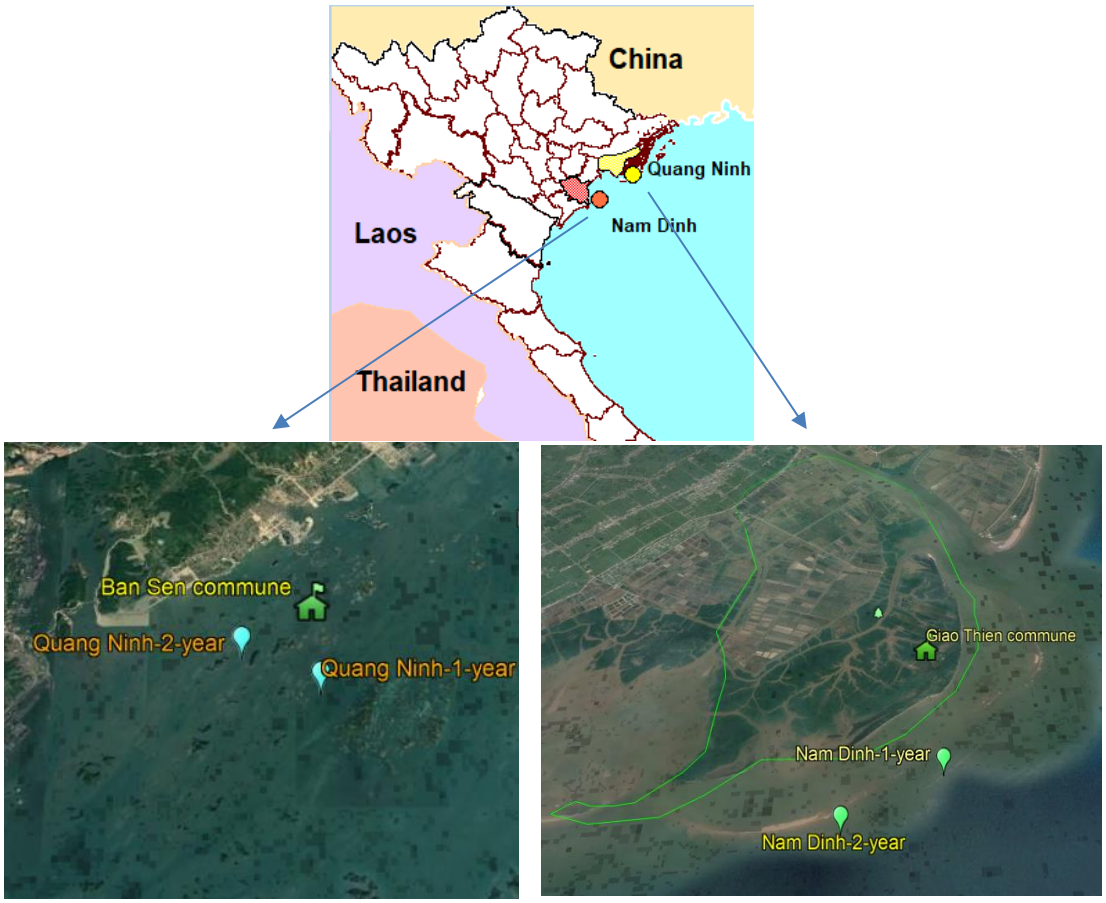

Figure 1. *Location map of studied areas*

Giao Thien commune, that is close to Xuan Thuy national park, is one of the nine Ramsars of Vietnam located in the ocean areas (latitude 20°16' N and longitude 106°32''E) (*Fig. 1*). Local people have aquaculture farms along the coast. There are around 350 households (of a total 8.250 local households) that have been working in aquacultural production, producing 1.360 tons of seafood from 320 ha, which provides the main income.

http://www.aloki.hu ● ISSN 1589 1623 (Print) ● ISSN 1785 0037 (Online)
DOI: http://dx.doi.org/10.15666/aeer/1906_49774991

Sample collection

Clam species are sampled from the aquacultural farms in the coastal waters of two locations, Ban Sen and Giao Thuy communes, in Quang Ninh (QN) and Nam Dinh (ND) provinces respectively. Clam samples were randomly collected from locations such as: 1-year (latitude 20°02′N; longitude 107°28′E) and 2-year (latitude 21°02′N; longitude 107°28′E) in Ban Sen; 1-year (latitude 20°12′N; longitude 106°34′E) and 2-year in Giao Thuy commune during August 2020 and February 2021 from an average sea depth of ~12 m (Hall et al., 2015). The clams were brought up by using local skin-divers from the commune. Information on clam aquaculture from farming households in the location were noted. There were sampling clam group (2 sites*10 sample groups = 20; total 20*10 = 200 sample clams) across all sites of Ban Sen commmune *(Meretrix lyrata)* and Giao Thuy commune *(Tapes dorsatus).* At each of the exposed intertidal sandy beaches clam specimens were transferred to the laboratory in an icebox (Li et al., 2018).

Sampling condition control

The clam samples were carefully cleaned, iced, and transported back to the Faculty of Environment, University of Science, Vietnam National University-Ho Chi Minh and stored under laboratory conditions from 2-4 weeks for analysing (Hue et al., 2018a). After a thorough washing with clean water, the clams were weighed and their lengths were measured, and they were then left in the refrigerator (*Fig. 2*). Each clam was measured in terms of age, and the location where it was found (Fig. 3) was recorded. The collected samples were held in a styrofoam case with sufficient ice and transported to the laboratory where they were quickly frozen and maintained at -19°C in the refrigerator (Cole and Galloway, 2015) to keep the stable sampled clams from decomposing until they were further needed (Azad et al., 2018) (*Fig. 2*). The tissues of 10 samples were randomly packed together as one sample (Narmatha Sathish et al., 2020) that were put into pouches made of aluminium foil (Li et al., 2018). The sampled clams from the refrigerator were slowly defrosted and thoroughly rinsed with clean water to remove sand and impurities from their bodies .

Figure 2. *Samples in electric refrigerator*

Figure 3. *Measurement of samples*

Chemical treatment

Clam samples were allowed to defrost for 2 h at normal temperature. The soft tissues of the clams on the cutting board were carefully separated from the shells with a knife, and the wet weight of each specimen was recorded (Narmatha Sathish et al., 2020)

http://www.aloki.hu ● ISSN 1589 1623 (Print) ● ISSN 1785 0037 (Online)
DOI: http://dx.doi.org/10.15666/aeer/1906_49774991

(*Fig. 4*). In brief, the soft tissues were washed with distilled water to separate the natural debris on the outside prior to working with the clams (e.g., sand, algae, and coral) (Li et al., 2018; Oceanography et al., 2018). The soft tissue was cut into 6-8 small pieces and put into Onelab 100 ml glass tubes (1 ml Ex 20^0C +-1 ml) for determining volume. The tissue was decomposed with Potassium hydroxide (KOH 10%; 3 x tissue volume) in an ED115 convection oven at 56^0C for a period of 48 h (12 h shaking-time) until a clear solution formed (Narmatha Sathish et al., 2020).

Floatation and filtration

After the tissue was decomposed in KOH in the electric oven and was washed in distilled water, all the rotten soft tissues were filtered through a 53 µm sieve and put into a WERTLAB GERMANY glass tube with 100 mL of a mixture of NaCl (1.2 g/ml) and $ZnCl_2$ (1.8 g/ml) (d=1.5 g/cm^3) for 24 hours to float the MPs. The filter paper (Glass microfiber filters) was weighed (*Fig. 4*). The floating residue was filtered through the filter paper with distilled water, using a Rocker 300 vacuum pump with the following settings: 105 m/bar, maximum flow rate, 20-23 liters/min, Rotation speed 1750 RPM, horsepower 1/8 HP, noise level 50 dB, and a voltage of 110 V/60 Hz and 220 V/50 Hz, was used to dry the filter paper at 56^0C (*Fig. 5*).

Figure 4. *Weight of soft clams*

Figure 5. *The soft clams in the ED115 autonomic oven*

Extraction of microplastic

The particles in the glass microfiber filter papers were examined using a USB Digital Microscope with 300x magnification and a 5M pixel image sensor connected to the computer. A visual assessment was made to identify the types of microplastics according to the physical characteristics of the particles (Li et al., 2015). The MP particles (size >0.25 mm) were removed to the diamond surface of FTIR-ATR by forceps, to investigate the polymer characters (Li et al., 2015). Furthermore, some MPs were identified using micro-Fourier Transformed Infrared Spectroscopy (FT/IR-6600 FT-IR made in Japan). The spectral resolution was in the range of 497.544 – 4003.5 cm^{-1} for the samples (*Fig. 6*).

Statistical analyses

In this study, microplastic particles refer to visually identified fibres, and there were few particles as plastic types (Baechler et al., 2020). Data collected on background

http://www.aloki.hu ● ISSN 1589 1623 (Print) ● ISSN 1785 0037 (Online)
DOI: http://dx.doi.org/10.15666/aeer/1906_49774991

characteristics of the sampled clams and microplastic particles were analysed in the Statistical Packages for Social Science (SPSS) version 20.0 and Microsoft Excel (Jeil et al., 2020) for means ± standard deviations, minimum, maximum, and percentages. Furthermore, to identify the differences in clam samples, types of variance (ANOVA) and post-hoc Tukey tests were analyzed (Hue et al., 2018a,b; Baechler et al., 2020). The models of linear regression were applied for observing the relationships between biological parameters (shell length, body wet weight) and MP load (per whole individual and g^{-1} tissue); the number of MPs per sample; g^{-1} tissue (wet weight; whole organisms) (Baechler et al., 2020). The significance was calculated for P ($P<0.05$). The statistical analyses were performed with the SPSS Statistic (Dong et al., 2018).

Figure 6. *FTIR spectrometer with ATR probe*

Results and discussion

Basic information on the sample clams

General sample clams

There are different sizes of clams in the study which are given as the mean ± SD such as clam_total_weight (17.12±6.23 g), clam_soft_tissues (4.13±2.45 g). Separately, the clam samples (10 clams altogether), four-locations and two year of age were illustrated in *Table 1*. The total weight of the soft tissues of clams in Quang Ninh (QN)-2-year was the highest, and Nam Dinh (ND)-1-year was the lowest, compared to others. The number of MPs per (g) was correlated with the clam's mean weight per (g) and clam's mean tissue weight per (g) on Spearman rank order correlations (rs) of 0.37 ($p < 0.05$), 0.36 ($p < 0.05$), respectively. Furthermore, the number of MPs was strongly correlated with MPs/clam's mean weight per (g) and MPs/clam's mean tissue weight per (g) 0.91 ($p < 0.01$), 0.71 ($p < 0.01$), respectively. The allometric relationship was disclosed between the clam's size and the MPs related to the considered clams as Saavedra et al. (2004) represented. Similarly, there was found to be a relationship between the rate of MPs/clam's size and the number of MPs as well (Narmatha Sathish et al., 2020).

Microplastic profusion in clam

The dispersion of MPs among the different ages of clams in the study is represented in *Table 2*. The highest variety of MPs was found in the clams of QN-2-year and the lowest abundance was found in ND-1-year. The number of clam bodies and MPs, varies from 0.25 ± 0.16 to 0.67 ± 2.98 items/ individual, from 0.11 ± 0.07 to 0.92 ± 0.59 items/g and from 0.02 ± 0.12 to 0.28 ± 0.13 items/soft tissues. However, Su et al. (2018) represented MPs extending from 0.4 to 5.0 items/individual (or 0.3 to 4.9 items/g) in

http://www.aloki.hu ● ISSN 1589 1623 (Print) ● ISSN 1785 0037 (Online)
DOI: http://dx.doi.org/10.15666/aeer/1906_49774991

Asian freshwater clams. In Quang Ninh, the young-sized clams contained a higher concentration of MPs (0.28 ± 0.13 items/soft tissues) than the older ones (0.25 ± 0.16 items/soft tissues). This was in contrast with Nam Dinh, where the older ones had a higher concentration of MPs. The level of microplastics was around one order of magnitude higher than those represented in mussels and oysters (Mathalon and Hill, 2014; Li et al., 2015). Furthermore, this might be growth of infiltration rate with the decline in the sampling size (Winter, 1974), which would increase in MPs in small-sized clams and decline in large-sized clams (Narmatha Sathish et al., 2020).

Table 1. *Mean values and range of measurements of sampled clams*

Location-age	Total mean clam weight (g)	Weight of soft tissues (g)
Quang Ninh-1-year	176.11±17.72	49.67±4.82
Quang Ninh-2-year	246.44±24.32	77.67±5.85
Nam Dinh-1-year	121.64±14.99	20.45±2.02
Nam Dinh-2-year	169.20±13.82	28.50±1.90

Table 2. *Mean values and range of microplastic and clam tissues*

Location-age	Number of miscroplatics *(Individual)*	Microplastic density/clam *(Individual)*	Microplastic /total weight *(g)*	Microplastic /tissues weight *(g)*
Quang Ninh-1-year	4.56±2.92	0.33±0.5	0.88±0.43	0.28±0.13
Quang Ninh-2-year	6.67±2.96	0.67±2.98	0.92±0.59	0.25±0.16
Nam Dinh-1-year	2.45±1.44	0.25±0.16	0.11±0.07	0.02±0.12
Nam Dinh-2-year	5.40±4.09	0.54±0.40	0.21±0.13	0.04±0.02

Futhermore, MPs/tissues were directly proportional to MPs/distance. Interestingly, younger clams (small-size) had an outstandingly greater concentration of MPs than the older ones (over medium-size). The highest rate of MPs/tissues and MPs/distance in 1-year-clams is 0.09 (ND) and 0.05 (QN) respectively (*Fig. 7*). However, according to research in India conducted by Narmatha Sathish et al. (2020) small-sized sample clams had higher concentrations of MPs. These fluctuations could be different according to the specific environments for the growing organisms (Cho et al., 2019).

Microplastics under digital microscope

Color of microplastics

The sample analysis showed MPs of various colors and sizes. Multiple colors of microplastics were recorded in clams, such as clear white, opalescent, blue, red, and black *(Fig. 8)*. The proportion of black colors was 55%, significantly larger than other colors. However, this finding was different from that of Lee et al. (2013), who reported that the transpearent MPs were the most commonly found category among all sample clams in China. The rate of clear-white, opalesent, and blue colors was around a mere 1%.

http://www.aloki.hu ● ISSN 1589 1623 (Print) ● ISSN 1785 0037 (Online)
DOI: http://dx.doi.org/10.15666/aeer/1906_49774991

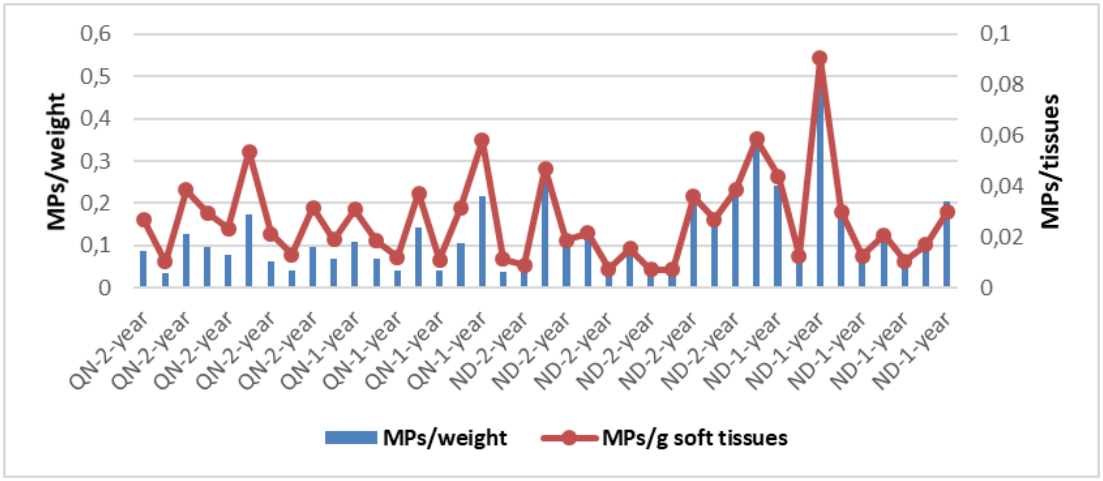

Figure 7. *The rate of MPs in sampling clam*

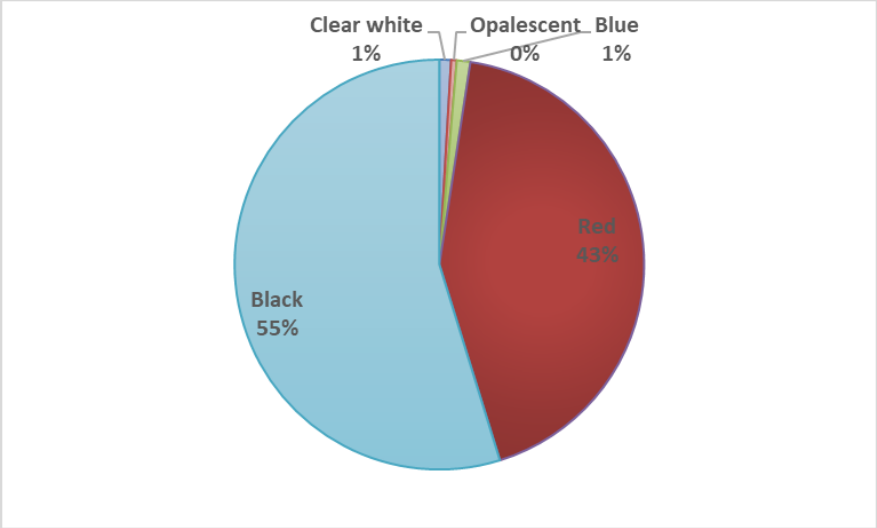

Figure 8. *Percentage of MPs colors from clams*

Shape of microplastics

Following clam shapes, there were three MP types such as fibers, fragments, and pellets. Fibers (68%) are the most common type of MPs in clams as reported by Narmatha Sathish et al. (2020) on the Tuticorin coast of the Gulf of Mannar (GoM), India (*Fig. 9*). Pellets were common in the sample clam but were not identified at all sampling locations. These research results were also supported by Li et al. (2015) when they reported the various MP types, including rich fibers in China. Davidson and Dudas (2016) also revealed that most commonly, fibers were observed in Manila clams. Additionally, De Witte et al. (2014) considered that fibers needed a longer time than other MPs to be eliminated. Further, Renzi et al. (2018) noted that the fibers found under gills and in the hepatopancreas could not be easily withdrawn.

http://www.aloki.hu ● ISSN 1589 1623 (Print) ● ISSN 1785 0037 (Online)
DOI: http://dx.doi.org/10.15666/aeer/1906_49774991

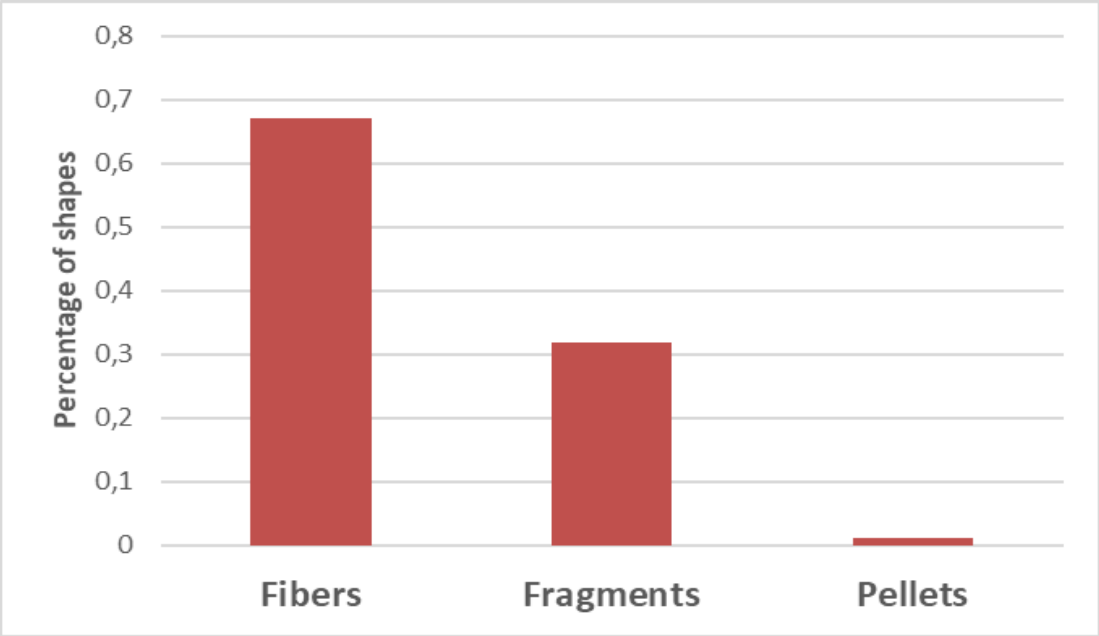

Figure 9. *The main abundance of microplastics shapes*

Size of microplastics

Interestingly, MPs were observed under Microscope (*Fig. 10*). The size of fibers (4.70±4.32 mm) and fragments (4.00±3.22 mm) were largest in ND-2-years and QN-2-years respectively, while both MP sizes were lowest in ND-1-year (*Table 3*). It is clear that the size of MPs in longer clams is greater than MP size in small ones which is similar to the findings of Narmatha Sathish et al. (2020), who considered that the direct proportionality of MP size to the size of clam body was significant. However, the overall size of MPs was different in QN-1-year (2.04±2.51mm), which was the biggest among others.

Table 3. *Mean values and range of microplastic sizes in different clams*

Location-clam-age	Microplastic size (mm)	Fibers (mm)		Fragments (mm)
Quang Ninh-1-year	2.04±2.51	2.56±2.24		1.89±1.05
Quang Ninh-2-year	1.50±1.80	3.44±2.24		4.00±3.22
Nam Dinh-1-year	1.49±0.78	2.10±1.29		1.00±0.00
Nam Dinh-2-year	1.61±1.05	4.70±4.32		1.17±0.41

Fig. 12 illustrates the spectrum of some resins found in clams at the two study sites, including Nylons in clams in Quang Ninh and unidentified resins, which are very diverse.

http://www.aloki.hu ● ISSN 1589 1623 (Print) ● ISSN 1785 0037 (Online)
DOI: http://dx.doi.org/10.15666/aeer/1906_49774991

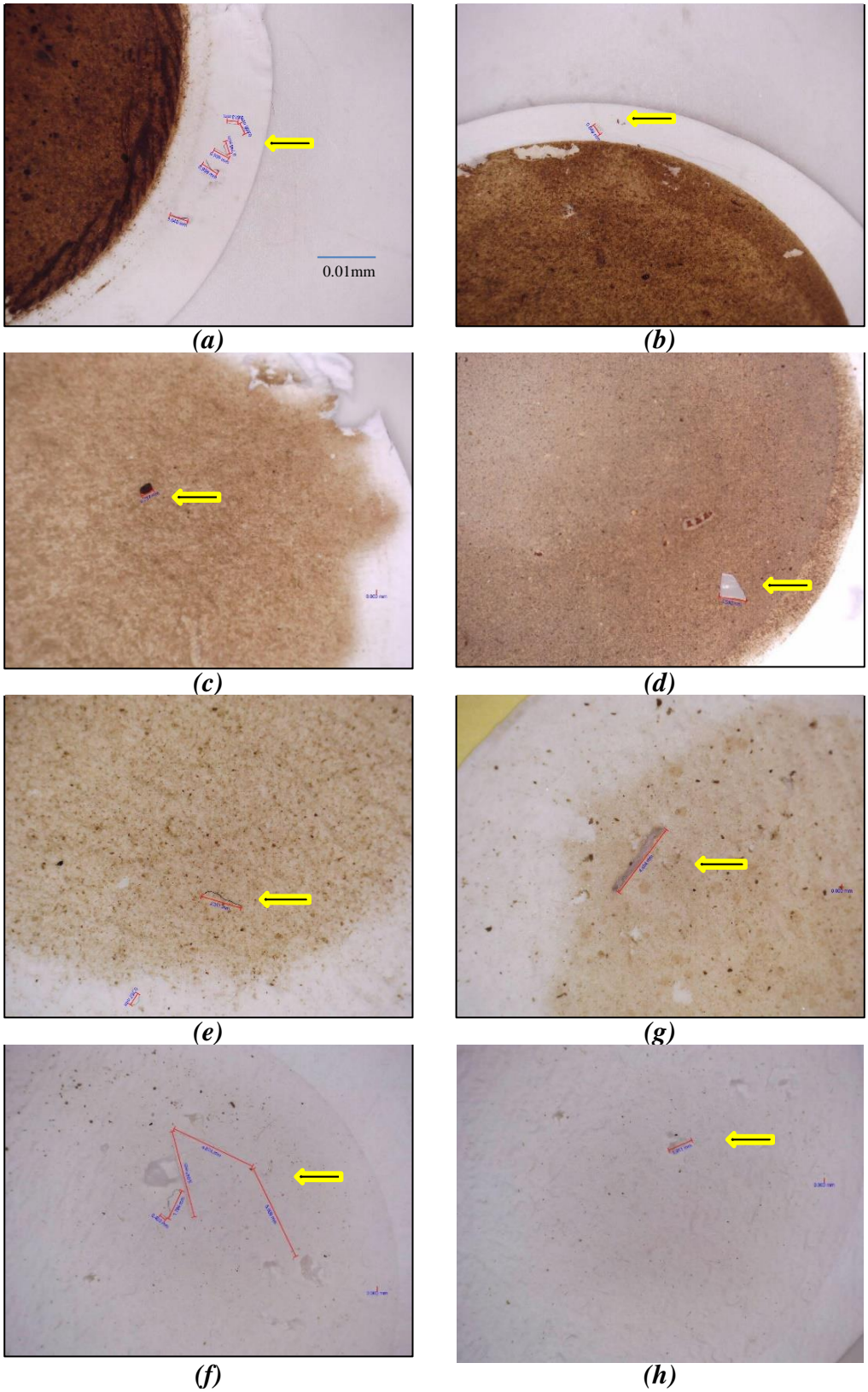

Figure 10. *Photographs of different types of microplastics in clams from the case study. The photographs were taken directly on the filter paper of Quang Ninh (2-year (a, b), 1-year (c,d)); Nam Dinh (2-year(e,g), 1-year (f,h)) samples; Black yarn beads (a,c,e,f); Opaque white fragments (b,d,g,h); Fibers (a,b,e,g,f) Fragments (d,h), Pellets (c)*

http://www.aloki.hu ● ISSN 1589 1623 (Print) ● ISSN 1785 0037 (Online)
DOI: http://dx.doi.org/10.15666/aeer/1906_49774991

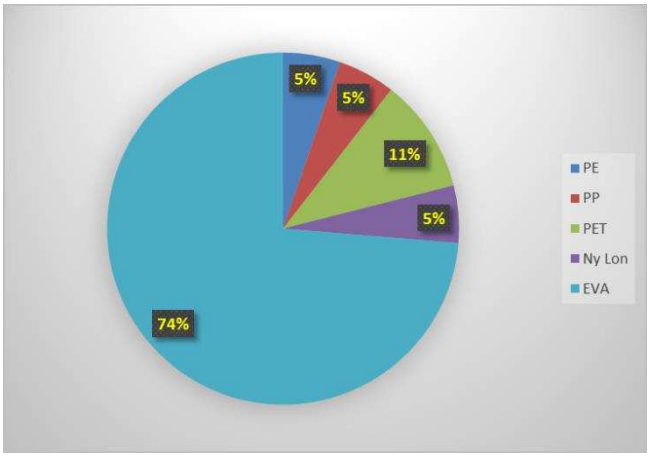

Figure 11. *The distribution of polymer composition of MPs in clam samples*

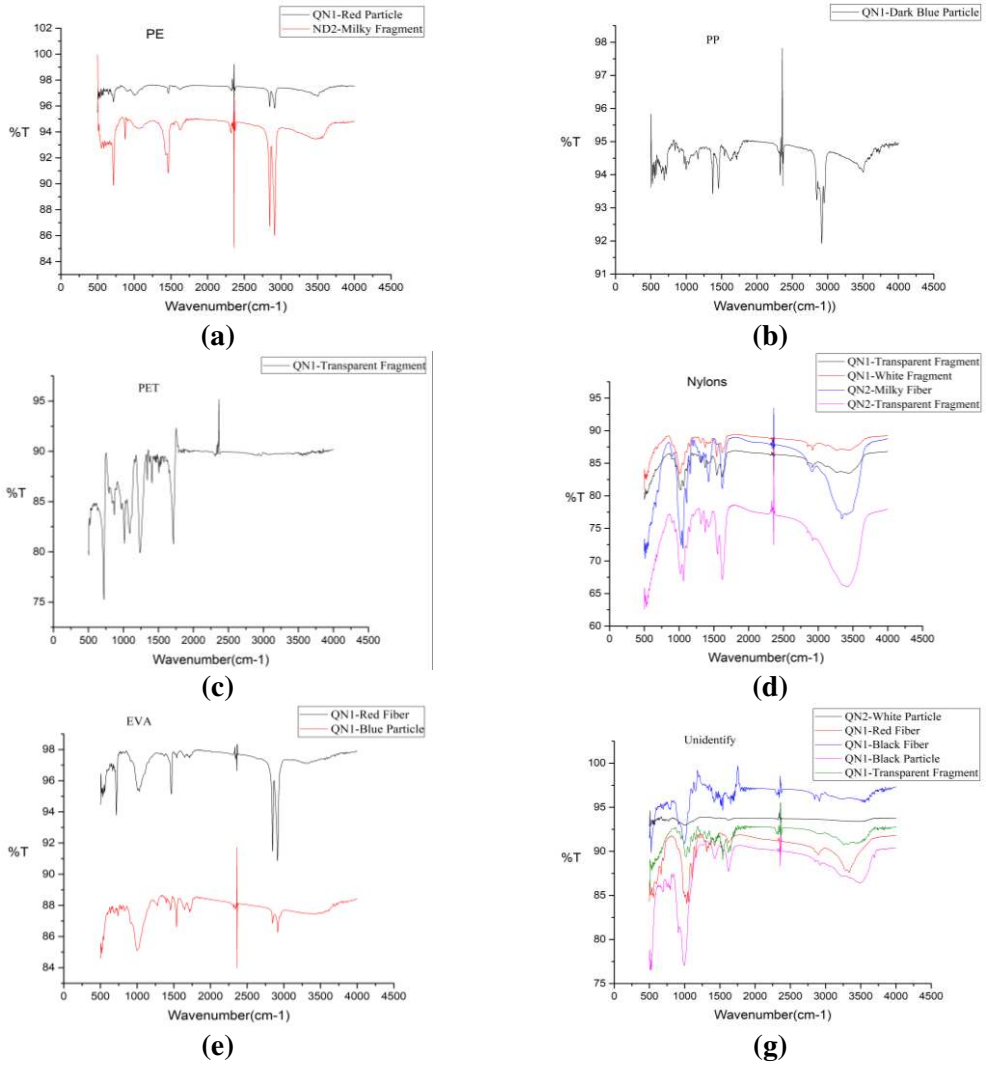

Figure 12. *Identification of different types of microplastic with micro-Fourier Transformed Infrared Spectroscopy (μ-FT-IR). The performed transmittance; a (PE: Polyetylen); b (PP: Polypropylene); c (PET: Polyethylene Terephthalate); d (Nylon); e (EVA: Ethylene vinyl acetate copolymer); g (identification)*

http://www.aloki.hu ● ISSN 1589 1623 (Print) ● ISSN 1785 0037 (Online)
DOI: http://dx.doi.org/10.15666/aeer/1906_49774991

Conclusion

This study used stereo microscopy and FTIR-ATR to explore the levels of contamination and characteristics of MPs in clam species (*Meretrix lyrata and Tapes dorsatus*) in two locations of common farming aquaculture in north Vietnam. The highest number of microplastics was found in the oldest clams. Similarly, the fiber types are the most common in the microplastic samples, thus fiber MPs should be considered in future environmental management. This research emphasized that the number of MPs is correlated with the clam's weight and soft tissues. Also, the clam is still a traditional food bivalve in humans and it will raise the risk of MP contamination through daily consumption (Narmatha Sathish et al., 2020). Further research investigating the impact of eating clams on human MP ingestion and its potential transfer through food consumption is needed. Furthermore, in this case, the question of correlation between microplastic pollution in clams and their living environment (such as waters, sediment, etc) should be considered, so environmental protection can be supported.

Acknowledgements. This research was supported by the Prince of Songkla University and the Ministry of Higher Education, Science, Research and Innovation, Thailand, under the Reinventing University Project (Grant Number REV64031). This paper also has been part of the project QG.20.44, with financial support from Vietnam National University, Ha Noi, Vietnam. We would like to acknowledge the staff in Ban Sen commune, Van Don district, Quang Ninh province for their efforts during the survey for the data collection in the field. We would further like to thank the two communities for allowing us to collect data in the study communities. Lastly, we would like to extend our gratitude towards farming households in the case study for their warm welcome and generosity.

Declaration of interest. The authors declare that there is no conflict of interests in this paper.

REFERENCES

[1] Arthur, C., Baker, J., Bamford, H. (eds.) (2009): Proceedings of the International Research Workshop on the Occurrence, Effects, and Fate of Microplastic Marine Debris. – NOAA Marine Debris Program.

[2] Azad, S. M. O., Towatana, P., Pradit, S., Patricia, B. G., Hue, H. T. T., Jualaong, S. (2018): First evidence of existence of microplastics in stomach of some commercial fishes in the lower gulf of Thailand. – Applied Ecology and Environmental Research 16(6): 7345-7360. doi: 10.15666/aeer/1606-73457360.

[3] Baechler, B. R., Granek, E. F., Mazzone, S. J., Nielsen-Pincus, M., Brander, S. M. (2020): Microplastic Exposure by Razor Clam Recreational Harvester-Consumers Along a Sparsely Populated Coastline. – Frontiers in Marince Science. https://doi.org/10.3389/fmars.2020.588481.

[4] Beer, S., Garm, A., Huwer, B., Dierking, J., Nielsen, T. G. (2018): No increase in marine microplastic concentration over the last three decades - A case study from the Baltic Sea. – Science of the Total Environment 621: 1272-1279. https://doi.org/10.1016/j.scitotenv.2017.10.101.

[5] Bergmann, M. (2009): Marine Anthropogenic Litter. – https://doi.org/10.1007/978-3-319-16510-3.

[6] Botterell, Z. L. R., Beaumont, N., Dorrington, T., Steinke, M., Thompson, R. C., Lindeque, P. K. (2019): Bioavailability and effects of microplastics on marine zooplankton: A review. – Environmental Pollution 245: 98-110. https://doi.org/10.1016/j.envpol.2018.10.065.

http://www.aloki.hu ● ISSN 1589 1623 (Print) ● ISSN 1785 0037 (Online)
DOI: http://dx.doi.org/10.15666/aeer/1906_49774991

[7] Browne, M. A., Dissanayake, A., Galloway, T. S., Lowe, D. M., Thompson, R. C. (2008): Ingested microscopic plastic translocates to the circulatory system of the mussel, Mytilus edulis (L.). – Environmental Science and Technology. https://doi.org/10.1021/es800249a.
[8] Carpenter, E. J., Anderson, S. J., Harvey, G. R., Miklas, H. P., Peck, B. B. (1972): Polystyrene spherules in coastal waters. – Science 178: 4062. https://doi.org/10.1126/science.178.4062.749.
[9] Chen, J. Y. S., Lee, Y. C., Walther, B. A. (2020): Microplastic contamination of three commonly consumed seafood species from Taiwan: A pilot study. – Sustainability 12(22): 9543. https://doi.org/10.3390/su12229543.
[10] Cho, S. A., Cho, W. B., Kim, S. B., Chung, J. H., Kim, H. J. (2019): Identification of microplastics in sea salts by Raman microscopy and FT-IR microscopy. – Analytical Science and Technology 32(6): 243-251. https://doi.org/10.5806/AST.2019.32.6.243.
[11] Cole, M., Galloway, T. S. (2015): Ingestion of Nanoplastics and Microplastics by Pacific Oyster Larvae. – Environmental Science and Technology 49(24): 14625-14632. https://doi.org/10.1021/acs.est.5b04099.
[12] Crosman, K. M., Petrou, E. L., Rudd, M. B., Tilotson, M. D. (2019): Clam hunger and the changing ocean: characterizing social and ecological risks to the Quinault razor clam fishery using participatory modeling. – Ecology and Society 24(2): 16. https://doi.org/https://doi.org/10.5751/ES-10928-240216.
[13] Davidson, K., Dudas, S. E. (2016): Microplastic Ingestion by Wild and Cultured Manila Clams (Venerupis philippinarum) from Baynes Sound, British Columbia. – Archives of Environmental Contamination and Toxicology 71(2): 147-156. https://doi.org/10.1007/s00244-016-0286-4.
[14] De Witte, B., Devriese, L., Bekaert, K., Hoffman, S., Vandermeersch, G., Cooreman, K., Robbens, J. (2014): Quality assessment of the blue mussel (Mytilus edulis): Comparison between commercial and wild types. – Marine Pollution Bulletin 85(1): 146-155. https://doi.org/10.1016/j.marpolbul.2014.06.006.
[15] Desforges, J. P. W., Galbraith, M., Ross, P. S. (2015): Ingestion of Microplastics by Zooplankton in the Northeast Pacific Ocean. – Archives of Environmental Contamination and Toxicology 69(3): 320-330. https://doi.org/10.1007/s00244-015-0172-5.
[16] Dong, K. L., Sutinee, S., Hoa, A. X., Anh, N. T., Thinh, N. V., Hai, L. V., Mano, P. K. T. (2018): Overview of improving patrolling efforts: A case study of forest staction in Pu Hu nature reserve. – Applied Ecology and Environmental Research 16(3): 2845-2859. https://doi.org/http://dx.doi.org/10.15666/aeer/1603_28452859.
[17] Groesbeck, A. S., Rowell, K., Lepofsky, D., Salomon, A. K. (2014): Ancient clam gardens increased shellfish production: Adaptive strategies from the past can inform food security today. – PLoS ONE 9(3). https://doi.org/10.1371/journal.pone.0091235.
[18] Hall, N. M., Berry, K. L. E., Rintoul, L., Hoogenboom, M. O. (2015): Microplastic ingestion by scleractinian corals. – Marine Biology 162: 725-732. https://doi.org/10.1007/s00227-015-2619-7.
[19] Hue, H. T. T., Pradit, S., Janunee, C., Lim, A., Nitiratsuwan, T., Goncalo, C. (2018a): Physical Properties of three Songkhla Lagoon fish species in the lower gulf of Thailand during and after the monsoon season. – Applied Ecology and Environmental Research 16(5): 6113-6127. doi: 10.15666/aeer. 1605_61136127.
[20] Hue, H. T. T., Pradit, S., Lim, A., Nitiratsuwan, T., Goncalo, C. (2018b): Seasonal aspects and the adaptation of fishermen in the Songkhla Lagoon, Thailand. – Asian Journal of Microbiolo. Biotech. Env. Sci. 20(4): 1349-1355. ISSN-0972-3005.
[21] Ivar, J. A., Costa, M. F. (2014): The present and future of microplastic pollution in the marine environment. – Environmental Pollution 185: 352-364. https://doi.org/10.1016/j.envpol.2013.10.036.
[22] Jeil, E. B., Segbefia, A. Y., Abass, K., Adjaloo, M. (2020): Livelihood security along beekeeping value chain: lessons from Ghana's beekeeping experience. – GeoJournal 85(2): 565-577. https://doi.org/10.1007/s10708-019-09982-4.

http://www.aloki.hu ● ISSN 1589 1623 (Print) ● ISSN 1785 0037 (Online)
DOI: http://dx.doi.org/10.15666/aeer/1906_49774991

[23] Lee, J., Hong, S., Song, Y. K., Hong, S. H., Jang, Y. C., Jang, M., Heo, N. W., Han, G. M., Lee, M. J., Kang, D., Shim, W. J. (2013): Relationships among the abundances of plastic debris in different size classes on beaches in South Korea. – Marine Pollution Bulletin 77(1-2): 349-354. https://doi.org/10.1016/j.marpolbul.2013.08.013.

[24] Li, J., Yang, D., Li, L., Jabeen, K., Shi, H. (2015): Microplastics in commercial bivalves from China. – Environmental Pollution 207: 190-195. https://doi.org/10.1016/j.envpol.2015.09.018.

[25] Li, H. X., Ma, L. S., Lin, L., Ni, Z. X., Xu, X. R., Shi, H. H., Yan, Y., Zheng, G. M., Rittschof, D. (2018): Microplastics in oysters Saccostrea cucullata along the Pearl River Estuary, China. – Environmental Pollution 236: 619-625. https://doi.org/10.1016/j.envpol.2018.01.083.

[26] Li, J., Huang, W., Xu, Y., Jin, A., Zhang, D., Zhang, C. (2020): Microplastics in sediment cores as indicators of temporal trends in microplastic pollution in Andong salt marsh, Hangzhou Bay, China. – Regional Studies in Marine Science 35: 101149. https://doi.org/10.1016/j.rsma.2020.101149.

[27] Lippiatt, S., Opfer, S., Arthur, C. (2013): Marine Debris Monitoring and Assessment. – NOAA Technical Memorandum.

[28] Mathalon, A., Hill, P. (2014): Microplastic fibers in the intertidal ecosystem surrounding Halifax Harbor, Nova Scotia. – Marine Pollution Bulletin 81(1): 69-79. https://doi.org/10.1016/j.marpolbul.2014.02.018.

[29] McNeish, R. E., Kim, L. H., Barrett, H. A., Mason, S. A., Kelly, J. J., Hoellein, T. J. (2018): Microplastic in riverine fish is connected to species traits. – Scientific Reports 8: 11639. https://doi.org/10.1038/s41598-018-29980-9.

[30] Naji, A., Nuri, M., Vethaak, A. D. (2018): Microplastics contamination in molluscs from the northern part of the Persian Gulf. – Environmental Pollution 235: 113-120. https://doi.org/10.1016/j.envpol.2017.12.046.

[31] Narmatha Sathish, M., Immaculate Jeyasanta, K., Patterson, J. (2020a): Monitoring of microplastics in the clam Donax cuneatus and its habitat in Tuticorin coast of Gulf of Mannar (GoM), India. – Environmental Pollution 266(1): 115219. https://doi.org/10.1016/j.envpol.2020.115219.

[32] Pradit, S., Towatana, P., Nitiratsuwanc, T., Jualaongd, S., Jirajarusa, M., Sornplang, K., Noppradita, P., Darakaia, Y., Weerawong, C. (2020): Occurrence of microplastics on beach sediment at Libong, a pristine island in Andaman Sea, Thailand. – ScienceAsia 46: 336-343. doi:10.2306/scienceasia1513-1874.2020.042.

[33] Pradit, S., Noppradit, P., Goh, B. P., Sornplang, K., Ong, M. C., Towatana, P. (2021): Occurrence of microplastics and trace metals in fish and shrimp from Songkhla Lake, Thailand during the covid 19 pandemeic. – Applied Ecology and Environmental Research 19(2): 1085-1106. DOI: http://dx.doi.org/10.15666/aeer/1902_10851106.

[34] Renzi, M., Guerranti, C., Blašković, A. (2018): Microplastic contents from maricultured and natural mussels. – Marine Pollution Bulletin 131(A): 248-251. https://doi.org/10.1016/j.marpolbul.2018.04.035.

[35] Rillig, M. C., Ziersch, L., Hempel, S. (2017): Microplastic transport in soil by earthworms. – Scientific Reports 7: 1362. https://doi.org/10.1038/s41598-017-01594-7.

[36] Saavedra, Y., Gonzalez, A., Fernandez, P., Blanco, J. (2004): The effect of size on trace metal levels in raft cultivated mussels (Mytilus galloprovincialis). – Science of The Total Environment 318(1-3): 115-124. https://doi.org/https://doi.org/10.1016/S0048-9697(03)00402-9.

[37] Strady, E., Dang, T. H., Dao, T. D., Dinh, H. N., Do, T. T. D., Duong, T. N., Duong, T. T., Hoang, D. A., Kieu-Le, T. C., Le, T. P. Q., Mai, H., Trinh, D. M., Nguyen, Q. H., Tran-Nguyen, Q. A., Tran, Q. V., Truong, T. N. S., Chu, V. H., Vo, V. C. (2020): Baseline assessment of microplastic concentrations in marine and freshwater environments of a developing Southeast Asian country, Viet Nam. – Marine Pollution Bulletin 162: 111870. https://doi.org/10.1016/j.marpolbul.2020.111870.

http://www.aloki.hu ● ISSN 1589 1623 (Print) ● ISSN 1785 0037 (Online)
DOI: http://dx.doi.org/10.15666/aeer/1906_49774991

[38] Su, L., Cai, H., Kolandhasamy, P., Wu, C., Rochman, C. M., Shi, H. (2018): Using the Asian clam as an indicator of microplastic pollution in freshwater ecosystems. – Environmental Pollution 234: 347-355. https://doi.org/10.1016/j.envpol.2017.11.075.

[39] Winter, J. E. (1974): The filtration rate of Mytilus edulis and its dependence on algal concentration, measured by a continuous automatic recording apparatus. – Marine Biology 22: 317-328.

[40] Wu, J., Lai, M., Zhang, Y., Li, J., Zhou, H., Jiang, R. (2020): Case Studies in Chemical and Environmental Engineering Microplastics in the digestive tracts of commercial fish from the marine ranching in east China sea, China. – Case Studies in Chemical and Environmental Engineering 2: 100066. https://doi.org/10.1016/j.cscee.2020.100066.

[41] Yang, Y., Cheng, W., Yin, B., Yang, M. B. (2019): Facile preparation of polymer coating on reduced graphene oxide sheets by plasma polymerization. – Nanocomposites 5(3): 74-83. https://doi.org/10.1080/20550324.2019.1647687.

http://www.aloki.hu ● ISSN 1589 1623 (Print) ● ISSN 1785 0037 (Online)
DOI: http://dx.doi.org/10.15666/aeer/1906_49774991

CORRELATION BETWEEN INTESTINAL MICROBIOTA AND GROWTH OF WHITE SHRIMP (*LITOPENAEUS VANNAMEI*)

WU, J. Y.[1,2] – YAN, M. C.[1,2] – SANG, Y.[1,2] – LI, F.[1,2] – LUO, K.[1,2] – HU, L. H.[1,2*]

[1]*Zhejiang Key Lab of Exploitation and Preservation of Coastal Bio-Resource, Zhejiang Mariculture Research Institute, Wenzhou 325005, China*

[2]*Wenzhou Key Laboratory of Marine Biological Genetics and Breeding, Zhejiang Mariculture Research Institute, Wenzhou 325005, China*

[*]*Corresponding author*
e-mail: 51275316@qq.com; phone: +86-138-6876-1896

(Received 15th Jun 2021; accepted 3rd Sep 2021)

Abstract. Although intestinal microbiota is closely related to the growth of the host, it is still unclear how it affects the growth of white shrimp. To elucidate the potential processes of intestinal microbiota affecting white shrimp growth, in this study, we compared the intestinal microbiota compositions and metabolisms of larger (11.11 ± 0.32 g) and smaller (5.30 ± 0.06 g) individuals in the same batch of white shrimp cultured in the same environment through high-throughput sequencing of 16S rRNA gene. Our results showed that there was no significant difference in the composition of intestinal microbiota between larger and smaller white shrimps. However, *Shewanella algae* and *Neptunomonas* sp. were significantly enriched in the larger group, while *Delftia* sp., *Hydrogenophaga* sp., *Pseudomonas* sp., *Synechococcus* sp., *Methylibium* sp., *Acidovorax* sp., *Limnohabitans* sp., *Burkholderia* sp., *Candidatus Koribacter* sp., and *Vogesella* sp. were enriched in the smaller group. Moreover, the intestinal microbiota might promote the energy metabolism and growth of white shrimps through regulating their metabolic characteristics and switching their metabolisms from material synthesis to energy metabolisms.
Keywords: *gut, microbiota structure, growth promoting probiotics, aquaculture, high-throughput sequencing*

Introduction

Shrimp is a good protein source with low-fat content, and it is the most popular seafood product around the world. According to the statistics of the Food and Agriculture Organization of the United Nations (FAO), crustacean culture productions have expanded from 5478.8 thousand tonnes in 2010 to 9386.5 thousand tonnes in 2018, with over 10% of annualized growth (FAO, 2020). The crustacean production is dominated by white shrimp (*Litopenaeus vannamei*), which has reached 4966.2 thousand tonnes and contributes to 52.9% of the crustacean production in 2018 (FAO, 2020). Therefore, shrimp aquaculture plays a significant role in the human nutrition supply and world economy, and exploration of low feed consumption, high efficiency, low pollution and ecological white shrimp aquaculture technology has been an important topic in aquaculture.

Trillions of microorganisms inhabit the metazoan intestinal tract (termed intestinal microbiota), and they play an important role in host nutrition, development, growth, and health (Nieuwdorp et al., 2014; Magnúsdóttir et al., 2015; Yan et al., 2016; Miyamoto et al., 2019; Butt and Volkoff, 2019). For instance, by colonizing conventional specific pathogen-free intestinal microbiota into sexually mature germ-free mice and antibiotic treatment of conventional mice, as well as supplementation of antibiotic-treated mice with short-chain fatty acids (SCFAs), Yan et al. (2016) demonstrate that intestinal microbiota

http://www.aloki.hu ● ISSN 1589 1623 (Print) ● ISSN 1785 0037 (Online)
DOI: http://dx.doi.org/10.15666/aeer/1906_49935005

promotes the production of insulin-like growth factor 1 (IFG-1) in liver and adipose tissue through producing SCFAs and improve serum levels of IFG-1, which causes an increase in bone formation and growth. Storelli et al. (2011) found that *Drosophila* microbiota promotes larval growth upon nutrient scarcity, and *Lactobacillus plantarum*, a commensal bacterium of the *Drosophila* intestine, is sufficient on its own to recapitulate the natural microbiota growth-promoting effect by modulating hormonal signals through TOR-dependent nutrient sensing. Zheng et al. (2017) report that intestinal microbiota promotes weight gain of both whole body and the gut in individual honey bees likely through mediating changes in host vitellogenin, insulin signaling, and gustatory response.

The role of intestinal microbiota in the growth and health of shrimps has also been widely investigated (Xiong et al., 2015, 2017; Anuta et al., 2016; Holt et al., 2020). For instances, Xiong et al. (2017) evaluated the composition and ecological processes of the intestinal bacterial communities in cohabitating retarded, overgrown, and normal white shrimps from identically managed ponds, and they found that intestinal bacterial community structures were distinct among the shrimp categories. Moreover, they found that changes in the intestinal microbiota were positively related to digestive activities, which subsequently affected shrimp growth rate (Xiong et al., 2017). Huang et al. (2020) reported that white shrimp intestinal microbiota may partly be derived from large particle of bioflocs, and these bacteria driven by large particles may play an important role in promoting shrimp growth.

Although the intestinal bacterial communities in cohabitating retarded, overgrown, and normal white shrimps were reported there were significant differences (Xiong et al., 2017), how these bacteria affect the growth of white shrimp remains unclear. Considering the intestinal microbiota is widely involved in the host's metabolic regulation through its own metabolic process, we speculated that there were significant differences in the metabolic processes of intestinal microbiota between fast-growing and slow-growing individuals in the same batch of white shrimp. To test the speculation, in this study, we compared the intestinal microbiota compositions and metabolic characteristics of fast-growing and slow-growing individuals in the same batch of white shrimp cultured in the same environment through high-throughput sequencing of 16S rRNA gene.

Materials and Methods

Sample collection

The experiment was conducted in the Qingjiang Base of the Zhejiang Institute of Marine Aquaculture. The seawater was taken from the Leqing Bay of East China Sea (salinity: 18.5±0.6‰). Mariculture seawater with salinity of 24 - 26‰ and pH of 8.2 ± 0.3 was obtained through secondary sand filtration in the impoundment pond. In the experiment, the larvae of the same pair of male and female white shrimps were cultured to approximately 1.0 cm, then 10000 of them were put into an indoor culture cement pond with 5 × 8 × 1.5 m for breeding. The water was changed 1/3 of total volume every 4 days, and the residual bait, shell, and dead prawns were cleaned. The larvae were bred for 130 days. During the experiment period, the larvae were fed with commercial prawn formula feed (Zhengda, Binzhou, China) at 6:00, 14:00, and 22:00. The daily feed weight was 15% of the prawn body weight. The pond was aerated continuously during the experiment period. The lighting cycle was natural light. The water temperature was 26 ± 0.5 °C.

http://www.aloki.hu ● ISSN 1589 1623 (Print) ● ISSN 1785 0037 (Online)
DOI: http://dx.doi.org/10.15666/aeer/1906_49935005

At the end of the experiment, the white shrimps were divided into two groups according to their body length and body weight: larger (L) and smaller (S) groups. Each 10 white shrimps of L and S groups were randomly collected. After measuring the body length, body weight, and body width, the intestinal tract of each sample was dissected under sterile condition and put into a 2 ml sterile centrifuge tube for subsequent extraction of total genomic DNA of intestinal microbiota. The hepatopancreas of the samples were also collected and stored at -80 °C for determination of the activities of amylase and lipase. In addition, each two white shrimps of L and S groups were randomly collected, and their intestines were dissected and stored in 4% paraformaldehyde universal tissue fixative (Biosharp, Hefei, China) for analysis of intestinal tissue section.

Determination of amylase and lipase activity of hepatopanceas

The α-amylase and lipase activity of hepatopancreas were determined using an α-amylase (α-AMS) assay kit (Nanjing Jiancheng Bioengineering Institute, Nanjing, China) and a lipase (LPS) assay kit (Nanjing Jiancheng Bioengineering Institute, Nanjing, China, China), respectively.

Analysis of intestinal tissue section

The fixed intestinal tissues of prawns were paraffin embedded and sectioned, and the sections were stained with hematoxylin and eosin according to the method described by Fischer et al. (2008a,b,c).

DNA extraction, PCR amplification and high-throughput sequencing

Fecal microbial DNA was extracted using a PowerSoil DNA isolation kit (QIAGEN, Germany). Then the V4-V5 hypervariable region of the prokaryotic 16S rRNA gene was amplified using the universal primers 515F and 909R with a 12-nt sample-specific barcode sequence included at the 5'-end of the 515F primer to distinguish samples (Ni et al., 2019, 2021). Polymerase chain reaction (PCR) was performed in duplicate with a 25-μL reaction mix containing 1 × PCR buffer, 0.25 U of Taq polymerase (Transgen, China), 0.2 mM of each deoxynucleoside triphosphate (Transgen, China), 10 μM of each primer (Sangon Biotech, China) and 10 ng microbial genomic DNA (Xiang et al., 2018). The thermal cycling procedure consisted at 94 °C for 10 min, followed by 30 cycles of 94 °C for 30 s, 56 °C for 30 s and 72 °C for 30 s, and finally 72 °C for 10 min (Xiang et al., 2018). Then the two PCR products from the same sample were mixed together and purified using a SanPrep DNA gel extraction kit (Sangon Biotech, China). All amplicons were pooled together with an equal molar amount from each sample and sequenced using an Illumina HiSeq system at Guangdong Meilikang Bio-Science, Ltd., China (Xiang et al., 2018).

Raw reads were merged using FLASH 1.2.8 (Magoc and Salzberg, 2011) and processed using QIIME pipeline 1.9.0 (Caporaso et al., 2010) as previously described (Xiang et al., 2018). Briefly, merged sequences were removed low-quality sequences and chimera sequences using QIIME pipeline 1.9.0 and UCHIME software (Edgar et al., 2011). Then, the high-quality sequences were clustered unto operational taxonomic units (OTUs) at 97% identity using UPARSE software (Edgar, 2013). Subsequently, all samples were randomly resampled to obtain the same number of sequences using the single_rarefaction.py command of QIIME pipeline 1.9.0. Taxonomy of each OTU was assigned using the RDP classifier (Wang et al., 2007) with gg_13_8_otus database.

http://www.aloki.hu ● ISSN 1589 1623 (Print) ● ISSN 1785 0037 (Online)
DOI: http://dx.doi.org/10.15666/aeer/1906_49935005

Metabolic characteristics of the intestinal microbiota were predicted using the PICRUSt software based on the intestinal microbiota compositions (Langille et al., 2013).

Data analysis

Data were presented as the mean ± standard error. Principal coordinate analysis (PCoA) was conducted using the QIIME pipeline 1.9.0. Nonparametric multivariate analysis of variance (PERMANOVA) (Anderson, 2001) was conducted using the vegan package (Dixon, 2003) of R 4.0.4 (R Core Team, 2013). Student's t test was used to compare the differences between larger and smaller prawn samples. Linear discriminant analysis effect size (LEfSe) (Segata et al., 2011) was analyzed on the Galaxy platform (http://huttenhower.sph.harvard.edu/galaxy/). Heatmap profiles of OUT compositions and KEGG ontologies were drown using pheatmap package of R 4.0.4.

Results

Differences in the size, the length of hindgut villi, and α-amylase and lipase activity of hepatopancreas between larger and smaller white shrimps

As expected, the body weight, body length, and body width of the L group were significantly higher than those of the S group (Student's t-test, $p < 0.001$; *Fig. 1A-1C*). The body weights of the L and S groups were 11.11 ± 0.32 g, and 5.30 ± 0.06 g (*Fig. 1A*). The body lengths of the L and S groups were 11.54 ± 0.16 cm, and 9.01 ± 0.07 cm (*Fig. 1B*). However, results of intestinal tissue sections showed that the lengths of hindgut villi between the L and S groups was no significant difference (Student's t-test, $p > 0.05$; *Fig. 1D-1F*). Moreover, α-amylase and lipase activities of hepatopancreas were also no significant difference between the L and S groups (Student's t-test, $p > 0.05$; *Fig. 2*).

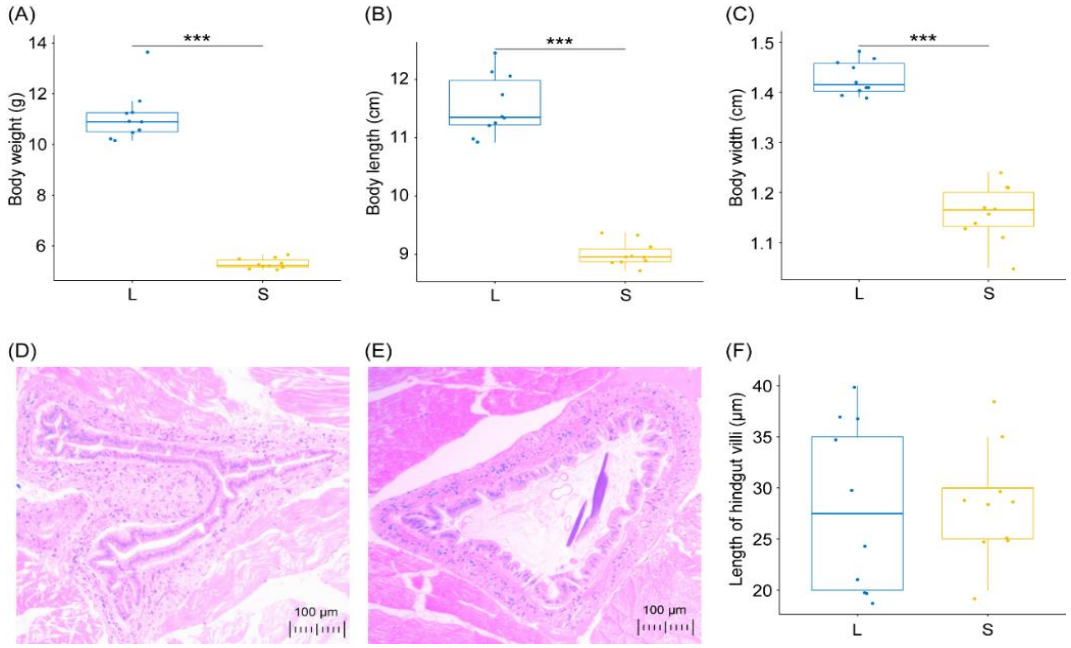

Figure 1. *Differences in the size and the length of hindgut villi of white shrimps. L, larger group; S, smaller group. (A), body weight; (B), body length; (C), body width; (D), hindgut section of larger group; (E), hindgut section of smaller group; (F), length of hindgut villi. ***, $p < 0.001$*

http://www.aloki.hu ● ISSN 1589 1623 (Print) ● ISSN 1785 0037 (Online)
DOI: http://dx.doi.org/10.15666/aeer/1906_49935005

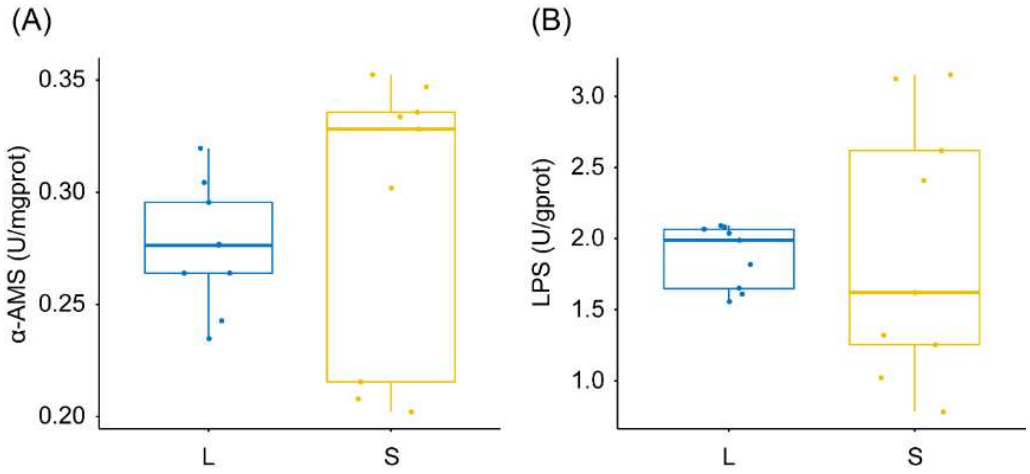

Figure 2. *α-Amylase and lipase activities of hepatopancreas between larger and smaller white shrimps. L, larger group; S, smaller group; α-AMS, α-amylase; LPS, lipase*

Composition differences of intestinal microbiota between larger and smaller white shrimps

A total of 1,336,738 high-quality sequences were obtained from the 20 intestinal samples. Finally, 26,747 high-quality sequences were randomly selected from each sample for further analysis. PCoA with PERMANOVA showed that there was no significant difference in the OTU compositions of intestinal microbiota between the L and S groups (PERMANOVA, $F = 1.002$, $p = 0.408$; *Fig. 3A*). Except for a few OTUs that could not be classified into any phylum, other OTUs were classified into 60 phyla (3 Archaea phyla and 57 Bacteria phyla), in which Proteobacteria, Bacteroidetes, Tenericutes, Acidobacteria, Actinobacteria, Chloroflexi, Cyanobacteria, Firmicutes, Fusobacteria, Nitrospirae, and Planctomycetes dominated the intestinal microbiota (*Fig. 3B*). Except the relative abundance of Tenericutes in the L group was significantly higher than that in the S group, there was no significant difference in other dominant phyla between the L and S groups (White's non-parametric t-test, $p > 0.05$; *Fig. 3C*). It was worth noting that Proteobacteria has an absolute dominance in these intestinal microbiota, and its relative abundance was over 70% in all samples, and reached to 98.20% in the sample L1 (*Fig. 3B* and *3C*). This was mainly due to the high relative abundance of *Vibrio* belonging to Proteobacteria in these intestinal microbiota, with a relative abundance of $68.95 \pm 0.04\%$. However, there was no significant difference in the relative abundance of *Vibrio* between the L and S groups (Student's t-test, $t = 0.16$, $p = 0.87$; *Fig. 3D*).

To confirm that there is no significant difference in the intestinal microbiota between the L and S groups, we further analyzed the dominant OTUs in more detail. Our results showed that *Shewanella algae* and *Neptunomonas* sp. were significantly enriched in the L group, while *Delftia* sp., *Hydrogenophaga* sp., *Pseudomonas* sp., *Synechococcus* sp., *Methylibium* sp., *Acidovorax* sp., *Limnohabitans* sp., *Burkholderia* sp., *Candidatus Koribacter* sp., and *Vogesella* sp. were enriched in the S group (LEfSe, $\log_{10}$ LDA score > 2; *Fig. 4A* and *4B*). Heatmap profile showed a similar result (*Fig. 4C*).

http://www.aloki.hu ● ISSN 1589 1623 (Print) ● ISSN 1785 0037 (Online)
DOI: http://dx.doi.org/10.15666/aeer/1906_49935005

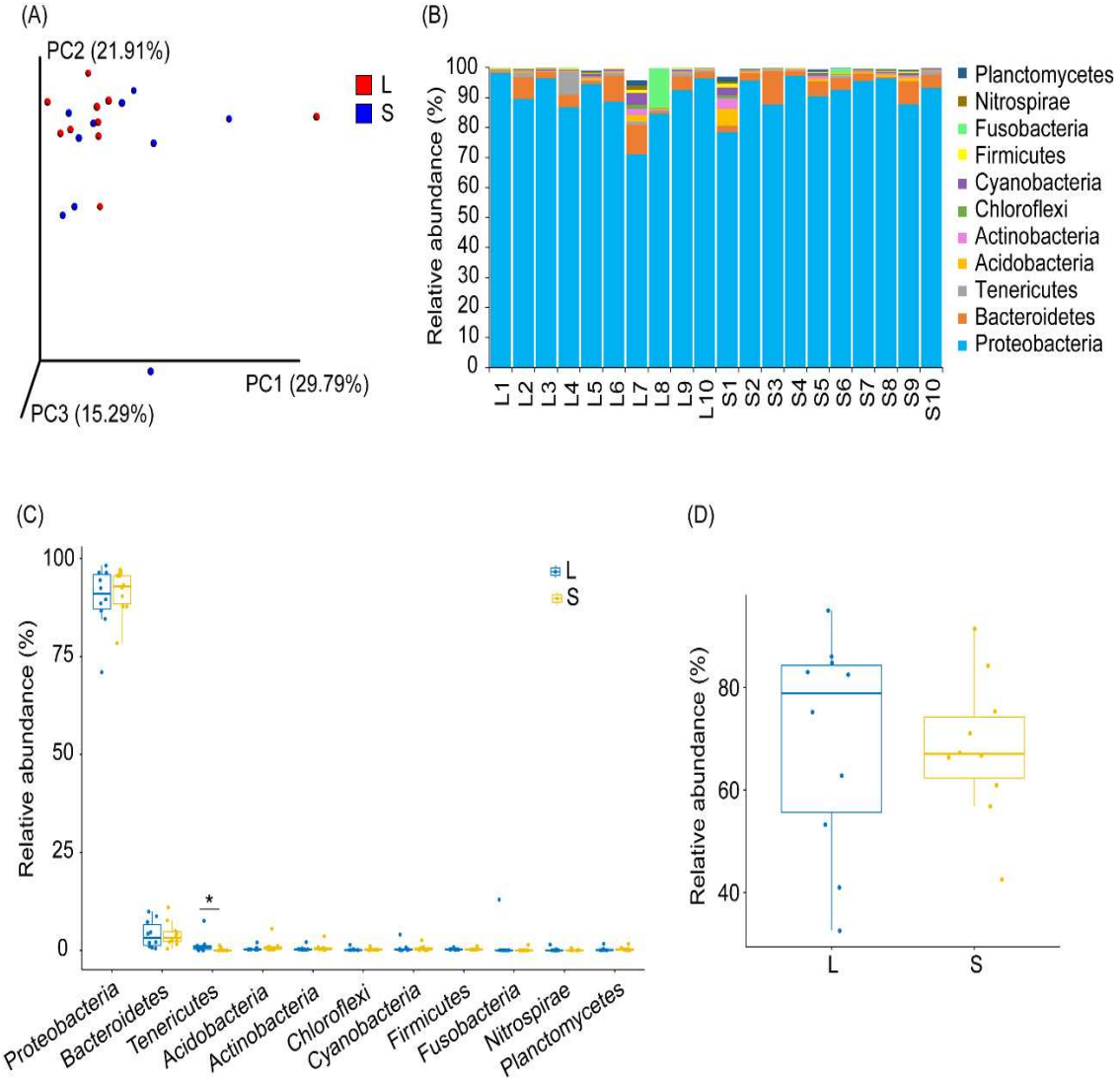

Figure 3. *Intestinal microbiota compositions of larger and smaller white shrimps. (A), PCoA profile; (B), relative abundances of dominant phyla; (C), boxplots showed difference of dominant phyla; (D), boxplot showed the relative abundance of Vibrio. L, larger group; S, smaller group. *, $P < 0.05$*

Potential metabolic differences of intestinal microbiota between larger and smaller prawn samples

To analyze the metabolic characteristics of intestinal microbiota of the L and S white shrimps, metabolic characteristics of the intestinal microbiota were predicted using the PICRUSt software based on the intestinal microbiota compositions. There were significant differences in 132 KEGG orthologies (KOs) between the L and S groups, in which the enhanced KOs in the L group were mainly involved in energy metabolisms and hydrolases, while the enhanced KOs in the S group were mainly involved in the cell structure synthesis, such as outer membrane protein, periplasmic protein, ribonucleotide synthase, and large subunit ribosomal protein (*Fig. 5*).

http://www.aloki.hu ● ISSN 1589 1623 (Print) ● ISSN 1785 0037 (Online)
DOI: http://dx.doi.org/10.15666/aeer/1906_49935005

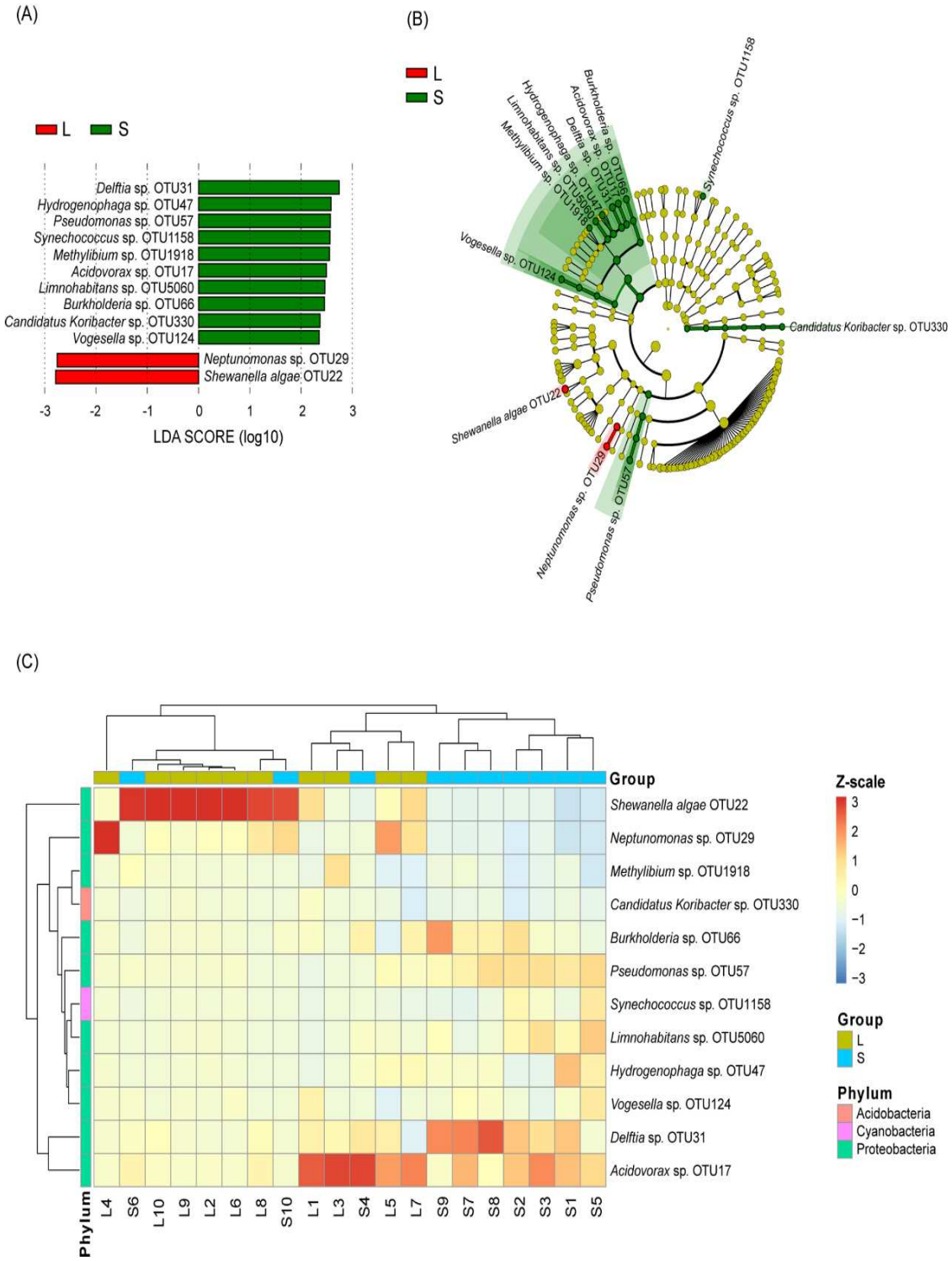

Figure 4. *Different OTUs of intestinal microbiota between larger and smaller white shrimps. L, larger group; S, smaller group*

http://www.aloki.hu ● ISSN 1589 1623 (Print) ● ISSN 1785 0037 (Online)
DOI: http://dx.doi.org/10.15666/aeer/1906_49935005

Figure 5. *Heatmap profile shows significantly different KEGG ontologies between larger and smaller white shrimps. L, larger group; S, smaller group. 4-HBCR, 4-hydroxybenzoyl-CoA reductase; PPIB, peptidyl-prolyl cis-trans isomerase B; 3-Oxsm, 3-oxoacyl-ACP synthase; OPDS, octaprenyl-diphosphate synthase; ANMK, anhydro-N-acetylmuramic acid kinase; CMT, cysteine methyltransferase; RPAR, regulatory protein of adaptative response*

http://www.aloki.hu ● ISSN 1589 1623 (Print) ● ISSN 1785 0037 (Online)
DOI: http://dx.doi.org/10.15666/aeer/1906_49935005

Discussion

Intestinal microbiota plays an important role in various physiological processes of host, such as growth, metabolism, immunity, and health through participating in the metabolism processes of host (Nieuwdorp et al., 2014; Magnúsdóttir et al., 2015; Yan et al., 2016; Wang et al., 2016; Oliphant and Allen Vercoe, 2019; Miyamoto et al., 2019; Butt and Volkoff, 2019; Ni et al., 2021). Although intestinal microbiota is closely related to host energy metabolism and obesity (Tremaroli and Bäckhed, 2012; Miyamoto et al., 2019), and it has been reported that there were significantly differences in intestinal microbiota between cohabitating retarded, overgrown, and normal shrimps (Xiong et al., 2017), our results did not show a significant difference in the whole intestinal microbiota compositions between the L and S groups of white shrimps (*Fig. 3*). Except for the significant differences in body length, body weight, and body width caused by sampling selection, the intestinal tissue structure and the α-amylase and lipase activities of hepatopancreas were no significant difference between the larger and smaller white shrimps (*Figs. 1* and *2*). These results indicated that the growth of white shrimp was not directly affected by the structure changes of intestinal microbiota. However, we still detected significantly different bacteria of intestinal microbiota between the S and L groups (*Fig. 4*).

Shewanella and *Neptunomonas* are two bacterial genera which are widely distributed in marine and participate in energy metabolism and material circulation (Dubiel et al., 2002; Beleneva et al., 2009; Bargiela et al., 2015; Light et al., 2019). Although there are a few reports about *Shewanella* pathogens (Beleneva et al., 2009), there is no *Shewanella* pathogen reported in shrimps. *Neptunomonas* sp. 0536 was reported as probiotic to suppress naturally occurring vibrios in the culture environment of healthy mussel larvae (Kesarcodi-Watson et al., 2010). The enriched bacteria in the S group, such as those in *Delftia*, *Hydrogenophaga*, *Synechococcus* and *Methylibium*, were also widely reported as degrading bacteria of organic pollutants (Streger et al., 2002; Moore et al., 2002; Choi et al., 2003; Kane et al., 2007; Jørgensen et al., 2009; Zhang et al., 2010). These results implied that these significantly different bacteria might affect the growth of enriched in the S group through participating in different material or energy metabolisms.

Intestinal microbiota plays an important role in host material and energy metabolisms (Tremaroli and Bäckhed, 2012). However, due to different characteristics of energy and substance transfer, energy is easier to be shared between the host and the intestinal microbiota, while substances are more difficult to be shared between the host and the intestinal microbiota except those extracellular secondary metabolites. Moreover, intestinal microbiota utilizes intestinal substances to synthesize their cell structures, and compete with the host for nutrients, which may limit the host's access to nutrients. Our results showed that the functional genes enhanced in the L group were mainly involved in enzymes of energy metabolism and hydrolases, while those in the S group were mainly involved in cell structure synthesis. This might be an important reason for the growth difference between the L and S groups.

Compositions of intestinal microbiota is easily affected by external environmental factors (Xiong et al., 2015; Zhao et al., 2018; Fan et al., 2019; Zhang et al., 2021). Therefore, in this study, the group internal error of intestinal microbiota caused by the undetected factors covered the difference between the L and S groups, which leaded to no significant difference in the compositions of intestinal microbiota between the L and S groups was detected. These results showed that in the study of the relationship between

http://www.aloki.hu ● ISSN 1589 1623 (Print) ● ISSN 1785 0037 (Online)
DOI: http://dx.doi.org/10.15666/aeer/1906_49935005

intestinal microbiota and host, we should not only focus on the composition of intestinal microbiota, especially if the environmental variables are not well controlled.

Conclusions

Our results showed that there was no significant difference in the composition of intestinal microbiota between larger and smaller white shrimps. However, *Shewanella algae* and *Neptunomonas* sp. were significantly enriched in the L group, while *Delftia* sp., *Hydrogenophaga* sp., *Pseudomonas* sp., *Synechococcus* sp., *Methylibium* sp., *Acidovorax* sp., *Limnohabitans* sp., *Burkholderia* sp., *Candidatus Koribacter* sp., and *Vogesella* sp. were enriched in the S group. Moreover, the intestinal microbiota might promote the energy metabolism and growth of white shrimps through regulating their metabolic characteristics and switching their metabolisms from material synthesis to energy metabolisms. However, further study is needed on what factors cause the differences of intestinal microbiota metabolic characteristics between the L and S groups, and how to regulate the intestinal microbiota metabolic characteristics to promote the growth of white shrimps.

Acknowledgements. This work was supported by the National Key Research and Development Plan of China (grant No. 2020YFD0900801), the Major Science and Technology Project of New Agricultural Varieties Breeding in Zhejiang Province (grant No. 2021C02025-5) and the Agricultural New Variety Selection and Breeding Cooperation Group Project of Wenzhou City (grant No. 2019ZX002-01). We would like to thank anonymous technicians at Guangdong Meilikang Bio-Science Ltd., China for assistance with data re-analysis.

REFERENCES

[1] Anderson, M. J. (2001): A new method for non-parametric multivariate analysis of variance. – Austral Ecology 26: 32-46.

[2] Anuta, J. D., Buentello, A., Patnaik, S., Hume, M. E., Mustafa, A., Gatlin, D. M. III, Lawrence, A. L. (2016): Effects of dietary supplementation of a commercial prebiotic Previda® on survival, growth, immune responses and gut microbiota of Pacific white shrimp, *Litopenaeus vannamei*. – Aquaculture Nutrition 22(2): 410-418. doi:10.1111/anu.12257.

[3] Bargiela, R., Mapelli, F., Rojo, D., Chouaia, B., Tornés, J., Borin, S., Richter, M., Del Pozo, M. V., Cappello, S., Gertler, C., et al. (2015): Bacterial population and biodegradation potential in chronically crude oil-contaminated marine sediments are strongly linked to temperature. – Scientific Reports 5: 11651.

[4] Beleneva, I. A., Magarlamov, T. Y., Eliseikina, M. G., Zhukova, N. V. (2009): Biochemical and pathogenic properties of the natural isolate of *Shewanella algae* from Peter the Great Bay, Sea of Japan. – Journal of Invertebrate Pathology 102: 250-255. doi:10.1016/j.jip.2009.09.001.

[5] Butt, R. L., Volkoff, H. (2019): Gut microbiota and energy homeostasis in fish. – Frontiers in Endocrinology 10: 9. doi:10.3389/fendo.2019.00009.

[6] Caporaso, J. G., Kuczynski, J., Stombaugh, J., Bittinger, K., Bushman, F. D., Costello, E. K., et al. (2010): QIIME allows analysis of high-throughput community sequencing data. – Nature Methods 7: 335-336. doi:10.1038/nmeth.f.303.

[7] Choi, M. H., Lee, H. J., Rho, J. K., Yoon, S. C., Nam, J. D., Lim, D., Lenz, R. W. (2003): Biosynthesis and local sequence specific degradation of poly (3-hydroxyvalerate-c o-4-hydroxybutyrate) in *Hydrogenophage pseudoflava*. – Biomacromolecules 4: 38-45.

http://www.aloki.hu ● ISSN 1589 1623 (Print) ● ISSN 1785 0037 (Online)
DOI: http://dx.doi.org/10.15666/aeer/1906_49935005

[8] Dixon, P. (2003): VEGAN, a package of R functions for community ecology. – Journal of Vegetation Science 14: 927-930. doi:10.1111/j.1654-1103.2003.tb02228.x.
[9] Dubiel, M., Hsu, C. H., Chien, C. C., Mansfeld, F., Newman, D. K. (2002): Microbial iron respiration can protect steel from corrosion. – Applied and Environmental Microbiology 68(3): 1440-1445. doi:10.1128/AEM.68.3.1440-1445.2002.
[10] Edgar, R. C. (2013): UPARSE: Highly accurate OTU sequences from microbial amplicon reads. – Nature Methods 10: 996-998. doi:10.1038/nmeth.2604.
[11] Edgar, R. C., Haas, B. J., Clemente, J. C., Quince, C., Knight, R. (2011): UCHIME improves sensitivity and speed of chimera detection. – Bioinformatics 27: 2194-2200. doi:10.1093/bioinformatics/btr381.
[12] Fan, J., Chen, L., Mai, G., Zhang, H., Yang, J., Deng, D., Ma, Y. (2019): Dynamics of the gut microbiota in developmental stages of *Litopenaeus vannamei* reveal its association with body weight. – Scientific Reports 9: 734. doi:10.1038/s41598-018-37042-3.
[13] FAO. (2020): The State of World Fisheries and Aquaculture 2020. Sustainability in action. – The Organization of Food and Agriculture of the United Nations, Rome. http://www.fao.org/3/ca9229en/ca9229en.
[14] Fischer, A. H., Jacobson, K. A., Rose, J., Zeller, R. (2008a): Paraffin embedding tissue samples for sectioning. – Cold Spring Harbor Protocols 3(5): prot4989. doi:10.1101/pdb.prot4989.
[15] Fischer, A. H., Jacobson, K. A., Rose, J., Zeller, R. (2008b): Cutting sections of paraffin-embedded tissues. – Cold Spring Harbor Protocols 3(5): prot4987. doi:10.1101/pdb.prot4987.
[16] Fischer, A. H., Jacobson, K. A., Rose, J., Zeller, R. (2008c): Hematoxylin and eosin staining of tissue and cell sections. – Cold Spring Harbor Protocols 3(5): prot4986. doi:10.1101/pdb.prot4986.
[17] Holt, C. C., Bass, D., Stentiford, G. D., van der Giezen, M. (2020): Understanding the role of the shrimp gut microbiome in health and disease. – Journal of Invertebrate Pathology, In press. doi:10.1016/j.jip.2020.107387.
[18] Huang, L., Guo, H., Chen, C., Huang, X., Chen, W., Bao, F., Liu, W., Wang, S., Zhang, D. (2020): The bacteria from large-sized bioflocs are more associated with the shrimp gut microbiota in culture system. – Aquaculture 523: 735159. doi:10.1016/j.aquaculture.2020.735159.
[19] Jørgensen, N. O. G., Brandt, K. K., Nybroe, O., Hansen, M. (2009): *Delftia lacustris* sp. nov., a peptidoglycan-degrading bacterium from fresh water, and emended description of *Delftia tsuruhatensis* as a peptidoglycan-degrading bacterium. – International Journal of Systematic and Evolutionary Microbiology 59: 2195-2199. doi:10.1099/ijs.0.008375-0.
[20] Kane, S. R., Chakicherla, A. Y., Chain, P. S. G., Schmidt, R., Shin, M. W., Legler, T. S., Scow, K. M., Larimer, F. W., Lucas, S. M., Richardson, P. M., Hristova, K. R. (2007): Whole-genome analysis of the methyl tert-butyl ether-degrading beta-proteobacterium *Methylibium petroleiphilum* PM1. – Journal of Bacteriology 189(5): 1931-1945.
[21] Kesarcodi-Watson, A., Kaspar, H., Lategan, J., Gibson, L. (2010): *Alteromonas macleodii* 0444 and *Neptunomonas* sp. 0536, two novel probiotics for hatchery-reared Greenshell™ mussel larvae, *Perna canaliculus*. – Aquaculture 309(1-4): 49-55. 10.1016/j.aquaculture.2010.09.019.
[22] Langille, M. G. I., Zaneveld, J., Caporaso, J. G., McDonald, D., Knights, D., Reyes, J. A., Clemente, J. C., Burkepile, D. E., Thurber, R. L. V., Knight, R., Beiko, R. G., Huttenhower, C. (2013): Predictive functional profiling of microbial communities using 16S rRNA marker gene sequences. – Nature Biotechnology 31(9): 814-921. doi:10.1038/nbt.2676.
[23] Light, S. H., Méheust, R., Ferrell, J. L., Cho, J., Deng, D., Agostoni, M., Iavarone, A. T., Banfield, J. F., D'Orazio, S. E. F., Portnoy, D. A. (2019): Extracellular electron transfer powers flavinylated extracellular reductases in Gram-positive bacteria. – Proceeding of the National Academy of Sciences of the United States of America 116(52): 26892-26899. doi:10.1073/pnas.1915678116.

http://www.aloki.hu ● ISSN 1589 1623 (Print) ● ISSN 1785 0037 (Online)
DOI: http://dx.doi.org/10.15666/aeer/1906_49935005

[24] Magnúsdóttir, S., Ravcheev, D., de Crécy-Lagard, V., Thiele, I. (2015): Systematic genome assessment of B-vitamin biosynthesis suggests co-operation among gut microbes. – Frontiers in Genetics 6: 148. doi:10.3389/fgene.2015.00148.

[25] Magoc, T., Salzberg, S. L. (2011): FLASH: Fast length adjustment of short reads to improve genome assemblies. – Bioinformatics 27: 2957-2963. doi:10.1093/bioinformatics/btr507.

[26] Miyamoto, J., Igarashi, M., Watanabe, K., Karaki, S.-I., Mukouyama, H., Kishino, S., Li, X., Ichimura, A., Irie, J., Sugimoto, Y., Mizutani, T., Sugawara, T., Miki, T., Ogawa, J., Drucker, D. J., Arita, M., Itoh, H., Kimura, I. (2019): Gut microbiota confers host resistance to obesity by metabolizing dietary polyunsaturated fatty acids. – Nature Communications 10: 4007. doi:10.1038/s41467-019-11978-0.

[27] Moore, L. R., Post, A. F., Rocap, G., Chisholm, S. W. (2002): Utilization of different nitrogen sources by the marine cyanobacteria *Prochlorococcus* and *Synechococcus*. – Limnology and Oceanography 47(4): 989-996.

[28] Ni, J., Huang, R., Zhou, H., Xu, X., Li, Y., Cao, P., Zhong, K., Ge, M., Chen, X., Hou, B., Yu, M., Peng, B., Li, Q., Zhang, P., Gao, Y. (2019): Analysis of the relationship between the degree of dysbiosis in gut microbiota and prognosis at different stages of primary hepatocellular carcinoma. – Frontiers in Microbiology 10: 1458. doi:10.3389/fmicb.2019.01458.

[29] Ni, J., Fu, C., Huang, R., Li, Z., Li, S., Cao, P., Zhong, K., Ge, M., Gao, Y. (2021): Metabolic syndrome cannot mask the changes of faecal microbiota compositions caused by primary hepatocellular carcinoma. – Letters in Applied Microbiology 73(1): 73-80. doi:10.1111/lam.13477.

[30] Nieuwdorp, M., Gilijamse, P. W., Pai, N., Kaplan, L. M. (2014): Role of the microbiome in energy regulation and metabolism. – Gastroenterology 146(6): 1525-1533.

[31] Oliphant, K., Allen-Vercoe, E. (2019): Macronutrient metabolism by the human gut microbiome: major fermentation byproducts and their impact on host health. – Microbiome 7: 91. doi:10.1186/s40168-019-0704-8.

[32] R Core Team. (2013): R: A Language and Environment for Statistical Computing. – R Foundation for Statistical Computing, Vienna, Austria. URL http://www.R-project.org/.

[33] Segata, N., Izard, J., Waldron, L., Gevers, D., Miropolsky, L., Garrett, W. S., Huttenhower, C. (2011): Metagenomic biomarker discovery and explanation. – Genome Biology 12: R60. doi:10.1186/gb-2011-12-6-r60.

[34] Storelli, G., Defaye, A., Erkosar, B., Hols, P., Royet, J., Leulier, F. (2011): *Lactobacillus plantarum* promotes *Drosophila* systemic growth by modulating hormonal signals through TOR-dependent nutrient sensing. – Cell Metabomism 14: 403-414. doi:10.1016/j.cmet.2011.07.012.

[35] Streger, S. H., Vainberg, S., Dong, H., Hatzinger, P. B. (2002): Enhancing transport of *Hydrogenophaga flava* ENV735 for bioaugmentation of aquifers contaminated with methyl *tert*-butyl ether. – Applied and Environmental Microbiology 68(11): 5571-5579. doi:10.1128/AEM.68.11.5571-5579.2002.

[36] Tremaroli, V., Bäckhed, F. (2012): Functional interactions between the gut microbiota and host metabolism. – Nature 489: 242-249. doi:10.1038/nature11552.

[37] Wang, Q., Garrity, G. M., Tiedje, J. M., Cole, J. R. (2007): Naïve Bayesian classifier for rapid assignment of rRNA sequences into the new bacterial taxonomy. – Applied and Environmental Microbiology 73: 5261-5267. doi:10.1128/AEM.00062-07.

[38] Wang, Z., Koonen, D., Hofker, M., Fu, J. (2016): Gut microbiome and lipid metabolism: from associations to mechanisms. – Current Opinion in Lipidology 27(3): 216-224. doi:10.1097/MOL.0000000000000308.

[39] Xiang, J., He, T., Wang, P., Xie, M., Xiang, J., Ni, J. (2018): Opportunistic pathogens are abundant in the gut of cultured giant spiny frog (*Paa spinosa*). – Aquaculture Research 49: 2033-2041. doi:10.1111/are.13660.

http://www.aloki.hu ● ISSN 1589 1623 (Print) ● ISSN 1785 0037 (Online)
DOI: http://dx.doi.org/10.15666/aeer/1906_49935005

[40] Xiong, J., Wang, K., Wu, J., Qiuqian, L., Yang, K., Qian, Y., Zhang, D. (2015): Changes in intestinal bacterial communities are closely associated with shrimp disease severity. – Applied Microbiology and Biotechnology 99: 6911-6919. doi:10.1007/s00253-015-6632-z.

[41] Xiong, J., Dai, W., Zhu, J., Liu, K., Dong, C., Qiu, Q. (2017): The underlying ecological processes of gut microbiota among cohabitating retarded, overgrown and normal shrimps. – Microbial Ecology 73: 988-999.

[42] Yan, J., Herzog, J. W., Tsang, K., Brennan, C. A., Bower, M. A., Garrett, W. S., Sartor, B. R., Aliprantis, A. O., Charles, J. F. (2016): Gut microbiota induce IGF-1 and promote bone formation and growth. – Proceeding of the National Academy of Sciences of the United States of America 113(47): E7554-E7563. doi.org/10.1073/pnas.1607235113.

[43] Zhang, L. L., He, D., Chen, J. M., Liu, Y. (2010): Biodegradation of 2-chloroaniline, 3-chloroaniline, and 4-chloroaniline by a novel strain *Delftia tsuruhatensis* H1. – Journal of Hazardous Materials 179(1-3): 875-882. doi: 10.1016/j.jhazmat.2010.03.086.

[44] Zhang, X., Li, X., Lu, J., Qiu, Q., Chen, J., Xiong, J. (2021): Quantifying the importance of external and internal sources to the gut microbiota in juvenile and adult shrimp. – Aquaculture 531: 735910. doi:10.1016/j.aquaculture.2020.735910.

[45] Zhao, Y., Duan, C., Zhang, X., Chen, H., Ren, H., Yin, Y., Ye, L. (2018): Insights into the gut microbiota of freshwater shrimp and its associations with the surrounding microbiota and environmental factors. – Journal of Microbiology and Biotechnology 28(6): 946-956. doi:10.4014/jmb.1710.09070.

[46] Zheng, H., Powell, J. E., Steele, M. I., Dietrich, C., Moran, N. A. (2017): Honeybee gut microbiota promotes host weight gain via bacterial metabolism and hormonal signaling. – Proceedings of the National Academy of Sciences of the United States of America 114(18): 4775-4780. doi:10.1073/pnas.1701819114.

http://www.aloki.hu ● ISSN 1589 1623 (Print) ● ISSN 1785 0037 (Online)
DOI: http://dx.doi.org/10.15666/aeer/1906_49935005

DETERMINATION OF THE RELATIONSHIP BETWEEN ORGANIC FARMING AREA AND AGRICULTURAL ADDED VALUE IN SOME EUROPEAN UNION COUNTRIES WITH PANEL ARDL ANALYSIS

ÇUKUR, F.[1] – IŞIN, F.[2] – ÇUKUR, T.[3*]

[1]*Department of Management and Organization, Milas Vocational School, Muğla Sıtkı Koçman University, 48200 Milas, Muğla, Turkey*

[2]*Department of Agricultural Economics, Agricultural Faculty, Ege University, 35100 Bornova, İzmir, Turkey*

[3]*Department of Marketing and Advertising, Milas Vocational School, Muğla Sıtkı Koçman University, 48200 Milas, Muğla, Turkey*

[*]*Corresponding author*
e-mail: tayfun.cukur@hotmail.com; phone: +90-252-211-3263; fax: +90-252-211-1879

(Received 1st Oct 2021; accepted 17th Jun 2021)

Abstract. In the current study, the relationship between organic farming area and agricultural added value in some European Union countries was examined for the period of 2010-2018. Germany, Austria, France, Spain, Italy, Greece, the Netherlands, Denmark and Sweden were included in the study. Dynamic panel ARDL model was used. In the countries examined according to the Pooled Mean-Group (PMG) estimator, a significant positive relationship was found between organic farming area and agricultural added value in the long-term. Since a positive correlation was found between organic farming area and agricultural added value in the study, it was concluded that that organic farming areas, correspondingly, organic agricultural production should be increased in order to increase agricultural added value. In the study, a bidirectional causality relationship was also determined between agricultural added value and organic farming area.
Keywords: *cointegration test, cross-section dependence test, unit root test, homogeneity test, PMG*

Introduction

Increasing world population and industrialization have created a significant pressure on the environment and natural resources. Chemical pesticides and fertilizers have been used extensively in order to feed the increasing population. Mankind has turned to conventional agricultural practices in order to meet the demand for agricultural products and increase their production. This has led to significant increases in the amount of agricultural production, and the amount of food and fibre production increased. However, the intensive use of inputs in agriculture has led to the deterioration of soil structure and land degradation. Thus, it has gained importance to develop environmentally friendly production methods that produce without the use of chemicals, do not harm the environment and natural resources, and are based on sustainability in production. On the other hand, the increase in people's demands for healthy food has led to the development of organic agriculture in the world. Organic agriculture has come to the fore around the world due to the observance that materials used and practices performed to increase yield in agricultural production harm the environment in different ways and due to the increase in environmental concerns (Bahsi, 2020).

http://www.aloki.hu ● ISSN 1589 1623 (Print) ● ISSN1785 0037 (Online)
DOI: http://dx.doi.org/10.15666/aeer/1906_50075016

Organic agriculture is a production system that sustains the health of soils, ecosystems, and people. It relies on ecological processes, biodiversity, and cycles adapted to local conditions, rather than the use of inputs with adverse effects. Organic agriculture combines tradition, innovation and science to benefit the shared environment and promote fair relationships and a good quality of life for all involved.

The four principles of organic agriculture are:

• Sustaining and enhancing the health of the soil, plants, animals, humans, and the planet as one and indivisible.

• It should be based on living ecological systems and cycles, and work with them, emulate them and help sustain them.

• Building on relationships that ensure fairness with regard to the common environment and life opportunities.

• Managing in a precautionary and responsible manner to protect the health and well-being of current and future generations and the environment (Cukur, 2015).

Organic production can be defined as a system that is carried out by using methods that reduce the damage to the environment as much as possible and is subject to the control of authorized institutions at every stage of the production and consumption chain (Ayla and Altıntaş, 2017).

Agricultural added value is to create an improvement in the physical condition and material value of the agricultural product produced. The improvement in the value of the agricultural raw material or product also adds originality to the product (Akyol, 2018). The agricultural sector provides added value to the country's economy by supplying the necessary raw materials for industrial production as well as meeting the need for animal and plant foodstuffs required for nutrition. Added value represents the difference between the monetary value of goods and services produced and the inputs used in their production. From a macro point of view, agricultural added value refers to the numerical net production reached as a result of the difference between the sum of the outputs in the agricultural sector and that of the inputs (Erdinç and Aydınbaş, 2021). There are two ways to increase agricultural added value. While the first of these is to widen the difference between gross output and inputs subject to production by increasing production efficiency, the other is to increase the margin between the gross output value and the cost of intermediate inputs as a result of changing the amount, function and shape as well as the characteristics of the product and production method (Akyol, 2018).

In the current study, the relationship between agricultural added value and organic farming area in some European Union countries was examined for the period of 2000-2018.

Materials and Methods

Agricultural added value (agriculture, forestry, fisheries) data of the countries used in the study were obtained from the Food and Agriculture Organization of the United Nations (FAO), and organic agricultural data were obtained from the Research Institute of Organic Agriculture (FIBL). Agricultural added values of the countries are in US$ obtained with the fixed prices of 2015. The organic agricultural areas of the countries represent the share (%) of the organic agricultural area in the total agricultural area. The years 2010-2018 were the period investigated in the study. Considering the data availability criterion, Germany, Austria, France, Spain, Italy, Greece, the Netherlands, Denmark and Sweden were included in the study.

http://www.aloki.hu ● ISSN 1589 1623 (Print) ● ISSN1785 0037 (Online)
DOI: http://dx.doi.org/10.15666/aeer/1906_50075016

In the current study, cross-section dependence test, unit root test, homogeneity test, panel Granger causality test and ARDL cointegration test were applied. In the study, panel data were used instead of time series. Due to the simultaneous presence of time series and cross-section data observations, the panel data allows the researcher to work with more data. In this case, the number of observations and thus the degree of freedom increase. Thus, the degree of multicollinearity between explanatory variables decreases and the efficiency and reliability of econometric estimates increase. In addition, the use of panel data also allows the analysis of economic problems that cannot be solved with only cross-section data or time series data (Tatoğlu, 2021). ARDL model is being used for decades to model the relationship between economic variables in time series analyses (Kripfganz and Schneider, 2016). In the analysis of the collected data, Stata program was used.

Results

Agricultural added values and share of organic farming areas of the countries

Agricultural added values of the countries examined are shown by years in *Figure 1*. In general, agricultural added values follow a stagnant course. As of 2018, the countries with the highest agricultural added value are France, Italy and Spain.

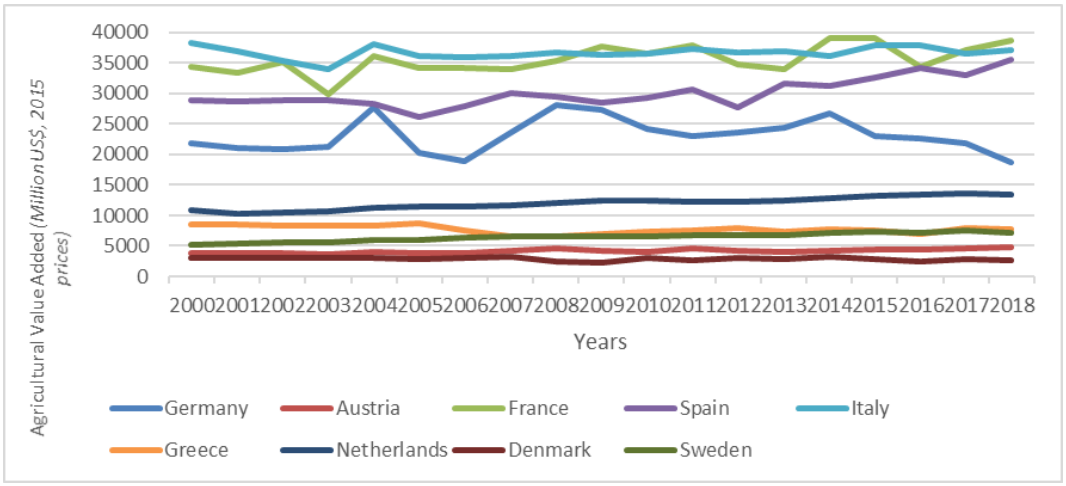

Figure 1. *Agricultural added values of the countries (Million US$, 2015 prices) (FAO, 2021)*

The share of organic farming areas (%) in the total agricultural area of the examined countries is shown in *Figure 2*. It can be said that organic farming areas tend to increase over time in all the countries. As of 2018, the countries with the highest share of organic farming areas in the total agricultural area are Austria, Sweden and Italy.

Cross-section dependence results

Cross-section dependence means that there is a correlation between the error terms calculated for each unit of the panel data model (Tatoğlu, 2021). The CD test was used to test the cross-section dependence in the study. The CD test is formulated as follows (Pesaran, 2004).

http://www.aloki.hu ● ISSN 1589 1623 (Print) ● ISSN1785 0037 (Online)
DOI: http://dx.doi.org/10.15666/aeer/1906_50075016

$$CD = \sqrt{\frac{2T}{N(N-1}}\left(\sum_{i=1}^{N-1}\sum_{j=i+1}^{N}\hat{p}_{ij}\right) \quad \text{(Eq.1)}$$

As seen in *Table 1*, p values are smaller than 0.05. In other words, the H_o hypothesis, which accepts that there is no cross-section dependence, is rejected. According to the test results, there is cross-section dependence in the series.

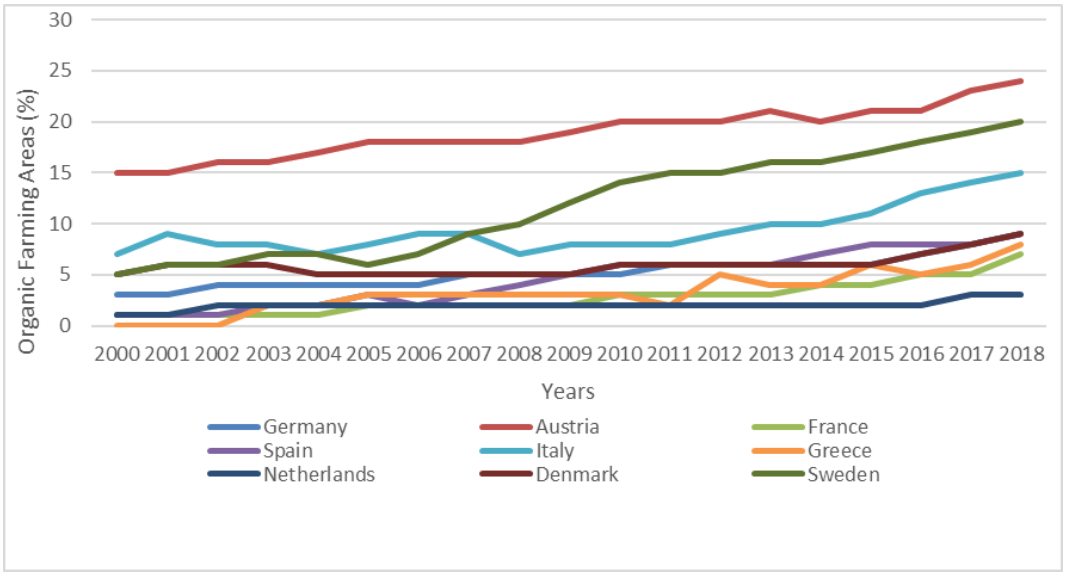

Figure 2. *Share of organic farming areas (%) (FIBL, 2021)*

Table 1. *Cross-section dependence test*

Variable	CD-test	p-value	corr.	abs(corr)
value_added	4.22	0.000	0.161	0.407
organic_area	21.61	0.000	0.826	0.826

Unit root test results

Since there is cross-section dependence between the series in the study, it will be appropriate to work with second generation unit root tests that take this situation into account. For this reason, the Fisher Extended Dickey Fuller Panel Unit Root test was used in the study.

The Dickey Fuller test is illustrated in theory and practice as follows:

$$\Delta Y_t = \delta Y_{t-1} + u_t \quad \text{(Eq.2)}$$

(constant and no trend)

$$\Delta Y_t = b_0 + \delta Y_{t-1} + u_t \quad \text{(Eq.3)}$$

(constant term and no trend)

http://www.aloki.hu ● ISSN 1589 1623 (Print) ● ISSN1785 0037 (Online)
DOI: http://dx.doi.org/10.15666/aeer/1906_50075016

$$\Delta Y_t = b_0 + b_1 t + \delta Y_{t-1} + u_t \quad \text{(Eq.4)}$$

By finding constant term and trend regressions in addition to these, MacKinnon critical values are obtained with the series τ or DF statistics.

If the error term is with u_t autocorrelation, then the *Equation (5)* is written as follows;

$$\Delta Y_t = b_0 + b_1 t + \delta Y_{t-1} + \alpha_i \sum_{i=1}^{m} \Delta Y_{t-i} + u_t \quad \text{(Eq.5)}$$

Here, lagged difference terms are used and the number of lagged difference terms is usually determined empirically. The main purpose of arranging the equation in this way is to include the terms that will ensure that the error term is free of autocorrelation in the model. Here, the null hypothesis is P = 1 or δ = 0. In other words, there is a unit root in Y and in this case, Y cannot be said to be stationary. If the DF test is applied to the models as the ones in equation (4), it is called the extended Dickey-Fuller (Augmented Dickey-Fuller) test, that is, the ADF test. The critical values of the test statistics of these tests are the same (Altun, 2017).

In the test run for the organic area series, the H_o hypothesis is "all units contain a unit root". When the p values are examined, it is seen that this hypothesis is accepted. That is, the organic area series contains a unit root (*Table 2*).

Table 2. *Fisher ADF panel unit root test results for organic area series*

	Statistic	**p-value**
Inverse chi-squared (18) P	19.3055	0.3732
Inverse normal Z	0.1066	0.5424
Inverse logit t (49) L*	0.4243	0.6634
Modified inv. chi-squared Pm	0.2176	0.4139

Since the organic area series contained a unit root, the model was reconstructed by taking the first difference. When the results presented in *Table 3* were examined, it was determined that the first difference organic area series became stationary.

Table 3. *Fisher ADF panel unit root test results for organic area*

	Statistic	**p-value**
Inverse chi-squared (18) P	81.5346	0.0000
Inverse normal Z	-6.5227	0.0000
Inverse logit t (49) L	-7.4993	0.0000
Modified inv. chi-squared Pm	10.5891	0.0000

In the test run for the agricultural value added series, when the p values are examined, it is seen that this hypothesis is rejected. In other words, it is determined that the value added series is stationary (*Table 4*).

http://www.aloki.hu ● ISSN 1589 1623 (Print) ● ISSN1785 0037 (Online)
DOI: http://dx.doi.org/10.15666/aeer/1906_50075016

Table 4. *Fisher ADF panel unit root test results for the agricultural value added series*

	Statistic	p-value
Inverse chi-squared (18) P	57.0006	0.0000
Inverse normal Z	-3.3437	0.0004
Inverse logit t (49) L	-4.3705	0.0000
Modified inv. chi-squared Pm	6.5001	0.0000

Homogeneity test

In panel data studies, the homogeneity or heterogeneity of the coefficients is an important factor in determining the cointegration and causality analyses to be made. While homogeneity refers to the state where the slope coefficients calculated for units such as all countries/regions, etc., are equal to β, which is a single slope coefficient, heterogeneity refers to the state where at least one of the βs belonging to the units is different (Gül and İnal, 2017). The homogeneity test developed by Pesaran and Yamagata (2008) was used in the current study. In the homogeneity test, the H_o hypothesis is "the slope coefficients are homogeneous". When the P values are examined, it is seen that this hypothesis is not accepted. In other words, it was determined that the series are heterogeneous (*Table 5*).

Table 5. *Homogeneity test*

Test	Test statistic	Probability value
Δ	5.412	0.000
$\Delta_{adj.}$	5.898	0.000

Panel causality analysis

Because the series were heterogeneous in the current study, Dumitrescu and Hurlin (2012) Granger Panel Causality Test was applied. The main advantages of this method are that it can take into account the cross-section dependence between the countries that make up the panel, it can be used when the time dimension (T) is larger or smaller than the cross-section dimension (N), and it can produce effective results in unbalanced panel data sets (Gülmez, 2015). The test statistic of this test is as follows:

$$yit = \alpha i + \sum_{k=1}^{K} \gamma i^{(k)} \; yi,t-k + \sum_{k=1}^{K} \beta i^{(k)} xi,t-k + \varepsilon i,t \qquad \text{(Eq.6)}$$

In the current study, a bidirectional causality relationship was determined between agricultural added value and organic agricultural area (*Table 6*).

Table 6. *Panel causality analysis results*

Ho	W-bar Stat.	Z-bar Stat.	Z-bar tilde
organic_area does not Granger-cause value_added	3.0749	4.4015*	3.1306*
value_added does not Granger-cause organic_area	2.6917	3.5887*	2.5062**

*, ** indicate the Granger causality at 1% and 5% significance level, respectively, lag order:1

http://www.aloki.hu ● ISSN 1589 1623 (Print) ● ISSN1785 0037 (Online)
DOI: http://dx.doi.org/10.15666/aeer/1906_50075016

Auto-regressive distributive lag cointegration test

Since agricultural value added and organic area series were stationary at different degrees (I(0) and I(1)), the relationship between them was investigated with ARDL model. Mean Group Estimator (MG) and Pooled Mean Group Estimator (PMG) were used to determine the relationship between agricultural added value and organic area, and Hausman test was used to determine which estimator's results would be taken into account.

The PMG estimator is a robust estimator that can cope with the omitted variable bias, endogeneity problem and country heterogeneity problem, and allows the long- and short-term coefficients to be calculated separately (Kar and Kar, 2019). This estimator allows estimating the long- and short-term coefficients together and accepts the long-term coefficients the same for all units, while allowing the short-term coefficients to change from unit to unit and averaging (Güven and Mert, 2016). The panel PMG estimator allows variables of different stationarity to be estimated in the same model. This estimator calculates the short-term and long-term relationships along with the error correction coefficient (Dam and Şanlı, 2019).

The format of the PMG model is as follows (Kutlar, 2017):

$$\Delta Y_{i,t} = \phi EC_{i,t} + \sum_{i=0}^{q-1} \Delta X_{i,t-j}{}' \beta_{i,j} + \sum_{i=1}^{p-1} \lambda_{i,j} \Delta y_{i,t-j} + u_{i,t} \quad \text{(Eq.7)}$$

$$EC_{i,t} = yi, t-1- X_{i,t}{}' \theta \quad \text{(Eq.8)}$$

In this model, independent variables and dependent variables have the same time lag for each cross-section. But this is not a mandatory condition (Kutlar, 2017).

Panel ARDL estimation results are presented in *Table 7*. When PMG results are analysed, it is seen that organic agriculture has a positive effect on agricultural added value in the long-term. When the error correction term was examined, the coefficient was found to be negative and significant at the 1% level. In the short term, the relationship between the two variables was found to be statistically insignificant at the 5% level. When the MG results were examined, it was determined that the organic farming area has no effect on the agricultural added value, neither in the short-term nor in the long-term (*Table 7*).

Table 7. *Panel ARDL estimation results*

Long-term coefficient	**PMG**	**MG**
organic_area	103.2494 (0.000)	565.7876 (0.095)
Error correction coefficient		
ECT	-0.6256404 (0.000)	-0.7302669 (0.000)
Short-term coefficient		
organic_area (D1)	-108.7267 (0.667)	-295.6065 (0.170)

Values in parentheses are p values

http://www.aloki.hu ● ISSN 1589 1623 (Print) ● ISSN1785 0037 (Online)
DOI: http://dx.doi.org/10.15666/aeer/1906_50075016

As can be seen, PMG and MG analyses yielded different results. For this reason, the Hausman test was used to determine which estimator's results would be taken as a basis. As the p value was greater than 0.05 in the Hausman test, it was determined that the PMG results were valid (*Table 8*). In other words, organic farming has a positive effect on agricultural added value in the long-term.

Table 8. *Hausman test results*

	mg	pmg	Difference	S.E.
fertilizer	565.7876	103.2494	462.5381	388.8182

chi2(1) = 1.42, Prob>chi2 = 0.2342

As a result of cointegration tests, long-term relationships between variables are estimated with the help of error correction models. If the error correction parameter is negative and significant, there is a long-term relationship between the variables (Tatoğlu, 2020). When the error correction coefficients by countries were analyzed separately, it was determined that there is a long-term relationship between organic farming area and agricultural added value in all the countries except for Spain and the Netherlands at different levels of importance (*Table 9*).

Table 9. *Error correction coefficients by country*

Countries	Coefficients	Standard Error	z	p
Germany	-0.8154798	0.2564646	-3.18	0.001
Austria	-0.8835147	0.2465509	-3.58	0.000
France	-1.01852	0.2540947	-4.01	0.000
Spain	-0.1878386	0.213034	-0.88	0.378
Italy	-1.169897	0.2588712	-4.52	0.000
Greece	-0.2872759	0.1386241	-2.07	0.038
Netherlands	-0.0257895	0.0673751	-0.38	0.702
Denmark	-0.8731309	0.2592194	-3.37	0.001
Sweden	-0.3693185	-0.3693185	-2.09	0.036

Discussion

In the current study conducted to determine whether there is a relationship between organic farming area and agricultural added value in some European Union countries, a positive relationship was determined between organic farming area and agricultural added value. When the literature was reviewed, no study investigating the relationship between organic agriculture and agricultural added value was found. However, studies on the subject indicate that organic agricultural production creates higher added value. Polushkina et al. (2020) found that Russia's GDP increased significantly as a result of value-added organic agriculture. In the study conducted by Saracin and Vasile (2015), it is stated that organic products create added value. In the research conducted by Sanders (2016), organic milk supply chain, organic apple supply chain and organic pasta supply chain in 9 European Union countries were examined and it was determined that higher added value occurred in the organic food chain compared to the conventional food chain.

http://www.aloki.hu ● ISSN 1589 1623 (Print) ● ISSN1785 0037 (Online)
DOI: http://dx.doi.org/10.15666/aeer/1906_50075016

Conclusion

Through organic agriculture, the use of chemicals in agricultural production is prevented, which makes significant contributions to the protection of the environment, nature and agricultural lands. In addition, organic agriculture has positive effects on human health, as consumers eat food that does not contain chemical inputs. On the other hand, organic agriculture can make significant contributions to the national economy.

Dynamic panel ARDL model was used in the current study carried out to determine the relationship between agricultural added value and organic farming area in 9 European Union countries for the period of 2000-2018. As a result of the statistical analyses, a significant positive relationship was determined between the organic farming area and the agricultural added value in the long term in the countries examined. In the short term, the relationship between the two variables was found to be statistically insignificant at the 5% significance level. In the current study, a bidirectional causality relationship was also determined between agricultural added value and organic farming area. When an evaluation was made by country, it was determined that there is a long-term relationship at different levels of importance between organic farming area and agricultural added value in all the countries except for Spain and the Netherlands. This result is considered to be important for policy makers. Since a positive relationship was found between organic farming area and agricultural added value in the current study, supports to organic farming should be increased to make a positive contribution to agricultural added value. On the other hand, it is thought that it is necessary to carry out more studies that reveal the relationship between organic agriculture and agricultural added value.

REFERENCES

[1] Akyol, M. (2018): An examination of the relationship between agricultural incentives and agricultural added value: panel simulated equations system analysis for new industrialized countries. – The Journal of International Scientific Researches 3(3): 226-236.
[2] Altun, N. (2017): The empirical analysis of sustainability of budget deficit in Turkey: 1950-2015 era. – The International Journal of Economic and Social Research 13(1): 13-22.
[3] Ayla, D., Altıntaş, D. (2017): A review of organic production and marketing issues. – Kastamonu University Journal of Faculty of Economics Administrative Sciences 19(4): 7-17.
[4] Bahsi, N. (2020): Investigation of factors affecting the organic agricultural production amount in Turkey: A panel data analysis. – Applied Ecology and Environmental Research 18(3): 4059-4073.
[5] Cukur, T. (2015): Conventional dairy farmers converting to organic dairy production in Turkey. – Polish Journal of Environmental Studies 24(4): 1543-1551.
[6] Dam, M. M., Şanlı, O. (2019): Impact of economic freedom on growth: a panel ARDL analysis on BRIC-T countries. – Atatürk University Journal of Economics and Administrative Sciences 33(4): 1027-1044.
[7] Dumitrescu, E. I., Hurlin, C. (2012): Testing for granger noncausality in heterogeneous panels. – Economic Modelling 29(4): 1450-1460.
[8] Erdinç, Z., Aydınbaş, G. (2021): Panel data analysis of value-added agriculture determinants. – Anadolu University Journal of Social Sciences 21(1): 213-232.
[9] FAO. (2021): Macro Indicators. – http://www.fao.org/faostat/en/#data/MK (accessed on 08.06.2021).
[10] FIBL. (2021): Data on Organic Agriculture in Europe. – https://statistics.fibl.org/europe.html (accessed on 08.06.2021).

http://www.aloki.hu ● ISSN 1589 1623 (Print) ● ISSN1785 0037 (Online)
DOI: http://dx.doi.org/10.15666/aeer/1906_50075016

[11] Gül, E., İnal, V. (2017): Air pollution and economic growth relation: time-varying panel causality analysis. – The Sakarya Journal of Economics 6(2): 70-82.
[12] Gülmez, A. (2015): The relationship between economic growth and air pollution in OECD countries: A Panel Data Analysis. – Kastamonu University Journal of Faculty of Economics Administrative Sciences 9: 18-30.
[13] Güven, S., Mert, M. (2016): Cointegration analysis of international tourism demand: a panel ARDL approach to Antalya case. – Cumhuriyet Universtity Journal of Economics and Administrative Science 17(1): 133-152.
[14] Kar, B. B., Kar, M. (2019): Financial development and income inequality: a dynamic heterogeneous approach for BRICS economies. – Anadolu University Journal of Social Sciences 19(1): 27-46.
[15] Kripfganz, S., Schneider, D. C. (2016): ARDL: Stata module to estimate autoregressive distributed lag models. – 2016 Stata Conference 18, Stata Users Group.
[16] Kutlar, A. (2017): Panel Data Econometrics Applications with Step-by-Step Eviews. – Umuttepe Publishing, Kocaeli (in Turkish).
[17] Pesaran, M. (2004): General Diagnostic Tests for Cross Section Dependence in Panels. – IZA Discussion Paper, 1240.
[18] Pesaran, M. H., Yamagata, T. (2008): Testing slope homogeneity in large panels. – Journal of Econometrics 142: 50-93.
[19] Polushkina, T., Akimova, Y., Kovalenko, E., Yakimova, O. (2020): Organic agriculture in the system of the sustainable use of natural resources. – BIO Web of Conferences 17.
[20] Sanders, J., Gambelli, D., Lernoud, J., Orsini, S., Padel, S., Stolze, M., Willer, H., Zanoli, R. (2016): Distribution of the added value of the organic food chain. – Braunschweig: Thünen Institute of Farm Economics.
[21] Saracin, V. C., Vasile, A. (2015): An exploratory research regarding Romanian organic farming sector. – Agrolife Scientific Journal 4(2): 119-123.
[22] Tatoğlu, F. Y. (2020): Panel Time Series Analysis Stata Applied. – Beta Publishing, İstanbul. (in Turkish).
[23] Tatoğlu, F. Y. (2021): Panel Data Analyses - Lecture Notes. – http://auzefkitap.istanbul.edu.tr/kitap/ekonometri_ue/panelverianalizi.pdf (accessed on 08.06.2021). (in Turkish).

http://www.aloki.hu ● ISSN 1589 1623 (Print) ● ISSN1785 0037 (Online)
DOI: http://dx.doi.org/10.15666/aeer/1906_50075016

THE EFFECT OF NITROGEN APPLICATION IN DIFFERENT DOSES BY FERTIGATION METHOD ON GRAIN YIELD, YIELD COMPONENTS AND QUALITY OF CORN (*Zea mays* L.)

SARACOGLU, M.[1] – OKTEM, A.[2*]

[1]*Ministry of Agriculture Provincial Directorate, Sanliurfa, Turkey*

[2]*Harran University, Faculty of Agriculture, Department of Field Crops, Sanliurfa, Turkey*

[*]*Corresponding author*
e-mail: aoktem@harran.edu.tr; phone: +90-414-318-3686; fax: +90-414-318-3682

(Received 1st Jul 2021; accepted 1st Oct 2021)

Abstract. This study was aimed to determine the most appropriate nitrogen amount for maize using fertigation method. Trials were conducted in 2018 and 2019 with 4 replicates according to the randomized blocks design in Sanliurfa, Turkey. Each plot area was 14 m^2 (5 m x 2.8 m) and consisted of four rows of 5 m in length. DKC-6664 maize variety was used in the study as a crop material. Drip irrigation system was used with 5-day intervals according to daily evaporation values. Irrigation water was given using 1.25 coefficient of Class A Pan evaporation. Ten separate nitrogen doses were applied with the irrigation water at 0 kg da^{-1}, 4 kg da^{-1}, 8 kg da^{-1}, 12 kg da^{-1}, 16 kg da^{-1}, 20 kg da^{-1}, 24 kg da^{-1} 28 kg da^{-1}, 32 kg da^{-1} and 36 kg da^{-1} (1 da = 1000 m^2). According to the results of the two-year average, grain yield ranged from 434 to 1594 kg da^{-1}. The leaf area per plant varied between 112 and 621 cm^2 $plant^{-1}$, protein content between 7.39% and 8.84%, starch content between 70.90% and 71.62%, and oil content between 4.20% and 4.66%. In general, the properties examined increased from the N0 application to the N28 application. Increasing nitrogen doses applied by fertigation method had a positive effect on the investigated properties. Based on average of years, the highest grain yield was determined in 28 kg da^{-1} nitrogen application with fertigation system. However, no statistical difference was observed between N24 and N28 applications.
Keywords: *maize, N, drip irrigation, protein, starch, oil*

Introduction

Corn is an annual hot climate cereal. It can be grown in tropical and subtropical temperate climates, and it can be cultivated almost anywhere in the world. Corn is a plant used as human food, animal feed and industrial raw material.

Stalk, leaves and grains are used as animal feed (Oktem and Oktem, 2020a). Grains and starch are used in human nutrition and in the food industry. In addition to these consumption areas, it is also consumed as a snack. Moreover, its use in the oil, sweetener industries and biofuel-bioethanol production has been increasing in recent years (Oktem and Oktem, 2020b).

Due to global warming and the gradual decrease of water resources, research and development studies on the effective use of water have increased. The use of pressurized irrigation systems such as drip irrigation has come to an important point concerning the use of water, which is an important input in the agricultural sector, at an optimum level. Drip irrigation system saves water compared to other irrigation systems and increases the effective use of water by the plant. In addition, drip irrigation system allows plant nutrients to be given in combination with irrigation water (Oktem, 2008a).

Nitrogen is absolutely essential and the most widely used plant macronutrient. The application of nitrogen fertilizers together with irrigation water in drip irrigation systems (fertigation) provides an increase in fertilizer use efficiency and yield. Therefore,

http://www.aloki.hu ● ISSN 1589 1623 (Print) ● ISSN 1785 0037 (Online)
DOI: http://dx.doi.org/10.15666/aeer/1906_50175031

irrigation methods and nitrogen fertilization application are key factors in increasing the yield of plants. Proper management of these two factors is necessary for environmental protection and high production (Oktem, 2008b).

Determining the appropriate fertilizer dose in the corn plant is important in terms of high efficiency, cost reduction and minimum damage to the environment. In previous studies, it was stated that the most appropriate nitrogen dose in corn plant was 25 kg N da^{-1} (Cokkızgın, 2002).

In another study, it was stated that increasing nitrogen doses had a positive effect on vegetative parameters; however, it was stated that the applications made above 25 kg N da^{-1} were not statistically significant (Kaplan and Aktas, 1993). Although the highest yield was obtained from 36 kg N da^{-1} dose in the study conducted on maize plant, it was stated that statistically 27 kg N da^{-1} dose was more appropriate (Kara, 2006).

In a study in which 5 different nitrogen doses (0, 24, 32, 40 and 48 kg N da^{-1}) were tested in two corn varieties (89MAY70 and Shemal), it was found that nitrogen doses positively affected the grain yield and the highest grain yields were obtained from 40 and 48 kg da^{-1} nitrogen doses (Tunalı et al., 2012). In a study where four different nitrogen doses (0, 7, 14 and 21 kg da^{-1}) were researched it has been reported that nitrogen doses have a statistically significant effect on plant height, first ear height and grain yield (Can and Akman, 2014).

It has been reported that the highest yield values were obtained from 15 kg da^{-1} N doses in the sweet corn plant, where 0, 7.5, 15, 22.5 and 30 kg da^{-1} pure nitrogen doses were applied by the fertigation method (Avsar et al., 2018).

The aim of this study is to determine the most appropriate amount of nitrogen to be applied by fertigation method in drip irrigation in maize plant and to find out the effects of applied nitrogen on yield and yield components of maize plant and quality.

Material and methods

Study design and experimental procedures

This study was carried out at the second crop conditions of the Harran Plain, Sanliurfa, Turkey in 2018 and 2019. The research was set up in a randomized block design with 4 replications. DKC-6664 single cross hybrid corn variety was used as plant material in the study. The climate data of the research area is given in *Table 1*, and the soil properties are given in *Table 2*. During the trial years, the temperature increased above 40 ^{0}C in June, July and August, and the average relative humidity was observed between 29.3% and 36.6%. There was no rainfall in July and August and rainfall was very low in June and September (*Table 1*). There was no climatic factor limiting corn cultivation, and the plants were grown without any problems with the irrigation.

The soil of the trial area is low in organic matter, calcareous, high in potassium, and has a harmless salinity (*Table 2*). The soil characteristics of the experimental area are alluvial, flat and deep soils. Typical red profiles have clay texture. The entire profile is very calcareous and has a pH between 7.3 and 7.8 (Dinc et al.,1988).

Before planting, the soil was first plowed with a mouldboard plough, then processed with a goble disc and made ready for planting by pulling the float. In the experiment, each plot consisted of 4 rows with a 5 m length. Row spacing was 70 cm, intra row spacing was 16 cm and sowing depth was 5-6 cm. Sowing was done on 25 June 2018 and 24 June 2019 with a pneumatic seed drill. Chemical spraying was done against weeds and pests. Harvesting was done when the plants were completely dry.

http://www.aloki.hu ● ISSN 1589 1623 (Print) ● ISSN 1785 0037 (Online)
DOI: http://dx.doi.org/10.15666/aeer/1906_50175031

Table 1. *Climatic data of 2018 and 2019 years of the research area*

	Lowest temperature (^{0}C)		Highest temperature (^{0}C)		Average temperature (^{0}C)		Average relative humidity (%)		Precipitation (mm)	
	2018	**2019**	**2018**	**2019**	**2018**	**2019**	**2018**	**2019**	**2018**	**2019**
April	9.3	5.9	32.1	26.8	19.9	14.4	38.4	67.0	35.8	97.4
May	12.2	10.1	36.3	40.3	23.0	25.2	50.1	35.8	64.5	7.3
June	16.2	18.6	43.1	44.1	28.6	30.7	36.6	30.6	10.1	8.9
July	21.2	19.7	43.2	42.3	31.9	31.7	34.2	29.6	0.0	0.0
August	20.8	20.7	42.2	45.8	32.2	32.8	33.6	29.3	0.0	0.0
September	17.7	15.9	41.5	39.5	28.8	27.9	31.3	30.3	2.2	0.2
October	9.3	11.3	34.2	36.2	21.6	22.9	45.6	44.9	39.4	45.1
November	5.4	-	27.5	-	13.0	-	72.5	-	106.6	0.0

Table 2. *Some physical and chemical properties of the trial area soil*

Soil properties	**2018**		**2019**	
Deep	**0-20**	**20-40**	**0-20**	**20-40**
pH	7.81	7.91	7.95	7.87
EC (ds/m)	1.31	1.00	0.91	0.90
Lime (%)	26.90	26.90	28.10	27.30
Phosphorus P_2O_5 (kg da-^{1})	6.42	4.12	4.69	4.69
Potassium K_2O (kg da-^{1})	213.30	171.60	145.20	150.30
Organic matter (%)	2.01	1.61	1.69	1.60
Nitrogen (%)	0.15	0.14	0.12	0.12
Sandy (%)	25.28	25.28	30.00	28.00
Clay (%)	56.00	52.00	48.88	48.80
Silt (%)	18.72	22.72	21.12	23.12

An analysis-of-variance (ANOVA) was performed using Jump statistical package program to evaluate statistical differences between research results. Means of the data obtained from research were compared using DUNCAN test at $P \leq 0.05$ (Yurtsever, 1984).

Application of irrigation water

Sprinkler irrigation was applied in all plots immediately after planting to obtain a sufficient output. When the plants have 3-4 leaf, nitrogen doses were started to be given to all plots with the drip irrigation system. During both trial years, laterals were placed in the drip irrigation system, one lateral to two plant rows, with 140 cm spacing (Oktem, 2008a).

The irrigation water to be given to the parcels was calculated as 1.25 times the 5-day cumulative evaporation amount obtained from the Class-A Pan container (Oktem, 2008a). Irrigation water was given to the parcels at 5-days intervals after correcting with the soil cover percentage of the plant (Oktem, 2006).

During the 2018 growing season of the experiment, 790 mm of total irrigation water was applied, and 759 mm during the 2019 growing season. Some chemical properties of irrigation water used in the research was given *Table 3*.

http://www.aloki.hu ● ISSN 1589 1623 (Print) ● ISSN 1785 0037 (Online)
DOI: http://dx.doi.org/10.15666/aeer/1906_50175031

Irrigation was continued until the end of the physiological maturity period of the plants. *Fig. 1* shows design of drip irrigation and fertigation system in the research.

Figure 1. *Design of drip irrigation and fertigation system in the reseach area*

The equation (*Eq.1*) given below was used in the calculation of irrigation water (Oktem and Oktem, 2009).

$$I = Ep \times Kcp \times P \times A \quad \text{(Eq.1)}$$

In the equality I is the amount of irrigation water (lt), EP is Evaporation from Class A-Pan (mm), Kcp is Pan coefficient (Kcp= 1.25), P is Cover percentage (%), A represents the parcel area (m^2).

The following equation (*Eq.2*) was used in the calculation of the cover percentage (Kanber and Gungor, 1986).

$$\% P = a/b \times 100 \quad \text{(Eq.2)}$$

In the equality a = The width of the projection of the above-ground part of the plant, b = It represents distance between two plants.

Application of fertilizers

Fertilization was done considering the soil analysis results of the experimental area. Ten pure nitrogen doses were used in the trial that is 0 kg da^{-1}, 4 kg da^{-1}, 8 kg da^{-1}, 12 kg da^{-1}, 16 kg da^{-1}, 20 kg da^{-1}, 24 kg da^{-1}, 28 kg da^{-1}, 32 kg da^{-1} and 36 kg da^{-1} (1 da = 1000 m^2). The total nitrogen doses were divided into 10 equal parts considering vegetation period of used variety and given with the drip irrigation system until the end of tasselling period. Nitrogen was given according to BBCH scale from phenological growth stage 1(13) to 5(59) (Lancashire et al., 1991). 1/10 of the total amount of pure nitrogen to be given and the whole amount of pure phosphorus (10 kg P_2O_5 da^{-1}) were given at once with planting. In the experiment, triple super phosphate $CaH_4(PO_4)_2.H_2O$ (43-44%) fertilizers were used as phosphorus source and urea (46% N) fertilizers were used as nitrogen source. In order to prevent the passage of nitrogen, a space of 2.0 m was left between the plots and 3.0 m between the blocks.

http://www.aloki.hu ● ISSN 1589 1623 (Print) ● ISSN 1785 0037 (Online)
DOI: http://dx.doi.org/10.15666/aeer/1906_50175031

Results and discussion

Plant height (cm)

It was determined that the effect of nitrogen amount applied at different doses by the fertigation method on plant height was statistically significant (P≤0.01). The plant height values in 2018, 2019 and the average of the two years of the study varied between 170.75 - 270.38 cm, 179.60 - 284.60 cm and 175.18 - 277.49 cm, respectively (*Table 3*). In both experimental years, the lowest plant height was obtained from the N0 application, and the highest plant height was obtained from the N28 application (*Fig. 2*). Although genetic factors affect plant height (Oktem and Oktem, 2013), in parallel with our findings, some researchers reported that plant height increased depending on nitrogen applications (Oktem, 2008b; Cerny et al., 2012; Ullah et al., 2015; Avsar et al., 2018).

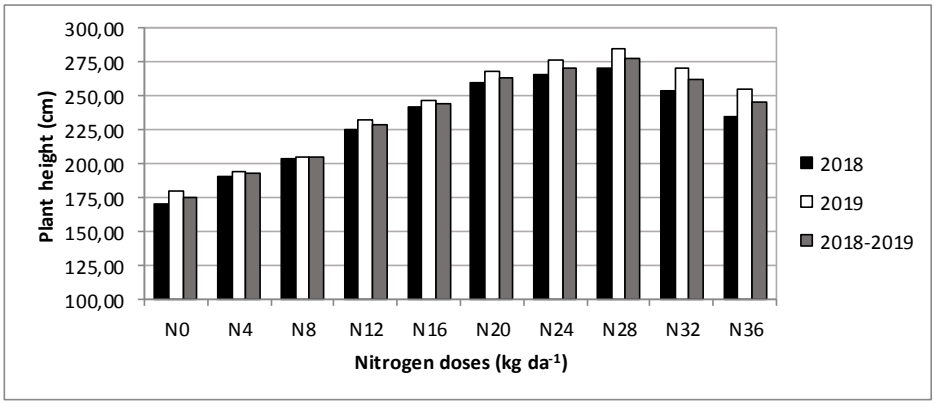

Figure 2. *Plant height values at different nitrogen doses given by fertigation method*

Table 3. *Plant height and stem diameter values at different nitrogen doses given by fertigation method*

N Doses	Plant height** (cm)			Stem diameter** (mm)		
(kg da^{-1})	2018	2019	2018-2019	2018	2019	2018-2019
N0	170.75 g†	179.60 g	175.19 g	10.65 e	10.85 g	10.75 g
N4	191.00 f	194.00 f	192.50 f	12.65 d	12.80 f	12.73 f
N8	204.13 e	205.50 f	204.81 e	15.03 c	14.80 e	14.91 e
N12	225.25 d	232.30 e	228.75 d	15.88 c	15.95 d	15.91 d
N16	242.50 c	246.30 d	244.38 c	15.78 c	16.05 d	15.91 d
N20	260.25 ab	267.60 bc	263.94 b	19.18 ab	19.55 b	19.36 b
N24	265.75 a	276.10 ab	270.94 ab	20.08 a	20.48 a	20.28 a
N28	270.38 a	284.60 a	277.50 a	20.10 a	20.45 a	20.28 a
N32	253.75 b	271.10 ab	262.44 b	17.95 b	18.63 c	18.29 c
N36	235.13 c	255.40 cd	245.25 c	12.98 d	13.28 f	13.13 f
Mean	231.89	241.25	236.57	16.03	16.28	16.15
CV	1.55	1.97	1.55	3.02	1.61	2.31

†: There is no significant difference at 0.05 level between the averages shown in the same letter according to Duncan test, **: denotes P≤0.01

http://www.aloki.hu ● ISSN 1589 1623 (Print) ● ISSN 1785 0037 (Online)
DOI: http://dx.doi.org/10.15666/aeer/1906_50175031

Stem diameter (mm)

According to the results of analysis of variance, the effect of different nitrogen doses applied by fertigation method on stem diameter was found to be statistically significant (P≤0.01). It was observed that the stem diameter varied between 10.65 mm (N0) and 20.10 mm (N28) in 2018, and between 10.85 mm (N0) and 20.48 mm (N24) in 2019 (*Table 3*). According to the combined analysis results of two years; stem diameter ranged from 10.75 to 20.28 mm (*Fig. 3*). The lowest stem diameter was obtained from the N0 application (10.75 mm), and the highest stem diameter (20.28 mm) was obtained from the N28 application (*Table 4*). Similar to our results, it has been reported that stem thickness increases depending on nitrogen applications (Oktem and Oktem, 2005; Kara, 2006; Kılınc et al., 2018; Kahriman et al., 2020).

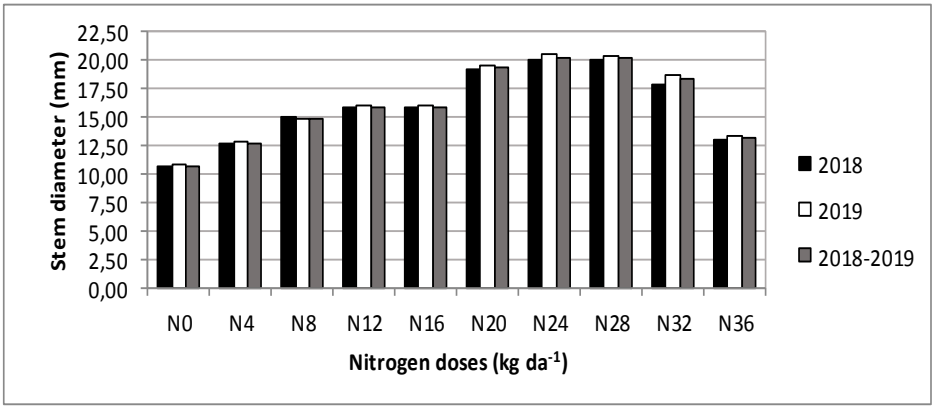

Figure 3. *Stem diameter values at different nitrogen doses given by fertigation method*

Table 4. *Ear length and ear diameter values at different nitrogen doses given by fertigation method*

N doses	Ear length** (mm)			Ear diameter** (mm)		
(kg da^{-1})	2018	2019	2018-2019	2018	2019	2018-20
N0	7.05 h†	6.93 i	6.99 i	34.53 e	33.90 g	34.22 f
N4	8.53 g	8.40 ı	8.47 ı	36.25 e	36.15 f	36.20 e
N8	12.13 f	10.90 h	11.52 h	41.23 d	41.73 e	41.48 d
N12	13.65 e	12.48 g	13.07 g	42.75 cd	43.68 de	43.22 c
N16	14.68 d	14.88 e	14.78 e	43.85 c	43.85 de	43.85 c
N20	16.85 c	16.45 d	16.65 d	47.78 b	47.95 ab	47.87 b
N24	18.68 b	18.90 b	18.79 b	48.50 ab	49.33 ab	48.92 ab
N28	20.88 a	21.45 a	21.17 a	50.60 a	50.73 a	50.67 a
N32	17.60 bc	17.60 c	17.60 c	46.68 ab	47.65 bc	47.17 b
N36	14.03 de	13.98 f	14.01 f	44.18 c	45.23 cd	44.71 c
Mean	7.05	6.93	6.99	43.64	44.02	43.83
CV	8.53	8.40	8.47	2.01	2.04	1.99

†: There is no significant difference at 0.05 level between the averages shown in the same letter according to Duncan test, **: denotes P≤0.01

http://www.aloki.hu ● ISSN 1589 1623 (Print) ● ISSN 1785 0037 (Online)
DOI: http://dx.doi.org/10.15666/aeer/1906_50175031

Ear length (cm)

The effect of different nitrogen doses applied by fertigation method on ear length was determined to be statistically significant (P≤0.01). In 2018, 2019 and the average of the two years, the ear lengths varied between 7.05 and 20.88 cm, 6.93 and 21.45 cm and 6.99 and 21.17 cm, respectively (*Fig. 4*).

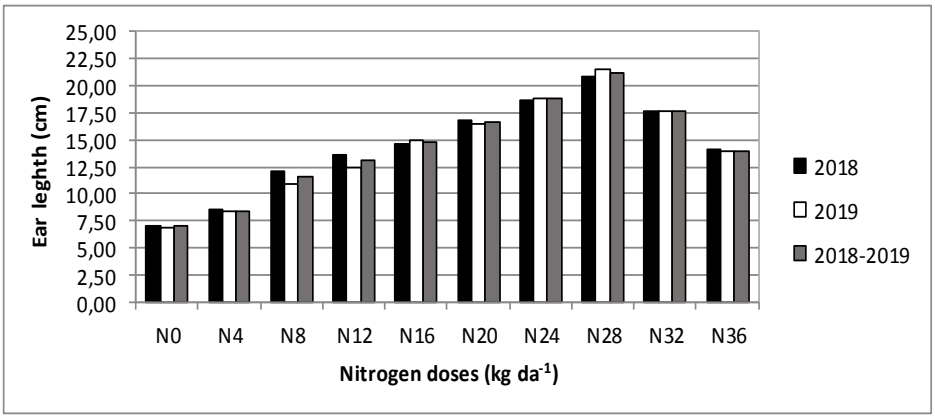

Figure 4. *Ear length values at different nitrogen doses given by fertigation method*

In both trial years, the lowest ear length was obtained from the N0 application, and the highest ear length was obtained from the N28 application (*Table 4*). Similar to our findings, it has been reported by some researchers that as the nitrogen dose increases, the ear length increases (Saruhan and Sireli, 2005; Oktem and Oktem, 2005; Kara, 2006; Oktem, 2008b; Safdarian et al., 2014).

Ear diameter (mm)

The effect of different nitrogen doses on ear diameter in corn plant grown by fertigation method was found to be statistically significant (P≤0.01). According to 2018 values, the lowest ear diameter was obtained from the N0 subject (34.53 mm), and the highest ear diameter was obtained from the N28 subject (50.60 mm). Ear diameter varied between 33.90 mm (N0) and 50.73 mm N28 in the 2019 growing season (*Table 4*).

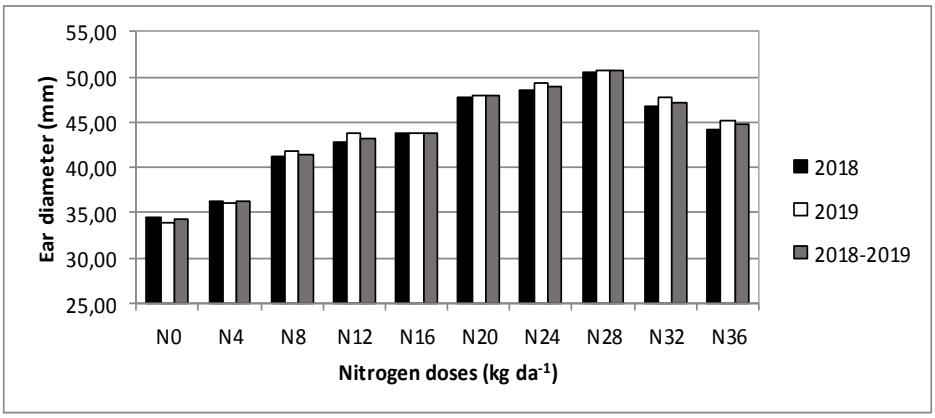

Figure 5. *Ear diameter values at different nitrogen doses given by fertigation method*

http://www.aloki.hu ● ISSN 1589 1623 (Print) ● ISSN 1785 0037 (Online)
DOI: http://dx.doi.org/10.15666/aeer/1906_50175031

According to the average of two years; the lowest ear diameter was found in N0 (34.22 mm), and the highest ear diameter (50.67 mm) was found in N28 (*Fig. 5*). In parallel with the increase in nitrogen doses, the ear diameter values also increased. Some researchers have stated in their studies that the ear diameter increases depending on the increased nitrogen doses (Saruhan and Sireli, 2005; Kara, 2006; Oktem, 2008b; Can and Akman, 2014).

Thousand kernel weight (g)

The effect of different nitrogen amounts on thousand kernel weight in corn plant was found to be statistically significant (P≤0.01). According to the 2018 values of the study, it was observed that the thousand-kernel weight varied between 274 g and 319 g, and in the 2019 growing season, it varied between 309 g and 373 g (*Table 5*).

Table 5. *Thousand kernel weight and grain yield values at different nitrogen doses given by fertigation method*

N doses	Thousand kernel weight** (g)			Grain yield** (kg da^{-1})		
(kg da^{-1})	2018	2019	2018-2019	2018	2019	2018-2019
N0	310 ab	309 d†	310 c	315 h	553 h	434 f
N4	299 abc	333 c	316 c	610 g	846 g	728 e
N8	274 c	344 bc	309 c	892 f	1047 f	970 d
N12	297 abc	331 c	314 c	1074 e	1189 e	1132 c
N16	300 abc	339 bc	320 bc	1229 c	1331 d	1280 b
N20	305 ab	349 b	327 abc	1301 bc	1393 c	1347 b
N24	315 a	369 a	342 ab	1428 ab	1499 b	1464 a
N28	319 a	373 a	346 a	1567 a	1621 a	1594 a
N32	297 ab	370 a	334 abc	1201 cd	1351 cd	1276 b
N36	289 bc	369 a	329 abc	1106 de	1105 f	1106 c
Mean	301	349	325	1072	1194	1133
CV	6.36	1.75	4.45	5.60	3.46	3.83

†: There is no significant difference at 0.05 level between the averages shown in the same letter according to Duncan test, **: denotes P≤0.01

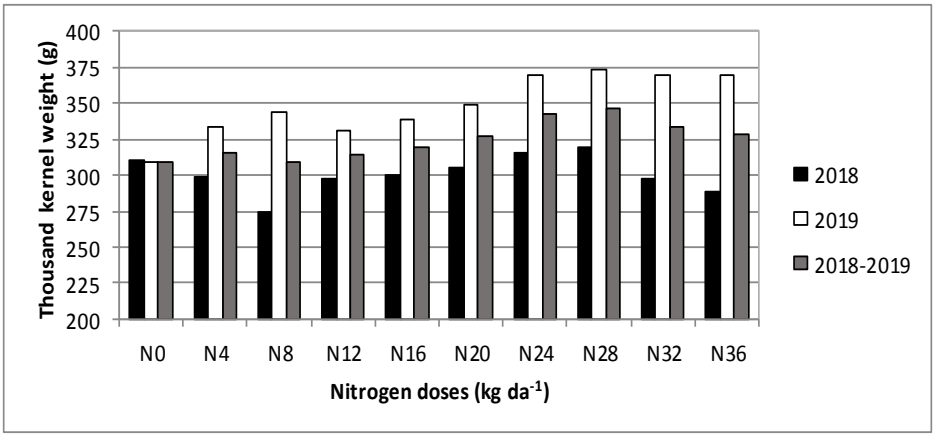

Figure 6. *Thousand kernel weight values at different nitrogen doses given by fertigation*

http://www.aloki.hu ● ISSN 1589 1623 (Print) ● ISSN 1785 0037 (Online)
DOI: http://dx.doi.org/10.15666/aeer/1906_50175031

According to the combined analysis results of two years; the thousand kernel weights varied between 310 g and 346 g in different N treatments. Increasing nitrogen doses had a positive effect on the grain weight (*Fig. 6*). Some researchers reported that the thousand kernel weight increased with increasing nitrogen doses and reported similar results with our findings (Amaral et al., 2005; Kara, 2006; Yururdurmaz, 2007).

Grain yield (kg da^{-1})

According to the results of analysis of variance, it was determined that the effect of different nitrogen doses given by fertigation method on grain yield was statistically significant (P≤0.01). In 2018, 2019 and the average of the two years of the research, it was observed that the grain yield values changed between 315 and 1567 kg da^{-1}, between 553 and 1621 kg da^{-1}, and between 434 and 1594 kg da^{-1}, respectively. In both trial years, the lowest grain yield was found in N0 application and the highest grain yield was found in N28 application (*Table 5*). But N24 and N28 applications were in the same statistical group at means of years. As the amount of nitrogen increased, the grain yield increased up to 28 kg da^{-1} nitrogen dose, after which a decrease was observed.

Increasing nitrogen doses had a positive effect on grain yield (*Fig. 7*). The nitrogen use efficiency can vary according to genotypes. Supporting our findings, some researchers stated that grain yield increased in response to increasing nitrogen dose (Allen et al., 2000; Oktem et al., 2001, 2010; Blumental et al., 2003; Tunalı et al., 2012; Yolcu, 2014; Avsar et al., 2018; Koca and Ibrikci, 2019). A significant second order polynomial relationship was found between grain yield and nitrogen doses in average of both years as shown in *Fig. 7* (P≤0.01). The relationship equation was $y = -28.831x^2 + 402.39x + 29.775$ ($R^2 = 0.9529$). From the regression analysis (*Fig. 7*), it seems appropriate to give 24 kg da^{-1} nitrogen to corn by fertigation method.

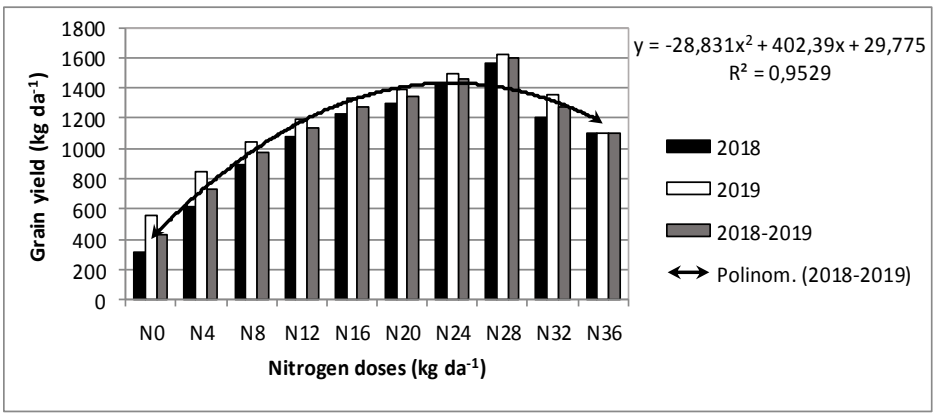

Figure 7. *Gain yield values at different nitrogen doses given by fertigation method*

Leaf area of plant (cm^2 bitki^{-1})

The effect of different nitrogen amounts on the leaf area of the plant was found to be statistically significant (P≤0.01). In the 2018 trial year, the leaf area per plant varied between 108 cm^2 plant^{-1} (N0) and 613 cm^2 plant^{-1} (N28). In 2019, the lowest leaf area was taken from the N0 application (116 cm^2 plant^{-1}), and the highest plant (629 cm^2 plant^{-1}) was taken from the N28 application (*Table 6*).

http://www.aloki.hu ● ISSN 1589 1623 (Print) ● ISSN 1785 0037 (Online)
DOI: http://dx.doi.org/10.15666/aeer/1906_50175031

Table 6. *Leaf area and protein content of kernel values at different nitrogen doses given by fertigation method*

N doses	Leaf area** (cm^2 $plant^{-1}$)			Protein content** (%)		
(kg da^{-1})	2018	2018	2018-2019	2018	2019	2018-2019
N0	108 f†	116 g	112 g	7.48 b	7.30 b	7.39 b
N4	151 ef	158 f	154 f	8.03 ab	7.95 ab	7.99 ab
N8	170 e	176 f	173 f	8.20 ab	8.03 ab	8.11 ab
N12	231 d	251 e	241 e	8.23 ab	8.10 ab	8.16 ab
N16	308 c	324 d	316 d	8.28 ab	8.13 ab	8.20 ab
N20	416 b	457 b	436 b	8.70 ab	8.20 ab	8.45 ab
N24	547 a	566 a	557 a	8.85 ab	8.35 ab	8.60 a
N28	613 a	629 a	621 a	8.88 a	8.80 a	8.84 a
N32	370 b	400 c	385 c	8.83 ab	8.43 ab	8.63 a
N36	227 d	244 e	236 e	8.73 ab	8.38 ab	8.55 a
Mean	314	332	323	8.42	8.17	8.29
CV	3.91	2.31	3.22	4.00	4.00	4.00

†: There is no significant difference at 0.05 level between the averages shown in the same letter according to Duncan test, **: denotes P≤0.01

According to the combined analysis results of two years, it was observed that the leaf area per plant varied between 112 cm^2 $plant^{-1}$ (N0) and 621 cm^2 $plant^{-1}$ (N28). Leaf area values increased in parallel with the increase in nitrogen (*Fig. 8*). Supporting our research findings, some researchers reported that leaf area values increased with increasing nitrogen doses (Yururdurmaz, 2007; Hokmalipour et al., 2011; Tunalı et al., 2012).

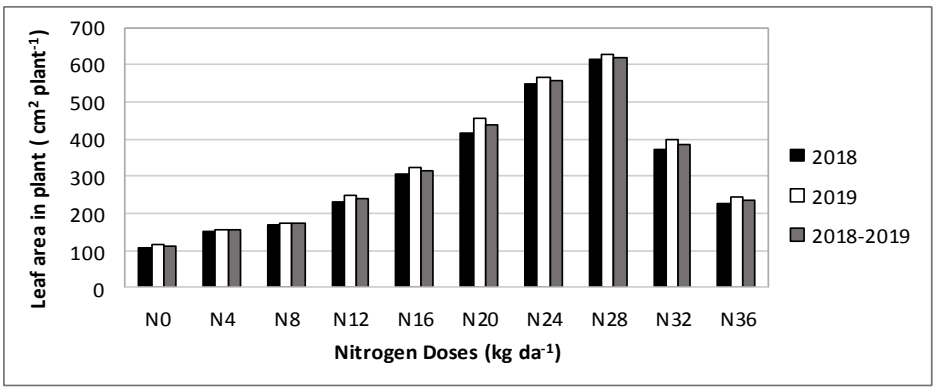

Figure 8. *Leaf area in plant values at different nitrogen doses given by fertigation method*

Protein content of kernel (%)

According to analysis of variance, the effect of different nitrogen amount on kernel protein content was found to be statistically significant (P≤0.01). According to the combined analysis results of two years it was observed that the protein content in the kernel varied between 7.39% and 8.84% in different N applications (*Fig. 9*).

http://www.aloki.hu ● ISSN 1589 1623 (Print) ● ISSN 1785 0037 (Online)
DOI: http://dx.doi.org/10.15666/aeer/1906_50175031

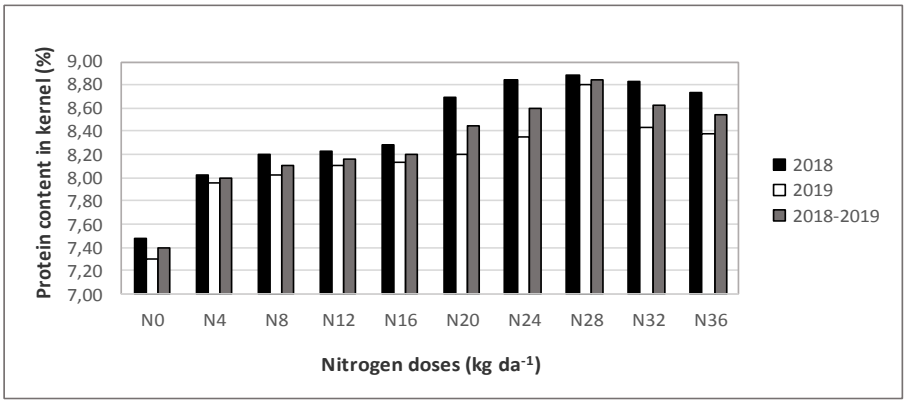

Figure 9. *Protein content of kernel values at different nitrogen doses given by fertigation*

The lowest kernel protein content was obtained from N0 application, and the highest kernel protein content (8.84%) was obtained from N28 application (*Table 6*). Parallel to our findings, some researchers stated that the protein ratio increased as the nitrogen dose increased (Patricio Soto et al., 2004; Oktem, 2008c; Oktem et al., 2010; Ullah et al., 2015; Avsar et al., 2018; Kılınc et al., 2018; Kahriman et al., 2020). Ozsisli (2010), on the other hand, reported higher protein content values than our findings.

Starch content of kernel (%)

The effect of different nitrogen amount applied by fertigation method on starch content in kernel was not found statistically significant. According to the combined analysis results of two years; the starch content in kernels varied between 70.90% and 71.62%. The lowest starch content in the kernel was obtained from the N36 application (70.90%), and the highest starch content in the kernel (71.62%) was obtained from the N8 application (*Table 7*).

Table 7. *Starch and oil content of kernel values at different nitrogen doses given by fertigation method*

N Doses	Starch content** (%)			Oil content** (%)		
(kg da^{-1})	2018	2019	2018-2019	2018	2019	2018-2019
N0	69.68	72.80	71.24	4.15 b†	4.25 b	4.20 c
N4	70.58	72.08	71.33	4.25 ab	4.35 ab	4.30 bc
N8	70.95	72.28	71.62	4.35 ab	4.40 ab	4.38 abc
N12	70.85	72.05	71.45	4.43 ab	4.48 ab	4.45 abc
N16	70.85	72.25	71.55	4.45 ab	4.48 ab	4.46 abc
N20	70.48	72.15	71.32	4.48 ab	4.50 ab	4.49 ab
N24	70.48	71.60	71.04	4.55 a	4.60 ab	4.58 ab
N28	69.90	72.05	70.98	4.59 a	4.73 a	4.66 a
N32	70.88	71.95	71.42	4.48 ab	4.55 ab	4.51 ab
N36	70.45	71.35	70.90	4.48 ab	4.55 ab	4.51 ab
Mean	70.51	72.06	71.28	4.42	4.49	4.45
CV	0.97	1.16	1.06	7.65	4.23	6.36

†: There is no significant difference at 0.05 level between the averages shown in the same letter according to Duncan test, **: denotes P≤0.01

http://www.aloki.hu ● ISSN 1589 1623 (Print) ● ISSN 1785 0037 (Online)
DOI: http://dx.doi.org/10.15666/aeer/1906_50175031

In parallel with our findings, similar starch content values in maize have been reported by some researchers (Ignjatovic-Micic et al., 2014; Kahriman et al., 2020). Some other researchers reported lower starch content values than our findings (Ozsisli, 2010; Kılınc et al., 2018).

Oil content of kernel (%)

According to the analysis of variance, it was determined that the effect of different nitrogen amounts applied by fertigation method on the oil content in the grain was statistically significant ($P \leq 0.01$). According to the values of the first year of the study, the lowest oil content in the grain was obtained from the N0 application (4.15%), and the highest oil content in the grain (4.59%) was obtained from the N28 application.

It was observed that the oil content in the grain varied between 4.25% (N0) and 4.73% (N28) in the 2019 growing season (*Table 7*). According to the combined analysis results of two years; the lowest oil content in the kernel was taken from the N0 application (4.20%), and the highest kernel oil content (4.66%) was taken from the N28 application. It has been reported that the oil content of the corn kernel is 4.3% (Watson, 2003). Josipovic et al. (2014) reported that grain oil ratios ranged from 3.50 to 4.17%.

The oil content in the kernel increased from N0 application to N28 application (*Fig. 10*). Increasing nitrogen doses had a positive effect on grain oil content. It has also been stated in previous studies that nitrogen doses have a positive effect on grain oil content (Paiva et al., 2011; Ignjatovic-Micic et al., 2014; Ozata and Kapar, 2014; Avsar et al., 2018; Kahriman et al., 2020).

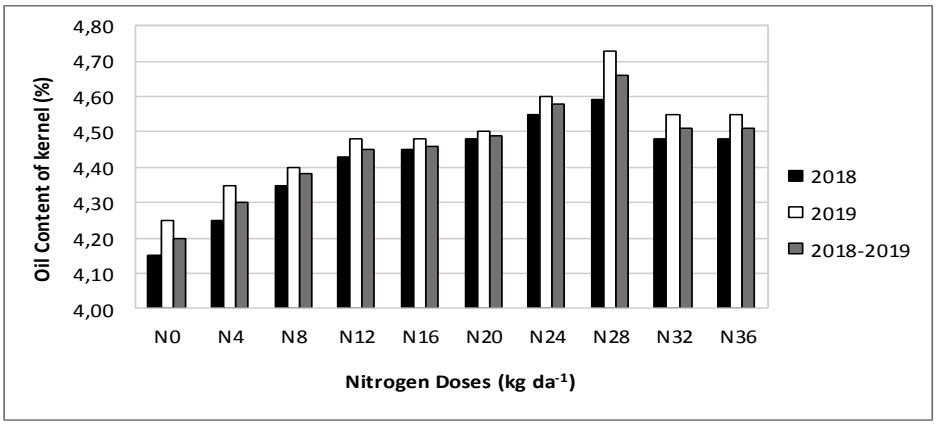

Figure 10. *Oil content of kernel values at different nitrogen doses given by fertigation*

Conclusion

As a result of this study which was carried out to determine the most appropriate nitrogen amount by fertigation method, according to the average of two years; plant height ranged from 175.18 to 277.49 cm, stem diameter 10.75 to 20.28 mm. Ear length varied from 6.99 to 21.17 mm, ear thickness 34.22 to 50.67 mm. Thousand kernel weight ranged from 309 to 373 g, grain yield from 434 to 1594 kg da^{-1}. The leaf area per plant was between 112 cm^2 $plant^{-1}$ and 621 cm^2 $plant^{-1}$, the protein content in the kernel was between 7.39% and 8.84%. The starch content was found between 70.90% and 71.62%, and the oil content in the kernel varied between 4.20% and 4.66%. The analyzed parameters were found to be statistically significant ($P<0.01$). In general, an increase was

http://www.aloki.hu ● ISSN 1589 1623 (Print) ● ISSN 1785 0037 (Online)
DOI: http://dx.doi.org/10.15666/aeer/1906_50175031

recorded in the properties examined from the N0 application to the N28 application, but a decrease was observed after N28 nitrogen dose. The nitrogen doses applied by the fertigation method had a positive effect on the investigated properties. According to two-years average, the highest grain yield was determined in 28 kg da^{-1} nitrogen application with fertigation system. But there were no statistical differences between N24 and N28 applications. When factors such as economic factors, protection of natural resources, environmental pollution, sustainable agriculture, and regression analysis (*Fig. 7*) are taken into consideration, 24 kg da^{-1} of nitrogen given by fertigation method seems more appropriate for corn. It is useful to repeat similar fertigation studies with nitrogen for different corn varieties and different locations in the world.

Acknowledgements. The authors are grateful to the Republic of Turkey, and the Ministry of Agriculture and Forestry for financial support. Project No: TAGEM/TSKAD/15/A13/P04/05.

REFERENCES

[1] Allen, T. H., Potter, K. N., Morrison, J. E. (2000): Tillage system, fertilizer nitrogen rate and timing effect on corn yields in the texas blackland prairie. – Agron. J. 93: 1119-1124.
[2] Amaral, C. P. R., Filho, D. F., Farinelli, R., Barbosa, J. K. (2005): Row spacing. population density and nitrogen fertilization in maize. – Rev. Bras. Cienc. Solo Vicosa 29: 467-473.
[3] Avsar, O., Kolay, B., Bilge, U., Bereketoglu, K., Atakul, S., Yasar, M. (2018): Determination of the effects of different amounts of nitrogen applications by fertigation method on yield and yield parameters of sweet corn. – Project Results Report GAP UTAEM, Diyarbakır, Turkey.
[4] Blumental, J. M., Lyon, D. J., Stroup, W. W. (2003): Optimal plant population and nitrogen fertility for dryland corn in Western Nebraska. – Agronomy Journal 95(4): 878-884.
[5] Can, M., Akman, Z. (2014): The effect of different nitrogen doses on yield and quality characteristics of sweet corn. – Journal of Suleyman Demirel University Faculty of Agriculture 9(2): 93-101.
[6] Cerny, J., Balık, J., Kulhanek, M., Vasak, F., Peklova, L., Sedlar, O. (2012): The effect of mineral N fertiliser and sewage sludge on yield and nitrogen efficiency of silage maize. – Plant Soil Environ 58(2): 76-83.
[7] Cokkızgın, A. (2002): The effect of different nitrogen doses and in-row sowing distances on yield components and physiological characteristics of second crop maize. – KSU Sutçu Imam University, Institute of Science, Master Thesis, K.Maras, Turkey, 73p.
[8] Dinc, U., Senol, S., Satın, M., Kapur, S., Güzel, N., Derici, R. (1988): Southeastern Anatolia soils of Turkey, I. Harran Plain. – TUBITAK, TOAG534, Final Result Report, Ankara, Turkey.
[9] Hokmalipour, S., Hamele Darbendi, M. (2011): Effects of nitrogen fertilizer on chlorophyll content and other leaf indicate in three cultivars of maize (*Zea mays* L.). – World Applied Sciences Journal 15(12): 1780-1785.
[10] Ignjatovic-Micic, D., Kostadinovic, M., Bozinovic, S., Andjelkovic, V., Vancetovic, J. (2014): High grain quality accessions within a maize drought tolerant core collection. – Scientia Agricola 71(5): 402-409.
[11] Josipovic, M., Plavsic, H., Kovacevic, V., Markovic, M., Iljkic D. (2014): Impacts of ırrigation and genotype on yield, protein, starch and oil contents in grain of maize ınbred lines. – Genetika Journal 46(1): 243-253.
[12] Kahriman, F., Ada, F., Uysal, Z., Songur, U. (2020): Investigation of yield and grain quality characteristics of Turkmenistan origin local corn populations. – Canakkale University, Journal of Agricultural Faculty, Special Issue, pp.79-86.

http://www.aloki.hu ● ISSN 1589 1623 (Print) ● ISSN 1785 0037 (Online)
DOI: http://dx.doi.org/10.15666/aeer/1906_50175031

[13] Kanber, R., Gungor, H. (1986): Use of Open Water Surface (Class A Pan) Evaporation in irrigation programs. – Rural Services, Plant Water Consumption Main Project No. 433, Eskisehir, Turkey, 25p.
[14] Kaplan, M., Aktas, M. (1993): Comparison of the effectiveness of ammonium nitrate and urea fertilizers in hybrid corn and determination of proper nitrogen doses of corn. – Journal of Agriculture and Forestry 17: 649-657.
[15] Kara, B. (2006): Determination of yield and yield characteristics, nitrogen uptake and utilization efficiency of maize at different plant frequencies and nitrogen doses in Çukurova conditions. – Cukurova Univ. Institute of Science, PhD Thesis, Adana, Turkey, 162p.
[16] Kılınc, S., Karademir, C., Ekin, Z. (2018): Determination of yield and quality characteristics of some maize (*Zea mays* L.) cultivars. – KSU Journal of Agriculture and Nature 21(6): 809-816.
[17] Koca, G., Ibrikci, H. (2019): Nitrogen and yield relations in maize plant in Çukurova conditions. – Cukurova J. Agric. Food Sci. 34(2): 119-125.
[18] Lancashire, P. D., Bleiholder, H., Langelüddecke, P., Stauss, R., Van Den Boom, T., Weber, E., Witzenberger, A. (1991): An uniform decimal code for growth stages of crops and weeds. – Ann. Appl. Biol. 119: 561-601.
[19] Oktem, A., Ulger, A. C., Kırtok, Y. (2001): The effect of different nitrogen doses and row spacing on grain yield and some agronomic traits in popcorn (*Zea mays everta* Sturt.). – Cukurova J. Agric. Food Sci. 16(2): 83-92.
[20] Oktem, A. G., Oktem, A. (2005): Effect of nitrogen and intra row spaces on sweet corn (*Zea mays saccharata* Sturt) ear characteristics. – Asian Journal of Plant Science 4(4): 361-364.
[21] Oktem, A. (2006): Effect of different irrigation intervals to drip irrigated dent corn *(Zea mays* L. *indentata)* water-yield relationship. – Pakistan Journal of Biological Sciences 9(8): 1476-1481.
[22] Oktem, A. (2008a): Effect of water shortage on yield, and protein and mineral compositions of drip-irrigated sweet corn in sustainable agricultural systems. – Agricultural Water Management 95(9): 1003-1010.
[23] Oktem, A. (2008b): Effects of deficit irrigation on some yield characteristics of sweet corn. – Bangladesh Journal of Botany 37(2): 127-131.
[24] Oktem, A. (2008c): Effect of nitrogen on fresh ear yield and kernel protein content of sweet corn (*Zea mays saccharata*) under upper Mesopotamia region of Turkey. – Indian Journal of Agricultural Sciences 78(1): 50-55.
[25] Oktem, A., Oktem, A. G. (2009): Yield characteristics of sweet corn under deficit irrigation in Southeastern Turkey. – The Philippine Agricultural Scientist 92(3): 39-44.
[26] Oktem, A., Oktem, A. G., Emeklier, H. Y. (2010): Effect of nitrogen to yield and some quality parameters of sweet corn. – Communications in Soil Science and Plant Analysis 41(7): 832-847.
[27] Oktem, A., Oktem, A. G. (2013): Determination of effective characteristics to green plant yield of corn as a selection criterion. – Soil-Water Journal 2(2): 1625-1632.
[28] Oktem, A. G., Oktem, A. (2020a): Effect of farmyard manure application on yield and some quality characteristics of popcorn (*Zea mays* L. *everta* Sturt) at the organic farming. – Journal of Agriculture and Ecology Research International 21(9): 35-42.
[29] Oktem, A. G., Oktem, A. (2020b): Effect of humic acid application methods on yield and some yield characteristics of corn plant (*Zea mays* L. *indentata*). – Journal of Applied Life Sciences International 23(11): 31-37.
[30] Ozata, E., Kapar, H. (2014): Determination of quality and performance of some dent hybrid maize (*Zea mays indentata* Sturt) genotypes under Samsun conditions. – Journal of Agricultural Sciences Research 7(2): 01-07.
[31] Ozsisli, B. (2010): Investigation of yield and quality characteristics of different corn varieties grown as main and second crop in Kahramanmaras conditions. – KSU Sutcu Imam University, Institute of Science, PhD Thesis, K. Maras, Turkey, 130p.

http://www.aloki.hu ● ISSN 1589 1623 (Print) ● ISSN 1785 0037 (Online)
DOI: http://dx.doi.org/10.15666/aeer/1906_50175031

[32] Paiva, P., Bezerra de Mello Monte, M. (2011): Yield, quality components, and nitrogen levels of silage corn fertilized with urea and zeolite. – Communications in Soil Science and Plant Analysis 42: 1266-1275.
[33] Patricio Soto, O., Ernesto Jahn, B., Susana Arredondo, S. (2004): Improvement of protein percentage in corn silage with an increase in and partitioning of nitrogen fertilization. – Agricultura Tecnia 64(2): 156-162.
[34] Safdarian, M., Razmjoo, J., Movahhedi Dehnavi, M. (2014): Effect of nitrogen sources and rates on yield and quality of silage corn. – Journal of Plant Nutrition 37(4): 611-617.
[35] Saruhan, V., Sireli, H. D. (2005): The effect of different nitrogen doses and plant density on ear, stem and leaf characteristics in maize plant (*Zea mays* L.). – Journal of Agriculture 9(2): 45-53.
[36] Tunalı, M., Budaklı, M., Carpıcı, E., Celik, N. (2012): The effects of different nitrogen doses on chlorophyll content, leaf area index and grain yield in some corn cultivars. – Journal of Agricultural Sciences Research 5(1): 131-133.
[37] Ullah, M. I., Khakwani, A. A., Sadiq, M., Awan, I., Munir, M., Ghazanfarullah, A. (2015): Effects of nitrogen fertilization rates on growth. quality and economic return of fodder maize (*Zea may*s L.). – Sarhad Journal of Agricul 31(1): 45-52.
[38] Watson, S. A. (2003): Description, development, structure and composition of the corn kernel. – In: White, P. J., Johnson, L. A. (eds.) Corn: chemistry and technology, 2nd ed. American Association of Cereal Chemists, St. Paul, MN, USA. pp.69-106.
[39] Yolcu, R. (2014): The effect of different irrigation levels and nitrogen fertilizer applied in different periods on yield and yield characteristics of silage corn irrigated with drip irrigation. – Cukurova Univ. Institute of Science, PhD Thesis, Adana, Turkey, 147p.
[40] Yurtsever, N. (1984): Experimental Statistics Methods. – Soil and Fertilizer Research Institute, General Publication No:121, Ankara, Turkey.
[41] Yururdurmaz, C. (2007): Determination of the effect of different fertilizer doses on different corn varieties in Kahramanmaras conditions and evaluation of the Ceres-Maize plant growth model. – Cukurova Univ. Institute of Science, PhD Thesis, Adana, Turkey, 242p.

http://www.aloki.hu ● ISSN 1589 1623 (Print) ● ISSN 1785 0037 (Online)
DOI: http://dx.doi.org/10.15666/aeer/1906_50175031

BIOPESTICIDE APPLICATION ON KINNOW MANDARIN (*CITRUS RETICULATA* BLANCO) WITH IMPROVED PRUNING CAN ENHANCE COSMETIC AND PHYSICAL CHARACTERS IN FRUIT

AFTAB, M.[1] – KHAN, M. A.[1*] – HABIB, U.[1] – AHMAD, M.[2]

[1]*Deparment of Horticulture, PMAS-Arid Agriculture University, Rawalpindi 46300, Pakistan*

[2]*Department of Entomology, PMAS-Arid Agriculture University, Rawalpindi 46300, Pakistan*

**Corresponding author*
email: drazam1980@uaar.edu.pk

(Received 4th Jul 2021; accepted 30th Sep 2021)

Abstract. Kinnow mandarin (*Citrus reticulata* Blanco) is a highly valued fruit crop with ever increasing demand in national and international markets. Farmers eagerly put their efforts to produce quality fruit even compromising food safety, which is a preliminary concern of every consumer due to increased awareness of the adverse impact of pesticide abuses in conventional farming system. Use of environment friendly non-hazardous biological agents is increasing particularly for perishable horticultural crops. The project was designed to evaluate ecofriendly approaches to improve plant vigor and fruit quality of Kinnow mandarin replacing unsafe synthetic pesticides. During first two years of trial (2014 and 2015) improved pruning practices (traditional, 10% and 20%) and biopesticides (neem oil and lemongrass oil each at 1.5%) were evaluated separately while in third year (2016) integrated treatment applications were designed to investigate cumulative effect of pruning and biopesticides on fruit quality in comparison with control and sole application of Bifenthrin at 2 ml/L. Cosmetic, physical and biochemical attributes were studied in fully ripened fruits. Initial experiments witnessed significant reduction in fruit blemishes with 20% pruning and 1.5% neem oil treatment with improved physical quality, while cumulative application resulted in prominent statistically significant improvement. Tree pruning along with foliar spray of neem oil significantly improved fruit physical quality and cosmetic appearance.
Keywords: *blemishes, fruit quality, neem oil, lemongrass oil, canopy management, non-hazardous, ecofriendly*

Introduction

Kinnow mandarin is the most prominent member of the citrus family particularly for juices and fresh consumption. Like any other commercial fruit crop quality is considered as driving force in supply chain for both Pakistan and international destinations (Dandekar, 2004). Determinants of fruit quality can be divided into factors affecting external quality and factors defining internal quality. Both are of critical importance, since external quality influences initial purchasing decision, while internal quality determines consumption and successive purchase (Chaparro, 2004). Cosmetic or external fruit quality deteriorates by several abiotic (wind, physical damage, physiological disorders) and biotic factors, including insects (thrips, mites, red scale, peel miner, fruit fly and others) and diseases (citrus scab, citrus melanose and citrus canker) which damage cuticle and epidermal cells of newly developed fruit (Fatima and Iram, 2019), while table quality of fruits is influenced by different biochemical factors such as TSS/TA ratio, pH, acidity and sugar profile (Ahmed, 2005).

Synthetic pesticides are aggressively used to reduce pathogen load on crops in agricultural industry. Excessive use of these pesticides is injurious as they are highly

http://www.aloki.hu ● ISSN 1589 1623 (Print) ● ISSN 1785 0037 (Online)
DOI: http://dx.doi.org/10.15666/aeer/1906_50335044

toxic, non-biodegradable and possess residual impact. Exposure to pesticides poses a continuous health hazard, especially in the agricultural working environment (Yadav et al., 2015). Within this context, pesticide use has raised serious concerns not only due to potential effects on human health, but also about impacts on wildlife and sensitive ecosystems (Ibitayo, 2006). Modern ecofriendly approaches discourage the use of chemicals all over the world (Chaudhary et al., 2017). Production of fresh produce with minimum pesticide residual levels has become a big challenge for the industry as most of the countries are demanding maximum residual limits (MRLs) report with every consignment (Khalid et al., 2012).

As an alternative and non-hazardous approach, many plant-based oils are reported to possess a broad spectrum of activity against insect pests and fungal pathogens (Hikal et al., 2017). These are generally termed as biopesticides. These biopesticides are reported to have insecticidal, antifeedant, repellent, oviposition, deterrent, growth regulatory and anti-vector activities (Dimetry et al., 2018). Recent investigations indicate that some chemical constituents of these oils interfere with the nervous system in insects. As the target site is not shared with mammals, most essential oil chemicals are relatively nontoxic to mammals and fish, meeting the criteria for "reduced risk" pesticides (Chaudhary et al., 2017). Thus, in the present concept of green pesticides, some rational attempts have been made to include substances such as plant extracts, hormones, pheromones (Koul, 2008). A number of source plants have been traditionally used for protection of stored commodities, but interest in the biopesticides is reintroduced due to their fumigant, repellent and contact insecticidal activities to a wide range of pests in field conditions (Priestley et al., 2003).

Along with some others, neem oil is widely known to use as a safe pest management technique. Studies witnessed that neem oil proved as a good substitute of synthetic insecticides to manage citrus insect pest like leaf miner (Arshad et al., 2019; Deka et al., 2018). Neem seeds contain numerous azadirachtin analogs which are well known as a potent antifeedant to many insects (Sirohi and Tandon, 2014). Azadiractin based products are recommended in the control of insects such as aphids, armyworms, caterpillars, beetles, borers, budworms, cutworms, leafhoppers, leaf miners, lepidopterous larvae, loopers, maggots, mealy bugs, psyllids, scale, stink bugs, weevils and whiteflies (Dayan et al., 2009). Several other plant extracts and essential oils are in general practice as repellents like lemongrass, marigold and basil. Some of the plant extracts especially leaf extract of chrysanthemum naturally contain pyrethrum and can be used as pesticide against many sucking pests.

Along with ecofriendly chemicals, orchard management and cultural practices are the key factor contributing to the quality of horticultural produce. Poor cultural practices can seriously impact fruit quality. Pruning is a valuable practice in citrus orchard suffering from negligence or decline to induce rejuvenation and enhance vegetative growth (Rani et al., 2018). In combination with regular schedule of pest control, removal of decadent wood will improve top root balance, resulting good quality fruit (Morales and Davies, 2000). Pruning in citrus is considered as a cheap and efficient practice to avoid physical damage like bruising of the fruit from rubbing with branches as reduction in crowded tree canopy decreases the risk of wind born blemishes. It also increases the light penetration in the tree, improves general health and vigor of the tree meanwhile pruning diseased and week branches also reduced the risk of fungal infestation (Dick, 2007; Marini, 2014). Pruning is done as a regular practice to reduce disease load and to improve light penetration to attain better fruit quality in many

http://www.aloki.hu ● ISSN 1589 1623 (Print) ● ISSN 1785 0037 (Online)
DOI: http://dx.doi.org/10.15666/aeer/1906_50335044

countries like USA (Fake, 2012). Pruning practices were never tested or standardized in Pakistan as a strategy to minimize fruit blemishes in Kinnow mandarin.

Putting all these factors under consideration, current study was designed to improve cosmetic, physical and biochemical aspects in Kinnow mandarin with application of non-hazardous biopesticides coupled with improved tree pruning practices in order to provide an alternative approach to cast off synthetic pesticides intensively used by citrus growers in Pakistan.

Materials and methods

Three-year study was conducted at commercial Kinnow mandarin (*Citrus reticulata*) orchard in prominent citrus growing District Sargodha of Punjab Province, Pakistan (32°05'N 72°40'E). Uniformly aged Kinnow mandarin trees, managed under similar cultural practices with same productivity potential, history and symptoms of identified potential issues were selected to perform the experiment.

During 2014 and 2015, impact of improved tree pruning practices and biopesticides applications were tested separately. The treatments included control (T_1), traditional pruning (Removal of dried and intermingled branched) (T_2), 10% pruning (removing additional 10% biomass) (T_3), 20% pruning (removing additional 20% biomass) (T_4), 1.5% neem oil (T_5), 1.5% lemongrass oil (T_6) and 2 ml/L bifenthrin (T_7), where bifenthrin was applied for comparison as it is one of the most widely used pesticides to overcome pest problems in citrus production. While in 2016, combinations of best performing treatments were tested in comparison with control and synthetic insecticides. The treatment combinations included control (T_1), 10% pruning (removing additional 10% biomass) * 1.5% neem oil (T_2), 20% pruning (removing additional 20% biomass) * 1.5% neem oil (T_3) and bifenthrin at 2ml/L (T_4). Selected trees were pruned at the end of February according to the treatment plan. Spray applications were carried out at three different developmental stages i.e. before flowering, at fruit set (when more than 90% petal fall reached) and at pea size fruit.

At commercial maturity, data regarding nature and extent of blemishes (fruit cosmetic quality) were recorded for randomly selected 100 fruits from each replicated tree. Data on nature of blemishes was divided into biotic and abiotic categories, among biotic factors, percent insect pest infected fruit (thrips, scales and mites) and percent disease infected fruits (scab, melanose and canker) were observed while among abiotic factors percent infected fruits due to wind scars, stem injury and styler end deformity (SED) were observed. Fruit was categorized for skin blemishes as described by Khalid et al. (2012).

Physical quality parameters included, fruit diameter, fruit weight, juice weight, peel thickness and number of seeds per fruit. Fruit diameter and peel thickness was recorded with the help of digital vernier caliper, while fruit and juice weight were recorded with weighing scale. The biochemical characters including ascorbic acid, pH, total soluble solids/titratable acidity (TSS/TA) ratio and total sugar were determined according to standard techniques, as described by Saleem et al. (2008) and Khan et al. (2011).

Experiment was laid out under randomized complete block design (RCBD) with three replications having one tree per replicate. Data regarding parameters was compared by HSD test with 5% significance level by using Statistix 8.1 (Steel et al., 1997).

http://www.aloki.hu ● ISSN 1589 1623 (Print) ● ISSN 1785 0037 (Online)
DOI: http://dx.doi.org/10.15666/aeer/1906_50335044

Results and discussion

Fruit cosmetic quality

To assess cosmetic quality fruits were analyzed for nature and extent of blemishes. Among nature of blemishes, fruits were expressed as percent infected fruits and categorized as insect pest induced (thrips, scales and mites), disease induced (scab, melanose and canker) and a biotic induced (wind scars, stem injury and SED) fruit blemishes against tree pruning and biopesticides as presented in *Figures 1* and *2.*

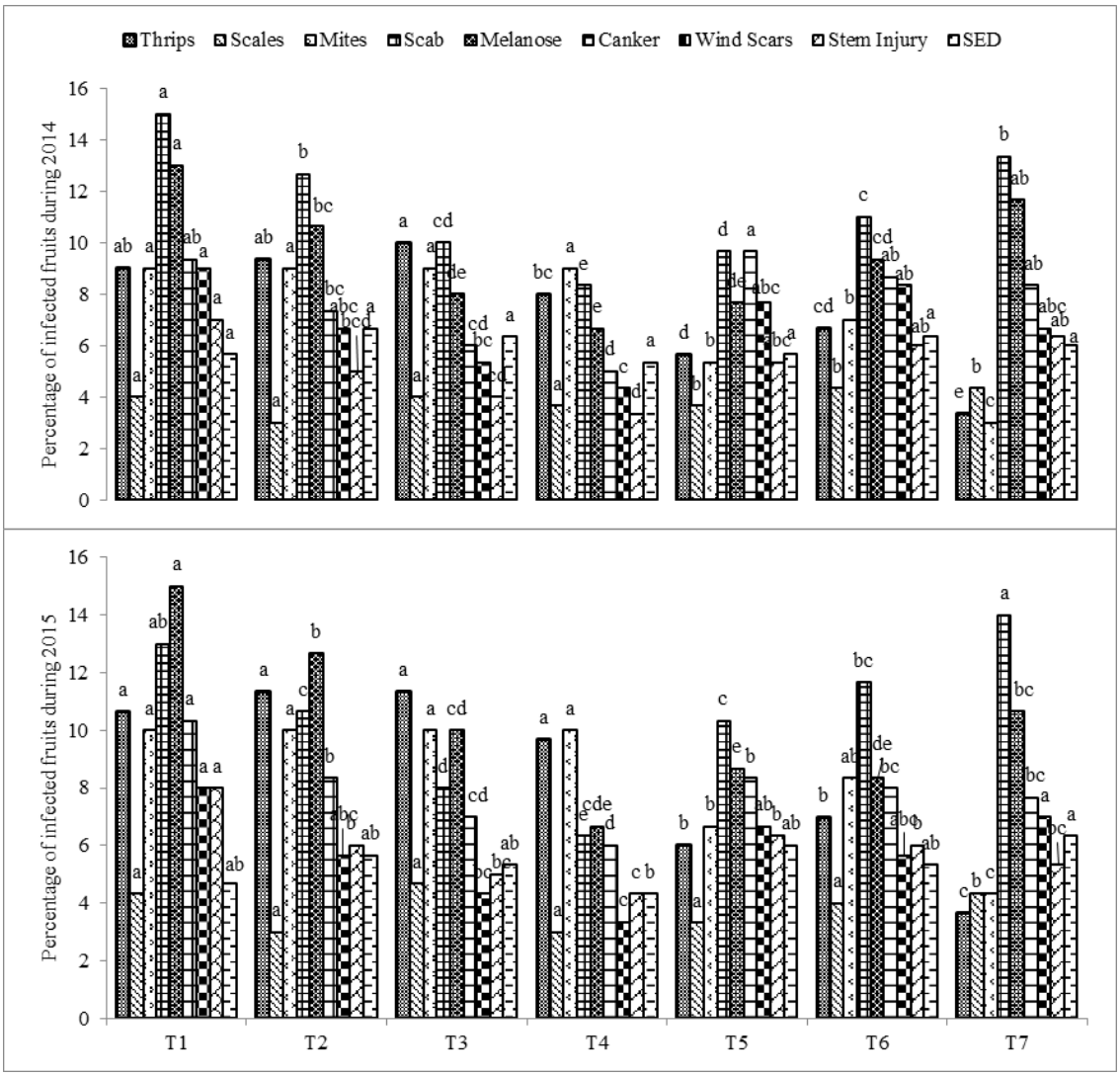

Figure 1. *Effect of biopesticides and tree pruning on nature of fruit blemishes during two consecutive years (2014 and 2015). T1 = Control, T2 = Traditional Pruning, T3 = pruning 10% T4 = Pruning 20%, T5 = Neem oil 1.5%, T6 = Lemongrass oil 1.5%, T7 = Bifenthrin 2 ml/L*

During 2014 and 2015 studies revealed that tree pruning at 20% alone proved beneficial to control blemishes on fruit skin due to fungus (scab 8.33% and 6.33%, melanose 6.67% and 6.67% and canker 5% and 6%), wind (4.33% and 3.33%) and stem injury (3.33% and 4.33%) as compared to other treatments, while tree pruning did not put any substantial impact on insect pest induced fruit blemishes. Biopesticides

http://www.aloki.hu ● ISSN 1589 1623 (Print) ● ISSN 1785 0037 (Online)
DOI: http://dx.doi.org/10.15666/aeer/1906_50335044

especially neem oil at 1.5% significantly reduced incidence of thrips (5.67 and 6%) and mites (5.33 and 6.67%) induced fruit blemishes as compared to other treatments while remained at par with synthetic insecticide i.e. Bifenthrin at 2 ml/L (thrips 3.33% and 3.67% and mites 3% and 4.33%). Chemical agent (Bifenthrin at 2 ml/L) failed to control fungal induced blemishes, however it provided most efficient control over insect pest induced blemishes on fruit skin in Kinnow mandarin. Fruit blemishes due to styler end deformity exhibited non-significant trend among all treatments.

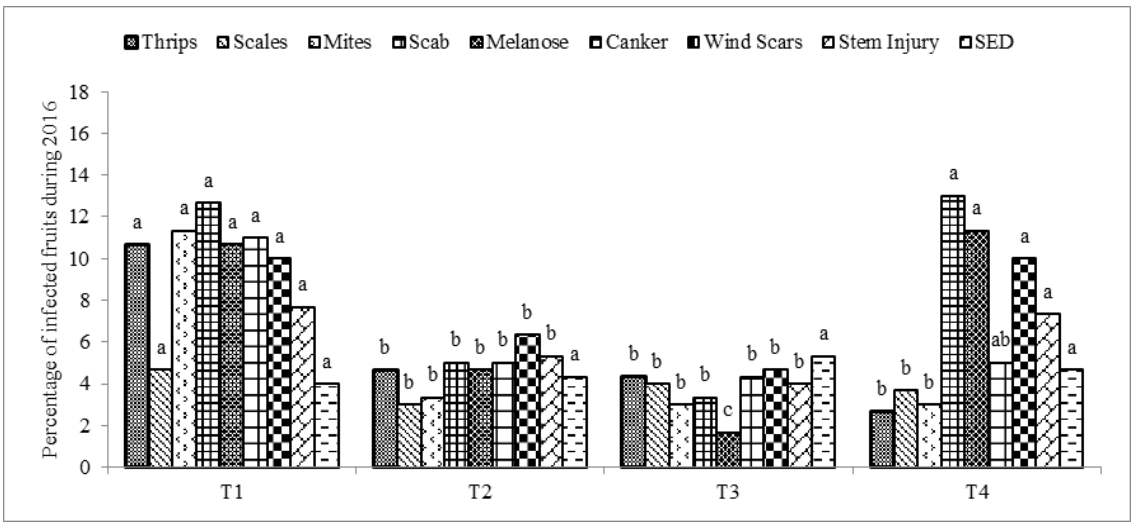

Figure 2. *Effect of biopesticides and tree pruning on nature of fruit blemishes during 2016. T_1 = Control, T_2 = Pruning 10% + Neem oil 1.5%, T_3 = Pruning 20% + Neem oil 1.5%, T_4 = Bifenthrin 2 ml/L*

While taking into account data collected in 2016, combination of pruning and neem oil significantly reduced abiotic and disease induced fruit blemishes. Maximum reduction in fruit blemishes due to scab (3.33%), melanose (1.67%), canker (4.33%), wind scars (4.67%) and stem injury (4%) were observed in plants pruned at 20% and sprayed with 1.5% neem. Among insect pest induced fruit blemishes again Bifenthrin proved to be most effective treatment (thrips: 2.67%, mites: 3%) as compared to other treatments.

Among extent of blemishes, fruits were categorized into six different grades having < 1%, 1-5%, 6-10%, 11-25%, 26-50% and > 50% blemished surface area against application of different treatments which reflected significant difference as shown in *Figures 3* and *4*. During 2014 and 2015, maximum number of fruit with less than 1% (29 and 26.67%), 1-5% (31.67 and 34%) and 6-10% (20.67 and 23%) blemished area were obtained from 2 ml/L bifenthrin treated Kinnow mandarin plants followed by 1.5% neem oil application for less than 1% (21.67 and 22.67%), 1-5% (30.33 and 30%) and 6-10% (20.33 and 21%) blemished area and pruning at 20% for less than 1% (21.67 and 23.67%), 1-5% (26 and 24.67%) and 6-10% (18.33 and 20.33%) blemished area as both were statistically at par with each other.

In 2016, when tree pruning was coupled with neem oil application, maximum number of fruits with less than 1% (28.67%), 1-5% (35.67%) and 6-10% (24.67%) blemished area was obtained from 20% pruning in combination with 1.5% neem oil application.

http://www.aloki.hu ● ISSN 1589 1623 (Print) ● ISSN 1785 0037 (Online)
DOI: http://dx.doi.org/10.15666/aeer/1906_50335044

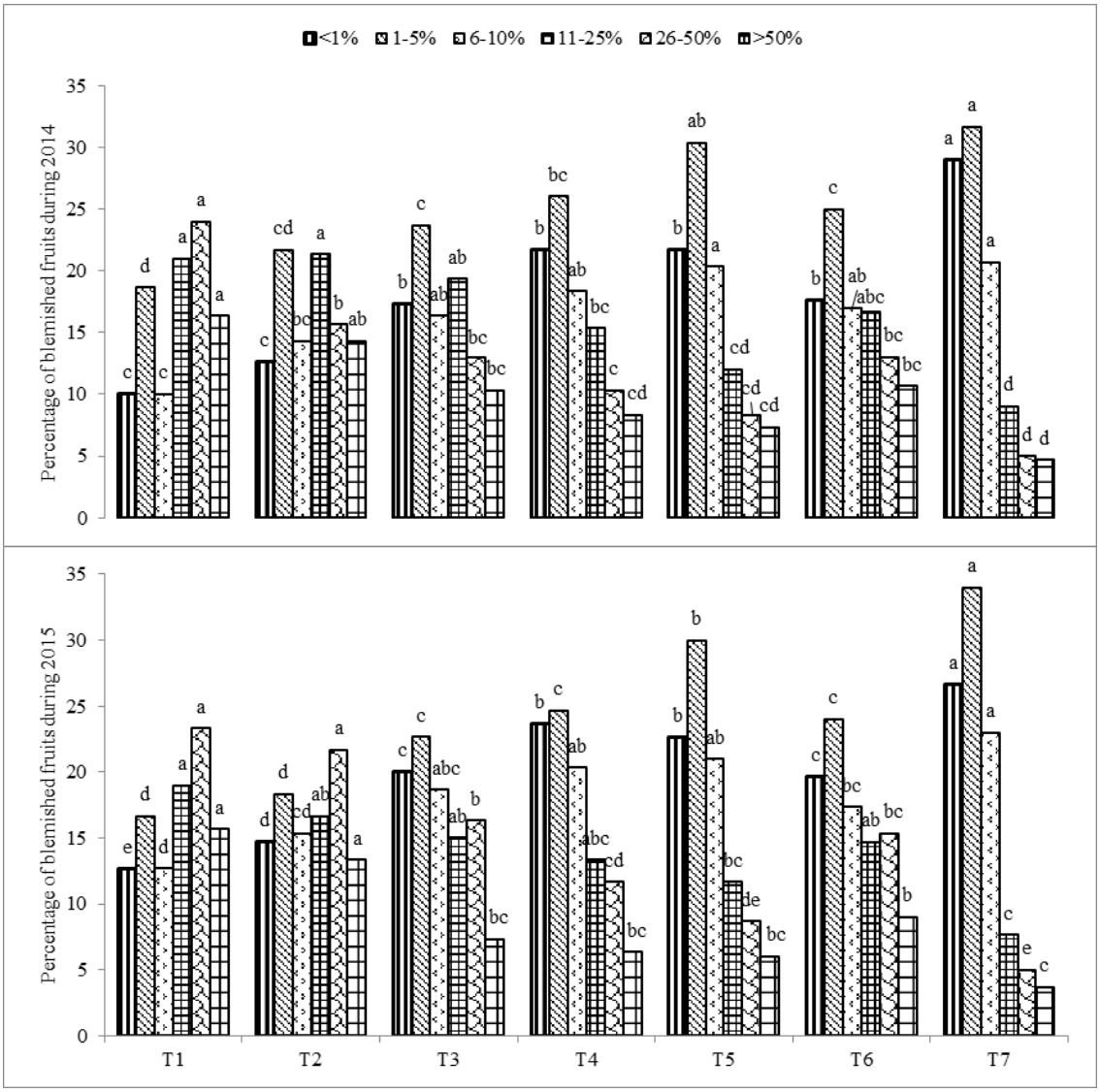

Figure 3. *Effect of biopesticides and tree pruning on extent of fruit blemishes during two consecutive years (2014 and 2015). T_1 = Control, T_2 = Traditional Pruning, T_3 = pruning 10% T_4 = Pruning 20%, T_5 = Neem oil 1.5%, T_6 = Lemongrass oil 1.5%, T_7 = Bifenthrin 2 ml/L*

Study revealed that pruning posed significant impact on disease born and wind born blemishes and when coupled with neem oil application insect pest born blemishes were also managed even more efficiently as compared to sole application of neem oil as shown in *Figure 5*. Pruning open up the canopy and improves pest control by allowing better spray penetration into the tree, hence while combined application of pruning and neem oil suppressed insect pest induced blemishes more efficiently (Khalid et al., 2012). While carrying out pruning most of diseased branches were removed which lower down fungal inoculums in the tree and uplift emergence and growth of healthy shoots (Rani et al. 2018), resulting aeration of tree canopy, reduced canopy moisture and suppressed the chance of fungal infestation and severity of many diseases (Marini, 2014).

The effect of neem oil on thrips, scales, mites, scab, melanose and canker induced fruit blemishes was statistically significant however, wind scars, stem injury and styler end deformation did not show significant response against neem oil application. It has

http://www.aloki.hu ● ISSN 1589 1623 (Print) ● ISSN 1785 0037 (Online)
DOI: http://dx.doi.org/10.15666/aeer/1906_50335044

been observed that various biopesticides can effectively be used to control different insects and diseases of fruits (Pavela and Benelli, 2016). Biopesticides have certain active chemicals which act as anti-fungal or insecticides (Hikal et al., 2017) to control pathogen and insects induced biotic stresses during pre-harvest stage of fruits (Hong et al., 2015). In the same way, neem essential oils were also known for their varied pest management characteristics (Koul et al., 2003).

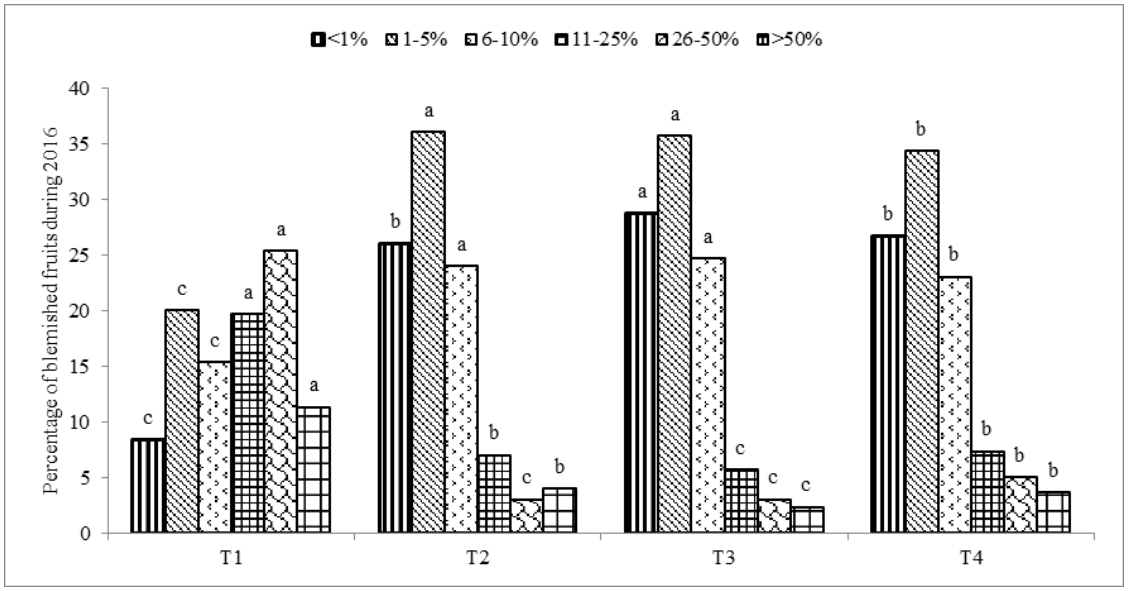

Figure 4. *Effect of biopesticides and tree pruning on extent of fruit blemishes during 2016. T_1 = Control, T_2 = Pruning 10% + Neem oil 1.5%, T_3 = Pruning 20% + Neem oil 1.5%, T_4 = Bifenthrin 2 ml/L*

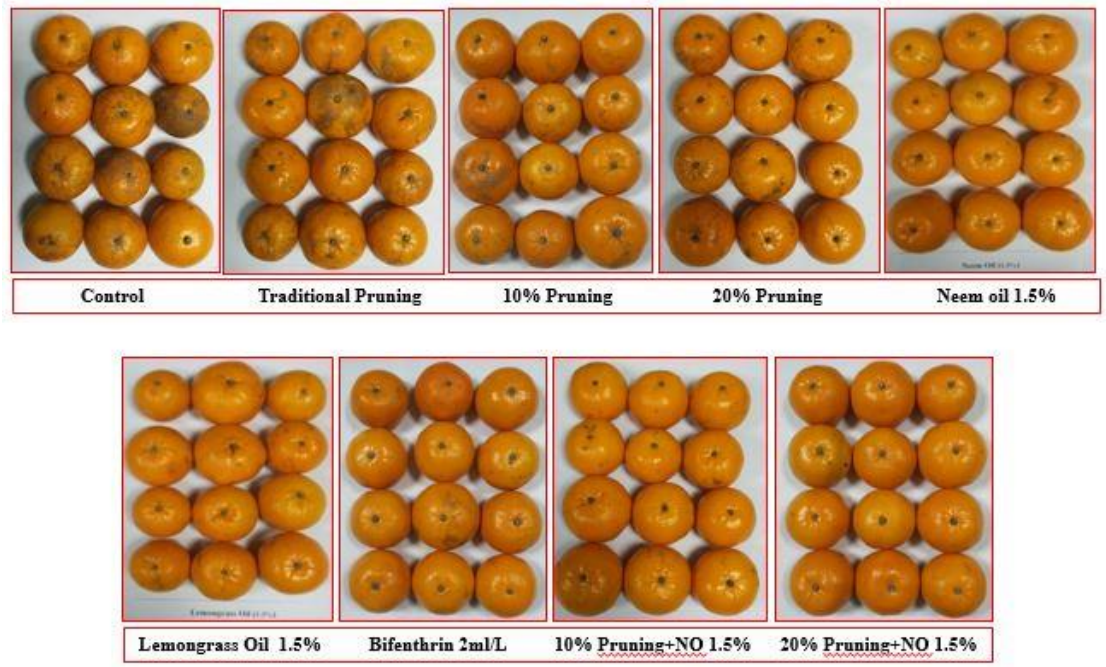

Figure 5. *Cosmetic quality of Kinnow mandarin fruits in response to tree pruning and biopesticides*

http://www.aloki.hu ● ISSN 1589 1623 (Print) ● ISSN 1785 0037 (Online)
DOI: http://dx.doi.org/10.15666/aeer/1906_50335044

Fruit physical quality

Fruits harvested from different treatments were observed for fruit diameter, fruit weight, juice weight, peel thickness and number of seeds per fruit. During the whole three years of study, tree pruning and biopesticides significantly improved fruit diameter as shown in *Figure 6,* fruit weight and juice weight but did not pose any substantial impact on number of seeds per fruit and peel thickness except during 2014, where peel thickness was observed maximum in 10% pruned trees and minimum in 2 ml/L Bifenthrin treated trees as shown in *Tables 1* and *2*.

During 2014 and 2015, 10% pruning resulted in maximum fruit diameter (76.82 mm and 75.87 mm), fruit weight (184.76 g and 181.71 g) and juice weight (44.97 g and 44.92 g) while in 2016 when pruning was combined with neem oil application again 10% pruning sprayed with 1.5% neem oil resulted in maximum fruit diameter (74.65 mm), fruit weight (178.36 g) and juice weight (47.43%) followed by 20% pruning sprayed with 1.5% neem oil for fruit diameter (73.63 mm), fruit weight (175.91 g) and juice weight (45.5%) and minimum in control (fruit diameter: 68.51 mm, fruit weight: 167.03 g, juice weight: 44.45%).

Pruning is an important orchard practice because pruning can influence fruit quality by creating balance between vegetative growth and fruiting. Annual pruning always enhances fruit quality. Pruning increases fruit size because excessive flower buds are removed and pruning encourages the growth of new shoots with high-quality flower buds. Pruning improves light penetration into the canopy, and light is required for flower bud development, photosynthesis and growth (Marini, 2014).

The importance of sunlight intercepted by the tree canopy in the production of high yield of good quality fruit cannot be over emphasized. Light becomes a limiting factor in crowded groves and pruning improves light access. Ahmad et al. (2006) studied the effect of pruning on the yield and quality of Kinnow fruit and conclusively found that pruning appeared to be the best method to obtain maximum yield, quality, fruit size, weight and juice in Kinnow fruit. Pruning increased the percentage of large fruit and reduced the percentage of small fruit (Morales and Davies, 2000).

Table 1. *Effect of biopesticides and tree pruning on physical fruit quality during 2014 and 2015*

Treatments	Fruit physical quality									
	Fruit diameter (mm)		Fruit weight (g)		Juice weight (%)		Peel thickness (mm)		No of seeds (No)	
	2014	2015	2014	2015	2014	2015	2014	2015	2014	2015
T_1	68.72c	69.78c	167.93d	164.88d	41.65b	42.03b	2.67ab	2.52a	20.7a	19.27a
T_2	72.76b	71.63b	172.98b	172.93c	42.63ab	43.01ab	2.63ab	2.28a	19.77a	20.33a
T_3	76.82a	75.87a	184.76a	181.71a	44.97a	44.92a	2.85a	2.67a	20.2a	19.17a
T_4	74.12a	74.44a	180.54ab	177.49ab	43.09ab	44.37ab	2.72ab	2.37a	20.97a	18.77a
T_5	75.68a	73.61ab	170.98bc	174.07b	44.04a	44.19a	2.03a	2.25a	20.20a	20.00a
T_6	72.82b	70.74b	170.61c	173.7b	43.33a	43.98ab	1.91b	2.13a	19.47a	19.27a
T_7	76.60a	74.53a	172.42bc	175.51ab	44.31a	44.42a	1.84b	2.06a	20.17a	19.97a
HSD($p \leq 0.05$)	2.869	2.683	2.960	2.960	2.674	2.592	NS	NS	NS	NS

Means sharing similar letter are not significantly different according to HSD test ($P \leq 0.05$). NS = Not significant. T_1 = Control, T_2 = Traditional Pruning, T_3 = pruning 10% T_4 = Pruning 20%, T_5 = Neem oil 1.5%, T_6 = Lemongrass oil 1.5%, T_7 = Bifenthrin 2 ml/L

http://www.aloki.hu ● ISSN 1589 1623 (Print) ● ISSN 1785 0037 (Online)
DOI: http://dx.doi.org/10.15666/aeer/1906_50335044

Table 2. *Effect of biopesticides and tree pruning on physical fruit quality during 2016*

	Fruit physical quality				
Treatments	**Fruit diameter (mm)**	**Fruit weight (g)**	**Juice weight (%)**	**Peel thickness (mm)**	**No of seeds (No)**
T_1	68.51c	167.03c	44.45b	2.46a	19.5a
T_2	74.65a	178.36a	47.43a	2.76a	19.2a
T_3	73.63ab	175.91ab	45.5ab	2.97a	19.53a
T_4	73.45b	174.55b	45.28ab	2.43a	20.63a
HSD($p \leq 0.05$)	2.34	13.32	NS	NS	NS

Means sharing similar letter are not significantly different according to HSD test ($P \leq 0.05$). NS = Not significant. T_1 = Control, T_2 = Pruning 10% + Neem oil 1.5%, T_3 = Pruning 20% + Neem oil 1.5%, T_4 = Bifenthrin 2 ml/L

Figure 6. *Pictorial description of fruit diameter influenced by tree pruning and biopesticides*

Fruit biochemical quality

Fruits harvested from different treatments were analyzed for ascorbic acid, pH, TSS/TA ratio and total sugar contents. During the whole 3 years of study, tree pruning and biopesticides did not put any substantial positive or negative impact on fruit biochemical features as shown in *Tables 3* and *4*.

Results indicated that pruning has non-significant changes on biochemical quality of Kinnow mandarin fruits, same trees were sprayed with neem oil as well. The results clearly indicate both pruning and biopesticides did not alter fruit quality when accessed on postharvest biochemical parameters. These management practices are useful to enhance external fruit quality without any impact on flavor, taste and sweetness in Kinnow mandarin.

Similar finding has already been reported by Ahmad et al. (2006), reporting non-significant response of pruning on TSS, TA and TSS/TA ratio in Kinnow mandarin

http://www.aloki.hu ● ISSN 1589 1623 (Print) ● ISSN 1785 0037 (Online)
DOI: http://dx.doi.org/10.15666/aeer/1906_50335044

fruit, and Khalid et al. (2012) revealing non-significant influence of pruning equipped with HMO application on Kinnow mandarin biochemical fruit quality. The application of biopesticides is known to effectively maintain higher TSS, TA and lower TSS/TA ratio during postharvest storage but not during pre-harvest situations (Sivakumar and Bautista-Banos, 2014).

Table 3. *Effect of biopesticides and tree pruning on biochemical fruit quality during 2014 and 2015*

Fruit biochemical quality								
Treatments	**Vitamin C (mg/100 g)**		**pH**		**TSS/TA**		**Total sugars (%)**	
	2014	**2015**	**2014**	**2015**	**2014**	**2015**	**2014**	**2015**
T_1	29.12a	29.8a	4.13a	4.09a	11.39a	10.55a	6.95a	7.31a
T_2	31.11a	31.6a	2.28a	4.22a	12.01a	10.66a	6.79a	7.39a
T_3	31.27a	30.31a	4.29a	4.27a	12.52a	11.59a	7.05a	7.35a
T_4	32.28a	31.76a	4.38a	4.24a	12.22a	12.62a	7.04a	7.37a
T_5	30.7a	29.12a	4.08a	4.50a	13.6a	12.95a	7.29a	6.95a
T_6	31.1a	30.37a	4.05a	4.78a	13.15a	14.67a	7.54a	7.73a
T_7	31.92	30.31a	4.07a	4.35a	13.3a	11.72a	7.68a	7.68a
HSD($p \leq 0.05$)	NS	NS	NS	NS	NS	NS	NS	NS

Means sharing similar letter are not significantly different according to HSD test ($P \leq 0.05$). NS = Not significant. T1 = Control, T2 = Traditional Pruning, T3 = pruning 10% T4 = Pruning 20%, T5 = Neem oil 1.5%, T6 = Lemongrass oil 1.5%, T7 = Bifenthrin 2ml/L

Table 4. *Effect of biopesticides and tree pruning on biochemical fruit quality during 2016*

Fruit biochemical quality				
Treatments	**Vitamin C (mg/100g)**	**pH**	**TSS/TA**	**Total sugars (%)**
T_1	30.7a	4.21a	11.01a	7.45a
T_2	28.84a	4.23a	11.91a	7.7a
T_3	31.95a	4.25a	12.42a	7.68a
T_4	29.44a	4.24a	11.18a	7.54a
HSD($p \leq 0.05$)	NS	NS	NS	NS

Means sharing similar letter are not significantly different according to HSD test ($P \leq 0.05$). NS = Not significant. T_1 = Control, T_2 = Pruning 10% + Neem oil 1.5%, T_3 = Pruning 20% + Neem oil 1.5%, T_4 = Bifenthrin 2 ml/L

Conclusion

Study witnessed that biopesticides coupled with improved tree pruning at 20% significantly improved fruit cosmetic quality meanwhile other quality aspects of Kinnow mandarin in comparison with synthetic insecticides. Although pruning at 10% put more significant impact on fruit size and weight but pruning at 20% resulted in better fruit cosmetic quality which will ultimately resulted in better pack out. It is need of the hour to screen out more available plant based biopesticides and to establish low-cost technology for its manufacturing and commercialization on large scale. Similarly,

http://www.aloki.hu ● ISSN 1589 1623 (Print) ● ISSN 1785 0037 (Online)
DOI: http://dx.doi.org/10.15666/aeer/1906_50335044

tree pruning should also be tested with other biopesticides and cultural practices like fruit thinning. These environmentally safe practices could be adopted by replacing hazardous synthetic pesticides to boost up blemish free citrus production without deteriorating internal fruit quality.

Acknowledgments. It is an honor to express deep sense of gratitude and thankfulness to my ex-supervisor, Prof. Dr. Nadeem Akhtar Abbasi (Late), Pro-Vice Chancellor, PMAS-AAUR, under whose dynamic and inspiring guidance as well as sympathetic attitude, I started my research work. I am also very much thankful to Roshan Enterprises, Sargodha, leading citrus producers and exporters of Pakistan, for providing citrus orchard to conduct research trials.

REFERENCES

[1] Ahmad, S., Chatha, Z. A., Nasir, M. A., Aziz, A., Virk, N. A., Khan, A. R. (2006): Effect of pruning on the yield and quality of Kinnow fruit. – Journal of Agriculture & Social Sciences 2(1): 51-53.

[2] Ahmed, M. (2005): Nature and extent of fruit blemishes in Kinnow mandarin. – M.Sc Research Thesis, Uni. Agri. Faisalabad, Pakistan.

[3] Arshad, M., Ullah, M. I., Afzal, M., Iftikhar, Y., Khalid, S., Hussain, Z. (2019): Evaluation of synthetic insecticides and essential oils for the management of Phyllocnistis citrella Stainton (Lepidoptera: Gracillariidae). – Pakistan Journal of Zoology 51(3): 1053-1058.

[4] Chaparro, J. X. (2004): Breeding a Red-Fleshed Mandarine (Candidate Gene Analysis). – Citrus Research Board, Annual Report, Horticultural Sciences, University of Florida, Gainesville.

[5] Chaudhary, S., Kanwar, R. K., Sehgal, A., Cahill, D. M., Barrow, C. J., Sehgal, R. (2017): Progress on Azadirachta indica based biopesticides in replacing synthetic toxic pesticides. – Frontiers in Plant Science 8: 610.

[6] Dandekar, A. M. (2004): Improving Peel Quality of California Citrus Fruit. – Citrus Research Board, Annual Report, Horticultural Sciences, University of Florida, Gainesville.

[7] Dayan, F. E., Cantrell, C. L., Duke, S. O. (2009): Natural products in crop protection. – Bioorganic & Medicinal Chemistry 17: 4022-4034.

[8] Deka, S., Sehgal, M., Kakoti, R. K., Barbora, A. C. (2018): Module analysis for insect pest management of khasi mandarin (Citrus reticulata Blanco) under climatic conditions of north-eastern India. – Journal of Entomology and Zoology Studies 6(4): 857-861.

[9] Dick, J. (2007): Pruning Citrus Trees. – Department of Agriculture, Western Australia.

[10] Dimetry, N. Z., Ibrahim, S. S., Metwally, H. M., El-Behery, H. (2018): Fumigant potential of some essential oils against the cowpea beetle "callosobruchus maculatus" under laboratory conditions. – Bioscience Research 15(3): 2364-2373.

[11] Fake, C. (2012): Pruning citrus. – University California Cooperative Extension, California. http://www. ucanr.edu/sites/ placernevadasmallfarms/files/134946. pdf (last accessed on 22 March 2018).

[12] Fatima, S., Iram, S. (2019): Identification of fungal pathotypes associated with skin disorders of Citrus reticulata Blanco through classical and molecular approach. – Pakistan Journal of Agricultural Research 32(1): 95-101.

[13] Hikal, W. M., Baeshen, R. S., Said-Al Ahl, H. A. (2017): Botanical insecticide as simple extractives for pest control. – Cogent Biology 3(1): 1404274.

[14] Hong, J. K., Yang, H. J., Jung, H., Dong, J. Y., Sang, M. K., Jeun, Y. C. (2015): Application of volatile antifungal plant essential oils for controlling pepper fruit anthracnose by Colletotrichum gloeosporioides. – Plant Pathology Journal 31: 269-277.

http://www.aloki.hu ● ISSN 1589 1623 (Print) ● ISSN 1785 0037 (Online)
DOI: http://dx.doi.org/10.15666/aeer/1906_50335044

[15] Ibitayo, O. O. (2006): Egyptian rural farmers' attitudes and behaviors regarding agricultural pesticides: Implications for pesticide risk communication. – Risk Anal. 26: 989-995.
[16] Khalid, M. S., Malik, A. U., Saleem, B. A., Khan, A. S., Javed, N. (2012): Horticultural mineral oil application and tree canopy management improve cosmetic fruit quality of Kinnow mandarin. – African Journal of Agricultural Research 7(23): 3464-3472.
[17] Khan, A. S., Ahmed, M. J., Singh, Z. (2011): Increased ethylene biosynthesis elevates incidence of chilling injury in cold store "Amber Jewel" Japanese plum (Prunus saliciana Lind L) during fruit ripening. – International Journal of Food Science and Technology 46: 642-650.
[18] Koul, O. (2008): Phytochemicals and insect control: an antifeed ant approach. – Critical Review of Plant Sciences 27: 1-24.
[19] Koul, O., Dhaliwal, G. S., Marwaha, S. S., Arora, J. K. (2003): Future perspectives in biopesticides. – Biopesticides and Pest Management 1: 386-388.
[20] Marini, R. (2014): Physiology of Pruning Fruit Trees. – Communications and Marketing, College of Agriculture and Life Sciences, Virginia Polytechnic Institute and State University.
[21] Morales, P., Davies, F. S. (2000): Pruning and skirting affect canopy microclimate, yields, and fruit quality of 'Orlando' tangelo. – Hortscience 35(1): 30-35.
[22] Pavela, R., Benelli, G. (2016): Essential oils as eco-friendly biopesticides? Challenges and constraints. – Trends in Plant Sciences. DOI: 10.1016/j.tplants.2016. 10.005.
[23] Priestley, C. M., Williamson, E. M., Wafford, K. A., Sattelle, D. B. (2003): Thymol, a constituent of thyme essential oil, is a positive allosteric modulator of human GABA receptors and a homo-oligomeric GABA receptor from Drosophila melanogaster. – Br. Journal of Pharmacology 140: 1363-1372.
[24] Rani, A., Misra, K. K., Rai, R., Singh, O. (2018): Effect of shoot pruning and paclobutrazol on vegetative growth, flowering and yield of lemon (Citrus limon Burm.) cv. pant lemon. – Journal of Pharmacognosy and Phytochemistry 7(1): 2588-2592.
[25] Saleem, B. A., Malik, A. U., Pervez, M. A., Khan, A. S., Khan, M. N. (2008): Spring application of growth regulators affects fruit quality of 'blood red' sweet orange. – Pakistan Journal of Botany 40(3): 1013-1023.
[26] Sirohi, A., Tandon, P. (2014): Insecticidal effects of various parts of *Azadirachta indica* on adults of Aulacophora foveicollis (Lucas) (Coleoptera: Chrysomelidae). – Trends in Biosciences 7: 3947-3949.
[27] Sivakumar, D., Bautista-Baños, S. (2014): A review on the use of essential oils for postharvest decay control and maintenance of fruit quality during storage. – Crop Protection 64: 27-37.
[28] Steel, R. G. D., Torrie, J. H., Dickey, D. (1997): Principles and Procedures of Statistics: A Biometrical Approach. 3rd Ed. – McGraw Hill Book Co. Inc., New York.
[29] Yadav, I. C., Devi, N. L., Syed, J. H., Cheng, Z., Li, J., Zhang, G. (2015): Current status of persistent organic pesticides residues in air, water and soil, and their possible effect on neighboring countries: a comprehensive review of India. – Science of the Total Environment 511: 123-137.

http://www.aloki.hu ● ISSN 1589 1623 (Print) ● ISSN 1785 0037 (Online)
DOI: http://dx.doi.org/10.15666/aeer/1906_50335044

THE EFFECTIVENESS OF ARBUSCULAR MYCORRHIZAL FUNGI AND SALICYLIC ACID AGAINST *VERTICILLIUM DAHLIAE* INFECTING PEPPER (*CAPSICUM ANNUUM* L.)

COŞKUN, F.[1] – DEMIR, S.[2] – ALPTEKIN, Y.[1*]

[1]*Department of Plant Protection, Faculty of Agriculture, Kahramanmaraş Sütçü İmam University, 46100 Kahramanmaraş, Turkey*

[2]*Department of Plant Protection, Faculty of Agriculture, Yüzüncü Yıl University, 65100 Van, Turkey*

[*]*Corresponding author*
e-mail: alptekin69@ksu.edu.tr

(Received 12th Jul 2021; accepted 1st Oct 2021)

Abstract. This study was carried out to determine the effects of arbuscular mycorrhizal fungi (AMF), and salicylic acid (SA) on plant growth parameters and severity of wilt disease caused by *Verticillium dahliae* Kleb. in pepper. Effects of two different AMFs (Commercial AMF and *Glomus intraradices*) and two different SA doses (0.5 and 1 mM) were compared with untreated control plants after ten weeks. Both AMF species caused 62.08% and 69.07% root colonization, and the mycorrhizal dependency ratio changed from 9.08% to 59.37% in pepper plants. Commercial AMF caused a significant increase in morphological growth parameters, root colonization, mycorrhizal dependency rates and suppression of the disease severity. SA (1 mM) resulted in improved morphological growth parameters and suppression of the severity of the disease. Besides, SA and AMF applications were found to suppress the severity of Verticillium wilt disease by 21.8% and 56% in pepper plants, respectively. Thus, the applications of SA and AMF had positive contributions to the pepper plant's morphological development.
Keywords: *wilt disease, Glomus spp., plant growth regulator, disease severity, plant morphology*

Introduction

Pepper (*Capsicum annuum* L.) is an essential vegetable that accounts for 9.8% of all cultivated land and 11.1% of all vegetable production (Wang et al., 2018). Fungal diseases, however, cause 14% annual yield loss in the global vegetable production (Duran and Özkaya, 2016). Verticillium wilt, caused by the fungal pathogen *Verticillium dahliae* Kleb., is the most economically important of all the diseases that affect pepper plants (Vasileva and Todorova, 2020). The fungus can survive as microsclerotia in the soil and plant debris. Microsclerotia germinate and infect the roots of sensitive pepper seedlings (Caroll et al., 2018). *V. dahliae* colonizes the host xylem vessels, where it might block nutrient and water movements upwards (Novo et al., 2017). As a result, the pathogen causes wilting symptoms in the host plants (Carroll et al., 2018).

There have not yet, been any effective chemicals that sufficiently control the diseases (Bilgili and Güldür, 2018). Researchers have been focused on the biological management of this disease by using environmentally friendly alternatives to chemicals (Adnan et al., 2019). Enhanced nutrition, which improves host defenses, or direct restriction of pathogen development and activity, is primarily associated with biocontrol of soil-borne diseases (Rajkumar et al., 2008).

As biological control agents, arbuscular mycorrhizal fungi (AMF) infect the roots of most terrestrial plants and improve resource absorption in return for photosynthate

http://www.aloki.hu ● ISSN 1589 1623 (Print) ● ISSN 1785 0037 (Online)
DOI: http://dx.doi.org/10.15666/aeer/1906_50455057

(Liang et al., 2015). Different AMFs can enhance plant root tolerance or resistance at various levels under different conditions (Demir and Akköprü, 2007). Among these AMFs, *Glomus intraradices* is one of the best performing species causing improved plant development and prevented soil-borne pathogens (Aguilera-Gomez et al., 1999; Akköprü and Demir, 2005; Zheang et al., 2005; Şavur, 2015).

Amendment with certain abiotic factors (inducers) stimulates disease resistance by indirectly stimulating indigenous populations of microorganism beneficial to plant growth and antagonistic to plant pathogens (Rajkumar et al., 2008). Salicylic acid (SA), a primary regulator of plant growth, development, interactions with other species, and reactions to environmental stress, is among the inducers (Hayat et al., 2010).

The objectives of the present study were to find out the effects of AMF and SA on plant growth parameters of pepper plants infected with *V. dahliae*.

Materials and methods

Materials

A local pepper (Sera Demre 8) variety susceptible to *Verticillium dahliae* (Vd) (Coşkun et al., 2019) was used as study materials. Commercial AMF (Endo Roots Soluble - Bioglobal A.Ş.) composed of different species (*Glomus intraradices, Glomus aggregatum, Glomus mosseae, Glomus clarum, Glomus monosporus, Glomus deserticola, Glomus brasillianum, Glomus etunicatum, Gigaspora margarita*) and *Glomus intraradices* (obtained from Department of Plant Protection, Faculty of Agriculture, Yüzüncü Yıl University, Turkey) which are known to have a high relative mycorrhizal dependency were employed. In the light of the findings obtained previously on SA treatments [Salicylic acid ($C_7H_6O_3$) 100%, İzmir Kimya, Turkey], the most appropriate SA doses (0.5 mM and 1 mM) were used, which would not cause adverse effects on plant growth. Vd, a highly virulent isolate obtained from pepper, was used in this study. The experiment was carried out in Turkey during 2019-2020.

Methods

Pathogen inoculation and assessment of disease severity

Pepper seeds were surface sterilized with 2% sodium hypochlorite. Seeds were sown in plastic viols 6 cm deep and 5 cm in diameter using a 1:1 perlite and peat growth mixture. AMF inocula [2.5 g (25 spores g^{-1})] and SA (0.5 mM and 1 mM) were applied to the soil concurrently with planting.

The seedlings were placed in a growth chamber with 12 hours of fluorescent illumination at 22 ± 2°C and relative humidity of 60 - 70%. Seedlings were irrigated with distilled water and fertilized three times, with 5 mL of diluted nutrient solution (Solution A: $Ca(NO_3)_2$, KNO_3; Solution B: K_2SO_4; Solution C: KH_2PO_4; Solution D: K_2HPO_4; Solution E: $C_6H_8O_7$, $C_4H_6O_5$; Oligo-elements; Fe (Sequestrene 138), $MnSO_4$, $CuSO_4$, $ZnSO_4$, $Na_2[B_4O_5(OH)_4]\cdot 8H_2O$) per seedling.

Vd isolate was subcultured on PDA (potato dextrose agar) medium in 9 mm diameter petri dishes for ten days at 24°C in a 12-hour dark-light cycle. Seedlings were transplanted to plastic pots (16 x 18 cm, 2-2.5 lt volume) with equal quantities of peat and perlite after six weeks. Roots of pepper seedlings were dipped in $1x10^6$ conidia/ml Vd spor suspension and let to grow for four weeks in a growth chamber. Control plants were dipped in tap water instead of Vd spor suspension.

http://www.aloki.hu ● ISSN 1589 1623 (Print) ● ISSN 1785 0037 (Online)
DOI: http://dx.doi.org/10.15666/aeer/1906_50455057

Four weeks after pathogen inoculation, disease symptoms were examined and evaluated (*Equation 1*). The severity of the disease was determined based on the degree of wilted leaves using a 0-5 scale (0= Healthy; 1= Less than 25% wilt in leaves; 2= 25% - 50% wilt (30% leaf loss); 3= 50% - 75% wilt (60% leaf loss); 4= 75% - 100% wilt (90% leaf loss) (Hwang et al., 1992) and vascular health 0-3 scale (0= The plants are healthy, no discoloration in the stem cross-section; 1= The plants are slightly diseased, small brown stains in the stem cross-section, 1-33% of the vascular bundles are browned; 2= The plants are moderately diseased, there are many black spots on the stem cross-section, 34-67% of the vascular bundles are browned; 3= The plants are heavily diseased, stem cross-sections are completely covered with black spots, and the plants are dried, 68-100% of the vascular bundles are browned) (Erwin et al., 1976). The following formula (*Equation 1*) was used to calculate the degree of disease severity on both scales:

$$\text{Disease Severity} = \sum \frac{(n*v)}{N*V} * 100 \qquad \text{(Eq.1)}$$

where n is the degree of disease severity on a scale, v is the number of plants in a category, N is the maximum degree of disease severity, and V is the total number of plants screened.

AMF root colonization and mycorrhizal dependency assessment

Plant roots were fixed and stained (Phillips and Hayman, 1970) and AMF root colonization was assessed under a stereoscope microscope (Leica/DFC295, Leica Microsystems Inc., Wetzlar, Germany) (4 × 10 and 10 × 10) using the grid-line intersect method according to Giovanetti and Mosse (1980). Mycorrhizal dependency assessment was determined using the method described by Declerck et al. (1995).

Plant growth parameters

A digital scale was used to determine the total fresh weight of the plants. Plants were dried at 70°C for 48 hours until they reached a consistent weight, and the dry weight was measured. The number of leaves, shoot length (cm), shoot diameter (cm), and root length (cm) of the plants were also recorded.

Statistical analysis

The study was conducted with a randomized block design with ten replications. The data were interpreted with SPSS program (v. 22.0, IBM Corp., Armonk, NY, USA). The data were analyzed using a one-way ANOVA. Duncan's multiple comparison test was used to differentiate the treatment means.

Results and discussion

Effects of two different AMF and Vd application on the plant morphology

Effects of two different AMF and Vd alone and in combination to plant growth parameters had been shown in *Table 1* and *Fig. 1*. Both AMFs caused a significant increase in plant growth parameters as compared to the untreated control plants. All plant growth parameters were declined in VD inoculated plants.

http://www.aloki.hu ● ISSN 1589 1623 (Print) ● ISSN 1785 0037 (Online)
DOI: http://dx.doi.org/10.15666/aeer/1906_50455057

Table 1. *Growth parameters of pepper plants treated with AMF and Vd*

Treatments	LN *	SD (cm)	RL (cm)	SL (cm)	RFW (g)	RDW (g)	SFW (g)	SDW (g)
Control	18.67 ±1.05 bc	4.17 ±0.10 c	35.48 ±0.98 ab	37.30 ±1.14 b	3.61 ±0.22 b	0.31 ±0.02 b	9.06 ±0.61 b	1.09 ±0.08 b
Vd	15.83 ±0.67 c	3.68 ±0.10 d	32.06 ±0.83 c	33.38 ±0.71 cd	3.04 ±0.19 b	0.29 ±0.01 b	5.66 ±0.35 c	0.95 ±0.05 b
AMF (Gi)	18.96 ±1.07 bc	4.66 ±0.16 b	34.31 ±0.85 bc	38.61 ±1.28 b	3.47 ±0.26 b	0.32 ±0.01 b	9.48 ±0.75 b	1.21 ±0.10 b
AMF (Gi) + Vd	16.13 ±1.05 c	3.73 ±0.11 d	33.06 ±1.07 bc	31.25 ±1.22 d	2.53 ±0.27 c	0.17 ±0.01 c	5.03 ±0.43 c	0.60 ±0.07 b
AMF (T)	26.20 ±1.45 a	5.24 ±0.11 a	37.73 ±1.12 a	42.35 ±0.59 a	5.11 ±0.29 a	0.44 ±0.03 a	14.25 ±0.80 a	1.80 ±0.11 a
AMF (T) + Vd	20.06 ±1.44 b	4.31 ±0.13 bc	34.13 ±0.94 bc	35.43 ±1.14 bc	3.68 ±0.35 b	0.28 ±0.03 b	8.22 ±0.61 b	1.11 ±0.11 b
df	5	5	5	5	5	5	5	5
F	10.64	22.99	4.10	14.03	9.93	11.98	28.45	18.39
Sig.	0.000	0.000	0.002	0.000	0.000	0.000	0.000	0.000

Vd: *Verticillium dahliae*, AMF (T): Commercial AMF, AMF (Gi): AMF (*Glomus intraradices*).
* LN: leaf number; SD: shoot diameter; RL: root length; SL: Shoot length; RFW: root fresh weight; RDW: root dry weight; SFW: shoot fresh weight; SDW: shoot dry weight.
The same letters in the same column indicate the insignificant differences ($P < 0.05$) according to the Duncan's test findings

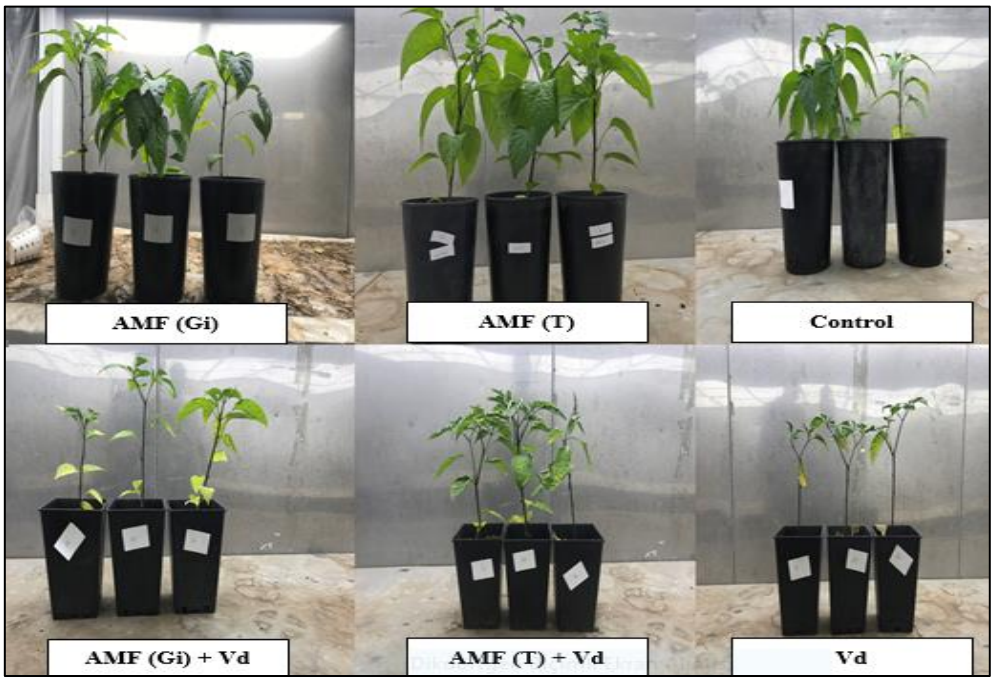

Figure 1. *The appearance of pepper plants treated with different AMFs and V. dahliae*

AMF inoculation improved the growth parameters in the plants inoculated with Vd; these parameters generally remained higher than those of the control plants (*Table 1*, *Fig. 1*). AMF (T) also significantly improved the number of leaves (26.20), shoot

http://www.aloki.hu ● ISSN 1589 1623 (Print) ● ISSN 1785 0037 (Online)
DOI: http://dx.doi.org/10.15666/aeer/1906_50455057

diameter (5.24 cm), root length (37.73 cm), shoot length (42.35 cm), root fresh weight (5.11 g), root dry weight (0.44 g), shoot fresh weight (14.25 g) and shoot dry weight (1.80 g). Given the vast range of reactions from different plant cultivars to AMFs, the best cultivar-AMF pairings must be discovered to maximize the benefits of symbiosis (Sensoy et al., 2007). Although AM fungi positively encourage many cultivated plants against both biotic and abiotic stress conditions, recent studies have shown that the positive effect on plants may differ between varieties depending on genetic variation (Demir et al., 2010). It was reported that AMF promotes plant growth and increases plant tolerance to biotic stress factors such as Fusarium and Verticillium, and increases photosynthetic water use efficiency and yield. (Kaya et al., 2009; Karipçin and Şatır, 2016). Şavur (2015) reported that AMF species have positive contributions to the morphological development of the tomato plant. Bilgili and Güldür (2018) stated that three different Glomus species alone and in combination contributed to the morphological development, especially they caused a significant increase shoot fresh weight in pepper plants inoculated with *Fusarium oxysporum*. Güneş et al. (2019) inferred that Commercial AMF performed better than other AMF species in terms of plant development when the interactions of commercial AMF, *G. intraradices, Gigaspora margarita* with radish, cauliflower, spinach and nettle were examined. As a result, the effect of mycorrhizal inoculation on the growth parameters can be linked to the plant's improved nutritional condition due to AMF.

Effects of different doses of salicylic acid (SA) on plant morphology

The effects of Vd alone and in combination with two different doses of SA, and single doses of 0.5 Mm SA and 1 Mm SA on plant growth parameters in pepper plants have been shown in *Table 2* and *Fig. 2*.

Table 2. *Growth parameters of pepper plants treated with SA and Vd*

Treatments	LN *	SD (cm)	RL (cm)	SL (cm)	RFW (g)	RDW (g)	SFW (g)	SDW (g)
Control	18.67 ± 1.05 b	4.17 ± 0.10 b	35.48 ±0.98 a	37.30 ±1.14 a	3.61 ±0.22 bc	0.31 ±0.02 ab	9.06 ±0.61 b	1.09 ±0.08 b
Vd	15.83 ± 0.67 b	3.68 ± 0.10 c	32.06 ±0.83 b	33.38 ±0.71 b	3.04 ±0.19 cd	0.29 ±0.01 ab	5.66 ±0.35 d	0.95 ±0.05 b
SA (0.5 mM)	17.40 ± 0.92 b	4.32 ± 0.08 b	34.80 ±0.85 a	33.76 ±0.86 b	4.53 ±0.27 a	0.34 ±0.02 a	8.08 ±0.53 bc	1.08 ±0.07 b
SA (0.5 mM) + Vd	17.06 ± 0.70 b	3.68 ±0.10 c	35.53 ±1.02 a	32.83 ±0.87 b	2.81 ±0.19 d	0.25 ±0.01 b	6.73 ±0.36 cd	1.00 ±0.05 b
SA (1 mM)	28.80 ± 1.00 a	5.39 ±0.09 a	35.01 ±0.90 a	35.16 ±0.65 ab	4.85 ±0.22 a	0.35 ±0.01 a	14.02 ±0.45 a	1.61 ±0.04 a
SA (1 mM) + Vd	18.47 ± 1.18 b	4.32 ±0.14 b	35.59 ±1.24 a	35.04 ±0.99 ab	3.81 ±0.26 b	0.33 ±0.02 a	7.35 ±0.51 c	1.10 ±0.08 b
df	5	5	5	5	5	5	5	5
F	28.12	37.90	2.02	3.48	12.67	3.25	38.90	12.75
Sig.	0.000	0.000	0.049	0.005	0.000	0.008	0.000	0.000

Vd: *Verticillium dahliae*, SA (0.5mM): Salicylic acid (0.5mM), SA (1 mM): Salicylic acid (1 mM).
* LN: leaf number; SD: shoot diameter; RL: root length; SL: shoot length; RFW: root fresh weight; RDW: root dry weight; SFW: shoot fresh weight; SDW: shoot dry weight.
The same letters in the same column indicate the insignificant differences ($P < 0.05$) according to the Duncan's test findings

http://www.aloki.hu ● ISSN 1589 1623 (Print) ● ISSN 1785 0037 (Online)
DOI: http://dx.doi.org/10.15666/aeer/1906_50455057

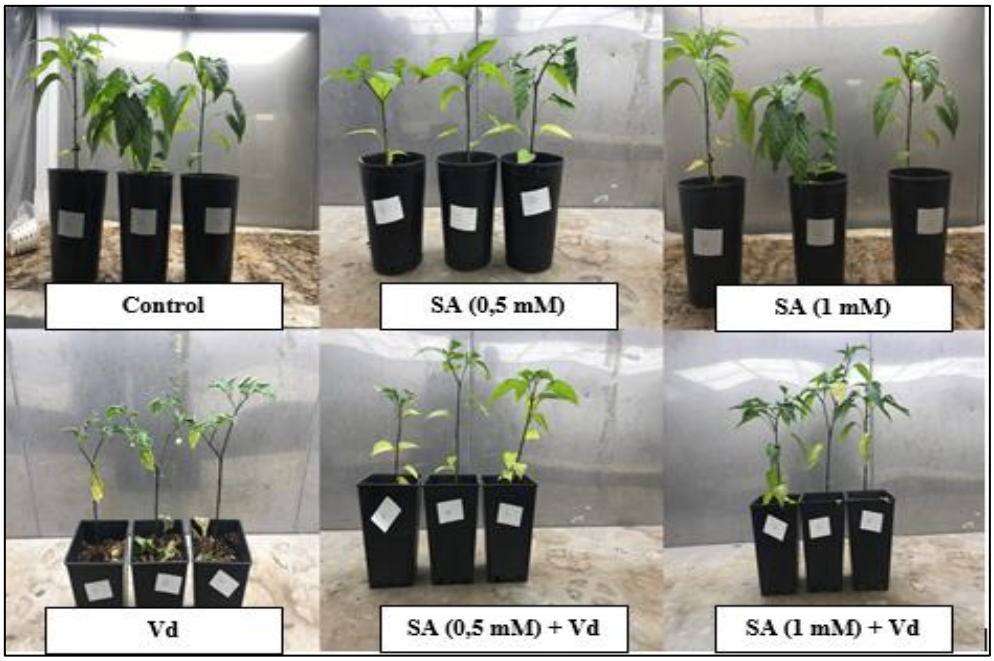

Figure 2. *The appearance of pepper plants treated with different doses of SA and Vd*

Vd caused a significant decline in shoot diameter, root length, shoot length, root fresh weight and shoot fresh weight, although it did not affect leaf number, root dry weight, and shoot dry weight. Vd combination with 0.5 Mm and 1 mM doses of SA resulted in decrease in all plant growth parameters. SA (1 mM) treatment improved in leaf number, shoot diameter, root fresh weight, root dry weight, shoot fresh weight and shoot dry weight except for root length and shoot length. SA (0.5 mM) treatment stimulated root fresh weight while it did not cause any increase in the other plant growth parameters (*Table 2*). It is shown that SA increases germination, flowering, rooting, yield and accelerates photosynthesis in plants in a number of different studies (Romanujam et al., 1998; Hayat et al., 2007; Dadaşoğlu and Ekinci, 2013; Algül et al., 2016). Elwan and El-Hamahmy (2009) examined the effect of foliar application of salicylic acid (SA 10^{-6} M and 10^{-4} M) on fruit yield and quality in pepper under salt stress conditions. They have reported that the application of SA 10^{-6} M increased the average fruit weight, fruit number and fruit yield. It is also reported that SA has a positive effect on increasing the plant height of the Kandıra pepper variety (Akpınar, 2011). Dura et al. (2016) investigated the effect of SA application against root-knot nematodes in 12 pepper cultivars of Yalova Chorba by applying different doses (3 mM/plant - 6 mM/plant -9 mM/plant) from leaves and soil. They determined that pepper plants with 9 mM SA application promoted plant growth parameters such as leaf number, plant height, root fresh and dry weight. Özdüven (2016) stated that SA applications increased yield, fruit number, leaf area, fruit firmness, total chlorophyll amount, protein content, single fruit weight and leaf K content. The study conducted by Ekbiç and Koşar (2020) studied the effects of SA doses (0, 0.5, 1 and 2 mM) on vine rootstocks and they concluded that the shoot growth was superior to the control and the degree of damage to the plants was lower with the application of 1 mM dose of SA for 1103 P rootstock. The studies conducted by other researchers earlier have been supported the current study. It has been proposed that SA's growth-promoting effects

http://www.aloki.hu ● ISSN 1589 1623 (Print) ● ISSN 1785 0037 (Online)
DOI: http://dx.doi.org/10.15666/aeer/1906_50455057

are linked to hormonal modifications or improvements in photosynthesis, transpiration, and stomatal conductance (Rivas-San Vicente and Plasencia, 2011).

Effects of AMF and SA application on the wilt disease caused by Vd in pepper

Effects of two different AMF and two different doses of SA on the disease development in pepper are shown in *Table 3*.

Table 3. *Effects of AMF, SA and Vd application on the wilt disease parameters (0-5 and 0-3 scale) in pepper*

Treatments	0-5 scale		0-3 scale	
	Wilting (%)*	Suppression rate (%)	Vascular discoloration (%)*	Suppression rate (%)
Vd (Control)	48.6 ±3,67 a*	-	30 ±3,69 a*	-
AMF (T) + Vd	22.6 ±3,36 c	53	13 ±3,42 b	56
AMF (Gi) + Vd	38 ±3,36 b	21.8	16 ±4,15 b	46.6
SA (0.5mM) + Vd	27.3 ±3,38 c	43.8	16 ±4,15 b	46.6
SA (1 mM) + Vd	31.4 ±3,79 bc	35.3	15 ±3,08 b	50
df	4	-	4	-
F	9.16	-	3.27	-
Sig.	0.000	-	0.013	-

Vd: *Verticillium dahliae*, AMF (T): Commercial AMF, AMF (Gi): AMF (*Glomus intraradices*), SA (0.5mM): Salicylic acid (0.5mM), SA (1 mM): Salicylic acid (1 mM).
*P < 0.05 (significant)

Vd inoculated control plants expressed the highest disease severity values for the wilted leaf index and vascular browning (48.6% and 30%, respectively). AMF (T) + Vd, AMF (Gi) + Vd, SA (0.5mM) + Vd and SA (1 mM) + Vd applications resulted in the suppression of the disease development, which was 53%, 21.8%, 43.8%, and 35.3% respectively; as well, the values of vascular health and suppression rate (56%, 46.6%, 46.6%, and 50%, respectively) should be noted. The best suppression of disease was observed in AMF (T) + Vd (53% - 56%) application according to 0-5 scale and 0-3 scales (*Table 3*).

AMF benefits plants by increasing the uptake of phosphorus and other nutrients from the soil and increasing disease tolerance in the host plant (Merina Prem Kumari and Jeberlin Prabina, 2019). Singh et al. (2010) reported that the applications of *Glomus hoi + Fusarium oxysporum*, *Glomus fasciculatum + Fusarium oxysporum* and *Rhizobium leguminosorum + Fusarium oxysporum* significantly reduced the severity of the disease compared to the control applications. Aljawasim et al. (2020) found that mycorrhizal plants reduced the disease severity by 46% (*Glomus clarum + Rhizoctonia solani*) and 41% (*Glomus mosseae + Rhizoctonia solani).* Ranjbar Sistani et al. (2020) examined the yield components of AMF application against *Didymella pinodes* to two different varieties of sensitive and tolerant pea plants grown in pots. They concluded that AMF

http://www.aloki.hu ● ISSN 1589 1623 (Print) ● ISSN 1785 0037 (Online)
DOI: http://dx.doi.org/10.15666/aeer/1906_50455057

application reduced the disease severity in both varieties. In our study, AMF (G) and AMF (T) applications significantly suppressed the severity of the disease caused by Vd in pepper plants. The above studies were in line with the results of the present study presented here.

Salicylic acid, as well as serving as a growth regulator, acts as a signal in the plant's defense mechanism against pests and diseases, promoting plant's resistance positively (Raskin, 1992; Arıcı and Yardımcı, 2001). Various studies have shown that SA increases the resistance to pathogens in different plants and decreases the disease severity. In this regard, Şahbaz and Akgül (2016) found that the application of SA at a dose of 50 g/100 L water three times, both *Fusarium oxysporum* f.sp. *vasinfectum* and *V. dahliae* have been the most successful application in reducing disease severity in cotton plants. Tutar and Erkılıç (2016) stated that the application of 500 and 1000-ppm concentrations of SA and BABA (DL-β-aminone-butyric acid) in the eggplant plant inhibited *V. dahliae* by 27.8% and 33.3%, respectively. Erkılıç et al. (2018) stated that three soil applications (SA, BABA and ASM (Acibenzolor S-Methyl)) in olive prevented the suppression of the *V. dahliae* in the vascular discoloration up to 90%. ASM also was seen as the most effective application, it was determined that different concentrations of SA prevented the development of disease at a rate of 52% to 76%.

Effects of different AMFs and Vd application on root colonization and mycorrhizal dependency

Effects of two different AMF and Vd application on root colonization and mycorrhizal dependency in pepper are shown in *Table 4*.

Table 4. *Effects of different AMFs and Vd application on root colonization and mycorrhizal dependency*

Treatments	Root colonization (%)	Mycorrhizal dependency (%)
AMF (Gi)	62.08 ±4.84 ab	9.08
AMF (Gi) + Vd	54.79 ±3.16 b	-
AMF (T)	69.07 ±2.19 a*	59.37
AMF (T) + Vd	54.95 ±4.87 b	-
df	3	-
F	2.98	-
Sig.	0.043	-

Vd: *Verticillium dahliae*, AMF (T): Commercial AMF, AMF (Gi): AMF (*Glomus intraradices*)
*P < 0.05 (significant)

The rates of colonization in pepper plants with different AMFs and Vd application varied between 54.95% and 69.07%. On the other hand, mycorrhizal dependence rates vary between AMF (Gi) 9.08% and AMF (T) 59.37%, but mycorrhizal dependence did not occur in applications with Vd. AMF root colonization and mycorrhizal dependency in the plant root were adversely affected by treatments that included the Vd pathogen (*Table 4*).

http://www.aloki.hu ● ISSN 1589 1623 (Print) ● ISSN 1785 0037 (Online)
DOI: http://dx.doi.org/10.15666/aeer/1906_50455057

AMF is under the influence of biotic and abiotic conditions; positively or negatively, it influences the colonization rates in the root zone (Akköprü and Demir, 2005). Çetinkaya and Dura (2009) determined that the fungal colonization rate was between 26% - 30% with Endo-Roots applications in corn plant under field conditions. Yıldız (2010) stated that the root colonization rate of *Glomus sp.* was recorded as 61% in pepper, 71% in cucumber, and 72% in tomato. Aslanpay (2011) reported that AMF colonization rates of pepper varieties varied between 3.05% - 38.66%, and mycorrhizal dependence rates varied between 2.52% and 20.64%. Different pathogens can reduce AMF colonization on a variety of hosts. Aysan (2008) investigated the effects of *G. mosseae, G. fasciculatum* and *Sclerotinia sclerotiorum* applications on root colonization in bean plants. It was determined that the lowest colonization rate was in *G. mosseae* + *Sclerotinia sclerotiorum* and *G. fasciculatum* + *Sclerotinia sclerotiorum* treatments. Demir et al. (2015) stated that different AMF applications, including Vd pathogen applications, had a negative effect on root colonization. Our study showed similar results with the above studies.

Conclusion

The use of beneficial biological agents or growth regulators in the crop production should be among the important objectives in ensuring sustainable, safe and healthy production and their contribution to plant development and yield. This study aimed to determine the effects of AMF and SA on plant growth parameters and disease severity against wilt disease caused by *V. dahliae* in pepper. It was determined that SA and AMF applications generally had positive contributions to the morphological development of pepper plants and disease severity. Commercial AMF resulted in the best in morphological growth parameters, root colonization, mycorrhizal dependency rates and suppressing severity of the disease. SA (1 mM) resulted in improved morphological growth parameters and suppression of the severity of the disease. After considering the beneficial effects of these agents on the plant's growth, their practical effect cannot be ignored. Besides, the obtained encouraging results against *V. dahliae* could help plant protection efforts. We believe that the results of our study can contribute to more detailed research in this direction.

Acknowledgements. This project was supported by the funds received from the Scientific and Technological Research Council of Turkey (TÜBİTAK Project No. 119O059).

REFERENCES

[1] Adnan, M., Islam, W., Shabbir, A., Khan, K. A., Ghramh, H. A., Huang, Z., Chen, H., Lu, G. D. (2019): Plant defense against fungal pathogens by antagonistic fungi with Trichoderma in focus. – Microbial Pathogenesis 129: 7-18.

[2] Aguilera-Gomez, L., Davies, F. J., Olalde-Portugal, V., Duray, S. A., Phavaphutanon, L. (1999): Influence of phosphorus and endomycorrhiza (*Glomus intraradices*) on gas exchange and plant growth of chile ancho pepper (*Capsicum annuum* L. cv. San Luis). – Photosynthetica 36(3): 441-449.

[3] Akköprü, A., Demir, S. (2005): Biological control of Fusarium wilt in tomato caused by *Fusarium oxysporum* f. sp. *lycopersici* by AMF *Glomus intraradices* and some rhizobacteria. – Journal of Phytopathology 153(9): 544-550.

http://www.aloki.hu ● ISSN 1589 1623 (Print) ● ISSN 1785 0037 (Online)
DOI: http://dx.doi.org/10.15666/aeer/1906_50455057

[4] Akpınar, S. T. (2011): Grafted plant production and yield in grafted plants of pepper (*Capsicum annuum* L.) (Biberde (*Capsicum annuum* L.) aşılı bitki üretme ve yetiştirme çalışmaları). – Yüksek Lisans Tezi, Namık Kemal Üniversitesi Fen Bilimleri Enstitüsü, Tekirdağ, Türkiye.

[5] Algül, B. E., Tekintaş, F. E., Günver Dalkılıç, G. (2016): The usage of plant growth regulators and hormone biosynthesis booster applications (Bitki büyüme düzenleyicilerinin kullanımı ve içsel hormonların biyosentezini arttırıcı uygulamalar). – Journal of Adnan Menderes University Agricultural Faculty 13(2): 87-95.

[6] Aljawasim, B. D. G., Khaeim, H. M., Manshood, M. A. (2020): Assessment of Biocontrol Potential of Arbuscular Mycorrhizal (*Glomus spp*.) against Damping-Off Disease (*Rhizoctonia solan*i) on Cucumber. – Mycorrhizal Fungi-Utilization in Agriculture and Industry Intech Open.

[7] Arıcı, Ş. E., Yardımcı, N. (2001): Induced resistance in plants (Bitkilerde uyarılmış dayanıklılık). – Atatürk Üniversitesi Ziraat Fakültesi Dergisi 32(1): 83-86.

[8] Aslanpay, B. (2011): The effects of arbuskular mycorrhizal fungus (AMF) and humic acid on the growth of pepper (*Capsicum annum* L.) plant and root rot disease caused by *Phytophthora capsici* Leonian (Arbusküler mikorhizal fungus (AMF) ve humik asitin biber (*Capsicum annum* L.) bitkisinin gelişimi ve *Phytophthora capsici* Leonian"ın neden olduğu kök boğazı çürüklüğü hastalığına etkileri). – Yüksek Lisans Tezi, Yüzüncü Yıl Üniversitesi Fen Bilimleri Enstitüsü, Van, Türkiye.

[9] Aysan, E. (2008): A research on the using of iniculation of arbuscular mycorrhizal fungus (AMF) and *Rhizobium bacteria* against rot root agents *Sclerotinia sclerotiorum* (Lib.) de Bary in the common bean (*Phaseolus vulgaris* L.) (Arbüsküler mikorhizal funguslar (AMF) ve rhizobium bakteri aşılamasının fasulye (*Phaseolus vulgaris* L.)'de kök çürüklüğü etmeni (*Sclerotinia Sclerotiorum* (Lib.) De Bary)'ne karşı kullanılma olanakları üzerine bir araştırma). – Yüksek Lisans Tezi, Yüzüncü Yıl Üniversitesi Fen Bilimleri Enstitüsü, Van, Türkiye.

[10] Bilgili, A., Güldür, M. E. (2018): The efficiency of arbuscular mycorrhizal fungi on *Fusarium oxysporum* f.sp *vasinfectum* root rot diseases of peppers in the GAP Region (GAP bölgesinde biberlerde *Fusarium oxysporum* f. sp *vasinfectum* kök çürüklüğü hastalığına arbüsküler mikorizal fungusların etkinliği). – Harran Tarım ve Gıda Bilimleri Dergisi 22(1): 88-108.

[11] Carroll, C. L., Carter, C. A., Goodhue, R. E., Lawell, C.-Y. C. L., Subbarao, K. V. (2018): A review of control options and externalities for Verticillium wilts. – Phytopathology 108(2): 160-171.

[12] Coşkun, F., Alptekin, Y., Demir, S. (2019): Response of some pepper (*Capsicum annuum* L.) varieties against wilt disease caused by *Verticillium dahliae* Kleb. – International Biological, Agricultural and Life Science Congress, November 7-8, 2019, Lviv, Ukraine, 164p.

[13] Çetinkaya, N., Dura, S. (2009): The effects of a endomycorrhizal preparate on yield and vegetative development of corn (Mısır vejetatif gelişimi ve verimi üzerinde bir endomikorizal preparatın etkileri). – Ege Üniversitesi Ziraat Fakültesi Dergisi 47(1): 53-59.

[14] Dadaşoğlu, E., Ekinci, M. (2013): Effects of different degrees of temperature, salt and salicylic acid applications on seed germination of bean (*Phaseolus vulgaris* L.) (Farklı sıcaklık dereceleri, tuz ve salisilik asit uygulamalarının fasulye (*Phaseolus vulgaris* L.) tohumlarında çimlenme üzerine etkisi). – Atatürk Üniversitesi Ziraat Fakültesi Dergisi 44(2): 145-150.

[15] Declerck, S., Plenchette, C., Strullu, D. G. (1995): Mycorrhizal dependency of banana (*Musa acuminata*, AAA group) cultivar. – Plant and Soil 176(1): 183-187.

[16] Demir, S., Akköprü, A. (2007): Using of Arbuscular Mycorrhizal Fungi (AMF) for Biocontrol of Soil-Borne Fungal Plant Pathogens. – In: Chincholkar, S. B., Mukerji, K. G. (eds.) Biological Control of Plant Diseases. USA: Haworth Press, pp. 124-138.

http://www.aloki.hu ● ISSN 1589 1623 (Print) ● ISSN 1785 0037 (Online)
DOI: http://dx.doi.org/10.15666/aeer/1906_50455057

[17] Demir, S., Orak, A. B., Demirer Durak, E. (2010): Arbuscular mycorrhizal fungus (AMF) dependency of some cotton cultivars indicating different response against Verticillium wilt (Verticillium solgunluğuna farklı reaksiyon gösteren bazı pamuk çeşitlerinin arbusküler mikorhizal funguslara (AMF) karşı mikorhizal bağımlılıkları). – Yüzüncü Yıl Üniversitesi Tarım Bilimleri Dergisi 20(3): 201-207.

[18] Demir, S., Şensoy, S., Ocak, E., Tüfenkçi, Ş., Demirer Durak, E., Erdinc, C., Ünsal, H. (2015): Effects of arbuscular mycorrhizal fungus, humic acid, and whey on wilt disease caused by *Verticillium dahliae* Kleb. in three solanaceous crops. – Turkish Journal of Agriculture and Forestry 39(2): 300-309.

[19] Dura, O., Sönmez, İ., Yıldırım, K. C. (2016): Effects of salicylic acid applications on root–knot nematodes (*Meloidogyne incognita*) and some growth parameters in pepper (*Capsicum annuum* L.) (Biberde (*Capsicum annuum* L.) salisilik asit uygulamalarının kök-ur nematodu (*Meloidogyne incognita*)'na ve bazı büyüme parametreleri üzerine etkileri). – Bahçe 45(1): 31-39.

[20] Duran, İ., Özkaya, H. Ö. (2016): Determination of soil-borne and foliar fungal disease agents of greenhouses in Kumluca district (Kumluca ilçesi sera alanlarında toprak ve yaprak kökenli fungal hastalık etmenlerinin belirlenmesi). – Süleyman Demirel Üniversitesi Fen Bilimleri Enstitüsü Dergisi 20(1): 111-122.

[21] Ekbiç, H. B., Koşar, S. (2020): Determination of the effect of salicylic acid on improving salt resistance of grapevine rootstocks in vitro (Salisilik asidin asma anaçlarının tuza dayanımının geliştirilmesi üzerine etkisinin in vitro koşullarda belirlenmesi). – Akademik Ziraat Dergisi 9(1): 33-42.

[22] Elwan, M. W. M., El-Hamahmy, M. A. M. (2009): Improved productivity and quality associated with salicylic acid application in greenhouse pepper. – Scientia Horticulturae 122(4): 521-526.

[23] Erkılıç, A., Özdemir, S. K., Akgül, D. S. (2018): Determination of the effects of some resistance promoting chemicals against *Verticillium dahliae* in olive trees (Zeytinde *Verticillium dahliae*'ya karşı bazı dayanıklılık teşvik edici kimyasalların etkilerinin belirlenmesi). – Çukurova Tarım ve Gıda Bilimleri Dergisi 33(1): 69-76.

[24] Erwin, D. C., Tsoti, S. D., Khan, R. A. (1976): Reduction of severity of Verticillium wilt of cotton by the growth retardant tributyl (5-chloro-2-thienyl methyl) phosphonium chloride. – Phytopathology 66: 106-110.

[25] Giovannetti, M., Mosse, B. (1980): An evaluation of techniques for measuring vesicular arbuscular mycorrhizal infection in roots. – New Phytologist 84(3): 489-500.

[26] Güneş, H., Demir, S., Demirer Durak, E. (2019): Relationship between *Brassicaceae, Chenopodiaceae* and *Urticaceae* families with arbuscular mycorrhizal fungi (AMF) (*Brassicaceae, Chenopodiaceae* ve *Urticaceae* familyalarına ait bazı bitkilerin arbusküler mikorhizal funguslar (AMF)'la ilişkisi). – Kahramanmaraş Sütçü İmam Üniversitesi Tarım ve Doğa Dergisi 22: 102-108.

[27] Hayat, S., Ali, B., Ahmad, A. (2007): Salicylic Acid: Biosynthesis, Metabolism and Physiological Role in Plants. – In: Hayat, S., Ahmad, A. (eds.) Salicylic Acid: A Plant Hormone. Springer, Dordrecht, pp. 1-14.

[28] Hayat, Q., Hayat, S., Irfan, M., Ahmad, A. (2010): Effect of exogenous salicylic acid under changing environment: a review. – Environmental and Experimental Botany 68(1): 14-25.

[29] Hwang, S. F., Chang, K. F., Chakravarty, P. (1992): Effects of vesicular-arbuscular mycorrhizal fungi on the development of Verticillium and Fusarium wilts of alfalfa. – Plant Disease 76(3): 239-243.

[30] Karipçin, M. Z., Şatır, N. Y. (2016): Effect of arbuscular mycorrhizal fungi (AMF) on growth and nutrient uptake of lettuce (*Lactuca sativa*) under water stress (Su stresi koşullarında yetiştirilen marul sebzesinin verim ve besin içeriğine arbusküler mikorizal fungus (AMF)'un etkileri). – Yüzüncü Yıl Üniversitesi Tarım Bilimleri Dergisi 26(3): 406-413.

http://www.aloki.hu ● ISSN 1589 1623 (Print) ● ISSN 1785 0037 (Online)
DOI: http://dx.doi.org/10.15666/aeer/1906_50455057

[31] Kaya, C., Ashraf, M., Sonmez, O., Aydemir, S., Tuna, A. L., Cullu, M. A. (2009): The influence of arbuscular mycorrhizal colonisation on key growth parameters and fruit yield of pepper plants grown at high salinity. – Scientia Horticulturae 121(1): 1-6.

[32] Liang, M., Liu, X., Etienne, R. S., Huang, F., Wang, Y., Yu, S. (2015): Arbuscular mycorrhizal fungi counteract the janzen-connell effect of soil pathogens. – Ecology 96(2): 562-574.

[33] Merina Prem Kumari, S., Jeberlin Prabina, B. (2019): Protection of tomato, *Lycopersicon esculentum* from wilt pathogen, *Fusarium oxysporum* f. sp. *lycopersici* by arbuscular mycorrhizal fungi, *Glomus sp*. – International Journal of Current Microbiology and Applied Sciences 8(4): 1368-1378.

[34] Novo, M., Silvar, C., Merino, F., Martínez-Cortés, T., Lu, F., Ralph, J., Pomar, F. (2017): Deciphering the role of the phenylpropanoid metabolism in the tolerance of *Capsicum annuum* L. to *Verticillium dahliae* Kleb. – Plant Science 258: 12-20.

[35] Özdüven, F. F. K. (2016): Effects of salicylic acid applications on plant growth and yield of summer squash (*Cucurbita pepo* L.) under different irrigation levels (Salisilik asit uygulamalarının farklı sulama seviyelerinde yetiştirilen yazlık kabakta (*Cucurbita pepo* L.) bitki gelişimi ve verime etkileri). – Doktora Tezi, Namık Kemal Üniversitesi, Fen Bilimleri Enstitüsü, Tekirdağ, Türkiye.

[36] Phillips, J. M., Hayman, D. S. (1970): Improved procedures for clearing roots and staining parasitic and vesicular-arbuscular mycorrhizal fungi for rapid assessment of infection. – Transactions of the British Mycological Society 55(1): 158-161.

[37] Rajkumar, M., Lee, K. J., Freitas, H. (2008): Effects of chitin and salicylic acid on biological control activity of *Pseudomonas spp.* against damping off of pepper. – South African Journal of Botany 74(2): 268-273.

[38] Ranjbar Sistani, N., Desalegn, G., Kaul, H., Wienkoop, S. (2020): Seed metabolism and pathogen resistance enhancement in *Pisum sativum* during colonization of arbuscular mycorrhizal fungi, an integrative metabolomics-proteomics approach. – Frontiers in Plant Science 11: 872.

[39] Raskin, I. (1992): Role of salicylic acid in plants. – Annual Review of Plant Biology 43(1): 439-463.

[40] Rivas-San Vicente, M., Plasencia, J. (2011): Salicylic Acid beyond defense, its role in plant growth and development. – Journal of Experimental Botany 62(10): 3321-3338.

[41] Romanujam, M. P., Jaleel, V. A., Kumaravelu, G. (1998): Effect of salicylic acid on nodultion, nitrogenous compounds and related enzymes of *Vigna mungo*. – Biologia Plantarum 41: 307-371.

[42] Sensoy, S., Demir, S., Turkmen, O., Erdinc, C., Savur, O. B. (2007): Responses of some different pepper (*Capsicum annuum* L.) genotypes to inoculation with two different arbuscular mycorrhizal fungi. – Scientia Horticulturae 113(1): 92-95.

[43] Singh, P. K., Singh, M., Vyas, D. (2010): Biocontrol of Fusarium wilt of chickpea using arbuscular mycorrhizal fungi and *Rhizobium leguminosorum* Biovar. – Caryologia 63(4): 349-353.

[44] Şahbaz, S., Akgül, S. (2016): Fungal wilt pathogens and their management in cotton growing areas in Reyhanlı county (Hatay). – The Journal of Turkish Phytopathology 45(1): 31-43.

[45] Şavur, O. B. (2015): The effects of arbuscular mycorrhizal fungi (AMF) and salicylic acid applications against crown and rot root disease (*Fusarium oxysporum* f.sp. *radicis-lycopersici* Jarvis & Shoemaker) on the some of growth and yield parameters and disease severity of tomato (*Lycopersicum esculantum* L.) plant (Domates kök ve kök boğazı çürüklüğü hastalığına (*Fusarium oxysporum* f. sp. *radicis- Lycopersici* Jarvis & Shoemaker) karşı arbusküler mikorhizal fungus (AMF) ve salisilik asit uygulamalarının domates (*Solanum lycopersicum* L.) bitkisinin bazı gelişim ve verim parametreleri ile hastalık şiddetine etkisi). – Doktora Tezi, Yüzüncü Yıl Üniversitesi Fen Bilimleri Ensititüsü,Van, Türkiye.

http://www.aloki.hu ● ISSN 1589 1623 (Print) ● ISSN 1785 0037 (Online)
DOI: http://dx.doi.org/10.15666/aeer/1906_50455057

[46] Tutar, F. K., Erkılıç, A. (2016): Determination of the effects of mycorrhizal fungi and abiotic inducers against eggplant wilt diseases (*Verticillium dahliae* and *Fusarium oxysporum* f.sp. *melongenae*) (Patlıcanda solgunluk hastaliklari (*Verticillium dahliae* ve *Fusarium oxysporum* f. sp. *melongenae*)'na karşı mikorizal fungusların ve abiyotik uyarıcıların etkilerinin belirlenmesi). – Çukurova Üniversitesi Fen ve Mühendislik Bilimleri Dergisi 34(5): 32-42.

[47] Vasileva, K., Todorova, V. (2020): Evaluation of pepper (*Capsicum annuum* L.) varieties to several methods of inoculation with *Verticillium dahliae* Kleb. in different conditions. – Bulgarian Journal of Agricultural Science 26(2): 423-430.

[48] Wang, X., Zou, C., Zhang, Y., Shi, X., Liu, J., Fan, S., Liu, Y., Du, Y., Zhao, Q., Tan, Y., Wu, C., Chen, X. (2018): Environmental impacts of pepper (*Capsicum annuum* L) production affected by nutrient management: a case study in southwest china. – Journal of Cleaner Production 171: 934-943.

[49] Yıldız, A. (2010): A native *Glomus sp.* from fields in Aydın Province and effects of native and commercial mycorrhizal fungi inoculants on the growth of some vegetables. – Turkish Journal of Biology 34(4): 447-452.

[50] Zheng, H., Cui, C., Zhang, Y., Wang, D., Jing, Y., Kim, K. Y. (2005): Active changes of lignification-related enzymes in pepper response to *Glomus intraradices* and/or *Phytophthora capsici*. – Journal of Zheijang University SCIENCE B - Biomedicine & Biotechnology 6(8): 778-786.

http://www.aloki.hu ● ISSN 1589 1623 (Print) ● ISSN 1785 0037 (Online)
DOI: http://dx.doi.org/10.15666/aeer/1906_50455057

EFFECTS OF CARBOHYDRATE AND ENDOGENOUS HORMONE CONTENT ON MORPHOLOGICAL STRUCTURE OF HETEROMORPHIC LEAVES OF *POPULUS PRUINOSA* SCHRENK.

LI, X.[1,2,3] – HAN, X. L.[1,2,3] – ZHAI, J. T.[1,2,3] – ZHANG, S. H.[1,2,3] – LI, Z. J.[1,2,3*]

[1]*Key Laboratory of Protection and Utilization of Biological Resources in Tarim Basin Xinjiang Production and Construction Corps, Alar, Xinjiang 843300, China*

[2]*Desert Poplar Research Center of Tarim University, Alar, Xinjiang 843300, China*

[3]*College of Life Science, Tarim University, Alar, Xinjiang 843300, China*

[*]*Corresponding author*
e-mail: lizhijun0202@126.com; phone: +86-997-468-1202

(Received 28th Jul 2021; accepted 20th Sep 2021)

Abstract. *Populus pruinosa* Schrenk. (*P. pruinose*) has the biological characteristic of heteromorphic leaves, which is related to growth and adaptation to extreme arid environments. The present study aimed to clarify whether carbohydrate and endogenous hormone content had an effect on the morphological structure of *P. pruinose* heteromorphic leaves on canopy height during ontogenesis. Petiole length, upper epidermal cell length, upper epidermal cell number, lower epidermal cell length, palisade tissue cell number, palisade tissue thickness, palisade tissue cell width and palisade tissue/spongy tissue ratio were very significantly positively correlated with diameter at breast height (DBH) and canopy height. Spongy tissue thickness is significantly negatively correlated with diameter at breast height and canopy height, with advancements in the developmental stage and increase in canopy height, the heterophil xerophytic structure is more and more obvious. Zeatin-riboside content and zeatin-riboside/abscisic acid ratio positively correlated with diameter at breast height, while gibberellin/abscisic acid ratio negatively correlated with canopy height. Soluble sugar and soluble protein contents significantly positively correlated with diameter at breast height and canopy height, starch contents significantly negatively correlated with diameter at breast height and canopy height. Regression analysis showed that soluble sugar content had positive effects on petiole length, leaf width, leaf area, leaf circumference, leaf thickness, upper epidermal cell length, lower epidermal cell number, palisade tissue thickness and spongy tissue thickness. The soluble protein content had a positive effect on leaf index and palisade tissue/spongy tissue ratio, starch content had a positive effect on upper epidermal cell width and palisade tissue thickness. It was concluded that the endogenous hormone and carbohydrate content could enhance the xerophytic structure of heteromorphic leaves during ontogenesis.
Keywords: *heteromorphic leaf, morphological anatomy, physiological characteristics, developmental stage, canopy height*

Abbreviations. LL = Leaf length; LW = Leaf width; LI = leaf index; LA = leaf area; LT = leaf thickness; LC = leaf circumference; PL = petiole length; UECN = upper epidermal cell number; LECN = lower epidermal cell number; UECL = upper epidermal cell length; LECL = lower epidermal cell length; UECW = upper epidermal cell width; LECW = lower epidermal cell width; PN = palisade tissue cell number; PTT = palisade tissue thickness; PTCL = palisade tissue cell length; PTCW = palisade tissue cell width; STT = spongy tissue thickness; PSR = palisade tissue/spongy tissue ratio; SS = soluble sugar; S = starch; SP = soluble protein; IAA = indole acetic acid; ZR = zeatin-riboside; GA_3 = gibberellin; ABA = abscisic acid; CH = canopy height; DBH = diameter at breast height

http://www.aloki.hu ● ISSN 1589 1623 (Print) ● ISSN1785 0037 (Online)
DOI: http://dx.doi.org/10.15666/aeer/1906_50595081

Introduction

The heteromorphic foliage of plants refers to the various shapes of leaves at different growth stages or changes in environmental conditions, which reflects the greater plasticity and variability of leaves (Bai, 2003). Heteromorphic leaves play an important role in the adaptation of plants to environmental changes (Winn, 1999; Wells and Pigliucci, 2000), changes in leaf morphology of aquatic plants, for example, promote gas exchange under underwater conditions (Kuwabara and Nagata, 2002; Mommer and Visser, 2005). Leaf morphology and physiological function show considerable plasticity within the canopy, and in very tall trees a distinct vertical gradient is usually shown for various leaf traits (Cai and Song, 2001; Burgess et al., 2007). Kenzo et al. (2015) showed that there was a significant linear relationship between leaf morphology and biochemical characteristics and tree height. With the increase of tree height, the leaf structure of *Parashorea chinensis* showed more obvious xerophytic characteristics (He et al., 2008). In addition, some studies have found that the morphology, structure and physiological characteristics of the heteromorphic leaves of *Populus euphratia* Oliv. are more obvious with the increase of ontogenetic stage and tree height (Zhai et al., 2020). Studies have pointed out that plant hormones such as abscisic acid and gibberellin are closely related to the regulation of profiled leaves (Nakayama et al., 2017; Li et al., 2020), Abscisic acid (ABA) is mainly involved in the establishment and maintenance of morphological characteristics of heterophyllous plants (Wanke, 2011). Nakayama et al. (2014) showed that the difference of gibberellin content in leaf primordium also determined the leaf shape changes of plants, and the content and distribution of auxins (IAA) regulated the leaf shape changes of *Arabidopsis thaliana*, *Cardamine hirsuta* and other plants (Barkoulas et al., 2008; Ben-gera et al., 2012). Many studies have shown that starch, soluble sugar and soluble protein are involved in the growth and development of plants, and these soluble substances can maintain cell turgor and protect the integrity of cell membrane when plants are stressed by drought, salt and alkali and other environmental conditions (Kuang et al., 2017; Liu et al., 2017; Liu et al., 2020). A few studies on herbaceous plants suggest that starch, or the ratio of soluble sugar to starch, is a major integrator of plant growth regulation (Selbig et al., 2009; Purdy et al., 2015).

P. pruinosa is an important tree species in arid desert areas with biological characteristics of heteromorphic leaves. It has three different leaf shapes: long oval, round, and broad oval (Wei, 1990). The long elliptic leaves, round leaves, and broad ovoid leaves on the crown of *P. pruinosa* appear regularly in different stages of individual development (Liu et al., 2016), and with the increase of ontogenetic stages, the heteromorphic leaves of *P. pruinosa* show more obvious xerophytic structural characteristics (Zhai et al., 2019). At present, the research on *P. pruinosa* in the world focuses on stress-resistant physiology (Zhang et al., 2014; Wang et al., 2017; Li, 2020), However, the relationship between the morphological and structural changes of *P. pruinosa* heteromorphic leaves and the endogenous hormones and carbohydrate in leaves has not been reported, which is of great significance to reveal the physiological regulation mechanism of the enhanced drought-resistant structure of *P. pruinosa* heteromorphic leaves.

In this study, *P. pruinosa* growing on the same site at different stages of development was selected as the research object. Through studying the change rules and their relationships of morphological structure, carbohydrate content, endogenous hormone content and their ratio of heteromorphous leaves of *P. pruinosa* at different stages of

http://www.aloki.hu ● ISSN 1589 1623 (Print) ● ISSN1785 0037 (Online)
DOI: http://dx.doi.org/10.15666/aeer/1906_50595081

development and vertical spatial changes of tree crown, the study aim to clarify the role of endogenous hormones and carbohydrate content in the morphological and structural changes of *P. pruinosa* heteromorphic leaves, and to lay a foundation for revealing the regulatory mechanism of morphological and structural changes of heteromorphic leaves at molecular level.

Materials and Methods

Study site

The study area is located in *P. pruinosa* forest in the northwest margin of Tarim Basin, Xinjiang, China (81°17′56.52″ E, 40°32′36.90″ N, 980 m above sea level). The study area has a hot and dry climate, with an average annual rainfall of about 50 mm, an average annual temperature of 10.8 ℃, a potential evaporation of 1900 mm and an average annual sunshine duration of 2900 h. It is a typical temperate desert climate. In the study area, the artificial *P. pruinosa* forest covers an area of 180.6 hm^2, and there are 293 *P. pruinosa* individuals at different development stages (different tree ages) in the forest. The accompanying species in the study area were *Tamarix chinensis* Lour., *Glycyrrhiza uralensis* Fisch., *Phragmites australis* (Cav.) trin.ex Steud, and *Aeluropus pungens* (M. Bieb.) C. Koch.

Experimental design and sampling

P. pruinosa with different diameters represented different developmental stages. Using the diameter at breast height (DBH) and 2 cm as class distance, the 293 *P. pruinosa* trees in the study area were divided into 9 diameter steps (2, 4, 6, 8, 10, 12, 14, 16 and 18), representing 9 developmental stages of *P. pruinosa* (*Table 1*). Three sample plants were selected in each diameter class. During the leaf maturity period, the sampling canopy height (CH) was divided into 5 equal parts (total stations (GTS-2002, TOPCON) to measure the tree heights and under branch heights of trees in the different diameter classes from base to top was defined as 1 to 5 layers). At each sampling layer, three one-year-old branches were collected from each of the four directions (east, south, west, and north). Sixty branches were collected from each sampling tree. A total of 60 leaves per sampling were used to measure the leaf morphological, anatomical, and physiological characteristics. The leaves used for the physiological characteristics were immediately stored in liquid nitrogen after collection.

Table 1. *Basic information of P. pruinosa*

Diameter classes	2	4	6	8	10	12	14	16	18
Breast diameter range（cm）	0-2	2-4	4-6	6-8	8-10	10-12	12-14	14-16	16-18
Number of plants	6	15	36	44	40	58	40	37	17
Number of samples	9	31	23	21	20	19	11	4	3
Mean breast diameter（cm）	2.2	4.1	6.1	8.2	10.5	11.8	13.9	15.8	17.8
Average tree height（m）	4.4	4.6	4.9	5.4	5.7	6.3	7.5	7.5	7.4
Average crown height（m）	4.4	5.7	7.1	8.5	10.7	11.6	12.2	12.7	13
Average tree age（year）	4.4	5.7	7.1	8.5	9.7	10.7	11.6	12.2	12.7

http://www.aloki.hu ● ISSN 1589 1623 (Print) ● ISSN1785 0037 (Online)
DOI: http://dx.doi.org/10.15666/aeer/1906_50595081

Leaf morphological and anatomical structure index determination

The leaves at the third node from the base of the current branch were selected as the sample leaves, leaf length (LL), leaf width (LW), leaf area (LA), leaf circumference (LC), leaf thickness (LT) and petiole length (PL) were measured using a scanner (MRS-9600TFU2) and LA-S plant image analysis software. The leaf shape index (LI) was calculated according to the ratio of leaf length to width.

The sample leaf was crosscut from the widest part and fixed with formalin-acetic acid-alcohol (FAA) solution. We used the paraffin section method to make tissue sections, the thickness of the sections was 8 μm, and the sections were stained with double saffron and solid green, and the sections were sealed with neutral resin. The upper epidermal cell number (UECN), lower epidermal cell number (LECN), upper epidermal cell length (UECL), lower epidermal cell length (LECL), upper epidermal cell width (UECW), lower epidermal cell width (LECW), palisade tissue thickness (PTT), palisade tissue cell number (PN), palisade tissue cell length (PTCL), palisade tissue cell width (PTCW) and spongy tissue thickness (STT) were measured under a Leica microscope (Leica DM4 B, Wetzlar, Germany). The palisade tissue/spongy tissue ratio (PSR) was calculated. Each blade has 5 fields of observation and 20 values of observation in each field. The average value of blade structure parameters in 5 fields of observation is taken as the parameter value of each blade structure.

Leaf physiological and biochemical index determination

The mixed sample of the leaves at the third node of the current branch in the same canopy of the sample plant was taken as the test sample, the soluble sugar content (SS) was determined by anthrone-sulfuric acid method, the starch content (S) was determined by anthrone-colorimetric method, and the soluble protein content (SP) was determined by Coomassie bright blue G-250 method (Gao, 2006).

Leaf hormone content determination

Stem tips of current shoots in the same canopy on the sample plant were mixed as test samples. Test samples were accurately weighed to 200 mg, and the contents of indole acetic acid (IAA), zeatin-riboside (ZR), gibberellin (GA_3) and abscisic acid (ABA) were determined by enzyme linked immunosorbent assay (ELISA) (Duan et al., 2009; Li et al., 2019).

Data processing method

A one-way ANOVA was used to compare the differences in the morphological structure and physiological characteristics of heteromorphic leaves. In SPSS 23.0, Duncan's new multiple range method was used for data analysis of variance. The significance of differences was determined at $a = 0.05$. Pearson correlation coefficient was used to test the correlation between each index, and stepwise regression analysis was conducted.

http://www.aloki.hu ● ISSN 1589 1623 (Print) ● ISSN1785 0037 (Online)
DOI: http://dx.doi.org/10.15666/aeer/1906_50595081

Results

Changes of morphological characteristics and structure of heteromorphic leaves with developmental stage and canopy height

Leaf index of heteromorphic leaves decreased with the increase of diameter class (*Figure 1A,C*), while leaf width, leaf area, leaf circumference, leaf thickness and petiole length increased with the increase of diameter class and canopy height (*Figure 1B,D,E,F,G*), and the changes of leaf index, leaf area and leaf thickness were more obvious.

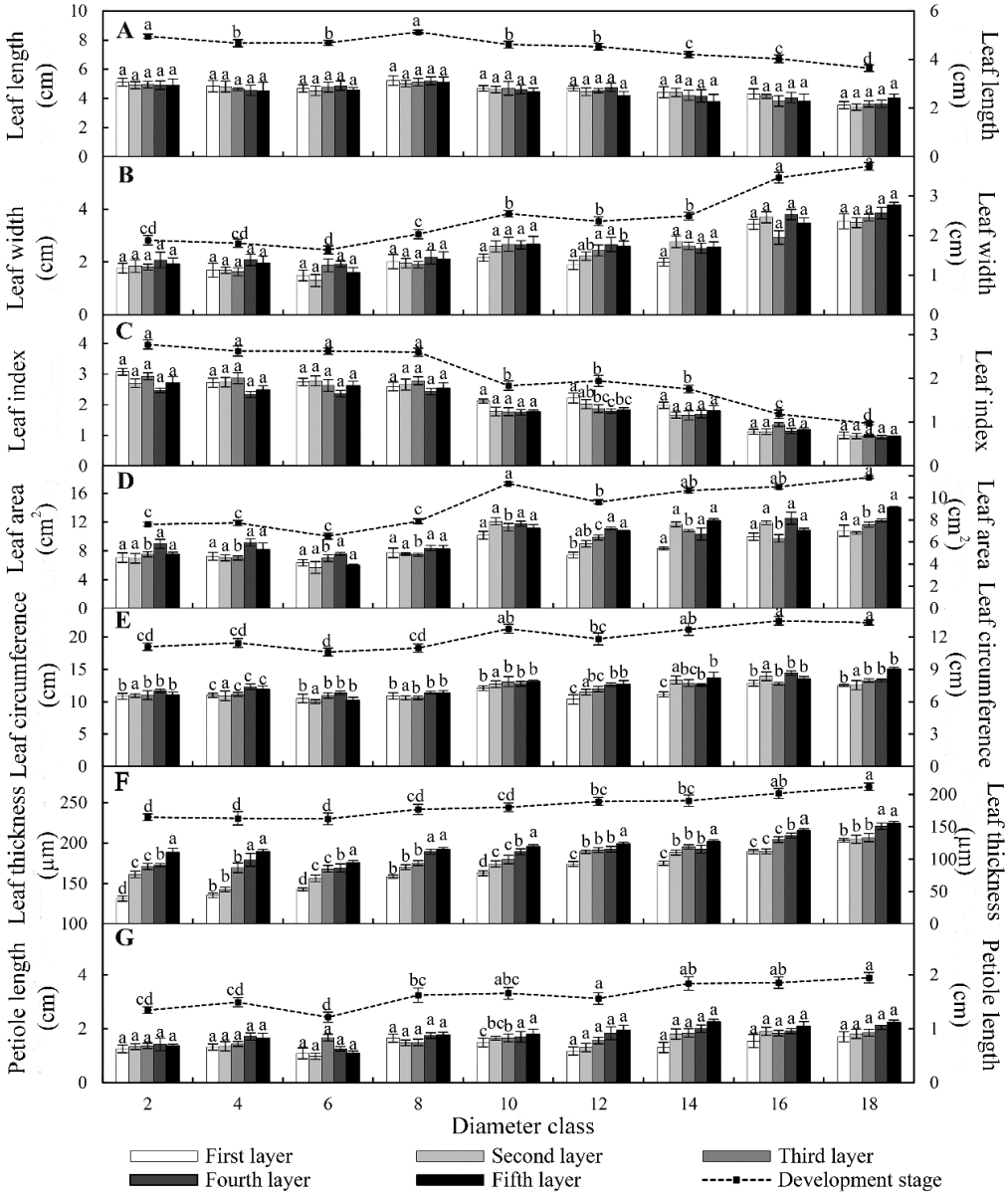

Figure 1. *Variation of heteromorphic leaf morphology with developmental stages and canopy height of P. pruinose. (A) leaf length, (B) leaf width, (C) leaf index, (D) leaf area, (E)Leaf circumference, (F) leaf thickness, (G) petiole length. Lowercase letters indicated significant differences, the same letters indicated not significant (P >0.05), and different letters indicated significant differences (P<0.05)*

http://www.aloki.hu ● ISSN 1589 1623 (Print) ● ISSN1785 0037 (Online)
DOI: http://dx.doi.org/10.15666/aeer/1906_50595081

The upper and lower epidermal cell number of leaves increased with the increase of diameter class and canopy height (*Figure S1E,F*), while the upper and lower epidermal cell number increased more obviously with the increase of diameter class from 2 to 10. In addition, the upper and lower epidermal cell length increased slowly with the increase of diameter class and canopy height, while the upper and lower epidermal cell width had no significant difference with the increase of diameter class and canopy height. The palisade tissue cell number, palisade tissue thickness and palisade tissue/spongy tissue ratio of leaves increased with the increase of diameter class and canopy height (*Figure S2A,D,F*), the spongy tissue thickness decreased with the increase of diameter class (*Figure S2E*), and the palisade tissue cell length increased with the increase of canopy height (*Figure S2B*). There were significant differences in the palisade tissue cell width between 2 and 4 diameter class.

Correlation analysis showed that (*Table S1*), petiole length, upper epidermal cell length, lower epidermal cell number, upper epidermal cell length, palisade tissue cell number, palisade tissue thickness, palisade tissue cell width and palisade tissue/spongy tissue ratio with DBH and canopy height was very significantly positively correlated, spongy tissue thickness with DBH and canopy height showed a significantly negative correlation. These results indicated that the morphological and structural changes of *P. pruinosa* heteromorphic leaves were closely related to the increase of diameter class and canopy height, and the xerophytic structural characteristics of heteromorphic leaves became more and more obvious with the increase of development stages and canopy height.

Changes of endogenous hormone content and their ratios in heteromorphic leaves with developmental stages and canopy height

We studied that the GA_3 content, IAA/ABA, GA_3/ABA, ZR/ABA, GA_3/IAA ratio of heteromorphic leaves in the 4 diameter were significantly lower than those in other diameters (*Figure 2* and *Figure S3A,B,C,D*), while ZR/GA_3 ratio was significantly higher than those of other diameter classes (*Figure S3F*). The ratios of IAA/ABA, GA_3/ABA and ZR/ABA in 4-12 diameter classes increased, while in 12-16 diameter classes decreased. In addition, the contents of GA_3, IAA and ZR in the 16 diameter special-shaped leaves were significantly higher than those in other diameter classes (*Figure 2A,B,D*), while the contents of ABA and IAA in the 18 diameter special-shaped leaves were lower than those in other diameter classes (*Figure 2B,C*).

From the vertical space of tree crown, the content of GA_3 in leaves basically decreased with the increase of canopy height at diameter classes 2, 12 and 14, but basically increased with the increase of CH at diameter classes 4 to 10, 16 and 18 (*Figure 2A*). The ratios of ZR/GA_3 and ZR /IAA of leaves basically increased with the increase of canopy height (*Figure S3E,F*), and there were significant differences between the first layer and the fifth layer. The content of IAA in leaves basically decreased with the increase of canopy height (*Figure 2B*), and the content of ZR in leaves basically increased with the increase of diameter classes, but the difference between tree crown levels was not significant (*Figure 2D*). The content of ABA in leaf of diameter classes 2, 6 and 8 showed a decreasing trend with the increase of CH, but the content of ABA in diameter classes 4 and 10 to 18 basically showed an increasing trend with the increase of canopy height (*Figure 2C*). The IAA/ABA ratio of leaves decreased with canopy height from 12 to 18 diameter classes, and the 3rd layer of individual canopies from 6 and 18 diameter classes had significant differences with

http://www.aloki.hu ● ISSN 1589 1623 (Print) ● ISSN1785 0037 (Online)
DOI: http://dx.doi.org/10.15666/aeer/1906_50595081

other canopies (*Figure S3A*). The ratios of GA_3/ABA and ZR/ABA in leaves were the highest in the third layer of the 6th diameter step, and there were significant differences with those in other canopy layers (*Figure S3B,C*).

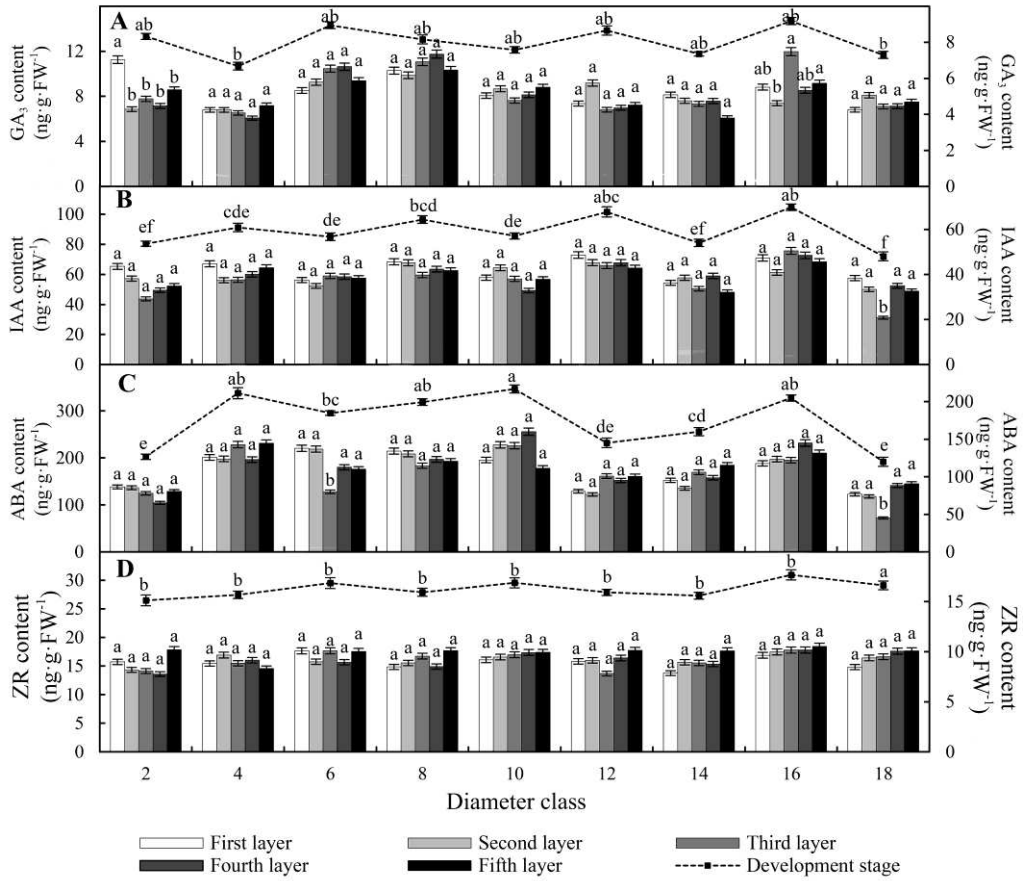

Figure 2. *Changes of endogenous hormone content in heteromorphic leaves with developmental stages and canopy height. (A) leaf GA_3 content, (B) leaf IAA content, (C) leaf ABA content, (D) leaf ZR content. Lowercase letters indicated significant differences, the same letters indicated not significant ($P > 0.05$), and different letters indicated significant differences ($P < 0.05$)*

Correlation analysis showed that (*Table S2*), ZR content and ZR/ABA ratio positively correlated with DBH, while GA_3/ABA ratio negatively correlated with canopy height, it shows that they are closely related to the Ontogenetic stage and canopy height where the heteromorphic leaves are located.

Changes of carbohydrate content in heteromorphic leaves with developmental stages and canopy height

It was found that the contents of SS and SP in leaves increased with the increase of diameter classes and canopy height (*Figure 3A,C*), while the content of starch in leaves decreased with the increase of diameter classes, but increased with the increase of canopy height (*Figure 3B*). In 2 - 6 diameter classes leaf soluble sugar, soluble protein, and starch content in the canopy layers between there was no significant change, but in

http://www.aloki.hu ● ISSN 1589 1623 (Print) ● ISSN1785 0037 (Online)
DOI: http://dx.doi.org/10.15666/aeer/1906_50595081

8 to 18 diameter classes there was a significant difference between the canopy height in each diameter class.

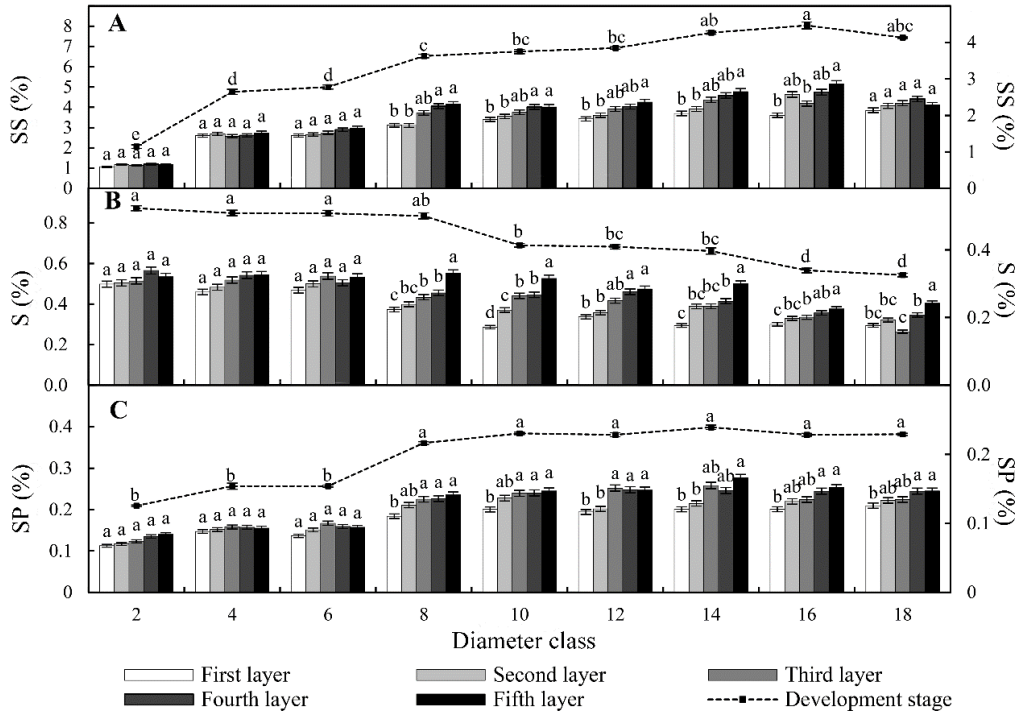

Figure 3. *Changes of soluble sugar, starch and soluble protein contents in heteromorphic leaves with developmental stages and canopy height. (A) leaf soluble sugar content (SS), (B) leaf starch content (S), (C) leaf soluble protein (SP). Lowercase letters indicated significant differences, the same letters indicated not significant (P >0.05), and different letters indicated significant differences (P<0.05)*

Correlation analysis showed that the soluble sugar and soluble protein contents significantly positively correlated with DBH and canopy height, starch contents significantly negatively correlated with DBH and canopy height (*Table S2*). These results indicated that the changes of the contents of soluble sugar, soluble protein and starch in heteromorphic leaves were closely related to the ontogenetic stage and canopy height.

Relationship between content and ratio of endogenous hormones in leaves and morphological structure of heteromorphic leaves

Correlation analysis was conducted on the contents and ratios of endogenous hormones and morphological structure of four kinds of *P. pruinosa* heteromorphic leaves (*Table 2*), indicating that the content of GA_3 and the ratio of ZR/IAA in *P. pruinosa* heteromorphic leaves significantly positively or negatively correlated with the lower epidermal cell width and lower epidermal cell length. The IAA content and IAA/ABA ratio significantly positively correlated with the palisade tissue cell length. ZR content and ZR/ABA ratio significantly positively correlated with Leaf width, leaf circumference, leaf area, leaf thickness, petiole length, upper epidermal cell length, palisade tissue thickness and palisade tissue/spongy tissue ratio, but negatively

http://www.aloki.hu ● ISSN 1589 1623 (Print) ● ISSN1785 0037 (Online)
DOI: http://dx.doi.org/10.15666/aeer/1906_50595081

correlated with leaf length and leaf index. ABA content significantly positively correlated with the Leaf length, but negatively correlated with the upper epidermal cell length. The GA_3/ABA ratio significantly positively correlated with leaf index, and significantly or negatively correlated with Leaf width, leaf area, leaf circumference, leaf thickness, petiole length, palisade tissue thickness, palisade tissue cell width and palisade tissue/spongy tissue ratio. The ratio of GA_3/IAA significantly negatively correlated with the upper epidermal cell number, lower epidermal cell width and lower epidermal cell number, and positively correlated with the spongy tissue, while the ratio of ZR/GA_3 negatively correlated with the leaf area, leaf thickness, leaf length and petiole length. The results indicated that the changes of morphological structure of heteromorphic leaves of *P. pruinosa* were closely related to the changes of contents and ratios of these 4 endogenous hormones.

Table 2. *The morphological and structural parameters of heteromorphic leaves correlated with Pearson's endogenous hormone content and ratio*

	GA_3	IAA	ZR	ABA	IAA/ABA	GA_3/ABA	ZR/ABA	GA_3/IAA	ZR/IAA	ZR/GA_3
LL	0.65	0.02	-0.97*	1.00**	0.01	0.86	-0.95*	0.37	-0.63	-0.74
LW	-0.34	0.33	0.99**	-0.9	0.34	-0.98*	1.00**	-0.67	0.32	0.93
LI	0.31	-0.36	-0.99*	0.88	-0.37	0.99**	-1.00**	0.7	-0.28	-0.94
LA	-0.09	0.56	0.93	-0.75	0.57	-1.00**	0.95*	-0.84	0.06	0.99**
LC	-0.34	0.33	0.99**	-0.9	0.34	-0.99*	1.00**	-0.68	0.31	0.93
LT	-0.21	0.46	0.97*	-0.83	0.47	-1.00**	0.98*	-0.77	0.18	0.97*
PL	-0.2	0.46	0.97*	-0.82	0.47	-1.00**	0.98*	-0.77	0.18	0.97*
UECL	-0.47	0.19	1.00**	-0.95*	0.2	-0.95	1.00**	-0.56	0.45	0.87
UECW	0.97*	0.6	-0.65	0.86	0.6	0.4	-0.59	-0.24	-0.97*	-0.21
UECN	0.17	0.76	0.8	-0.56	0.76	-0.94	0.84	-0.95*	-0.2	0.99*
LECL	-0.99*	-0.67	0.57	-0.81	-0.67	-0.31	0.52	0.33	0.99*	0.12
LECW	0.18	0.76	0.8	-0.55	0.77	-0.94	0.84	-0.96*	-0.21	0.99*
LECN	0.18	0.76	0.8	-0.55	0.77	-0.94	0.84	-0.96*	-0.21	0.99*
PN	0.03	0.17	0.5	0.07	-0.03	-0.12	0.11	-0.2	0.09	0.14
PTT	-0.35	0.32	0.99**	-0.9	0.33	-0.98*	1.00**	-0.67	0.33	0.93
PTCW	0.06	0.68	0.86	-0.65	0.69	-0.97*	0.9	-0.91	-0.09	1.00**
PTCL	0.74	1.00**	0.27	0.07	1.00**	-0.53	0.33	-0.94	-0.76	0.69
STT	-0.18	-0.76	-0.8	0.55	-0.77	0.94	-0.84	0.95*	0.2	-0.99*
PSR	-0.15	0.51	0.95*	-0.79	0.52	-1.00**	0.97*	-0.81	0.13	0.98*

* $p<0.05$, ** $p<0.01$

The content and ratio of endogenous hormones in leaves were taken as independent variables, and the leaf morphology was taken as dependent variable for stepwise regression analysis. The results showed that there was an extremely significant linear relationship between dependent variable Y and independent variable X (*Table S3*).

The results showed that the increase of ZR content had positive effects on leaf length, leaf circumference, leaf thickness, upper epidermal cell length, palisade tissue thickness and palisade tissue/spongy tissue ratio. The increase of ZR/ABA and ZR/GA_3 ratio had a positive effect on petiole length. The increase of GA_3/IAA ratio had a positive effect on the lower epidermal cell width, indicating that ZR content, ZR/ABA, ZR/GA_3 and GA_3/IAA ratio played an important role in the enhancement of xerophytic structure in heteromorphic leaves.

http://www.aloki.hu ● ISSN 1589 1623 (Print) ● ISSN1785 0037 (Online)
DOI: http://dx.doi.org/10.15666/aeer/1906_50595081

Relationship between leaf carbohydrate content and morphological structure of heteromorphic leaves

Correlation analysis showed (*Table 3*) that the soluble sugar and soluble protein content in heteromorphic leaves significantly or extremely significantly positively correlated with Leaf width, leaf area, leaf circumference, leaf thickness, petiole length, length of upper and lower epidermal cells, number of upper and lower epidermal cells, lower epidermal cell width, palisade tissue thickness, palisade tissue cell width and palisade tissue/spongy tissue ratio. There was a significant or extremely significant negative correlation between leaf index and spongy tissue thickness, while the starch content showed the opposite, namely an extremely significant positive correlation with Leaf length, indicating that the change of leaf morphology and structure was closely related to the significant increase of leaf soluble sugar and soluble protein and the significant decrease of starch content.

Table 3. *The morphological and structural parameters of heteromorphic leaves correlated with the carbohydrate content of leaves by Pearson*

	Soluble sugar	Starch	Soluble protein
LL	-0.63	0.90**	-0.53
LW	0.69*	-0.95**	0.67*
LI	-0.78**	0.99**	-0.76*
LA	0.74*	-0.93**	0.81**
LC	0.71*	-0.94**	0.72*
LT	0.79**	-0.96**	0.80**
PL	0.80**	-0.87**	0.82**
UECL	0.78**	-0.85**	0.71*
UECW	-0.14	0.23	-0.08
UECN	0.93**	-0.86**	0.94**
LECL	0.08	-0.09	-0.02
LECW	0.93**	-0.88**	0.96**
LECN	0.93**	-0.88**	0.96**
PN	0.69*	0.6	0.94**
PTT	0.80**	-0.85**	0.68*
PTCW	0.76*	-0.88**	0.83**
PTCL	0.14	-0.11	0.14
STT	-0.94**	0.65*	-0.88**
PSR	0.92**	-0.83**	0.82**

* $p<0.05$, ** $p<0.01$

Stepwise regression analysis was conducted with leaf carbohydrate as the independent variable and leaf morphology as the dependent variable, and the results showed that there was an extremely significant linear relationship between the dependent variable Y and the independent variable X (*Table S4*).

The results showed that the increase of soluble sugar content had positive effects on petiole length, leaf width, leaf area, petiole length, leaf thickness, upper epidermal cell length, upper epidermal cell number, palisade tissue thickness and spongy tissue thickness. The increase of soluble protein content had a positive effect on leaf index and palisade tissue/spongy tissue ratio. The increase of starch content had a positive effect on the lower epidermal cell width and palisade tissue thickness, indicating that the increase of carbohydrate content played an important role in the enhancement of xerophytic structure of heteromorphic leaves.

http://www.aloki.hu ● ISSN 1589 1623 (Print) ● ISSN1785 0037 (Online)
DOI: http://dx.doi.org/10.15666/aeer/1906_50595081

Discussion

The relationship between the morphological structure of heteromorphic leaves and the developmental stage and canopy height of P. pruinosa

To adapt to dry conditions, plants in desert areas try their best to change their morphological characteristics, such as stomatal depression and leaf thickening, so as to resist the adverse effects of drought stress on plants (Mendes et al., 2001). Thicker leaves can maintain a higher water content, and at the same time avoid the burning of mesophyll caused by intense light in arid areas. In addition, scattered light can be effectively used for photosynthesis, which is conducive to the improvement of time-concordant efficiency of leaves under water stress (Chartzoulakis et al., 2002; Velikova et al., 2020), therefore, trees adapt to the environment by adjusting their leaf morphology and biochemical characteristics (Kenzo et al., 2006). However, with the increase of ontogenetic stage and tree height, the demand for nutrients and water will continue to increase, and at the same time, a stronger ability to adapt to the environment such as drought resistance is required. On one hand, it is possible to increase the photosynthetically available area of leaves by increasing leaf area, leaf perimeter and leaf thickness, and further improve photosynthesis (Oikawa et al., 2016; Wang et al., 2017). On the other hand, increasing petiole length, palisade tissue thickness and palisade to sea ratio of leaves can effectively reduce leaf temperature, reduce transpiration, and water loss, and maintain high water content (Bridge et al., 2013; Velikova et al., 2020). Studies have shown that with the increase of ontogenetic stage and tree height, leaf thickness, epidermal cell number, palisade tissue cell number, palisade tissue thickness and palisade tissue/spongy tissue ratio of heteromorphic leaves increase, and their drought resistance is gradually enhanced (Zhang et al., 2017; Zhai et al., 2019, 2020).

In this study, the morphological and structural differences of *P. pruinosa* heteromorphic leaves during ontogeny reflect the synergistic or trade-off strategy between different traits and functions of leaves during ontogeny (Pan et al., 2018). Studies have found that the morphological and structural differences of *P. pruinosa* heteromorphic leaves are closely related to the increase of developmental stage and canopy height. From sapling to mature leaves, leaf thickness, leaf area, leaf quality and other traits showed significant changes with the DBH of trees (Martin et al., 2013), which was consistent with our research results. In addition, studies showed that the xerophytic structural characteristics of heteromorphic leaves became more and more obvious with the increase of development stage and canopy height, such as the enlargement of leaf area, the thickening of leaves, the increasingly developed palisade tissue, and the degeneration of spongy tissue in the cross section of leaves (*Figure 1* and *Figure S1,2*). England and Attiwill (2006) found that the leaf shape of eucalyptus changed significantly with the increase of tree age and height, for example, the leaf length became shorter, the leaf thickness increased, and the leaf area index and specific leaf area decreased. Some studies showed that the palisade tissue thickness, palisade to sea ratio and epidermal thickness of leaves increased with the increase of tree height. The more obvious xerophytic structure is adapted to the water stress caused by arid environment and the increase of tree height (He et al., 2008; Zhai et al., 2020), water stress may eventually limit leaf expansion and photosynthesis to further increase tree height (Koch et al., 2004), and at the same time, the trend of changes in leaf structural traits is often interpreted as an adaptive response to light availability (Lusk et al., 2008).

http://www.aloki.hu ● ISSN 1589 1623 (Print) ● ISSN1785 0037 (Online)
DOI: http://dx.doi.org/10.15666/aeer/1906_50595081

Therefore, it is speculated that the obvious xerophytic structure of the heteromorphic leaves of *P. pruinosa* is a self-protection to adapt to the water stress caused by the growth stage and the increase of tree height and to avoid the intense light.

Effect of carbohydrate on morphological structure of heteromorphic leaves of P. pruinose

Many studies have shown that starch, soluble sugar, and soluble protein are closely related to plant growth and development (Kuang et al., 2017; Liu et al., 2017, 2020). Starch is a key factor in mediating plant responses to abiotic stresses such as drought, as it compensates for changes in carbon assimilation to maintain levels of soluble sugars (Thalmann and Santelia, 2017). Previous studies have shown that the growth of trees under drought stress depends on the relationship between soluble sugar and starch, and there is a negative correlation between starch concentration and growth, and a positive correlation between soluble sugar/starch ratio and growth (Liu et al., 2017). In this study, it was found that the contents of soluble sugar, soluble protein and starch in heteromorphic leaves were closely related to the stage of ontogeny and canopy height. Göttlicher et al. (2006) found that the starch content of leaves gradually increased from the lower canopy to the higher canopy. Some studies showed that the starch content of leaves significantly negatively correlated with the diameter at breast height (Li et al., 2015). However, it showed an increasing trend with the increase of canopy height (*Figure 3B*), which was consistent with the results of our study. Some authors found that the higher photosynthetic capacity was related to the increase of leaf carbohydrates (Aspinwall et al., 2016). Kenzo et al. (2006) found that the photosynthetic capacity of dipterocarp species depends on the height of the tree, and the trees adapt to the light environment by changing their leaf morphology and biochemical characteristics. The results showed that the content of osmotic regulatory substances such as soluble sugar could improve the photosynthetic capacity of heteromorphic leaves with the increase of canopy height.

Leaves mainly reduce osmotic potential and maintain turgor pressure through soluble osmotic regulatory substances, so that physiological processes related to turgor in plants can proceed normally (Patakas et al., 2002). In some studies, it has been found that the down-regulation of photosynthesis will offset the accumulation of starch in leaves in the long term (Quentin et al., 2013; Hagedorn et al., 2016). Soluble sugar produced by photosynthesis in leaves is exported from source leaves to phloem and is directly used for leaf growth (Lemoine et al., 2013). Some studies have found that soluble protein can be used as the main nitrogen source for leaf growth (Gonçalves et al., 2016; Liu et al., 2018). We found that the increase of soluble sugar and soluble protein and the decrease of starch content played an important role in enhancing the xerophytic structure of heteromorphic leaves. Drought stress results in the degradation of starch reserves in plant leaves into soluble sugars (Svensk et al., 2020), which can be used directly in physiological activities, including maintaining leaf turgor to resist drought (Martínez-Villata et al., 2016). Woodruff et al. (2011) found that leaf cell turgor pressure decreased with the increase of height. Therefore, with the increase of canopy height, leaves need to maintain turgor pressure by increasing the content of soluble substances to further drive leaf cell growth (Woodruff et al., 2015). Therefore, it can adapt to water stress caused by tree height and improve drought resistance ability. It was preliminarily speculated that the increase of soluble sugar and soluble protein and the

http://www.aloki.hu ● ISSN 1589 1623 (Print) ● ISSN1785 0037 (Online)
DOI: http://dx.doi.org/10.15666/aeer/1906_50595081

decrease of starch content might regulate the enhancement of drought resistance ability in heteromorphic leaves of *P. pruinose*.

Effects of endogenous hormone content and ratio on morphological structure of heteromorphic leaves of P. pruinose

Plant hormones play an important role in regulating plant growth and development and coping with stress environment. Plant hormones, especially gibberellin (GA_3), auxin (IAA), abscisic acid (ABA) and corn nucleosides (ZR), can affect the formation and development of profiled leaves in many plants (Nakayama et al., 2017; Li et al., 2019). ZR can promote the cell division of stems and leaves, which is beneficial to the formation of leaves (Debnath, 2009). ABA controls the growth and development of plants, such as leaf shedding, fruit ripening and drought stress response (Nakayama et al., 2017). Studies on various plants show that osmotic stress induces ABA production, and ABA plays a controlling role in the stress response and tolerance of plants (Yamaguchi-Shinozaki and Shinozaki, 2006; Nakashima and Yamaguchi-Shinozaki, 2013), and ABA accumulation in leaves helps to improve drought resistance (He et al., 2020). Some studies have found that IAA affects leaf morphology and development (Barkoulas et al., 2008; Koenig et al., 2009). In this study, it was found that the changes of ZR content and ZR/ABA ratio in leaves were closely related to the increase of DBH, and the ZR content in leaves basically increased with the increase of diameter class, but there was no significant difference among crown levels (*Figure 2D*). Li et al. (2017) found that the contents of ZR and ABA in leaves showed an overall trend of increase with the increase of tree age (diameter class). Our study showed that ZR content and ZR/ABA ratio significantly or extremely significantly positively correlated with leaf width, leaf circumference, leaf area, leaf thickness, petiole length, upper epidermal cell length, palisade tissue thickness and gate to sea ratio. It was preliminarily speculated that ZR content and ZR/ABA ratio of heteromorphic leaves of *P. pruinose* were involved in the regulation of leaf morphology and structure changes with the increase of diameter step.

When plants suffer from adversity stress, they can balance the growth regulation substances by changing the way of synthesis, conduction, and metabolism of endogenous hormones to improve the stress resistance of plants. In this study, it was found that ZR content, ZR /ABA, ZR /GA_3, and GA_3/IAA ratios played an important role in the structure enhancement of heteromorphic leaves. Some studies have shown that the number of upper and lower epidermal cells, the width of upper epidermal cells, the length of palisade tissue and the ratio of gate to sea of leaves reflect the drought resistance of plants (Chartzoulakis et al., 2002; Zhang et al., 2017), our study showed that leaf ZR content had significant positive effects on leaf length decrease, leaf circumference increase, leaf thickness increase, upper epidermal cell length increase, palisade tissue thickness increase and gate sea ratio increase, and ZR/ABA and ZR/GA_3 ratios had significant positive effects on petiole length increase. In addition, GA_3/IAA ratio had a significant positive effect on the decrease of lower epidermal cell width. It was suggested that the increase of ZR content, the ratio of ZR/ABA and ZR/GA_3 and the decrease of GA_3/IAA might play an important regulatory role in improving the drought resistance in heteromorphic leaves of *P. pruinose*.

http://www.aloki.hu ● ISSN 1589 1623 (Print) ● ISSN1785 0037 (Online)
DOI: http://dx.doi.org/10.15666/aeer/1906_50595081

Conclusion

This study shows that *P. pruinose* in different developmental stages and different shaped leaf canopy height in different forms, and the xerophytic structure of heteromorphic leaves increased obviously with the developmental stage and canopy height. The increase of soluble sugar and soluble protein content and the decrease of starch content may enhance the xerophytic structure of heteromorphic leaves by improving photosynthetic capacity and osmotic regulation ability. In addition, the increase of ZR content, ZR/ABA, ZR/GA_3 ratio and the decrease of GA_3/IAA ratio may play an important regulatory role in the enhancement of xerophilous structure of heteromorphic leaves. The results indicated that the formation of heteromorphic leaves was regulated by the synergistic changes of leaf morphology, structure and physiological characteristics during the individual growth and development of *P. pruinose* and could better adapt to the water stress caused by tree height, which provide a theoretical basis for further research on the molecular mechanism of how leaf morphological structure and physiological characteristics resist extreme environments through coordinated changes.

Acknowledgements. This work was financially supported by the National Natural Sciences Foundation of China (31860198, 31460042, 31060026), Innovative team Building Plan for key areas of Xinjiang Production and Construction Corps (2018CB003).

REFERENCES

[1] Aspinwall, M. J., Drake, J. E., Campany, C., Vårhammar, A., Ghannoum, O., Tissue, D. T., Reich, P. B., Tjoelker, M. G. (2016): Convergent acclimation of leaf photosynthesis and respiration to prevailing ambient temperatures under current and warmer climates in Eucalyptus tereticornis. – New Phytol 212(2): 354-367.

[2] Bai, S. N. (2003): Plant development biology. – Peking University Press, Beijing, pp. 72-73.

[3] Barkoulas, M., Hay, A., Kougioumoutzi, E., Tsiantis, M. (2008): A developmental framework for dissected leaf formation in the Arabidopsisrelative Cardamine hirsuta. – Nature genetics 40(9): 1136-1141.

[4] Ben-Gera, H., Shwartz, I., Shao, M. R., Shani, E., Estelle, M., Ori, N. (2012): ENTIRE and GOBLET promote leaflet development in tomato by modulating auxin response. – Plant J. 70(6): 903-915.

[5] Bridge, L. J., Franklin, K. A., Homer, M. E. (2013): Impact of plant shoot architecture on leaf cooling: a coupled heat and mass transfer model. – J R Soc Interface. 10(85): 20130326.

[6] Burgess, S. S. O., Dawson, T. E. (2007): Predicting the limits to tree height using statistical regressions of leaf traits. – New Phytol. 174(3): 626-636.

[7] Cai, Y. L., Song, Y. C. (2001): Adaptive ecology of lianas in Tiantongevergreen broadleaved forest, Zhejiang, China- I. Leaf anatomical characters. – Acta Phytoecol. Sin. 25: 90-98.

[8] Chartzoulakis, K., Loupassaki, M., Bertaki, M., Androulakis, I. (2002): Effects of NaCl salinity on growth, ion content and CO_2 assimilation rate of six olive cultivars. – Scientia Horticulturae 96: 235-247.

[9] Debnath, S. C. (2009): A two-step procedure for adventitious shoot regeneration on excised leaves of lowbush blueberry. – Vitro Cellular & Developmental Biology Plant 45(2): 122-128.

http://www.aloki.hu ● ISSN 1589 1623 (Print) ● ISSN1785 0037 (Online)
DOI: http://dx.doi.org/10.15666/aeer/1906_50595081

[10] Duan, B., Li, Y., Zhang, X., Helena, K., Li, C. (2009): Water deficit affects mesophyll limitation of leaves more strongly in sun than in shade in two contrasting Picea asperata populations. – Tree Physiology 29(12): 1551-1561.
[11] England, J. R., Attiwill, P. (2006): Changes in leaf morphology and anatomy with tree age and height in the broadleaved evergreen species, Eucalyptus regnans F. Muell. – Trees 20: 79-90.
[12] Gao, J. F. (2006): Experimental Guide of Plant Physiology. – China Higher Education Press, Beijing, pp. 122-125.
[13] Gonçalves, A. Z., Mercier, H., Oliveira, R. S., Romero, G. Q. (2016): Trade-off between soluble protein production and nutritional storage in Bromeliaceae. – Ann Bot. 118(6): 1199-1208.
[14] Göttlicher, S., Knohl, A., Wanek, W., Buchmann, N., Richter, A. (2006): Short-term changes in carbon isotope composition of soluble carbohydrates and starch: from canopy leaves to the root system. – Rapid Commun Mass Spectrom 20(4): 653-60.
[15] Hagedorn, F., Joseph, J., Peter, M., Luster, J., Pritsch, K., Geppert, U., Kerner, R., Molinier, V., Egli, S., Schaub, M., Liu, J. F., Li, M., Sever, K., Weiler, M., Siegwolf, R. T., Gessler, A., Arend M. (2016): Recovery of trees from drought depends on belowground sink control. – Nature Plants 2: 16111.
[16] He, C. X., Li, J. Y., Zhou, P., Guo, M., Zheng, Q. S. (2008): Changes of leaf morphological, anatomical structure and carbon isotope ratio with the height of the Wangtian tree (Parashorea chinensis) in Xishuangbanna, China. – J Integr Plant Biol. 50(2): 168-73.
[17] He, X., Xu, L., Pan, C., Gong, C., Wang, Y., Liu, X., Yu, Y. (2020): Drought resistance of Camellia oleifera under drought stress: Changes in physiology and growth characteristics. – PLoS One 15(7): e0235795.
[18] Kenzo, T., Ichie, T., Watanabe, Y., Yoneda, R., Ninomiya, I., Koike, T. (2006): Changes in photosynthesis and leaf characteristics with tree height in five dipterocarp species in a tropical rain forest. – Tree Physiol. 26(7): 865-873.
[19] Kenzo, T., Inoue, Y., Yoshimura, M., Yamashita, M., Tanaka-Oda, A., Ichie, T. (2015): Height-related changes in leaf photosynthetic traits in diverse Bornean tropical rain forest trees. – Oecologia 177(1): 191-202.
[20] Koch, G. W., Sillett, S. C., Jennings, G. M. (2004): Davis SD. The limits to tree height. – Nature 428(6985): 851-854.
[21] Koenig, D., Bayer, E., Kang, J., Kuhlemeier, C., Sinha, N. (2009): Auxin patterns Solanum lycopersicum leaf morphogenesis. – Development 136: 2997-3006.
[22] Kuang, Y., Xu, Y., Zhang, L., Hou, E., Shen, W. (2017): Dominant Trees in a Subtropical Forest Respond to Drought Mainly via Adjusting Tissue Soluble Sugar and Proline Content. – Frontiers in plant science 8: 802.
[23] Kuwabara, A., Nagata, T. (2002): Views on developmental plasticity of plants through heterophylly. – Recent Res Dev Plant Physiol. 3: 45-59.
[24] Lemoine, R., La Camera, S., Atanassova, R., Dédaldéchamp, F., Allario, T., Pourtau, N., Bonnemain, J. L., Laloi, M., Coutos-Thévenot, P., Maurousset, L., Faucher, M., Girousse, C., Lemonnier, P., Parrilla, J. (2013): Durand, M. Source-to-sink transport of sugar and regulation by environmental factors. – Frontiers in Plant Science 4: 272.
[25] Li, J. H., Feng, M., Li, Z. J. (2015): Carbohydrate, Soluble Protein and Morphometric Changes of Leaves of *Populus euphratica* Oliv. Individuals under Different Developmental Stages. – Bulletin of Botanical Research 35(4): 521-527.
[26] Li, Y. L., Zhang, X., Feng, M., Han, Z. J., Li, Z. J. (2017): Characteristics of Endhormones in Leaf Blade of *Populus euphratica* Heteromorphic Leaves. – Journal of Tarim University 29(3): 7-13.
[27] Li, X., He, D., Guo, Y. (2019): Morphological structure and physiological research of heterophylly in Potamogeton octandrus. – Plant Systematics and Evolution 305: 223-232.

http://www.aloki.hu ● ISSN 1589 1623 (Print) ● ISSN1785 0037 (Online)
DOI: http://dx.doi.org/10.15666/aeer/1906_50595081

[28] Li, G., Hu, S., Hou, H., Kimura, S. (2019): Heterophylly: Phenotypic Plasticity of Leaf Shape in Aquatic and Amphibious Plants. – Plants (Basel) 8(10): 420.
[29] Li, Z. J. (2020): Physiological and Molecular Mechanisms of Drought Resistance of *Populus euphratica* and *Populus pruinosa*. – China Science Press, Beijing, pp. 11-15.
[30] Li, G. J., Hu, S. Q., Yang, J. J., Hou, H. W. (2020): Advances of heterophylly studies in plant. – Plant Physiology Journal 56(10): 2067-2078.
[31] Liu, S. F., Jiao, P. P., Li, Z. J. (2016): Diversifolious Types and Spatiotemporal Characteristics of *Populus pruinosa* Schrenk. – Arid Zone Research 33(5): 1098-1103.
[32] Liu, J. F., Arend, M., Yang, W. J., Schaub, M., Ni, Y. Y., Gessler, A., Jiang, Z. P., Rigling, A., Li, M. H. (2017): Effects of drought on leaf carbon source and growth of European beech are modulated by soil type. – Sci Rep. 7: 42462.
[33] Liu, T., Ren, T., White, P. J., Cong, R., Lu, J. (2018): Storage nitrogen co-ordinates leaf expansion and photosynthetic capacity in winter oilseed rape. – J Exp Bot. 69(12): 2995-3007.
[34] Liu, Q., Huang, Z., Wang, Z., Chen, Y., Wen, Z., Liu, B., Tigabu, M. (2020): Responses of leaf morphology, NSCs contents and C:N:P stoichiometry of Cunninghamia lanceolata and Schima superba to shading. – BMC plant biology 20(1): 354.
[35] Lusk, C. H., Reich, P. B., Montgomery, R. A., Ackerly, D. D., Cavender-Bares, J. (2008): Why are evergreen leaves so contrary about shade? – Trends Ecol Evol. 23(6): 299-303.
[36] Martin, A. R., Thomas, S. C. (2013): Size-dependent changes in leaf and wood chemical traits in two Caribbean rainforest trees. – Tree Physiol 33(12): 1338-1353.
[37] Martínez-Vilalta, J., Sala, A., Asensio, D., Galiano, L., Hoch, G., Palacio, S., Piper, F., Lloret, F. (2016): Dynamics of non-structural carbohydrates in terrestrial plants: a global synthesis. – Ecological Monographs 86: 495-516.
[38] Mendes, M. M., Gazarini, L. C., Rodrigues, M. L. (2001): Acclimation of Myrtus communis to contrasting Mediterranean light environments - Effects on structure and chemical composition of foliage and plant water relations. – Environmental & Experimental Botany 45(2): 165-178.
[39] Mommer, L., Visser, E. J. W. (2005): Underwater photosynthesis in flooded terrestrial plants: a matter of leaf plasticity. – Annals of Botany 96: 581-589.
[40] Nakashima, K., Yamaguchi-Shinozaki, K. (2013): ABA signaling in stress-response and seed development. – Plant Cell Rep. 32: 959-970.
[41] Nakayama, H., Nakayama, N., Seiki, S., Kojima, M., Sakakibara, H., Sinha, N., Kimura, S. (2014): Regulation of the KNOX-GA Gene Module Induces Heterophyllic Alteration in North American Lake Cress. – Plant Cell 26(12): 4733-4748.
[42] Nakayama, H., Sinha, N., Kimura, S. (2017): How Do Plants and Phytohormones Accomplish Heterophylly, Leaf Phenotypic Plasticity, in Response to Environmental Cues. – Frontiers in Plant Science 8: 1717.
[43] Oikawa, S., Ainsworth, E. A. (2016): Changes in leaf area, nitrogen content and canopy photosynthesis in soybean exposed to an ozone concentration gradient. – Environ Pollut. 215: 347-355.
[44] Pan, Y. P., Chen, Y. P., Wang, H. J., Ren, Z. G. (2018): Leaf Structure and Functional Traits of *Populus euphratica*. – Journal of Desert Research 38(4): 765-771.
[45] Patakas, A., Nikolaou, N., Zioziou, E., Radoglou, K., Noitsakis, B. (2002): The role of organic solute and ion accumulation in osmotic adjustment in drought-stressed grapevines. – Plant Science 163: 361-367.
[46] Purdy, S. J., Maddison, A. L., Cunniff, J., Donnison, I., Clifton-Brown, J. (2015): Non-structural carbohydrate profiles and ratios between soluble sugars and starch serve as indicators of productivity for a bioenergy grass. – AoB Plants. 7: 32.
[47] Quentin, A. G., Close, D. C., Hennen, L. M., Pinkard, E. A. (2013): Down-regulation of photosynthesis following girdling, but contrasting effects on fruit set and retention, in two sweet cherry cultivars. – Plant Physiol Biochem 73: 359-367.

http://www.aloki.hu ● ISSN 1589 1623 (Print) ● ISSN1785 0037 (Online)
DOI: http://dx.doi.org/10.15666/aeer/1906_50595081

[48] Selbig, J., Fernie, A. R., Altmann, T., Stitt, M. (2009): Starch as a major integrator in the regulation of plant growth. – Proc Natl Acad Sci USA 106(25): 10348-10353.
[49] Svensk, M., Coste, S., Gérard, B., Gril, E., Julien, F., Maillard, P., Stahl, C., Leroy, C. (2020): Drought effects on resource partition and conservation among leaf ontogenetic stages in epiphytic tank bromeliads. – Physiol Plant 170(4): 488-507.
[50] Thalmann, M., Santelia, D. (2017): Starch as a determinant of plant fitness under abiotic stress. – New Phytol 214(3): 943-951.
[51] Velikova, V., Arena, C., Izzo, L. G., Tsonev, T., Koleva, D., Tattini, M., Roeva, O., De, M. A., Loreto, F. (2020): Functional and Structural Leaf Plasticity Determine Photosynthetic Performances during Drought Stress and Recovery in Two Platanus orientalis Populations from Contrasting Habitats. – Int J Mol Sci. 21(11): 3912.
[52] Wang, H. Z., Han, L., Xu, Y. L., Niu, J. L., Yu, J. (2017): Effects of soil water gradient on photosynthetic characteristics and stress resistance of *Populus pruinosa* in the Tarim Basin, China. – Acta Ecologica Sinica 37(2): 432-442.
[53] Wanke, D. (2011): The ABA-mediated switch between submersed and emersed life-styles in aquatic macrophytes. – J Plant Res 124(4): 467-475.
[54] Wei, Q. J. (1990): *Populus euphratica* Oliv. – China Forestry Publishing House, Beijing, pp. 1-99.
[55] Wells, C. L., Pigliucci, M. (2000): Adaptive phenotypic plasticity: the case of heterophylly in aquatic plants. – Perspectives in Plant Ecology Evolution and Systematics 3(1): 0-18.
[56] Winn, A. A. (1999): The functional significance and fitness consequences of heterophylly. – International Journal of Plant Sciences 160: 113-121.
[57] Woodruff, D. R., Meinzer, F. C. (2011): Water stress, shoot growth and storage of non-structural carbohydrates along a tree height gradient in a tall conifer. – Plant Cell Environ 34(11): 1920-30.
[58] Woodruff, D. R., Meinzer, F. C., Marias, D. E., Sevanto, S., Jenkins, M. W., McDowell, N. G. (2015): Linking nonstructural carbohydrate dynamics to gas exchange and leaf hydraulic behavior in Pinus edulis and Juniperus monosperma. – New Phytol. 206(1): 411-421.
[59] Yamaguchi-Shinozaki, K., Shinozaki, K. (2006): Transcriptional regulatory networks in cellular responses and tolerance to dehydration and cold stresses. – Annu Rev Plant Biol. 57: 781-803.
[60] Zhai, J. T., Han, X. L., Li, Z. J. (2019): Evaluation of Drought Resistance of Different Development Stages of *Populus pruinosa* Based on the Leaf Anatomical Structure. – Journal of Tarim University 31(4): 12-21.
[61] Zhai, J. T., Li, Y. L., Han, Z. J., Li, Z. J. (2020): Morphological, structural and physiological differences in heteromorphic leaves of Euphrates poplar during development stages and at crown scales. – Plant Biol. 22(3): 366-375.
[62] Zhang, J., Jiang, D., Liu, B., Luo, W., Lu, J., Ma, T., Wan, D. (2014): Transcriptome dynamics of a desert poplar (*Populus pruinosa*) in response to continuous salinity stress. – Plant Cell Reports 33(9): 1565-1579.
[63] Zhang, J. L., Li, Y. L., Pang, M. L., Zhu, C. G., Bi, Z. L. (2017): Comparison of Resistance of Anatomical Structure in the Heterophylly Mechanism of Sabina vulgaris. – Acta Bot. Boreal.-Occident. Sin. 37(9): 1756-1763.

http://www.aloki.hu ● ISSN 1589 1623 (Print) ● ISSN1785 0037 (Online)
DOI: http://dx.doi.org/10.15666/aeer/1906_50595081

APPENDIX

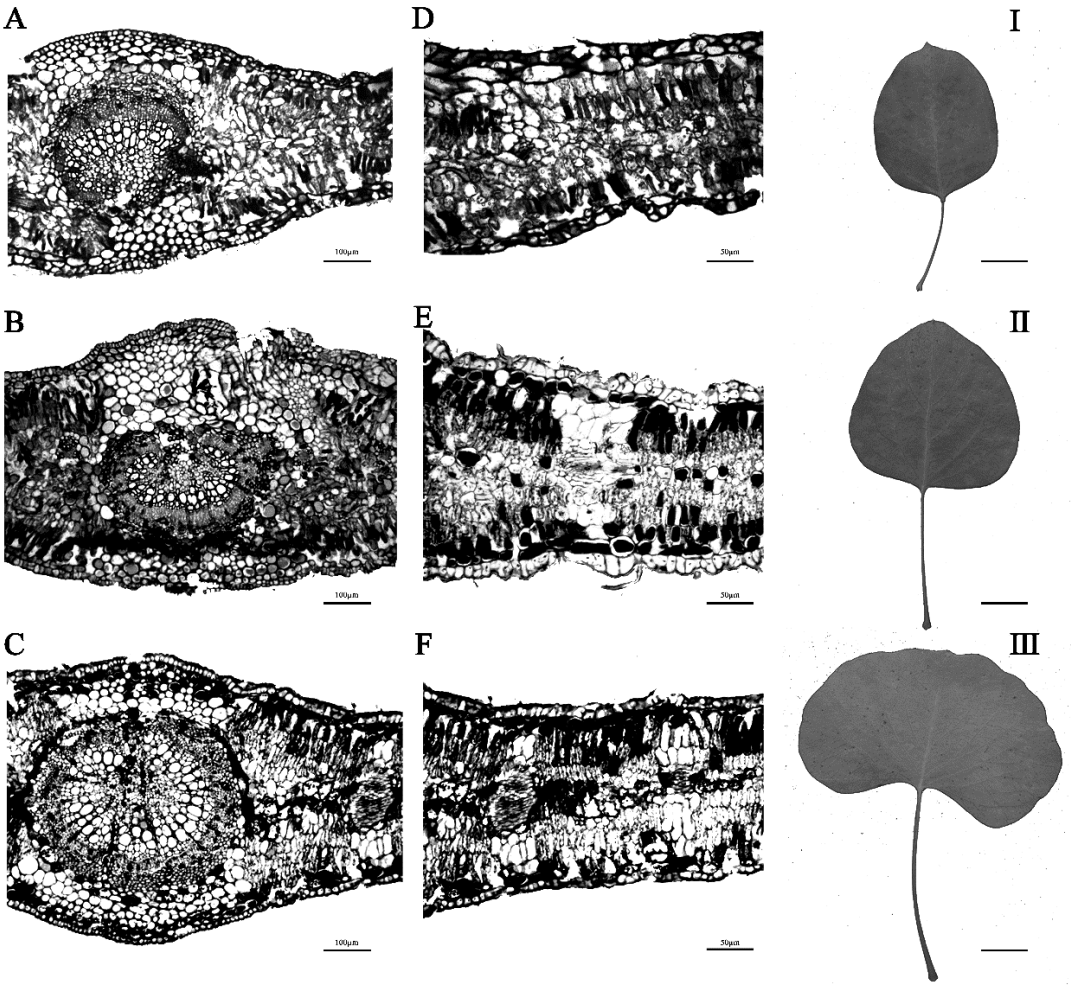

Plate I. *Anatomic structure of long elliptic, round and broadly ovate leaves of P. pruinosa (From top to bottom corresponding to the long elliptic (Ⅰ), circular (Ⅱ), broad ovate (Ⅲ) anatomical structure; A-C represents A 10X10 times field of view, and D-F represents A 20X20 times field of view*

http://www.aloki.hu ● ISSN 1589 1623 (Print) ● ISSN1785 0037 (Online)
DOI: http://dx.doi.org/10.15666/aeer/1906_50595081

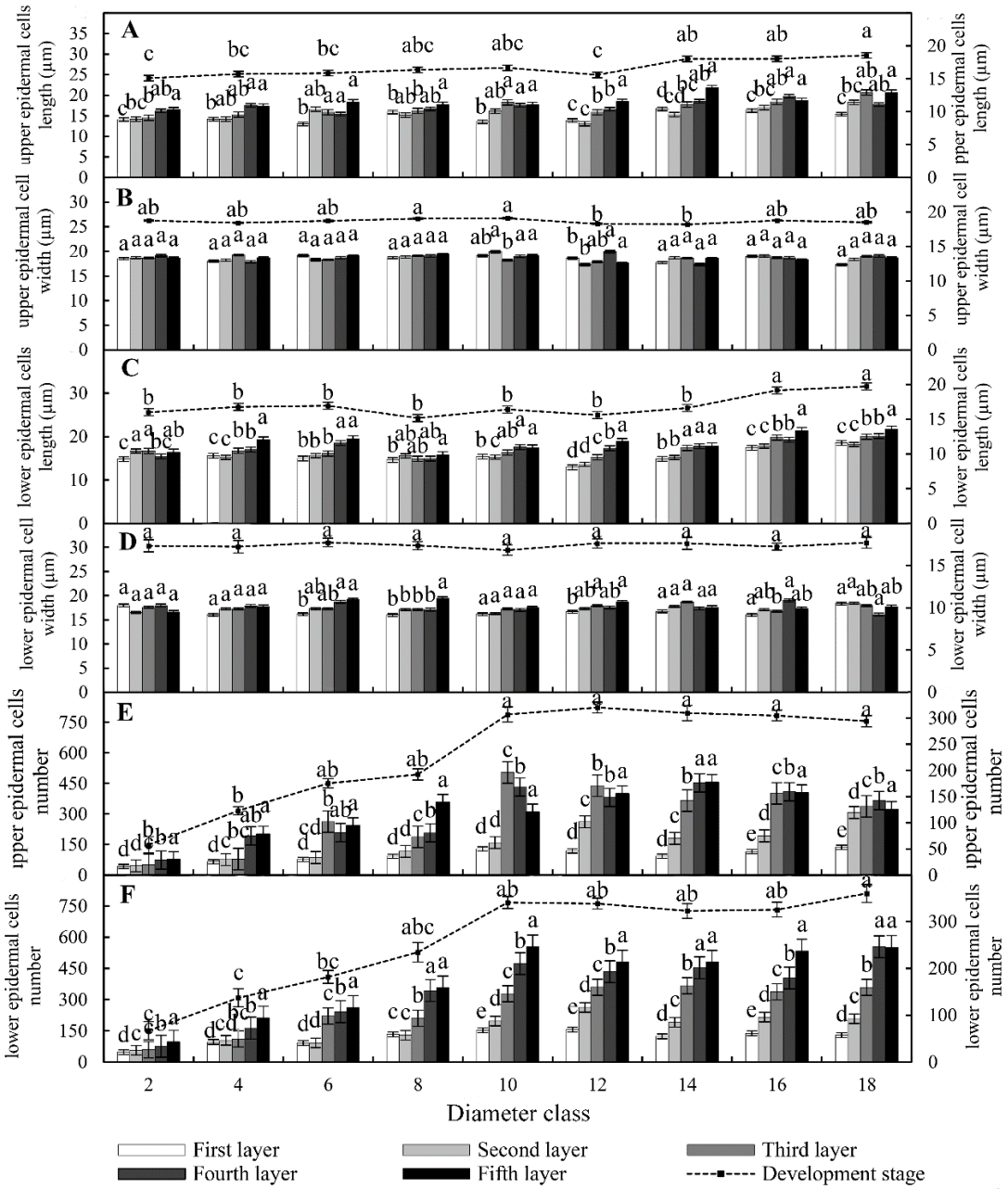

Figure S1. *Changes of leaf epidermis with developmental stages and canopy height in cross section of heteromorphic leaves of P. pruinose. (A) length of upper epidermal cells, (B) width of upper epidermal cells, (C) length of lower epidermal cells, (D) width of upper epidermal cells, (E) number of upper epidermal cells, and (F) number of lower epidermal cells. Lowercase letters indicated significant differences, the same letters indicated not significant (P >0.05), and different letters indicated significant differences (P<0.05)*

http://www.aloki.hu ● ISSN 1589 1623 (Print) ● ISSN1785 0037 (Online)
DOI: http://dx.doi.org/10.15666/aeer/1906_50595081

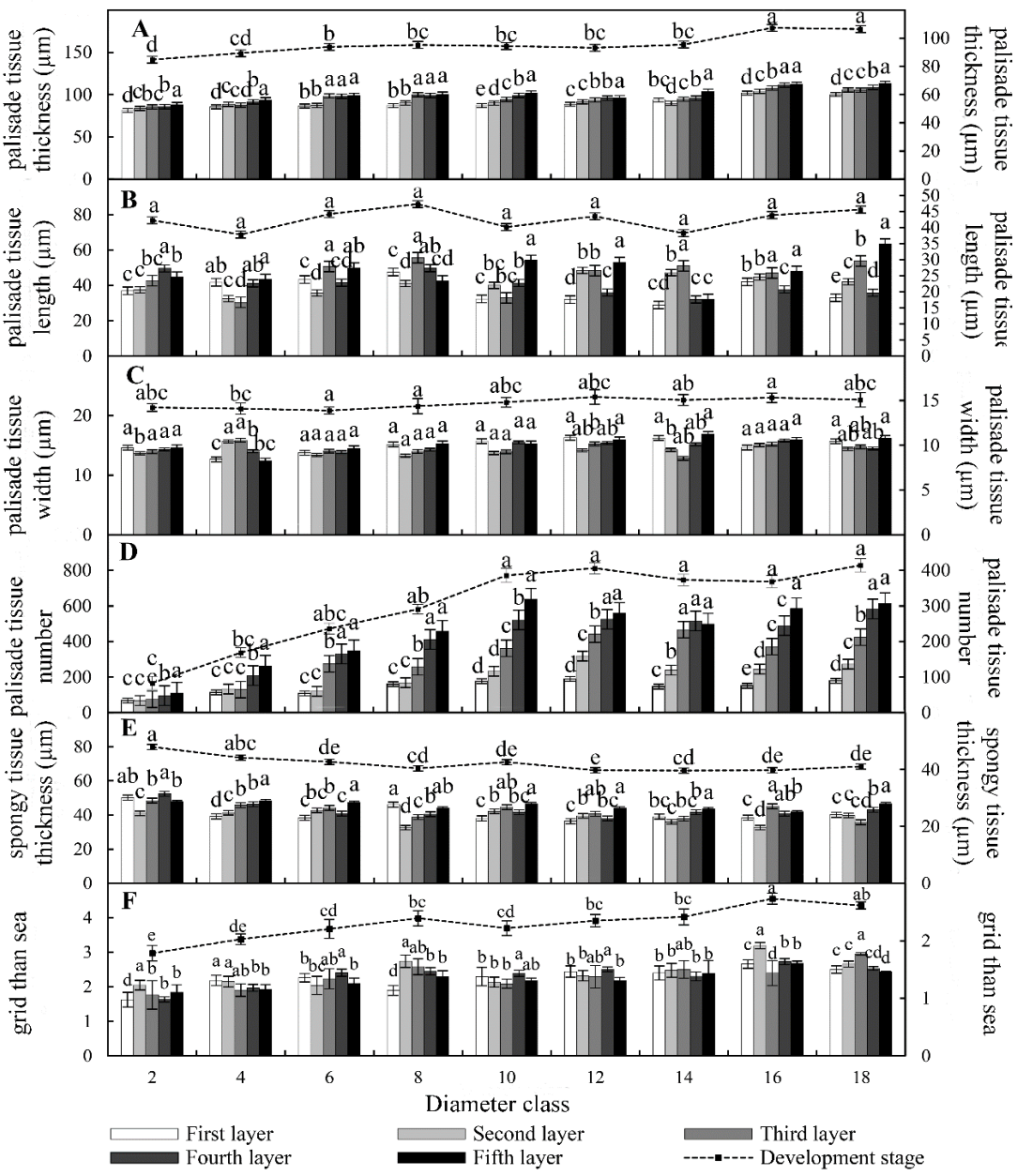

Figure S2. *Changes of mesophyll tissue in cross section of heteromorphic leaves of P. pruinose with developmental stages and canopy height. (A) tissue thickness of fence, (B) tissue length of fence, (C) tissue width of fence, (D) tissue number of fence, (E) tissue thickness of sponge fence, (F) ratio of fence to sea. Lowercase letters indicated significant differences, the same letters indicated not significant (P >0.05), and different letters indicated significant differences (P<0.05)*

http://www.aloki.hu ● ISSN 1589 1623 (Print) ● ISSN1785 0037 (Online)
DOI: http://dx.doi.org/10.15666/aeer/1906_50595081

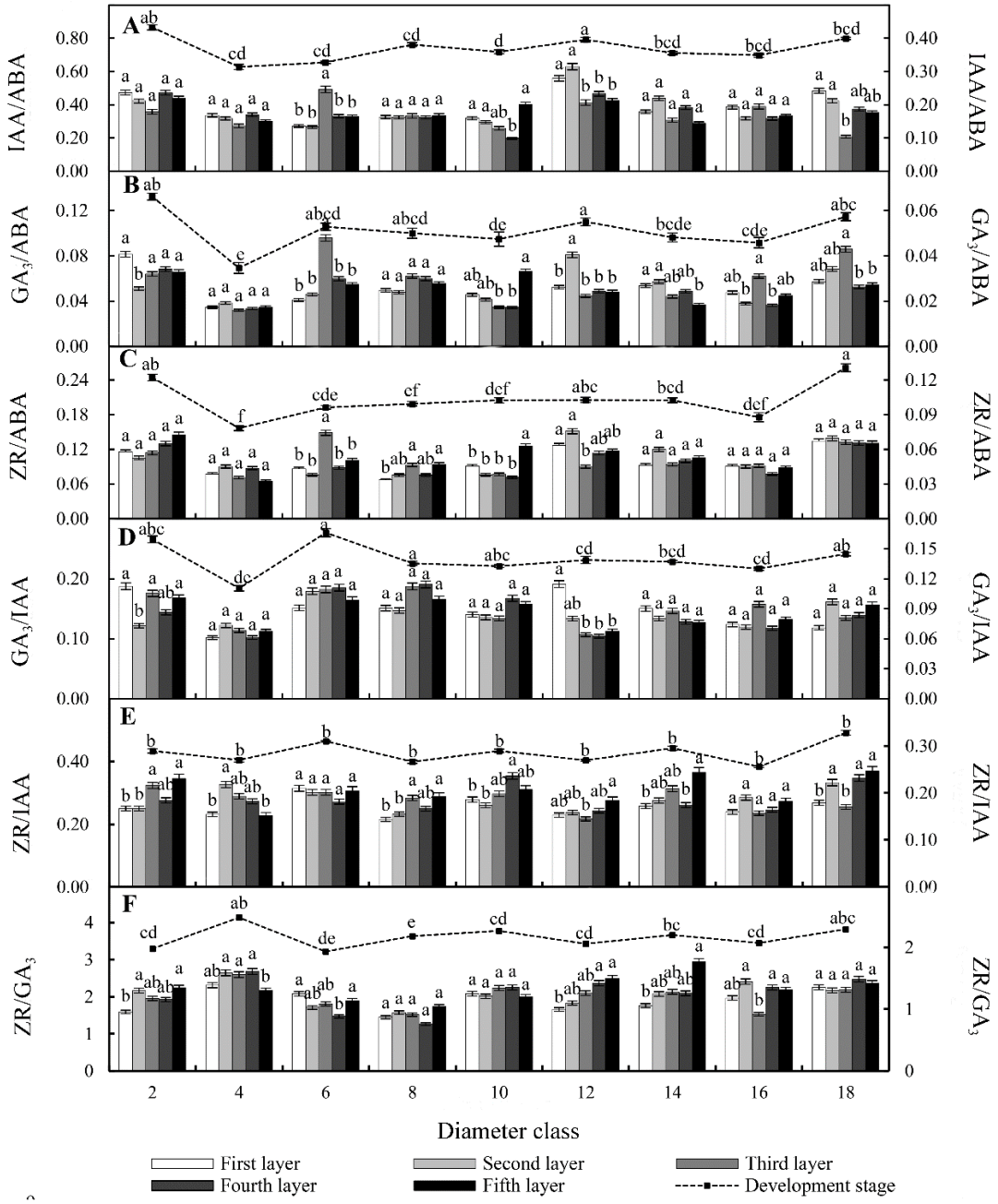

Figure S3. *Changes of endogenous hormone ratio in heteromorphic leaves of P. pruinose with individual crown height and various developmental stages. (A)IAA/ABA, (B)GA₃/ABA, (C)ZR/ABA, (D)GA₃/IAA, (E)ZR/IAA, (F)ZR/GA₃. Lowercase letters indicated significant differences, the same letters indicated not significant (P >0.05), and different letters indicated significant differences (P<0.05)*

http://www.aloki.hu ● ISSN 1589 1623 (Print) ● ISSN1785 0037 (Online)
DOI: http://dx.doi.org/10.15666/aeer/1906_50595081

Table S1. *The morphological and structural changes of heteromorphic leaves were related to the Pearson of DBH and crown height of P. pruinosa*

	PL	LL	LW	LI	LA	LC	BT	UECL	UECW	LECL	LECW	UECN	LECN	PN	PTT	PTCL	PTCW	STT	PSR
DBH	0.89**	0.38	0.54	0.37	0.53	0.67*	0.54	0.89**	-0.22	0.64*	0.21	0.91**	0.92**	0.91**	0.89**	0.22	0.85**	-0.79**	0.92**
CH	0.83**	0.34	0.48	0.43	0.48	0.6	0.49	0.81**	-0.22	0.5	0.15	0.97**	0.97**	0.96**	0.81**	0.16	0.89**	-0.84**	0.89**

Table S2. *Four endogenous hormones and their ratios and carbohydrate of heteromorphic leaves were related to the Pearson of DBH and crown height of P. pruinosa*

	GA_3	IAA	ZR	ABA	IAA/ABA	GA_3/ABA	ZR/ABA	GA_3/IAA	ZR/IAA	SS	S	SP
DBH	-0.18	0.48	0.96*	-0.81	0.49	-1.00**	0.98*	-0.79	0.15	0.90**	-0.97**	0.86**
CH	-0.02	0.62	0.9	-0.71	0.63	-0.99*	0.93	-0.88	-0.01	0.94**	-0.94**	0.94**

http://www.aloki.hu ● ISSN 1589 1623 (Print) ● ISSN1785 0037 (Online)
DOI: http://dx.doi.org/10.15666/aeer/1906_50595081

Table S3. *Optimal regression model for predicting the content and ratio of endogenous hormones and leaf morphology of P. pruinosa*

Dependent variable(Y)	Regression equation	R	R^2	F	Sig.
Y_1	$Y_1=1.60+0.12X_1+10.53X_3$	0.52	0.27	1.08	0.00
Y_2	$Y_2=0.10-0.00026X_3$	0.85	0.72	18.31	0.00
Y_3	$Y_3=2.14+0.63X_1$	0.54	0.29	2.89	0.00
Y_4	$Y_4= -47.64+17.14X_1$	0.52	0.27	2.54	0.00
Y_5	$Y_5=5.88-83.70X_2+36.50X_3-1.72X_5$	0.77	0.59	2.43	0.00
Y_6	$Y_6=4.63+0.75X_1$	0.45	0.20	1.80	0.00
Y_7	$Y_7=16.16+8.84X_4$	0.49	0.24	2.21	0.00
Y_8	$Y_8=-20.13+7.17X_1$	0.74	0.55	8.58	0.00
Y_9	$Y_9=-1.85+0.26X_1$	0.68	0.46	5.99	0.00

Y_1, leaf length; Y_2, leaf width; Y_3, leaf circumference; Y_4, leaf thickness; Y_5, petiole length; Y_6, length of upper epidermal cells; Y_7, width of lower epidermal cells; Y_8, thickness of palisade tissue; Y_9, ratio of grid to sea; X_1,ZR; X_2,GA_3/ABA; X_3,ZR/ABA; X4,GA_3/IAA; X5,ZR/GA_3

Table S4. *Optimal Regression Model for the Prediction of Carbohydrate and Leaf Morphological Structure of P. pruinosa Leaves*

Dependent variable(Y)	Regression equation	R	R^2	F	Sig.
Y_1	$Y_1=1.08+0.17X_3$	0.85	0.72	18.45	0.00
Y_2	$Y_2=2.73+0.10X_3$	0.53	0.28	2.78	0.00
Y_3	$Y_3= 1.17+25.41X_1$	0.62	0.38	4.33	0.00
Y_4	$Y_4= 7.56+0.57X_3$	0.52	0.27	2.64	0.00
Y_5	$Y_5= 10.53+0.50X_3$	0.59	0.36	3.92	0.00
Y_6	$Y_6= 185.56+12.69X_3$	0.53	0.28	2.72	0.00
Y_7	$Y_7= 13.50+0.93X_3$	0.78	0.61	10.74	0.00
Y_8	$Y_8=17.45+19.19X_1-7.62X_2$	0.54	0.29	1.24	0.00
Y_9	$Y_9= -62.10+89.85X_3$	0.93	0.87	47.11	0.00
Y_{10}	$Y_{10}= -64.13+94.11X_3$	0.93	0.87	46.93	0.00
Y_{11}	$Y_{11}= 78.89-154.87X_2+7.25X_3$	0.89	0.81	12.42	0.00
Y_{12}	$Y_{12}= 13.33+0.40X_3$	0.76	0.57	9.37	0.00
Y_{13}	$Y_{13}= 50.37-2.46X_3$	0.94	0.89	57.96	0.00
Y_{14}	$Y_{14}=1.51-4.44X_2+0.30X_3$	0.97	0.94	47.55	0.00

Y_1, long petiole; Y_2, blade width; Y_3, leaf shape index; Y_4, leaf area; Y_5, leaf circumference; Y_6, leaf thickness; Y_7, length of upper epidermis; Y_8, width of lower epidermis; Y_9, number of upper epidermis; Y_{10}, number of lower epidermis; Y_{11}, thick fence tissue; Y_{12}, wide fence organization; Y_{13}, spongy tissue is thick; Y_{14}, ratio of grid to sea; X_1, soluble protein content; X_2, starch content; X_3, soluble sugar content

http://www.aloki.hu ● ISSN 1589 1623 (Print) ● ISSN1785 0037 (Online)
DOI: http://dx.doi.org/10.15666/aeer/1906_50595081

GROWTH ESTIMATION AND LENGTH–WEIGHT RELATIONSHIPS OF SPOTTAIL MANTIS SHRIMP (*SQUILLA MANTIS,* LINNEAUS 1758) IN THE ALGIERS REGION (SOUTH-WEST OF MEDITERRANEAN SEA)

KENNOUCHE, H.[1*] – KACIMI, A.[2]

[1]*Management and enhancement of agricultural and aquatic ecosystems laboratory, Institute of Sciences, Morsli Abdellah University Center, 42000 Tipaza, Algeria (phone: +213-2437-1003; fax: +213-2437-1006)*

[2]*Marine and Coastal Ecosystems Laboratory (ECOSYSMarL), National Higher School of Marine Sciences and Coastal Management (ENSSMAL), 16320 Algiers, Algeria (phone: +213-2191-7743; fax: +213-2191-7791)*

[*]*Corresponding author*
e-mail: kennouchehanane@yahoo.fr

(Received 5th Aug 2021; accepted 1st Oct 2021)

Abstract. This study concerns the growth and biometric relations of the mantis shrimp *Squilla mantis* from the region of Algiers. A total of 1064 individuals were sampled from the trawl fishery landings, between December 2016 and December 2017. The results show the different growth parameters, established on cephalothorax measurements (Lc_∞ = 48.06 mm; K = 0.34 yr^{-1}; t_0 = -0.69 year) and total length values (Lt_∞ = 189.9 mm; K = 0.48 yr^{-1}; t_0 = -0.66 year). The decomposition of size structures according to the Bhattacharya method yielded four age classes based on the cephalothorax and total length (0^+-3). The total mortality (Z) calculated from Ricker curve was 1.32 $year^{-1}$, and the natural mortality coefficient M was calculated at 0.95 $year^{-1}$ indicating an under-exploitation of the *S. mantis* stock in this area. Different biometric relationships are established of the size-size and size weight type highlighting an allometry coefficient higher than 1 and lower than 3, respectively for the size-size and size-weight relationships, translating a major growth of the total size and a minor growth of the weight. Researchers and decision makers can integrate these results in analytical, bioenergetic and bioeconomic models to better manage the exploitation of the *S. mantis* stock in the western Mediterranean basin.
Keywords: *S. mantis mortality, population dynamic, age structure, biometric relationship, Algeria, Mediterranean-Western basin*

Introduction

Of the nine species of Mediterranean Stomatopods, only the spottail mantis shrimp, *Squilla mantis*, is of appreciable economic importance (Maynou et al., 2004). Its range extends from Angola to the Gulf of Cadiz (Manning, 1977). In the Atlantic, this species seems to be present only in the Gulf of Cadiz (Maynou et al., 2004), while in the Mediterranean, it is reported in Egypt, Syria, Greece, Turkey, Italy, France, Spain, Palestine, Algeria (Schram and Muller, 2004) and on the Tunisian coast (Mili et al., 2011). It is found at sublittoral depths greater than 3 m on sandy and muddy bottoms up to 200 m deep, but generally at less than 50 m (Holthuis, 1987). Its presence is reported on the entire Algerian coast, and studies carried out in the Algerian basin have highlighted its relatively high abundance in the center of the basin, in particular, in the bay of Bou Ismail between 50 and 100 m. *S mantis* prefers compact and sandy liquid muds and fine sand, and average temperatures of 13.2 to 15.3°C (Campilo, 1982). Its

http://www.aloki.hu ● ISSN 1589 1623 (Print) ● ISSN 1785 0037 (Online)
DOI: http://dx.doi.org/10.15666/aeer/1906_50835101

catch on the Algerian coast in the last five years has recorded a maximum landing rate of 3232.9 Kg in 2016 (*Fig. 1*; Ministry of Fisheries and Fisheries Production, 2021).

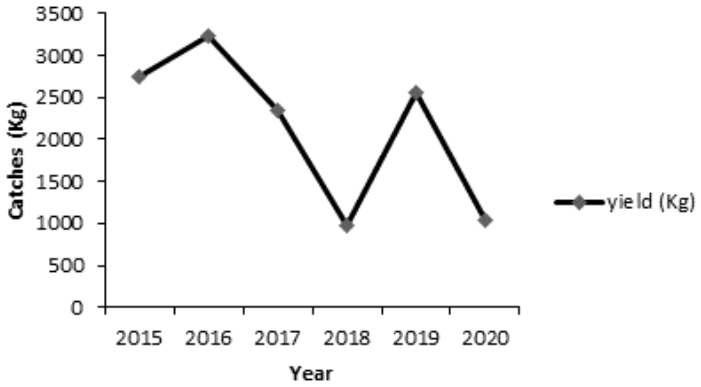

Figure 1. *Catch of S. mantis in Algeria between 2015 and 2020 (Ministry of Fisheries and Fisheries Production, 2021)*

S. mantis has been the subject of numerous research studies in the Mediterranean and Atlantic. Among these works, we mention those of Ragonese et al. (2012) in the southern coast of Sicily, Vasconcelos et al. (2017) in algarve coast, Erdogan-Saglam et al. (2017) in the bay of Izmir, Vila et al. (2013) in the Gulf of Cadiz, Kampouris et al. (2018) in the Thermaikos Gulf, Veneroni and Fernandes (2021) in the northern Adriatic sea; Mili et al. (2008, 2013, 2014) in Tunisia; but no study has been undertaken on this species in Algeria.

S. mantis is caught in limited quantities and essentially on trawlable bottoms by means of demersal trawls. In the past, this species was considered as a fishing product of low market value not appreciated by Algerians for lack of culinary tradition and was consequently rejected at sea after its capture. But given the high price of wild shrimp in recent years, this species has begun to attract interest by the Algerian consumer (*Fig. 1*). Indeed, *S. mantis* has become popular in fish shops in the central region with prices/kg ranging between 400 and 500 Algerian dinars at retail (about 3 euros). Compared to the numerous investigations undertaken on Peneidae (Derbal and Soltani, 2008; Kennouche, 2009), Aristeidae (Mouffok et al., 2005, 2008; Nouar and Kennouche, 2013) or Pandalidae (Derbal and Kara, 2006) from the Algerian coasts, Stomatopods have not attracted the same scientific interest. Moreover, there is no comprehensive information on the biology, ecology or exploitation level of Stomatopods in Algeria. In order to better understand the available stocks of Stomatopods along the Algerian coasts, this study aims to provide new data on the growth and biometric relationships of *S. mantis* in the Algerian region in a perspective of rational exploitation and valorization of this carcinological resource.

Material and methods

Sampling

Between December 2016 and December 2017, 1064 individuals of *S. mantis* were sampled from the landings of the commercial trawl fishery conducted in the Algiers region (*Fig. 2*).

http://www.aloki.hu ● ISSN 1589 1623 (Print) ● ISSN 1785 0037 (Online)
DOI: http://dx.doi.org/10.15666/aeer/1906_50835101

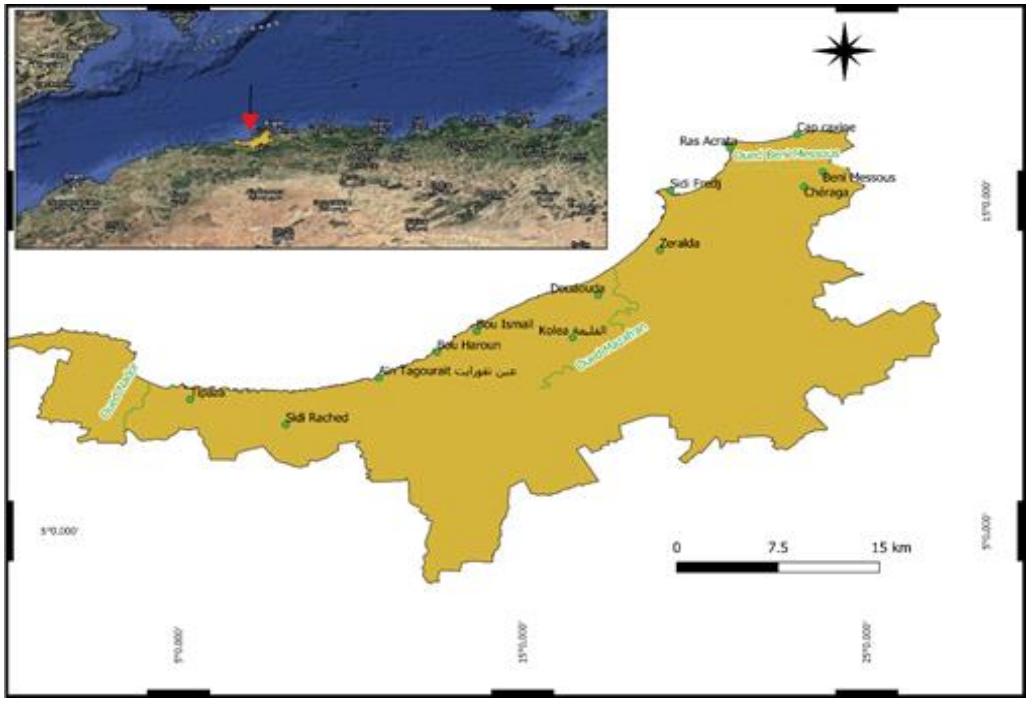

Figure 2. *Map of the study area in the central region of the Algerian basin*

Measurements were made on each individual using an ichthyometer, for the measurement of total length (*Lt*) and telson (*Ltel*), and a caliper, for the measurement of cephalothoracic length (*Lc*). Total weight (*Wt*) was determined with a 0.01 g precision scale (*Fig. 3*). The sex of *S. mantis* is easily identified by the presence of a pair of copulatory organs from the base of the third pair of pereiopods corresponding to the 8th thoracic segment in males and by the presence of the genital plate on the sternite of the 6th thoracic segment in females (Abelló and Martín, 1993). Also, other individuals (152 specimens) were measured and considered without distinction of sex, because of the deterioration of some frozen individuals.

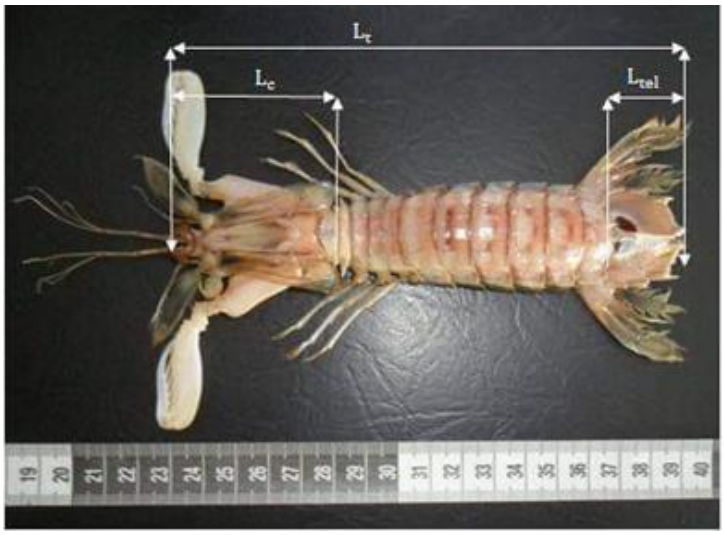

Figure 3. *The different measurements made on S. mantis*

http://www.aloki.hu ● ISSN 1589 1623 (Print) ● ISSN 1785 0037 (Online)
DOI: http://dx.doi.org/10.15666/aeer/1906_50835101

Age and growth

The age of the specimens was determined from length-frequency data analysis using Bhattacharya's method in the FISAT II software. This method, which is based on logarithmic differences, was outlined by Bhattacharya (1967), taken up by Masson (1970) and applied by Gayanilo et al. (2002). The growth in length of this species has been described using the Von Bertalanffy equation (Ricker, 1975; Beverton and Holt, 2012; *Eq. 1*):

$$\mathrm{Lt} = L\infty\,(1 - e^{-K(t-t0)}) \qquad \text{(Eq.1)}$$

with: Lt: total length at age t (cm), L∞: asymptotic length (cm), K: growth coefficient (yr^{-1}), t: age (yr), t0: the hypothetical age corresponding to zero theoretical length (Sparre and Venema, 1992; King, 2013). The Von Bertalanffy exponential growth models were evaluated using the root mean square error (RMSE). The RMSE gives an overview of the overall difference between the predicted (VBGE) and observed (Bhattacharya decomposition) values.

The length performance (∅') was estimated using the equation (*Eq. 2*), given by Moreau et al. (1986):

$$\emptyset' = \log K + 2\log L\infty \qquad \text{(Eq.2)}$$

The asymptotic length L_∞ was estimated from the size frequency distribution by the method of Powell (1979); Wetherall (1986) using the FISAT II software, version 1.2.0 (Gayanilo et al., 2002). This same software also allowed us to estimate the growth rate *K* by analyzing the age-length key obtained by Bhattacharya (1967) multimodal decomposition. The analysis of this age-length key was performed according to the iterative method of Tomlinson and Abramson (1961), a method based on a "least square" type of adjustment by integrating the L_∞ obtained by Powell (1979) and Wetherall (1986). This method estimates the parameter *K* so that the sum of the squares of the differences between the model and the observations is minimal (Gayanilo et al., 2002).

The age at time "zero", represented by t_0 is calculated by Pauly (1980) (*Eq. 3*):

$$\log 10\,(\mathrm{t0}) = -0.3922 - 0.2752\log 10\,L\infty - 1.038\,log10\,K \qquad \text{(Eq.3)}$$

Biometric relations

For the biometric study of the mantis shrimp, we established the following morphometric relationships: *Ltel* = *F* (*Lc*), *Lt* = *F* (*Ltel*), *Lt* = *F* (*Lc*), *Wt* = *F* (*Lc*), *Wt* = *F* (*Ltel*) and *Wt* = *F* (*Lt*). With: *Ltel*: telson length, *Lc*: cephalothoracic length, *Lt*: total length and *Wt*: total weight. These relationships were expressed by a linear model of the form y= a x + b for length-length relationships and log w= log a +b log L for length-weight relationships. Where *W* = total weight, *L* = *Lt*, *Lc*, or *Ltel*, *a* = intercept and *b* = slope of the regression line for length-weight relationships, these parameters are inverted for length-length relationships (*a*: slope of the regression line and *b*: intercept). The exponent *b* is the allometry coefficient reflecting the proportionality of the growth of a given trait to the reference trait (*b* < 3 negative

http://www.aloki.hu ● ISSN 1589 1623 (Print) ● ISSN 1785 0037 (Online)
DOI: http://dx.doi.org/10.15666/aeer/1906_50835101

allometry, $b = 3$ isometry, $b > 3$ positive allometry). For length-length relationships, the slope coefficient a reflects the nature of the allometry ($a < 1$ minor allometry, $a > 1$ major allometry, $a = 1$ isometry).

In addition, *t*-test for slope conformity was performed to confirm the type of allometry for the length-weight and length-length relationships (*Eqs. 4,5*) for the size-weight relationships and length-length relationships, respectively:

$$t = \frac{[(b-3)]}{sd\ (b)} \quad \text{(Eq.4)}$$

$$t = \frac{[(b-1)]}{sd\ (b)} \quad \text{(Eq.5)}$$

with:

$$sd(b) = \sqrt{\frac{\frac{\delta y^2}{\delta x^2}(1-R^2)}{n-2}} \quad \text{(Eq.6)}$$

with δy^2: Variance of variable y, δx^2: variance of variable x, R^2: coefficient of determination, n-2: degree of freedom and $\alpha = 0.05$. If $t < 1.96$ non-significant difference, if $t > 1.96$ significant difference. In addition, statistical analyses were performed to test the significance of the difference between the calculated and observed values. Differences in sex ratios, based on a theoretical ratio of 1:1, were assessed using Chi-square ($\chi 2$) analysis in R (4.0.3). Sample normality was tested by the Kolmogorov Smirnov test and homogeneity of variances with the Levene test using STATISTICA 6.1. ANOVA of the regression models (length-weight and length-length) was used to test the significance of the latter (R 4.0.3).

Mortality

The instantaneous coefficient of total mortality (Z) was calculated by the capture curve given by Ricker (1975); where Z is equal to the slope of the descending part of the curve. Natural mortality (M) was estimated using the empirical equation of Pauly (1983) (*Eq. 7*):

$$\log M = -0.0066 - 0.279 \log L\infty + 0{,}6543 \log K + \log T° \quad \text{(Eq.7)}$$

with $T°$: temperature of the seawater (°C). The mortality coefficient (F) was deduced from the formula $F=Z-M$ (Gulland, 1971). The exploitation rate (E) was estimated according to the ratio: $E=F/Z$ (Gulland, 1971). All statistical analyses were conducted using STATISTICA 6.1, R 4.0.3 and Microsoft Excel® software.

Results

Statistical analysis

The mean total length (*Lt*), cephalothoracic length (*Lc*), telson length (*Ltel*), and mean weight of 1064 *Squilla mantis* specimens were 13.39±0.16 (cm), 2.99±0.04 (cm), 2.35±0.03 (cm), and 29.18±0.99 (g), respectively (*Table 1*). Males were slightly larger

http://www.aloki.hu ● ISSN 1589 1623 (Print) ● ISSN 1785 0037 (Online)
DOI: http://dx.doi.org/10.15666/aeer/1906_50835101

than females, but the difference was statistically insignificant ($P > 0.05$). The sex ratio was 52.82% for females versus 47.18% for males. Chi-square analyses show that the difference between males (47.18%) and females (52.82%) is not statistically significant (*Table 2*). Males and females were equally represented in the western Mediterranean population of *S. mantis*.

Table 1. *Sex, mean total length (cm), carapace length (cm) and weight (g) of Squilla mantis from the Mediterranean Sea-Western Basin*

Sex	Total length (cm) (min-max)	Carapace length (cm) (min-max)	Telson length (cm) (min-max)	Weigth (g) (min-max)
Male N= 422	13.71±0.24 (9.5-17.3)	3.26±0.0.6 (2.35-4.15)	2.42±0.05 (1.6-3.1)	31.56±1.57 (8.88-61.56)
Female N= 490	13.28±0.2 (9.5-16.3)	3.08±0.05 (2.25-3.8)	2.30±0.04 (1.6-2.9)	26.98±1.16 (9.68-50.5)
Total N = 1064	13.39±0.16 (6-18.5)	2.99±0.04 (2.35-4.5)	2.35±0.03 (1.6-3.1)	29.18±0.99 (8.88-61.56)

Table 2. *Statistical tests applied on the different measurements of S.mantis*

Male vs Female	Total length (cm)	Carapace length (cm)	Telson length (cm)	Weigth (g)
Levene's Test for Equality of Variances	P=0.37	P=0.01	P=0.013	P=0.02
t test for independent samples	P=0.0052	$P=10^{-6}$	$P=6.3\times10^{-5}$	$P=3\times10^{-6}$
Kolmogorov-Smirnov normality test	P_{male}=0.119 P_{female}=0.087	P_{male}=0.1 P_{female}=0.092	P_{male}=0.113 P_{female}=0.089	P_{male}=0.052 P_{female}=0.06
Chi-squared test for sex ratio (*F*/*M*)	P=0.07			

Significant difference marked at $P<0.05$. For the Kolmogorov-Smirnov test, the normality of the distribution is accepted at $P>0.05$

Levene's test of homogeneity of variances, applied between males and females indicates a non-significant difference for total length. However, this same test asserts a heterogeneity of variances for cephalothoracic length, telson length and weight (*Table 2*). The Kolmogorov-Smirnov normality test shows that the different distributions of size and weight follow a normal distribution. The *t*-test for independent samples shows a significant difference in the growth of male and female *S. mantis* (*Table 2*), which suggests a sex-dependent growth study.

Linear growth estimation

Figure 4 shows the frequency-size distributions of the sample. The decomposition of these distributions with Bhattacharya's logarithmic difference method, revealed four age groups of 0^+-3 years for the different measurements *Lt*, *Lc*, *Ltel* (*Fig. 4* and *Fig. 5*).

http://www.aloki.hu ● ISSN 1589 1623 (Print) ● ISSN 1785 0037 (Online)
DOI: http://dx.doi.org/10.15666/aeer/1906_50835101

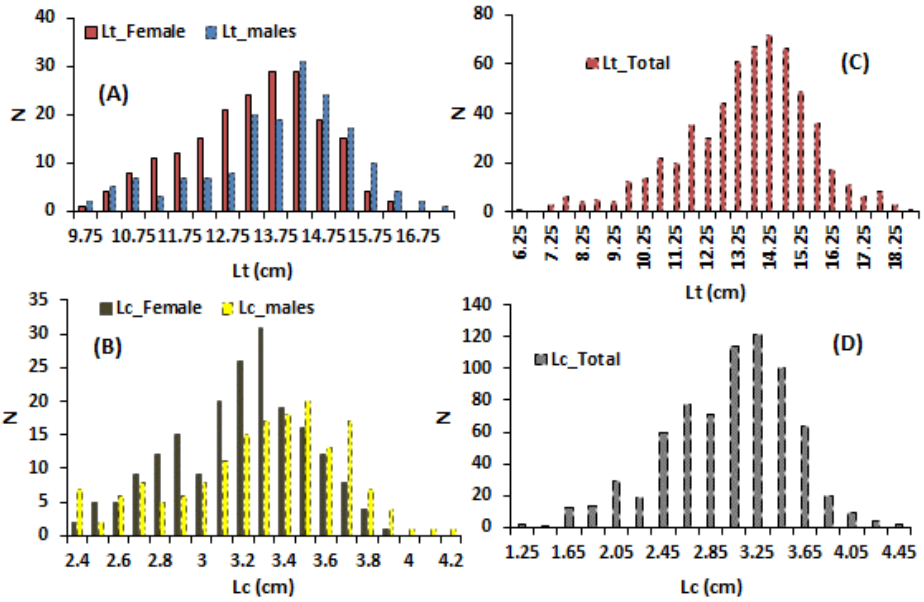

Figure 4. *Length frequency distribution for males and females of S. mantis, (A): Total length for male and female, (B): Carapace length for male and female, (C): Total length for both sex, (D): Carapace length for both sex*

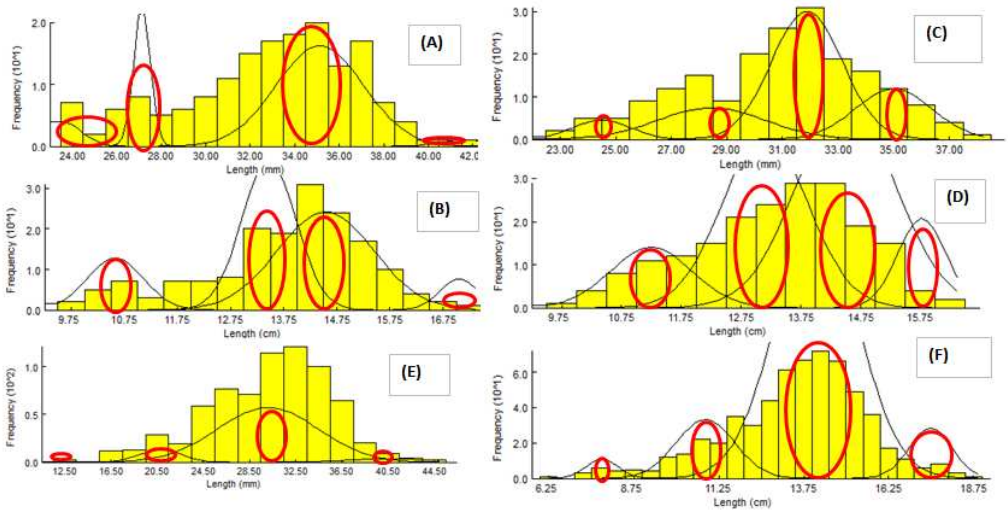

Figure 5. *Decomposition of length frequency structures by the Bhattacharya's method in FISAT II. (A): Carapace length for male. (B): Total length for male. (C): Carapace length for females. (D): Total length for females. (E): Carapace length for both sex. (F): Total length for both sex. The red circles represent the age groups*

These results indicate that *S. mantis* can be considered a fast growing species. The fastest growth occurs mostly in the age interval 0-1.

Bhattacharya's method consists of separating normal components, each representing a cohort of *S. mantis*, from the overall distribution, starting from a left side (*Fig. 4*). *Fig. 5* shows different multimodal distributions with several peaks that can be divided

http://www.aloki.hu ● ISSN 1589 1623 (Print) ● ISSN 1785 0037 (Online)
DOI: http://dx.doi.org/10.15666/aeer/1906_50835101

into four subsamples. These distributions result from a length frequency table with a step of 0.1 cm for cephalothoracic lengths and 0.5 cm for total lengths.

For mean male sizes of 13.71±0.24, 3.26±0.06 and for mean female sizes of 13.28±0.2, 3.08±0.05; the method of Powell (1979); Wetherall (1986) allowed to estimate asymptotic lengths for males and females: 18.25 cm, 39.40 mm, 18.56 cm, 42.50 cm, respectively for total and cephalothorax lengths. The calculated asymptotic lengths are consistent with the differences in growth observed between males and females of *S. mantis* in the Algerian region, i.e. males show a slightly faster growth than females in this bay (*Table 3*). The coefficients of catabolism *K* estimated from total and cephalothorax length are very close to each other, with a slight difference in favor of females, and a slight underestimation when sex is taken together. Calculation of the performance index Ø' gives an overall view on the rapid growth of *S. mantis* (2.36-3.06); highly similar for both sexes (*Table 3*). The growth equations as a function of *Lt* and *Lc* are: $Lt = 18.25\,(1 - e^{-0.69\,(t+0.56)})$, $Lc = 39.40\,(1 - e^{-0.71\,(t+0.51)})$ for females $Lt = 18.56\,(1 - e^{-0.67\,(t+0.57)})$, $Lc = 45.50\,(1 - e^{-0.64\,(t+0.53)})$ for males, $\mathrm{Lt} = 18.99\,(1 - e^{-0.48(t+0.66)})$, $\mathrm{Lc} = 48.06\,(1 - e^{-0.34(t+0.69)})$ for all sexes combined.

Table 3. *Growth parameters obtained for the mantis shrimp S. mantis from the western Mediterranean basin*

Sex	Length measurements (cm)	L_∞ (Powell, 1979; Wetherall, 1986)	K (year-1) (Tomlinson and Abramson, 1961)	t_0 (Pauly, 1980)	Ø'
Male N= 422	Lt (cm)	18.25	0.69	-0.56	2.36
	Lc (mm)	39.40	0.71	-0.51	3.04
Female N= 490	Lt (cm)	18.56	0.67	-0.57	2.36
	Lc (mm)	42.50	0.64	-0.53	3.06
Total N = 1064	Lt (cm)	18.99	0.48	-0.66	2.24
	Lc (mm)	48.06	0.34	-0.69	2.9

The age-length key developed for the mantis shrimp *S. mantis* highlighted age groups ranging from 0^+ to 3 regardless of the length used (*Lt* or *Lc*) (*Table 4*). Bhattacharya's multimodal decomposition led to mean lengths of 13.91 cm, 31.88 mm for males and 13.67 cm, 29.96 mm for females; 12.57 cm, 25.76 mm for all sexes combined; which is very close to the means actually sampled in the population.

RMSE values are expressed as the percentage of the mean observed in each sampled length to give more meaning to this statistical estimator. For males, the overall variance of the Von Bertalanffy model was 17.77% for “total length” and 18.70% based on “cephalothorax length”; this means that the two growth models estimated for males explained 82.23%, 81.3% of the observations. The RMSE for females was 20.57%, 21.47%, based on “total” and “cephalothorax length”. For all sexes combined, the growth model developed performed well, explaining 87.06%, 87.29% of the average observations. The calculated growth rate indicates rapid growth during early stages, followed by slower growth as the species approaches L_∞. The two growth rates estimated for Bhattacharya's age-length key and from Von Bertalanffy's growth equation (Eq.1), show a divergence for the early age groups, suggesting that the size range is not fully sampled due to gear selectivity.

http://www.aloki.hu ● ISSN 1589 1623 (Print) ● ISSN 1785 0037 (Online)
DOI: http://dx.doi.org/10.15666/aeer/1906_50835101

Table 4. *Age-length key, growth rate, root mean square error obtained for the mantis-shrimp S. mantis from the central Algerian region*

Sex	Measurement (cm)	Age group	Bhattacharya	VBGE	RMSE	RMSE/MEAN (%)	Growth rate (Bhattacharya-VBGE)
Male	Lt (cm)	0	10.58	5.89	2.47	17.77	
		1	13.47	12.08			2.89/6.19
		2	14.54	15.24			1.07/3.17
		3	17.05	16.86			2.51/1.62
	Mean		13.91				
	Lc (mm)	0	23.5	12.23	5.96	18.70	
		1	27.14	26.54			3.64/14.31
		2	35.13	34.08			7.99/7.55
		3	41.75	38.06			6.62/3.9
	Mean						
Female	Lt (cm)	0	11.25	5.85	2.81	20.57	
		1	13.15	12.03			1.9/6.18
		2	14.51	15.13			1.36/3.10
		3	15.78	16.69			1.27/1.55
	Mean		13.6725				
	Lc (mm)	0	24.5	11.97	6.43	21.47	
		1	28.45	25.91			3.95/13.94
		2	31.88	32.77			3.43/6.86
		3	35	36.14			3.12/3.37
	Mean		29.9575				
Combined	Lt (cm)	0	7.82	5.16	1.63	12.94	
		1	10.86	10.43			3.04/5.27
		2	14.12	13.69			3.26/3.26
		3	17.48	15.71			3.36/2.02
	Mean		12.57				
	Lc (mm)	0	11.5	10.05	3.27	12.71	
		1	20.81	21.01			9.31/10.96
		2	30.11	28.80			9.3/7.80
		3	40.6	34.35			10.49/5.55
	Mean		25.755				

Biometric relations

From the different measurements, linear relationships were established of the "length-length" and "length-weight" type. *Tables 5* and *6* summarize the equations, the correlation coefficients linking the "length-length" and "length-weight" measurements as well as the different results of the statistical tests applied to each model. These models were obtained using the least squares method which consists of determining the parameters of the intercept and the slope of the regression line so that the sum of the squares of the residual errors is as small as possible.

http://www.aloki.hu ● ISSN 1589 1623 (Print) ● ISSN 1785 0037 (Online)
DOI: http://dx.doi.org/10.15666/aeer/1906_50835101

Table 5. *Length-length relationship parameters obtained for the mantis-shrimp S.mantis from the Algiers region (R 4.0.3)*

Biometric relation	Sex	a	b	Std.Error (a and b)	t value	Pr (>|t|)	R^2	F-Statistic
Ltel=a×Lc+b	Female	0.668 (0.608-0.729)	0.24 (0.058-0.43)	0.03	21.96	$<2\times10^{-16}$ ***	0.715	482.1
				0.09	2.59	0.0102 *		
	Male	0.6716 (0.61-0.735)	0.23 (0.023-0.437)	0.032	21.070	$<2\times10^{-16}$ ***	0.729	444
				0.105	2.194	0.0296		
	Total	0.669 (0.627-0.71)	0.244 (0.11-0.38)	0.02118	31.550	$<2\times10^{-16}$ ***	0.735	995.4
				0.06747	3.611	3.49×10-4 ***		
Lt=a×Ltel+b	Female	4.4774 (4.045-4.91)	2.9731 (1.971-3.974)	0.2193	20.417	$<2\times10^{-16}$ ***	0.684	416.9
				0.5079	5.845	2.05×10^{-8}***		
	Male	4.33 (3.95-4.71)	3.22 (2.29-4.15)	0.1928	22.471	$<2\times10^{-16}$ ***	0.754	504.9
				0.4709	6.831	1.54×10^{-10} ***		
	Total	4.36 (4.08-4.64)	3.19 (2.54-3.86)	0.1416	30.796	$<2\times10^{-16}$ ***	0.73	948.4
				0.3364	9.506	$<2\times10^{-16}$ ***		
Lt=a×Lc+b	Female	3.7953 (3.51-4.077)	1.60 (0.73-2.48)	0.1428	26.573	$<2\times10^{-16}$ ***	0.786	706.1
				0.4417	3.637	3.5×10^{-4} ***		
	Male	3.46 (3.18-3.75)	2.40 (1.47-3.34)	0.1438	24.083	$<2\times10^{-16}$ ***	0.779	580
				0.4729	5.087	9.8×10^{-7} ***		
	Total	3.78 (3.63-3.92)	1.70 (1.26-2.15)	0.07226	52.241	$<2\times10^{-16}$ ***	0.82	2729
				0.22649	7.519	2.05×10^{-13} ***		

Significant codes: 0 '***' 0.001 '**' 0.01 '*' 0.05 '.' 0.1 ' ' 1

The linear biometric relationships (*Table 5*) show a majoring allometry ($a > 1$) for the relationships $Lt=a\times Ltel+b$, $Lt=a\times Lc+b$ and a minoring allometry for relationships of the type $Ltel=a\times Lc+b$ ($a<1$). The *F*-test based on Fisher's statistic shows a very high overall significance of all models ($P_{\_value} <2\times10^{-16}$ and $416.9 \leq F \leq 2729$). Student's *t* test applied on the regression coefficients *a* and *b* (*Table 5*) indicates a high significance of the slope coefficients *a* ($Pr(>|t|) <2\times10^{-16}$), which is significant at the error rate $\alpha = 0.001$. The values of the intercept coefficients *b* are highly significant for all models ($2\times10^{-16} \leq Pr \leq 0.0102$), except for the model $Lt=a\times Lc+b$ established for males ($Pr = 0.0296$) (*Table 5*). The Standard error ranged from 0.03-0.4729, which led to confidence intervals between 0.608-4.71 for the *a* coefficient and between 0.023-3.94 for the *b* coefficient (*Table 5*). This metric of how the values of *a* and those of *b* vary under repeated sampling reflects a very high quality of the fitted "length-length" models for *S. mantis*. The estimated coefficient of determination R^2 for all linear models ranged from 0.684-0.82, showing a high degree of linear independence between "total", "cephalothorax" and "telson length" (*Table 5*). The linear growth model of "telson

http://www.aloki.hu ● ISSN 1589 1623 (Print) ● ISSN 1785 0037 (Online)
DOI: http://dx.doi.org/10.15666/aeer/1906_50835101

length" versus "cephalothorax length" shows slope coefficients *a* less than 1 for both sexes and for the overall population, resulting in a majoring allometry. These results sub-imply that cephalothorax grows faster than telson for *S. mantis* specimens. On the other hand, models that relate "total length" to either "cephalothorax" or "telson" reflect growth with minor allometry ($a < 1$), i.e., "total length" grows faster than both "cephalothorax" and "telson" (*Table 5*). The observed *a*-slope values were compared to the theoretical value of 1 and the difference was statistically significant ($t<1.96$) for all models developed.

Table 6. *Size-weight relationship parameters obtained for the mantis-shrimp S.mantis from the Algiers region (R 4.0.3)*

Biometric relation	Sex	log a	b	Std.Error	t value	Pr (>|t|)	R^2	F-Statistic
Log Wt = log a + b log Lc	F	0.056 (-0.045-0.158)	2.78	0.05153	1.092	0.276	0.79	695.2
				0.10547	26.367	$<2\times10^{-16}$ ***		
	M	0.084 (-0.034-0.204)	2.7 (2.47-2.93)	0.06	1.4	0.163	0.77	529.6
				0.117	23.01	$<2\times10^{-16}$ ***		
	Total	0.075 (0.029-0.12)	2.77 (2.67-2.86)	0.023	3.20	0.00145	0.853	3388
				0.047	58.21	$<2\times10^{-16}$ ***		
Log Wt= log a + b log Ltel	F	0.50 (0.42-0.59)	2.52 (2.29-2.75)	0.04297	11.69	$<2\times10^{-16}$ ***	0.71	453.1
				0.11831	21.29	$<2\times10^{-16}$ ***		
	M	0.51 (0.42-0.61)	2.50 (2.26-2.74)	0.04699	10.95	$<2\times10^{-16}$ ***	0.73	424.3
				0.12123	20.60	$<2\times10^{-16}$ ***		
	Total	0.51 (0.44-0.57)	2.52 (2.35-2.67)	0.031	16.41	$<2\times10^{-16}$ ***	0.73	937.6
				0.082	30.62	$<2\times10^{-16}$ ***		
Log Wt= log a+ b log Lt	F	-1.83 (-2.05,-1.62)	2.89 (2.7-3.079)	0.10781	-17	$<2\times10^{-16}$ ***	0.83	905.6
				0.09602	30.09	$<2\times10^{-16}$ ***		
	M	-2.16 (-2.31,-2.003)	3.19 (3.06-3.33)	0.07811	-27.62	$<2\times10^{-16}$ ***	0.93	2163
				0.06865	46.51	$<2\times10^{-16}$ ***		
	Total	-1.92 (-1.99,-1.84)	2.97 (2.91-3.05)	0.03962	-48.50	$<2\times10^{-16}$ ***	0.92	7132
				0.03524	84.45	$<2\times10^{-16}$ ***		

Significant codes: 0 '***' 0.001 '**' 0.01 '*' 0.05 '.' 0.1 ' ' 1

Log transformation of the data for the length-weight relationships linearizes the relationship and erases problems of heteroscedasticity (*Table 6*). Fisher's *F* statistic applied on the "log-log" models shows a very high overall significance of the models with varying values between 424.3-7132 and a $P_{\_value} <2.2\times10^{-16}$, which is significant at $\alpha = 0.001$. Student's *t*-test shows high significance of the slope coefficients *b* at the 99.9% confidence level ($Pr(>|t|< 2\times10^{-16})$ (*Table 6*). The values of the intercept *a* are significant for all models except for the model log Wt = log a + b log Lc. The value of this parameter for the total weight-cephalothoracic height relationship being: $a = 1$. The standard error calculated for each of the models indicates confidence interval values

http://www.aloki.hu ● ISSN 1589 1623 (Print) ● ISSN 1785 0037 (Online)
DOI: http://dx.doi.org/10.15666/aeer/1906_50835101

ranging from 2.26-3.33 and -2.31-0.57 for the parameters *b* and *log a* respectively (*Table 6*).

The estimated R^2 for each model is very close to 1 (0.71-0.93) indicating a very good fit and a strong linear relationship between the logarithm of weight and the logarithm of length (*Table 6*). The set of tests applied show a very good fit of the length-weight relationships. The slope coefficients *b* of the models of the length-weight relationship indicates a negative allometry ($b < 3$) and a positive allometry for males of the total weight-total length relationship. This results in a relatively lower weight growth than the "total", "cephalothorax" and "telson length" for both sexes and for the whole population. However, *S. mantis* males show faster growth in "total length" than weight ($b > 3$) (*Table 6*). The calculated reduced difference *t*-test indicates a significant difference between the observed slope values and the theoretical value of 3 for the length-weight relationships ($t < 1.96$, $\alpha = 0.05$), except for the two "total length-total weight" relationships for females and combined sex ($t = 1.15$, $0.83 < 1.96$). This result suggests that "total weight" growth is proportional to the cube of "total length" growth for females and for the sex-mixed *S. mantis* population (isometry).

Mortality

The instantaneous total mortality coefficient (*Z*) for *S. mantis* was 1.32/year. According to Pauly (1983) (*Eq. 3*), natural mortality (*M*) was calculated as 0.95/year using $L_\infty = 18.99$ cm and $K = 0.48$ yr^{-1} and a water temperature (*T*°) of 15.3°C (Shaltout and Omstedt, 2014). Fishing mortality (*F*) was 0.37/year (*Fig. 6*). Exploitation rate (*E*) indicates whether a stock is overfished based on the fishing mortality rate (*F*), while assuming that the optimal value of *E* is approximately equal to 0.5 (Gulland, 1971). The value of *E* obtained in the present study (0.28) was lower than the optimal value, which is in line with the catches actually observed in the field (under-exploited stock).

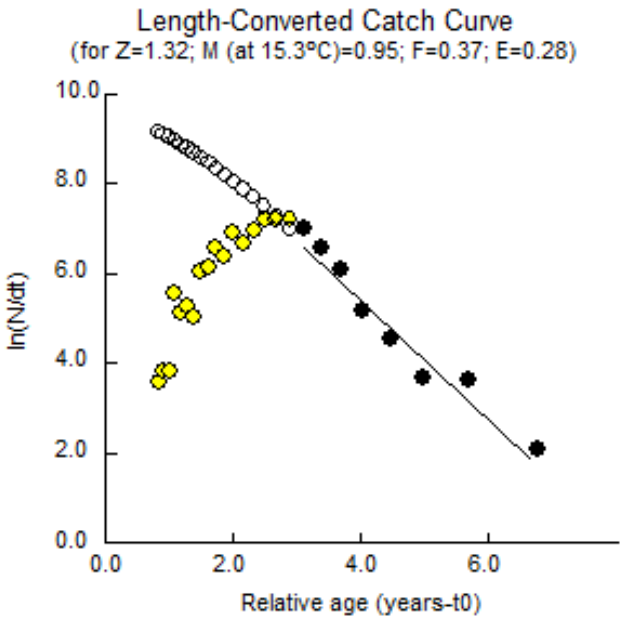

Figure 6. *Length-converted catch curve of mantis shrimp from the Mediterranean-Western basin. (Yellow represents points on the ascending part of the catch curve that were not included in the regression analysis to estimate total mortality Z. The black dots represent the descenting part used in the estimation of Z.)*

http://www.aloki.hu ● ISSN 1589 1623 (Print) ● ISSN 1785 0037 (Online)
DOI: http://dx.doi.org/10.15666/aeer/1906_50835101

Discussion

The average lengths obtained by the different measurements considered as well as the average total weight are compared with the results of other authors. The average total length (*Lt*) of males (13.7 cm) is the same as that obtained by Ragonese et al. (2012) and is very close to that observed by Mili et al. (2013) in the Tunis area (13.92 cm). For females, the average cephalothoracic length (*Lc*) (3.08 cm) is comparable with those of Mili et al. (2013) in the Gabes area (3.089 cm) (*Table 1*). The average total weight (29.18 g) remains between the values of Erdoğan Sağlam et al. (2017): 22.14 g and Torres et al. (2017): 35.3 g.

For each growth parameter (L_∞, K, and t_0) obtained, the calculation was performed using "total length" and "cephalothoracic length". The asymptotic "total length" of females (18.25 cm) is lower than those of other Mediterranean authors, whereas for males this parameter is very close to that found by Erdoğan Sağlam et al. (2017). The asymptotic "cephalothoracic" length of females (39.4 cm) is identical to that obtained by Abelló and Martín (1993) (*Table 7*). For all sexes combined, the present results of growth parameters are very similar than those noted by Erdoğan Sağlam et al. (2017) and Ragonese et al. (2012) (*Table 7*). The coefficients of catabolism K estimated from "total" and "cephalothoracic lengths" are very similar, with a slight difference in favor of females. These estimated coefficients are consistent with the more or less low longevity character of the squilla *S. mantis* (Maynou et al., 2004).

Table 7. *Growth parameters obtained by different authors in the Mediterranean Sea*

Authors	Region	Length measurment	Sexe	N	L_∞(mm)	K (y^{-1})	t_0 (y)	Ø'
Froglia (1996)	Central Adriatic Sea	Lc	*F*		41.88	0.448	-0.038	2.90
			M		41.18	0.532	-0.059	2.96
			F+M		41.53	0.49	-0.010	2.93
Righini & Baino (1996)	Ligurian Sea	Lt	*F*		220	1.45		4.85
			M		225	1.3		4.82
Ragonese et al (2012)	Southern coasts of Sicily	Lt	*F+M*	484	190	0.41	-0.52	4.17
Mili et al. 2013	Gulf of Tunis	Lt	*F*	1564	179.1	1.44	-0.57	4.66
			M	1726	188.3	1.400	-0.39	4.70
	Gulf of Hammamet		*F*	1404	187.1	1.430	-0.24	4.70
			M	1620	198.2	1.330	-0.26	4.72
	Gulf of Gabes		*F*	7799	188.4	1.560	-0.31	4.74
			M	8770	204.6	1.330	-0.3	4.75
Erdogan Saglam et al. (2017)	Izmir Bay (Aegean Sea)	Lt	*F*	549	192.8	0.510	-0.36	4.28
			M	387	183.43	0.420	-0.45	4.15
			F+M	936	196.9	0.500	-0.37	4.29
		Lc	*F*	549	46.3			
			M	387	45.7			
			F+M	936	47.4			
Present study	Algiers region (SW Medit.)	Lt	*F*	490	182.5	0.69	-0.56	4.36
			M	422	185.6	0.67	-0.57	4.36
			F+M	1064	189.9	0.48	-0.66	4.24
		Lc	*F*	490	39.40	0.71	-0.51	3.04
			M	422	42.50	0.64	-0.53	3.06
			F+M	1064	48.06	0.34	-0.69	2.90

http://www.aloki.hu ● ISSN 1589 1623 (Print) ● ISSN 1785 0037 (Online)
DOI: http://dx.doi.org/10.15666/aeer/1906_50835101

The determination of the age-length key, established from the method of Bhattacharya (1967) and the Von Bertalanffy curve (*Eq. 1*), has given satisfactory results. Indeed, between three and four age classes are observed in most Mediterranean authors (*Figs. 4,5*); the studies carried out in the Bay of Cadiz (northeastern Atlantic Ocean), based on the length of the carapace, have determined two age groups in females and males (Vila et al., 2013); this same result was also observed by Mili et al. (2013) on the Tunisian coast. On the southern coasts of Sicily, three age groups are observed (1-3) (Ragonese et al., 2012). Erdoğan Sağlam et al. (2017) note four age groups in Izmir Bay (Aegean Sea), a result similar to this work (*Figs. 4,5*). The differences found with previous authors may be due to the methods used for size structure decomposition or simply the vagaries of sampling. The difference between the study areas where the samples were taken could be the first source of variability in the results.

The length versus age correspondence presented by Bhattacharya's method of total length in males and females shows very similar lengths with Ragonese et al. (2012) and the same size of 15.7 cm obtained at age 3 in females with Erdoğan Sağlam et al. (2017) (*Table 4*).

The growth parameters given by this study are very comparable with other Mediterranean research (*Table 7*). Indeed, Mili et al. (2013) presented very similar values in the Gulf of Tunis, Hammamet and Gabes. This emphasizes the current results given the proximity of the two study regions. For all sexes, the asymptotic total length is identical to that found by Ragonese et al. (2012). As for the results based on "cephalothorax length", the asymptotic length of males (Lc_∞) is close to that obtained by Froglia (1996) in the central Adriatic Sea. The growth rate K is between 0.41/year and 1.56/year for *S. mantis*, the results obtained in this study are within this range except for both sexes combined considering "cephalothorax length" (0.34/year) (*Table 7*).

This difference found with other authors who determined the growth parameters of *S. mantis* can likely be attributed to the environmental conditions (temperature, salinity, nutrients) or to the fishing pressure exerted on the stock of this species which differs according to the region. According to the growth performance estimated in this study (*Table 7*), the values of Ø' are greater in the Ligurian Sea (Righini and Baino, 1996) and in the Gulfs of Tunis, Hammamet, and Gabes (Mili et al., 2013) but are highly similar compared to those in the central Adriatic Sea and Izmir Bay (Froglia, 1996; Erdoğan Sağlam et al., 2017) (*Table 7*).

Concerning the biometric relationships, the "length-length" relationships are strong (R^2 = 0.68-0.82), with a slope a for both sexes between 0.67 and 4.88: for females ($0.67 < a < 4.88$) and males ($0.67 < a < 4.33$) indicating a growth with minoring allometry ($a < 1$) for telson size versus cephalothorax. A growth with majoring allometry ($a > 1$) was recorded for the "total-length-cephalothorax" and "total-length-telson" relationships for both sexes, reflecting a higher total growth than both sizes; cephalothorax and that of telson (*Table 5*). As for the "total weight-cephalothorax length", "total weight-telson length" and "total weight-total length" relationships, the coefficient of determination R^2 is very high (0.71-0.93), reflecting a strong body response of weight to length changes in the *S. mantis* population (*Table 6*). Erdoğan Sağlam et al. (2017) found isometry in the "total length-weight" relationship for males and females, with slope values equal to 2.95 and 3.02, respectively, reflecting isometry (*Table 8*).

The "length-length" relationship (*Lt-Lc*) gives values close to those of Mili et al. (2008) in the Gabes region (*Table 8*). This author is the only one who considered the

http://www.aloki.hu ● ISSN 1589 1623 (Print) ● ISSN 1785 0037 (Online)
DOI: http://dx.doi.org/10.15666/aeer/1906_50835101

length of the telson and their results are very comparable to this study (*Tables 5,8*). Indeed, the calculated *Ltel-Lc* relationship gives an "*a*" in males and females (0.67 and 0.66, respectively) close to the one obtained by Mili et al (2008) in Gabes (0.73 and 0.70). The "length-weight" relationship (*Wt-Lt*) of our results, showing an isometry between length growth and weight growth, are also very comparable to those of Ragonese et al. (2012) and Erdoğan Sağlam et al. (2017) for females, males and for both sexes combined. As for the *Wt-Lc* relationship, the results are supported by those reported by Righini and Baino (1996), Abelló (1989), Mili et al. (2008) (Hammamet), Vila et al. (2013) and Erdoğan Sağlam et al. (2017).

Table 8. *Length-weight and length-length relationship parameters obtained by different authors in the Mediterranean*

Authors	Region	Relation	Male		Female		Combined	
			a	b	a	b	a	b
Giovanardi and Piccinetti Manfrin (1984)	Adriatic Sea	Lc-Wt	0.0116	3.0431	0.0138	2.9168		
Abello and Sarda (1989)	Ebro delta (NW Mediterranean	Lc-Wt	0.0026	2.8305	0.0020	2.9026		
		Lc-Lt	0.7637	0.8937	0.6164	0.9523		
Froglia (1996)	Adriatic Sea	Lc-Wt	0.0014	3.0425	0.0014	3.0419		
Righini and Baino (1996)	Ligurian Sea	Lc-Wt	0.0356	2.6100	0.0526	2.4100		
Mili et al.(2008)	Tunisian water (Tunis)	Ltel-Lc	0.786	1.0135	0.8592	0.99	0.821	1.0021
		Lc-Lt	5.4649	0.9374	4.8955	0.9712	5.2613	0.9526
		Lc-Wt	0.0008	3.026	0.0006	3.11	0.0007	3.0673
	Tunisian water (Hammamet)	Ltel-Lc	0.9387	0.9644	0.9168	0.972	0.9269	0.9684
		Lc-Lt	5.5116	0.9389	5.1155	0.6909	5.299	0.9505
		Lc-Wt	0.0013	2.8864	0.0011	2.9165	0.0012	2.9019
	Tunisian water (Gabes)	Ltel-Lc	0.7302	1.0414	0.7087	1.0624	0.7211	1.0461
		Lc-Lt	4.9131	0.9776	4.494	1.0553	4.7074	0.9909
		Lc-Wt	0.0006	3.1279	0.0006	3.1555	0.0006	3.1431
Ragonese et al. (2012)	South of Sicily	Lt-Wt	-11.561	3.031	-11.534	3.027		
Vila et al. (2013)	Gulf of Cadiz (E-C Atlantic)	Lc-Lt	6.8589	0.8879	7.2757	0.8766	7.3949	0.8693
		Lc-Wt	0.00677	2.5465	0.004347	2.6725	0.005118	2.6263
Erdogan Saglam et al. (2017)	Izmir Bay	Lc-Lt	0.2317	0.1087	0.2410	0.0117	0.2373	0.0378
		Lc-Wt	0.7733	2.92	0.8670	2.87	0.8046	2.91
		Lt-Wt	0.0111	2.95	0.0098	3.02	0.0098	3.02
Torres et al. (2017)	Gulf of Cadiz	Lc-Wt					1.709	2.842
Kampouris et al. (2018)	Gulf of Thermaikos Aegean Sae	Lc-Wt	2.670	2.737	2.941	3.189	2.881	3.087
Present study	Algiers region (SW Medit.)	Lc-Wt	1.0876	2.7	1.0575	2.78	1.0778	2.77
		Ltel-Wt	1.6652	2.50	1.6487	2.52	1.6652	2.52
		Lt-Wt	0.1153	3.19	0.1604	2.89	0.1466	2.97
		Ltel-Lc	0.67	0.23	0.668	0.24	0.669	0.24
		Ltel- Lt	3.33	3.22	4.477	2.973	4.36	3.19
		Lc-Lt	3.46	2.40	3.795	1.60	3.78	1.70

http://www.aloki.hu ● ISSN 1589 1623 (Print) ● ISSN 1785 0037 (Online)
DOI: http://dx.doi.org/10.15666/aeer/1906_50835101

The calculation of exploitation indices provided insight into the status of the stock. Fishing mortality *F* is 0.95/year, a value very close to that recorded in southern Sicily by Ragonese et al. (2012), but still lower than that found by Erdoğan Sağlam et al. (2017) in Izmir Bay in 2017 (1.16/year). The latter Mediterranean region exploits mantis shrimp weakly with an exploitation rate of 0.39. In the central Algerian region, this exploitation is even lower; *E* is equal to 0.28 because the fishery does not target this species (*Fig. 6*).

Conclusion

This study is the first of its kind to give results on the growth parameters and mortality of *S. mantis* from Algeria. It was based on length-frequency data which can, provide valuable information on the life history of the mantis shrimp in this country.

Overall, the study contributed to the knowledge of the population dynamics of *S. mantis* exploited in the central region of Algeria and provided basic parameters essential for the management of the stock of this species in this area. We showed that the spottail mantis shrimp has a rapid growth in this area and a low longevity. The study of biometric relationships revealed the following findings: a) growth in "total weight" is proportional to the cube of growth in "total length" for females and for the mixed-sex population of *S. mantis* (isometry) and b) growth with a major allometry for males. For growth in length, cephalothorax grows faster than telson for all *S. mantis* specimens and "total length" grows faster than "cephalothorax" and "telson".

This study carried out from the catches of the commercial fishery in the central region of Algeria shows an under-exploitation of the *S. mantis* stock. Nevertheless, the fishing statistics of this species show an evolution of the catches in 2016. This limited fishing pressure may be considered as an important issue to protect the *S. mantis* population in this region. In this study, it is noted that the fishery is carried out by trawls with a large horizontal opening, but it is discarded at sea. In our country, the discarding of this species, which is beginning to attract consumers, represents a loss for the national economy and the regional fishery.

In other countries such as Italy, Spain, France and Slovenia, this species is economically valued. As a result of this study, the population parameters of *S. mantis* are similar to those of the European countries that fish this species economically. It could be exported to European countries or fished as a target species instead of being discarded in Algeria. The lack of knowledge concerning the biology of *S. mantis* is evident and further research is needed. The present study is the first one carried out in Bou-Ismail Bay (central region of Algeria). Future studies should focus more on this species in order to enhance its value.

Acknowledgements. The authors express their thanks to Michael Sievers of Griffith University in Australia for editing the scientific English of this manuscript. Thanks are also expressed to the reviewers for their advice and suggestions.

REFERENCES

[1] Abelló, P., Sardá, F. (1989): Some observations on the biology and fishery of *Squilla mantis* L. in the Catalan area (NW Mediterranean Sea). – Biology of Stomatopods: Selected Symposia and Monographs UZI, 3.- Mucchi: 229-239.

http://www.aloki.hu ● ISSN 1589 1623 (Print) ● ISSN 1785 0037 (Online)
DOI: http://dx.doi.org/10.15666/aeer/1906_50835101

[2] Abelló, P., Martín, P. (1993): Fishery dynamics of the mantis shrimp *Squilla mantis* (Crustacea: Stomatopoda) population off the Ebro delta (northwestern Mediterranean). – Fisheries Research 16: 131-145.
[3] Beverton, R. J., Holt, S. J. (2012): On the dynamics of exploited fish populations. – Springer Science and Business Media.
[4] Bhattacharya, C. G. (1967): A simple method of resolution of a distribution into Gaussian components. – Biometrics 23(1): 115-135.
[5] Campilo, A. (1982): Algerie 82 (THALASSA) cruise. – Thalassa R/V.
[6] Derbal, F., Kara, M. (2006): Données préliminaires sur la biologie de la crevette *Plesionika edwardsii* (Crustacea, Pandalidae) du golfe d'Annaba (Algérie, est). – Bull. INSTM, NS (9) - Actes des 7èmes Journées de L'ATSMer, Zarzis, Tunisie.
[7] Derbal, F., Soltani, N. (2008): Cycle cuticulaire et variations de la protéinémie et de la lipémie chez la crevette royale *Penaeus kerathurus* (Forskal, 1775) des côtes Est algériennes. Sciences and Technologie. – Biotechnologies, pp. 80-86.
[8] Erdoğan Sağlam, N., Demir Sağlam, Y., Sağlam, C. (2017): A study on some population parameters of mantis shrimp (*Squilla mantis* L., 1758) in Izmir Bay (Aegean Sea). – Journal of the Marine Biological Association of the United Kingdom 98: 721-726.
[9] Froglia, C. (1996): Growth and behaviour of *Squilla mantis* (mantis shrimp) in the Adriatic Sea. – EU Study DG XIV. MED/93/016, Final Report.
[10] Gayanilo, J., Sparre, P., Pauly, D. (2002): FAO–ICLARM fish stock assessment tools (FiSAT II): user's manual. – Rome: International Center for Living Aquatic Resources Management and Food and Agriculture Organization of the United Nations.
[11] Giovanardi, C., Piccinetti-Manfrin, G. (1984): Summary of biological parameters of *Squilla mantis* L. in the Adriatic Sea. – FAO Fish. Rep 290: 131-134.
[12] Gulland, J. (1971): The fish resources of the ocean. – West Byfleet, Surrey. Fishing News (Books), Ltd., for FAO, 255.
[13] Holthuis, L. (1987): Stomatopodes. Fiches FAO d'identification des espèces pour les besoins de la pêche. – Méditerranée et Mer Noire 1: 181-187.
[14] Kampouris, T. E., Kouroupakis, E., Lazaridou, M., Batjakas, I. E. (2018): Length-weight relationships of *Squilla mantis* (Linnaeus, 1758) (Crustacea, Stomatopoda, Squillidae) from Thermaikos Gulf, North-West Aegean Sea, Greece. – International Journal of Fisheries and Aquatic Studies 6: 241-246.
[15] Kennouche, H. (2009): Biologie, ecologie et exploitation de la crevette rouge *Aristeus antennatus* dans la région d'Alger. – Thesis USTHB, 87p.
[16] King, M. (2013): Fisheries biology, assessment and management. – John Wiley & Sons.
[17] Manning, R. B. (1977): A monograph of the West African stomatopod Crustacea. – Scandinavian Science Press.
[18] Masson, J. (1970): Estimation des paramètres d'un mélange de distributions gaussiennes. – Station.
[19] Maynou, F., Abelló, P., Sartor, P. (2004): A review of the fisheries biology of the mantis shrimp, *Squilla mantis* (L., 1758) (Stomatopoda, Squillidae) in the Mediterranean. – Crustaceana: 1081-1099.
[20] MFFP. (2021): Regional report on fishing statistics in the central region of Algeria. – Ministry of Fisheries and Fisheries Production, Algiers.
[21] Mili, S., Jarboui, O., Missaoui, H. (2008): Caractères biométriques de la squille *Squilla mantis* dans les eaux tunisiennes. – Bulletin de l'institut national des sciences et technologies de la mer Salommbo 35: 1-14.
[22] Mili, S., Bouriga, N., Missaoui, H., Jarboui, O. (2011): Morphometric, reproductive parameters and seasonal variations in fatty acid composition of the mantis shrimp *Squilla mantis* (Crustacea: Stomatopoda) in the Gulf of Gabes (Tunisia). – Journal of Life Sciences 5: 1058-1071.
[23] Mili, S. (2013): La squille *Squilla mantis* des eaux tunisiennes: eco-biologie, pêche et opportunités de valorisation. – Thesis, Institut national agronomique de Tunis, 196p.

http://www.aloki.hu ● ISSN 1589 1623 (Print) ● ISSN 1785 0037 (Online)
DOI: http://dx.doi.org/10.15666/aeer/1906_50835101

[24] Mili, S., Ennouri, R., Jarboui, O., Missawi, H. (2013): Premiere approche de la croissance de la squille *Squilla mantis* (*L.*, 1758) dans les eaux tunisienneas. – Bulletin de l'institut national des sciences et technologies de la mer Salommbo 40: 27-42.
[25] Mili, S., Ennouri, R., Jarboui, O., Missaoui, H. (2014): Étude de la biologie de reproduction chez la squille ocellée *Squilla mantis* pêchée dans trois golfes tunisiens: Tunis, Hammamet et Gabès. – Bulletin de Société zoologique de France 139: 215-232.
[26] Moreau, J., Bambino, C., Pauly, D. (1986): A comparison of four indices of overal fish growth performance, based on 100 tilapia population (Cichlidae): 201-206. – In: Maclean, J. L., Dizon, L. B., Hosillo, L. V. (eds.) The first Asian fisheries forum. Asian Fisheries Society, Manilla, Philippines.
[27] Mouffok, S., Kherraz, A., Bouras, D., Bennoui, A., Boutiba, Z. (2005): Premières observations biologiques de la crevette profonde *Aristeus antennatus* (Decapoda: Aristeidae) exploitée le long du littoral occidental algérien (Méditérannée du sud-ouest). – Editorial Advisory Board E: 817.
[28] Mouffok, S., Massuti, E., Boutiba, Z., Guijarro, B., Ordines, F., Fliti, K. (2008): Ecology and fishery of the deep-water shrimp, *Aristeus antennatus* (Risso, 1816) off Algeria (South-western Mediterranean). – Crustaceana 81(10): 1177-1199.
[29] Nouar, A., Kennouche, H. (2013): Régime alimentaire de la crevette rouge *Aristeus antennatus* (Risso, 1816) (Decapoda, Penaeoidea) dans la région algéroise (Algérie centre). – Crustaceana 86: 553-563.
[30] Pauly, D. (1980): On the interrelationships between natural mortality, growth parameters, and mean environmental temperature in 175 fish stocks. – ICES Journal of Marine Science 39: 175-192.
[31] Pauly, D. (1983): Some simple methods for the assessment of tropical fish stocks. – FAO, Fishery Technics Reports 234, 52p.
[32] Powell, D. (1979): Estimation of mortality and growth parameters from the length frequency of a catch [model]. – Rapports et Proces-Verbaux des Reunions (Denmark).
[33] R Core Team (2020): R: A language and environment for statistical computing. – R Foundation for Statistical Computing, Vienna, Austria. URL http://www.R-project.org/.
[34] Ragonese, S., Morara, U., Canali, E., Pagliarino, E., Bianchini, M. L. (2012): Abundance and biological traits of the spottail mantis shrimp, *Squilla mantis* (L., 1758) (Crustacea: Stomatopoda), off the southern coast of Sicily. – Cahiers de Biologie Marine 53: 485.
[35] Ricker, W. E. (1975): Computation and interpretation of biological statistics of fish populations. – Bulletin of Fisheries Research 191: 1-382.
[36] Righini, P., Baino, R. (1996): Parametri popolazionistici della pannocchia (Squilla mantis, Crustacea, Stomatopoda). – Biologia Marina Mediterranea 3: 565-566.
[37] Schram, F. R., Muller, H. G. (2004): Catalog and bibliography of the fossil and Recent Stomatopoda. – Backhuys, 264p.
[38] Shaltout, M., Omstedt, A. (2014): Recent sea surface temperature trends and future scenarios for the Mediterranean Sea. – Oceanologia 56: 411-443.
[39] Sparre, P., Venema, C. S. (1992): Introduction to tropical fish stock assessment. – Part. 1 Manual, FAO.
[40] Tomlinson, P. K., Abramson, N. J. (1961): Fitting a von Bertalanffy growth curve by least squares. – Fisheries Bulletin 116: 3-69.
[41] Torres, M. A., Vila, Y., Silva, L., Acosta, J. J., Ramos, F., Palomares, M. L. D., Sobrino, I. (2017): Length–weight relationships for 22 crustaceans and cephalopods from the Gulf of Cadiz (SW Spain). – Aquatic Living Resources 30: 12.
[42] Vasconcelos, P., Carvalho, A. N., Pilo, D., Gaspar, M. B., Cristo, M. (2017): First record of the spottail mantis shrimp, *Squilla mantis* (Stomatopoda, Squillidae), in the Ria Formosa lagoon (Algarve coast, southern Portugal). – Crustaceana 90: 1665-1671.
[43] Veneroni, B., Fernandes, P. G. (2021): Fishers' knowledge detects ecological decay in the Mediterranean Sea. – Ambio 50: 1159-1171.

http://www.aloki.hu ● ISSN 1589 1623 (Print) ● ISSN 1785 0037 (Online)
DOI: http://dx.doi.org/10.15666/aeer/1906_50835101

[44] Vila, Y., Sobrino, I., Jiménez, M. P. (2013): Fishery and life history of spot-tail mantis shrimp, Squilla mantis (Crustacea: Stomatopoda), in the Gulf of Cadiz (eastern central Atlantic). – Scientia Marina 77: 137-148.
[45] Wetherall, J. (1986): A new method for estimating growth and mortality parameters from length frequency data. – Fishbyte 4: 12-14.

http://www.aloki.hu ● ISSN 1589 1623 (Print) ● ISSN 1785 0037 (Online)
DOI: http://dx.doi.org/10.15666/aeer/1906_50835101

EFFECTS OF CADMIUM EXPOSURE ON PROXIMATE ANALYSIS AND METALLIC ELEMENT CONTENTS OF WEDGE CLAM (*DONAX TRUNCULUS*)

KROINI, H.[1] – HAMDANI, A.[1*] – SOLTANI, N.[1] – ZAIDI, N.[2] – SLEIMI, N.[3]

[1]*Laboratory of Applied Animal Biology, Faculty of Sciences, Department of Biology, Badji Mokhtar University, 23000 Annaba, Algeria*

[2]*Laboratory for the Optimization of Agricultural in Subhumid Areas, Department of Natural and Life Sciences, Faculty of Sciences, University of Skikda, 21000 Skikda, Algeria*

[3]*Laboratory RME-Resources, Materials and Ecosystems, Faculty of Sciences of Bizerte, University of Carthage, Carthage, Tunisia*

**Corresponding author*
e-mail: a_hamdaniamel@yahoo.fr; phone: +213-55-786-3661

(Received 6th Aug 2021; accepted 28th Oct 2021)

Abstract. The present study was designed to investigate the proximate (moisture, dry matter, ash, and fat content) composition and metallic element contents (Ca, Zn, Fe, and Cd) in an edible Bivalve, *Donax trunculus* from the gulf of Annaba, and to evaluate the effect of cadmium (Cd) on these parameters. The clams were collected from the El-Battah site during the morphologically ripe and reared stages under laboratory conditions. Physicochemical parameters of seawater samples including temperature, pH, salinity, and dissolved oxygen were determined. Cadmium at two sub-lethal concentrations (LC_{10} and LC_{25}-96h as determined previously) was added to the rearing water. The results revealed significant effects of Cd concentrations, exposure time, and sex on all the studied parameters. Indeed, the contents of dry matter, fat and metallic elements, excluding Cd were significantly decreased, while the moisture, ash, and Cd contents were significantly increased in both sexes at two sub-lethal concentrations. Moreover, the measurement of proximate composition and minerals contents in *D. trunculus* could be a very useful approach to evaluate the nutritive value changes in case of exposure to cadmium contamination, and subsequently to avoid health-associated problems.
Keywords: *pollution, mollusk, heavy metals, acute toxicity, bioindicator, seafood, nutritive value*

Introduction

Heavy metals are one of the major persistent wastewater pollutants, non-biodegradable and naturally toxic within a short period (Zhang et al., 2016). Recently, a great concern has been raised for the impact of heavy metals on the environment (Bankaji et al., 2019; Sall et al., 2020; Sleimi et al., 2021). Indeed, marine ecosystems are vulnerable to trace element contamination posing a considerable hazard to the environment and human health (Dhinamala et al., 2017; Obaiah et al., 2020). Most seafood products, including Mollusk Bivalves are considered biological indicators of heavy metal pollution through the food web (Tulonenet al., 2006; Vieira et al., 2021). Overall, these mollusks are excellent sources of nutrients due to their high-value in protein contents, low-fat contents and marked contents in essential micronutrients (e.g., vitamins D, A and B, water, and minerals) (Orban et al., 2002; Gil and Gil, 2015; Wright et al., 2018). Further, the proximate composition is a valuable tool to identify the quality of meat and to understand the nutritive value changes (Margret, 2015; Ogidi et al., 2020). Besides, some metals like calcium (Ca), Zinc (Zn), iron (Fe) required in

http://www.aloki.hu ● ISSN 1589 1623 (Print) ● ISSN 1785 0037 (Online)
DOI: http://dx.doi.org/10.15666/aeer/1906_51035128

minute quantities for the organisms' metabolism and growth are referred to as essential metallic elements (Yusoff and Long, 2011; Hossen et al., 2015). These essential metallic elements are important components for hormones, activators of enzymes, and are effectively involved in various oxidation-reduction reactions (Khan, 1992; Wright et al., 2018), and the process of muscle contraction, nerve conductance, and energy production (Margret et al., 2013). In addition, these metallic elements (ME) become toxic to organisms at concentrations exceeding the recommended limits (Beldi et al., 2006), meanwhile certain other metallic elements like Cd are not essential for any biological process in the organism, and become toxic even at low concentrations (Astudillo et al., 2005). According to the United States, Environmental Protection Agency (U.S. EPA), and the International Agency for Research on Cancer (IARC), Cd ranks among the highly hazardous metals for the public health. Also, it is reported to induce the generation of free radicals causing chronic oxidative kidney damages and cancers (Salama and Radwan, 2005; Obaiah, 2020). In this context, the assessment of trace element contents in seafood is an important step in ensuring food safety for the sake of human health.

Donax trunculus, an edible Mollusk Bivalve, is a suitable species for the aquatic environment biomonitoring, and also successfully used as a bioindicator to monitor seawater quality worldwide (Künili et al., 2020; Costa et al., 2021; Patino et al., 2021). This wedge clam is chosen as sentinel species due to their typical properties, including life traits, wide geographical distribution, suitable size, facility of collection, transplantation and maintenance in the laboratory, in addition to their ability to concentrate pollutants (Tlili and Mouneyrac, 2019; Hamdani et al., 2020). In the gulf of Annaba (Northeast Algeria), *D. trunculus* is the most widely distributed bivalve in sand beaches (Beldi et al., 2006; Hafsaoui et al., 2016), and the most consumed by the local population (Merad et al., 2017). Thus, *D. trunculus* can be mainly targeted by several environmental pollutants from different sources including heavy metals, in particular, Cd that has been found in tissues of *D. trunculus* and sediments (Beldi et al., 2006; Drif et al., 2010; Amira et al., 2018). The research investigating the sub-lethal Cd exposure was performed in order to understand the toxic effects other than lethal effects, which are usually expressed by the real environmental pollution states (Mouabad, 1991; Dutta et al., 2017).

Previous studies conducted in the gulf of Annaba have investigated the sub-lethal toxic effects of LC_{10} and LC_{25}-96h of Cd on *D. trunculus* on the contents of metallothioneins (Mts) (Merad et al., 2015; Rabei et al., 2018), protein carbonyls (Pc) (Merad et al., 2016), omega-3 fatty acids (Merad et al., 2017) and nucleic acid (Merad and Soltani, 2015), and the biochemical components of gonads (Merad and Soltani, 2017). So, the essential previous results showed a significant reduction in the main essential omega-3 fatty acid (EPA and DHA concentrations), in the level of ARN, in the level of biochemical composition. A significant elevation in the Pc level and MTS level was also detected. The current study, is in continuation to previous studies, was undertaken to assess the sub-lethal Cd exposure (LC_{10} and LC_{25}-96h) on the proximate composition and minerals contents of *D. trunculus* females and males in order to compare the data obtain with previous reports we have chosen to test similar sublethal concentrations. Noteworthy, the nutritive value, considered as an important index for determining the quality of meat and the understanding of the nutritive value changes under metallic contamination, has not been examined until now in the gulf of Annaba.

http://www.aloki.hu ● ISSN 1589 1623 (Print) ● ISSN 1785 0037 (Online)
DOI: http://dx.doi.org/10.15666/aeer/1906_51035128

Review of literature

Our results are original data for proximate composition and minerals contents of an edible mollusk bivalve *D. trunculus* from gulf of Annaba (Algeria). Also, it is the first study to elucidate the toxicity of Cd on proximate and essential metallic elements of *D. trunculus*.

Materials and methods

Animal collection and treatment with sub-lethal concentrations of cadmium

The experiments were performed in March 2019 where the majority of individuals were in the stage of morphologically ripe (Hamdani et al., 2020), and all individuals tested were in the morphologically ripe. The Gulf of Annaba city (northeast Algeria) is surrounded from the East by the Cap Rosa (8°15′ E and 36° 38′ N), and from the West by the Cap Garde (7° 16′ E and 36° 68′ N). *D. trunculus* samples were collected from El Battah beach (36° 50’ N - 7° 50’ E) located approximately 30 km East from Annaba city, and precisely in the eastern area close to the Mafragh estuary characterized by low levels of all nutrients (Ounissi et al., 2014). El Battah site, distant site from any anthropogenic pressures, is subjected to an important hydrodynamic regime, likely contributing to the pollutants dilution (Rabei et al., 2018) (*Fig. 1*). Of note, the suspension feeder bivalve *D. trunculus* is preferentially present between 0 and 2 m in depth in the Mediterranean Sea (Gaspar et al., 2002; La Valle, 2006; Tlili and Mouneyrac, 2019), and hence samples were collected by a hand rake as described elsewhere (Hafsaoui et al., 2016). The experimental animals were brought to the laboratory and macroscopically separated by sex based on the color of gonads (dark blue gonads indicate females, and the yellow-white ones indicate males) according to Gaspar (1999). Further, the rearing was conducted in aquaria taken from the sandy and seawater of the sampling area. During all the experiments, the water was constantly aerated with air pumps (Nirox X5) and photoperiod approximately 12 h dark and 12 h light. Adults *D. trunculus* were acclimatized for 48 h in filtered seawater before the experimental procedures (Belabed and Soltani, 2013). The physicochemical parameters of seawater measured by a multi-parameter water analyzer (Multi 340 i, Germany) were temperature (16.21 ± 0.5 °C), salinity (32.6 ± 1.5 g/l), pH (8.10 ± 0.1), and dissolved oxygen (8.20 ± 1.2 mg/l). After the laboratory acclimation period, the aquariums containing *D. trunculus* were separated into control and experimental groups (*Fig. 2*). The sub-lethal acute exposure to cadmium chloride ($CdCl_2$: Sigma, USA) as a commercial form of cadmium was performed according to preliminary bioassay applied on *D. trunculus* as previously reported (Merad and Soltani, 2015). Here, *D. trunculus* females and males were exposed to two sub-lethal concentrations (LC_{10} and LC_{25}) of cadmium chloride ($CdCl_2$) for 96 h for each sex (females: LC_{10} (0.94 mg/l) and LC_{25} (1.6 mg/l); males: LC_{10} (1.15 mg/l) and LC_{25} (2.02 mg/l) (Merad and Soltani, 2015; Merad et al., 2017). *D. trunculus* were fed every day with a commercial food mixture (Marine Invertebrate Diet. Carolina Ltd., NC, and USA). Animals were dissected at various point times (0, 48 and 96 h) to remove their soft tissues.

Proximate composition determination

The soft tissues of four individuals of *D. trunculus* per treatment were used each 48 h, and the basic proximate composition of *D. trunculus* (moisture, dry matter, ash,

http://www.aloki.hu ● ISSN 1589 1623 (Print) ● ISSN 1785 0037 (Online)
DOI: http://dx.doi.org/10.15666/aeer/1906_51035128

and fat) was determined according to the Association of Official Analytical Chemists methods (AOAC, 2000). All measured values were presented in percentages.

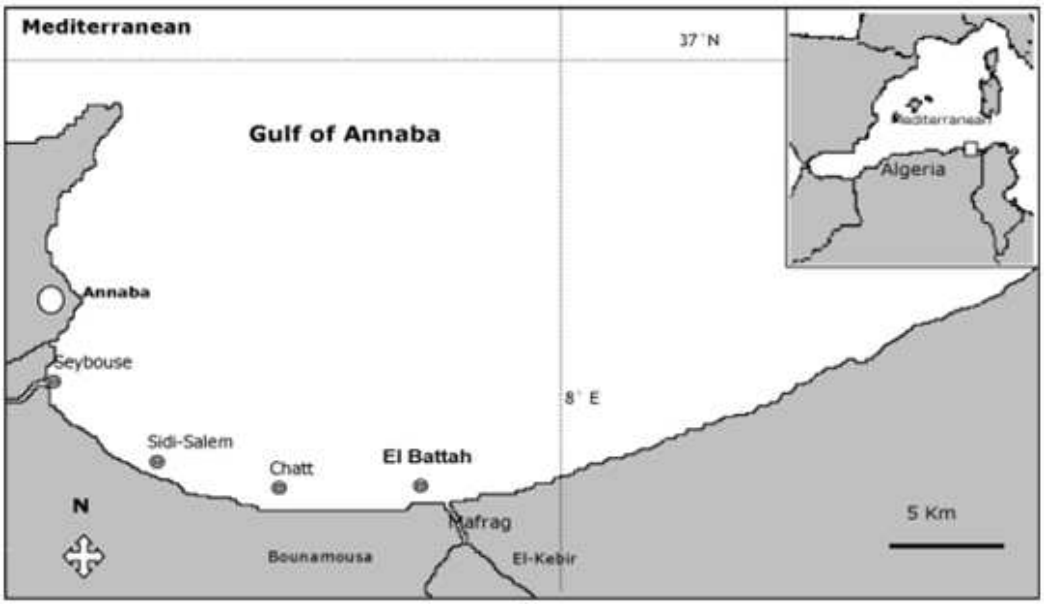

Figure1. *Location of El Battah site in the Gulf of Annaba (Northeast Algeria)*

Figure2. *Experimental culture of D. trunculus in the laboratory*

Moisture and dry matter determination

Moisture defined as the main component of the feed nutrient or ingredients was determined from the weight difference before and after drying the samples at 105 °C overnight to constant weight (Bhobe and Pai, 1986) according to the following formula (*Eq. 1*):

$$\% \text{ moisture content} = \frac{M1}{M2} \times 100 \qquad \text{(Eq.1)}$$

where M1 is the weight sample loss (grams); M2 is the mass of the used sample (grams).

http://www.aloki.hu ● ISSN 1589 1623 (Print) ● ISSN 1785 0037 (Online)
DOI: http://dx.doi.org/10.15666/aeer/1906_51035128

The percentage of dry matter content in the sample was calculated by the following formula (*Eq. 2*):

$$\% \text{ Dry matter content} = 100\% - \text{moisture content} \quad \text{(Eq.2)}$$

Ash content determination

Ash content, the residues of the inorganic matter (mineral) of the sample after burning, was estimated after incinerating the sample in a muffle furnace at 550 °C for 12 h until constant weight as described by AOAC method 920.153 (*Eq. 3*):

$$\% \text{ Ash content} = \frac{M1}{M2} \times 100 \quad \text{(Eq.3)}$$

where M1 is the weight of ash (grams); and M2 is the weight of the used sample (grams).

Fat content determination

Fat content in *D. trunculus* sample determined by Soxhlet method contains only free lipids, but not all lipid forms (Larpent, 1997). The Soxhlet extraction experiment was performed with a Franz Von Soxhlet according to AOAC method 960.39 using petroleum ether as solvent. In brief, 10 g of samples were included in a cartridge to enable to proceed the extraction procedure for 5 h. After the subsequent extraction, the residual solvent evaporates, and the results fall in the round bottom flask which was thereafter, heated in an oven to achieve permanent weight and then cooled in a desiccator. Fat content was measured and expressed as percent by weight as follows (*Eq. 4*):

$$\% \text{ Fat content} = \frac{\text{g fat of sample}}{\text{g weight of sample}} \times 100 \quad \text{(Eq.4)}$$

Determination of metallic elements

Three pool replicates of three individuals of *D. trunculus* per treatment were used each 48 h; the contents of Cd, Ca, Fe, and Zn were measured by atomic absorption spectrometry using a Perkin Elmer 900T instrument (Perkin Elmer PinAAcle 900T, USA). In brief, as previously described by Bryan et al. (1977), the soft tissues were dried at 110 °C to a constant weight, homogenized and crushed in a mortar to obtain a fine powder which afterward was kept away from metallic materials to avoid contamination until analyze. Thereafter, 0.20 g of dry sample was mineralized with muffle furnace at 350 °C to 450 °C, and two milliliters of nitric acid were added. After evaporation, ashes were cooled and the resulting residue was dissolved in 25 ml of nitric acid 1%, and filtered through a filter paper (Whatman N°1). The filtered sample was aspirated into the atomic absorption spectrophotometer at mode flame, and the reading was registered. The blank was used to adjust the zero of the instrument and to detect possible cross-contamination. All reagents were obtained from Merck and were of analytical grade. Metallic element contents were expressed in µg/g of dry weight (dw).

Statistical analyses

Data are expressed as mean ± standard deviation (SD). Statistical analyses were performed using the MINITAB Software (Version 17, Penn State College, PA, USA)

http://www.aloki.hu ● ISSN 1589 1623 (Print) ● ISSN 1785 0037 (Online)
DOI: http://dx.doi.org/10.15666/aeer/1906_51035128

where $p < 0.05$ was considered statistically significant. The normality was tested by the Kolmogorov-Smirnov test, and the homogeneity of variances was checked by Levine's test. One-way analysis of variance (ANOVA) followed by Tukey's post-hoc test was used to evaluate the difference between treatment means. The effects of concentrations, exposure time, and sex were tested by a three-way analysis of variance (ANOVA). The correlation between all parameters was examined by the Pearson correlation test (R = coefficient of correlation, p-value of correlation = significance at $p < 0.05$).

Results

Effects of sub-lethal concentrations of cadmium on the proximate composition

Tables 1 and *2* showed the effect of Cd on proximate composition in females and males of *D. trunculus* respectively. The proximate composition varies as a function of cadmium concentration and exposure time, and sex.

Sub-lethal effects of Cd on the percentage of moisture contents

As shown in *Tables 1* and *2,* a significant increase in moisture contents was observed in the two treated series as compared to control series in both sexes. Also, there was a significant difference in the LC_{10} and LC_{25}-treated series at 48 h ($F_{2,\ 11} = 9.34$; $p = 0.006$) and 96 h ($F_{2,\ 11} = 48.17$; $p = 0.000$) as compared to control series (0 h) in females (*Table 1; Tables A1* and *A2* in the *Appendix*). The males presented a significant difference in the two treated series at 48 h ($F_{2,\ 11} = 6.45$; $p = 0.018$) and 96 h ($F_{2,\ 11} = 26.58$; $p = 0.000$) as compared to control series (*Tables 2, A3* and *A4*). The three-way ANOVA indicated significant effects of concentrations ($F_{2,\ 71} = 49.05$; $p = 0.000$), exposure time ($F_{2,\ 71} = 63.96$; $p = 0.000$) and sex ($F_{1,71} = 73.16$; $p = 0.000$) (*Table A5*).

Sub-lethal effects of cadmium on the percentage of dry matter contents

As indicated in *Tables 1* and *2,* a significant decrease in the percentage of dry matter contents was detected in the two tested concentrations as compared to control groups in both sexes. The dry matter contents differed significantly in the two tested concentrations at 48 h ($F_{2,\ 11} = 9.34$; $p = 0.006$) and 96 h ($F_{2,\ 11} = 44.24$; $p = 0.000$) as compared to control in females (*Tables 1, A6* and *A7*). Meanwhile, this parameter differed significantly in the two treated series at 48 h ($F_{2,\ 11} = 6.45$; $p = 0.018$) and 96 h ($F_{2,\ 11} = 26.58$; $p = 0.000$) as compared to control in males (*Tables 2, A8* and *A9*). The three-way ANOVA showed significant effects of concentration ($F_{2,\ 71} = 47.36$; $p = 0.000$), exposure time ($F_{2,\ 71} = 61.59$; $p = 0.000$), and sex ($F_{1,\ 71} = 72.83$; $p = 0.000$) (*Table A10*).

Sub-lethal effects of cadmium on the percentage of ash contents

As presented in *Table 1* and 2, the percentage of ash contents was significantly increased in the two treated series when compared with control series of both sexes. This parameter differs significantly in the LC_{10} and LC_{25}-treated series at 48 h ($F_{2,\ 11} = 19.82$; $p = 0.001$) and 96 h ($F_{2,\ 11} = 34.57$; $p = 0.000$) as compared to control in females, with marked effect in Cl_{25} treated series (*Tables 1, A11* and *A12*). Similarly, males showed a significant difference in ash contents in the two treated series at 48 h ($F_{2,\ 11} = 19.62$; $p = 0.001$) and 96 h ($F_{2,\ 11} = 32.64$; $p = 0.000$) as compared to control, with pronounced effect in Cl_{25} treated series (*Tables 2, A13* and *A14*). The three-way

http://www.aloki.hu ● ISSN 1589 1623 (Print) ● ISSN 1785 0037 (Online)
DOI: http://dx.doi.org/10.15666/aeer/1906_51035128

ANOVA revealed significant effects of concentrations ($F_{2.\ 71} = 60.98$; $p = 0.000$) and exposure time ($F_{2.\ 71} = 70.50$; $p = 0.000$), and sex ($F_{1.71} = 66.38$; $p = 0.000$) (*Table A15*).

Table 1. *Effect of Cd on proximate composition (%) in D. trunculus females (m ± SD. n = 4). (Means for the same time exposure (the rows) followed by the different letter in miniscule are significantly different, while for each treatment (the columns), values followed by the different letter in majuscule are significantly different at p ≤ 0.05)*

Proximate composition (%)	Exposure time (h)	Treatment		
		Control	LC_{10}	LC_{25}
Moisture content	0	77.21 ± 1.11**aA**	77.21 ± 1.11**aA**	77.21 ± 1.11**aA**
	48	77.39 ± 0.97 **aA**	79.59 ± 1.09 **bB**	80.56 ± 1.12 **bB**
	96	77.61 ± 0.81 **aA**	82.16 ± 0.86 **bC**	82.49 ± 0.66 **bC**
Dry matter	0	22.54 ± 0.94 **aA**	22.54 ± 0.94 **aA**	22.54 ± 0.94 **aA**
	48	22.59 ± 0.97 **aA**	20.40 ± 1.09 **bB**	19.43 ± 1.11 **bB**
	96	22.34 ± 0.89 **aA**	17.82 ± 0.86 **bC**	17.49 ± 0.67 **bC**
Ash content	0	1.96 ± 0.73 **aA**	1.96 ± 0.73 **aA**	1.96 ± 0.73 **aA**
	48	1.89 ± 0.30 **aA**	3.03 ± 0.40 **bAB**	4.12 ± 0.64 **cB**
	96	2.33 ± 0.12 **aA**	3.95 ± 0.65 **bB**	4.89 ± 0.37 **cB**
Fat content	0	1.82 ± 0.05 **aA**	1.82 ± 0.05 **aA**	1.82 ± 0.05 **aA**
	48	1.77 ± 0.07 **aA**	1.70 ± 0.06 **aB**	1.53 ± 0.08 **bB**
	96	1.75 ± 0.06 **aA**	1.35 ± 0.05 **bC**	1.20 ± 0.05 **cC**

Table 2. *Effect of Cd on proximate composition (%) in D. trunculus males (m ± SD. n = 4). (Means for the same time exposure (the rows) followed by the different letter in miniscule are significantly different, while for each treatment (the columns), values followed by the different letter in majuscule are significantly different at p ≤ 0.05)*

Proximate composition (%)	Exposure time (h)	Treatment		
		Control	LC_{10}	LC_{25}
Moisture content	0	75.44 ± 0.91**aA**	75.44 ± 0.91**aA**	75.44 ± 0.91**aA**
	48	75.35 ± 0.84 **aA**	77.17 ± 1.70 **abA**	78.60 ± 1.14 **bB**
	96	75.43 ± 1.0 **aA**	80.28 ± 1.2 **bB**	80.47 ± 1.1 **bB**
Dry matter	0	24.56 ± 0.91 **aA**	24.56 ± 0.91 **aA**	24.56 ± 0.91 **aA**
	48	24.64 ± 0.84 **aA**	22.84 ± 1.70 **abA**	21.40 ± 1.14 **bB**
	96	24.57 ± 1.0 **aA**	19.72 ± 1.20 **bB**	19.53 ± 1.12 **bB**
Ash content	0	1.15 ± 0.16 **aA**	1.15 ± 0.16 **aA**	1.15 ± 0.16 **aA**
	48	1.12 ± 0.11 **aA**	2.03 ± 0.49 **bAB**	3.09 ± 0.58 **cB**
	96	1.35 ± 0.06 **aA**	2.87 ± 0.65 **bB**	3.82 ± 0.38 **cB**
Fat content	0	1.31 ± 0.04 **aA**	1.31 ± 0.04 **aA**	1.31 ± 0.04 **aA**
	48	1.27 ± 0.05 **aA**	1.17 ± 0.02 **bB**	1.08 ± 0.03 **cB**
	96	1.24 ± 0.03 **aA**	0.91 ± 0.08 **bC**	0.56 ± 0.08 **cC**

Sub-lethal effects of cadmium on the percentage of fat contents

As given in *Tables 1* and *2,* the percentage of fat contents was significantly decreased in the two tested Cd concentrations as compared with those in controls of both sexes.

http://www.aloki.hu ● ISSN 1589 1623 (Print) ● ISSN 1785 0037 (Online)
DOI: http://dx.doi.org/10.15666/aeer/1906_51035128

Females exhibit a significant difference in this parameter in the LC_{10} and LC_{25}-treated series at 48 h ($F_{2.\ 11} = 11.37$; $p = 0.003$) and 96 h ($F_{2.\ 11} = 91.17$; $p = 0.000$) as compared to control, with more effect in Cl_{25} treated series at 96 h (*Tables 1, A16* and *A17*). Also, the fat contents differ significantly in males in the two treated series at 48 h ($F_{2.\ 11} = 24.84$; $p = 0.000$) and 96 h ($F_{2.\ 11} = 83.33$; $p = 0.000$) (*Tables 2, A18* and *A19*) as compared to control, with distinct effect in Cl_{25} treated series. The three-way ANOVA revealed significant effects of concentration ($F_{2.\ 71} = 130.50$; $p = 0.000$), and exposure time ($F_{2.\ 71} = 277.73$; $p = 0.000$) and sex ($F_{1.71} = 1344.20$; $p = 0.000$) (*Table A20*).

Effects of sub-lethal concentrations of cadmium on metallic element

Tables 3 and *4* show the effect of Cd on ME in females and males of *D. trunculus* respectively. The ME contents vary as a function of cadmium concentration and exposure time, and sex.

Calcium contents

The Ca contents were significantly decreased in the two treated series as compared to control series in both sexes. A significant difference was observed in the level of this element in the LC_{10} and LC_{25}-treated series at 48 h ($F_{2.\ 8} = 49667.29$; $p = 0.000$) and 96 h ($F_{2.\ 8} = 13938.86$; $p = 0.000$) as compared to control in females, with marked effect in Cl_{25} treated series (*Tables 3, A21* and *A22*). Additionally, the Ca level element differed significantly in the two treated series at 48 h ($F_{2.\ 8} = 823.03$; $p = 0.000$) and 96 h ($F_{2.\ 8} = 5624.86$; $p = 0.000$) as compared to control in males, with pronounced effect in Cl_{25} treated series (*Tables 4, A23* and *A24*). The three-way ANOVA showed significant effects of Cd concentrations ($F_{2.\ 53} = 14560.76$; $p = 0.000$), and exposure time ($F_{2.\ 53} = 14597.25$; $p = 0.000$) and sex ($F_{1.\ 53} = 79623.14$; $p = 0.000$) (*Table A25*)

Iron contents

The Fe contents in females and males of *D. trunculus* were significantly decreased in the two treated series as compared to control series in both sexes. There was a significant difference in the two tested concentrations at 48 h ($F_{2.\ 8} = 182.74$; $p = 0.000$) and 96 h ($F_{2.\ 8} = 928.63$; $p = 0.000$) as compared to control in females, with more effect in Cl_{25} treated series (*Tables 3, A26* and *A27*). In parallel, *D. trunculus* males revealed a significant difference in Fe content in the two treated series at 48 h ($F_{2.\ 8} = 7.42$; $p = 0.024$) and 96 h ($F_{2.\ 8} = 100.77$; $p = 0.000$) as compared to control, with remarkable effect in Cl_{25} treated series at 96 h (*Tables 4, A28* and *A29*). The three-way ANOVA revealed significant effects of Cd concentration ($F_{2.53} = 325.15$; $p = 0.000$) and exposure time ($F_{2.53} = 496.49$; $p = 0.000$) and sex ($F_{1.\ 53} = 8324.47$; $p = 0.000$) (*Table A30*).

Zinc contents

A significant decrease of Zn contents was observed in two groups of treated series as compared to control series in both sexes. In addition, the Zn contents were significantly differed in the LC_{10} and LC_{25}-treated series at 48 h ($F_{2.\ 8} = 954.29$; $p = 0.000$) and 96 h ($F_{2.\ 8} = 1636.34$; $p = 0.000$) as compared to control in *D. trunculus* females, with distinct effect in Cl_{25} treated series (*Tables 3, A31* and *A32*). In *D. trunculus* males (*Tables 4, A33* and *A34*), the Zn contents revealed a significant difference in the two treated series at 48 h ($F_{2.\ 8} = 208.19$; $p = 0.000$) and 96 h ($F_{2.\ 8} = 7025.45$; $p = 0.000$) as compared to

http://www.aloki.hu ● ISSN 1589 1623 (Print) ● ISSN 1785 0037 (Online)
DOI: http://dx.doi.org/10.15666/aeer/1906_51035128

control, with pronounced effect in Cl_{25} treated series. The three-way ANOVA showed significant effects of Cd concentration ($F_{2.53} = 2074.06$; $p = 0.000$) and exposure time ($F_{2.53} = 2470.09$; $p = 0.000$), and sex ($F_{1.53} = 506.26$; $p = 0.000$) (*Table A35*).

Table 3. *Effect of Cd on metallic elements (µg/g of dry weight) in D. trunculus females (m ± SD. n = 3). (Means for the same time exposure (the rows) followed by the different letter in miniscule are significantly different, while for each treatment (the columns), values followed by the different letter in majuscule are significantly different at p ≤ 0.05)*

Metallic elements (µg/g dry weight)	Exposure time (h)	Treatment		
		Control	LC_{10}	LC_{25}
Ca	0	624.54 ± 4.75 **aA**	624.54 ± 4.75 **aA**	624.54 ± 4.75 **aA**
	48	621.61 ± 1.64 **aA**	619.83 ± 0.57 **bB**	310.66 ± 1.00 **cB**
	96	621.21 ± 1.20 **aA**	354.37 ± 2.57 **bC**	305.04 ± 3.26 **cB**
Fe	0	149.71 ± 1.94 **aA**	149.71 ± 1.94 **aA**	149.71 ± 1.94 **aA**
	48	148.83 ± 0.06 **aA**	130.50 ± 4.69 **bB**	104.83 ± 1.45 **cB**
	96	147.33 ± 0.47 **aA**	95.58 ± 2.70 **bC**	86.66 ± 1.70 **cC**
Zn	0	91.12 ± 0.45 **aA**	91.12 ± 0.45 **aA**	91.12 ± 0.45 **aA**
	48	90.33 ± 0.06 **aA**	76.29 ± 0.79 **bB**	70.83 ± 0.56 **cB**
	96	89.70 ± 0.90 **aA**	60.99 ± 0.64 **bC**	54.04 ± 0.85 **cC**
Cd	0	4.45 ± 0.90 **aA**	4.45 ± 0.90 **aA**	4.45 ± 0.90 **aA**
	48	4.87 ± 0.21 **aA**	14.79 ± 0.06 **bB**	21.04 ± 0.40 **cB**
	96	5.24 ± 0.33 **aA**	15.25 ± 0.43 **bB**	22.04 ± 1.23 **cB**

Table 4. *Effect of Cd on metallic elements (µg/g of dry weight) in D. trunculus males (m ± SD. n = 3). (Means for the same time exposure (the rows) followed by the different letter in miniscule are significantly different, while for each treatment (the columns), values followed by the different letter in majuscule are significantly different at p ≤ 0.05)*

Metallic elements (µg/g dry weight)	Exposure time (h)	Treatment		
		Control	LC_{10}	LC_{25}
Ca	0	340.95 ± 0.80 **aA**	340.95 ± 0.80 **aA**	340.95 ± 0.80 **aA**
	48	339.95 ± 0.87 **aA**	282.70 ± 3.09 **bB**	270.29 ± 2.19 **cB**
	96	339.66 ± 0.28 **aA**	264.21 ± 1.79 **bC**	212.91 ± 1.80 **cC**
Zn	0	86.54 ± 0.25 **aA**	86.54 ± 0.25 **aA**	86.54 ± 0.25 **aA**
	48	84.33 ± 2.74 **aA**	74.25 ± 1.11 **bB**	53.75 ± 1.32 **cB**
	96	85.62 ± 0.66 **aA**	63.03 ± 0.38 **bC**	41.66 ± 0.18 **cC**
Fe	0	73.71 ± 4.19 **aA**	73.71 ± 4.19 **aA**	73.71 ± 4.19 **aA**
	48	70.45 ± 0.58 **aA**	68.50 ± 0.56 **abAB**	66.12 ± 2.25 **bB**
	96	68.74 ± 0.37 **aA**	63.33 ± 1.82 **bB**	53.12 ± 1.47 **cC**
Cd	0	4.20 ± 0.40 **aA**	4.20 ± 0.40 **aA**	4.20 ± 0.40 **aA**
	48	4.87 ± 0.43 **aA**	5.20 ± 0.40 **aA**	13.75 ± 1.21**bB**
	96	4.58 ± 0.57 **aA**	7.53 ± 0.94 **bB**	15.45 ± 0.38 **cB**

Cadmium contents

A significant increase of Cd contents was observed in two groups of treated series as compared to control series in both sexes. Also, the Cd contents differed significantly in the two treated series at 48 h ($F_{2.8} = 2811.72$; $p = 0.000$) and 96 h ($F_{2.8} = 352.97$;

http://www.aloki.hu ● ISSN 1589 1623 (Print) ● ISSN 1785 0037 (Online)
DOI: http://dx.doi.org/10.15666/aeer/1906_51035128

p = 0.000) as compared to control in females, with marked effect in Cl_{25} treated series (*Tables 3, A36* and *A37*). In *D. trunculus* males (*Tables 4, A38* and *A39*), the Cd contents were significantly different significantly in the two treated series at 48 h ($F_{2.\ 8}$ = 126.27; p = 0.000) and 96 h ($F_{2.\ 8}$ = 206.78; p = 0.000) as compared to control, with more effect in Cl_{25} treated series at 96 h. The three-way ANOVA indicated significant effects of concentration ($F_{2.\ 53}$ = 770.06; p = 0.000) and exposure time ($F_{2.\ 53}$ = 636.93; p = 0.000) and sex ($F_{1.\ 53}$ = 390.76; p = 0.001) (*Table A40*).

Regarding all ME, our results showed that the order of ME in *D. trunculus* females is as follows: Ca >Fe >Zn > Cd. Ca and Fe are the most abundant elements, and Cd is a scarce element. In *D. trunculus* males, the gradient of ME becomes as follows: Ca >Zn >Fe > Cd. It is worth noting that Ca and Zn are the main abundant elements in males.

Correlation tests

Pearson correlation tests between cadmium and proximate composition

Pearson correlation tests between the proximate composition and the contents of Cd in both sexes of *D. trunculus* are displayed in *Table 5*. Here, the results revealed a highly significant (p = 0.000) negative correlation between Cd and dry matter; and Cd and Fat content in both sexes. Conversely, a highly significant (0.000) positive correlation was noticed between Cd content and moisture content, and Cd content and ash content in both sexes.

Pearson correlation tests between cadmium and metallic elements

The relationships between ME in both sexes of *D. trunculus* are illustrated in *Table 5*. The Pearson correlation displayed a highly significant (p = 0.000) negative correlation between Cd and other ME in both sexes.

Table 5. *Pearson correlation tests between all parameters studies in D. trunculus females and males (R = coefficient of correlation. p = significance at P < 0.05)*

Pearson correlation	Females		Males	
	R	P	R	P
Dry matter – Cd	-0.875	0.000	-0.779	0.000
Fat– Cd	-0.838	0.000	-0.826	0.000
Moisture – Cd	0.917	0.000	0.779	0.000
Ash – Cd	0.924	0.000	0.875	0.000
Zn – Cd	-0.921	0.000	-0.950	0.000
Fe – Cd	-0.930	0.000	-0.799	0.000
Ca – Cd	-0.981	0.000	-0.861	0.000

Discussion

The consumers' awareness about proximate composition and ME contents of any edible organism which are commonly threatened by the usage of the coastal waters (simple wastes repository) is exceedingly important (Akpor et al., 2014; Ehsanuddin et al., 2019). Our study provides a helpful understanding of the changes in the nutritive value of *D. trunculus* exposed to cadmium contaminated Gulf of Annaba. Very limited

http://www.aloki.hu ● ISSN 1589 1623 (Print) ● ISSN 1785 0037 (Online)
DOI: http://dx.doi.org/10.15666/aeer/1906_51035128

studies investigating the impact of heavy metals (no essential metallic elements) on the proximate and essential ME of bivalvia (Bejaoui et al., 2020) are available.

Impact of sub-lethal concentrations of cadmium on moisture contents

In this study, we found that the mean percentage of moisture contents in *D. trunculus* controls was 77.40% and 75.40% for females and males respectively. Similar results were previously reported for the same and other species of bivalvia (Appukuttan and Aravindan, 1995; Mc Lean and Bulling, 2005; Hussein, 2015; Ogidi et al., 2020). In fact, the significant change in the percentage of moisture contents could reflect an index of the freshness of edible mollusks (Ghribi et al., 2018; Bejaoui et al., 2020). Besides, our results revealed an increase in the percentage of moisture contents with the two test concentrations in both sexes during the exposure periods. This is likely due to tissue alterations following an intense uptake of body water after an energetic metabolic degradation (Vargasmachuca et al., 2017; Hussain et al., 2018). Our results are in agreement with a previous study (Krishnakumari and Nair, 1984) conducted in oyster *Saccostrea cucullata* from different sites (polluted site and a relatively clean site). Of note, the moisture content was influenced by the surrounding environment (Hussein, 2015).

Impact of sub-lethal concentrations of cadmium on dry matter contents

D. trunculus controls showed values of the mean percentage of dry matter contents between 22.49% and 24.59% for females and males, respectively. This result is alike to that found in *Mercenaria mercenaria* from Nigeria (Ogidi et al., 2020). Findings showed also a marked decrease in the percentage of dry matter contents in both sexes treated with the two concentrations during the exposure period. This result could be due to the increased moisture contents, indicating thus that the dry matter is the remaining material after the removal process of water.

Impact of sub-lethal concentrations of cadmium on ash contents

The mean percentage of ash content in *D. trunculus* controls is 2.06% and 1.20% for females and males respectively. This was similar to that reported in other bivalve species such as *Laternula elliptica* (Ahn et al., 2003); *Anodonta woodiana* (Hartono, 2007); *Meretrix meretrix* and *Pholas dactylus* (Ghifari, 2011); *Batissa violacea* (Jamaluddin et al., 2016). A significant increase in the percentage of ash contents was detected in both sexes exposed to the two tested concentrations as compared to the controls. This result might be related to the increase of the Cd in soft tissues. Similarly, a previous study conducted on *Anodonta anatine* exposed to various doses of Pb, Cu, and Cr in water has reported a marked increase in the ash content (Sohail et al., 2016). Furthermore, the moisture content exhibited a positive correlation with ash content, because the acquisition of moisture leads to an acquisition of inorganic water-soluble compounds (Bochi et al., 2008).

Impact of sub-lethal concentrations of cadmium on fat contents

The obtained results revealed that the mean percentage of fat contents in *D. trunculus* controls is between 1.78% and 1.27% for females and males respectively. Previous studies, including those conducted on *Anodonta woodiana* (Hartono, 2007); *Meretrix*

http://www.aloki.hu ● ISSN 1589 1623 (Print) ● ISSN 1785 0037 (Online)
DOI: http://dx.doi.org/10.15666/aeer/1906_51035128

meretrix and *Pholas dactylus* (Ghifari, 2011) concord with our finding. The low-fat content represents a nutritional characteristic of the mollusk flesh (Bellisle et al., 1999; Wen et al., 2020). Further, the percentage of fat contents was significantly decreased in *D. trunculus* subjected to the two tested concentrations as compared to the control group of both sexes. This result might be owed to the increase of the Cd content in soft tissues, exhibiting a negative correlation with fat contents. In this context, a comparable tendency was estimated by Bejaoui et al. (2020) for lipids and reserve lipids in *Venerupis decussata* tissue from two Tunisian lagoons exposed to different anthropogenic contaminants.

Impact of sub-lethal concentrations of cadmium on essential metallic elements contents

Regarding the contents of EM, our study indicated that the predominant EM detected in both sexes of *D. trunculus* controls is Ca. This finding concords with other previous studies conducted on *Donax cuneatus* (Idayachandiran et al., 2014), *Perna viridis* and *Villoritta cyprinoids* (Ragi et al., 2017), *Anomalocardia brasiliensis* and *Mytella guyanensis* (Costa et al., 2019). Moreover, a negative correlation between Cd and Ca has been noticed in both sexes, and the Cd exposure at two sub-lethal concentrations was found to likely reduce the levels of Ca. Also, Cd was reported to affect Ca metabolism in bivalve mollusks (Faubel et al., 2008), through a competitive interaction in the plasma membrane binding site of Ca. Additionally, Cd affects the SH groups of Ca-ATPase (Verbost et al., 1988), resulting consequently in decreased Ca levels in soft tissue. This finding is similar to previous studies performed on *Donax rugosus* (Sidoumou et al., 1997), *Crassostrea gaster* (Javanshir and Shapoori, 2011) and *Anodonta anatina* (Ngo et al., 2011).

In this study, Fe was proved as the second most abundant element in *D. trunculus* female controls, and this was similarly reported in previous studies performed on same-sex of the same species or other species (Romeo and Gnassia-Barelli, 1988; El-Serehy et al., 2013; Richir and Gobert, 2014). Furthermore, a negative correlation between Cd and Fe was observed in both sexes, and accordingly, the decreased level of Fe at two sub-lethal concentrations was also detected in *Mizuhopecten yessoensis* (Chelomin et al., 1995). Fe plays an essential role in antioxidant enzyme activities like catalase whose activity can be affected by Fe variations. In this regard, Soltani et al. (2012) have reported disruption in catalase activity in a mantle of *D. trunculus* collected from Cd polluted northeast Algeria sites (Sidi Salem beach, Annaba city). Besides, *D. trunculus* controls males were found to contain abundantly zinc element whose cellular uptake is higher in sperm than eggs in *M. edulis* (Latouche and Mix, 1981; Akberali et al., 1985 in Earnshaw et al., 1986). Whilst, *D. trunculus* females are rich in Zn after Fe as compared to males. Similar results have been found in *D. trunculus* females from Italy (Marina and Enzo, 1983) and *Mytilus galloprovincialis* females from Belgium (Richir and Gobert, 2014). Findings showed also a negative correlation between Cd and Zn, in addition to a decrease in Zn contents in soft tissues of *D. trunculus* in both sexes at two sub-lethal concentrations. This result was similar to that of a previous study conducted on *Lamellidans marginalis* (Das and Jana, 1999) and *Anodonta anatine* (Ngo et al., 2011). The plausible explanation of this result is that Cd can affect the active sites of DNA-binding proteins, MTs, and Zn-containing enzymes (Pruskiand Dixon, 2002; Golovanova, 2008; Ngo et al., 2011). As reported, Zn protects against the toxicity of Cd (Kaji et al., 1988) whose each atom coordinates with seven zinc atoms (Giles, 1988).

http://www.aloki.hu ● ISSN 1589 1623 (Print) ● ISSN 1785 0037 (Online)
DOI: http://dx.doi.org/10.15666/aeer/1906_51035128

As Cd is a non-essential element, both sexes showed the lowest contents of these elements in the control series. Importantly, these values are less than the permissible limit recommended by CEFAS (1997) and NHMRC (1987). Also, the incorporation of Cd increased as a function of the concentration and the exposure time in both sexes. Our results are in line with the study of Belabed and Solatni (2018) reporting that *D. trunculus* is sensitive to Cd toxicity. This metal was gradually incorporated into the body. *D. trunculus* responds quickly with a relatively effective detoxification process, since a reduction in the levels of Cd in tissue was observed starting at 96 h during the recovery period. Moreover, the effect of LC_{25} was relatively more significant, and accordingly, the Cd toxicity on PC, omega-3 fatty acids, EPA, DHA, carbohydrates, proteins, lipids for the same species and same concentrations have been previously reported (Merad et al., 2016, 2017; Merad and Soltani, 2017).

According to the literature, the values of EM contents in *Donax* were varied in different areas. This variation is strongly dependent on geochemical and biological factors (Gupta and Singh, 2011; Katsallah et al., 2013), including sexes, size, age, phenotype, genotype, feeding activity, and reproductive stage (Boening, 1997). The geochemical factors include organic carbon, water hardness, salinity, temperature, pH, dissolved oxygen, sediment grain size, and hydrologic features of the system (Elder et al., 1991; Caçador et al., 2016).

Alike to previous studies (Laxmilatha, 2009; Richir and Gobert, 2014; Hussein, 2015) investigating the differences between the sexes in the proximate and EM contents, our data indicated higher contents on moisture, ash, fat, and EM in females than males of *D. trunculus*. This is likely due to the reason that the formation of reserves during the respawning period is more pronounced in females, suggesting that the accumulation of proximate and EM in this sex could be faster (Sokolowski et al., 2004). Accordingly, Merad et al. (2015) have reported a higher rate of MTs in *D. trunculus* females than males**.**

Conclusion

The present study provides valuable knowledge on the proximate and EM contents in *D. trunculus* from the gulf of Annaba (Northeast Algeria), as well as the impact of Cd on these parameters. *D. trunculus* was found to be rich in moisture contents and contains low ash and fat contents. Ca, Zn and Fe were the main compounds in the flesh of *D. trunculus*. The contents of Cd in tissues can vary as a function of its concentration, exposure time, and sexes, which hence significantly affected the proximate and EM contents in *D. trunculus.* Thus, it is necessary to continue monitoring programs to control the metal concentrations and, subsequently to avoid health-associated problems.

Acknowledgements. This work was supported by the National Fund for Scientific Research to Pr. N. Soltani (Laboratory of Applied Animal Biology) and the Ministry of High Education and Scientific Research of Algeria (CNEPRU Project to Dr. A. Hamdani).

REFERENCES

[1] Ahn, I. Y., Surh, J., Park, Y. G., Kwon, H., Choi, K. S., Kang, S. H., Chung, H. (2003): Growth and seasonal energetics of the Antarctic bivalve *Laternula elliptica* from King

http://www.aloki.hu ● ISSN 1589 1623 (Print) ● ISSN 1785 0037 (Online)
DOI: http://dx.doi.org/10.15666/aeer/1906_51035128

George Island, Antarctica. – Marine Ecology Progress Series 257: 99−110. https://doi.org/10.3354/meps257099.

[2] Akberali, H. B., Earnshaw, M. J., Marriott, R. M. (1985): The action of heavy metals on the gametes of the marine mussel, *Mytilus edulis* (L.)-II. Uptake of copper and zinc and their effect on respiration in the sperm and unfertilized egg. – Marine Environmental Research 16(1): 37-59. https://doi.org/10.1016/0141-1136(85)90019-4.

[3] Akpor, O. B., Ohiobor, G. O., Olaolu, T. D. (2014): Heavy metal pollutants in waste water effluents: Sources, effects, and remediation. – Advances in Bioscience and Bioengineering 2(4): 37-43. https://doi.org/10.11648/J.ABB.20140204.11.

[4] Amira, A., Merad, I., Marisa, R., Almeida, G. L., Soltani, N. (2018): Seasonal variation in biomarker responses of *Donax trunculus* from the Gulf of Annaba (Algeria): implication of metal accumulation in sediments. – Comptes Rendus Geoscience 350(4): 173-179. https://doi.org/10.1016/j.crte.2018.02.002.

[5] AOAC Official Method 920.153-Ash of Meat (2000): Official Method of Analytical Chemists. 17th Ed. – Association of Official Analytical Chemists, Maryland.

[6] AOAC Official Method 960.39-Fat (Crude) or Ether Extract in Meat (2000): Official Method of Analytical Chemists. 17th Ed. – Association of Official Analytical Chemists, Maryland.

[7] Appukuttan, K. K., Aravindan, C. M. (1995): Studies on the biochemical composition of the short neck clam, *Paphia malabarica* from Ashtamudi estuary, Southwest coast of India. – Seafood Export Journal 26(5): 17−21.

[8] Astudillo, L. R., Yen, I. C., Bekele, I. (2005): Heavy metals in sediments, mussels and oysters from Trinidad and Venezuela. – Revista de Biología Tropical 53(1): S41-53.

[9] Bankaji, I., Pérez-Clemente, R. M., Caçador, I., Sleimi, N. (2019): Accumulation potential of *Atriplex halimus* to zinc and lead combined with NaCl: effects on physiological parameters and antioxidant enzymes activities. – South African Journal of Botany 123: 51-61. https://doi.org/10.1016/j.sajb.2019.02.011.

[10] Bejaoui, S., Bouaziz, M., Ghribi, F., Chetoui, I., El Cafsi, M. (2020): Assessment of the biochemical and nutritional values of *Venerupis decussata* from Tunisian lagoons submitted to different anthropogenic ranks. – Environmental Science and Pollution Research 27: 1734-1751. https://doi.org/10.1007/s11356-019-06851-y.

[11] Belabed, S., Soltani, N. (2013): Acute toxicity of cadmium on *Donax trunculus*: acetylcholinesterase, glutathione S-transferase activities and pattern of recovery. – European Journal of Experimental Biology 3(2): 54-61.

[12] Belabed, S., Soltani, N. (2018): Effects of cadmium concentrations on bioaccumulation and depuration in the marine bivalve *Donax trunculus*. – Euro-Mediterranean Journal for Environmental Integration 3: 19. https://doi.org/10.1007/s41207-018-0054-0.

[13] Beldi, H., Gimbert, F., Maas, S., Scheifler, R., Soltani, N. (2006): Seasonal variations of Cd, Cu, Pb and Zn in the edible mollusc *Donax trunculus* (Mollusca Bivalvia) from the gulf of Annaba, Algeria. – African Journal Agricultural of Research 1(4): 85-90. https://doi.org/10.5897/AJAR-0AE486A36567.

[14] Bellisle, F. (1999): Glutamate and the umami taste: sensory, metabolic, nutritional and behavioural considerations. A review of the literature published in the last 10 years. – Neuroscience Biobehavioral Reviews 23(3): 423-438. https://doi.org/10.1016/S0149-7634(98)00043-8.

[15] Bhobe, A. M., Pai, J. S. (1986): Study of the properties of frozen shrimps. – Journal of Food Science and Technology 23: 143-147.

[16] Bochi, V. C., Weber, J., Ribeiro, C. P., Victório, A. M., Emanuelli, T. (2008): Fishburgers with silver cat fish (*Rhamdia quelen*) filleting residue. – Bioresources Technology 99: 8844-8849. https://doi.org/10.1016/j.biortech.2008.04.075.

[17] Boening, D. W. (1997): An evaluation of bivalves as biomonitors of heavy metals pollution in marine waters. – Environmental Monitoring and Assessment 55: 459-470. http://dx.doi.org/10.1023/A: 1005995217901.

http://www.aloki.hu ● ISSN 1589 1623 (Print) ● ISSN 1785 0037 (Online)
DOI: http://dx.doi.org/10.15666/aeer/1906_51035128

[18] Bryan, G. W., Potts, G. W., Forester, G. R. (1977): Heavy metals in the gastropod mollusc *Haliotis tuberculata* (L.). – Journal of the Marine Biological Association UK (JMBA) 57: 379-390.
[19] Caçador, I., Duarte, B., Marques, J. C., Sleimi, N. (2016): Carbon Mitigation: A Salt Marsh Ecosystem Service in Times of Change. – In: Khan, M. A., Ozturk, M., Gul, B., Ahmed, M. Z. (eds.) Halophytes for Food Security in Dry Lands. Elsevier Academic Press, Cambridge, MA, pp. 83-110. https://doi.org/10.1016/B978-0-12-801854-5.00006-6.
[20] CEFAS, Centre for Environment, Fisheries and Aquaculture Science (1997): Monitoring and surveillance of non-radioactive contaminants in the aquatic environment and activities regulating the disposal of waste at sea (1994). – Aquatic Environment Monitoring Report 47. Centre for Environment, Fisheries, and Agriculture Science, Lowestoft, UK.
[21] Chelomin, V. P., Bobkova, E. A., Lukyanova, O. N., Chekmasova, N. M. (1995): Cadmium-induced alterations in essential trace element homoeostasis in the tissues of scallop *Mizuhopecten yessoensis*. – Comparative Biochemistry & Physiology Part C 110: 329-335.
[22] Costa, V. C., Carqueija, A. F. A., Babos, D. V., Pereira-Filho, E. R. (2019): Direct determination of Ca, K, Mg, Na, P, S, Fe and Zn in bivalve mollusks by wavelength dispersive X-ray fluorescence (WDXRF) and laser-induced breakdown spectroscopy (LIBS). – Food Chemistry 273: 91-98. https://doi.org/10.1016/j.foodchem.2018.02.016.
[23] Costa, L. L., Costa, M. F., Zalmon, I. R. (2021): Macroinvertebrates as biomonitors of pollutants on natural sandy beaches: overview and meta-analysis. – Review Environmental Pollution 275: 116629. https://doi.org/10.1016/j.envpol.2021.116629.
[24] Das, S., Jana, B. B. (1999): Dose-dependent uptake and Eichhornia-induced elimination of cadmium in various organs of the freshwater mussel, *Lamellidens marginalis* (Linn.). – Ecological Engineering 12(3-4): 207-29. https://doi.org/10.1016/S0925-8574(98)00062-7.
[25] Dhinamala, K., Pushpalatha, M., Meeran, M., Arivoli, S., Tennyson, S., Raveen, R. (2017): Bioaccumulation of cadmium in gills and muscles of shellfish from Pulicat lake, Tamil Nadu, India. – Journal of Coastal Life Medicine 5(2): 47-50. https://doi.org/10.12980/jclm.5.2017J6-210.
[26] Drif, F., Abdennour, C. (2010): Trace metals in the mussel *Donax trunculus* Linnaeus 1758 from urban and industrial contaminated locations. – Journal of Applied Sciences Research 6(12): 2063-2067.
[27] Dutta, M., Rajak, P., Khatun, S. (2017): Toxicity assessment of sodium fluoride in *Drosophila melanogaster* after chronic sub-lethal exposure. – Chemosphere 166: 255-266. https://doi.org/10.1016/j.chemosphere.2016.09.112.
[28] Earnshaw, M. J., Wilson, S., Akberali, H. B. (1986): The action of heavy metals on the gametes of the marine mussel, *Mytilus edulis* (L.)—III. The effect of applied copper and zinc on sperm motility in relation to ultrastructural damage and intracellular metal localisation. – Marine of Environmental Research 20(4): 261-278.
[29] Ehsanuddin, N. A., Shafie, F. A., Abdullah, A. H., Mahalingam, S. R., Tiong, C. S., Arshad, K. (2019): Heavy metals in dried squids (*Loligo* sp.) in Melaka Tengah District. – MAEH Journal of Environmental Health 1(1): 24-27.
[30] Elder, J. F., Collins, J. J. (1991): Freshwater molluscs as indicators of bioavailability and toxicity of metals in surface water systems. – Reviews of Environmental Contamination and Toxicology 122: 37-79. https://doi.org/10.1007/978-1-4612-3198-1_2.
[31] El-Serehy, H. A., Aboulela, H., Al-Misned, F., Bahgat, M., Shafik, H., Al-Rasheid, K., Kaiser, M., Ezz, H. (2013): The potential use of the bivalve *Donax trunculus* as bioindicator for heavy metal pollution of port said western coast on the Mediterranean Sea. – Life Science Journal 10(4): 1094-1101.

http://www.aloki.hu ● ISSN 1589 1623 (Print) ● ISSN 1785 0037 (Online)
DOI: http://dx.doi.org/10.15666/aeer/1906_51035128

[32] Faubel, D., Lopes-Lima, M., Freitas, S., Pereira, L., Andrade, J., Checa, A., Frank, H., Matsuda, T., Machado, J. (2008): Effects of Cd2+ on the calcium metabolism and shell mineralization of bivalve *Anodonta cygnea*. – Marine Freshwater Behaviour and Physiology 41(2): 93-108. https://doi.org/10.1080/10236240802194123.

[33] Gaspar, M. B., Ferreira, R., Monteiro, C. (1999): Growth and reproductive cycle of *Donax trunculus* L. (Mollusca: Bivalvia) in Faro, southern Portugal. – Fish Research 41(3): 309-316. https://doi.org/10.1016/S0165-7836(99)00017-X.

[34] Gaspar, M. B., Chícharo, L. M., Vasconcelos, P., Garcia, A., Santos, A. R., Monteiro, C. C. (2002): Depth segregation phenomenon in *Donax trunculus* (Bivalvia: Donacidae) populations of the Algarve coast (southern Portugal). – Science Marine 66(2): 111-121. https://doi.org/10.3989/scimar.2002.66n2111.

[35] Ghifari, A. (2011): Karakteristik Asam Lemak Daging Keong Macan (*Babylonia spirata*), Kerang Tahu (*Meretrix meretrix*), Dan Kerang Salju (*Pholas dactylus*). – [skripsi], Departemen Teknologi Hasil Perairan Fakultas Perikanan Dan Ilmu Kelautan Institut Pertanian Bogor, Bogor.

[36] Ghribi, F., Boussoufa, D., Aouini, F., Bejaoui, S., Chetoui, I., Rabeh, I., EL Cafsi, M. (2018): Seasonal variation of biochemical composition of Noah's ark shells (Arcanoae L. 1758) in Tunisian coastal lagoon in relation to its reproductive cycle and environmental conditions. – Aquatic Living Resources 31: 14. https://doi.org/10.1051/alr/2018002.

[37] Gil, A., Gil, F. (2015): Fish, a Mediterranean source of n−3 PUFA: benefits do not justify limiting consumption. – British Journal of Nutrition 113: 58-67. https://doi: 10.1017/S0007114514003742.

[38] Giles, M. A. (1988): Accumulation of cadmium by rainbow trout, *Salmo gairdneri*, during extended exposure. – Canadian Journal of Fisheries Aquatic Sciences 45: 1045-1053.

[39] Golovanova, I. L. (2008): Effects of heavy metals on the physiological and biochemical status of fishes and aquatic invertebrates. – Inland Water Biology 1: 93-101. https://doi.org/10.1007/s12212-008-1014-1.

[40] Gupta, S. K., Singh, J. (2011): Evaluation of mollusc as sensitive indicator of heavy metal pollution in aquatic system. A review. – Institute of Integrative Omics and Applied Biotechnology Journal 2(1): 49-57.

[41] Hafsaoui, I., Draredja, B., Lasota, R., Como, S., Magni, P. (2016): Population dynamics and secondary production of *Donax trunculus* (Mollusca, Bivalvia) in the Gulf of Annaba (Northeast Algeria). – Mediterranean Marine Science 17(3): 738-750. https://doi.org/10.12681/mms.1760.

[42] Hamdani, A., Soltani, N., Zaidi, N. (2020): Growth and reproduction of *Donax trunculus* from the Gulf of Annaba (Northeast Algeria) in relation to environmental conditions. – Environmental Science and Pollution Research 27: 41656-41667. https://doi.org/10.1007/s11356-020-10103-9.

[43] Hartono, N. (2007): Pengaruh Berbagai Metode Pemaaakan Terhadap Kelarutan Mineral Kijing Taiwan (*Anodonta woodiana* Lea) [Skripsi]. – Departemen Teknologi Hasil Perairan, Fakultas Perikanan dan Ilmu Kelautan, IPB. http://repository.ipb.ac.id/handle/123456789/48718.

[44] Hossen, M. F., Hamdan, S., Rahman, M. R. (2015): Review on the risk assessment of heavy metals in Malaysian clams. – Science World Journal 1-7. https://doi.org /10. 1155 /2015/905497.

[45] Hussain, B., Sultana, T., Sultana, S., Ahmed, Z., Mahboob, S. (2018): Study on impact of habitat degradation on proximate composition and amino acid profile of Indian major carps from different habitats. – Saudi Journal of Biological Sciences 25(4): 755-759. https://doi.org/10.1016/j.sjbs.2018.02.004.

http://www.aloki.hu ● ISSN 1589 1623 (Print) ● ISSN 1785 0037 (Online)
DOI: http://dx.doi.org/10.15666/aeer/1906_51035128

[46] Hussein, S. M. (2015): Water content as a new tool for discrimination between some shellfishes. – Pakistan Journal of Biological Sciences 18: 204-214. https://doi.org/10.3923/pjbs.2015.204.214.
[47] Idayachandiran, G., Muthukumar, A., Kumaresan, S., Balasubramanian, T. (2014): Nutritional value of marine bivalve, *Donax cuneatus* (Linnaeus, 1758) from Cuddalore coastal waters, southeast coast of India. – Inventi Impact: Life Style 1: 15-19.
[48] Jamaluddin, M., Septiawan, Y., Yonelian, Y. (2016): Analysis of fatty acid and amino acid profile of "Meti" mussels (*Batissa violacea* L. von Lamarck, 1818) in La'a river of Petasia District North Morowali regency. – Rasayan Jounal of Chemistry 9(4): 673-679.
[49] Javanshir, A., Shapoori, M. (2011): Influence of water hardness (calcium concentration) on the absorption of cadmium by the mangrove oyster *Crassostrea gaster* (Ostreidae; Bivalvia). – Journal of Food, Agriculture and Environment 9(2): 724-727.
[50] Kaji, T., Takata, M., Hoshino, T., Miyahara, T., Kozuka, H., Kurashige, Y., Koizumi, F. (1988): Role of zinc in protection against cadmium induced toxicity in formation of embryonic chick bone in tissue culture. – Toxicology Letters 44: 219-27. https://doi.org/10.1016/0378-4274(88)90149-X.
[51] Katsallah, G. I. M., Rukayya, M., Sambo, D., Sule, T. G. (2013): Comparative metal analysis of the soft tissues of three species of Anodonta (Class: Bivalvia) from Kubanni Lake in Zaria Nigeria. – Journal of Environmental Science, Toxicology and Food Technology 6(3): 18-23. https://doi.org/10.9790/2402-0631823.
[52] Khan, P. A. (1992): Biochemical composition, minerals (calcium and iron) and chitin content of two portunid crabs Scylla *serrata Forskal* and *Portunus pelagicus* Linnaeus available in and around the coastal regions of Bangladesh. – M.Sc. Thesis, Institute of Marine Sciences, Chittagong University.
[53] Krishnakumari, L., Nair, V. R. (1984): On the water quality of selected environments along Bombay coast. – Journal of the Indian Fisheries Association 14-15: 49-57.
[54] Künili, I. E., Çolakoğlu, S., Çolakoğlu, F. (2020): Levels of PAHs, PCBs, and toxic metals in *Ruditapes philippinarum* and *Donax trunculus* in Marmara Sea, Turkey. – Journal of the Science of Food and Agriculture 101(3): 1167-1173. https://doi.org/10.1002/jsfa.10728.
[55] La Valle, P. (2006): *Donax trunculus* (Bivalvia: Donacidae) quale indicatore biologico degli equilibri costieri e del bilancio sedimentario. – Doctoral Thesis. University of Rome La Sapienza.
[56] Larpent, J. P. (1997): Microbiologie alimentaire technique de laboratoire. – Technique et documentation. Lavoisier, Paris, pp. 882-883.
[57] Latouche, Y. D., Mix, M. C. (1981): Seasonal variation in soft tissue weights and trace metal burdens in the bay mussel, *Mytilus edulis*. – Bulletin of Environmental Contamination and Toxicology 27(1): 821-828.
[58] Laxmilatha, P. (2009): Proximate composition of the surf clam *Mactra violacea* (Gmelin 1791). – Indian Journal of Fisheries 56(2): 147-150.
[59] Margret, S. M. (2015): A Survey on biodiversity of molluscs in trash fish landing of Colachal and Kadipatinam and searching of gastropods and bivalves for human consumption. – Ph. D. Thesis, Manonmaniam Sundaranar University, India, pp. 25−31.
[60] Margret, S. M., Santhiya, M., Mary, M. T., Jansi, M. (2013): Comparative study on the biochemical composition of four gastropods along the Kanyakumari coast. – World Journal of Fish and Marine Sciences 5: 637−40.
[61] Marina, M., Enzo, O. (1983): Variability of zinc and manganese concentrations in relation to sex and season in the bivalve *Donax trunculus*. – Marine Pollution Bulletin 14: 342-346.
[62] Mc Lean, C. H., Bulling, K. R. (2005): Differences in lipid profile of New Zealand marine species over four seasons. – Journal of Food Lipids 12(4): 313−326. https://doi.org/10.1111/j.1745-4522.2005.00026.x.

http://www.aloki.hu ● ISSN 1589 1623 (Print) ● ISSN 1785 0037 (Online)
DOI: http://dx.doi.org/10.15666/aeer/1906_51035128

[63] Merad, I., Soltani, N. (2015): Environmental risks of cadmium on *Donax trunculus* (Mollusca, Bivalvia): sublethal effect on nucleic acid contents of gonads. – Proceeding of INOC International Congress "Estuaries & Coastal Protected Areas" ECPA 2014, 04-06 November 2014, Izmir, Turkey, pp. 260-267.

[64] Merad, I., Soltani, N. (2017): Sublethal effects of cadmium on energy reserves in the edible mollusk *Donax trunculus*. – Journal Entomology Zoology Studies 5(1): 100-105.

[65] Merad, I., Rabei, A., Soltani, N. (2015): Réponse de la métallothionéine au cours de l'exposition au cadmium et la restauration chez *Donax trunculus*. Bulletin de l'Institut National des Sciences de la Mer (INSTM Salammbo). – Numéro Spécial (18): Actes du IXème Congrès Maghrébin des Sciences de la Mer Sousse, 2014.

[66] Merad, I., Bairi, Y., Sifi, K., Soltani, N. (2016): Protein carbonyls as biomarkers of oxidative stress induced by cadmium in *Donax trunculus* gonad contents during exposure and recovery. – Fresenius Environmental Bulletin 25: 5889-5895.

[67] Merad, I., Bellenger, S., Hichami, A., Khan, N. A., Soltani, N. (2017): Effect of cadmium exposure on essential omega-3 fatty acids in the edible bivalve *Donax trunculus.* – Environmental Science and Pollution Research 25: 18242-18250. https://doi.org/10.1007/s11356-017-9031-4.

[68] Mouabad, A. (1991): Toxicité comportementale et physiologique (filtration, respiration) des métaux lourds (cu, zn, hg, cd et pb) chez la moule d'eau douce *Dreissena polymorpha pallas*. – Thése de Doctorat en Ecotoxicologie, Université de Metz.

[69] Ngo, S., Gu, L., Guo, Z. (2011): Hierarchical organization in the amyloid core of yeast prion protein Ure2. – Journal of Biological Chemistry 286(34): 29691-9.

[70] NHMRC (National Health and Medical Research Council) (1987): National Food Standard A l2: Metals and Contaminants in Food. – Australia Australian Government Publishing Service, Canberra.

[71] Obaiah, J., Vivek, Ch., Padmaja, B., Sridhar, D., Peera, K. (2020): Cadmium toxicity impact on aquatic organisms oxidative stress: implications for human health safety and environmental aspects. A review. – International Journal of Science and Research 9: 2277-8616.

[72] Ogidi, O. I., Charles, E. E., Onimisi, A. M., Amugeh, R. (2020): Assessment of Nutritional Properties and Heavy Metal Composition of African Giant Land Snails (*Archachatina marginata*) and Clams (*Mercenaria mercenaria*) from Ekowe Community. – European Journal of Nutrition Food and Safety. https://doi.org/ 10.9734/EJNFS/2020/v12i630242.

[73] Orban, E., Di Lena, G., Nevigato, T., Casini, I., Marzetti, A., Caproni, A. (2002): Seasonal changes in meat content, condition index and chemical composition of mussels (*Mytilus galloprovincialis*) cultured in two different Italian sites. – Food Chemistry 77(1): 57-65. https://doi.org/10.1016/S0308-8146(01)00322-3.

[74] Ounissi, M., Ziouch, O. R., Aounallah, O. (2014): Variability of the dissolved nutrient (N, P, Si) concentrations in the bay of Annaba in relation to the inputs of the Seybouse and Mafragh estuaries. – Marine Pollution Bulletin 80(1-2): 234-244. https://doi.org/10.1016/j.marpolbul.2013.12.030.

[75] Patino, D. M., Otero, J., Louza´n, A., Ojea, J., Vazquez, S. N., Alvarez-Salgado, X. A. (2021): Wedge clam (*Donax trunculus* Linnaeus, 1758) reproduction: reproductive traits and environmental influence in the NW Iberian coast and contrast across Atlantic and Mediterranean waters. – Hydrobiologia 848: 1347-1366. https://doi.org/10.1007/s10750-021-04532-x.

[76] Pruski, A. M., Dixon, D. R. (2002): Effects of cadmium on nuclear integrity and DNA repair efficiency in the gill cells of *Mytilus edulis* L. – Aquatic Toxicology 57(3): 127-37. https://doi.org/10.1016/s0166-445x(01)00192-8.

[77] Rabei, A., Hichami, A., Beldi, H., Bellenger, S., Akhtar Khan, N. A., Soltani, N. (2018): Fatty acid composition, enzyme activities and metallothioneins in *Donax trunculus* (Mollusca, Bivalvia) from polluted and reference sites in the Gulf of Annaba (Algeria):

http://www.aloki.hu ● ISSN 1589 1623 (Print) ● ISSN 1785 0037 (Online)
DOI: http://dx.doi.org/10.15666/aeer/1906_51035128

Pattern of recovery during transplantation. – Environmental Pollution 237: 900-907. https://doi.org/10.1016/j.envpol.2018.01.041.

[78] Ragi, A. S., Leena, P. P., Cheriyan, E., Nair, S. M. (2017): Heavy metal concentrations in some gastropods and bivalves collected from the fishing zone of South India. – Marine Pollution Bulletin 118(1-2): 452-458. https://doi.org/10.1016/j.marpolbul.2017.03.029.

[79] Richir, J., Gobert, S. (2014): The effect of size, weight, body compartment, sex and reproductive status on the bioaccumulation of 19 trace elements in rope-grown *Mytilus galloprovincialis*. – Ecology Indicators 36: 33-47. https://doi.org/10.1016/j.ecolind.2013.06.021.

[80] Romeo, M., Gnassia-Barelli, M. (1988): *Donax trunculus* and *Venus verrucosa* as bioindicators of trace metal concentrations in Mauritanian costal waters. – Marine Biology 99: 223-227.

[81] Salama, A., Radwan, M. (2005): Heavy metals (Cd, Pb) and trace elements (Cu, Zn) contents in some foodstuffs from the Egyptian market. – Emirates Journal of Food and Agriculture 17(1): 34-42. https://doi.org/10.9755/ejfa.v12i1.5046.

[82] Sall, M. L., Diagne, D. A. K., Gningue-Sall, D., Aaron, S. E., Aaron, J. J. (2020): Toxic heavy metals: impact on the environment and human health, and treatment with conducting organic polymers, a review. – Environmental Science and Pollution Research 27: 29927-29942. https://doi.org/10.1007/s11356-020-09354-3.

[83] Sidoumou, Z., Gnassia-Barelli, M., Roméo, M. (1997): Cadmium and calcium uptake in the mollusc *Donax rugosus* and effect of a calcium channel blocker. – Bulletin of Environmental Contamination and Toxicology 58(2): 318-25. https://doi.org/10.1007/s001289900337.

[84] Sleimi, N., Kouki, R., HadjAmmar, M., Ferreira, R., Perez-Clemente, R. (2021): Barium effect on germination, plant growth, and antioxidant enzymes in *Cucumis sativus* L. plants. – Food Science & Nutrition 9(4): 2086-2094. https://doi.org/10.1002/fsn3.2177.

[85] Sohail, M., Khan, M. N., Chaudhry, A. S., Qureshi, N. A. (2016): Bioaccumulation of heavy metals and analysis of mineral element alongside proximate composition in foot, gills and mantle of freshwater mussels (*Anodonta anatina*). – Rendiconti Lincei. Scienze Fisiche e Naturali 27: 687-696. https://doi.org/ 10.1007/s12210-016-0551-5.

[86] Sokolowski, A., Bawazir, A. S., Wolowicz, M. (2004): Trace metals in the brown mussel *Perna perna* from the coastal waters off Yemen (Gulf of Aden): how concentrations are affected by weight, sex, and seasonal cycle. – Archives of Environmental Contamination and Toxicology 46: 67-80. https://doi.org/ 10.1007/s00244-003-2164-0.

[87] Soltani, N., Amira, A., Sifi, K., Beldi, H. (2012): Environmental monitoring of the Annaba gulf (Algeria): measurement of biomarkers in *Donax trunculus* and metallic pollution. – Bullettin de la Société Zoologique de France 137(1-4): 47-56.

[88] Tlili, S., Mouneyrac, C. (2019): The wedge clam *Donax trunculus* as sentinel organism for Mediterranean coastal monitoring in a global change context. – Regional Environmental Change 19: 995-1007. https://doi.org/10.1007/s10113-018-1449-9.

[89] Tulonen, T., Pihlström, M., Lauri, A., Martti, R., 2006. Concentration of heavy metals in food wed components of small, boreal lakes. – Boreal Environmental Research 11: 185-194.

[90] Vargasmachuca, S. G. C., Ponce-Palafox, J., Arambul-Munoz, E., Lopez- Gomez, C., Arredondo-Figueroa, J. L., Spanopoulos-Herandez, M. (2017): The combined effects of salinity and temperature on the proximate composition and energetic value of spotted rose snapper *Lutjanus guttatus* (Steindachnar, 1869). – Latin American Journal Aquatic Research 45: 1054-1058. http://dx.doi.org/10.3856/vol45-issue5-fulltext-20.

[91] Verbost, P. M., Flik, G., Lock, R. A. C., Bonga, S. E. W. (1988): Cadmium inhibits plasma membrane calcium transport. – The Journal of Membrane Biology 102: 97-104.

[92] Vieira, K. S., Crapez, M. A. C., Lima, L. S., Delgado, J. F., Brito, E. B. C. C., Fonseca E. M., Baptista, N. J. A., Aguia, V. M. C. (2021): Evaluation of bioavailability of trace

http://www.aloki.hu ● ISSN 1589 1623 (Print) ● ISSN 1785 0037 (Online)
DOI: http://dx.doi.org/10.15666/aeer/1906_51035128

metals through bioindicators in an urbanized estuarine system in southeast Brazil. – Environmental Monitoring and Assessment 193-18. https://doi.org/10.1007/s10661-020-08809-x.

[93] Wen, X., Chen, A., Wu, Y., Yang, Y., Xu, Y., Xia, W., Zhang, Y., Cao, Y., Chen, S. (2020): Comparative evaluation of proximate compositions and taste attributes of three Asian hard clams (*Meretrix meretrix*) with different shell colors. – International Journal of Food Properties 23(1): 400-411. https://doi.org/10.1080/10942912.2020.1733015.

[94] Wright, A. C., Fan, Y., Baker, G. L. (2018): Nutritional value and food safety of bivalve mollusc and shellfish. – Journal of Shellfish Research (37) 4: 695-708. https://doi.org/10.2983/035.037.0403.

[95] Yusoff, N. A. M., Long, S. M. (2011): Comparative bioaccumulation of heavy metals (Fe, Zn, Cu, Cd, Cr, Pb) in different edible mollusc collected from the estuary area of Sarawak River. – Proceedings of the University Malaysia Terengganu, 10th International Annual Symposium (UMTAS'11) 4−10. https://doi.org/10.1155/2014/924360.

[96] Zhang, Y., Jacob, D. J., Horowitz, H. M., Chen, L., Amos, H. M., Krabbenhoft, D. P., Sunderland, E. M. (2016): Observed decrease in atmospheric mercury explained by global decline in anthropogenic emissions. – Proceedings of the National Academy of Sciences 113(3): 526-531. https://doi.org/10.1 073/pnas.1516312113.

APPENDIX

Table A1. *One-way analysis of variance (ANOVA) of moisture contents for females at 48 h*

Source	df	SS	MS	F	P value
Concentration	2	21.05	10.527	9.34	0.006
Error	9	10.15	1.127		
Total	11	31.20			

Table A2. *One-way analysis of variance (ANOVA) of moisture contents for females at 96 h*

Source	df	SS	MS	F	P value
Concentration	2	59.655	29.8275	48.17	0.000
Error	9	5.573	0.6192		
Total	11	65.228			

Table A3. *One-way analysis of variance (ANOVA) of moisture contents for males at 48 h*

Source	df	SS	MS	F	P value
Concentration	2	21.15	10.576	6.45	0.018
Error	9	14.75	1.639		
Total	11	35.90			

Table A4. *One-way analysis of variance (ANOVA) of moisture contents for males at 96 h*

Source	df	SS	MS	F	P value
Concentration	2	65.44	32.722	26.58	0.000
Error	9	11.08	1.231		
Total	11	76.52			

http://www.aloki.hu ● ISSN 1589 1623 (Print) ● ISSN 1785 0037 (Online)
DOI: http://dx.doi.org/10.15666/aeer/1906_51035128

Table A5. *Three-way analysis of variance (ANOVA) of moisture contents*

Source	df	SS	MS	F	P value
Concentration	2	101.247	50.6233	49.05	0.000
Time	2	132.016	66.0081	63.96	0.000
Sex	1	75.502	75.5016	73.16	0.000
Error	54	55.729	1.0320		
Total	71	430.641			

Table A6. *One-way analysis of variance (ANOVA) of dry matter contents for females at 48 h*

Source	df	SS	MS	F	P value
Time	2	21.03	10.513	9.34	0.006
Error	9	10.13	1.125		
Total	11	31.15			

Table A7. *One-way analysis of variance (ANOVA) of dry matter contents for females at 96 h*

Source	df	SS	MS	F	P value
Time	2	58.680	29.3400	44.24	0.000
Error	9	5.969	0.6632		
Total	11	64.649			

Table A8. *One-way analysis of variance (ANOVA) of dry matter contents for males at 48 h*

Source	df	SS	MS	F	P value
Concentration	2	21.15	10.576	6.45	0.018
Error	9	14.75	1.639		
Total	11	35.90			

Table A9. *One-way analysis of variance (ANOVA) of dry matter contents for males at 96 h*

Source	df	SS	MS	F	P value
Concentration	2	65.44	32.722	26.58	0.000
Error	9	11.08	1.231		
Total	11	76.52			

Table A10. *Three-way analysis of variance (ANOVA) of dry matter contents*

Source	df	SS	MS	F	P value
Concentration	2	100.709	50.3543	47.36	0.000
Time	2	130.981	65.4905	61.59	0.000
Sex	1	77.439	77.4390	72.83	0.000
Error	54	57.419	1.0633		
Total	71	432.197			

http://www.aloki.hu ● ISSN 1589 1623 (Print) ● ISSN 1785 0037 (Online)
DOI: http://dx.doi.org/10.15666/aeer/1906_51035128

Table A11. *One-way analysis of variance (ANOVA) of ash contents for females at 48 h*

Source	df	SS	MS	F	P value
Concentration	2	9.881	4.9406	19.82	0.001
Error	9	2.243	0.2493		
Total	11	12.125			

Table A12. *One-way analysis of variance (ANOVA) of ash contents for females at 96 h*

Source	df	SS	MS	F	P value
Concentration	2	13.388	6.6938	34.57	0.000
Error	9	1.742	0.1936		
Total	11	15.130			

Table A13. *One-way analysis of variance (ANOVA) of ash contents for males at 48 h*

Source	df	SS	MS	F	P value
Concentration	2	7.797	3.8985	19.62	0.001
Error	9	1.788	0.1987		
Total	11	9.585			

Table A14. *One-way analysis of variance (ANOVA) of ash contents for males at 96 h*

Source	df	SS	MS	F	P value
Concentration	2	12.453	6.2264	32.64	0.000
Error	9	1.717	0.1908		
Total	11	14.170			

Table A15. *Three-way analysis of variance (ANOVA) of ash contents*

Source	df	SS	MS	F	P value
Concentration	2	28.518	14.2588	60.98	0.000
Time	2	32.972	16.4858	70.50	0.000
Sex	1	15.522	15.5217	66.38	0.000
Error	54	12.628	0.2338		
Total	71	104.814			

Table A16. *One-way analysis of variance (ANOVA) of fat contents for females at 48 h*

Source	df	SS	MS	F	P value
Concentration	2	0.12740	0.063700	11.37	0.003
Error	9	0.05040	0.005600		
Total	11	0.17780			

http://www.aloki.hu ● ISSN 1589 1623 (Print) ● ISSN 1785 0037 (Online)
DOI: http://dx.doi.org/10.15666/aeer/1906_51035128

Table A17. *One-way analysis of variance (ANOVA) of fat contents for females at 96 h*

Source	df	SS	MS	F	P value
Concentration	2	0.63112	0.315558	91.17	0.000
Error	9	0.03115	0.003461		
Total	11	0.66227			

Table A18. *One-way analysis of variance (ANOVA) of fat contents for males at 48 h*

Source	df	SS	MS	F	P value
Concentration	2	0.07052	0.035258	24.84	0.000
Error	9	0.01278	0.001419		
Total	11	0.08329			

Table A19. *One-way analysis of variance (ANOVA) of fat contents for males at 96 h*

Source	df	SS	MS	F	P value
Concentration	2	0.91805	0.459025	83.33	0.000
Error	9	0.04958	0.005508		
Total	11	0.96763			

Table A20. *Three-way analysis of variance (ANOVA) of fat contents*

Source	df	SS	MS	F	P value
Concentration	2	0.91301	0.45650	130.50	0.000
Time	2	1.94311	0.97155	277.73	0.000
Sex	1	4.70222	4.70222	1344.20	0.000
Error	54	0.18890	0.00350		
Total	71	8.58500			

Table A21. *One-way analysis of variance (ANOVA) of Ca contents for females at 48 h*

Source	df	SS	MS	F	P value
Concentration	2	156452	78226.0	49667.29	0.000
Error	6	9	1.6		
Total	8	156461			

Table A22. *One-way analysis of variance (ANOVA) of Ca contents for females at 96 h*

Source	df	SS	MS	F	P value
Concentration	2	173595	86797.6	13938.86	0.000
Error	6	37	6.2		
Total	8	173633			

http://www.aloki.hu ● ISSN 1589 1623 (Print) ● ISSN 1785 0037 (Online)
DOI: http://dx.doi.org/10.15666/aeer/1906_51035128

Table A23. *One-way analysis of variance (ANOVA) of Ca contents for males at 48 h*

Source	df	SS	MS	F	P value
Concentration	2	8284.63	4142.32	823.03	0.000
Error	6	30.20	5.03		
Total	8	8314.83			

Table A24. *One-way analysis of variance (ANOVA) of Ca contents for males at 96 h*

Source	df	SS	MS	F	P value
Concentration	2	24391.6	12195.8	5624.86	0.000
Error	6	13.0	2.2		
Total	8	24404.6			

Table A25. *Three-way analysis of variance (ANOVA) of Ca contents*

Source	df	SS	MS	F	P value
Concentration	2	185511	92755	14560.76	0.000
Time	2	185975	92988	14597.25	0.000
Sex	1	507217	507217	79623.14	0.000
Error	36	229	6		
Total	53	1110808			

Table A26. *One-way analysis of variance (ANOVA) of Fe contents for females at 48 h*

Source	df	SS	MS	F	P value
Concentration	2	2930.89	1465.44	182.74	0.000
Error	6	48.12	8.02		
Total	8	2979.00			

Table A27. *One-way analysis of variance (ANOVA) of Fe contents for females at 96 h*

Source	df	SS	MS	F	P value
Concentration	2	6437.73	3218.86	928.63	0.000
Error	6	20.80	3.47		
Total	8	6458.53			

Table A28. *One-way analysis of variance (ANOVA) of Fe contents for males at 48 h*

Source	df	SS	MS	F	P value
Concentration	2	28.30	14.151	7.42	0.024
Error	6	11.47	1.908		
Total	8	39.75			

http://www.aloki.hu ● ISSN 1589 1623 (Print) ● ISSN 1785 0037 (Online)
DOI: http://dx.doi.org/10.15666/aeer/1906_51035128

Table A29. *One-way analysis of variance (ANOVA) of Fe contents for males at 96 h*

Source	df	SS	MS	F	P value
Concentration	2	377.60	188.802	100.77	0.000
Error	6	11.24	1.874		
Total	8	388.85			

Table A30. *Three-way analysis of variance (ANOVA) of Fe contents*

Source	df	SS	MS	F	P value
Concentration	2	3959.3	1979.7	325.15	0.000
Time	2	6045.8	3022.9	496.49	0.000
Sex	1	50683.5	50683.5	8324.47	0.000
Error	36	219.2	6.1		
Total	53	68488.0			

Table A31. *One-way analysis of variance (ANOVA) of Zn contents for females at 48 h*

Source	df	SS	MS	F	P value
Concentration	2	607.183	303.592	954.29	0.000
Error	6	1.909	0.318		
Total	8	609.092			

Table A32. *One-way analysis of variance (ANOVA) of Zn contents for females at 96 h*

Source	df	SS	MS	F	P value
Concentration	2	2144.77	1072.39	1636.34	0.000
Error	6	3.93	0.66		
Total	8	2148.70			

Table A33. *One-way analysis of variance (ANOVA) of Zn contents for males at 48 h*

Source	df	SS	MS	F	P value
Concentration	2	1457.19	728.597	208.19	0.000
Error	6	21.00	3.500		
Total	8	1478.19			

Table A34. *One-way analysis of variance (ANOVA) of Zn contents for males at 96 h*

Source	df	SS	MS	F	P value
Concentration	2	2899.01	1449.51	7025.45	0.000
Error	6	1.24	0.21		
Total	8	2900.25			

http://www.aloki.hu ● ISSN 1589 1623 (Print) ● ISSN 1785 0037 (Online)
DOI: http://dx.doi.org/10.15666/aeer/1906_51035128

Table A35. *Three-way analysis of variance (ANOVA) of Zn contents*

Source	df	SS	MS	F	P value
Concentration	2	4175.1	2087.57	2074.06	0.000
Time	2	4972.4	2486.18	2470.09	0.000
Sex	1	509.6	509.56	506.26	0.000
Error	36	36.2	1.01		
Total	53	12662.3			

Table A36. *One-way analysis of variance (ANOVA) of Cd contents for females at 48 h*

Source	df	SS	MS	F	P value
Concentration	2	398.764	199.382	2811.72	0.000
Error	6	0.425	0.071		
Total	8	399.189			

Table A37. *One-way analysis of variance (ANOVA) of Cd contents for females at 96 h*

Source	df	SS	MS	F	P value
Concentration	2	428.030	214.015	352.97	0.000
Error	6	3.638	0.606		
Total	8	431.668			

Table A38. *One-way analysis of variance (ANOVA) of Cd contents for males at 48 h*

Source	df	SS	MS	F	P value
Concentration	2	151.840	75.9201	126.27	0.000
Error	6	3.608	0.6013		
Total	8	155.448			

Table A39. *One-way analysis of variance (ANOVA) of Cd contents for males at 96 h*

Source	df	SS	MS	F	P value
Concentration	2	189.553	94.7763	206.78	0.000
Error	6	2.750	0.4583		
Total	8	192.303			

Table A40. *Three-way analysis of variance (ANOVA) of Cd contents*

Source	df	SS	MS	F	P value
Concentration	2	697.70	348.850	770.06	0.000
Time	2	577.08	288.541	636.93	0.000
Sex	1	177.02	177.018	390.76	0.000
Error	36	16.31	0.453		
Total	53	2016.23			

http://www.aloki.hu ● ISSN 1589 1623 (Print) ● ISSN 1785 0037 (Online)
DOI: http://dx.doi.org/10.15666/aeer/1906_51035128

IMPACT OF EXPERIMENTAL FREEZE-THAW EVENTS ON BACTERIAL COMMUNITY DYNAMICS IN PETROLEUM POLLUTED TEMPERATE SOILS

OKONKWO, C. J.[1] – LIU, N.[1,2*] – LI, J.[1] – AHMED, A.[1]

[1]*Key Laboratory of Groundwater Resources and Environment, Ministry of Education, College of New Energy and Environment, Jilin University, Changchun 130021, China*

[2]*Institute of Groundwater and Earth Science, Jinan University, Guangzhou City 510632, China*

**Corresponding author*
email: liuna@jlu.edu.cn

(Received 1st Sep 2021; accepted 28th Oct 2021)

Abstract. Soil bacteria are important drivers of biogeochemical cycles and they participate in the degradation of contaminants in petroleum polluted soils. Here, we investigated the influence of freeze-thaw events on bacterial community structure and diversity in petroleum-polluted temperate soils. Four temperate soils from Northern China (clean (CS), short-term diesel fuel-pollution (SS1), short-term crude oil-pollution (SS2), and weathered petroleum-pollution (PS)) were subjected to freeze-thaw events with a temperature range of -20 to + 20 °C for 47 days. In this study, polymerase chain reaction and high-throughput sequencing of soil microbial DNA were applied to investigate the compositions of microorganisms including alpha and beta diversity in the soils. Results showed that after the freezing and thawing treatments, Proteobacteria was still the predominant phylum but its relative abundance in the clean and short-term polluted soils changed whereas it remained constant in PS. The bacterial community compositions in the short-term polluted soils were the most affected by freeze-thaw events. Overall, our results established that the dissimilarities in bacterial communities in the soils were more of a result of their contamination profiles than their exposure to freeze-thaw events.
Keywords: *temperature variation, oil pollution, α-diversity, beta-diversity*

Introduction

Petroleum pollution represents a major source of soil and groundwater contamination in the cold temperate regions (Aislabie et al., 2004). The impact of contamination is usually more severe in colder environments as the ecosystems present are generally more sensitive to temperature variations (Bell et al., 2012). Consequently, the remediation of petroleum contaminants in cold environments faces challenges such as nutrient deficiency and slower degradation rates due to lower surface temperatures (Yang et al., 2019). Hence, the successful bioremediation of petroleum-contaminated sites in most cold climate regions requires an in-depth understanding of the diversity and dynamics of the indigenous petroleum degrading microorganisms and their responses to changing temperature regimes (Gavazov et al., 2017).

The freeze-thaw event in soils is a common but complicated process which occurs in temperate and cold climate soils (Ren et al., 2018). Most temperate environments experience significant annual variations in freeze thaw cycles with seasonal transitions occurring about twice in a year (Guoqing et al., 2014). Freeze-thaw cycles (FTCs) can be categorized into annual and diurnal FTCs with the frequency of the latter changing under climate warming scenarios (Wang et al., 2017). Both the annual and diurnal FTCs exert great influence on soil physicochemical and biological properties (Børresen et al., 2007). Their influence is mainly due to the creation of different soil microenvironments

http://www.aloki.hu ● ISSN 1589 1623 (Print) ● ISSN 1785 0037 (Online)
DOI: http://dx.doi.org/10.15666/aeer/1906_51295157

especially in terms of unfrozen water availability in the soil matrices and nutrient release (Henry, 2007; Olsson et al., 2003). Skogland and colleagues (1988) estimated that a single FTC resulted in respiratory losses equivalent to 15% microbial mass carbon. In another study by Schimel et al. (2007), they observed that one FTC could release carbon to the atmosphere corresponding to as much as 25% of the net annual primary production in an Alaskan tussock tundra region. This release of carbon is expected to exacerbate climate change (Kumar et al., 2013).

In a changing climate, the temperate regions including the Eurasia drylands where Northern China is situated are expected to undergo substantial warming with a projected increase in average air temperature of 2-4 °C in this century (IPCC, 2007; Schmidhuber and Tubiello, 2007). Climate modelling studies have also confirmed that reduced snow cover in winter and consequentially decreased insulation of soils against freezing results in increased freeze-thaw frequency (Christensen et al., 2007; Kimoto, 2005). Such increases in the frequency of freeze-thaw processes are of ecological interest because of their impacts on soil microbial communities and nutrient transformation especially in petroleum polluted environments. The distribution of microbes in petroleum polluted soils has been well interpreted (Wu et al., 2016). For instance, in oil-contaminated soils, the microbial community composition has been shown to shift in favour of the petroleum hydrocarbon degraders (Siles and Margesin, 2018). Previous studies conducted using high-throughput sequencing technology have shown that the changes in soil microbial population and diversity in oil-polluted sites are higher compared to clean, uncontaminated soil, and their metabolic activities were susceptible to sensitivity by the external environment (Trellu et al., 2016; Igun et al., 2019). It is essential to mention that the nature and duration of contamination (short or long term) could be a critical factor in determining how microbial communities respond as tolerance may be developed over time. Additionally, as these polluted soils undergo episodes of freezing and thawing induced by climate change, the associated temperature variations can further influence the distribution characteristics of microbial communities occurring in ecosystems where organisms may be at the limit of their physiological tolerance. Therefore, monitoring the responses of soil microbes in petroleum polluted soils to variations in simulated freeze/thaw temperature regimes would provide useful information that can be applied in optimizing the current or designing new bioremediation strategies for contaminated sites in the temperate region as it experiences climate change.

Although some studies have been conducted on the effects of FTCs on microbial communities in soils from temperate regions (Ren et al., 2018; Han et al., 2018; Juan et al., 2018) detailed datasets on the effects of freeze-thaw events on microbial communities in petroleum polluted soils are still lacking. Our research here addressed the following questions: Can the freeze-thaw processes triggered by climate change affect the distribution characteristics of bacterial communities in weathered petroleum polluted soils and ones affected by short-term pollution? What happens to the petroleum hydrocarbon degraders in short-term and weathered petroleum polluted soils when they are subjected to an hypothetical freezing and thawing rate of 2 °C per day similar to the global climate change projection for Asia (Li et al., 2018; Lin et al., 2018)? We hypothesized that freeze-thaw events can have a direct impact on the diversity, abundance, and responsiveness of soil bacterial communities in short-term and weathered petroleum contaminated soils. To test this hypothesis, a controlled soil incubation experiment to simulate freeze-thaw conditions (-20 to 20 °C) was conducted

http://www.aloki.hu ● ISSN 1589 1623 (Print) ● ISSN 1785 0037 (Online)
DOI: http://dx.doi.org/10.15666/aeer/1906_51295157

using four soils (clean soil, short-term diesel polluted soil, short-term crude oil-polluted soil and weathered petroleum polluted soil). Polymerase chain reaction and high-throughput sequencing of soil microbial DNA were applied to investigate the compositions of microorganisms and alpha diversity in the soils at ten temperature points. Our objectives were (1) to compare differences in the abundance and diversity of bacterial communities across the four soil types during freezing and thawing periods. (2) to investigate the microbial community dynamics in each soil as a function of contamination type.

Materials and methods

Soil sampling and analysis

The weathered petroleum-polluted soil (PS) sample was collected near the petroleum well (sampling depth < 20 cm) which had been exploited for about twenty years in Songyuan city of Jilin Province, China (45.1375° N, 124.8348° E) while the clean natural soil (CS) was collected from a site in Changchun city, Jilin Province, China (39° 7'55" N, 117°11'53" E), with no history of petroleum contamination and also confirmed by GC-MS analysis of C10 – C36 petroleum hydrocarbons. The methods of sampling, collection and transportation were according to the description of Wu et al. (2016). Both sampling sites (situated in Jilin Provinces) are located in a cold temperate continental monsoon climate with an average precipitation of 500-650 nm, an annual average temperature of 1-2 °C, and an average frost-free period of 120-140 days (Guo et al., 2013).

In this study, two types of short-term petroleum polluted soil were used, SS1 and SS2 represent diesel-oil amended and crude-oil amended soil, respectively. SS1 was prepared by adding diesel oil to the clean soil at a percentage of 10% (volume/weight) while for SS2, crude oil was added to clean soil at a percentage of 10% (volume/weight) and thoroughly homogenized with a glass rod. The amended soils (short-term petroleum polluted soils) were left at room temperature for two days before subjecting them to the freeze-thaw cycles. The physical and chemical properties of the soils have been previously characterized in our earlier published study (Okonkwo et al., 2021).

Freeze-thaw microcosm

The soil samples (an equivalent of 150 g of dry soil) were incubated in a specialised temperature and humidity programmable machine (HD-GDJS, China). The samples were incubated for 47 days, starting with a pre-incubation step at + 20 °C for 48 h, then a gradual decrease to -20 °C over 20 days, followed by -20 °C for five days and a thawing phase with increasing temperature over 20 days to + 20 °C thereby providing a simulation of repeated freezing and thawing periods (9). The freezing and thawing rates were hypothetically set at 2 °C per day and the experiment involved four extended phases: pre-incubation phase (20 °C), freezing phase (10 °C to -20 °C), transition phase (-20 °C) and thawing phase (-10 °C to 20 °C) (*Fig. 1*). Samples were obtained between five-day intervals at + 20, + 10, 0, -10, -20 °C during the freezing phase; these samples will be referred to as $F_{20°C}$, $F_{10°C}$, $F_{0°C}$, $F_{-10°C}$, and $F_{-20°C}$ respectively. Following the five days at -20 °C, samples were obtained at five-day intervals -20, -10, 0, + 10, + 20 °C in the thawing phase; these samples will be referred to as $T_{-20°C}$, $T_{-10°C}$, $T_{0°C}$, $T_{+10°C}$, $T_{+20°C}$ respectively.

http://www.aloki.hu ● ISSN 1589 1623 (Print) ● ISSN 1785 0037 (Online)
DOI: http://dx.doi.org/10.15666/aeer/1906_51295157

At each of the ten sampling points, two replicates were collected, labelled and immediately stored at -80 °C until DNA extraction.

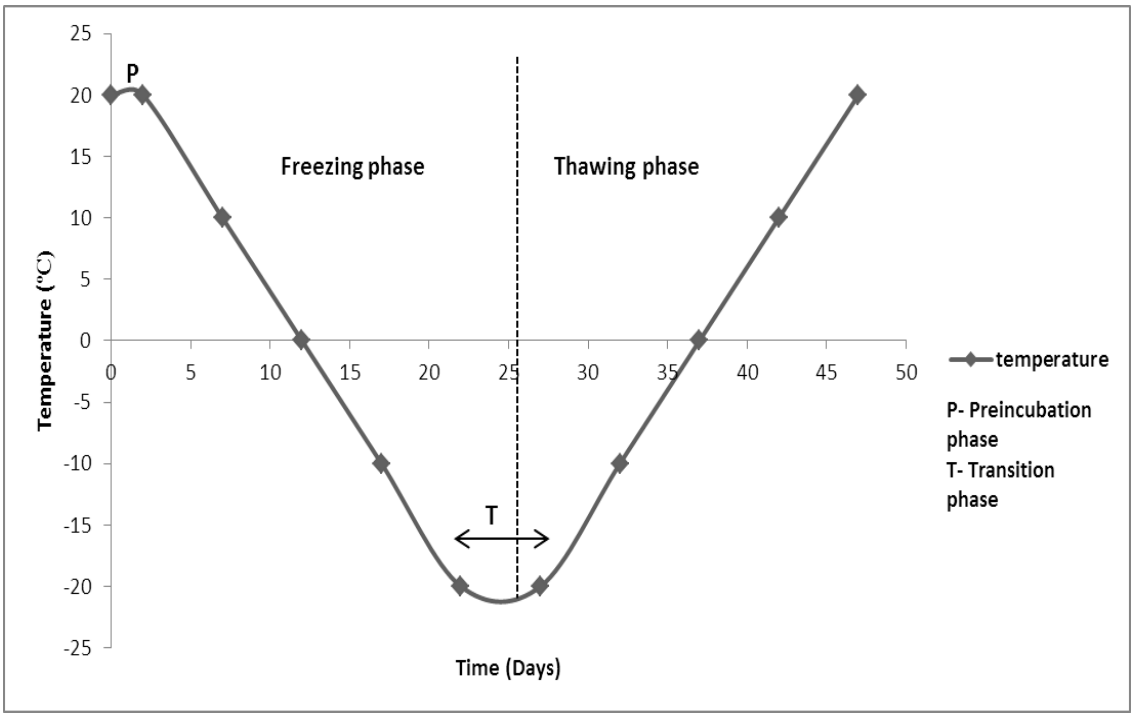

Figure 1. *Temperature regimes for the freeze-thaw experiment*

Microbial community analyses

Microbial community in the soil samples at each of the ten previously mentioned time points was determined by the following steps;

A total of 40 DNA samples were obtained from the four different soil groups (CS, PS, SS1 and SS2) after the freeze-thaw experiment. The DNA samples were labelled F1 to F40 for easy identification (*Table 1*). Soil DNA was extracted by OMEGA E.Z.N.A^{TM} Mag-Bind Soil DNA kit (Omega Bio-tek, Inc, GA, USA) according to manufacturer's instruction. DNA quality was assayed on 1% agarose gel and the quantity of DNA was determined by Qubit 3.0 DNA detection kit (Invitrogen, Carlsbad, CA, USA). A total of 10 – 20 ng of DNA was used to generate amplicons using MetaVx^{TM}Library Preparation kit (GENEWIZ, Inc, NJ, USA).

The microbial diversity was evaluated by amplicon-based metagenomic sequencing using the primers NOBAR_341F (5'-CCTACGGGNGGCWGCAG-3') and NOBAR_805R (5'-GACTACHVGGGTATCTAATCC-3') for the bacterial V3-V4 region of the 16S rRNA gene (White et al., 1990; Cisneros-de la Cueva et al., 2016). Next-generation sequencing was conducted on an Illumina Miseq Platform (Illumina, San-Diego, USA) at Sangon Biotech Co., Ltd., Shanghai, China.

Statistical and bioinformatics analyses

All merged raw sequences were trimmed using the Quantitative Insights into Microbial Ecology (QIIME) toolkit v.1.7.0 (Caporaso et al., 2010). After ambiguous bases containing "N" were trimmed, joined sequences with lengths between 240 and

http://www.aloki.hu ● ISSN 1589 1623 (Print) ● ISSN 1785 0037 (Online)
DOI: http://dx.doi.org/10.15666/aeer/1906_51295157

260 base pairs were subjected to chimera removal by U-Chime (Edgar et al., 2011) in Mothur (v.1.30.1). Lastly, OTU clustering was performed using UCLUST at a similarity level of 97% (Wang et al., 2007), and taxonomic groups were assigned using RDP Classifier (Jia et al., 2017) with a minimal 50% confidence estimate. The Mothur software (version v.1.30.1) was used to estimate coverage according to Good's estimator. Alpha (α)-diversity metrics (observed species (OTUs), Chao1 richness, Shannon's Index) were calculated for soil samples (at various freeze thaw incubation temperature points) using Mothur while Beta (β)-diversity metrics were calculated using weighted UniFrac metrics, unweighted UniFrac measures and Bray-Curtis dissimilarity matrix. The β-diversity (unweighted UniFrac and weighted UniFrac distances) were visualized using Prinicipal Co-ordinate Analysis (PCoA) ordination method (Shankar et al., 2017). Venn diagram was constructed using R statistical package (R Core Team, 2014) to visualise unique species present in the clean and polluted soils. The taxa shifts along with different incubation temperatures in the four soil groups were presented in pie charts based on the percent relative abundances of the top abundant bacteria at the genus and phylum levels respectively.

Table 1. *Sample identification codes for microbial community analyses*

Code	Soil sample	Sampling temperature (°C)	Phase	Code	Soil sample	Sampling temperature (°C)	Phase
F1	CS	20	Pre-incubation	F21	SS2	20	Pre-incubation
F2	CS	10	Freezing	F22	SS2	10	Freezing
F3	CS	0	Freezing	F23	SS2	0	Freezing
F4	CS	-10	Freezing	F24	SS2	-10	Freezing
F5	CS	-20	Freezing	F25	SS2	-20	Freezing
F6	CS	-20	Transition	F26	SS2	-20	Transition
F7	CS	-10	Thawing	F27	SS2	-10	Thawing
F8	CS	0	Thawing	F28	SS2	0	Thawing
F9	CS	10	Thawing	F29	SS2	10	Thawing
F10	CS	20	Thawing	F30	SS2	20	Thawing
F11	SS1	20	Pre-incubation	F31	PS	20	Pre-incubation
F12	SS1	10	Freezing	F32	PS	10	Freezing
F13	SS1	0	Freezing	F33	PS	0	Freezing
F14	SS1	-10	Freezing	F34	PS	-10	Freezing
F15	SS1	-20	Freezing	F35	PS	-20	Freezing
F16	SS1	-20	Transition	F36	PS	-20	Transition
F17	SS1	-10	Thawing	F37	PS	-10	Thawing
F18	SS1	0	Thawing	F38	PS	0	Thawing
F19	SS1	10	Thawing	F39	PS	10	Thawing
F20	SS1	20	Thawing	F40	PS	20	Thawing

CS: Clean soil, SS1: Short-term diesel-oil polluted soil, SS2: Short-term crude-oil polluted soil, PS: Weathered petroleum polluted soil

Prediction and analysis of gene functions of the bacterial microbiota

PICRUSt software package was used to predict predictive functional profiling of microbial communities using 16S rRNA marker gene sequences (Langille et al., 2013).

http://www.aloki.hu ● ISSN 1589 1623 (Print) ● ISSN 1785 0037 (Online)
DOI: http://dx.doi.org/10.15666/aeer/1906_51295157

The metagenomic functions and pathways are predicted against COG and KEGG pathways. Heatmap was generated using the pheatmap and Gplots packages in R.

Results and discussion

Bacterial community compositions in the clean, short-term and weathered petroleum polluted soils

Illumina MiSeq sequencing of the 40 soil samples after the FTCs produced 2143348 raw and 2069096 quality sequence reads. OTU clustering at a similarity level of 97% resulted in 133264 OTUs. The obtained bacterial sequences were classified into 46 known phyla.

According to the pie charts, the relative abundance of the genus differed dramatically among the clean, short-term and weathered polluted soils during the preincubation phase (*Fig. 2a-d*). *Arthrobacter* (7.11%)*, Janthinobacterium*, (8.40%) and *Flavobacterium* (7.96%) were the dominant groups in the clean soil group (*Fig. 2a*). The dominant genus groups in the SS1 were *Pseudomonas* (13.60%)*, Massilia* (7.19%)*,* and Arthrobacter (5.96%) (*Fig. 2b*). *Thermomonas, Arenimonas* and *Aquabacterium* accounted for > 50% of the total bacterial community in the SS2 (*Fig. 2c*) while *Pseudomonas (6.92%), Rhodoferax (5.97%), Lutibacter* (3.96%), and *Thiobacillus* (3.75%) were the predominant genus groups in PS (*Fig. 2d*). In this study, although the pre-incubation phase lasted for 48 h, it is interesting to note the rapid changes that occurred in the short-term polluted soils within the short time frame. There was a distinct redistribution in the relative abundance of the bacterial community in the short-term polluted soils SS1 and SS 2 with community composition shifting in favour of the petroleum hydrocarbon degraders *Pseudomonas* and *Massilia* in SS1 while *Thermomonas and Arenimonas* were the dominant petroleum hydrocarbon degraders in SS2. This finding is consistent with previous studies in which petroleum contamination led to the selective enrichment of oil-degrading bacteria while others were suppressed (Jia et al., 2017; Wyszkowska and Kucharski, 2005). We further observed that the selective enrichment of petroleum degraders in SS1 and SS2 differed with respect to the oil types i.e., diesel fuel and crude oil suggesting that there may be a strong association between the predominant oil-degraders found in a soil and nature of oil contaminant present in that soil. A reasonable explanation for this occurrence is that petroleum products often differ in their abilities to disrupt of soil trophic and aerobic conditions and contribute to organic carbon pools (Borowik et al., 2019). The class level results (*Fig. A1*) in the short-term polluted soils further highlights the difference in selective enrichment of bacterial classes as a function of oil contamination type. The diesel amended soil SS1 was dominated by Betaproteobacteria while Gammaproteobacteria exhibited highest abundance in the crude oil amended soil SS2 during this phase. The increase in the abundance of Beta- and Gammaproteobacterial classes in the short-term polluted soils is in line with observations made in previous studies on bacterial shifts upon contamination with petroleum (Korenblum et al., 2012; Baek et al., 2007). Hence, pollution of soil with different petroleum products may not produce similar changes in the soil microbiome.

At the phylum level, Proteobacteria was the dominant group in the clean and polluted soils during this phase of the study (*Fig. A2a-d*). They accounted for 48.56% in the clean soil, for 53. 51%, 88.98% and 74.84% in polluted soils SS1, SS2 and PS

http://www.aloki.hu ● ISSN 1589 1623 (Print) ● ISSN 1785 0037 (Online)
DOI: http://dx.doi.org/10.15666/aeer/1906_51295157

respectively. The short-term pollution of soil with petroleum products elicited notable changes in the abundance of the dominant phylum. Proteobacteria in SS1 and SS2 was higher by 4.95% and 40.42% respectively than in the clean soil CS. This finding was consistent with previous reports on cold temperate soils where Proteobacteria was the predominant phylum (Shen et al., 2014; Sun et al., 2015). Borowik et al. (2019) reported that Proteobacteria was higher by 35.3% in the soil exposed to diesel contamination compared to the control soil. The difference in relative abundance of Proteobacteria between the clean and polluted soils could be attributed to presence of alternative carbon sources. In addition, Wu et al. (2019) and Liu et al. (2020) found that the relative abundance of Proteobacteria in soil was positively correlated with hydrocarbon content. Hence, the higher hydrocarbon contents in the polluted soils might partly account for the increase in Proteobacteria in SS1, SS2 and PS.

During the freezing phase (F 10 ℃ to F -20 ℃), the identified sequences from the different soil types were affiliated with 47 bacterial genera (*Figs. 3-6*). At the beginning of the freezing phase (*Fig. 3a-d*), the bacterial genera *Arthrobacter* (8.67%) and *Janthinobacterium* (8.09%) were predominant in the clean soil. The short-term polluted soil SS1 was characterized by lower relative abundance of *Pseudomonas* (12.51%) whereas SS2 showed higher relative abundance of *Thermomonas* (55.89%) when compared to their population during the pre-incubation phase. Consistent decrease in temperature at the hypothetical rate of 2 °C per day resulted in decreased relative abundance of the predominant bacterial genera in SS1 while the abundance of *Thermomonas* in SS2 increased in response to lower temperatures (*Figs. 3c, 4c, 5c* and *6c*). *Thermomonas* is a gamma proteobacterium that has been identified as psychrotolerant with a wide growth range from 18-50 ℃ (52). In this study, *Thermomonas* was able to adapt to sub-zero freezing temperatures and selective pressure exerted by pollutants in the short-term polluted soil SS2. Further studies are however needed to confirm its suitability as a bioaugmentation candidate in remediating oil polluted temperate soils.

Among the abiotic environmental factors, temperature exerts a more direct influence on microbial populations in soil (Buckeridge et al., 2013). The relative abundance of the dominant bacterial genus (*Pseudomonas*) in the weathered polluted soil PS however remained constant through-out the freezing phase. This buffering potential observed in PS may be attributed to the ability of the dominant bacterial genus to adapt to the presence of hydrocarbon contaminants over extended period, hence they were very stable and not affected by perturbations likely to arise from the freezing phase. Ramadass et al. (2015) reported a similar trend in their microcosm study of the microbial community in weathered hydrocarbon contaminated arid soils. In this study, we also found that bacterial populations related to sulphur cycling (*Sulfuritalea* and *Sulfuricurvum*) occurred only in the weathered polluted soil PS. This was a major difference among the four soils in our study as the sulphur oxidizing genera were absent in CS and the short-term polluted soils SS1 and SS2. Generally, sulfur oxidation processes occur wherever reduced inorganic sulphur compounds are available (Meyer and Kuever, 2007). This suggests that sulphur mineralization was higher in PS compared to the clean soil and short-term polluted soils.

At the phylum level, the members of *Proteobacteria* were dominant in all the soil samples, accounting for more than 45% of bacterial phyla in both clean and polluted samples (*Figs. A3–A6* in the *Appendix*). After repeated freezing processes, SS2 had the

http://www.aloki.hu ● ISSN 1589 1623 (Print) ● ISSN 1785 0037 (Online)
DOI: http://dx.doi.org/10.15666/aeer/1906_51295157

highest relative abundance of *Proteobacteria* (91.79%) among the soils in the study. We found that the average abundance of *Proteobacteria* increased in SS2 during the freezing phase when compared to the Pre-incubation phase whereas it remained constant in PS. The results correspond roughly with previous reports. Labbe et al. (2007) suggested that cold-adapted bacteria belonging to *Proteobacteria* phylum can rapidly adapt to low sub-zero temperatures and retain metabolic activity for growth and survival. From our results, it was evident that repeated freezing did not influence the abundance of the dominant bacterial phyla present in PS. This means that the bacterial community composition in PS may have attained a form of equilibrium and stability prior to this phase.

During the transition phase (T -20 ℃), temperature was kept constant at -20 ℃ over a period of five days and we observed that there were some distinct changes in the relative abundance of the predominant genera in the experimental soil groups (*Fig. 7a-d*). In the clean soil CS, *Arthrobacter* increased in relative abundance while the abundance of *Pseudomonas* and *Thermomonas* decreased in SS1 and SS2 respectively when compared to the freezing phase. Of the classified genera in PS, the relative abundance of *Pseudomonas* (9.07%) and *Lutibacter* (5.85%) were higher when compared to their respective values during both pre-incubation and freezing phase. The observed variations in the soil types suggested that apart from temperature and the nature of oil contaminants present in the soil, there may be some other factors that might affect the composition of bacterial communities in the soil.

The thawing phase (T -10 ℃ to T 20 ℃) in this study was of particular importance because it represented a projection of increasing temperature consistent with global warming indices in Asia (Lin et al., 2018). During this phase, we observed higher relative abundance in the predominant bacterial genera in all the soil groups (*Figs. 8-11*). By the end of this phase, *Janthinobacterium* (9.28%), *Pseudomonas* (11.31%), *Thermomonas* (80.27%) and *Pseudomonas* (7.09%) were the predominant genera in CS, SS1, SS2 and PS. Although this pattern of dominance was similar to what was observed during in the initial pre-incubation and freezing phases, there was a remarkable increase in their relative abundance. For instance, the relative abundance of *Thermomonas* by the end of thawing phase (*Fig. 11c*) was 2.04 and 1.50 times higher when compared to the pre-incubation (*Fig. 2c*) and freezing phases (*Fig. 6c*) respectively. The thawing phase in soil has been well interpreted. Koponen et al. (2006) earlier reported that soil freeze-thaw events can increase nutrient concentration by destroying microbes resulting in the increased activity of the surviving microbes. This phenomenon was most evident in SS2, where the relative abundance of the predominant genus *Thermomonas* responded most positively to the warm thawing phase. Another distinct occurrence during the thawing phase was the appearance of some new genera such as *Hydrogenophaga* (0.77%), *Shingomonas* (0.16%) and *Tolumonas* (0.7%) in SS1, SS2 and PS respectively. Overall, our findings suggest that rising temperatures in the thawing phase favoured the growth of both predominant and rare petroleum degrading genera in the polluted soils.

Figures A7–A11 displayed the bacterial community composition at the phylum level, and we found that the thawing phase compensated for the decreases in relative abundance of the predominant phylum (*Proteobacteria*) in CS, SS1 and SS2 that occurred during the freezing phase. This is consistent with previous report that relative warmer temperature resulted in increased bacterial growth (Jiang et al., 2018).

http://www.aloki.hu ● ISSN 1589 1623 (Print) ● ISSN 1785 0037 (Online)
DOI: http://dx.doi.org/10.15666/aeer/1906_51295157

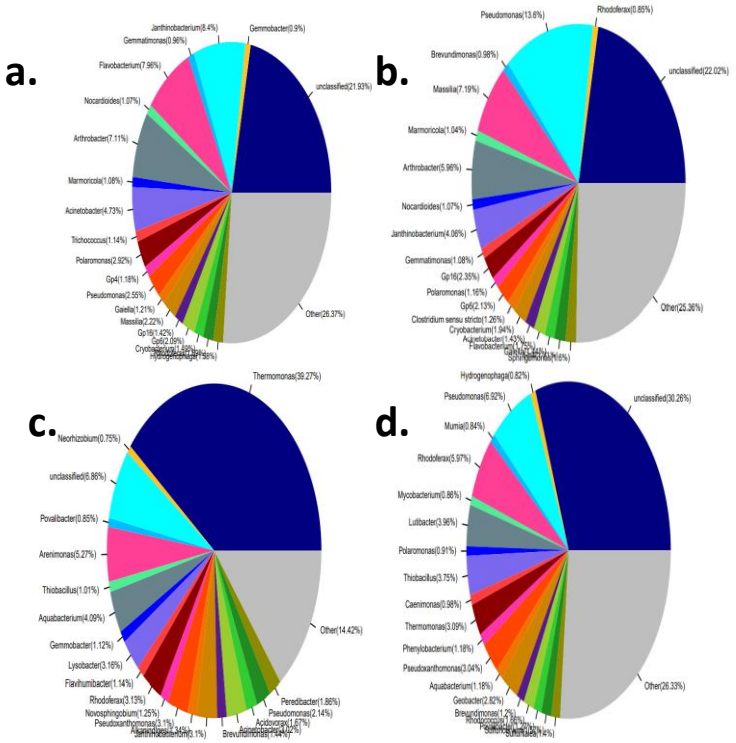

Figure 2. a-d *Bacterial genus composition in (a) Clean natural soil CS (b) Diesel-oil amended soil SS1 (c) Crude-oil amended soil SS2 (d) weathered petroleum-polluted soil PS at Pre-incubation phase (F 20 ℃)*

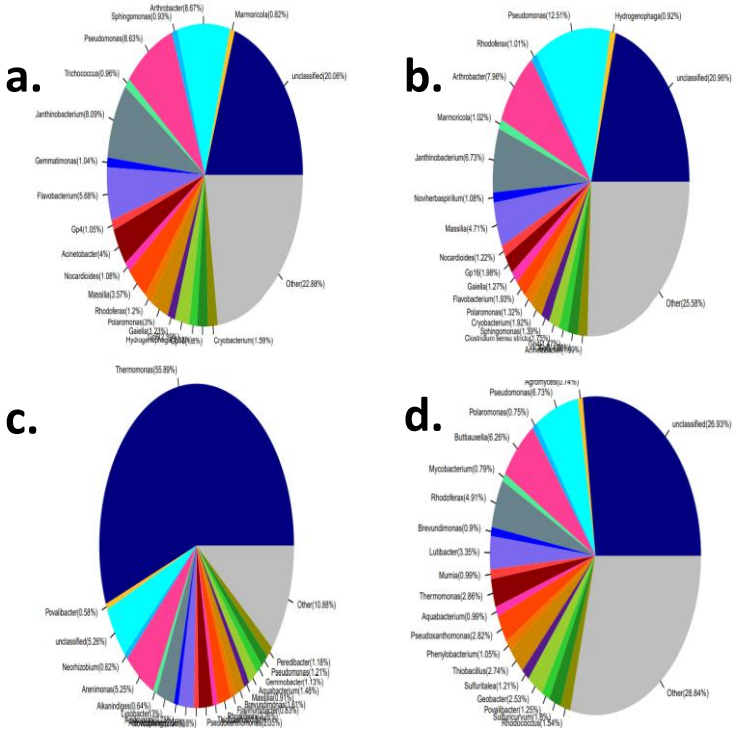

Figure 3. a-d *Bacterial genus composition in (a) Clean natural soil CS (b) Diesel-oil amended soil SS1 (c) Crude-oil amended soil SS2 (d) weathered petroleum-polluted soil PS during Freezing phase (F 10 ℃)*

http://www.aloki.hu ● ISSN 1589 1623 (Print) ● ISSN 1785 0037 (Online)
DOI: http://dx.doi.org/10.15666/aeer/1906_51295157

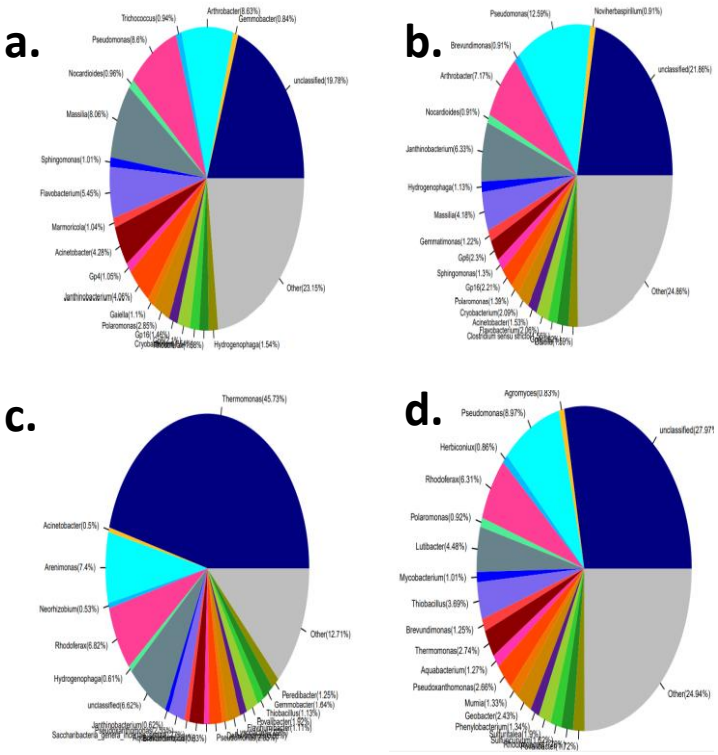

Figure 4. a-d *Bacterial genus composition in (a) Clean natural soil CS (b) Diesel-oil amended soil SS1 (c) Crude-oil amended soil SS2 (d) weathered petroleum-polluted soil PS during Freezing phase (F 0 ℃)*

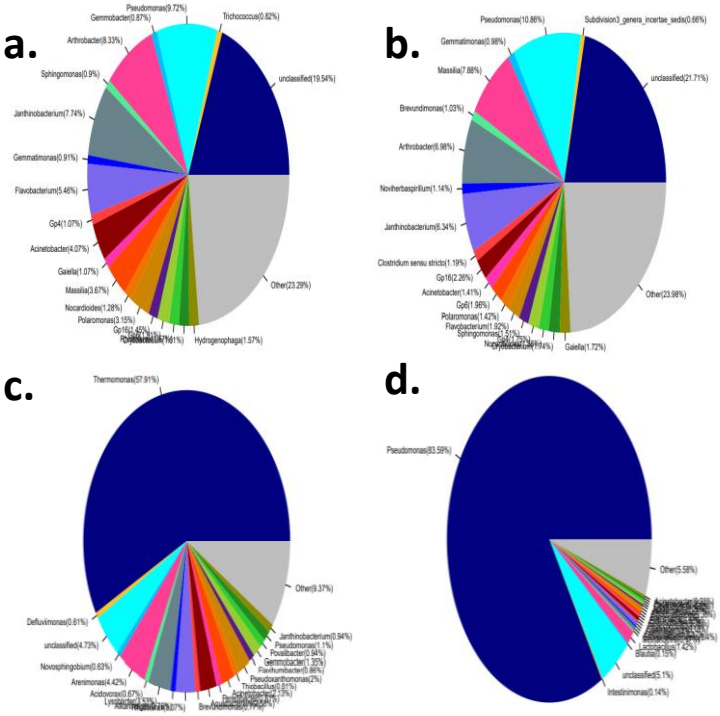

Figure 5. a-d *Bacterial genus composition in (a) Clean natural soil CS (b) Diesel-oil amended soil SS1 (c) Crude-oil amended soil SS2 (d) weathered petroleum-polluted soil PS during Freezing phase (F -10 ℃)*

http://www.aloki.hu ● ISSN 1589 1623 (Print) ● ISSN 1785 0037 (Online)
DOI: http://dx.doi.org/10.15666/aeer/1906_51295157

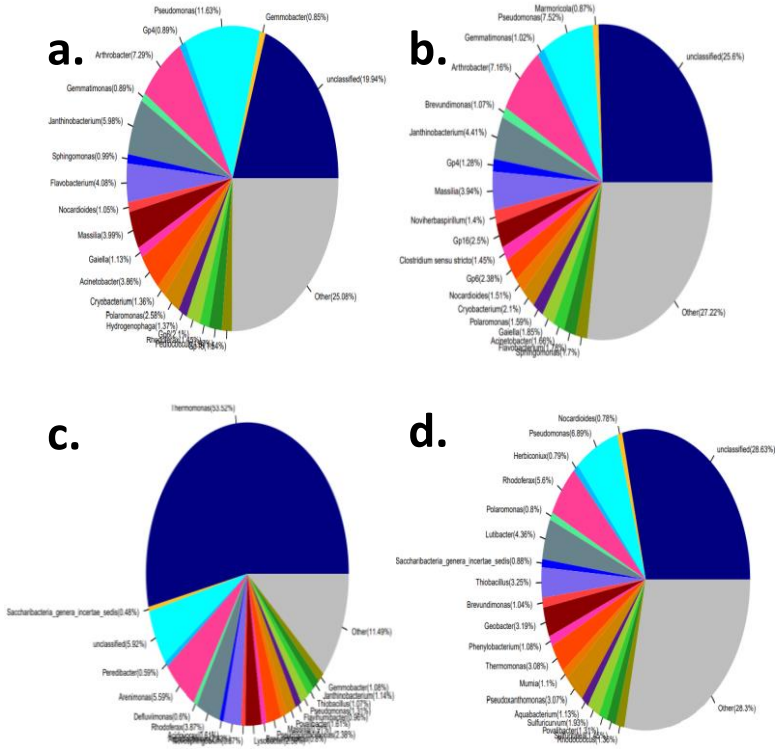

Figure 6. a-d *Bacterial genus composition in (a) Clean natural soil CS (b) Diesel-oil amended soil SS1 (c) Crude-oil amended soil SS2 (d) weathered petroleum-polluted soil PS during Freezing phase (F -20 ℃)*

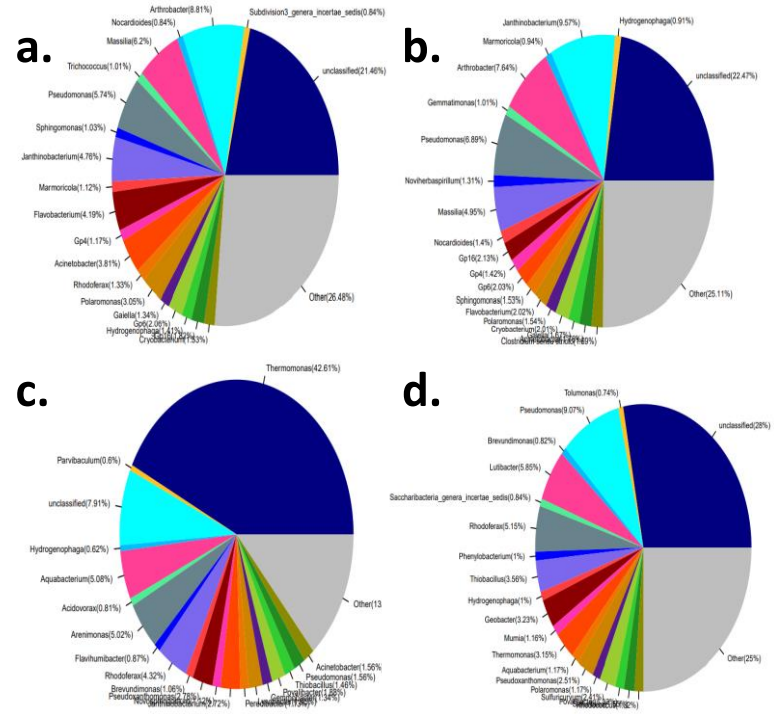

Figure 7. a-d *Bacterial genus composition in (a) Clean natural soil CS (b) Diesel-oil amended soil SS1 (c) Crude-oil amended soil SS2 (d) weathered petroleum-polluted soil PS during Transition phase (T -20 ℃)*

http://www.aloki.hu ● ISSN 1589 1623 (Print) ● ISSN 1785 0037 (Online)
DOI: http://dx.doi.org/10.15666/aeer/1906_51295157

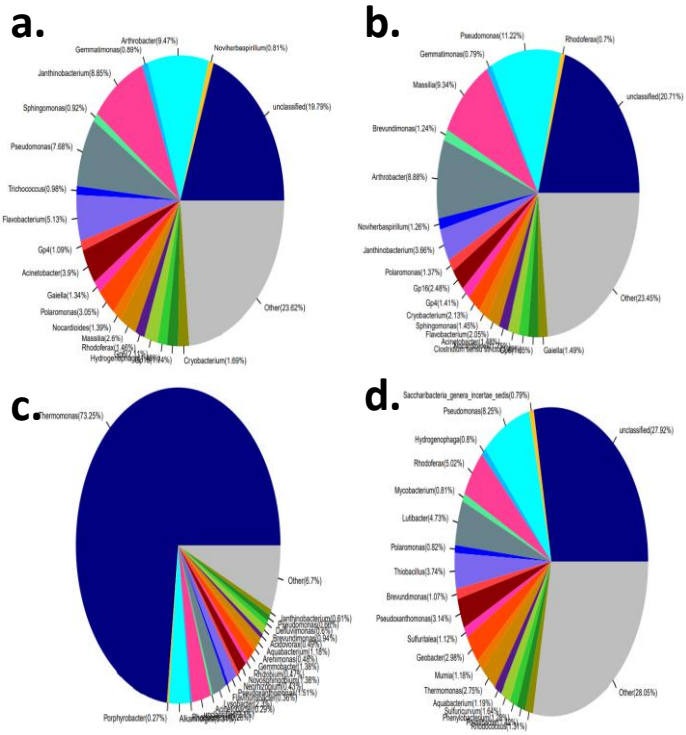

Figure 8 a-d. *Bacterial genus composition in (a) Clean natural soil CS (b) Diesel-oil amended soil SS1 (c) Crude-oil amended soil SS2 (d) weathered petroleum-polluted soil PS during Thawing phase (T -10 ℃)*

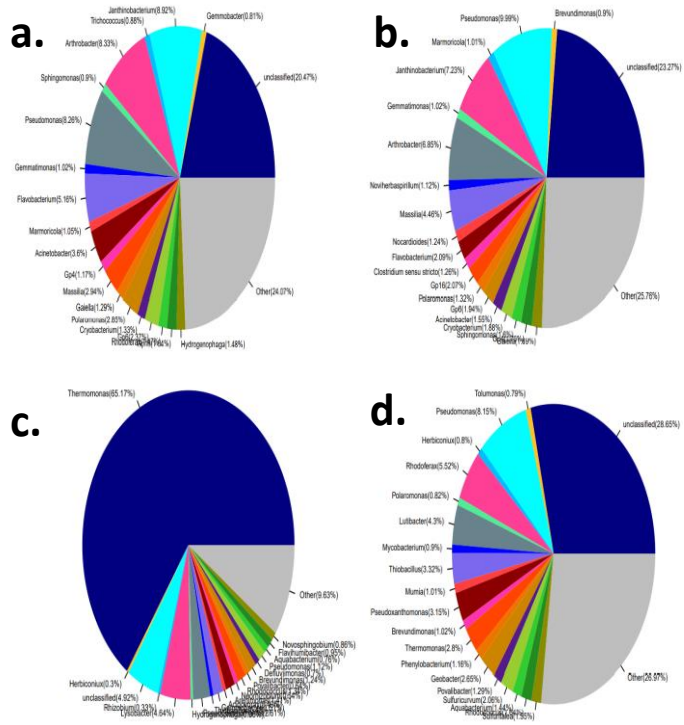

Figure 9 a-d. *Bacterial genus composition in (a) Clean natural soil CS (b) Diesel-oil amended soil SS1 (c) Crude-oil amended soil SS2 (d) weathered petroleum-polluted soil PS during Thawing phase (T 0 ℃)*

http://www.aloki.hu ● ISSN 1589 1623 (Print) ● ISSN 1785 0037 (Online)
DOI: http://dx.doi.org/10.15666/aeer/1906_51295157

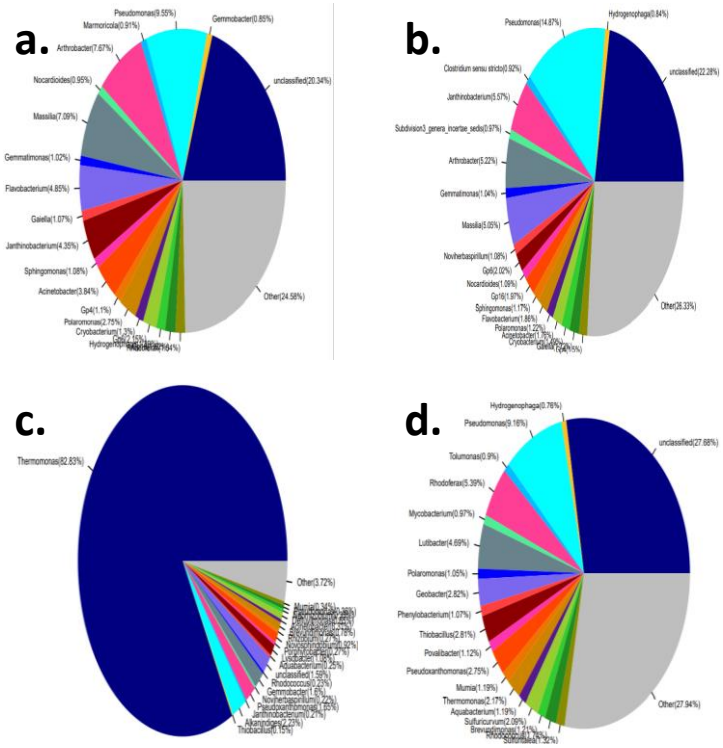

Figure 10. a-d *Bacterial genus composition in (a) Clean natural soil CS (b) Diesel-oil amended soil SS1 (c) Crude-oil amended soil SS2 (d) weathered petroleum-polluted soil PS during Thawing phase (T 10 ℃)*

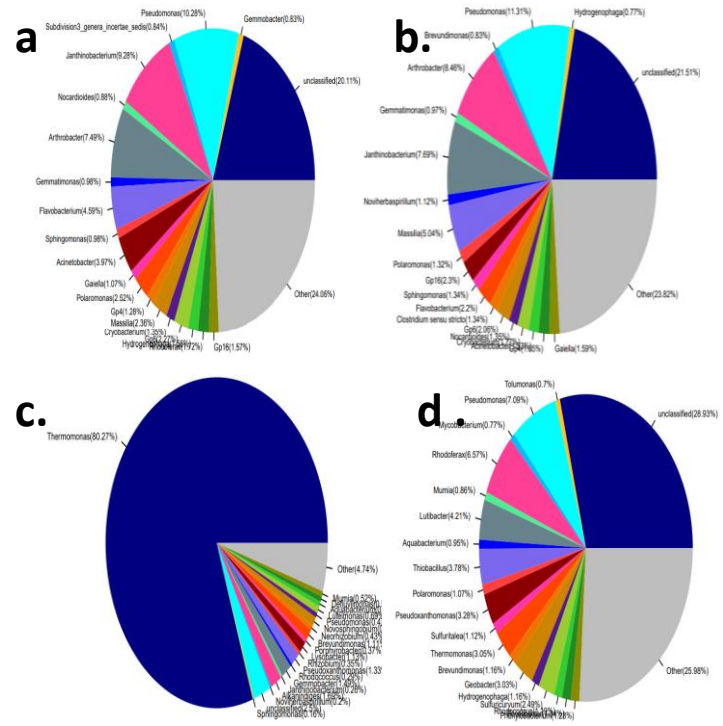

Figure 11. a-d *Bacterial genus composition in (a) Clean natural soil CS (b) Diesel-oil amended soil SS1 (c) Crude-oil amended soil SS2 (d) weathered petroleum-polluted soil PS during Thawing phase (T 20 ℃)*

http://www.aloki.hu ● ISSN 1589 1623 (Print) ● ISSN 1785 0037 (Online)
DOI: http://dx.doi.org/10.15666/aeer/1906_51295157

Bacterial community alpha diversity and presence of unique bacterial species

The results of the OTU richness and diversity analyses at the beginning of the study (F 20 °C) showed that the richness index (ACE and Chao 1) and the uniformity index (Shannon) varied among the soil samples (*Table 2*). It can be seen that the alpha diversity indices of CS was the highest while the Simpson index of SS2 was the highest. In all the samples, the order was CS > PS > SS1 > SS2 for ACE index and CS > SS1 > PS > SS2 for Shannon index. Therefore, compared to the polluted soils the bacterial diversity and richness in the clean soil was higher. Further comparison of the weathered petroleum contaminated soil PS to the short-term polluted soils revealed that the bacterial community diversity was reduced in SS1 and SS2 and this decrease was more evident in the SS2. Sutton et al. (2013) have previously reported that the presence of oil contamination significantly influences bacterial community structure and diversity, regardless of the soil matrix type, and suggested that clean samples had higher diversity than contaminated soil. From our results, we infer that the duration of oil contamination is a crucial factor that could affect bacterial community diversity and richness. The higher diversity seen in the weathered polluted soil may be attributed to a form of community adaptation to long term oil exposure. Earlier investigations conducted on long-term petroleum polluted soils also reported a trend of higher diversity when compared to newly contaminated soils (Bourceret et al., 2016; Jeanbille et al., 2016). Venn diagram (*Fig. A12*) showed the occurrence of unique bacterial species in the soil samples; 76, 85, 3 and 109 unique species were identified in the clean CS, diesel amended SS1, crude oil amended SS2, and weathered petroleum polluted PS soil respectively during the pre-incubation phase. This result indicated that the introduction of petroleum products in the soil had immediate impacts on the unique bacterial species with the number of unique species increasing and decreasing notably in the short-term polluted soils SS1 and SS2 respectively. In particular, sequences related to *Thermomonas* were found to constitute 39.27% of total sequences in the short-term polluted soil SS1 suggesting that the selective enrichment of the genus *Themomonas* may have led to the suppression of other unique bacterial species in SS2. Hence, the number of unique bacterial species in the soil samples varied as a result of contamination type with diesel and crude-oil amended soils showing distinct bacterial responses. Borowik and Wyszkowska (2018) also reported that petroleum products induced noticeable changes at the species level in polluted soils. Our results are consistent with their findings.

The alpha diversity indices of the clean and polluted soils during the freezing phase are presented in *Table 3*. The ACE index identified differences between the clean soil and the polluted soils indicating that PS had more variety of organisms than CS, SS1 and SS2 after repeated freezing. This suggests that the bacterial population in the weathered polluted soil PS are most likely cold-adapted microorganisms which are able to tolerate and survive sub-zero freezing temperatures. By the end of the freezing phase, the order in the soil was PS > CS > SS1 > SS2 for ACE index and SS2 > CS = PS > SS1 for Simpson index. Interestingly, the richness remained constant in both CS and PS during the freezing phase while community decreased and increased in SS1 and SS2 respectively. In this study, we inferred that the observed changes in richness in the newly contaminated soils SS1 and SS2 were more likely as a result of their recent pollution status rather than the exposure to freezing temperature amplitude since the community richness in the clean (control) soil remained constant. The environmental disturbance of oil contamination is one of the most significant anthropogenic activities that affect soil microbial communities (Liu et al., 2017).

http://www.aloki.hu ● ISSN 1589 1623 (Print) ● ISSN 1785 0037 (Online)
DOI: http://dx.doi.org/10.15666/aeer/1906_51295157

Table 2. *Bacterial diversity indices in the clean and polluted soils during the pre-incubation phase of the study*

Pre-incubation phase (20 °C)				
Soil type	**CS**	**SS1**	**SS2**	**PS**
Sequencing analysis				
Sequence number	46700	50682	33068	30015
OTUs number	4772	4413	1611	3118
Diversity indices				
OTU diversity				
Ace index	9288.75	6492.4	5231.8	8832.5
Chao1 index	7268.28	6144.1	3585.2	5814.3
OTU richness				
Shannon index	6.09	6.03	3.67	5.56
Simpson index	0.02	0.02	0.16	0.02
Coverage	0.95	0.97	0.97	0.94

CS: Clean soil, SS1: Short-term diesel-oil polluted soil, SS2: Short-term crude-oil polluted soil, PS: Weathered petroleum polluted soil

Table 3. *Bacterial diversity indices in the clean and polluted soils during the freezing phase (10 to -20 °C) of the study*

SOIL TYPE	**CS**				**SS1**				**SS2**				**PS**			
Temp (°C)	10	0	-10	-20	10	0	-10	-20	10	0	-10	-20	10	0	-10	-20
Sequencing analysis																
Sequence number	40660	48121	44967	49853	40853	49482	52643	55260	34280	32302	29937	33077	33299	20717	44020	47781
OTUs number	4282	4715	4483	4724	4079	4522	4396	4709	1493	1692	1377	1653	2739	2631	441	3620
Diversity indices																
OTU Richness																
Ace index	9538	10774	9906	7745	78921	8318	8333	6713,.6	5177	5713	4982	5637	7654	8090	451.3	9679
Chao1 index	7097	7916	7470	7338	6196	6699	6581	6476	3072	3465	2999	3548	5250	5189	463.6	6672
OTU Diversity																
Shannon index	5.87	5.87	5.91	5.98	5.91	6.04	5.96	6.3	2.93	3.39	2.86	3.13	5.47	5.61	1.93	5.51
Simpson index	0.02	0.02	0.02	0.02	0.02	0.02	0.02	0.01	0.31	0.21	0.33	0.28	0.02	0.02	0.36	0.02
Coverage	0.95	0.95	0.95	0.96	0.96	0.96	0.96	0.97	0.97	0.97	0.97	0.97	0.97	0.93	0.99	0.96

CS: Clean soil, SS1: Short-term diesel-oil polluted soil, SS2: Short-term crude-oil polluted soil, PS: Weathered petroleum polluted soil

The analysis of diversity indices during transition phase showed that CS had the highest bacterial diversity and richness when compared to the polluted soils (*Table 4*). The transition phase was characterized by a marked increase in the diversity in all the soil groups compared to the freezing phase thereby suggesting that the bacterial populations in the soil eventually develop coping mechanisms for extended period of lower temperature. Chattopadhyay (2002) reported that certain soil bacteria contain cryoprotective compounds such as mannitol, sorbitol, betaine etc. These low molecular weight compounds suppress the aggregation of cellular proteins during stress conditions. Other cold adapted bacterial populations have been reported to prevent cell death by using endogenous biopolymers such as extracellular polymeric substances (EPS, primarily polysaccharides). The EPS forms a capsule around the cell and prevents cell death from osmotic stress, and mechanical ice damage (Junge et al., 2006). The

http://www.aloki.hu ● ISSN 1589 1623 (Print) ● ISSN 1785 0037 (Online)
DOI: http://dx.doi.org/10.15666/aeer/1906_51295157

presence of bacterial cryoprotectants may be responsible for the increased diversity in all the soil groups. However, further studies may be required to confirm the nature and mechanism of cryoprotection in the oil polluted temperate soils.

Table 4. *Bacterial diversity indices in the clean and polluted soils during the transition phase of the study*

	Transition phase (-20 °C)			
Soil type	**CS**	**SS1**	**SS2**	**PS**
Sequencing analysis				
Sequence number	44899	59493	35225	35520
OTUs number	4623	5039	1800	3143
Diversity indices				
OTU richness				
Ace index	10203	10014	5939.8	8905
Chao1 index	7715.6	7893.8	3785.1	6078.2
OTU diversity				
Shannon index	6.09	5.98	3.61	5.51
Simpson index	0.02	0.02	0.18	0.02
Coverage	0.95	0.96	0.97	0.95

CS: Clean soil, SS1: Short-term diesel-oil polluted soil, SS2: Short-term crude-oil polluted soil, PS: Weathered petroleum polluted soil

The results of the OTU richness and diversity analyses during the thawing phase showed that bacterial diversity varied among the soil samples (*Table 5*). The order was PS > SS1 > CS > SS2 for ACE index and SS1 > CS > PS > SS1 for Shannon index. The diversity was higher in the polluted soils compared to the clean soil. In a previous study by Peng and colleagues (2015), they reported that oil-polluted soils supported more diverse bacterial community compared to the clean soil. Our findings during the thawing phase agree with their report. Although their study was for a single temperature regime, the present study highlights the changes in bacterial diversity that occurs when polluted soils are continuously subjected to warmer temperature regimes after a period of freezing. Similarly, the bacterial community richness changed after the thawing phase. A higher bacterial richness was observed in the crude oil contaminated soils when compared to the clean soil.

Beta diversity of bacterial communities

The principal component analysis (PCA) based on UniFrac distances (*Fig. 12*) revealed that the bacterial communities in the four soil samples clustered separately based on soil contamination levels. However, the bacterial communities of CS and SS1 were grouped in a cluster. The result indicated that the bacterial communities in the clean soil and diesel polluted soil were more similar to each other than the bacterial communities in the crude-oil polluted soils SS1 and PS during freezing and thawing phases. When the bacterial communities in the clean and polluted soils were compared at the phylum level, the communities in the soil groups were clustered in different axes (*Fig. 12*). Regardless of the temperature regime, samples from each of the soil groups clustered in the same axis. The result indicated that the dissimilarity in bacterial

http://www.aloki.hu ● ISSN 1589 1623 (Print) ● ISSN 1785 0037 (Online)
DOI: http://dx.doi.org/10.15666/aeer/1906_51295157

communities in the soil groups were more as a function of their contamination level rather than the freeze-thaw regime. Borowik et al. (2019) reported that the presence of petroleum product in a soil creates a new microenvironment which may greatly alter its biological properties. Our results are in consonance with their finding.

Table 5. *Bacterial diversity indices in the clean and polluted soils during the thawing phase of the study*

THAWING PHASE (-10 to 20 °C)																
SOIL TYPE	**CS**				**SS1**				**SS2**				**PS**			
Temp (°C)	-10	0	10	20	-10	0	10	20	-10	0	10	20	-10	0	10	20
Sequence numbe	45310	49162	45362	53116	49803	42728	41318	47468	36278	36982	35132	46393	27844	34179	38974	37844
OTUs num	4623	4895	4530	4787	4499	4229	3833	4485	1066	1521	801	1031	2596	3224	3330	3464
OTU Diversity																
ACE index	10249	10343	9137	7446	8992	8602	5565	9057	4432	5485	3349	3521	7325	8506	9257	10134
Chao1 index	7641	7807	7087	6977	7067	6586	5334	6992	2729	3401	1796	2328	5001	5895	6294	6738
OTU Richness																
Shannon index	5.88	5.97	5.97	5.89	5.89	6.05	6	5.91	1.93	2.48	1.32	1.56	5.49	5.56	5.55	5.53
Simpson index	0.02	0.02	0.02	0.02	0.02	0.02	0.02	0.02	0.52	0.42	0.68	0.62	0.02	0.02	0.02	0.02
Coverage	0.95	0.95	0.95	0.96	0.96	0.95	0.96	0.96	0.98	0.98	0.99	0.99	0.95	0.95	0.95	0.95

CS: Clean soil, SS1: Short-term diesel-oil polluted soil, SS2: Short-term crude-oil polluted soil, PS: Weathered petroleum polluted soil

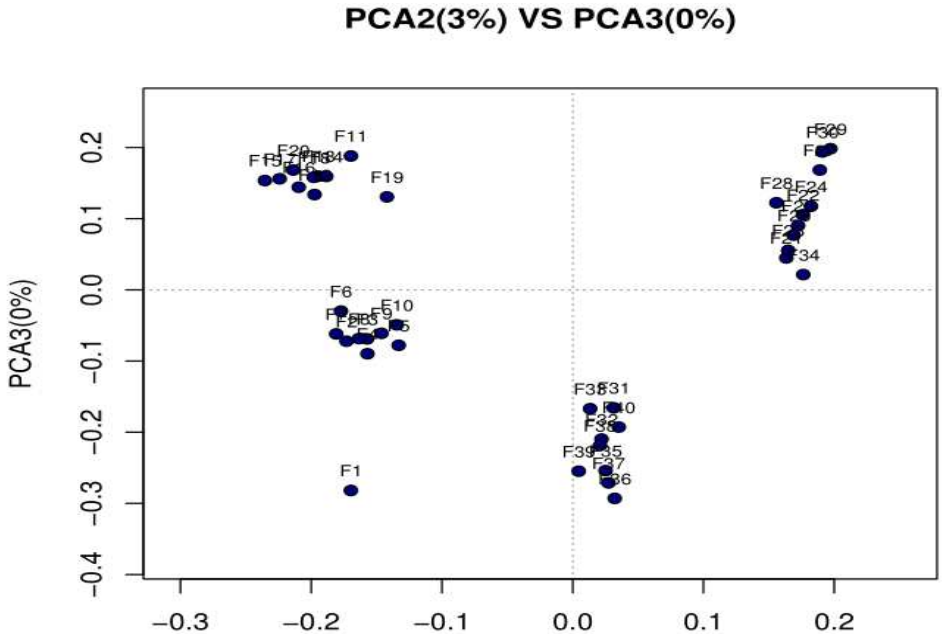

Figure 12. *Weighted UniFrac principal component analysis (PCA) at the phylum level based on the 16S rDNA gene sequence in the soil samples. F1: CS, F11: SS1, F21: SS2, F31: PS (F 20 °C, Pre-incubation phase). F2: CS, F12: SS1, F22: SS2, F32: PS (F 10 °C, Freezing phase). F3: CS, F13: SS1, F23: SS2, F33: PS (F 0 °C, Freezing phase). F4: CS, F14: SS1, F24: SS2, F34: PS (F -10 °C, Freezing phase). F5: CS, F15: SS1, F25: SS2, F35: PS (F -20 °C, Freezing phase). F6: CS, F16: SS1, F26: SS2, F36: PS (T -10 °C, Transition phase). F7: CS, F17: SS1, F27: SS2, F37: PS (T 0 °C, Thawing phase). F8: CS, F18: SS1, F28: SS2, F38: PS (T 0 °C, Thawing phase). F9: CS, F19: SS1, F29: SS2, F39: PS (T 0 °C, Thawing phase). F10: CS, F20: SS1, F30: SS2, F40: PS (T 0 °C, Thawing phase)*

http://www.aloki.hu ● ISSN 1589 1623 (Print) ● ISSN 1785 0037 (Online)
DOI: http://dx.doi.org/10.15666/aeer/1906_51295157

Functional prediction of bacterial communities

For pathways prediction (*Figs. 13* and *14*), the clean and polluted soil samples were aggregated into two major clusters.

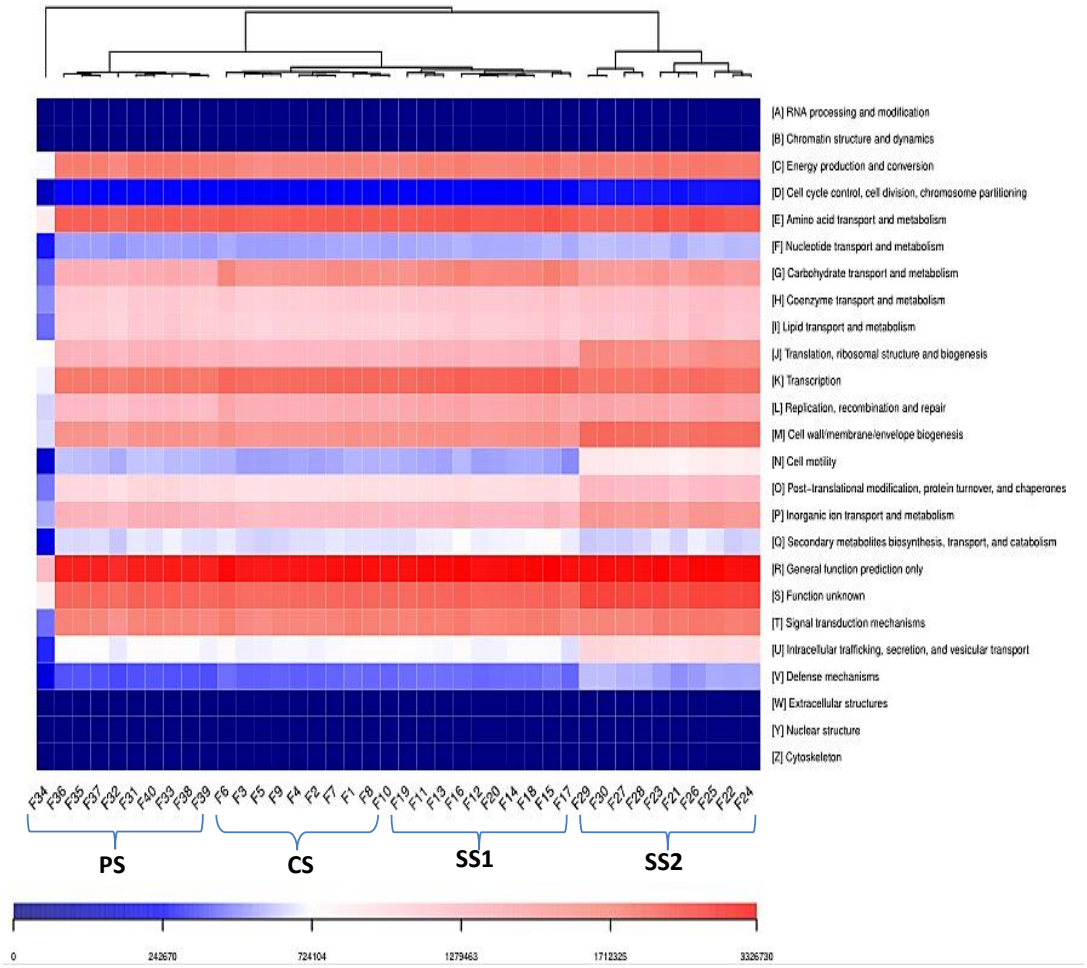

Figure 13. *Heat map showing relative abundances of clusters of orthologous group (COG) categories predicted by PICRUSt. The relationship among specimens is determined by the complete clustering method with Bray-Curtis distance. In the heat map, the red and blue colors indicate high and low relative abundance, respectively*

Bacteria indicated that the pathways of amino acid and carbohydrate metabolism, cellular processes and signalling, energy production and conversion, glycan synthesis and metabolism, xenobiotic biodegradation and translation mechanisms were the functions most abundant in all samples during the freeze-thaw experiments. There was no clear cluster based on the freezing and thawing phases in the samples except SS2. This indicated that the predicted function of bacteria population was more related to their contamination level than freeze-thaw temperature regimes. Previous study by Auti et al. (2016) also identified xenobiotic biosynthesis, carbohydrate metabolism and glycan biosynthesis terms in their petroleum polluted soil samples. The results were indicative of the predictive microbiomes of polluted soils SS1, SS2 and PS having the metabolic capacity associated with the degradation of xenobiotic compounds in the company of carbohydrate metabolism.

http://www.aloki.hu ● ISSN 1589 1623 (Print) ● ISSN 1785 0037 (Online)
DOI: http://dx.doi.org/10.15666/aeer/1906_51295157

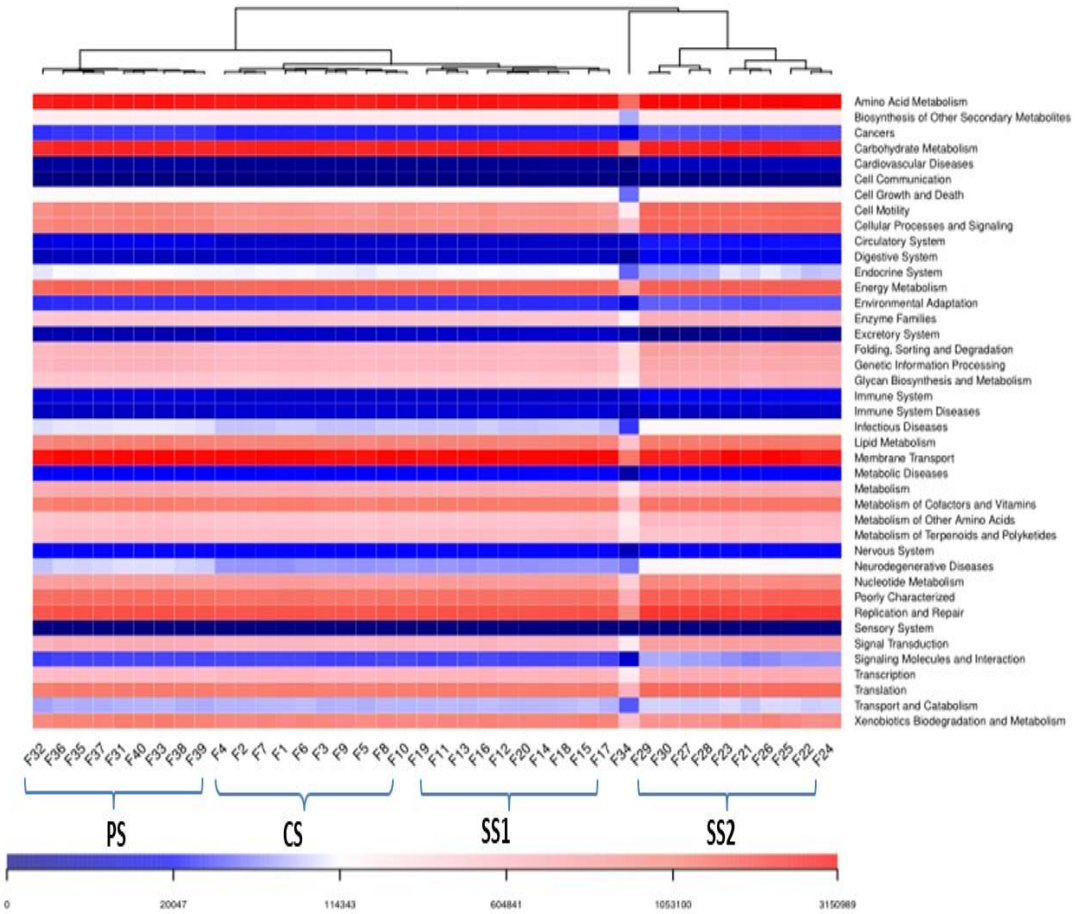

Figure 14. *Clustered heatmap of KEGG pathway enrichment analysis. F1: CS, F11: SS1, F21: SS2, F31: PS (F 20 ℃, Pre-incubation phase). F2: CS, F12: SS1, F22: SS2, F32: PS (F 10 ℃, Freezing phase). F3: CS, F13: SS1, F23: SS2, F33: PS (F 0 ℃, Freezing phase). F4: CS, F14: SS1, F24: SS2, F34: PS (F -10 ℃, Freezing phase). F5: CS, F15: SS1, F25: SS2, F35: PS (F -20 ℃, Freezing phase). F6: CS, F16: SS1, F26: SS2, F36: PS (T -10 ℃, Transition phase). F7: CS, F17: SS1, F27: SS2, F37: PS (T 0 ℃, Thawing phase). F8: CS, F18: SS1, F28: SS2, F38: PS (T 0 ℃, Thawing phase). F9: CS, F19: SS1, F29: SS2, F39: PS (T 0 ℃, Thawing phase). F10: CS, F20: SS1, F30: SS2, F40: PS (T 0 ℃, Thawing phase)*

Conclusion

This study provides important information on the impact of freeze-thaw events on the distribution characteristics of the bacterial communities in clean and petroleum polluted temperate soils with varying duration of oil exposure. The bacterial community compositions in the short-term polluted soils were more responsive to the freezing and thawing events while community richness remained relatively constant in the clean and weathered polluted soils during the freezing and thawing phases of the study. The important and interesting phenomenon found in the study was that the bacterial community composition in the short-term and weathered polluted temperate soils were more responsive to the presence of oil contaminants than the freezing and thawing events. Overall, our results provide insight on how the compositional structure of soil microbial communities in soils are modified as a result of oil contamination and freeze-thaw events. Nonetheless, the results reported in the study must be interpreted with

http://www.aloki.hu ● ISSN 1589 1623 (Print) ● ISSN 1785 0037 (Online)
DOI: http://dx.doi.org/10.15666/aeer/1906_51295157

caution considering the small sample size involved. Future work may focus on the studying the comparative influence of freeze-thaw events on polluted soils from different cold regions and also the biodegradation potentials of isolated microorganisms from short-term polluted soils and their application in on-field remediation approaches for cold sites.

Acknowledgements. This work was supported by the National Water Pollution Control and Treatment Science and Technology Major Project (No. 2018ZX07109-003) of China. The first author is grateful to the Petroleum Technology Development Fund for the doctoral scholarship award.

REFERENCES

[1] Aislabie, J. M., Balks, M. R., Foght, J. M., Waterhouse, E. J. (2004): Hydrocarbon spills on Antarctic soils: Effects and management. – Environmental Science and Technology 38(5): 1265-1274.

[2] Baek, K. H., Yoon, B. D., Kim, B. H., Cho, D. H., Lee, I. S., Oh, H. M., Kim, H. S. (2007): Monitoring of microbial diversity and activity during bioremediation of crude oil-contaminated soil with different treatments. – Journal of Microbiology and Biotechnology 17: 67-73.

[3] Bell, T. W., Menzer, O., Troyo-Diéquez, E., Oechel, W. C. (2012): Carbon dioxide exchange over multiple temporal scales in an arid shrub ecosystem near La Paz, Baja California Sur, Mexico. – Global Change Biology 18(8): 2570-2582.

[4] Borowik, A., Wyszkowska, J., Kucharski, M., Kucharski, J. (2019): Implications of soil pollution with diesel oil and BP petroleum with ACTIVE technology for soil health. – International Journal of Environmental Research and Public Health 16(14): 2474-2485.

[5] Børresen, M. H., Barnes, D. L., Rike, A. G. (2007): Repeated freeze-thaw cycles and their effects on mineralization of hexadecane and phenanthrene in cold climate soils. – Cold Region Science and Technology 49(3): 215-25.

[6] Buckeridge, K. M., Banerjee, S., Siciliano, S. D., Grogan, P. (2013): The seasonal pattern of soil microbial community structure in mesic low arctic tundra. – Soil Biology and Biochemistry 65: 338-347.

[7] Caporaso, J., Kuczynsk, J., Stombaugh, J., Bittinger, K., Bushman, F. D., Costello, E. K., et al. (2010): QIIME allows analysis of high-throughput community sequencing data. – Nature Methods 7(5): 335-336.

[8] Christensen, J. H., Hewitson, B., Busuioc, A., Chen, A., Gao, X., Held, I., et al. (2007): Regional Climate Projections. – In: Solomon, S., Qin, D., Manning, M., Chen, Z., Marquis, M., Averyt, K. B. (eds.) Climate Change 2007: The Physical Science Basis Contribution of Working Group I to the Fourth Assessment Report of the Intergovernmental Panel. Cambridge University Press, Cambridge, UK.

[9] Cisneros-de la Cueva, S., Martinez-Prado, M., Lopez-Miranda, J., Rojas-Contreras, J., Medrano-Roldan, H. (2016): Aerobic degradation of diesel by a pure culture of *Aspergillus terreus* KP862582. – Rev Mex Ing Quim. 15(2): 347-60.

[10] Edgar, R. C., Haas, B. J., Clemente, J. C., Quince, C., Knight, R. (2011): UCHIME improves sensitivity and speed of chimera detection. – Bioinformatics. 27(16): 2194-200.

[11] Gavazov, K., Ingrisch, J., Hasibeder, R., Mills, R. T. E., Buttler, A., Gleixner, G., Bahn, M. (2017): Winter ecology of a subalpine grassland: effects of snow removal on soil respiration, microbial structure and function. – Science of the Total Environment 590: 316-324.

[12] Guo, W. L., Hong-Bo, S., Jing-Jin, M., Ying-Juan, Z., Ji, W., Wen-Jun, S., Zi-Yin, Z. (2013): Basic features of climate change in North China during 1961-2010. – Advances in Climate Change Research, 4(2): 73-83.

http://www.aloki.hu ● ISSN 1589 1623 (Print) ● ISSN 1785 0037 (Online)
DOI: http://dx.doi.org/10.15666/aeer/1906_51295157

[13] Guoqing, L., Huadong, G., Xinwu, L., Lu, Z. (2014): Research on the temporal-spatial changes of near-surface soil freeze/thaw cycles in China based on Radiometer. – IOP Conference Series Earth and Environmental Science. https://doi.org/10.1088/1755-1315/17/1/012142.
[14] Han, Z., Deng, M., Yuan, A., Wang, J., Li, H., Ma, J. (2018): Vertical variation of a black soil's properties in response to freeze-thaw cycles and its links to shift of microbial community structure. – Science of the Total Environment 625: 106-113.
[15] Henry, A. (2007): Soil freeze–thaw cycle experiments: trends, methodological weaknesses and suggested improvements. – Soil Biology and Biochemistry 39: 977-986.
[16] Igun, O. T., Meynet, P., Davenport, R. J., Werner, D. (2019): Impacts of activated carbon amendments, added from the start or after five months, on the microbiology and outcomes of crude oil bioremediation in soil. – International Biodeterioration and Biodegradation 142: 1-10.
[17] Intergovernmental Panel on Climate Change, IPCC (2007): Climate Change 2007: The Physical Science Basis. – In: Solomon, S., Qin, D., Manning, M., Chen, Z., Marquis, M., Averyt, K. B. (eds.) Contribution of Working Group I to the Fourth Assessment Report of the Intergovernmental Panel on Climate Change. Cambridge University Press, Cambridge, UK and New York.
[18] Jia, J., Zong, S., Hu, L., Shi, S., Zhai, X., Wang, B. (2017): The dynamic change of microbial communities in crude oil-contaminated soils from oilfields in China. – Soil and Sediment Contamination 18: 1-30.
[19] Jiang, N., Juan, Y., Tian, L., Chen, X., Sun, W., Chen, L. (2018): Modification of the composition of dissolved nitrogen forms, nitrogen transformation processes, and diversity of bacterial communities by freeze–thaw events in temperate soils. – Pedobiologia Journal of Soil Ecology 71: 41-49.
[20] Juan, Y., Jiang, N., Tian, L., Chen, X., Sun, W., Chen, L. (2018): Effect of freeze-thaw on a midtemperate soil bacterial community and the correlation network of its members. – Biomed Research International 8412429: 1-13.
[21] Kimoto, M. (2005): Simulated change of the east Asian circulation under global warming scenario. – Geophysics Research Letters 32(16): 1-5.
[22] Koponen, H. T., Jaakkola, T., Keina, M. M. (2006): Microbial communities, biomass, and activities in soils as affected by freeze thaw cycles. – Soil Biology and Biochemistry 38: 1861-1871.
[23] Korenblum, E., Souza, D., Penna, M., Seldin, L. (2012): Molecular analysis of the bacterial communities in crude oil samples from two Brazilian offshore petroleum platforms. – International Journal of Microbiology 156537: 1-8.
[24] Kumar, N., Grogan, P., Chu, H., Christiansen, C. T., Walker, V. K. (2013): The effect of freeze-thaw conditions on arctic soil bacterial communities. – Biology (Basel) 2(1): 356-377.
[25] Labbé, D., Margesin, R., Schinner, F., Whyte, L. G., Greer, C. W. (2007): Comparative phylogenetic analysis of microbial communities in pristine and hydrocarbon-contaminated Alpine soils. – FEMS Microbiology Ecology 59(2): 466-475.
[26] Langille, M. G., Zaneveld, J., Caporaso, J. G., Mcdonald, D., Knights, D., Reyes, J. A., et al. (2013): Predictive functional profiling of microbial communities using 16S rRNA marker gene sequences. – Nature Biotechnology 31: 814-821.
[27] Li, W., Jiang, Z., Zhang, X., Li, L., Sun, Y. (2018): Additional risk in extreme precipitation in China from 1.5 °C to 2.0 °C global warming levels. – Science Bulletin 63(4): 228-234.
[28] Lin, L., Wang, Z., Yang, Y., Zhang, H., Dong, W. (2018): Additional intensification of seasonal heat and flooding extreme over China in 2 °C warmer world compared to 1.5 °C. – Earths Future 6: 968-978.

http://www.aloki.hu ● ISSN 1589 1623 (Print) ● ISSN 1785 0037 (Online)
DOI: http://dx.doi.org/10.15666/aeer/1906_51295157

[29] Liu, Q., Tang, J., Gao, K., Gurav, R., Giesy, J. P. (2017): Aerobic degradation of crude oil by microorganisms in soils from four geographic regions of China. – Science Reports 7: 1-12.
[30] Meyer, B., Kuever, J. (2007): Molecular analysis of the diversity of sulfate-reducing and sulfur oxidizing prokaryotes in the environment, using aprA as functional marker gene. – Applied Environmental Microbiology 73(23): 7664-7679.
[31] Okonkwo, C. J., Liu, N., Li, J., Ahmed, A. (2021): Experimental thawing events enhance petroleum hydrocarbon attenuation and enzymatic activities in polluted temperate soils. – International Journal Environment Science and Technology. https://doi.org/10.1007/s13762-021-03175-8.
[32] Olsson, P. Q., Sturm, M., Racine, C. H., Romanovsky, V., Liston, G. E. (2003): Five stages of the Alaskan Arctic cold season with ecosystem implications. – Arctic, Antarctic and Alpine Research 35(1): 74-81.
[33] Peng, M., Zi, X., Wang, Q. (2015): Bacterial community diversity of oil-contaminated soils assessed by high throughput sequencing of 16S rRNA genes. – International Journal of Environmental Research and Public Health 12(10): 12002-12015.
[34] R Core Team (2014): R: A language and Environment for Statistical Computing. – R Foundation for Statistical Computing, Vienna, Austria. URL http://www.R-project.org/.
[35] Ramadass, K., Smith, E., Palanisami, T., Mathieson, G., Srivastava, P., Megharaj, M., et al. (2015): Evaluation of constraints in bioremediation of weathered hydrocarbon-contaminated arid soils through microcosm biopile study. – International Journal of Environmental Science and Technology 12(11): 3597-3612.
[36] Ren, J., Song, C., Hou, A., Song, Y., Zhu, X., Cagle, G. A. (2018): Shifts in soil bacterial and archaeal communities during freeze-thaw cycles in a seasonal frozen marsh, Northeast China. – Science of the Total Environment 625: 782-791.
[37] Schimel, J., Balser, T. C., Wallenstein, M. (2007): Microbial stress-response physiology and its implication. – Ecology 88(6): 1386-1394.
[38] Schmidhuber, J., Tubiello, F. (2007): The mixing phenomena of SLUSH hydrogen in ducts. – PNAS 104(50): 19703-19708.
[39] Shankar, V., Agans, R., Paliy, O. (2017): Advantages of phylogenetic distance based constrained ordination analyses for the examination of microbial communities. – Scientific Reports 7: 1-10.
[40] Shen, R. C., Xu, M., Chi, Y. G., Yu, S., Wan, S. Q. (2014): Soil microbial responses to experimental warming and nitrogen addition in a temperate steppe of Northern China. – Pedosphere 24(4): 427-436.
[41] Siles, J. A., Margesin, R. (2018): Insights into microbial communities mediating the bioremediation of hydrocarbon-contaminated soil from an Alpine former military site. – Applied Microbiology and Biotechnology 102: 4409-4421.
[42] Skogland, T., Lomeland, S., Goksøyr, J. (1988): Respiratory burst after freezing and thawing of soil: experiments with soil bacteria. – Soil Biology and Biochemistry 20(6): 851-856.
[43] Sun, W., Li, J., Jiang, L., Sun, Z. (2015): Profiling microbial community structures across six large oilfields in China and the potential role of dominant microorganisms in bioremediation. – Applied Microbiology and Biotechnology 99(20): 8751-8764.
[44] Trellu, C., Mousset, E., Pechaud, Y., Huguenot, D., van Hullebusch, E. D., Esposito, G., et al. (2016): Removal of hydrophobic organic pollutants from soil washing/flushing solutions: a critical review. – Journal of Hazardous Materials 306: 149-174.
[45] Wang, Q., Garrity, G. M, Tiedje, J. M., Cole, J. R. (2007): Naïve Bayesian classifier for rapid assignment of rRNA sequences into the new bacterial taxonomy. – Applied Environmental Microbiology 73(16): 5261-5267.
[46] Wang, Q., Liu, J., Wang, L. (2017): An experimental study on the effects of freeze-thaw cycles on phosphorus adsorption-desorption processes in brown soil. – RSC Advances 7(59): 37441-37446.

http://www.aloki.hu ● ISSN 1589 1623 (Print) ● ISSN 1785 0037 (Online)
DOI: http://dx.doi.org/10.15666/aeer/1906_51295157

[47] White, T., Bruns, T. D., Lee, S. B., Taylor, J. W. (1990): Amplification and Direct Sequencing of Fungal Ribosomal RNA Genes for Phylogenetics. – Academic Press, Inc., Cambridge, MA, pp. 315-321.
[48] Wu, M., Dick, W. A., Li, W., Wang, X., Yang, Q., Wang, T., Wang, L., Chen, L. (2016): Bioaugmentation and biostimulation of hydrocarbon degradation and the microbial community in a petroleum-contaminated soil. – International Biodeterioration and Biodegradation 107: 158-64.
[49] Wu, M. L., Wu, J. L., Zhang, X. H., Ye, X. Q. (2019): Effect of bioaugmentation and biostimulation on hydrocarbon degradation and microbial community composition in petroleum-contaminated loessal soil. – Chemosphere 237: 124456.
[50] Wyszkowska, J., Kucharski, J. (2005): Correlation between the number of microorganisms and soil contamination with diesel oil. – Polish Journal of Environmental Studies 14: 359-368.
[51] Yang, S. Z., Jin, H. J., Wei, Z., He, R. X., Ji, Y. J., Li, X. M. (2019): Bioremediation of oil spills in cold environments: a review. – Pedosphere 19(3): 371-381.
[52] Zheng, Z., Zhang, Y., Su, X., Cui, X. (2016): Responses of hydrochemical parameters, community structures, and microbial activities to the natural biodegradation of petroleum hydrocarbons in a groundwater–soil environment. – Environmental Earth Science 75(21): 1400-1413.

APPENDIX

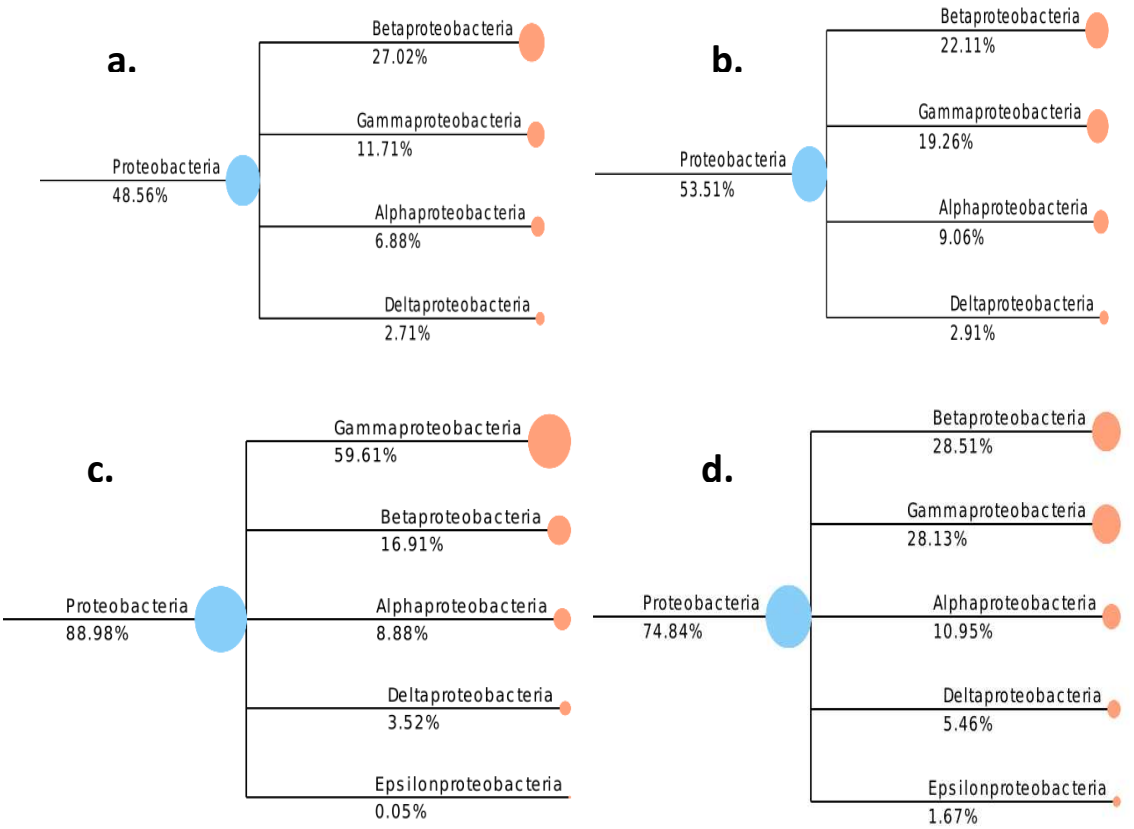

Figure A1. *Bacterial class composition in (a) Clean natural soil CS (b) Diesel-oil amended soil SS1 (c) Crude-oil amended soil SS2 (d) weathered petroleum-polluted soil PS during Pre-incubation phase (F -20 ℃)*

http://www.aloki.hu ● ISSN 1589 1623 (Print) ● ISSN 1785 0037 (Online)
DOI: http://dx.doi.org/10.15666/aeer/1906_51295157

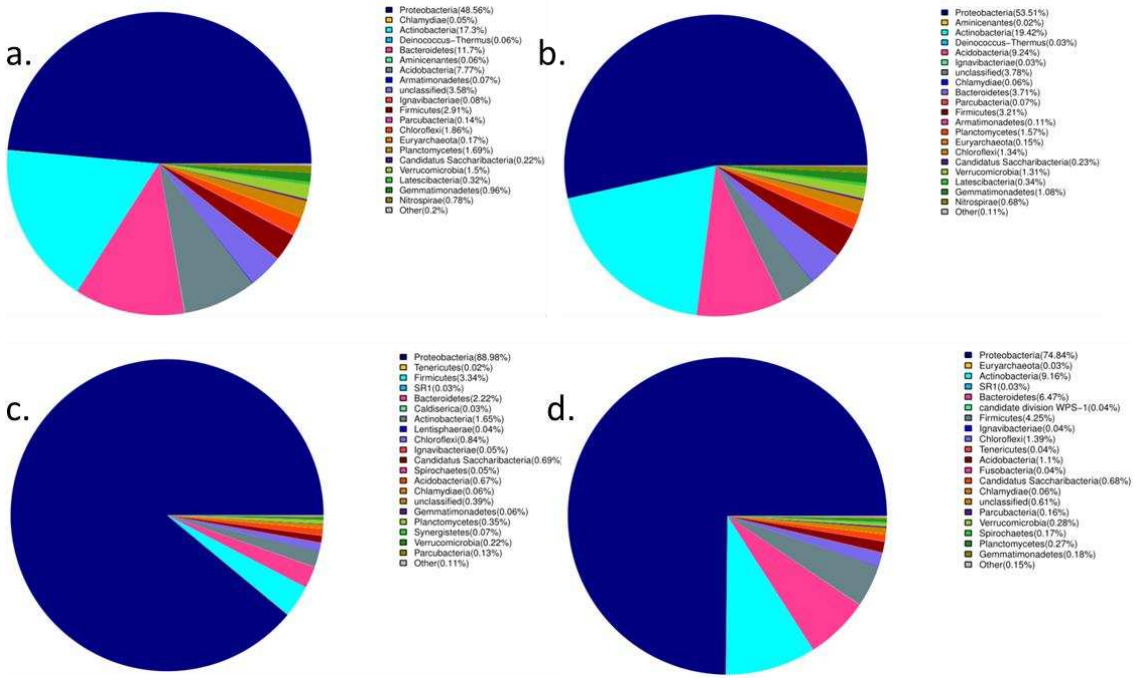

Figure A2. a-d *Bacterial phylum composition in (a) Clean natural soil CS (b) Diesel-oil amended soil SS1 (c) Crude-oil amended soil SS2 (d) weathered petroleum-polluted soil PS at Pre-incubation phase (F 20 ℃)*

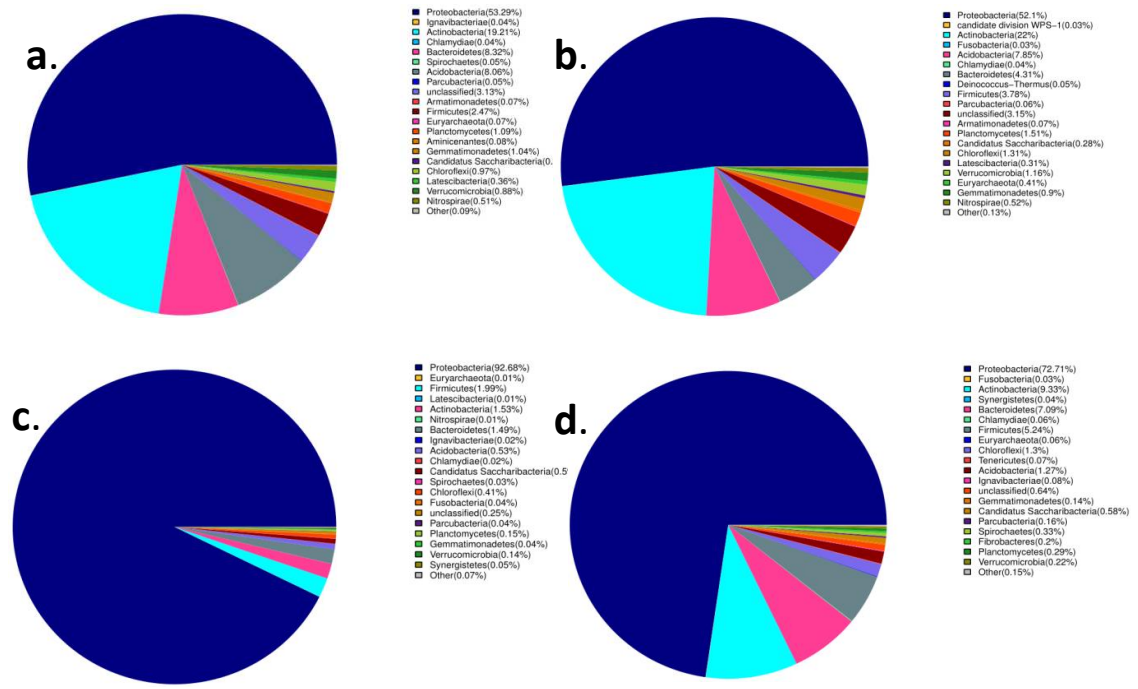

Figure A3. a-d *Bacterial phylum composition in (a) Clean natural soil CS (b) Diesel-oil amended soil SS1 (c) Crude-oil amended soil SS2 (d) weathered petroleum-polluted soil PS at freezing phase (F 10 ℃)*

http://www.aloki.hu ● ISSN 1589 1623 (Print) ● ISSN 1785 0037 (Online)
DOI: http://dx.doi.org/10.15666/aeer/1906_51295157

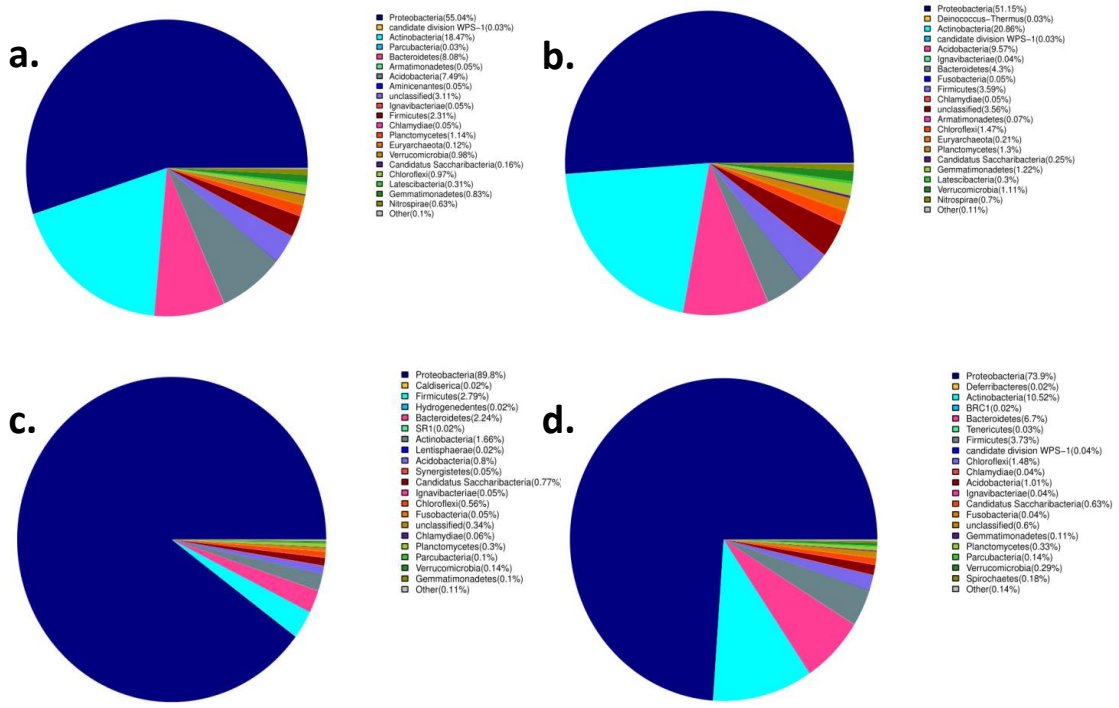

Figure A4. a-d *Bacterial phylum composition in (a) Clean natural soil CS (b) Diesel-oil amended soil SS1 (c) Crude-oil amended soil SS2 (d) Weathered petroleum-polluted soil PS at freezing phase (F 0 ℃)*

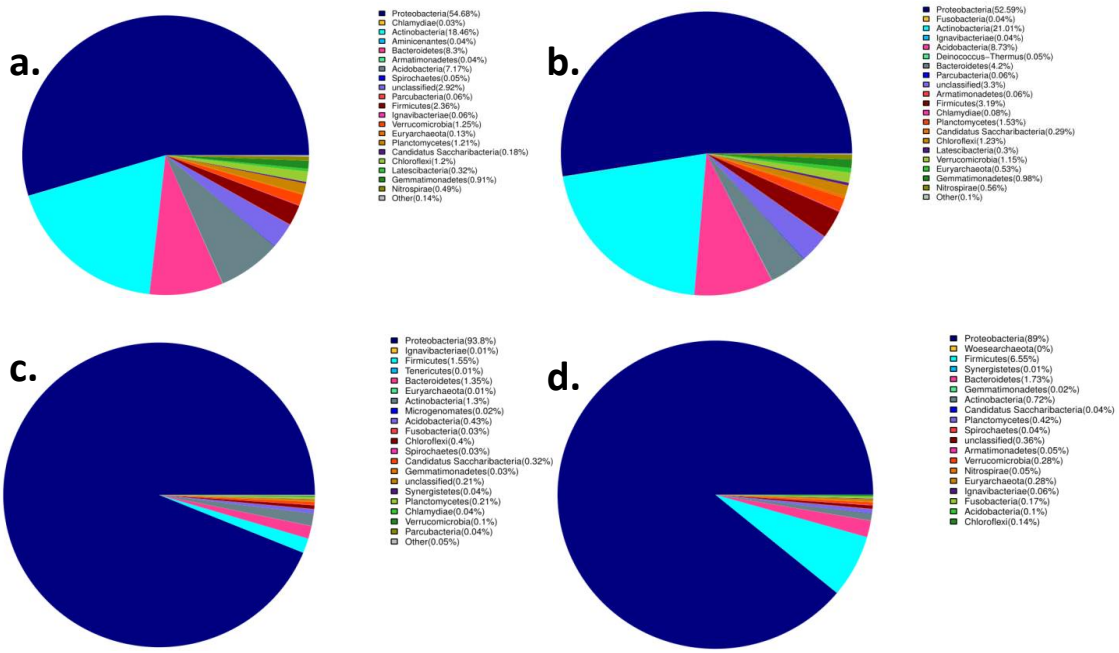

Figure A5. a-d *Bacterial phylum composition in (a) Clean natural soil CS (b) Diesel-oil amended soil SS1 (c) Crude-oil amended soil SS2 (d) Weathered petroleum-polluted soil PS at freezing phase (F -10 ℃)*

http://www.aloki.hu ● ISSN 1589 1623 (Print) ● ISSN 1785 0037 (Online)
DOI: http://dx.doi.org/10.15666/aeer/1906_51295157

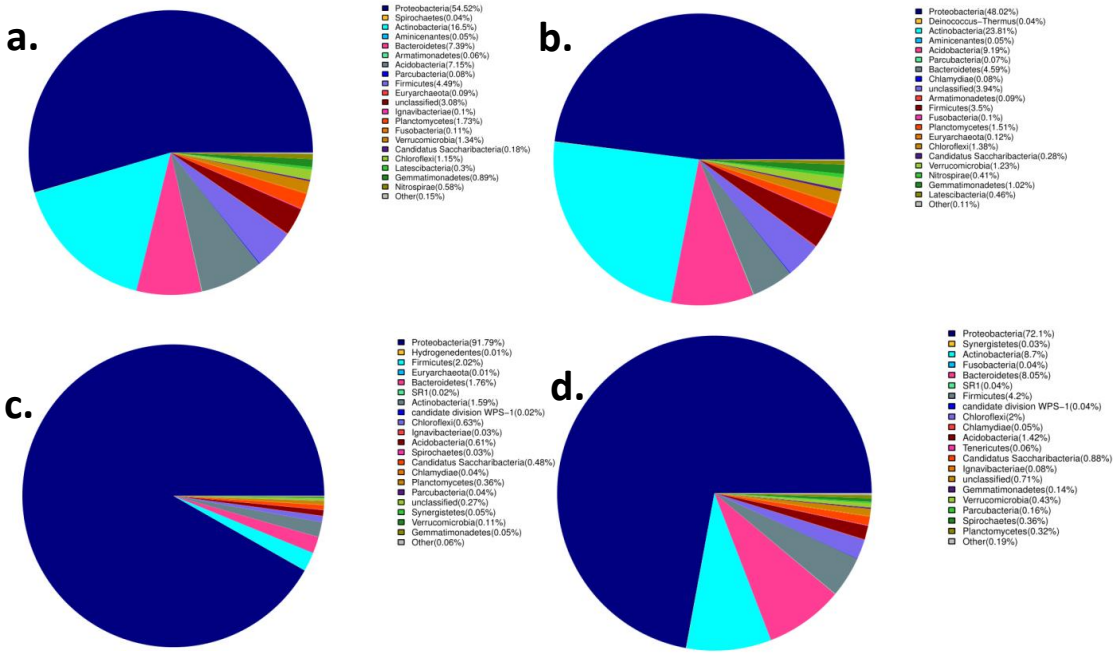

Figure A6. a-d *Bacterial phylum composition in (a) Clean natural soil CS (b) Diesel-oil amended soil SS1 (c) Crude-oil amended soil SS2 (d) Weathered petroleum-polluted soil PS at freezing phase (F -20 ℃)*

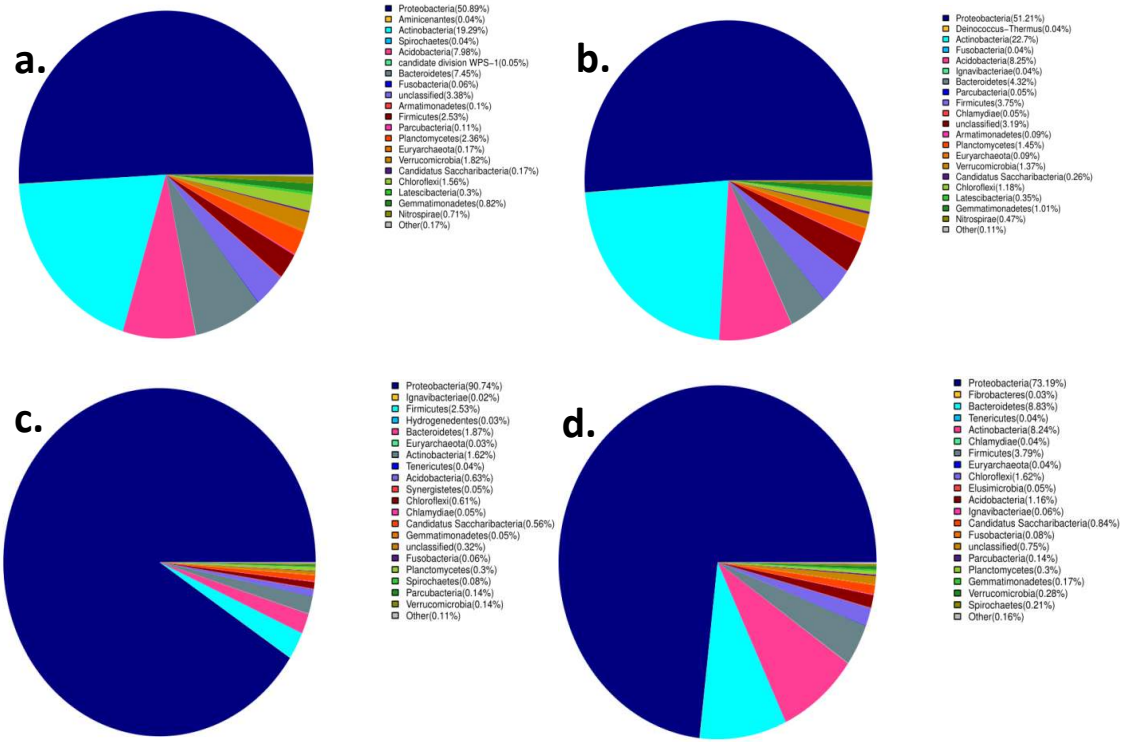

Figure A7. a-d *Bacterial phylum composition in (a) Clean natural soil CS (b) Diesel-oil amended soil SS1 (c) Crude-oil amended soil SS2 (d) Weathered petroleum-polluted soil PS at transition phase (T -20 ℃)*

http://www.aloki.hu ● ISSN 1589 1623 (Print) ● ISSN 1785 0037 (Online)
DOI: http://dx.doi.org/10.15666/aeer/1906_51295157

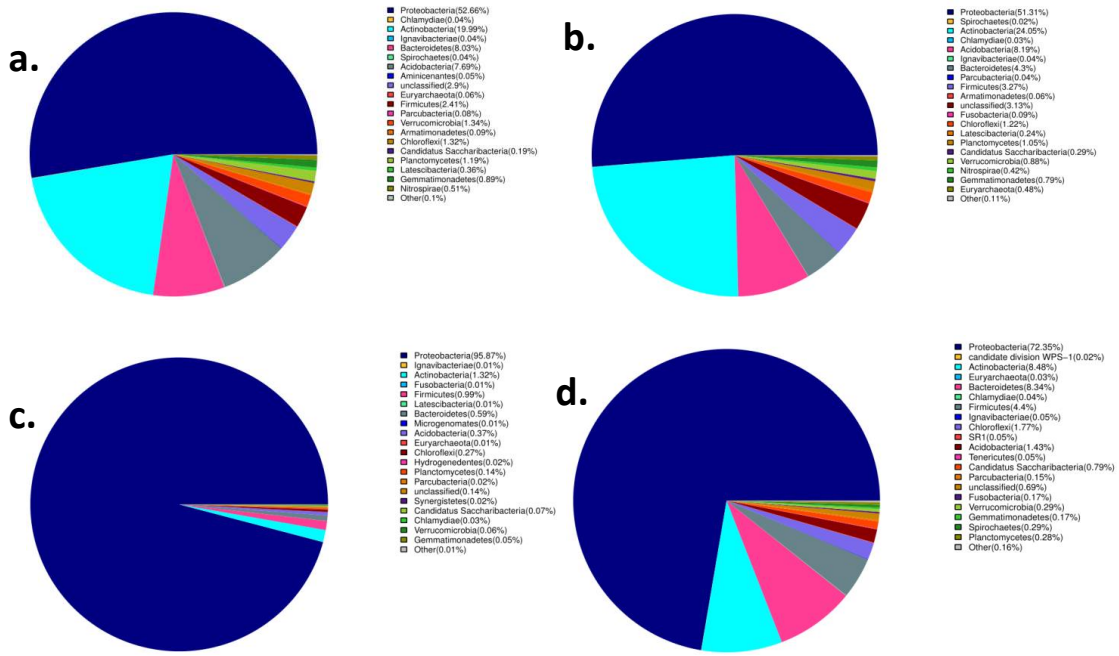

Figure A8. a-d *Bacterial phylum composition in (a) Clean natural soil CS (b) Diesel-oil amended soil SS1 (c) Crude-oil amended soil SS2 (d) Weathered petroleum-polluted soil PS at thawing phase (T -10 ℃)*

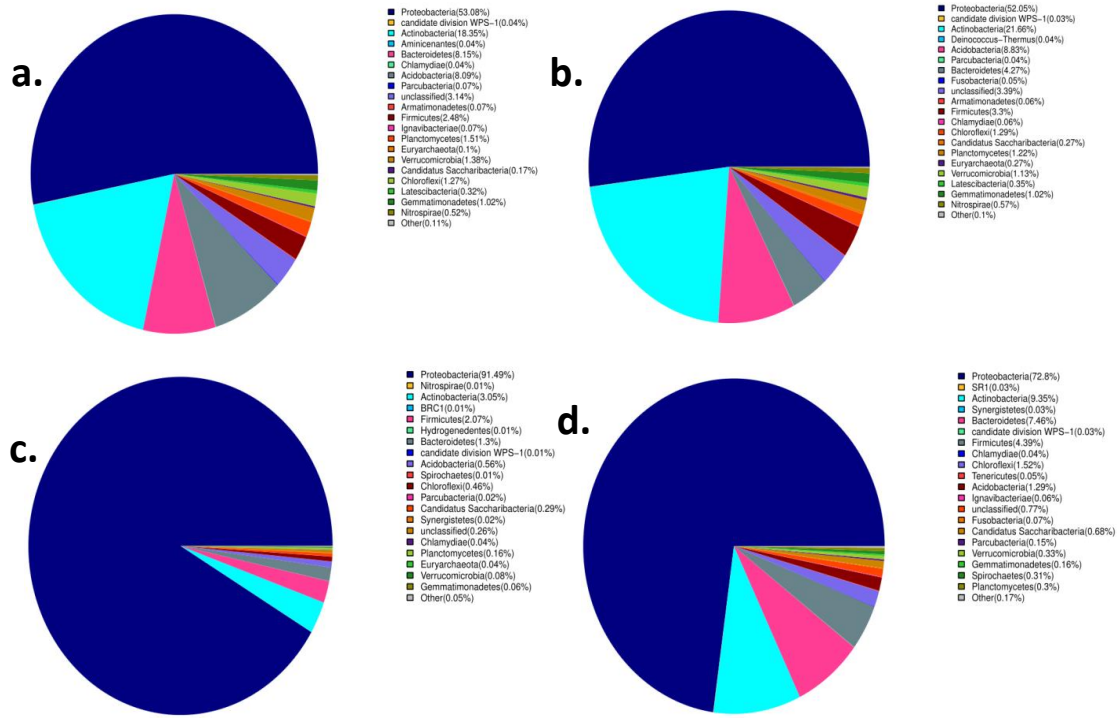

Figure A9. a-d *Bacterial phylum composition in (a) Clean natural soil CS (b) Diesel-oil amended soil SS1 (c) Crude-oil amended soil SS2 (d) Weathered petroleum-polluted soil PS at thawing phase (T 0 ℃)*

http://www.aloki.hu ● ISSN 1589 1623 (Print) ● ISSN 1785 0037 (Online)
DOI: http://dx.doi.org/10.15666/aeer/1906_51295157

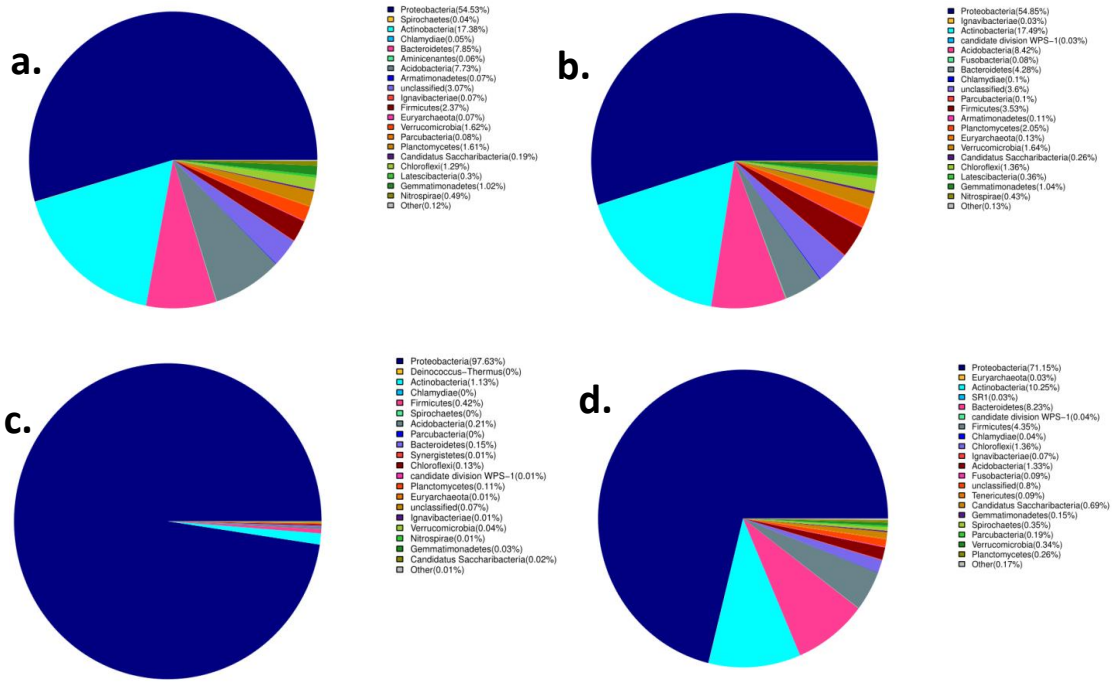

Figure A10. a-d *Bacterial phylum composition in (a) Clean natural soil CS (b) Diesel-oil amended soil SS1 (c) Crude-oil amended soil SS2 (d) Weathered petroleum-polluted soil PS at thawing phase (T 10 ℃)*

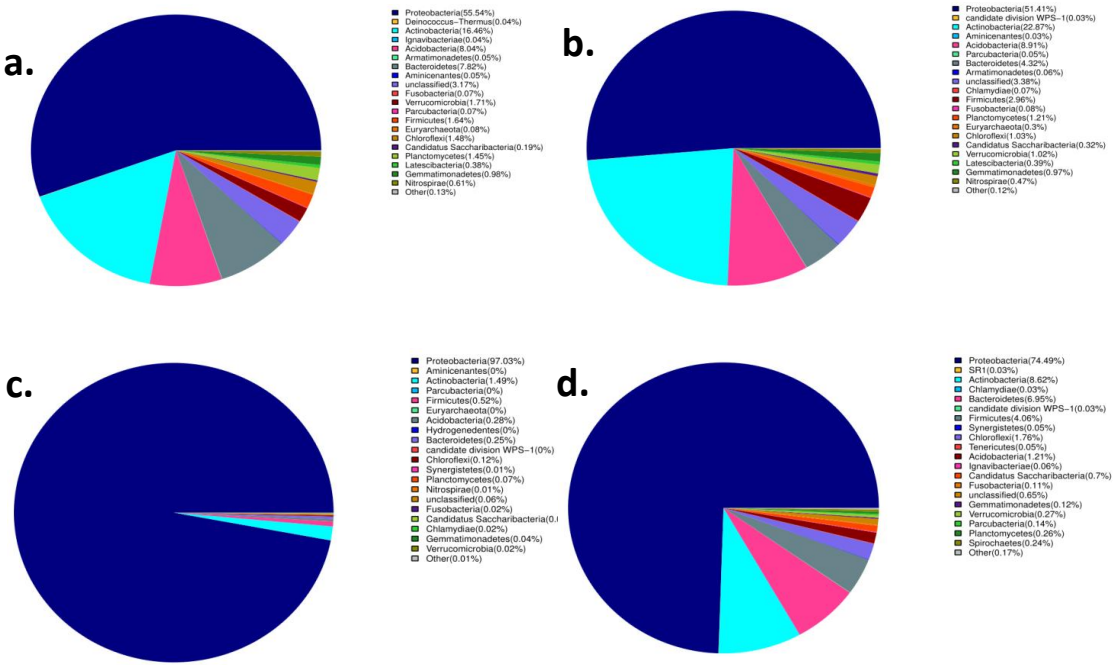

Figure A11. a-d *Bacterial phylum composition in (a) Clean natural soil CS (b) Diesel-oil amended soil SS1 (c) Crude-oil amended soil SS2 (d) Weathered petroleum-polluted soil PS at thawing phase (T 20 ℃)*

http://www.aloki.hu ● ISSN 1589 1623 (Print) ● ISSN 1785 0037 (Online)
DOI: http://dx.doi.org/10.15666/aeer/1906_51295157

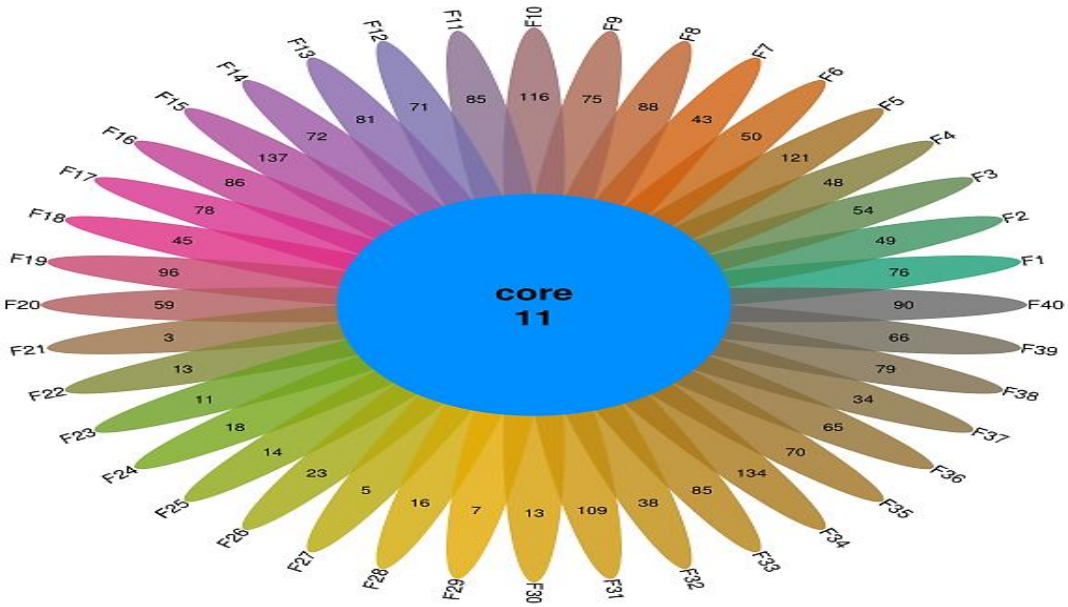

Figure A12. *Venn diagram showing the unique bacterial species in the soil samples CS, SS1, SS2 and PS. F1: CS, F11: SS1, F21: SS2, F31: PS (F 20 °C, Pre-incubation phase). F2: CS, F12: SS1, F22: SS2, F32: PS (F 10 °C, Freezing phase). F3: CS, F13: SS1, F23: SS2, F33: PS (F 0 °C, Freezing phase). F4: CS, F14: SS1, F24: SS2, F34: PS (F -10 °C, Freezing phase). F5: CS, F15: SS1, F25: SS2, F35: PS (F -20 °C, Freezing phase). F6: CS, F16: SS1, F26: SS2, F36: PS (T -10 °C, Transition phase). F7: CS, F17: SS1, F27: SS2, F37: PS (T 0 °C, Thawing phase). F8: CS, F18: SS1, F28: SS2, F38: PS (T 0 °C, Thawing phase). F9: CS, F19: SS1, F29: SS2, F39: PS (T 0 °C, Thawing phase). F10: CS, F20: SS1, F30: SS2, F40: PS (T 0 °C, Thawing phase)*

http://www.aloki.hu ● ISSN 1589 1623 (Print) ● ISSN 1785 0037 (Online)
DOI: http://dx.doi.org/10.15666/aeer/1906_51295157